NEUROENDOCRINE-IMMUNOLOGICAL INTERACTIONS IN HEALTH AND DISEASE

EDITED BY: Vinicius Frias Carvalho, Ana Rosa Pérez and Clarissa M. Maya-Monteiro
PUBLISHED IN: Frontiers in Endocrinology and Frontiers in Neuroscience

frontiers Research Topics

frontiers

ISSN 1664-8714
ISBN 978-2-88971-525-1
DOI 10.3389/978-2-88971-525-1

About Frontiers

Frontiers is more than just an open-access publisher of scholarly articles: it is a pioneering approach to the world of academia, radically improving the way scholarly research is managed. The grand vision of Frontiers is a world where all people have an equal opportunity to seek, share and generate knowledge. Frontiers provides immediate and permanent online open access to all its publications, but this alone is not enough to realize our grand goals.

Frontiers Journal Series

The Frontiers Journal Series is a multi-tier and interdisciplinary set of open-access, online journals, promising a paradigm shift from the current review, selection and dissemination processes in academic publishing. All Frontiers journals are driven by researchers for researchers; therefore, they constitute a service to the scholarly community. At the same time, the Frontiers Journal Series operates on a revolutionary invention, the tiered publishing system, initially addressing specific communities of scholars, and gradually climbing up to broader public understanding, thus serving the interests of the lay society, too.

Dedication to Quality

Each Frontiers article is a landmark of the highest quality, thanks to genuinely collaborative interactions between authors and review editors, who include some of the world's best academicians. Research must be certified by peers before entering a stream of knowledge that may eventually reach the public - and shape society; therefore, Frontiers only applies the most rigorous and unbiased reviews.
Frontiers revolutionizes research publishing by freely delivering the most outstanding research, evaluated with no bias from both the academic and social point of view. By applying the most advanced information technologies, Frontiers is catapulting scholarly publishing into a new generation.

What are Frontiers Research Topics?

Frontiers Research Topics are very popular trademarks of the Frontiers Journals Series: they are collections of at least ten articles, all centered on a particular subject. With their unique mix of varied contributions from Original Research to Review Articles, Frontiers Research Topics unify the most influential researchers, the latest key findings and historical advances in a hot research area! Find out more on how to host your own Frontiers Research Topic or contribute to one as an author by contacting the Frontiers Editorial Office: frontiersin.org/about/contact

NEUROENDOCRINE-IMMUNOLOGICAL INTERACTIONS IN HEALTH AND DISEASE

Topic Editors:
Vinicius Frias Carvalho, Oswaldo Cruz Foundation (Fiocruz), Brazil
Ana Rosa Pérez, Consejo Nacional de Investigaciones Científicas y Técnicas (CONICET), Argentina
Clarissa M. Maya-Monteiro, Oswaldo Cruz Foundation (Fiocruz), Brazil

Citation: Carvalho, V. F., Pérez, A. R., Maya-Monteiro, C. M., eds. (2021). Neuroendocrine-Immunological Interactions in Health and Disease. Lausanne: Frontiers Media SA. doi: 10.3389/978-2-88971-525-1

Table of Contents

frontiers in Endocrinology

EDITORIAL
published: 06 September 2021
doi: 10.3389/fendo.2021.718893

Editorial: Neuroendocrine-Immunological Interactions in Health and Disease

Ana Rosa Pérez[1,2*], *Clarissa M. Maya-Monteiro*[3,4,5*] *and Vinicius Frias Carvalho*[6*]

[1] Instituto de Inmunología Clínica y Experimental de Rosario, Consejo Nacional de Investigaciones Científicas y Técnicas (CONICET), Rosario, Argentina, [2] Facultad de Ciencias Médicas, Universidad Nacional de Rosario, Rosario, Argentina, [3] Laboratory of Immunopharmacology, Oswaldo Cruz Institute (IOC), Oswaldo Cruz Foundation (FIOCRUZ), Rio de Janeiro, Brazil, [4] Department of Endocrinology and Metabolism, Amsterdam University Medical Centers (Amsterdam UMC), Amsterdam, Netherlands, [5] Metabolism and Reward Group, Netherlands Institute for Neuroscience (NIN), Amsterdam, Netherlands, [6] Laboratory of Inflammation, Oswaldo Cruz Institute (IOC), Oswaldo Cruz Foundation (FIOCRUZ), Rio de Janeiro, Brazil

Keywords: neuroendocrine, immunoendocrine, neuroimmune, metabolism, hormones, adipocytokines, cytokines

Editorial on the Research Topic

Neuroendocrine-Immunological Interactions in Health and Disease

Historically, scientists have delimited the immune, endocrine, and neural systems to study physiology and disease (**Figure 1**). Although questions relating to whether there is a strict boundary between these systems do persist today, we do not believe in that. Biology does not seem to "respect" the established limits between these systems. Indeed, since Claude Bernard's early studies in physiology, we know that the different organs and systems must communicate in an integrative way to maintain homeostasis. During recent decades, we have investigated these systems in an integrative way, since both the tools and the information to perform these studies are now available. In this Research Topic, we gathered diverse studies that increase our knowledge about the complex interactions among the immune, endocrine, and neural systems in both homeostasis and disease, and the potential therapeutic or disrupting agents of these circuits.

The similarities between nervous, immune, and endocrine systems are remarkable, and there are a number of shared mechanisms, agents, and receptors. As an example, cytokines and hormones are both important mediators of the hypothalamus–pituitary–adrenal (HPA) and hypothalamus–pituitary–thyroid (HPT) axes in response to stress and promoting immune modulation. Activation of the HPA axis triggers the synthesis of hypothalamic corticotropin-releasing hormone (CRH), followed by the release of the pituitary adrenocorticotropic hormone (ACTH) and activation of adrenal glands to secrete cortisol and dehydroepiandrosterone (DHEA). An imbalance of these components affects both positive and negative regulatory loops, leading to the predisposition for, and/or exacerbation of several infectious diseases. This imbalance was well described by Fernandez et al. as they studied the immune-endocrine system in the presence of tuberculosis and diabetes comorbidity, and demonstrated opposite effects on DHEA and cortisol. In humans, the immune response developed against *B. abortus* is also influenced by DHEA and cortisol secretions. Here, Gentilini et al. evaluated the consequence of both adrenal steroids on synoviocytes during *B. abortus* infection, contributing to knowledge about this infectious osteoarthritis. Furthermore, infectious-driven immune stimulation could sustain glucocorticoid production through changes in the intra-adrenal catabolic pathways or induced cellular damage, as shown by Silva Barbosa et al. and by Chen et al. in experimental models of Chagas disease and sepsis, respectively.

OPEN ACCESS

Edited and reviewed by:
Hubert Vaudry,
Université de Rouen, France

***Correspondence:**
Ana Rosa Pérez
perez@idicer-conicet.gob.ar
Clarissa M. Maya-Monteiro
clarissa@ioc.fiocruz.br
Vinicius Frias Carvalho
vfrias@ioc.fiocruz.br

Specialty section:
This article was submitted to Neuroendocrine Science, a section of the journal Frontiers in Endocrinology

Received: *01 June 2021*
Accepted: *07 July 2021*
Published: *06 September 2021*

Citation:
Pérez AR, Maya-Monteiro CM and Carvalho VF (2021) Editorial: Neuroendocrine-Immunological Interactions in Health and Disease. Front. Endocrinol. 12:718893. doi: 10.3389/fendo.2021.718893

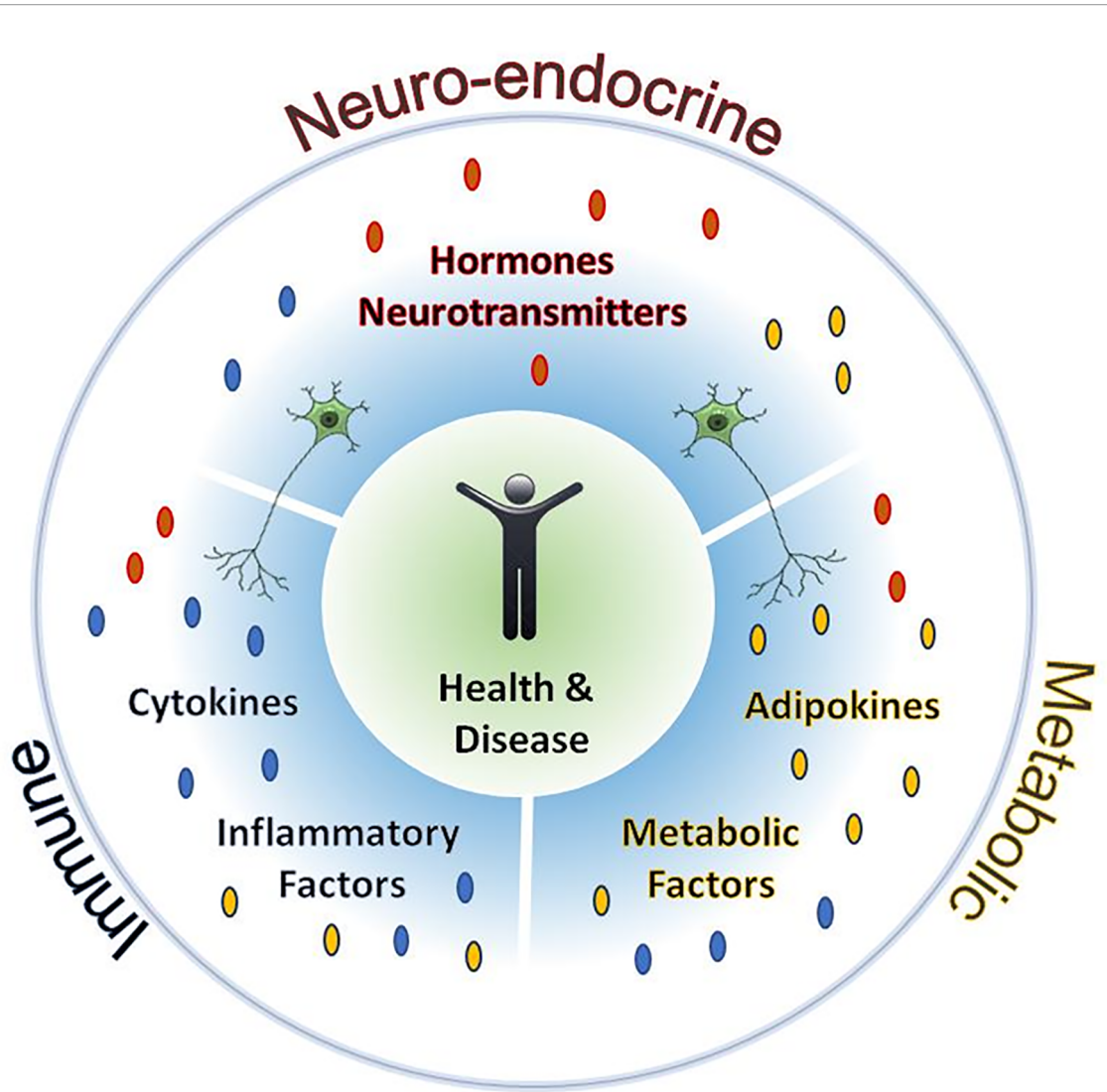

FIGURE 1 | Neuroendocrine, immune and even metabolic systems are interconnected by a profuse network of mediators.

It is known that endogenous hypercortisolism or exposure to exogenous glucocorticoids can lead to Cushing's syndrome. Liu et al. report on a rare case of an ectopic ACTH-dependent Cushing's syndrome and proposed a mechanism for this unique clinical phenotype. Despite the adverse effects that sustained hypercortisolism may cause, the chronic use of corticosteroids to treat inflammatory diseases is widely accepted in clinical settings. As reported here, Ferreira et al. revealed a promising use of flunisolide as a pharmacological treatment for silicosis. Another important neuro-endocrine circuit, essential for dealing with stress, is the sympatho-adrenal system. Pilipovic et al. summarized the data, pointing to an immunopathogenic role for the sympathoadrenal axis in the pathogenesis of experimental autoimmune encephalomyelitis and multiple sclerosis.

Activation of the HPT axis induces the production of hypothalamic thyrotropin-releasing hormone (TRH), followed by the release of the thyroid-stimulating hormone (TSH), and synthesis of thyroid hormones. Hashimoto's encephalopathy (HE) is an unusual neuropsychiatric syndrome characterized by elevated levels of autoantibodies against several thyroid antigens. Yu et al. described a case report of HE in a patient whose clinical symptoms and laboratory test results mimicked viral encephalitis. The effective diagnosis enabled the successful use of immunosuppressive therapy. In addition, Ferraris et al. showed that octyl methoxycinnamate, one of the most used UV filters, disrupted thyroid regulation and modulated the immune system in mice pups.

The adipose tissue is considered to be an immunoendocrine organ capable of producing a wide variety of mediators; the main adipose tissue specific cytokines, the adipocytokines, are leptin and adiponectin. Disruption of adipose tissue homeostasis can lead to alterations in many critical aspects of immunity. Pesce Viglietti et al. showed how *B. abortus* can modulate the transcription of adipocytokines and affect the process of

adipogenesis both directly and indirectly. Palhinha et al. described for the first time that leptin autocrine signaling pathways induce adipogenesis and proinflammatory profile. This effect may have particular importance during obesity when leptin central nervous system signaling is defective. Amorim et al. showed that leptin can also trigger an eosinophilic inflammatory response *in vivo*, by an indirect mechanism dependent on the activation of resident mast cell secretory activity and mediated by TNFα, CCL5, and PGD2.

Immunometabolism can be regarded as a branch of neuroendocrine-immunology examining the crosstalk between metabolism and the immune response. Smitka et al. summarized evidence showing that the gut microbiome is a potential modulator of adipose tissue, energy homeostasis, and appetite satiety in eating disorders, like anorexia and bulimia. The work from Silva et al. proposed that short-chain fatty acids from gut microbiota can be used as a therapy for central nervous system (CNS) disorders through its capacity to regulate the neuro-immunoendocrine function. Milanova et al. showed that hypothalamic microglia from high-fat diet fed mice were activated and lost rhythm, displaying immuno-metabolic functions different from those observed in microglia from control animals. Huang et al. demonstrated that high glucose or glucose fluctuations caused M2 phenotype polarization in a microglial cell line *in vitro*. They also showed that miR-146a overexpression inhibited high-glucose-induced M1/M2 polarization transitions in those cells.

In literature, activation of immune system secondary lymphoid organs (SLOs) has been observed to coincide with the decrease in noradrenergic activity and/or retraction of sympathetic fibers. Bottasso *(part I) and* Bottasso *(part II)* introduced a challenging hypothesis for the existence of a neural plasticity program in the sympathetic fibers innervating both SLOs and non-lymphoid peripheral tissues during inflammation. According to the author, this plasticity implies a retraction and degeneration of sympathetic fibers during immune activation and their re-generation once homeostasis is re-established. The activation of the immune system can be important in the disruption of neural circuits and induction of nervous system disorders. In this regard, Li et al. showed that IFN-α, administered by i.c.v. routes induced depression-like behavior in monkeys. This was associated with a dysfunction in some monoamine neurotransmitters founded in the cerebrospinal fluid. Stary et al. found that nursing in the post-partum period protected the mouse nervous system in a model of middle cerebral artery occlusion-induced stroke. They showed a reduced neurological deficit, lower pro-inflammatory cytokine levels, and lower migration of blood leukocytes into the brain, apparently by an increase of local oxytocin levels in the nursing mice. Along these lines, Kang et al. summarized the protective effects of exosomes on ischemic and hypoxic brain injury by inhibiting neuronal apoptosis, mediating axon reconstruction and neurogenesis, and alleviating inflammatory response and immune suppression.

Neuroendocrine disorders interfere with the interactions between the nervous and the endocrine systems, causing excessive or deficient hormone production with a negative impact on metabolism. The Prader-Willi syndrome (PWS) was the first neuroendocrine disease to be related to genomic imprinting errors. Costa et al. reviewed and summarized the disrupted genes related to the clinical phenotypes of PWS. Another important neuroendocrine disorder is Alzheimer's disease (AD), where deficiency of the tau protein in the CNS is an important feature in AD pathology. Gonçalves et al. showed that an AD mouse model knockout for tau protein presented anxiety-related behavior and memory impairment. They also verified that the introduction of human tau, in tau knockout mice, did not restore anxiety or metabolic alterations and triggered insulin resistance and further impairments in learning and memory features. Finally, Alvarez-Herrera et al. summarize the peripheral immunological, endocrine, and intestinal microbiome changes induced by atypical antipsychotics used for the treatment of schizophrenia and other psychiatric disorders.

In recent decades, our understanding of the intricate network between nervous, immune, and endocrine systems, and the development of diseases has remarkably increased. However, extensive challenges remain in providing a more comprehensive picture. The articles presented in this Research Topic show the complex circuitry affecting the neuroendocrine-immunological interactions in different diseases and indicate future directions for research in this area.

AUTHOR CONTRIBUTIONS

All authors contributed equally to the Topic (Topic Image, ARP). All authors contributed to the article and approved the submitted version.

FUNDING

This study obtained funding from Capes (Brazil), PICT 2016-0312 (Argentina).

Conflict of Interest: The authors declare that the research was conducted in the absence of any commercial or financial relationships that could be construed as a potential conflict of interest.

Publisher's Note: All claims expressed in this article are solely those of the authors and do not necessarily represent those of their affiliated organizations, or those of the publisher, the editors and the reviewers. Any product that may be evaluated in this article, or claim that may be made by its manufacturer, is not guaranteed or endorsed by the publisher.

frontiers in Endocrinology

ORIGINAL RESEARCH
published: 26 June 2019
doi: 10.3389/fendo.2019.00424

Diet-Induced Obesity Disturbs Microglial Immunometabolism in a Time-of-Day Manner

*Irina V. Milanova[1,2], Martin J. T. Kalsbeek[1,2], Xiao-Lan Wang[1,2], Nikita L. Korpel[1,2], Dirk Jan Stenvers[1,2], Samantha E. C. Wolff[1,2], Paul de Goede[1,2], Annemieke C. Heijboer[2,3], Eric Fliers[1,2], Susanne E. la Fleur[1,2,4], Andries Kalsbeek[1,2,4] and Chun-Xia Yi[1,2]**

[1] Department of Endocrinology and Metabolism, Amsterdam University Medical Center, University of Amsterdam, Amsterdam, Netherlands, [2] Laboratory of Endocrinology, Amsterdam University Medical Center, Amsterdam Gastroenterology & Metabolism, University of Amsterdam, Amsterdam, Netherlands, [3] Endocrine Laboratory, Department of Clinical Chemistry, Amsterdam University Medical Center, Amsterdam Gastroenterology & Metabolism, Vrije Universiteit Amsterdam, Amsterdam, Netherlands, [4] NetherlandsInstitute for Neuroscience, Royal Netherlands Academy of Arts and Sciences, Amsterdam, Netherlands

Background: Disturbance of immunometabolic signaling is a key process involved in the progression of obesity. Microglia—the resident immune cells in the brain, initiate local immune responses. It is known that hypercaloric diets lead to microglial activation. Previously, we observed that hypothalamic microglial cells from mice fed high-fat diet (HFD) lose their day/night rhythm and are constantly activated. However, little is known about daily rhythmicity in microglial circadian, immune and metabolic functions, either in lean or obese conditions. Therefore, we hypothesized that HFD disturbs microglial immunometabolism in a day/night-dependent manner.

Methods: Obesity was induced in Wistar rats by feeding them HFD *ad libitum* for the duration of 8 weeks. Microglia were isolated from HFD- and chow-fed control animals at six time points during 24 h [every 4 h starting 2 h after lights on, i.e., Zeitgeber Time 2 (ZT2)]. Gene expression was evaluated using quantitative RT-PCR. JTK_Cycle software was used to estimate daily rhythmicity. Statistical analysis was performed with two-way ANOVA test.

Results: Consumption of the obesogenic diet resulted in a 40 g significantly higher body weight gain in week 8, compared to chow diet ($p < 0.0001$), associated with increased adiposity. We observed significant rhythmicity of circadian clock genes in microglia under chow conditions, which was partially lost in diet-induced obesity (DIO). Microglial immune gene expression also showed time-of-day differences, which were disrupted in HFD-fed animals. Microglia responded to the obesogenic conditions by a shift of substrate utilization with decreased glutamate and glucose metabolism in the active period of the animals, and an overall increase of lipid metabolism, as indicated by gene expression evaluation. Additionally, data on mitochondria bioenergetics and dynamics suggested an increased energy production in microglia during the inactive period on HFD. Finally, evaluation of monocyte functional gene expression showed small or absent effect of HFD on peripheral myeloid cells, suggesting a cell-specific microglial inflammatory response in DIO.

OPEN ACCESS

Edited by:
Vinicius Frias Carvalho, Oswaldo Cruz Foundation (Fiocruz), Brazil

Reviewed by:
Licio A. Velloso, Campinas State University, Brazil
Yinghua Yu, Xuzhou Medical University, China

***Correspondence:**
Chun-Xia Yi
c.yi@amsterdamumc.nl

Specialty section:
This article was submitted to Neuroendocrine Science, a section of the journal Frontiers in Endocrinology

Received: *12 April 2019*
Accepted: *12 June 2019*
Published: *26 June 2019*

Citation:
Milanova IV, Kalsbeek MJT, Wang X-L, Korpel NL, Stenvers DJ, Wolff SEC, de Goede P, Heijboer AC, Fliers E, la Fleur SE, Kalsbeek A and Yi C-X (2019) Diet-Induced Obesity Disturbs Microglial Immunometabolism in a Time-of-Day Manner. Front. Endocrinol. 10:424. doi: 10.3389/fendo.2019.00424

Conclusions: An obesogenic diet affects microglial immunometabolism in a time-of-day dependent manner. Given the central role of the brain in energy metabolism, a better knowledge of daily rhythms in microglial immunometabolism could lead to a better understanding of the pathogenesis of obesity.

Keywords: microglia, immunometabolism, neuroinflammation, diet-induced obesity, high-fat diet, daily rhythms

INTRODUCTION

Arising evidence highlights the disturbed interaction between immunity and metabolism as a key player in the pathogenesis of obesity (1–3). Immune cell function is highly dependent on metabolic adaptation of the immune cells, allowing for abrupt shifts in energy utilization, thus promoting either a resting or an activated state (4). Moreover, distinct immune cell populations show specific metabolic patterns, modulating their functional properties (4). In the brain, microglia are involved in maintaining brain homeostasis by surveying the environment, sensing invading pathogens and phagocyting dead neurons, and cellular debris, thus eliciting an innate immune response (5, 6). Microglial metabolic reprogramming is associated with polarization to pro- or anti-inflammatory state, which involves both functional and phenotypic plasticity (7, 8). It has been shown that hypercaloric environment induces a proinflammatory response in the hypothalamus via NF-kB and toll-like receptor activation, leading to disturbed energy homeostasis (9–13). This could be due to hypothalamic microglial activation as seen in rodents fed an obesogenic diet (14–17). We observed that under physiological conditions in mice, microglial cells exert their function in a strict time-of-day manner with higher activity during the dark, active phase, compared to the light, sleep phase (18). However, this day-night rhythm was abolished in animals fed an obesogenic, high-fat diet (HFD), suggesting an interaction of diet content and daily rhythms. Indeed, recent evidence suggest an involvement of circadian function in the progression of obesity (19, 20). It is well-known now that a master circadian clock in mammals generates daily rhythms in behavioral, physiological, and hormonal processes to allow adaptation to daily environmental changes, thus optimizing metabolic function to the time of day (21). However, little is known about daily rhythms in microglial function. Therefore, we performed a detailed investigation of daily rhythmicity in microglial immunometabolism in lean and obese rats. As mentioned earlier, many studies have focused on hypothalamic microglial inflammatory response due to the clear relation between the hypothalamus and energy homeostasis. Here, we chose to evaluate cortical microglial activation, to expand on available knowledge on microglial immunometabolism in obesity outside of the hypothalamus.

We induced obesity with HFD for the duration of 8 weeks in rats and evaluated the expression of key clock genes involved in maintaining circadian rhythms (**Figure 1**). Microglial cells, as many other immune cells, have a high metabolic demand (22). Therefore, we also evaluated the expression of key genes involved in microglial glucose, lipid, and glutamate metabolism. As higher activity and substrate utilization require higher energy production we also assessed the state of mitochondria bioenergetics and dynamics in response to either healthy or obesogenic diet. The immune state of the cells was studied by evaluating cytokine production and phagocytosis (**Figure 1**). Our results showed time-of-day disturbances in microglial circadian and inflammatory functions in the obesogenic conditions, accompanied with changes in substrate utilization and energy production. We compared these data to monocytes, isolated from the same animals, to evaluate the state of peripheral myeloid cells in a hypercaloric environment. We observed a small effect of HFD on monocyte function, suggesting a microglia-specific response to hypercaloric intake. These results shed further light on microglial time-of-day innate immunometabolism in health and obesity.

Abbreviations: (Abbreviations in italic represent target genes tested) *Atp5b*, ATP synthase subunit b; *Atp5g*, ATP synthase subunit g; *bactin*, Beta-actin; *Bmal1*, Brain and muscle ARNT-Like 1; *Cd36*, Cluster of differentiation 36; *Cd68*, Cluster of differentiation 68; *Clock*, Circadian locomotor output cycles kaput; *Cox4*, Cytochrome C oxidase subunit 4; *Cry1*, Cryptochrome 1; *Cry2*, Cryptochrome 2; *Dbp*, D-box binding protein; DIO, Diet-induced obesity; *Drp1*, Dynamin-related protein 1; EDTA, Ethylenediaminetetraacetic acid; FA, Fatty acid; *Fas*, Fatty acid synthesis; *Fis1*, Fission 1; *Gdh*, Glutamate dehydrogenase; *Gls*, Glutaminase; *Glut5*, Glucose transporter type 5; *Gpx1*, Glutathione peroxidase 1; HFD, High-carbohydrate-high-fat diet; *Hk2*, Hexokinase 2; *Hprt*, Hypoxanthine phosphoribosyltransferase 1; *Ikbkb*, Inhibitor of nuclear factor kappa B kinase subunit betta; *Il1b*, Interleukin 1 betta; *Lpl1*, Lipoprotein lipase 1; *Mfn2*, Mitofusin 2; *Myd88*, Myeloid differentiation primary response 88; NEFA, Non-esterified fatty acids; *Opa1*, Optic atrophy 1; *Pdk4*, Pyruvate dehydrogenase kinase 4; *Per1*, Period 1; *Per2*, Period 2; POMC, Proopiomelanocortin; *Ppard*, Peroxisome proliferator activated receptor delta; pWAT, Perirenal white adipose tissue; *Reverba*, Reverse viral erythroblastosis oncogene product alfa; RIA, Radioimmunoassay; ROS, Reactive oxygen species; SEM, Standard error of the mean; *Sirt1*, Sirtuin 1; *Tnfa*, Tumor necrosis factor alfa; ZT, Zeitgeber Time.

METHODS

Animals

Seventy-two male Wistar rats (Charles River, Germany) were group housed on a 12-h-light/12-h-dark cycle [lights on at 7:00 am; Zeitgeber time zero (ZT0)] at 22 ± 2°C with access to food and water *ad libitum*. Obesity was induced for the duration of 8 weeks, with a diet containing 60 kcal% fat and 20 kcal% carbohydrates (HFD, 5.24 kcal/g, D12492, Research Diets Inc.). Control animals were fed a standard chow diet (3.1 kcal/g, 2018, Teklad diets, Invigo). Body weight was monitored once per week, and food intake twice per week. All studies were approved by the Animal Ethics Committee of the Royal Dutch Academy of Arts and Sciences (KNAW, Amsterdam) and performed according

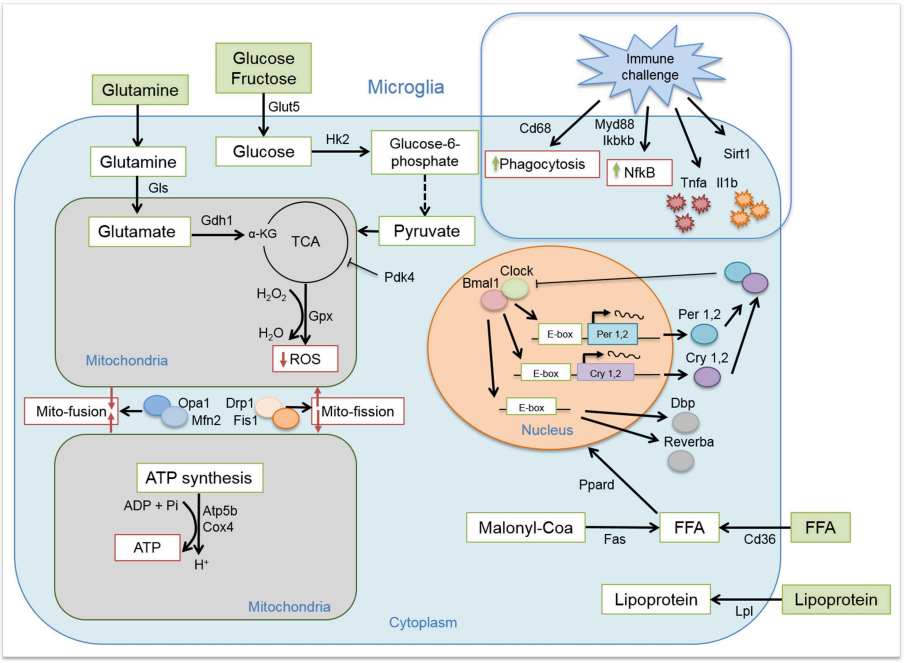

FIGURE 1 | Microglial circadian, immune, metabolic, and mitochondrial profile. Schematic representation of the pathways and/or functions tested on microglial cells from chow- and HFD-fed rats.

to the guidelines on animal experimentation of the Netherlands Institute for Neuroscience (NIN, Amsterdam).

Microglia/Monocyte Isolation and Plasma Collection

Animals were sacrificed at six time points during 24 h (every 4 h starting at ZT2) by euthanasia with 60% CO_2/40% O_2, followed by decapitation. Perirenal white adipose tissue (pWAT) was dissected for evaluation of fat mass gain, evaluating the amount of pWAT in grams weight. Microglial cells from cerebral cortex were isolated for gene expression analysis using the Percoll isopycnic isolation, as it provides a high cell number (23). Briefly, brains were mechanically homogenized with RPMI 1640 medium (Ref.: 11875-093, Gibco™) and filtered through 70 µm cell strainer (Ref.: 431751, Corning®) in a 15 mL Falcon tube. Brain homogenate was centrifuged for 5′ (380 g, 4°C). Pellets were resuspended with 7 mL RPMI medium and mixed with 100% Percoll solution [for 10 mL: 9 mL Percoll® stock (Ref.: 17-5445-01, GE Healthcare, Sigma-Aldrich®) with 1 mL 10x HBSS (Ref.: 14185-045, Gibco™)]. The cell suspension was layered slowly on 70% Percoll solution [for 10 mL: 7 mL 100% Percoll solution with 3 mL 1x HBSS (Ref.: 14175-053, Gibco™)] and centrifuged for 30′ (500 g, 18°C, break 1/0). Cell debris on the surface was discarded and fuse interphase, containing microglial cells were collected in 8 mL 1x HBSS, followed by centrifuging for 7′ (500 g, 18°C, break 9/9). Supernatant was discarded and the microglial cell pellet was used directly for RNA extraction.

During decapitation trunk blood was collected for measurement of different parameters. Briefly, blood was collected in 50 mL Falcon tubes, containing 0.5 M EDTA (ethylenediaminetetraacetic acid). Blood was filtered through a 70 µm cell strainer in a 15 mL Falcon tube and separated for monocyte isolation. For plasma collection, 2 mL blood was centrifuged for 15′ (4,000 rpm, 4°C, break 9/9). Plasma was collected in a new tube and stored at −80°C until usage. For monocyte isolation, 30 mL lysis buffer (containing 1× ACK; 155 mM NH_4Cl; 10 mM $KHCO_3$; 0.1 mM EDTA) was added to ∼3 mL blood and vortexed gently, followed by incubation at RT for 10–15′. The cell suspension was centrifuged for 5′ (200 g, RT, 9/9 break), supernatant was discarded and cells were resuspended in 2 mL PBS-FBS (PBS containing 1% FBS). The new cell suspension was again centrifuged for 5′ (200 g, RT, 9/9 break), supernatant was discarded and cells were resuspended in 0.5 mL PBS-FBS. The cell suspension was added to 4.5 mL RPMI medium and layered slowly on 5 mL Ficoll® (Ref.: 17-1440-02, GE Healthcare, Sigma-Aldrich®), followed by centrifuging for 30′ (400 g, 20°C, break 1/1). The fuse interphase, containing monocytes, was collected in 8 mL 1x HBSS, followed by centrifuging for 5′ (200 g, RT). Supernatant was discarded and the monocyte pellet was used for RNA extraction.

Real-Time PCR

For gene expression analysis, RNA from microglial cells and monocytes was extracted using the RNeasy Micro Kit (Cat No. 74004, Qiagen®) according to the manufacturer's guidelines. RNA was quantified by spectrophotometry at 260 nm (DS 11; Denovix). RNA was reverse transcribed using Transcriptor First Strand cDNA Synthesis Kit (04897030001; Roche) according to the manufacturer's guidelines. Levels of mRNA for *Tnfa, Bmal1,*

Per1, Per2, Cry1, Cry2, Dbp, Reverba, Clock, Gls, Gdh, Gpx1, Cd36, Fas, Lpl1, Opa1, Mfn2, Fis1, Drp1, Pdk4, Ppard, Ikbkb, Cd68, Il1b, Cox4, Atp5b, Atp5g, Hk2, Glut5, Myd88, Sirt1, Hprt (internal control), and *bactin* (internal control) were measured by semiquantitative real-time PCR on a LightCycler LC480 (Roche), using the SensiFAST SYBR® No-ROX Kit (BIO-98020, GC-Biotech) according to the manufacturer's guidelines. Expression levels of all genes were normalized to the geometric mean of the internal controls. Primer sequences (see **Table S1**) were designed using the Basic Local Alignment Search Tool (BLAST) from the National Center for Biotechnology Information (NCBI). Primers were purchased from Sigma-Aldrich® and validated by melt curve analysis and DNA band size and/or purity on agarose gel electrophoresis (data not shown).

Glucose, Insulin, and Non-esterified Fatty Acids (NEFA) Measurements in Plasma

Plasma glucose concentrations were measured using the Glucose GOD-PAP kit (Ref. 80009, Biolabo S.A.S.), following the manufacturer's guidelines. Absorbance of colored samples, proportional to glucose concentration, was measured at 500 nm with Varioskan® Flash spectral scanning multimode reader (Version 40053; Thermo Scientific). Insulin concentrations were measured using Rat Insulin Radioimmunoassay (RIA) Kit (RI-13K; Millipore, Merck), according to the manufacturer's guidelines. Non-esterified fatty acids (NEFA) concentration in plasma was measured using the NEFA HR(2) reagents (R1 set, Ref. 434-91795; R2 set, Ref. 436-91995; Standard, Ref. 270-77000, Wako Chemicals GmbH) following the adjusted protocol from the Mouse Metabolic Phenotyping Centers [https://www.mmpc.org/shared/document.aspx?id=196&docType=Protocol]. Within-run variations for all measurements fall in the range suggested by the manufacturers.

Statistical Analyses

All results are expressed as mean ± SEM. Statistical analyses were performed using Graph-Pad PRISM (version 7.03, GraphPad Software, Inc.) and JTK_Cycle software (24). Two-way ANOVA analysis was used for effects of *Diet*, *Time,* (ZT) and *Interaction*. Unpaired *t*-tests were used to evaluate the effect of diet for each time point, unless stated otherwise. Sidak's multiple comparison test was used to compare the effect of diet for the food intake, body weight gain, and plasma measurements data (**Figures 2A,B,D–F**). One-way ANOVA analysis was used to assess the effect of *Time* for the chow and HFD groups separately. JTK_Cycle analysis *p*-values were obtained by fitting the data on a curve with fixed 24 h period. Results were considered statistically significant when $p < 0.05$.

RESULTS

HFD Intake Induces Obesity in Rats

We observed that chronic feeding with HFD for 8 weeks induced obesogenic phenotype in adult male rats, compared to control animals on the standard chow diet. The HFD rats had a higher caloric intake (**Figure 2A**) and a 40 g higher body weight gain after 8 weeks as compared to controls (**Figure 2B**). Moreover, there was a 2-fold increase in pWAT mass in HFD-fed animals compared to controls (**Figure 2C**). These results were in line with other literature available on diet-induced obesity (DIO) in rodents (14, 25). To assess glycemic status at the time of death, we evaluated glucose and insulin concentrations in plasma over the 24 h cycle. Control animals showed the expected daily rhythm in glucose concentrations in the plasma (26). However, HFD-fed animals showed increased glucose concentrations during the light phase at ZT6 (inactive period) (**Figure 2D**). The overall high levels of glucose concentration in both conditions could be explained by our choice of euthanasia (60% CO_2/40% O_2), as it has been shown previously that CO_2 causes acidosis which stimulates enzymes of the glycolytic pathway, leading to decreased liver glycogen stores and increased plasma glucose concentrations, both in fed and fasted animals (27, 28). Insulin concentrations were significantly elevated in HFD-fed animals during the dark phase (active period) at ZT18, which could indicate an impaired insulin sensitivity, as glucose concentrations during this period were not elevated, but overall maintained during 24 h (**Figure 2E**). A similar trend of increased insulin secretion during the dark phase has also been observed in mice on a HFD (29). Evaluation of the NEFA concentrations in plasma showed a significant increase in HFD-fed animals during the light phase (ZT2-ZT10) compared to chow controls (**Figure 2F**). Together, these data indicate metabolic changes toward obesity in animals fed HFD.

HFD Disturbs Microglial Circadian Gene Expression

It has been shown previously that microglial cells express clock genes (30, 31). Diets rich in fat and/or sugar are known to alter circadian rhythms of clock gene expression in peripheral tissue (32, 33). To test whether HFD also disturbs daily microglial rhythmicity, we studied expression of genes within the transcriptional feedback loop—circadian locomotor output cycles kaput (*Clock)* and brain and muscle ARNT-Like 1 (*Bmal1)*—the so-called activators and the repressors—period and cryptochrome genes (*Per1*, *Per2*, *Cry1,* and *Cry2)*. Additionally, we assessed the expression of two other clock genes—reverse viral erythroblastosis oncogene product alfa (*Reverbα),* a *Clock* and *Bmal1* repressor, and D-box binding protein (*Dbp*), a regulator of peripheral circadian input (34).

Control animals fed chow diet showed a clear rhythmic expression for all genes, except *Clock* and *Cry2* (see **Table S2**). Rhythmicity of *Bmal1*, *DBP,* and *Reverbα* was not influenced by HFD, although a reduced amplitude was observed for *DBP* and *Reverbα*. There was a gain of rhythm for *Clock* expression. However, *Per1*, *Per2,* and *Cry1* showed a loss of rhythmic expression during HFD, as evaluated with JTK_Cycle (see **Table S2**). Moreover, all genes showed a significant *Interaction* effect, as well as difference between HFD and chow-fed animals at the transition period between dark and light phase (ZT22 and/or ZT2) (**Figures 3A–H**; **Table 1**). These data point to a clock disturbance, which could lead to irregularity in the expression of other key microglial genes, as it is known that clock genes regulate the expression of 10–20% of all cell genes (34).

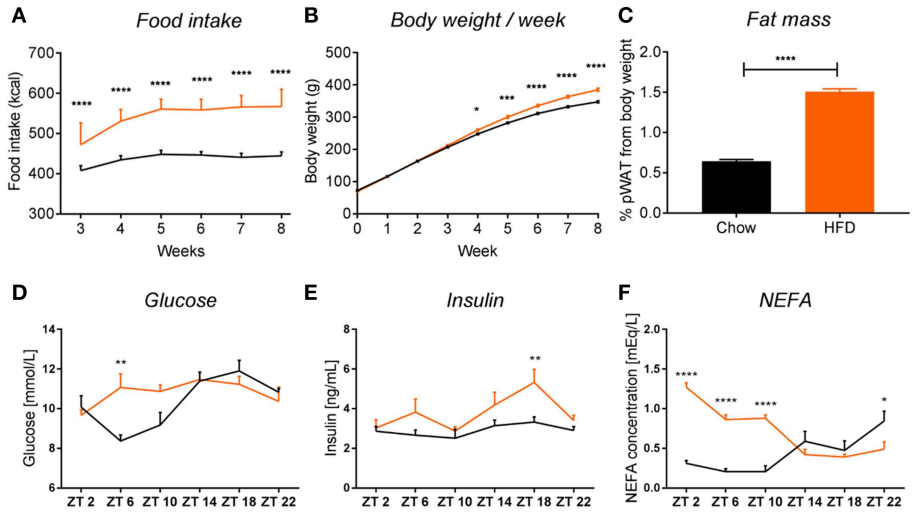

FIGURE 2 | HFD intake leads to obesity in rats. HFD (orange) leads to an increase in food intake **(A)** ($p_{int} < 0.0001$, $p_{time} < 0.0001$, $p_{diet} < 0.0001$), body weight **(B)** ($p_{int} < 0.0001$, $p_{time} < 0.0001$, $p_{diet} = 0.0003$), and fat mass gain, seen as 2-fold increase in perirenal white adipose tissue **(C)** in rats, compared to chow-fed controls (black). Plasma measurements in non-fasted HFD-fed animals show an increase in glucose at ZT6 **(D)** ($p_{int} = 0.0032$, $p_{time} = 0.0003$, $p_{diet} = 0.0874$), increased insulin at ZT18 **(E)** ($p_{int} = 0.2802$, $p_{time} = 0.0042$, $p_{diet} = 0.0006$), and significant increase in non-esterified fatty acids during the light phase **(F)** ($p_{int} < 0.0001$, $p_{time} = 0.0006$, $p_{diet} < 0.0001$). Data are presented as means ± SEM. Statistical significance was determined using Two-way ANOVA **(A,B,D–F)** or unpaired *t*-test **(C)**. Effect of diet within each time point was evaluated with Sidak's multiple comparison test **(A,B,D–F)** (*$p < 0.05$; **$p < 0.01$, ***$p < 0.001$, ****$p < 0.0001$).

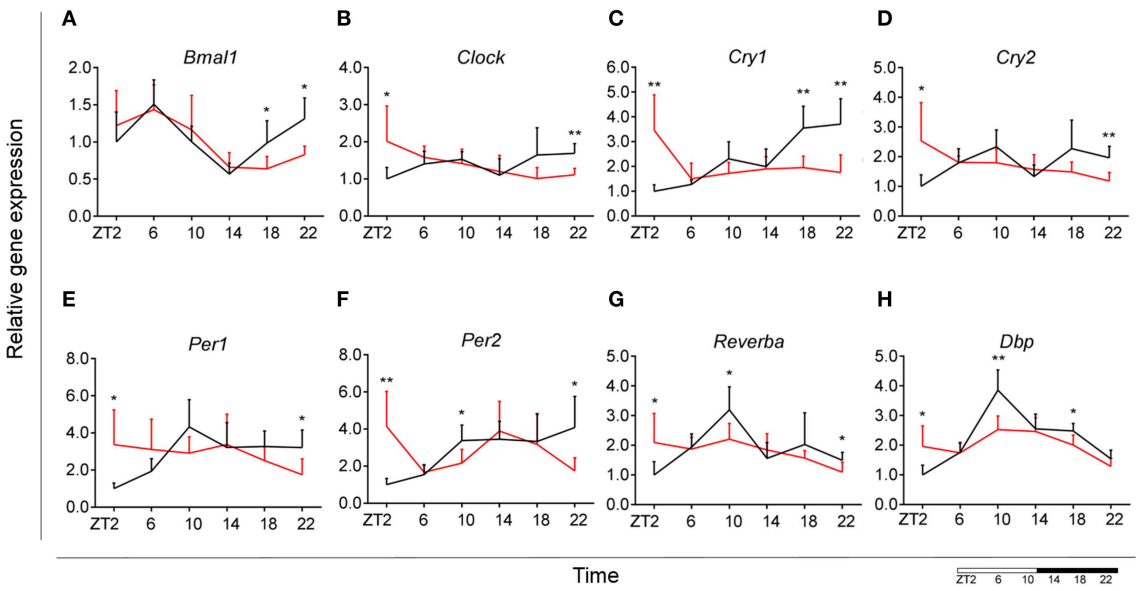

FIGURE 3 | Microglial circadian clock system in HFD-fed and control animals. Relative gene expression of circadian genes *Bmal1* **(A)**, *Clock* **(B)**, *Cry1* **(C)**, *Cry2* **(D)**, *Per1* **(E)**, *Per2* **(F)**, *Reverba* **(G),** and *Dbp* **(H)** in HFD-fed rats (red) compared to Chow-fed controls (black). Data are presented as means ± SEM. Statistical significance was determined using Two-way ANOVA effects for *Interaction*, *Diet,* and *Time* (ZT); Student *t*-test is used for diet effect within a separate time point (*$p < 0.05$; **$p < 0.01$). Scale (bottom right) represents light (ZT0-12) and dark (ZT12-24) phase.

Microglial Time-of-Day Disturbance of Inflammatory Signaling During HFD

To evaluate the effect of HFD on daily changes in microglial activation, we assessed the relative gene expression of the main cytokines secreted by microglia—tumor necrosis factor α (*Tnfa*) and interleukin 1β (*Il1b*). We observed an increased expression of *Tnfa* at the transition between dark and light phase, as well as increased *Il1b* production at the end of the light period for animals fed HFD, pointing to an increased microglial activation in the obesogenic group, compared

TABLE 1 | Two-way ANOVA assessment of effect of *Time, Diet,* and *Interaction* in microglia.

Genes	Two-way ANOVA analysis		
	p-value		
	Interaction	***Time***	***Diet***
Circadian			
Bmal1	**0.0356**	**<0.0001**	0.3308
Clock	**0.0006**	0.4015	0.9599
Cry1	**<0.0001**	**0.0002**	0.1484
Cry2	**<0.0001**	0.1616	0.7026
Per1	**0.0011**	**0.0437**	0.9673
Per2	**<0.0001**	**0.0035**	0.9989
Reverba	**0.0023**	**<0.0001**	0.5351
Dbp	**<0.0001**	**<0.0001**	0.0573
Inflammatory			
Tnfa	0.1547	**0.0042**	0.1705
Il1b	**0.0085**	0.2610	0.4658
Myd88	**0.0378**	**0.0022**	**0.0140**
Ikbkb	**<0.0001**	**0.0165**	0.7572
Cd68	0.0685	**0.0226**	**0.0014**
Sirt1	**0.0004**	0.2071	0.4654
Metabolic			
Gls	**0.0138**	0.4456	0.0888
Gdh	**0.0095**	0.8306	0.8648
Gpx1	**0.0009**	0.9390	0.8424
Hk2	**0.0023**	**0.0274**	**0.0024**
Glut5	**0.0058**	0.0935	**0.0025**
Cd36	**0.0031**	**0.0004**	0.1116
Lpl	0.0554	**0.0064**	**0.0412**
Ppard	**0.0034**	0.6143	0.7868
Fas	**0.0030**	0.5214	0.6840
Mitochondrial			
Cox4	**<0.0001**	0.1598	0.8468
Atp5b	**0.0020**	**0.0257**	**0.0194**
Pdk4	0.2512	**<0.0001**	0.7817
Fis1	**0.0001**	0.3438	0.0934
Drp1	**<0.0001**	0.2189	0.6340
Mfn2	**0.0001**	0.4675	0.1899
Opa1	**0.0056**	0.9284	0.6975

Diet, Time, and Interaction effects were evaluated in microglia for circadian, inflammatory, metabolic, and mitochondrial genes. Statistical significance was determined using Two-way ANOVA effect for Interaction, Diet, and Time (ZT). Data are presented as means ± SEM. Genes are considered rhythmic when $p < 0.05$ (Bold).

to controls (**Figures 4A,B**). However, myeloid differentiation primary response 88 (*Myd88)* gene expression, an adaptor for inflammatory signaling pathways, located downstream of Il1b, showed a decrease at ZT2 in HFD-fed animals (**Figure 4C**). Therefore, we assessed the expression of inhibitor of nuclear factor kappa B kinase subunit betta (*Ikbkb*) as the protein it encodes phosphorylates the inhibitor in the inhibitor/NFkB complex, leading to activation of nuclear factor kappa-light-chain-enhancer of activated B cells NFkB—a transcriptional activator of key genes involved in cell survival, proliferation and inflammatory response. We observed an inverted daily pattern of *Ikbkb* expression between chow and HFD animals, with higher expression at the beginning of the light phase, but lower expression at the end of the dark phase for HFD-fed animals, compared to chow diet controls (**Figure 4D**). We also studied gene parameters reflecting the phagocytic capacity of microglia as this is a key function of their immune response in health, as well as different pathologies (35). We evaluated the gene expression of cluster of differentiation 68 (*Cd68*), which encodes for a microglial lysosomal protein, and is a good indicator of phagocytic activity (36). Our results showed an overall steady expression of *Cd68* during the day-night cycle for HFD-fed animals, with a loss of the time-of-day differences, as observed in control animals (**Figure 4E**). One-Way ANOVA evaluation of the effect of *Time* for each group showed a loss of significance during HFD (see **Table S3**). Recent studies have shown that Sirtuin 1 (*Sirt1*) deficiency in microglia is associated with increased Il1b production (37). We observed an inverted pattern of expression of *Sirt1* expression in animals fed HFD, compared to controls. Moreover, the significantly lower *Sirt1* expression at ZT10 coincided with an increased expression of *Il1b* at the same time point (**Figure 4F**). No significant daily rhythmicity was observed for any of the genes, apart from *Myd88* in Chow-fed animals and *Ikbkb* in HFD-fed animals (see **Table S2**). These data demonstrate that microglial innate immunity is affected in HFD-fed animals, suggesting a disruptive effect of obesogenic diets on the microglial inflammatory response.

Microglial Glutamate Metabolism Decreases During the Dark Phase During HFD

Glutamate metabolism is a key component in the biosynthesis of nucleic acids and proteins (38, 39). Microglial cells have been shown to be involved in glutamate uptake under physiological conditions, which can be directly converted to glutathione as a defense response against oxidative stress (40). This mechanism has also been observed under pathological conditions, where it has been shown that microglial cells express glutamate transporters (41). We wanted to assess the state of glutamate substrate utilization in microglial cells under control and obesogenic conditions. We observed that glutaminase (*Gls*)—a key enzyme in the glutamate pathway that converts glutamine to glutamate, showed an effect of *Time* in control animals, which was lost during HFD, with a decrease in expression during the dark phase (ZT18) (**Figure 5A**) (see **Table S3**). Similar observations were made for glutamate dehydrogenase 1 (*Gdh1*), a mitochondrial matrix enzyme that converts glutamate to α-ketoglutarate, a key intermediate in the tricarboxylic acid cycle. *Gdh1* expression showed a lower expression during the dark phase for HFD-fed animals (**Figure 5B**). Moreover, both genes show a significant *Interaction* effect between time and diet (**Table 1**). These data indicate a decrease in conversion of glutamate during the active state of the animals. Microglial activation leads to production of reactive oxygen species (ROS), therefore self-produced antioxidants could have a protective role

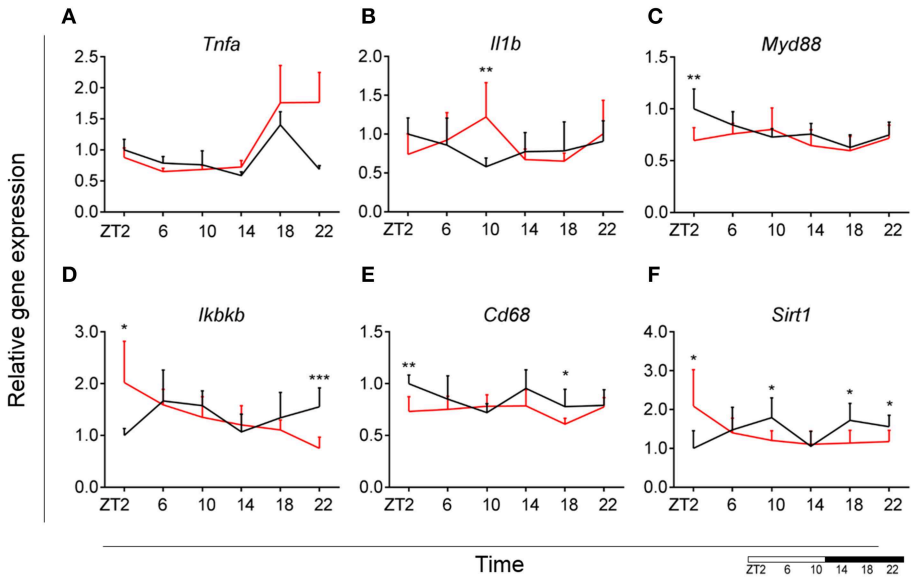

FIGURE 4 | Microglial inflammatory signaling is disturbed in DIO. Relative gene expression of innate immunity genes *Tnfa* **(A)**, *Il1b* **(B)**, *Myd88* **(C)**, *Ikbkb* **(D)** as well as phagocytic indicator gene *Cd68* **(E)** and *Sirt1* **(F)** in HFD-fed rats (red) compared to Chow-fed controls (black) evaluated at six time points, starting at ZT2. Data are presented as means ± SEM. Statistical significance was determined using Two-way ANOVA effect for *Interaction*, *Diet,* and *Time* (ZT); Student *t*-test is used for diet effect within a separate time point (*$p < 0.05$; **$p < 0.01$; ***$p < 0.001$). Scale (bottom right) represents light (ZT0-12) and dark (ZT12-24) phase.

in the cells. Expression of glutathione peroxidase 1 (*Gpx1*)—an important antioxidant enzyme, involved in reduction of organic hydroperoxides and hydrogen peroxide by glutathione, showed an inverted pattern of expression during the light phase between both groups (**Figure 5C**), suggesting a change in this protective mechanism. No significant daily rhythmicity according to JTK_Cycle analysis was observed for any of the genes under control and obesogenic conditions (see **Table S2**). Together, these data point to an overall decrease of glutamate utilization during the active period of HFD-fed animals.

Decrease of Microglial Glucose Utilization During the Dark Phase During HFD

It has been shown that glycolysis is crucial for immune cell function (42). Moreover, it has been suggested that upregulation of expression of glycolytic genes leads to M1 polarization in macrophages, known for its proinflammatory function (43). To assess the involvement of glucose metabolism in microglial immune function when rats are fed HFD, we evaluated gene expression of hexokinase 2 (*Hk2*)—the first glycolytic enzyme converting glucose to glucose-6-phosphate. We observed a decrease of *Hk2* expression during the dark phase (ZT18-22) for animals fed HFD, suggesting a decrease in glucose utilization in microglial cells (**Figure 5D**). Moreover, there was a gain of rhythm for *Hk2* in animals, fed HFD (see **Table S2**). To investigate this further, we evaluated the expression of glucose transporter type 5 (*Glut5*)—a fructose transporter, which is known to be highly specific for microglial cells (44). We observed a similar trend for *Glut5* in HFD-fed animals, with a steady decreased expression toward the end of the dark phase ZT22 (**Figure 5E**). Both genes show a significant *Interaction* effect between time and diet (**Table 1**). Together these data on glutamate and glucose metabolism, suggest that under obesogenic conditions microglial cells switch their substrate utilization to other sources during their active state.

HFD Leads to an Increase in Lipid Utilization and Sensing in Microglia During the Light Phase

Fatty acid oxidation can contribute 20% of total brain energy production (45). A recent study has shown that microglial cells determine hypothalamic inflammation in response to excess saturated fat intake through a direct and specific sensing mechanism (16). To assess microglial fatty acid (FA) metabolism in DIO, we evaluated genes involved in FA substrate utilization and sensing. Expression of cluster of differentiation 36 (*Cd36*)—a FA translocase responsible for import of FA inside the cell, showed a flattening of the time-of-day differences in animals fed HFD, compared to controls (**Figure 5F**). Evaluation of daily rhythmicity of *Cd36* gene expression confirms this observation, with a loss of rhythm under obesogenic conditions (see **Table S2**). This suggests an overall steady import of FA during the day/night cycle under HFD. Previous research from our group has shown that HFD stimulates the expression of microglial lipoprotein lipase (*Lpl*)—a triglyceride hydrolase receptor involved in receptor-mediated lipoprotein uptake, and that lack of LPL impairs microglial immune reactivity (46). Here, we show that this increase of *Lpl* expression takes place during the light phase in animals fed HFD (**Figure 5G**). These data highlight LPL as a key player in microglial immunometabolism in

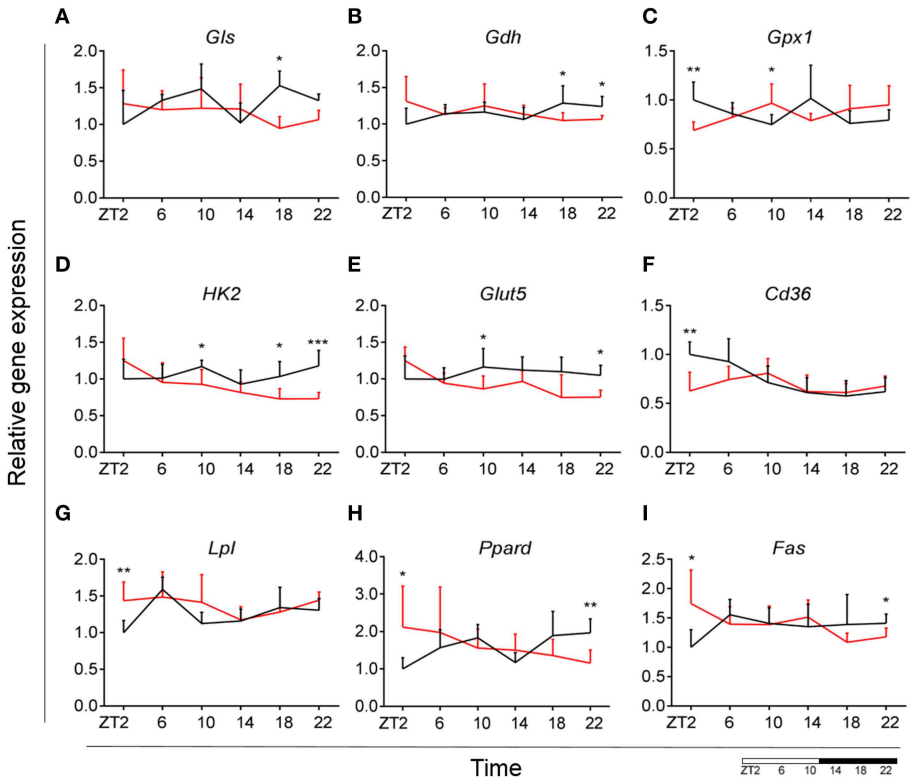

FIGURE 5 | HFD effect on glutamate, glucose and lipid microglial metabolism in rats. Relative gene expression of (top) glutamate substrate utilization genes *Gls* **(A)** and *Gdh* **(B)**, as well as antioxidant enzyme gene *Gpx1* **(C)**; (middle) glucose metabolism genes *Hk2* **(D)** and *Glut5* **(E)**, fatty acid sensing gene *Cd36* **(F)**; (bottom) fatty acid sensing genes *Lpl* **(G)** and *Ppard* **(H)**, as well as fatty acid synthesis gene *Fas* **(I)** in HFD-fed rats (red) compared to Chow-fed controls (black) evaluated at six time points, starting at ZT2. Data are presented as means ± SEM. Statistical significance was determined using Two-way ANOVA effect for *Interaction*, *Diet,* and *Time* (ZT); Student *t*-test is used for diet effect within a separate time point (*$p < 0.05$; **$p < 0.01$; ***$p < 0.001$). Scale (bottom right) represents light (ZT0-12) and dark (ZT12-24) phase.

DIO. Peroxisome proliferator-activated receptors (PPARs) have an important physiological role in lipid sensing and regulation of lipid metabolism during normal healthy conditions, as well in the development of pathologies like obesity and type two diabetes (47). PPAR delta (*Ppard*) is highly expressed by microglia and its activity increases oxidative capacity. Our results showed an inverted pattern of *Ppard* day/night expression in obesogenic animals, with highest expression during ZT2, but lowest at ZT22 (**Figure 5H**). To assess the effect of HFD-induced obesity on fatty acid synthesis we evaluated gene expression of fatty acid synthase (*Fas*)—a key enzyme catalyzing the synthesis of palmitate from malonyl coenzyme A. *Fas* expression in microglia from HFD-fed animals showed a lower expression at the end of the dark phase and higher expression at the beginning of the light phase, compared to control chow-fed animals (**Figure 5I**). These data suggest a shift of FA synthesis to the light phase in HFD-fed animals.

Taken together, these data suggest an overall increase in lipid metabolism during the light, i.e., sleep, phase of animals fed HFD. This increase could be partially explained by the higher levels of NEFA in HFD-fed rodents during the light phase (**Figure 2F**) (48, 49). Moreover, we observed a decrease in glutamate and glucose utilization as shown above. This could suggest a microglial metabolic switch to lipid substrate utilization in HFD-induced obesity.

HFD Increases Mitochondrial Bioenergetics and Dynamics Gene Expression During the Light Phase

To assess whether microglial mitochondria bioenergetics are affected by DIO, we evaluated the gene expression of cytochrome c oxidase subunit 4 (*Cox4*), encoding a terminal enzyme of the mitochondrial respiratory chain that catalyzes the reduction of oxygen to water, and ATP synthase subunit beta (*Atp5b*)—encoding a part of the enzyme, catalyzing ATP synthesis. We observed a decrease in *Cox4* and *Atp5b* expression in animals fed HFD at ZT18 (dark phase), but an increase during the beginning of the light phase (ZT2), suggesting a shift of energy production to the resting state in obese animals (**Figures 6A,B**). These data are in line with our observation on lipid metabolism; therefore, we selected another mitochondrial target, involved in FA metabolism. Pyruvate dehydrogenase kinase 4 (*Pdk4*) is an enzyme located in the mitochondrial matrix, inhibiting the pyruvate dehydrogenase complex and exerting a regulatory function on substrate utilization by suppressing

glycolysis and enhancing FA oxidation. *Pdk4* expression showed the same trend for HFD-fed animals, with an increase at ZT2 (beginning of the light phase) (**Figure 6C**). This has also been previously observed in heart tissue and soleus muscle of rats fed HFD (49). Moreover, all three genes show a daily rhythm under control conditions, which was lost in HFD-fed animals, suggesting that hypercaloric diet impairs time-of-day mitochondrial bioenergetics in microglial cells (see **Table S2**).

To test if this trend was also observed in mitochondrial dynamics, as they adjust to mitochondrial demand, we evaluated key genes involved in mitochondrial fusion—mitofusin 2 (*Mfn2*) and optic atrophy 1 (*Opa1*); as well as mitochondrial fission—fission 1 (*Fis1*) and dynamin-related protein 1 (*Drp1*). Results were supportive of changes in the bioenergetics state, with a significant increase of expression for all four genes (*Mfn2, Opa1, Fis1, Drp1*) at ZT2 for HFD-fed animals (**Figures 6D–G**). Two-way ANOVA test showed a significant *Interaction* effect for all four genes (**Table 1**).

Taken together these data suggest an increased energy production in microglia of DIO animals during the light phase, which could be explained by an increased demand to sustain the increase in lipid metabolism. Another recent study indeed showed that mitochondrial fission is elevated as a consequence of high-fat concentrated diets (50). This indicates that mitochondrial dynamics adapt to changes in the bioenergetics state in response to nutritional status.

The Effect of HFD-Induced Obesity on Blood Monocyte Immunometabolism Is Less Robust Than on Brain Microglial Cells

Following our observations in microglia, we were interested if the same effects could be seen in monocytes—peripheral myeloid cells. Originating from hematopoietic stem cells in the bone marrow, monocytes circulate in the blood and migrate to other tissue where they differentiate into tissue resident macrophages. It is known that under obesogenic conditions, circulating monocytes could infiltrate adipose tissue, leading to macrophage activation and increasing proinflammatory activity (51–53).

Our results indicated an overall loss of daily rhythmicity of circadian gene expression, with *Clock*, *Per2,* and *Dbp* showing daily rhythmicity in control animals, which was only maintained for *Per2* gene expression under obesogenic conditions (see **Table S2**). *Bmal1* and *Per1* showed a significant increase in expression at the beginning of the light phase (ZT2) in HFD-fed animals compared to control chow (**Figures 7A,C**). Gene expression of *Reverba* and *Dbp* in monocytes showed a higher expression at ZT6 in HFD-fed animals (**Figures 7E,F**). There was no difference in *Clock*, *Per2*, *Cry1* and *Cry2* gene expression between both conditions (**Figures 7B,D**) (see **Figures S1A,B**). Moreover, One-Way ANOVA analysis showed lack of *Time* effect for all circadian genes during HFD (see **Table S3**).

We did not find any difference in monocyte immune response between both groups for *Tnfa*, *Ikbkb*, *Cd68,* and *Sirt1* gene expression (see **Figures S1C–F**). However, we did observe a daily rhythm in *Tnfa* and *Cd68* in control animals, as well as gain of rhythm for *Sirt1* gene expression in HFD-fed animals (see **Table S2**). There was an increase in *Il1b* expression at ZT2 for the HFD group (**Figure 7G**). *Il1b* showed daily rhythmicity under control conditions, which was maintained under obesogenic conditions with a shift in acrophase of 6 h (see **Table S2**). Il1b-induced inflammation has been shown to be indirectly involved in insulin resistance in type 2 diabetes (54, 55). Thus, these data could indicate a reduction in insulin sensitivity. Moreover, we observed an increased expression of *Myd88* at ZT2 for HFD-fed animals (**Figure 7H**).

No differences between obese and control animals were found for representative genes of the glutamate pathway *Gls* and *Gdh* (see **Figures S1G,H**). However, there was a gain of daily rhythm for *Gls* gene expression in HFD-fed animals (see **Table S2**). We found an increase in *Gpx1* expression at ZT2 for HFD group with an overall stable day/night expression, suggesting a mechanism of constant anti-oxidant production (**Figure 7I**). This observation was supported by a loss of daily rhythmicity under obesogenic conditions (see **Table S2**). Expression of the glucose metabolic gene *Hk2* was decreased at ZT22 in HFD-fed animals, similar to what was observed in microglia (**Figure 7J**). We observed no difference in FA metabolism and sensing genes *Fas* and *Ppard* (see **Figures S1I,J**), apart from *Cd36* expression (**Figure 7K**). *Cd36* expression showed a strong daily rhythm under control conditions, which was significant also in HFD-fed animals with an acrophase shift of 6 h (see **Table S2**). The expression of the FA translocase in monocytes has also been shown to be associated with insulin resistance, supporting our observation for *Il1b* expression (56). *Lpl* evaluation showed low expression (data not shown).

We observed no difference in mitochondrial bioenergetics gene expression between both dietary groups for *Atp5b, Atp5g,* and *Cox4* (see **Figures S1K–M**). Mitochondria dynamics gene expression was affected only at ZT2 for *Opa1* and *Drp1* expression (**Figures 7L,M**), with no difference in *Mfn2* expression (see **Figure S1N**) and low expression of *Fis1* (data not shown). Interestingly, HFD led to a decrease in mitochondrial bioenergetics gene expression in monocytes at the start of the inactive period, opposite to the increase we observed in microglia under obesogenic conditions. We found no daily rhythm for any of the mitochondria genes, both under control and obesogenic conditions (see **Table S2**). One-Way ANOVA analysis showed lack of *Time* effect for all genes both during control and HFD (see **Table S3**). Two-way ANOVA analysis data is shown the in Supplementary Material (see **Table S4**).

Overall, these data suggest a small effect of the obesogenic diet on monocyte immunometabolism, suggesting that HFD specifically affects microglial immunometabolism.

DISCUSSION

It is well-known now that a hypercaloric environment is a potent inducer of microglial activation, which ultimately leads to chronic neuroinflammation (14–17). However, the daily rhythm of microglial innate immune function is poorly known,

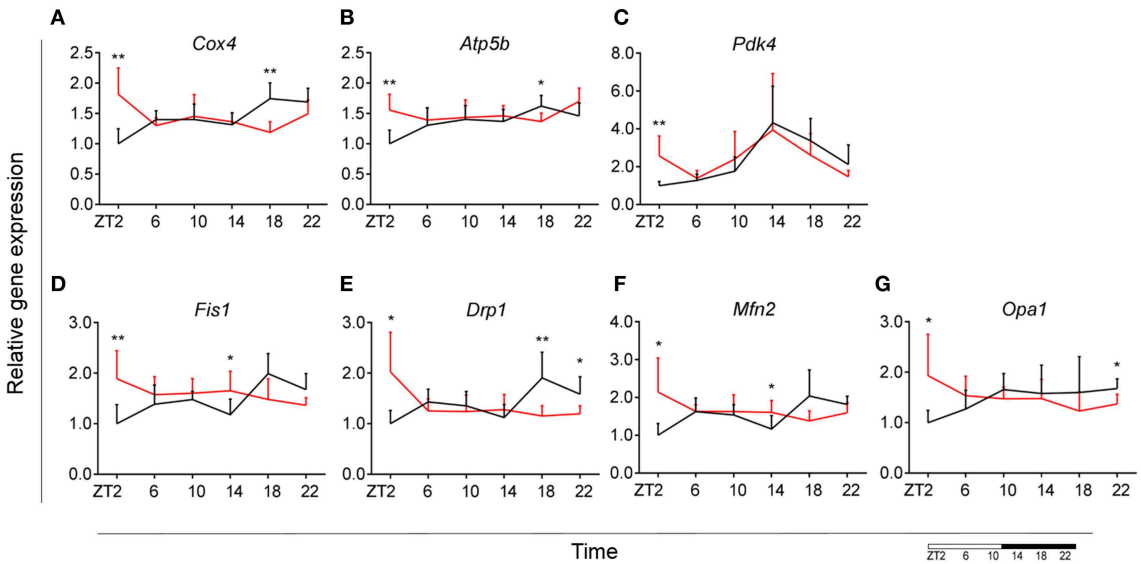

FIGURE 6 | Microglial mitochondria signaling during DIO. Relative gene expression of mitochondria bioenergetics genes *Cox4* **(A)**, *Atp5b* **(B)**, and *Pdk4* **(C)**, as well as mitochondria dynamics gene *Fis1* **(D)**, *Drp1* **(E)**, *Mfn2* **(F)**, and *Opa1* **(G)** in HFD-fed rats (red) compared to Chow-fed controls (black) evaluated at six time points, starting at ZT2. Data are presented as means ± SEM. Statistical significance was determined using Two-way ANOVA effect for *Interaction*, *Diet,* and *Time* (ZT); Student *t*-test is used for diet effect within a separate time point (*$p < 0.05$; **$p < 0.01$). Scale (bottom right) represents light (ZT0-12) and dark (ZT12-24) phase.

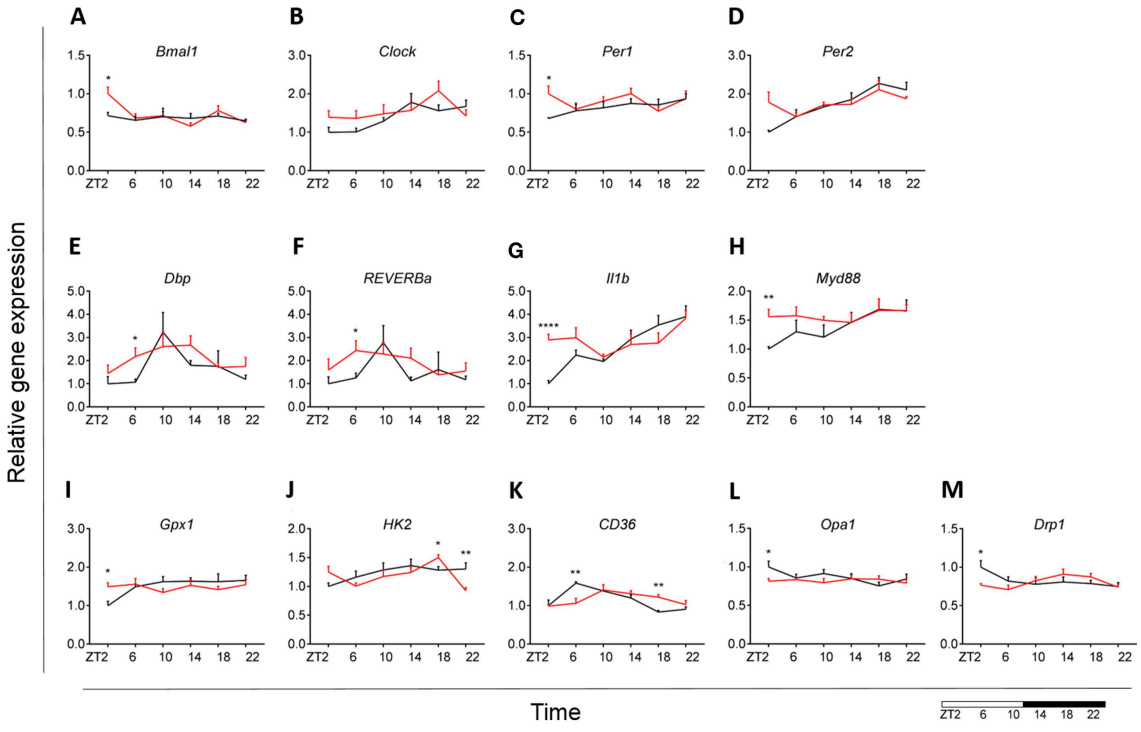

FIGURE 7 | Monocyte immunometabolism in DIO. Relative gene expression of circadian genes *Bmal1* **(A)**, *Clock* **(B)**, *Per1* **(C)**, *Per2* **(D)**, *Dbp* **(E)**, and *Reverba* **(F)**; immune genes *Il1b* **(G)** and *Myd88* **(H)**, antioxidant enzyme gene *Gpx1* **(I)**, glycolysis gene *Hk2* **(J)**, fatty acid sensing gene *Cd36* **(K)**, and mitochondria dynamic genes *Opa1* **(L)** and *Drp1* **(M)** in HFD-fed rats (red) compared to Chow-fed controls (black) evaluated at six time points, starting at ZT2. Data are presented as means ± SEM. Statistical significance was determined using Two-way ANOVA effect for *Interaction*, *Diet,* and *Time* (ZT); Student *t*-test is used for diet effect within a separate time point (*$p < 0.05$; **$p < 0.01$; ****$p < 0.0001$). Scale (bottom right) represents light (ZT0-12) and dark (ZT12-24) phase.

both in obesity and health. The purpose of this study was to evaluate the effect of an obesogenic diet on daily changes in microglial immunometabolism. Our data showed a disturbance of the microglial interaction between metabolism and immunity during DIO. We report that HFD-induced obesity leads to loss of daily rhythm of circadian genes and impaired microglial immunometabolic functions primarily at the transition period between dark and light phase (ZT22-ZT2).

To evaluate the effect of DIO on daily rhythms in microglial function and activity, we studied the microglial expression of major circadian and immune genes. Under normal conditions, microglia circadian genes were expressed in a rhythmic manner, which is disturbed by HFD, mainly due to a loss of its rhythmicity. Comparable changes have also been observed in different peripheral tissues like liver, brown adipose tissue and skeletal muscle in animals on an obesogenic diet (57–59). However, to our knowledge, we are the first to report an effect of HFD on expression rhythms of microglial clock genes. The presently reported difference in time-of-day expression of microglial cytokine genes, is in line with our previous results (18). Fonken et al. have shown previously that *Il1b* and *Tnfa* gene expression have a peak during the middle of the day, contrary to our observations (31). Possible explanation to this contradiction is the heterogeneous transcriptional identities of microglia, specific for each brain region, in this case hippocampal vs. cortical microglia (60).

Microglial cells are known to exhibit bioenergetics shifts in energy substrate, for example during aging (61). Such a shift in substrate utilization is known to have an effect on the activation status of immune cells (42, 62). We studied microglial substrate utilization, focusing on glutamate, glucose and FA metabolism and observed a difference between control and HFD-fed animals, particularly during the transition period from the dark to light phase. Key players in the glutamate pathway have been shown to be involved in macrophage immune function, *e.g.,* glutamine availability was shown to modulate macrophage phagocytic capacity, while α-ketoglutarate, generated through glutaminolysis, is crucial in eliciting an anti-inflammatory phenotype in macrophages (63, 64). We report a decrease in microglial glutamate utilization in the active period of HFD-fed animals as seen in glutamine conversion to glutamate and glutamate conversion to α-ketoglutarate. Additionally, a similar change was observed for glucose metabolism with decreased glucose utilization in the active period of HFD-fed animals. However, we observed an increase in FA sensing and synthesis at the beginning of the light period under obesogenic conditions, suggesting a shift to FA utilization during the sleep phase of the animal. It has been shown that FA treatment of BV2 cells (a microglial cell line) is a potent inducer of cytokine production via TLR4 signaling, thus leading to low-grade inflammation even in the absence of immune challenge (65). This FA metabolism increase could be a possible explanation for our previously observed constant day/night activation of hypothalamic microglia under HFD (66). Additionally, we know that immune cell activation requires higher energy production. We here show that microglial mitochondrial function in DIO is increased during the inactive period, suggesting an increase in ATP production, which could be explained by the increased FA metabolism demand. These data support the view that mitochondrial function adapts to nutritional status (50).

To investigate whether the observed effect of HFD on immunometabolism is restricted to microglial cells, we also studied monocyte immunometabolism in obesity. We report small or no effect of the hypercaloric diet on monocyte immunometabolic function, which suggests a microglia-specific functional disturbance in HFD-induced obesity. Taken together, our data suggest that microglial innate immunity is highly dependent on metabolic changes, as well as the time of day. Microglial cells are highly active cells, with a high energy demand, which is achieved by a strictly regulated cellular metabolism. A robust switch of substrate utilization is a suitable mechanism, in response to the high demands of immune defense.

The data currently presented suggest a deleterious effect of an obesogenic diet on microglial function by inducing chronic activation. It has been shown that chronic microglial activation has a negative impact on neuronal function and could play a role in obesity-associated cognitive decline (16, 67). Our data point out to the importance of microglial integrity and the negative impact of chronic exposure to a hypercaloric environment on cortical microglial function, which could ultimately lead to cognitive impairment. Previously we observed that obesity induces microglial activation in close proximity to the anorexigenic proopiomelanocortin (POMC) neurons located in the arcuate nucleus of the hypothalamus (18). Moreover, chronic HFD feeding leads to POMC neuronal loss, which would lead to further progression of obesity (66). It is possible that the current observation on cortical microglia could be translated to the hypothalamus, which would give insight in the mechanisms behind this neuronal loss.

Finally, three issues need to be addressed: firstly, we observed a clear effect of HFD on microglial immunometabolism, leading to an increase in expression of many of the presented genes around the end of the dark period, i.e., ZT22/ZT2. In order to check whether or not a higher food intake at the end of the dark period in the HFD-fed group could be responsible for these changes, we re-analyzed the food intake data from metabolic cage experiments from a separate cohort of rats fed a similar HFD (68). With respect to consumed grams, no difference in timing of food intake was found between control and obesogenic diet (see **Figure S2**). However, with respect to consumed calories, the obesogenic diet group showed a larger increase of kcal intake at the beginning and the end of the dark period, although only significant for the beginning of the dark period, suggesting that higher energy consumption (but not higher food intake) may be partially responsible for the differences in gene expression between the HFD and control group at the end of the dark period (see **Figure S2**). Secondly, we cannot distinguish between the effect of obesity and the hypercaloric diet itself. However, a hypercaloric diet can induce microglial activation in the hypothalamus after 1 day, prior to any changes in body weight, pointing to an effect of diet rather than obesity itself (69). Thirdly, the data presented only show

the transcriptional state of selected target genes, representative of the different functions investigated. Future studies should be aimed at a further understanding of activity changes in each of the represented pathways.

CONCLUSIONS

An obesogenic diet affects microglial immunometabolism in a time-of-day specific manner. The aim of this study was to increase the knowledge of microglial cell function in obesity in general and its daily rhythms in specific. To our knowledge, we are the first to point out (loss of) time-of-day differences for microglial cells during HFD. Our data are supportive of the ongoing research, focused on the interaction between immune cells and metabolism. Further studies should focus on addressing the time-of-day differences in microglial function, as more detailed knowledge of microglial immunometabolism could lead to a better understanding of the neuroinflammatory process taking place in the CNS under chronic hypercaloric environment.

DATA AVAILABILITY

All data generated or analyzed during this study are included in this published article (and its **Supplementary Information Files**).

ETHICS STATEMENT

All studies were approved by the Animal Ethics Committee of the Royal Dutch Academy of Arts and Sciences (KNAW, Amsterdam) and performed according to the guidelines on animal experimentation of the Netherlands Institute for Neuroscience (NIN, Amsterdam).

AUTHOR CONTRIBUTIONS

IM performed the animal experiments, microglia isolation, RNA extraction, cDNA synthesis, qPCR experiments, glucose and NEFA measurements in plasma, and constructed the manuscript. MK and XW helped with the animal experiments and monocyte isolation. NK performed the monocyte isolation and helped with the animal experiments. DS performed the time-of-day food intake data and helped with data analysis. SW helped with qPCR experiments. PG helped with data statistical analysis. AH supervised the measuring of the insulin plasma concentration. EF, SF, and AK provided intellectual input and drafted the manuscript. CY designed the study, supervised the experiments, interpreted the findings, and drafted the manuscript. All authors have read and approved the final manuscript.

FUNDING

This work was supported by an AMC fellowship (CY, 2014, Amsterdam University Medical Center), the Dutch Diabetes Research Foundation (CY, Diabetes Fonds, 2015.82.1826), and the ZonMW TOP grant (MK, PG, and AK, #91214047), The Netherlands.

ACKNOWLEDGMENTS

We would like to thank the Laboratory of Endocrinology, Amsterdam University Medical Center (UMC).

SUPPLEMENTARY MATERIAL

The Supplementary Material for this article can be found online at: https://www.frontiersin.org/articles/10.3389/fendo.2019.00424/full#supplementary-material

REFERENCES

1. Mathis D, Shoelson SE. Immunometabolism: an emerging frontier. *Nat Rev Immunol*. (2011) 11:81. doi: 10.1038/nri2922
2. Lee YS, Wollam J, Olefsky JM. An integrated view of immunometabolism. *Cell*. (2018) 172:22–40. doi: 10.1016/j.cell.2017.12.025
3. Hotamisligil GS. Foundations of immunometabolism and implications for metabolic health and disease. *Immunity*. (2017) 47:406–20. doi: 10.1016/j.immuni.2017.08.009
4. Norata Giuseppe D, Caligiuri G, Chavakis T, Matarese G, Netea Mihai G, Nicoletti A, et al. The cellular and molecular basis of translational immunometabolism. *Immunity*. (2015) 43:421–34. doi: 10.1016/j.immuni.2015.08.023
5. Mariani MM, Kielian T. Microglia in infectious diseases of the central nervous system. *J Neuroimmune Pharmacol*. (2009) 4:448–61. doi: 10.1007/s11481-009-9170-6
6. Yang I, Han SJ, Kaur G, Crane C, Parsa AT. The role of microglia in central nervous system immunity and glioma immunology. *J Clin Neurosci*. (2010) 17:6–10. doi: 10.1016/j.jocn.2009.05.006
7. Orihuela R, McPherson CA, Harry GJ. Microglial M1/M2 polarization and metabolic states. *Br J Pharmacol*. (2016) 173:649–65. doi: 10.1111/bph.13139
8. Butovsky O, Weiner HL. Microglial signatures and their role in health and disease. *Nat Rev Neurosci*. (2018) 19:622–35. doi: 10.1038/s41583-018-0057-5
9. De Souza CT, Araujo EP, Bordin S, Ashimine R, Zollner RL, Boschero AC, et al. Consumption of a fat-rich diet activates a proinflammatory response and induces insulin resistance in the hypothalamus. *Endocrinology*. (2005) 146:4192–9. doi: 10.1210/en.2004-1520
10. Morari J, Anhe GF, Nascimento LF, de Moura RF, Razolli D, Solon C, et al. Fractalkine (CX3CL1) is involved in the early activation of hypothalamic inflammation in experimental obesity. *Diabetes*. (2014) 63:3770–84. doi: 10.2337/db13-1495
11. Milanski M, Degasperi G, Coope A, Morari J, Denis R, Cintra DE, et al. Saturated fatty acids produce an inflammatory response predominantly through the activation of TLR4 signaling in hypothalamus: implications for the pathogenesis of obesity. *J Neurosci*. (2009) 29:359–70. doi: 10.1523/JNEUROSCI.2760-08.2009
12. Zhang X, Zhang G, Zhang H, Karin M, Bai H, Cai D. Hypothalamic IKKbeta/NF-kappaB and ER stress link overnutrition to energy imbalance and obesity. *Cell*. (2008) 135:61–73. doi: 10.1016/j.cell.2008.07.043
13. Kleinridders A, Schenten D, Konner AC, Belgardt BF, Mauer J, Okamura T, et al. MyD88 signaling in the CNS is required for development of fatty acid-induced leptin resistance and diet-induced obesity. *Cell Metab*. (2009) 10:249–59. doi: 10.1016/j.cmet.2009.08.013
14. Gao Y, Bielohuby M, Fleming T, Grabner GF, Foppen E, Bernhard W, et al. Dietary sugars, not lipids, drive hypothalamic inflammation. *Mol Metab*. (2017) 6:897–908. doi: 10.1016/j.molmet.2017.06.008

15. Gao Y, Ottaway N, Schriever SC, Legutko B, Garcia-Caceres C, de la Fuente E, et al. Hormones and diet, but not body weight, control hypothalamic microglial activity. *Glia*. (2014) 62:17–25. doi: 10.1002/glia.22580
16. Valdearcos M, Robblee MM, Benjamin DI, Nomura DK, Xu AW, Koliwad SK. Microglia dictate the impact of saturated fat consumption on hypothalamic inflammation and neuronal function. *Cell Rep*. (2014) 9:2124–38. doi: 10.1016/j.celrep.2014.11.018
17. Baufeld C, Osterloh A, Prokop S, Miller KR, Heppner FL. High-fat diet-induced brain region-specific phenotypic spectrum of CNS resident microglia. *Acta Neuropathol*. (2016) 132:361–75. doi: 10.1007/s00401-016-1595-4
18. Yi C-X, Walter M, Gao Y, Pitra S, Legutko B, Kälin S, et al. TNFα drives mitochondrial stress in POMC neurons in obesity. *Nat Commun*. (2017) 8:15143. doi: 10.1038/ncomms15143
19. Froy O. Metabolism and circadian rhythms—implications for obesity. *Endocr Rev*. (2010) 31:1–24. doi: 10.1210/er.2009-0014
20. Sun M, Feng W, Wang F, Li P, Li Z, Li M, et al. Meta-analysis on shift work and risks of specific obesity types. *Obesity Rev*. (2018) 19:28–40. doi: 10.1111/obr.12621
21. Kalsbeek A, Palm IF, La Fleur SE, Scheer FA, Perreau-Lenz S, Ruiter M, et al. SCN outputs and the hypothalamic balance of life. *J Biol Rhythms*. (2006) 21:458–69. doi: 10.1177/0748730406293854
22. Olenchock BA, Rathmell JC, Vander Heiden MG. Biochemical underpinnings of immune cell metabolic phenotypes. *Immunity*. (2017) 46:703–13. doi: 10.1016/j.immuni.2017.04.013
23. Nikodemova M, Watters JJ. Efficient isolation of live microglia with preserved phenotypes from adult mouse brain. *J Neuroinflamm*. (2012) 9:147. doi: 10.1186/1742-2094-9-147
24. Hughes ME, Hogenesch JB, Kornacker K. JTK_CYCLE: an efficient nonparametric algorithm for detecting rhythmic components in genome-scale data sets. *J Biol Rhythms*. (2010) 25:372–80. doi: 10.1177/0748730410379711
25. Bahceci M, Tuzcu A, Akkus M, Yaldiz M, Ozbay A. The effect of high-fat diet on the development of obesity and serum leptin level in rats. *Eat Weight Disord*. (1999) 4:128–32. doi: 10.1007/BF03339728
26. La Fleur SE, Kalsbeek A, Wortel J, Buijs RM. A suprachiasmatic nucleus generated rhythm in basal glucose concentrations. *J Neuroendocrinol*. (1999) 11:643–52. doi: 10.1046/j.1365-2826.1999.00373.x
27. Zardooz H, Rostamkhani F, Zaringhalam J, Faraji Shahrivar F. Plasma corticosterone, insulin and glucose changes induced by brief exposure to isoflurane, diethyl ether and CO2 in male rats. *Physiol Res*. (2010) 59:973–8.
28. Artwohl J, Brown P, Corning B, Stein S. Report of the ACLAM task force on rodent euthanasia. *J Am Assoc Lab Anim Sci*. (2006) 45:98–105.
29. Kohsaka A, Laposky AD, Ramsey KM, Estrada C, Joshu C, Kobayashi Y, et al. High-fat diet disrupts behavioral and molecular circadian rhythms in mice. *Cell Metab*. (2007) 6:414–21. doi: 10.1016/j.cmet.2007.09.006
30. Nakazato R, Takarada T, Yamamoto T, Hotta S, Hinoi E, Yoneda Y. Selective upregulation of Per1 mRNA expression by ATP through activation of P2X7 purinergic receptors expressed in microglial cells. *J Pharmacol Sci*. (2011) 116:350–61. doi: 10.1254/jphs.11069FP
31. Fonken LK, Frank MG, Kitt MM, Barrientos RM, Watkins LR, Maier SF. Microglia inflammatory responses are controlled by an intrinsic circadian clock. *Brain Behav Immun*. (2015) 45:171–9. doi: 10.1016/j.bbi.2014.11.009
32. Pendergast JS, Branecky KL, Yang W, Ellacott KLJ, Niswender KD, Yamazaki S. High-fat diet acutely affects circadian organization and eating behavior. *Eur J Neurosci*. (2013) 37:1350–6. doi: 10.1111/ejn.12133
33. Blancas-Velazquez AS, Unmehopa UA, Eggels L, Koekkoek L, Kalsbeek A, Mendoza J, et al. A free-choice high-fat high-sugar diet alters day–night Per2 gene expression in reward-related brain areas in rats. *Front Endocrinol*. (2018) 9:154. doi: 10.3389/fendo.2018.00154
34. Takahashi JS. Transcriptional architecture of the mammalian circadian clock. *Nat Rev Genet*. (2016) 18:164. doi: 10.1038/nrg.2016.150
35. Wolf SA, Boddeke HWGM, Kettenmann H. Microglia in physiology and disease. *Annu Rev Physiol*. (2017) 79:619–43. doi: 10.1146/annurev-physiol-022516-034406
36. Zotova E, Bharambe V, Cheaveau M, Morgan W, Holmes C, Harris S, et al. Inflammatory components in human Alzheimer's disease and after active amyloid-β42 immunization. *Brain*. (2013) 136:2677–96. doi: 10.1093/brain/awt210
37. Cho SH, Chen JA, Sayed F, Ward ME, Gao F, Nguyen TA, et al. SIRT1 deficiency in microglia contributes to cognitive decline in aging and neurodegeneration via epigenetic regulation of IL-1beta. *J Neurosci*. (2015) 35:807–18. doi: 10.1523/JNEUROSCI.2939-14.2015
38. Yelamanchi SD, Jayaram S, Thomas JK, Gundimeda S, Khan AA, Singhal A, et al. A pathway map of glutamate metabolism. *J Cell Commun Signal*. (2016) 10:69–75. doi: 10.1007/s12079-015-0315-5
39. Schousboe A, Scafidi S, Bak LK, Waagepetersen HS, McKenna MC. Glutamate metabolism in the brain focusing on astrocytes. *Adv Neurobiol*. (2014) 11:13–30. doi: 10.1007/978-3-319-08894-5_2
40. Persson M, Sandberg M, Hansson E, Ronnback L. Microglial glutamate uptake is coupled to glutathione synthesis and glutamate release. *Eur J Neurosci*. (2006) 24:1063–70. doi: 10.1111/j.1460-9568.2006.04974.x
41. Persson M, Ronnback L. Microglial self-defence mediated through GLT-1 and glutathione. *Amino Acids*. (2012) 42:207–19. doi: 10.1007/s00726-011-0865-7
42. O'Neill LA, Kishton RJ, Rathmell J. A guide to immunometabolism for immunologists. *Nat Rev Immunol*. (2016) 16:553–65. doi: 10.1038/nri.2016.70
43. Wang T, Liu H, Lian G, Zhang S-Y, Wang X, Jiang C. HIF1α-induced glycolysis metabolism is essential to the activation of inflammatory macrophages. *Mediators Inflamm*. (2017) 2017:9029327. doi: 10.1155/2017/9029327
44. Payne J, Maher F, Simpson I, Mattice L, Davies P. Glucose transporter Glut 5 expression in microglial cells. *Glia*. (1997) 21:327–31. doi: 10.1002/(SICI)1098-1136(199711)21:3<27::AID-GLIA7>3.0.CO;2-1
45. Ebert D, Haller RG, Walton ME. Energy contribution of octanoate to intact rat brain metabolism measured by 13C nuclear magnetic resonance spectroscopy. *J Neurosci*. (2003) 23:5928–35. doi: 10.1523/JNEUROSCI.23-13-05928.2003
46. Gao Y, Vidal-Itriago A, Kalsbeek MJ, Layritz C, Garcia-Caceres C, Tom RZ, et al. Lipoprotein lipase maintains microglial innate immunity in obesity. *Cell Rep*. (2017) 20:3034–42. doi: 10.1016/j.celrep.2017.09.008
47. Berger J, Moller DE. The mechanisms of action of PPARs. *Annu Rev Med*. (2002) 53:409–35. doi: 10.1146/annurev.med.53.082901.104018
48. Shostak A, Meyer-Kovac J, Oster H. Circadian regulation of lipid mobilization in white adipose tissues. *Diabetes*. (2013) 62:2195–203. doi: 10.2337/db12-1449
49. Stavinoha MA, RaySpellicy JW, Hart-Sailors ML, Mersmann HJ, Bray MS, Young ME. Diurnal variations in the responsiveness of cardiac and skeletal muscle to fatty acids. *Am J Physiol Endocrinol Metab*. (2004) 287:E878–E87. doi: 10.1152/ajpendo.00189.2004
50. Putti R, Sica R, Migliaccio V, Lionetti L. Diet impact on mitochondrial bioenergetics and dynamics. *Front Physiol*. (2015) 6:109. doi: 10.3389/fphys.2015.00109
51. Xu H, Barnes GT, Yang Q, Tan G, Yang D, Chou CJ, et al. Chronic inflammation in fat plays a crucial role in the development of obesity-related insulin resistance. *J Clin Investig*. (2003) 112:1821–30. doi: 10.1172/JCI200319451
52. Ghanim H, Aljada A, Hofmeyer D, Syed T, Mohanty P, Dandona P. Circulating mononuclear cells in the obese are in a proinflammatory state. *Circulation*. (2004) 110:1564–71. doi: 10.1161/01.CIR.0000142055.53122.FA
53. Krinninger P, Ensenauer R, Ehlers K, Rauh K, Stoll J, Krauss-Etschmann S, et al. Peripheral monocytes of obese women display increased chemokine receptor expression and migration capacity. *J Clin Endocrinol Metab*. (2014) 99:2500–9. doi: 10.1210/jc.2013-2611
54. Ehses JA, Lacraz G, Giroix MH, Schmidlin F, Coulaud J, Kassis N, et al. IL-1 antagonism reduces hyperglycemia and tissue inflammation in the type 2 diabetic GK rat. *Proc Natl Acad Sci USA*. (2009) 106:13998–4003. doi: 10.1073/pnas.0810087106
55. Bing C. Is interleukin-1β a culprit in macrophage-adipocyte crosstalk in obesity? *Adipocyte*. (2015) 4:149–52. doi: 10.4161/21623945.2014.979661
56. Love-Gregory L, Abumrad NA. CD36 genetics and the metabolic complications of obesity. *Curr Opin Clin Nutr Metab Care*. (2011) 14:527–34. doi: 10.1097/MCO.0b013e32834bbac9
57. Branecky KL, Niswender KD, Pendergast JS. Disruption of daily rhythms by high-fat diet is reversible. *PLoS ONE*. (2015) 10:e0137970. doi: 10.1371/journal.pone.0137970
58. de Goede P, Sen S, Oosterman JE, Foppen E, Jansen R, la Fleur SE, et al. Differential effects of diet composition and timing of feeding behavior on rat

brown adipose tissue and skeletal muscle peripheral clocks. *Neurobiol Sleep Circ Rhythms*. (2018) 4:24–33. doi: 10.1016/j.nbscr.2017.09.002
59. Wang X, Xue J, Yang J, Xie M. Timed high-fat diet in the evening affects the hepatic circadian clock and PPARα-mediated lipogenic gene expressions in mice. *Genes Nutr*. (2013) 8:457–63. doi: 10.1007/s12263-013-0333-y
60. Grabert K, Michoel T, Karavolos MH, Clohisey S, Baillie JK, Stevens MP, et al. Microglial brain region-dependent diversity and selective regional sensitivities to ageing. *Nat Neurosci*. (2016) 19:504–16. doi: 10.1038/nn.4222
61. Flowers A, Bell-Temin H, Jalloh A, Stevens SM Jr., Bickford PC. Proteomic anaysis of aged microglia: shifts in transcription, bioenergetics, and nutrient response. *J Neuroinflamm*. (2017) 14:96. doi: 10.1186/s12974-017-0840-7
62. Kelly B, O'Neill LAJ. Metabolic reprogramming in macrophages and dendritic cells in innate immunity. *Cell Res*. (2015) 25:771. doi: 10.1038/cr.2015.68
63. Liu P-S, Wang H, Li X, Chao T, Teav T, Christen S, et al. α-ketoglutarate orchestrates macrophage activation through metabolic and epigenetic reprogramming. *Nat Immunol*. (2017) 18:985. doi: 10.1038/ni.3796
64. de Oliveira DC, da Silva Lima F, Sartori T, Santos ACA, Rogero MM, Fock RA. Glutamine metabolism and its effects on immune response: molecular mechanism and gene expression. *Nutrire*. (2016) 41:14. doi: 10.1186/s41110-016-0016-8
65. Button EB, Mitchell AS, Domingos MM, Chung JH, Bradley RM, Hashemi A, et al. Microglial cell activation increases saturated and decreases monounsaturated fatty acid content, but both lipid species are proinflammatory. *Lipids*. (2014) 49:305–16. doi: 10.1007/s11745-014-3882-y
66. Thaler JP, Yi CX, Schur EA, Guyenet SJ, Hwang BH, Dietrich MO, et al. Obesity is associated with hypothalamic injury in rodents and humans. *J Clin Investig*. (2012) 122:153–62. doi: 10.1172/JCI59660
67. Cope EC, LaMarca EA, Monari PK, Olson LB, Martinez S, Zych AD, et al. Microglia play an active role in obesity-associated cognitive decline. *J Neurosci*. (2018) 38:8889–904. doi: 10.1523/JNEUROSCI.0789-18.2018
68. Stenvers DJ, van Dorp R, Foppen E, Mendoza J, Opperhuizen AL, Fliers E, et al. Dim light at night disturbs the daily sleep-wake cycle in the rat. *Sci Rep*. (2016) 6:35662. doi: 10.1038/srep35662
69. Waise TMZ, Toshinai K, Naznin F, NamKoong C, Md Moin AS, Sakoda H, et al. One-day high-fat diet induces inflammation in the nodose ganglion and hypothalamus of mice. *Biochem Biophys Res Commun*. (2015) 464:1157–62. doi: 10.1016/j.bbrc.2015.07.097

Conflict of Interest Statement: The authors declare that the research was conducted in the absence of any commercial or financial relationships that could be construed as a potential conflict of interest.

frontiers in Neuroscience

ORIGINAL RESEARCH
published: 08 July 2019
doi: 10.3389/fnins.2019.00609

Nursing Markedly Protects Postpartum Mice From Stroke: Associated Central and Peripheral Neuroimmune Changes and a Role for Oxytocin

Creed M. Stary[1], Lijun Xu[1], Ludmilla A. Voloboueva[1], Marcela Alcántara-Hernández[2,3], Oiva J. Arvola[1], Juliana Idoyaga[2,3] and Rona G. Giffard[1]*

[1] Department of Anesthesiology, Perioperative and Pain Medicine, Stanford, CA, United States, [2] Department of Microbiology and Immunology, Stanford, CA, United States, [3] Program in Immunology, Stanford University School of Medicine, Stanford, CA, United States

OPEN ACCESS

Edited by:
Ana Rosa Pérez, National Scientific and Technical Research Council (CONICET), Argentina

Reviewed by:
Benedetta Leuner, The Ohio State University, United States
Ana María Franchi, National Scientific and Technical Research Council (CONICET), Argentina

***Correspondence:**
Creed M. Stary
cstary@stanford.edu

Specialty section:
This article was submitted to Neuroendocrine Science, a section of the journal Frontiers in Neuroscience

Received: *27 March 2019*
Accepted: *28 May 2019*
Published: *08 July 2019*

Citation:
Stary CM, Xu L, Voloboueva LA, Alcántara-Hernández M, Arvola OJ, Idoyaga J and Giffard RG (2019) Nursing Markedly Protects Postpartum Mice From Stroke: Associated Central and Peripheral Neuroimmune Changes and a Role for Oxytocin. Front. Neurosci. 13:609. doi: 10.3389/fnins.2019.00609

Recent studies demonstrate significant neuroimmune changes in postpartum females, a period that also carries an increased risk of stroke. Oxytocin, a major hormone upregulated in the brains of nursing mothers, has been shown to both modulate neuroinflammation and protect against stroke. In the present study we assessed whether and how nursing modulates the neuroimmune response and injury after stroke. We observed that postpartum nursing mice were markedly protected from 1 h of transient middle cerebral artery occlusion (MCAO) relative to either non-pregnant/non-postpartum or non-nursing (pups removed) postpartum females. Nursing mice also expressed reduced levels of pro-inflammatory cytokines, had decreased migration of blood leukocytes into the brain following MCAO, and displayed peripheral neuroimmune changes characterized by increased spleen weight and increased fraction of spleen monocytes. Intranasal oxytocin treatment in non-pregnant females in part recapitulated the protective and anti-inflammatory effects associated with nursing. In summary, the results of the present study demonstrate that nursing in the postpartum period provides relative protection against transient ischemic stroke associated with decreased brain leukocytes and increased splenic monocytes. These effects appear to be regulated, at least in part, by oxytocin.

Keywords: MCAO, FACS, ischemia, innate, adaptive, focal ischemia, inflammation, cytokine

INTRODUCTION

Over the past decades significant progress has been achieved in understanding the complex cellular and molecular mechanisms of stroke pathology. Various physiological conditions and interventions that modulate stroke outcome have been identified and extensively investigated (Lo et al., 2003; Lakhan et al., 2009; Moskowitz et al., 2010), but clinical translation has been elusive. While stroke is uncommon in young women, the peripartum period is associated with a significantly increased risk of stroke (Kittner et al., 1996; James et al., 2005). Notably, approximately 15% of pregnant women who experience a stroke die as a result, making it the 8th leading cause of pregnancy-associated

deaths in the United States (Kochanek et al., 2013), and retrospective clinical studies demonstrate the risk of stroke remains significantly elevated in the postpartum period (Jaigobin and Silver, 2000; Kamel et al., 2014; Cheng et al., 2017). However, to date, essentially no research has been conducted on stroke in the postpartum period in rodent models.

Strong evidence supports the notion that modulation of the neuroimmune response critically influences lesion volume and overall outcome after ischemic stroke. While the healthy brain maintains an anti-inflammatory local milieu limiting destructive inflammation (Carson and Sutcliffe, 1999), stroke initiates both acute and long-lasting inflammatory processes characterized by release of pro-inflammatory molecules and infiltration of inflammatory cells into the ischemic brain (Stoll et al., 1998; Schwab et al., 2001; Iadecola and Anrather, 2011). Stroke-induced release of pro-inflammatory mediators and cytokines leads to brain cell damage and apoptosis (Choe et al., 2011; Vogelgesang et al., 2014), specifically tied to increased levels of pro-inflammatory cytokines IL-6 and TNF-α (Campbell et al., 1993; Rothwell and Relton, 1993; Meistrell et al., 1997; Lavine et al., 1998). Induction of stroke results not only in brain damage and local neuroinflammation, but also has profound effects on peripheral immune responses, promoting peripheral immune suppression, splenic atrophy and changes in circulating leukocytes (Offner et al., 2006; Lafargue et al., 2012).

Sex differences in outcome from stroke have long been appreciated (Sohrabji et al., 2017), with female animals generally being protected compared to male animals (Alkayed et al., 1998; Murphy et al., 2004). A recent review summarizes the current clinical evidence for sex differences in ischemic stroke, and highlights immune/inflammatory pathways that may contribute to these clinical differences (Chauhan et al., 2017). While pregnancy, parturition and lactation are major important physiological changes in females, these factors have been little studied in the context of stroke. The postpartum period induces significant changes in brain physiology and plasticity including altered neurogenesis (Darnaudery et al., 2007; Leuner et al., 2007), neuronal morphology and synaptic plasticity (Tomizawa et al., 2003; Haim et al., 2014), and astrocytic and oligodendrocytes function (Salmaso and Woodside, 2006; Maheu et al., 2009). Only recently have studies reported changes in maternal neuroimmune function during the postpartum period (Haim et al., 2014; Sherer et al., 2017). In particular, the postpartum period is associated with changes in pro- and anti-inflammatory cytokine levels (Haim et al., 2017). Oxytocin, a hormone produced in the paraventricular and supraoptic nuclei of the hypothalamus, is best known for its role in lactation and parturition. In addition, oxytocin signaling modulates social behaviors, feeding, and pain perception. It has been demonstrated that oxytocin administration provides neuroprotection after cerebral ischemia in male mice, preventing the increased injury seen with social isolation (Karelina et al., 2011). In addition, oxytocin treatment inhibited pro-inflammatory microglial activation both *in vivo* and *in vitro* (Yuan et al., 2016), and mitigated neuroinflammatory responses associated with maternal separation (Amini-Khoei et al., 2017).

In the present study we compared infarct volume and neurological function following transient middle cerebral artery occlusion (MCAO) in acute postpartum nursing female mice with age-matched, postpartum non-nursing (pups removed) mice and age-matched nulliparous female mice. We observed marked protection in nursing mice accompanied by decreased migration of leukocytes and reduced levels of brain pro-inflammatory cytokines in the brain, and increased numbers of leukocytes in the spleen. Because oxytocin is a major hormone upregulated during nursing, we also performed comparative studies between nursing, non-pregnant, and oxytocin-treated non-pregnant female mice following MCAO.

MATERIALS AND METHODS

Animals

The study was conducted in accordance with National Institutes of Health guidelines for the use of experimental animals, and the protocols were approved by the Stanford Animal Care and Use Committee. Female 10 week old Swiss Webster mice (Charles River Laboratory, Wilmington, MA, United States) were used. All animals were housed in air-conditioned rooms in a controlled environment at 21 ± 2°C with seasonal lighting conditions (12 h of light and 12 h of darkness), with unrestricted food and water. Pregnant mice were allowed to deliver and nurse the newborn pups for 3 days before use in stroke studies. Control postpartum mice were deprived of all their pups after delivery and did not nurse for 3 days prior to use in studies. MCAO was performed in each experimental group immediately after the 3 day treatment period. Control non-pregnant female mice were also studied, with and without 3 days of oxytocin treatment. The total number of female mice used was 147 (MCAO 83, non-stroke 64).

Intranasal Oxytocin Treatment

Oxytocin was administered intranasally for 3 days with a dose previously demonstrated to significantly increase brain oxytocin levels in male mice (Neumann et al., 2013). Briefly, synthetic oxytocin (Tocris Bristol, United Kingdom), 12 μl of a 1 μg/μl in saline solution, or control saline vehicle alone, was administered, the solution was applied alternately into each nares, using a pipette. The solution was allowed to diffuse into the squamous epithelium of both the left and right tunica mucosa nasi.

Transient Focal Cerebral Ischemia

Focal cerebral ischemia was induced, and neuroscore and edema corrected infarct volume (percent of hemisphere) were assessed as described previously (Xu et al., 2015). In brief, mice were randomized to treatment groups. Under 1.5–2.0% isoflurane anesthesia, the common carotid artery was exposed and the external carotid artery ligated and cauterized. Unilateral MCAO occlusion was performed by inserting a 6-0 nylon monofilament surgical suture from Doccol Corporation (Sharon, MA, United States). The suture was secured, and the animal allowed to awaken. After 60 min, the animal was briefly re-anesthetized and reperfusion was initiated by filament withdrawal. Sham-operated mice were treated identically with

the exception that no filament was inserted. Intraoperative rectal temperature was controlled in all animals between 36.5 and 37.5°C.

Neurological deficit score (Yang et al., 1994) was determined after 24 h reperfusion. Scores were (0) no deficit, (1) forelimb weakness, failure to extend forepaw; (2) torso turning to the ipsilateral side when held by tail, circling to affected side, (3) inability to bear weight on affected side, falling (4) no spontaneous locomotor activity. Any animal without a visible deficit, score of 0, was excluded from the study. The number of animals excluded from the study was four for control, three for oxytocin and three for the nursing group. Ischemic injury resulted in five deaths in the control group, and three deaths in each of the oxytocin and nursing groups.

Brain Oxytocin and Cytokine Measurements

For *ex vivo* measurements of oxytocin and proinflammatory cytokines, mice were killed and perfused with 0.9% saline. The brains were removed and the peri-infarct areas and corresponding brain areas in sham control animals were isolated and immediately homogenized in cold phosphate buffered saline using a ratio of 1 g of tissue to 10 ml of reagent plus protease inhibitor mixture (G-Biosciences, St. Louis, MO, United States). The samples were centrifuged at 10,000 × *g* for 20 min at 4°C and the supernatants were used for measurements. Oxytocin levels in brain tissue were assayed by ELISA kit according to manufacturer's instructions (DLdevelop Wuxi, China 214031). Levels of proinflammatory cytokines were determined by TNF-α and IL-6 ELISA kits (Invitrogen). Protein concentrations were measured by BCA protein assay (Pierce).

Brain and Spleen FACS Studies

For FACS studies of brain immune cells, mice were euthanized and perfused with 20 mL of 0.9% saline. The brains were removed, chopped with dissecting scissors and digested with 400 mU/mL Collagenase-D (Roche, Germany) and 50 μg/mL DNase I (Roche) for 1 h in a 37°C incubator. 10 μM EDTA (Life Technologies, Grand Island, NY, United States) was added for the last 5 min. The samples were centrifuged at 450 × g for 10 min, resuspended in 4 mL of 67.5% Percoll (Sigma, St. Louis, MO, United States) and carefully overlaid with 4 mL of 30% Percoll. The Percoll gradient mix was centrifuged at 800 × g for 20 min at room temperature. The cells were collected at the Percoll interface (lymphocytes and monocytes) and bottom pellet (granulocytes).

Spleen cell suspensions were obtained by mechanical disruption and enzymatic digestion with 400 mU/ml Collagenase D and 50 μg/ml DNase I for 30 min at 37°C, and 10 μM EDTA was added for the last 5 min. Cell suspensions were lysed with ACK lysis buffer (Lonza, Walkersville, MD, United States) and filtered through a 70 μm filter. Total leukocyte count ($CD45^+$) from spleen and brain were obtained using Countbright Beads (Thermo Fisher Scientific, Eugene, OR, United States) following manufacturer's instructions. Cell suspensions were incubated 15 min at 4°C with CD16/CD32 (produced in house from 2.4G2 hybridoma, ATCC) to prevent binding of antibodies through Fc-receptor. Cell suspensions were then stained using the following antibodies obtained from eBiosciences, BD or Biolegend: F4/80 PerCPCy5.5 (BM8 clone), CD115 PE (clone AFS98), CD11c PE-Cy7 (clone N418), CD19 APC-A780 and APC-A700 (clone eBio1D3), CD3e APC-A780 (clone145-2C11), Ly6C efluor450 (clone HK1.4), MHCII A700 (clone M5/114.15.2), CD4 BUV395 GK1.5, Ly6G BUV395 (clone 1A8), CD8 BV510 (clone 53-6.7) and CD11b BV785 (clone M1/70). For lymphocyte quantification, cells were stained with the surface cocktail: CD49b FITC (clone DX5), CD25 PerCPCy5.5 (clone PC61), CD19 APC-A700 (clone 1D3), CD62L APC-A780 (clone MLE14), CD44 BV785 (clone IM7), CD4 BUV396 (clone GK1.5), TCRbeta eFluor450 (H57-597), and CD8 BV510 (clone 53-6.7). All surface stainings were performed at 4°C for 20 min. After surface staining, cell were fixed using FoxP3 transcription factor detection kit (eBiosciences) for at least 2 h. Cells were permebealized and stained with FoxP3 APC (clone FJK-16s) for 30 min at 4°C. Stained cells were acquired in a Fortessa X-20 and fcs files were analyzed using FlowJo.

Statistical Analyses

Numbers of animals/group are indicated in figure legends. Data reported are means + SEM. Statistical difference was determined using *T*-test for comparison of two groups or ANOVA followed by Tukey correction for experiments with >2 groups using SigmaPlot (Systat Software, San Jose, CA, United States). $P < 0.05$ was considered significant.

RESULTS

Infarction volume was assessed by TTC staining 24 h after MCAO in non-pregnant/non-postpartum females, nursing postpartum females and postpartum females from which the pups had been removed after delivery (experimental overview illustrated in **Figure 1A**). We observed marked (>70%) reduction in nursing postpartum mice relative to either non-pregnant/non-postpartum mice or when nursing was inhibited by removing the pups in the postpartum period (**Figures 1B,C**). In parallel we evaluated changes in neurological score associated with nursing. **Figure 1D** demonstrates that nursing was associated with significantly improved neurological performance relative to non-pregnant/non-postpartum or non-nursing postpartum females. Because both stroke injury and neurobehavioral outcomes after MCAO were comparable between non-pregnant/non-postpartum mice and non-nursing postpartum mice, non-pregnant/non-postpartum mice were used as the "control" group in the remainder of studies.

We next determined the effects of intranasally delivered oxytocin on stroke outcome (experimental overview illustrated in **Figure 2A**). We observed (**Figure 2B**) that 3d of intranasal oxytocin resulted in elevated brain oxytocin levels (5.2-fold) in control female mice relative to intranasal saline treatment, were comparable to levels observed in nursing females (4.1-fold). Administration of oxytocin resulted in a significant ∼(32%) decrease in the post-MCAO infarction volume (**Figures 2C,D**),

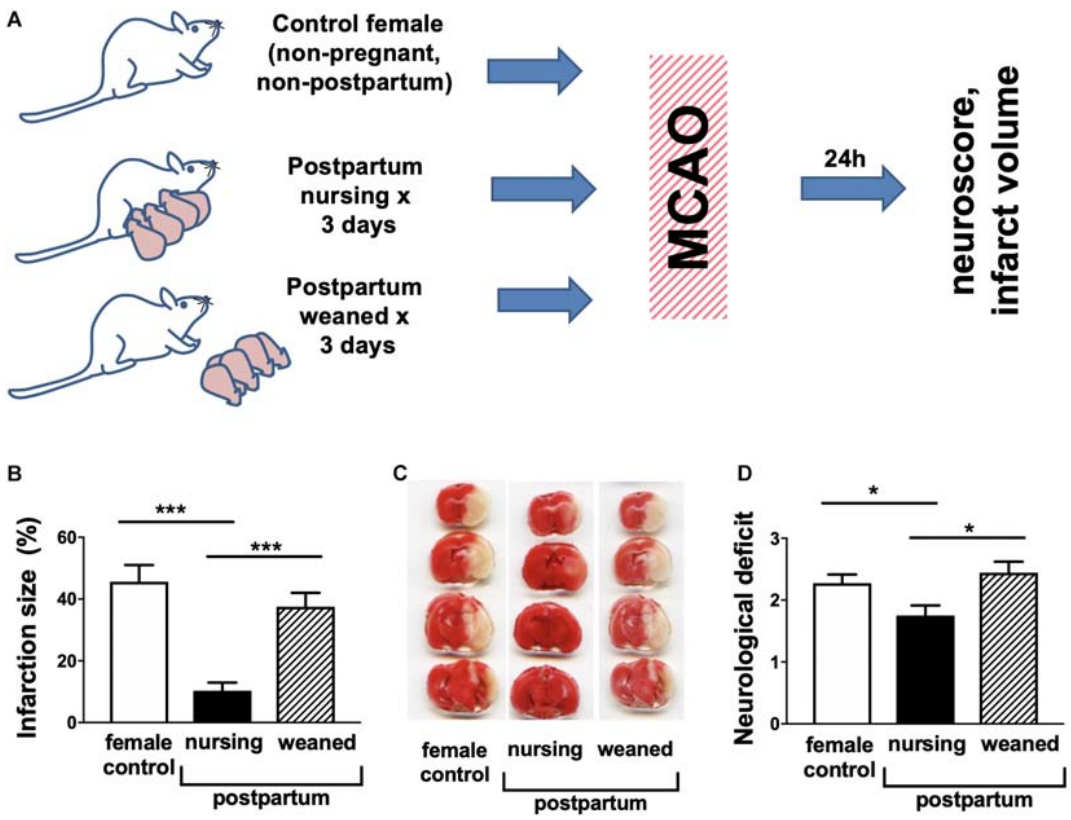

FIGURE 1 | Nursing mice demonstrate marked protection from middle cerebral artery occlusion (MCAO). **(A)** Experimental overview. **(B)** representative TTC stained brain sections, **(C)** quantification of infarction volume as % of hemisphere, and **(D)** post-ischemic neurological deficit. Control are non-pregnant, age-matched females. (N = 8–10/group, $^{***}p < 0.001$ and $^{*}p < 0.05$ compared to control).

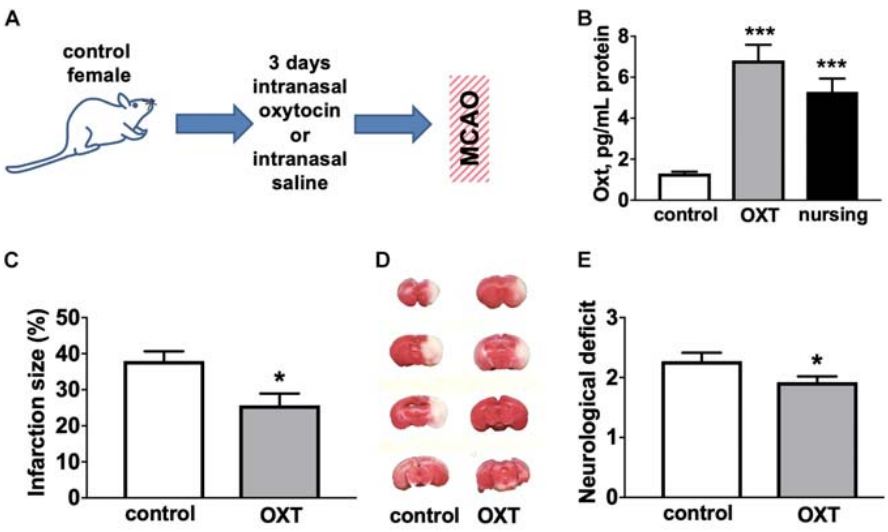

FIGURE 2 | Oxytocin treatment improves post-MCAO outcome in female mice. **(A)** Experimental overview. **(B)** Intranasal oxytocin (Oxt) treatment for 3 days resulted in significantly higher brain levels of oxytocin than seen in non-nursing females and comparable to levels in nursing mice, N = 8–12. Oxytocin treated female mice demonstrated reduced infarction volume compared to control (Ctrl). **(C)** representative TTC stained brain sections, **(D)** quantification of percent of hemisphere infarct volume (N = 9–12), and **(E)** post-ischemic neurological deficit (N = 11–13) $^{***}p < 0.001$ and $^{*}p < 0.05$ compared to control (Ctrl) non-nursing.

significantly improved neurological scores (**Figure 2E**) compared to intranasal saline treated female controls.

Since it has been reported that both lactation and oxytocin treatment are associated with significant neuroimmunological changes (Yuan et al., 2016; Haim et al., 2017; Sherer et al., 2017), we measured brain levels of two major cytokines involved in post-ischemic brain injury, IL-6 and TNF-α, in non-pregnant/non-postpartum mice with and without intranasal oxytocin treatment and in nursing postpartum mice after MCAO (experimental overview illustrated in **Figure 3A**). We observed that brain TNF-α levels were significantly (4.2-fold) increased after MCAO in saline-treated control females, and this increase was significantly attenuated in both nursing postpartum and oxytocin-treated control females (**Figure 3B**). Similarly, brain IL-6 levels were significantly (3.3-fold) increased after MCAO in saline-treated control females, and this increase was also significantly attenuated in both nursing postpartum, and oxytocin-treated control females (**Figure 3C**). We did not observe any significant differences in brain TNF-α or IL-6 levels between the three groups in the absence of ischemic injury (sham surgery).

It has been shown that MCAO induces major changes in the peripheral immune system, including significant spleen atrophy in male mice (Offner et al., 2006). Therefore we assessed spleen weight and immune cell composition in non-pregnant/non-postpartum mice with and without intranasal oxytocin treatment and in nursing postpartum mice after MCAO (experimental overview illustrated in **Figure 3A**). **Figure 4A** demonstrates that oxytocin induced a moderate 1.4-fold increase in spleen weight in females, while nursing resulted in a stronger 2.2-fold increase in spleen weight compared to control sham. MCAO caused small but significant decreases in spleen weights in all groups (17% decrease in control, 26% in oxytocin treated, and 14% in nursing mice). We then studied male Swiss Webster mice and found modest decreases in spleen weight following MCAO, with no significant effect of oxytocin treatment on spleen weight (**Supplementary Material**).

Analyses of spleen cell suspensions by flow cytometry indicate that nursing was associated with a significant 1.7-fold increase in total spleen leukocytes, while oxytocin treatment resulted in only a non-significant increase in non-ischemic animals. Ischemia caused a significant 37% decrease in total spleen leukocyte numbers in control animals. Significant MCAO-associated decreases in total spleen leukocytes were also observed in oxytocin-treated and nursing mice (45 and 36%, respectively, **Figure 4B**). We observed nursing-associated changes in spleen myeloid cells, monocytes and granulocytes. **Figures 4C,D** demonstrate sequential gating strategies used to analyze myeloid cells in the spleen and in the brain, respectively. Analysis of monocyte frequency and total counts showed a markedly increased frequency in nursing post-MCAO animals, compared to all other groups (**Figure 5A**). This translated to significantly higher spleen monocyte counts in the nursing mice, without significant differences between non-ischemic and post-MCAO animals, due to the differences in overall leukocyte count (**Figure 5B**). Granulocyte frequency

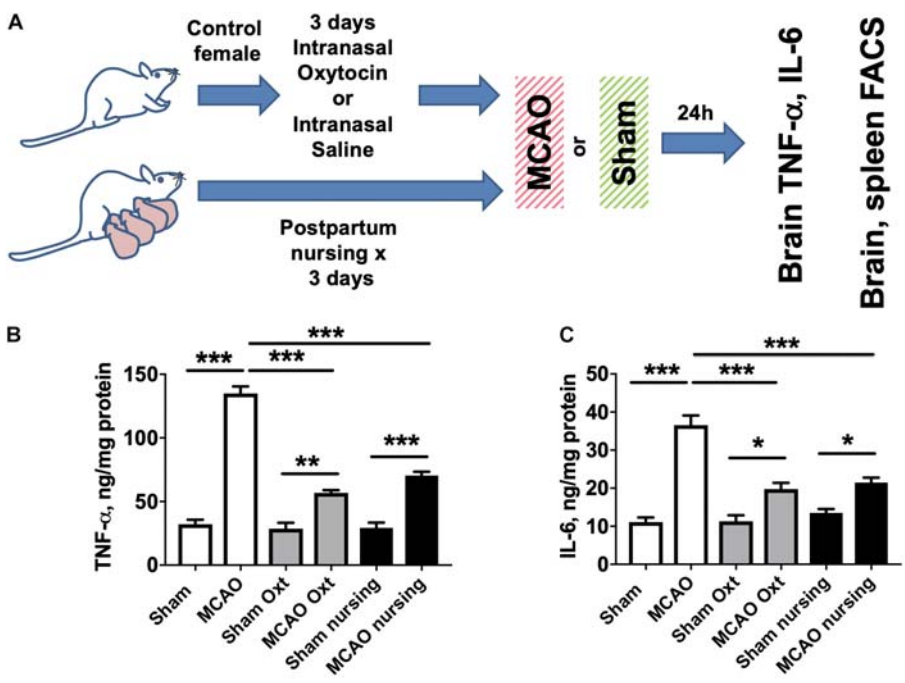

FIGURE 3 | Increases in brain TNF- and IL-6 levels induced by MCAO are moderated by nursing or oxytocin treatment. **(A)** Experimental overview. Brain cytokine levels were assessed in sham operated or MCAO mice either nursing or treated with vehicle or oxytocin. TNF-α **(B)** and IL-6 **(C)** levels were significantly increased in mouse brain 24 h after MCAO compared to sham operated animals. This increase was significantly attenuated in both nursing and oxytocin (Oxt) treated mice $N = 6$ for MCAO animals, $N = 4$ for sham, $^{***}p < 0.001$ $^{**}p < 0.01$, and $^{*}p < 0.05$ for comparisons indicated by the horizontal bars.

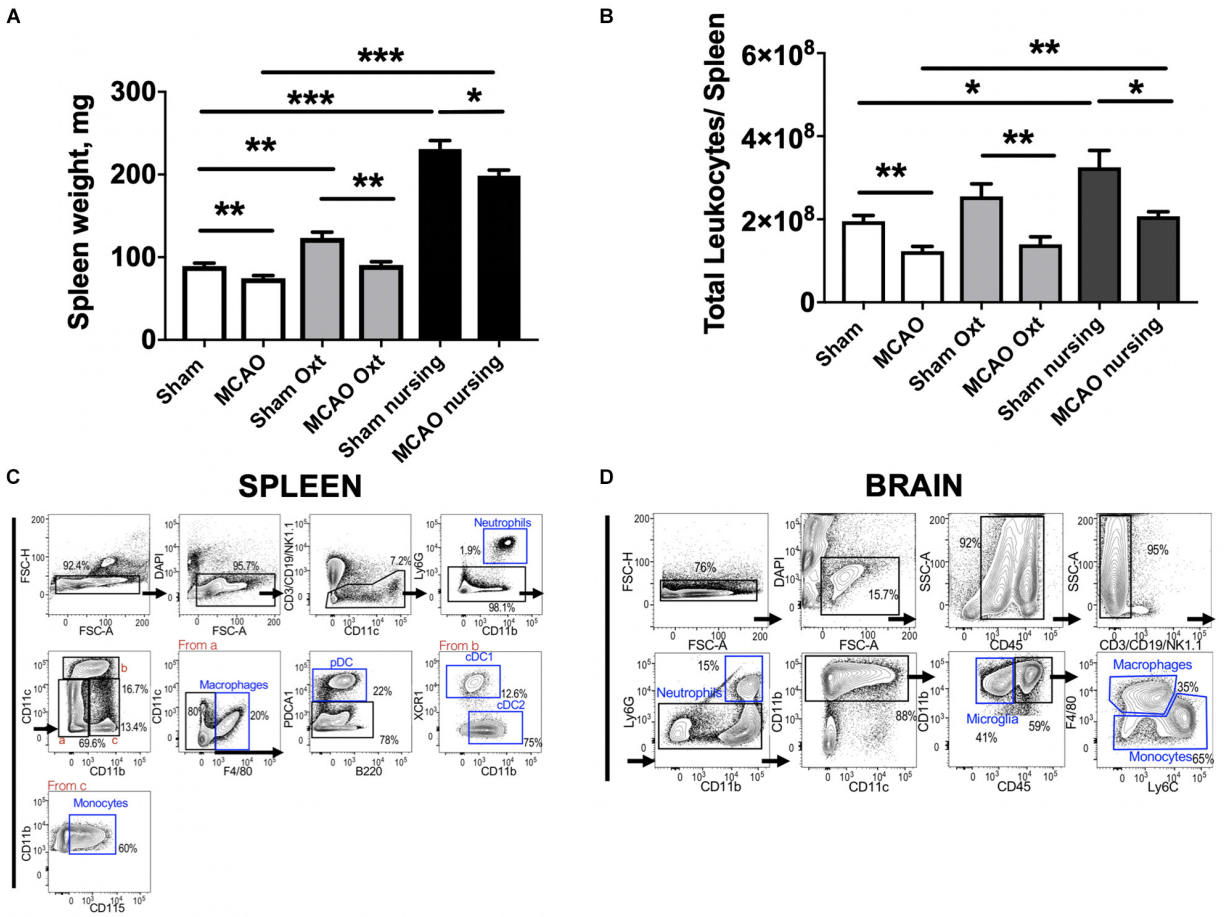

FIGURE 4 | Changes in spleen 24 h past ischemia in nursing and oxytocin treated mice evaluated by spleen weight and FACS studies of leukocytes. Oxytocin (Oxt) treated and nursing animals demonstrated significantly bigger spleen weights **(A)**. Changes in total leukocyte numbers promoted by nursing and oxytocin treatment **(B)**. Sequential gating strategy to analyze myeloid cells in the spleen **(C)** and the brain **(D)**. Number represent frequency of parent. $N = 11$ for A, $N = 4$ for B, $^{***}p < 0.001$, $^{**}p < 0.01$, and $^{*}p < 0.05$, for comparisons indicated by horizontal bars.

was significantly increased in non-ischemic nursing mice, compared to non-ischemic sham control (**Figure 5C**). The total spleen granulocyte numbers were significantly increased in both ischemic and post-MCAO nursing mice, compared to corresponding sham controls (**Figure 5D**). However oxytocin supplementation did not recapitulate the effects observed with nursing (**Figures 5A–D**).

Lymphocyte populations in the spleen were also analyzed. We observed a significant 2.1-fold increase in total regulatory T cells (Treg) numbers in spleens of post-MCAO nursing animals compared to control ischemic animals, while only a non-significant 1.4-fold increase was observed in oxytocin-treated mice. Results of FACS studies for different leukocyte types, frequency and total counts, are included in **Supplementary Material**. Because leukocyte migration into the brain develops over time and peaks around 3 days post-stroke (Jin et al., 2010), we performed FACS studies of brain immune cells at this time point. MCAO induced a strong 3.3-fold increase in total leukocyte numbers in the stroke affected (ipsilateral) brain hemisphere compared to the contralateral hemisphere in control mice (33583 vs. 15077 total leukocytes in ipsilateral vs. contralateral hemispheres). This MCAO-associated increase was significantly attenuated in nursing mice (13052 total leukocytes per hemisphere) only reaching levels comparable to the non-ischemic hemispheres of controls. This was paralleled by significant increases in frequencies (**Figure 6A**) and total cell numbers of monocytes (**Figure 6B**) and granulocytes (**Figures 6C,D**) in the ipsilateral hemispheres of MCAO animals. Together our observations demonstrate that nursing significantly attenuated the MCAO-induced increase of immune cell types that are considered central to the development of ischemic injury (Shi and Pamer, 2011).

DISCUSSION

Oxytocin is essential for lactation and postpartum maternal behavior (Gimpl and Fahrenholz, 2001). Recent studies report significant neuroimmunological changes in postpartum animals (Haim et al., 2017; Sherer et al., 2017), and immune responses

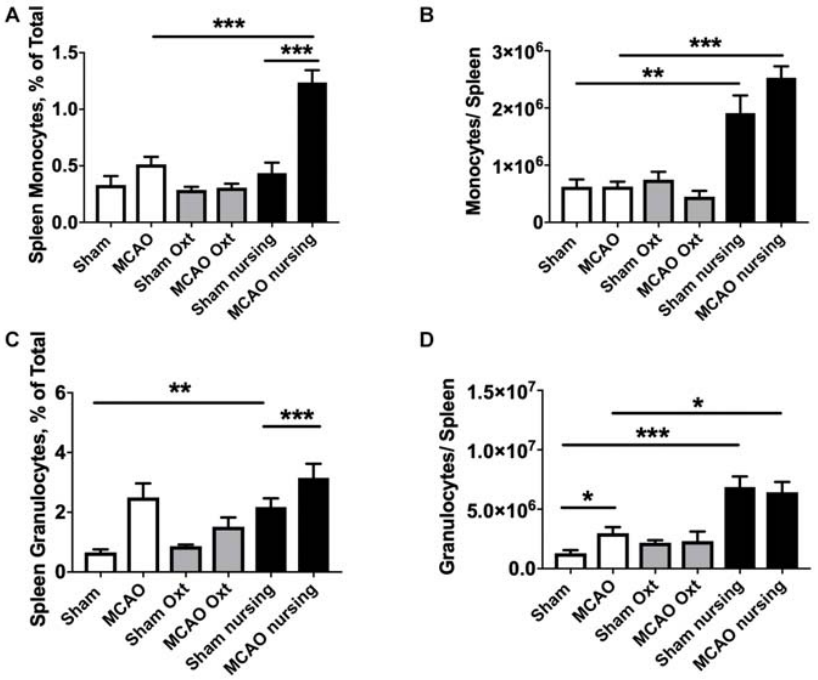

FIGURE 5 | Nursing- and oxytocin (Oxt)-associated changes in spleen myeloid cells. Monocyte frequency **(A)** and total counts **(B)** demonstrated significant increase in nursing animals. Granulocyte frequencies **(C)** and total counts **(D)** were also increased in nursing animals. $N = 4$, $^{***}p < 0.001$, $^{**}p < 0.01$, and $^{*}p < 0.05$ for comparisons indicated by horizontal bars.

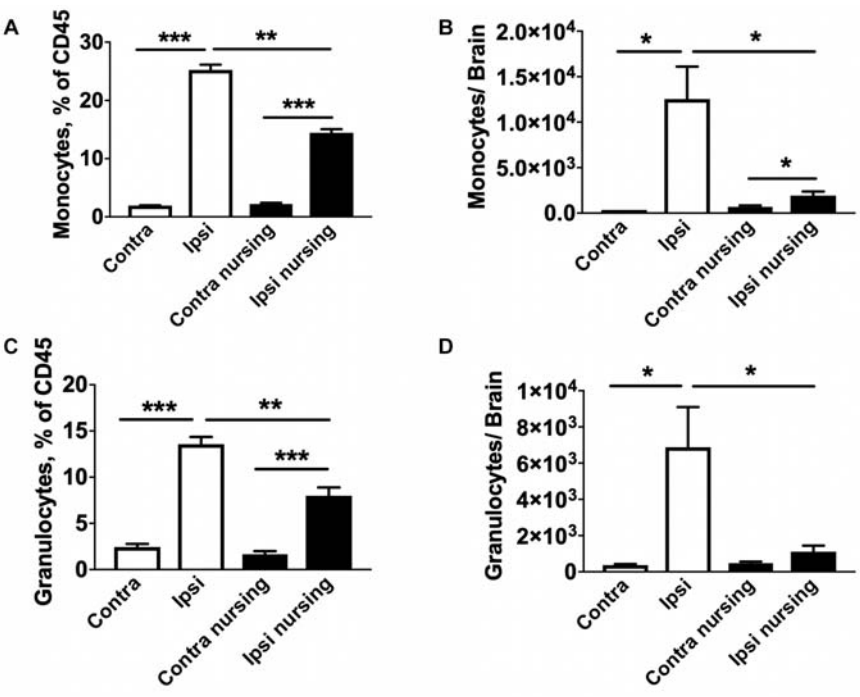

FIGURE 6 | MCAO-induced brain migration of monocytes and granulocytes is reduced in nursing mice. In non-nursing mice MCAO promoted strong migration of monocytes **(A,B)** and granulocytes **(C,D)** into the ipsilateral ischemic hemispheres (Ipsi) compared to the non-ischemic contralateral hemispheres (Contra). This migration was significantly attenuated in nursing mice. $N = 4$, $^{*}p < 0.05$, $^{**}p < 0.01$, and $^{***}p < 0.001$ for comparisons indicated by horizontal bars.

are crucial to stroke outcome (Stoll et al., 1998; Schwab et al., 2001; Iadecola and Anrather, 2011). Our results show for the first time that nursing animals have markedly smaller infarct volumes and improved neurological outcome following MCAO injury. To compare the protective effects of nursing and oxytocin treatment we administered oxytocin intranasally and achieved brain oxytocin levels comparable to those in nursing animals. We observed reduced infarct volume and improved neurological outcome in oxytocin-treated female mice. These results support related observations in male mice whereby oxytocin treatment improved stroke outcome after cerebral ischemia when caged alone, but provided no protection to group-housed male mice that had higher brain oxytocin levels (Karelina et al., 2011).

Oxytocin inhibited LPS-induced inflammation in microglial cells and attenuated microglial activation associated with LPS treatment and maternal separation *in vivo* (Yuan et al., 2016; Amini-Khoei et al., 2017). Stroke induces significant inflammation in the brain (Choe et al., 2011; Vogelgesang et al., 2014); however, to the best of our knowledge, the effects of oxytocin on post-stroke inflammation have not been studied. Our studies indicate that the levels of two major pro-inflammatory cytokines associated with stroke injury, TNF-α and IL-6 (Campbell et al., 1993; Rothwell and Relton, 1993; Meistrell et al., 1997; Lavine et al., 1998), were elevated following MCAO injury. Independently, both oxytocin treatment and nursing significantly attenuated this pro-inflammatory cytokine release. The decrease in pro-inflammatory cytokine levels in nursing mice was accompanied by reduced brain migration of blood leukocytes, particularly monocytes and granulocytes. These cell types have been shown to be central to the development of post-ischemic brain inflammation and damage, especially due to pro-inflammatory cytokine generation (Shi and Pamer, 2011). Thus one major mechanism of protection is likely reduced migration of monocytes and granulocytes to the brain.

Peripheral immune responses are activated by stroke and interact with the development of brain damage. The spleen is a key lymphatic organ and a major reservoir of blood cells that come into the circulation and brain following brain injury (Mebius and Kraal, 2005). Therefore, splenic responses after stroke have gained attention (Seifert and Offner, 2018). It is well established that the spleen shrinks in animal stroke models (Offner et al., 2006; Ajmo et al., 2009). Spleen shrinkage is associated with early release of splenocytes and splenocyte apoptosis (Liu et al., 2015). Our studies demonstrate that nursing is associated with a marked increase in spleen size, and reduced MCAO-associated spleen atrophy. Spleen responses have been shown to correlate inversely with infarct volume (Vendrame et al., 2006), and, in turn, influence the development of ischemic brain injury (Liu et al., 2015). Prior studies have shown that splenectomy, preceding or immediately after stroke, or spleen irradiation is protective (Dotson et al., 2014; Chauhan et al., 2018). To the best of our knowledge this study describes the first observations of nursing-associated reduced spleen atrophy in post-MCAO animals, with associated improvements in stroke outcomes. In the present study we also observed that nursing independently promoted significant increases in spleen weight and total leukocyte numbers prior to injury. Importantly, nursing resulted in higher numbers of spleen monocytes and granulocytes, and this increase was retained after stroke induction. Both monocytes and granulocytes have been shown to contribute to post-ischemic brain damage and inflammation, and their increased numbers in the spleen apparently inversely correlate with the observed decrease in those cell types in post-ischemic brain (Shi and Pamer, 2011). Notably, in the present study we observed that oxytocin treatment alone failed to significantly reduce the MCAO-associated spleen atrophy.

It has been demonstrated that pro-inflammatory cytokine production induced by LPS stimulation is attenuated during pregnancy and in the postpartum period (Sherer et al., 2017). Whether lactation or oxytocin treatment leads to reduced peripheral immunosuppression remains to be determined. Post- and peripartum changes in baseline microglial density, and brain levels of interleukins 6 and 10, have been previously described in rat brains (Haim et al., 2017). Notably, the brain immune response to stress (forced swim test) is also altered in pregnant versus non-pregnant females. Most relevant to the present study, Ritzel et al. (2017) recently described reduced baseline microglial activity in multiparous female rats compared with nulliparous rats. This translated to reduced inflammatory activation after experimental stroke, reduced injury and faster recovery. Because infection is a major factor in post-stroke mortality this will be an important future direction to pursue.

Recent studies also suggest that Treg cells, a subset of T lymphocytes, are beneficial for stroke outcome (Liesz et al., 2009; Li et al., 2013). While significant Treg brain migration is generally observed at later time points than studied here, it has been shown that Treg depletion promotes increased levels of pro-inflammatory cytokines in the blood of post-ischemic animals within hours after MCAO (Liesz et al., 2009). In the present study we observed that nursing was associated with increased total spleen Treg cells, suggesting that this mechanism may also contribute to the observed protection, though future studies at later time points will be required.

SUMMARY

This study is the first to assess the effects of nursing and exogenous oxytocin treatment in stroke outcomes in female mice. Our study demonstrates for the first time strong nursing-associated neuroprotection against experimental stroke, along with observed oxytocin-associated anti-inflammatory mechanisms. Spleen and brain monocyte numbers were also increased with nursing, whereas in nursing mouse brains monocyte number and fraction were both decreased following MCAO. These studies suggest that: (1) intranasal oxytocin may be a novel neuroimmunological approach to reduce injury from stroke in females; and, (2) that nursing confers protection against neuroinflammatory changes and resultant stroke injury. One limitation of the present study is that the effect of oxytocin replacement therapy on stroke outcomes and neuroimmune

modulation was not assessed in non-nursing postpartum females. As these studies did not include a non-nursing group for all comparisons, changes in postpartum females following MCAO cannot necessarily be attributed to nursing *per se*, as other features associated with pup presence/absence could also underlie our observations. Litter size may also have an effect on postpartum stroke outcomes, as nulliparity versus multiparity have bene shown to determine stroke outcomes (Ritzel et al., 2017), however this was not controlled for in this study. A final limitation is that we did not identify the cell-type specific source of brain cytokine modulation associated with oxytocin treatment. Further studies incorporating cell-type specific mechanistic studies will be required to develop a more comprehensive understanding of the regulatory pathways responsible for lactation-associated neuroprotection, to advance therapeutic applications for this specific, at-risk population.

DATA AVAILABILITY

The datasets generated for this study are available on request to the corresponding author.

ETHICS STATEMENT

This study was carried out in accordance with the recommendations of the National Institutes of Health guidelines for the use of experimental animals. The protocol was approved by the Stanford Animal Care and Use Committee.

AUTHOR CONTRIBUTIONS

CS contributed to study design, data analysis, and manuscript preparation. LX performed the animal surgeries. LV performed the ELISA experiments. MA-H performed the FACS experiments. OA performed the blinded treatments, tissue collection, and histological analyses. JI contributed to study design and data analysis. RG contributed to study design, data analysis, and manuscript preparation.

FUNDING

This work was supported by American Heart Association grant FTF-19970029 to CS, Finnish Cultural Foundation grant 00171200 to OA, and NIH grants R01NS084396 and R01NS080177 to RG.

SUPPLEMENTARY MATERIAL

The Supplementary Material for this article can be found online at: https://www.frontiersin.org/articles/10.3389/fnins.2019.00609/full#supplementary-material

REFERENCES

Ajmo, C. T. Jr., Collier, L. A., Leonardo, C. C., Hall, A. A., Green, S. M., Womble, T. A., et al. (2009). Blockade of adrenoreceptors inhibits the splenic response to stroke. *Exp. Neurol.* 218, 47–55. doi: 10.1016/j.expneurol.2009.03.044

Alkayed, N. J., Harukuni, I., Kimes, A. S., London, E. D., Traystman, R. J., and Hurn, P. D. (1998). Gender-linked brain injury in experimental stroke. *Stroke* 29, 159–165; discussion 166.

Amini-Khoei, H., Mohammadi-Asl, A., Amiri, S., Hosseini, M. J., Momeny, M., Hassanipour, M., et al. (2017). Oxytocin mitigated the depressive-like behaviors of maternal separation stress through modulating mitochondrial function and neuroinflammation. *Prog. Neuropsychopharmacol. Biol. Psychiatry* 76, 169–178. doi: 10.1016/j.pnpbp.2017.02.022

Campbell, I. L., Abraham, C. R., Masliah, E., Kemper, P., Inglis, J. D., Oldstone, M. B., et al. (1993). Neurologic disease induced in transgenic mice by cerebral overexpression of interleukin 6. *Proc. Natl. Acad. Sci. U.S.A.* 90, 10061–10065. doi: 10.1073/pnas.90.21.10061

Carson, M. J., and Sutcliffe, J. G. (1999). Balancing function vs. Self defense: the cns as an active regulator of immune responses. *J. Neurosci. Res.* 55, 1–8. doi: 10.1002/(sici)1097-4547(19990101)55:1<1::aid-jnr1>3.0.co;2-9

Chauhan, A., Al Mamun, A., Spiegel, G., Harris, N., Zhu, L., and McCullough, L. D. (2018). Splenectomy protects aged mice from injury after experimental stroke. *Neurobiol. Aging* 61, 102–111. doi: 10.1016/j.neurobiolaging.2017.09.022

Chauhan, A., Moser, H., and McCullough, L. D. (2017). Sex differences in ischaemic stroke: potential cellular mechanisms. *Clin. Sci.* 131, 533–552. doi: 10.1042/CS20160841

Cheng, C. A., Lee, J. T., Lin, H. C., Lin, H. C., Chung, C. H., Lin, F. H., et al. (2017). Pregnancy increases stroke risk up to 1 year postpartum and reduces long-term risk. *QJM* 110, 355–360. doi: 10.1093/qjmed/hcw222

Choe, C. U., Lardong, K., Gelderblom, M., Ludewig, P., Leypoldt, F., Koch-Nolte, F., et al. (2011). Cd38 exacerbates focal cytokine production, postischemic inflammation and brain injury after focal cerebral ischemia. *PLoS One* 6:e19046. doi: 10.1371/journal.pone.0019046

Darnaudery, M., Perez-Martin, M., Del Favero, F., Gomez-Roldan, C., Garcia-Segura, L. M., and Maccari, S. (2007). Early motherhood in rats is associated with a modification of hippocampal function. *Psychoneuroendocrinology* 32, 803–812. doi: 10.1016/j.psyneuen.2007.05.012

Dotson, A. L., Zhu, W., Libal, N., Alkayed, N. J., and Offner, H. (2014). Different immunological mechanisms govern protection from experimental stroke in young and older mice with recombinant tcr ligand therapy. *Front. Cell Neurosci.* 8:284.

Gimpl, G., and Fahrenholz, F. (2001). The oxytocin receptor system: structure, function, and regulation. *Physiol. Rev.* 81, 629–683. doi: 10.1152/physrev.2001.81.2.629

Haim, A., Julian, D., Albin-Brooks, C., Brothers, H. M., Lenz, K. M., and Leuner, B. (2017). A survey of neuroimmune changes in pregnant and postpartum female rats. *Brain Behav. Immun.* 59, 67–78. doi: 10.1016/j.bbi.2016.09.026

Haim, A., Sherer, M., and Leuner, B. (2014). Gestational stress induces persistent depressive-like behavior and structural modifications within the postpartum nucleus accumbens. *Eur. J. Neurosci.* 40, 3766–3773. doi: 10.1111/ejn.12752

Iadecola, C., and Anrather, J. (2011). The immunology of stroke: from mechanisms to translation. *Nat. Med.* 17, 796–808. doi: 10.1038/nm.2399

Jaigobin, C., and Silver, F. L. (2000). Stroke and pregnancy. *Stroke* 31, 2948–2951. doi: 10.1161/01.str.31.12.2948

James, A. H., Bushnell, C. D., Jamison, M. G., and Myers, E. R. (2005). Incidence and risk factors for stroke in pregnancy and the puerperium. *Obstet. Gynecol.* 106, 509–516. doi: 10.1097/01.aog.0000172428.78411.b0

Jin, R., Yang, G., and Li, G. (2010). Inflammatory mechanisms in ischemic stroke: role of inflammatory cells. *J. Leukoc. Biol.* 87, 779–789. doi: 10.1189/jlb.1109766

Kamel, H., Navi, B. B., Sriram, N., Hovsepian, D. A., Devereux, R. B., and Elkind, M. S. (2014). Risk of a thrombotic event after the 6-week postpartum period. *N. Engl. J. Med.* 370, 1307–1315. doi: 10.1056/NEJMoa1311485

Karelina, K., Stuller, K. A., Jarrett, B., Zhang, N., Wells, J., Norman, G. J., et al. (2011). Oxytocin mediates social neuroprotection after cerebral ischemia. *Stroke* 42, 3606–3611. doi: 10.1161/STROKEAHA.111.628008

Kittner, S. J., Stern, B. J., Feeser, B. R., Hebel, R., Nagey, D. A., Buchholz, D. W., et al. (1996). Pregnancy and the risk of stroke. *N. Engl. J. Med.* 335, 768–774.

Kochanek, K. D., Murphy, S. L., Xu, J., and Arias, E. (2013). Mortality in the united states. *NCHS Data Brief.* 2014, 1–8.

Lafargue, M., Xu, L., Carles, M., Serve, E., Anjum, N., Iles, K. E., et al. (2012). Stroke-induced activation of the alpha7 nicotinic receptor increases *pseudomonas aeruginosa* lung injury. *FASEB J.* 26, 2919–2929. doi: 10.1096/fj.11-197384

Lakhan, S. E., Kirchgessner, A., and Hofer, M. (2009). Inflammatory mechanisms in ischemic stroke: therapeutic approaches. *J. Transl. Med.* 7:97. doi: 10.1186/1479-5876-7-97

Lavine, S. D., Hofman, F. M., and Zlokovic, B. V. (1998). Circulating antibody against tumor necrosis factor-alpha protects rat brain from reperfusion injury. *J. Cereb. Blood Flow Metab.* 18, 52–58. doi: 10.1097/00004647-199801000-00005

Leuner, B., Mirescu, C., Noiman, L., and Gould, E. (2007). Maternal experience inhibits the production of immature neurons in the hippocampus during the postpartum period through elevations in adrenal steroids. *Hippocampus* 17, 434–442. doi: 10.1002/hipo.20278

Li, P., Gan, Y., Sun, B. L., Zhang, F., Lu, B., Gao, Y., et al. (2013). Adoptive regulatory t-cell therapy protects against cerebral ischemia. *Ann. Neurol.* 74, 458–471. doi: 10.1002/ana.23815

Liesz, A., Suri-Payer, E., Veltkamp, C., Doerr, H., Sommer, C., Rivest, S., et al. (2009). Regulatory t cells are key cerebroprotective immunomodulators in acute experimental stroke. *Nat. Med.* 15, 192–199. doi: 10.1038/nm.1927

Liu, Z. J., Chen, C., Li, F. W., Shen, J. M., Yang, Y. Y., Leak, R. K., et al. (2015). Splenic responses in ischemic stroke: new insights into stroke pathology. *CNS Neurosci. Ther.* 21, 320–326. doi: 10.1111/cns.12361

Lo, E. H., Dalkara, T., and Moskowitz, M. A. (2003). Mechanisms, challenges and opportunities in stroke. *Nat. Rev. Neurosci.* 4, 399–415.

Maheu, M. E., Akbari, E. M., and Fleming, A. S. (2009). Callosal oligodendrocyte number in postpartum sprague-dawley rats. *Brain Res.* 1267, 18–24. doi: 10.1016/j.brainres.2009.02.029

Mebius, R. E., and Kraal, G. (2005). Structure and function of the spleen. *Nat. Rev. Immunol.* 5, 606–616. doi: 10.1038/nri1669

Meistrell, M. E. III, Botchkina, G. I., Wang, H., Di Santo, E., Cockroft, K. M., Bloom, O., et al. (1997). Tumor necrosis factor is a brain damaging cytokine in cerebral ischemia. *Shock* 8, 341–348.

Moskowitz, M. A., Lo, E. H., and Iadecola, C. (2010). The science of stroke: mechanisms in search of treatments. *Neuron* 67, 181–198. doi: 10.1016/j.neuron.2010.07.002

Murphy, S. J., McCullough, L. D., and Smith, J. M. (2004). Stroke in the female: role of biological sex and estrogen. *ILAR J.* 45, 147–159. doi: 10.1093/ilar.45.2.147

Neumann, I. D., Maloumby, R., Beiderbeck, D. I., Lukas, M., and Landgraf, R. (2013). Increased brain and plasma oxytocin after nasal and peripheral administration in rats and mice. *Psychoneuroendocrinology* 38, 1985–1993. doi: 10.1016/j.psyneuen.2013.03.003

Offner, H., Subramanian, S., Parker, S. M., Wang, C., Afentoulis, M. E., Lewis, A., et al. (2006). Splenic atrophy in experimental stroke is accompanied by increased regulatory t cells and circulating macrophages. *J. Immunol.* 176, 6523–6531. doi: 10.4049/jimmunol.176.11.6523

Ritzel, R. M., Patel, A. R., Spychala, M., Verma, R., Crapser, J., Koellhoffer, E. C., et al. (2017). Multiparity improves outcomes after cerebral ischemia in female mice despite features of increased metabovascular risk. *Proc. Natl. Acad. Sci. U.S.A.* 114, E5673–E5682. doi: 10.1073/pnas.1607002114

Rothwell, N. J., and Relton, J. K. (1993). Involvement of cytokines in acute neurodegeneration in the cns. *Neurosci. Biobehav. Rev.* 17, 217–227. doi: 10.1016/s0149-7634(05)80152-6

Salmaso, N., and Woodside, B. (2006). Upregulation of astrocytic basic fibroblast growth factor in the cingulate cortex of lactating rats: time course and role of suckling stimulation. *Horm. Behav.* 50, 448–453. doi: 10.1016/j.yhbeh.2006.05.006

Schwab, J. M., Nguyen, T. D., Meyermann, R., and Schluesener, H. J. (2001). Human focal cerebral infarctions induce differential lesional interleukin-16 (il-16) expression confined to infiltrating granulocytes, cd8+ t-lymphocytes and activated microglia/macrophages. *J. Neuroimmunol.* 114, 232–241. doi: 10.1016/s0165-5728(00)00433-1

Seifert, H. A., and Offner, H. (2018). The splenic response to stroke: from rodents to stroke subjects. *J. Neuroinflam.* 15:195. doi: 10.1186/s12974-018-1239-9

Sherer, M. L., Posillico, C. K., and Schwarz, J. M. (2017). An examination of changes in maternal neuroimmune function during pregnancy and the postpartum period. *Brain Behav. Immun.* 66, 201–209. doi: 10.1016/j.bbi.2017.06.016

Shi, C., and Pamer, E. G. (2011). Monocyte recruitment during infection and inflammation. *Nat. Rev. Immunol.* 11, 762–774. doi: 10.1038/nri3070

Sohrabji, F., Park, M. J., and Mahnke, A. H. (2017). Sex differences in stroke therapies. *J. Neurosci. Res.* 95, 681–691. doi: 10.1002/jnr.23855

Stoll, G., Jander, S., and Schroeter, M. (1998). Inflammation and glial responses in ischemic brain lesions. *Prog. Neurobiol.* 56, 149–171. doi: 10.1016/s0301-0082(98)00034-3

Tomizawa, K., Iga, N., Lu, Y. F., Moriwaki, A., Matsushita, M., Li, S. T., et al. (2003). Oxytocin improves long-lasting spatial memory during motherhood through map kinase cascade. *Nat. Neurosci.* 6, 384–390. doi: 10.1038/nn1023

Vendrame, M., Gemma, C., Pennypacker, K. R., Bickford, P. C., Davis Sanberg, C., Sanberg, P. R., et al. (2006). Cord blood rescues stroke-induced changes in splenocyte phenotype and function. *Exp. Neurol.* 199, 191–200. doi: 10.1016/j.expneurol.2006.03.017

Vogelgesang, A., Becker, K. J., and Dressel, A. (2014). Immunological consequences of ischemic stroke. *Acta Neurol. Scand.* 129, 1–12. doi: 10.1111/ane.12165

Xu, L. J., Ouyang, Y. B., Xiong, X., Stary, C. M., and Giffard, R. G. (2015). Post-stroke treatment with mir-181 antagomir reduces injury and improves long-term behavioral recovery in mice after focal cerebral ischemia. *Exp. Neurol.* 264, 1–7. doi: 10.1016/j.expneurol.2014.11.007

Yang, G., Chan, P. H., Chen, J., Carlson, E., Chen, S. F., Weinstein, P., et al. (1994). Human copper-zinc superoxide dismutase transgenic mice are highly resistant to reperfusion injury after focal cerebral ischemia. *Stroke* 25, 165–170. doi: 10.1161/01.str.25.1.165

Yuan, L., Liu, S., Bai, X., Gao, Y., Liu, G., Wang, X., et al. (2016). Oxytocin inhibits lipopolysaccharide-induced inflammation in microglial cells and attenuates microglial activation in lipopolysaccharide-treated mice. *J. Neuroinflamm.* 13:77. doi: 10.1186/s12974-016-0541-7

Conflict of Interest Statement: The authors declare that the research was conducted in the absence of any commercial or financial relationships that could be construed as a potential conflict of interest.

frontiers in Endocrinology

HYPOTHESIS AND THEORY
published: 18 September 2019
doi: 10.3389/fendo.2019.00633

Toward the Existence of a Sympathetic Neuroplasticity Adaptive Mechanism Influencing the Immune Response. A Hypothetical View—Part II

*Emanuel Bottasso**

Departments of Pathology and Physiology, Faculty of Medicine, Centro de Altos Estudios en Ciencias Humanas y de la Salud, Universidad Abierta Interamericana, Rosario, Argentina

OPEN ACCESS

Edited by:
Ana Rosa Pérez, National Council for Scientific and Technical Research (CONICET), Argentina

Reviewed by:
Lenin Pavón, National Institute of Psychiatry Ramon de la Fuente Muñiz (INPRFM), Mexico
Ciro De Luca, Second University of Naples, Italy
Moisés Evandro Bauer, Pontifical Catholic University of Rio Grande do Sul, Brazil

***Correspondence:**
Emanuel Bottasso
emanuelbottasso@hotmail.com

Specialty section:
This article was submitted to Neuroendocrine Science, a section of the journal Frontiers in Endocrinology

Received: *30 April 2019*
Accepted: *30 August 2019*
Published: *18 September 2019*

Citation:
Bottasso E (2019) Toward the Existence of a Sympathetic Neuroplasticity Adaptive Mechanism Influencing the Immune Response. A Hypothetical View—Part II. Front. Endocrinol. 10:633. doi: 10.3389/fendo.2019.00633

In the preceding work, a hypothesis on the existence of a specific neural plasticity program from sympathetic fibers innervating secondary lymphoid organs was introduced. This proposed adaptive mechanism would involve segmental retraction and degeneration of noradrenergic terminals during the immune system (IS) activation followed by regeneration once the IS returns to the steady-state. Starting from such view, this second part presents clinical and experimental evidence allowing to envision that this sympathetic neural plasticity mechanism is also operative on inflamed non-lymphoid peripheral tissues. Importantly, the sympathetic nervous system regulates most of the physiological bodily functions, ranging from cardiovascular, respiratory and gastro-intestinal functions to endocrine and metabolic ones, among others. Thus, it seems sensible to think that compensatory programs should be put into place during inflammation in non-lymphoid tissues as well, to avoid the possible detrimental consequences of a sympathetic blockade. Nevertheless, in many pathological scenarios like severe sepsis, chronic inflammatory diseases, or maladaptive immune responses, such compensatory programs against noradrenergic transmission impairment would fail to develop. This would lead to a manifest sympathetic dysfunction in the above-mentioned settings, partly accounting for their underlying pathophysiological basis; which is also discussed. The physiological/teleological significance for the whole neural plasticity process is postulated, as well.

Keywords: neuro-immune interaction, sympathetic nervous system, inflammation, neural plasticity, peripheral immune tolerance

INTRODUCTION

In the preceding work (1) evidence regarding changes in the sympathetic innervation of secondary lymphoid organs (SLOs) during the activation of the immune system (IS) was presented. Different authors interpreted this phenomenon as "damage" or "injury" of the noradrenergic axons, probably due to the action of endogenous mediators. In contrast to this view, the hypothesis of a neural plasticity adaptive mechanism was postulated –involving axonal degeneration during the activation of the IS with subsequent axonal regeneration once the immune response ceases, thus recovering

the innervation pattern of the steady-state. It was also proposed that this mechanism may be mediated by molecules such as neurotrophins and semaphorins.

One of the main remaining questions was whether these changes in innervation would also occur in other non-lymphoid organs and tissues during inflammation, encompassing recruitment of immune cells and/or presence of inflammatory cytokines. Given that the above-mentioned molecules mediating neural plasticity can be produced by immune cells or by other different cell types under cytokine influence (2–6), this hypothetical view seems plausible. In support of this, clinical and experimental evidence regarding the loss of sympathetic innervation during different inflammatory conditions is now presented. As part of the autonomic nervous system (ANS), the sympathetic nervous system (SNS), regulates nearly all bodily functions (7). Hence, a sympathetic dysfunction would become clinically manifest, in cases wherein a compensation against this hypothetical impaired noradrenergic transmission is insufficient, implying life-threatening consequences in some circumstances.

Nature is unlikely to orchestrate complex and energy-wasting mechanisms for nothing. As the nervous system (NS) regulates most phases of the immune response, mainly through the SNS (8–11), the immunological meaning for this postulated retraction of the noradrenergic terminals both in SLOs and in non-lymphoid tissues during immune-mediated processes is also proposed.

Sepsis and Septic Shock

Sepsis is one of the main causes of morbidity and mortality throughout the world consisting of a dysregulated systemic inflammatory response syndrome against a specific pathogen infection. Sepsis with organic dysfunction is called severe sepsis, which can progress to septic shock, characterized by persistent hypotension <65 mmHg leading to a state of acute circulatory failure (12–15). Organic dysfunction in severe sepsis can include renal, hepatic, cardiac or pulmonary failure, lactic acidosis, thrombocytopenia with abnormalities in coagulation or multiple organ failure. Bacterial endotoxins such as LPS activate the NF-κB pathway in immune cells with the subsequent production and release to the circulation of inflammatory mediators such as TNF, IL-1, IL-6, IL-8, and macrophage migration inhibitory factor, presumably involved in the above-referred clinical alterations.

Vasoplegia and myocardial dysfunction are the two complications of septic shock leading to hemodynamic instability (16, 17). Vasoplegia is defined as a lack of vasculature response to vasopressors (18, 19) leading to a state of persistent peripheral vasodilation, hypotension, and hypoperfusion. Nitric oxide (NO), synthesized by the vascular smooth muscle inducible nitric oxide synthase (iNOS) under the control of cytokines, may play a central role in this regard (20). As to cardiac function, at the beginning of sepsis, patients have a hyperdynamic phase characterized by an increased cardiac output as a reaction to the decreased peripheral vascular resistance. After that, progression toward septic shock is characterized by a depressed activity of the ventricular myocardium along with a reduced ejection fraction. Since this depression cannot be simply explained by hypoperfusion and coronary ischemia, a direct action of inflammatory mediators, as depressants, was postulated (21–23). It is currently believed that such depression is multifactorial, involving metabolic alterations and mitochondrial dysfunction of the cardiomyocytes, reduced calcium release from the sarcoplasmic reticulum and impaired electromechanical coupling at the myofibrillar level (17). These alterations seem to be caused by different cytokines produced and released from activated immune cells, as well as NO.

The first-line treatment for the maintenance of hemodynamic stability in septic shock is norepinephrine (NA) -or other sympathomimetics such as dopamine or dobutamine through their effects on α- and β-adrenoreceptors (ARs) and their high vasoconstrictive action and inotropic effect on the vascular and cardiac muscle, respectively (12–15). Vasopressin can also be used, to reduce NA doses.

Sympathetic noradrenergic fibers normally mediate vasoconstriction by acting on α_1-ARs from the smooth muscle of arteries and veins, thus regulating peripheral vascular resistance. On the other hand, by acting on β_1-ARs, the sympathetic activity increases myocardial contractility -both atrial and ventricular- as well as the heart rate (7). As commented, during sepsis and septic shock inflammatory mediators can lead to vasodilation and a decrease in peripheral vascular resistance as well as depression of myocardial activity. Regardless of the action of inflammatory mediators, the question emerges as to why the SNS fails to overcome this alteration to maintain hemodynamic stability, raising the need for exogenous sympathomimetics administration to keep the patient alive. It follows that some impairment in the noradrenergic transmission is likely to exist during sepsis and septic shock. Considering that sepsis is a systemic inflammatory response, it may be hypothesized that even in the absence of immune cells infiltrating the vessel walls or the heart, circulating inflammatory mediators favor a probable retraction of the noradrenergic terminals, leading to an impairment in sympathetic transmission, as it may happen in SLOs during IS activation (1). In line with the proposed hypothesis, this impairment may be due to the action of neurotrophins and semaphorins with possible re-expression of p75 neurotrophin receptor (p75NTR) in vascular and cardiac sympathetic nerves in an inflammatory milieu (**Figure 1**). These molecules might be locally produced under the influence of cytokines, as found in different tissues (2–6). A possible action of netrin-1, an axon guidance molecule able to mediate neural fibers retraction, expressed in epithelial and endothelial cells under inflammatory influences, may not be discarded (24, 25); in addition to a probably direct action of some inflammatory cytokines, given their regulatory role in neurogenesis and synaptic function (26, 27).

This sympathetic dysfunction may not only explain the lack of vasoconstriction reflex, but also other alterations observed in sepsis and septic shock, like myocardial metabolic alterations and reduced intracellular calcium in cardiomyocytes, contributing to a decreased contractility (**Figure 1**). In fact, sympathetic action has very important metabolic functions since NA increases glucose uptake in brown fat and heart (28, 29), by mechanisms other than insulin (30), like the important enhancement of GLUT1 functional activity (31). NA

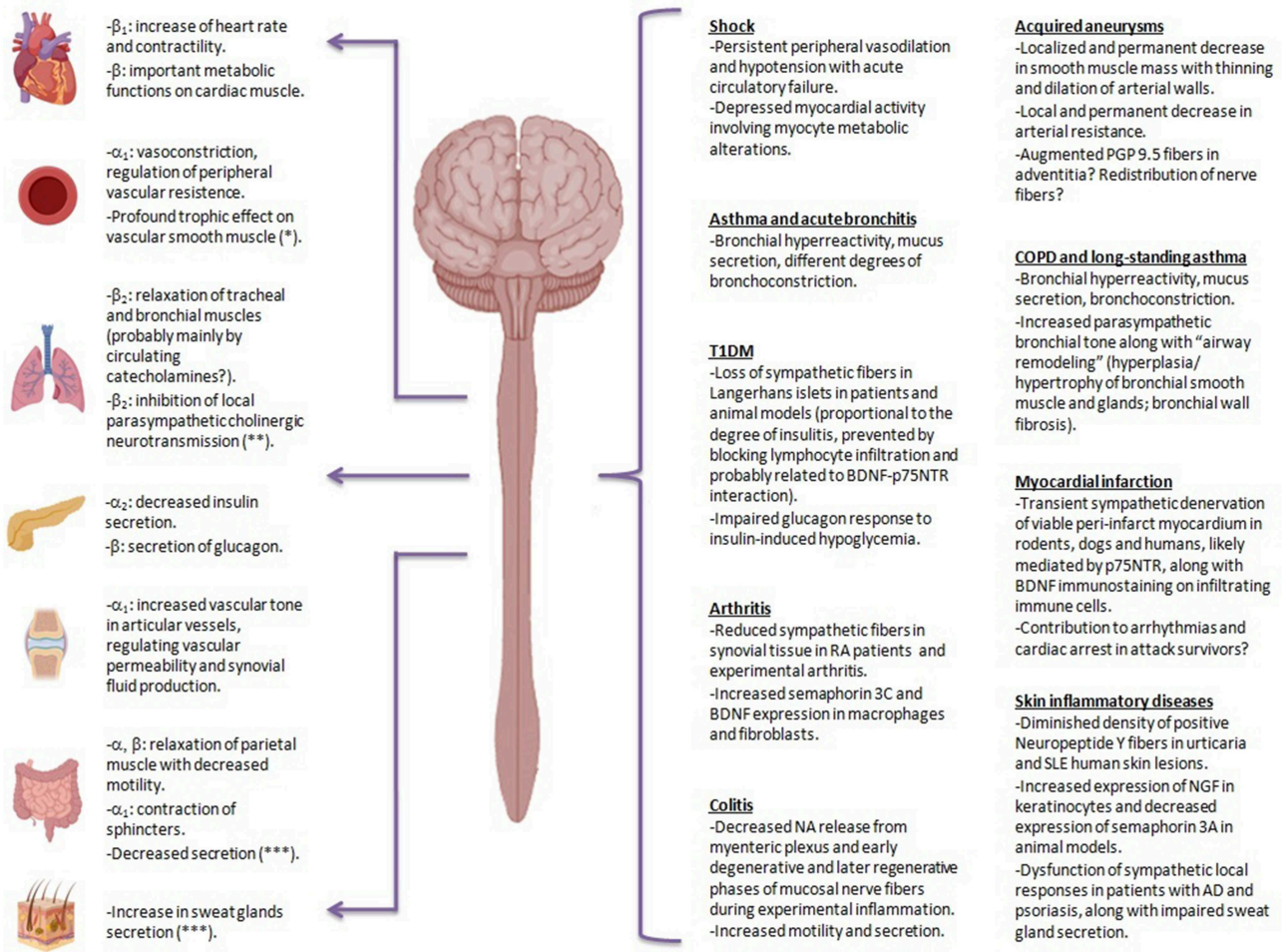

FIGURE 1 | Clinical and experimental evidence of sympathetic structural and functional alterations in many inflammatory scenarios. In different situations in which compensatory mechanisms against sympathetic blockade may be insufficient or may have failed to evolve, sympathetic dysfunction is likely to become evident. This may apply to chronic inflammatory diseases, the ones due to hypersensitivity reactions (maladaptive immune reactions *per se*), and situations of protracted and dysregulated immune responses failing to eradicate pathogens, i.e., prolonged septicemia. Physiological effects of sympathetic nervous system on different organs are depicted on the left, together with the involved adrenergic-receptor. Evidence suggestive of sympathetic impairment in different pathological conditions is shown on the right. PGP 9.5, protein gene product 9.5; COPD, chronic obstructive pulmonary disease; T1DM, type 1 diabetes mellitus; BDNF, brain-derived neurotrophin factor; p75NTR, p75 neurotrophin receptor; RA, rheumatoid arthritis; SLE, systemic lupus erythematosus; NGF, nerve growth factor; AD, atopic dermatitis: NA, norepinephrine. *Mediated by sympathetic adrenergic and non-adrenergic transmission.**Parasympathetic cholinergic neurotransmission elicits in turn bronchoconstriction, increases mucus production and favors airway remodeling (through muscarinic mediated proliferation of bronchial smooth myocytes and fibroblasts). ***Mediated by sympathetic non-adrenergic transmission.

also stimulates glucose utilization by myocytes (32), thyrocytes and platelets. As to calcium levels, endotoxins and cytokines alter and suppress L-type calcium currents in cardiomyocytes, possibly via changes in the autonomic regulation of this channel (33–35). Calcium trafficking is also linked to mitochondrial function and integrity (17).

Different authors raised the view of an autonomic dysfunction in multiple organ failure as contributing significantly to the pathogenesis of this syndrome (36–38). In fact, a decreased sympathetic activity has been observed in the early course of severe sepsis that may contribute to circulatory and cardiac failure (39). In anesthetized cats, the injection of *Escherichia coli* endotoxin causes a significant decrease in mean blood pressure with a drop in sympathetic activity of the splanchnic nerve (40). Post-mortem examinations in humans dying from septic shock reveal neuronal and glial apoptosis within cardiovascular autonomic centers with a significantly increased brain expression of TNF and iNOS (41). Provided a noradrenergic transmission blockade does occur in sepsis, as part of the proposed adaptive neural plasticity mechanism involving sympathetic decreased activity during inflammation, the question remains on how it has evolved when causing hemodynamic instability and even patient death? Being so, other compensatory mechanisms must also exist tending to maintain peripheral vascular resistance and cardiac functionality. Progression toward septic shock with hemodynamic instability

may then represent the exhaustion of compensatory programs given the immune incapability to eliminate the pathogen and the persistence of systemic inflammation.

Activation of the renin-angiotensin-aldosterone system is a well-characterized physiologic mechanism to prevent hypotension during sepsis (42). Also, it is worth reminding that vertebrates have two main sources of NA and adrenaline (Adr): the sympathetic nerves and the adrenal medulla. The function of the catecholamines released by the adrenal medulla in the septic scenario is yet poorly understood. Perhaps it may be basically compensatory to preserve hemodynamic stability given the transient blockade of noradrenergic transmission, mainly at the vascular level. Thus, the perpetuation of the sympathetic blockade may exhaust the adrenal medulla in its compensatory attempt along with a certain degree of tissue hypo-responsiveness due to prolonged exposure to circulating catecholamines favoring circulatory instability. In parallel, immunoinflammatory responses are known to also activate the hypothalamic-pituitary-adrenal (HPA) axis, leading to the release of corticosteroids, a major immunomodulatory compound (43, 44). Adrenal insufficiency, at least in terms of corticosteroid production, is present during sepsis (45), and likely detrimental in this regard considering that corticosteroids regulate vascular reactivity to vasoconstrictors (46).

The adrenal medulla releases both NA and Adr, in a very variable proportion depending on species [for review, (47)]. There are also two independent sympathetic innervation pathways in the adrenal medulla, one mediating the release of Adr and the other one NA. Rat preganglionic sympathetic neurons innervating the Adr-releasing adrenal cells are not influenced by baroreceptor arterial reflexes but stimulated by hypoglycemia. Unlike this, preganglionic neurons that innervate the noradrenergic cells from the adrenal medulla are under a potent baroreceptor arterial reflex control. Thus, Adr released from the adrenal medulla to circulation primarily exerts metabolic effects by mediating glycogenolysis in the liver and skeletal muscle, with no significant effect on the maintenance of circulatory homeostasis. On the other hand, NA released into the plasma from the adrenal medulla has neither metabolic nor hemodynamic effects under physiological conditions. In this sense, it is important to note that, in neuro-effector vascular junctions, NA reaches concentrations in the micromolar range, while circulating NA barely reaches concentrations in the picomolar range, being normally unable to exert any effect. However, under pathophysiological circumstances, this situation changes markedly. In fact, after sympathetic denervation, some effector organs, like vascular smooth and cardiac muscles, develop an adaptive hyper-responsiveness to adrenal circulating NA, viewed as a compensatory mechanism (48).

During sepsis and septic shock, both Adr and NA plasma levels and ARs expression in different tissues undergo important and varied modifications. In this sense, high levels of circulating catecholamines have been observed during human and experimental sepsis (39, 49–51). On the other hand, the α_1-ARs from human hepatocytes experience dynamic changes during sepsis showing an increased, normal or decreased expression in mild, moderate, or severe sepsis, respectively (52). In septic rats, myocardial ARs were found to be decreased (53, 54). From a hypothetical viewpoint, these variations throughout the sepsis spectrum may reflect an initial blockade of sympathetic neurotransmission and a subsequent over-exposure to circulating adrenal catecholamines.

Anaphylaxis and Anaphylactic Shock

The term anaphylaxis is used to describe a rapid and widespread immunological reaction occurring after exposure to certain substances in previously sensitized persons [for review (55, 56)]. The most frequent triggers are food, medicines, and insect bites, causing a type I immediate hypersensitivity reaction. Clinically, the most common life-threatening manifestations include angioedema, pulmonary edema, bronchospasm, and hemodynamic instability in cases of anaphylactic shock, characterized by hypotension due to decreased peripheral vascular resistance, and occasionally myocardial depression.

Cells implicated in this reaction are mast cells and granulocytes, which upon degranulation release pre-formed and newly and rapidly synthesized inflammatory mediators into the systemic circulation. Among these mediators, the most important ones are histamine, tryptase, chymase, bradykinin, and heparin as well as metabolites from the arachidonic acid, including products of the lipoxygenase and cyclooxygenase pathways such as prostaglandins and leukotrienes. During severe anaphylaxis episodes, there is concomitant activation of complement and coagulation pathways, and the kallikrein-kinin contact system. These mediators are capable of inducing vasodilation and mucosal edema, bronchial smooth muscle contraction, and increased mucus production. As in septic shock, the first-line treatment is the administration of fluids and sympathomimetics like Adr (57, 58), which reverses all features of anaphylaxis. In fact, stimulation of α-ARs increases peripheral vascular resistance, raising the blood pressure while reversing peripheral vasodilation and decreasing angioedema. Stimulation of β_1-ARs has positive inotropic and chronotropic effects on the cardiac muscle, whereas β_2-ARs stimulation leads to bronchodilation. β-ARs also increase the production of intracellular cyclic AMP, which stabilizes mast cells, inhibiting further mediator release. At this point, one might wonder why the organism does not respond with an increased sympathetic tone to such a massive systemic release of these inflammatory mediators and hence maintaining homeostasis with no need of exogenous catecholamine administration. Once again, there may exist a blockade of sympathetic transmission during anaphylactic shock, probably mediated by mechanisms like those proposed for septic shock (**Figure 1**). Several years ago, the group of Levi-Montalcini described the production, storage, and release of nerve growth factor (NGF) by mast cells, suggesting interactions between the NS and IS (59). Probably the adrenal production and release of catecholamines may be insufficient in these cases to counterbalance the SNS dysfunction in front to such a massive maladaptive reaction.

Supporting the hypothesis of the sympathetic transmission blockade in the pathophysiology of distributive shock, it is worth remembering that the disruption of descending pathways

from central centers to spinal sympathetic neurons may also lead to hemodynamic instability. In fact, spinal cord injury provokes different clinical manifestations that will depend on the localization and severity of the lesion, with some patients developing neurogenic shock in the acute phase, and even multi-organ dysfunction syndrome, mainly in severe cervical lesions (60). The initial response in these cases consists of a massive sympathetic stimulation and parasympathetic reflex activity lasting 3–4 min due to the release of catecholamines by adrenal glands immediately after the injury. This results in severe hypertension and heart rhythm alterations. After this short initial phase, there is a massive decrease in sympathetic activity, with a reduction in peripheral vascular resistance, marked hypotension and, occasionally, bradycardia due to the absence of sympathetic tone and unimpeded vagal tone, which characterizes the state of shock (61, 62). In contrast, during the chronic phase, some patients display autonomic dysreflexia, after spinal shock resolution, which constitutes a life-threatening syndrome of massive imbalanced reflex sympathetic discharge.

It follows that the solely traumatic lesion of the sympathetic pathway reproduces, in the acute phase, a hemodynamic instability state, like the one seen in sepsis or anaphylaxis (**Figure 1**). Furthermore, the treatment of neurogenic shock is also based on the replacement of volume and the administration of sympathomimetic vasopressors.

Acquired Vascular Aneurysms

One of the most frequent forms of acquired aneurysms is the abdominal aortic aneurysm—AAA—(63). AAA consists of a localized and permanent weakening and dilation of this vessel over 50% of its usual diameter or >3 cm, which in most cases compromises the infrarenal segment. In 65–80-year old men, the prevalence is between 1–2 and 8% according to the series; being 6 times less frequent in women [for review (64, 65)]. The most important complication is the rupture, which leads to significant bleeding and an estimated 150,000–200,000 deaths yearly worldwide.

Although the pathogenesis of AAA is not yet clearly elucidated, most researchers agree that its development is related to atherosclerosis along with chronic inflammation (63). In fact, atherosclerosis, previously considered as a disease of lipid storage, involves an important inflammatory response, with presence within the arterial wall of cells from innate and adaptive immunity, and locally produced cytokines (66–69). Moreover, targeting of inflammatory adhesion molecules reduces atherosclerosis, whereas, removing or blocking IL-10 or TGF-β accelerates its development.

Apparently, the release of proteolytic enzymes, oxidation-derived free radicals and cytokines during such a chronic inflammatory response leads to a reduction in elastin content, a distorted elastin configuration, increased deposition of type I collagen and reduced type III collagen, in both tunica media and adventitia. These phenomena may also diminish the number of smooth muscle cells leading to a marked thinning of the tunica media, typical of AAA, resulting in a decreased resistance of the arterial wall (70, 71). Search into the literature revealed one study on the AAA innervation through immunohistochemistry for protein gene product 9.5 (PGP 9.5), indicating an apparent increase in the number of nerve fibers in AAA only in the adventitia (71), without identifying the proper fiber type. Beyond this fact, the question remains whether this increased immunostaining does correspond to a real increase in nerve terminals or to a redistribution within the AAA wall.

Not only in AAA but also in other pathological settings, i.e., tertiary syphilis and "mycotic" aneurysms, the existence of localized chronic inflammation of the arterial wall results in thinning of the tunica media and dilation of the vessel with aneurysm formation. Noticeably, the occurrence of these pathologies is very low nowadays compared to the one recorded in the pre-antibiotic era (72–75).

As it is widely known, the SNS innervates the vascular smooth muscle leading to vasoconstriction by acting on α_1-ARs, thus increasing flow resistance in large and small arteries and arterioles (7). Beyond this effect, *in vivo,* and *in vitro* studies showed that sympathetic fibers exert a profound trophic effect on vascular smooth muscle, stimulating its proliferation and differentiation, probably not only through NA but also through co-transmitters such as ATP and neuropeptide Y (76–81).

Within the setting of the proposed adaptive neural plasticity mechanism, chronic inflammation of the vessel wall may mediate a retraction of the sympathetic fibers and probably the apoptosis of neurons innervating such arterial segment, through p75NTR stimulation (82–84). Considering the localized and chronic nature of the inflammatory process, sympathetic denervation may lead to a marked decrease in the trophism of the tunica media of the arterial wall, which may partly explain the weakening and dilation of vessels, with the ensuing aneurysm formation (**Figure 1**).

Asthma

Asthma is a heterogeneous inflammatory disease of the lower airways causing recurrent symptoms and exacerbations. It can develop at any age, but the disease onset is more frequent in childhood or young adulthood, affecting about 7.5% of the adult population [reviewed in (85–87)]. It is characterized by bronchial hyperreactivity, cough, mucus secretion, different degrees of bronchoconstriction and dyspnea. Even when allergic and non-allergic phenotypes are described (88, 89), the immunopathological characteristics of both patient groups are similar and this distinction is not easy. The bronchial mucosa is infiltrated by a series of inflammatory cells, like eosinophils, mast cells, neutrophils, and lymphocytes.

The chemical mediators released by the inflammatory cells in the context of an immediate hypersensitivity reaction (like histamine and arachidonic acid metabolites) seem to be the cause of asthma symptoms. Nevertheless, it has long been thought that the mechanisms put into place by such mediators, linked to disease symptoms, may be of neural nature. For instance, the β-adrenergic blocking theory proposed by Szentivanyi (90) argued that a diminished responsiveness to β-adrenergic stimulation could increase impulse transmission or receptor stimulation through α-adrenergic or cholinergic pathways. Since then an important body of evidence suggests the existence of an autonomic dysfunction in patients with asthma. Some groups

have observed increased bronchial cholinergic responsiveness and β-adrenergic hyporesponsiveness (91), which would lead to bronchospasm, mucosal edema, augmented mucous secretion, cough, and dyspnea (92). Moreover, according to some authors, not only asthma symptoms but also the most common ones seen in other respiratory diseases may be explained by a dysfunction in the ANS (93, 94). Furthermore, asthma treatment is currently addressed to reduce inflammation through local or systemic corticosteroids as well as to promote β_2-adrenergic stimulation or cholinergic inhibition. Other drugs like leukotriene receptor antagonist and leukotriene synthesis inhibitor, along with biological therapies such as antibodies against IgE or IL-5 are also employed (86, 87).

The autonomic innervation of the lower airway is somewhat complex, regulating tones from the bronchial smooth muscle, the vessel wall and the activity of bronchial glands (7). Parasympathetic nerves are the dominant neural pathway in the control of airway smooth muscle tone and mucus secretion in humans, with acetylcholine (ACh) acting on type 3 muscarinic receptors, promoting bronchoconstriction (95). The sympathetic innervation in the human airways is fundamentally present in the vicinity of the submucosal glands and the bronchial arteries. The bronchial smooth muscle, on the other hand, does not appear to be directly innervated by adrenergic fibers. However, β-ARs, which mediate bronchorelaxation, are widely distributed in the human lung. It has been postulated that circulating Adr may act on these receptors facilitating the dilation of the bronchial smooth muscle, but there is no convincing evidence in this regard. Nevertheless, the SNS does influence bronchial muscle tone through adrenergic fibers indirectly (96). In fact, adrenergic transmission can inhibit cholinergic neurotransmission at different levels. In parasympathetic ganglia, which are predominantly and physically associated with larger airways, sympathetic nerves stimulate ARs, thus preventing cholinergic activity (97). Moreover, in the bronchial walls themselves, sympathetic fibers end on parasympathetic postganglionic nerves, probably inhibiting cholinergic output through stimulation of prejunctional β_2-ARs (98). In this sense, it is well-known that the sympathetic blockade induced by treatment with β-blockers produces bronchospasm and precipitates asthma (99, 100). This effect is thought to be caused by blockade of presynaptic β_2-ARs on cholinergic nerves, which normally inhibits ACh release (98). In addition to the cholinergic and adrenergic fibers, a non-adrenergic non-cholinergic nervous system exists in the airways, exhibiting inhibitory (bronchodilator) or excitatory (bronchoconstrictor) actions (95).

To support the hypothesis that symptoms of inflammatory airway diseases are caused by an autonomic dysfunction, some authors have postulated that the different mediators produced and released locally during an inflammatory response may stimulate action potential discharge in parasympathetic nerves leading to bronchoconstriction (93). Even if this turns out to be true, it cannot be excluded that a primary decreased adrenergic transmission leads to increased cholinergic activity, thus contributing to the development of asthma, within the hypothetical mechanism involving neurotrophins and semaphorins effects on sympathetic nerves (**Figure 1**). As commented, these molecules can be produced by the immune cells themselves or by bronchial smooth muscle cells under cytokine influence (2). As proposed for anaphylaxis, compensatory programs against a possible noradrenergic transmission blockade may simply be insufficient to counterbalance bronchoconstriction in asthma, due to the maladaptive type of the immune response, predominantly immediate hypersensitivity.

Bronchial Hyperreactivity During Acute Inflammation of the Airways

Formerly healthy subjects undergoing viral infections in the respiratory tract are largely known to experience bronchial hyperreactivity without developing clinical asthma. In fact, the inhalation of histamine diphosphate aerosol produces a significantly higher increase in airway resistance from normal subjects with flu, compared to the increase recorded in healthy individuals. Moreover, isoproterenol hydrochloride (a β-adrenergic agonist), and atropine sulfate aerosol (a muscarinic antagonist) inhibit and reverse such increased histamine-induced airway resistance, implying that increased cholinergic and/or decreased adrenergic activity play a role in the contraction of the smooth bronchial muscle in this scenario (101, 102).

In parallel, it is well-known that bronchoconstriction and wheezing resulting from increased bronchial reactivity are much more frequent in childhood during viral respiratory diseases caused by the respiratory syncytial virus (RSV), human metapneumovirus, rhinovirus, parainfluenza virus, influenza virus, and adenovirus, among others (103). Also, RSV infection of the lower respiratory tract in children is associated with an increased risk for the subsequent development of recurrent asthma/wheezing, becoming less likely as age increases (104). Such association was seen in viral respiratory infections other than the one caused by RSV, as well (105).

The reason for this persistence of bronchial hyperreactivity beyond the resolution of the infectious disease in early childhood is not currently understood. Viral infections may increase asthma susceptibility by acting onto the neural control of the respiratory tract. Indeed, the airway inflammation may lead to some degree of blockade of adrenergic transmission, thus facilitating cholinergic transmission, through the proposed neural plasticity mechanism (**Figure 1**). In theory, previously healthy adults would not experience bronchial obstruction, but rather a certain degree of bronchial hyperreactivity, probably due to the existence of compensatory programs. By opposite, symptoms may be more florid in early childhood, when the NS is still developing. Moreover, since the p75NTR is capable to mediate neuronal apoptosis (82–84), it may be speculated that severe airway inflammation in early developmental stages alters the normal innervation of the respiratory tract, perhaps further progressing to wheezing or asthma, as described in children.

Chronic Obstructive Pulmonary Disease (COPD) and Long-Standing Asthma

COPD comprises a heterogeneous group of pathologies affecting the respiratory tract and pulmonary parenchyma, such as chronic

bronchitis and emphysema, which are characterized by an incompletely reversible obstruction to the expiratory flow [for review (106–108)]. Although there are many risk factors, most cases are smoking-related and develop after the fourth decade of life. It manifests with periodic exacerbations due to viral or bacterial respiratory infections, causing an estimated of 3.2 million people deaths yearly worldwide.

Although in asthma airflow obstruction is usually intermittent and reversible, it can progress to an irreversible obstructive pattern, like COPD, in older people with a history of long-standing asthma. Thus, asthma and COPD overlap and converge, sharing three basic common clinical features: airway inflammation and obstruction along with bronchial hyperresponsiveness (109–112). Like asthma, COPD treatment is based on the use of inhaled corticosteroids and bronchodilators such as β-adrenergic and anticholinergic drugs, as well as oxygen therapy in some cases (106).

Regardless of the type of immune response seen in COPD or asthma, airway chronic inflammation may lead by itself to bronchial histo-structural changes usually referred to as "airway remodeling" partly accounting for the phenotypic clinical overlap of asthmatic and COPD patients (109, 113). Although there exist some differences in remodeling patterns between COPD and asthma, both cases are characterized by increased thickness of the basal membrane, changes in the extracellular matrix (fibrosis of the bronchial wall), angiogenesis, increased permeability of mucosal vessels, with hyperplasia/hypertrophy of glandular structures and the bronchial smooth muscle. This increased airway smooth muscle mass is the most important contributor to airway hyperresponsiveness and obstruction (114).

As well as the parasympathetic bronchial tone was found increased in patients with COPD and asthma, non-neuronal cells -including inflammatory cells and airway structural cells- can synthesize and release ACh (115, 116). Beyond its traditional role as a bronchoconstrictor, ACh may also play a pro-inflammatory immunological role favoring airway remodeling via pro-fibrotic and pro-proliferative mechanisms mediated by muscarinic receptors. In fact, stimulation of muscarinic receptors induces the proliferation of fibroblasts and collagen production. Notably, ACh may play an important role in the increase of bronchial smooth muscle mass, by enhancing the effect of different mediators (TGF-β, epidermal growth factor and platelet-derived growth factor) on proliferation, hypertrophy, and differentiation of smooth myocytes of the airway wall. Current clinical and experimental evidence suggests that anticholinergic drugs, mostly the long-acting tiotropium bromide, may reduce airway remodeling and the degradation of lung function, beyond its bronchodilator effect (117, 118).

As proposed for asthma and acute respiratory infections, chronic bronchial inflammation may lead to a blockade of sympathetic adrenergic transmission, giving rise to a sustained and unopposed increased parasympathetic cholinergic tone, responsible for the irreversibility of the bronchial hyperreactivity, mucus production and bronchoconstriction observed in COPD and long-standing asthma (**Figure 1**). The chronic nature of this condition would have prevented any adaptive compensatory program from evolving. Furthermore, since p75NTR can mediate neuronal apoptosis (82–84), the adrenergic innervation may be definitively lost in this context.

Type 1 Diabetes Mellitus

Diabetes mellitus is characterized by a deregulation of carbohydrate, lipid and protein metabolism. There are two major types of diabetes, type 1 (T1DM) and type 2 (T2DM). T2DM is the most common form (accounting for more than 90% of cases) and develops in adult life over a background of peripheral insulin resistance with subsequent exhaustion of pancreatic β cells to produce it (119). On the other hand, T1DM is an autoimmune disease (120), presumably caused by T cell-mediated destruction of pancreatic β cells, with inflammation of the islets of Langerhans—insulitis—composed of T cells, B cells, macrophages and dendritic cells—DCs—(121–124).

The ANS innervates the islets of Langerhans, contributing to the regulation of endocrine pancreas function (7, 125). Accordingly, parasympathetic nerves stimulate insulin secretion whereas sympathetic nerves inhibit basal and glucose-stimulated insulin secretion. Regarding autonomic regulation of glucagon secretion, there are three mechanisms of direct stimulation of adrenergic and cholinergic receptors from α cells, which are activated in the brain during hypoglycemia and tend to facilitate glucagon release to normalize glycemia: (1) sympathoadrenal system, which culminates with the release of Adr by the adrenal medulla; (2) islet parasympathetic nerves, eliciting a modest glucagon response; (3) islet sympathetic nerves, that provoke a robust glucagon response (126, 127). It is known that the physiological glucagon response to insulin-induced hypoglycemia is impaired in T1DM, but not in T2DM (128). Interestingly, Taborsky's group linked this impaired glucagon response to a loss of sympathetic innervation of Langerhans islets in the context of the T1DM insulitis (129).

In fact, rodent models of T1DM (Bio-Breeder rats and NOD mice), in which an impaired glucagon response to insulin-induced hypoglycemia is also observed, showed an early and selective loss of sympathetic innervation in the islets of Langerhans. Such loss does not affect the exocrine pancreas and has not been observed in other models of non-autoimmune diabetes, like streptozotocin-induced diabetes (130, 131). In the above-referred T1DM models, the loss of sympathetic fibers is fully established in the first 2–3 weeks after the onset of diabetes and does not progress any further, thus differing from diabetic neuropathy, due to chronic hyperglycemia, which develops much later in the course of this disease and does progress. It was also shown that islet sympathetic nerve loss was proportional to the degree of invasive insulitis and that could be prevented by blocking lymphocyte infiltration. In another experimental animal model, they demonstrated that p75NTR was required for the loss of islet sympathetic fibers during insulitis, since mice lacking p75NTR retained most of their islet sympathetic nerves (132). Further studies in pancreas necropsy samples from patients with T1DM and T2DM and non-diabetic controls, revealed a severe loss of sympathetic fibers in islets of T1DM patients, either of recent onset (<2 weeks) or long-term disease (>10 years). This loss was observed neither in patients with T2DM nor in the exocrine pancreas of both patients with T1DM and

T2DM (133). Apparently, such early loss of islet sympathetic nerves may be mediated by the brain-derived neurotrophic factor (BDNF) acting on p75NTR, being unclear which cells within the infiltrated islets of Langerhans will produce this neurotrophin (134).

As proposed in other cases of chronic inflammation, it may be hypothesized that semaphorins and pro-neurotrophins, produced by immune cells infiltrating the islets of Langerhans in T1DM–or by other cytokine-influenced local cells–act on sympathetic nerves, thus mediating their retraction. P75NTR stimulation may also induce neural apoptosis, with a definitive loss of sympathetic islet innervation (82–84). According to Taborsky's group (129), this loss of sympathetic innervation may partly explain the impaired glucagon response to insulin-induced hypoglycemia during T1DM (**Figure 1**).

Myocardial Infarction-Related Inflammation

Myocardial infarction (MI) is one of the most important causes of morbidity and mortality worldwide, with an annual incidence in the United States of 525,000 and 210,000 first and recurrent attacks, respectively. An estimated number of 155,000 silent attacks also occur annually (135). MI causes sterile inflammation of the myocardium characterized by the recruitment of innate and adaptive IS cells (136, 137). In fact, a rapid influx of neutrophils and monocytes-derived macrophages has been demonstrated, followed by DCs, T cells, B cells, NK, and NKT cells. The resolutive phase of the inflammatory process culminates with apoptosis of immune cells and reparative fibrosis of the necrotic myocardium.

Interestingly, it has been observed that MI causes two distinct types of myocardial sympathetic denervation: a permanent denervation of the infarct area, because of tissue ischemic necrosis, and a transient denervation of viable peri-infarct myocardium (138). This transient sympathetic denervation of the non-infarct myocardium, apical to the infarct, was demonstrated in dogs, rodents and even in humans, through imaging techniques consisting of the use of radiolabeled compounds (139–141). On the other hand, it has also been observed an up-regulation of NGF and BDNF in the infarct myocardium and its viable border zone, respectively (142). The role of p75NTR in this cardiac sympathetic transient denervation after ischemia has been demonstrated in mice (143). Three days after MI, it was observed a significant sympathetic denervation in the proximal peri-infarct region in WT mice but not in p75NTR-/- counterparts. Since the loss of sympathetic nerve fibers adjacent to the infarct required p75NTR, it was suggested that ischemia induced the expression of a p75NTR ligand mediating axon degeneration outside of the infarct. In addition, BDNF immunostaining was shown on immune cells, within the infarct area (**Figure 1**).

As it is widely known, sympathetic innervation increases heart rate as well as atrial and ventricle contractility, through β_1-adrenergic stimulation (7). Some clinical studies have indicated that sympathetic denervation following MI is a risk factor for the development of arrhythmias and cardiac arrest in attack survivors (144–146). However, the transient sympathetic denervation of the viable non-infarct myocardium seems to have a minimal impact on the development of electrical complications (138).

Skin Inflammatory Diseases

Since a common manifestation of cutaneous inflammatory diseases is pruritus, the interest in the investigation of changes in the innervation in these conditions was placed mainly in the sensory fibers and not in the sympathetic ones (147). As such, it was observed an increase of fibers containing gastrin-releasing peptide and calcitonin gene-related peptide (CGRP), both in the dermis and epidermis of patients suffering from atopic dermatitis (AD), as well as in murine models of AD and acute dry skin (148, 149). In these cases, it has also been shown an increased expression of NGF in keratinocytes, as well as a decrease in the expression of semaphorin 3A, which has been shown to inhibit NGF-induced sprouting of sensory nerves (3–6). On the other hand, TNF-α was shown to enhance NGF production in human keratinocytes (150). Likewise, mast cells, and mast cell-derived TNF-α, promoted the elongation of epidermal and dermal PGP 9.5+ nerves and dermal CGRP+ nerves in a mouse model of oxazolone-induced contact hypersensitivity (151).

Only a few studies evaluated the sympathetic innervation and activity in the skin during inflammation. In frozen tissue sections from skin biopsies of patients with AD, it was observed an increased expression of markers of different fibers by immunohistochemistry, except those for sympathetic fibers (neuropeptide Y and tyrosine-β-hydroxylase). A diminished density of fibers immunolabeled for neuropeptide Y was also observed in biopsies from patients with urticaria and systemic lupus erythematosus skin lesions (152). In the same line, another group evaluated the electrophysiological functioning of the ANS in patients with AD (153) and psoriasis (154). In both cases, a dysfunction in local sympathetic responses was observed, probably accounting for the impairment in sweat glands secretion and skin dryness seen in those conditions (**Figure 1**).

Colitis

During the 1990s, early degenerative and later regenerative phases of mucosal nerve fibers were reported in the rat acute inflammation model of intestinal infection with the nematode *Nippostrongylus brasiliensis* (155, 156). The type of nerve fibers was not characterized in these studies. A decrease in the NA release from the myenteric plexus of rats infected with *Trichinella spiralis* was also reported in those years (157). More recently, Boissé et al. (158) demonstrated an abnormal sympathetic neural activity and decreased NA release from sympathetic nerve fibers in bowels during experimental inflammatory bowel disease (IBD). On the other hand, in a mouse model of dextran sulfate sodium-induced colitis, an inhibition of N-type voltage-gated calcium channels in prevertebral sympathetic neurons was observed (159). According to this study, this inhibition may explain the decreased NA release observed both in inflamed and uninflamed regions of experimental IBD.

It's worth noting that the enteric nervous system constitutes a very complex network, with autonomic extrinsic innervation and neuronal plexuses present in the very wall of the gastrointestinal organs (myenteric and submucosal plexuses), exhibiting intricate interactions (160). Importantly, authors working in the field agree that intestinal inflammation leads to significant changes in the structure and functionality of nearly all these different nerve fibers (161–164). Since many of these neural plasticity phenomena involve non-sympathetic nerve fibers, discussing these issues is beyond the scope of this work. However, as above-referred, concerning changes in local SNS functioning, this neural plasticity mainly comprises an impaired sympathetic activity. Since sympathetic innervation of the gastrointestinal tract modulates motility, blood flow, and secretion, these authors proposed that this impairment may contribute to symptom generation during IBD and intestinal inflammation in general (**Figure 1**).

Arthritis

Innervation changes were also noted in rheumatoid arthritis (RA). Straub's group assessed the presence of sympathetic fibers and sensory nerve fibers by immunohistochemistry in fresh synovial tissue of 52 patients with RA, 59 patients with osteoarthritis (OA) and 26 controls. They observed a significant reduction in sympathetic fibers along with an increased number of sensory nerve fibers in RA patients, compared to OA patients and controls. At the same time, they found an increased semaphorin 3C and BDNF expression by *in situ* hybridization in samples from RA patients, with double immunohistochemistry revealing that these molecules were expressed in macrophages and fibroblasts (165, 166). In the same line, higher plasma levels of BDNF were also observed in RA patients, as compared to controls (167).

This loss of sympathetic fibers in the joints was consistently replicated in rat type II collagen-induced arthritis [collaborative studies between Straub's group with del Rey and Besedovsky; (168–170)]. Since sympathetic stimulation increases vascular tone in articular vessels, regulating vascular permeability, and synovial fluid production (171, 172) its loss does not have major clinical consequences (**Figure 1**).

Chagas Disease

Chagas disease is an anthropozoonosis of the American continent, caused by the protozoan *Trypanosoma cruzi*. It affects an estimated 8–10 million people worldwide with 25 million people living in endemic areas of Latin America (173). Current migration flows have also led to an increased incidence in non-endemic countries (174, 175). Among chronically infected patients, 30–40% can develop organ involvement 10–30 years after acute infection. This chronic phase of the disease is characterized by cardiomyopathy, arrhythmias, and megavisceras like megaesophagus and megacolon. It constitutes a disabling condition, responsible for significant morbidity and mortality among relatively young patients since primo-infection which mostly occurs during childhood in endemic areas is generally symptomless. Whereas the loss of autonomic innervation of involved organs (i.e., the gastrointestinal tract and the myocardium) was found to underlie clinical manifestations decades ago (176), very little is known about mechanisms leading to this sympathetic and parasympathetic impairment. Auto-immune phenomena secondary to chronic inflammation have been proposed in this regard, but definitive evidence is lacking (177). To the best of my knowledge, the existence of inflammation-related neural plasticity in affected organs during chronic Chagas disease has not been investigated so far but would be worth testing.

Sympathetic Plasticity as a Whole: Potential Clinical and Immunological Significance

The clinical and experimental evidence reviewed here points out to a neural plasticity phenomenon in inflamed non-lymphoid tissues with a particular focus on changes involving sympathetic nerve fibers, the branch of the ANS that is thought to be the main regulator of the activity of the IS (8–11). ACh-immunomodulatory action has also been shown (178, 179), depending on the integrity of the SNS pathway, as well as an immunomodulatory action of the sensory fibers through different neuropeptides (180, 181). Most authors reporting innervation changes in SLOs and non-lymphoid tissues during an inflammatory/immunological response interpreted these findings as pathological and non-specific phenomena (1). On the contrary, there are firm reasons to believe they correspond to a specific neural plasticity adaptive mechanism -leading to a decreased sympathetic activity during such a situation-, likely mediated by neurotrophins and semaphorins acting on their receptors.

Regarding the clinical consequences of decreased sympathetic activity during inflammation, it is worth remembering that SNS modulate nearly all physiological functions, i.e., cardiovascular, gastrointestinal, respiratory, endocrine, sexual, and temperature regulation, transmitting signals from the central nervous system (CNS) and favoring the homeostatic adaptation to different situations (7). Then, as commented in the present work, an autonomic dysfunction would become clinically evident in many organs and tissues during inflammation, partially accounting for symptom generation and clinical manifestations. This would be particularly true in situations in which compensatory programs counterbalancing the impact of an autonomic blockade during the inflammatory/immunological response were insufficient or had failed to evolve (**Figure 1**). As above stated, this may apply to chronic inflammatory diseases, hypersensitivity reactions (maladaptive immune reactions *per se*), or protracted immune responses failing to eradicate pathogens (i.e., prolonged septicemia). On the other hand, compensatory mechanisms against sympathetic blockade may involve the release of catecholamines by the adrenal medulla -as proposed for shock- or perhaps peptides/amines release by cells from the diffuse neuroendocrine system, present in different organs, since these compounds parallel in some cases ANS actions (182). Provided this hypothesis is true, sympathetic dysfunction may be at the basis of pathophysiological processes in different inflammatory

conditions, opening new research horizons and future directions for novel therapeutic approaches.

As to the immunological significance of the proposed sympathetic neural plasticity mechanism, it may be addressed to change the way by which the NS modulates the IS in its diverse functional-associated activation states. Then, it is necessary to underscore issues about the influence of SNS on IS, both in SLOs and in non-lymphoid organs, along with evidence indicating how the immune response develops in the absence of sympathetic nerves. Importantly, the immune processes that occur in the peripheral non-lymphoid tissues and the SLOs are diverse. In general, DCs recognize, capture and process a given antigen in peripheral tissues and then mature and migrate to SLOs where priming takes place. Subsequently, activated adaptive immune cells are recruited into tissues where the antigen is expressed. Cells of innate immunity are also recruited to the target tissue to eliminate non-self-antigens (183). The SNS has been shown to influence most of these processes (8–11), modulating the different phases of the immune response. But what happens if the sympathetic nerve fibers are not there? Does this process still develop in the same way?

First, as regards to priming in SLOs in absence of sympathetic fibers, to the best of my knowledge, there are no *ad hoc* experiments. Nevertheless, some evidence concerning this was reported in a study employing superantigens, which usually induce a strong proliferative response followed by clonal deletion of a substantial portion of defined VβT cells, with the remaining cells displaying *in vitro* anergy (184, 185). Del Rey and Besedovsky observed that sympathetic denervation prior to the superantigen staphylococcal enterotoxin B (SEB) challenge resulted in decreased SEB-induced T cell proliferation and IL-2 production while hindering the specific deletion of splenic CD4Vβ8 cells seen in intact animals (186, 187). In the same sense, mice lacking dopamine β-hydroxylase (and hence unable to produce NA or Adr but capable of dopamine production) have normal numbers of blood leukocytes, as well as normal T and B cell development and *in vitro* function. However, when challenged *in vivo* with *Listeria monocytogenes* or *Mycobacterium tuberculosis*, they are more susceptible to infection displaying an impaired T cell function, and Th1 cytokine production (188). Similarly, in a murine tuberculosis model, sympathetic denervation with 6-hydroxydopamine (6-OHDA) at the time of mouse infection led to a three-fold higher pulmonary bacillary load at different time-points post-infection. Treated mice also showed a significant increase in the lung parenchyma affected by pneumonia, along with a significant decrease of pro-inflammatory cytokines IFN-γ, TNF-α, IL-12, and IL-17. The same trend of results was observed when administering α/β adrenergic antagonists from day one of infection (189). Likewise, injection of 6-OHDA into rat lateral ventricles–leading to a significant reduction of brain and splenic catecholamine contents–is known to result in a decreased lymphocyte proliferation from spleen and peripheral blood samples, as well as a reduced splenic IL-2 and IFN-γ production and IL-2 mRNA expression (190). Coincidently, mice injected intrastriatally with 6-OHDA have impaired resistance to *L. monocytogenes* along with a reduced immune response to keyhole limpet hemocyanin (191). Rat studies also revealed an age-associated decline in sympathetic innervation in the SLOs accompanied by a significant reduction in IL-2 and IFN-γ production, and T cell proliferation (192). Moreover, peripheral sympathectomy induced by 6-OHDA has been shown to significantly increase CD4+Foxp3+ Treg compartment within SLOs in mice, inhibiting the induction of experimental autoimmune encephalomyelitis (193, 194).

On the other hand, it is well-known that whereas preganglionic sympathetic neurons lie in the intermediate zone of the thoracolumbar spinal cord, sympathetic premotor neurons, and sympathetic neurons antecedent to them, are located in the brain stem, hypothalamus, and telencephalon. Thus, CNS injury affecting those centers may lead to significant changes in SLOs' sympathetic activity, probably influencing the immune response. Remarkably, patients with CNS damage are known to present a secondary immunodeficiency—CNS injury-induced immunodepression—(195–200), characterized by an impaired T- and NK-cell function, both in the acute and chronic phases of the CNS injury. High levels of circulating catecholamines—most likely from adrenal origin—, along with increased plasma corticosteroids levels are observed in the acute phase of CNS injury, as a part of an acute stress response (195–201). Since the immunosuppressive effect of NA is widely accepted (8–11), most authors linked CNS injury-induced immunodepression to an alleged increased SNS activity. However, direct evidence concerning SNS innervation state and activity in lymphoid organs after CNS injury is lacking; for which such immunosuppressive state may be due instead to a loss of noradrenergic nerve fibers integrity within the spleen. In the same sense, decreased cell-mediated immune functions were related to chronic stress and major depressive disorder (202). In both situations, changes in corticosteroid and catecholamines plasma levels along with splenic histological alterations were found (203, 204), setting the basis for future studies addressing whether such alterations are accompanied by modifications in the splenic noradrenergic fibers activity and structure.

Secondly, concerning the point on how inflammation in non-lymphoid organs develops in the absence of sympathetic innervation, studies in this setting also revealed a reduced recruitment of immune cells to target sites. In patients who developed autoimmune pathologies following a hemiplegia-associated CNS injury, there were unilateral cases of RA (205), scleroderma skin changes (206), psoriatic arthritis (207), and asymmetric rheumatoid vasculitis (208), with unique or predominant involvement of the neurologically non-compromised side. In the same line, a patient developing RA after human immunodeficiency virus-1 infection and hemiplegia experienced a complete clinical remission only in the paralytic limbs (209). Since all these patients with stroke and autoimmune disorders not only presented a deficient motor and sensory innervation but also an autonomic one, it was early thought that these surprising phenomena were due to sympathetic dysfunction. As a matter of fact, in the early '50 sympathectomy was used in the treatment of RA with satisfactory

results (210). In the same line, patients with stroke showed a significant correlation of side asymmetries between delayed-type hypersensitivity responses and axon reflex vasodilation, a cutaneous test used to assess sympathetic activity (211).

Experimentally, a couple of studies in rat models of RA showed that the prior destruction of the sympathetic innervation by injection of 6-OHDA drastically reduced the joint inflammation compared to untreated controls (212, 213). Nevertheless, it is worth noting that in these models not only joints but also SLOs were sympathetically denervated, for which such reduced joint inflammation may be due to a lack of sympathetic action both on priming and migration of inflammatory cells to joints. More recently, Stangenberg et al. (214) designed an elegant model of experimental arthritis in which a group of mice was unilaterally paralyzed by transecting the sciatic and femoral nerves from one hindlimb. These animals developed asymmetrical arthritis, with highly attenuated inflammation of the denervated paw. To explain results, they studied the transcriptome of endothelial cells (ECs) of denervated hind paws to find that the expression of several genes coding for proteins involved in controlling vascular permeability, rolling, adhesion, and transmigration of immune cells was altered, either negatively or positively. This evidence may be taken to imply that vascular innervation may provide signals to ECs that regulate the transmigration of immune cells. While this denervation-related protective effect could not be associated with a single nerve quality in the above-mentioned work (i.e., with the sympathetic, parasympathetic, or sensory nerves), it is worth reminding that most if not all vessels only possess sympathetic innervation. Hence, the presence of sympathetic fibers seems to be essential for immune cells to infiltrate peripheral tissues.

When addressing the potential immunological significance of decreased noradrenergic activity during an ongoing immune response, Besedovsky and del Rey stated that it represents "*a way of releasing immune cells from the inhibitory effects of NA*" (215). This is in line with the immunosuppressive effect of NA, mainly by acting on β-ARs, the most accepted action of the ANS on immune cells (8–11). Although this may be true, evidence discussed in this section indicates that prior presence of noradrenergic fibers is necessary for the effector immune response to start normally, both in the SLOs as in non-lymphoid peripheral tissues, with increased sympathetic activity at the very onset of such response likely exerting a pro-inflammatory effect (11, 216–219). These apparently opposed actions may depend on a different neurotransmitter concentration, distinct types of receptor stimulation, the existence of cotransmitters acting concomitantly, the timing of neurotransmitters release, the different receptor expression pattern and the type and activation state of the immune cells (11, 220), among other factors probably acting *in vivo*. While discussing these issues is beyond the scope of the present work, provided this neural plasticity program does actually occur once the IS is fully activated, it may also represent a sort of "extrinsic" neural-regulated mechanism of peripheral immune tolerance, encompassing cell-mediated innate and adaptive immune responses, probably attempting to limit their extent and magnitude. Hypothetically, within SLOs where priming occurs, once the IS is already activated against a specific antigen, this mechanism would prevent new antigenic challenges from leading to further and successive immune activations, potentially detrimental. In this way, during an ongoing immune response against a given antigen, the IS would remain in a kind of "relative refractory state" for other antigens. On the other hand, in non-lymphoid organs and tissues during active inflammation, the proposed mechanism would preclude a massive recruitment of immune cells to the target site, once cells needed to clear the antigen are already there, and hence hindering more tissue damage. Under such evolutionary pressure, this neural plasticity mechanism might have evolved.

Additional findings favoring the present hypothesis come from the field of neuroscience. The emergence of the placenta allowed viviparity in most mammals, affording survival advantages, like a more complex fetal development and protection. Nevertheless, since the fetus represents a semi-allogeneic graft expressing paternally inherited alloantigens, the establishment of local mechanisms ensuring tolerance by the maternal innate and adaptive IS are essential. In this way, several overlapping mechanisms protect the fetus from the maternal IS (221–224). As known for several decades, during pregnancy the uterus undergoes an extensive axonal degeneration of sympathetic fibers followed by regeneration after delivery (225). This remarkable neural plasticity process is mediated by a range of molecules produced by the myometrium under estrogen's influence, including neurotrophins and pro-neurotrophins acting on Trk receptors and p75NTR, and proteins of the semaphorins family (226–233). The significance of this phenomenon is presently unknown. However, when considering the complex relationship between the IS and the SNS, and the viviparity need of an immune-privileged uterus, this neural plasticity process may emerge as an additional mechanism of peripheral immune tolerance allowing pregnancy.

Another important issue to consider is the effect that changes in tissue innervation may have on DCs, which link the innate and the adaptive immune responses and migrate from peripheral tissues to SLOs. Several years ago, Maestroni showed that DCs expressed functional ARs, with receptor stimulation being able to affect their migration, cytokine production, Th1 and Th17 polarization capacities, and antigen uptake (234–240). Other groups showed that DCs also express functional dopamine receptors through which dopamine—the precursor of NA in sympathetic terminals—, may also modify DCs-mediated Th2 differentiation, CD4+ T cell activation, and Th17 differentiation (241, 242). Nevertheless, while the SNS exerts a marked influence on multiple DCs functions [for review (243)], the same neurotransmitter can mediate different and apparently opposed effects depending on the receptor interactions. Perhaps *in vitro* experiments and the use of agonists/antagonists of adrenergic or dopaminergic receptors may not faithfully reproduce what happens *in vivo*. On the other hand, sympathetic fibers also release cotransmitters like ATP and neuropeptide Y (244) that probably may affect DCs functions, as suggested for peptidergic nerve fibers (245), and hence relevant considering that sensory innervation seems to be increased in inflamed non-lymphoid tissues (147–149, 151). Taken together, there seems to be no conclusive experimental evidence as to the meaning of an

immune response to an antigen presented by DCs coming from a peripheral tissue lacking sympathetic innervation or having other possible changes such as increased sensory innervation. Whatever the case, if the retraction of the sympathetic terminals does really represent an extrinsic mechanism of peripheral immune tolerance, DCs migrating from tissues with reduced sympathetic innervation may convey tolerance.

Although much work is needed to corroborate or not the experimental consequences of this hypothesis, it could have a critical impact on fundamental clinical settings wherein peripheral immune tolerance mechanisms are put into place, like transplantation, cancer, and autoimmune pathology, as well as in mucosal immune tolerance (246–248). Accordingly, it seems crucial to study the sympathetic innervation state in these circumstances, both in SLOs and in non-lymphoid target tissues.

AUTHOR CONTRIBUTIONS

The author confirms being the sole contributor of this work and has approved it for publication.

ACKNOWLEDGMENTS

The author acknowledges the support from the Fundación Iberoamericana de Estudios Superiores.

REFERENCES

1. Bottasso E. Toward the existence of a sympathetic neuroplasticity adaptive mechanism influencing the immune response. A hypothetical view-part I. *Front Endocrinol.* (2019) 10:632. doi: 10.3389/fendo.2019.00632
2. Kemi C, Grunewald J, Eklund A, Höglund CO. Differential regulation of neurotrophin expression in human bronchial smooth muscle cells. *Respir Res.* (2006) 7:18. doi: 10.1186/1465-9921-7-18
3. Tominaga M, Ogawa H, Takamori K. Decreased production of semaphorin 3A in the lesional skin of atopic dermatitis. *Br J Dermatol.* (2008) 158:842–4. doi: 10.1111/j.1365–2133.2007.08410.x
4. Tominaga M, Ozawa S, Ogawa H, Takamori K. A hypothetical mechanism of intraepidermal neurite formation in NC/Nga mice with atopic dermatitis. *J Dermatol Sci.* (2007) 46:199–210. doi: 10.1016/j.jdermsci.2007.02.002
5. Tominaga M, Ozawa S, Tengara S, Ogawa H, Takamori K. Intraepidermal nerve fibers increase in dry skin of acetone-treated mice. *J Dermatol Sci.* (2007) 48:103–11. doi: 10.1016/j.jdermsci.2007.06.003
6. Kamo A, Tominaga M, Tengara S, Ogawa H, Takamori K. Inhibitory effects of UV-based therapy on dry skin-inducible nerve growth in acetone-treated mice. *J Dermatol Sci.* (2011) 62:91–7. doi: 10.1016/j.jdermsci.2011.01.004
7. Jänig W, editor. Functional anatomy of the peripheral sympathetic and parasympathetic system. In: *The Integrative Action of the Autonomic Nervous System: Neurobiology of Homeostasis*. Cambridge, UK: Cambridge University Press (2006). p. 13–34. doi: 10.1017/CBO9780511541667.004
8. Elenkov IJ, Wilder RL, Chrousos GP, Vizi ES. The sympathetic nerve–an integrative interface between two supersystems: the brain and the immune system. *Pharmacol Rev*. (2000) 52:595–638.
9. Padro CJ, Sanders VM. Neuroendocrine regulation of inflammation. *Semin Immunol.* (2014) 26:357–68. doi: 10.1016/j.smim.2014.01.003
10. Kenney MJ, Ganta CK. Autonomic nervous system and immune system interactions. *Compr Physiol.* (2014) 4:1177–200. doi: 10.1002/cphy.c130051
11. Bellinger DL, Lorton D. Sympathetic nerve hyperactivity in the spleen: causal for nonpathogenic-driven chronic Immune-Mediated Inflammatory Diseases (IMIDs)? *Int J Mol Sci.* (2018) 19:E1188. doi: 10.3390/ijms19041188
12. Singer M, Deutschman CS, Seymour CW, Shankar-Hari M, Annane D, Bauer M, et al. The Third International Consensus Definitions for Sepsis and Septic Shock (Sepsis-3). *JAMA*. (2016) 315:801–10. doi: 10.1001/jama.2016.0287
13. Gotts JE, Matthay MA. Sepsis: pathophysiology and clinical management. *BMJ.* (2016) 353:i1585. doi: 10.1136/bmj.i1585
14. Gyawali B, Ramakrishna K, Dhamoon AS. Sepsis: The evolution in definition, pathophysiology, and management. *SAGE Open Med.* (2019) 7:2050312119835043. doi: 10.1177/2050312119835043
15. László I, Trásy D, Molnár Z, Fazakas J. Sepsis: from pathophysiology to individualized patient care. *J Immunol Res.* (2015) 2015:510436. doi: 10.1155/2015/510436
16. Sharawy N. Vasoplegia in septic shock: do we really fight the right enemy? *J Crit Care*. (2014) 29:83–7. doi: 10.1016/j.jcrc.2013.08.021
17. Kakihana Y, Ito T, Nakahara M, Yamaguchi K, Yasuda T. Sepsis-induced myocardial dysfunction: pathophysiology and management. *J Intensive Care.* (2016) 4:22. doi: 10.1186/s40560-016-0148-1
18. Burgdorff AM, Bucher M, Schumann J. Vasoplegia in patients with sepsis and septic shock: pathways and mechanisms. *J Int Med Res*. (2018) 46:1303–10. doi: 10.1177/0300060517743836
19. Levy B, Collin S, Sennoun N, Ducrocq N, Kimmoun A, Asfar P, Perez P, et al. Vascular hyporesponsiveness to vasopressors in septic shock: from bench to bedside. *Intensive Care Med.* (2010) 36:2019–29. doi: 10.1007/s00134-010-2045-8
20. Shaefi S, Mittel A, Klick J, Evans A, Ivascu NS, Gutsche J, et al. Vasoplegia after cardiovascular procedures-pathophysiology and targeted therapy. *J Cardiothorac Vasc Anesth.* (2018) 32:1013–22. doi: 10.1053/j.jvca.2017.10.032
21. Cunnion RE, Parrillo JE. Myocardial dysfunction in sepsis. *Crit Care Clin*. (1989) 5:99–118. doi: 10.1016/S0749-0704(18)30452-4
22. Lefer AM, Martin J. Origin of myocardial depressant factor in shock. *Am J Physiol*. (1970) 218:1423–7. doi: 10.1152/ajplegacy.1970.218.5.1423
23. Rudiger A, Singer M. Mechanisms of sepsis-induced cardiac dysfunction. *Crit Care Med.* (2007) 35:1599–608. doi: 10.1097/01.CCM.0000266683.64081.02
24. Ly NP, Komatsuzaki K, Fraser IP, Tseng AA, Prodhan P, Moore KJ, et al. Netrin-1 inhibits leukocyte migration *in vitro* and *in vivo*. *Proc Natl Acad Sci USA*. (2005) 102:14729–34. doi: 10.1073/pnas.0506233102
25. Rosenberger P, Schwab JM, Mirakaj V, Masekowsky E, Mager A, Morote-Garcia JC, et al. Hypoxia-inducible factor-dependent induction of netrin-1 dampens inflammation caused by hypoxia. *Nat Immunol.* (2009) 10:195–202. doi: 10.1038/ni.1683
26. Borsini A, Zunszain PA, Thuret S, Pariante CM. The role of inflammatory cytokines as key modulators of neurogenesis. *Trends Neurosci.* (2015) 38:145–57. doi: 10.1016/j.tins.2014.12.006
27. Poon VY, Choi S, Park M. Growth factors in synaptic function. *Front Synaptic Neurosci.* (2013) 5:6. doi: 10.3389/fnsyn.2013.00006
28. Chernogubova E, Cannon B, Bengtsson T. Norepinephrine increases glucose transport in brown adipocytes via β3-adrenoceptors through a cAMP, PKA, and PI3-kinase-dependent pathway stimulating conventional and novel PKCs. *Endocrinology*. (2004) 145:269–80. doi: 10.1210/en.2003-0857
29. Cooney GJ, Caterson ID, Newsholme EA. The effect of insulin and noradrenaline on the uptake of 2-[1-14C]deoxyglucose *in vivo* by brown adipose tissue and other glucose-utilising tissues of the mouse. *FEBS Lett.* (1985) 188:257–61. doi: 10.1016/0014-5793(85)80383-5
30. Shimizu Y, Kielar D, Minokoshi Y, Shimazu T. Noradrenaline increases glucose transport into brown adipocytes in culture by a mechanism different from that of insulin. *Biochem J.* (1996) 314:485–90. doi: 10.1042/bj3140485
31. Shimizu Y, Satoh S, Yano H, Minokoshi Y, Cushman SW, Shimazu T. Effects of noradrenaline on the cell-surface glucose transporters in cultured brown adipocytes: novel mechanism for selective activation of GLUT1 glucose transporters. *Biochem J.* (1998) 330:397–403. doi: 10.1042/bj3300397

32. Inokuma K, Ogura-Okamatsu Y, Toda C, Kimura K, Yamashita H, Saito M. Uncoupling protein 1 is necessary for norepinephrine-induced glucose utilization in brown adipose tissue. *Diabetes*. (2005) 54:1385–91. doi: 10.2337/diabetes.54.5.1385
33. Abi-Gerges N, Tavernier B, Mebazaa A, Faivre V, Paqueron X, Payen D, et al. Sequential changes in autonomic regulation of cardiac myocytes after *in vivo* endotoxin injection in rat. *Am J Respir Crit Care Med*. (1999) 160:1196–204. doi: 10.1164/ajrccm.160.4.9808149
34. Zhong J, Hwang TC, Adams HR, Rubin LJ. Reduced L-type calcium current in ventricular myocytes from endotoxemic guinea pigs. *Am J Physiol*. (1997) 273:H2312–24. doi: 10.1152/ajpheart.1997.273.5.H2312
35. Liu S, Schreur KD. G protein-mediated suppression of L-type Ca2+ current by interleukin-1 beta in cultured ratventricular myocytes. *Am J Physiol*. (1995) 268:C339–49. Erratum in: *Am J Physiol*. (1995) 268:section C following table of contents. doi: 10.1152/ajpcell.1995.268.2.C339
36. Schmidt H, Hoyer D, Wilhelm J, Söffker G, Heinroth K, Hottenrott K, et al. The alteration of autonomic function in multiple organ dysfunction syndrome. *Crit Care Clin*. (2008) 24:149–63. doi: 10.1016/j.ccc.2007.10.003
37. Hoyer D, Friedrich H, Zwiener U, Pompe B, Baranowski R, Werdan K, et al. Prognostic impact of autonomic information in multiple organ dysfunction syndrome patients. *Int J Cardiol*. (2006) 108:359–69. doi: 10.1016/j.ijcard.2005.05.031
38. Godin PJ, Buchman TG. Uncoupling of biological oscillators: a complementary hypothesis concerning the pathogenesis of multiple organ dysfunction syndrome. *Crit Care Med*. (1996) 24:1107–16. doi: 10.1097/00003246-199607000-00008
39. Annane D, Trabold F, Sharshar T, Jarrin I, Blanc AS, Raphael JC, et al. Inappropriate sympathetic activation at onset of septic shock: a spectral analysis approach. *Am J Respir Crit Care Med*. (1999) 160:458–65. doi: 10.1164/ajrccm.160.2.9810073
40. Koyoama S, Manning JW. Role of sympathetic nerve activity in endotoxin induced hypotension in cats. *Cardiovasc. Res*. (1985) 19:32–37. doi: 10.1093/cvr/19.1.32
41. Sharshar T, Gray F, Lorin de la Grandmaison G, Hopkinson NS, Ross E, Dorandeu A, et al. Apoptosis of neurons in cardiovascular autonomic centres triggered by inducible nitric oxidesynthase after death from septic shock. *Lancet*. (2003) 362:1799–805. doi: 10.1016/S0140-6736(03)14899-4
42. Corrêa TD, Takala J, Jakob SM. Angiotensin II in septic shock. *Crit Care*. (2015) 19:98. doi: 10.1186/s13054-015-0802-3
43. Torpy DJ, Chrousos GP. The three-way interactions between the hypothalamic-pituitary-adrenal and gonadal axes and the immune system. *Baillieres Clin Rheumatol*. (1996) 10:181–98. doi: 10.1016/S1521-6942(06)80039-2
44. Silverman MN, Pearce BD, Biron CA, Miller AH. Immune modulation of the hypothalamic-pituitary-adrenal (HPA) axis during viral infection. *Viral Immunol*. (2005) 18:41–78. doi: 10.1089/vim.2005.18.41
45. Polito A, Aboab J, Annane D. Adrenal insufficiency in sepsis. *Rev Bras Ter Intensiva*. (2006) 18:86–94. doi: 10.1590/S0103-507X2006000100014
46. Annane D, Bellissant E, Sebille V, Lesieur O, Mathieu B, Raphael JC, et al. Impaired pressor sensitivity to noradrenaline in septic shock patients with and without impaired adrenal function reserve. *Br J Clin Pharmacol*. (1998) 46:589–97. doi: 10.1046/j.1365–2125.1998.00833.x
47. Jänig W, editor. The peripheral sympathetic and parasympathetic pathways. In: *The Integrative Action of the Autonomic Nervous System: Neurobiology of Homeostasis*. Cambridge, UK: Cambridge University Press (2006). p. 106–67. doi: 10.1017/CBO9780511541667.007
48. Kopin, IJ. Plasma Levels of Catecholamines and Dopamine-β-Hydroxylase. In: Trendelemburg U, Weiner N, editors. *Catecholamines II. Handbook of Experimental Pharmacology, Vol 90/2*. Berlin; Heidelberg: Springer (1989). p. 211–75. doi: 10.1007/978-3-642-73551-6_6
49. Bocking JK, Sibbald WJ, Holliday RL, Scott S, Viidik T. Plasma catecholamine levels and pulmonary dysfunction in sepsis. *Surg Gynecol Obstet*. (1979) 148:715–9.
50. Bernardin G, Strosberg AD, Bernard A, Mattei M, Marullo S. β-adrenergic receptor-dependent and –independent stimulation of adenylate cyclase is impaired during severe sepsis in humans. *Intensive Care Med*. (1998) 24:1315–22. doi: 10.1007/s001340050768
51. Hahn PY, Wang P, Tait SM, Ba ZF, Reich SS, Chaudry IH. Sustained elevation in circulating catecholamine levels during polymicrobial sepsis. *Shock*. (1995) 4:269–73. doi: 10.1097/00024382-199510000-00007
52. Hwang TL, Lau YT, Huang SF, Chen MF, Liu MS. Changes of α_1-adrenergic receptors in human liver during intraabdominal sepsis. *Hepatology*. (1994) 20:638–42. doi: 10.1002/hep.1840200314
53. Tang C, Liu MS. Initial externalization followed by internalization of beta-adrenergic receptors in rat heart during sepsis. *Am J Physiol*. (1996) 270:254–63. doi: 10.1152/ajpregu.1996.270.1.R254
54. Shepherd RE, Lang CH, McDonough KH. Myocardial adrenergic responsiveness after lethal and nonlethal doses of endotoxin. *Am J Physiol*. (1987) 252:H410–6. doi: 10.1152/ajpheart.1987.252.2.H410
55. Reber LL, Hernandez JD, Galli SJ. The pathophysiology of anaphylaxis. *J Allergy Clin Immunol*. (2017) 140:335–348. doi: 10.1016/j.jaci.2017.06.003
56. Kemp SF, Lockey RF. Anaphylaxis: a review of causes and mechanisms. *J Allergy Clin Immunol*. (2002) 110:341–8. doi: 10.1067/mai.2002.126811
57. Campbell RL, Li JT, Nicklas RA, Sadosty AT; Members of the Joint Task Force; Practice Parameter Workgroup. Emergency department diagnosis and treatment of anaphylaxis: a practice parameter. *Ann Allergy Asthma Immunol*. (2014) 113:599–608. doi: 10.1016/j.anai.2014.10.007
58. Ring J, Beyer K, Biedermann T, Bircher A, Duda D, Fischer J, et al. Guideline for acute therapy and management of anaphylaxis: S2 Guideline of the German Society for Allergology and Clinical Immunology (DGAKI), the Association of German Allergologists (AeDA), the Society of Pediatric Allergy and Environmental Medicine (GPA), the German Academy of Allergology and Environmental Medicine (DAAU), the German Professional Association of Pediatricians (BVKJ), the Austrian Society for Allergology and Immunology (ÖGAI), the Swiss Society for Allergy and Immunology (SGAI), the German Society of Anaesthesiology and Intensive Care Medicine (DGAI), the German Society of Pharmacology (DGP), the German Society for Psychosomatic Medicine (DGPM), the German Working Group of Anaphylaxis Training and Education (AGATE) and the patient organization German Allergy and Asthma Association (DAAB). *Allergo J Int*. (2014) 23:96–112. doi: 10.1007/s40629-014-0009-1
59. Leon A, Buriani A, Dal Toso R, Fabris M, Romanello S, Aloe L, et al. Mast cells synthesize, store, and release nerve growth factor. *Proc Natl Acad Sci USA*. (1994) 91:3739–43. doi: 10.1073/pnas.91.9.3739
60. Casha S, Christie S. A systematic review of intensive cardiopulmonary management after spinal cord injury. *J Neurotrauma*. (2011) 28:1479–95. doi: 10.1089/neu.2009.1156
61. Popa C, Popa F, Grigorean VT, Onose G, Sandu AM, Popescu M, et al. Vascular dysfunctions following spinal cord injury. *J Med Life*. (2010) 3:275–85.
62. Partida E, Mironets E, Hou S, Tom VJ. Cardiovascular dysfunction following spinal cord injury. *Neural Regen Res*. (2016) 11:189–94. doi: 10.4103/1673–5374.177707
63. Mitchell RN, Schoen FJ. Blood Vessels. In: Kumar V, Abbas AK, Aster JC, editors. *Robbins Basic Pathology*. Philadelphia, PA: Elsevier Saunders (2018). p. 361–98.
64. Golledge J. Abdominal aortic aneurysm: update on pathogenesis and medical treatments. *Nat Rev Cardiol*. (2019) 16:225–42. doi: 10.1038/s41569-018-0114-9
65. Nordon IM, Hinchliffe RJ, Loftus IM, Thompson MM. Pathophysiology and epidemiology of abdominal aortic aneurysms. *Nat Rev Cardiol*. (2011) 8:92–102. doi: 10.1038/nrcardio.2010.180
66. Li H, Bai S, Ao Q, Wang X, Tian X, Li X, et al. Modulation of immune-inflammatory responses in abdominal aortic aneurysm: emerging molecular targets. *J Immunol Res*. (2018) 2018:7213760. doi: 10.1155/2018/7213760
67. Galkina E, Ley K. Immune and inflammatory mechanisms of atherosclerosis (*). *Annu Rev Immunol*. (2009) 27:165–97. doi: 10.1146/annurev.immunol.021908.132620
68. Libby P. Inflammation in atherosclerosis. *Arterioscler Thromb Vasc Biol*. (2012) 32:2045–51. doi: 10.1161/ATVBAHA.108.179705
69. Fredman G, Tabas I. Boosting inflammation resolution in atherosclerosis: the next frontier for therapy. *Am J Pathol*. (2017) 187:1211–21. doi: 10.1016/j.ajpath.2017.01.018

70. Hellenthal FA, Geenen IL, Teijink JA, Heeneman S, Schurink GW. Histological features of human abdominal aortic aneurysm are not related to clinical characteristics. *Cardiovasc Pathol*. (2009) 18:286–93. doi: 10.1016/j.carpath.2008.06.014
71. Rodella LF, Rezzani R, Bonomini F, Peroni M, Cocchi MA, Hirtler L, et al. Abdominal aortic aneurysm and histological, clinical, radiological correlation. *Acta Histochem*. (2016) 118:256–62. doi: 10.1016/j.acthis.2016.01.007
72. Paulo N, Cascarejo J, Vouga L. Syphilitic aneurysm of the ascending aorta. *Interact Cardiovasc Thorac Surg*. (2012) 14:223–5. doi: 10.1093/icvts/ivr067
73. Roberts WC, Barbin CM, Weissenborn MR, Ko JM, Henry AC. Syphilis as a cause of thoracic aortic aneurysm. *Am J Cardiol*. (2015) 116:1298–303. doi: 10.1016/j.amjcard.2015.07.030
74. Brown SL, Busuttil RW, Baker JD, Machleder HI, Moore WS, Barker WF. Bacteriologic and surgical determinants of survival in patients with mycotic aneurysms. *J Vasc Surg*. (1984) 1:541–7. doi: 10.1016/0741-5214(84)90040-5
75. Lee WK, Mossop PJ, Little AF, Fitt GJ, Vrazas JI, Hoang JK, et al. Infected (mycotic) aneurysms: spectrum of imaging appearances and management. *Radiographics*. (2008) 28:1853–68. doi: 10.1148/rg.287085054
76. Bevan RD. Effect of sympathetic denervation on smooth muscle cell proliferation in the growing rabbit ear artery. *Circ Res*. (1975) 37:14–9. doi: 10.1161/01.RES.37.1.14
77. Chamley JH, Campbell GR. Trophic influences of sympathetic nerves and cyclic AMP on differentiation and proliferation of isolated smooth muscle cells in culture. *Cell Tissue Res*. (1975) 161:497–510. doi: 10.1007/BF00224140
78. Fronek K. Trophic effect of the sympathetic nervous system on vascular smooth muscle. *Ann Biomed Eng*. (1983) 11:607–15. doi: 10.1007/BF02364090
79. Erlinge D, Yoo H, Edvinsson L, Reis DJ, Wahlestedt C. Mitogenic effects of ATP on vascular smooth muscle cells vs. other growth factors and sympathetic cotransmitters. *Am J Physiol*. (1993) 265:H1089–97. doi: 10.1152/ajpheart.1993.265.4.H1089
80. Erlinge D, Brunkwall J, Edvinsson L. Neuropeptide Y stimulates proliferation of human vascular smooth muscle cells: cooperation with noradrenaline and ATP. *Regul Pept*. (1994) 50:259–65. doi: 10.1016/0167-0115(94)90006-X
81. Zhang H, Faber JE. Trophic effect of norepinephrine on arterial intima-media and adventitia is augmented by injury and mediated by different alpha1-adrenoceptor subtypes. *Circ Res*. (2001) 89:815–22. doi: 10.1161/hh2101.098379
82. Dechant G, Barde YA. The neurotrophin receptor p75(NTR): novel functions and implications for diseases of the nervous system. *Nat Neurosci*. (2002) 5:1131–6. doi: 10.1038/nn1102-1131
83. Kenchappa RS, Tep C, Korade Z, Urra S, Bronfman FC, Yoon SO, et al. p75 neurotrophin receptor-mediated apoptosis in sympathetic neurons involves a biphasic activation of JNK and up-regulation of tumor necrosis factor-alpha-converting enzyme/ADAM17. *J Biol Chem*. (2010) 285:20358–68. doi: 10.1074/jbc.M109.082834
84. Kraemer BR, Snow JP, Vollbrecht P, Pathak A, Valentine WM, Deutch AY, et al. A role for the p75 neurotrophin receptor in axonal degeneration and apoptosis induced by oxidative stress. *J Biol Chem*. (2014) 289:21205–16. doi: 10.1074/jbc.M114.563403
85. Bush A. Pathophysiological mechanisms of asthma. *Front Pediatr*. (2019) 7:68. doi: 10.3389/fped.2019.00068
86. Olin JT, Wechsler ME. Asthma: pathogenesis and novel drugs for treatment. *BMJ*. (2014) 349:g5517. doi: 10.1136/bmj.g5517
87. McCracken JL, Veeranki SP, Ameredes BT, Calhoun WJ. Diagnosis and management of asthma in adults: a review. *JAMA*. (2017) 318:279–90. doi: 10.1001/jama.2017.8372
88. Schatz M, Rosenwasser L. The allergic asthma phenotype. *J Allergy Clin Immunol Pract*. (2014) 2:645-8; quiz 649. doi: 10.1016/j.jaip.2014.09.004
89. Peters SP. Asthma phenotypes: nonallergic (intrinsic) asthma. *J Allergy Clin Immunol Pract*. (2014) 2:650–2. doi: 10.1016/j.jaip.2014.09.006
90. Szentivanyi A. The beta-adrenergic theory of the atopic abnormality in bronchial asthma. *J Allergy Clin Immunol*. (1968) 42:203–32. doi: 10.1016/S0021-8707(68)90117-2
91. Lemanske RF Jr, Kaliner MA. Autonomic nervous system abnormalities and asthma. *Am Rev Respir Dis*. (1990) 141:S157–61. doi: 10.1164/ajrccm/141.3_Pt_2.S157
92. Jartti T. Asthma, asthma medication and autonomic nervous system dysfunction. *Clin Physiol*. (2001) 21:260–9. doi: 10.1046/j.1365–2281.2001.00323.x
93. Mazzone SB, Undem BJ. Vagal afferent innervation of the airways in health and disease. *Physiol Rev*. (2016) 96:975–1024. doi: 10.1152/physrev.00039.2015
94. Undem BJ, Carr MJ. The role of nerves in asthma. *Curr Allergy Asthma Rep*. (2002) 2:159–65. doi: 10.1007/s11882-002-0011-4
95. van der Velden VH, Hulsmann AR. Autonomic innervation of human airways: structure, function, and pathophysiology in asthma. *Neuroimmunomodulation*. (1999) 6:145–59. doi: 10.1159/000026376
96. de Jongste JC, Jongejan RC, Kerrebijn KF. Control of airway caliber by autonomic nerves in asthma and in chronic obstructive pulmonary disease. *Am Rev Respir Dis*. (1991) 143:1421–6. doi: 10.1164/ajrccm/143.6.1421
97. Grundstrom N, Andersson ROO. Inhibition of the cholinergic neurotransmission in human airways via prejunctional alpha-2-adrenoceptors. *Acta Physiol Scand*. (1985) 125:513–7. doi: 10.1111/j.1748–1716.1985.tb07749.x
98. Davis C, Kannan MS. Sympathetic innervations of human tracheal and bronchial smooth muscle. *Respir Physiol*. (1987) 68:53–61. doi: 10.1016/0034-5687(87)90076-4
99. Morales DR, Dreischulte T, Lipworth BJ, Donnan PT, Jackson C, Guthrie B. Respiratory effect of beta-blocker eye drops in asthma: population-based study and meta-analysis of clinical trials. *Br J Clin Pharmacol*. (2016) 82:814–22. doi: 10.1111/bcp.13006
100. Morales DR, Jackson C, Lipworth BJ, Donnan PT, Guthrie B. Adverse respiratory effect of acute β-blocker exposure in asthma: a systematic review and meta-analysis of randomized controlled trials. *Chest*. (2014) 145:779–786. doi: 10.1378/chest.13-1235
101. Empey DW, Laitinen LA, Jacobs L, Gold WM, Nadel JA. Mechanisms of bronchial hyperreactivity in normal subjects after upper respiratory tract infection. *Am Rev Respir Dis*. (1976) 113:131–9.
102. Laitinen LA, Elkin RB, Empey DW, Jacobs L, Mills J, Nadel JA. Bronchial hyperresponsiveness in normal subjects during attenuated influenza virus infection. *Am Rev Respir Dis*. (1991) 143:358–61. doi: 10.1164/ajrccm/143.2.358
103. Freymuth F, Vabret A, Gouarin S, Petitjean J, Campet M: [Epidemiology of respiratory virus infections]. *Allerg Immunol*. (2001) 33:66–9.
104. Pérez-Yarza EG, Moreno A, Lázaro P, Mejías A, Ramilo O. The association between respiratory syncytial virus infection and the development of childhood asthma: a systematic review of the literature. *Pediatr Infect Dis J*. (2007) 26:733–9. doi: 10.1097/INF.0b013e3180618c42
105. Fjaerli HO, Farstad T, Rød G, Ufert GK, Gulbrandsen P, Nakstad B. Acute bronchiolitis in infancy as risk factor for wheezing and reduced pulmonary function by seven years in Akershus County, Norway. *BMC Pediatr*. (2005) 5:31. doi: 10.1186/1471-2431-5-31
106. Mirza S, Clay RD, Koslow MA, Scanlon PD. COPD Guidelines: a review of the 2018 GOLD Report. *Mayo Clin Proc*. (2018) 93:1488–502. doi: 10.1016/j.mayocp.2018.05.026
107. Rossi A, Butorac-Petanjek B, Chilosi M, Cosío BG, Flezar M, Koulouris N, et al. Chronic obstructive pulmonary disease with mild airflow limitation: current knowledge and proposal for future research - a consensus document from six scientific societies. *Int J Chron Obstruct Pulmon Dis*. (2017) 12:2593–610. doi: 10.2147/COPD.S132236
108. GBD 2015 Chronic Respiratory Disease Collaborators. Global, regional, and national deaths, prevalence, disability-adjusted life years, and years lived with disability for chronic obstructive pulmonary disease and asthma, 1990-2015: a systematic analysis for the Global Burden of Disease Study 2015. *Lancet Respir Med*. (2017) 5:691–706. doi: 10.1016/S2213-2600(17)30293-X
109. Papaiwannou A, Zarogoulidis P, Porpodis K, Spyratos D, Kioumis I, Pitsiou G, et al. Asthma-chronic obstructive pulmonary disease overlap syndrome (ACOS): current literature review. *J Thorac Dis*. (2014) 6 Suppl 1:S146–51. doi: 10.3978/j.issn.2072-1439.2014.03.04

110. Brown PJ, Greville HW, Finucane KE. Asthma and irreversible airflow obstruction. *Thorax*. (1984) 39:131–6. doi: 10.1136/thx.39.2.131
111. Backman KS, Greenberger PA, Patterson R. Airways obstruction in patients with long-term asthma consistent with irreversible asthma. *Chest*. (1997) 112:1234–40. doi: 10.1378/chest.112.5.1234
112. Vonk JM, Jongepier H, Panhuysen CIM, Schouten JP, Bleecker ER, Postma DS. Risk factors associated with the presence of irreversible airflow limitation and reduced transfer coefficient in patients with asthma after 26 years of follow up. *Thorax*. (2003) 58:322–7. doi: 10.1136/thorax.58.4.322
113. Grzela K, Litwiniuk M, Zagorska W, Grzela T. Airway remodeling in chronic obstructive pulmonary disease and asthma: the role of matrix metalloproteinase-9. *Arch Immunol Ther Exp (Warsz)*. (2016) 64:47–55. doi: 10.1007/s00005-015-0345-y
114. Lambert RK, Wiggs BR, Kuwano K, Hogg JC, Paré PD. Functional significance of increased airway smooth muscle in asthma and COPD. *J Appl Physiol*. (1993) 74:2771–81. doi: 10.1152/jappl.1993.74.6.2771
115. Meurs H, Dekkers BG, Maarsingh H, Halayko AJ, Zaagsma J, Gosens R. Muscarinic receptors on airway mesenchymal cells: novel findings for an ancient target. *Pulm Pharmacol Ther*. (2013) 26:145–55. doi: 10.1016/j.pupt.2012.07.003
116. Kistemaker LE, Oenema TA, Meurs H, Gosens R. Regulation of airway inflammation and remodeling by muscarinic receptors: perspectives on anticholinergic therapy in asthma and COPD. *Life Sci*. (2012) 91:1126–33. doi: 10.1016/j.lfs.2012.02.021
117. Koarai A, Ichinose M. Possible involvement of acetylcholine-mediated inflammation in airway diseases. *Allergol Int*. (2018) 67:460–6. doi: 10.1016/j.alit.2018.02.008
118. Gosens R, Gross N. The mode of action of anticholinergics in asthma. *Eur Respir J*. (2018) 52:1701247. doi: 10.1183/13993003.01247-2017
119. DeFronzo RA, Ferrannini E, Groop L, Henry RR, Herman WH, Holst JJ, et al. Type 2 diabetes mellitus. *Nat Rev Dis Primers*. (2015) 1:15019. doi: 10.1038/nrdp.2015.39
120. Katsarou A, Gudbjörnsdottir S, Rawshani A, Dabelea D, Bonifacio E, Anderson BJ, et al. Type 1 diabetes mellitus. *Nat Rev Dis Primers*. (2017) 3:17016. doi: 10.1038/nrdp.2017.16
121. Krogvold L, Wiberg A, Edwin B, Buanes T, Jahnsen FL, Hanssen KF, et al. Insulitis and characterisation of infiltrating T cells in surgical pancreatic tail resections from patients at onset of type 1 diabetes. *Diabetologia*. (2016) 59:492–501. doi: 10.1007/s00125-015-3820-4
122. Krogvold L, Edwin B, Buanes T, Ludvigsson J, Korsgren O, Hyöty H, et al. Pancreatic biopsy by minimal tail resection in live adult patients at the onset of type 1 diabetes: experiences from the DiViD study. *Diabetologia*. (2014) 57:841–3. doi: 10.1007/s00125-013-3155-y
123. Imagawa A, Hanafusa T, Tamura S, Moriwaki M, Itoh N, Yamamoto K, et al. Pancreatic biopsy as a procedure for detecting in situ autoimmune phenomena in type 1 diabetes: close correlation between serological markers and histological evidence of cellular autoimmunity. *Diabetes*. (2001) 50:1269–73. doi: 10.2337/diabetes.50.6.1269
124. Bottazzo GF, Dean BM, McNally JM, MacKay EH, Swift PG, Gamble DR. In situ characterization of autoimmune phenomena and expression of HLA molecules in the pancreas in diabetic insulitis. *N Engl J Med*. (1985) 313:353–60. doi: 10.1056/NEJM198508083130604
125. Ahrén B. Autonomic regulation of islet hormone secretion–implications for health and disease. *Diabetologia*. (2000) 43:393–410. doi: 10.1007/s001250051322
126. Taborsky GJ Jr. The physiology of glucagon. *J Diabetes Sci Technol*. (2010) 4:1338–44. doi: 10.1177/193229681000400607
127. Taborsky GJ Jr, Mundinger TO. The role of the autonomic nervous system in mediating the glucagon response to hypoglycemia. *Endocrinology*. (2012) 153:1055–62. doi: 10.1210/en.2011-2040
128. Gerich JE, Langlois M, Noacco C, Karam JH, Forsham PH. Lack of glucagon response to hypoglycemia in diabetes: evidence for an intrinsic pancreatic alpha cell defect. *Science*. (1973) 182:171–3. doi: 10.1126/science.182.4108.171
129. Mundinger TO, Taborsky GJ Jr. Early sympathetic islet neuropathy in autoimmune diabetes: lessons learned and opportunities for investigation. *Diabetologia*. (2016) 59:2058–67. doi: 10.1007/s00125-016-4026-0
130. Mei Q, Mundinger TO, Lernmark A, Taborsky GJ Jr. Early, selective, and marked loss of sympathetic nerves from the islets of BioBreeder diabetic rats. *Diabetes*. (2002) 51:2997–3002. Erratum in: *Diabetes*. (2002) 51:3591. doi: 10.2337/diabetes.51.10.2997
131. Taborsky GJ Jr, Mei Q, Hackney DJ, Figlewicz DP, LeBoeuf R, Mundinger TO. Loss of islet sympathetic nerves and impairment of glucagon secretion in the NOD mouse: relationship to invasive insulitis. *Diabetologia*. (2009) 52:2602–11. doi: 10.1007/s00125-009-1494-5
132. Taborsky GJ Jr, Mei Q, Bornfeldt KE, Hackney DJ, Mundinger TO. The p75 neurotrophin receptor is required for the major loss of sympathetic nerves from islets under autoimmune attack. *Diabetes*. (2014) 63:2369–79. doi: 10.2337/db13-0778
133. Mundinger TO, Mei Q, Foulis AK, Fligner CL, Hull RL, Taborsky GJ Jr. Human Type 1 diabetes is characterized by an early, marked, sustained, and islet-selective loss of sympathetic nerves. *Diabetes*. (2016) 65:2322–30. doi: 10.2337/db16-0284
134. Taborsky GJ Jr, Mei Q, Hackney DJ, Mundinger TO. The search for the mechanism of early sympathetic islet neuropathy in autoimmune diabetes. *Diabetes Obes Metab*. (2014) 16(Suppl. 1):96–101. doi: 10.1111/dom.12341
135. Mozaffarian D, Benjamin EJ, Go AS, Arnett DK, Blaha MJ, Cushman M, et al. Heart disease and stroke statistics—2015 update: a report from the American Heart Association. *Circulation*. (2015) 131:e29–322. doi: 10.1161/CIR.0000000000000152
136. Francis Stuart SD, De Jesus NM, Lindsey ML, Ripplinger CM. The crossroads of inflammation, fibrosis, and arrhythmia following myocardial infarction. *J Mol Cell Cardiol*. (2016) 91:114–22. doi: 10.1016/j.yjmcc.2015.12.024
137. Ong SB, Hernández-Reséndiz S, Crespo-Avilan GE, Mukhametshina RT, Kwek XY, Cabrera-Fuentes HA, et al. Inflammation following acute myocardial infarction: Multiple players, dynamic roles, and novel therapeutic opportunities. *Pharmacol Ther*. (2018) 186:73–87. doi: 10.1016/j.pharmthera.2018.01.001
138. Parrish DC, Francis Stuart SD, Olivas A, Wang L, Nykjaer A, Ripplinger CM, et al. Transient denervation of viable myocardium after myocardial infarction does not alter arrhythmia susceptibility. *Am J Physiol Heart Circ Physiol*. (2018) 314:H415–23. doi: 10.1152/ajpheart.00300.2017
139. Stanton MS, Tuli MM, Radtke NL, Heger JJ, Miles WM, Mock BH, et al. Regional sympathetic denervation after myocardial infarction in humans detected noninvasively using I-123-metaiodobenzylguanidine. *J Am Coll Cardiol*. (1989) 14:1519–26. doi: 10.1016/0735-1097(89)90391-4
140. Kammerling JJ, Green FJ, Watanabe AM, Inoue H, Barber MJ, Henry DP, et al. Denervation supersensitivity of refractoriness in noninfarcted areas apical to transmural myocardial infarction. *Circulation*. (1987) 76:383–93. doi: 10.1161/01.CIR.76.2.383
141. Li W, Knowlton D, Van Winkle DM, Habecker BA. Infarction alters both the distribution and noradrenergic properties of cardiac sympathetic neurons. *Am J Physiol Heart Circ Physiol*. (2004) 286:H2229–36. doi: 10.1152/ajpheart.00768.2003
142. Hiltunen JO, Laurikainen A, Väkevä A, Meri S, Saarma M. Nerve growth factor and brain-derived neurotrophic factor mRNAs are regulated in distinct cell populations of rat heart after ischaemia and reperfusion. *J Pathol*. (2001) 194:247–53. doi: 10.1002/path.878
143. Lorentz CU, Parrish DC, Alston EN, Pellegrino MJ, Woodward WR, Hempstead BL, et al. Sympathetic denervation of peri-infarct myocardium requires the p75 neurotrophin receptor. *Exp Neurol*. (2013) 249:111–9. doi: 10.1016/j.expneurol.2013.08.015
144. Boogers MJ, Borleffs CJ, Henneman MM, van Bommel RJ, van Ramshorst J, Boersma E, et al. Cardiac sympathetic denervation assessed with 123-iodine metaiodobenzylguanidine imaging predicts ventricular arrhythmias in implantable cardioverter-defibrillator patients. *J Am Coll Cardiol*. (2010) 55:2769–77. doi: 10.1016/j.jacc.2009.12.066
145. Fallavollita JA, Heavey BM, Luisi AJ Jr, Michalek SM, Baldwa S, Mashtare TL Jr, et al. Regional myocardial sympathetic denervation predicts the risk of sudden cardiac arrest in ischemic cardiomyopathy. *J Am Coll Cardiol*. (2014) 63:141–9. doi: 10.1016/j.jacc.2013.07.096
146. Nishisato K, Hashimoto A, Nakata T, Doi T, Yamamoto H, Nagahara D, et al. Impaired cardiac sympathetic innervation and myocardial perfusion are related to lethal arrhythmia: quantification of cardiac tracers in

patients with ICDs. *J Nucl Med*. (2010) 51:1241–9. doi: 10.2967/jnumed.110.074971
147. Tominaga M, Takamori K. Recent advances in pathophysiological mechanisms of itch. *Expert Rev Dermatol*. (2010) 5:197–212. doi: 10.1586/edm.10.7
148. Tominaga M, Takamori K. Itch and nerve fibers with special reference to atopic dermatitis: therapeutic implications. *J Dermatol*. (2014) 41:205–12. doi: 10.1111/1346–8138.12317
149. Tominaga M, Ogawa H, Takamori K. Histological characterization of cutaneous nerve fibers containing gastrin-releasing peptide in NC/Nga mice: an atopic dermatitis model. *J Invest Dermatol*. (2009) 129:2901–5. doi: 10.1038/jid.2009.188
150. Takaoka K, Shirai Y, Saito N. Inflammatory cytokine tumor necrosis factor-alpha enhances nerve growth factor production in human keratinocytes, HaCaT cells. *J Pharmacol Sci*. (2009) 111:381–91. doi: 10.1254/jphs.09143FP
151. Kakurai M, Monteforte R, Suto H, Tsai M, Nakae S, Galli SJ. Mast cell-derived tumor necrosis factor can promote nerve fiber elongation in the skin during contact hypersensitivity in mice. *Am J Pathol*. (2006) 169:1713–21. doi: 10.2353/ajpath.2006.060602
152. Tobin D, Nabarro G, Baart de la Faille H, van Vloten WA, van der Putte SC, Schuurman HJ. Increased number of immunoreactive nerve fibers in atopic dermatitis. *J Allergy Clin Immunol*. (1992) 90:613–22. doi: 10.1016/0091-6749(92)90134-N
153. Cicek D, Kandi B, Berilgen MS, Bulut S, Tekatas A, Dertlioglu SB, et al. Does autonomic dysfunction play a role in atopic dermatitis? *Br J Dermatol*. (2008) 159:834–8. doi: 10.1111/j.1365–2133.2008.08756.x
154. Haligür BD, Cicek D, Bulut S, Berilgen MS. The investigation of autonomic functions in patients with psoriasis. *Int J Dermatol*. (2012) 51:557–63. doi: 10.1111/j.1365–4632.2011.05111.x
155. Stead RH, Kosecka-Janiszewska U, Oestreicher AB, Dixon MF, Bienenstock J. Remodeling of B-50 (GAP-43)- and NSE-immunoreactive mucosal nerves in the intestines of rats infected with Nippostrongylus brasiliensis. *J Neurosci*. (1991) 11:3809–21. doi: 10.1523/JNEUROSCI.11-12–03809.1991
156. Stead RH. Nerve remodelling during intestinal inflammation. *Ann N Y Acad Sci*. (1992) 664:443–55. doi: 10.1111/j.1749–6632.1992.tb39782.x
157. Swain MG, Blennerhassett PA, Collins SM. Impaired sympathetic nerve function in the inflamed rat intestine. *Gastroenterology*. (1991) 100:675–82. doi: 10.1016/0016-5085(91)80011-W
158. Boissé L, Chisholm SP, Lukewich MK, Lomax AE. Clinical and experimental evidence of sympathetic neural dysfunction during inflammatory bowel disease. *Clin Exp Pharmacol Physiol*. (2009) 36:1026–33. doi: 10.1111/j.1440–1681.2009.05242.x
159. Motagally MA, Neshat S, Lomax AE. Inhibition of sympathetic N-type voltage-gated Ca2+ current underlies the reduction in norepinephrine release during colitis. *Am J Physiol Gastrointest Liver Physiol*. (2009) 296:G1077–84. doi: 10.1152/ajpgi.00006.2009
160. Jänig W, editor. The enteric nervous system. In: *The Integrative Action of the Autonomic Nervous System: Neurobiology of Homeostasis*. Cambridge, UK: Cambridge University Press (2006). p. 168–207. doi: 10.1017/CBO9780511541667
161. Lomax AE, Sharkey KA, Furness JB. The participation of the sympathetic innervation of the gastrointestinal tract in disease states. *Neurogastroenterol Motil*. (2010) 22:7–18. doi: 10.1111/j.1365–2982.2009.01381.x
162. Brierley SM, Linden DR. Neuroplasticity and dysfunction after gastrointestinal inflammation. *Nat Rev Gastroenterol Hepatol*. (2014) 11:611–27. doi: 10.1038/nrgastro.2014.103
163. Moynes DM, Lucas GH, Beyak MJ, Lomax AE. Effects of inflammation on the innervation of the colon. *Toxicol Pathol*. (2014) 42:111–7. doi: 10.1177/0192623313505929
164. Lomax AE, Pradhananga S, Bertrand PP. Plasticity of neuroeffector transmission during bowel inflammation[1]. *Am J Physiol Gastrointest Liver Physiol*. (2017) 312:G165–70. doi: 10.1152/ajpgi.00365.2016
165. Weidler C, Holzer C, Harbuz M, Hofbauer R, Angele P, Schölmerich J, et al. Low density of sympathetic nerve fibres and increased density of brain derived neurotrophic factor positive cells in RA synovium. *Ann Rheum Dis*. (2005) 64:13–20. doi: 10.1136/ard.2003.016154
166. Miller LE, Weidler C, Falk W, Angele P, Schaumburger J, Schölmerich J, et al. Increased prevalence of semaphorin 3C, a repellent of sympathetic nerve fibers, in the synovial tissue of patients with rheumatoid arthritis. *Arthritis Rheum*. (2004) 50:1156–63. doi: 10.1002/art.20110
167. Petersen LE, Baptista TSA, Molina JK, Motta JG, do Prado A, Piovesan DM, et al. Cognitive impairment in rheumatoid arthritis: role of lymphocyte subsets, cytokines and neurotrophic factors. *Clin Rheumatol*. (2018) 37:1171–81. doi: 10.1007/s10067-018-3990-9
168. del Rey A, Wolff C, Wildmann J, Randolf A, Hahnel A, Besedovsky HO, et al. Disrupted brain-immune system-joint communication during experimental arthritis. *Arthritis Rheum*. (2008) 58:3090–9. doi: 10.1002/art.23869
169. del Rey A, Wolff C, Wildmann J, Randolf A, Straub RH, Besedovsky HO. When immune-neuro-endocrine interactions are disrupted: experimentally induced arthritis as an example. *Neuroimmunomodulation*. (2010) 17:165–8. doi: 10.1159/000258714
170. Wolff C, Straub RH, Hahnel A, Randolf A, Wildmann J, Besedovsky HO, et al. Mimicking disruption of brain-immune system-joint communication results in collagen type II-induced arthritis in non-susceptible PVG rats. *Mol Cell Endocrinol*. (2015) 415:56–63. doi: 10.1016/j.mce.2015.08.005
171. Levick JR. Microvascular architecture and exchange in synovial joints. *Microcirculation*. (1995) 2:217–33. doi: 10.3109/10739689509146768
172. Ferrell WR, Khoshbaten A. Responses of blood vessels in the rabbit knee to electrical stimulation of the joint capsule. *J Physiol*. (1990) 423:569–78. doi: 10.1113/jphysiol.1990.sp018040
173. Pereira PC, Navarro EC. Challenges and perspectives of Chagas disease: a review. *J Venom Anim Toxins Incl Trop Dis*. (2013) 19:34. doi: 10.1186/1678-9199-19-34
174. Malik LH, Singh GD, Amsterdam EA. Chagas heart disease: an update. *Am J Med*. (2015) 128:1251.e7–9. doi: 10.1016/j.amjmed.2015.04.036
175. Lidani KCF, Andrade FA, Bavia L, Damasceno FS, Beltrame MH, Messias-Reason IJ, et al. Chagas disease: from discovery to a worldwide health problem. *Front Public Health*. (2019) 7:166. doi: 10.3389/fpubh.2019.00166
176. Meneghelli UG. Chagas' disease: a model of denervation in the study of digestive tract motility. *Braz J Med Biol Res*. (1985) 18:255–64.
177. Pérez-Molina JA, Molina I. Chagas disease. *Lancet*. (2018) 391:82–94. doi: 10.1016/S0140-6736(17)31612-4
178. Chavan SS, Tracey KJ. Essential neuroscience in immunology. *J Immunol*. (2017) 198:3389–97. doi: 10.4049/jimmunol.1601613
179. Pavlov VA, Chavan SS, Tracey KJ. Molecular and functional neuroscience in immunity. *Annu Rev Immunol*. (2018) 36:783–812. doi: 10.1146/annurev-immunol-042617-053158
180. McMahon SB, La Russa F, Bennett DL. Crosstalk between the nociceptive and immune systems in host defence and disease. *Nat Rev Neurosci*. (2015) 16:389–402. doi: 10.1038/nrn3946
181. Pinho-Ribeiro FA, Verri WA Jr, Chiu IM. Nociceptor sensory neuron-immune interactions in pain and inflammation. *Trends Immunol*. (2017) 38:5–19. doi: 10.1016/j.it.2016.10.001
182. Pearse AG. The cytochemistry and ultrastructure of polypeptide hormone-producing cells of the APUD series and the embryologic, physiologic and pathologic implications of the concept. *J Histochem Cytochem*. (1969) 17:303–13. doi: 10.1177/17.5.303
183. Abbas AK, Lichtman AH, Pillai S. *Cellular and Molecular Immunology*. 9th ed. Philadelphia, PA: Saunders Elsevier (2017).
184. Herman A, Kappler JW, Marrack P, Pullen AM. Superantigens: mechanism of T-cell stimulation and role in immune responses. *Annu Rev Immunol*. (1991) 9:745–72. doi: 10.1146/annurev.iy.09.040191.003525
185. MacDonald HR, Lees RK, Baschieri S, Herrmann T, Lussow AR. Peripheral T-cell reactivity to bacterial superantigens in vivo: the response/anergy paradox. *Immunol Rev*. (1993) 133:105–17. doi: 10.1111/j.1600-065X.1993.tb01512.x
186. del Rey A, Kabiersch A, Petzoldt S, Randolf A, Besedovsky HO. Sympathetic innervation affects superantigen-induced decrease in CD4V beta 8 cells in the spleen. *Ann N Y Acad Sci*. (2000) 917:575–81. doi: 10.1111/j.1749–6632.2000.tb05423.x
187. del Rey A, Kabiersch A, Petzoldt S, Besedovsky HO. Involvement of noradrenergic nerves in the activation and clonal deletion of T cells stimulated by superantigen *in vivo*. *J Neuroimmunol*. (2002) 127:44–53. doi: 10.1016/S0165-5728(02)00096-6

188. Alaniz RC, Thomas SA, Perez-Melgosa M, Mueller K, Farr AG, Palmiter RD, et al. Dopamine beta-hydroxylase deficiency impairs cellular immunity. *Proc Natl Acad Sci USA*. (1999) 96:2274–8. doi: 10.1073/pnas.96.5.2274
189. Barrios-Payán J, Revuelta A, Mata-Espinosa D, Marquina-Castillo B, Villanueva EB, Gutiérrez ME, et al. The contribution of the sympathetic nervous system to the immunopathology of experimental pulmonary tuberculosis. *J Neuroimmunol.* (2016) 298:98–105. doi: 10.1016/j.jneuroim.2016.07.012
190. Pacheco-López G, Niemi MB, Kou W, Bildhäuser A, Gross CM, Goebel MU, et al. Central catecholamine depletion inhibits peripheral lymphocyte responsiveness in spleen and blood. *J Neurochem*. (2003) 86:1024–31. doi: 10.1046/j.1471–4159.2003.01914.x
191. Filipov NM, Cao L, Seegal RF, Lawrence DA. Compromised peripheral immunity of mice injected intrastriatally with six-hydroxydopamine. *J Neuroimmunol*. (2002) 132:129–39. doi: 10.1016/S0165-5728(02)00321-1
192. ThyagaRajan S, Madden KS, Teruya B, Stevens SY, Felten DL, Bellinger DL. Age-associated alterations in sympathetic noradrenergic innervation of primary and secondary lymphoid organs in female Fischer 344 rats. *J Neuroimmunol*. (2011) 233:54–64. doi: 10.1016/j.jneuroim.2010.11.012
193. Wirth T, Westendorf AM, Bloemker D, Wildmann J, Engler H, Mollerus S, et al. The sympathetic nervous system modulates $CD4^+Foxp3^+$ regulatory T cells via noradrenaline-dependent apoptosis in a murine model of lymphoproliferative disease. *Brain Behav Immun.* (2014) 38:100–10. doi: 10.1016/j.bbi.2014.01.007
194. Bhowmick S, Singh A, Flavell RA, Clark RB, O'Rourke J, Cone RE. The sympathetic nervous system modulates $CD4^+FoxP3^+$ regulatory T cells via a TGF-β-dependent mechanism. *J Leukoc Biol.* (2009) 86:1275–83. doi: 10.1189/jlb.0209107
195. Prass K, Meisel C, Höflich C, Braun J, Halle E, Wolf T, et al. Stroke-induced immunodeficiency promotes spontaneous bacterial infections and is mediated by sympathetic activation reversal by poststroke T helper cell type 1-like immunostimulation. *J Exp Med.* (2003) 198:725–36. doi: 10.1084/jem.20021098
196. Meisel C, Schwab JM, Prass K, Meisel A, Dirnagl U. Central nervous system injury-induced immune deficiency syndrome. *Nat Rev Neurosci*. (2005) 6:775–86. doi: 10.1038/nrn1765
197. Prass K, Braun JS, Dirnagl U, Meisel C, Meisel A. Stroke propagates bacterial aspiration to pneumonia in a model of cerebral ischemia. *Stroke.* (2006) 37:2607–12. doi: 10.1161/01.STR.0000240409.68739.2b
198. Walter U, Kolbaske S, Patejdl R, Steinhagen V, Abu-Mugheisib M, Grossmann A, et al. Insular stroke is associated with acute sympathetic hyperactivation and immunodepression. *Eur J Neurol.* (2013) 20:153–9. doi: 10.1111/j.1468–1331.2012.03818.x
199. Winklewski PJ, Radkowski M, Demkow U. Cross-talk between the inflammatory response, sympathetic activation and pulmonary infection in the ischemic stroke. *J Neuroinflammation.* (2014) 11:213. doi: 10.1186/s12974-014-0213-4
200. Allison DJ, Ditor DS. Immune dysfunction and chronic inflammation following spinal cord injury. *Spinal Cord*. (2015) 53:14–8. doi: 10.1038/sc.2014.184
201. Tibbs PA, Young B, Ziegler MG, McAllister RG Jr. Studies of experimental cervical spinal cord transection. Part II: Plasma norepinephrine levels after acute cervical spinal cord transection. *J Neurosurg.* (1979) 50:629–32. doi: 10.3171/jns.1979.50.5.0629
202. Reiche EM, Nunes SO, Morimoto HK. Stress, depression, the immune system, and cancer. *Lancet Oncol.* (2004) 5:617–25. doi: 10.1016/S1470-2045(04)01597-9
203. Veith RC, Lewis N, Linares OA, Barnes RF, Raskind MA, Villacres EC, et al. Sympathetic nervous system activity in major depression. Basal and desipramine-induced alterations in plasma norepinephrine kinetics. *Arch Gen Psychiatry.* (1994) 51:411–22. doi: 10.1001/archpsyc.1994.03950050071008
204. Hernandez ME, Martinez-Mota L, Salinas C, Marquez-Velasco R, Hernandez-Chan NG, Morales-Montor J, et al. Chronic stress induces structural alterations in splenic lymphoid tissue that are associated with changes in corticosterone levels in wistar-kyoto rats. *Biomed Res Int.* (2013) 2013:868742. doi: 10.1155/2013/868742
205. Thompson M, Bywaters EG. Unilateral rheumatoid arthritis following hemiplegia. *Ann Rheum Dis*. (1962) 21:370–7. doi: 10.1136/ard.21.4.370
206. Sethi S, Sequeira W. Sparing effect of hemiplegia on scleroderma. *Ann Rheum Dis*. (1990) 49:999–1000. doi: 10.1136/ard.49.12.999
207. Veale D, Farrell M, Fitzgerald O. Mechanism of joint sparing in a patient with unilateral psoriatic arthritis and a longstanding hemiplegia. *Br J Rheumatol.* (1993) 32:413–6. doi: 10.1093/rheumatology/32.5.413
208. Dolan AL. Asymmetric rheumatoid vasculitis in a hemiplegic patient. *Ann Rheum Dis*. (1995) 54:532. doi: 10.1136/ard.54.6.532
209. Lapadula G, Iannone F, Zuccaro C, Covelli M, Grattagliano V, Pipitone V. Recovery of erosive rheumatoid arthritis after human immunodeficiency virus-1 infection and hemiplegia. *J Rheumatol.* (1997) 24:747–51.
210. Herfort RA. Extended sympathectomy in the treatment of advanced rheumatoid arthritis; a preliminary report. *N Y State J Med.* (1956) 56:1292–4.
211. Tarkowski E, Naver H, Wallin BG, Blomstrand C, Tarkowski A. Lateralization of T-lymphocyte responses in patients with stroke. Effect of sympathetic dysfunction? *Stroke.* (1995) 26:57–62. doi: 10.1161/01.STR.26.1.57
212. Aloe L, Tuveri MA, Levi-Montalcini R. Studies on carrageenan-induced arthritis in adult rats: presence of nerve growth factor and role of sympathetic innervation. *Rheumatol Int*. (1992) 12:213–6. doi: 10.1007/BF00302155
213. Härle P, Möbius D, Carr DJ, Schölmerich J, Straub RH. An opposing time-dependent immune-modulating effect of the sympathetic nervous system conferred by altering the cytokine profile in the local lymph nodes and spleen of mice with type II collagen-induced arthritis. *Arthritis Rheum*. (2005) 52:1305–13. doi: 10.1002/art.20987
214. Stangenberg L, Burzyn D, Binstadt BA, Weissleder R, Mahmood U, Benoist C, et al. Denervation protects limbs from inflammatory arthritis via an impact on the microvasculature. *Proc Natl Acad Sci USA*. (2014) 111:11419–24. doi: 10.1073/pnas.1410854111
215. del Rey A, Besedovsky HO. Immune-neuro-endocrine reflexes, circuits, and networks: physiologic and evolutionary implications. *Front Horm Res*. (2017) 48:1–18. doi: 10.1159/000452902
216. MacNeil BJ, Jansen AH, Greenberg AH, Nance DM. Activation and selectivity of splenic sympathetic nerve electrical activity response to bacterial endotoxin. *Am J Physiol*. (1996) 270:R264–70. doi: 10.1152/ajpregu.1996.270.1.R264
217. Pardini BJ, Jones SB, Filkins JP. Cardiac and splenic norepinephrine turnovers in endotoxic rats. *Am J Physiol*. (1983) 245:H276–83. doi: 10.1152/ajpheart.1983.245.2.H276
218. Fuchs BA, Campbell KS, Munson AE. Norepinephrine and serotonin content of the murine spleen: its relationship to lymphocyte beta-adrenergic receptor density and the humoral immune response *in vivo* and *in vitro*. *Cell Immunol.* (1988) 117:339–51. doi: 10.1016/0008-8749(88)90123-2
219. Kohm AP, Tang Y, Sanders VM, Jones SB. Activation of antigen-specific CD4+ Th2 cells and B cells *in vivo* increases norepinephrine release in the spleen and bone marrow. *J Immunol.* (2000) 165:725–33. doi: 10.4049/jimmunol.165.2.725
220. Kin NW, Sanders VM. It takes nerve to tell T and B cells what to do. *J Leukoc Biol*. (2006) 79:1093–104. doi: 10.1189/jlb.1105625
221. Thellin O, Heinen E. Pregnancy and the immune system: between tolerance and rejection. *Toxicology*. (2003) 185:179–84. doi: 10.1016/S0300-483X(02)00607-8
222. Koch CA, Platt JL. Natural mechanisms for evading graft rejection: the fetus as an allograft. *Springer Semin Immunopathol*. (2003) 25:95–117. doi: 10.1007/s00281-003-0136-0
223. Guleria I, Sayegh MH. Maternal acceptance of the fetus: true human tolerance. *J Immunol.* (2007) 178:3345–51. doi: 10.4049/jimmunol.178.6.3345
224. Samstein RM, Josefowicz SZ, Arvey A, Treuting PM, Rudensky AY. Extrathymic generation of regulatory T cells in placental mammals mitigates maternal-fetal conflict. *Cell*. (2012) 150:29–38. doi: 10.1016/j.cell.2012.05.031
225. Owman C. Pregnancy induces degenerative and regenerative changes in the autonomic innervation of the female reproductive tract. *Ciba Found Symp*. (1981) 83:252–79. doi: 10.1002/9780470720653.ch13

226. Varol FG, Duchemin AM, Neff NH, Hadjiconstantinou M. Nerve growth factor (NGF) and NGF mRNA change in rat uterus during pregnancy. *Neurosci Lett*. (2000) 294:58–62. doi: 10.1016/S0304-3940(00)01533-0
227. Zoubina EV, Smith PG. Sympathetic hyperinnervation of the uterus in the estrogen receptor alpha knock-out mouse. *Neuroscience*. (2001) 103:237–44. doi: 10.1016/S0306-4522(00)00549-2
228. Krizsan-Agbas D, Pedchenko T, Hasan W, Smith PG. Oestrogen regulates sympathetic neurite outgrowth by modulating brain derived neurotrophic factor synthesis and release by the rodent uterus. *Eur J Neurosci*. (2003) 18:2760–8. doi: 10.1111/j.1460–9568.2003.03029.x
229. Richeri A, Bianchimano P, Mármol NM, Viettro L, Cowen T, Brauer MM. Plasticity in rat uterine sympathetic nerves: the role of TrkA and p75 nerve growth factor receptors. *J Anat*. (2005) 207:125–34. doi: 10.1111/j.1469–7580.2005.00435.x
230. Brauer MM. Cellular and molecular mechanisms underlying plasticity in uterine sympathetic nerves. *Auton Neurosci*. (2008) 140:1–16. doi: 10.1016/j.autneu.2008.02.002
231. Latini C, Frontini A, Morroni M, Marzioni D, Castellucci M, Smith PG. Remodeling of uterine innervation. *Cell Tissue Res*. (2008) 334:1–6. doi: 10.1007/s00441-008-0657-x
232. Brauer MM, Smith PG. Estrogen and female reproductive tract innervation: cellular and molecular mechanisms of autonomic neuroplasticity. *Auton Neurosci*. (2015) 187:1–17. doi: 10.1016/j.autneu.2014.11.009
233. Brauer MM. Plasticity in uterine innervation: state of the art. *Curr Protein Pept Sci*. (2017) 18:108–19. doi: 10.2174/1389203717666160322145411
234. Maestroni GJ. Dendritic cell migration controlled by alpha 1b-adrenergic receptors. *J Immunol*. (2000) 165:6743–7. doi: 10.4049/jimmunol.165.12.6743
235. Maestroni GJ, Mazzola P. Langerhans cells beta 2-adrenoceptors: role in migration, cytokine production, Th priming and contact hypersensitivity. *J Neuroimmunol*. (2003) 144:91–9. doi: 10.1016/j.jneuroim.2003.08.039
236. Maestroni GJ. Sympathetic nervous system influence on the innate immune response. *Ann N Y Acad Sci*. (2006) 1069:195–207. doi: 10.1196/annals.1351.017
237. Maestroni GJ. Short exposure of maturing, bone marrow-derived dendritic cells to norepinephrine: impact on kinetics of cytokine production and Th development. *J Neuroimmunol*. (2002) 129:106–14. doi: 10.1016/S0165-5728(02)00188-1
238. Maestroni GJ. Adrenergic modulation of dendritic cells function: relevance for the immune homeostasis. *Curr Neurovasc Res*. (2005) 2:169–73. doi: 10.2174/1567202053586776
239. Manni M, Granstein RD, Maestroni G. β2-Adrenergic agonists bias TLR-2 and NOD2 activated dendritic cells towards inducing an IL-17 immune response. *Cytokine*. (2011) 55:380–6. doi: 10.1016/j.cyto.2011.05.013
240. Yanagawa Y, Matsumoto M, Togashi H. Enhanced dendritic cell antigen uptake via α_2 adrenoceptor-mediated PI3K activation following brief exposure to noradrenaline. *J Immunol*. (2010) 185:5762–8. doi: 10.4049/jimmunol.1001899
241. Nakano K, Higashi T, Takagi R, Hashimoto K, Tanaka Y, Matsushita S. Dopamine released by dendritic cells polarizes Th2 differentiation. *Int Immunol*. (2009) 21:645–54. doi: 10.1093/intimm/dxp033
242. Prado C, Contreras F, González H, Díaz P, Elgueta D, Barrientos M, et al. Stimulation of dopamine receptor D5 expressed on dendritic cells potentiates Th17-mediated immunity. *J Immunol*. (2012) 188:3062–70. doi: 10.4049/jimmunol.1103096
243. Takenaka MC, Guereschi MG, Basso AS. Neuroimmune interactions: dendritic cell modulation by the sympathetic nervous system. *Semin Immunopathol*. (2017) 39:165–176. doi: 10.1007/s00281-016-0590-0
244. Burnstock G. Cotransmission in the autonomic nervous system. *Handb Clin Neurol*. (2013) 117:23–35. doi: 10.1016/B978-0-444-53491–0.00003-1
245. Beresford L, Orange O, Bell EB, Miyan JA. Nerve fibres are required to evoke a contact sensitivity response in mice. *Immunology*. (2004) 111:118–25. doi: 10.1111/j.1365–2567.2004.01786.x
246. Alonso R, Flament H, Lemoine S, Sedlik C, Bottasso E, Péguillet I, et al. Induction of anergic or regulatory tumor-specific CD4+ T cells in the tumor-draining lymph node. *Nat Commun*. (2018) 9:2113. doi: 10.1038/s41467-018-04524-x
247. Mowat AM. Anatomical basis of tolerance and immunity to intestinal antigens. *Nat Rev Immunol*. (2003) 3:331–41. doi: 10.1038/nri1057
248. Holmgren J, Czerkinsky C. Mucosal immunity and vaccines. *Nat Med*. (2005) 11:S45–53. doi: 10.1038/nm1213

Conflict of Interest Statement: The author declares that the research was conducted in the absence of any commercial or financial relationships that could be construed as a potential conflict of interest.

frontiers in Endocrinology

HYPOTHESIS AND THEORY
published: 20 September 2019
doi: 10.3389/fendo.2019.00632

Toward the Existence of a Sympathetic Neuroplasticity Adaptive Mechanism Influencing the Immune Response. A Hypothetical View—Part I

*Emanuel Bottasso**

Department of Pathology and Physiology, Faculty of Medicine, Centro de Altos Estudios en Ciencias Humanas y de la Salud, Universidad Abierta Interamericana, Rosario, Argentina

The nervous system exerts a profound influence on the function of the immune system (IS), mainly through the sympathetic arm of the autonomic nervous system. In fact, the sympathetic nervous system richly innervates secondary lymphoid organs (SLOs) such as the spleen and lymph nodes. For decades, different research groups working in the field have consistently reported changes in the sympathetic innervation of the SLOs during the activation of the IS, which are characterized by a decreased noradrenergic activity and retraction of these fibers. Most of these groups interpreted these changes as a pathological phenomenon, referred to as "damage" or "injury" of the noradrenergic fibers. Some of them postulated that this "injury" was probably due to toxic effects of released endogenous mediators. Others, working on animal models of chronic stimulation of the IS, linked it to the very chronic nature of processes. Unlike these views, this first part of the present work reviews evidence which supports the hypothesis of a specific adaptive mechanism of neural plasticity from sympathetic fibers innervating SLOs, encompassing structural and functional changes of noradrenergic nerves. This plasticity mechanism would involve segmental retraction and degeneration of these fibers during the activation of the IS with subsequent regeneration once the steady state is recovered. The candidate molecules likely to mediate this phenomenon are also here introduced. The second part will extend this view as to the potential changes in sympathetic innervation likely to occur in inflamed non-lymphoid peripheral tissues and its possible immunological implications.

Keywords: neuro-immune interaction, sympathetic fibers, secondary lymphoid organs, neural plasticity, semaphorins, neurotrophins

OPEN ACCESS

Edited by:
Ana Rosa Pérez, National Council for Scientific and Technical Research (CONICET), Argentina

Reviewed by:
Lenin Pavón, National Institute of Psychiatry Ramon de la Fuente Muñiz (INPRFM), Mexico
Moisés Evandro Bauer, Pontifical Catholic University of Rio Grande do Sul, Brazil
Ciro De Luca, Second University of Naples, Italy

***Correspondence:**
Emanuel Bottasso
emanuelbottasso@hotmail.com

Specialty section:
This article was submitted to Neuroendocrine Science, a section of the journal Frontiers in Endocrinology

Received: *30 April 2019*
Accepted: *30 August 2019*
Published: *20 September 2019*

Citation:
Bottasso E (2019) Toward the Existence of a Sympathetic Neuroplasticity Adaptive Mechanism Influencing the Immune Response. A Hypothetical View—Part I. Front. Endocrinol. 10:632. doi: 10.3389/fendo.2019.00632

INTRODUCTION

The nervous (NS) and immune (IS) systems have aroused increasing interest in biomedical research during the last 50 years accompanied by important advances in the understanding of their functioning. Since the 1970s many research groups have attempted to understand the complex relationship between both systems and how the NS modulates the immune response, considering that the IS works in a physiological framework instead of being a self-regulated

system. The two major pathways involved in such neuroendocrine-immune interactions are the hypothalamic-pituitary-adrenal (HPA) axis and the autonomic nervous system (ANS), mainly the sympathetic nervous system -SNS- [reviewed in (1, 2)]. However, the proper mechanisms mediating this crosstalk are only partly understood. The present review will provide some clues compatible with the existence of a still hypothetical neural plasticity mechanism arising during the development of an immune response in secondary lymphoid organs (SLOs), probably influential in immunological terms.

Sympathetic Innervation of SLOs

In 1984 Felten et al. (3) made a detailed description of the sympathetic innervation of mouse lymph nodes by means of fluorescent histochemistry. Noradrenergic fibers enter the hilus and distribute either into a subcapsular nerve plexus or travel via blood vessels through the medullary cords. These fibers go along with small vessels into the parenchyma of paracortical region (the T zone, where the antigenic presentation takes place) and cortical region (the B zone), surrounding the lymphoid follicles. Individual lymph nodes receive their sympathetic input from postganglionic neurons depending on the region where this lymphoid organ is located (4).

After these initial studies, noradrenergic innervation in the rat spleen was identified by the same group by using immunohistochemistry for tyrosine-β-hydroxylase -TβH- (the rate-limiting enzyme of catecholamine biosynthesis and specific marker for sympathetic fibers) and electron microscopy (5–7). Noradrenergic fibers enter the spleen around the splenic artery, travel with the vasculature in plexuses, and continue along the trabeculae in trabecular plexuses. Fibers from both the vascular and trabecular plexuses go into the white pulp and continue along the central artery and its branches. Noradrenergic varicosities radiate from these plexuses into the T zone, that is, the periarterial lymphatic sheath (PALS). The B zone is also innervated, and the red pulp contains scattered fibers, primarily associated with the plexuses along trabeculae and surrounding tissues. The well-characterized co-transmission phenomenon of sympathetic fibers, assures the release of neuropeptide Y (NPY) and adenosine triphosphate (ATP) together with adrenaline and noradrenaline (NA) by the sympathetic terminals and varicosities (8), for which NPY positive fibers can also be identified in the rat spleen (9). In addition, the prevertebral sympathetic ganglia associated with the celiac-mesenteric plexus were found to provide the major sympathetic input to the spleen (10). A similar noradrenergic innervation pattern has recently been demonstrated in the human spleen (11).

NA released from the sympathetic nerves mediate its effects by primarily interacting with the α- and β-adrenergic receptors (12, 13) expressed on immune cells (4). Furthermore, immune cells also express functional purinergic (14–16) and NPY-Y receptors (17, 18), allowing ATP and NPY to respectively interact with them. A non-synaptic neurotransmission has been suggested at this level, so the released neurotransmitters may act in a paracrine fashion (19), with no synaptic neuro-immune communication being demonstrated so far (20).

Changes in Noradrenergic Innervation of SLOs During the Immune Response

Upon activation, the IS elicits a rapid and selective increase in splenic sympathetic activity in the early phase of the immune response (21–24). Conversely, many studies seem to indicate that once the IS becomes fully activated, such sympathetic activity significantly decreases in SLOs. Pioneering work from Besedovsky and del Rey's group (25, 26) described a very important decrease in NA content in lymphoid organs like the spleen and lymph nodes during the IS activation. They initially showed that 3 days after challenging rats with a harmless antigen such as sheep red blood cells -the timepoint when the IS begins to get fully activated- there was a substantial decline of NA in SLOs. Following that, it was observed that specific-pathogen-free rats, which usually have contact with environmental antigens and therefore possess a stimulated IS, had lower concentrations of NA within their spleens, compared to germ-free rats from the same strain. Importantly, this decrease in NA was observed regardless of the results were expressed as NA content per gram tissue or per total spleen. There were no changes in NA content from non-lymphoid organs.

Expanding these studies (27), the same group also reported a positive correlation between the magnitude of the immune response and the decrease of splenic NA. Investigations on whether the development of sympathetic innervation in the spleen was affected by lymphoid cells (28), revealed no difference in NA content in the spleen from newborn athymic nude mice and normal thymus-bearing littermates, but demonstrated higher NA levels in 7-, 11-, and 21-day old athymic mice. Remarkably, the reconstitution of newborn nude mice by thymus transplantation or thymocyte injection resulted in splenic NA levels comparable to those seen in normal mice. Fluorescence histochemistry for the visualization of splenic sympathetic fibers showed a higher number of fluorescent fibers and enhanced fluorescence intensity within the spleens from 21-day old athymic mice, compared to normal counterparts or thymus-grafted mice.

Following these demonstrations, other studies consistently observed a decreased sympathetic activity in different animal models, both during acute and chronic immune responses. For instance, decreased levels of NA were observed in the spleens of mice challenged with staphylococcal enterotoxin B superantigen (29). In the same way, MRL-lpr/lpr male and female mice -lacking functional Fas expression and prone to develop lymphoproliferative autoimmune diseases- presented decreased levels of splenic NA prior to the onset of splenomegaly (30–32). Decreased levels of splenic NA were also observed in acute *Trypanosoma cruzi*-infected mice (33), in a murine AIDS model induced by the LP-BM5 mixture of murine retroviruses (34), and in Lewis rats with adjuvant-induced arthritis (35). More recently, a marked loss of sympathetic noradrenergic nerves in patients who died from sepsis has also been shown (11). In fact, spleens from half of septic patients lacked noradrenergic fibers whereas presence of these nerves from the septic group was significantly reduced as compared to control samples obtained from patients with no inflammatory diseases.

Some of these studies also assessed the presence of noradrenergic fibers, by fluorescence histochemistry for catecholamines (28, 30), immunohistochemistry for TβH (11, 32–34) or both (35). In all cases, there was a consistently marked decrease in sympathetic fibers in the non-vascular areas within the spleen during the IS activation. In some studies fibers were only present around vascular structures whereas in other samples only very rare positive fibers were found. Interestingly, one of these studies (34) assessed total nerve fibers density through immunohistochemistry for protein gene product 9.5 (PGP 9.5), a constitutive protein found in the cytoplasm of all central and peripheral neurons, whose presence is independent of neural activity. The PGP 9.5 staining pattern resulted to be very similar to the TβH one, that is, a much less PGP 9.5 staining in spleens from mice in the acute phase of the viral infection, compared to control spleens. Also, PGP 9.5 positive nerve fibers were rarely found once the IS was already activated.

Most researchers regarded this decreased sympathetic activity as a pathological process, referred to as an "injury," "damage," or even "destruction" of sympathetic fibers within the spleen during immune activation. In this sense, different hypotheses were postulated concerning possible toxic effects of the high levels of NA released at the very onset of the response, prior to full activation of the IS, or oxidative stress caused by the immune response itself. The use of models of chronic inflammation led other research groups to propose that the phenomenon was due to the chronicity of the process. In this regard, Besedovsky and del Rey interpreted this observation, from the very beginning, as a part of a physiological mechanism, by which the "*decrease in noradrenergic activity late during the immune response*" was "*a way of releasing immune cells from the inhibitory effects of NA, favoring the take-off of the adaptive response*" (36).

Based on currently available evidence, the existence of an adaptive mechanism of neural plasticity involving sympathetic terminals retraction during IS activation within SLOs can be envisioned (**Figure 1**). In fact, activated immune cells can produce different molecules likely to mediate axonal retraction and/or segmental axonal degeneration of sympathetic fibers innervating SLOs. On the other hand, in an inflammatory milieu, cytokines can also stimulate the production of these same molecules by other non-immune cells. Within this hypothetical neural plasticity adaptive mechanism that may modify the way by which the NS modulate the IS functioning, two major compounds are quite likely to play a role, semaphorins and neurotrophins (see **Box 1** and **Table 1**).

On the Potential Role of Semaphorins and Neurotrophins

There is reason to believe that semaphorins and their receptors may be involved in potential changes in the innervation of SLOs, i.e., in the spleen, during activation of the IS leading to a retraction in sympathetic fibers. Plexin A3 and Plexin A4 (receptors for 3A and 3F Semaphorins) are expressed in sympathetic fibers together with Neuropilin-1 and Neuropilin-2, which collectively are essential for the migration of sympathetic neurons during the development of the ANS (105–107). *In vitro* experiments showed that both Sema3A and Sema3F can repel dissociated neurons from wild-type sympathetic superior cervical ganglia (108). Apparently, Plexin-A3 would be preferentially used in Sema3F/Neuropilin-2 signaling while Plexin-A4 primarily signals downstream of Sema3A/Neuropilin-1. Production of Semaphorin 3A during activation of the IS (54) opens the possibility that this molecule could interact with its canonical receptors Plexin A4 and Neuropilin 1, conceivable expressed in the sympathetic fibers innervating the SLOs, and hence mediating their retraction. On the other hand, in an inflammatory milieu, semaphorins may not only be produced by the immune cells themselves but by other cell types under the influence of cytokines, as reported in other experimental settings (109). Moreover, it cannot be excluded that cytokines induce the expression of other types of plexins or neuropilins on the sympathetic fibers on which other types of semaphorins may act. Alternatively, semaphorins produced during an activation of the IS may bind receptors different from the canonical ones on sympathetic nerves, like the soluble form of 4D semaphorin interacting with CD72 (110).

The proper mechanism by which semaphorins exert their effects has not been fully clarified. It was first described that by binding to plexins (using neuropilins as co-receptors for type 3 semaphorins), semaphorins induce a dramatic depolymerization of the actin cytoskeleton, which normally forms lamellipodia and filipodia (111, 112). A depolymerization of the fascin-associated actin bundles may afford the substrate for actomyosin contractions, thus mediating retraction. In addition, plexin activation leads to a fast disassembling of integrin-based focal adhesive structures, preventing cell adhesion to components of the extracellular matrix (113). Thus, the neurite's entire structure collapses and retracts. The integrity of the actin cytoskeleton is not only essential for the axonal growth cone, but also indispensable at the synaptic terminal level for the maintenance and regulation of vesicles pools, their attachment to the active zone and their exocytosis, thus allowing neurotransmitters release (114). Hence, it may be speculated that semaphorins effects on sympathetic terminals within SLOs not only led to their retraction and collapse but may also elicit a rapid interruption of the release of different neurotransmitters.

Finally, the semaphorins and plexins/neuropilins system can mediate both the retraction and the attraction of nerves. It has already been mentioned the case of 3A and 7A Semaphorins acting on Neuropilin-1 or on Plexin C1 from hypothalamic gonadotropin releasing hormone neurons (43, 44). Moreover, the repulsion elicited by 3D Semaphorin on growth cones of cultured *Xenopus* spinal neurons can be transformed into attraction upon pharmacological activation of the guanosine 3′, 5′-monophosphate (cGMP) and adenosine 3′, 5′-monophosphate (cAMP) signaling pathways (115). In the same way, studies in *Caenorhabditis elegans* with lowered levels of specific RAC GTPases revealed a conversion of cell movement responses to Semaphorin-1 and Plexin-1 from attraction to repulsion (116). In another interesting study, it was shown that Sema5A displays both attractive and inhibitory guidance activities on the development of *fasciculus retroflexus*, a diencephalon fiber tract from rat brains (117).

Apparently, the type-1 thrombospondin repeats domain of this semaphorin can mediate regulatory functional interactions with different components of the extracellular matrix determining how Sema5A affects neuronal growth cones. On the other hand, in the zebrafish brain Sema3D seems to conduct axons from the nucleus of the medial longitudinal fasciculus by repulsion, acting through receptors containing Neuropilin-1A (118). Unlike this, the same semaphorin seems to attract telencephalic neurons that form the anterior commissure via receptors containing Neuropilin-1A and Neuropilin-2B. Thus, axons may respond differentially to a single semaphorin, depending on their neuropilin composition. Hence, several signals involving semaphorin and plexin/neuropilin interactions may regulate actin polymerization and depolymerization causing attraction (cytoskeletal growth) or repulsion (cytoskeletal collapse), respectively. In this scenario, it may be assumed that once the immune response is terminated, different signals may concur to mediate sympathetic fibers attraction, thus favoring the reconstitution of the innervation pattern from the steady state. These may include changes in the cytokine environment, changes in the type of semaphorins produced by the immune cells themselves or by other cells under the influence of cytokines, or changes in the type of receptors expressed on sympathetic nerves.

However, regardless of their repelling or attracting action on nerve fibers, semaphorins would not be mediating the physical "disappearance" of sympathetic nerves by axonal degeneration which seems to occur within SLOs during an IS activation (11, 28, 30, 32–35). Therefore, other molecules may be acting concomitantly (**Figure 1**).

In this regard, neurotrophins and pro-neurotrophins and their receptors are likely to mediate a transient and segmental axonal degeneration of sympathetic nerves -followed by regeneration once the IS returns to a resting state. Importantly, the expression of neurotrophins in lymphocytes and other immune cells in basal conditions, along with a remarkable increase in their production after their activation is well-recognized. In 1999, activated human T cells, B cells and monocytes were shown to secrete bioactive BDNF *in vitro* (82). The same group demonstrated that in T cell lines specific for myelin autoantigens, such as myelin basic protein or myelin oligodendrocyte glycoprotein, BDNF production increased upon antigen stimulation. Moreover, BDNF immunoreactivity was also identified in inflammatory infiltrates in brain from patients

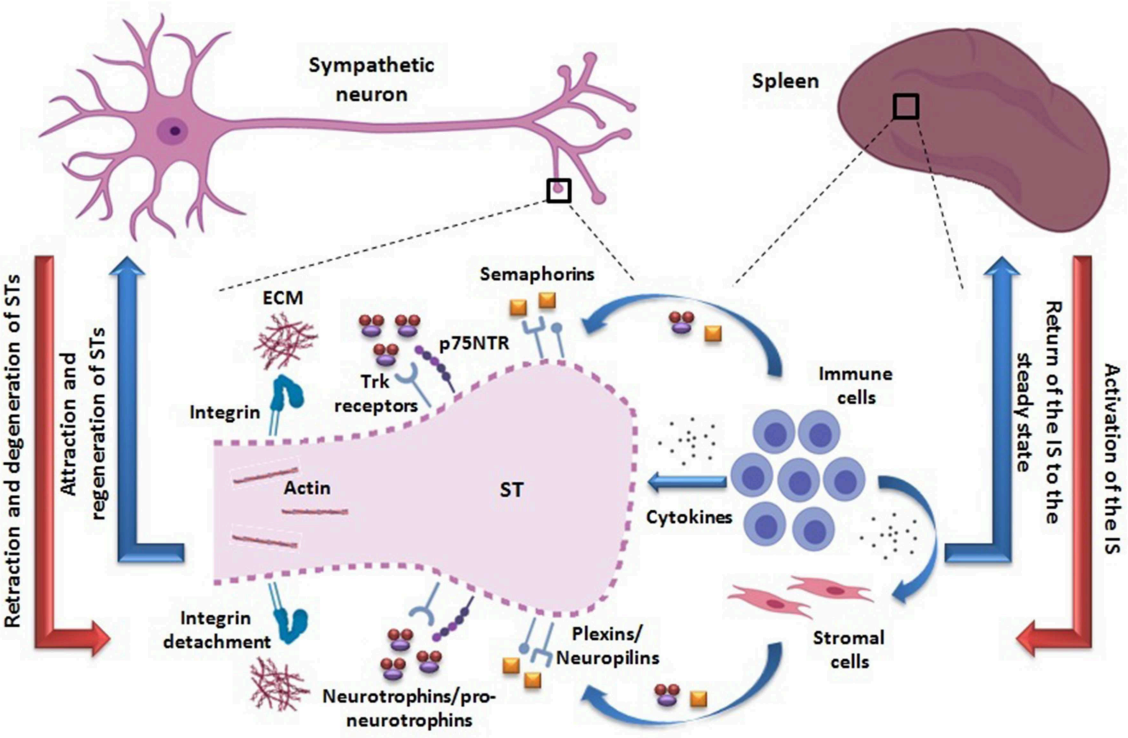

FIGURE 1 | Proposed adaptive mechanism of neural plasticity from STs innervating secondary lymphoid organs such as the spleen. The activation of the IS may be accompanied by retraction and axonal degeneration of STs (red arrows). The activated immune cells are able to produce semaphorins and pro-neurotrophins/neurotrophins, binding to their receptors -plexins/neuropilins and Trk/p75NTR, respectively- probably expressed on STs. In particular, p75NTR may be re-expressed in a pro-inflammatory milieu. The action of these molecules may lead to an inhibition of STs integrin-mediated adhesion to ECM and depolymerization of their actin cytoskeleton, thus favoring their retraction and axonal degeneration (dotted line). In addition, semaphorins and neurotrophins/pro-neurotrophins may be produced by other non-lymphoid cell types as well (i.e., stromal cells), under cytokine influence. A direct action of cytokines as playing a role on STs retraction cannot be disregarded. Once the immune response ceases, the IS returns to the steady state and STs may regenerate, recovering the usual splenic innervation pattern (blue arrows). Neural and immunological phenomena are summarized on the left and right sides, respectively. STs, sympathetic terminals; IS, immune system; Trk, tropomyosin-related kinase; p75NTR, p75 neurotrophin receptor; ECM, extracellular matrix.

BOX 1 | Semaphorins and their receptors

Semaphorins are a family of soluble, transmembrane or cell-anchored proteins that contain a common "sema" domain of about 400 amino acids [reviewed in (37–39)]. They were initially described as guiding molecules during the development of the NS, with capacity to attract or repel axonal growth cones so that they could reach the appropriate targets. They have been grouped into 8 classes based on their structural characteristics. Semaphorins of class 1 and 2 belong to invertebrates, those of class 3–7 to vertebrates and those of class 8 are coded by viruses. There are also subclasses that are designated with letters (for example, Sema3A or Sema4D) and currently there are more than 30 different types of semaphorins. Class 1, 4–6 semaphorins are transmembrane proteins, class 7 members are glycosylphosphatidylinositol-linked, while class 2, 3 and viral semaphorins are soluble proteins. Class 4, 5, and 7 semaphorins can be cleaved and released extracellularly.

Semaphorins bind receptors expressed in neurons called plexins. Plexins are grouped into four classes called A–D. Four types of plexin A, three types of plexin B, one plexin C, and one plexin D have been described. There are also two types of plexins in invertebrates. In contrast to the remaining classes, class 3 semaphorins require a co-receptor binding to signal through class A plexins (40). These co-receptors are transmembrane proteins called neuropilins. They have a short intracellular domain devoid of intrinsic catalytic activity and functioning as a ligand-binding partner in co-receptor complexes for both plexins and vascular endothelial growth factor receptors.

Beyond their role in the development of the NS (37–39, 41), these proteins continued to be expressed in the adult brain, where they are linked to processes such as the modulation of synaptic activity in the hippocampus (42). As well as participating in the modulation of intrinsic NS functions, two elegant studies (43, 44) demonstrated that the 65KDa isoform of Semaphorin 3A (produced by endothelial cells of the medial eminence of the hypothalamus) and Semaphorin 7A produced by tanycytes (in both cases under steroid stimuli) can act on Neuropilin-1 or on Plexin C1. This is followed by an attraction or retraction, respectively, of the nerve terminals of the gonadotropin releasing hormone neurons, thus favoring the release of the neurohormone toward the anterior pituitary in different phases of the ovarian cycle.

Remarkably, it has also been shown that these proteins play a role in processes unrelated to axon guidance or to synaptic plasticity, such as organogenesis, vascularization, angiogenesis, neuronal apoptosis and tumor progression (45, 46). Finally, it has been demonstrated that both semaphorins and plexins are expressed in immune cells, where they interact and exert influences on functions as diverse and critical as cell-to-cell contact, modulation of immunological synapses, regulation of immune cell activation (by serving as costimulatory molecules), proliferation, differentiation, cell migration or production of cytokines [(47, 48), reviewed in (49–51)]. For instance, a transmembrane semaphorin, 4D Semaphorin, is weakly expressed on T cells, B cells and antigen presenting cells such as dendritic cells (DCs). Its expression increases radically after activation with different immunological stimuli and in these circumstances, 4D Semaphorin suffers a proteolytic cleavage resulting a soluble form of it. 6D Semaphorin is present in T cells, B cells and NK cells, whereas 7D Semaphorin is found in activated T cells and in double positive thymocytes. Sema4A is expressed on antigen-presenting cells and Sema4C is upregulated on follicular T helper cells (52, 53). Regarding plexins, Plexin-A1 is highly expressed by mature DCs, while Plexin-A4 is located in T cells, DCs, and macrophages. Plexin-B1 is expressed on activated T cells and follicular dendritic cells. As to Plexin-B2, its expression was found in macrophages, DCs, and plasmacytoid dendritic cells, being also highly expressed by germinal center B cells (53). Plexin-D1 is present in $CD4^+$ $CD8^+$ double positive thymocytes (49, 51).

Current data on soluble semaphorins, which can be released into the extracellular medium and exert their action in the vicinity without any cell-to-cell contact, is perhaps even more intriguing for the purposes of this viewpoint. For instance, 3A Semaphorin is produced by activated T cells and one of its functions would be to inhibit the proliferation of T cells themselves and the production of cytokines (54). The same study shows that $CD4^+$ T cells express higher levels of 3A Semaphorin than $CD8^+$ T cells. Expression of 3A Semaphorin has also been observed in human blood peripheral monocytes, further increasing when monocytes are differentiated with macrophage colony-stimulating factor under conditions that promote a macrophage M2 phenotype (alternatively activated macrophages). DCs also express 3A Semaphorin and their maturation induced by both TNF-α and IL-1β or by CD40L significantly increases the expression of Sema3A mRNA (55). More recently, T-cell precursors in the thymus of humans were also found to express another soluble semaphorin, 3F Semaphorin (56).

Neurotrophins and their receptors

Since the discovery of nerve growth factor (NGF) by Rita Levi Montalcini (57), great advances have been made in the field of neurotrophins. These molecules, defined primarily as neural survival stimulants during development in sympathetic neurons, constitute a group of soluble proteins produced by many different cell types. They are called NGF, brain derived neurotrophin factor (BDNF), neurotrophin 3 (NT-3) and neurotrophin 4 (NT-4) [reviewed in (58–61)], acting on transmembrane receptors expressed primarily on neural cells: the tropomyosin-related kinase (Trk) receptors and p75 neurotrophin receptor (p75NTR). NGF binds preferably to TrkA, BDNF and NT-4 to TrkB and NT-3 to TrkC. All neurotrophins can interact with p75NTR. The interactions of neurotrophins with Trk receptors are of high affinity, whereas the binding of neurotrophins to p75NTR has a very low affinity. However, the binding of NGF to TrkA and that of BDNF to TrkB are of low affinity. Furthermore, p75NTR can act as a co-receptor by increasing the affinity of neurotrophins for Trk receptors.

The signaling systems of these receptors, mainly those of the p75NTR, are very complex and some controversies exist in this regard (62–65). Acting on Trk receptors, the neurotrophins promote cell survival and growth, mostly by stimulating the activation of PI-3 kinase-AKT and Ras-ERK pathways. On the other hand, p75NTR, a member of the tumor necrosis factor (TNF) receptor superfamily, lacks intrinsic catalytic activity and signals through a series of interactions with different proteins through its intracellular juxtamembrane and death domains. This receptor contributes to cell survival or to neurite outgrowth (by activating or regulating the NF-κB pathway and Rho activity, respectively), as well as cell migration. Nevertheless, when Trk receptors activation is reduced or absent, high levels of p75NTR expression can mediate axonal degeneration or induce apoptosis through increased ceramide production and activation of c-Jun N-terminal kinase, caspases, and p53 (66–68).

Since the binding affinity of neurotrophins to p75NTR is very low compared to their affinity for Trk receptors, the view that neurotrophins were just cell survival promotors prevailed for a long time. However, it had been proven that during development NGF and BDNF exerted functionally antagonistic actions on sympathetic neuron growth and target innervation, acting via TrkA or p75NTR to promote or inhibit growth, respectively (69). Even so, the high-affinity *bona fide* ligands of p75NTR that may mediate cell death remained largely elusive. Finally, in 2001 Lee et al. (70), showed that pro-NGF was a high-affinity ligand for p75NTR. It was also demonstrated that pro-NGF induces p75NTR-dependent apoptosis in cultured sympathetic neurons with minimal activation of TrkA-mediated differentiation or survival. Like many other proteins, neurotrophins are synthesized as proforms that are further cleaved intracellularly by furin or other proconvertases to release their mature form. Pro-neurotrophins had always been considered biologically inactive precursors until the work by Lee et al. (70) showed that neurotrophins may be released as pro-neurotrophins into the extracellular medium and then undergo extracellular cleavage by extracellular proteases such as serine protease plasmin and selective matrix metalloproteinases. Thus, the biological action of neurotrophins is regulated by proteolytic cleavage, with proforms preferentially activating p75NTR to mediate apoptosis or axonal degeneration and mature forms conversely promoting survival, axonal and dendritic growth, via Trk receptors (71).

Neurotrophins and pro-neurotrophins not only act during development but also in the adult brain, for instance, mediating synaptic plasticity. Within the hippocampus, mature BDNF facilitates long-term potentiation through TrkB, whereas long-term depression is facilitated by pro-BDNF through p75NTR activation (72–74). At the

BOX 1 | Continued

peripheral level the application of pro-BDNF induces a dramatic decrease in synaptic efficacy in the neuro-muscular plaque followed by a retraction of the presynaptic terminals, this effect being mediated by p75NTR (75). This lend support to the view that post-synaptic secretion of pro-BDNF may stabilize or cause retraction of the presynaptic terminal depending on the proteolytic conversion of this molecule to its mature form, or not.

On the other hand, vascular endothelial cells are able to synthesize BDNF (76), whereas platelets store and release it upon activation, predominately through proteinase-activated receptor-1 stimulation by thrombin, and plasmin, among other mediators (77, 78). Hemostasis and the IS are linked in different physiological and pathological conditions, mainly via the complement system. Then, some authors have proposed that these interactions are particularly relevant in adaptive and maladaptive neural plasticity within the central nervous system, at the level of the neurovascular unit (the blood-brain barrier on the one side, and neurons, glia, and extracellular matrix on the other side). Such interactions are thought to be quite influential in the development of different conditions, like Alzheimer's disease, neuro-inflammation, stroke, neoplastic, and psychiatric disorders (79–81).

Beyond these considerations, it is important to highlight the well-recognized expression of neurotrophins in different inflammatory milieu and unstimulated immune cells, further increasing upon their activation (82–95). This will constitute a central issue as to the view proposed in the present work.

TABLE 1 | Summary of different types of semaphorins and neurotrophins, along with their receptors, actions and presence in immune cells.

Molecules	Types	Receptors on neural cells	Activities	Expression on immune cells
Semaphorins	Class 1 and 2 in invertebrates; class 3, 4, 5, 6, and 7 in vertebrates; class 8 in viruses Subclasses designated with letters (i.e., Sema3A or Sema4D, etc.) Class 1 and 4–7 semaphorins are transmembrane proteins; class 2, 3 and viral semaphorins are soluble proteins Sema4D has a soluble form	Plexins: grouped into four classes (A–D), and presenting many different subtypes Neuropilins: co-receptors for class 3 semaphorins	Axon guidance molecules with capacity to attract or repel axonal growth cones Modulation of synaptic activity in the hippocampus Plasticity in uterine sympathetic nerves Modulation of hormone release in the pituitary Organogenesis, angiogenesis, neuronal apoptosis and tumor progression Many immune functions: cell-to-cell contact, modulation of immunological synapses, regulation of immune cell activation (by serving as costimulatory molecules), proliferation, differentiation, cell migration, and cytokine production	4A Semaphorin: expressed on antigen-presenting cells (52) 4C Semaphorin: upregulated on follicular T helper cells (53) 4D Semaphorin: expressed on T cells, B cells and dendritic cells (DCs), markedly increased upon activation [reviewed in (49–51)] 6D Semaphorin: present in T cells, B cells and NK cells (49–51) 7D Semaphorin: seen in activated T cells and in double positive thymocytes (49–51) 3A Semaphorin: produced by activated $CD4^+$ and $CD8^+$ T cells, human blood peripheral monocytes, macrophages and DCs (54, 55) 3F Semaphorin: present in T-cell precursors in the human thymus (56)
Neurotrophins (all of them are soluble proteins)	Nerve growth factor (NGF) Brain derived neurotrophin factor (BDNF) Neurotrophin 3 (NT-3) Neurotrophin 4 (NT-4) Pro-forms and mature forms are released. Pro-forms can be cleaved intra or extracellularly	Tropomyosin-related kinase (Trk) receptors A, B and C, high-affinity receptors for mature forms of neurotrophins p75 neurotrophin receptor (p75NTR), "low-affinity receptor," showing high affinity for pro-forms p75NTR is specifically re-expressed under cytokine influence and during injury [reviewed in (96–104)]	Mature forms promote cell survival, axonal and dendritic outgrowth, mainly via Trk receptors Neurotrophins (mainly their pro-forms) can also mediate axonal degeneration or apoptosis via p75NTR, when Trk receptors activation is reduced or absent Synaptic plasticity within the hippocampus Plasticity in uterine sympathetic nerves Immune functions: modulation of immune cells apoptosis, proliferation and cytokine production	BDNF: *in vitro* on activated human T cells, B cells and monocytes (82) NT-3, BDNF, TrkB, and TrkC: human immune cells (83) NGF, BDNF, NT-3, and NT-4/5: rat T cells, significantly increased upon antigen activation (84) BDNF, pro-BDNF, and Trk receptors: human B cells (92) TrkA: human monocytes (95) p75NTR: murine and human plasmacytoid dendritic cells (94) p75NTR and pro-BDNF: murine innate immune cells (93) Elevated levels of neurotrophins found in many different inflammatory scenarios (85–91)

These molecules are widely expressed in many different cell types, in some cases under the influence of cytokines in an inflammatory milieu.

with acute disseminated encephalitis and multiple sclerosis. By the same time, another group observed that human immune cells also produced NT-3 mRNA, secreted BDNF, and expressed their specific receptors TrkB and TrkC (83). The Th1 cytokine IL-2 stimulated the expression of TrkB mRNA but not of TrkC, whereas the Th2 cytokine IL-4 enhanced NT-3 but not BDNF mRNA expression. Following that, it was shown that rat T cells expressed NGF, BDNF, NT-3, and NT-4/5 and that the secretion

of neurotrophins by T cells was significantly increased by antigen activation (84). By then the dual role of neurotrophins and pro-neurotrophins acting on Trk receptors and p75NTR facilitating antagonistic processes was unknown (70, 71), therefore there was no interest in assessing whether immune cells released mature forms of neurotrophins or pro-neurotrophins. Moreover, since neurotrophins were thought to stimulate only neuronal survival and most of these experiments were conducted in animal models of central nervous system (CNS) inflammatory diseases, inflammatory infiltrates in conditions like multiple sclerosis were supposed to exert a "neuroprotective" role (119, 120).

The relationship between neurotrophins and immune-mediated phenomena was initially envisioned by Aloe et al. (85) and Bracci-Laudiero et al. (86) who reported elevated levels of NGF in the synovial fluid of patients with chronic arthritis and in sera from patients with systemic lupus erythematosus (SLE), in the latter case positively correlated with disease severity. More recently, it was also demonstrated that circulating levels of NGF and BDNF are increased in SLE patients, with severe lupus flares showing augmented NT-3 levels (87). Other studies also demonstrate increased values of neurotrophins in the cerebrospinal fluid of children with viral meningoencephalitis (88), in plasma from rheumatoid arthritis patients (89) as well as in many other inflammatory and autoimmune states [reviewed in (90)], including the bronchoalveolar lavage fluid of patients with pulmonary sarcoidosis (91). In this study, immunohistochemistry revealed the expression of NGF, BDNF and NT-3 in sarcoid granulomas. Again, no characterization on whether it corresponded to pro-forms or the mature ones was attempted.

Further work led to envisage different immunological functions for neurotrophins. Apparently, they would act primarily in autocrine loops on immune cells by virtue of the expression of both neurotrophins and Trk receptors on these cells. In this sense, B lymphocytes have been shown to produce and release both the mature form of BDNF and pro-BDNF to the extracellular medium that may modulate apoptosis on the same B cells (92). On the other hand, neurotrophin signaling has also been shown to regulate immune cell proliferation and cytokine secretion, via the p75NTR and TrkA receptors (93–95).

Independently of the type of neurotrophins produced and released by immune cells during activation, analyzing the expression of their receptors in neural cells in an inflammatory context is critical to support the above-stated neural plasticity hypothesis. As regards p75NTR, this receptor is widely expressed in the developing NS, including sympathetic neurons, while most cells no longer express it at adult stages. Surprisingly, many different types of injury and cellular stressors are potent inducers of p75NTR re-expression in neuronal and glial cells [reviewed in (121)]. For instance, p75NTR is up-regulated in rat dorsal root ganglion neurons after peripheral nerve transection (96), in corticospinal neurons after axotomy in mice (97), in rat retina following ischemic injury (98), in ischemic stroke in rat striatal interneurons (99), in hippocampal neurons during rodent seizures (100), in spinal cord motor neurons in murine and human amyotrophic lateral sclerosis (101), as well as in glial cells in multiple sclerosis plaques (102) and in basal forebrain neurons of patients with Alzheimer's disease (103). Interestingly, inflammatory cytokines such as IL-1β and TNF-α have been shown to up-regulate p75NTR in neurons and glial cells of the CNS (104). In this study IL-1β induced p75NTR expression via p38 MAPK in hippocampal neurons, and via p38 MAPK and NF-kB in astrocytes, whereas TNF-α induced p75NTR expression via NF-kB both in hippocampal neurons and in astrocytes. Hence, a pro-inflammatory cytokine milieu, common to some of the pathological conditions reproduced in these models of neural injury, may regulate the re-expression of p75NTR on neural cells. Whether sympathetic fibers innervating SLOs react by up-regulating p75NTR upon cytokine signals during an immune response remains and intriguing possibility.

It is worth noting that, p75NTR mediated axonal degeneration should not always be regarded as a pathological process, but as a physiological mechanism, in some cases. *In vitro* models of sympathetic axon competition revealed how winning axons release BDNF, further interacting with p75NTR on losing axons to promote their degeneration. This mechanism is essential for the normal development of neuronal circuits (122, 123). Moreover, axonal degeneration takes place in the intact rodent adult brain via a p75NTR and myelin-dependent mechanism (124), thus precluding septal cholinergic axons (where the expression of p75NTR is maintained in adult life), from an abnormal growth onto myelinated tracts, in the *corpus callosum*. In the same vein, transient loss of sympathetic nerves in SLOs should not be necessarily regarded as harmful but as part of a neural plasticity adaptive mechanism (**Figure 1**).

Accordingly, the pro-inflammatory cytokine environment present during the IS activation may lead to the re-expression of p75NTR in the sympathetic nerves innervating the SLOs, with neurotrophins produced by lymphocytes mediating a segmental and transient physiological axonal degeneration of those fibers, and hence explaining some of the former observations (11, 28, 30, 32–35). On the other hand, released cytokines may also induce the expression of neurotrophins in other non-immune cell types, further contributing to this mechanism (**Figure 1**). For instance, IL-1β, IFN-γ, and IL-4 were found to regulate NGF and BDNF expression in human culture bronchial smooth muscle cells (125) whereas NGF was significantly increased in keratinocytes during different skin inflammatory diseases, with TNF-α probably mediating this effect (126–129). As seen with semaphorins eliciting both attraction and retraction of nerve fibers, neurotrophins may promote antagonistic effects being able to mediate either degeneration or axonal growth. In this way the restoration of the innervation pattern of SLOs once the immune response is over, may be explained by modifications in different signals (i.e., changes in the cytokine environment leading to possible alterations in the expression of Trk receptors and p75NTR in sympathetic nerves, changes in the production of neurotrophins and pro-neurotrophins, or changes in factors favoring their intracellular or extracellular cleavage).

Sensitive and Parasympathetic Innervation of SLOs

Concerning sensory spleen innervation, the presence and distribution of positive fibers for substance P -SP-, one of the main neurotransmitters of sensitive fibers, was described in rats (130). In this study, SP positive nerve fibers entered the spleen

with the splenic artery in the hilar region, arborized along the venous sinuses, and extended from these larger plexuses into trabeculae and the surrounding red pulp. In the white pulp, SP positive nerve fibers were found in the marginal zone, and in the outer regions of the PALS among T lymphocytes. SP positive nerve fibers were observed in association with the splenic capsule, the central arteries of the white pulp, or the follicles. However, retrograde tracing studies were unable to find the neuronal cell bodies of such fibers in dorsal root ganglia or nodose ganglia in the rat (10). So, no definitive evidence was found for the sensory input to the spleen and according to the more influential authors in this issue, sensory neuropeptide-positive fibers identified in the spleen would not be involved in providing sensory feedback from this immune organ (4).

Although there are only a few studies on this subject, one report did obtain neuroanatomical evidence in the sense that lymph nodes may receive a sensory afferent supply (131) because retrograde tracing studies in the tracheobronchial lymph nodes of guinea pigs identified neurons in cervical dorsal root ganglia. According to some authors this may have a functional sense, since unlike the spleen, lymph nodes play fundamental roles in local immune responses of the organism (4). On the other hand, careful search of the literature revealed no studies as to possible changes in the sensitive innervation of lymph nodes, and density, quantity or distribution of SP positive fibers within the spleen during an immune activation.

In relation to cholinergic fibers, neuroanatomical evidence for a parasympathetic input to the lymph nodes or to the spleen is lacking (4, 132, 133). Nevertheless, a particular subset of splenic memory T cells has been shown to produce acetylcholine (ACh), able to elicit anti-inflammatory responses via α7 nicotinic ACh receptors on macrophages (134). Apparently, vagal nerve stimulation may result in splenic sympathetic release of NA, stimulating β2-adrenergic receptors on cholinergic T cells and thus provoking ACh release (134, 135).

AN INTEGRATIVE VIEW

The adaptive branch of the IS has the impressive capacity to produce a specific response against a given non-self-antigen upon its encounter. This response involves antigen recognition, the activation and clonal expansion of specific lymphocytes, followed by the production of cytokines or other molecular mediators, the synthesis of specific antibodies, and migration of immune cells to specific sites; collectively implying a huge energetic and metabolic cost. Provided the response eliminates the triggering insult, the entire storm ceases and the system recovers its steady state.

As stated, many observations from the last four decades have shown that, after an initial increase in sympathetic activity at the very onset of the immune response (21–24), a significant decrease of noradrenergic transmission within the SLOs occurs once the IS becomes activated (11, 25–35). Expanding the view of a physiological mechanism (36), it can be now hypothesized that such phenomena reflect the existence of an adaptive neural plasticity program of the sympathetic fibers innervating SLOs. Thus, retraction and segmental and transient axonal degeneration would occur during an ongoing immune response, with further regeneration once the response achieves its goal and the system returns to a resting state (**Figure 1**).

Axonal degeneration does occur in a physiological manner, as it was found in certain areas of the brain during development and adult life (122–124). P75NTR up-regulation was also induced by IL-1β and TNF-α, two of the major pro-inflammatory cytokines released during immune activation (104). Moreover, in different neural stress/injury situations and inflammatory scenarios, a re-expression of p75NTR was observed in diverse types of neurons and glial cells (96–103). Considering current knowledge about the p75NTR-mediated effects, many neuroscientists have wondered why the system would respond to neural injury by up-regulating a receptor capable to mediate axonal degeneration and even neuronal apoptosis. While seeming initially unsound, Ibáñez et al. (121) suggested that injury and inflammation induction of p75NTR in cells that expressed the receptor earlier in development may mirror the existence of neural plasticity programs in those situations that to some extend recapitulate a developmental mechanism. Whether sympathetic nerves innervating SLOs react by up-regulating p75NTR during an activation of the IS remains to be established. If so, the existence of a neural plasticity program working in this context would be strengthened.

Although neurotransmitters of the ANS released from the axonal terminals and varicosities are thought to act on the immune cells in a paracrine fashion [non-synaptic neurotransmission (19)], it can be speculated that the neuro-immune interface within the SLOs constitutes a sort of synapse. Therefore, the immune post-synaptic component may generate positive and negative signals that further modify, retrogradely, the structure and function of the pre-synaptic component. The existence of such post-synaptic signals has long been described, like those from the neuro-muscular plaque (136–138).

It is now clear that the NS possesses a remarkable and unexpected plasticity, allowing to modulate critical physiological functions. As above-mentioned, steroid-stimulated endothelial cells from the hypothalamic medial eminence and tanycytes produce and release different semaphorins. These molecules cause attraction or retraction of the nerve terminals of the gonadotropin releasing hormone neurons, regulating the release of the neurohormone toward the anterior pituitary in different phases of the ovarian cycle (43, 44). Another impressive example of neural plasticity, of currently unknown significance, occurs in the uterus, in which sympathetic axons degenerate or regenerate depending on whether estrogen levels rise or decline, respectively (139–147). This phenomenon was found to be mediated by different molecules produced by the myometrium under estrogen's influence, including neurotrophins and pro-neurotrophins acting on Trk receptors and p75NTR, as well as semaphorins.

The above-mentioned evidence suggests that semaphorins and neurotrophins or pro-neurotrophins, and their respective receptors, are quite likely candidates to mediate this hypothetical neural plasticity phenomenon of sympathetic fibers innervating SLOs. These molecules, essential during the development of the NS, continue to be expressed in adult life, fulfilling fundamental

and very different functions. For instance, the expression of transmembrane and soluble semaphorins and neurotrophins by activated immune cells and in different inflammatory settings was widely documented (47–56, 82–95), as did their production by non-immune cell types under the influence of cytokines in an inflammatory milieu (109, 125–129). As stated, by acting on their receptors expressed in axons, they can mediate both the collapse, retraction and degeneration of neural processes as well as their attraction and regeneration (70, 71, 115–118). Changes either in the type of molecules produced by immune cells or other cell types or in the receptor expressed in the neural processes on which they act, along with modifications in the local cytokine environment may explain such antagonistic actions. Far from exerting their actions separately, neurotrophins and semaphorins were shown to activate cellular pathways that can interact downstream (148–150). Accordingly, neurotrophins may be able, in some cases, to quickly modulate the response of a given axon to semaphorins, so that the final response would be dynamic, relying on the interaction of cytoplasmic signals elicited concurrently by both types of molecules.

The possible participation of molecules other than semaphorins and neurotrophins in this mechanism cannot be excluded. There is evidence for inflammatory cytokines to exert both positive and negative direct regulatory roles in neurogenesis, neural stem cell proliferation, fate specification, young neuron migration and neuronal maturation (151) as well as synaptic plasticity (152). On the other hand, as happened with semaphorins, netrin-1, a protein formerly described as an axon guidance molecule (153), seems to be involved in multiple physiological and pathological conditions, such as organogenesis (154), angiogenesis (155), tumorigenesis (156), and inflammation (157, 158). Netrin-1 is a bifunctional axonal guidance cue, capable of attracting or repelling developing axons via activation of different receptors (159). Interestingly, it has been shown that netrin-1 is essential for the development of arterial sympathetic innervation in mice. Netrin-1 is produced by arterial smooth muscle cells and arterial innervation required its interaction with one of its receptors on sympathetic growth cones (160). A participation of this molecule in the proposed mechanism is therefore possible.

Also, the existence of signals from de CNS contributing to this hypothetical mechanism should be considered. Very early, it was observed that the immune response elicits the activation of different areas of the CNS, such as the hypothalamus (161). In these circumstances the activation of the HPA and gonadal axes is a well-known physiological response (162, 163). Moreover, the activation of other centers within the cortico-limbic region is involved in the so-called sickness behavior (164). Hence, as different areas of the CNS become activated during an ongoing immune response, central responses may be elaborated in turn, thus affecting autonomic activity in the periphery and probably contributing to the decreased sympathetic activity during immune activation.

Much research is needed to properly demonstrate the existence of this putative neural plasticity mechanism and the processes accounting for it. Even when the intimate machinery mediating changes in sympathetic innervation in SLOs were unveiled, too many questions would remain unanswered. Evidence for changes in lymph nodes innervation is less abundant than that for the spleen. This may be due to the technical advantages of this latter organ and to the characteristics of the animal models used in these studies. Since the lymph nodes apparently do possess sensory innervation, it would also be interesting to know what happens to SP positive fibers during an immune activation.

Another essential question is whether changes in the sympathetic, sensitive and/or parasympathetic innervation within peripheral non-lymphoid tissues accompany the development of an inflammatory process, together with the recruitment of activated immune cells at the site of phlogosis. If molecules proposed to mediate changes in local innervation -semaphorins and neurotrophins- are released by activated immune cells or other cytokine-stimulated cell types, this may be the case. If so, the emerging question deals with the potential clinical consequences of this, considering the ANS regulates many biological functions.

Perhaps the most intriguing matter is what would be the physiological and immunological goal of this hypothetical neural plasticity mechanism. Considering the accumulated evidence on the broad relationship between the NS and the IS (1, 2), this neural plasticity mechanism may ensure a differential neural modulation of the IS in its diverse functional-associated activation states. It was stated that decreased noradrenergic activity during an ongoing immune response is "*a way of releasing immune cells from the inhibitory effects of NA*" for a proper adaptive response to be developed (36). This interpretation is in line with the β-adrenergic-receptor-mediated immunosuppressive effects of NA on such cells, particularly on Th1-type responses (1, 2, 165–167); the most consistent view on the immunomodulating effect of the ANS. Even if this turns out to be true, current evidence also supports a proinflammatory role of the SNS. In fact, SNS signaling has also been shown to play an important role in the induction of proinflammatory cytokines (168, 169), as well as in contributing to proliferation and mobilization of myeloid lineage immune cells in the first steps of inflammation [reviewed in (170)]. Moreover, two different groups have reported that peripheral sympathectomy in mice led to a significant increase in $CD4^{+}Foxp3^{+}$ Treg compartment in SLOs (171, 172). Consequently, the physiological meaning of this neural plasticity mechanism may be even more complex. Some of these issues will be better addressed in the second part of this work.

AUTHOR CONTRIBUTIONS

The author confirms being the sole contributor of this work and has approved it for publication.

FUNDING

The author acknowledges the support from the Fundación Iberoamericana de Estudios Superiores.

REFERENCES

1. Elenkov IJ, Wilder RL, Chrousos GP, Vizi ES. The sympathetic nerve–an integrative interface between two supersystems: the brain and the immune system. *Pharmacol Rev*. (2000) 52:595–638.
2. Padro CJ, Sanders VM. Neuroendocrine regulation of inflammation. *Semin Immunol*. (2014) 26:357–68. doi: 10.1016/j.smim.2014.01.003
3. Felten DL, Livnat S, Felten SY, Carlson SL, Bellinger DL, Yeh P. Sympathetic innervation of lymph nodes in mice. *Brain Res Bull*. (1984) 13:693–9. doi: 10.1016/0361-9230(84)90230-2
4. Nance DM, Sanders VM. Autonomic innervation and regulation of the immune system (1987–2007). *Brain Behav Immun*. (2007) 21:736–45. doi: 10.1016/j.bbi.2007.03.008
5. Felten DL, Ackerman KD, Wiegand SJ, Felten SY. Noradrenergic sympathetic innervation of the spleen: I. Nerve fibers associate with lymphocytes and macrophages in specific compartments of the splenic white pulp. *J Neurosci Res*. (1987) 18:28–36, 118–21. doi: 10.1002/jnr.490180107
6. Felten SY, Olschowka J. Noradrenergic sympathetic innervation of the spleen: II. Tyrosine hydroxylase (TH)-positive nerve terminals form synapticlike contacts on lymphocytes in the splenic white pulp. *J Neurosci Res*. (1987) 18:37–48. doi: 10.1002/jnr.490180108
7. Ackerman KD, Felten SY, Bellinger DL, Felten DL. Noradrenergic sympathetic innervation of the spleen: III. Development of innervation in the rat spleen. *J Neurosci Res*. (1987) 18:49–54, 123–5. doi: 10.1002/jnr.490180109
8. Burnstock G. Cotransmission. *Curr Opin Pharmacol*. (2004) 4:47–52. doi: 10.1016/j.coph.2003.08.001
9. Romano TA, Felten SY, Felten DL, Olschowka JA. Neuropeptide-Y innervation of the rat spleen: another potential immunomodulatory neuropeptide. *Brain Behav Immun*. (1991) 5:116–31. doi: 10.1016/0889-1591(91)90011-X
10. Nance DM, Burns J. Innervation of the spleen in the rat: evidence for absence of afferent innervation. *Brain Behav Immun*. (1989) 3:281–90. doi: 10.1016/0889-1591(89)90028-7
11. Hoover DB, Brown TC, Miller MK, Schweitzer JB, Williams DL. Loss of sympathetic nerves in spleens from patients with end stage sepsis. *Front Immunol*. (2017) 8:1712. doi: 10.3389/fimmu.2017.01712
12. Grisanti LA, Perez DM, Porter JE. Modulation of immune cell function by α(1)-adrenergic receptor activation. *Curr Top Membr*. (2011) 67:113–38. doi: 10.1016/B978-0-12-384921-2.00006-9
13. Lorton D, Bellinger DL. Molecular mechanisms underlying β-adrenergic receptor-mediated cross-talk between sympathetic neurons and immune cells. *Int J Mol Sci*. (2015) 16:5635–65. doi: 10.3390/ijms16035635
14. Jacob F, Pérez Novo C, Bachert C, Van Crombruggen K. Purinergic signaling in inflammatory cells: P2 receptor expression, functional effects, and modulation of inflammatory responses. *Purinergic Signal*. (2013) 9:285–306. doi: 10.1007/s11302-013-9357-4
15. Burnstock G, Boeynaems JM. Purinergic signalling and immune cells. *Purinergic Signal*. (2014) 10:529–64. doi: 10.1007/s11302-014-9427-2
16. Cekic C, Linden J. Purinergic regulation of the immune system. *Nat Rev Immunol*. (2016) 16:177–92. doi: 10.1038/nri.2016.4
17. Petitto JM, Huang Z, McCarthy DB. Molecular cloning of NPY-Y1 receptor cDNA from rat splenic lymphocytes: evidence of low levels of mRNA expression and [125I]NPY binding sites. *J Neuroimmunol*. (1994) 54:81–6. doi: 10.1016/0165-5728(94)90234-8
18. Wheway J, Mackay CR, Newton RA, Sainsbury A, Boey D, Herzog H, et al. A fundamental bimodal role for neuropeptide Y1 receptor in the immune system. *J Exp Med*. (2005) 202:1527–38. doi: 10.1084/jem.20051971
19. Burnstock G. Non-synaptic transmission at autonomic neuroeffector junctions. *Neurochem Int*. (2008) 52:14–25. doi: 10.1016/j.neuint.2007.03.007
20. Murray K, Godinez DR, Brust-Mascher I, Miller EN, Gareau MG, Reardon C. Neuroanatomy of the spleen: mapping the relationship between sympathetic neurons and lymphocytes. *PLoS ONE*. (2017) 12:e0182416. doi: 10.1371/journal.pone.0182416
21. MacNeil BJ, Jansen AH, Greenberg AH, Nance DM. Activation and selectivity of splenic sympathetic nerve electrical activity response to bacterial endotoxin. *Am J Physiol*. (1996) 270:R264–70. doi: 10.1152/ajpregu.1996.270.1.R264
22. Pardini BJ, Jones SB, Filkins JP. Cardiac and splenic norepinephrine turnovers in endotoxic rats. *Am J Physiol*. (1983) 245:H276–83. doi: 10.1152/ajpheart.1983.245.2.H276
23. Fuchs BA, Campbell KS, Munson AE. Norepinephrine and serotonin content of the murine spleen: its relationship to lymphocyte beta-adrenergic receptor density and the humoral immune response *in vivo* and *in vitro*. *Cell Immunol*. (1988) 117:339–51. doi: 10.1016/0008-8749(88)90123-2
24. Kohm AP, Tang Y, Sanders VM, Jones SB. Activation of antigen-specific $CD4^+$ Th2 cells and B cells *in vivo* increases norepinephrine release in the spleen and bone marrow. *J Immunol*. (2000) 165:725–33. doi: 10.4049/jimmunol.165.2.725
25. Besedovsky HO, del Rey A, Sorkin E, Da Prada M, Keller HH. Immunoregulation mediated by the sympathetic nervous system. *Cell Immunol*. (1979) 48:346–55. doi: 10.1016/0008-8749(79)90129-1
26. del Rey A, Besedovsky HO, Sorkin E, da Prada M, Arrenbrecht S. Immunoregulation mediated by the sympathetic nervous system, II. *Cell Immunol*. (1981) 63:329–34. doi: 10.1016/0008-8749(81)90012-5
27. del Rey A, Besedovsky HO, Sorkin E, Da Prada M, Bondiolotti GP. Sympathetic immunoregulation: difference between high- and low-responder animals. *Am J Physiol*. (1982) 242:R30–3. doi: 10.1152/ajpregu.1982.242.1.R30
28. Besedovsky HO, del Rey A, Sorkin E, Burri R, Honegger CG, Schlumpf M, et al. T lymphocytes affect the development of sympathetic innervation of mouse spleen. *Brain Behav Immun*. (1987) 1:185–93. doi: 10.1016/0889-1591(87)90020-1
29. del Rey A, Kabiersch A, Petzoldt S, Randolf A, Besedovsky HO. Sympathetic innervation affects superantigen-induced decrease in CD4V beta 8 cells in the spleen. *Ann N Y Acad Sci*. (2000) 917:575–81. doi: 10.1111/j.1749-6632.2000.tb05423.x
30. Breneman SM, Moynihan JA, Grota LJ, Felten DL, Felten SY. Splenic norepinephrine is decreased in MRL-lpr/lpr mice. *Brain Behav Immun*. (1993) 7:135–43. doi: 10.1006/brbi.1993.1015
31. del Rey A, Kabiersch A, Petzoldt S, Besedovsky HO. Sympathetic abnormalities during autoimmune processes: potential relevance of noradrenaline-induced apoptosis. *Ann N Y Acad Sci*. (2003) 992:158–67. doi: 10.1111/j.1749-6632.2003.tb03146.x
32. del Rey A, Roggero E, Kabiersch A, Schäfer M, Besedovsky HO. The role of noradrenergic nerves in the development of the lymphoproliferative disease in Fas-deficient, lpr/lpr mice. *J Immunol*. (2006) 176:7079–86. doi: 10.4049/jimmunol.176.11.7079
33. Roggero E, Pérez AR, Pollachini N, Villar SR, Wildmann J, Besedovsky H, et al. The sympathetic nervous system affects the susceptibility and course of *Trypanosoma cruzi* infection. *Brain Behav Immun*. (2016) 58:228–236. doi: 10.1016/j.bbi.2016.07.163
34. Kelley SP, Moynihan JA, Stevens SY, Grota LJ, Felten DL. Sympathetic nerve destruction in spleen in murine AIDS. *Brain Behav Immun*. (2003) 17:94–109. doi: 10.1016/S0889-1591(02)00101-0
35. Lorton D, Lubahn C, Lindquist CA, Schaller J, Washington C, Bellinger DL. Changes in the density and distribution of sympathetic nerves in spleens from Lewis rats with adjuvant-induced arthritis suggest that an injury and sprouting response occurs. *J Comp Neurol*. (2005) 489:260–73. doi: 10.1002/cne.20640
36. del Rey A, Besedovsky HO. Immune-neuro-endocrine reflexes, circuits, and networks: physiologic and evolutionary implications. *Front Horm Res*. (2017) 48:1–18. doi: 10.1159/000452902
37. Kruger RP, Aurandt J, Guan KL. Semaphorins command cells to move. *Nat Rev Mol Cell Biol*. (2005) 6:789–800. doi: 10.1038/nrm1740
38. Pasterkamp RJ, Giger RJ. Semaphorin function in neural plasticity and disease. *Curr Opin Neurobiol*. (2009) 19:263–74. doi: 10.1016/j.conb.2009.06.001
39. Alto LT, Terman JR. Semaphorins and their signaling mechanisms. *Methods Mol Biol*. (2017) 1493:1–25. doi: 10.1007/978-1-4939-6448-2_1
40. Nakamura F, Kalb RG, Strittmatter SM. Molecular basis of semaphorin-mediated axon guidance. *J Neurobiol*. (2000) 44:219–29. doi: 10.1002/1097-4695(200008)44:2<219::AID-NEU11>3.0.CO;2-W

41. Mohan V, Sullivan CS, Guo J, Wade SD, Majumder S, Agarwal A, et al. Temporal regulation of dendritic spines through NrCAM-semaphorin3F receptor signaling in developing cortical pyramidal neurons. *Cereb Cortex*. (2019) 29:963–977. doi: 10.1093/cercor/bhy004
42. Sahay A, Kim CH, Sepkuty JP, Cho E, Huganir RL, Ginty DD, et al. Secreted semaphorins modulate synaptic transmission in the adult hippocampus. *J Neurosci*. (2005) 25:3613–20. doi: 10.1523/JNEUROSCI.5255-04.2005
43. Giacobini P, Parkash J, Campagne C, Messina A, Casoni F, Vanacker C, et al. Brain endothelial cells control fertility through ovarian-steroid-dependent release of semaphorin 3A. *PLoS Biol*. (2014) 12:e1001808. doi: 10.1371/journal.pbio.1001808
44. Parkash J, Messina A, Langlet F, Cimino I, Loyens A, Mazur D, et al. Semaphorin7A regulates neuroglial plasticity in the adult hypothalamic median eminence. *Nat Commun*. (2015) 6:6385. doi: 10.1038/ncomms7385
45. Tran TS, Kolodkin AL, Bharadwaj R. Semaphorin regulation of cellular morphology. *Annu Rev Cell Dev Biol*. (2007) 23:263–92. doi: 10.1146/annurev.cellbio.22.010605.093554
46. Neufeld G, Sabag AD, Rabinovicz N, Kessler O. Semaphorins in angiogenesis and tumor progression. *Cold Spring Harb Perspect Med*. (2012) 2:a006718. doi: 10.1101/cshperspect.a006718
47. Ueda Y, Kondo N, Ozawa M, Yasuda K, Tomiyama T, Kinashi T. Sema3e/Plexin D1 modulates immunological synapse and migration of thymocytes by Rap1 Inhibition. *J Immunol*. (2016) 196:3019–31. doi: 10.4049/jimmunol.1502121
48. Duke-Cohan JS, Ishikawa Y, Yoshizawa A, Choi YI, Lee CN, Acuto O, et al. Regulation of thymocyte trafficking by Tagap, a GAP domain protein linked to human autoimmunity. *Sci Signal*. (2018) 11:eaan8799. doi: 10.1126/scisignal.aan8799
49. Kumanogoh A, Kikutani H. Immune semaphorins: a new area of semaphorin research. *J Cell Sci*. (2003) 116:3463–70. doi: 10.1242/jcs.00674
50. Roney K, Holl E, Ting J. Immune plexins and semaphorins: old proteins, new immune functions. *Protein Cell*. (2013) 4:17–26. doi: 10.1007/s13238-012-2108-4
51. Chapoval SP. Neuroimmune semaphorins as costimulatory molecules and beyond. *Mol Med*. (2018) 24:13. doi: 10.1186/s10020-018-0014-9
52. Lu N, Li Y, Zhang Z, Xing J, Sun Y, Yao S, Chen L. Human semaphorin-4A drives Th2 responses by binding to receptor ILT-4. *Nat Commun*. (2018) 9:742. doi: 10.1038/s41467-018-03128-9
53. Yan H, Wu L, Shih C, Hou S, Shi J, Mao T, et al. Plexin B2 and semaphorin 4C guide T cell recruitment and function in the germinal center. *Cell Rep*. (2017) 19:995–1007. doi: 10.1016/j.celrep.2017.04.022
54. Catalano A. The neuroimmune semaphorin-3A reduces inflammation and progression of experimental autoimmune arthritis. *J Immunol*. (2010) 185:6373–83. doi: 10.4049/jimmunol.0903527
55. Ji JD, Park-Min KH, Ivashkiv LB. Expression and function of semaphorin 3A and its receptors in human monocyte-derived macrophages. *Hum Immunol*. (2009) 70:211–7. doi: 10.1016/j.humimm.2009.01.026
56. Mendes-da-Cruz DA, Brignier AC, Asnafi V, Baleydier F, Messias CV, Lepelletier Y, et al. Semaphorin 3F and neuropilin-2 control the migration of human T-cell precursors. *PLoS ONE*. (2014) 9:e103405. doi: 10.1371/journal.pone.0103405
57. Levi-Montalcini R. The nerve growth factor: its mode of action on sensory and sympathetic nerve cells. *Harvey Lect*. (1966) 60:217–59.
58. Bibel M, Barde YA. Neurotrophins: key regulators of cell fate and cell shape in the vertebrate nervous system. *Genes Dev*. (2000) 14:2919–37. doi: 10.1101/gad.841400
59. Lee FS, Kim AH, Khursigara G, Chao MV. The uniqueness of being a neurotrophin receptor. *Curr Opin Neurobiol*. (2001) 11:281–6. doi: 10.1016/S0959-4388(00)00209-9
60. Chao MV. Neurotrophins and their receptors: a convergence point for many signalling pathways. *Nat Rev Neurosci*. (2003) 4:299–309. doi: 10.1038/nrn1078
61. Bothwell M. Recent advances in understanding neurotrophin signaling. *F1000Res*. (2016) 5:F1000 Faculty Rev-1885. doi: 10.12688/f1000research.8434.1
62. Charalampopoulos I, Vicario A, Pediaditakis I, Gravanis A, Simi A, Ibáñez CF. Genetic dissection of neurotrophin signaling through the p75 neurotrophin receptor. *Cell Rep*. (2012) 2:1563–70. doi: 10.1016/j.celrep.2012.11.009
63. Yuan W, Ibáñez CF, Lin Z. Death domain of p75 neurotrophin receptor: a structural perspective on an intracellular signalling hub. *Biol Rev Camb Philos Soc*. (2019) 94:1282–1293. doi: 10.1111/brv.12502
64. Becker K, Cana A, Baumgärtner W, Spitzbarth I. p75 Neurotrophin receptor: a double-edged sword in pathology and regeneration of the central nervous system. *Vet Pathol*. (2018) 55:786–801. doi: 10.1177/0300985818781930
65. Tanaka K, Kelly CE, Goh KY, Lim KB, Ibáñez CF. Death domain signaling by disulfide-linked dimers of the p75 neurotrophin receptor mediates neuronal death in the CNS. *J Neurosci*. (2016) 36:5587–95. doi: 10.1523/JNEUROSCI.4536-15.2016
66. Dechant G, Barde YA. The neurotrophin receptor p75(NTR): novel functions and implications for diseases of the nervous system. *Nat Neurosci*. (2002) 5:1131–6. doi: 10.1038/nn1102-1131
67. Kenchappa RS, Tep C, Korade Z, Urra S, Bronfman FC, Yoon SO, et al. p75 neurotrophin receptor-mediated apoptosis in sympathetic neurons involves a biphasic activation of JNK and up-regulation of tumor necrosis factor-alpha-converting enzyme/ADAM17. *J Biol Chem*. (2010) 285:20358–68. doi: 10.1074/jbc.M109.082834
68. Kraemer BR, Snow JP, Vollbrecht P, Pathak A, Valentine WM, Deutch AY, et al. A role for the p75 neurotrophin receptor in axonal degeneration and apoptosis induced by oxidative stress. *J Biol Chem*. (2014) 289:21205–16. doi: 10.1074/jbc.M114.563403
69. Kohn J, Aloyz RS, Toma JG, Haak-Frendscho M, Miller FD. Functionally antagonistic interactions between the TrkA and p75 neurotrophin receptors regulate sympathetic neuron growth and target innervation. *J Neurosci*. (1999) 19:5393–408. doi: 10.1523/JNEUROSCI.19-13-05393.1999
70. Lee R, Kermani P, Teng KK, Hempstead BL. Regulation of cell survival by secreted proneurotrophins. *Science*. (2001) 294:1945–8. doi: 10.1126/science.1065057
71. Ibáñez CF. Jekyll-Hyde neurotrophins: the story of proNGF. *Trends Neurosci*. (2002) 25:284–6. doi: 10.1016/S0166-2236(02)02169-0
72. Pang PT, Teng HK, Zaitsev E, Woo NT, Sakata K, Zhen S, et al. Cleavage of proBDNF by tPA/plasmin is essential for long-term hippocampal plasticity. *Science*. (2004) 306:487–91. doi: 10.1126/science.1100135
73. Rösch H, Schweigreiter R, Bonhoeffer T, Barde YA, Korte M. The neurotrophin receptor p75NTR modulates long-term depression and regulates the expression of AMPA receptor subunits in the hippocampus. *Proc Natl Acad Sci U S A*. (2005) 102:7362–7. doi: 10.1073/pnas.0502460102
74. Woo NH, Teng HK, Siao CJ, Chiaruttini C, Pang PT, Milner TA, et al. Activation of p75NTR by proBDNF facilitates hippocampal long-term depression. *Nat Neurosci*. (2005) 8:1069–77. doi: 10.1038/nn1510
75. Yang F, Je HS, Ji Y, Nagappan G, Hempstead B, Lu B. Pro-BDNF-induced synaptic depression and retraction at developing neuromuscular synapses. *J Cell Biol*. (2009) 185:727–41. doi: 10.1083/jcb.200811147
76. Nakahashi T, Fujimura H, Altar CA, Li J, Kambayashi J, Tandon NN, et al. Vascular endothelial cells synthesize and secrete brain-derived neurotrophic factor. *FEBS Lett*. (2000) 470:113–7. doi: 10.1016/S0014-5793(00)01302-8
77. Fujimura H, Altar CA, Chen R, Nakamura T, Nakahashi T, Kambayashi J, et al. Brain-derived neurotrophic factor is stored in human platelets and released by agonist stimulation. *Thromb Haemost*. (2002) 87:728–34 doi: 10.1055/s-0037-1613072
78. Tamura S, Suzuki H, Hirowatari Y, Hatase M, Nagasawa A, Matsuno K, et al. Release reaction of brain-derived neurotrophic factor (BDNF) through PAR1 activation and its two distinct pools in human platelets. *Thromb Res*. (2011) 128:e55–61. doi: 10.1016/j.thromres.2011.06.002
79. De Luca C, Papa M. Matrix metalloproteinases, neural extracellular matrix, and central nervous system pathology. *Prog Mol Biol Transl Sci*. (2017) 148:167–202. doi: 10.1016/bs.pmbts.2017.04.002
80. De Luca C, Virtuoso A, Maggio N, Papa M. Neuro-coagulopathy: blood coagulation factors in central nervous system diseases. *Int J Mol Sci*. (2017) 18:E2128. doi: 10.3390/ijms18102128
81. De Luca C, Colangelo AM, Alberghina L, Papa M. Neuro-immune hemostasis: homeostasis and diseases in the central nervous system. *Front Cell Neurosci*. (2018) 12:459. doi: 10.3389/fncel.2018.00459

82. Kerschensteiner M, Gallmeier E, Behrens L, Leal VV, Misgeld T, Klinkert WE, et al. Activated human T cells, B cells, and monocytes produce brain-derived neurotrophic factor *in vitro* and in inflammatory brain lesions: a neuroprotective role of inflammation? *J Exp Med*. (1999) 189:865–70. doi: 10.1084/jem.189.5.865
83. Besser M, Wank R. Cutting edge: clonally restricted production of the neurotrophins brain-derived neurotrophic factor and neurotrophin-3 mRNA by human immune cells and Th1/Th2-polarized expression of their receptors. *J Immunol*. (1999) 162:6303–6.
84. Moalem G, Gdalyahu A, Shani Y, Otten U, Lazarovici P, Cohen IR, et al. Production of neurotrophins by activated T cells: implications for neuroprotective autoimmunity. *J Autoimmun*. (2000) 15:331–45. doi: 10.1006/jaut.2000.0441
85. Aloe L, Tuveri MA, Carcassi U, Levi-Montalcini R. Nerve growth factor in the synovial fluid of patients with chronic arthritis. *Arthritis Rheum*. (1992) 35:351–5. doi: 10.1002/art.1780350315
86. Bracci-Laudiero L, Aloe L, Levi-Montalcini R, Galeazzi M, Schilter D, Scully JL, et al. Increased levels of NGF in sera of systemic lupus erythematosus patients. *Neuroreport*. (1993) 4:563–5. doi: 10.1097/00001756-199305000-00025
87. Fauchais AL, Lise MC, Marget P, Lapeybie FX, Bezanahary H, Martel C, et al. Serum and lymphocytic neurotrophins profiles in systemic lupus erythematosus: a case-control study. *PLoS ONE*. (2013) 8:e79414. doi: 10.1371/journal.pone.0079414
88. Chiaretti A, Capozzi D, Mariotti P, Valentini P, Manni L, Buonsenso D, et al. Increased levels of neurotrophins in the cerebrospinal fluid of children with Epstein-Barr virus meningoencephalitis. *Int J Infect Dis*. (2014) 20:52–7. doi: 10.1016/j.ijid.2013.11.006
89. Petersen LE, Baptista TSA, Molina JK, Motta JG, do Prado A, Piovesan DM, et al. Cognitive impairment in rheumatoid arthritis: role of lymphocyte subsets, cytokines and neurotrophic factors. *Clin Rheumatol*. (2018) 37:1171–1181. doi: 10.1007/s10067-018-3990-9
90. Skaper SD. Nerve growth factor: a neuroimmune crosstalk mediator for all seasons. *Immunology*. (2017) 151:1–15. doi: 10.1111/imm.12717
91. Dagnell C, Grunewald J, Kramar M, Haugom-Olsen H, Elmberger GP, Eklund A, et al. Neurotrophins and neurotrophin receptors in pulmonary sarcoidosis—granulomas as a source of expression. *Respir Res*. (2010) 11:156. doi: 10.1186/1465-9921-11-156
92. Fauchais AL, Lalloué F, Lise MC, Boumediene A, Preud'homme JL, Vidal E, et al. Role of endogenous brain-derived neurotrophic factor and sortilin in B cell survival. *J Immunol*. (2008) 181:3027–38. doi: 10.4049/jimmunol.181.5.3027
93. Düsedau HP, Kleveman J, Figueiredo CA, Biswas A, Steffen J, Kliche S, et al. p75NTR regulates brain mononuclear cell function and neuronal structure in Toxoplasma infection-induced neuroinflammation. *Glia*. (2019) 67:193–211. doi: 10.1002/glia.23553
94. Bandoła J, Richter C, Ryser M, Jamal A, Ashton MP, von Bonin M, et al. Neurotrophin receptor p75NTR regulates immune function of plasmacytoid dendritic cells. *Front Immunol*. (2017) 8:981. doi: 10.3389/fimmu.2017.00981
95. Datta-Mitra A, Kundu-Raychaudhuri S, Mitra A, Raychaudhuri SP. Cross talk between neuroregulatory molecule and monocyte: nerve growth factor activates the inflammasome. *PLoS One*. (2015) 10:e0121626. doi: 10.1371/journal.pone.0121626
96. Zhou XF, Rush RA, McLachlan EM. Differential expression of the p75 nerve growth factor receptor in glia and neurons of the rat dorsal root ganglia after peripheral nerve transection. *J Neurosci*. (1996) 16:2901–11. doi: 10.1523/JNEUROSCI.16-09-02901.1996
97. Giehl KM, Röhrig S, Bonatz H, Gutjahr M, Leiner B, Bartke I, et al. Endogenous brain-derived neurotrophic factor and neurotrophin-3 antagonistically regulate survival of axotomized corticospinal neurons *in vivo*. *J Neurosci*. (2001) 21:3492–502. doi: 10.1523/JNEUROSCI.21-10-03492.2001
98. Lönngren U, Näpänkangas U, Lafuente M, Mayor S, Lindqvist N, Vidal-Sanz M, et al. The growth factor response in ischemic rat retina and superior colliculus after brimonidine pre-treatment. *Brain Res Bull*. (2006) 71:208–18. doi: 10.1016/j.brainresbull.2006.09.005
99. Kokaia Z, Andsberg G, Martinez-Serrano A, Lindvall O. Focal cerebral ischemia in rats induces expression of P75 neurotrophin receptor in resistant striatal cholinergic neurons. *Neuroscience*. (1998) 84:1113–25. doi: 10.1016/S0306-4522(97)00579-4
100. Volosin M, Trotter C, Cragnolini A, Kenchappa RS, Light M, Hempstead BL,et al. Induction of proneurotrophins and activation of p75NTR-mediated apoptosis via neurotrophin receptor-interacting factor in hippocampal neurons after seizures. *J Neurosci*. (2008) 28:9870–9. doi: 10.1523/JNEUROSCI.2841-08.2008
101. Lowry KS, Murray SS, McLean CA, Talman P, Mathers S, Lopes EC, et al. A potential role for the p75 low-affinity neurotrophin receptor in spinal motor neuron degeneration in murine and human amyotrophic lateral sclerosis. *Amyotroph Lateral Scler Other Motor Neuron Disord*. (2001) 2:127–34. doi: 10.1080/146608201753275463
102. Dowling P, Ming X, Raval S, Husar W, Casaccia-Bonnefil P, Chao M, et al. Up-regulated p75NTR neurotrophin receptor on glial cells in MS plaques. *Neurology*. (1999) 53:1676–82. doi: 10.1212/WNL.53.8.1676
103. Ernfors P, Lindefors N, Chan-Palay V, Persson H. (1990). Cholinergic neurons of the nucleus basalis express elevated levels of nerve growth factor receptor mRNA in senile dementia of the Alzheimer type. *Dement Geriatr Cogn Disord*. (1990) 1:138–145. doi: 10.1159/000107133
104. Choi S, Friedman WJ. Inflammatory cytokines IL-1β and TNF-α regulate p75NTR expression in CNS neurons and astrocytes by distinct cell-type-specific signalling mechanisms. *ASN Neuro*. (2009) 1:e00010. doi: 10.1042/AN20090009
105. Cheng HJ, Bagri A, Yaron A, Stein E, Pleasure SJ, Tessier-Lavigne M. Plexin-A3 mediates semaphorin signaling and regulates the development of hippocampal axonal projections. *Neuron*. (2001) 32:249–63. doi: 10.1016/S0896-6273(01)00478-0
106. Chen H, Chédotal A, He Z, Goodman CS, Tessier-Lavigne M. Neuropilin-2, a novel member of the neuropilin family, is a high affinity receptor for the semaphorins Sema E and Sema IV but not Sema III. *Neuron*. (1997) 19:547–59. doi: 10.1016/S0896-6273(00)80371-2
107. Waimey KE, Huang PH, Chen M, Cheng HJ. Plexin-A3 and plexin-A4 restrict the migration of sympathetic neurons but not their neural crest precursors. *Dev Biol*. (2008) 315:448–58. doi: 10.1016/j.ydbio.2008.01.002
108. Yaron A, Huang PH, Cheng HJ, Tessier-Lavigne M. Differential requirement for Plexin-A3 and -A4 in mediating responses of sensory and sympathetic neurons to distinct class 3 Semaphorins. *Neuron*. (2005) 45:513–23. doi: 10.1016/j.neuron.2005.01.013
109. Kang HR, Lee CG, Homer RJ, Elias JA. Semaphorin 7A plays a critical role in TGF-beta1-induced pulmonary fibrosis. *J Exp Med*. (2007) 204:1083–93. doi: 10.1084/jem.20061273
110. Wang X, Kumanogoh A, Watanabe C, Shi W, Yoshida K, Kikutani H. Functional soluble CD100/Sema4D released from activated lymphocytes: possible role in normal and pathologic immune responses. *Blood*. (2001) 97:3498–504. doi: 10.1182/blood.V97.11.3498
111. Luo Y, Raible D, Raper JA. Collapsin: a protein in brain that induces the collapse and paralysis of neuronal growth cones. *Cell*. (1993) 75:217–27. doi: 10.1016/0092-8674(93)80064-L
112. Brown JA, Bridgman PC. Disruption of the cytoskeleton during Semaphorin 3A induced growth cone collapse correlates with differences in actin organization and associated binding proteins. *Dev Neurobiol*. (2009) 69:633–46. doi: 10.1002/dneu.20732
113. Barberis D, Artigiani S, Casazza A, Corso S, Giordano S, Love CA, et al. Plexin signaling hampers integrin-based adhesion, leading to Rho-kinase independent cell rounding, and inhibiting lamellipodia extension and cell motility. *FASEB J*. (2004) 18:592–4. doi: 10.1096/fj.03-0957fje
114. Cingolani LA, Goda Y. Actin in action: the interplay between the actin cytoskeleton and synaptic efficacy. *Nat Rev Neurosci*. (2008) 9:344–56. doi: 10.1038/nrn2373
115. Song H, Ming G, He Z, Lehmann M, McKerracher L, Tessier-Lavigne M, et al. Conversion of neuronal growth cone responses from repulsion to attraction by cyclic nucleotides. *Science*. (1998) 281:1515–8. doi: 10.1126/science.281.5382.1515
116. Dalpé G, Zhang LW, Zheng H, Culotti JG. Conversion of cell movement responses to Semaphorin-1 and Plexin-1 from attraction to repulsion by

lowered levels of specific RAC GTPases in *C. elegans*. *Development*. (2004) 131:2073–88. doi: 10.1242/dev.01063
117. Kantor DB, Chivatakarn O, Peer KL, Oster SF, Inatani M, Hansen MJ, et al. Semaphorin 5A is a bifunctional axon guidance cue regulated by heparan and chondroitin sulfate proteoglycans. *Neuron*. (2004) 44:961–75. doi: 10.1016/j.neuron.2004.12.002
118. Wolman MA, Liu Y, Tawarayama H, Shoji W, Halloran MC. Repulsion and attraction of axons by semaphorin3D are mediated by different neuropilins *in vivo*. *J Neurosci*. (2004) 24:8428–35. doi: 10.1523/JNEUROSCI.2349-04.2004
119. Hammarberg H, Lidman O, Lundberg C, Eltayeb SY, Gielen AW, Muhallab S, et al. Neuroprotection by encephalomyelitis: rescue of mechanically injured neurons and neurotrophin production by CNS-infiltrating T and natural killer cells. *J Neurosci*. (2000) 20:5283–91. doi: 10.1523/JNEUROSCI.20-14-05283.2000
120. Kerschensteiner M, Stadelmann C, Dechant G, Wekerle H, Hohlfeld R. Neurotrophic cross-talk between the nervous and immune systems: implications for neurological diseases. *Ann Neurol*. (2003) 53:292–304. doi: 10.1002/ana.10446
121. Ibáñez CF, Simi A. p75 neurotrophin receptor signaling in nervous system injury and degeneration: paradox and opportunity. *Trends Neurosci*. (2012) 35:431–40. doi: 10.1016/j.tins.2012.03.007
122. Singh KK, Miller FD. Activity regulates positive and negative neurotrophin-derived signals to determine axon competition. *Neuron*. (2005) 45:837–45. doi: 10.1016/j.neuron.2005.01.049
123. Singh KK, Park KJ, Hong EJ, Kramer BM, Greenberg ME, Kaplan DR, et al. Developmental axon pruning mediated by BDNF-p75NTR-dependent axon degeneration. *Nat Neurosci*. (2008) 11:649–58. doi: 10.1038/nn.2114
124. Park KJ, Grosso CA, Aubert I, Kaplan DR, Miller FD. p75NTR-dependent, myelin-mediated axonal degeneration regulates neural connectivity in the adult brain. *Nat Neurosci*. (2010) 13:559–66. doi: 10.1038/nn.2513
125. Kemi C, Grunewald J, Eklund A, Höglund CO. Differential regulation of neurotrophin expression in human bronchial smooth muscle cells. *Respir Res*. (2006) 7:18. doi: 10.1186/1465-9921-7-18
126. Takaoka K, Shirai Y, Saito N. Inflammatory cytokine tumor necrosis factor-alpha enhances nerve growth factor production in human keratinocytes, HaCaT cells. *J Pharmacol Sci*. (2009) 111:381–91. doi: 10.1254/jphs.09143FP
127. Tominaga M, Ozawa S, Ogawa H, Takamori K. A hypothetical mechanism of intraepidermal neurite formation in NC/Nga mice with atopic dermatitis. *J Dermatol Sci*. (2007) 46:199–210. doi: 10.1016/j.jdermsci.2007.02.002
128. Tominaga M, Ozawa S, Tengara S, Ogawa H, Takamori K. Intraepidermal nerve fibers increase in dry skin of acetone-treated mice. *J Dermatol Sci*. (2007) 48:103–11. doi: 10.1016/j.jdermsci.2007.06.003
129. Kamo A, Tominaga M, Tengara S, Ogawa H, Takamori K. Inhibitory effects of UV-based therapy on dry skin-inducible nerve growth in acetone-treated mice. *J Dermatol Sci*. (2011) 62:91–7. doi: 10.1016/j.jdermsci.2011.01.004
130. Lorton D, Bellinger DL, Felten SY, Felten DL. Substance P innervation of spleen in rats: nerve fibers associate with lymphocytes and macrophages in specific compartments of the spleen. *Brain Behav Immun*. (1991) 5:29–40. doi: 10.1016/0889-1591(91)90005-U
131. Kurkowski R, Kummer W, Heym C. Substance P-immunoreactive nerve fibers in tracheobronchial lymph nodes of the guinea pig: origin, ultrastructure and coexistence with other peptides. *Peptides*. (1990) 11:13–20. doi: 10.1016/0196-9781(90)90103-C
132. Bellinger DL, Lorton D, Hamill RW, Felten SY, Felten DL. Acetylcholinesterase staining and choline acetyltransferase activity in the young adult rat spleen: lack of evidence for cholinergic innervation. *Brain Behav Immun*. (1993) 7:191–204. doi: 10.1006/brbi.1993.1021
133. Schäfer MK, Eiden LE, Weihe E. Cholinergic neurons and terminal fields revealed by immunohistochemistry for the vesicular acetylcholine transporter. II. The peripheral nervous system. *Neuroscience*. (1998) 84:361–76. doi: 10.1016/S0306-4522(97)80196-0
134. Rosas-Ballina M, Olofsson PS, Ochani M, Valdés-Ferrer SI, Levine YA, Reardon C, et al. Acetylcholine-synthesizing T cells relay neural signals in a vagus nerve circuit. *Science*. (2011) 334:98–101. doi: 10.1126/science.1209985
135. Pavlov VA, Tracey KJ. Neural regulation of immunity: molecular mechanisms and clinical translation. *Nat Neurosci*. (2017) 20:156–66. doi: 10.1038/nn.4477
136. Balice-Gordon RJ, Chua CK, Nelson CC, Lichtman JW. Gradual loss of synaptic cartels precedes axon withdrawal at developing neuromuscular junctions. *Neuron*. (1993) 11:801–15. doi: 10.1016/0896-6273(93)90110-D
137. Lo YJ, Lin YC, Sanes DH, Poo MM. Depression of developing neuromuscular synapses induced by repetitive postsynaptic depolarizations. *J Neurosci*. (1994) 14:4694–704. doi: 10.1523/JNEUROSCI.14-08-04694.1994
138. Cash S, Dan Y, Poo MM, Zucker R. Postsynaptic elevation of calcium induces persistent depression of developing neuromuscular synapses. *Neuron*. (1996) 16:745–54. doi: 10.1016/S0896-6273(00)80095-1
139. Owman C. Pregnancy induces degenerative and regenerative changes in the autonomic innervation of the female reproductive tract. *Ciba Found Symp*. (1981) 83:252–79. doi: 10.1002/9780470720653.ch13
140. Varol FG, Duchemin AM, Neff NH, Hadjiconstantinou M. Nerve growth factor (NGF) and NGF mRNA change in rat uterus during pregnancy. *Neurosci Lett*. (2000) 294:58–62. doi: 10.1016/S0304-3940(00)01533-0
141. Zoubina EV, Smith PG. Sympathetic hyperinnervation of the uterus in the estrogen receptor alpha knock-out mouse. *Neuroscience*. (2001) 103:237–44. doi: 10.1016/S0306-4522(00)00549-2
142. Krizsan-Agbas D, Pedchenko T, Hasan W, Smith PG. Oestrogen regulates sympathetic neurite outgrowth by modulating brain derived neurotrophic factor synthesis and release by the rodent uterus. *Eur J Neurosci*. (2003) 18:2760–8. doi: 10.1111/j.1460-9568.2003.03029.x
143. Richeri A, Bianchimano P, Mármol NM, Viettro L, Cowen T, Brauer MM. Plasticity in rat uterine sympathetic nerves: the role of TrkA and p75 nerve growth factor receptors. *J Anat*. (2005) 207:125–34. doi: 10.1111/j.1469-7580.2005.00435.x
144. Brauer MM. Cellular and molecular mechanisms underlying plasticity in uterine sympathetic nerves. *Auton Neurosci*. (2008) 140:1–16. doi: 10.1016/j.autneu.2008.02.002
145. Latini C, Frontini A, Morroni M, Marzioni D, Castellucci M, Smith PG. Remodeling of uterine innervation. *Cell Tissue Res*. (2008) 334:1–6. doi: 10.1007/s00441-008-0657-x
146. Brauer MM, Smith PG. Estrogen and female reproductive tract innervation: cellular and molecular mechanisms of autonomic neuroplasticity. *Auton Neurosci*. (2015) 187:1–17. doi: 10.1016/j.autneu.2014.11.009
147. Brauer MM. Plasticity in uterine innervation: state of the art. *Curr Protein Pept Sci*. (2017) 18:108–119. doi: 10.2174/1389203717666160322145411
148. Tuttle R, O'Leary DD. Neurotrophins rapidly modulate growth cone response to the axon guidance molecule, collapsin-1. *Mol Cell Neurosci*. (1998) 11:1–8. doi: 10.1006/mcne.1998.0671
149. Dontchev VD, Letourneau PC. Nerve growth factor and semaphorin 3A signaling pathways interact in regulating sensory neuronal growth cone motility. *J Neurosci*. (2002) 22:6659–69. doi: 10.1523/JNEUROSCI.22-15-06659.2002
150. Atwal JK, Singh KK, Tessier-Lavigne M, Miller FD, Kaplan DR. Semaphorin 3F antagonizes neurotrophin-induced phosphatidylinositol 3-kinase and mitogen-activated protein kinase kinase signaling: a mechanism for growth cone collapse. *J Neurosci*. (2003) 23:7602–9. doi: 10.1523/JNEUROSCI.23-20-07602.2003
151. Borsini A, Zunszain PA, Thuret S, Pariante CM. The role of inflammatory cytokines as key modulators of neurogenesis. *Trends Neurosci*. (2015) 38:145–57. doi: 10.1016/j.tins.2014.12.006
152. Poon VY, Choi S, Park M. Growth factors in synaptic function. *Front Synaptic Neurosci*. (2013) 5:6. doi: 10.3389/fnsyn.2013.00006
153. Serafini T, Colamarino SA, Leonardo ED, Wang H, Beddington R, Skarnes WC, et al. Netrin-1 is required for commissural axon guidance in the developing vertebrate nervous system. *Cell*. (1996) 87:1001–14. doi: 10.1016/S0092-8674(00)81795-X
154. Salminen M, Meyer BI, Bober E, Gruss P. Netrin 1 is required for semicircular canal formation in the mouse inner ear. *Development*. (2000) 127:13–22.
155. Bouvrée K, Larrivée B, Lv X, Yuan L, DeLafarge B, Freitas C, et al. Netrin-1 inhibits sprouting angiogenesis in developing avian embryos. *Dev Biol*. (2008) 318:172–83. doi: 10.1016/j.ydbio.2008.03.023

156. Delloye-Bourgeois C, Brambilla E, Coissieux MM, Guenebeaud C, Pedeux R, Firlej V, et al. Interference with netrin-1 and tumor cell death in non-small cell lung cancer. *J Natl Cancer Inst*. (2009) 101:237–47. doi: 10.1093/jnci/djn491
157. Ly NP, Komatsuzaki K, Fraser IP, Tseng AA, Prodhan P, Moore KJ, et al. Netrin-1 inhibits leukocyte migration *in vitro* and *in vivo*. *Proc Natl Acad Sci USA*. (2005) 102:14729–34. doi: 10.1073/pnas.0506233102
158. Rosenberger P, Schwab JM, Mirakaj V, Masekowsky E, Mager A, Morote-Garcia JC, et al. Hypoxia-inducible factor-dependent induction of netrin-1 dampens inflammation caused by hypoxia. *Nat Immunol*. (2009) 10:195–202. doi: 10.1038/ni.1683
159. Chisholm A, Tessier-Lavigne M. Conservation and divergence of axon guidance mechanisms. *Curr Opin Neurobiol*. (1999) 9:603–15. doi: 10.1016/S0959-4388(99)00021-5
160. Brunet I, Gordon E, Han J, Cristofaro B, Broqueres-You D, Liu C, et al. Netrin-1 controls sympathetic arterial innervation. *J Clin Invest*. (2014) 124:3230–40. doi: 10.1172/JCI75181
161. Besedovsky H, Sorkin E, Felix D, Haas H. Hypothalamic changes during the immune response. *Eur J Immunol*. (1977) 7:323–5. doi: 10.1002/eji.1830070516
162. Torpy DJ, Chrousos GP. The three-way interactions between the hypothalamic-pituitary-adrenal and gonadal axes and the immune system. *Baillieres Clin Rheumatol*. (1996) 10:181–98. doi: 10.1016/S1521-6942(06)80039-2
163. Silverman MN, Pearce BD, Biron CA, Miller AH. Immune modulation of the hypothalamic-pituitary-adrenal (HPA) axis during viral infection. *Viral Immunol*. (2005) 18:41–78. doi: 10.1089/vim.2005.18.41
164. Engler H, Doenlen R, Engler A, Riether C, Prager G, Niemi MB, et al. Acute amygdaloid response to systemic inflammation. *Brain Behav Immun*. (2011) 25:1384–92. doi: 10.1016/j.bbi.2011.04.005
165. Panina-Bordignon P, Mazzeo D, Lucia PD, D'Ambrosio D, Lang R, Fabbri L, et al. Beta2-agonists prevent Th1 development by selective inhibition of interleukin 12. *J Clin Invest*. (1997) 100:1513–9. doi: 10.1172/JCI119674
166. Cole SW, Korin YD, Fahey JL, Zack JA. Norepinephrine accelerates HIV replication via protein kinase A-dependent effects on cytokine production. *J Immunol*. (1998) 161:610–6.
167. Ramer-Quinn DS, Swanson MA, Lee WT, Sanders VM. Cytokine production by naive and primary effector $CD4^+$ T cells exposed to norepinephrine. *Brain Behav Immun*. (2000) 14:239–55. doi: 10.1006/brbi.2000.0603
168. Johnson JD, Campisi J, Sharkey CM, Kennedy SL, Nickerson M, Greenwood BN, et al. Catecholamines mediate stress-induced increases in peripheral and central inflammatory cytokines. *Neuroscience*. (2005) 135:1295–307. doi: 10.1016/j.neuroscience.2005.06.090
169. Grebe KM, Takeda K, Hickman HD, Bailey AL, Embry AC, Bennink JR, et al. Cutting edge: sympathetic nervous system increases proinflammatory cytokines and exacerbates influenza A virus pathogenesis. *J Immunol*. (2010) 184:540–4. doi: 10.4049/jimmunol.0903395
170. Wohleb ES, Franklin T, Iwata M, Duman RS. Integrating neuroimmune systems in the neurobiology of depression. *Nat Rev Neurosci*. (2016) 17:497–511. doi: 10.1038/nrn.2016.69
171. Wirth T, Westendorf AM, Bloemker D, Wildmann J, Engler H, Mollerus S, et al. The sympathetic nervous system modulates $CD4^+Foxp3^+$ regulatory T cells via noradrenaline-dependent apoptosis in a murine model of lymphoproliferative disease. *Brain Behav Immun*. (2014) 38:100–10. doi: 10.1016/j.bbi.2014.01.007
172. Bhowmick S, Singh A, Flavell RA, Clark RB, O'Rourke J, Cone RE. The sympathetic nervous system modulates $CD4^+FoxP3^+$ regulatory T cells via a TGF-beta-dependent mechanism. *J Leukoc Biol*. (2009) 86:1275–83. doi: 10.1189/jlb.0209107

Conflict of Interest Statement: The author declares that the research was conducted in the absence of any commercial or financial relationships that could be construed as a potential conflict of interest.

frontiers in Endocrinology

ORIGINAL RESEARCH
published: 22 October 2019
doi: 10.3389/fendo.2019.00722

Adrenal Steroids Modulate Fibroblast-Like Synoviocytes Response During *B. abortus* Infection

*María Virginia Gentilini, Guillermo Hernán Giambartolomei and María Victoria Delpino**

Instituto de Inmunología, Genética y Metabolismo (INIGEM), Universidad de Buenos Aires (UBA), Consejo Nacional de Investigaciones Científicas y Técnicas (CONICET), Buenos Aires, Argentina

Brucella abortus stimulates an inflammatory immune response that stimulates the endocrine system, inducing the secretion of dehydroepiandrosterone (DHEA) and cortisol. In humans, the active disease is generally present as osteoarticular brucellosis. In previous studies we showed that *B. abortus* infection of synoviocytes creates a proinflammatory microenvironment. We proposed to determine the role of cortisol and DHEA on synoviocytes and infiltrating monocytes during *B. abortus* infection. Cortisol inhibited IL-6, IL-8, MCP-1, and MMP-2 secretion induced by *B. abortus* infection in synovial fibroblast. Cortisol-mediated MMP-2 inhibition during *B. abortus* infection was reversed by IL-6. DHEA inhibited *B. abortus*-induced RANKL up-regulation in synovial fibroblast through estrogen receptor (ER). *B. abortus* infection did not modulate glucocorticoid receptor (GR) expression. Cell responses to cortisol also depended on its intracellular bioavailability, according to the activity of the isoenzymes 11β-hydroxysteroid dehydrogenase (HSD) type-1 and 11β-HSD2 (which are involved in cortisone-cortisol interconversion). *B. abortus* infection did not modify 11β-HSD1 expression and GRα/β ratio in the presence or absence of adrenal steroids. Supernatants from *B. abortus*-infected monocytes induced 11β-HSD1 in synovial cells. Administration of cortisone was capable of inhibiting the secretion of RANKL by synoviocytes mimicking cortisol's effect. These results go along with previous observations that highlighted the ability of synovial tissue to secrete active steroids, making it an intracrine tissue. This is the first study that contributes to the knowledge of the consequence of adrenal steroids on synoviocytes in the context of a bacterial infection.

Keywords: DHEA, cortisol, *Brucella*, synovial fibroblast (FLS), RANKL

OPEN ACCESS

Edited by:
Vinicius Frias Carvalho, Oswaldo Cruz Foundation (Fiocruz), Brazil

Reviewed by:
Cristiana Couto Garcia, Oswaldo Cruz Foundation (Fiocruz), Brazil
Patrícia Paiva Corsetti, University of José de Rosário Vellano, Brazil
Huynh Tan Hop, Gyeongsang National University, South Korea

****Correspondence:***
María Victoria Delpino
mdelpino@ffyb.uba.ar

Specialty section:
This article was submitted to Neuroendocrine Science, a section of the journal Frontiers in Endocrinology

Received: *11 July 2019*
Accepted: *07 October 2019*
Published: *22 October 2019*

Citation:
Gentilini MV, Giambartolomei GH and Delpino MV (2019) Adrenal Steroids Modulate Fibroblast-Like Synoviocytes Response During B. abortus Infection. Front. Endocrinol. 10:722. doi: 10.3389/fendo.2019.00722

INTRODUCTION

Brucellosis is an infection caused by bacteria of the genus *Brucella*. This is one of the infectious diseases transmissible between animals and humans. *Brucella* osteoarthritis is one of the most common features of human brucellosis. The most frequent joint involvements are spondylitis, arthritis, and osteomyelitis (1, 2). The acute and the chronic forms of human brucellosis present joint involvement. Clinical characteristics include joint pain, which increased local warmth, tenderness, and limitation of movement. In brucellar arthritis, cartilage loss, and bone erosion affecting different joints may eventually lead to permanent joint dysfunction (3, 4). In about 50% of the cases of osteoarciular brucellosis, bacteria are isolated from synovial fluid samples. In the affected joint, the synovial membrane may present a lymphomononuclear infiltrate in the chronic phase of the disease, but usually this takes place in the acute setting (5, 6).

Synovial damage caused by *Brucella* infection involves different immune mechanisms. We have demonstrated that *Brucella* infects and survives within human synoviocytes, and this infection elicits a proinflammatory microenvironment with the secretion of interleukin (IL)-6 and the chemokines IL-8; chemoattractant of neutrophils and monocyte chemoattractant protein 1 (MCP-1); chemoattractant of monocytes; and the secretion of matrix metalloproteases (MMPs) and RANKL—with concomitant osteoclastogenesis (7, 8).

During *Brucella* infection different cytokines generated, including those produced in the local osteoarticular site, exerted a direct effect on immune or bone cells and also influenced indirectly these cells through their capacity to influence several neuroendocrine mechanisms, including the stimulation of the hypothalamus-pituitary-adrenal axis (HPA) (9). A cross-regulation between adrenal steroids (glucocorticoids and dehydroepiandrosterone [DHEA]) and the immune response modulation (10) has been established. The effects of DHEA are frequently opposed by the adrenal steroid cortisol (11). Further, in the course of immune response, hormones are endogenously released. The type of immune response that humans develop against Brucella infection is influenced by glucocorticoids and DHEA. Accordingly, it has been demonstrated that in patients with acute brucellosis, cortisol levels were more elevated than those of healthy individuals (12, 13). In addition, we have previously demonstrated that steroid hormones are implicated in the modulation of osteoblast differentiation and macrophage response during *B. abortus* infection (13, 14). In synoviocytes, the link between inflammation and the endocrine system at local level may be due to the presence of functional receptors for glucocorticoids, androgens, and estrogens.

The potential mechanism that is involved in synoviocytes and bone damage during *Brucella* infection has been partially deciphered (7, 8). Considering our previous results which demonstrate an inappropriate secretion of steroid hormones in patients with acute brucellosis (12, 13), the aim of this work was to determine if this hormonal dysregulation is implicated in the development and evolution of osteoarticular disease.

To this end we investigated the consequence of cortisol and DHEA on synoviocyte responses during *B. abortus* infection.

METHODS

Bacterial Culture

Brucella abortus S2308 was grown overnight in 10 ml of tryptic soy broth (Merck, Buenos Aires, Argentina) with constant agitation at 37°C. To prepare the bacteria inocula, we performed the procedure previously described (14). All live *Brucella* manipulations were carried out in biosafety level 3 facilities located at the at the Instituto de Investigaciones Biomédicas en Retrovirus y SIDA (INBIRS).

Cell Culture

The immortalized human FLS cell line SW982 was obtained from the ATCC (Rockville, MD). The SW982 cell line was cultured in an α-Minimum Essential Medium (α-MEM) (Gibco) supplemented with 2 mM L-glutamine, 10% heat-inactivated fetal bovine serum (FBS) (Gibco), 100 U/ml penicillin, and 100 μg/ml streptomycin. The human monocytic cell line THP-1 was cultured in RPMI 1640 medium (Gibco) supplemented with 2 mM L-glutamine, 10% heat inactivated FBS, 100 U/ml penicillin, and 100 μg/ml. The cultures were maintained in a 5% CO2 atmosphere at 37°C.

Cellular Infection

SW982 at a concentration of 3×10^5 cells/well (for cytokine determination by ELISA) and at 5×10^4 cells/well (for intracellular survival assay) were seeded in 24-well plates, and at 5.2×10^5 cells/well (for mRNA extraction) it was seeded in 6-well plates. It was infected at different multiplicities of infection (MOI) in the presence or absence of DHEA (1×10^{-8} M) and cortisol (1×10^{-6} M) and incubated for 1 h at 37°C in a 5% CO_2 atmosphere. Cells were extensively washed with DMEM-F12 to remove extracellular bacteria and were incubated in medium supplemented with 100 μg/ml of gentamicin and 50 μg/ml of streptomycin to kill extracellular bacteria in the presence or absence of DHEA and cortisol at the indicated concentrations. SW982 cells and culture supernatants were harvested at 24 h to obtain whole cell extracts and determine cytokines, chemokine production, matrix metalloproteinase (MMP) secretion, and mRNA extractions. To determine *Brucella* intracellular survival, cells were lysed with a sterile solution of 0.1% (vol/vol) Triton X-100 in H_2O. To enumerate CFU, lysates from serial dilutions were plated on tryptic soy agar plates.

THP-1 cells were seeded at 5×10^5 cells/well in 24-well plates and infected at MOI 100 for 1 h, then washed with RPMI and incubated during 24 h with medium supplemented with antibiotics as was described above.

Neutralization experiments were performed with anti-TNF receptor (anti-TNFRc, BD biosciences) at a concentration of 20 μg/ml. Synoviocytes were preincubated with the anti-TNFRc neutralizing antibody (20 mg/ml) or its corresponding isotype controls for 1 h at 37°C, and then stimulated with supernatants from *B. abortus*-infected monocytes.

Fulvestrant treatment was performed by using a concentration of 10 μM of Fulvestrant (Sigma).

Measurement of Cytokine Concentrations

Secretion of IL-6, TNF-α, IL-1β, IL-10, IL-8, and monocyte chemotactic protein 1 (MCP-1) was quantified by enzyme-linked immunosorbent assay (ELISA; BD Biosciences, San Jose, CA) and RANKL was quantified by ELISA (R&D systems) in culture supernatants.

Zymography

The method of Hibbs et al. with modifications was used to determine gelatinase activity (7, 15). The reversion of the inhibitory effect of cortisol on MMP production was carried out in the presence of human recombinant IL-6 at a concentration of 20 ng/ml (rhIL-6, R&D Systems).

mRNA Preparation and Quantitative PCR

RNA was extracted using the Quick-RNA MiniPrepKit (Zymo Research) and 1 μg of RNA was subjected to reverse transcription

using Improm-II Reverse Transcriptase (Promega). PCR analysis was performed with a Mx3000P real-time PCR detection system (Stratagene) using SYBR Green as fluorescent DNA binding dye. The primer sets used for amplification were: CycA sense: 5′-GCATACGGGTCCTGGCATCTTG−3′, antisense: 5′- TGCC ATCCAACCACTCAGTCTTG−3′; 11β-HSD1 sense 5′- ATGA TATTCACCATGTGCGCA−3′ antisense 5′- ATAGGCAG CAACCATTGGATAAG-3′; 11β-HSD2 sense 5′- TCGCGCGG TGCTCATCAC−3′antisense 5′- GTACGCAGCTCGATGGCA CC−3′; GRα sense 5′- GAAGGAAACTCCAGCCAGAAC−3′ antisense 5′- GATGATTTCAGCTAACATCTCG−3′; GRβ sense 5′- GAAGGAAACTCCAGCCAGAAC−3′antisense 5′- TGAG CGCCAAGATTGTTGG−3′; DKK1 sense 5′- TCCCCTGT GATTGCAGTAAA-3′antisense 5′- TCCAAGAGATCCTTGC GTTC-3′.

The amplification cycle for GRα and GRβ was 95°C for 15 s, 65°C for 30 s and 72°C for 60 s while for 11β-HSD1 and DKK1 it was 95°C for 15 s, 62,5°C for 30 s and 72°C for 60 s. The fold change (relative expression) in gene expression was calculated using the relative quantitation method ($2^{-\Delta\Delta Ct}$). Relative expression levels were normalized against CycA.

Statistical Analysis

Statistical analysis was performed with one-way analysis of variance, followed by the *post-hoc* Tukey test, using GraphPad Prism 5.0 software. The data are represented as means ± standard error of the mean (SEM).

RESULTS

Cortisol and DHEA Modulate *B. abortus* Intracellular Replication in Synovial Cells

We have previously demonstrated that primary human synovial fibroblast and SW982 cell line support *B. abortus* invasion and replication (7, 8). Taking into account that adrenal steroids do not only alter the function of host cells but can also affect the intracellular replication of bacteria (13, 16, 17), we aimed to determine if these hormones could modify *B. abortus* replication in synovial fibroblast. The capacity of *B. abortus* to replicate in synovial fibroblast was significantly increased by cortisol with respect to untreated controls. In contrast, DHEA treatment had no effect. However, during the administration of cortisol and DHEA in conjunction, no differences were observed in intracellular bacterial survival with respect to untreated cells, indicating that DHEA avoided the effect of cortisol These differences were significant at 24, 48, and 72 h post-infection (**Figures 1A,B**). Taken together, these results indicate the intracellular replication of *Brucella* was increased by cortisol treatment whereas DHEA treatment avoided this effect.

Cortisol Inhibits IL-6, IL-8, and MCP-1 Induced by *B. abortus* Infection in Synovial Fibroblast

B. abortus-infected synovial fibroblasts secrete the proinflammatory cytokine IL-6, chemokines, and MMP-2, but not the anti-inflammatory cytokine IL-10 (data not shown). In the migration of innate inflammatory cells, chemokines, and MMPs participated (18) in the concomitant tissue damage. Adrenal steroids can modulate the expression of cytokines, chemokines and MMPs in several cell types. When synovial fibroblasts were infected with *B. abortus* in the presence of cortisol, these cells secreted significantly lower quantities of IL-6, IL-8, MCP-1, and MMP-2 in respect to untreated cells. DHEA treatment could not avoid the effect of cortisol on IL-6, IL-8, and MCP-1 expression but could partially avoid the inhibitory effect of cortisol on MMP-2 expression, as was demonstrated when infection experiments were performed in the presence of both cortisol and DHEA (**Figures 1B–E**). Our results show that cortisol reduces the expression of secreted mediators induced by *B. abortus* infection in synoviocytes and DHEA could only partially avoid the effect in MMP-2 expression.

IL-6 Avoids the Effect of Cortisol Inhibition of MMP-2 Secretion Induced by *B. abortus* Infection in Synovial Fibroblast

Proinflammatory cytokines have been previously implicated in MMP induction in different cell types (19–24). The role of IL-6 in the downmodulation of MMP-2 induced by cortisol in *B. abortus*-infected synovial fibroblast was determined by adding recombinant human IL-6 exogenously at the time of treatment. IL-6 was able to avoid the inhibitory effect on MMP-2 secretion induced by cortisol in *B. abortus*-infected synovial fibroblasts (**Figure 1F**). This indicates that cortisol downmodulated MMP-2 secretion in a mechanism that at least involved the dampening of IL-6 production.

DHEA Inhibits *B. abortus*-Induced RANKL Up-Regulation in Synovial Fibroblast Through Estrogen Receptor (ER)

RANKL is the master regulator of bone metabolism involved in osteoclast differentiation (cell type implicated in bone resorption) in physiological conditions. In pathological conditions, the increase of RANKL expression could induce an exacerbation of bone resorption. We have previously demonstrated that *B. abortus* infection induced an increase of RANKL expression in synoviocytes. Then, experiments were conducted to determine if adrenal steroids could modulate RANKL expression during *B. abortus* infection in synoviocytes. To this end, infection experiments were performed in the presence of cortisol and DHEA. Cortisol treatment significantly reduced the secretion of RANKL with respect to untreated cells. In addition, DHEA treatment could also partially inhibit RANKL secretion induced by *B. abortus* infection (**Figure 2A**). These results indicate that adrenal hormones reduced the expression of RANKL induced by *B. abortus* infection in synoviocytes.

Infiltrating monocytes could be infected by *B. abortus* and then secrete proinflammatory cytokines and a low amount of IL-10 in response to this infection (**Figure 2C**) (25–27). This in turn could modulate synovial fibroblast responses (7, 27). Thus, we aimed to determine if supernatants from *B. abortus*-infected monocytes could modulate RANKL expression and if this response could be modified by the presence of adrenal

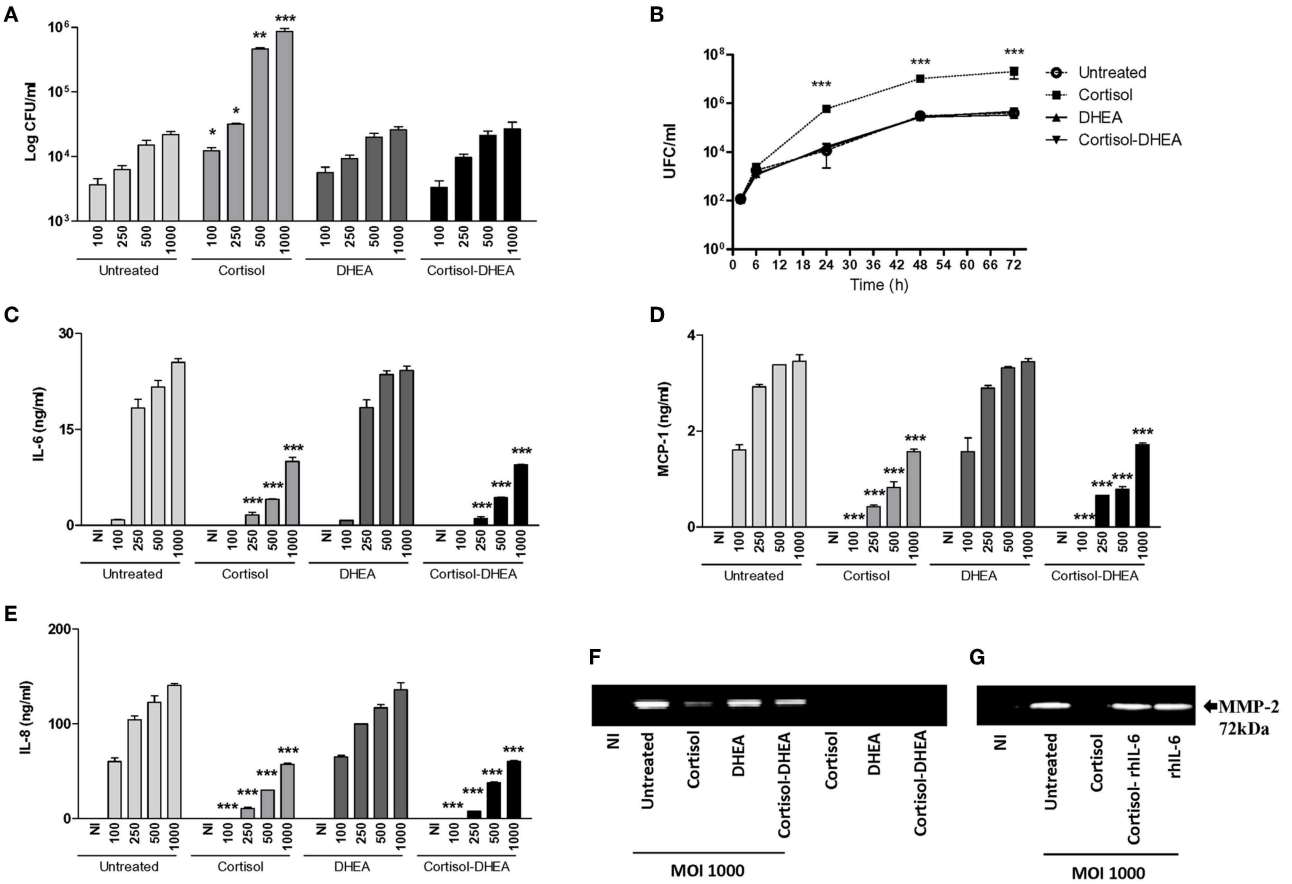

FIGURE 1 | Adrenal steroids modulate *B. abortus* intracellular replication, cytokines, and chemokine secretion by synoviocytes. **(A)** After infection at different multiplicities of infection (MOI, 100 to 1000) in the presence or absence of cortisol (1×10^{-6} M), dehydroepiandrosterone (DHEA) (1×10^{-8} M), or cortisol plus DHEA (1×10^{-6} and 1×10^{-8} M, respectively); cells were incubated with antibiotics to kill extracellular bacteria. Cell lysates obtained at 24 h post-infection were plated onto agar to determine intracellular colony forming units (CFU). At 2, 6, 24, and 48 h post-infection at MOI 1000, synovial cells treated or not with cortisol, DHEA, and Cortisol-DHEA were plated on agar to determine intracellular CFU **(B)**. After 24 h post-infection IL-6, MCP-1 and IL-8 were measured in culture supernatants by ELISA **(C–E)**. MMP-2 production by *B. abortus* infected synoviocytes at MOI of 1000 was measured by gelatin zymography **(F)**. Reversion of the inhibitory effect of cortisol on MMP-2 secretion by recombinant IL-6 (rhIL-6, 20 ng/ml) **(G)**. Data are given as the mean ± SEM from at least three individual experiments. $^{*}P < 0.1$; $^{**}P < 0.01$; and $^{***}P < 0.001$ vs. untreated cells. NI, non-infected.

steroids. Our results indicate that supernatants from *B. abortus*-infected monocytes induce RANKL expression by synoviocytes. When stimulation experiments were performed in the presence of cortisol, the expression of RANKL was completely abrogated. DHEA was able to reduce the levels of the expression of RANKL induced by supernatants from *B. abortus*-infected monocytes (**Figure 2B**). These results indicate that RANKL expression induced by supernatants from *B. abortus*-infected monocytes was inhibited by cortisol and DHEA treatment.

Most of the action of DHEA is mediated through ER (28). Then, experiments were conducted to evaluate the role of ER in the inhibition of the effect of *B. abortus* infection or supernatants from *B. abortus*-infected monocytes on RANKL expression in synoviocytes. To this end, fulvestran-mediated ER inhibition was employed to investigate the role of ER in regulating the DHEA effect on RANKL expression in synoviocytes infected with *B. abortus* or stimulated with conditioned medium. Fulvestrant was able to avoid the effect of DHEA in the inhibition of RANKL in *B. abortus*-infected synoviocytes or when stimulated with supernatants from *B. abortus*-infected synoviocytes (**Figures 2A,B**). Therefore, these results indicate that DHEA modulates the secretion of RANKL by synoviocytes mainly through ER.

B. ABORTUS INFECTION INDUCES DICKKOPF-1 (DKK1) EXPRESSION IN SYNOVIOCYTES

A main factor involved in the regulation of bone biology is DKK-1, and it is deemed a contributing factor in bone resorption (29). Since DKK-1 is produced by synoviocytes, experiments were conducted to determine if *B. abortus* infection could induce DKK-1 expression and the ability of adrenal steroids to modulate this response. *B. abortus* infection induced DKK-1 expression with respect to uninfected cells (**Figure 3A**). Cortisol

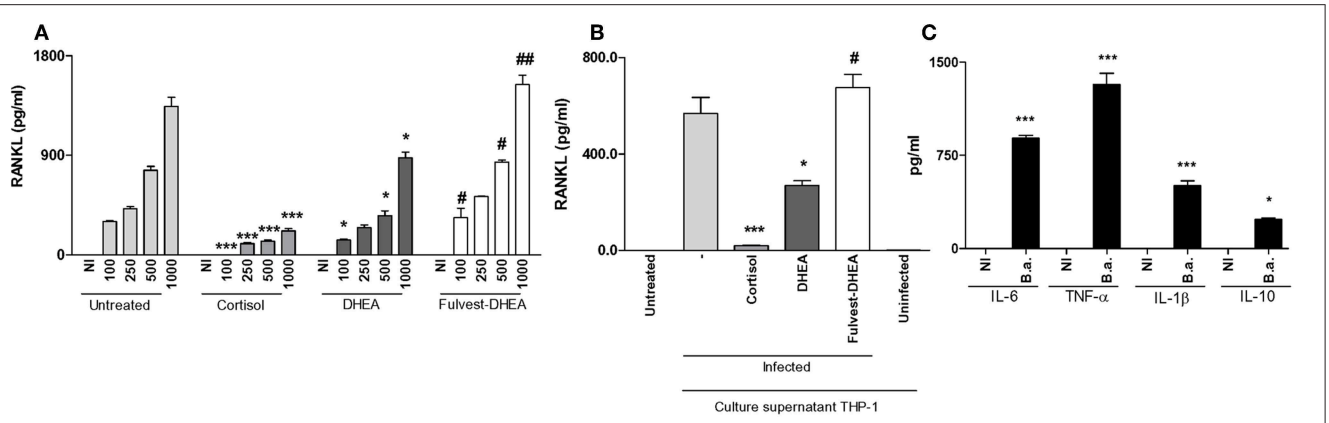

FIGURE 2 | DHEA inhibits RANKL induced by *B. abortus* infection and culture supernatants from *B. abortus*-infected monocytes via estrogen receptor (ER). Synoviocytes were infected at different MOI or stimulated with 1/2 dilution of culture supernatants from *B. abortus* infected or uninfected THP-1 cells, in the presence or not of cortisol (1×10^{-6} M), dehydroepiandrosterone (DHEA) (1×10^{-8} M), and in the presence or not of the ER inhibitor, fulvestrant (Fulvest, 10 μM). RANKL was measured by ELISA in culture supernatants from *B. abortus*-infected synoviocytes **(A)** or in culture supernatants from synoviocytes stimulated with culture supernatants from *B. abortus* infected THP-1 cells (culture supernatants THP-1, infected) or culture supernatants from uninfected THP-1 cells (culture supernatants THP-1, uninfected) **(B)**. IL-6, TNF-α, IL-1β, and IL-10 levels were determined in culture supernatants from *B. abortus*-infected THP-1 cells **(C)**. Data are given as the mean ± SEM from at least three individual experiments. $^{*}P < 0.1$ and $^{***}P < 0.001$ vs. untreated cells. $^{\#}P < 0.05$ and $^{\#\#}P < 0.01$ vs. DHEA treated cells. NI, non-infected.

and DHEA had no effect on the expression of DKK-1 in *B. abortus*-infected cells at least at 24 h (**Figure 3A**). It has been previously shown that inflammatory mediators can induce the expression of DKK-1. *B. abortus*-infected macrophages secrete proinflammatory cytokines (25–27). Thus, we decided to investigate if supernatants from *B. abortus*-infected monocytes could induce DKK-1 expression by synoviocytes. Supernatants from *B. abortus*-infected monocytes failed to induce DKK-1 expression as was determined at 24 h post-stimulation. Cortisol and DHEA had no effect on this response (**Figure 3B**). Taken together, our results indicated that *B. abortus*-infected synoviocytes express DKK-1 that could contribute to bone damage and *B. abortus*- infected monocytes did not contribute to DKK-1 expression at the mentioned time of stimulation. In addition, in these conditions, cortisol and DHEA did not participate in the modulation of DKK-1.

B. abortus Infection Does Not Modulate Cortisol Intracellular Bioavailability in Synovial Fibroblasts

The capacity of cells to respond to cortisol depends not only on levels of circulating cortisol, but it is also dependent on GR expression and its intracellular bioavailability. This depends on the activity of the isoenzymes 11β-hydroxysteroid-dehydrogenase type 1 (11β-HSD1) and type 2 (11β-HSD2) that catalyze the interconversion of inactive cortisol (cortisone) to active cortisol and vice versa, respectively. Thus, experiments were conducted to establish if *B. abortus* infection could modulate the two GR receptor isoforms, termed GRα and GRβ; as well as 11β-HSD1 and 11β-HSD2 expression and to establish if this phenomenon could be modulated by adrenal steroid treatment during the infection. *B. abortus* infection did not induce the expression of GRα, GRβ, and 11β-HSD1, with respect to uninfected cells (**Figure 4**). In addition, adrenal steroids were unable to modulate the expression of GRα, GRβ, and 11β-HSD1 during *B. abortus* infection. In concordance of previous reports, 11β-HSD2 was not detectable in synovial fibroblast (30). These results indicated that *B. abortus* infection did not modulate GR and 11β-HSD1 in synoviocytes.

Adrenal Steroids Modulate 11β-HSD1, GRα, and GRβ Expression in *B. abortus*-Infected Monocytes

Brucella-infected synovial fibroblasts have the ability to secrete MCP-1, a key cytokine involved in monocyte migration, and monocytes could be attracted to the site of infection and contribute to modulate synovial responses. Experiments were then performed to determine if *B. abortus* infection could modulate 11β-HSD1, 11β-HSD2, GRα, and GRβ expression in THP-1 monocytes. *B. abortus* infection did not induce 11β-HSD1 expression in monocytes (**Figure 5A**). Infection experiments in the presence of cortisol or DHEA indicated that both steroids were able to reduce 11β-HSD1 expression. In accordance with previous results by others, the type 2 enzyme, 11β-HSD2, which converts cortisol to cortisone, was not detectable in monocytes (31).

B. abortus infection was also able to induce GRα and GRβ expression in monocytes. When infection experiments were performed in the presence of adrenal steroids, our results indicate that cortisol had no significant effect on GRα and GRβ expression. In contrast, DHEA was able to reduce GRα and GRβ up to basal levels (**Figures 5B,C**). When we analyze the GRα/β ratio, our results demonstrate that *B. abortus* infection induced a reduction of GRα/β ratio, the treatment with cortisol had no effect, and the infection experiments in the presence of DHEA increased the GRα/β ratio up to basal levels present in uninfected cells (**Figure 5D**).

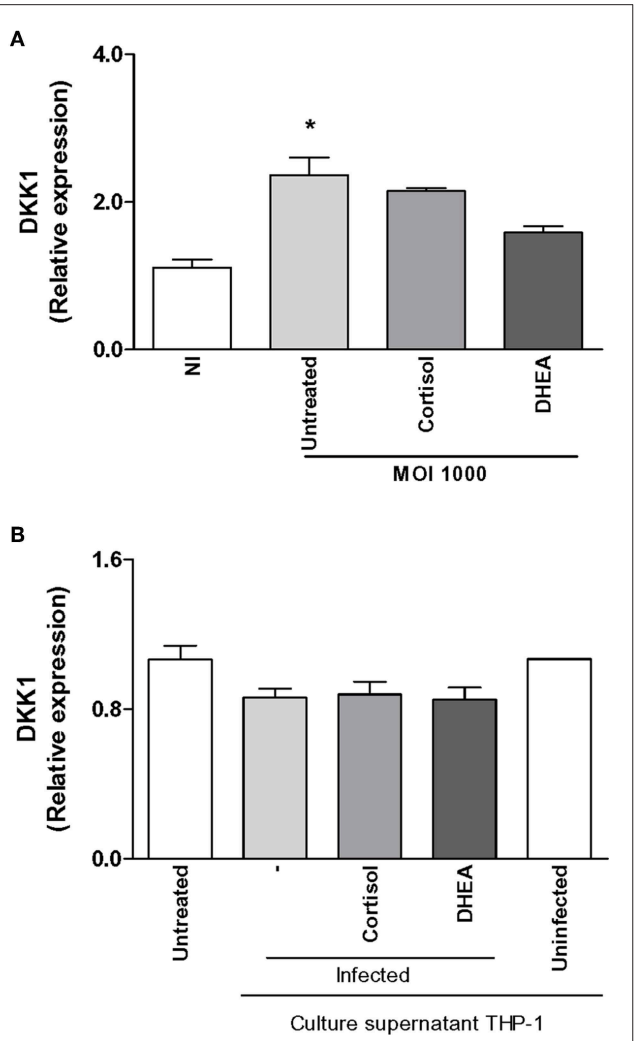

FIGURE 3 | Effect of *B. abortus* infection and culture supernatants from *B. abortus*-infected monocytes on dickkopf-1 (DKK1) expression in synoviocytes. DKK1 expression was determined by RT-qPCR in synoviocytes infected by *B. abortus* at a MOI of 1000 or stimulated with 1/2 dilution of culture supernatants from *B. abortus*-infected or uninfected THP-1 cells, in the presence or not of cortisol (1×10^{-6} M) and dehydroepiandrosterone (DHEA) (1×10^{-8} M) for 24 h. Data are given as the mean ± SEM from at least three individual experiments. *$P < 0.1$ vs. untreated infected cells. NI, non-infected.

Together, our results indicate that *B. abortus* infection did not increase the ability of the cells to respond to cortisol since it did not significantly increase 11β-HSD1 expression or the GRα/β ratio.

Supernatants From *B. abortus*-Infected Monocytes Modulate GR and 11β-HSD1 Expression in Synoviocytes

As was mentioned before, infiltrating monocytes could be infected by *B. abortus* and secrete proinflammatory cytokines in response to this infection that could modulate synovial fibroblasts responses. Thus, we aimed to determine if supernatants from *B. abortus*-infected monocytes could modulate GRα, GRβ, and 11β-HSD1 expression in synovial fibroblasts.

Supernatants from *B. abortus*-infected monocytes induced an increase of 11β-HSD1 with respect to cells stimulated with supernatants from uninfected monocytes. Cortisol significantly increased the induction in 11β-HSD1 mRNA transcription induced by supernatants from *B. abortus*-infected monocytes; in contrast, DHEA had no effect (**Figure 6A**). When we analyzed the modulation of supernatants from *B. abortus*-infected monocytes on the expression of GR in synoviocytes, our results indicate that supernatants from *B. abortus*-infected monocytes did not modulate GRα expression in synovial fibroblasts (**Figure 6B**). In addition, when stimulation with *B. abortus*-infected monocytes was performed in the presence of cortisol and DHEA, our results indicated that cortisol and DHEA had no effect. When we analyzed the expression of GRβ, supernatants from *B. abortus*-infected monocytes induced GRβ expression (**Figure 6C**). The presence of cortisol was able to inhibit the stimulatory effect of supernatants from *B. abortus*-infected monocytes on GRβ expression. In contrast, the presence of DHEA had no effect. It is well-known that GRβ lacks the capacity to bind glucocorticoids, and it seems to act as an inhibitor of GRα-mediated transcriptional activation through the formation of GRα/GRβ heterodimers (32). In this context, stimulation with supernatants from *B. abortus*-infected monocytes did not have a significant effect on GRα/β ratio, and the treatment with cortisol or DHEA had no effect (**Figure 6D**).

Supernatants From *B. abortus*-Infected Monocytes Induce 11β-HSD1 Expression Through TNF-α

TNF-α is abundant in sites of osteoarticular inflammation (33). At the local level it has been described that TNF-α modulates 11β-HSD1 in order to convert cortisone in their active form cortisol (34).

Then, we asked if the increment of 11β-HSD1 transcription observed in synoviocytes treated with supernatants from *B. abortus*-infected monocytes was mediated by TNF-α. To this end, stimulation of synoviocytes with supernatants from *B. abortus*-infected monocytes was performed in the presence of an anti-TNFRc-blocking antibody. TNFRc-blocking antibody significantly inhibits the expression of 11β-HSD1, whereas an isotype control had no effect (**Figure 7A**). These results indicated that TNF-α secreted by *B. abortus*-infected monocytes could be involved in the induction of 11β-HSD1.

Cortisone Fails to Enhance 11β-HSD1 but Inhibits RANKL Induced by Supernatants From *B. abortus*-Infected Monocytes

We demonstrated that supernatants from *B. abortus*-infected monocytes induce 11β-HSD1 expression, and this expression is increased when stimulation was performed in the presence of cortisol. Thus, we decided to determine the effect of added cortisone instead of cortisol with culture supernatants from *B. abortus*-infected monocytes on 11β-HSD1 expression in synoviocytes. To this end, stimulation experiments were

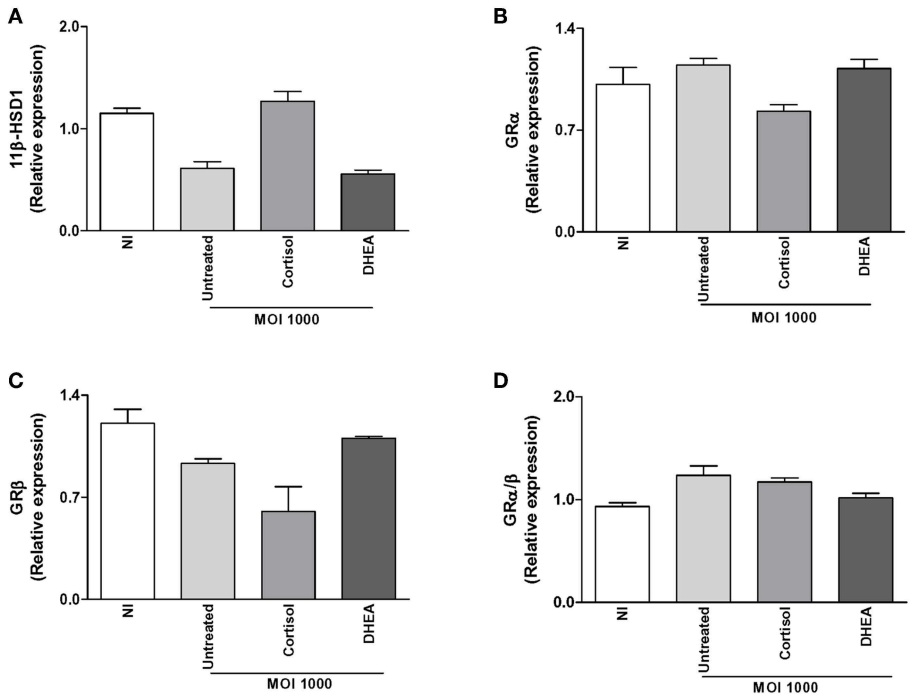

FIGURE 4 | Adrenal steroids do not modulate glucocorticoid receptor (GR) and 11β-hydroxysteroid dehydrogenase (HSD)-1 during *B. abortus* infection. 11β-HSD1, GRα, and GRβ expression were determined by RT-qPCR in *B. abortus*-infected synoviocytes at MOI of 1000 in the presence or not of cortisol (1×10^{-6} M) and dehydroepiandrosterone (DHEA) (1×10^{-8} M) for 24 h. 11β-HSD1 **(A)**, GRα **(B)**, GRβ **(C)**, GRα/β ratio **(D)**. Data are given as means ± SEM from at least three individual experiments. NI, non-infected.

performed by added culture supernatants from *B. abortus*-infected monocytes, and after 24 h of stimulation they were treated with cortisone or cortisol as a control. After 24 h, cells were harvested to determine the expression of 11β-HSD1. Addition of cortisone to cells stimulated with culture supernatants from *B. abortus*-infected monocytes had no effect on 11β-HSD1 expression with respect to cells stimulated with supernatants from *B. abortus*-infected monocytes alone (**Figure 7B**). However, cortisone inhibits RANKL secretion induced by supernatants from *B. abortus*-infected monocytes (**Figure 7C**). These results indicate that although supernatants from *B. abortus*-infected monocytes were able to induce 11β-HSD1, cortisone was unable to enhance the expression of 11β-HSD1 but mimicked the effect of cortisol on the modulation of RANKL expression.

DISCUSSION

The immune system does not respond in isolation. The immune system along with the endocrine axis and the neural system act together to fight diseases. Adrenal glands secrete cortisol, a glucocorticoid hormone that plays a role in the stress response, and DHEA that has frequently opposing actions to cortisol (35).

Although the role of adrenal steroids on synovial cells has been previously studied, the impact in the context of bacterial infection has not been elucidated until now. In this context, in brucellosis, it has been previously shown that this infection elicits an imbalance in the cortisol/DHEA ratio that could impact the immune response (12, 13). Our results indicated that in synoviocytes, cortisol treatment increased *B. abortus* intracellular proliferation. This phenomenon was avoided when both cortisol and DHEA were administrated in conjunction. This increase in bacterial load has been previously described during intracellular infection of other bacteria—*Salmonella typhimurium, Mycobacterium tuberculosis,* and inclusive *B. abortus* (13, 14, 16, 17). However, the mechanisms involved in the increase of intracellular growth were not completely elucidated. While some hormones induce and increase in bacteria virulence factor expression in *Mycoplasma hyopneumoniae*, *Vibrio parahaemolyticus,* and *Candida albicans* (36–38), cortisol was unable to induce an increase of virulence factors in *Salmonella typhymurium* (16).

Accordingly, with its opposite effect with respect to cortisol, DHEA treatment avoided the effect of cortisol, as was revealed in cells treated with cortisol and DHEA in conjunction. On the other hand, cortisol was able to promote *B. abortus* infection not only through its intracellular replication but also by the inhibition of the immune response and cell function in synoviocytes (39). In agreement with other observations, cortisol suppressed proinflammatory mediator secretion by *B. abortus-infected* synoviocytes, and DHEA was able to partially avoid this effect at least for MMP-2. These results again support the antagonist effect of DHEA (11). The role of proinflammatory

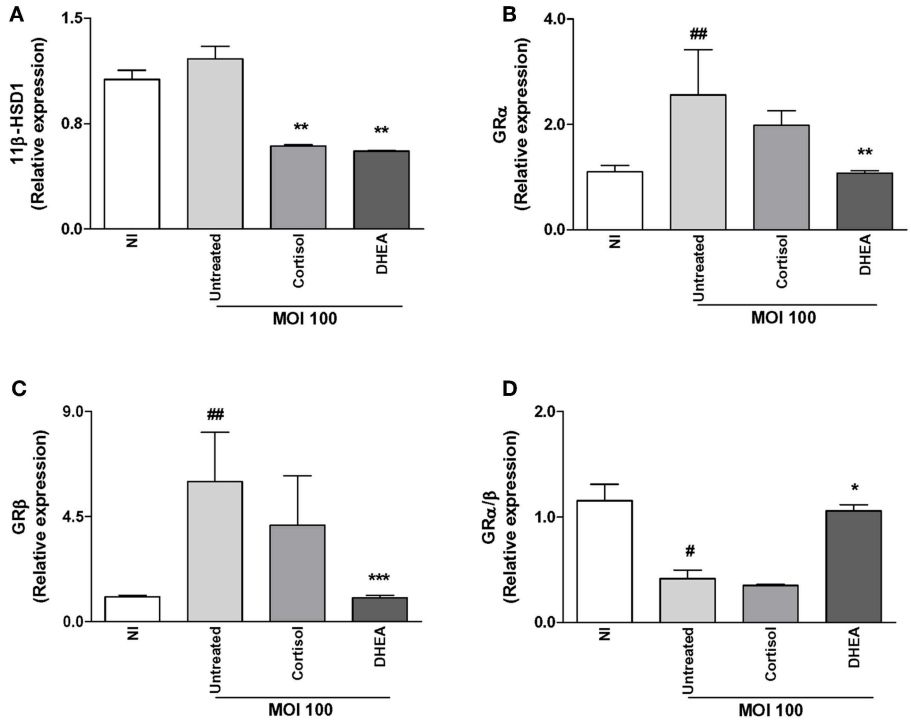

FIGURE 5 | Effect of adrenal steroids on glucocorticoid receptor (GR) and 11β-hydroxysteroid dehydrogenase (HSD)-1 expression in *B. abortus*-infected monocytes. 11β-HSD1, GRα, and GRβ expression were determined by RT-qPCR in *B. abortus*-infected THP-1 cells at MOI of 100 in the presence or not of cortisol (1×10^{-6} M), dehydroepiandrosterone (DHEA) (1×10^{-8} M) for 24 h. 11β-HSD1 **(A)**, GRα **(B)**, GRβ **(C)**, GRα/β ratio **(D)**. Data are given as the mean ± SEM from at least three individual experiments. $^{*}P < 0.1$; $^{**}P < 0.01$; and $^{***}P < 0.001$ vs. untreated cells: $^{\#}P < 0.1$; and $^{\#\#}P < 0.01$ vs. untreated infected cells. NI, non-infected.

cytokines on MMP induction has been extensively reported in osteoarticular diseases (19–24). *B. abortus* infection induces IL-6 but not TNF-α and IL-1β production by synovial cells. Since rhIL-6 was able to reverse the inhibitory effect of cortisol on MMP-2 secretion in *B. abortus*-infected synovial cells, it suggests that IL-6 could be involved in such induction.

In osteoarthritis, osteoclast formation is enhanced by proinflammatory cytokines from infiltrating immune cells but also synoviocytes enhance osteoclast formation via expression of RANKL (40). During osteoarticular brucellosis, the expression of RANKL could be increased by *B. abortus* infection and by the proinflammatory environment created by *B. abortus*-infected monocytes. In this context, DHEA was able to inhibit RANKL expression. The role of DHEA in the modulation of RANKL expression was described in the context of inflammatory non-infectious osteoarticular disease (41, 42). In addition, DHEA mediated this effect through ER receptor as evidenced when infections and the treatment with supernatants from *B. abortus*-infected monocytes were performed in the presence of fulvestrant. The ability of DHEA and its metabolites to signal through androgen receptor (AR) and ER has been previously described (43, 44). However, since the addition of ER antagonist, fulvestrant, completely avoids the effect of DHEA on RANKL expression, we could affirm that the main signaling of DHEA during *B. abortus* infection in sinoviocytes is via ER.

The presence of functional ER in synoviocytes might link the endocrine system and inflammation at the local level (45). The ability of DHEA to regulate RANKL through ER has been demonstrated previously at least in osteoblast cells (44). This indicated that ER could play a role in the modulation of osteoclastogénesis through the modulation of the key molecule implicated in osteoclastogenesis, RANKL in *B. abortus*-infected synoviocytes.

DKK-1 is the master regulator of bone remodeling in osteoarticular inflammatory disease (46). DKK-1 expression inhibits osteoblast differentiation and increases osteoclastogenesis with concomitant bone resorption. *B. abortus* induces the increase of DKK-1 expression in synoviocytes; this is in concordance with the bone resorption observed in patients with osteoarticular brucellosis. However, supernatants from *B. abortus*-infected monocytes were unable to induce DKK-1 expression. This could be explained, at least in part, by the role of TNF-α, IL-6, and IL-1β present in culture supernatants from *B. abortus*-infected monocytes on DKK-1 expression. While TNF-α suppresses bone formation by inducing DKK-1, IL-6, and IL-1β have been reported as inhibitors of DKK-1 expression (47, 48). Then, the cytokines combined in the culture supernatants from *B. abortus*-infected monocytes were unable to induce DKK-1 expression.

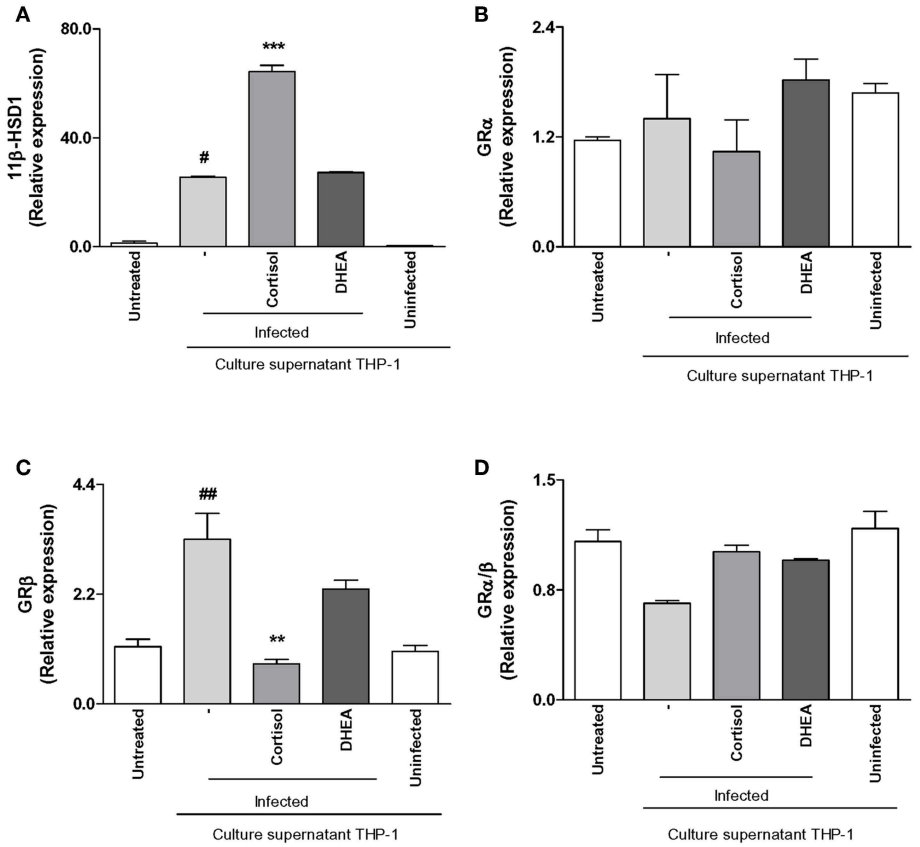

FIGURE 6 | Adrenal steroids modulate 11β-hydroxysteroid dehydrogenase (HSD)-1 and glucocorticoid receptor (GR) in synoviocytes stimulated with culture supernatants from *B. abortus*-infected monocytes. 11β-HSD1, GRα, and GRβ expression were determined by RT-qPCR in synoviocytes stimulated with 1/2 dilution of culture supernatants from *B. abortus* infected or uninfected THP-1 cells, in the presence or not of cortisol (1×10^{-6} M) and dehydroepiandrosterone (DHEA) (1×10^{-8} M) for 24 h. 11β-HSD1 **(A)**, GRα **(B)**, GRβ **(C)**, GRα/β ratio **(D)**. Data are given as means ± SEM from at least three individual experiments. $^{**}P < 0.01$, and $^{***}P < 0.001$ vs. absence of cortisol. $^{\#}P < 0.1$; and $^{\#\#}P < 0.01$ vs. non-infected culture supernatant THP-1.

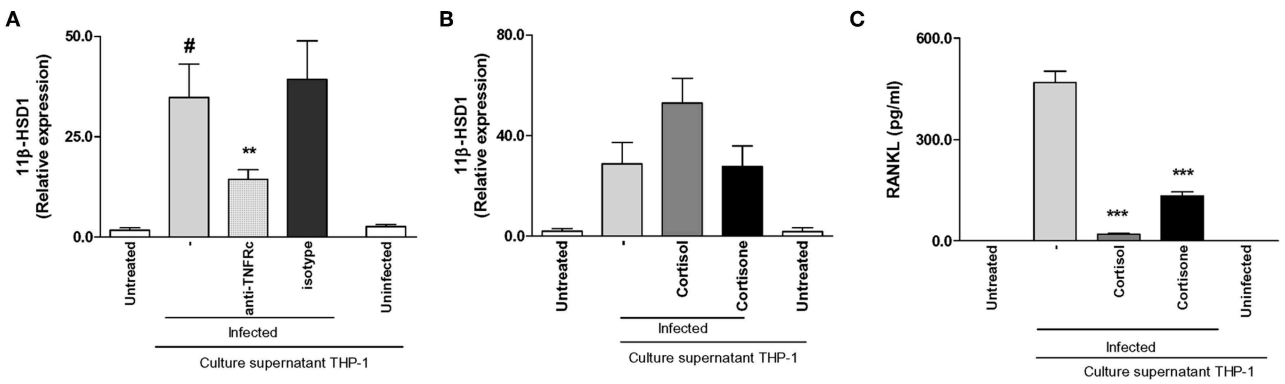

FIGURE 7 | Supernatants from *B. abortus*-infected monocytes induce 11β-hydroxysteroid dehydrogenase (HSD)-1 expression in a mechanism that is dependent on the presence of TNF-α. Synoviocytes were stimulated with 1/2 dilution of culture supernatants from *B. abortus* infected or uninfected THP-1 cells in the presence or not of cortisol (1×10^{-6} M), or cortisone (1×10^{-6} M) in the presence or not of anti-TNF receptor neutralizing antibody (anti-TNFRc) at a concentration of 20 μg/ml for 24 h; and 11β-HSD1 expression was determined by RT-qPCR **(A,B)**. RANKL was determined in culture supernatants by ELISA **(C)**. Data are given as means ± SEM from at least three individual experiments. $^{*}P < 0.1$, vs. anti-TNFRc. $^{***}P < 0.001$ vs. cortisol and cortisone treatment. $^{\#}P < 0.1$ vs. non-infected culture supernatant THP-1. NI, non-infected.

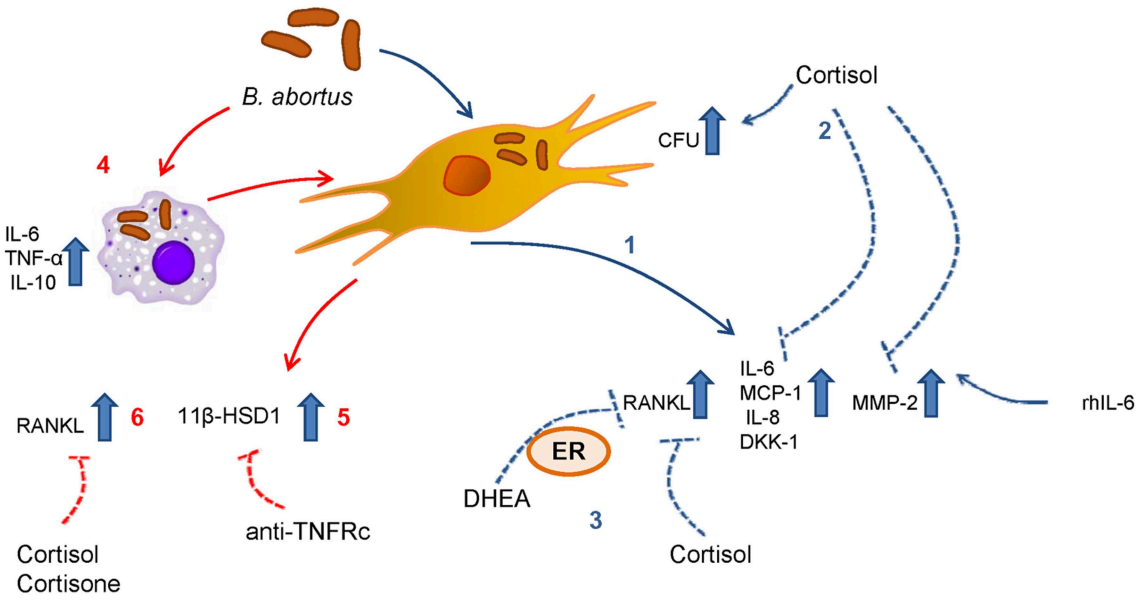

FIGURE 8 | Scheme summarized the results for the mechanisms involved in the modulation of synoviocytes by adrenal steroids during *B. abortus* infection. (1) Infection with *B. abortus* induces the secretion of RANKL, IL-6, MCP-1, IL-8, DKK-1, and MMP-2. (2) When cortisol is present, the intracellular CFU is increased with respect to untreated cells. (3) DHEA and cortisol avoid the increase of RANKL induced by *B. abortus* infection. The action of DHEA is mediated through the ER. (4) *B. abortus* infection induces the secretion of IL-6, TNF-α, and IL-10 by monocytes. (5) Supernatants from *B. abortus*-infected monocytes induce 11β-HSD1 in a mechanism that is dependent on TNFRc. (6) In addition, supernatants from *B. abortus*-infected monocytes induce RANKL, cortisol, and cortisone avoid this effect.

The effect of cortisol in synovial cells does not dependent on an increase of their bioavailability, as was demonstrated by the non-modification of 11β-HSD1 and GRα/β ratio in response to *B. abortus* infection in the presence or absence of adrenal steroids. A similar situation was found for *B. abortus*-infected monocytes in which *B. abortus* infection had no effect on 11β-HSD1 but cortisol and DHEA treatment inhibited its expression in the context of the infection. In addition, *B. abortus* infection in the presence or not of cortisol inhibited GRα/β ratio and DHEA could avoid this effect. In synoviocytes and monocytes, the absence of detectable expression of 11β-HSD2 deserves to be discussed since this enzyme is involved in the conversion of cortisol in its inactive form, cortisone. The absence of negligible levels of 11β-HSD2 in human monocytes, macrophages and dendritic cells has been reported (31, 49). In synovial cells, a high expression of 11β-HSD1 has been demonstrated, mainly in synovial fibroblast, whereas 11β-HSD2 is primarily restricted to synovial macrophages (30). Taking into account that we evaluated the effect of *B. abortus* infection in synovial fibroblast, our findings are in line with previous results.

Although the ability of monocytes to induce proinflammatory cytokines in response to *B. abortus* infection has been widely demonstrated (25, 27), supernatants from *B. abortus*-infected monocytes appear to have some anti-inflammatory effect, as was revealed by the induction of 11β-HSD1 in synovial cells. Despite this, cortisone does not seem to increase the expression of 11β-HSD1 as it does cortisol. However, the administration of cortisone is capable of inhibiting the secretion of RANKL by synoviocytes mimicking the cortisol effect. This indicates the importance of the increase of 11β-HSD1 in the utilization of cortisone. This is in accordance with previous observations that highlight the ability of synovial tissue to make active steroids, and this tissue has been considered an intracrine tissue (45). The increase of 11β-HSD1 expression induced by cortisol in synoviocytes treated with culture supernatants from *B. abortus*-infected monocytes also deserves to be discussed. The interactions between proinflammatory cytokines and glucocorticoids are often antagonistic. However, in some cases it can be additive or synergistic (50–52); even this synergistic effect of glucocorticoids on the production of 11β-HSD1 in the presence of proinflammatory cytokines was previously described in synovial fibroblasts (53). Our experiments in synovial cells treated with culture supernatants from *B. abortus*-infected monocytes in the presence of a neutralizing antibody anti-TNFRc significantly reduced 11β-HSD1; however, the remaining expression of 11β-HSD1 indicates that the contribution of other proinflammatory cytokines cannot be ruled out (**Figure 8**).

Finally, this is the first study that contributes to the knowledge of the effect of adrenal steroids on synoviocytes in the context of a bacterial infection. Our findings reveal that DHEA could modulate some synoviocytes function. Considering that and taking into account the modulation exerted by DHEA on other cell types in bone damage (13, 14), we can conclude that antibiotic therapy with supplementation with DHEA or its derivates could be a potential new treatment in order to reduce the bone damage during osteoarticular brucellosis.

DATA AVAILABILITY STATEMENT

The datasets generated for this study are available on request to the corresponding author.

AUTHOR CONTRIBUTIONS

All authors were involved in the design of the study, the preparation of the manuscript, and approve the final version for publication. MG: conceptualization, methodology, validation, formal analysis, investigation, funding acquisition, writing review and editing. GG: conceptualization, funding acquisition, writing review and editing. MD: conceptualization, methodology, validation, formal analysis, investigation, funding acquisition—supervision, validation, visualization, and writing original draft.

FUNDING

This work was supported by grants PICT 2014-1111 and PICT 2015-0316 from Agencia Nacional of Promoción Científica y Tecnológica (ANPCYT, Argentina), by grant PIP 2015-2017-0200 from Consejo Nacional de Investigaciones científicas y técnicas (CONICET). Funding agencies had no role in study design, data collection and analysis, decision to publish, or preparation of the manuscript.

ACKNOWLEDGMENTS

We thank Horacio Salomón and the staff of the Instituto de Investigaciones Biomédicas en Retrovirus y Sida (INBIRS) for their assistance with biosafety level 3 laboratory uses. MG, GG, and MD are members of the Carrera del Investigador of CONICET.

REFERENCES

1. Pourbagher A, Pourbagher MA, Savas L, Turunc T, Demiroglu YZ, Erol I, et al. Epidemiologic, clinical, and imaging findings in brucellosis patients with osteoarticular involvement. *AJR Am J Roentgenol*. (2006) 187:873–80. doi: 10.2214/AJR.05.1088
2. Madkour MM. *Osteoarticular brucellosis*. In: Madkour MM, editor. *Madkour's brucellosis*. 2nd edn. Berlin: Springer-Verlag (2001). p. 74–84. doi: 10.1007/978-3-642-59533-2_8
3. Bosilkovski M, Krteva L, Caparoska S, Dimzova M. Osteoarticular involvement in brucellosis: study of 196 cases in the Republic of Macedonia. *Croat Med J*. (2004) 45:727–33.
4. Madkour MM. Bone and joint imaging. In: Madkour MM, editor. *Madkour's brucellosis*. 2nd edn. Berlin: Springer-Verlag (2001). p. 90–132. doi: 10.1007/978-3-642-59533-2_10
5. Gotuzzo E, Alarcon GS, Bocanegra TS, Carrillo C, Guerra JC, Rolando I, et al. Articular involvement in human brucellosis: a retrospective analysis of 304 cases. *Semin Arthritis Rheum*. (1982) 12:245–55. doi: 10.1016/0049-0172(82)90064-6
6. Madkour MM. *Osteoarthicular brucellosis*. In: Madkour MM, editor. *Madkour's brucellosis*. 2nd edn. Berlin: Springer-Verlag (2001). p. 150–8. doi: 10.1007/978-3-642-59533-2_13
7. Scian R, Barrionuevo P, Giambartolomei GH, De Simone EA, Vanzulli SI, Fossati CA, et al. Potential role of fibroblast-like synoviocytes in joint damage induced by *Brucella abortus* infection through production and induction of matrix metalloproteinases. *Infect Immun*. (2011) 79:3619–32. doi: 10.1128/IAI.05408-11
8. Scian R, Barrionuevo P, Rodriguez AM, Arriola Benitez PC, Garcia Samartino C, Fossati CA, et al. *Brucella abortus* invasion of synoviocytes inhibits apoptosis and induces bone resorption through RANKL expression. *Infect Immun*. (2013) 81:1940–51. doi: 10.1128/IAI.01366-12
9. Besedovsky HO, del Rey A. Immune-neuro-endocrine interactions: facts and hypotheses. *Endocr Rev*. (1996) 17:64–102. doi: 10.1210/edrv-17-1-64
10. McEwen BS, Biron CA, Brunson KW, Bulloch K, Chambers WH, Dhabhar FS, et al. The role of adrenocorticoids as modulators of immune function in health and disease: neural, endocrine and immune interactions. *Brain Res Brain Res Rev*. (1997) 23:79–133. doi: 10.1016/S0165-0173(96)00012-4
11. Loria RM. Antiglucocorticoid function of androstenetriol. *Psychoneuroendocrinology*. (1997) 22 (Suppl. 1):S103–8. doi: 10.1016/S0306-4530(97)00005-X
12. Yildiz O, Gokce C, Alp E, Durak AC, Aygen B, Kelestimur F, et al. Investigation of the hypothalamo-pituitary-adrenal axis and changes in the size of adrenal glands in acute brucellosis. *Endocr J*. (2005) 52:183–8. doi: 10.1507/endocrj.52.183
13. Gentilini MV, Velasquez LN, Barrionuevo P, Arriola Benitez PC, Giambartolomei GH, Delpino MV. Adrenal steroids modulate the immune response during *Brucella abortus* infection by a mechanism that depends on the regulation of cytokine production. *Infect Immun*. (2015) 83:1973–82. doi: 10.1128/IAI.03090-14
14. Gentilini MV, Pesce Viglietti AI, Arriola Benitez PC, Iglesias Molli AE, Cerrone GE, Giambartolomei GH, et al. Inhibition of osteoblast function by *Brucella abortus* is reversed by dehydroepiandrosterone and involves ERK1/2 and estrogen receptor. *Front Immunol*. (2018) 9:88. doi: 10.3389/fimmu.2018.00088
15. Hibbs MS, Hasty KA, Seyer JM, Kang AH, Mainardi CL. Biochemical and immunological characterization of the secreted forms of human neutrophil gelatinase. *J Biol Chem*. (1985) 260:2493–500.
16. Verbrugghe E, Boyen F, Van Parys A, Van Deun K, Croubels S, Thompson A, et al. Stress induced *Salmonella Typhimurium* recrudescence in pigs coincides with cortisol induced increased intracellular proliferation in macrophages. *Vet Res*. (2011) 42:118. doi: 10.1186/1297-9716-42-118
17. Bongiovanni B, Mata-Espinosa D, D'Attilio L, Leon-Contreras JC, Marquez-Velasco R, Bottasso O, et al. Effect of cortisol and/or DHEA on THP1-derived macrophages infected with *Mycobacterium tuberculosis*. *Tuberculosis*. (2015) 95:562–9. doi: 10.1016/j.tube.2015.05.011
18. Elkington PT, O'Kane CM, Friedland JS. The paradox of matrix metalloproteinases in infectious disease. *Clin Exp Immunol*. (2005) 142:12–20. doi: 10.1111/j.1365-2249.2005.02840.x
19. Alsalameh S, Amin RJ, Kunisch E, Jasin HE, Kinne RW. Preferential induction of prodestructive matrix metalloproteinase-1 and proinflammatory interleukin 6 and prostaglandin E2 in rheumatoid arthritis synovial fibroblasts via tumor necrosis factor receptor-55. *J Rheumatol*. (2003) 30:1680–90.
20. Harris JE, Fernandez-Vilaseca M, Elkington PT, Horncastle DE, Graeber MB, Friedland JS. IFNgamma synergizes with IL-1beta to up-regulate MMP-9 secretion in a cellular model of central nervous system tuberculosis. *Faseb J*. (2007) 21:356–65. doi: 10.1096/fj.06-6925com
21. Nagase H, Brew K. Designing TIMP (tissue inhibitor of metalloproteinases) variants that are selective metalloproteinase inhibitors. *Biochem Soc Symp*. (2003) 70:201–12. doi: 10.1042/bss0700201
22. Panagakos FS, Kumar S. Modulation of proteases and their inhibitors in immortal human osteoblast-like cells by tumor necrosis factor-alpha *in vitro*. *Inflammation*. (1994) 18:243–65. doi: 10.1007/BF01534267
23. Uchida M, Shima M, Shimoaka T, Fujieda A, Obara K, Suzuki H, et al. Regulation of matrix metalloproteinases (MMPs) and tissue inhibitors of metalloproteinases (TIMPs) by bone resorptive factors in osteoblastic cells. *J Cell Physiol*. (2000) 185:207–14. doi: 10.1002/1097-4652(200011)185:2<207::AID-JCP5>3.0.CO;2-J

24. Wright KM, Friedland JS. Regulation of monocyte chemokine and MMP-9 secretion by proinflammatory cytokines in tuberculous osteomyelitis. *J Leukoc Biol*. (2004) 75:1086–92. doi: 10.1189/jlb.0903433
25. Giambartolomei GH, Zwerdling A, Cassataro J, Bruno L, Fossati CA, Philipp MT. Lipoproteins, not lipopolysaccharide, are the key mediators of the proinflammatory response elicited by heat-killed *Brucella abortus*. *J Immunol*. (2004) 173:4635–42. doi: 10.4049/jimmunol.173.7.4635
26. Zhan Y, Cheers C. Differential induction of macrophage-derived cytokines by live and dead intracellular bacteria *in vitro*. *Infect Immun*. (1995) 63:720–3.
27. Delpino MV, Barrionuevo P, Macedo GC, Oliveira SC, Genaro SD, Scian R, et al. Macrophage-elicited osteoclastogenesis in response to *Brucella abortus* infection requires TLR2/MyD88-dependent TNF-alpha production. *J Leukoc Biol*. (2012) 91:285–98. doi: 10.1189/jlb.04111185
28. Miller KK, Al-Rayyan N, Ivanova MM, Mattingly KA, Ripp SL, Klinge CM, et al. DHEA metabolites activate estrogen receptors alpha and beta. *Steroids*. (2013) 78:15–25. doi: 10.1016/j.steroids.2012.10.002
29. Huang Y, Liu L, Liu A. Dickkopf-1: current knowledge and related diseases. *Life Sci*. (2018) 209:249–54. doi: 10.1016/j.lfs.2018.08.019
30. Hardy R, Cooper MS. Adrenal gland and bone. *Arch Biochem Biophys*. (2010) 503:137–45. doi: 10.1016/j.abb.2010.06.007
31. Thieringer R, Le Grand CB, Carbin L, Cai TQ, Wong B, Wright SD, et al. 11 Beta-hydroxysteroid dehydrogenase type 1 is induced in human monocytes upon differentiation to macrophages. *J Immunol*. (2001) 167:30–5. doi: 10.4049/jimmunol.167.1.30
32. Oakley RH, Cidlowski JA. Cellular processing of the glucocorticoid receptor gene and protein: new mechanisms for generating tissue-specific actions of glucocorticoids. *J Biol Chem*. (2011) 286:3177–84. doi: 10.1074/jbc.R110.179325
33. Zhang YH, Heulsmann A, Tondravi MM, Mukherjee A, Abu-Amer Y. Tumor necrosis factor-alpha (TNF) stimulates RANKL-induced osteoclastogenesis via coupling of TNF type 1 receptor and RANK signaling pathways. *J Biol Chem*. (2001) 276:563–8. doi: 10.1074/jbc.M008198200
34. Heiniger CD, Rochat MK, Frey FJ, Frey BM. TNF-alpha enhances intracellular glucocorticoid availability. *FEBS Lett*. (2001) 507:351–6. doi: 10.1016/S0014-5793(01)03004-6
35. Sacco M, Valenti G, Corvi Mora P, Wu FC, Ray DW. DHEA, a selective glucocorticoid receptor antagonist: its role in immune system regulation and metabolism. *J Endocrinol Invest*. (2002) 25(10 Suppl.):81–2.
36. Oneal MJ, Schafer ER, Madsen ML, Minion FC. Global transcriptional analysis of Mycoplasma hyopneumoniae following exposure to norepinephrine. *Microbiology*. (2008) 154(Pt 9):2581–8. doi: 10.1099/mic.0.2008/020230-0
37. Nakano M, Takahashi A, Sakai Y, Nakaya Y. Modulation of pathogenicity with norepinephrine related to the type III secretion system of *Vibrio parahaemolyticus*. *J Infect Dis*. (2007) 195:1353–60. doi: 10.1086/513275
38. Banerjee D, Martin N, Nandi S, Shukla S, Dominguez A, Mukhopadhyay G, et al. A genome-wide steroid response study of the major human fungal pathogen *Candida albicans*. *Mycopathologia*. (2007) 164:1–17. doi: 10.1007/s11046-007-9025-8
39. Miyazawa K, Mori A, Okudaira H. Regulation of interleukin-1beta-induced interleukin-6 gene expression in human fibroblast-like synoviocytes by glucocorticoids. *J Biochem*. (1998) 124:1130–7. doi: 10.1093/oxfordjournals.jbchem.a022231
40. Takayanagi H, Iizuka H, Juji T, Nakagawa T, Yamamoto A, Miyazaki T, et al. Involvement of receptor activator of nuclear factor kappaB ligand/osteoclast differentiation factor in osteoclastogenesis from synoviocytes in rheumatoid arthritis. *Arthritis Rheum*. (2000) 43:259–69. doi: 10.1002/1529-0131(200002)43:2<259::AID-ANR4>3.0.CO;2-W
41. Wang YD, Wang L, Li DJ, Wang WJ. Dehydroepiandrosterone inhibited the bone resorption through the upregulation of OPG/RANKL. *Cell Mol Immunol*. (2006) 3:41–5.
42. Harding G, Mak YT, Evans B, Cheung J, MacDonald D, Hampson G. The effects of dexamethasone and dehydroepiandrosterone (DHEA) on cytokines and receptor expression in a human osteoblastic cell line: potential steroid-sparing role for DHEA. *Cytokine*. (2006) 36(1–2):57–68. doi: 10.1016/j.cyto.2006.10.012
43. Engdahl C, Lagerquist MK, Stubelius A, Andersson A, Studer E, Ohlsson C, et al. Role of androgen and estrogen receptors for the action of dehydroepiandrosterone (DHEA). *Endocrinology*. (2014) 155:889–96. doi: 10.1210/en.2013-1561
44. Wang YD, Tao MF, Wang L, Cheng WW, Wan XP. Selective regulation of osteoblastic OPG and RANKL by dehydroepiandrosterone through activation of the estrogen receptor beta-mediated MAPK signaling pathway. *Horm Metab Res*. (2012) 44:494–500. doi: 10.1055/s-0032-1311567
45. Cutolo M, Straub RH, Bijlsma JW. Neuroendocrine-immune interactions in synovitis. *Nat Clin Pract Rheumatol*. (2007) 3:627–34. doi: 10.1038/ncprheum0601
46. Diarra D, Stolina M, Polzer K, Zwerina J, Ominsky MS, Dwyer D, et al. Dickkopf-1 is a master regulator of joint remodeling. *Nat Med*. (2007) 13:156–63. doi: 10.1038/nm1538
47. Yeremenko N, Zwerina K, Rigter G, Pots D, Fonseca JE, Zwerina J, et al. Tumor necrosis factor and interleukin-6 differentially regulate Dkk-1 in the inflamed arthritic joint. *Arthritis Rheumatol*. (2015) 67:2071–5. doi: 10.1002/art.39183
48. Yoshida Y, Yamasaki S, Oi K, Kuranobu T, Nojima T, Miyaki S, et al. IL-1beta Enhances Wnt Signal by Inhibiting DKK1. *Inflammation*. (2018) 41:1945–54. doi: 10.1007/s10753-018-0838-z
49. Freeman L, Hewison M, Hughes SV, Evans KN, Hardie D, Means TK, et al. Expression of 11beta-hydroxysteroid dehydrogenase type 1 permits regulation of glucocorticoid bioavailability by human dendritic cells. *Blood*. (2005) 106:2042–9. doi: 10.1182/blood-2005-01-0186
50. Hermoso MA, Matsuguchi T, Smoak K, Cidlowski JA. Glucocorticoids and tumor necrosis factor alpha cooperatively regulate toll-like receptor 2 gene expression. *Mol Cell Biol*. (2004) 24:4743–56. doi: 10.1128/MCB.24.11.4743-4756.2004
51. Trujillo ME, Lee MJ, Sullivan S, Feng J, Schneider SH, Greenberg AS, et al. Tumor necrosis factor alpha and glucocorticoid synergistically increase leptin production in human adipose tissue: role for p38 mitogen-activated protein kinase. *J Clin Endocrinol Metab*. (2006) 91:1484–90. doi: 10.1210/jc.2005-1901
52. Homma T, Kato A, Hashimoto N, Batchelor J, Yoshikawa M, Imai S, et al. Corticosteroid and cytokines synergistically enhance toll-like receptor 2 expression in respiratory epithelial cells. *Am J Respir Cell Mol Biol*. (2004) 31:463–9. doi: 10.1165/rcmb.2004-0161OC
53. Kaur K, Hardy R, Ahasan MM, Eijken M, van Leeuwen JP, Filer A, et al. Synergistic induction of local glucocorticoid generation by inflammatory cytokines and glucocorticoids: implications for inflammation associated bone loss. *Ann Rheum Dis*. (2009) 69:1185–90. doi: 10.1136/ard.2009.107466

Conflict of Interest: The authors declare that the research was conducted in the absence of any commercial or financial relationships that could be construed as a potential conflict of interest.

frontiers in Endocrinology

ORIGINAL RESEARCH
published: 22 October 2019
doi: 10.3389/fendo.2019.00719

Overexpression of miR-146a Might Regulate Polarization Transitions of BV-2 Cells Induced by High Glucose and Glucose Fluctuations

Yinqiong Huang[1†], Zhenling Liao[2†], Xiahong Lin[1], Xiaohong Wu[1], Xiaoyu Chen[1], Xuefeng Bai[1], Yong Zhuang[1], Yingxia Yang[3] and Jinying Zhang[3]*

[1] Department of Endocrinology, The Second Affiliated Hospital of Fujian Medical University, Quanzhou, China, [2] Department of Endocrinology, The First People's Hospital of Shaoguan City, Shaoguan, China, [3] Department of Neurology, The Second Affiliated Hospital of Fujian Medical University, Quanzhou, China

Microglia are critical in neuroinflammation. M1/M2 polarization transitions of microglial phenotypes determine the states of neuroinflammation and are regulated by multiple pathways, including miRNAs and other epigenetic regulations. This study investigated the polarization transitions of microglia induced by high glucose and glucose fluctuations, and the role of miR-146a in regulating M1/M2 polarization transitions of microglia. BV-2 cells were cultured with 25 mmol/L glucose, 75 mmol/L glucose, and 25 mmol/L—75 mmol/L glucose fluctuation for 48 h. BV-2 cells overexpressing miR-146a were generated using a lentiviral vector. Quantitative real-time polymerase chain reaction (qRT-PCR) was used to measure mRNA expression of miR-146a, CD11b, iNOS, Arg-1, IRAK1, TRAF6, and NF-κB. Immunofluorescence was used to measure CD11b expression. Western blot was used to measure protein expression of CD11b, iNOS, and Arg-1. Compared with those in the 25 mmol/L glucose control group, expression of CD11b, iNOS, TNF-α, and IL-6 in the 75 mmol/L glucose or glucose fluctuation groups of cultured BV-2 cells were significantly increased, while Arg-1 and IL-10 was significantly decreased. These effects were reversed by overexpression of miR-146a. Furthermore, expression of IRAK1, TRAF6, and NF-κB was significantly increased in the high glucose and glucose fluctuation groups; this was reduced after miR-146a overexpression. In sum, high glucose and glucose fluctuations induced polarization transitions from M1 to M2 phenotype in BV-2 cells. Overexpression of miR-146a might protect BV-2 cells from high glucose and glucose fluctuation associated with M1/M2 polarization transitions by downregulating the expression of IRAK1, TRAF6, and NF-κB.

Keywords: microglia, polarization transitions, miR-146a, neuroinflammation, glucose fluctuation

OPEN ACCESS

Edited by:
Vinicius Frias Carvalho, Oswaldo Cruz Foundation (Fiocruz), Brazil

Reviewed by:
Zhen-Zhen Wang, Institute of Drugs (CAMS), China
Rudimar Luiz Frozza, Oswaldo Cruz Foundation (Fiocruz), Brazil

****Correspondence:***
Xiahong Lin
linxiahongdr@fjmu.edu.cn

† These authors have contributed equally to this work

Specialty section:
This article was submitted to Neuroendocrine Science, a section of the journal Frontiers in Endocrinology

Received: *04 July 2019*
Accepted: *04 October 2019*
Published: *22 October 2019*

Citation:
Huang Y, Liao Z, Lin X, Wu X, Chen X, Bai X, Zhuang Y, Yang Y and Zhang J (2019) Overexpression of miR-146a Might Regulate Polarization Transitions of BV-2 Cells Induced by High Glucose and Glucose Fluctuations. Front. Endocrinol. 10:719. doi: 10.3389/fendo.2019.00719

INTRODUCTION

Diabetic encephalopathy (DE) is a chronic complication of diabetes mellitus (DM), which can cause cognitive decline, dementia, and mental disorders, which significantly affects the quality of life of diabetic patients (1). Since the concept of DE was proposed by Nieleson in 1965, our understanding of DE has deepened. Its pathogenesis involves various aspects, including neuroinflammation (2, 3), blood-brain barrier (BBB) (2), vascular factors (4), insulin resistance,

insulin deficiency (5, 6), and oxidative stress (3, 6). However, controversy in the literature remains. Neuroinflammation plays an important role in the pathogenesis of DE (7). Neuroinflammation is a complex innate immune response of the central nervous system that inhibits infection; removes pathogens, cell debris, and misfolded proteins; and plays an important role in nerve repair and evolution (8, 9). However, the persistence or excessive activation of neuroinflammation can lead to various neurological diseases.

Microglia are critical nervous system-specific immune cells involved in the response to neuroinflammation. Microglial polarization states comprise M1 and M2 phenotypes. M1 polarized microglia have pro-inflammatory effects and phagocytic functions (10), mainly secreting pro-inflammatory factors such as inducible nitric oxide synthase (iNOS), tumor necrosis factor (TNF)-α, interleukin (IL)-6, and nitric oxide (NO) to further aggravate neuronal damage. M2 polarized microglia inhibit inflammatory responses, regulate neuroinflammation (7), nourish nerves, and promote nerve repair (8, 11), with overexpression of arginase-1 (Arg-1), IL-10, IL-4, and transforming growth factor (TGF)-β. Polarization transitions to M1 phenotype induced by high glucose and glucose fluctuations have been observed in microglia both *in vivo* and *in vitro*. The expression of iNOS in the hippocampus of diabetic mice was significantly increased by inflammatory factors induced by high glucose (11). Compared with that in the control group, the expression of iNOS in microglia was upregulated after glucose fluctuations. The expression of iNOS also significantly increased after high glucose induction (12). Activation of nuclear factor (NF)-κB and signal transducer and activator of transcription 1 (STAT1) may regulate M1 polarization of microglia, whereas STAT6 and STAT3 activation may regulate M2 polarization (13). Nevertheless, it remains unclear how hyperglycemia and glucose fluctuations regulate polarization transitions of microglia.

In recent years, studies have reported that miRNAs are involved in the regulation of microglia polarization. miR-29b and miR-125a induce polarization transitions to M1 phenotype by inhibiting the expression of TNF-α-inducible protein 3 (TNFAIP3) downstream of the NF-κB signaling pathway (14). miR-146a plays an important role in the regulation of inflammatory responses (15). Previous studies confirmed that miR-146a directly regulates IRAK1 and TRAF6, thereby regulating the pro-inflammatory factor NF-κB and expression of inflammatory factors (16).

The present study therefore aimed to evaluate the role of miR-146a on high glucose and glucose fluctuation-associated polarization transitions of microglia. We hypothesized that miR-146a was involved in the regulation of polarization transitions of microglia induced by hyperglycemia and glucose fluctuations.

MATERIALS AND METHODS

Cell Culture

BV-2 cells were obtained from Chinese Academy of Sciences (CAS) Kunming Cell Bank (Kunming, China) and cultured in 25 mmol/L glucose Dulbecco's Modified Eagle Medium (DMEM) (Gibco, USA) supplemented with 10% fetal bovine serum (FBS) (Gibco, USA) and 1% penicillin-streptomycin (Hyclone, USA). Cells were maintained in a humidified atmosphere containing 5% CO_2 at 37°C.

For glucose fluctuation BV-2 group culture, after cell attachment, the cell culture medium was replaced with 25 or 75 mmol/L glucose in DMEM every 6 h and cultured for 48 h. High glucose was the last fluctuation.

Stably transfected BV-2 cells overexpressing miR-146a were generated using the overexpression plasmid vector GV369 (Addgene). miR-146a was amplified using the following primers: forward primer, 5′-GAGGATCCCCGGGTACCGGT ACAGGGCTGGCAGGATCTG-3; reverse primer, 5′- CACA CATTCCACAGGCTAGCCCCACTCTCTCCACTCTTC AAG-3 (Shanghai Gene Company, Shanghai, China). The amplified sequences were inserted into GV369 by a recombinant method (Genechem Company, Shanghai, China) according to the manufacturer's instructions. The resultant plasmid was then transfected into 293T cells to construct a lentivirus overexpressing miR-146a.

BV-2 at 3×10^4/well (six well plates) were seeded and cultured for 12 h. A volume of 2 mL enhanced infection solution containing Lv-mmu-miR-146a (Genechem Company, Shanghai, China) with the corresponding viral load and control virus expressing spontaneous green fluorescent protein (GFP) with puromycin acetyltransferase was incubated with cells. The load of viral particles was quantified and normalized before the addiction to the cells. At 12 h after infection, the medium was replaced with conventional culture medium. After 72 h, GFP expression was observed under a fluorescence microscope (Leica, Germany). Complete medium containing 2 μg/mL puromycin (Sigma, Aldrich, USA) was used to screen virus-infected cells, and 1 g/mL was used for further screening. Quantitative real-time polymerase chain reaction (qRT-PCR) was used to assess relative expression levels of miR-146a in the Lv-mmu-miR-146a infection group.

Immunofluorescence Staining of CD11b

Cells grown on glass coverslips were fixed with 4% paraformaldehyde, 0.1% Triton X-100, permeabilized, blocked with 1% bovine serum albumin (BSA), and incubated with anti-CD11b antibody (rat monoclonal antibody; Abcam, USA; 1: 500) at 4°C overnight. After washes with 1× phosphate-buffered saline (PBS), cells were incubated with the corresponding secondary antibody conjugated with Alexa Fluor® 647 (donkey polyclonal secondary antibody to rat IgG, H&L; Abcam, USA; 1:100) in the dark for 1 h and analyzed using an inverted fluorescence microscope (Leica, Germany). 4′,6-diamidino-2-phenylindole (DAPI) was used to label cell nuclei. To assess BV-2 cell activation. ImageJ was used to calculate the expression of CD11b fluorescence intensity per scaffold. At least five slides were examined per treatment group for each experiment. A comparison of the fluorescence intensity of CD11b between the indicated groups was performed.

Quantitative RT-PCR (qRT-PCR)

Total RNA was extracted with TRIzol (RNAiso Plus) (Takara, Japan). RNA was reversed transcribed into cDNA using the

TABLE 1 | Primers of qRT-PCR.

Gene		Primers sequence
CD11b	Forward	5′ GAGCATCAATAGCCAGCCTCAGTG 3′
	Reverse	5′ CCAACAGCCAGGTCCATCAAGC 3′
iNOS	Forward	5′ GTTTACCATGAGGCTGAAATCC 3′
	Reverse	5′ CCTCTTGTCTTTGACCCAGTAG 3′
Arg-1	Forward	5′ CATATCTGCCAAAGACATCGTG 3′
	Reverse	5′ GACATCAAAGCTCAGGTGAATC 3′
β-actin	Forward	5′ CTACCTCATGAAGATCCTGACC 3′
	Reverse	5′ CACAGCTTCTCTTTGATGTCAC 3′
NF-κB	Forward	5′ CAAAGACAAAGAGGAAGTGCAA 3′
	Reverse	5′ GATGGAATGTAATCCCACCGTA 3′
TRAF6	Forward	5′ GAAAATCAACTGTTTCCCGACA3′
	Reverse	5′ ACTTGATGATCCTCGAGATGTC 3′
IRAK1	Forward	5′ GTTATGTGCCGCTTCTACAAAG 3′
	Reverse	5′ GATGTGAACGAGGTCAGCTAC 3′
TNF-α	Forward	5′ ATGTCTCAGCCTCTTCTCATTC 3′
	Reverse	5′ GCTTGTCACTCGAATTTTGAGA 3′
IL-6	Forward	5′ CTCCCAACAGACCTGTCTATAC 3′
	Reverse	5′ CCATTGCACAACTCTTTTCTCA 3′
IL-10	Forward	5′ TGCTAACCGACTCCTTAATGCAGGAC 3′
	Reverse	5′ CCTTGATTTCTGGGCCATGCTTCTC 3′
U6	Forward	5′ CTCGCTTCGGCAGCACA 3′
	Reverse	5′ AACGCTTCACGAATTTGCGT 3′
miR-146a−5p	Forward	5′ CGCTGAGAACTGAATTCCATGGGTT 3′

β-actin was used as mRNA and U6 as miRNA reference gene, with the $2^{-\Delta\Delta Ct}$ method used for quantitation. Triplicate experiments were performed and repeated at least 3 times.

twostep method with PrimeScript™ RT reagent Kit with gDNA Eraser (Takara, Japan). Genomic DNA of miRNA was removed using Recombinant DNase I (RNase-free) (Takara, Japan). miRNA was reversed transcribed into cDNA using the Mir-X® miRNA FirstStrand Synthesis and SYBR® qRT-PCR (Takara, Japan). mRNA qRT-PCR was performed with the TB Green™ Premix Ex Taq™ (Tli RNaseH Plus) (Takara, Japan). miRNA qRT-PCR was performed with Mir-X™ miRNA FirstStrand Synthesis and SYBR® qRT-PCR (Takara, Japan). The primers used are shown in **Table 1**.

Western Blot

Total cell proteins were extracted and equal amounts of protein (20 μg/sample) were separated by 10% SDS-PAGE and transferred onto PVDF membranes (Millipore, USA). After blocking with 5% skim milk at room temperature for 2 h, the membranes were incubated with primary antibodies targeting β-actin (mouse monoclonal antibody; Bioworld Technology, USA; 1:10,000), Cd11b (rabbit polyclonal antibody; Abcam, USA; 1:2,000), iNOS (rabbit polyclonal antibody; Abcam, USA; 1:600), and Arg-1 (rabbit polyclonal antibody; Abcam, USA; 1:1,000) overnight at 4°C. Then, membranes were incubated with secondary antibodies (anti-rabbit or anti-mouse IgG/HRP; CST; 1:5,000) for 2 h with shaking. After enhanced chemiluminescence (ECL) (Merck Millipore, Germany) reaction, protein bands were revealed on a Gel Imaging System (Syngene, USA). Gray values were analyzed with Image Lab software (Bio-Rad, USA) using β-actin as a loading control.

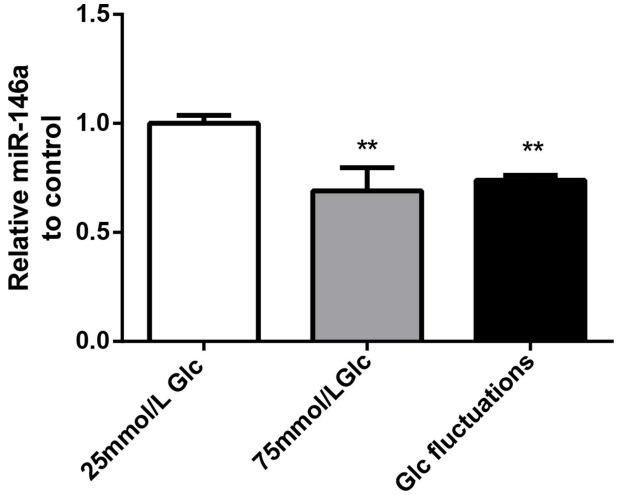

FIGURE 1 | Effects of high glucose and glucose fluctuations on miR-146a levels in BV-2 cells. Expression levels of miR-146a, $^{**}p < 0.01$ 75 mmol/L Glc vs. control, $^{**}p < 0.01$ Glc fluctuation vs. control.

Enzyme-Linked Immunosorbent Assay (ELISA)

The levels of TNF-α, IL-6, and IL-10 in cell culture supernatants were evaluated with an ELISA kit (ABclonal, China), according to the manufacturer's instructions.

Statistical Analysis

SPSS 22.0 software (SPSS, USA) was used for data analysis. Data are expressed as mean ± standard deviation (SD). Group pairs were compared by *t*-tests. Normally distributed data were analyzed 292 using one-way analysis of variance (ANOVA), and non-normal 293 distributions were analyzed with the Kruskal–Wallis *H*-test. Statistical differences were 297 considered as significant if the $P < 0.05$.

RESULTS

Effects of High Glucose and Glucose Fluctuation on miR-146a Expression in BV-2 Cells

Compared with that in the 25 mmol/L glucose group, the expression of miR-146a in the 75 mmol/L glucose group and glucose fluctuation group was significantly decreased (0.69 ± 0.107 vs. 1.00 ± 0.037, $^{**}p = 0.001$ and 0.74 ± 0.208 vs. 1.00 ± 0.037, $^{**}p = 0.003$, respectively) (**Figure 1**).

miR-146a Overexpression in BV-2 Cells

Green fluorescent protein was expressed by more than 80% of BV-2 cells 72 h after transfection with miR-146a lentivirus and control virus (**Figure 2A**). After stable transfection and

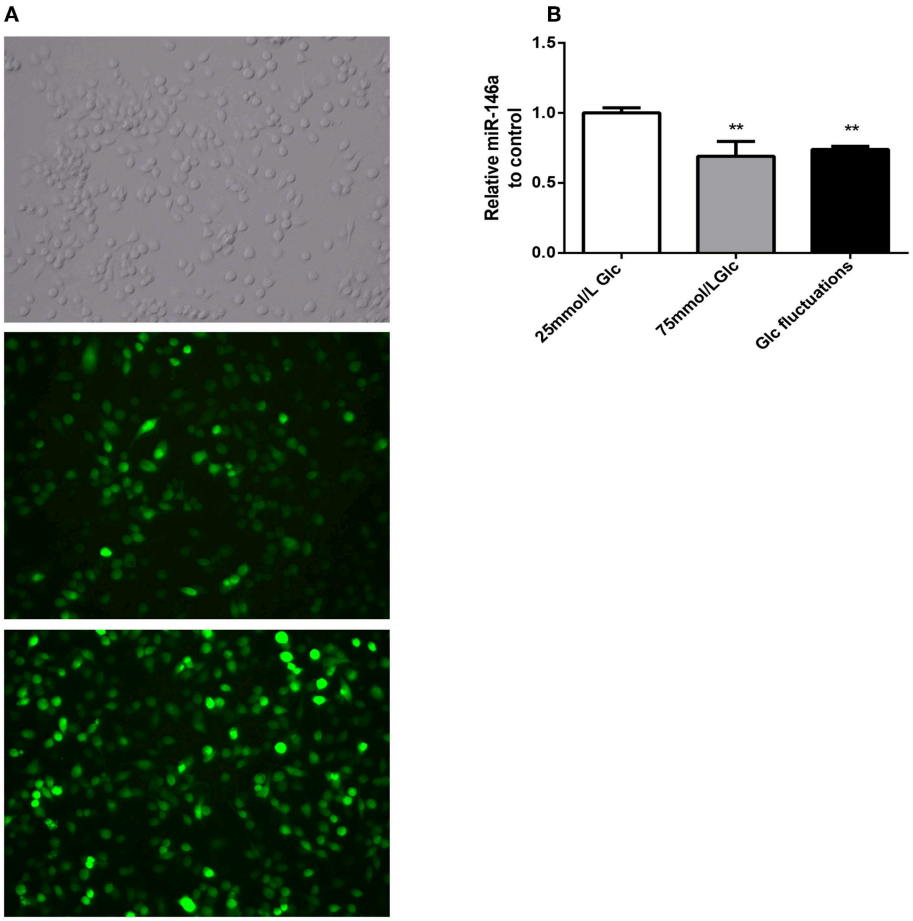

FIGURE 2 | GFP expression and miR-146a expression levels after lentiviral infection in BV-2. **(A)** GFP expression after BV-2 transfection with over-expression of miR-146a lentivirus and control virus. **(B)** miR-146a expression levels before and after BV-2 transfection with over-expression of miR-146a lentivirus, $^{***}p < 0.001$ Lv-mmu-miR-146a group vs. control.

puromycin screening, miR-146a levels in the Lv-mmu-miR-146a group were significantly higher than those of the control group (3.63 ± 0.208 vs. 1.00 ± 0.086, $^{***}p < 0.001$) (**Figure 2B**). These findings indicated that miR-146a overexpressing lentiviruses were successfully transfected into BV-2.

Effects of miR-146a Overexpression on M1/M2 Polarization Transitions

Microglial Activation Marker CD11b

Immunofluorescence analysis (**Figure 3**) indicated that the expression of the M1 phenotype polarization marker, CD11b, was significantly increased in the 75 mmol/L glucose (15.75 ± 3.98 vs. 6.47 ± 0.996, $^{###}p < 0.001$) and fluctuation group (11.5 ± 1.952 vs. 6.47 ± 0.996, $^{##}p = 0.008$) compared to that in the control group. The expression of CD11b was significantly decreased in the 75 mmol/L glucose+Lv-mmu-miR-146a group compared with that in the 75 mmol/L glucose group (6.74 ± 0.916 vs. 15.75 ± 3.98, $^{***}p < 0.001$). Similar results were observed in the glucose fluctuation+Lv-mmu-miR-146a group when compared with the glucose fluctuation group (6.76 ± 1.487 vs. 11.50 ± 1.952, $^{***}p < 0.001$).

BV-2 cells were cultured in 25 mmol/L glucose, 75 mmol/L glucose, or glucose fluctuation groups for 24 h, and qRT-PCR was used to measure the expression of CD11b (**Figure 4A**). Compared with that in the 25 mmol/L glucose group, the expression of *CD11b* mRNA was significantly increased in the 75 mmol/L glucose group (2.13 ± 0.269 vs. 1.00 ± 0.093, $^{###}p < 0.001$) and glucose fluctuation group (1.57 ± 0.141 vs. 1.00 ± 0.093, $^{##}p = 0.002$). The expression of *CD11b* mRNA was significantly decreased in the 75 mmol/L glucose+Lv-mmu-miR-146a group compared with that in the 75 mmol/L glucose group (1.16 ± 0.074 vs. 2.13 ± 0.2691, $^{***}p < 0.001$). Similar results were observed in the glucose fluctuation+Lv-mmu-miR-146a group when compared with the glucose fluctuation group (1.015 ± 0.266 vs. 1.57 ± 0.141, $^{**}p = 0.002$).

Western blot (**Figures 4B,C**) revealed that the expression of CD11b protein was significantly increased in the 75 mmol/L glucose (2.13 ± 0.422 vs. 1.00 ± 0.110, $^{##}p = 0.007$) and fluctuation group (1.80 ± 0.360 vs. 1.00 ± 0.110, $^{##}p = 0.003$) compared with that in the control group. The expression of CD11b protein was significantly decreased in the 75 mmol/L glucose+Lv-mmu-miR-146a group compared

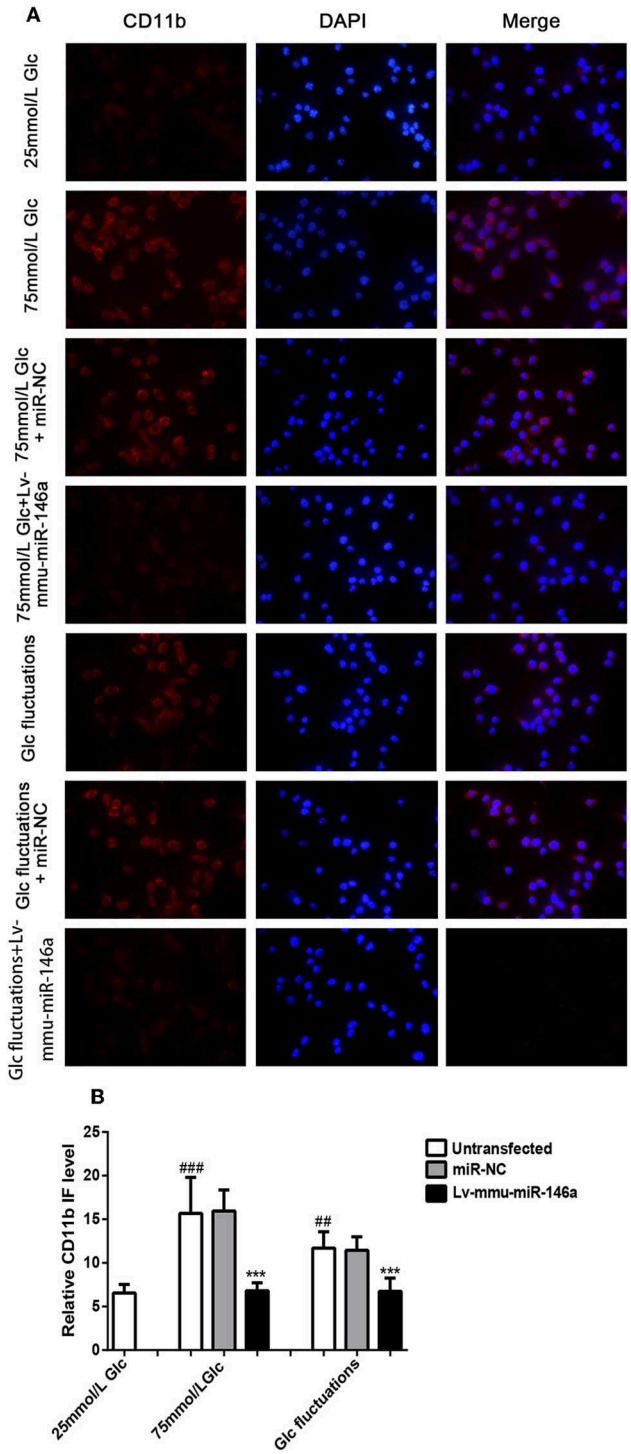

FIGURE 3 | Immunofluorescence for CD11b in BV-2 cells overexpressing miR-146a induced by high glucose and glucose fluctuations for 48 h. **(A)** Immunofluorescence was used to measure the expression of CD11b protein in BV-2 cells overexpressing miR-146a induced by high glucose and glucose fluctuation. **(B)** Comparison of CD11b protein immunofluorescence intensity. $^{###}p < 0.001$, 75 mmol/L Glc vs. control; $^{##}p < 0.01$, Glc fluctuation group vs. control. $^{***}p < 0.001$, 75 mmol/L Glc+Lv-mmu-miR-146a group vs. 75 mmol/L Glc group, Glc fluctuation+Lv-mmu-miR-146a group vs. Glc fluctuation group.

with that in the 75 mmol/L glucose group (1.01 ± 0.102 vs. 2.13 ± 0.422, $^{***}p < 0.001$). Similar results were observed in the glucose fluctuation+Lv-mmu-miR-146a group when compared with the glucose fluctuation group (0.899 ± 0.077 vs. 1.80 ± 0.360, $^{***}p < 0.001$).

M1 Phenotype Polarization Marker iNOS

BV-2 cells were cultured in 25 mmol/L glucose, 75 mmol/L glucose, or glucose fluctuation groups for 24 h, and qRT-PCR was used to detect the expression of iNOS (**Figure 4D**). Compared with that in the 25 mmol/L glucose group, the expression of *iNOS* mRNA was significantly increased in the 75 mmol/L glucose group (2.45 ± 0.071 vs. 1.00 ± 0.030, $^{###}p < 0.001$) and glucose fluctuation group (1.35 ± 0.173 vs. 1.00 ± 0.030, $^{#}p = 0.02$). The expression of *iNOS* mRNA was significantly decreased in the 75 mmol/L glucose+Lv-mmu-miR-146a group compared with that in the 75 mmol/L glucose group (1.36 ± 0.188 vs. 2.45 ± 0.071, $^{***}p < 0.001$). Similar results were observed in the glucose fluctuation+Lv-mmu-miR-146a group when compared with the glucose fluctuation group (0.98 ± 0.072 vs. 1.35 ± 0.173, $^{*}p = 0.014$).

Western blot results (**Figures 4B,E**) revealed that the expression of iNOS protein was significantly increased in the 75 mmol/L glucose (2.07 ± 0.449 vs. 1.00 ± 0.055, $^{#}p = 0.028$) and fluctuation group (1.96 ± 0.104 vs. 1.00 ± 0.055, $^{#}p = 0.03$) compared with that in the control group. The expression of iNOS protein was significantly decreased in the 75 mmol/L glucose+Lv-mmu-miR-146a group compared with that in the 75 mmol/L glucose group (1.53 ± 0.257 vs. 2.07 ± 0.449, $^{***}p < 0.001$). Similar results were observed in the glucose fluctuation+Lv-mmu-miR-146a group when compared with the glucose fluctuation group (1.43 ± 0. 239 vs. 1.96 ± 0.104, $^{**}p = 0.001$).

M2 Phenotype Polarization Marker Arg-1

BV-2 cells were cultured in 25 mmol/L glucose, 75 mmol/L glucose, or glucose fluctuation groups for 24 h, and qRT-PCR was used to measure the expression of Arg-1 (**Figure 4F**). Compared to that in the 25 mmol/L glucose group, the expression of *Arg-1* mRNA was significantly decreased in the 75 mmol/L glucose group (0.38 ± 0.005 vs. 1.00 ± 0. 095, $^{###}p < 0.001$) and glucose fluctuation group (0.56 ± 0.055 vs. 1.00 ± 0.095, $^{###}p < 0.001$). The expression of *Arg-1* mRNA was significantly increased in the 75 mmol/L glucose+Lv-mmu-miR-146a group compared with that in the 75 mmol/L glucose group (0.57 ± 0.112 vs. 0.38 ± 0.005, $^{*}p = 0.018$). Similar results were observed in the glucose fluctuation+Lv-mmu-miR-146a group when compared with the glucose fluctuation group (0.91 ± 0.131 vs. 0.56 ± 0.055, $^{***}p < 0.001$).

Western blot results (**Figures 4B,G**) revealed that the expression of Arg-1 protein was significantly decreased in the 75 mmol/L glucose (0.41 ± 0.150 vs. 1.00 ± 0.269, $^{#}p = 0.016$) and fluctuation group (0.52 ± 0.170 vs. 1.00 ± 0.269, $^{#}p = 0.042$) compared with that in the control group. The expression of Arg-1 protein was significantly increased in the 75 mmol/L glucose+Lv-mmu-miR-146a group compared with that in the 75 mmol/L glucose group (0.96 ± 0.274 vs. 0.41 ± 0.150, $^{*}p = 0.023$). Similar

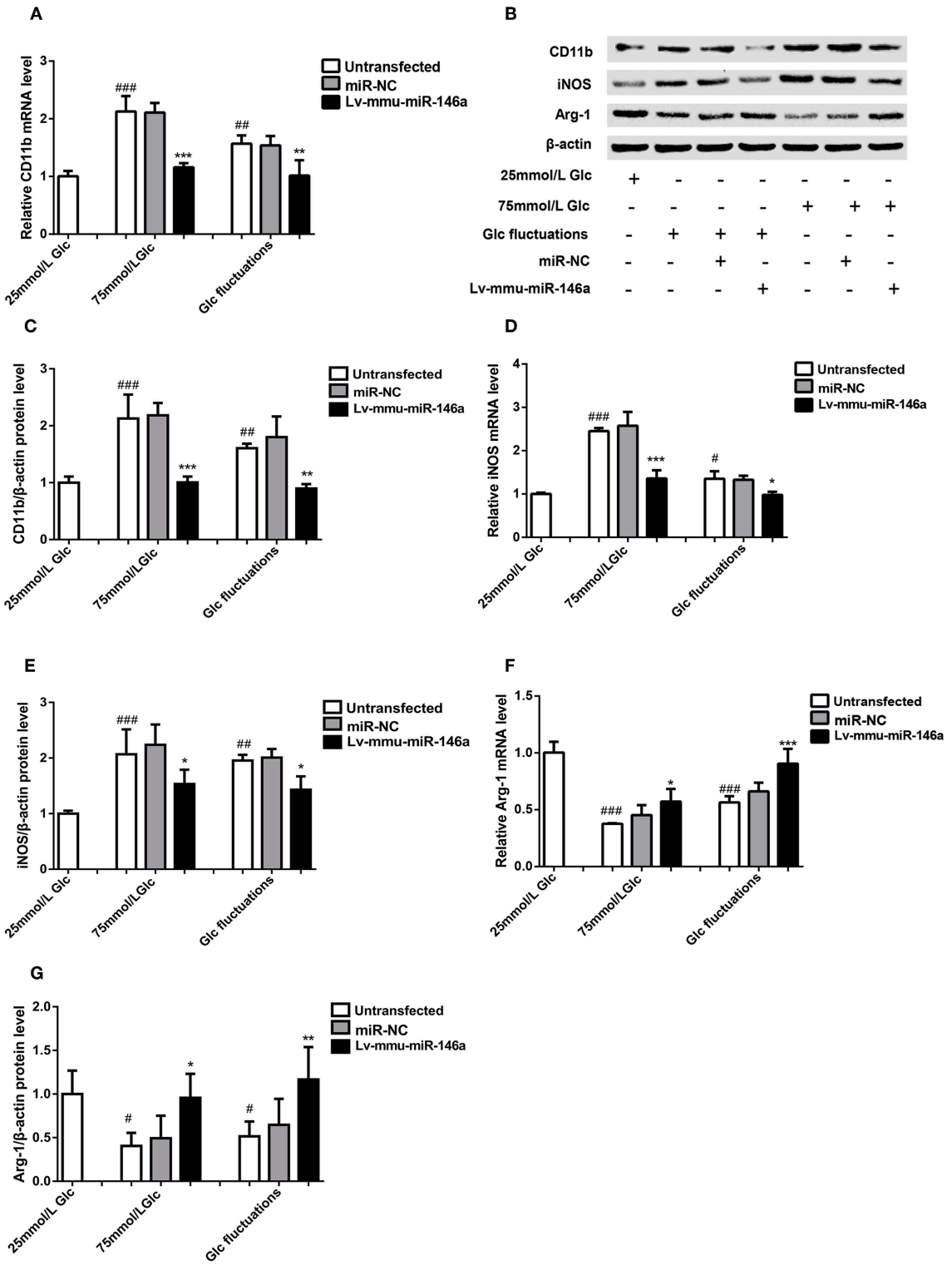

FIGURE 4 | Effects of miR-146a on polarization transitions in BV-2 cells induced by high glucose and glucose fluctuation. **(A)** *CD11b* mRNA expression levels. ***$p <$ 0.001, 75 mmol/L Glc+Lv-mmu-miR-146a group vs. 75 mmol/L Glc group; **$p < 0.01$, Glc fluctuation+Lv-mmu-miR-146a group vs. Glc fluctuation group; ###$p <$ 0.001, 75 mmol/L Glc vs. control; ##$p < 0.01$, Glc fluctuation group vs. control. **(B)** Western blot for CD11b, iNOS, and Arg-1 protein detection. **(C)** Expression levels of CD11b protein. ***$p < 0.001$, 75 mmol/L Glc+Lv-mmu-miR-146a group vs. 75 mmol/L Glc group; **$p < 0.01$, Glc fluctuation+Lv-mmu-miR-146a group vs.

(Continued)

FIGURE 4 | Glc fluctuation group; $^{\#\#}p < 0.01$, 75 mmol/L Glc vs. control; $^{\#\#}p < 0.01$ Glc fluctuation group vs. control. **(D)** *iNOS* mRNA expression levels. $^{***}p < 0.001$, 75 mmol/L Glc+Lv-mmu-miR-146a group vs. 75 mmol/L Glc group; $^{*}p < 0.05$ Glc fluctuation+Lv-mmu-miR-146a group vs. Glc fluctuation group, $^{\#\#\#}p < 0.001$, 75 mmol/L Glc vs. control, $^{\#}p < 0.05$, Glc fluctuation group vs. control. **(E)** Expression levels of iNOS protein. $^{*}p < 0.05$ 75 mmol/L Glc+Lv-mmu-miR-146a group vs. 75 mmol/L Glc group; $^{*}p < 0.05$, Glc fluctuation+Lv-mmu-miR-146a group vs. Glc fluctuation group; $^{\#\#\#}p < 0.001$, 75 mmol/L Glc vs. control; $^{\#\#}p < 0.01$ Glc fluctuation group vs. control. **(F)** *Arg-1* mRNA expression levels. $^{*}p < 0.05$ 75 mmol/L, Glc+Lv-mmu-miR-146a group vs. 75 mmol/L Glc group; $^{***}p < 0.001$ Glc fluctuation+Lv-mmu-miR-146a group vs. Glc fluctuation group; $^{\#\#\#}p < 0.001$, 75 mmol/L Glc vs. control; $^{\#\#\#}p < 0.001$, Glc fluctuation group vs. control. **(G)** Expression levels of Arg-1 protein. $^{*}p < 0.05$, 75 mmol/L Glc+Lv-mmu-miR-146a group vs. 75 mmol/L Glc group; $^{**}p < 0.01$, Glc fluctuation+Lv-mmu-miR-146a group vs. Glc fluctuation group; $^{\#}p < 0.05$, 75 mmol/L Glc vs. control; $^{\#}p < 0.05$, Glc fluctuation group vs. control.

results were observed in the glucose fluctuation+Lv-mmu-miR-146a group compared with that in the glucose fluctuation group (1.17 ± 0.373 vs. 0.52 ± 0.170, $^{**}p = 0.009$).

Inflammation Cytokines

TNF-α

BV-2 cells were cultured in 25 mmol/L glucose, 75 mmol/L glucose, or glucose fluctuation groups for 24 h, and qRT-PCR was used to measure the expression of TNF-α (**Figure 5A**). Compared to that in the 25 mmol/L glucose group, the expression of TNF-α mRNA was significantly increased in the 75 mmol/L glucose (1.23 ± 0.056 vs. 1.0 ± 0.134, $^{\#}p = 0.022$). There was no significant difference between the fluctuation group and control group(1.11 ± 0.02 vs. 1.0 ± 0.134, $p = 0.161$). The expression of TNF-α mRNA was significantly decreased in the 75 mmol/L glucose+Lv-mmu-miR-146a group compared to the 75 mmol/L glucose group (1.0 ± 0.051 vs. 1.23 ± 0.056, $^{*}p = 0.017$). No significant difference between the glucose fluctuation+Lv-mmu-miR-146a group and the glucose fluctuation group (1.00 ± 0.172 vs. 1.11 ± 0.020, $p = 0.368$) was observed.

ELISA (**Figure 5B**) results showed that compared to that in the 25 mmol/L glucose group, the expression of TNF-α protein was significantly increased in the 75 mmol/L glucose (993.11 ± 5.06 vs. 828.09 ± 20.953, $^{\#}p = 0.02$). No significant difference between the fluctuation group and control groups (919.70 ± 5.025 vs. 828.09 ± 20.953, $p = 0.071$) was observed. The expression of TNF-α protein was significantly decreased in the 75 mmol/L glucose+Lv-mmu-miR-146a group compared to the 75 mmol/L glucose group (857.74 ± 13.91 vs. 993.11 ± 5.06, $^{**}p = 0.009$), and significantly decreased in the glucose fluctuation+Lv-mmu-miR-146a group compared to the glucose fluctuation group (871.03 ± 4.649 vs. 919.7 ± 5.025, $^{**}p = 0.003$).

IL-6

BV-2 cells were cultured in 25 mmol/L glucose, 75 mmol/L glucose, or glucose fluctuation groups for 24 h, and qRT-PCR was used to measure the expression of IL-6 (**Figure 5C**). Compared to that in the 25 mmol/L glucose group, the expression of IL-6 mRNA was significantly increased in the 75 mmol/L glucose (1.27 ± 0.072 vs. 1.0 ± 0.114, $^{\#\#}p = 0.009$). The expression of IL-6 mRNA was significantly decreased in the 75 mmol/L glucose+Lv-mmu-miR-146a group compared to the 75 mmol/L glucose group (0.21 ± 0.052 vs. 1.27 ± 0.072, $^{*}p < 0.001$), and similarly significantly decreased in the glucose fluctuation+Lv-mmu-miR-146a group compared to the glucose fluctuation group (0.30 ± 0.047 vs. 1.02 ± 0.064, $^{***}P < 0.001$).

ELISA (**Figure 5D**) results showed that compared to that in the 25 mmol/L glucose group, the expression of IL-6 protein was significantly increased in the 75 mmol/L glucose (12.830 ± 0.125 vs. 11.36 ± 0.032, $^{\#\#}p = 0.008$ compared with control groups. No significant difference was observed between the fluctuation group and control groups (111.79 ± 0.483 vs. 11.36 ± 0.032, $p = 0.826$). The expression of IL-6 protein was significantly decreased in the 75 mmol/L glucose+Lv-mmu-miR-146a group compared to the 75 mmol/L glucose group (5.84 ± 0.828 vs. 12.830 ± 0.125, $^{*}p = 0.02$), and similarly significantly decreased in the glucose fluctuation+Lv-mmu-miR-146a group compared with the glucose fluctuation group (6.17 ± 0.343 vs 11.79 ± 0.483, $^{**}p = 0.001$).

IL-10

BV-2 cells were cultured in 25 mmol/L glucose, 75 mmol/L glucose, or glucose fluctuation groups for 24 h, and qRT-PCR was used to measure the expression of IL-10 (**Figure 5E**). Compared to that in the 25 mmol/L glucose group, the expression of IL-10 mRNA was significantly decreased in the 75 mmol/L glucose (0.434 ± 0.017 vs. 1.0 ± 0.045, $^{\#\#\#}p < 0.001$)and in the fluctuation group (0.63 ± 0.089 vs. 1.0 ± 0.045, $^{\#\#\#}p < 0.001$).The expression of IL-10 mRNA was significantly increased in the 75 mmol/L glucose+Lv-mmu-miR-146a group compared with the 75 mmol/L glucose group(1.52 ± 0.042 vs. 0.434 ± 0.017, $^{***}p < 0.001$), and similarly significantly increased in the glucose fluctuation+Lv-mmu-miR-146a group compared with the glucose fluctuation group (1.32 ± 0.078 vs. 0.63 ± 0.089, $^{***}p < 0.001$).

ELISA (**Figure 5F**) results showed that compared to that in the 25 mmol/L glucose group, the expression of IL-10 protein was significantly decreased in the 75 mmol/L glucose (4.53 ± 0.276 vs. 8.55 ± 0.296, $^{\#\#}p = 0.001$). No significant difference was observed between the fluctuation group and control groups (5.56 ± 1.788 vs. 8.55 ± 0.296, $p = 0.083$). The expression of IL-10 protein was significantly increased in the 75 mmol/L glucose Lv-mmu-miR-146a group compared with the 75 mmol/L glucose group(10.0 ± 0.915 vs. 4.53 ± 0.276, $^{*}p = 0.01$), and similarly significantly increased in the glucose fluctuation Lv-mmu-miR-146a group compared with the glucose fluctuation group (12.21 ± 1.046 vs. 5.56 ± 0.788, $^{*}p = 0.011$).

miR-146a Regulation of Polarization Transitions via IRAK1/TRAF6/NF-κB Signaling

The expression of *IRAK1* mRNA (**Figure 6A**) was significantly increased in the 75 mmol/L glucose (1.82 ± 0.151 vs. $1.0 \pm$

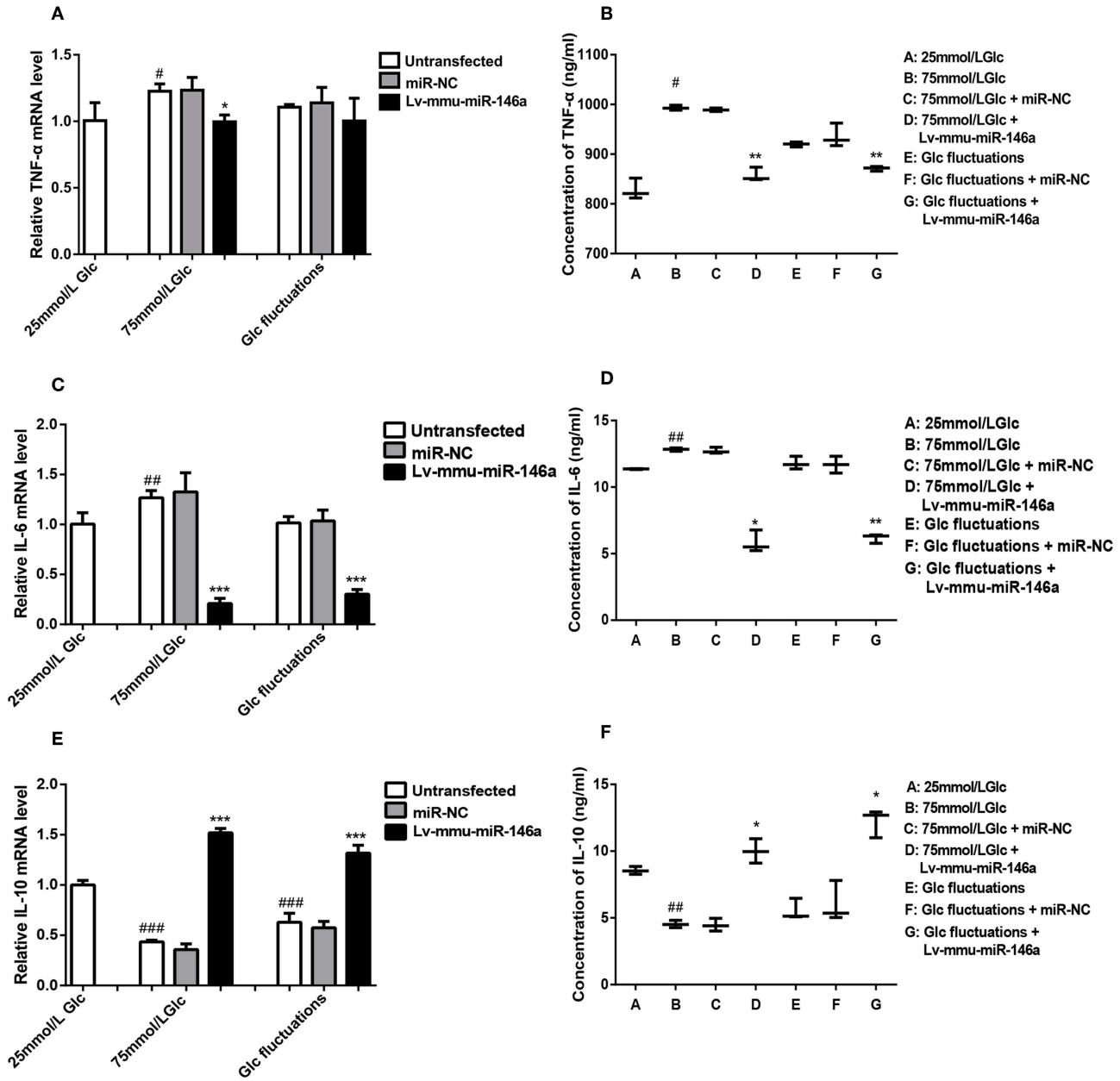

FIGURE 5 | Effects of miR-146a on inflammatory cytokines expression in BV-2 cells induced by high glucose and glucose fluctuation. **(A)** TNF-α mRNA expression levels. $^{\#}p < 0.05$, 75 mmol/L Glc vs. control; $^{*}p < 0.05$, 75 mmol/L Glc+Lv-mmu-miR-146a group vs. 75 mmol/L Glc group. **(B)** ELISA results of TNF-α. $^{\#}p < 0.05$, 75 mmol/L Glc vs. control; $^{**}p < 0.01$, 75 mmol/L Glc+Lv-mmu-miR-146a group vs. 75 mmol/L Glc group; Glc fluctuation+Lv-mmu-miR-146a group vs. Glc fluctuation group. **(C)** IL-6 mRNA expression levels. $^{\#\#}p < 0.01$, 75 mmol/L Glc vs. control; $^{***}p < 0.001$, 75 mmol/L Glc+Lv-mmu-miR-146a group vs. 75 mmol/L Glc group; $^{***}p < 0.001$, Glc fluctuation+Lv-mmu-miR-146a group vs. Glc fluctuation group. **(D)** ELISA results of IL-6. $^{\#\#}p < 0.01$, 75 mmol/L Glc vs. control; $^{*}p < 0.05$, 75 mmol/L Glc+Lv-mmu-miR-146a group vs. 75 mmol/L Glc group; $^{**}p < 0.01$, Glc fluctuation+Lv-mmu-miR-146a group vs. Glc fluctuation group. **(E)** IL-10 mRNA expression levels. $^{\#\#\#}p < 0.001$, 75 mmol/L Glc vs. control; $^{\#\#\#}p < 0.001$, Glc fluctuation vs. control; $^{***}p < 0.001$, 75 mmol/L Glc+Lv-mmu-miR-146a group vs. 75 mmol/L Glc group. $^{***}p < 0.001$, Glc fluctuation+Lv-mmu-miR-146a group vs. Glc fluctuation group. **(F)** ELISA results of IL-10. $^{\#\#}p < 0.01$, 75 mmol/L Glc vs. control; $^{*}p < 0.05$, 75 mmol/L Glc+Lv-mmu-miR-146a group vs. 75 mmol/L Glc group; $^{*}p < 0.05$, Glc fluctuation+Lv-mmu-miR-146a group vs. Glc fluctuation group.

0.079, $^{\#\#\#}p < 0.001$) compared with that in the control group. No significant difference between the fluctuation group and control group was observed (1.23 ± 0.05 vs. 1.0 ± 0.079, $p = 0.067$). The expression of *IRAK1* mRNA was significantly decreased in the 75 mmol/L glucose+Lv-mmu-miR-146a group compared with that in the 75 mmol/L glucose group (1.3 ± 0.247 vs. $1.82 \pm$

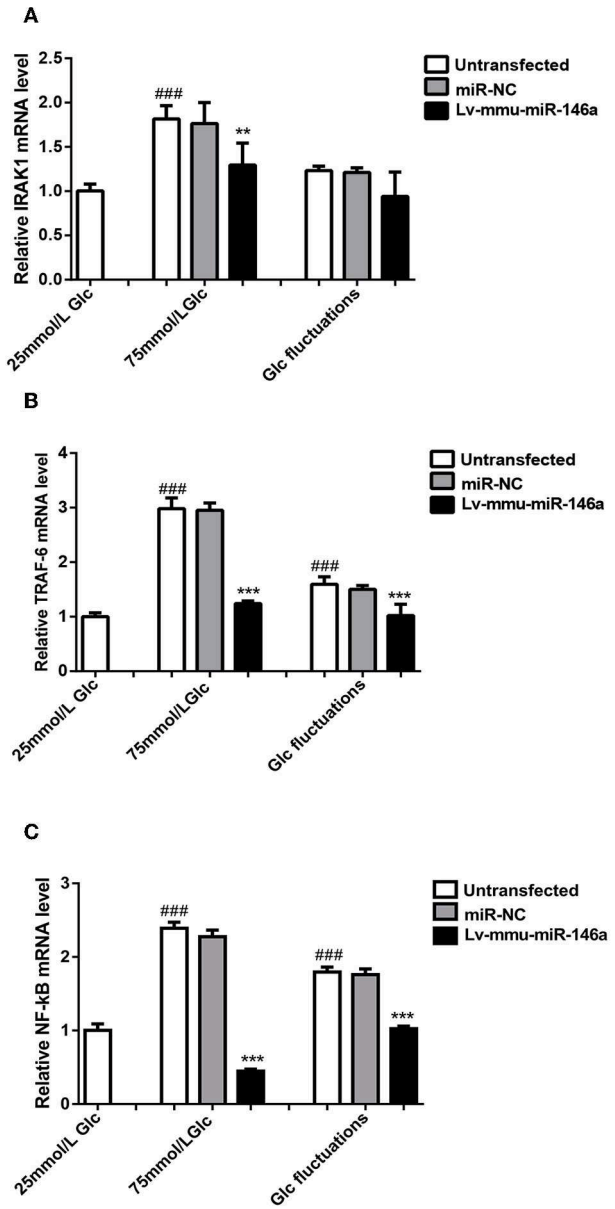

FIGURE 6 | miR-146a regulation of polarization transitions via the IRAK1/TRAF6/NF-κB signaling pathway. **(A)** IRAK1 mRNA expression levels. $^{###}p < 0.001$, 75 mmol/L Glc vs. control; $^{**}p < 0.01$, 75 mmol/L Glc+Lv-mmu-miR-146a group vs. 75 mmol/L Glc group. **(B)** TRAF6 mRNA expression levels. $^{###}p < 0.001$, 75 mmol/L Glc vs. control, Glc fluctuation group vs. control; $^{***}p < 0.001$, 75 mmol/L Glc+Lv-mmu-miR-146a group vs. 75 mmol/L Glc group, Glc fluctuation+Lv-mmu-miR-146a group vs. Glc fluctuation group. **(C)** NF-κB mRNA expression levels. $^{###}p < 0.001$, 75 mmol/L Glc vs. control, Glc fluctuation group vs. control; $^{***}p < 0.001$, 75 mmol/L Glc+Lv-mmu-miR-146a group vs. 75 mmol/L Glc group, Glc fluctuation+Lv-mmu-miR-146a group vs. Glc fluctuation group.

0.151, $^{**}p = 0.03$). No significant difference between the glucose fluctuation+Lv-mmu-miR-146a group and glucose fluctuation group was observed (0.94 ± 0.275 vs. 1.23 ± 0.05, $p = 0.14$).

The expression of *TRAF6* mRNA (**Figure 6B**) was significantly increased in the 75 mmol/L glucose (2.98 ± 0.199 vs. 1.0 ± 0.071, $^{###}p < 0.001$) and fluctuation group (1.59 ± 0.137 vs. 1.0 ± 0.071, $^{###}p < 0.001$) compared with that in the control group. The expression of *TRAF6* mRNA was significantly decreased in the 75 mmol/L glucose+Lv-mmu-miR-146a group compared with that in the 75 mmol/L glucose group (1.24 ± 0.048 vs. 2.98 ± 0.199, $^{***}p < 0.001$), as well as in the glucose fluctuation+Lv-mmu-miR-146a group compared with that in the glucose fluctuation group (1.02 ± 0.207 vs. 1.59 ± 0.137, $^{***}p < 0.001$).

The expression of NF-κB mRNA (**Figure 6C**) was significantly increased in the 75 mmol/L glucose (2.39 ± 0.083 vs. 1.0 ± 0.088, $^{###}p < 0.001$) and fluctuation group (1.8 ± 0.07 vs. 1.0 ± 0.088, $^{###}p < 0.001$) compared with that in the control group. The expression of NF-κB mRNA was significantly decreased in the 75 mmol/L glucose+Lv-mmu-miR-146a group compared with that in the 75 mmol/L glucose group (0.6 ± 0.287 vs. 2.39 ± 0.083, $^{***}p < 0.001$), as well as in the glucose fluctuation+Lv-mmu-miR-146a group compared with that in the glucose fluctuation group (1.03 ± 0.036 vs. 1.8 ± 0.07, $^{***}p < 0.001$).

DISCUSSION

This study demonstrated that high glucose and glucose fluctuations induced polarization transitions to M1 phenotype in BV-2 cells. M1 phenotype parameters including CD11b and iNOS were significantly increased while the expression of M2 phenotype polarizing parameter Arg-1 was significantly decreased. These effects were reversed by overexpression of miR-146a. Furthermore, IRAK1, TRAF6, and NF-κB expression was significantly increased in the high glucose group and glucose fluctuation group. Similarly, these effects were reduced after miR-146a overexpression.

Neuroinflammation is a double-edged sword. Neuroinflammation plays an important role in suppressing infection, removing pathogens, clearing cell debris and misfolded proteins in the nervous system, and nerve repair. However, persistent neuroinflammation induces damage to the nervous system. The role of neuroinflammation depends primarily on the polarization transitions of M1/M2 phenotypes of microglia. Microglia are critical cells that mediate neuroinflammation and have different effects according to polarization phenotype. The M1-polarized phenotype secretes inflammatory cytokines and damages nerve cells, while the M2-polarized phenotype exerts protective effects on nerve cells. Most microglia in the central nervous system are in a relative "quiescent state." Upon changes to the surrounding environment, microglia are activated, which induces M1/M2 polarization transitions. An *in vitro* study suggested that hyperglycemia induced polarization transitions to M1 polarization in microglia (17). In the cortex of diabetic mice, M1 phenotype polarization of microglia was increased, whereas M2 phenotype polarization of microglia was decreased. Similarly, microglia in the hypothalamus of streptozotocin-induced diabetic rats demonstrated M1 phenotype polarization transition (18). The deleterious effects of glucose fluctuations on diabetic macroangiopathy has been reported (19, 20). However, few studies on the effects of diabetic encephalopathy have been

performed. An *in vitro* study indicated that glucose fluctuations significantly activated microglia (12). Nevertheless, more studies are required to confirm these findings.

In this study, we use 25 mmol/L glucose DMEM for BV-2 cell culture. We found that 25 mmol/L glucose didn't impact the level of miR-146a, while in the high glucose group, miR-146a expression was reduced. However, Chen et al. demonstrated that 25 mmol/L of glucose decreased the expression of miR-146a in human retinal microvascular endothelial cells (21).

We measured the microglial activation marker CD11b as well as M1 and M2 phenotype markers. We observed that both hyperglycemia and glucose fluctuations induced polarization transitions to M1 phenotype in microglia, leading to increased expression of pro-inflammatory factors including TNF-α and IL-6. Previous studies suggested that excessive M1 phenotype polarization induces inflammatory factor secretion in diabetic encephalopathy, leading to central nervous system damage in diabetes. The expression of iNOS was up-regulated in the hippocampus of diabetic mice and aggravated neuronal damage (22). Our study verified that high glucose and glucose fluctuations induced M1 phenotype polarization transitions in microglia *in vitro*, which is a possible mechanism underpinning diabetic encephalopathy.

Hyperglycemia and blood glucose fluctuations induce cell activation through multiple pathways (23). Of these, the TLR4/NF-κB signaling pathway is one of the main pathways involved. Dasu et al. reported that high glucose induced up-regulation of toll-like receptors (TLR; including TLR2 and TLR4) in human monocytic THP-1 cell lines and initiated intracellular myeloid differentiation factor 88 (MyD88)/IRAK-1/NF-κB signaling pathway, which induced inflammatory responses (24). In recent years, a growing number of studies has reported that epigenetic regulation is an important regulatory mechanism underscoring neuroinflammation, especially microRNAs (25–28). Different miRNAs are expressed depending on phenotype polarization of microglia; in turn, miRNA affect polarization transitions of microglia (29). For example, high expression of miR-155 in microglia induced M1 phenotype polarization and inhibited M2 phenotype polarization (30). miR-124 induced M2 phenotype polarization by targeting inhibition of M1 phenotype polarization to maintain the resting state of microglia and macrophages (31). miR-689, miR-124, and miR-155 are involved in M1 phenotype polarization. In contrast, miR-124, miR-711, and miR-145 are implicated in M2 phenotype polarization in lipopolysaccharide (LPS) or IL-4 stimulated primary mouse microglia based on miRNA expression profiling and bioinformatics analysis (29). To date, there have been no reports on miR-146a in the context of microglial phenotype polarization. Previous studies reported that miRNA-146a played an important role in the regulation of inflammation mainly through the NF-κB pathway. Taganov et al. reported that miR-146a regulated two key adapter molecules, TRAF-6 and IRAK1, which were downstream of the TLR signaling pathway, thereby regulating the activation of the pro-inflammatory factor NF-κB and negatively regulating the release of pro-inflammatory factors (16). Yang et al. reported that miRNA-146a negatively regulated mouse T-cell activation, and the regulatory mechanism also affected the expression of NF-κB by regulating the expression of TRAF-6 and IRAK1 (32). Studies have indicated that miR-146a inhibited M1 polarization and induced M2 polarization in mouse alveolar macrophages induced by LPS (33). Further, the M1 phenotype polarizing factors IL-6 and TNF-α were increased, while the M2 phenotype polarizing factor MGL-1 was decreased in alveolar macrophages by inhibiting the expression of miR-155 or miR-146a. miR-146a and miR-155 may be involved in the anti-inflammatory activity of macrophages and participate in the mechanisms underpinning M1 and M2 polarization transitions (34).

miR-146a induced M2 phenotype polarization and up-regulated tumor-associated macrophages expression to regulate breast cancer tumor growth (35). Our results showed that high glucose increased TNF-α and IL-6 expression while reduced IL-10 expression, which was reversed by overexpression of miR-146a. Similar results was observed in another study. Overexpression of miR-146a attenuated the inhibitory effects of NIFK-AS1 M2 phenotype polarization in macrophages, while the expression of IL-10 and Arg-1 were increased (36). Altered expression of miR-146a in the brains of patients with Alzheimer's disease (AD) underpinned inflammatory senile plaque lesions in AD brains (37, 38). miR-146a expression was decreased in DRG cells in hyperglycemia studies of diabetic peripheral neuropathy; cell survival rate was decreased, but this was attenuated by miR-146a mimics (39, 40). Rong et al. reported that the expression of miR-146a in plasma of patients with type 2 diabetes was significantly decreased (29). Our study revealed that the expression of miR-146a was significantly decreased in cell cultures by high glucose and glucose fluctuations, which partially verified that low levels of miR-146a expression were induced by hyperglycemia (41). Both *in vitro* and *in vivo* studies suggest that miR146a is involved in the regulation of neuroinflammation and plays an important role in various diseases such as diabetes and neurodegenerative diseases. Therefore, we speculated that miR-146a was involved in regulating the polarization transitions of microglia induced by high glucose and glucose fluctuations. Overexpression of miR-146a regulated polarization transitions induced by high glucose and glucose fluctuations promoting M1 to M2 phenotype polarization.

A negative feedback loop between miR-146a and NF-κB may be at play in this process. The expression of miR-146a was decreased in the hippocampus of diabetic rats, while increased expression of IRAK1, TRAF6, and NF-kB aggravated hippocampal inflammation and apoptosis (42). However, compared with that in the control group, the expression of miR-146a and NF-κB were increased, expression of TRAF6 was decreased, and expression of TNF-α, IL-6, and IL-1β were increased in the sciatic nerve of DM rats, indicating that loss of NF-κB/miR-146a in the negative feedback loop may underpin the pathogenesis of diabetic peripheral neuropathy (43). Further, miR-146a regulates the expression of target genes *IRAK1, TRAF6,* and NF-κB. Thus, the regulation may be involved in the NF-κB pathway. In this study, overexpression of miR-146a regulated M1/M2 polarization transitions by

downregulating the expression of IRAK1, TRAF6, and NF-κB in microglia. This could be a regulatory mechanism in the response of microglial inflammation induced by high glucose and glucose fluctuation.

Central nervous system inflammation is a complex process involving various glial cells, macrophages, neuronal cells, and vascular endothelial cells. The results of this study were only observed *in vitro*, which precludes inferences on the neuroinflammatory effects of polarization transitions of microglia in diabetic encephalopathy. However, this study provides insight into the pathogenesis of diabetic encephalopathy. We observed that overexpression of miR-146a contributed to polarization transitions from M1 to M2 phenotype in microglia. Our results provide a potential strategy for the treatment of diabetic encephalopathy. Future studies should further investigate how miR-146a regulates polarization transitions in microglia induced by high glucose and glucose fluctuations.

DATA AVAILABILITY STATEMENT

All datasets generated for this study are included in the manuscript.

AUTHOR CONTRIBUTIONS

YH, ZL, and XL conceptualized and designed these studies, performed them, and wrote the manuscript. XW, XC, XB, YZ, YY, and JZ contributed through data analyses, data interpretation, and manuscript preparation. All authors contributed to manuscript revision and read and approved the submitted version.

FUNDING

This work was funded by the Science and Technology Plan Project of Quanzhou City (2018Z114, 2018Z115, and 2019N104S).

REFERENCES

1. Wang Y, Xu XY, Feng CH, Li YL, Ge X, Zong GL, et al. Patients with type 2 diabetes exhibit cognitive impairment with changes of metabolite concentration in the left hippocampus. *Metab Brain Dis.* (2015) 30:1027–34. doi: 10.1007/s11011-015-9670-4
2. Takechi R, Lam V, Brook E, Giles C, Fimognari N, Mooranian A, et al. Blood-brain barrier dysfunction precedes cognitive decline and neurodegeneration in diabetic insulin resistant mouse model: an implication for causal link. *Front Aging Neurosci.* (2017) 9:399. doi: 10.3389/fnagi.2017.00399
3. Xuyan Z, Ping YJ, Zhongjing W, Sheng D, Li L, Fan Y, et al. Melatonin reverses type 2 diabetes-induced cognitive deficits via attenuation of oxidative/nitrosative stress and NF-κB-mediated neuroinflammation in rat hippocampus. *Trop J Pharm Res.* (2018) 16:2865. doi: 10.4314/tjpr.v16i12.10
4. Chung CC, Pimentel D, Jor'dan AJ, Hao Y, Milberg W, Novak V. Inflammation-associated declines in cerebral vasoreactivity and cognition in type 2 diabetes. *Neurology.* (2015) 85:1–9. doi: 10.1212/WNL.0000000000001820
5. Willette AA, Johnson SC, Birdsill AC, Sager MA, Christian B, Baker LD, et al. Insulin resistance predicts brain amyloid deposition in late middle-aged adults. *Alzheimers Dement.* (2015) 11:504–10.e1. doi: 10.1016/j.jalz.2014.03.011
6. Liu Y, Fu X, Lan N, Li S, Zhang J, Wang S, et al. Luteolin protects against high fat diet-induced cognitive deficits in obesity mice. *Behav Brain Res.* (2014) 267:178–88. doi: 10.1016/j.bbr.2014.02.040
7. Oliveira WH, Nunes AK, Franca ME, Santos LA, Los DB, Rocha SW, et al. Effects of metformin on inflammation and short-term memory in streptozotocin-induced diabetic mice. *Brain Res.* (2016) 1644:149–60. doi: 10.1016/j.brainres.2016.05.013
8. Baldwin KT, Carbajal KS, Segal BM, Giger RJ. Neuroinflammation triggered by beta-glucan/dectin-1 signaling enables CNS axon regeneration. *Proc Natl Acad Sci USA.* (2015) 112:2581–6. doi: 10.1073/pnas.1423221112
9. Bartus K, James ND, Didangelos A, Bosch KD, Verhaagen J, Yanez-Munoz RJ, et al. Large-scale chondroitin sulfate proteoglycan digestion with chondroitinase gene therapy leads to reduced pathology and modulates macrophage phenotype following spinal cord contusion injury. *J Neurosci.* (2014) 34:4822–36. doi: 10.1523/JNEUROSCI.4369-13.2014
10. Lampron A, Elali A, Rivest S. Innate immunity in the CNS: redefining the relationship between the CNS and Its environment. *Neuron.* (2013) 78:214–32. doi: 10.1016/j.neuron.2013.04.005
11. Tang Y, Li T, Li J, Yang J, Liu H, Zhang XJ, et al. Jmjd3 is essential for the epigenetic modulation of microglia phenotypes in the immune pathogenesis of Parkinson's disease. *Cell Death Differ.* (2014) 21:369–80. doi: 10.1038/cdd.2013.159
12. Hsieh CF, Liu CK, Lee CT, Yu LE, Wang JY. Acute glucose fluctuation impacts microglial activity, leading to inflammatory activation or self-degradation. *Sci Rep.* (2019) 9:840. doi: 10.1038/s41598-018-37215-0
13. Orihuela R, McPherson CA, Harry GJ. Microglial M1_M2 polarization and metabolic states. *Br J Pharmacol.* (2016) 173:649–65. doi: 10.1111/bph.13139
14. Graff JW, Dickson AM, Clay G, McCaffrey AP, Wilson ME. Identifying functional microRNAs in macrophages with polarized phenotypes. *J Biol Chem.* (2012) 287:21816–25. doi: 10.1074/jbc.M111.327031
15. Feng B, Chen S, Gordon AD, Chakrabarti S. miR-146a mediates inflammatory changes and fibrosis in the heart in diabetes. *J Mol Cell Cardiol.* (2017) 105:70–6. doi: 10.1016/j.yjmcc.2017.03.002
16. Konstantin D. Taganov MPB, Chang KJ, Baltimore D. NF-kB-dependent induction of microRNA miR-146, an inhibitor targeted to signaling proteins of innate immune responses. *PNAS.* (2006) 103:12481–6. doi: 10.1073/pnas.0605298103
17. Ma S, Wang J, Wang Y, Dai X, Xu F, Gao X, et al. Diabetes mellitus impairs white matter repair and long-term functional deficits after cerebral ischemia. *Stroke.* (2018) 49:2453–63. doi: 10.1161/STROKEAHA.118.021452
18. Richa R, Yadawa AK, Chaturvedi CM. Hyperglycemia and high nitric oxide level induced oxidative stress in the brain and molecular alteration in the neurons and glial cells of laboratory mouse, Mus musculus. *Neurochem Int.* (2017) 104:64–79. doi: 10.1016/j.neuint.2016.12.008
19. Teraguchi I, Imanishi T, Ozaki Y, Tanimoto T, Ueyama M, Orii M, et al. Acute-phase glucose fluctuation is negatively correlated with myocardial salvage after acute myocardial infarction. *Circ J.* (2014) 78:170–9. doi: 10.1253/circj.CJ-13-0723
20. Xia J, Xu J, Li B, Liu Z, Hao H, Yin C, et al. Association between glycemic variability and major adverse cardiovascular and cerebrovascular events (MACCE) in patients with acute coronary syndrome during 30-day follow-up. *Clin Chim Acta.* (2017) 466:162–6. doi: 10.1016/j.cca.2017.01.022
21. Chen S, Feng B, Thomas AA, Chakrabarti S. miR-146a regulates glucose induced upregulation of inflammatory cytokines extracellular matrix proteins in the retina and kidney in diabetes. *PLoS ONE.* (2017) 12:e0173918. doi: 10.1371/journal.pone.0173918
22. Mastrocola R, Barutta F, Pinach S, Bruno G, Perin PC, Gruden G. Hippocampal heat shock protein 25 expression in

streptozotocin-induced diabetic mice. *Neuroscience.* (2012) 227:154–62. doi: 10.1016/j.neuroscience.2012.09.038
23. Shanmugam N, Reddy MA, Guha M, Natarajan R. High glucose–induced expression of proinflammatory cytokine and chemokine genes in monocytic cells. *Diabetes.* (2003) 52:1256–64. doi: 10.2337/diabetes.52.5.1256
24. Dasu MR, Devaraj S, Zhao L, Hwang DH, Jialal I. High glucose induces toll-like receptor expression in human monocytes: mechanism of activation. *Diabetes.* (2008) 57:3090–8. doi: 10.2337/db08-0564
25. Li TR, Jia YJ, Ma C, Qiu WY, Wang Q, Shao XQ, et al. The role of the microRNA-146a/complement factor H/interleukin-1beta-mediated inflammatory loop circuit in the perpetuate inflammation of chronic temporal lobe epilepsy. *Dis Model Mech.* (2018) 11:dmm031708. doi: 10.1242/dmm.031708
26. Yang Z, Zhong L, Zhong S, Xian R, Yuan B. miR-203 protects microglia mediated brain injury by regulating inflammatory responses via feedback to MyD88 in ischemia. *Mol Immunol.* (2015) 65:293–301. doi: 10.1016/j.molimm.2015.01.019
27. Ashraf U, Zhu B, Ye J, Wan S, Nie Y, Chen Z, et al. MicroRNA-19b-3p modulates Japanese encephalitis virus-mediated inflammation via targeting RNF11. *J Virol.* (2016) 90:4780–95. doi: 10.1128/JVI.02586-15
28. Yao L, Ye Y, Mao H, Lu F, He X, Lu G, et al. MicroRNA-124 regulates the expression of MEKK3 in the inflammatory pathogenesis of Parkinson's disease. *J Neuroinflammation.* (2018) 15:13. doi: 10.1186/s12974-018-1053-4
29. Freilich RW, Woodbury ME, Ikezu T. Integrated expression profiles of mRNA and miRNA in polarized primary murine microglia. *PLoS ONE.* (2013) 8:e79416. doi: 10.1371/journal.pone.0079416
30. O'Connell RM, Taganov KD, Boldin MP, Cheng G, Baltimore D. MicroRNA-155 is induced during the macrophage inflammatory response. *PNAS.* (2007) 104:1604–9. doi: 10.1073/pnas.0610731104
31. Ponomarev ED, Veremeyko T, Barteneva N, Krichevsky AM, Weiner HL. microRNA-124 promotes microglia quiescence and suppresses EAE by deactivating macrophages via the C/EBP-alpha-PU.1 pathway. *Nat Med.* (2011) 17:64–70. doi: 10.1038/nm.2266
32. Yang L, Boldin MP, Yu Y, Liu CS, Ea CK, Ramakrishnan P, et al. miR-146a controls the resolution of T cell responses in mice. *J Exp Med.* (2012) 209:1655–70. doi: 10.1084/jem.20112218
33. Vergadi E, Vaporidi K, Theodorakis EE, Doxaki C, Lagoudaki E, Ieronymaki E, et al. Akt2 deficiency protects from acute lung injury via alternative macrophage activation and miR-146a induction in mice. *J Immunol.* (2014) 192:394–406. doi: 10.4049/jimmunol.1300959
34. Yang Y, Wu BQ, Wang YH, Shi YF, Luo JM, Ba JH, et al. Regulatory effects of miR-155 and miR-146a on repolarization and inflammatory cytokine secretion in human alveolar macrophages *in vitro*. *Immunopharmacol Immunotoxicol.* (2016) 38:502–9. doi: 10.1080/08923973.2016.1248845
35. Li Y, Zhao L, Shi B, Ma S, Xu Z, Ge Y, et al. Functions of miR-146a and miR-222 in tumor-associated macrophages in breast cancer. *Sci Rep.* (2015) 5:18648. doi: 10.1038/srep18648
36. Zhou YX, Zhao W, Mao LW, Wang YL, Xia LQ, Cao M, et al. Long non-coding RNA NIFK-AS1 inhibits M2 polarization of macrophages in endometrial cancer through targeting miR-146a. *Int J Biochem Cell Biol.* (2018) 104:25–33. doi: 10.1016/j.biocel.2018.08.017
37. Lukiw WJ, Zhao Y, Cui JG. An NF-kappaB-sensitive micro RNA-146a-mediated inflammatory circuit in Alzheimer disease and in stressed human brain cells. *J Biol Chem.* (2008) 283:31315–22. doi: 10.1074/jbc.M805371200
38. Cui JG, Li YY, Zhao Y, Bhattacharjee S, Lukiw WJ. Differential regulation of interleukin-1 receptor-associated kinase-1 (IRAK-1) and IRAK-2 by microRNA-146a and NF-kappaB in stressed human astroglial cells and in Alzheimer disease. *J Biol Chem.* (2010) 285:38951–60. doi: 10.1074/jbc.M110.178848
39. Wang L, Chopp M, Szalad A, Zhang Y, Wang X, Zhang RL, et al. The role of miR-146a in dorsal root ganglia neurons of experimental diabetic peripheral neuropathy. *Neuroscience.* (2014) 259:155–63. doi: 10.1016/j.neuroscience.2013.11.057
40. Jia L, Wang L, Chopp M, Zhang Y, Szalad A, Zhang ZG. MicroRNA 146a locally mediates distal axonal growth of dorsal root ganglia neurons under high glucose and sildenafil conditions. *Neuroscience.* (2016) 329:43–53. doi: 10.1016/j.neuroscience.2016.05.005
41. Rong Y, Bao W, Shan Z, Liu J, Yu X, Xia S, et al. Increased microRNA-146a levels in plasma of patients with newly diagnosed type 2 diabetes mellitus. *PLoS ONE.* (2013) 8:e73272. doi: 10.1371/journal.pone.0073272
42. Habibi F, Ghadiri Soufi F, Ghiasi R, Khamaneh AM, Alipour MR. Alteration in inflammation-related miR-146a expression in NF-KB signaling pathway in diabetic rat hippocampus. *Adv Pharm Bull.* (2016) 6:99–103. doi: 10.15171/apb.2016.015
43. Yousefzadeh N, Alipour MR, Ghadiri Soufi F. Deregulation of NF-κB–miR-146a negative feedback loop may be involved in the pathogenesis of diabetic neuropathy. *J Physiol Biochem.* (2015) 71:51–8. doi: 10.1007/s13105-014-0378-4

Conflict of Interest: The authors declare that the research was conducted in the absence of any commercial or financial relationships that could be construed as a potential conflict of interest.

frontiers in Neuroscience

REVIEW
published: 29 October 2019
doi: 10.3389/fnins.2019.01149

Progress of Research on Exosomes in the Protection Against Ischemic Brain Injury

Xianhui Kang[1,2†], Ziyi Zuo[3†], Wandong Hong[4†], Hongli Tang[1] and Wujun Geng[1*]*

[1] Department of Anesthesiology, The First Affiliated Hospital of Wenzhou Medical University, Wenzhou, China, [2] Department of Anesthesiology, The First Affiliated Hospital, College of Medicine, Zhejiang University, Hangzhou, China, [3] The First Clinical College, Wenzhou Medical University, Wenzhou, China, [4] Department of Gastroenterology and Hepatology, The First Affiliated Hospital of Wenzhou Medical University, Wenzhou, China

Exosomes, as a type of extracellular vesicle (EV), are lipid bilayer vesicles 20–100 nm in diameter that can cross the blood-brain barrier. Exosomes are important transport vesicles in the human body that participate in many conduction pathways and play an important physiological role. Because of their high biocompatibility and low immunogenicity and toxicity, exosomes have attracted increasing attention as an attractive drug delivery system. This article reviews the relevant studies that have shown that exosomes play an important role in protective mechanisms against ischemic brain injury.

Keywords: exosomes, brain protection, ischemic brain injury, stroke, drug delivery

OPEN ACCESS

Edited by:
Clarissa M. Maya-Monteiro, Oswaldo Cruz Foundation (Fiocruz), Brazil

Reviewed by:
Nils Lambrecht, VA Long Beach Healthcare System, United States
David Vaudry, Institut National de la Santé et de la Recherche Médicale (INSERM), France

***Correspondence:**
Hongli Tang
tanghongliok@126.com
Wujun Geng
gengwujun@wzhospital.cn

† These authors have contributed equally to this work

Specialty section:
This article was submitted to Neuroendocrine Science, a section of the journal Frontiers in Neuroscience

Received: *23 July 2019*
Accepted: *11 October 2019*
Published: *29 October 2019*

Citation:
Kang X, Zuo Z, Hong W, Tang H and Geng W (2019) Progress of Research on Exosomes in the Protection Against Ischemic Brain Injury. Front. Neurosci. 13:1149. doi: 10.3389/fnins.2019.01149

INTRODUCTION

For ischemic brain injury, pharmacological and non-pharmacological brain protection methods are commonly used in the clinic. Pharmacological methods include ion channel blockers, lipid peroxidation inhibitors, excitatory amino acid (EAA) antagonists, blood sugar reduction, barbiturates, and traditional Chinese medicine, whereas non-pharmacological methods include mild hypothermia treatment and acupuncture. Research has examined both ischemic postconditioning and ischemic preconditioning.

In recent years, an increasing number of studies have shown that exosomes can act on the central nervous system through crossing the blood-brain barrier due to their own properties and contents and protect brain tissues through various mechanisms; these findings suggest that exosomes from various sources can protect the brain through cerebral ischemic preconditioning and ameliorate nervous system diseases in the clinic. Exosomes are derived from the intracellular lysosome pathway. Intracellular lysosome particles invade and form multivesicular bodies (MVBs). Then, the extracellular membrane of these vesicles fuses with the cell membrane and secretes them to the extracellular matrix (Colombo et al., 2014). Exosomes, which are between 20 and 100 nm in diameter, are important transport vesicles that can cross the blood-brain barrier and participate in multiple signaling pathways. Exosomes play an important role in the normal physiological function of cells and the occurrence and development of diseases, but research on exosomes is relatively new. Exosomes have been found to mediate the occurrence and development of related diseases such as Alzheimer's disease and Parkinson's disease by participating in the production, secretion, aggregation and uptake of related "toxic" proteins, suggesting that exosomes may be an important marker for the early diagnosis of related diseases. This article reviews the latest progress of research on exosomes in the field of ischemic brain injury protection.

OVERVIEW OF EXOSOMES

Discovery of Exosomes

Pan and Johnstone (1983) studied the transformation of sheep reticulocytes to mature erythrocytes *in vitro*. Through ultracentrifugation, a small vesicle was isolated from the supernatant of sheep erythrocytes. Under electron microscopy, the vesicle was found to be composed of a lipid bilayer with a round or concave cup-like structure and was later named an exosome. For some time afterward, exosomes were considered carriers of waste transported by cells to the outside world. In Raposo et al. (1996) discovered that B lymphocyte-derived exosomes have multiple functions, including antigen presentation, T lymphocyte activation, and immune cell function regulation. Related functions of exosomes began to be discovered gradually. After further study, exosomes were found to be widely present in human blood, cerebrospinal fluid, saliva, urine and so on. In Valadi et al. (2007) discovered for the first time that exosomes contained both RNA and microRNA and confirmed that the RNA carried by exosomes had certain biological activities. With the gradual discovery of substances carried by exosomes, the important roles of proteins, lipids and RNA carried by exosomes in intercellular information exchange and genetic material transfer have increasingly become hot research subjects in the fields of disease occurrence, disease treatment and disease prevention.

Biogenesis and Composition of Exosomes

Extracellular vesicles (EVs) include exosomes with a diameter of 20–100 nm, microvesicles with a diameter of 20–1000 nm and apoptotic bodies with a diameter of 500–2000 nm. Exosomes originate from the endolysosome pathway, whereas microvesicles originate from the direct germination of cells, making the composition of microvesicles much simpler than that of exosomes. The exosome formation process mainly includes early endosomal formation by invagination of the cytoplasmic membrane and early endosomal formation by regulation of the endosomal sorting complex (ESCRT) to form multiple intraluminal vesicles (ILVs), which then constitute MVBs. MVBs mature and fuse with lysosomes for lysosome degradation or fuse with plasmalemma, releasing ILVs to the cell surface to form exosomes (Samanta et al., 2018).

The composition of exosomes has been examined by trypsin digestion, mass spectrometry, Western blot and fluorescence-activated cell sorting (FACS). Exosomes are lipid bilayer vesicles rich in cholesterol, ceramide, sphingomyelin and phospholipids with long saturated ester chains. Exosomes contain a variety of proteins: protein membrane transport fusion proteins (GTPases, annexins, flotillin), transmembrane proteins (CD9, CD63, CD81 and CD82), heat shock proteins (Hsp70, Hsp60, Hsp20, Hsp90) (Gupta and Knowlton, 2007; Zhang et al., 2012) and other proteins (Alix, TSG101), lipoproteins and phospholipases (Roucourt et al., 2015) involved in the formation of vesicles. In addition, exosomes contain many microRNAs, RNAs and other non-coding RNAs, which can be transferred between cells and then regulate the expression of related genes (Pegtel et al., 2010). Many scholars are now focusing on the RNA contained in exosomes and its corresponding regulatory role. An increasing number of scholars are examining the mechanisms of exosomes in mediating disease and tissue protection. The biogenesis and composition of exosomes as shown in **Figure 1** (Shahabipour et al., 2017).

Regulation of Exosome Secretion

Precise regulation of exosome secretion is important for various cell functions. The molecular mechanisms that directly regulate exosome secretion have been studied in recent year. Increasing numbers of studies have shown that some essential regulators of exosome biogenesis and secretion in diverse cell types (Hessvik et al., 2016; Wei et al., 2017). Endosomal sorting complexes required for transport proteins (e.g., HRS and Tsg101), tetraspanins (e.g., CD81 and CD9), lipids (e.g., ceramide) and Rab GTPases (e.g., Rab11, Rab27, and Rab35) have been identified to regulate exosome secretion and release (Hsu et al., 2010; Ostrowski et al., 2010; Colombo et al., 2013; Sims et al., 2018). However, the upstream platform for exosome regulators is not well understood. Song L. et al. (2019) revealed that KIBRA controls exosome secretion via inhibiting the proteasomal degradation of Rab27a. Given that Exosomes play a vital role in intercellular communication and numerous biological processes, the exact molecular mechanisms implicated in Exosomes secretion warrant further exploration.

Purification of Exosomes

Separation of exosomes is the first step in functioning as a carrier, and thus, appropriate separation is the key to maintenance of their physical, chemical, and biological functions. Given the substantial differences in exosome size and surface markers, the methods for separation of exosomes must have high specificity and high efficiency. The commonly used methods of separation include ultracentrifugation, ultrafiltration, precipitation, immunoaffinity procedures and microfluidics (Ayala-Mar et al., 2019).

Ultracentrifugation

An effective method for separation of exosomes is the key to the value of exosomes, and therefore, it is essential to reserve the physical, chemical, and biological functions, structure and content of the exosomes to the greatest extent. At present, the golden standard for separation of exosomes is ultracentrifugation (Li P. et al., 2017). By utilizing the differences in the sedimentation rates of components of different molecular weights in a homogeneous suspension and by increasing the centrifugal force gradually, this technique separates cells, cell debris, vesicles, and proteins of different molecular weights and thus purifies exosomes. Distinguishing exosomes, small vesicles and some proteins following ultracentriguation is difficult. Purification is usually achieved by sucrose density gradient centrifugation combined with ultracentrifugation (Gupta et al., 2018).

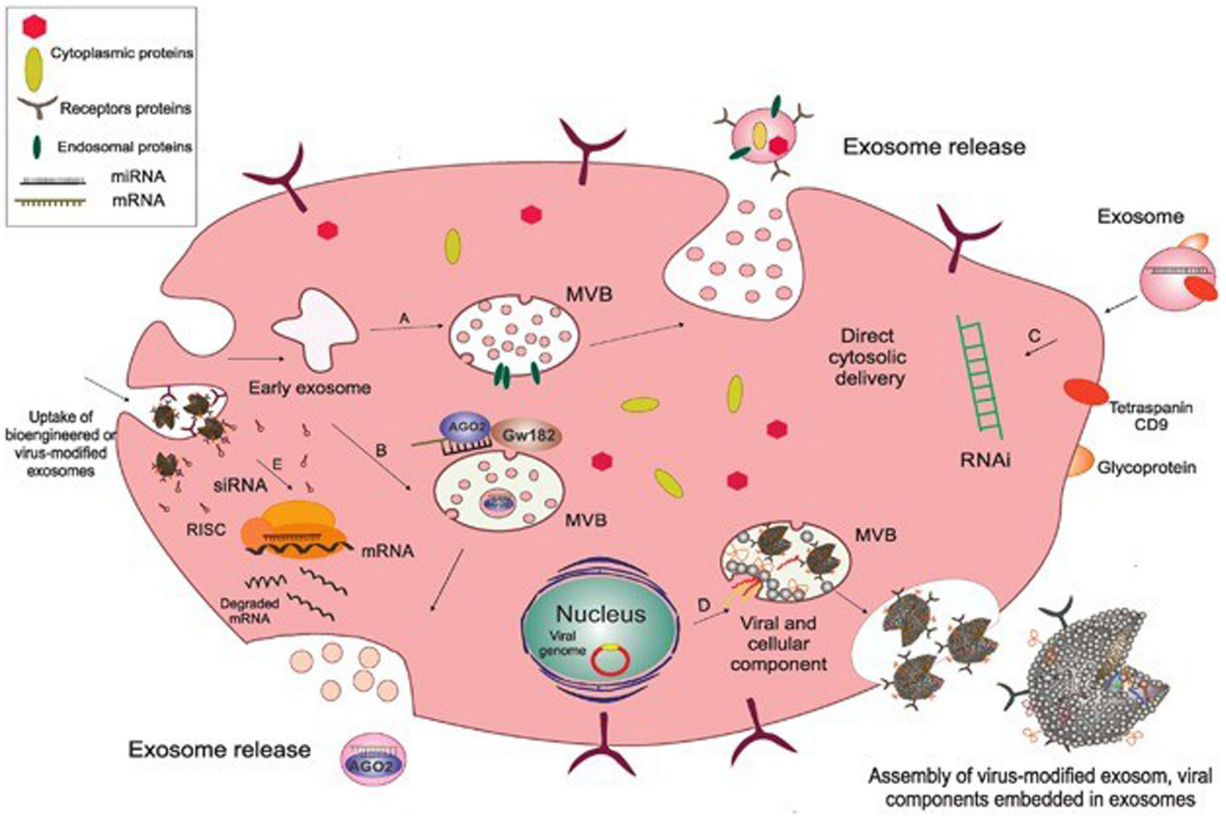

FIGURE 1 | The biogenesis and composition of exosomes. Exosomes originate as endocytic vesicles through invagination of the cell membrane, which results in the formation of early exosomes and, subsequently, late exosome called MVBs. MVBs contain ILV which are formed from budding of the endosomal membrane and are called exosomes. When MVBs fuse with the plasma membrane, they give rise to the release of exosomes into the extracellular space. (A) Endosomal proteins such as CD9, Alix, and TSG101 may be incorporated into exosomes during their assembly to facilitate this process. (B) AGO2 and GW182 are two important components of the RNA-induced silencing complex (RISC), which associate with MVBs so as to mediate miRNA sorting into exosomes. (C) Subsequent fusion of cell-derived exosomes with the plasma membrane through their CD9 (tetraspanin) interaction with surface glycoproteins on target cells gives rise to cytosolic delivery of the siRNA directly. This process is involved in the creation of temporary RNAi. (D) Exosomes originate from inward budding in the lumen of the MVB through which the cytoplasmic content from the cell of origin and also viral components, including mRNA and small non-coding RNA and viral glycoproteins are incorporated into the exosome, and then released as a selective cargo in viral-infected cells. These virus-modified exosomes display the original surface markers and cell membrane as the parent cells. (E) Bioengineered or virus-modified exosomes are designed to express a selective set of proteins and small, non-coding RNAs to target specific receptors. Exosomes then fuse with the endosomal membrane to release their non-coding RNAs into the cytoplasm so as to load siRNA into the RNAi (RISC) complex of the target cells in order to prevent mRNA translation into protein. Acronyms: RISC, RNA-induced silencing complex; RNAi, RNA interference; siRNA, small interference RNA; MVBs, multivesicular bodies.

Ultrafiltration

Ultrafiltration allows EVs to pass or remain on a selective membrane based on their different sizes through application of different forces, thereby achieving the purpose of isolating the exosomes of a specific size.

Precipitation

Exosomes are precipitated by mixing the sample with a highly hydrophilic polymer to change the solubility or dispersibility of the exosomes. Polyethylene glycol (PEG) is commonly used for this process and has extensive applications, including the extraction of exosomes from serum, plasma, ascites, and urine.

Immunoaffinity Procedures

Immunoblotting based on immunoaffinity is an effective means for identifying the separated exosomes. In addition, immunoaffinity techniques can be used to selectively separate exosomes in complex liquid environments. Exosomes separated using this method have high quality and purity. At present, the magnetic beads are coated with monoclonal antibody microparticles and then specifically bound to the exosome surface proteins to achieve the separation.

Microfluidics

Microfluidic techniques, an emerging separation method, include immunoaffinity, screening, and porous structure capture (Liga et al., 2015). Because this method requires a much smaller volume of samples and reagents than other methods, these techniques can complete the processing of small samples in a short period of time and thus have been widely applied in biomedicine, analytical chemistry and other fields.

Relevance of Exosomes for Occurrence and Development of Diseases

Related studies have discovered that exosomes contain many miRNAs, mRNAs, and other non-coding RNAs, and therefore, as a new form of intercellular communication, these molecules play a very important role in the information transfer between cells (Salem and Fan, 2017). In recent years, the role of exosomes in the development of various diseases has been discovered gradually. For their biological effects, exosomes transfer information from the original cells to the recipient cells mainly through the information transfer between cells and simultaneously release the encoded information into the intercellular fluid or blood circulation, thereby inducing corresponding changes in the recipient cells. Therefore, the occurrence of many diseases is closely related to exosomes. In the course of diabetes development, a variety of miRNAs carried by exosomes, including miR-155 and miR-204, can facilitate the occurrence of diabetes by causing insulin resistance, reducing the sensitivity of the body to insulin, and activating mitochondrial apoptosis in β cells.

Among the exosome-mediated diseases related to the central nervous system, Alzheimer's disease has been extensively studied. Dinkins et al. found that astrocyte-derived exosomes can aggravate cognitive dysfunction by enriching and blocking the degradation of Aβ42 as a component of the senile plaques of Alzheimer's disease (Dinkins et al., 2016). Moreover, microglia can internalize and release Tau protein through exosomes. Exosomes can carry overphosphorylated Tau protein into peripheral cells, causing damage to the functions of cells when intracellular regulatory functions are dysfunctional.

Exosomes also play a vital role in the development of various blood-related diseases. In recent years, many studies have found that exosomes are closely linked to hypertension (Pironti et al., 2015), atherosclerosis (Moreno et al., 2013), cardiac hypertrophy and other diseases and can carry and transfer miR-21-3p, miR-133b and other miRNAs, playing an important role in the occurrence and development of the above cardiovascular diseases.

Advantages of Exosomes as a Natural Carrier System

As an important barrier to isolate plasma and cerebrospinal fluid, the blood-brain barrier plays a crucial role in preventing harmful substances from entering the brain and maintaining the basic stability of the brain environment. However, the restriction of the transport of macromolecule proteins by the blood-brain barrier makes entering the brain through the blood-brain barrier difficult for some macromolecule drugs that would be otherwise effective for the treatment of nervous system diseases, thereby limiting their clinical application. To enable these drugs to be used effectively in the clinic, an effective carrier system is needed to participate in the delivery of drugs.

Currently, carrier systems including liposomes and nanoparticles are widely used, but their high immunogenicity, low biocompatibility, short half-life and lack of specificity are limiting. As a natural carrier system, exosomes have a low immunogenicity, high biocompatibility, long half-life (Ha et al., 2016), and strong targeting ability (Lakhal and Wood, 2011). Exosomes can freely cross the blood-brain barrier (Zhuang et al., 2011) and maintain high activity during long-term storage, giving them major advantages as an ideal drug delivery system. A large number of studies have shown that exosomes can deliver different pharmacological molecules to target cells or tissues. These molecules can be further modified and reinserted into exosomes for different therapeutic applications (see **Figure 2**), opening up a new method for clinical drug delivery for central nervous system diseases (Samanta et al., 2018).

Brain Tissue Protection and Treatment in Central Nervous System Diseases

A series of studies have shown that exosomes play a therapeutic role in ischemic diseases of the central nervous system, creating treatment options. Exosomes have a variety of sources (endothelial cells, adipose tissue-derived mesenchymal stem cells, astrocytes, etc.) and can protect against and repair ischemic central nervous system injury. A key characteristic of exosomes is their ability to penetrate the blood-brain barrier and release the associated RNA, protein, etc. into the central nervous system (Valadi et al., 2007) and then pass through it. There are many pathways that promote the growth and repair of blood vessels, inhibit the apoptosis of nerve cells, and promote the repair and regeneration of nerve cells. Long et al. (2017) found that the adult exudate of mesenchymal stem cells administered through the nasal spray administration route can be absorbed by neurons and microglia in the motor cortex, thereby alleviating neuronal inflammation, indicating that exosomes can penetrate the blood-brain barrier and play a therapeutic role in relevant regions of the brain. Among all the sources of exosomes, mesenchymal

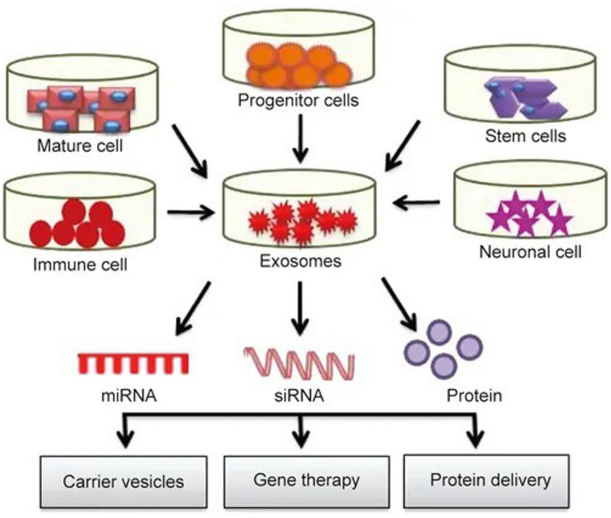

FIGURE 2 | Exosomes play roles in drug delivery: exosomes isolated from different cell types are rich in miRNA, RNA and protein. These molecules can further modified and reinserted into the exosomes for different therapeutic applications.

stem cell-derived exosomes have been extensively studied for their ability to promote the protection and repair of the central nervous system. The neuroprotective effect of mesenchymal stem cell-derived exosomes was found to be related to their dose and number of generations. The smaller the generation, the stronger neuroprotective effect of the exosomes is. Low-dose exosomes could inhibit neuronal injury through antiapoptotic effects and oxidation, while high-dose exosomes had the opposite effect on neurons (Venugopal et al., 2017).

Protective and Reparative Effects of Exosomes on Brain Tissue Injury

Relevant studies on the protection and repair of brain tissue mediated by exosomes have shown that exosomes can protect and repair neurons by (1) improving the microenvironment and regulating the corresponding immune function; (2) inhibiting neuronal apoptosis and mediating axon reconstruction and neurogenesis; (3) promoting vascular regeneration and remodeling; and (4) alleviating inflammation. Exosomes also play a role in the sexual response and immunosuppression. Dosage and route of administration of exosomes in animal experiments (see **Table 1**).

Improving the Microenvironment and Regulating Immune-Mediated Tissue Protection and Repair

In acute brain injury, insufficient cerebral perfusion can lead to ischemic stroke. White et al. (2000) showed that during stroke, high levels of glutamate accumulate in cells, which opens voltage-dependent and glutamate-regulated calcium channels, resulting in a substantial calcium influx and activation and production of large quantities of nitric oxide synthase. Excessive consumption of superoxide dismutase (SOD) leads to an accumulation of free radicals in cells, causing cell apoptosis, DNA damage, and brain tissue damage. Wei et al. (2016) showed that in a glutamate-induced neuronal injury model, adipose-derived mesenchymal stem cell-derived exosomes can protect brain tissue from glutamate-induced neuronal injury by transporting and releasing cytokines such as insulin-like growth factor (IGF) and hepatocyte growth factor (HGF), which are potentially associated with activation of the phosphatidylinositol 3-kinase (PI3K)/Akt pathway. In addition, Kalani et al. (2016) found that exosomes could reduce the infarct volume and degree of edema in the brain of ischemia-reperfusion mice by reducing the expression of the glutamate receptor *N*-methyl-D-aspartate receptor (NMDAR) in the central nervous system.

Neurons, as permanent cells, are difficult to repair after damage. Although neural stem cells provide hope for regeneration of neurons through self-differentiation, this process is very difficult due to the poor peripheral microenvironment of damaged tissues. Han et al. (2019) showed that intravenous injection of mesenchymal stem cell-derived exosomes into a intracerebral hemorrhage rat model improved the brain microenvironment through crossing the blood-brain barrier and promoting vascular remodeling and neurological function by regulating angiogenesis and neuron regeneration. These results indicated that mesenchymal stem cell-derived exosomes could enter the brain microenvironment and improve it to promote the repair of damaged neurons.

Promoting Vascular Regeneration and Reconstruction

The protective effect of exosomes is also reflected in their ability to promote the regeneration and reconstruction of blood vessels. Du et al. (2018) co-cultured mesenchymal stem cell-derived exosomes with high expression of microRNA-132-3p and bEnd.3 with mouse brain microvascular endothelial cells damaged by glucose and oxygen deprivation/reoxygenation (H/R). The mesenchymal stem cell-derived exosomes expressing high levels of microRNA-132-3p effectively improved the proliferation and migration function of H/R-induced damaged cerebrovascular endothelial cells and reduced Akt phosphorylation levels, thereby promoting blood vessel regeneration through the PI3K/Akt pathway. These observations indicated that exosomes can promote the regeneration of cerebrovascular endothelial cells by promoting the proliferation of cerebrovascular endothelial cells, providing a new method for stem cell therapy for the treatment of cerebrovascular injury.

Inhibiting Neuronal Apoptosis and Mediating Axon Remodeling and Neurogenesis

Shen et al. (2018) showed that the number of apoptotic and degenerative neurons in the rat brain was significantly reduced by transfecting exosomes with microRNA-133b and transfusing them back into the rat tail vein after intracerebral hemorrhage, indicating that microRNA-133b-containing exosomes had a protective effect on the brain tissue after intracerebral hemorrhage. Similarly, Li et al. (2018) found that neural stem cell (NSC)-derived exosomes could inhibit neuronal apoptosis and promote neuronal survival by studying the role of NSC-derived exosomes in a cobalt chloride ($CoCl_2$)-induced hypoxia

TABLE 1 | Dosages and routes of administration of exosomes in animal experiments.

Administration route	Protein dosage	Quantity	References
Intranasal (IN)	15 μg	7.5×10^9 exosomes	Long et al., 2017
Intranasal (IN)	10 μg	–	Kalani et al., 2016
Tail vein injection (TV)	100 μg	3×10^9 exosomes	Zhang et al., 2017c
Intravenous injection (IV)	250 μL	EVs released by 2×10^6 MSCs	Doeppner et al., 2015
Tail vein injection (TV)	100 μg	–	Xin et al., 2013
Tail vein injection (TV)	100 μg/day for 3 days	–	Song Y. et al., 2019
Tail vein injection (TV)	100 μg	–	Shen et al., 2018

model. Furthermore, Xin et al. (2013) showed that exosomes can promote neuronal axon remodeling, neurogenesis and angiogenesis in stroke models. In addition, culturing neurons and glial cells in the presence of mesenchymal stem cell-derived exosomes expressing abundant microRNA-133b promoted neuronal cell growth, indicated by an increase in neuron neurites (Xin et al., 2012). Similarly, Zhang et al. (2017b) found that exosomes derived from mesenchymal stem cells promoted axon formation in nerve cells, which may be related to microRNA-17-92. Song Y. et al. (2019) observed mouse infarction and neuronal apoptosis 3 days after an ischemic attack induced by blocking the middle cerebral artery of the mouse, followed by immediate intravenous injection of M2 microglia-derived exosomes; M2 BV2-derived exosomes were shown to promote neuronal-mediated neuroprotection via miR-124 and through downregulation of miR-124 target proteins, which inhibited neurological deficits and neuronal apoptosis in the mouse model of stroke, thereby increasing the survival rate of neuronal cells.

Antagonizing Immunosuppression and the Inflammatory Response

Li Y. et al. (2017) showed that exosomes of dental pulp mesenchymal stem cells could inhibit the neuroinflammatory response induced by traumatic brain injury. Huang et al. (2018) also showed that under traumatic brain injury, an increase in microglial exosome miRNA-124-3p not only reduced the occurrence of the inflammatory response but also promoted the growth of axons. Similarly, Zhang et al. (2017c) found that neurological function was improved by extracting mesenchymal stem cell-derived exosomes and transfusing them back into a traumatic brain injury (TBI) animal model. The exosomes may act by promoting vascular remodeling and nerve regeneration and alleviating inflammatory reactions. In addition, Doeppner et al. (2015) found that mesenchymal stem cell-derived exosomes not only promoted cerebral vascular regeneration in mice with focal cerebral ischemia but also provided an appropriate external environment for brain remodeling by antagonizing the immunosuppressive response. This study indicated that exosomes from various sources have various mechanisms by which they provide protection of brain tissues after a trauma. Exosomes are able to protect and repair damaged tissues by antagonizing immune and inflammatory responses, promoting neuron regeneration and providing a suitable reconstructed external environment.

Protection of Brain Tissue Mediated by Secretion of Exosome in Ischemic Preconditioning

As research on the function of exosomes has been performed and our knowledge of their role has deepened, researchers' views on exosomes have changed. At an early stage, exosomes were considered a medium for cells to discharge waste to the outside world. In recent years, the above studies showed that exosomes play an important role in the protection and repair of brain tissue after brain injury. The research not only suggests that exosomes can be used as a new therapeutic approach with great potential but also that exosomes play an important role in alleviating or even preventing brain tissue damage caused by ischemia and hypoxia. At present, non-pharmacological approaches such as mild hypothermia and ion channel blockers are mostly used to prevent ischemic brain damage in the clinic, as well as other pharmacological approaches such as ion channel blockers. In recent years, an increasing number of researchers have found that exosomes may play an important role in brain protection mediated by ischemic preconditioning.

Ischemic conditioning refers to a process involving short-term blockade and reperfusion of blood flow to activate various endogenous protective mechanisms and alleviate tissue damage. This method is widely used in various cardiovascular operations. However, because the protection of brain tissue using this process requires the separation of the brain tissue for blood flow blockage and reflux, the process has many advantages. In recent years, the concept of ischemic conditioning has been extended to remote ischemic conditioning (RIC), i.e., a short series of blood flow blockade and reperfusion in the distal limbs through cuff suppression, which has also been found to have protective effects on brain tissue after multiple cycles. Although ischemic preconditioning and RIC have great potential for development as effective, low-cost and simple methods, few researchers have studied the mechanism of ischemic preconditioning.

Xiao et al. (2017) studied the protective effect of RIC in acute cerebral ischemia. RIC on the limbs of experimental animals increased the content of exosomes in the blood, the morphology of which was similar to that of endothelial cell-derived exosomes. Further experiments showed that endothelial cell-derived exosomes could be induced by upregulation of transcription and translation through sugar deprivation/reoxygenation in the SH-SY5Y nerve cell line. In this process, the expression of Bcl-2 inhibits the expression of Bax, thus alleviating nerve cell apoptosis and achieving a protective effect. The mechanism of this process may be related to the Janus kinase 2 (JAK2)/signal transducer and activator of transcription-3 (STAT3) pathway (Cheng et al., 2014) and the PI3K/Akt pathway (Zhang et al., 2017a); the latter pathway has been extensively studied, and the former requires further testing.

In Xiao et al. (2017), the CD63, HSP70 and TSG101 expression levels in exosomes in the hippocampus of the RIP group did not increase, but the expression in plasma increased, indicating that RIP can promote the release of exosomes. This finding indicates that in light of the spatial distribution of exosomes in a model of acute cerebral ischemia, exosomes are extensively distributed in the blood circulation. Moreover, the brain protection mediated by remote ischemic preconditioning also indicates that exosomes are extensively distributed in the whole body through the blood circulation, and due to the size of the exosomes themselves and the specificity of their physical and chemical properties, these molecules can further mediate brain protection by passing through the BBB and releasing miRNAs and other substances. Furthermore, based on the elevated blood exosomes induced by remote ischemic preconditioning, these molecules are likely associated with the protection of other organs. The dependent interaction of exosomes in the damage of organism has been outlined above. In recent year, increasing numbers of studies have shown that in addition to the brain protection mediated by exosomes, exosomes can act on tissues such as the myocardium in

a similar manner and mediate the corresponding tissue protective functions, indicating that the effect of exosomes is not specific to brain tissue. Given the diversity of these mechanisms, multiple organ protective mechanisms may be present simultaneously, and further exploration of these mechanisms is needed.

OUTLOOK

As a new therapeutic carrier, exosomes have attracted increasing attention because of their unique biological characteristics. Our understanding of exosomes has also changed from an excreta carrier in earlier years to a new therapeutic carrier with tremendous research potential in recent years, with an ability to mediate the repair process of multiple brain tissue injuries. Many studies have shown that exosomes can ameliorate ischemic and hypoxic brain tissue by improving the microenvironment, regulating the corresponding immune effects, inhibiting neuronal apoptosis, mediating axon reconstruction and neurogenesis, promoting vascular regeneration and remodeling, alleviating the inflammatory response and immune suppression, etc. Moreover, these repairing effects of exosomes also suggest that they can play a protective role in preventing ischemic brain necrosis by improving the resistance of brain tissue to acute ischemic injury. Through the study of animal models of acute ischemia, we see that RIC can produce exosomes and transfer them to brain tissue to play a protective role, not only indicating that exosomes can play a protective role in preventing ischemic brain necrosis but also showing tremendous research value in the study of their involvement in mediating brain protection. Research has also shown that exosomes, with their high biocompatibility, low immunogenicity and toxicity, can effectively participate in brain protection. In addition to traditional non-pharmacological approaches such as mild hypothermia and pharmacological approaches, exosomes can protect against cerebral ischemia injury. At the same time, the protective effect mediated by exosomes found in remote ischemic preconditioning experiments indicates that exosomes are related to the traditional ischemic preconditioning mechanism.

However, our knowledge of the protective effect of exosomes on brain tissue is limited; most experiments are limited to the protective effect of exosomes on the tissue itself, and the interaction between exosomes and signaling pathways is not discussed in detail. In addition to studies on the use of exosomes as an effective therapeutic approach, more research examining the specific mechanism of exosome-mediated brain tissue protection is needed.

AUTHOR CONTRIBUTIONS

WG and HT were the guarantor of integrity of the entire study. WG and WH contributed to study concepts. XK and WH contributed to manuscript preparation. XK and ZZ contributed to manuscript editing. HT helped to manuscript review.

FUNDING

This study was funded by the Natural Science Foundation of China (81774109 and 81973620), Natural Science Foundation of Zhejiang Provincial (Y19H310028), Zhejiang Public Welfare Technology Research Plan (GD20H290004), and Wenzhou Science and Technology project (ZY2019015 and Y20180496).

REFERENCES

Ayala-Mar, S., Donoso-Quezada, J., Gallo-Villanueva, R. C., Perez-Gonzalez, V. H., and Gonzalez-Valdez, J. (2019). Recent advances and challenges in the recovery and purification of cellular exosomes. *Electrophoresis* doi: 10.1002/elps.201800526 [Epub ahead of print].

Cheng, Z., Li, L., Mo, X., Zhang, L., Xie, Y., Guo, Q., et al. (2014). Non-invasive remote limb ischemic postconditioning protects rats against focal cerebral ischemia by upregulating STAT3 and reducing apoptosis. *Int. J. Mol. Med.* 34, 957–966. doi: 10.3892/ijmm.2014.1873

Colombo, M., Moita, C., van Niel, G., Kowal, J., Vigneron, J., Benaroch, P., et al. (2013). Analysis of ESCRT functions in exosome biogenesis, composition and secretion highlights the heterogeneity of extracellular vesicles. *J. Cell Sci.* 126, 5553–5565. doi: 10.1242/jcs.128868

Colombo, M., Raposo, G., and Thery, C. (2014). "Biogenesis, secretion, and intercellular interactions of exosomes and other extracellular vesicles," in *Annual Review of Cell and Developmental Biology*, Vol. 30, eds R. Schekman and R. Lehmann (California, CA: Annual Reviews), 255–289. doi: 10.1146/annurev-cellbio-101512-122326

Dinkins, M. B., Enasko, J., Hernandez, C., Wang, G., Kong, J., Helwa, I., et al. (2016). Neutral sphingomyelinase-2 deficiency ameliorates Alzheimer's Disease pathology and improves cognition in the 5XFAD Mouse. *J. Neurosci.* 36, 8653–8667. doi: 10.1523/jneurosci.1429-16.2016

Doeppner, T. R., Herz, J., Goergens, A., Schlechter, J., Ludwig, A.-K., Radtke, S., et al. (2015). Extracellular vesicles improve post-stroke neuroregeneration and prevent postischemic immunosuppression. *Stem Cells Transl. Med.* 4, 1131–1143. doi: 10.5966/sctm.2015-2078

Du, D., Wang, Y., Xu, X., Zheng, J., Zhang, H., Kuang, X., et al. (2018). Improving effect of exosomes of mesenchymal stem cells with high expression of miR-132-3p on hypoxia/reoxygenation impaired brain microvascular endothelial cell function. *Chin. J. Cerebrovasc. Dis.* 15, 584–591.

Gupta, S., and Knowlton, A. A. (2007). HSP60 trafficking in adult cardiac myocytes: role of the exosomal pathway. *Am. J. Physiol. Heart Circ. Physiol.* 292, H3052–H3056. doi: 10.1152/ajpheart.01355.2006

Gupta, S., Rawat, S., Arora, V., Kottarath, S. K., Dinda, A. K., Vaishnav, P. K., et al. (2018). An improvised one-step sucrose cushion ultracentrifugation method for exosome isolation from culture supernatants of mesenchymal stem cells. *Stem Cell Res. Ther.* 9:180. doi: 10.1186/s13287-018-0923-920

Ha, D., Yang, N., and Nadithe, V. (2016). Exosomes as therapeutic drug carriers and delivery vehicles across biological membranes: current perspectives and future challenges. *Acta Pharm. Sin. B* 6, 287–296. doi: 10.1016/j.apsb.2016.02.001

Han, Y., Seyfried, D., Meng, Y., Yang, D., Schultz, L., Chopp, M., et al. (2019). Multipotent mesenchymal stromal cell-derived exosomes improve functional recovery after experimental intracerebral hemorrhage in the rat. *J. Neurosurg.* 131, 290–300. doi: 10.3171/2018.2.jns171475

Hessvik, N. P., verbye, A., Brech, A., Torgersen, M. L., Jakobsen, I. S., Sandvig, K., et al. (2016). PIKfyve inhibition increases exosome release and induces secretory autophagy. *Cell. Mol. Life Sci.* 73, 4717–4737. doi: 10.1007/s00018-016-2309-2308

Hsu, C., Morohashi, Y., Yoshimura, S. I, Manrique-Hoyos, N., Jung, S., Lauterbach, M. A., et al. (2010). Regulation of exosome secretion by Rab35 and its GTPase-activating proteins TBC1D10A-C. *J. Cell Biol.* 189, 223–232. doi: 10.1083/jcb.200911018

Huang, S., Ge, X., Yu, J., Han, Z., Yin, Z., Li, Y., et al. (2018). Increased miR-124-3p in microglial exosomes following traumatic brain injury inhibits neuronal inflammation and contributes to neurite outgrowth via their transfer into neurons. *FASEB J.* 32, 512–528. doi: 10.1096/fj.201700673R

Kalani, A., Chaturvedi, P., Kamat, P. K., Maldonado, C., Bauer, P., Joshuaa, I. G., et al. (2016). Curcumin-loaded embryonic stem cell exosomes restored neurovascular unit following ischemia-reperfusion injury. *Int. J. Biochem. Cell Biol.* 79, 360–369. doi: 10.1016/j.biocel.2016.09.002

Lakhal, S., and Wood, M. J. A. (2011). Exosome nanotechnology: an emerging paradigm shift in drug delivery exploitation of exosome nanovesicles for systemic in vivo delivery of RNAi heralds new horizons for drug delivery across biological barriers. *Bioessays* 33, 737–741. doi: 10.1002/bies.201100076

Li, B., Wei, H., Yang, Y., Ying, M., Hu, C., Lu, Y., et al. (2018). Neural stem cell-derived exosomes inhibit apoptosis of neurons induced by hypoxia neural cells. *Chinese J. Pathophysiol.* 34, 717–722, 728.

Li, P., Kaslan, M., Lee, S. H., Yao, J., and Gao, Z. (2017). Progress in exosome isolation techniques. *Theranostics* 7, 789–804. doi: 10.7150/thno.18133

Li, Y., Yang, Y.-Y., Ren, J.-L., Xu, F., Chen, F.-M., and Li, A. (2017). Exosomes secreted by stem cells from human exfoliated deciduous teeth contribute to functional recovery after traumatic brain injury by shifting microglia M1/M2 polarization in rats. *Stem Cell Res. Ther.* 8:198. doi: 10.1186/s13287-017-0648-645

Liga, A., Vliegenthart, A. D. B., Oosthuyzen, W., Dear, J. W., and Kersaudy-Kerhoas, M. (2015). Exosome isolation: a microfluidic road-map. *Lab Chip* 15, 2388–2394. doi: 10.1039/c5lc00240k

Long, Q., Upadhya, D., Hattiangady, B., Kim, D.-K., An, S. Y., Shuai, B., et al. (2017). Intranasal MSC-derived A1-exosomes ease inflammation, and prevent abnormal neurogenesis and memory dysfunction after status epilepticus. *Proc. Natl. Acad. Sci. U.S.A.*114, E3536–E3545. doi: 10.1073/pnas.1703920114

Moreno, J. A., Sastre, C., Madrigal-Matute, J., Munoz-Garcia, B., Ortega, L., Burkly, L. C., et al. (2013). HMGB1 expression and secretion are increased Via TWEAK-Fn14 interaction in atherosclerotic plaques and cultured monocytes. *Arterioscler. Thromb. Vasc. Biol.* 33, 612–620. doi: 10.1161/atvbaha.112.300874

Ostrowski, M., Carmo, N. B., Krumeich, S., Fanget, I., Raposo, G., Savina, A., et al. (2010). Rab27a and Rab27b control different steps of the exosome secretion pathway. *Nat. Cell Biol.* 12, 19–30. doi: 10.1038/ncb2000

Pan, B. T., and Johnstone, R. M. (1983). Fate of the transferrin receptor during maturation of sheep reticulocytes invitro - selective externalization of the receptor. *Cell* 33, 967–977. doi: 10.1016/0092-8674(83)90040-90045

Pegtel, D. M., Cosmopoulos, K., Thorley-Lawson, D. A., van Eijndhoven, M. A. J., Hopmans, E. S., Lindenberg, J. L., et al. (2010). Functional delivery of viral miRNAs via exosomes. *Proc. Natl. Acad. Sci. U.S.A.* 107, 6328–6333. doi: 10.1073/pnas.0914843107

Pironti, G., Strachan, R. T., Abraham, D., Yu, S. M.-W., Chen, M., Chen, W., et al. (2015). Circulating exosomes induced by cardiac pressure overload contain functional Angiotensin II Type 1 receptors. *Circulation* 131, 2120–2130. doi: 10.1161/circulationaha.115.015687

Raposo, G., Nijman, H. W., Stoorvogel, W., Leijendekker, R., Harding, C. V., Melief, C. J. M., et al. (1996). B lymphocytes secrete antigen-presenting vesicles. *J. Exp. Med.* 183, 1161–1172. doi: 10.1084/jem.183.3.1161

Roucourt, B., Meeussen, S., Bao, J., Zimmermann, P., and David, G. (2015). Heparanase activates the syndecan-syntenin-ALIX exosome pathway. *Cell Res.* 25, 412–428. doi: 10.1038/cr.2015.29

Salem, E. S. B., and Fan, G.-C. (2017). "Pathological effects of exosomes in mediating diabetic cardiomyopathy," in *Exosomes in Cardiovascular Diseases: Biomarkers, Pathological and Therapeutic Effects*, eds J. Xiao and S. Cretoiu (Berlin: Springer), 113–138. doi: 10.1007/978-981-10-4397-0_8

Samanta, S., Rajasingh, S., Drosos, N., Zhou, Z., Dawn, B., and Rajasingh, J. (2018). Exosomes: new molecular targets of diseases. *Acta Pharmacol. Sin.* 39, 501–513. doi: 10.1038/aps.2017.162

Shahabipour, F., Barati, N., Johnston, T. P., Derosa, G., Maffioli, P., and Sahebkar, A. (2017). Exosomes: nanoparticulate tools for RNA interference and drug delivery. *J. Cell. Physiol.* 232, 1660–1668. doi: 10.1002/jcp.25766

Shen, H., Yao, X., Li, H., Li, X., Zhang, T., Sun, Q., et al. (2018). Role of exosomes derived from miR-133b modified mscs in an experimental rat model of intracerebral hemorrhage. *J. Mol. Neurosci.* 64, 421–430. doi: 10.1007/s12031-018-1041-1042

Sims, B., Farrow, A. L., Williams, S. D., Bansal, A., Krendelchtchikov, A., and Matthews, Q. L. (2018). Tetraspanin blockage reduces exosome-mediated HIV-1 entry. *Arch. Virol.* 163, 1683–1689. doi: 10.1007/s00705-018-3737-3736

Song, L., Tang, S., Han, X. L., Jiang, Z. Y., Dong, L. L., Liu, C. C., et al. (2019). KIBRA controls exosome secretion via inhibiting the proteasomal degradation of Rab27a. *Nat. Commun.* 10:1639. doi: 10.1038/s41467-019-09720-x

Song, Y., Li, Z., He, T., Qu, M., Jiang, L., Li, W., et al. (2019). M2 microglia-derived exosomes protect the mouse brain from ischemia-reperfusion injury via exosomal miR-124. *Theranostics* 9, 2910–2923. doi: 10.7150/thno.30879

Valadi, H., Ekstrom, K., Bossios, A., Sjostrand, M., Lee, J. J., and Lotvall, J. O. (2007). Exosome-mediated transfer of mRNAs and microRNAs is a novel mechanism of genetic exchange between cells. *Nat. Cell Biol.* 9, 654–659. doi: 10.1038/ncb1596

Venugopal, C., Shamir, C., Senthilkumar, S., Babu, J. V., Sonu, P. K., Nishtha, K. J., et al. (2017). Dosage and passage dependent neuroprotective effects of exosomes derived from rat bone marrow mesenchymal stem cells: an in vitro analysis. *Curr. Gene Ther.* 17, 379–390. doi: 10.2174/1566523218666180125091952

Wei, J. J., Chen, Y. F., Xue, C. L., Ma, B. T., Shen, Y. M., Guan, J., et al. (2016). Protection of nerve injury with Exosome extracted from mesenchymal stem cell. *Zhongguo Yi Xue Ke Xue Yuan Xue Bao* 38, 33–36. doi: 10.3881/j.issn.1000-503X.2016.01.006

Wei, Y., Wang, D., Jin, F., Bian, Z., Li, L., Liang, H., et al. (2017). Pyruvate kinase type M2 promotes tumour cell exosome release via phosphorylating synaptosome-associated protein 23. *Nat. Commun.* 8:14041. doi: 10.1038/ncomms14041

White, B. C., Sullivan, J. M., DeGracia, D. J., O'Neil, B. J., Neumar, R. W., Grossman, L. I., et al. (2000). Brain ischemia and reperfusion: molecular mechanisms of neuronal injury. *J. Neurol. Sci.* 179, 1–33. doi: 10.1016/s0022-510x(00)00386-385

Xiao, B., Chai, Y., Lv, S., Ye, M., Wu, M., Xie, L., et al. (2017). Endothelial cell-derived exosomes protect SH-SY5Y nerve cells against ischemia/reperfusion injury. *Int. J. Mol. Med.* 40, 1201–1209. doi: 10.3892/ijmm.2017.3106

Xin, H., Li, Y., Buller, B., Katakowski, M., Zhang, Y., Wang, X., et al. (2012). Exosome-mediated transfer of mir-133b from multipotent mesenchymal stromal cells to neural cells contributes to neurite outgrowth. *Stem Cells* 30, 1556–1564. doi: 10.1002/stem.1129

Xin, H., Li, Y., Cui, Y., Yang, J. J., Zhang, Z. G., and Chopp, M. (2013). Systemic administration of exosomes released from mesenchymal stromal cells promote functional recovery and neurovascular plasticity after stroke in rats. *J. Cereb. Blood Flow Metab.* 33, 1711–1715. doi: 10.1038/jcbfm.2013.152

Zhang, W., Wang, Y., and Bi, G. (2017a). Limb remote ischaemic postconditioning-induced elevation of fibulin-5 confers neuroprotection to rats with cerebral ischaemia/reperfusion injury: activation of the Akt pathway. *Clin. Exp. Pharmacol. Physiol.* 44, 656–663. doi: 10.1111/1440-1681.12742

Zhang, Y., Chopp, M., Liu, X. S., Katakowski, M., Wang, X., Tian, X., et al. (2017b). Exosomes derived from mesenchymal stromal cells promote axonal growth of cortical neurons. *Mol. Neurobiol.* 54, 2659–2673. doi: 10.1007/s12035-016-9851-9850

Zhang, Y., Chopp, M., Zhang, Z. G., Katakowski, M., Xin, H., Qu, C., et al. (2017c). Systemic administration of cell-free exosomes generated by human bone marrow derived mesenchymal stem cells cultured under 2D and 3D conditions improves functional recovery in rats after traumatic brain injury. *Neurochem. Int.* 111, 69–81. doi: 10.1016/j.neuint.2016.08.003

Zhang, X., Wang, X., Zhu, H., Kranias, E. G., Tang, Y., Peng, T., et al. (2012). Hsp20 functions as a novel Cardiokine in promoting angiogenesis via activation of VEGFR2. *PLoS One* 7:e32765. doi: 10.1371/journal.pone.0032765

Zhuang, X., Xiang, X., Grizzle, W., Sun, D., Zhang, S., Axtell, R. C., et al. (2011). Treatment of brain inflammatory diseases by delivering exosome encapsulated anti-inflammatory drugs from the nasal region to the brain. *Mol. Ther.* 19, 1769–1779. doi: 10.1038/mt.2011.164

Conflict of Interest: The authors declare that the research was conducted in the absence of any commercial or financial relationships that could be construed as a potential conflict of interest.

frontiers in Endocrinology

REVIEW
published: 13 December 2019
doi: 10.3389/fendo.2019.00864

Genotype-Phenotype Relationships and Endocrine Findings in Prader-Willi Syndrome

*Régis Afonso Costa†, Igor Ribeiro Ferreira†, Hiago Azevedo Cintra, Leonardo Henrique Ferreira Gomes and Letícia da Cunha Guida**

Laboratório de Alta Complexidade, Instituto Nacional da Saúde da Mulher, da Criança e Do Adolescente Fernandes Figueira, Fiocruz, Rio de Janeiro, Brazil

Prader-Willi syndrome (PWS) is a complex imprinting disorder related to genomic errors that inactivate paternally-inherited genes on chromosome 15q11-q13 with severe implications on endocrine, cognitive and neurologic systems, metabolism, and behavior. The absence of expression of one or more genes at the PWS critical region contributes to different phenotypes. There are three molecular mechanisms of occurrence: paternal deletion of the 15q11-q13 region; maternal uniparental disomy 15; or imprinting defects. Although there is a clinical diagnostic consensus criteria, DNA methylation status must be confirmed through genetic testing. The endocrine system can be the most affected in PWS, and growth hormone replacement therapy provides improvement in growth, body composition, and behavioral and physical attributes. A key feature of the syndrome is the hypothalamic dysfunction that may be the basis of several endocrine symptoms. Clinical and molecular complexity in PWS enhances the importance of genetic diagnosis in therapeutic definition and genetic counseling. So far, no single gene mutation has been described to contribute to this genetic disorder or related to any exclusive symptoms. Here we proposed to review individually disrupted genes within the PWS critical region and their reported clinical phenotypes related to the syndrome. While genes such as *MKRN3*, *MAGEL2*, *NDN*, or *SNORD115* do not address the full spectrum of PWS symptoms and are less likely to have causal implications in PWS major clinical signs, *SNORD116* has emerged as a critical, and possibly, a determinant candidate in PWS, in the recent years. Besides that, the understanding of the biology of the PWS SNORD genes is fairly low at the present. These non-coding RNAs exhibit all the hallmarks of RNA methylation guides and can be incorporated into ribonucleoprotein complexes with possible hypothalamic and endocrine functions. Also, DNA conservation between SNORD sequences across placental mammals strongly suggests that they have a functional role as RNA entities on an evolutionary basis. The broad clinical spectrum observed in PWS and the absence of a clear genotype-phenotype specific correlation imply that the numerous genes involved in the syndrome have an additive deleterious effect on different phenotypes when deficiently expressed.

Keywords: Prader-Willi syndrome, genotype, phenotype, endocrine, imprinting, SNORDs

OPEN ACCESS

Edited by:
Ana Rosa Pérez, National Council for Scientific and Technical Research, Argentina

Reviewed by:
Christian P. Schaaf, Heidelberg University, Germany
Dag H. Yasui, University of California, Davis, United States

***Correspondence:**
Letícia da Cunha Guida
leticia.guida@iff.fiocruz.br

†These authors have contributed equally to this work

Specialty section:
This article was submitted to Neuroendocrine Science, a section of the journal Frontiers in Endocrinology

Received: *30 September 2019*
Accepted: *26 November 2019*
Published: *13 December 2019*

Citation:
Costa RA, Ferreira IR, Cintra HA, Gomes LHF and Guida LdC (2019) Genotype-Phenotype Relationships and Endocrine Findings in Prader-Willi Syndrome. Front. Endocrinol. 10:864. doi: 10.3389/fendo.2019.00864

INTRODUCTION

Prader-Willi syndrome (PWS; OMIM 176270) was first described in 1956 by Andrea Prader, Alexis Labhart and Heinrich Willi based on a study of nine children with a common clinical tetrad: short stature, intellectual disability, obesity, and small hands and feet (1, 2). The phenotypic analysis was expanded in the following years and decades, revealing the complexity of the syndrome, affecting endocrine, cognitive and neurologic systems, metabolism, and behavior. PWS was the first human disease to be related to genomic imprinting errors, and also the first one shown to be caused by uniparental disomy (3, 4). This rare genetic disorder has a prevalence of 1 in 10,000–30,000 live births, males and females are affected equally in all ethnic groups (5).

The PWS critical region on chromosome 15q11-q13 is monoallelically expressed by paternally inherited genes, exclusively. The absence of expression of one or more of these genes contributes to different phenotypes of PWS (6, 7) and there are three main mechanisms of occurrence: paternal deletion of the 15q11-q13 region; maternal uniparental disomy 15; or imprinting defects (8–10). On the other hand, in the same region, the loss of expression of the *UBE3A* gene (preferentially maternally expressed) drives to Angelman syndrome, with completely different clinical characteristics. By their common implicated region and mechanisms, both syndromes are considered sister imprinted disorders (11, 12).

Clinical manifestations vary with age, impacting multiple body systems (**Table 1**). Fetal size is usually within the normal range. Compared to unaffected siblings, birth weight and body mass index (BMI) are 15% lower on average. Prenatal hypotonia may cause decreased fetal movement, abnormal fetal position at delivery, and increased incidence of assisted delivery or cesarean section (14, 15).

TABLE 1 | Clinical characteristics and the nutritional phases in PWS.

Median ages	Clinical characteristics
Prenatal—birth	Decreased fetal movements
	Lower birth weight and body mass compared to sibs
0–9 months	Severe hypotonia
	Feeding problems and failure to thrive
9–25 months	Improved feeding and appetite
	Normal growth
	Delayed physical and social milestones
2.1–4.5 years	Weight increasing without appetite increase or excess calories
4.5–8 years	Weight increasing with appetite increase
	Global developmental delay
8 years—adulthood	Hyperphagic, rarely feels satiety
	Mild intellectual disability and behavior problems
	Hypogonadism
Adulthood	Appetite no longer insatiable for some
	Short stature and small hands and feet

Gunay-Aygun et al. (13); Miller et al. (14); Driscoll et al. (5).

Severe hypotonia is a clinical hallmark of PWS, leading to failure to thrive during infancy due to lethargy and poor suck. Other common neonatal findings are decreased movement and spontaneous arousal, weak cry, thick saliva, and poor reflexes (13, 16). Around 9 months of life, eating behavior starts to normalize, and the hypotonic status tends to improve, but mild-to-moderate hypotonia persists throughout life, with reduced muscle mass and tone (9, 17).

Physical and social milestones (as sitting, walking, first words, and reading) are delayed and can be achieved at about double the normal age (18). Most individuals have mild intellectual disability, learning difficulties, and poor academic performance. During early infancy, characteristic behavioral problems are common, such as stubbornness, manipulation, compulsiveness, self-injury, and difficulty with change in routine (5, 19, 20). Another common feature in the syndrome is sleep disruption, related to sleep apnea that impairs the quality and efficiency of sleep, frequently associated with excessive daytime sleepiness, and sedentary behavior with a higher predisposition to obesity (13, 21).

In later childhood, individuals with PWS will reach severe obesity unless food intake is strictly controlled by family and caretakers. The lack of satiety (hypothalamic origin) results in hyperphagia, with obsessive food seeking. In uncontrolled cases, obesity, and its complications are the major causes of morbidity and mortality: respiratory insufficiency, cardiovascular problems, metabolic syndrome, sleep apnea, and type 2 diabetes mellitus (22, 23). Mortality rates range between 1.25 and 3% per year (24, 25). Hyperphagia in PWS is still not fully understood and controlling appetite remains a challenge.

The endocrine system can be the most affected in PWS. Growth hormone (GH) deficiency is present in up to 74% of cases and is associated with short stature, small hands and feet, low motor strength, increased fat mass, and decreased movement and energy expenditure (26, 27). GH replacement therapy has shown positive effects not only on growth and body composition but also on development, behavior, and nocturnal respiratory abnormalities, although a careful respiratory follow up is mandatory during long-term GH administration (28–34). Hypogonadism affects both sexes and is manifested as hypogenitalism, incomplete pubertal development and infertility in most individuals (35). Hypogonadism is thought to have a hypothalamic origin, and subsequent insufficient secretion of pituitary gonadotropins and sexual hormones (testosterone or estrogen) (7, 36, 37). Other endocrine abnormalities include hypothyroidism (20–30%), central adrenal insufficiency (about 5%) and type 2 diabetes (up to 25%) due to obesity complications (24, 38–41).

MOLECULAR GENETICS AND DIAGNOSTIC

The hypothalamic dysfunction observed in PWS may be the basis of several symptoms (such as hypotonia, developmental delay or obesity) that overlaps features of other conditions on clinical grounds, like normal obesity and intellectual disability (42).

Definitive diagnosis requires DNA testing. The PWS region spans ∼6 Mb on the long arm of chromosome 15 (**Figure 1**). Within this region, at least 2.5 Mb comprises genes with differential expression depending on parental origin. This locus holds protein-coding genes and several non-coding RNAs, which are believed to be involved in the regulation of alternative splicing, mainly in the brain (10, 16).

The bicistronic gene *SNURF-SNRPN* is central to the PWS region and crucial to understanding the methylation pattern in the syndrome. The CpG island at the 5′ end of *SNURF-SNRPN* (encompassing the promoter region, exon 1 and intron 1) is differentially imprinted according to parental origin: the unmethylated paternal allele is expressed while the methylated maternal allele is repressed (43). The PWS imprinting center (PWS-IC, **Figure 1**) involves the CpG island and exon 1 within the 4.3 Kb smallest region of overlap (44). Furthermore, *SNURF-SNRPN* expression produces a long transcript also including PWS-IC, Six snoRNA genes, *IPW* and *UBE3A* antisense (**Figure 1**), which is hypothesized to repress paternal *UBE3A* (45–48).

Most PWS patients (65–75%) present a 5–6 Mb deletion at 15q11-q13 from the paternal origin (16, 49). There are two proximal breakpoints and a common distal breakpoint (**Figure 1**), these regions are flanked by low copy repeat sequences that predispose to abnormal chromosomal pairing and uneven crossing-over, resulting in errors during meiosis (50, 51). Maternal Uniparental Disomy (mDUP) occurs when both chromosomes 15 are inherited from the mother and accounts

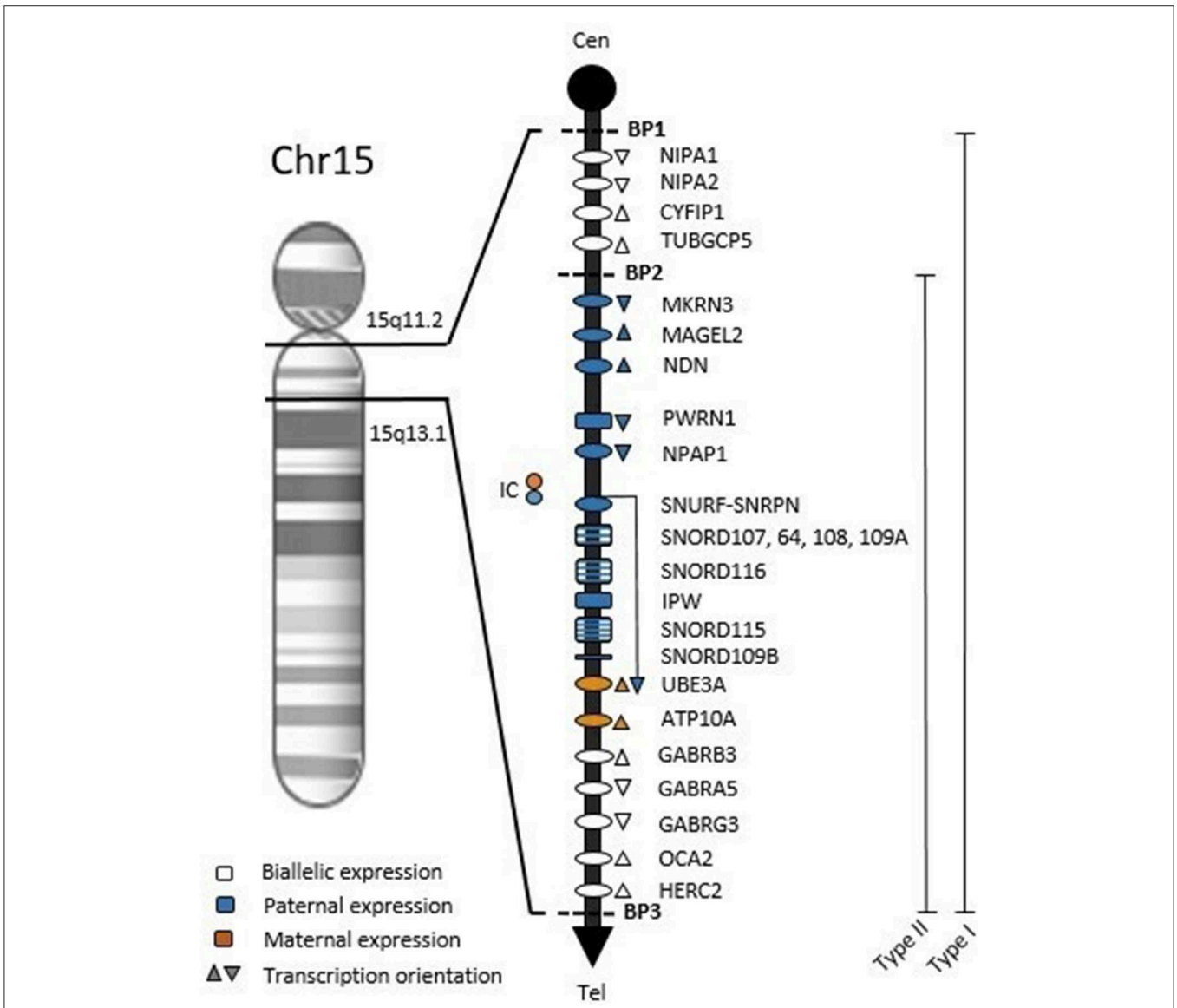

FIGURE 1 | Chromosome map of 15q11.2-q13.1 region. Symbols: ovals, protein-coding genes; rectangles, RNA genes; BP1, breakpoint 1; BP2, breakpoint 2; BP3, breakpoint 3; Type 1, BP1-BP3 deletion with ∼6 Mb; Type 2, BP2-BP3 deletion with ∼5.3 Mb; Cen, Centromere; Tel, Telomere; IC, Imprinting Center.

for ∼20–30% of cases, being associated with advanced maternal age (9, 15). Imprinting defects are caused by epimutations or microdeletions in the PWS-IC in 1–3% of PWS cases. These individuals have biparental allele inheritance, but a maternal-only DNA methylation pattern (11, 52).

Clinical and molecular complexity in PWS enhances the importance of genetic diagnosis in therapeutic definition and genetic counseling. Only DNA methylation analysis can consistently diagnose the syndrome in all three molecular classes (deletion, mUPD, and imprinting defects) and differentiate it from Angelman Syndrome (9, 52). The methylation analysis targets the 5′ CpG island of the *SNURF-SNRPN* locus and will correctly diagnose more than 99% of cases. Currently, there are three assays with this detection capacity: methylation-specific PCR (MS-PCR, the gold standard), methylation-specific multiplex ligation-dependent probe amplification (MS-MLPA) and methylation-sensitive high-resolution melting (MS-HRM) (53–58).

After methylation status confirmation, defining the exact molecular mechanism behind the syndrome origin is important for genetic counseling. Sporadic deletion cases have <1% risk of recurrence, while rare cases of structural abnormalities involving chromosome 15 (such as translocations, ring formation, isochromosome or inversions) can be as high as 25–50% and fluorescence *in situ* hybridization (FISH) can address the deletion source (59–65). mUPD 15 is typically *de novo* (recurrence <1%), proband and parents should be investigated by small nucleotide polymorphisms (SNP) microarray for accurate counseling (66, 67). Most imprinting defects cases are classified as epimutations with no alteration in the DNA sequence and have <1% recurrence risk. However, 15% of individuals with imprinting defects present a paternally inherited microdeletion (7.5–100 kb) in the PWS-IC, in which cases the risk of recurrence is 50%. IC analysis by MS-MLPA or DNA sequencing will address the exact origin of this event (5, 44).

GENOTYPE-PHENOTYPE RELATIONSHIPS IN PRADER-WILLI SYNDROME

None of the PWS genetic errors are associated with exclusive symptoms. However, the most prevalent molecular classes (deletion and mUPD) show statistical differences in frequency or severity in some clinical characteristics. Patients with paternal deletion were more related to feeding problems, sleep disturbances, hypopigmentation and speech and language deficits (68). Individuals with the larger type 1 deletion (**Figure 1**) have been reported to have better academic performance and intellectual abilities, and more compulsiveness when compared to type 2 deletion patients (69, 70). Several other features are more common in mUPD individuals, such as post-term delivery, higher verbal IQ, psychosis and autism spectrum disorder (15, 69, 71–75). On the other hand, mUPD patients are less likely to have the typical PWS facial appearance or hypopigmentation (16). So far, no single gene mutation has been described to contribute to this genetic disorder. Here we proposed to review genes individually disrupted within the PWS critical region and their reported clinical phenotypes related to the syndrome.

The Makorin Ring Finger Protein 3 (*MKRN3*, *ZNF127*) gene encodes a zinc finger protein of the Makorin family and is paternally expressed ubiquitously in human adult tissues, with the highest level in testis, although its exact mechanism of action remains to be elucidated (76). This gene is associated with inhibition of puberty initiation, and loss of function mutations in *MKRN3* are recognized as the main genetic cause of Central Precocious Puberty (77). This correlation has been described by distinct studies with different ethnic groups, affecting equally both sexes, with all mutations segregated in a paternal manner at *MKRN3* (78–81). Experimental models with mice also support the correlation between mutations in *Mkrn3* and puberty dysfunctions, suggesting it may play a role in the hypothalamic-pituitary-gonadal axis (77–79). Altogether, this makes *MKRN3* a strong candidate gene for hypogonadism and infertility in PWS.

The physiological consequence of loss of expression of MAGE Family Member L2 (*MAGEL2*) has been related to phenotypic characteristics of PWS (82). *Magel2*-null mice exhibited endocrine dysfunction similar to PWS: neonatal growth retardation; excessive weight gain; increased adiposity after weaning; impaired hypothalamic regulation and changes in circadian rhythm (83, 84). Hyperphagia, commonly observed in individuals with PWS, is associated with a defect in the hypothalamic arcuate nucleus, which is the major action site of multiple complex interactions between neuropeptide Y (NPY), agouti-related peptide (AgRP), proopiomelanocortin (POMC), and leptin, regulating the food intake and body weight (85, 86). NPY/AgRP interaction stimulates food intake, whereas POMC reduces it. Loss of *MAGEL2* expression disturbs leptin-mediated depolarization of POMC neurons, indicating that food intake is being less repressed and fat storage regulated by leptin is uncontrolled (87, 88). Additionally, loss of expression of *Magel2* impairs reproductive function in mice. *Magel2*-null females showed extended and irregular estrous cycles, while males displayed decreased testosterone levels, and reduced pheromone detection, which has a direct relationship between the main olfactory epithelium and the hypothalamic GnRH neuronal system (89, 90). These results suggest that lack of expression of *MAGEL2* contributes to the reproductive deficiencies observed in PWS and also highlights the role of normal circadian rhythm in maintaining fertility.

Therein, specific point mutations on the paternal allele of *MAGEL2* were reported in 4 individuals with PWS spectrum phenotype: muscle hypotonia, weight gain, developmental delay, and hypogonadism. Although all clinical characteristics were consistent with PWS clinical diagnosis, methylation analysis on the promoter-exon 1 region of the *SNURF-SNRPN* gene showed normal allelic patterns (82). All four subjects were diagnosed with an autism spectrum disorder, intellectual disability, and different degrees of clinical and behavioral features of PWS. Although not a main characteristic, autism is present in 19% of individuals with PWS (71). These four individuals presented a normal methylation pattern, not compatible with PWS, despite similar clinical conditions, which was subsequently called Schaaf-Yang Syndrome (SYS) (91).

Recent data of an international cohort of 78 patients with truncating *MAGEL2* mutations emphasized that SYS overlaps with PWS on clinical grounds in the early stages of life but diverges with the advance of childhood and adolescence (92). PWS features such as hypopigmentation, facial appearance, small hands and feet, thick saliva, behavioral problems are not commonly seen in SYS. And above all distinct symptoms, SYS does not usually cause the high appetite and severe obesity observed in PWS, which can disassociate *MAGEL2* and the hyperphagia condition.

The Necdin (*NDN*) gene encodes a DNA binding protein highly expressed in mature hypothalamic neurons (93). It has been postulated as a key regulator of GnRH levels both *in vitro* and *in vivo*, modulating essential intracellular processes for neurite and axonal outgrowth (94–96). Lack of *NDN* reduces GnRH gene expression, leads to decreased numbers of GnRH neurons, and decreased targeting of GnRH axons to the median eminence of the hypothalamus during development, which can contribute to hypogonadism and infertility in PWS. Also, Necdin paternal-deficient mice were associated with alterations in serotonin and respiratory systems, resulting in irregular breathing and sleep apneas, commonly observed in PWS. Another important evidence reported with *Ndn*-KO mice was sudden death due to respiratory disorders, which is the main side effect associated with GH therapy (97–99). *NDN* might be a genetic factor contributing to apneas and respiratory dysfunctions of PWS.

Interestingly, (100) described three patients with atypical deletions related to PWS. Patient 1 was deleted for *MKRN3*, *MAGEL2*, and *NDN* with no PWS major clinical criteria, except for obesity, developmental delay, and high pain threshold. Patients 2 and 3 had a deletion encompassing *NPAP1*, *SNURF-SNRPN*, and the SNORD genes, but did not reach *MKRN3*, *MAGEL2*, and *NDN*, and presented PWS major clinical signs (100). This report suggests that a paternal deficiency of *MKRN3*, *MAGEL2*, and *NDN* is not sufficient to generate the full PWS phenotype and postulates *NPAP1*, *SNURF-SNRPN*, and the SNORD genes (discussed ahead) to be the critical region for PWS. These results contradict other studies and exemplify the complexity to establish a genotype-phenotype relationship in PWS (78, 82, 83, 98, 99, 101, 102).

The Prader-Willi region encompasses a series of long non-coding RNAs (lncRNAs) which are characteristically more than 200 nucleotides long and can be involved in epigenetic modifications of DNA, and regulation of gene expression at transcriptional and post-transcriptional levels (103–105). The first lncRNA inside the PWS region is the Prader-Willi Region Non-Protein Coding RNA 1 (*PWRN1*), biallelically expressed in the testis and kidneys, and monoallelic expressed in the brain, in addition to being an alternative 5′ part of SNURF–SNRPN (106). Wawrzik et al. (107) hypothesized that the action of *PWRN1* on the imprinting mechanism may be indirect through keeping the paternal allele in an open chromatin configuration, allowing access to transcription factors (107). The main limitation for further confirmation studies is the lack of gene orthology in mice (108–110).

The Nuclear Pore Associated Protein 1 (*NPAP1*), formerly known as Chromosome 15 Open Reading Frame 2 (C15orf2), is an intronless gene that is biallelically expressed in adult testis and monoallelically expressed in fetal brain, including the hypothalamus which is related to several endocrine features of PWS (106, 111). Moreover, this gene is associated with the Nuclear Pore Complex (NPC), in which the main function is to regulate macromolecular transport between the nucleus and the cytoplasm. NPCs also participates in several nuclear processes, such as gene regulation, mRNA biogenesis, and cell cycle control. Likewise *PWRN1*, due to the lack of orthology in mice the exact role of the *NPAP1* gene in the development of PWS is not clear (112).

The Small Nuclear Ribonucleoprotein Polypeptide N (*SNRPN*) gene is located within the central region associated with PWS and has an important regulatory role over the imprinted genes located in chromosome 15 (113, 114), while the SNRPN Upstream Reading Frame (*SNURF*) gene is encoded by an evolutionarily-conserved upstream open reading frame and is localized to the nucleus (115). *SNURF-SNRPN* is a complex bicistronic gene encoding two different proteins, and the PWS-IC is found at its 5' end. *SNURF* is encoded by exons 1–3 and produces a small nuclear protein of unknown function (113), exons 4–10 correspond to the *SNRPN* portion and encode the protein SmN, involved in mRNA splicing (43). It also holds six snoRNA genes located telomerically which are expressed as a long transcript (46). The SmN protein shows the highest expression in the brain and heart (115–117). Despite its central position in PWS, the function and regulation of the many alternative transcripts of *SNURF-SNRPN* are still poorly understood (48).

Within the long *SNURF-SNRPN* transcript, there are a series of Small Nucleolar RNAs (snoRNAs) thought to participate in DNA methylation, alternative splicing and post-transcriptional regulation (10, 118). The PWS region encompasses five single copy snoRNA genes (*SNORD64*, *SNORD107*, *SNORD108*, *SNORD109A*, and *SNORD109B*) and two snoRNA gene clusters (*SNORD115* and *SNORD116*). The expression of SNORD genes varies in different human and mouse tissues, suggesting specificity in post-transcriptional activity (46, 119–122). Although most of the SNORDs are ubiquitously expressed in human tissues, *SNORD115* and *SNORD109B* appear to be restricted to the brain. Our understanding of the single-copy SNORDs in PWS remains extremely limited, but some progress has been made with the clusters: *SNORD116* has 29 tandemly repeats and *SNORD115* is composed of 48 gene copies (118). Given that SNORD sequences are well-conserved across placental mammals (especially in primates and rodents), this suggests they have an evolutionary functional role (123, 124).

A minimal critical region has emerged implicating that the *SNORD116* cluster is crucial for most of the PWS phenotype, based on clinical evidence on rare patients with small deletions (150–200 Kb) or translocations (11, 125–128). Experimental studies on *Snord116*-KO mice displayed PWS features such as post-natal growth retardation and hyperphagia (129–132). Remarkably, a *Snord116*-KO mice model specifically in NPY neurons in the hypothalamic arcuate nucleus summarized the

same overall phenotype observed in mice lacking *Snord116* globally; low birth weight, increased body weight gain in early adulthood, increased energy expenditure and hyperphagia (130). This suggests an important role of *Snord116* in controlling NPY neuronal functions, and thus food intake and energy homeostasis. Also, a recent study reported *Snord116*-deficient mice with decreased activity of the hypothalamic prohormone convertase PC1 impairing the prohormone processing of proinsulin, pro-GH-releasing hormone, and proghrelin, pointing to an important part of *SNORD116* and PC1 deficiency in the main neuroendocrine features of PWS (133). Interestingly, it was shown that a mouse *Snord116* deletion model displayed loss or shift in methylation dynamics in 97% of CpG islands in the cerebral cortex dependent on the circadian cycle. And this disrupted epigenetic rhythm had a strong overlap between mouse and human genes related to meal timing, circadian biology, and obesity (134). In the recent years, *SNORD116* has emerged as a critical, and possibly, determinant candidate in PWS not only by its highly conserved sequence in the minimal critical region, but also because paternal deletions affecting the expression of *NDN*, *MKRN3*, *MAGEL2*, or *SNORD115* genes do not address the full spectrum of PWS symptoms (10, 100, 123, 135, 136).

The Imprinted in Prader-Willi Syndrome (*IPW*) gene is a lncRNA known to modulate another evolutionarily distinct imprinted gene cluster at the human chromosomal region 14q32 expressed only from maternally inherited alleles (137). *IPW* is widely expressed both in fetal and adult tissues, exclusively from the paternal allele (138). It has been postulated that *IPW* has no biological consequences in PWS, based on the relatively poor conservation between human and mouse sequences (138), and the fact that mice with a paternally inherited deletion including *Ipw* did not show PWS symptoms (139). However, Stelzer et al. (137) proposed that lack of expression of *IPW* results in aberrant upregulation of maternally expressed genes at the 14q32 imprinted cluster, pointing that the action of *IPW* on the imprinting mechanism of this locus occurs by histone modification, and consequently, transcription reduction (137). This hypothesis is supported by clinical reports of affected individuals with mUPD 14 (overexpression of maternal genes) presenting PWS-like phenotypes, such as neonatal hypotonia, small hands and feet, intellectual disability and hyperphagia (140–142). These findings pinpoint a regulatory cross-talk between 15q11-13 and 14q32 imprinted loci, but further, suggest that some PWS phenotypes may arise from different chromosomal regions other than the PWS critical locus (143, 144).

SNORD115 gene is the most characterized SNORD within the PWS region. It presents a complementary sequence of 18 nucleotides with the mRNA encoding the serotonin receptor 5-HT2C, perfectly base pairing with exon V that undergoes both alternative RNA splicing and RNA editing (post-transcriptional changes to specific nucleotide sequences) (118). Mice with a large deletion encompassing the *Snord115* cluster developed normally to adulthood with apparently no significant defects (139). And there are also clinical reports on patients with an entire deletion of the *SNORD115* gene cluster that did not present any PWS major clinical signs (135, 136). Taken together, these findings suggest that lack of *SNORD115* is not sufficient to cause PWS, but a phenotypic effect when absent along with other genes in the PWS critical region cannot be excluded. Actually, the *5-HT2C* gene encodes G protein-coupled receptor specific to the brain, whose activation is associated with a variety of physiological processes, such as dopamine modulation, anxiety, sleep regulation, satiety response, energy balance, and locomotor activity (145). Interestingly, experimental studies have described 5-HT2C receptor knockout mice that developed are hyperphagia and late-onset obesity, two major clinical features of PWS in humans (146, 147). Therefore, the absence of *SNORD115* expression in PWS accompanied by the possible post-transcriptional impairment of the 5-HT2C receptor activity may be partly responsible for some of the behavioral and metabolic features of the syndrome.

The establishment of a causal genotype-phenotype relationship can bring light to new therapeutic approaches for PWS. Epigenetic therapy has been used in cancer treatment mostly focusing on the identification of small molecules and compounds with the capacity to reverse the epigenetic changes (epigenome reprogramming) (145, 148). The successful experience obtained from the epigenetic-cancer therapies contributes to the development of similar approaches for genomic imprinting disorders. Recent studies have shown that histone methyltransferase inhibitors are capable of reactivating the expression of paternally expressed SNRPN and *SNORD116* from the maternal chromosome, both in PWS mouse models and in cultured PWS patient-derived fibroblasts (149, 150). Although further investigation needs to be performed *in vivo*, epigenetic therapy aiming PWS genes in the maternal chromosome could reverse, or at least regulate, some PWS clinical conditions such as hyperphagia and behavioral problems (151). This data supports future studies to assess translational epigenetic-based therapies for PWS in humans.

CONCLUSION

PWS is a complex imprinting disorder caused by the lack of expression of paternally-inherited genes on chromosome 15q11-q13 with severe implications on endocrine, cognitive and neurologic systems, metabolism, and behavior. The PWS critical region encompasses five protein-coding genes (*MKRN3*, *MAGEL2*, *NDN*, *NPAP1*, and *SNURF-SNRPN*) and more than 80 RNA genes (*PWRN1*, *IPW*, and several SNORDs) but their contribution to unique PWS phenotypes is still unclear. The broad clinical spectrum and the absence of a clear genotype-phenotype specific correlation imply that the numerous genes involved in PWS have an additive deleterious effect when deficiently expressed. So far, the lack of expression of the *SNORD116* gene cluster has arisen as the best explanation for most of the PWS phenotype, yet there is a clear need to investigate more of its mechanism of action, especially the incorporation into ribonucleoprotein complexes, possibly acting in hypothalamic and endocrine functions in adulthood and perinatal period. Besides *SNORD115* and *SNORD116*, our understanding of the

biology of the PWS SNORD genes is still rather shallow. These SNORDs exhibit all the hallmarks of RNA methylation guides and can associate with other proteins to form functional ribonucleoprotein complexes. Also, the SNORD sequences are well-conserved across placental mammals, strongly asserting that they have a functional role as RNA entities under evolutionary pressure. A better understanding about genotype-phenotype in PWS can open space for new therapeutic approaches especially for patients that present side effects related to the current standard treatment, and develop genetic counseling for the different levels of severity in PWS that require specific and constant medical follow-up, improving the life quality of patients, family, and caretakers.

AUTHOR CONTRIBUTIONS

RC, IF, HC, and LGu contributed to the writing of the manuscript. LGo provided consultation and contributed to the writing of the manuscript.

FUNDING

This work was supported by Conselho Nacional de Desenvolvimento Científico e Tecnológico (CNPQ) and was financed in part by the Coordenação de Aperfeiçoamento de Pessoal de Nível Superior - Brasil (CAPES) - Finance Code 001.

REFERENCES

1. Prader A, Labhart A, Willi H. Ein syndrom von adipositas, kleinwuchs, kryptorchismus und oligophrenie nach myatonieartigem zustand im neugeborenenalter. *Schweiz Med Wochenschr*. (1956) 86:1260–1.
2. Butler MG, Meaney FJ, Palmer CG, Opitz JM, Reynolds JF. Clinical and cytogenetic survey of 39 individuals with Prader-Labhart-Willi syndrome. *Am J Med Genet*. (1986) 23:793–809. doi: 10.1002/ajmg.1320230307
3. Nicholls RD, Knoll JH, Butler MG, Karam S, Lalande M. Genetic imprinting suggested by maternal heterodisomy in nondeletion Prader-Willi syndrome. *Nature*. (1989) 342:281–5. doi: 10.1038/342281a0
4. Butler MG. Genomic imprinting disorders in humans: a mini-review. *J Assist Reprod Genet*. (2009) 26:477–86. doi: 10.1007/s10815-009-9353-3
5. Driscoll DJ, Miller JL, Schwartz S, Cassidy SB. Prader-Willi Syndrome. In: Adam MP, Ardinger HH, Pagon RA, Wallace SE, Bean LJH, Stephens K, et al., editors. *GeneReviews*. Seattle, WA: University of Washington (2017). p. 1–38.
6. Whittington JE, Butler JV, Holland AJ. Changing rates of genetic subtypes of Prader-Willi syndrome in the UK. *Eur J Hum Genet*. (2007) 15:127–30. doi: 10.1038/sj.ejhg.5201716
7. Cassidy SB, Driscoll DJ. Prader–Willi syndrome. *Eur J Hum Genet*. (2009) 17:3–13. doi: 10.1038/ejhg.2008.165
8. Nicholls RD, Knepper JL. Genome organization, function, and imprinting in Prader-Willi and Angelman syndromes. *Annu Rev Genomics Hum Genet*. (2001) 2:153–75. doi: 10.1146/annurev.genom.2.1.153
9. Angulo MA, Butler MG, Cataletto ME. Prader-Willi syndrome: a review of clinical, genetic, and endocrine findings. *J Endocrinol Invest*. (2015) 38:1249–63. doi: 10.1007/s40618-015-0312-9
10. Cheon CK. Genetics of Prader-Willi syndrome and Prader-Will-Like syndrome. *Ann Pediatr Endocrinol Metab*. (2016) 21:126–35. doi: 10.6065/apem.2016.21.3.126
11. Buiting K. Prader-Willi syndrome and Angelman syndrome. *Am J Med Genet Part C Semin Med Genet*. (2010) 154:365–76. doi: 10.1002/ajmg.c.30273
12. Chamberlain SJ, Lalande M. Neurobiology of disease neurodevelopmental disorders involving genomic imprinting at human chromosome 15q11 – q13. *Neurobiol Dis*. (2010) 39:13–20. doi: 10.1016/j.nbd.2010.03.011
13. Gunay-Aygun M, Schwartz S, Heeger S, O'Riordan MA, Cassidy SB. The changing purpose of Prader-Willi syndrome clinical diagnostic criteria and proposed revised criteria. *Pediatrics*. (2001) 108:e92–e92. doi: 10.1542/peds.108.5.e92
14. Miller JL, Lynn CH, Driscoll DC, Goldstone AP, Gold JA, Kimonis V, et al. Nutritional phases in Prader-Willi syndrome. *Am J Med Genet Part A*. (2011) 155:1040–9. doi: 10.1002/ajmg.a.33951
15. Butler MG, Sturich J, Myers SE, Gold J, Kimonis V, Driscoll DJ. Is gestation in Prader-Willi syndrome affected by the genetic subtype? *J Assist Reprod Genet*. (2009) 26:461–6. doi: 10.1007/s10815-009-9341-7
16. Cassidy SB, Schwartz S, Miller JL, Driscoll DJ. Prader-Willi syndrome. *Genet Med*. (2012) 14:10–26. doi: 10.1038/gim.0b013e31822bead0
17. Richer LP, Shevell MI, Miller SP. Diagnostic profile of neonatal hypotonia: an 11-year study. *Pediatr Neurol*. (2001) 25:32–7. doi: 10.1016/S0887-8994(01)00277-6
18. Whittington J, Holland A, Webb T, Butler J, Clarke D, Boer H. Academic underachievement by people with Prader-Willi syndrome. *J Intellect Disabil Res*. (2004) 48:188–200. doi: 10.1111/j.1365-2788.2004.00473.x
19. Jauregi J, Arias C, Vegas O, Alén F, Martinez S, Copet P, et al. A neuropsychological assessment of frontal cognitive functions in Prader-Willi syndrome. *J Intellect Disabil Res*. (2007) 51:350–65. doi: 10.1111/j.1365-2788.2006.00883.x
20. Copet P, Jauregi J, Laurier V, Ehlinger V, Arnaud C, Cobo AM, et al. Cognitive profile in a large french cohort of adults with Prader-Willi syndrome: differences between genotypes. *J Intellect Disabil Res*. (2010) 54:204–15. doi: 10.1111/j.1365-2788.2010.01251.x
21. Gillett E, Perez I. Disorders of sleep and ventilatory control in Prader-Willi Syndrome. *Diseases*. (2016) 4:23. doi: 10.3390/diseases4030023
22. Brambilla P, Crinò A, Bedogni G, Bosio L, Cappa M, Corrias A, et al. Metabolic syndrome in children with Prader-Willi syndrome: the effect of obesity. *Nutr Metab Cardiovasc Dis*. (2011) 21:269–76. doi: 10.1016/j.numecd.2009.10.004
23. Crinò A, Fintini D, Bocchini S, Grugni G. Diabetes, metabolic syndrome and obesity: targets and therapy dovepress obesity management in Prader-willi syndrome: current perspectives. *Diabetes Metab Syndr Obes Targets Ther*. (2018) 11:579–93. doi: 10.2147/DMSO.S141352
24. Butler JV, Whittington JE, Holland AJ, Boer H, Clarke D, Webb T. Prevalence of, and risk factors for, physical ill-health in people with Prader-Willi syndrome: a population-based study. *Dev Med Child Neurol*. (2002) 44:248–55. doi: 10.1017/S001216220100202X
25. Whittington JE, Holland AJ, Webb T. Ageing in people with Prader-Willi syndrome: mortality in the UK population cohort and morbidity in an older sample of adults. *Psychol Med*. (2015) 45:615–21. doi: 10.1017/S0033291714001755
26. Tauber M, Cutfield W. KIGS highlights: growth hormone treatment in Prader-Willi Syndrome. *Horm Res*. (2007) 68(Suppl 5):48–50. doi: 10.1159/000110475
27. Grugni G, Sartorio A, Crinò A. Growth hormone therapy for Prader–Willi syndrome: challenges and solutions. *Ther Clin Risk Manag*. (2016) 12:873–81. doi: 10.2147/TCRM.S70068
28. Lindgren AC. Somatropin therapy for children with Prader-Willi syndrome: guidelines for use. *Treat Endocrinol*. (2006) 5:223–8. doi: 10.2165/00024677-200605040-00003
29. Höybye C. Five-years growth hormone (GH) treatment in adults with Prader-Willi syndrome. *Acta Paediatr*. (2007) 96:410–3. doi: 10.1111/j.1651-2227.2006.00051.x
30. Mogul HR, Lee PDK, Whitman BY, Zipf WB, Frey M, Myers S, et al. Growth hormone treatment of adults with Prader-Willi syndrome and growth hormone deficiency improves lean body mass, fractional body fat, and serum triiodothyronine without glucose impairment: results from the

United States multicenter trial. *J Clin Endocrinol Metab*. (2008) 93:1238–45. doi: 10.1210/jc.2007-2212
31. Siemensma EPC, Tummers-de Lind van Wijngaarden RFA, Festen DAM, Troeman ZCE, van Alfen-van der Velden AAEM, Otten BJ, et al. Beneficial effects of growth hormone treatment on cognition in children with Prader-Willi syndrome: a randomized controlled trial and longitudinal study. *J Clin Endocrinol Metab*. (2012) 97:2307–14. doi: 10.1210/jc.2012-1182
32. Berini J, Spica Russotto V, Castelnuovo P, Di Candia S, Gargantini L, Grugni G, et al. Growth hormone therapy and respiratory disorders: long-term follow-up in PWS children. *J Clin Endocrinol Metab*. (2013) 98:E1516–23. doi: 10.1210/jc.2013-1831
33. Deal CL, Tony M, Höybye C, Allen DB, Tauber M, Christiansen JS, et al. Growth hormone research society workshop summary: consensus guidelines for recombinant human growth hormone therapy in Prader-Willi syndrome. *J Clin Endocrinol Metab*. (2013) 98:E1072–87. doi: 10.1210/jc.2012-3888
34. Dykens EM, Roof E, Hunt-Hawkins H. Cognitive and adaptive advantages of growth hormone treatment in children with Prader-Willi syndrome. *J Child Psychol Psychiatry Allied Discip*. (2017) 58:64–74. doi: 10.1111/jcpp.12601
35. Crinò A, Schiaffini R, Ciampalini P, Spera S, Beccaria L, Benzi F, et al. Hypogonadism and pubertal development in Prader-Willi syndrome. *Eur J Pediatr*. (2003) 162:327–33. doi: 10.1007/s00431-002-1132-4
36. Heksch R, Kamboj M, Anglin K, Obrynba K. Review of Prader-Willi syndrome: the endocrine approach. *Transl Pediatr*. (2017) 6:274–85. doi: 10.21037/tp.2017.09.04
37. Muscogiuri G, Formoso G, Pugliese G, Ruggeri RM, Scarano E, Colao A. Prader- Willi syndrome: an uptodate on endocrine and metabolic complications. *Rev Endocr Metab Disord*. (2019) 20:239–50. doi: 10.1007/s11154-019-09502-2
38. Tauber M, Barbeau C, Jouret B, Pienkowski C, Malzac P, Moncla A, et al. Auxological and endocrine evolution of 28 children with Prader-Willi syndrome: effect of GH therapy in 14 children. *Horm Res Paediatr*. (2000) 53:279–87. doi: 10.1159/000053184
39. Corrias A, Grugni G, Crinò A, Di Candia S, Chiabotto P, Cogliardi A, et al. Assessment of central adrenal insufficiency in children and adolescents with Prader-Willi syndrome. *Clin Endocrinol.* (2012) 76:843–50. doi: 10.1111/j.1365-2265.2011.04313.x
40. Beauloye V, Dhondt K, Buysse W, Nyakasane A, Zech F, De Schepper J, et al. Evaluation of the hypothalamic-pituitary-adrenal axis and its relationship with central respiratory dysfunction in children with Prader-Willi syndrome rare endocrinological diseases. *Orphanet J Rare Dis*. (2015) 10:4–11. doi: 10.1186/s13023-015-0312-z
41. Grugni G, Beccaria L, Corrias A, Crinò A, Cappa M, De Medici C, et al. Central adrenal insufficiency in young adults with Prader-Willi Syndrome. *Clin Endocrinol*. (2013) 79:371–8. doi: 10.1111/cen.12150
42. Smith A, Hung D. The dilemma of diagnostic testing for Prader-Willi syndrome. *Transl Pediatr*. (2017) 5:46–56. doi: 10.21037/tp.2016.07.04
43. Glenn CC, Saitoh S, Jong MTC, Filbrandt MM, Surti U, Driscoll DJ, et al. Gene structure, DNA methylation, and imprinted expression of the human SNRPN gene. *Am J Hum Genet*. (1996) 58:335–46.
44. Ohta T, Gray TA, Rogan PK, Buiting K, Gabriel JM, Saitoh S, et al. Imprinting-mutation mechanisms in Prader-Willi Syndrome. *AGHG*. (1999) 64:397–413. doi: 10.1086/302233
45. Yazdi PG, Su H, Ghimbovschi S, Fan W, Coskun PE, Nalbandian A, et al. Differential gene expression reveals mitochondrial dysfunction in an imprinting center deletion mouse model of prader-willi syndrome. *Clin Transl Sci*. (2013) 6:347–55. doi: 10.1111/cts.12083
46. Galiveti CR, Raabe CA, Konthur Z, Rozhdestvensky TS. Differential regulation of non-protein coding RNAs from Prader-Willi Syndrome locus. *Sci Rep*. (2014) 4:6445. doi: 10.1038/srep06445
47. Butler MG, Wang K, Marshall JD, Naggert JK, Rethmeyer JA, Gunewardena SS, et al. Coding and noncoding expression patterns associated with rare obesity-related disorders: Prader-Willi and Alstrom syndromes. *Adv Genomics Genet*. (2015) 50:53–75. doi: 10.2147/AGG.S74598
48. Koufaris C, Alexandrou A, Papaevripidou I, Alexandrou I, Christophidou-Anastasiadou V, Sismani C. Deletion of SNURF/SNRPN U1B and U1B* upstream exons in a child with developmental delay and excessive weight. *J Genet*. (2016) 95:621–4. doi: 10.1007/s12041-016-0666-6
49. Bittel DC, Butler MG. Prader-Willi syndrome: clinical genetics, cytogenetics and molecular biology. *Expert Rev Mol Med*. (2005) 7:1–20. doi: 10.1017/S1462399405009531
50. Christian SL, Robinson WP, Huang B, Mutirangura A, Line MR, Nakao M, et al. Molecular characterization of two proximal deletion breakpoint regions in both Prader-Willi and Angelman syndrome patients. *Am J Hum Genet*. (1995) 57:40–8.
51. Hartin SN, Hossain WA, Francis D, Godler DE, Barkataki S, Butler MG. Analysis of the Prader–Willi syndrome imprinting center using droplet digital PCR and next-generation whole-exome sequencing. *Mol Genet Genomic Med*. (2019) 7:1–10. doi: 10.1002/mgg3.575
52. Glenn CC, Driscoll DJ, Yang TP, Nicholls RD. Genomic imprinting: potential function and mechanisms revealed by the Prader-Willi and Angelman syndromes. *Mol Hum Reprod*. (1997) 3:321–32. doi: 10.1093/molehr/3.4.321
53. Kosaki K, McGinniss MJ, Veraksa AN, McGinnis WJ, Jones KL. Prader-Willi and Angelman syndromes: diagnosis with a bisulfite-treated methylation-specific PCR method. *Am J Med Genet*. (1997) 73:308–13. doi: 10.1002/(SICI)1096-8628(19971219)73:3<308::AID-AJMG15>3.0.CO;2-N
54. Botezatu A, Puiu M, Cucu N, Diaconu CC, Badiu C, Arsene C, et al. Comparative molecular approaches in Prader-Willi syndrome diagnosis. *Gene*. (2016) 575:353–8. doi: 10.1016/j.gene.2015.08.058
55. Bittel DC, Kibiryeva N, Butler MG. Methylation-specific multiplex ligation-dependent probe amplification analysis of subjects with chromosome 15 abnormalities. *Genet Test*. (2007) 11:467–76. doi: 10.1089/gte.2007.0061
56. Henkhaus RS, Kim SJ, Kimonis VE, Gold J-A, Dykens EM, Driscoll DJ, et al. Methylation-specific multiplex ligation-dependent probe amplification and identification of deletion genetic subtypes in Prader-Willi syndrome. *Genet Test Mol Biomarkers*. (2011) 16:178–86. doi: 10.1089/gtmb.2011.0115
57. White HE, Hall VJ, Cross NCP. Methylation-sensitive high-resolution melting-curve analysis of the SNRPN gene as a diagnostic screen for Prader-Willi and Angelman syndromes. *Clin Chem*. (2007) 53:1960–2. doi: 10.1373/clinchem.2007.093351
58. Ferreira IR, Darleans dos Santos Cunha W, Henrique Ferreira Gomes L, Azevedo Cintra H, Lopes Cabral Guimarães Fonseca L, Ferreira Bastos E, et al. A rapid and accurate methylation-sensitive high-resolution melting analysis assay for the diagnosis of Prader Willi and Angelman patients. *Mol Genet Genomic Med*. (2019) 7:1–10. doi: 10.1002/mgg3.637
59. Hawkey CJ, Smithies A. The Prader-Willi syndrome with a 15/15 translocation. Case report and review of the literature. *J Med Genet*. (1996) 13:152–7. doi: 10.1136/jmg.13.2.152
60. Smith A, Lindeman R, Volpato F, Kearney A, White S, Haan E, et al. A *de novo* unbalanced reciprocal translocation identified as paternal in origin in the Prader-Willi syndrome. *Hum Genet*. (1991) 86:534–6. doi: 10.1007/BF00194651
61. Robinson WP, Dutly F, Nicholls RD, Bernasconi F, Pefiaherrera M, Michaelis RC, et al. The mechanisms involved in formation of deletions. *J Med Genet*. (1998) 35:130–6. doi: 10.1136/jmg.35.2.130
62. Kuslich CD, Kobori JA, Mohapatra G, Gregorio-King C, Donlon TA. Prader-Willi syndrome is caused by disruption of the SNRPN gene. *Am J Hum Genet*. (1999) 64:70–6. doi: 10.1086/302177
63. Flori E, Biancalana V, Girard-Lemaire F, Favre R, Flori J, Doray B, et al. Difficulties of genetic counselling and prenatal diagnosis in a consanguineous couple segregating for the same translocation (14;15)(q11;q13) and at risk for Prader-Willi and Angelman syndromes. *Eur J Hum Genet*. (2004) 12:181–6. doi: 10.1038/sj.ejhg.5201134
64. Kim SJ, Miller JL, Kuipers PJ, German JR, Beaudet AL, Sahoo T, et al. Unique and atypical deletions in Prader-Willi syndrome reveal distinct phenotypes. *Eur J Hum Genet*. (2012) 20:283–90. doi: 10.1038/ejhg.2011.187
65. Yip MY. Uniparental disomy in Robertsonian translocations: strategies for uniparental disomy testing. *Transl Pediatr*. (2014) 3:98–107. doi: 10.3978/j.issn.2224-4336.2014.03.03
66. Santoro SL, Hashimoto S, McKinney A, Mihalic Mosher T, Pyatt R, Reshmi SC, et al. Assessing the clinical utility of SNP microarray for Prader-Willi syndrome due to uniparental disomy. *Cytogenet Genome Res*. (2017) 152:105–9. doi: 10.1159/000478921

67. Beygo J, Buiting K, Ramsden SC, Ellis R, Clayton-Smith J, Kanber D. Update of the EMQN/ACGS best practice guidelines for molecular analysis of Prader-Willi and Angelman syndromes. *Eur J Hum Genet*. (2019) 15:1326–40. doi: 10.1038/s41431-019-0435-0
68. Torrado M, Araoz V, Baialardo E, Abraldes K, Mazza C, Krochik G, et al. Clinical-etiologic correlation in children with Prader-Willi syndrome (PWS): an interdisciplinary study. *Am J Med Genet Part A*. (2007) 143A:460–8. doi: 10.1002/ajmg.a.31520
69. Butler MG, Bittel DC, Bittel N, Talebizadeh KZ, Thompson T. Behavioral differences among subjects with Prader-Willi Syndrome and type I or type II deletion and maternal disomy. *Pediatrics*. (2004) 113:565–73. doi: 10.1542/peds.113.3.565
70. Hartley SL, MacLean WE, Butler MG, Zarcone J, Thompson T. Maladaptive behaviors and risk factors among the genetic subtypes of Prader-Willi syndrome. *Am J Med Genet Part A*. (2005) 136A:140–5. doi: 10.1002/ajmg.a.30771
71. Descheemaeker MJ, Govers V, Vermeulen P, Fryns JP. Pervasive developmental disorders in Prader–Willi syndrome: the Leuven experience in 59 subjects and controls. *Am J Med Genet Part A*. (2006) 140A:1136–42. doi: 10.1002/ajmg.a.31235
72. Dykens EM. Are Jigsaw Puzzle skills 'spared' in persons with Prader-Willi syndrome? *J Child Psychol Psychiatry*. (2002) 43:343–52. doi: 10.1111/1469-7610.00025
73. Whittington J, Holland A, Webb T, Butler J, Clarke D, Boer H. Cognitive abilities and genotype in a population-based sample of people with Prader-Willi syndrome. *J Intellect Disabil Res*. (2004) 48:172–87. doi: 10.1111/j.1365-2788.2004.00556.x
74. Yang L, Zhan G, Ding J, Wang H, Ma D, Huang G, et al. Psychiatric illness and intellectual disability in the Prader–Willi syndrome with different molecular defects - a meta analysis. *PLoS ONE*. (2013) 8:e72640. doi: 10.1371/journal.pone.0072640
75. Dykens EM, Roof E, Hunt-Hawkins H, Dankner N, Lee EB, Shivers CM, et al. Diagnoses and characteristics of autism spectrum disorders in children with Prader-Willi syndrome. *J Neurodev Disord*. (2017) 9:18. doi: 10.1186/s11689-017-9200-2
76. Jong MTC, Gray TA, Ji Y, Glenn CC, Saitoh S, Driscoll DJ, et al. A novel imprinted gene, encoding a RING Zinc-finger protein, and overlapping antisense transcript in the Prader-Willi syndrome critical region. *Hum Mol Genet*. (1999) 8:783–93. doi: 10.1093/hmg/8.5.783
77. Valadares LP, Meireles CG, De Toledo IP, Santarem de Oliveira R, Gonçalves de Castro LC, Abreu AP, et al. *MKRN3* mutations in central precocious puberty: a systematic review and meta-analysis. *J Endocr Soc*. (2019) 3:979–95. doi: 10.1210/js.2019-00041
78. Abreu AP, Delanie BM, Brito VN, Kaiser UB, Latronico AC. A new pathway in the control of the initiation of puberty: the *MKRN3* gene. *J Mol Endocrinol*. (2015) 54:R131–9. doi: 10.1530/JME-14-0315
79. Macedo DB, Abreu AP, Reis ACS, Montenegro LR, Dauber A, Beneduzzi D, et al. Central precocious puberty that appears to be sporadic caused by paternally inherited mutations in the imprinted gene makorin ring finger 3. *J Clin Endocrinol Metab*. (2014) 99:E1097–103. doi: 10.1210/jc.2013-3126
80. Schreiner F, Gohlke B, Hamm M, Korsch E, Woelfle J. *MKRN3* mutations in familial central precocious puberty. *Horm Res Paediatr*. (2014) 82:122–6. doi: 10.1159/000362815
81. Settas N, Dacou-Voutetakis C, Karantza M, Kanaka-Gantenbein C, Chrousos GP, Voutetakis A. Central precocious puberty in a girl and early puberty in her brother caused by a novel mutation in the *MKRN3* gene. *J Clin Endocrinol Metab*. (2014) 99:E647–51. doi: 10.1210/jc.2013-4084
82. Schaaf CP, Gonzalez-Garay ML, Xia F, Potocki L, Gripp KW, Zhang B, et al. Truncating mutations of *MAGEL2* cause Prader-Willi phenotypes and autism. *Nat Genet*. (2013) 45:1405–8. doi: 10.1038/ng.2776
83. Bischof JM, Stewart LC, Wevrick R. Inactivation of the mouse *MAGEL2* gene results in growth abnormalities similar to Prader-Willi syndrome. *Hum Mol Genet*. (2007) 16:2713–9. doi: 10.1093/hmg/ddm225
84. Devos J, Weselake SV, Wevrick R. *MAGEL2*, a Prader-Willi syndrome candidate gene, modulates the activities of circadian rhythm proteins in cultured cells. *J Circadian Rhythms*. (2011) 9:12. doi: 10.1186/1740-3391-9-12
85. Fliers E. The human hypothalamus: basic and clinical aspects. *J Neuroendocrinol*. (2004) 16:1009–10. doi: 10.1111/j.1365-2826.2005.01255.x
86. Myers SE, Davis A, Whitman BY, Santiago JV, Landt M. Leptin concentrations in Prader-Willi syndrome before and after growth hormone replacement. *Clin Endocrinol*. (2000) 52:101–5. doi: 10.1046/j.1365-2265.2000.00868.x
87. Mercer RE, Michaelson SD, Chee MJS, Atallah TA, Wevrick R, Colmers WF. *MAGEL2* is required for leptin-mediated depolarization of POMC neurons in the hypothalamic arcuate nucleus in mice. *PLoS Genet*. (2013) 9:e1003207. doi: 10.1371/journal.pgen.1003207
88. Varela L, Horvath TL. Leptin and insulin pathways in POMC and AgRP neurons that modulate energy balance and glucose homeostasis. *EMBO Rep*. (2012) 13:1079–86. doi: 10.1038/embor.2012.174
89. Mercer RE, Wevrick R. Loss of *MAGEL2*, a candidate gene for features of Prader-Willi syndrome, impairs reproductive function in mice. *PLoS ONE*. (2009) 4:e4291. doi: 10.1371/journal.pone.0004291
90. Yoon H, Enquist LW, Dulac C. Olfactory inputs to hypothalamic neurons controlling reproduction and fertility. *Cell*. (2005) 123:669–82. doi: 10.1016/j.cell.2005.08.039
91. Fountain MD, Schaaf CP. Prader-Willi syndrome and Schaaf-Yang syndrome: neurodevelopmental diseases intersecting at the *MAGEL2* gene. *Diseases*. (2016) 4:E2. doi: 10.3390/diseases4010002
92. McCarthy J, Lupo PJ, Kovar E, Rech M, Bostwick B, Scott D, et al. Schaaf-Yang syndrome overview: report of 78 individuals. *Am J Med Genet Part A*. (2018) 176:2564–74. doi: 10.1002/ajmg.a.40650
93. Miller NLG, Wevrick R, Mellon PL. Necdin, a Prader-Willi syndrome candidate gene, regulates gonadotropin-releasing hormone neurons during development. *Hum Mol Genet*. (2008) 18:248–60. doi: 10.1093/hmg/ddn344
94. Jay P, Rougeulle C, Massacrier A, Moncla A, Mattei M, Malzac P, et al. The human necdin gene, *NDN*, is maternally imprinted and located in the Prader-Willi syndrome chromosomal region. *Nat Genet*. (1997) 17:357–61. doi: 10.1038/ng1197-357
95. Lee S, Walker CL, Karten B, Kuny SL, Tennese AA, O'Neill MA, et al. Essential role for the Prader–Willi syndrome protein necdin in axonal outgrowth. *Hum Mol Genet*. (2005) 14:627–37. doi: 10.1093/hmg/ddi059
96. Watrin F, Roëckel N, Lacroix L, Mignon C, Mattei MG, Disteche C, et al. The mouse Necdin gene is expressed from the paternal allele only and lies in the 7C region of the mouse chromosome 7, a region of conserved synteny to the human Prader-Willi syndrome region. *Eur J Hum Genet*. (1997) 5:324–32. doi: 10.1159/000484784
97. Miller J, Silverstein J, Shuster J, Driscoll DJ, Wagner M. Short-term effects of growth hormone on sleep abnormalities in Prader-Willi syndrome. *J Clin Endocrinol Metab*. (2006) 91:413–7. doi: 10.1210/jc.2005-1279
98. Muscatelli F. Disruption of the mouse necdin gene results in hypothalamic and behavioral alteratio ns reminiscent of the human Prader-Willi syndrome. *Hum Mol Genet*. (2000) 9:3101–10. doi: 10.1093/hmg/9.20.3101
99. Zanella S, Watrin F, Mebarek S, Marly F, Roussel M, Gire C, et al. Necdin plays a role in the serotonergic modulation of the mouse respiratory network: implication for Prader-Willi syndrome. *J Neurosci*. (2008) 28:1745–55. doi: 10.1523/JNEUROSCI.4334-07.2008
100. Kanber D, Giltay J, Wieczorek D, Zogel C, Hochstenbach R, Caliebe A, et al. A paternal deletion of MKRN3, MAGEL2 and NDN does not result in Prader-Willi syndrome. *Eur J Hum Genet*. (2009) 17:582–90. doi: 10.1038/ejhg.2008.232
101. Lee S. Expression and imprinting of *MAGEL2* suggest a role in Prader-Willi syndrome and the homologous murine imprinting phenotype. *Hum Mol Genet*. (2000) 9:1813–9. doi: 10.1093/hmg/9.12.1813
102. Pagliardini S, Ren J, Wevrick R, Greer JJ. Developmental abnormalities of neuronal structure and function in prenatal mice lacking the Prader-Willi syndrome gene necdin. *Am J Pathol*. (2005) 167:175–91. doi: 10.1016/S0002-9440(10)62964-1
103. Dhanoa JK, Sethi RS, Verma R, Arora JS, Mukhopadhyay CS. Long non-coding RNA: its evolutionary relics and biological implications in mammals: a review. *J Anim Sci Technol*. (2018) 60:25. doi: 10.1186/s40781-018-0183-7
104. Fernandes J, Acuña S, Aoki J, Floeter-Winter L, Muxel S. Long non-coding RNA*s* in the regulation of gene expression: physiology and disease. *Non-Coding RNA*. (2019) 5:17. doi: 10.3390/ncrna5010017
105. Mercer TR, Dinger ME, Mattick JS. Long non-coding RNAs: insights into functions. *Nat Rev Genet*. (2009) 10:155–9. doi: 10.1038/nrg2521

106. Buiting K, Nazlican H, Galetzka D, Wawrzik M, Groβ S, Horsthemke B. C15orf2 and a novel noncoding transcript from the Prader–Willi/Angelman syndrome region show monoallelic expression in fetal brain. *Genomics.* (2007) 89:588–95. doi: 10.1016/j.ygeno.2006.12.008
107. Wawrzik M, Spiess A-N, Herrmann R, Buiting K, Horsthemke B. Expression of SNURF–SNRPN upstream transcripts and epigenetic regulatory genes during human spermatogenesis. *Eur J Hum Genet*. (2009) 17:1463–70. doi: 10.1038/ejhg.2009.83
108. Chen Z, Ju H, Yu S, Zhao T, Jing X, Li P, et al. Prader–Willi region non-protein coding RNA 1 suppressed gastric cancer growth as a competing endogenous RNA of MiR-425-5p. *Clin Sci.* (2018) 132:1003–19. doi: 10.1042/CS20171588
109. Kung JTY, Colognori D, Lee JT. Long noncoding RNAs: past, present, and future. *Genetics.* (2013) 193:651–69. doi: 10.1534/genetics.112.146704
110. Lee S, Wevrick R. Identification of novel imprinted transcripts in the Prader-Willi syndrome and angelman syndrome deletion region: further evidence for regional imprinting control. *Am J Hum Genet*. (2000) 66:848–58. doi: 10.1086/302817
111. Färber C, Groß S, Neesen J, Buiting K, Horsthemke B. Identification of a testis-specific gene (C15orf2) in the Prader–Willi syndrome region on chromosome 15. *Genomics.* (2000) 65:174–83. doi: 10.1006/geno.2000.6158
112. Neumann LC, Markaki Y, Mladenov E, Hoffmann D, Buiting K, Horsthemke B. The imprinted *NPAP1*/C15orf2 gene in the Prader–Willi syndrome region encodes a nuclear pore complex associated protein. *Hum Mol Genet*. (2012) 21:4038–48. doi: 10.1093/hmg/dds228
113. Gray TA, Saitoh S, Nicholls RD. An imprinted, mammalian bicistronic transcript encodes two independent proteins. *Proc Natl Acad Sci USA*. (1999) 96:5616–21. doi: 10.1073/pnas.96.10.5616
114. Özçelik T, Leff S, Robinson W, Donlon T, Lalande M, Sanjines E, et al. Small nuclear ribonucleoprotein polypeptide N (SNRPN), an expressed gene in the Prader–Willi syndrome critical region. *Nat Genet*. (1992) 2:265–9. doi: 10.1038/ng1292-265
115. Rodriguez-Jato S, Nicholls RD, Driscoll DJ, Yang TP. Characterization of cis-and trans-acting elements in the imprinted human *SNURF-SNRPN* locus. *Nucleic Acids Res*. (2005) 33:4740–53. doi: 10.1093/nar/gki786
116. Cao Y, AlHumaidi SS, Faqeih EA, Pitel BA, Lundquist P, Aypar U. A novel deletion of SNURF/SNRPN Exon 1 in a patient with Prader-Willi-like phenotype. *Eur J Med Genet.* (2017) 60:416–20. doi: 10.1016/j.ejmg.2017.05.003
117. Geuns E. Methylation imprints of the imprint control region of the SNRPN-gene in human gametes and preimplantation embryos. *Hum Mol Genet*. (2003) 12:2873–9. doi: 10.1093/hmg/ddg315
118. Cavaillé J, Buiting K, Kiefmann M, Lalande M, Brannan CI, Horsthemke B, et al. Identification of brain-specific and imprinted small nucleolar RNA genes exhibiting an unusual genomic organization. *Proc Natl Acad Sci USA*. (2000) 97:14311–6. doi: 10.1073/pnas.250426397
119. Castle JC, Armour CD, Löwer M, Haynor D, Biery M, Bouzek H, et al. Digital genome-wide NcRNA expression, including SnoRNAs, across 11 human tissues using polyA-neutral amplification. *PLoS ONE.* (2010) 5:e11779. doi: 10.1371/journal.pone.0011779
120. Chamberlain SJ, Chen PF, Ng KY, Bourgois-Rocha F, Lemtiri-Chlieh F, Levine ES, et al. Induced pluripotent stem cell models of the genomic imprinting disorders angelman and Prader-Willi Syndromes. *Proc Natl Acad Sci USA*. (2010) 107:17668–73. doi: 10.1073/pnas.1004487107
121. Martins-Taylor K, Hsiao JS, Chen P-F, Glatt-Deeley H, De Smith AJ, Blakemore AIF, et al. Imprinted expression of *UBE3A* in non-neuronal cells from a Prader–Willi syndrome patient with an atypical deletion. *Hum Mol Genet*. (2014) 23:2364–73. doi: 10.1093/hmg/ddt628
122. Vitali P, Royo H, Marty V, Bortolin-Cavaille M-L, Cavaille J. Long nuclear-retained non-coding RNAs and allele-specific higher-order chromatin organization at imprinted snoRNA gene arrays. *J Cell Sci*. (2010) 123:70–83. doi: 10.1242/jcs.054957
123. Cavaillé J. Box C/D small nucleolar RNA genes and the Prader-Willi syndrome: a complex interplay: box C/D SnoRNA genes and the Prader-Willi syndrome. *Wiley Interdiscipl. Rev. RNA*. (2017) 8:e1417. doi: 10.1002/wrna.1417
124. Zhang YJ, Yang JH, Shi QS, Zheng LL, Liu J, Zhou H, et al. Rapid birth-and-death evolution of imprinted snoRNAs in the Prader-Willi syndrome locus: implications for neural development in *Euarchontoglires*. *PLoS ONE.* (2014) 9:e100329. doi: 10.1371/journal.pone.0100329
125. Bieth E, Eddiry E, Gaston V, Lorenzini F, Buffet A, Conte AF, et al. Highly restricted deletion of the *SNORD116* region is implicated in Prader–Willi syndrome. *Eur J Hum Genet*. (2015) 23:252–5. doi: 10.1038/ejhg.2014.103
126. Duker AL, Ballif BC, Bawle EV, Person RE, Mahadevan S, Alliman S, et al. Paternally inherited microdeletion at 15q11.2 confirms a significant role for the *SNORD116* C/D box SnoRNA cluster in Prader–Willi syndrome. *Eur J Hum Genet.* (2010) 18:1196–201. doi: 10.1038/ejhg.2010.102
127. Sahoo T, del Gaudio D, German JR, Shinawi M, Peters SU, Person RE, et al. Prader-Willi phenotype caused by paternal deficiency for the HBII-85 C/D box small nucleolar RNA cluster. *Nat Genet*. (2008) 40:719–21. doi: 10.1038/ng.158
128. de Smith AJ, Purmann C, Walters RG, Ellis RJ, Holder SE, Van Haelst MM, et al. A deletion of the HBII-85 class of small nucleolar RNAs (snoRNAs) is associated with hyperphagia, obesity and hypogonadism. *Hum Mol Genet*. (2009) 18:3257–65. doi: 10.1093/hmg/ddp263
129. Ding F, Li HH, Zhang S, Solomon NM, Camper SA, Cohen P, et al. SnoRNA *SNORD116* (Pwcr1/MBII-85) deletion causes growth deficiency and hyperphagia in mice. *PLoS ONE.* (2008) 3:e1709. doi: 10.1371/journal.pone.0001709
130. Qi Y, Purtell L, Fu M, Lee NJ, Aepler J, Zhang L, et al. *SNORD116* is critical in the regulation of food intake and body weight. *Sci Rep*. (2016) 6:18614. doi: 10.1038/srep18614
131. Rozhdestvensky TS, Robeck T, Galiveti CR, Raabe CA, Seeger B, Wolters A, et al. Maternal transcription of non-protein coding RNAs from the PWS-critical region rescues growth retardation in mice. *Sci Rep*. (2016) 6:20398. doi: 10.1038/srep20398
132. Skryabin BV, Gubar LV, Seeger B, Pfeiffer J, Handel S, Robeck T, et al. Deletion of the MBII-85 snoRNA gene cluster in mice results in postnatal growth retardation. *PLoS Genet*. (2007) 3:e235. doi: 10.1371/journal.pgen.0030235
133. Burnett LC, LeDuc CA, Sulsona CR, Paull D, Rausch R, Eddiry S, et al. Deficiency in prohormone convertase PC1 impairs prohormone processing in Prader-Willi syndrome. *J Clin Invest*. (2017) 127:293–305. doi: 10.1172/JCI88648
134. Coulson RL, Yasui DH, Dunaway KW, Laufer BI, Vogel Ciernia A, Zhu Y, et al. Snord116-dependent diurnal rhythm of DNA methylation in mouse cortex. *Nat Commun*. (2018) 9:1616. doi: 10.1038/s41467-018-03676-0
135. Bürger J, Horn D, Tönnies H, Neitzel H, Reis A. Familial interstitial 570 Kbp deletion of the *UBE3A* gene region causing angelman syndrome but not Prader-Willi syndrome: familial *UBE3A* gene deletion. *Am J Med Genet*. (2002) 111:233–7. doi: 10.1002/ajmg.10498
136. Runte M, Varon R, Horn D, Horsthemke B, Buiting K. Exclusion of the C/D box snoRNA gene cluster HBII-52 from a major role in Prader? Willi syndrome. *Hum Genet*. (2005) 116:228–30. doi: 10.1007/s00439-004-1219-2
137. Stelzer Y, Sagi I, Yanuka O, Eiges R, Benvenisty N. The noncoding RNA *IPW* regulates the imprinted DLK1-DIO3 locus in an induced pluripotent stem cell model of Prader-Willi syndrome. *Nat Genet*. (2014) 46:551–7. doi: 10.1038/ng.2968
138. Wevrick R, Francke U. An imprinted mouse transcript homologous to the human imprinted in Prader-Willi syndrome (*IPW*) gene. *Hum Mol Genet*. (1997) 6:325–32. doi: 10.1093/hmg/6.2.325
139. Ding F, Prints Y, Dhar MS, Johnson DK, Montero CC, Nicholls RD, et al. Lack of Pwcr1/MBII-85 SnoRNA is critical for neonatal lethality in Prader–Willi syndrome mouse models. *Mammalian Genome.* (2005) 16:424–31. doi: 10.1007/s00335-005-2460-2
140. Falk MJ, Curtis C, Bass NE, Zinn AB, Schwartz S. Maternal uniparental disomy chromosome 14: case report and literature review. *Pediatric Neurol.* (2005) 32:116–20. doi: 10.1016/j.pediatrneurol.2004.07.007
141. Hordijk R, Wierenga H, Scheffer H, Leegte B, Hofstra R, Stolte-Dijkstra I. Maternal uniparental disomy for chromosome 14 in a boy with a normal karyotype. *J Med Genet.* (1999) 36:782–5. doi: 10.1136/jmg.36.10.782
142. Hosoki K, Kagami M, Tanaka T, Kubota M, Kurosawa K, Kato M, et al. Maternal Uniparental Disomy 14 Syndrome Demonstrates

Prader-Willi Syndrome-Like Phenotype. *J Pediatr.* (2009) 155:900–03.e1. doi: 10.1016/j.jpeds.2009.06.045
143. Murrell A. Cross-talk between imprinted loci in Prader-Willi syndrome. *Nat Genet.* (2014) 46:528–30. doi: 10.1038/ng.2994
144. Patten MM, Cowley M, Oakey RJ, Feil R. Regulatory links between imprinted genes: evolutionary predictions and consequences. *Proc R Soc B Biol Sci.* (2016) 283:20152760. doi: 10.1098/rspb.2015.2760
145. Wold EA, Wild CT, Cunningham KA, Zhou J. Targeting the 5-HT2C receptor in biological context and the current state of 5-HT2C receptor ligand development. *Curr Top Med Chem.* (2019) 19:1381–98. doi: 10.2174/1568026619666190709101449
146. Nonogaki K, Strack AM, Dallman MF, Tecott LH. Leptin-independent hyperphagia and type 2 diabetes in mice with a mutated serotonin 5-HT2C receptor gene. *Nat Med.* (1998) 4:1152–6. doi: 10.1038/2647
147. Tecott LH, Sun LM, Akana SF, Strack AM, Lowenstein DH, Dallman MF, et al. Eating disorder and epilepsy in mice lacking 5-HT2C serotonin receptors. *Nature.* (1995) 374:542–6. doi: 10.1038/374542a0
148. Biswas S, Rao CM. Epigenetic tools (the writers, the readers and the erasers) and their implications in cancer therapy. *Eur J Pharmacol.* (2018) 837:8–24. doi: 10.1016/j.ejphar.2018.08.021
149. Kim Y, Wang SE, Jiang Y. Epigenetic therapy of Prader–Willi syndrome. *Transl Res.* (2019) 208:105–18. doi: 10.1016/j.trsl.2019.02.012
150. Wang SE, Jiang Y. Potential of epigenetic therapy for Prader-Willi syndrome. *Trends Pharmacol Sci.* (2019) 40:605–8. doi: 10.1016/j.tips.2019.07.002
151. Kim Y, Lee H-M, Xiong Y, Sciaky N, Hulbert SW, Cao X, et al. Targeting the histone methyltransferase G9a activates imprinted genes and improves survival of a mouse model of Prader–Willi syndrome. *Nat Med.* (2017) 23:213–22. doi: 10.1038/nm.4257

Conflict of Interest: The authors declare that the research was conducted in the absence of any commercial or financial relationships that could be construed as a potential conflict of interest.

frontiers in Endocrinology

ORIGINAL RESEARCH
published: 13 December 2019
doi: 10.3389/fendo.2019.00841

Leptin Induces Proadipogenic and Proinflammatory Signaling in Adipocytes

*Lohanna Palhinha[1], Sally Liechocki[1], Eugenio D. Hottz[1,2], Jéssica Aparecida da Silva Pereira[3,4], Cecília J. de Almeida[1], Pedro Manoel M. Moraes-Vieira[3,4,5], Patrícia T. Bozza[1] and Clarissa Menezes Maya-Monteiro[1]**

[1] Laboratory of Immunopharmacology, Oswaldo Cruz Institute (IOC), Oswaldo Cruz Foundation (FIOCRUZ), Rio de Janeiro, Brazil, [2] Laboratory of Glycoconjugates Analysis, Department of Biochemistry, Federal University of Juiz de Fora (UFJF), Juiz de Fora, Brazil, [3] Laboratory of Immunometabolism, Department of Genetics, Evolution, Microbiology and Immunology, Institute of Biology, University of Campinas, Campinas, Brazil, [4] Post-Graduate Program in Immunology, Institute of Biological Sciences, University of Sao Paulo, São Paulo, Brazil, [5] Experimental Medicine Research Cluster, EMRC, University of Cammpinas, Campinas, Brazil

Background: Leptin is an adipokine with well-known effects on the central nervous system including the induction of energy expenditure and satiety. Leptin also has major relevance when activating immune cells and modulating inflammatory response. In obesity, increases in white adipose tissue accumulation and leptin levels are accompanied by hypothalamic resistance to leptin. Even though the adipose tissue is a leptin-rich environment, the local actions of leptin regarding adipogenesis were not thoroughly investigated until now. Here we evaluate the contributions of leptins direct signaling in preadipocytes and adipose tissue-derived stromal cells (ASCs) for adipogenesis.

Methods: Adipocytes were differentiated from the murine lineage of preadipocytes 3T3-L1 or ASCs from subcutaneous and visceral (retroperitoneal) fat depots from C57Bl/6J mice. Differentiating cells were treated with leptin in addition to or in replacement of insulin. The advance of adipogenesis was assessed by the expression and secretion of adipogenesis- and lipogenesis-related proteins by Western blot and immunoenzimatic assays, and the accumulation of lipid droplets by fluorescence microscopy.

Results: Leptin treatment in 3T3-L1 preadipocytes or ASCs increased the production of the adipogenesis- and lipogenesis-related proteins PLIN1, CAV-1, PPARγ, SREBP1C, and/or adiponectin at earlier stages of differentiation. In 3T3-L1 preadipocytes, we found that leptin induced lipid droplets' formation in an mTOR-dependent manner. Also, leptin induced a proinflammatory cytokine profile in 3T3-L1 and ASCs, modulating the production of TNF-α, IL-10, and IL-6. Since insulin is considered an essential factor for preadipocyte differentiation, we asked whether leptin would support adipogenesis in the absence of insulin. Importantly, leptin induced the formation of lipid droplets and the expression of adipogenesis-related proteins independently of insulin during the differentiation of 3T3-L1 cells and ASCs.

Conclusions: Our results demonstrate that leptin induces intracellular signaling in preadipocytes and adipocytes promoting adipogenesis and modulating the secretion

OPEN ACCESS

Edited by:
Riccarda Granata, University of Turin, Italy

Reviewed by:
Philipp E. Scherer, UT Southwestern Medical Center, United States
Lourdes Mounien, Aix-Marseille Université, France

****Correspondence:***
Clarissa Menezes Maya-Monteiro
clarissa@ioc.fiocruz.br;
clarissamayam@gmail.com

Specialty section:
This article was submitted to Neuroendocrine Science, a section of the journal Frontiers in Endocrinology

Received: *24 July 2019*
Accepted: *19 November 2019*
Published: *13 December 2019*

Citation:
Palhinha L, Liechocki S, Hottz ED, Pereira JAdS, de Almeida CJ, Moraes-Vieira PMM, Bozza PT and Maya-Monteiro CM (2019) Leptin Induces Proadipogenic and Proinflammatory Signaling in Adipocytes. Front. Endocrinol. 10:841. doi: 10.3389/fendo.2019.00841

of inflammatory mediators. Also, leptin restores adipogenesis in the absence of insulin. These findings contribute to the understanding of the local signaling of leptin in precursor and mature adipose cells. The proadipogenic role of leptin unraveled here may be of especial relevance during obesity, when its central signaling is defective.

Keywords: adipogenesis, leptin, insulin, lipid droplet, adipose tissue, adipose-derived stromal cells, preadipocyte differentiation, mTOR

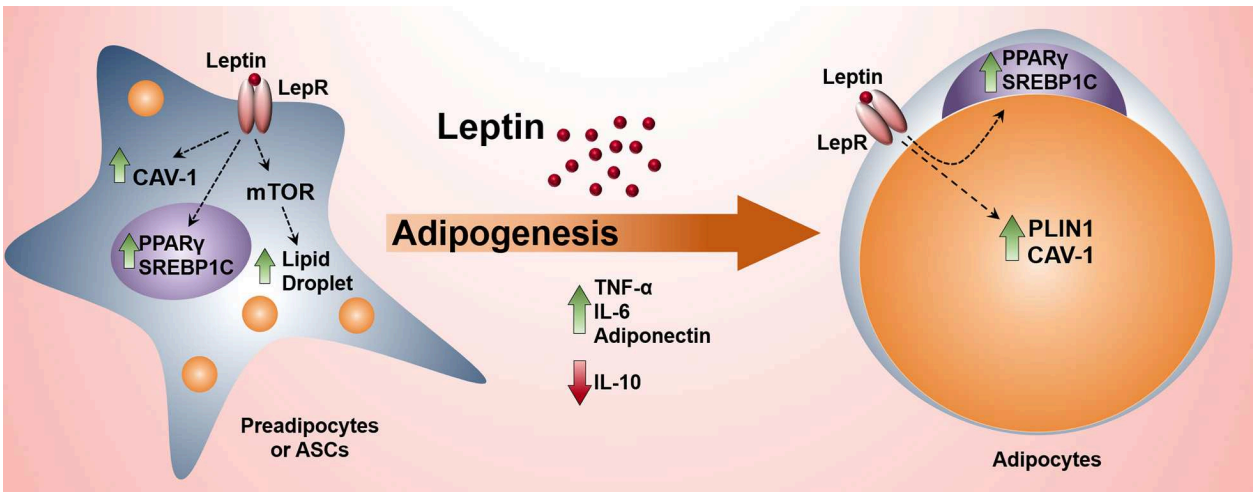

GRAPHICAL ABSTRACT | The activation of leptin signaling pathway in preadipocytes induces adipogenesis and the production of proinflammatory cytokines.

HIGHLIGHTS

- Leptin anticipates adipocyte differentiation in an mTOR-dependent manner.
- Leptin sustains adipogenesis of 3T3-L1 and ASCs in the absence of insulin.
- Leptin induces a proinflammatory cytokine profile in adipocytes.

INTRODUCTION

According to the World Health Organization, obesity prevalence nearly tripled since 1975 (1). Obesity is characterized by the expansion of the white adipose tissue with a subsequent imbalance in the production and signaling of adipokines accompanied by the development of chronic low-grade inflammation (2). Due to the obesity-associated inflammation and metabolic reprogramming, obese individuals have increased risk of developing comorbidities such as cancer, type II diabetes, stroke, among others (1, 3, 4). Thus, the understanding of the onset of obesity is of major importance, including adipogenesis itself.

The white adipose tissue (WAT) is recognized as an essential immunoendocrine organ that controls energy balance and metabolism (5). Adipocytes, the main cell type within adipose tissue, secrete hormones/cytokines collectively classified as adipokines. The first-described adipokine was leptin (6), one of the first links between the adipose tissue and the neuroendocrine control of energy homeostasis (6, 7). Leptin binds to the long leptin receptor isoform (LepRb), leading to the activation of JAK2/STAT3 and PI3K/AKT/mTOR pathways (8–10). In the hypothalamus, activation of the mTOR pathway by leptin is important for the induction of energy expenditure and satiety and consequently, a long-term effect on preventing excessive WAT accumulation (10). On the other hand, mTOR has been shown to be essential for adipogenesis (11, 12). We have previously shown that leptin can induce formation of lipid droplets in an mTOR-dependent manner, in different cell types (13–15). In peripheral tissues, leptin participates in reproduction (16), activation of immune cells (15, 17, 18), cell proliferation (14), osteogenesis (19), among many other functions. Leptin levels are increased during obesity but leptin signaling in the hypothalamus is impaired, a phenomenon called central leptin resistance (9, 20, 21). The concentration of leptin in the white adipose tissue depots may be much higher than its circulating serum levels. Although the hypertrophy and hyperplasia of

Abbreviations: ASCs, adipose tissue-derived stromal cells; WAT, white adipose tissue; PLIN, perilipin; CAV-1, caveolin-1; PPARγ, peroxisome proliferatoractivated receptor γ; SREBP1C, sterol regulatory element-binding protein-1; TNF-α, tumor necrosis factor-α; IL-10, interleukin-10.

adipocytes occur in this leptin-rich environment, leptin's paracrine, and autocrine effects on adipocyte differentiation are still not clear.

Here we tested leptin's ability to modulate adipogenesis in 3T3-L1 and primary adipose-derived stromal cells (ASCs) of subcutaneous and visceral WAT depots. Our data show that leptin is able to accelerate the differentiation of preadipocytes. Further, we describe that leptin induces adipogenesis even in the absence of insulin—which is considered an essential hormone for the induction of adipogenesis (22). The results presented here indicate an unexpected new role for leptin as a proadipogenic factor.

MATERIALS AND METHODS

3T3-L1 Preadipocyte Differentiation

The murine lineage of preadipocytes NIH3T3-L1 was obtained from the National Bank of Cells, Federal University of Rio de Janeiro, Brazil. To keep preadipocytes in their undifferentiated state, we cultured the cells with medium containing Dulbecco's Modified Eagle Medium (DMEM) (Gibco) with 4.5 g/L of glucose (Invitrogen) supplemented with penicillin (100 U/mL) and streptomycin (100 μg/mL) (Gibco) and with 10% of bovine serum (Invitrogen). Preadipocytes (1.05×10^4 cells/cm^2 of adherence area) were seeded in polystyrene culture plates (Biofil). Four days after the seeding (day 0) medium was replaced by the differentiation-inducting medium containing DMEM with 4.5 g/L of glucose, penicillin (100 U/mL), streptomycin (100 μg/mL), 10% of fetal bovine serum, 1 μM of dexamethasone (Sigma Aldrich), 0.5 mM of isobutylmethylxantine (IBMX) (Sigma Aldrich) and 0.3 units of insulin/mL (Regular Humulin—Lily). The differentiation induction medium was maintained for 3 days and then replaced by the maturation medium, containing DMEM with 4.5 g/L of glucose, penicillin (100 U/mL), streptomycin (100 μg/mL), 10 % of fetal bovine serum and 0.3 units/mL of insulin. Seventy-five percent of the maturation medium was renewed every 2–3 days.

For the experiments in which cells were differentiated in the presence of leptin, the first supplementation with leptin [4 or 40 nM, doses approximately matched to the circulating levels of leptin in obese and morbidly obese individuals (23–25)] occurred at day−3 (1 day after plating) and leptin was added at every medium renewal.

To investigate the ability of leptin to induce preadipocyte differentiation in the absence of insulin, insulin was replaced by leptin at day 0 and differentiation was performed as aforementioned.

Murine Mesenchymal Stromal Cells (ASCs) Isolation and Differentiation

Subcutaneous and retroperitoneal fat pads were isolated from male C57Bl/6J mice of 6 weeks of age. In order to achieve a considerable amount of stem cells to expand and differentiate we pooled right and left tissue depots from three animals for each experimental replicate. For the experiments using LepR-deficient mouse, we pooled the right and left tissue depots (subcutaneous, retroperitoneal and epididymal) from one BKS.Cg-m$^+$/$^+$Lepr^{db}/JUnib male mouse (UNICAMP, Campinas, SP, Brazil). Tissues were washed with phosphate-buffered saline (PBS) solution with penicillin (100 U/mL) and streptomycin (100 μg/mL) (Sigma) and 5 μg/mL of ciprofloxacin (Sigma) and then cut into small pieces. These pieces were rewashed with the same solution and incubated for 2 h with 2 mg/mL of collagenase (Sigma) in a volume of 2.5 mL per mg of tissue with constant shaking at 37°C. Collagenase was inactivated by doubling the volume with media containing antibiotics and 10% fetal bovine serum (Life Sciences). Digested tissues were then filtered in cell strainers of 100 μm pore size and centrifuged at 500 × g for 7 min. The superior fraction which contained mainly lipids and mature adipocytes was discarded and the pellet was resuspended in PBS plus penicillin (100 U/mL) and streptomycin (100 μg/mL), 5 μg/mL of ciprofloxacin, filtered again in cell strainers of 40 μm pore size and centrifuged at 500 × *g* for 7 min. The pellet of stromal vascular cells was then resuspended in culture media containing DMEM with 4.5 g/L glucose, penicillin (100 U/mL) and streptomycin (100 μg/mL), 5 μg/mL of ciprofloxacin, and 20% of fetal bovine serum (Life Sciences) and cultured. Cells were expanded 3–4 times before plating. All animal procedures were approved by the Committee of Ethics in Animal Research L011.2015.

Characterization of ASCs by Flow Cytometry

Stromal vascular cells expanded up to two times were labeled with ASCs' positive (CD44, CD29, CD106, and CD105) and negative (MHC-class II, CD11b, CD31, CD45, and CD144) markers. Cells were incubated (30 min) with FITC-conjugated anti-CD45 (eBioscience, cat 12-1051-81, dilution 1:20); -CD31 (eBioscience, cat 11-0311-81, dilution 1:20) and -MHC class II (eBioscience, cat: 11-5320-82, dilution 1:20); APC-conjugated anti-CD11b (BD Pharmingen, cat 553312, dilution 1:20), and PE-conjugated anti-CD29 (eBioscience, cat 12-0291-81, dilution 1:20) or -CD105 (eBioscience, cat 12-1051-81, dilution 1:10). For evaluation of CD106 expression, cells were incubated (30 min) with rat anti-mouse CD106 (eBioscience, cat 14-1061-81, dilution 1:10) followed by 30 min incubation with Alexa Fluor® 546-conjugated anti-rat IgG (Molecular Probes, cat: A-11081, dilution 1:250); unbound antibodies were washed out and cells were incubated (30 min) with FITC-conjugated anti-CD45, -CD31, and -MHC class II, and APC-conjugated anti-CD11b. For evaluation of CD44 (eBioscience, cat 11-0441-81, dilution 1:20) expression, cells were incubated (30 min) with unconjugated rat antibodies against CD45 (BD Biosciences, cat: 550539, dilution 1:10) and CD144 (eBioscience, cat: 16-1441-85, dilution 1:20) followed by 30 min incubation with AlexaFluor 546-conjugated anti-rat IgG; unbound antibodies were washed out and cells were incubated (30 min) with FITC-conjugated anti-CD44 and APC-conjugated anti-CD11b antibodies. Cells incubated with isotype-matched IgG conjugated with the same fluorochromes or unconjugated IgG followed by incubation with the secondary antibody were used as a negative control. Cells were acquired in a Beckman Coulter CytoFLEX S using CytExpert software and analyzed using FlowJo v10 software.

For analysis, cells were gated by the exclusion of leucocytes and endothelial cells markers (CD45, MHC class II, CD11b, CD31, and CD144) and the expression of ASCs markers evaluated as shown in **Supplementary Figure 3**.

Fluorescence Microscopy Analysis

Cells were fixed for 15 min with formaldehyde 3.7 %, washed with buffered saline, and stained with BODIPY^{TM} 493/503 (ThemoFisher Scientific) for 30 min and DAPI (ThemoFisher Scientific) for 5 min. Images were acquired with the microscope Olympus BX60 and analyzed with the software Fiji (26) version 1.49 m (National Institutes of Health, USA) with Java version 1.6.0_24 (64-bit). We developed a macro to analyze the total Bodipy stained area (green) in each field adjusting the same parameters of color balance, contrast, background, and noise. Images were processed so that the threshold setting for quantifying the total and relative area of Bodipy staining excluded most of the interferences from the image acquisition. A different macro was developed for the counting of nuclei numbers in each field (DAPI—blue). Then, total Bodipy stained area was normalized by the number of cells in each field and the mean of these measurements was plotted for each group.

Western Blot Analysis

Cells were washed with phosphate-buffered saline (PBS) solution and then subjected to lysis directly by 95°C-heated Laemmli buffer with concomitant cell scraping from the wells. Protein content was separated by 10–15% sodium dodecyl sulfate-polyacrylamide gel electrophoresis (SDS-PAGE) and transferred to nitrocellulose membranes. Membranes were blocked with 5% non-fat dried milk diluted in Tris-Buffered Saline supplemented with 0.1% Tween 20 (Sigma) (TBS-T) for 1 h before incubation overnight with primary antibodies against PLIN1 (Cell Signaling, cat 3470, dilution 1:500), JAK2 (Cell Signaling, cat 3230, dilution 1:1,000), pTyr1007/1008 JAK2 (Cell Signaling, cat 3771, dilution 1:1,000), pTyr389 S6K (Cell Signaling, cat 9205, dilution 1:1,000), S6K (Cell Signaling, cat 2708, dilution 1:1,000), pTyr705 STAT3 (Cell Signaling, cat 9131, dilution 1:1,000), STAT3 (Cell Signaling, cat 9139, dilution 1:1,000), PPARγ (Santa Cruz, cat sc-7196, dilution 1:1,000), SREBP1 (Santa Cruz, cat sc-13551, dilution 1:1,000), and for 1–2 h with anti-β-actin (Sigma, cat A2228, dilution 1:10,000) or CAV-1 (Santa Cruz, cat sc-894, dilution 1:2,000). Membranes were then washed with TBS-T and proteins were detected using fluorescent dye-conjugated secondary antibodies (anti-mouse, IRDye 800CW, cat 926-32210 or anti-rabbit, IRDye 680RD cat 926-68071, LI-COR) or horseradish peroxidase-conjugated secondary antibodies (anti-rabbit, cat PI-1000 or anti-mouse, cat PI-2000; Vector).

Quantification of Cytokines

Supernatants were harvested from cultured preadipocytes and adipocytes or differentiating ASCs at different timepoints and the levels of leptin, adiponectin, TNF-α, IL-10, IL-6, KC/CXCL1, and MCP-1were measured using standard ELISA protocols according to manufacturer's instructions (R&D Systems).

Statistical Analysis

Statistics were performed using GraphPad Prism (San Diego, CA) version 6.05. All numeric variables were tested for normal distribution using the Kolmogorov-Smirnov normality test. For comparison among three or more groups, we used One-way ANOVA with Dunnet's post-test to compare differentiated cells with preadipocytes, or Tukey's post-test to compare leptin-treated with untreated cells among groups following a normal distribution. In cases of non-parametric distribution among three or more groups, we used One-way ANOVA, followed by Kruskal-Wallis' test with Dunn's correction. To analyze the effect of rapamycin over the effect of leptin we used Two-way ANOVA with Sidak's post-test to locate the differences among groups. For comparison between two groups we used the Mann-Whitney *U*-test for non-parametric distribution. For comparisons when the groups were normalized by the control group (thus containing repeated value) we used the Kolmogorov-Smirnov non-parametric test.

RESULTS

Leptin Increases Preadipocyte Differentiation

3T3-L1 cells progressively differentiated into adipocytes up to 17 days after the induction of adipogenesis (day 0) with increased formation of lipid droplets accompanied by enhanced secretion leptin and adiponectin (**Supplementary Figures 1A–D**). Briefly, the adipocyte differentiation protocol (**Figure 1A**) consisted of plating cells at day−4, followed by administration of the adipogenic medium (insulin, IBMX, dexamethasone) at day 0—so called for being the start-point of adipogenesis *in vitro*—which was maintained until day 3. Afterwards, cells were incubated in insulin-containing medium and kept in this medium until the end of the assay (**Figure 1A**) as described in more details in section Materials and Methods. In order to evaluate the effects of leptin in the adipogenic process, 3T3-L1 cells were incubated with leptin supplementation from the first day post-plating (day−3) until the end of the differentiation protocol (day 17). The cells were analyzed at the preadipocyte stage (day−1) and at the three stages of adipocyte maturation (days 3, 10, or 17) (**Figure 1A**). Leptin significantly enhanced lipid accumulation in preadipocytes, showing an anticipation of this adipogenic feature when compared to the control cells, without leptin (**Figures 1B,C**). Leptin lead to increased expression of the lipid droplet protein PLIN1 in adipocytes (**Figure 1D**). In addition, preadipocytes and adipocytes cultured with leptin exhibited increased levels of the adipogenesis- and lipogenesis-related factors PPARγ, SREBP1C and Caveolin-1 (CAV-1), mainly in preadipocytes and adipocytes at the first stages of differentiation (**Figure 2D**; **Supplementary Figure 2** shows the replicates of all Western blots). These results show a synergistic proadipogenic effect of leptin and insulin.

Leptin-Induced Adipogenesis Depends on the mTOR Pathway

Leptin binds to its LepRb receptor and activates JAK2, which can activate STAT3 and PI3K/AKT/mTOR pathways (9, 10, 15).

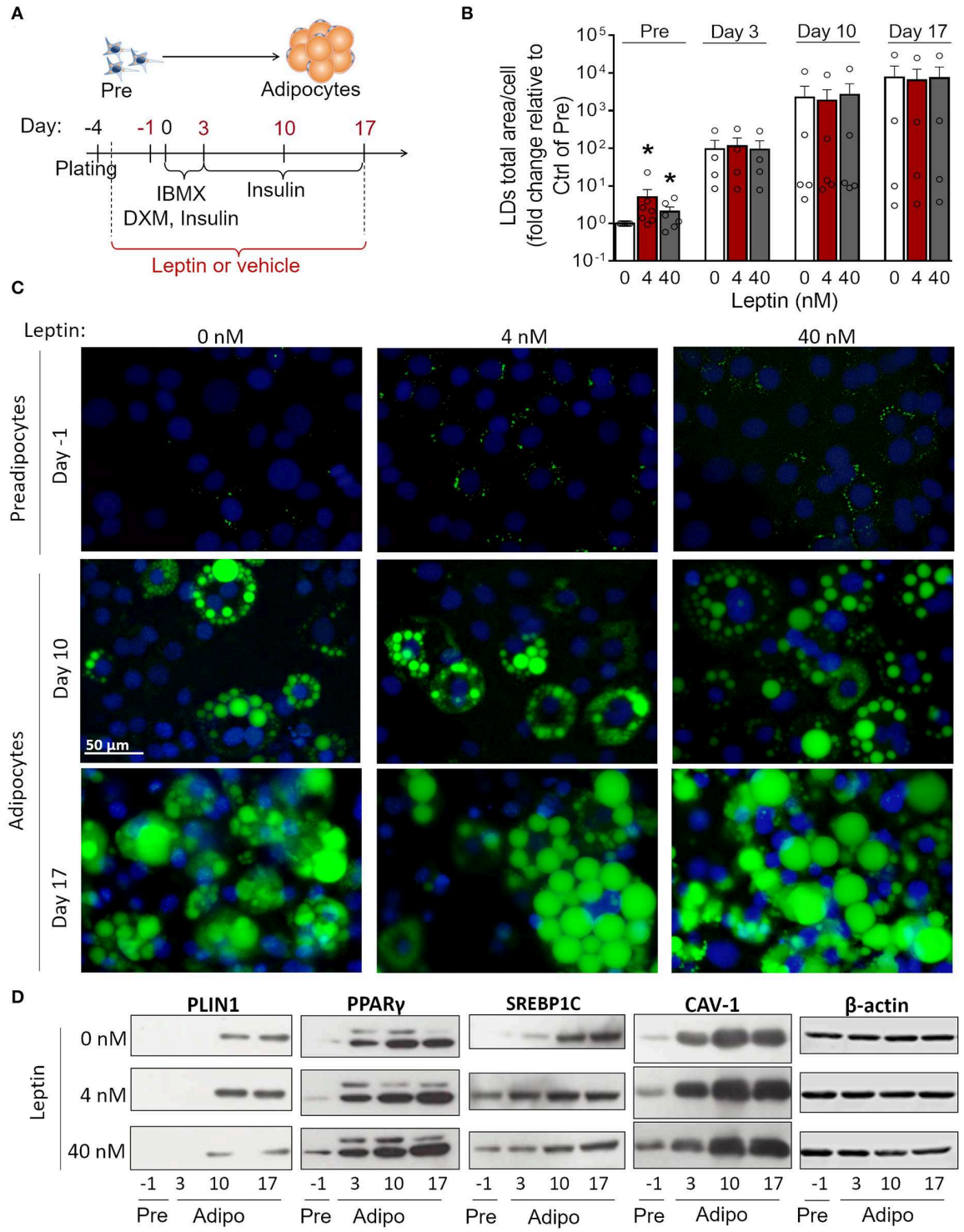

FIGURE 1 | Leptin treatment enhances the expression of adipogenesis- and lipogenesis-related proteins. **(A)** Schematic representation of experimental design: leptin was administered from day−3 up to days−1, 3, 10, or 17 of differentiation. Day 0 represents the day of the induction of differentiation (with IBMX – isobutylmethylxantine, DXM—Dexamethazone and insulin). **(B,C)** Preadipocytes (day−1) and adipocytes (days 3–17) were differentiated with leptin (4 or 40 nM) and stained with Bodipy (green) for lipid droplets and DAPI (blue) for nuclei. **(B)** Quantification of the green area per cell in each condition. Bars represent mean ± standard error of the mean of 4–7 independent experiments. *Means $p < 0.05$ in a Kolmogorov-Smirnov non-parametric test. **(C)** Representative images of 4–7 independent experiments. Scale bar represents 50 µm in range. All images have the same dimensions. **(D)** Western blot analysis of PLIN1, PPARγ, SREBP1C, caveolin-1 (CAV-1), and β-actin in 3T3-L1 preadipocytes and adipocytes differentiated with or without leptin. Blots are representative of 3–5 independent experiments. Lysates from cells differentiated with 0, 4, or 40 nM were analyzed in the same gel and cropped for clearer comparison among groups.

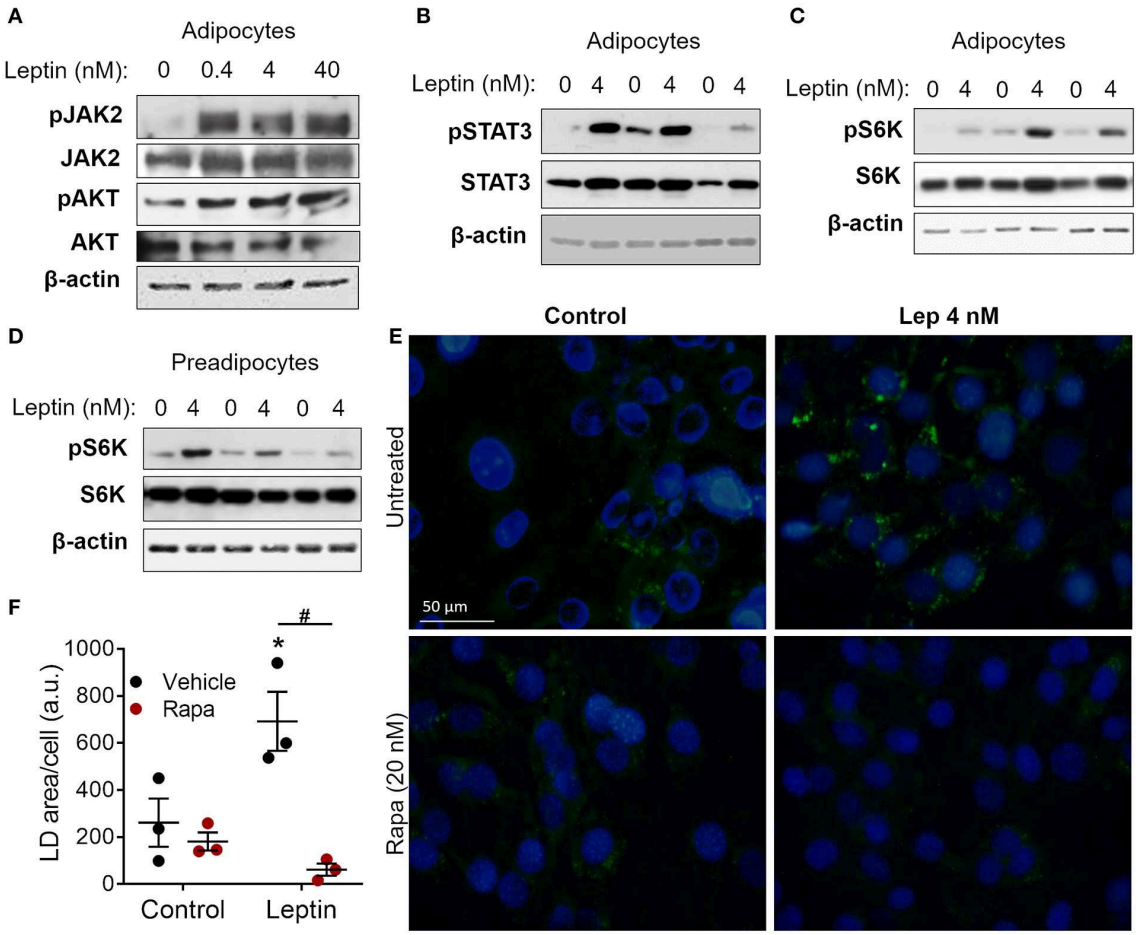

FIGURE 2 | Leptin-induced adipogenesis depends on mTOR/p70 S6K pathway. **(A–D)** 3T3-L1 cells were cultured as described in methods up to day−1 (preadipocytes) and day 17 (adipocytes) and then stimulated with leptin at the indicated concentrations for 20 min. **(A)** Western blot analysis of phosphorylated JAK2 (pJAK2), total JAK2, pAKT, total AKT, and β-actin. Blots are representative of three independent experiments. **(B)** Western blot analysis of pSTAT3, total STAT3, and β-actin in adipocytes from three independent experiments analyzed in the same gel. **(C,D)** Western blot analysis of pS6K, total S6K, and β-actin in adipocytes **(C)** and preadipocytes **(D)** from three independent experiments. **(E,F)** Preadipocytes were cultured for 48 h with no stimulus (control), leptin (4 nM), rapamycin (20 nM), or both. Cells were stained with Bodipy (green) for lipid droplets and with DAPI (blue) for nuclei. **(E)** Shows images representative of three independent experiments. Scale bar represents 50 µm in range. **(F)** Quantification of the green area per cell in each condition. Dots represent the replicates of one experiment representative of three. Horizontal lines represent mean ± standard error of the mean. *Means $p < 0.05$ relative to control, #means $p < 0.05$ between vehicle and rapamycin treated cells. Statistical analyzes were performed by using Two-way ANOVA with Sidak's post-test.

To dissect leptin signaling pathways in adipocytes, differentiated adipocytes were stimulated with leptin for 20 min and the phosphorylated proteins of each pathway were analyzed through Western blot. We observed increased phosphorylation of JAK2, AKT, and STAT3 in adipocytes after stimulation with leptin (**Figures 2A,B**; **Supplementary Figure 2**), confirming the activation of the two branches of the leptin signaling pathway in adipocytes. Leptin also induced the phosphorylation of p70 S6 kinase (S6K), a substrate of mTOR (**Figure 2C**). Considering the importance of mTOR signaling in the induction of adipogenesis (11, 12, 27, 28), we asked whether leptin can modulate this pathway in undifferentiated cells (**Figure 2D**). We found that leptin also activated the mTOR pathway in preadipocytes, as evidenced by the increased phosphorylation of p70 S6K (**Figure 2D**). To gain insights into the role of mTOR signaling in leptin-induced adipogenesis, we stimulated preadipocytes with leptin in the presence of rapamycin, a selective mTOR inhibitor, and evaluated the biogenesis of lipid droplets after 48 h. Rapamycin treatment completely abolished the leptin-induced biogenesis of lipid droplets in preadipocytes (**Figures 2E,F**), indicating that the pro-adipogenic effects of leptin depend on mTOR activation.

Leptin Shifts Adipocyte Cytokine Production Toward a Proinflammatory Pattern

Adipose tissue is an important source of cytokines and chemokines, which are collectively called adipokines (29). We observed increased production of TNF-α

in 3T3-L1 control cells as adipogenesis progressed (**Figures 3A,B**; **Supplementary Figure 2**). Treatment with leptin further increased TNF-α expression by preadipocytes (day−1) and immature adipocytes (day 3) (**Figure 3A**; **Supplementary Figure 2**). In addition, treatment with leptin (40 nM) also induced the secretion of TNF-α and adiponectin at earlier stages of differentiation (**Figures 3B,C**), which is consistent with the anticipation of adipogenesis described above. Also, leptin treatment decreased the secretion of the anti-inflammatory cytokine IL-10 (**Figure 3D**). The levels of the chemokines KC/CXCL1 and MCP-1/CCL2, on the other hand, were not modulated by leptin treatment (**Figures 3E,F**). These results suggest that, in addition to adipogenesis, leptin induces a proinflammatory cytokine balance in 3T3-L1 adipocytes.

Adipocyte Differentiation in the Absence of Insulin Is Recovered by Leptin

Insulin is considered essential for the proper differentiation of preadipocytes due to the induction of cell growth and fatty

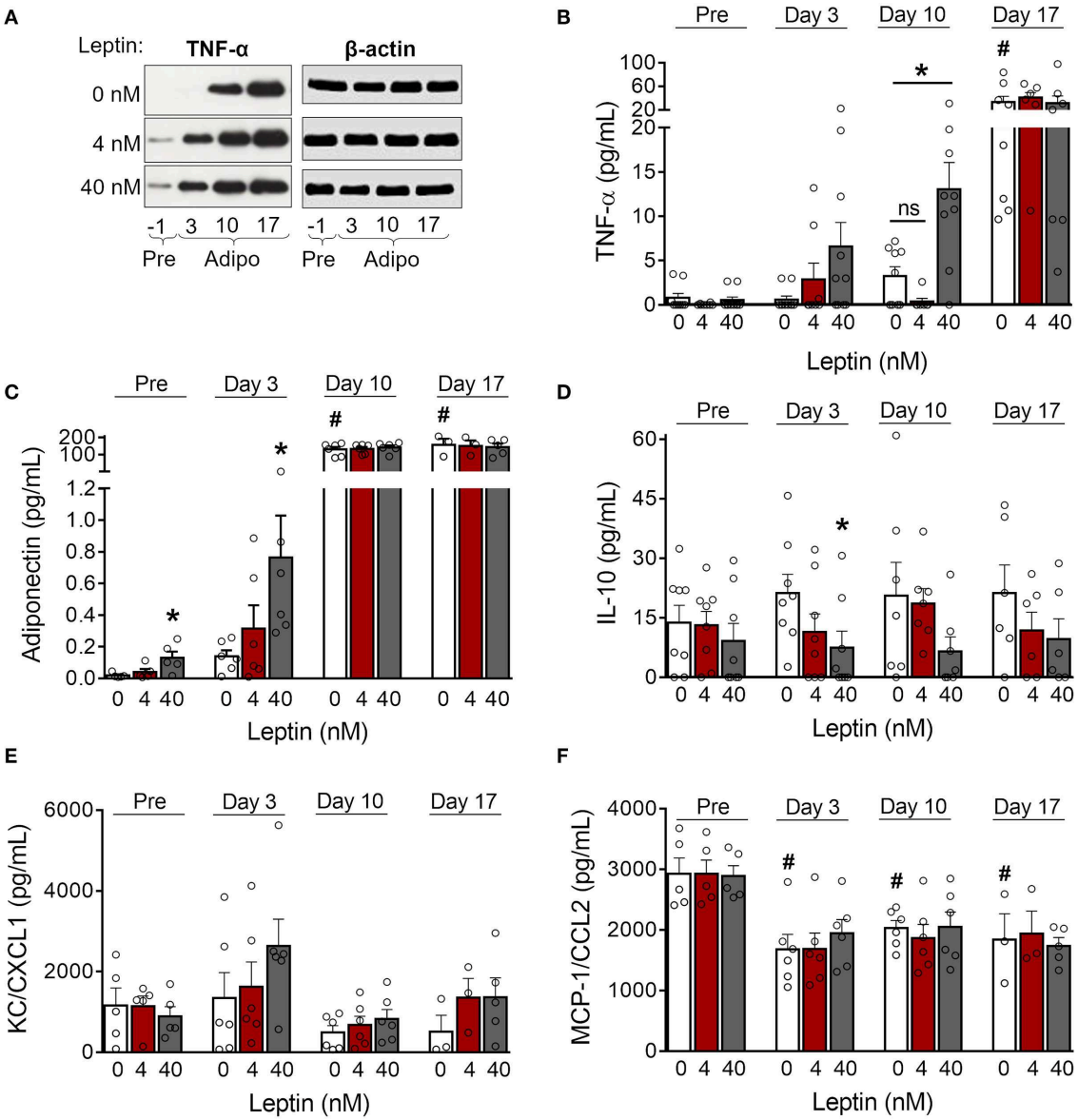

FIGURE 3 | Leptin induces a proinflammatory cytokine profile during adipocyte differentiation. **(A,B)** 3T3-L1 preadipocytes (day−1) and adipocytes at days 3, 10, and 17 were cultured in the presence of leptin (0, 4, or 40 nM). **(A)** Western blot analysis of TNF-α and β-actin in cell lysates from each condition. Blots are representative of three independent experiments. Cell lysates from a representative experiment were analyzed in the same gel and cropped for clearer comparison among the groups. **(B–F)** Concentration of **(B)** TNF-α, **(C)** adiponectin, **(D)** IL-10, **(E)** KC/CXCL1, and **(F)** MCP-1/CCL2 in the supernatant of preadipocytes and adipocytes differentiated under distinct leptin stimulus. Bars represent mean ± standard error of the mean of 3–11 independent experiments. $^{\#}p < 0.05$ compared to preadipocytes (day−1). *Represents $p < 0.05$ between leptin-treated and untreated cells at the same stage of differentiation. Statistical analyzes were performed by using **(B–E)** One-way ANOVA followed by Kruskal-Wallis' test with Dunn's correction or **(F)** One-way ANOVA with Dunnet's post-test. "ns" stands for non-significant.

acid synthesis and is an important constituent of adipogenic cocktails (22, 30). Considering the proadipogenic effects of leptin observed above, we investigated whether leptin, in the absence of insulin, would be sufficient for the induction of adipogenesis in 3T3-L1 cells. As shown in **Figure 4**, 3T3-L1 cells cultured without insulin or leptin supplementation showed impaired lipid droplets' formation (**Figures 4A,B**) and reduced expression of the adipogenesis-related proteins PLIN1, SREBP1C, PPARγ, and CAV-1 (**Figure 4C**; **Supplementary Figure 2**) compared to insulin-differentiated cells. Importantly, replacement of insulin by leptin during 3T3-L1 differentiation recovered the biogenesis of lipid droplets and the expression of adipogenesis-related proteins (**Figures 4A–C**; **Supplementary Figure 2**). These data indicate that leptin exerts proadipogenic effects independently of insulin.

Leptin Induces Proadipogenic and Proinflammatory Signaling in Primary Adipose Tissue-Derived ASCs

Next, we investigated whether leptin has proadipogenic effects in ASCs obtained from the stromal vascular fraction of subcutaneous and retroperitoneal fat pads from C57Bl/6J mice. Characterization of ASCs is described in Methods and shown in **Supplementary Figure 3**. Similar to 3T3-L1 cells, leptin also synergized with insulin and anticipated the differentiation of ASCs into adipocytes (**Figure 5**). As shown in **Figures 5A,B**, concomitant treatment of retroperitoneal—but not subcutaneous—ASCs with leptin and insulin increased lipid accumulation at day 5 of differentiation compared to control cells cultured with insulin only. Morphologically, ASCs cultured with insulin had already achieved maximal

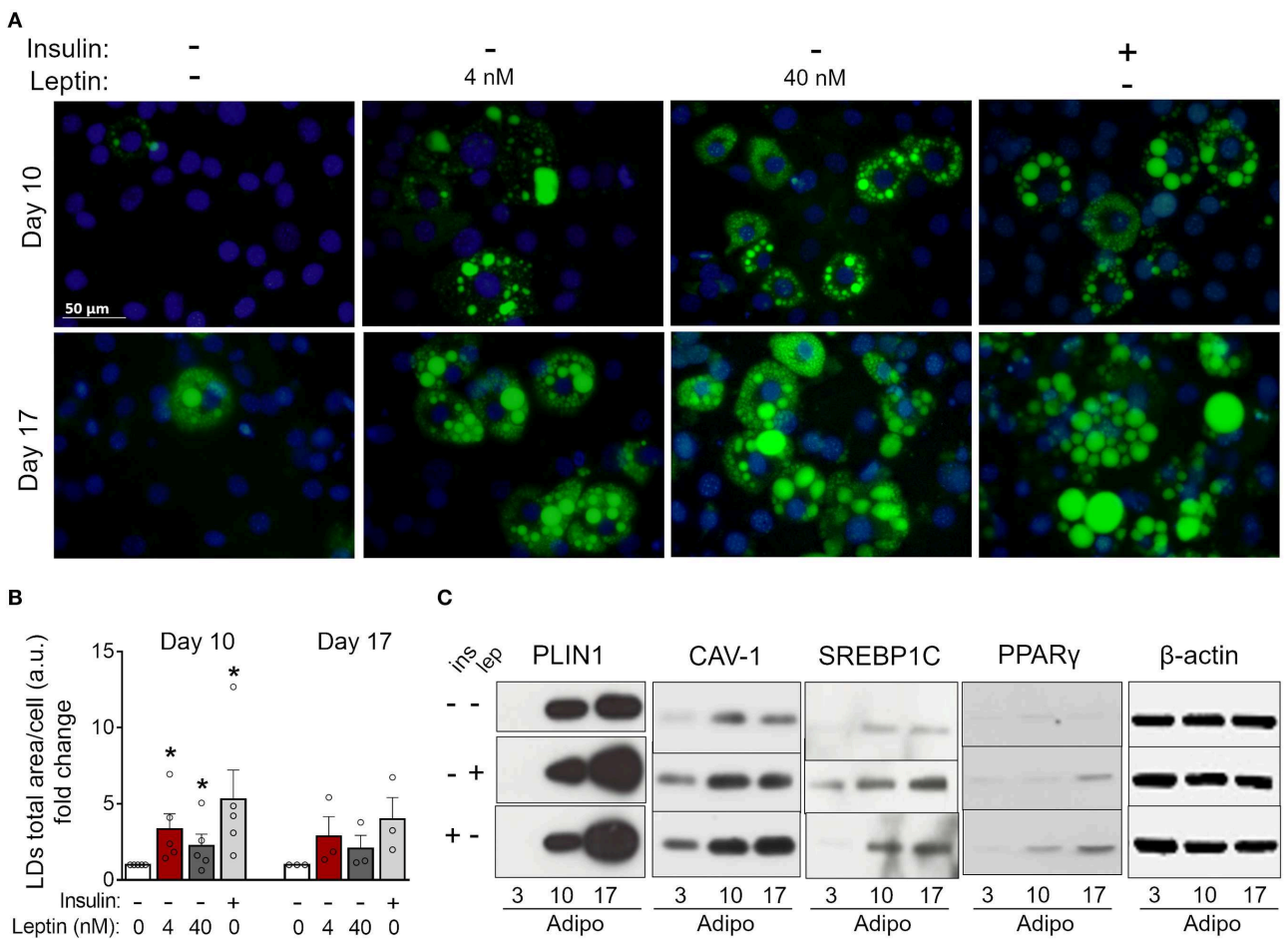

FIGURE 4 | Leptin recovers 3T3-L1 differentiation in the absence of insulin. 3T3-L1 adipocytes were cultured with no hormone, insulin or leptin (4 or 40 nM) up to 3, 10, or 17 days after induction of differentiation. **(A)** Fluorescence images of cells stained with Bodipy (green) for lipid droplets and DAPI (blue) for nuclei. Images are representative of 3–5 independent experiments. Scale bar represents 50 µm. **(B)** Quantification of the green area per cell in each field. Data are depicted as the fold change relative to the group with no hormone supplementation. Bars represent mean ± standard error of the mean of 3–5 independent experiments. **(C)** Western blot analysis of PLIN1, CAV-1, SREBP1C, PPARγ, and β-actin. Blots are representative of three independent experiments in the cases of PLIN1, CAV-1, and PPARγ and two independent experiments in the case of SREBP1C. Cell lysates were analyzed in the same gel and cropped for clearer comparison among groups. *$p < 0.05$ relative to the group in which cells were cultured with neither insulin nor leptin. Statistical analyzes were performed by using the Kolmogorov-Smirnov test.

lipid accumulation at day 12, so there was no observable effect of leptin in potentiating insulin-induced lipid droplet biogenesis at this time point (**Figures 5A,B**). On the other hand, induction of adipogenesis and anticipation of differentiation were evidenced by the increased expression of CAV-1, PPARγ, SREBP1C and/or PLIN1 at days 5 and 12 in ASCs obtained from both depots (**Figures 5C,D**; **Supplementary Figure 2**). As shown with 3T3-L1, leptin treatment was able to modulate the expression of the adipogenic markers in ASCs. These data show that leptin is able to potentiate insulin-induced ASCs differentiation into adipocytes. In addition, leptin treatment induced a proinflammatory cytokine profile in differentiated ASCs by increasing the levels of TNF-α and IL-6 without affecting IL-10 levels (**Figure 6**).

As previously mentioned, adipocyte differentiation can be achieved by the combination of adipogenesis induction factors, with insulin being considered indispensable for this purpose (30). We then investigated the ability of leptin to support ASCs commitment to adipocytes in the absence of insulin. As shown in **Figure 7**, leptin induces lipid accumulation at day 12 of differentiation in subcutaneous and retroperitoneal ASCs when compared to the cells cultured without leptin or insulin supplementation (**Figures 7A–C**). Also, stimulation with leptin alone supported the expression of the adipogenesis-related proteins CAV-1, PLIN-1, PPAR-γ, and/or SREBP1C in ASCs from both adipose tissue depots (**Figures 7D,E**; **Supplementary Figure 2**). In addition, leptin did not induce adipogenesis in ASCs from LepRb-deficient (db/db) mouse, albeit these cells were still able to differentiate in response to insulin (**Supplementary Figures 4A,B**). Also, leptin signaling through mTOR pathway was absent in ASCs from db/db mice (**Supplementary Figure 4C**). Our data show that leptin supports the induction of adipocyte differentiation through LepRb signaling, even in the absence of insulin.

DISCUSSION

Leptin is a key adipokine in the control of energy balance and satiety through its signaling in the central nervous system (9, 22). Several effects of leptin regarding the systemic control of metabolism in various organs and systems are well-documented and still very explored by many groups (9, 31). However, one simple question remained elusive so far: what are the autocrine and paracrine effects of leptin on its own producer cells? Our data provide a new branch in leptin signaling regarding the local modulation of the adipogenic process. Here we show that leptin has direct effects in 3T3-L1 preadipocytes and adipocytes, as well as in ASCs, anticipating the commitment with the adipocyte lineage and adipogenesis.

Continuous leptin supplementation had similar effects on the differentiation of primary mouse ASCs and the murine lineage of preadipocytes 3T3-L1, anticipating and enhancing several adipogenic features. Expression of the adipogenesis- and lipogenesis-related proteins PPARγ, SREBP1C, PLIN1, and CAV-1 were enhanced both in 3T3-L1 and ASCs from subcutaneous and retroperitoneal depots. We also observed that leptin anticipated the secretion of the adipokine adiponectin, which is expressed exclusively by mature adipocytes, corroborating the advanced state of differentiation upon leptin treatment (32).

Previous studies showed that leptin induced lipolysis in rat adipose tissue (33–35). In these studies, most experiments were performed with the whole explant of WAT or isolated mature adipocytes stimulated with leptin, acutely, for 1 or 2 h (33, 35). As a matter of fact, these studies do not oppose to ours since adipogenesis is not the opposite of lipolysis: increased adipocyte differentiation only means that adipogenesis is prevailing over lipolysis in the time points observed. In other studies the cells were stimulated also for a short period and/or with high concentrations of leptin, above the physiological or obesity-associated levels (34, 36). These short incubations and the elevated doses of leptin can indeed acutely activate lipolytic pathways in mature adipocytes. There is also evidence of inhibition of lipolysis when tissue explants were incubated for longer periods (i.e., 18 h) with leptin (37). Rhee et al. (36) state that leptin stimulus inhibits rosiglitazone-induced adipogenesis in primary cells from ob/ob mice, The effects of leptin on rosiglitazone-treated cells may differ from leptin stimulation alone. Another report indicates an indirect proadipogenic effect of leptin showing that leptin inhibits the anti-adipogenic effects of vitamin D (38). Finally, in previous reports (36, 39) the cells were stimulated with leptin only after the induction of differentiation. We believe that the contact of the cells with leptin when they are still undifferentiated is a better model to evaluate the pro-adipogenic effect. The control of lipolysis in the mature adipocyte can also be regulated by infiltrating macrophages that can be present in different amounts depending on the inflammatory activation (40, 41). The activation of recruited and adipose tissue-resident immune cells—including macrophages—by leptin has been shown to induce the production of the potent prolipolytic and proinflammatory cytokine TNF-α (18, 42–44). In our work, we show that chronic leptin treatment increases the expression and secretion of TNF-α by adipocytes. Although TNF-α clearly induces lipolysis through diverse mechanisms including the inhibition of PPARγ (29, 45) and reduction of PLIN1 expression (46), we show that leptin treatment is able to significantly increase the expression of PPARγ, PLIN1, and many other features related to lipogenesis and adipogenesis. It has also been shown that leptin, TNF-α and other adipokines stimulate the expression of the proadipogenic miR-378 (47) and the adipogenesis-related miR-355 (48). We do not exclude the acute effect of leptin in the induction of lipolysis directly in mature adipocytes, but we clearly show that the proadipogenic effect prevails in a long-term incubation.

As stated above, the timing of leptin's treatment is of paramount importance for the outcomes observed in differentiated cells, with an early treatment of precursor cells leading to a proadipogenic leptin signaling. Sustaining this hypothesis, the specific knockout of LepR in already mature adipocytes did not have important effects on adipogenesis (49), while the specific knockout or knockdown of LepR in precursor cells impaired their ability to commit to the adipocyte fate (19, 50). Yue et al. (19) showed that the specific deletion of the leptin receptor LepR gene in the bone marrow-derived mesenchymal stromal cells (BM-MSCs) favored osteogenesis at the expense of adipogenesis within the bone marrow (19).

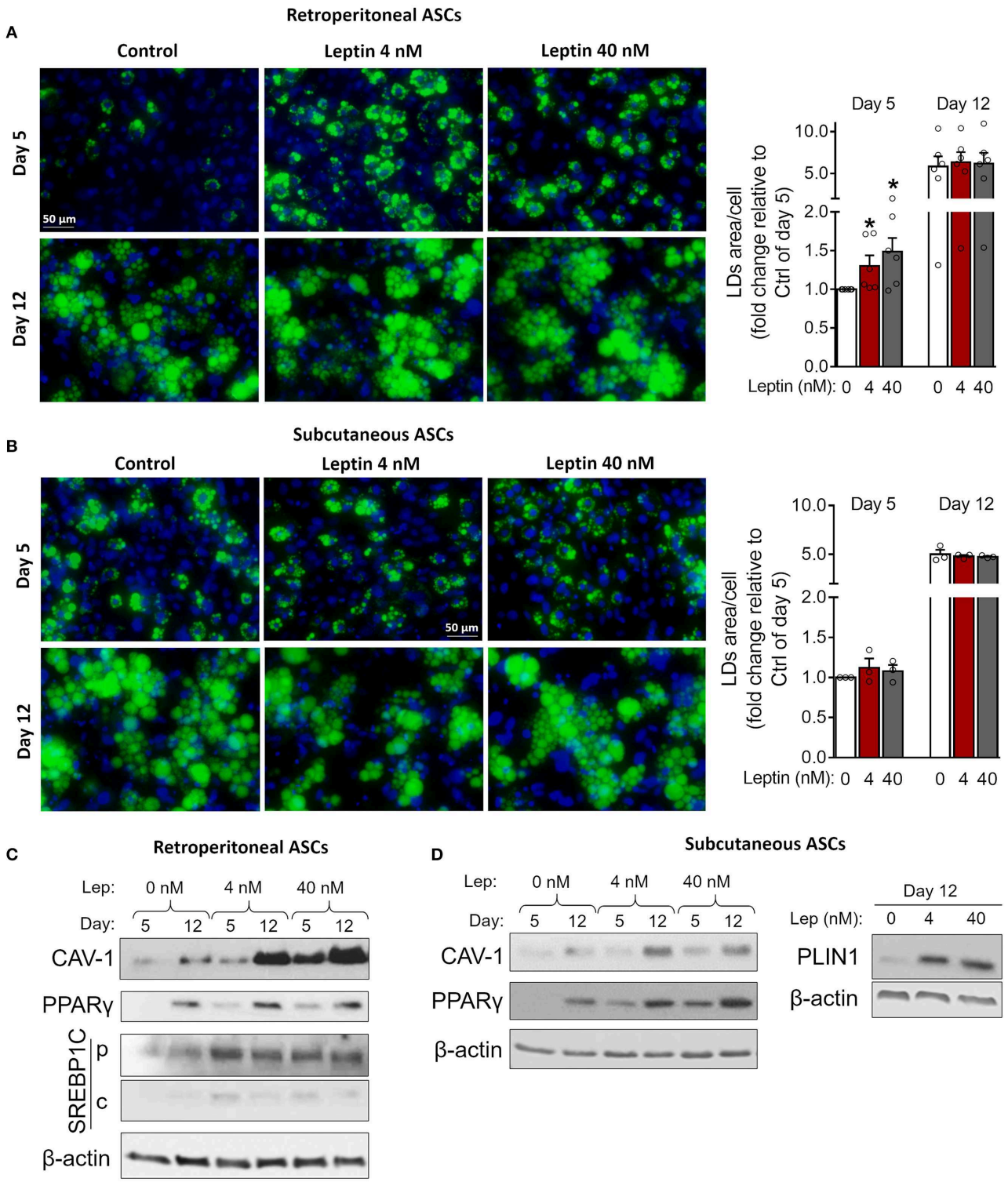

FIGURE 5 | Leptin potentiates insulin-induced adipogenesis in ASCs. Adipose-derived stem cells from subcutaneous and retroperitoneal depots were isolated and then differentiated with insulin alone or insulin plus leptin (4 or 40 nM). **(A,B)** Fluorescence images of ASCs from **(A)** retroperitoneal and **(B)** subcutaneous depots that were differentiated into adipocytes and stained with Bodipy (green) for lipid droplets and with DAPI (blue) for nuclei. Images are representative of 3–6 independent experiments. Scale bar represents 50 µm. Graphs show the quantification of the green area per cell relative to the control group (insulin only) at day 5. Bars represent mean ± standard error of the mean of 3–5 independent experiments. *$p < 0.05$ relative to the control group of the same day. Statistical analyzes were performed by using Kolmogorov-Smirnov test. **(C,D)** Western blot analysis of CAV-1 and PPARγ and β-actin in ASCs differentiated at the conditions specified. Blots are representative of 3–5 independent experiments.

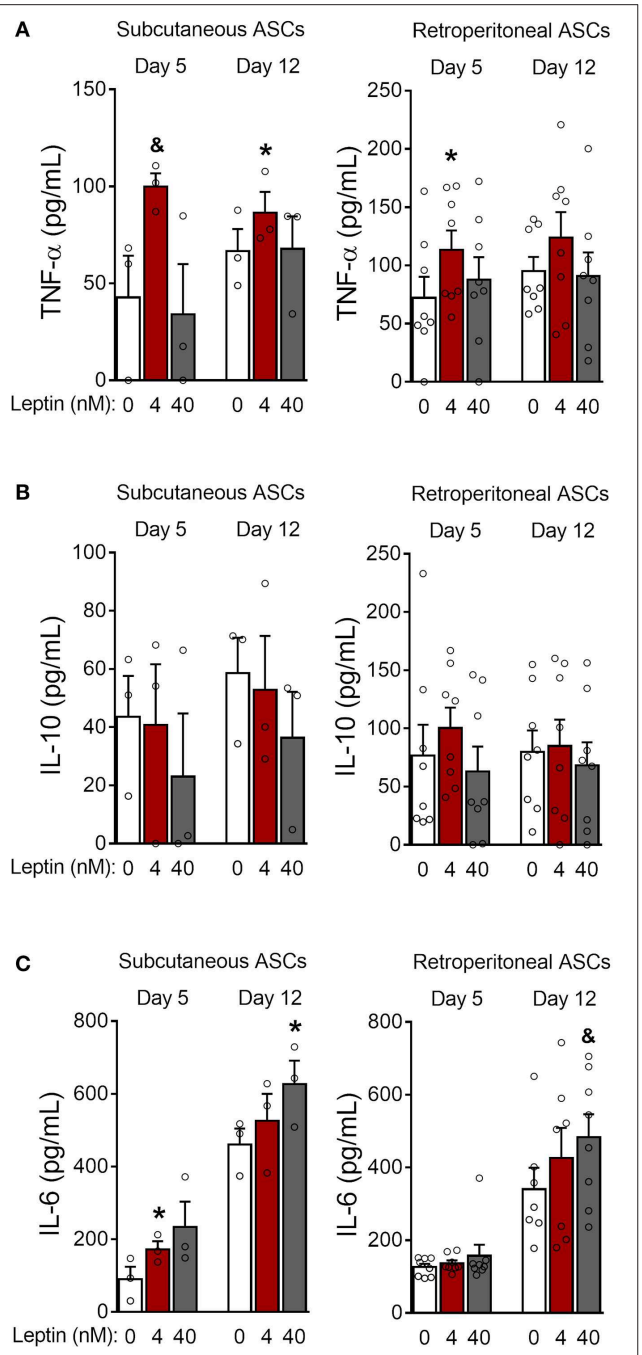

FIGURE 6 | Leptin induces a proinflammatory cytokine profile during ASCs differentiation. **(A–C)** ASCs from subcutaneous and retroperitoneal fat depots were differentiated for 5 and 12 days in the presence of leptin (0, 4, or 40 nM) and the concentrations of **(A)** TNF-α, **(B)** IL-10, and **(C)** IL-6 were measured in the supernatants. Bars represent mean ± standard error of the mean of 3–8 independent experiments. $^{*}p < 0.05$ and $^{\&}p < 0.06$ compared to ASCs differentiated in the absence of leptin at the respective timepoint. Statistical analyzes were performed using paired *t*-test.

Also, high fat diet increased the numbers of adipocytes in the limb bone and reduced bone volume in wild type mice, but not in mice with the deletion of LepR in BM-MSCs (19). The authors clearly show that the local signaling of leptin in bone marrow stromal precursors, during obesity, is essential for the adipocyte commitment and differentiation (19). In another work, Tencerova et al. (50) showed that LepR-positive BM-MSCs of obese individuals are more likely to differentiate into adipocytes, and that the silencing of LepR in BM-MSCs from obese individuals favored osteogenesis and reduced adipogenesis, with decreased expression of several adipogenesis-associated genes, alongside the impairment of the staining for lipid droplets (50). These results indicate that leptin's local effect may contribute *in vivo* to adipogenesis. Even though they used *in vivo* or *ex vivo* models and different sets of stromal cells, their results are in accordance with our data showing that leptin has local adipogenic effects in stromal cells. In addition, our work supports that leptin may be important throughout the adipogenic process, not only at the commitment phase.

Insulin is a classic inductor of adipogenesis and therefore is present in the majority of the adipogenesis *in vitro* protocols (22, 30). Indeed, when we remove insulin from the culture media, we see a dramatic reduction in differentiation. As aforementioned, when we differentiate cells with leptin in addition to insulin, we boost differentiation. These results may be explained by the fact that both leptin and insulin signal through PI3K/AKT/mTOR pathway (31, 51). Interestingly, here we also show that leptin sustains adipocyte maturation of cells cultured in insulin-free medium. These findings highlight that leptin can compensate for insulin absence when it comes to adipogenesis, with potential implications in pathological conditions such as types 1 and 2 diabetes. In patients with type 1 diabetes (T1D), who have little or no production of insulin, there are several metabolic alterations as hyperglycemia, weight loss and enhanced lipolysis with augmented lipotoxicity (52, 53). For these patients, insulin long-term usage often leads to unwanted side effects such as ectopic fat deposition and disabling episodes of hypoglycemia. In animal models of T1D, plasma levels of leptin are diminished compared to healthy animals (52–54). In these models, leptin administration improved survival, weight gain and glycemia, which were associated with metabolic recovery toward a reduction of hepatic gluconeogenesis, adipocyte lipolysis and diminished circulation of free fatty acids (52–54). Although leptin was not able to recover β-cell function and insulin secretion in neither of these studies, these findings point out beneficial actions of leptin in the absence of insulin that can overcome several caveats f insulin therapy. The described insulin-independent actions of leptin, especially regarding the recovery of body weight and decreased lipolysis, corroborate with our findings on the insulin-independent induction of adipocyte differentiation and maturation. Enhancement of adipogenesis may help to increase the lipid storage capacity of cells, dumping the circulation of free fatty acids and the deposition of ectopic fat *in vivo*. Similarly, the leptin analog metreleptin is the main treatment to human lipodystrophy syndromes, also improving several metabolic parameters (55). Even though metreleptin does not recover the deficiency in subcutaneous adipose tissue in lipodystrophic patients, most of these patients lack the major adipogenic pathways, including those involving CAV-1 and PLIN-1, among others. Moreover, these patients are also treated with metformin, which inhibits the mTOR pathway (55). There will be little or no possibility for leptin to induce adipogenesis and recover subcutaneous WAT in these cases, since either the

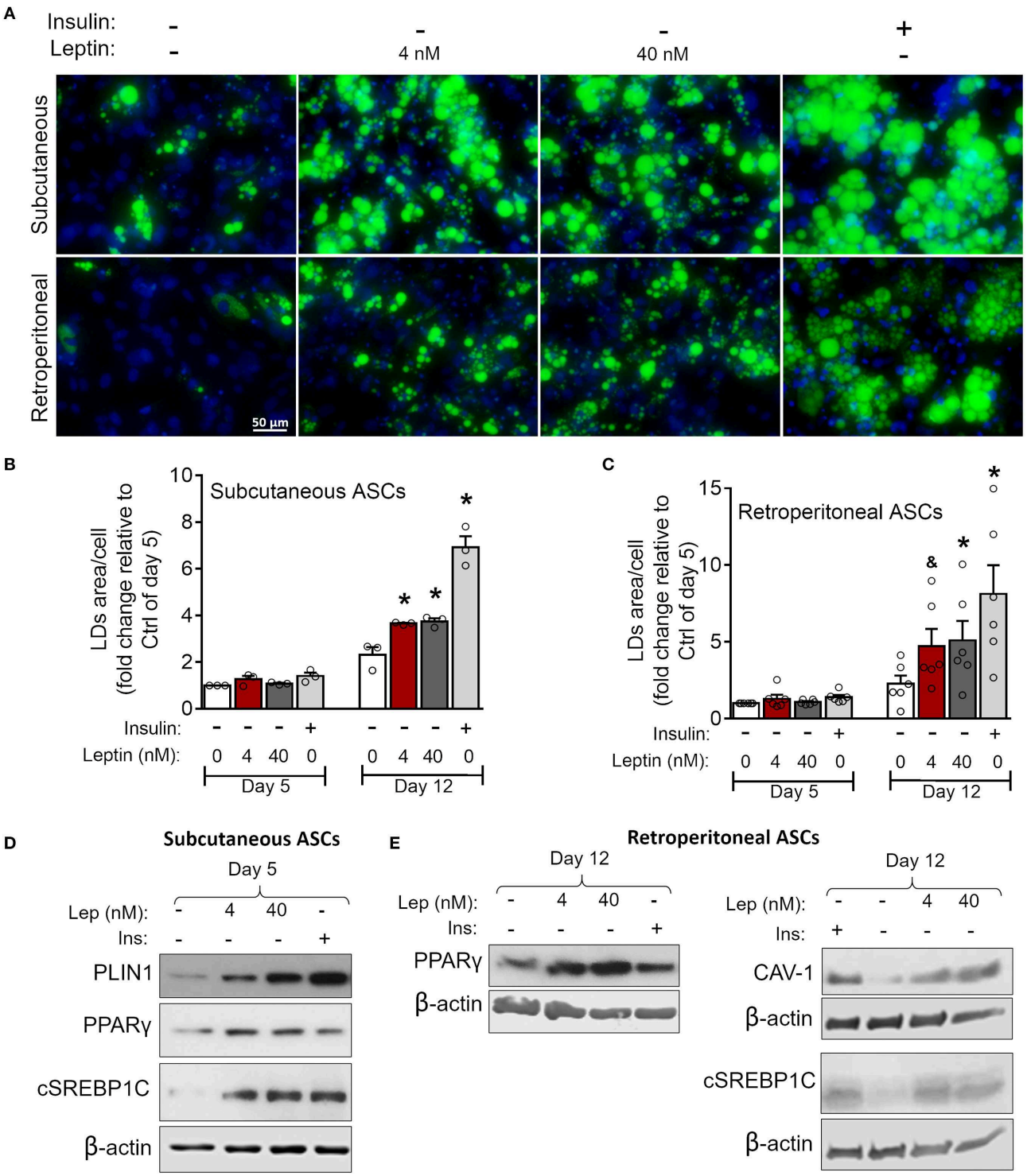

FIGURE 7 | Leptin induces adipogenesis in ASCs independently on insulin. ASCs from subcutaneous and retroperitoneal depots were isolated and then differentiated up to 5 or 12 days with neither insulin nor leptin, leptin (4 or 40 nM), or insulin. **(A)** Fluorescence images of ASCs differentiated for 12 days and stained with Bodipy (green) for lipid droplets and with DAPI (blue) for nuclei. Images are representative of 3–6 independent experiments from different animal pools. Scale bar represents 50 µm. **(B,C)** Quantification of the green area per cell in adipocytes differentiated from **(B)** subcutaneous or **(C)** retroperitoneal ASCs. Graphs depict the fold change relative to the group with no hormone supplementation at day 5. Bars represent mean ± standard error of the mean of 3–5 independent experiments. *Means $p < 0.05$ and & means $p = 0.06$ relative to the control group at the same day. Statistical analyzes were performed by using One-way ANOVA with Dunnet's post-test. **(D)** Western blot analysis of PLIN1, PPARγ, cleaved SREBP1C (cSREBP1C), and β-actin in subcutaneous ASCs or **(E)** CAV-1, cSREBP1C, PPARγ, and β-actin in retroperitoneal ASCs after 12 days of differentiation in each condition. Blots are representative of 3–5 independent experiments.

major adipogenic pathways are primarily absent or inhibited by the treatment for diabetes. Specific studies should be done to determine the capacity of leptin in restoring adipogenesis within the different forms of lipodystrophy.

As previously mentioned, leptin and insulin share the activation of the mTOR pathway (31). It was shown that adipocyte-specific deletion of the mTOR gene in mice dramatically reduced white and brown fat masses but did not change body weight (11). This was explained by the ectopic fat accumulation in the heart, spleen and liver, with greater circulation of free fatty acids (11). These and other studies establish mTOR as an indispensable protein for lipid uptake (56), storage and adipogenesis (11, 57–59). With that in mind, we sought to determine if the proadipogenic effects of leptin in preadipocytes were also mediated by activation of the mTOR pathway. For this purpose, we treated 3T3-L1 preadipocytes—which had no insulin supplementation at all—with leptin in the presence or absence of rapamycin. Confirming our hypothesis, leptin effect on the increase of lipid droplet's biogenesis in preadipocytes was mediated by the mTOR signaling pathway as rapamycin treatment completely abolished lipid accumulation in leptin-treated cells.

Besides its clear role in the control of energy homeostasis and adipose tissue function, leptin is also very important in immune processes. For instance, it has been shown to participate in the activation and recruitment of immune cells, such as macrophages (15, 60), neutrophils (18), and eosinophils (13). In obesity, adipose cells secrete large amounts of immunometabolic mediators that usually cause a derange in homeostasis (2, 5, 61, 62). Adipose tissue, which includes adipocytes and stromal cells, becomes chronically inflamed with enhanced secretion of proinflammatory mediators, such as TNF-α and IL-6, and a decrease in anti-inflammatory ones, such as IL-10 (5, 63). Leptin was found to participate in the induction of proinflammatory cytokines in dendritic cells (17), T cells (17), and macrophages (15, 44, 60). In this report we show that leptin is a proinflammatory factor also in adipocytes, as shown by the increase in TNF-α and the decrease in IL-10 production by 3T3-L1 cells, and increased TNF-α and IL-6 in differentiated ASCs. Although the secretion of the chemokines KC/CXCL1 and MCP-1/CCL2 remained unchanged in 3T3-L1, our results show that leptin's actions on adipocytes contribute to the inflammatory profile characteristic of obesity.

In obesity, leptin central effects (i.e., induction of energy expenditure) is impaired, therefore its local effects may prevail and contribute to white adipose tissue expansion and enhanced inflammatory milieu. In addition, the direct induction of leptin signaling pathways in preadipocytes and adipocytes is sufficient to support adipogenesis regardless of the presence of insulin. Our data open a new perspective for the study of leptin as an inductor of adipogenesis and associated inflammation.

DATA AVAILABILITY STATEMENT

All datasets generated for this study are included in the article/**Supplementary Material**.

ETHICS STATEMENT

The animal study was reviewed and approved by Committee of Ethics in Animal Research from Oswaldo Cruz Institute/CEUA-IOC L011.2015.

AUTHOR CONTRIBUTIONS

All authors had critically revised and approved the final version of the manuscript. LP participated in the conception of the study, designed and executed experiments, analyzed and interpreted the data, and wrote the manuscript. SL participated in the conception of the study and in scientific discussions. EH participated in the design and execution of experiments, analysis and interpretation of data, and in scientific discussions. JP participated in the design and execution of experiments and in scientific discussions. CA participated in the conception of the study and in scientific discussions. PM-V participated in the design of experiments and in scientific discussions. PB participated in the conception and direction of the study, design of experiments, analysis, and interpretation of data. CM-M participated in the conception and direction of the study, design and execution of experiments, analysis, and interpretation of data.

FUNDING

This work was supported by grants from Conselho Nacional de Desenvolvimento Científico e Tecnológico (CNPq) (LP, CM-M, and PB), Fundação de Amparo à Pesquisa do Estado do Rio de Janeiro (FAPERJ) (CM-M and PB), Programa Estratégico de Apoio à Pesquisa em Saúde (PAPES)/Fiocruz (CM-M), Instituto Oswaldo Cruz/Fiocruz grant (PB), Coordenação de Aperfeiçoamento de Pessoal de Nível Superior - Brasil (CAPES) - Finance Code 001, and (LP, PB, and CM-M), FAPESP (2015/15626-8; PM-V).

ACKNOWLEDGMENTS

The authors thank the Multiuser Research Facility of flow cytometry and Daniela Gois Beghini's technical assistance for the characterization of the adipose stromal cells. Also, the authors thank Jens Rietdorf and Edson Fernandes de Assis for technical assistance and Christianne Bandeira de Melo for the important scientific discussions. We also thank the PrInt-Fiocruz-CAPES Program and the Molecular and Cellular Biology Postgraduate Program, Oswaldo Cruz Institute - Fiocruz/RJ for the support.

SUPPLEMENTARY MATERIAL

The Supplementary Material for this article can be found online at: https://www.frontiersin.org/articles/10.3389/fendo.2019.00841/full#supplementary-material

REFERENCES

1. WHO. *Obesity and Overweight*. (2018). Available online at: http://www.who.int/en/news-room/fact-sheets/detail/obesity-and-overweight (accessed February 16, 2018).
2. Unamuno X, Gómez-Ambrosi J, Rodríguez A, Becerril S, Frühbeck G, Catalán V. Adipokine dysregulation and adipose tissue inflammation in human obesity. *Euro J Clin Invest.* (2018) 48:e12997. doi: 10.1111/eci.12997
3. Gallagher EJ, LeRoith D. Obesity and diabetes: the increased risk of cancer and cancer-related mortality. *Physiol Rev.* (2015) 95:727–48. doi: 10.1152/physrev.00030.2014
4. Koliaki C, Liatis S, Kokkinos A. Obesity and cardiovascular disease: revisiting an old relationship. *Metabolism.* (2018) 92:98–107. doi: 10.1016/j.metabol.2018.10.011
5. Vegiopoulos A, Rohm M, Herzig S. Adipose tissue: between the extremes. *EMBO J.* (2017) 36:1999–2017. doi: 10.15252/embj.201696206
6. Zhang Y, Proenca R, Maffei M, Barone M, Leopold L, Friedman JM. Positional cloning of the mouse obese gene and its human homologue. *Nature.* (1994) 372:425–32. doi: 10.1038/372425a0
7. Coleman DL. Obese and diabetes: two mutant genes causing diabetes-obesity syndromes in mice. *Diabetologia.* (1978) 14:141–8. doi: 10.1007/BF00429772
8. Xu J, Bartolome CL, Low CS, Yi X, Chien C-H, Wang P, et al. Genetic identification of leptin neural circuits in energy and glucose homeostases. *Nature.* (2018) 556:505–9. doi: 10.1038/s41586-018-0049-7
9. Amitani M, Asakawa A, Amitani H, Inui A. The role of leptin in the control of insulin-glucose axis. *Front Neurosci.* (2013) 7:1–12. doi: 10.3389/fnins.2013.00051
10. Cota D, Proulx K, Smith KAB, Kozma SC, Thomas G, Woods SC, et al. Hypothalamic mTOR signaling regulates food intake. *Science.* (2006) 312:927–30. doi: 10.1126/science.1124147
11. Shan T, Zhang P, Jiang Q, Xiong Y, Wang Y, Kuang S. Adipocyte-specific deletion of mTOR inhibits adipose tissue development and causes insulin resistance in mice. *Diabetologia.* (2016) 59:1995–2004. doi: 10.1007/s00125-016-4006-4
12. El-Chaâr D, Gagnon A, Sorisky A. Inhibition of insulin signaling and adipogenesis by rapamycin: effect on phosphorylation of p70 S6 kinase vs eIF4E-BP1. *Int J Obesity Relat Metab Disord.* (2004) 28:191–8. doi: 10.1038/sj.ijo.0802554
13. Amorim NRT, Luna-Gomes T, Gama-Almeida M, Souza-Almeida G, Canetti C, Diaz BL, et al. Leptin elicits LTC4 synthesis by eosinophils mediated by sequential two-step autocrine activation of CCR3 and PGD2 receptors. *Front Immunol.* (2018) 9:2139. doi: 10.3389/fimmu.2018.02139
14. Fazolini NPB, Cruz ALS, Werneck MBF, Viola JPB, Maya-Monteiro CM, Bozza PT. Leptin activation of mTOR pathway in intestinal epithelial cell triggers lipid droplet formation, cytokine production and increased cell proliferation. *Cell Cycle.* (2015) 14:2667–76. doi: 10.1080/15384101.2015.1041684
15. Maya-Monteiro CM, Almeida PE, D'Avila H, Martins AS, Rezende AP, Castro-Faria-Neto H, et al. Leptin induces macrophage lipid body formation by a phosphatidylinositol 3-kinase- and mammalian target of rapamycin-dependent mechanism. *J Biol Chem.* (2008) 283:2203–10. doi: 10.1074/jbc.M706706200
16. Chehab FF. 20 years of leptin: leptin and reproduction: past milestones, present undertakings, and future endeavors. *J Endocrinol.* (2014) 223:T37–48. doi: 10.1530/JOE-14-0413
17. Moraes-Vieira PMM, Larocca RA, Bassi EJ, Peron JPS, Andrade-Oliveira V, Wasinski F, et al. Leptin deficiency impairs maturation of dendritic cells and enhances induction of regulatory T and Th17 cells. *Eur J Immunol.* (2014) 44:794–806. doi: 10.1002/eji.201343592
18. Souza-Almeida G, D'Avila H, Almeida PE, Luna-Gomes T, Liechocki S, Walzog B, et al. Leptin mediates *in vivo* neutrophil migration: involvement of tumor necrosis factor-alpha and CXCL1. *Front Immunol.* (2018) 9:111. doi: 10.3389/fimmu.2018.00111
19. Yue R, Zhou BO, Shimada IS, Zhao Z, Morrison SJ. Leptin receptor promotes adipogenesis and reduces osteogenesis by regulating mesenchymal stromal cells in adult bone marrow. *Cell Stem Cell.* (2016) 18:782–96. doi: 10.1016/j.stem.2016.02.015
20. Balland E, Cowley MA. New insights in leptin resistance mechanisms in mice. *Front Neuroendocrinol.* (2015) 39:59–65. doi: 10.1016/j.yfrne.2015.09.004
21. Myers MG, Leibel RL, Seeley RJ, Schwartz MW, Schwartz MW. Obesity and leptin resistance: distinguishing cause from effect. *Trends Endocrinol Metab.* (2010) 21:643–51. doi: 10.1016/j.tem.2010.08.002
22. Green H, Kehinde O. An established preadipose cell line and its differentiation in culture. II Factors affecting the adipose conversion. *Cell.* (1975) 5:19–27. doi: 10.1016/0092-8674(75)90087-2
23. Iwan-Zietek I, Ruszkowska-Ciastek B, Michalska M, Overskaug E, Goralczyk K, Dabrowiecki S, et al. Association of adiponectin and leptin-to-adiponectin ratio with the function of platelets in morbidly obese patients. *J Physiol Pharmacol.* (2016) 67:555–61.
24. Morel O, Luca F, Grunebaum L, Jesel L, Meyer N, Desprez D, et al. Short-term very low-calorie diet in obese females improves the haemostatic balance through the reduction of leptin levels, PAI-1 concentrations and a diminished release of platelet and leukocyte-derived microparticles. *Int J Obesity.* (2011)35:1479–86. doi: 10.1038/ijo.2011.19
25. Wing RR, Sinha MK, Considine RV, Lang W, Caro JF. Relationship between weight loss maintenance and changes in serum leptin levels. *Horm Metab Res.* (1996) 28:698–703. doi: 10.1055/s-2007-979881
26. Schindelin J, Arganda-Carreras I, Frise E, Kaynig V, Longair M, Pietzsch T, et al. Fiji: an open-source platform for biological-image analysis. *Nat Methods.* (2012) 9:676–82. doi: 10.1038/nmeth.2019
27. Cai H, Dong LQ, Liu F. Recent advances in adipose mTOR signaling and function: therapeutic prospects. *Trends Pharmacol Sci.* (2016) 37:303–17. doi: 10.1016/j.tips.2015.11.011
28. Laplante M, Sabatini DM. An emerging role of mTOR in lipid biosynthesis. *Curr Biol.* (2009) 19:R1046–52. doi: 10.1016/j.cub.2009.09.058
29. Luo L, Liu M. Adipose tissue in control of metabolism. *J Endocrinol.* (2016) 231:R77–99. doi: 10.1530/JOE-16-0211
30. Boucher J, Softic S, El Ouaamari A, Krumpoch MT, Kleinridders A, Kulkarni RN, et al. Differential roles of insulin and IGF-1 receptors in adipose tissue development and function. *Diabetes.* (2016) 65:2201–13. doi: 10.2337/db16-0212
31. Varela L, Horvath TL. Leptin and insulin pathways in POMC and AgRP neurons that modulate energy balance and glucose homeostasis. *EMBO Rep.* (2012) 13:1079–86. doi: 10.1038/embor.2012.174
32. Wang ZV, Scherer PE. Adiponectin, the past two decades. *J Mol Cell Biol.* (2016) 8:93–100. doi: 10.1093/jmcb/mjw011
33. Siegrist-Kaiser CA, Pauli V, Juge-Aubry CE, Boss O, Pernin A, Chin WW, et al. Direct effects of leptin on brown and white adipose tissue. *J Clin Invest.* (1997) 100:2858–64. doi: 10.1172/JCI119834
34. Rodríguez VM, Macarulla MT, Echevarría E, Portillo MP. Lipolysis induced by leptin in rat adipose tissue from different anatomical locations. *Eur J Nutr.* (2003) 42:149–53. doi: 10.1007/s00394-003-0405-7
35. Jaubert A-M, Penot G, Niang F, Durant S, Forest C. Rapid nitration of adipocyte phosphoenolpyruvate carboxykinase by leptin reduces glyceroneogenesis and induces fatty acid release. *PLoS ONE.* (2012) 7:e40650. doi: 10.1371/journal.pone.0040650
36. Rhee SD, Sung YY, Jung WH, Cheon HG. Leptin inhibits rosiglitazone-induced adipogenesis in murine primary adipocytes. *Mol Cell Endocrinol.* (2008) 294: 61–9. doi: 10.1016/j.mce.2008.08.018
37. Niang F, Benelli C, Ribière C, Collinet M, Mehebik-Mojaat N, Penot G, et al. Leptin induces nitric oxide-mediated inhibition of lipolysis and glyceroneogenesis in rat white adipose tissue. *J Nutr.* (2011) 141:4–9. doi: 10.3945/jn.110.125765
38. Nobre JL, Lisboa PC, Carvalho JC, Martins MR, Vargas S, Barja-Fidalgo C, et al. Leptin blocks the inhibitory effect of vitamin D on adipogenesis and cell proliferation in 3T3-L1 adipocytes. *Gen Comp Endocrinol.* (2018) 266:1–8. doi: 10.1016/j.ygcen.2018.01.014
39. Ambati S, Kim H-K, Yang J-Y, Lin J, Della-Fera MA, Baile CA. Effects of leptin on apoptosis and adipogenesis in 3T3-L1 adipocytes. *Biochem Pharmacol.* (2007) 73:378–84. doi: 10.1016/j.bcp.2006.10.009
40. Weisberg SP, McCann D, Desai M, Rosenbaum M, Leibel RL, Ferrante AW. Obesity is associated with macrophage accumulation in adipose tissue. *J Clin Invest.* (2003) 112:1796–808. doi: 10.1172/JCI200319246

41. Li C, Xu MM, Wang K, Adler AJ, Vella AT, Zhou B. Macrophage polarization and meta-inflammation. *Transl Res.* (2018) 191:29–44. doi: 10.1016/j.trsl.2017.10.004
42. Zeng W, Pirzgalska RM, Pereira MMA, Kubasova N, Barateiro A, Seixas E, et al. Sympathetic neuro-adipose connections mediate leptin-driven lipolysis. *Cell.* (2015) 163:84–94. doi: 10.1016/j.cell.2015.08.055
43. Ingalls AM, Dickie MM, Snell GD. Obese, a new mutation in the house mouse. *J Heredity.* (1950) 41:317–8. doi: 10.1093/oxfordjournals.jhered.a106073
44. Monteiro L, da Silva Pereira JA, Palhinha L, Moraes-Vieira PMM. Leptin in the regulation of the immunometabolism of adipose tissue-macrophages. *J Leukocyte Biol.* (2019) 106:703–16. doi: 10.1002/JLB.MR1218-478R
45. Guilherme A, Virbasius JV, Puri V, Czech MP. Adipocyte dysfunctions linking obesity to insulin resistance and type 2 diabetes. *Nat Rev Mol Cell Biol.* (2008) 9:367–77. doi: 10.1038/nrm2391
46. Souza SC, de Vargas LM, Yamamoto MT, Lien P, Franciosa MD, Moss LG, et al. Overexpression of perilipin A and B blocks the ability of tumor necrosis factor alpha to increase lipolysis in 3T3-L1 adipocytes. *J Biol Chem.* (1998) 273:24665–9. doi: 10.1074/jbc.273.38.24665
47. Xu L, Shi C, Xu G, Chen L, Zhu L, Zhu L, et al. TNF-α, IL-6, and leptin increase the expression of miR-378, an adipogenesis-related microRNA in human adipocytes. *Cell Biochem Biophys.* (2014) 70:771–6. doi: 10.1007/s12013-014-9980-x
48. Zhu L, Chen L, Shi C-M, Xu G-F, Xu L-L, Zhu L-L, et al. MiR-335, an adipogenesis-related MicroRNA, is involved in adipose tissue inflammation. *Cell Biochem Biophys.* (2014) 68:283–90. doi: 10.1007/s12013-013-9708-3
49. Pereira S, O'Dwyer SM, Webber TD, Baker RK, So V, Ellis CE, et al. Metabolic effects of leptin receptor knockdown or reconstitution in adipose tissues. *Sci Rep.* (2019) 9:3307. doi: 10.1038/s41598-019-39498-3
50. Tencerova M, Frost M, Figeac F, Nielsen TK, Ali D, Lauterlein JJL, et al. Obesity-associated hypermetabolism and accelerated senescence of bone marrow stromal stem cells suggest a potential mechanism for bone fragility. *Cell Rep.* (2019) 27:2050–62.e6. doi: 10.1016/j.celrep.2019.04.066
51. Zhang Z-Y, Dodd GT, Tiganis T. Protein tyrosine phosphatases in hypothalamic insulin and leptin signaling. *Trends Pharmacol Sci.* (2015) 36:661–74. doi: 10.1016/j.tips.2015.07.003
52. Mittendorfer B, Klein S. Absence of leptin triggers type 1 diabetes. *Nat Med.* (2014) 20:705–6. doi: 10.1038/nm.3629
53. Fujikawa T, Chuang JC, Sakata I, Ramadori G, Coppari R. Leptin therapy improves insulin-deficient type 1 diabetes by CNS-dependent mechanisms in mice. *Proc Natl Acad Sci USA*. (2010) 107:17391–6. doi: 10.1073/pnas.1008025107
54. Perry RJ, Zhang X-M, Zhang D, Kumashiro N, Camporez J-PG, Cline GW, et al. Leptin reverses diabetes by suppression of the hypothalamic-pituitary-adrenal axis. *Nat Med.* (2014) 20:759–63. doi: 10.1038/nm.3579
55. Brown RJ, Araujo-Vilar D, Cheung PT, Dunger D, Garg A, Jack M, et al. The diagnosis and management of lipodystrophy syndromes: a multi-society practice guideline. *J Clin Endocrinol Metab.* (2016) 101:4500–11. doi: 10.1210/jc.2016-2466
56. Blanchard P-G, Festuccia WT, Houde VP, St-Pierre P, Brûlé S, Turcotte V, et al. Major involvement of mTOR in the PPARγ-induced stimulation of adipose tissue lipid uptake and fat accretion. *J Lipid Res.* (2012) 53:1117–25. doi: 10.1194/jlr.M021485
57. Haissaguerre M, Saucisse N, Cota D. Influence of mTOR in energy and metabolic homeostasis. *Mol Cell Endocrinol.* (2014) 397: 67–77. doi: 10.1016/j.mce.2014.07.015
58. Caron A, Richard D, Laplante M. The roles of mTOR complexes in lipid metabolism. *Ann Rev Nutr.* (2015) 35:321–48. doi: 10.1146/annurev-nutr-071714-034355
59. Ricoult SJH, Manning BD. The multifaceted role of mTORC1 in the control of lipid metabolism. *EMBO Rep.* (2013) 14:242–51. doi: 10.1038/embor.2013.5
60. Desai HR, Sivasubramaniyam T, Revelo XS, Schroer SA, Luk CT, Rikkala PR, et al. Macrophage JAK2 deficiency protects against high-fat diet-induced inflammation. *Sci Rep.* (2017) 7:7653. doi: 10.1038/s41598-017-07923-0
61. Hernandez-Carretero A, Weber N, La Frano MR, Ying W, Lantero Rodriguez J, Sears DD, et al. Obesity-induced changes in lipid mediators persist after weight loss. *Int J Obes.* (2018) 42:728–36. doi: 10.1038/ijo.2017.266
62. Reilly SM, Saltiel AR. Adapting to obesity with adipose tissue inflammation. *Nat Rev Endocrinol.* (2017) 13:633–43. doi: 10.1038/nrendo.2017.90
63. Rakotoarivelo V, Variya B, Ilangumaran S, Langlois M-F, Ramanathan S. Inflammation in human adipose tissues-Shades of gray, rather than white and brown. *Cytokine Growth Factor Rev.* (2018) 44:28–37. doi: 10.1016/j.cytogfr.2018.10.001

Conflict of Interest: The authors declare that the research was conducted in the absence of any commercial or financial relationships that could be construed as a potential conflict of interest.

frontiers in Endocrinology

ORIGINAL RESEARCH
published: 08 January 2020
doi: 10.3389/fendo.2019.00866

Evidence in Favor of an Alternative Glucocorticoid Synthesis Pathway During Acute Experimental Chagas Disease

Esdras da Silva Oliveira Barbosa[1], *Eduardo A. Roggero*[1], *Florencia B. González*[1], *Rocío del Valle Fernández*[1], *Vinicius Frias Carvalho*[2,3], *Oscar A. Bottasso*[1], *Ana R. Pérez*[1,4] *and Silvina R. Villar*[1,4]*

[1] *Institute of Clinical and Experimental Immunology of Rosario (IDICER-CONICET-UNR), Rosario, Argentina,* [2] *Laboratory of Inflammation, Oswaldo Cruz Institute, Oswaldo Cruz Foundation, Rio de Janeiro, Brazil,* [3] *National Institute of Science and Technology on Neuroimmunomodulation (INCT-NIM), Rio de Janeiro, Brazil,* [4] *Center for Research and Production of Biological Reagents (CIPREB), Faculty of Medical Sciences, National University of Rosario, Rosario, Argentina*

OPEN ACCESS

Edited by:
James A. Carr,
Texas Tech University, United States

Reviewed by:
Phileno Pinge-Filho,
State University of Londrina, Brazil
Aparecida Donizette Malvezi,
State University of Londrina, Brazil
Fabiana Simão Machado,
Federal University of Minas Gerais, Brazil

***Correspondence:**
Silvina R. Villar
villar@idicer-conicet.gob.ar;
villar_silvina@hotmail.com

Specialty section:
This article was submitted to Neuroendocrine Science, a section of the journal Frontiers in Endocrinology

Received: *16 July 2019*
Accepted: *26 November 2019*
Published: *08 January 2020*

Citation:
da Silva Oliveira Barbosa E, Roggero EA, González FB, Fernández RdV, Carvalho VF, Bottasso OA, Pérez AR and Villar SR (2020) Evidence in Favor of an Alternative Glucocorticoid Synthesis Pathway During Acute Experimental Chagas Disease. Front. Endocrinol. 10:866. doi: 10.3389/fendo.2019.00866

It is well-established that infectious stress activates the hypothalamus–pituitary–adrenal axis leading to the production of pituitary adrenocorticotropin (ACTH) and adrenal glucocorticoids (GCs). Usually, GC synthesis is mediated by protein kinase A (PKA) signaling pathway triggered by ACTH. We previously demonstrated that acute murine Chagas disease courses with a marked increase of GC, with some data suggesting that GC synthesis may be ACTH-dissociated in the late phase of this parasitic infection. Alternative pathways of GC synthesis have been reported in sepsis or mental diseases, in which interleukin (IL)-1β, prostaglandin E2 (PGE2), and/or cAMP-activated guanine nucleotide exchange factor 2 (EPAC2) are likely to play a role in this regard. Accordingly, we have searched for the existence of an ACTH-independent pathway in an experimental model of a major parasitic disease like Chagas disease, in addition to characterizing potential alternative pathways of GC synthesis. To this end, C57BL/6 male mice were infected with *T. cruzi* (Tc), and evaluated throughout the acute phase for several parameters, including the kinetic of GC and ACTH release, the adrenal level of MC2R (ACTH receptor) expression, the p-PKA/PKA ratio as ACTH-dependent mechanism of signal transduction, as well as adrenal expression of IL-1β and its receptor, EPAC2 and PGE2 synthase. Our results reveal the existence of two phases involved in GC synthesis during Tc infection in mice, an initial one dealing with the well-known ACTH-dependent pathway, followed by a further ACTH-hyporesponsive phase. Furthermore, inflamed adrenal microenvironment may tune the production of intracellular mediators that also operate upon GC synthesis, like PGE2 synthase and EPAC2, as emerging driving forces for GC production in the advanced course of Tc infection. In essence, GC production seems to be associated with a biphasic action of PGE2, suggesting that the effect of PGE2/cAMP in the ACTH-independent second phase may be mediated by EPAC2.

Keywords: adrenal glands, glucocorticoid, ACTH, *Trypanosoma cruzi*, EPAC2, IL-1β, PGE2, ACTH-independent

INTRODUCTION

The hypothalamus–pituitary–adrenal (HPA) axis is activated in diverse stressful situations, like pathological and metabolic disorders (1) or infectious diseases (2, 3), to preserve homeostasis (4) by controlling the availability of glucocorticoid (GC) hormones: corticosterone (CT) in rodents and cortisol in humans (4–6). Adrenocorticotropic hormone (ACTH) is the main stimulus for GC synthesis and release, acting through the melanocortin 2 receptor (MC2R). MC2R activation induces the synthesis of the second messenger cAMP, which, in a protein kinase A (PKA)-dependent fashion, induces the expression of many steroidogenic enzymes transforming cholesterol to GC (7).

Since pituitary disorders lead to secondary adrenal insufficiency (8), elevated GC concentrations have been traditionally ascribed as being due to a pituitary-stimulated increase of ACTH. Nevertheless, in the last decades, it became evident that alternative pathways of GC steroidogenesis may also occur in the context of some pathological situations. Patients with sepsis (9–12), or undergoing surgery (13, 14), as well as presenting malignant diseases or depression (15) often show in plasma-augmented GC amounts without changes in ACTH levels (16, 17). The dissociation between the ACTH and GC levels during critical illnesses may be envisioned as an adaptive phenomenon addressed to preserve elevated GC levels to respond as appropriately as possible to the stress-related needs. One possible alternative pathway involves the production of cAMP (in an ACTH-independent fashion), and the so-called cAMP-activated guanine nucleotide exchange factor 2 (EPAC2) (18–21), whose positive effects upon the steroideogenic pathway are exerted through mechanisms not yet fully described. Diverse mediators may be involved in the cAMP rise in the absence of ACTH, like prostaglandins (22, 23), and indirectly, some inflammatory cytokines (24, 25).

Trypanosoma cruzi (Tc) is a protozoan parasite causing Chagas disease, a main parasitic disease in Latin America. Chagas disease is currently spreading in a non-vector way throughout the world due to migratory flows. The parasite usually elicits an intense systemic response able to damage essential organs, i.e., heart and digestive tract (26, 27), causing disability. Moreover, oral breaks course with high lethality (28, 29). We previously demonstrated that Tc acute infection in C57BL/6 mice induces a strong release of GC, which is critical to mice survival (30, 31). Further studies developed in Tc-infected mice suggested that an ACTH-GC dissociation phenomenon may also occur in this protozoan infection. In fact, findings recorded from a single time point along the course of the acute infection showed that higher circulating levels of GC coexisted with slight ACTH amounts (32, 33), raising the view of a GC-driven negative feedback as playing a role in this regard.

Given this background, we searched for the occurrence of an ACTH-independent pathway in an experimental model of acute Chagas disease in addition to characterizing potential alternative pathways of GCs synthesis. Here, we evaluated throughout infection the kinetics of ACTH and GC production and intracellular pathways involved in GC synthesis in the adrenal gland. To discriminate ACTH-dependent from -independent pathways, Tc-infected mice were also assessed for MC2R expression and the PKA-pathway activation as a correlate of the ACTH-pathway activation, with the adrenal expression of interleukin (IL)-1β and its receptor (IL-1R), prostaglandin E2 (PGE2) synthase, and EPAC2 being studied as factors involved in the ACTH-independent pathway.

MATERIALS AND METHODS

Mice and Experimental Infection

C57BL/6 male mice, aged 6–8 weeks, were obtained from the Animal Facilities of Faculty of Medical Sciences, National University of Rosario (FCM-UNR). Trypomastigotes of the Tulahuen strain of Tc, corresponding to Tc lineage VI (34) were used. Mice were infected with 200 viable trypomastigotes subcutaneously. Parasitemia and the survival time were recorded following infection, to monitor the systemic repercussion of the acute disease, as previously reported (32).

Plasma ACTH and CT

Assessment of basal and infection-induced hormones was performed as previously reported (30, 32). Mice were housed individually 1 week before the beginning of the experiments and kept single-caged throughout the infection in temperature, and light-controlled rooms (light cycle from 7:00 a.m. to 7:00 p.m.). Plasma samples for hormone measurements were obtained from the tip of the tail between 8:00 and 10:00 a.m. (30, 32). Following that, blood was taken by cardiac puncture and adrenal glands were removed for other approaches detailed below. Plasma CT (IBL International, Hamburg, Germany) and ACTH levels (MD Bioproducts, Zurich, Switzerland) were determined by ELISA.

Plasma and Intra-adrenal Cytokine Measurements

Plasma and adrenal glands were obtained from control and Tc-infected animals throughout acute infection. Plasma IL-1β was measured by specific two-site enzyme-linked immunosorbent assay (ELISA) using an ELISA kit according to the manufacturer's specifications (Pharmingen, USA). Plasma TNF-α, IFN-γ, and IL-6 were measured using a murine BD Cytometric Bead Array (BD Biosciences, USA). Intra-adrenal IL-1β mRNA levels were assessed by RT-qPCR, as below described. All samples were assayed in duplicate.

Immunoblot Assays

Adrenal glands were homogenized in 4 volumes of 300 mmol/L sucrose with 1× protease inhibitor cocktail and 1× phosphatase inhibitor cocktail (SIGMA, Saint Louis, USA). Homogenates were centrifuged at 1,000*g* to remove unbroken cells, nuclei, and heavy membranes, based on previous studies (35). Proteins were quantified according to Lowry technique (36). For protein detection, samples were subjected to sodium dodecyl sulfate–polyacrylamide gel electrophoresis (SDS-PAGE) and electroblotted onto polyvinyl difluoride (PVDF) membranes (PerkinElmer Life Sciences, Inc., Boston, MA). Membranes were incubated with primary anti-mouse antibodies (anti-IL-1R, anti-PKA, anti-p-PKA, anti-EPAC2, anti-GAPDH, and anti-PGE2

TABLE 1 | Primer sequences and expected amplification products.

Transcript	Forward primers	Reverse primers	Product size (bp)
RPL13a Rpl13a, Gene ID: *22121*	*RPL13a-F* 5′-gca tga ggt cgg gtg gaa g-3′	*RPL13a-R* 5′-ctc cac att ctt ttc tgc ctg ttt-3′	133
IL-1r1 Il1r1, Gene ID: *16177*	*IL-1r1-F* 5′-tac agg gac tcc tgc tct ggt t-3′	*IL-1r1-R* 5′-ccc tcc aag acc tca ggc aa-3′	152
IL-1β Il1b, Gene ID: *16176*	*IL-1β-F* 5′-agc tga aag ctc tcc acc tca at-3′	*IL-1β-R* 5′-gtg ggt gtg ccg tct ttc att a-3′	163
EPAC2 Rapgef4, Gene ID: *56508*	*EPAC2-F* 5′-gta cta cag gag cca gcc ctt-3′	*EPAC2-R* 5′-atg gcc ttc gag gct cta atc t-3′	149
Ptgs2 Ptgs2, Gene ID: *19225*	*Ptgs2-F* 5′-agt tca tcc ctg acc ccc aag-3′	*Ptgs2-R* 5′-gaa aag gcg cag ttt atg ttg tct-3′	185
Mc2r Mc2r, Gene ID: 17200	*Mc2r-F* 5′-gac ctt ctg ccc aaa taa ccc tt-3′	*Mc2r -R* 5′-cgg ttg cag aag agc atc ctt t-3′	159

Specific selected primers for IL-1β, IL-1r1, EPAC2, Ptgs2, Mc2r, and RPL13a transcripts (quantitative polymerase chain reaction). RPL13a, ribosomal protein L13A; IL-1r1, interleukin 1 receptor type I; IL-1β, interleukin 1 beta; EPAC2, rap guanine nucleotide exchange factor (GEF) 4; Ptgs2, prostaglandin-endoperoxide synthase 2; Mcr2, melanocortin 2 receptor; bp, base pair.

synthase from Santa Cruz Biotechnology). The expression of total and phosphorylated isoforms of both PKA was analyzed by stripping in the same membrane. Finally, protein levels were detected by an enhanced chemiluminescence detection system (Pierce ECL, Thermo Fisher Scientific, USA). Immunoreactive bands were quantified by densitometry using the Image J software (imagej.nih.gov).

Immunohistochemical Staining

Immunohistochemistry studies were performed on 4-μm paraffin sections from adrenal glands. Sections were deparaffinized with xylene, rehydrated in a gradient series of alcohol (100, 95, and 45% alcohol) and rinsed in PBS. Each section was covered with 0.3% peroxyacetic acid for 15 min to block endogenous peroxidase activity and microwaved for antigen retrieval (100 W, 5 min × 3 min), and cooled at room temperature (RT) for 20 min. Then, sections were incubated with the anti-MC2R (Santa Cruz Biotechnology, dilution 1/50) at RT during 60 min, and then rinsed again. This step was followed by incubation with a streptavidin–biotin–peroxidase antibody complex (BD Pharmingen) for 30 min at RT. Slides were then treated with streptavidin peroxidase reagent for 10 min. The sections were visualized with 3,3′-diaminobenzidine (DAB), counterstained with hematoxylin, and mounted in mounting medium for microscopical observation.

RNA Isolation, cDNA Synthesis, and qPCR

Total RNA was isolated from adrenals using TRI Reagent (Genbiotech). cDNA was synthesized from 2 μg of total RNA by extension of oligo dT primers (Invitrogen, Carlsbad, CA, USA) with M-MuLV reverse transcriptase (Fermentas, Vilnius, Lithuania) according to the manufacturer's instructions. qPCR using 5X HOT FIREPol® Eva Green qPCR Mix Plus (Solis BioDyne, Tartu, Estonia) was performed in a StepOne Plus Real-Time PCR System (Thermo Fisher Scientific). Thermal cycling conditions were 15 min at 95°C followed by 40 PCR cycles of denaturing at 95°C for 15 s, 25 s for annealing at 60°C, and 25 s for elongation at 72°C. Fluorescence readings were performed during 10 s at 80°C before each elongation step. RPL13a (Gene ID: 22121) transcript was also measured and used as endogenous control to normalize the expression of mRNA determinations. External curves constituted by serial dilutions of cDNA of the transcript to be quantified were included in each run. Data are expressed as fold change with respect to RPL13a. Primer sequences are detailed in **Table 1**.

Statistics

Data are shown as mean ± standard error of the mean (SEM), unless otherwise stated. Statistical analysis was performed by the non-parametric analysis of variance Kruskal–Wallis followed by Dunn post-test ($k > 2$) or U de Mann–Whitney test ($k = 2$). The GraphPad Instat 4.0 software (GraphPad, California, USA) was used for statistical analyses, and differences were considered significant when p value was <0.05.

RESULTS

Tc Infection Induces Both ACTH-Dependent and -Independent Phases of GC Secretion

In Tc-infected C57BL/6 mice, parasitemia begins to be evident from day 7 post-infection (pi), followed by a marked and progressive increase (data not shown). As seen in earlier studies, infection was lethal in all animals with a mean survival time of 24–26 days (31, 32).

To investigate the dynamic of ACTH and GC secretion in Tc-infected mice, plasma samples were obtained at different time points following infection. The main GC hormone present in rodents is CT and in humans cortisol. Basal CT levels in blood from non-infected mice were 2.1 ± 1.3 μg/dl, while basal ACTH concentrations were 16.2 ± 2.8. GC rise began to be observed from day 7 pi and increased progressively until day 21 pi (20-fold

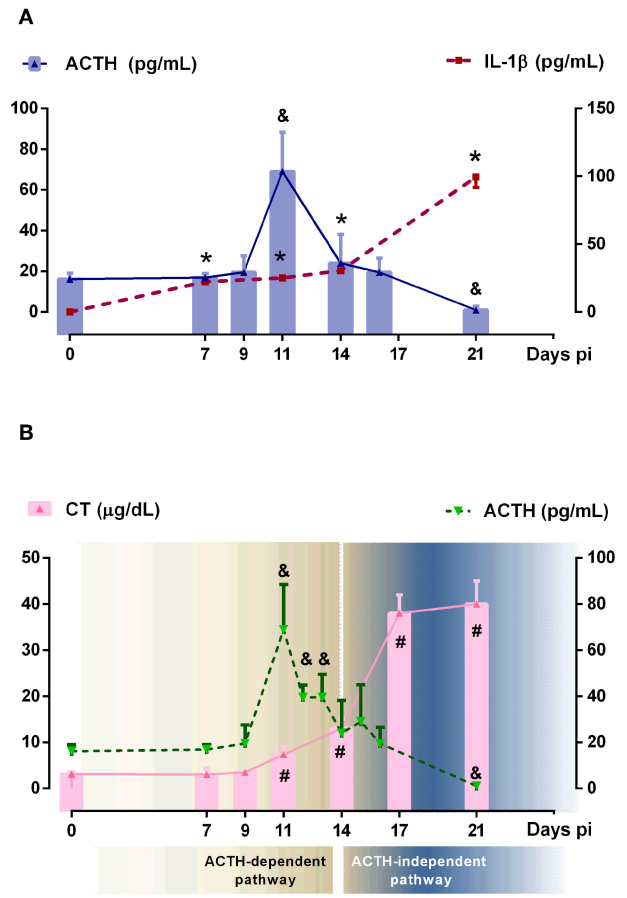

FIGURE 1 | Relationship between ACTH, CT and IL-1β systemic levels. **(A)** IL-1β and ACTH showed an independent behavior after 14 days pi. Solid bars represent mean serum ACTH levels and dashed lines indicated serum IL-1β concentrations [ACTH: $^{\&}p < 0.05$ vs. day 0 pi; IL-1β: $^{*}p < 0.05$ vs. day 0 pi]. **(B)** ACTH and CT showed the classical coupled pattern of secretion until day 14 pi (defined as ACTH-dependent pathway) and a dissociated behavior afterwards (defined as ACTH-independent pathway) Solid bars correspond to CT levels and dashed line represents ACTH levels [ACTH: $^{\&}p < 0.05$ vs. day 0 pi; CT: $^{\#}p < 0.05$ vs. day 0 pi]. In all cases, lines are interpolations of mean values, thus approximating the time course of parameter levels between the measured time points. pi, post-infection.

increase), while ACTH peaked by day 11 pi (4.3-fold increase), further lowering to values seen in control mice at day 14 pi, to reach quite reduced amounts by day 21 pi. These results showed that GC secretion is only matched to ACTH levels nearly during the first 2 weeks of infection, being ACTH-uncoupled afterwards (**Figure 1A**).

Tc infection increased plasma levels of IL-1β as well as other HPA axis-activating cytokines such as TNF-α, IFN-γ, or IL-6 (**Supplementary Figure 1A**). Among pro-inflammatory cytokines involved in the HPA axis activation, IL-1β is the most potent one. As can be seen in **Figure 1A**, the rise of IL-1β was observed at day 7 pi, probably constituting the main stimulus for ACTH-triggered CT synthesis in the initial response, whereas in more advanced infection, ACTH release seems not to be fueled by IL-1β (the same was true for TNF-α, IFN-γ, and IL-6). It follows that, during Tc infection in C57BL/6 mice, GC secretion does exhibit a dual control: an initial ACTH-dependent mechanism followed by an ACTH-uncoupled one (**Figure 1B**).

ACTH-Dependent Functional Response Is Evidenced by the P-PKA/PKA Ratio

ACTH stimulates GC production through MC2R and also regulates MC2R gene and protein expression. The ligation of ACTH to MC2R activates the adenylyl cyclase cascade, leading to cAMP production. This step is followed by phosphorylation of cAMP-dependent PKA and the subsequent activation of several transcription factors inducing the expression of steroidogenic enzymes, like StAR (**Supplementary Figure 1B**). The latter in fact occurred during Tc. As seen in **Figure 2A**, MC2R protein expression peaked at day 11 pi, matching with higher ACTH levels. In the following days, MCR2 expression decreased, coinciding with the lowest ACTH plasma concentration. Consistent with protein data, MC2R gene expression decreased after 16 days pi (**Figure 2B**). In line with higher MCR2 protein expression, the p-PKA/PKA ratio revealed its highest point at day 11 pi (**Figure 2C**). Moreover, we also verify that MC2R expression was restricted to the zona fasciculata in Tc-infected animals (**Figure 2D**). The poor signaling shown by the MC2R/PKA pathway after 14 days pi indicates that mediators other than ACTH sustain the late GC synthesis in Tc-infected animals, reinforcing the view that GC synthesis is ACTH-dependent only in the first period of infection, and further becomes ACTH-independent.

IL-1β and IL-1RI Are Expressed in Adrenal Glands During Infection

Besides the hypothalamic effects of IL-1β, some studies showed that it also stimulates the steroidogenesis *in vitro* (37, 38), whereas human adrenal cells are also able to produce IL-1β (25). Since intra-adrenal production of IL-1β may represent an autocrine/paracrine factor involved in GC synthesis during the ACTH-independent phase, adrenal glands from Tc-infected mice were next studied for the expression of IL-1β and their receptor. In Tc-infected mice, the increase in GC levels not only occurred in parallel with the systemic elevation of IL-1β, but also with an increase in the IL-1β synthesis within adrenal glands (**Figure 3A**). Adrenal IL-1β transcripts begin to increase after 14 days pi, coinciding with the onset of the ACTH-independent phase.

Since IL-1β may locally signal through its receptor to enhance GC secretion in the ACTH-independent phase, the intra-adrenal expression of IL-1R1 was also investigated (**Figures 3B,C**). IL-1RI mRNA contents paralleled protein counterparts, showing no gross changes throughout infection, except on days 17 and 15 pi where both levels are, respectively, diminished (**Figures 3B,C**). These results suggest that IL-1β/IL-1RI signaling was off in the ACTH-independent phase.

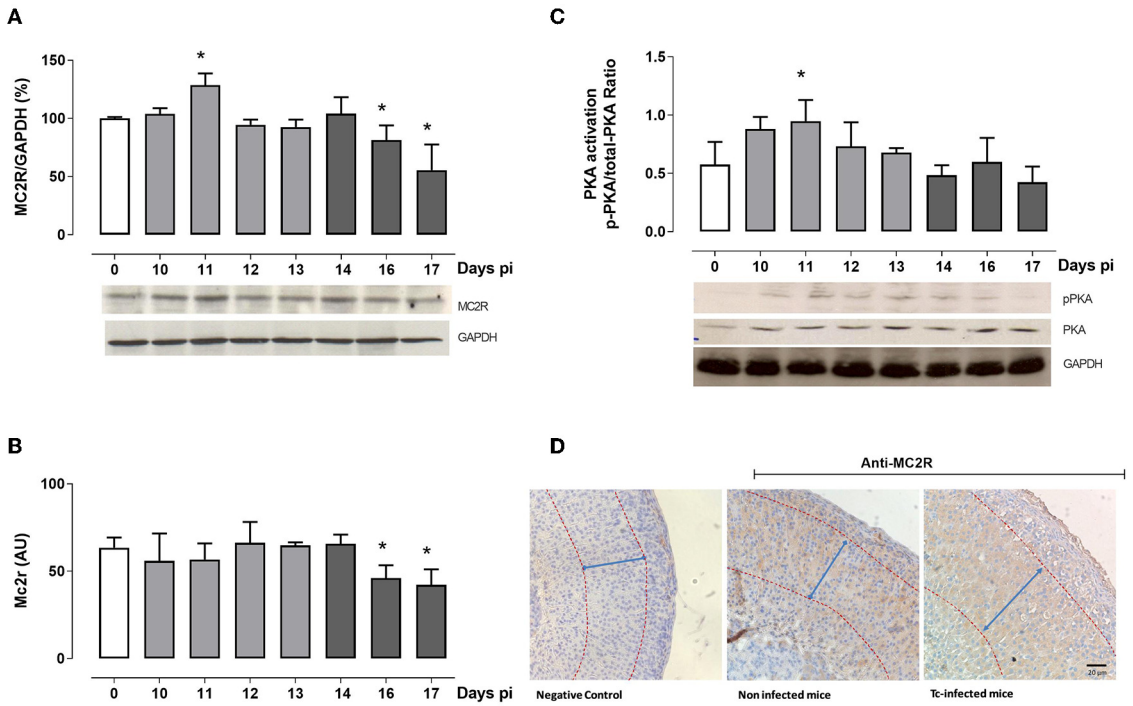

FIGURE 2 | ACTH-dependent pathway analysis. **(A)** Western blot analyses of the MC2R expression throughout infection. Bars represent the densitometry with data from day 0 pi taken as 100%. Optical density was normalized to GAPDH. In the representative blot, lines are numbered according to the day pi. **(B)** MC2R mRNA levels in adrenal cells from Tc-infected mice at different days pi. **(C)** Western blot analyses of the p-PKA/PKA ratio at different days pi. In the representative blot, lines are numbered according to the day pi. Basal levels are represented by a white column; light gray columns represent p-PKA/PKA ratio levels during the ACTH-dependent phase; and dark gray columns represent p-PKA/PKA ratio levels during the ACTH-independent phase. **(D)** Immunohistochemical localization of MC2R in the adrenal cortex (magnification 20×). Positive immunoreactivity was observed in the fascicular zone from both non-infected (middle panel) and Tc-infected mice (14-day pi; right panel). Left panel shows the negative control. Tc-infected animals evidenced a clear hyperplasia of the *zona fasciculata* (demarcated with arrows). Results are expressed as mean ± SEM, from 3 to 5 mice/group/day. A representative experiment from three independent series is shown. $^*p < 0.05$ vs. day 0 pi. AU, arbitrary units; Tc, *Trypanosoma cruzi*; pi, post-infection.

EPAC2 and PGE2 Synthase Cell Signaling-Related Factors Are Linked to GC Synthesis During the ACTH-Independent Phase

Besides PKA, EPAC2 may be involved in GC synthesis. Aimed at evaluating whether EPAC2 may play a role in the ACTH-independent phase, we next assessed EPAC2 expression. As depicted in **Figure 4**, EPAC2 mRNA reached high levels between 13 and 15 days pi (**Figure 4A**), whereas its protein content attained elevated concentrations after 14 days pi (**Figure 4B**), pointing out that EPAC2 is likely to be involved in the alternative pathway for steroidogenesis from Tc-infected mice.

Additionally, in the ACTH-independent phase, the cAMP supply may be sustained by PGE2. Measurements of PGE2 synthase mRNA and its protein showed two peaks of expression (**Figures 4C,D**). The first one coincides with the maximum release of ACTH, while the second weave is evident from 15 to 17 days pi, paralleling the ACTH-independent phase.

Overall, present data support the view that PGE2 may stimulate the adrenal cAMP production during both the ACTH-dependent and -independent phases, likely exerting a positive regulatory role on GC production via EPAC2 during the ACTH-independent phase.

DISCUSSION

The HPA axis is a dynamic system regulating the synthesis and release of adrenal GC during stressful conditions. Particularly, during states of immune hyperactivity, a rapid increase of GC is critical to mount an efficient anti-inflammatory response and hence preserving the energy supply required by immune cells. In the context of acute experimental Chagas disease, the relevance of HPA activation and the consequent role of GC as endogenous anti-inflammatory agents are undoubtful (30, 31). The fact that GC rise coincided with the highest circulating amounts of ACTH, together with an intensified adrenal MC2R expression and an enhanced p-PKA/PKA ratio, corroborate the existence of an ACTH-dependent pathway of GC synthesis at the early stage of Tc infection. Furthermore, these findings match with our earlier observations showing an evident adrenal hyperplasia accompanied by an enhanced steroidogenic

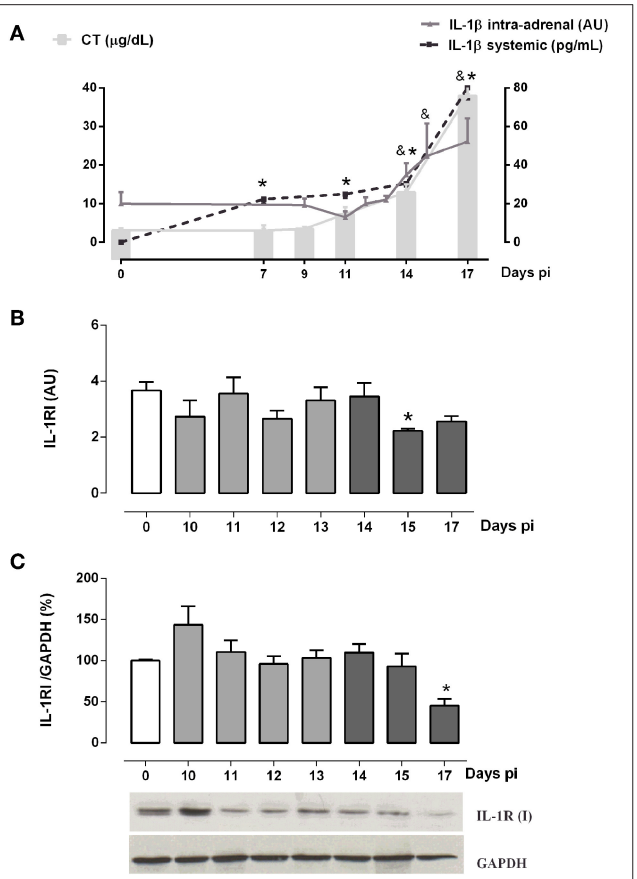

FIGURE 3 | Intra-adrenal expression of IL-1β and IL-1RI in Tc-infected mice. **(A)** IL-1β and CT exhibited similar secretion kinetics throughout infection. Mean serum levels of CT are indicated by solid bars, while dashed lines illustrate IL-1β levels [IL-1β systemic: $^{*}p < 0.05$ vs. day 0 pi; IL-1β intra-adrenal: $^{\&}p < 0.05$ vs. day 0 pi]. **(B)** IL-1RI mRNA expression was diminished at day 15 pi. **(C)** Western blot analyses of IL-1RI expression throughout infection showed a down-regulation at day 17 pi. Basal levels are represented by a white column; light gray and dark gray columns represent IL-1β transcription levels during the ACTH-dependent phase and ACTH-independent phases, respectively. Results are expressed as mean ± SEM, from 3 to 5 mice/group/day. IL-1β and IL-1RI transcripts were normalized against RPL13a gene (Gene ID: 22121) as endogenous control. Data correspond to a representative experiment from three independent rounds. $^{*}p < 0.05$ vs. basal expression (day 0 pi). AU, arbitrary units; pi, post-infection.

machinery since StAR, CYP11A1, CYP11B1, and 11β-HSD1 expression are increased in this period (32).

Expanding our former results (32), we now reveal that infection-driven GC rise is coupled to ACTH solely during the first 2 weeks, to further become dissociated. The uncoupled ACTH-GC response observed in the second phase of infection denote the existence of ACTH-independent mechanisms maintaining the supply of GC. The occurrence of changes in the adrenal microenvironment conditioned by the infection may be central for such ACTH-independent GC secretion.

For instance, constitutive activation of MC2R or their signaling molecules has been thought as likely accounting for GC production in an ACTH-independent form (39, 40). However, this scenario does not occur in the late phase of Tc infection, since the MC2R/PKA pathway was evidently downregulated just after 2 weeks, favoring the lack of response to ACTH even in the presence of hormone basal levels. *In vitro* studies in 24-h LPS-exposed adrenal cells revealed a reduced MC2R expression accompanied by an ameliorated CT production (41), suggesting that ACTH-independent mechanisms underlying GC production may require a more prolonged stimulus. In this regard, MC2R internalization seems to be triggered by a prolonged ACTH binding to MC2R followed by an increase in p-PKA (42, 43). Moreover, *in vitro* evidence showed that, at least, MC2R desensitization results from a regulatory mechanism implicating MC2R internalization by clathrin-mediated endocytosis (42, 44, 45), which also appears to be insensitive to PKA activation from heterologous sources other than ACTH (44). Under non-stressful conditions, nearly 28% of internalized MC2R may be recycling to the cell surface, while the remaining fraction may be subjected to lysosomal degradation (43). Since MCR2 immunoreactivity after 14 days pi seems to be mostly localized within cell cytoplasm, it is conceivable that under prolonged stressful conditions like Tc infection, mechanisms about MC2R protein internalization and degradation are boosted, reinforcing MCR2 desensitization. Moreover, transcriptional activity of the Mc2r gene may be upregulated by diverse transcription factors, like JDP2 (Jun dimerization protein 2) (46), FOXL2 (Forkhead box protein L2), or NR5A1 (steroidogenic factor 1) (47), which, in the context of Tc infection, may be disturbed. Further studies are needed to address such issue.

The ACTH-GC dissociation taking place in the late phase of infection may be explained by PGE2 stimulation of fasciculate cells. PGE2 is produced in response to inflammation, injury or mechanical stress and may also stimulate steroid production partly by triggering adrenal cAMP production (48). PGE2 synthase is the enzyme responsible for the PGE2 synthesis, being likely that autocrine PGE2-stimulated expression of the PGE2 receptor (22, 49, 50) was exerting a positive regulatory role on GC synthesis. Strikingly, during Tc infection, PGE2 synthase showed a noticeable biphasic response, compatible with both ACTH-dependent and -independent phases, suggesting that autocrine PGE2 production may favor CT secretion. In the early phase, PGE2 may stimulate CT release from adrenal cells synergistically with ACTH, increasing cAMP. On the other hand, during the ACTH-hyporesponsive period, CT secretion may be sustained by the PGE2 produced because of increased PGE2 synthase bioavailability, as shown in **Figure 4C**. Furthermore, induction of cAMP by PGE2 when the PKA signaling cascade was shutting off may favor EPAC-mediated actions (51, 52). The abundance of EPAC2 protein in adrenal glands from infected mice after 14 days pi, along with its increased mRNA the day before, is highly suggestive that cAMP-activated EPAC, rather than PKA, mediates GC production during the late phase of infection.

Studies in human adrenal adenomas led to propose the existence of an alternative pathway of GC synthesis governed by IL-1β and IL-1RI, instead of ACTH (53). Indeed, similar mechanisms have been proposed for IL-1α (38). In our model, both systemic and intra-adrenal IL-1β may elicit its effects by promoting the local secretion of PGE2 or other factors

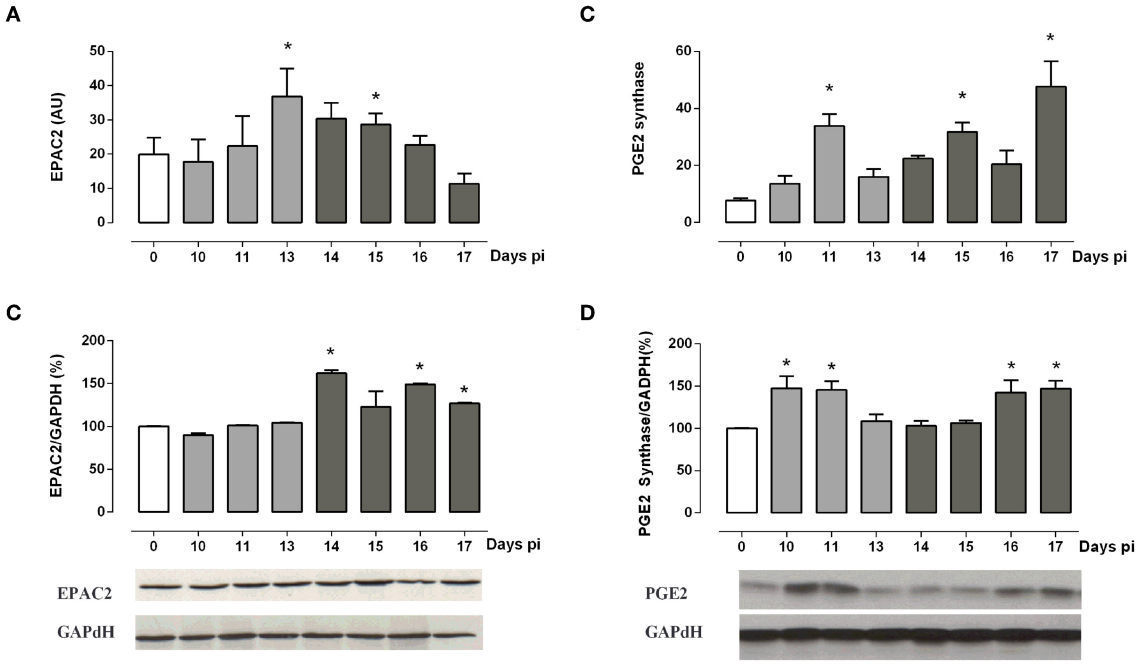

FIGURE 4 | ACTH-independent pathway analysis. **(A,B)** EPAC2 mRNA and protein expression are increased during the ACTH-independent phase. **(C,D)** PGE2 synthase mRNA and protein are expressed throughout infection, showing a peak during both the ACTH-dependent and independent phases. Bars from immunoblots represent the densitometry with data from day 0 pi taken as 100%. Optical density was normalized to GAPDH. Basal levels are represented by a white column; light gray and dark gray columns represent IL-1β transcription levels during the ACTH-dependent phase and ACTH-independent phases, respectively. EPAC2 and PGE2 synthase transcripts were normalized against RPL13a gene (Gene ID: 22121) as endogenous control. Results are expressed as mean ± SEM, from 3 to 5 mice/group/day. A representative experiment from three independent series is shown. *$p < 0.05$ vs. basal expression (day 0 pi). AU, arbitrary units; pi, post-infection.

that stimulate the steroidogenic machinery in both ACTH-dependent and independent phases. However, IL-1β/IL-1RI signaling seemed to be slightly depressed in the second phase; in this sense, IL-1β does not seem to contribute to the mechanisms sustaining the ACTH-independent GC production. While IL-1β was found to promote catecholamine production by adrenomedullar cells (54, 55), a synergy between IL-1β and catecholamines in driving GC secretion in this experimental model sounds unlikely. Our previous studies in the late phase of experimental Chagas disease in C57BL/6 female mice indicated that neither infection nor sympathectomy affected noradrenaline contents in adrenal glands (56).

Collectively, our data strongly point to the existence of two phases dealing with GC synthesis during Tc infection in mice, an initial phase that matches with the well-known ACTH-dependent pathway, followed by a second one characterized by an ACTH-hyporesponsive state. The inflamed adrenal microenvironment may also tune the production of intracellular mediators influencing GC synthesis like PGE2 synthase and EPAC2, which emerge as driving forces for GC production during progressive Tc infection. Lastly, CT production seems to be associated to a biphasic action of PGE2, implying that the effect of PGE2/cAMP in the ACTH-independent phase may be mediated by EPAC2.

Increasing amount of the experimental evidence indicated that the degree of dissociation between ACTH and GC secretion is of clinical relevance, as it has been associated with the level of complications of sepsis, surgery, malignant disease, and depression. In the context of human Chagas disease, beyond the disturbed HPA response in terms of the CG/dehydroepiandrosterone ratio, GC levels fell within normal levels (57, 58). Nevertheless, it is possible that during the acute symptomatic phase of human Chagas disease, as seen in the highly lethal oral acute infection (28, 29), the regulation of GC production may be like the one seen in the experimental model. Further studies are needed to address whether oral Chagas disease outcomes are linked to ACTH-GC decoupling response.

DATA AVAILABILITY STATEMENT

The raw data supporting the conclusions of this article will be made available by the authors, without undue reservation, to any qualified researcher.

ETHICS STATEMENT

All animal procedures were performed according to the Guide for the Care and Use of Laboratory Animals (NIH), and approved by Institutional Committees (Bioethics, Animal Care and Use, and Biosecurity Committees, FCM-UNR; Resolutions No. 3486/2013 and 4976/2013).

AUTHOR CONTRIBUTIONS

VC, AP, and SV conceived and designed the experiments and contributed reagents, materials, analysis tools. ES, ER, FG, RF, AP, and SV performed the experiments. ES, RF, AP, and SV analyzed the data. AP, OB, and SV interpreted the data and wrote the paper.

FUNDING

AP, OB, and SV are members of the National Scientific and Technical Research Council (CONICET). This work was supported by grants from ANPCyT (Grant Nos. PICT 2013-1892 and PICT 2015-3777) and SECYTUNR (Grant Nos. 1MED372 and 1MED408), Argentina.

ACKNOWLEDGMENTS

We thank Marisa Derio for her technical assistance.

SUPPLEMENTARY MATERIAL

The Supplementary Material for this article can be found online at: https://www.frontiersin.org/articles/10.3389/fendo.2019.00866/full#supplementary-material

REFERENCES

1. Lee JK, Tran T, Tansey MG. Neuroinflammation in Parkinson's disease. *J Neuroimmune Pharmacol.* (2009) 4:419–29. doi: 10.1007/s11481-009-9176-0
2. Vezzani A, Maroso M, Balosso S, Sanchez MA, Bartfai T. IL-1 receptor/Toll-like receptor signaling in infection, inflammation, stress and neurodegeneration couples hyperexcitability and seizures. *Brain Behav Immun.* (2011) 25:1281–9. doi: 10.1016/j.bbi.2011.03.018
3. Hotamisligil GS. Endoplasmic reticulum stress and the inflammatory basis of metabolic disease. *Cell.* (2010) 140:900–17. doi: 10.1016/j.cell.2010.02.034
4. Smith SM, Vale WW. The role of the hypothalamic-pituitary-adrenal axis in neuroendocrine responses to stress. *Dialogues Clin Neurosci.* (2006) 8:383–95.
5. Charmandari E, Tsigos C, Chrousos G. Endocrinology of the Stress Response. *Annu Rev Physiol.* (2005) 67:259–84. doi: 10.1146/annurev.physiol.67.040403.120816
6. Sapolsky RM, Romero LM, Munck AU. How do glucocorticoids influence stress responses? Integrating permissive, suppressive, stimulatory, and preparative actions. *Endocr Rev.* (2000) 21:55–89. doi: 10.1210/er.21.1.55
7. Gallo-Payet N, Martinez A, Lacroix A. Editorial: ACTH action in the adrenal cortex: from molecular biology to pathophysiology. *Front Endocrinol.* (2017) 8:101. doi: 10.3389/fendo.2017.00101
8. Charmandari E, Nicolaides NC, Chrousos GP. Adrenal insufficiency. *Lancet.* (2014) 383:2152–67. doi: 10.1016/S0140-6736(13)61684-0
9. Kanczkowski W, Sue M, Zacharowski K, Reincke M, Bornstein SR. The role of adrenal gland microenvironment in the HPA axis function and dysfunction during sepsis. *Mol Cell Endocrinol.* (2015) 408:241–8. doi: 10.1016/j.mce.2014.12.019
10. Lipiner-Friedman D, Sprung CL, Laterre PF, Weiss Y, Goodman SV, Vogeser M, et al. Adrenal function in sepsis: the retrospective corticus cohort study. *Crit Care Med.* (2007) 35:1012–8. doi: 10.1097/01.CCM.0000259465.92018.6E
11. Loisa P, Rinne T, Kaukinen S. Adrenocortical function and multiple organ failure in severe sepsis. *Acta Anaesthesiol Scand.* (2002) 46:145–51. doi: 10.1034/j.1399-6576.2002.460204.x
12. Vermes I, Beishuizen A. The hypothalamic-pituitary-adrenal response to critical illness. *Best Pract Res Clin Endocrinol Metab.* (2001) 15:495–511. doi: 10.1053/beem.2001.0166
13. Roth-Isigkeit AK, Schmucker P. Postoperative dissociation of blood levels of cortisol and adrenocorticotropin after coronary artery bypass grafting surgery. *Steroids.* (1997) 62:695–9. doi: 10.1016/S0039-128X(97)00069-X
14. Cho YM, Kim SY, Cho BY, Lee HK, Yang HK, Lee KU. Dissociation between plasma adrenocorticotropin and serum cortisol level during the early postoperative period after gastrectomy. *Horm Res.* (2000) 53:246–50. doi: 10.1159/000023574
15. Carroll BJ, Cassidy F, Naftolowitz D, Tatham NE, Wilson WH, Iranmanesh A, et al. Pathophysiology of hypercortisolism in depression. *Acta Psychiatr Scand.* (2007) 115:90–103. doi: 10.1111/j.1600-0447.2007.00967.x
16. Boonen E, Langouche L, Janssens T, Meersseman P, Vervenne H, De Samblanx E, et al. Impact of duration of critical illness on the adrenal glands of human intensive care patients. *J Clin Endocrinol Metab.* (2014) 99:4214–22. doi: 10.1210/jc.2014-2429
17. Vermes I, Beishuizen A, Hampsink RM, Haanen C. Dissociation of plasma adrenocorticotropin and cortisol levels in critically ill patients: possible role of endothelin and atrial natriuretic hormone. *J Clin Endocrinol Metab.* (1995) 80:1238–42. doi: 10.1210/jcem.80.4.7714094
18. Enyeart JJ. Biochemical and ionic signaling mechanisms for ACTH-stimulated cortisol production. *Vitam Horm.* (2005) 70:265–79. doi: 10.1016/S0083-6729(05)70008-X
19. Enyeart JA, Enyeart JJ. Metabolites of an Epac-selective cAMP analog induce cortisol synthesis by adrenocortical cells through a cAMP-independent pathway. *PLoS ONE.* (2009) 4:e6088. doi: 10.1371/journal.pone.0006088
20. Holz GG, Chepurny OG, Schwede F. Epac-selective cAMP analogs: new tools with which to evaluate the signal transduction properties of cAMP-regulated guanine nucleotide exchange factors. *Cell Signal.* (2008) 20:10–20. doi: 10.1016/j.cellsig.2007.07.009
21. Lewis AE, Aesoy R, Bakke M. Role of EPAC in cAMP-mediated actions in adrenocortical cells. *Front Endocrinol.* (2016) 7:63. doi: 10.3389/fendo.2016.00063
22. Spät A, Jozan S. Effect of prostaglandin E2 and A2 on steroid synthesis by the rat adrenal gland. *J Endocrinol.* (1975) 65:55–63. doi: 10.1677/joe.0.0650055
23. Tachibana T, Nakai Y, Makino R, Khan MSI, Cline MA. Effect of central and peripheral injection of prostaglandin E2 and F2α on feeding and the crop-emptying rate in chicks. *Prostaglandins Other Lipid Mediat.* (2017) 130:30–7. doi: 10.1016/j.prostaglandins.2017.03.005
24. Tkachenko IV., Jääskeläinen T, Jääskeläinen J, Palvimo JJ, Voutilainen R. Interleukins 1α and 1β as regulators of steroidogenesis in human NCI-H295R adrenocortical cells. *Steroids.* (2011) 76:1103–15. doi: 10.1016/j.steroids.2011.04.018
25. González-Hernández JA, Bornstein SR, Ehrhart-Bornstein M, Gschwend JE, Gwosdow A, Jirikowski G, et al. IL-1 is expressed in human adrenal gland *in vivo*. Possible role in a local immune-adrenal axis. *Clin Exp Immunol.* (1995) 99:137–41. doi: 10.1111/j.1365-2249.1995.tb03484.x
26. Rassi A, Rassi A, Marin-Neto JA. Chagas disease. *Lancet.* (2010) 375:1388–402. doi: 10.1016/S0140-6736(10)60061-X
27. World Health Organisation. *WHO Chagas Disease (American Trypanosomiasis)* [Fact sheet]. World Heal Organisation. (2015). Available online at: http://www.who.int/mediacentre/factsheets/fs340/en/
28. Shikanai-Yasuda MA, Carvalho NB. Oral transmission of chagas disease. *Clin Infect Dis.* (2012) 54:845–52. doi: 10.1093/cid/cir956
29. Filigheddu MT, Górgolas M, Ramos JM. Enfermedad de chagas de transmisión oral. *Med Clin.* (2017) 148:125–31. doi: 10.1016/j.medcli.2016.10.038
30. Roggero E, Pérez AR, Tamae-Kakazu M, Piazzon I, Nepomnaschy I, Besedovsky HO, et al. Endogenous glucocorticoids cause thymus atrophy but are protective during acute *Trypanosoma cruzi* infection. *J Endocrinol.* (2006) 190:495–503. doi: 10.1677/joe.1.06642
31. Pérez AR, Roggero E, Nicora A, Palazzi J, Besedovsky HO, del Rey A, et al. Thymus atrophy during *Trypanosoma cruzi* infection is caused by an immuno-endocrine imbalance. *Brain Behav Immun.* (2007) 21:890–900. doi: 10.1016/j.bbi.2007.02.004

32. Villar SR, Ronco MT, Fernández Bussy R, Roggero E, Lepletier A, Manarin R, et al. Tumor necrosis factor-α regulates glucocorticoid synthesis in the adrenal glands of *Trypanosoma cruzi* acutely-infected mice. The role of TNF-R1. *PLoS ONE.* (2013) 8:e63814. doi: 10.1371/journal.pone.0063814
33. Corrêa-De-Santana E, Paez-Pereda M, Theodoropoulou M, Kenji Nihei O, Gruebler Y, Bozza M, et al. Hypothalamus-pituitary-adrenal axis during *Trypanosoma cruzi* acute infection in mice. *J Neuroimmunol.* (2006) 173:12–22. doi: 10.1016/j.jneuroim.2005.08.015
34. Zingales B, Miles MA, Campbell DA, Tibayrenc M, Macedo AM, Teixeira MMG, et al. The revised *Trypanosoma cruzi* subspecific nomenclature: rationale, epidemiological relevance and research applications. *Infect Genet Evol.* (2012) 12:240–53. doi: 10.1016/j.meegid.2011.12.009
35. Pérez AR, Lambertucci F, González FB, Roggero EA, Bottasso OA, de Meis J, et al. Death of adrenocortical cells during murine acute *T. cruzi* infection is not associated with TNF-R1 signaling but mostly with the type II pathway of Fas-mediated apoptosis. *Brain Behav Immun.* (2017) 65:284–95. doi: 10.1016/j.bbi.2017.05.017
36. Lowry OH, Rosebrough NJ, Farr AL, Randall RJ. Protein measurement with the Folin phenol reagent. *J Biol Chem.* (1951) 193:265–75.
37. Bornstein SR, Rutkowski H, Vrezas I. Cytokines and steroidogenesis. *Mol Cell Endocrinol.* (2004) 215:135–41. doi: 10.1016/j.mce.2003.11.022
38. O'Connell NA, Kumar A, Chatzipanteli K, Mohan A, Agarwal RK, Head C, et al. Interleukin-1 regulates corticosterone secretion from the rat adrenal gland through a catecholamine-dependent and prostaglandin E2-independent mechanism. *Endocrinology.* (1994) 135:460–7. doi: 10.1210/endo.135.1.8013385
39. Hiroi N, Chrousos GP, Kohn B, Lafferty A, Abu-Asab M, Bonat S, et al. Adrenocortical-pituitary hybrid tumor causing Cushing's syndrome. *J Clin Endocrinol Metab.* (2001) 86:2631–7. doi: 10.1210/jcem.86.6.7590
40. Latronico AC, Reincke M, Mendonça BB, Arai K, Mora P, Allolio B, et al. No evidence for oncogenic mutations in the adrenocorticotropin receptor gene in human adrenocortical neoplasms. *J Clin Endocrinol Metab.* (1995) 80:875–7. doi: 10.1210/jcem.80.3.7883845
41. Liu S, Zhu X, Liu Y, Wang C, Wang S, Tang X, et al. Endotoxin tolerance of adrenal gland: attenuation of corticosterone production in response to lipopolysaccharide and adrenocorticotropic hormone*. *Crit Care Med.* (2011) 39:518–26. doi: 10.1097/CCM.0b013e318206b980
42. Baig AH, Swords FM, Noon LA, King PJ, Hunyady L, Clark AJL. Desensitization of the Y1 cell adrenocorticotropin receptor. *J Biol Chem.* (2001) 276:44792–7. doi: 10.1074/jbc.M108572200
43. Roy S, Roy SJ, Pinard S, Taillefer L-D, Rached M, Parent J-L, et al. Mechanisms of melanocortin-2 receptor (MC2R) internalization and recycling in human embryonic kidney (hek) cells: identification of Key Ser/Thr (S/T) amino acids. *Mol Endocrinol.* (2011) 25:1961–77. doi: 10.1210/me.2011-0018
44. Baig AH, Swords FM, Szaszák M, King PJ, Hunyady L, Clark AJL. Agonist activated adrenocorticotropin receptor internalizes via a clathrin-mediated G protein receptor kinase dependent mechanism. *Endocr Res.* (2002) 28:281–9. doi: 10.1081/ERC-120016798
45. Kilianova Z, Basora N, Kilian P, Payet MD, Gallo-Payet N. Human melanocortin receptor 2 expression and functionality: effects of protein kinase A and protein kinase C on desensitization and internalization. *Endocrinology.* (2006) 147:2325–37. doi: 10.1210/en.2005-0991
46. Wang C-M, Wang R, Liu R, Yang W-H. Jun dimerization protein 2 activates Mc2r transcriptional activity: role of phosphorylation and SUMOylation. *Int J Mol Sci.* (2017) 18:304. doi: 10.3390/ijms18020304
47. Yang W-H, Gutierrez NM, Wang L, Ellsworth BS, Wang C-M. Synergistic activation of the Mc2r promoter by FOXL2 and NR5A1 in mice1. *Biol Reprod.* (2010) 83:842–51. doi: 10.1095/biolreprod.110.085621
48. Rainey WE, Naville D, Cline N, Mason JI. Prostaglandin E2 is a positive regulator of adrenocorticotropin receptors, 3 beta-hydroxysteroid dehydrogenase, and 17 alpha-hydroxylase expression in bovine adrenocortical cells. *Endocrinology.* (1991) 129:1333–9. doi: 10.1210/endo-129-3-1333
49. Dazord A, Morera AM, Bertrand J, Saez JM. Prostaglandin receptors in human and ovine adrenal glands: binding and stimulation of adenyl cyclase in subcellular preparations. *Endocrinology.* (1974) 95:352–9. doi: 10.1210/endo-95-2-352
50. Saruta T, Kaplan NM. Adrenocortical steroidogenesis: the effects of prostaglandins. *J Clin Invest.* (1972) 51:2246–51. doi: 10.1172/JCI107033
51. Samuchiwal SK, Balestrieri B, Raff H, Boyce JA. Endogenous prostaglandin E_2 amplifies IL-33 production by macrophages through an E prostanoid (EP) $_2$ /EP $_4$ -cAMP-EPAC-dependent pathway. *J Biol Chem.* (2017) 292:8195–206. doi: 10.1074/jbc.M116.769422
52. Shrestha K, Meidan R. The cAMP-EPAC pathway mediates PGE2-induced FGF2 in bovine granulosa cells. *Endocrinology.* (2018) 159:3482–91. doi: 10.1210/en.2018-00527
53. Willenberg HS, Stratakis CA, Marx C, Ehrhart-Bornstein M, Chrousos GP, Bornstein SR. Aberrant interleukin-1 receptors in a cortisol-secreting adrenal adenoma causing cushing's syndrome. *N Engl J Med.* (1998) 339:27–31. doi: 10.1056/NEJM199807023390105
54. Lujan HJ, Mathews HL, Gamelli RL, Jones SB. Human immune cells mediate catecholamine secretion from adrenal chromaffin cells. *Crit Care Med.* (1998) 26:1218–24. doi: 10.1097/00003246-199807000-00024
55. Weidenfeld J, Abramsky O, Ovadia H. Evidence for the involvement of the central adrenergic system in interleukin 1-induced adrenocortical response. *Neuropharmacology.* (1989) 28:1411–4. doi: 10.1016/0028-3908(89)90018-X
56. Roggero E, Pérez AR, Pollachini N, Villar SR, Wildmann J, Besedovsky H, et al. The sympathetic nervous system affects the susceptibility and course of *Trypanosoma cruzi* infection. *Brain Behav Immun.* (2016) 58:228–36. doi: 10.1016/j.bbi.2016.07.163
57. Pérez AR, Silva-Barbosa SD, Berbert LR, Revelli S, Beloscar J, Savino W, et al. Immunoneuroendocrine alterations in patients with progressive forms of chronic Chagas disease. *J Neuroimmunol.* (2011) 235:84–90. doi: 10.1016/j.jneuroim.2011.03.010
58. González F, Villar S, D'Attilio L, Leiva R, Marquez J, Lioi S, et al. Dysregulated network of immune, endocrine and metabolic markers is associated to more severe human chronic chagas cardiomyopathy. *Neuroimmunomodulation.* (2018) 25:119–28. doi: 10.1159/000491699

Conflict of Interest: The authors declare that the research was conducted in the absence of any commercial or financial relationships that could be construed as a potential conflict of interest.

frontiers in Endocrinology

MINI REVIEW
published: 14 January 2020
doi: 10.3389/fendo.2019.00921

Role of the End-Point Mediators of Sympathoadrenal and Sympathoneural Stress Axes in the Pathogenesis of Experimental Autoimmune Encephalomyelitis and Multiple Sclerosis

Ivan Pilipović[1], *Zorica Stojić-Vukanić*[2], *Ivana Prijić*[1] *and Gordana Leposavić*[3]*

[1] *Branislav Jankovic Immunology Research Centre, Institute of Virology, Torlak Vaccines and Sera, Belgrade, Serbia,* [2] *Department of Microbiology and Immunology, Faculty of Pharmacy, University of Belgrade, Belgrade, Serbia,* [3] *Department of Pathobiology, Faculty of Pharmacy, University of Belgrade, Belgrade, Serbia*

OPEN ACCESS

Edited by:
Ana Rosa Pérez, National Council for Scientific and Technical Research (CONICET), Argentina

Reviewed by:
Djordje Miljkovic, Institute for Biological Research Sinisa Stankovic, University of Belgrade, Serbia
James William Crane, University of Tasmania, Australia

***Correspondence:**
Gordana Leposavić
gordana.leposavic@pharmacy.bg.ac.rs

Specialty section:
This article was submitted to Neuroendocrine Science, a section of the journal Frontiers in Endocrinology

Received: *16 September 2019*
Accepted: *17 December 2019*
Published: *14 January 2020*

Citation:
Pilipović I, Stojić-Vukanić Z, Prijić I and Leposavić G (2020) Role of the End-Point Mediators of Sympathoadrenal and Sympathoneural Stress Axes in the Pathogenesis of Experimental Autoimmune Encephalomyelitis and Multiple Sclerosis. Front. Endocrinol. 10:921. doi: 10.3389/fendo.2019.00921

The role of stress effector systems in the initiation and progression of multiple sclerosis (MS) and experimental autoimmune encephalomyelitis (EAE), the most commonly used experimental model of MS, has strongly been suggested. To corroborate this notion, alterations in activity of the sympathoadrenal and sympathoneural axes of sympathoadrenal system (a major communication pathway between the central nervous system and the immune system), mirrored in altered release of their end-point mediators (adrenaline and noradrenaline, respectively), are shown to precede (in MS) and/or occur during development of MS and EAE in response to immune cell activation (in early phase of disease) and disease-related damage of sympathoadrenal system neurons and their projections (in late phase of disease). To add to the complexity, innate immunity cells and T-lymphocytes synthesize noradrenaline that may be implicated in a local autocrine/paracrine self-amplifying feed-forward loop to enhance myeloid-cell synthesis of proinflammatory cytokines and inflammatory injury. Furthermore, experimental manipulations targeting noradrenaline/adrenaline action are shown to influence clinical outcome of EAE, in a disease phase-specific manner. This is partly related to the fact that virtually all types of cells involved in the instigation and progression of autoimmune inflammation and target tissue damage in EAE/MS express functional adrenoceptors. Although catecholamines exert majority of immunomodulatory effects through β_2-adrenoceptor, a role for α-adrenoceptors in EAE pathogenesis has also been indicated. In this review, we summarize all aforementioned aspects of immunopathogenetic action of catecholamines in EAE/MS as possibly important for designing new strategies targeting their action to prevent/mitigate autoimmune neuroinflammation and tissue damage.

Keywords: sympathoadrenal system, noradrenaline, β-adrenoceptor, α-adrenoceptor, experimental autoimmune encephalomyelitis, multiple sclerosis

INTRODUCTION

Multiple sclerosis (MS) is one of the most common neurological disorders and cause of disability of young adults (1–3). Patogenetically, MS is the prototype of the autoimmune inflammatory diseases of the central nervous system (CNS), and is characterized by breakdown of the blood-brain barrier (BBB), neuroinflammation, and axonal damage (4, 5). Its pathogenesis is largely deciphered using experimental autoimmune encephalomyelitis (EAE), a group of neuroantigen-induced animal diseases (4). These models are mainly based on neuroinflammation induced by auto-reactive T helper (Th) cells (4, 6). Upon activation in draining lymph nodes (dLNs), neuroantigen-specific Th cells synthesize IL-17, IFN-γ and/or GM-CSF, and express chemokine receptors (CCR2, CCR6) to gain access in the CNS (4, 6, 7). In the CNS, upon reactivation by resident antigen-presenting cells (APCs), Th cells activate neighboring microglia and attract peripheral cells (T-cells, B-cells, inflammatory monocytes) to perpetuate neuroinflammation and cause demyelination (4, 7). With EAE development, apart from CD4+Foxp3+ regulatory T-cells (Tregs) (8), activated microglia may assume regulatory functions (through phagocytosis, anti-inflammatory mediator and growth factor release) to limit the CNS damage and promote recovery (9). Noteworthy, so far, no single experimental model covers the entire spectrum of MS immunopathological features (particularly role of CD8+ T-cells and B-cells in propagating inflammation and tissue damage in established MS), so the relevance of results from EAE models has to be critically validated (5).

MS is multifactorial disease involving genetic traits and non-genetic triggers (1, 2). Generally, physical and psychological stressors are important triggers of MS (10–12). To corroborate this notion, war veterans with stress-related disorders (associated with low levels of morning cortisol and elevated levels of noradrenaline), were found to exhibit the higher risk of being diagnosed with MS compared to those without any psychiatric disorders (13). However, not only does stress contribute to MS development, but the disease itself causes stress, creating a vicious cycle (10, 12, 14). Additionally, stress contributes to exacerbations of MS (12, 15). The pathogenetic role of stress has been ascribed not only to action of glucocorticoids, end-point mediators of hypothalamo-pituitary-adrenal system (16, 17), but also to catecholamines, end-point mediators of sympathoadrenal system consisting of sympathoneural (the key end-point mediator noradrenaline) and sympathoadrenal (the key end-point mediator adrenaline) axes (15, 16, 18). This review focuses the role of catecholamines in development of EAE/MS.

In MS, aside from sensory, motor and cognitive impairments, autonomic dysfunction (mirrored in fatigue, bladder, bowel, cardiovascular, and sexual disorders) considerably contributes to disability (19–21). It has been speculated that (i) altered sympathoadrenal system activity induced by various stressors, including the disease itself (in early phase and at the onset of exacerbations), and (ii) damage of central sympathoadrenal system neurons and their projections with the disease progression (12, 22–24) is not only consequence, but also mechanism involved in MS pathogenesis.

The sympathoadrenal system, a major communication pathway between the CNS and the immune system (25), originates from locus coeruleus (LC) (18, 26). Activation of LC leads to (i) central effects reflecting noradrenaline release (primarily via non-junctional varicosities to enable its action on non-neural cells) throughout the brain and spinal cord (SC), and (ii) peripheral effects due to release of catecholamines from adrenal medulla and sympathetic nerve fibers (18, 27–30). On the other hand, activation of peripheral immune cells activates sympathoadrenal system to secure control of the ongoing response (18, 31). Namely, cytokines released upon their activation signal to the sympathoadrenal system by stimulating proinflammatory mediator release from the CNS resident cells or by activation of afferent signaling pathways (32–36). In inflammatory autoimmune diseases, this activational effect is suggested to be superimposed on elevated sympathoadrenal system activity due to chronic stress and/or stressful adverse life events leading to its hyperactivity and proinflammatory action (31). In MS, the release of proinflammatory cytokines from activated immune cells in the CNS also contributes to sympathoadrenal hyperactivity (32, 33, 36). Stress-induced sympathoadrenal activation prior to these diseases is suggested to induce low grade self-perpetuating lymphoid tissue and systemic inflammation that further increases sympathoadrenal activity and alters immune system reactivity to enable autoreactive lymphocyte activation (31). This, in return, contributes to sympathoadrenal activation and the promotion of inflammation (31, 37). Adding to the complexity, innate and adaptive "catecholaminergic" immune cells also synthesize catecholamines (29, 30, 38) to regulate inflammatory/immune responses (39). However, in inflammatory autoimmune diseases, they may form an alternative catecholamine source with role in promotion of inflammation (40–43). Namely, activated immune cell-derived catecholamines are suggested to drive an autocrine/paracrine self-amplifying feed-forward loop to increase synthesis of proinflammatory cytokines in myeloid cells (41, 44). Thus, in early phases of the diseases neurocrine/endocrine- and autocrine/paracrine-derived catecholamines may synergistically act to promote inflammation.

Catecholamines exert immunomodulatory effects through β- and α-adrenoceptors expressed on almost all types of immune cells, but majority of their effects are β_2-adrenoceptor-mediated (18, 25, 43, 45–60). Monocytes/macrophages, together with dendritic cells, constitute the mononuclear phagocyte system, which plays a key role in maintaining tissue integrity, its restoration after injury, and the initiation, direction and resolution of innate and adaptive immunity. Catecholamines modulate their activity in a context-dependent manner, so they exert both proinflammatory (61–63) and anti-inflammatory (64, 65) effects depending on a number of factors (25), including adrenoceptor subtype (66, 67), adrenoceptor agonist concentrations (68), and the timing of adrenoceptor engagement in relation to antigen stimulation (69). Thus, it seems obvious that their action in EAE/MS has to be disease phase-dependent. In this review, considering EAE/MS pathogenesis, catecholamine influence on microglia

and Th17/Treg axis is focused. Several stress paradigms induce β-adrenoceptor antagonist (propranolol) preventable microglial activation and synthesis of inflammatory mediators exaggerating proinflammatory responses to subsequent immunological stimuli (70). β_2-adrenoceptor activation in lipopolysaccharide-stimulated dendritic cells diminishes IL-12 secretion, leading to a shift in the IL-12/IL-23 ratio and thereby promotes the generation of CD4+ T cells that produce lower amounts of IFN-γ (Th1 signature cytokine) and higher levels of IL-17 (Th17 signature cytokine) (71).

CENTRAL NORADRENALINE IN PATHOGENESIS OF EAE/MS

Human Data

It has been shown that in MS noradrenaline levels decrease in the tissue surrounding LC (72) reflecting the disease-induced neuronal damage in LC (72). At present, there is no data on effects of the disease on the other "descending catecholaminergic system neurons" projecting to the spinal cord. On the other hand, several studies showed that cerebrospinal fluid levels of noradrenaline metabolite 3-methoxy-4-hydroxyphenylglycol, a marker of central noradrenergic activity, do not change in MS (73, 74). Given that peripheral and central administration of cytokines to rodents increased noradrenaline synthesis and 3-methoxy-4-hydroxyphenylglycol levels in brain (75), it may be assumed that elevated noradrenaline synthesis and turnover in non-damaged brain structures overcame diminished noradrenaline synthesis in those affected by the disease. On the other hand, combination of lofepramine or maprotiline (noradrenaline reuptake inhibitors) with levodopa (after conversion to dopamine metabolizes to noradrenaline) exhibited therapeutic effects in MS (76). However, given that dopamine itself exerts beneficial effects on the disease (77), these effects cannot be ascribed to the rise in the central noradrenaline level. On the other hand, although combined treatment with lofepramine and phenylalanine (upstream noradrenaline precursor) was initially shown to moderate clinical symptoms of MS (78), follow-up rigorously controlled study put the benefits of this therapy into question (79). Additionally, there are limited and inconsistent data on the therapeutic effects of β_2-adrenoceptor agonists, such as salbutamol (albuterol), in MS. Namely, depending on type and phase of MS both adverse and benefitial effects have been described (80–82). To potentiate need for further studies on role of central noradrenaline in MS, several studies provided evidence that anti-stress therapies, including exercise (83–85), mindfulness meditation (86–88), and yoga (89), moderate MS symptoms (depression, anxiety, fatigue, cognitive dysfunction). In the same line are data from a population-based study indicating that the incidence of MS was negatively associated with use of fenoterol, a β_2-adrenoceptor agonist, but not salbutamol belonging to the same drug class (90). This was ascribed to differences in their functionality, as fenoterol differently from salbutamol significantly stimulates cyclic-adenosine monophosphate (90).

Animal Data

The study encompassing dogs suffering from EAE showed that cerebrospinal fluid and white matter noradrenaline levels rise early after the immunization, but decrease in the clinical phase of the disease (91). Consistently, decline in SC and/or brainstem noradrenaline concentration was found at the peak of EAE in Lewis and Dark Agouti (DA) rats (45, 92–94). Noradrenaline concentration in SC also decreased with EAE progression in C57BL/6 mice (72, 95). This was attributed to disease-related damage of LC noradrenergic neurons (72) and/or axonal damage in SC (92). Additionally, it was reported that electrolytic destruction of LC noradrenergic neurons attenuates the disease in Wistar rats (96). Furthermore, central noradrenaline depletion (decrease in noradrenaline level by ∼85% without changes in dopamine) by intracisternal-ventricular 6-hydroxydopamine injections reduced motor deficit in Lewis EAE rats (97, 98). Conversely, in C57BL/6 mice developing chronic EAE, treatment with N-(2-chloroethyl)-N-ethyl-2 bromobenzylamine, selective neurotoxin for rodent LC neurons, exacerbated the disease (99). This discrepancy could be related to N-(2-chloroethyl)-N-ethyl-2 bromobenzylamine–induced increase in the central extraneuronal noradrenaline level due to its inflow from non-lesioned regions, so that noradrenaline levels were reduced by only 10–30% (100). Additionally, treatment with propranolol, a non-selective β-adrenoceptor antagonist, depending on its onset relative to immunization, produced different effects on clinical outcome of EAE in rats (101, 102). Propranolol treatment starting 3 days before immunization moderated clinical and histological picture of EAE in DA rats (102), whereas the treatment beginning at immunization prolonged the disease duration in Lewis rats (101). When administered over effector phase of EAE to Lewis rats, propranolol exacerbated the disease (103), or produced no effect (101), while propranolol treatment in DA rats starting before the onset of clinical EAE decreased the disease severity (45). Given that propranolol crosses the BBB (104), the latter findings were consistent with data indicating that chemical depletion of central noradrenaline starting before the effector phase of EAE may remove an effector amplification mechanism leading to suppression of the paralysis (97). The inconsistencies in data from different propranolol studies may be associated with differences in drug dose regimen and/or treatment onset/duration, as well as animal genetic makeup, immunization protocols (possibly affecting the kinetics in development of sympathoadrenal neuron damage).

The ameliorating effect of propranolol on the clinical outcome of EAE in DA rats was linked with upregulated expression of nuclear factor (erythroid-derived 2)-like 2 (Nrf2) and heme oxygenase-1, a Nrf2-regulated gene with a crucial role in the prevention of neuroinflammation (105, 106). This partly reflected propranolol-induced upregulation of CX3CR1, the receptor for fractalkine (CX3CL1), which activates the Nrf2 signaling in microglial cells to limit their activation (107). Nrf2 recognizes an enhancer sequence termed antioxidant response element that is present in the regulatory regions of over 250 genes (108), and is implicated in the modulation of inflammation through crosstalk with the transcription factor NF-κB, the principal regulator of

inflammation (109). Consistently, compared with saline-injected controls, in propranolol-treated rats the frequencies of IL-1β- and IL-23-expressing cells among microglia, and microglia expression level of IL-6 and CCL-2, the chemokine recruiting inflammatory monocytes and T-cells to the sites of inflammation (110), was decreased (45). Additionally, in accordance with role of CX3CR1 in regulation of the expression of TAM receptors (111), which are essential in apoptotic cell phagocytosis (112), so that their deficiency is linked with autoimmune disease progression (110), the frequency of phagocytic cells among microglia was significantly increased in propranolol-treated rats (45). As expected (9, 113, 114), this correlated with the increased proportion of anti-inflammatory CD163- and IL-10-expressing microglia (45). In keeping with alterations in phenotypic and functional profile of microglia, in propranolol-treated EAE rats the infiltration of SC with blood-borne inflammatory monocytes and Th cells, their reactivation/proliferation and differentiation toward highly pathogenic IL-17/IFN-γ/GM-CSF co-producing Th17 cells was impaired (45).

On the other hand, administration of prazosin, an α_1-adrenoceptor antagonist, throughout the disease or effector phase alone suppressed active and passively transferred EAE in rats (103, 115, 116). This was related to blockade of disease-promoting α_1-adrenoceptor–mediated vascular action (115).

Putative Research Directions

Considering all the aforementioned, it is clear that many important issues still remain to be addressed to fully enlighten the role of sympathoadrenal system in EAE/MS pathogenesis, but to mention a few. To confirm changes in sympathoadrenal system reactivity during EAE development, noradrenaline concentration in SC along with development of sympathoadrenal neuron lesions, should be examined in distinct EAE models and distinct phases and types of MS. Additionally, considering that rodent microglia synthesize catecholamines (45), it should be investigated whether these cells, as macrophages (41), may enhance local inflammation by an autocrine/paracrine feedback mechanism. Furthermore, given that functional β_1- and β_2-adrenoceptors were revealed on microglia (46), further research to delineate β_1-adrenoceptor-mediated from β_2-adrenoceptor-mediated effects on microglia in this model is necessary. Moreover, given that microglia express α_1-adrenoceptor (47), putative α_1-adrenoceptor-mediated effects of catecholamines on microglia from EAE rats are also worth examining.

PERIPHERAL CATECHOLAMINES IN PATHOGENESIS OF EAE/MS

Human Data

In favor of peripheral sympathoadrenal dysregulation in MS, in chronic progressive (CP) MS increase in circulating noradrenaline level was found (117). Differently, in relapsing-remitting (RR) MS its level is decreased (118). Additionally, in active RR MS, circulating levels of adrenaline and noradrenaline are lower than in stable disease (23). Alterations in lymphocyte catecholamine levels also occur in MS (119), so higher adrenaline in the first-attack MS patients and lower noradrenaline in RR MS were found (119). Higher noradrenaline level was also measured in peripheral blood mononuclear cells (PBMC) from MS patients (120). Additionally, upregulated β-adrenoceptor on T-lymphocytes from CP MS patients (121, 122), and on PBMC from RR and secondary progressive MS patients was reported (123–125). There is no data on the expression of α-adrenoceptors on peripheral immune cells from MS patients.

Animal Data

In Lewis EAE rats, splenic noradrenaline concentration decreased during the inductive phase of the disease (126). Our recent study demonstrated reduced noradrenaline concentration in dLNs from DA rats on the 7th day post-immunization (59). However, noradrenaline content was increased in dLN cells constituting, most likely, a compensatory mechanism (42, 127, 128). Early studies in active (129) and adoptively transferred (130) Lewis rat EAE showed more severe disease in adult rats subjected to 6-hydroxydopamine–induced sympathectomy at birth. These findings should be interpreted with caution, as neonatally administered 6-hydroxydopamine crosses the BBB (129), so aside from peripheral sympathectomy, it permanently increases noradrenergic innervation in hind brain (131). Administration of isoproterenol, a non-selective β-adrenergic agonist, during preclinical phase of EAE in Lewis rats suppressed the disease severity, while propranolol did not produce any effects (101). Conversely, we showed that propranolol administration throughout preclinical phase of EAE in DA rats moderated the disease severity (132). This discrepancy could be related to recent findings indicating that isoproterenol represents a novel type of α_{1A}-adrenoceptor partial agonist (133), and differences in propranolol dose, particularly as in the rat there are strain differences in its metabolism. Furthermore, it has recently been reported that increased systemic noradrenaline levels due to sympathoneural system hyperactivity (134) in mice constitutively lacking $\alpha_{2a/c}$-adrenoceptor (constituting an important negative-feedback mechanism required for the presynaptic control of neurotransmitter release from sympathetic fibers) is associated with diminished pathogenic T-cell responses and CNS inflammation in EAE (135). These findings might be explained by data suggesting that prolonged sympathoneural activation (as it is in late phases of inflammatory autoimmune diseases) leads to anti-inflammatory sympathoneural action (31). The moderating effect of propranolol on clinical outcome of EAE in DA rat model was ascribed to diminished CD4+ T-cell activation/proliferation and Th17 cell generation in dLNs (132), due to impaired migration of neuroantigen-carrying APCs from the site of immunization to dLNs, reflecting decreased expression of CCL19/21, chemokines driving their migration in dLNs (132). On the other hand, study on propranolol effects on dLN cells recovered in the inductive phase of EAE in the presence of arterenol (synthetic noradrenaline) or its absence showed that it enhanced CD4+ cell IL-2 synthesis and proliferation (43). Additionally, propranolol augmented differentiation of Th17 cells in dLN cell cultures by increasing RORγt expression in CD4+ cells, and production of cytokines driving/maintaining Th17 cell differentiation (IL-1β and IL-23) by APCs (43). The discrepancy between the effects of propranolol

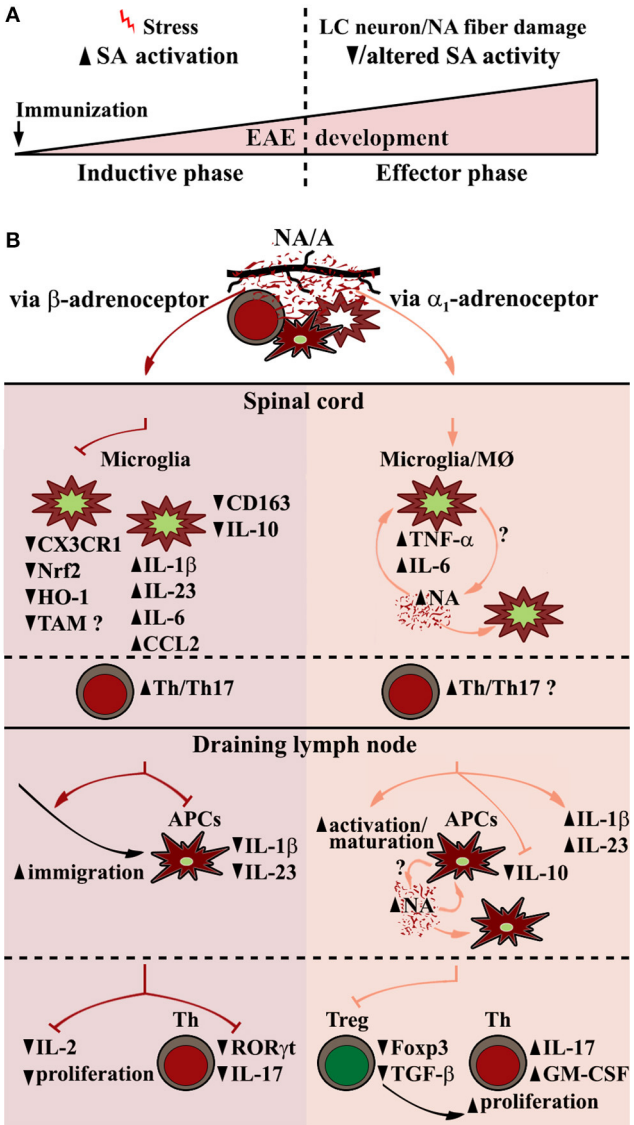

FIGURE 1 | EAE-related alterations in sympathoadrenal system (SA) and putative central and peripheral effects of its key end-point mediators (noradrenaline and adrenaline) contributing to EAE pathogenesis. **(A)** Biphasic changes in SA over the course of EAE encompass SA overactivation in preclinical EAE stage (premorbid/disease-related stress), followed by its diminished and possibly qualitatively altered activity in clinical stage of the disease partly due to locus coeruleus (LC) neuron damage. **(B)** (Spinal cord) Central noradrenaline (NA)/adrenaline (A) acting through β-adrenoceptor in early phases of the disease downregulate microglial expression of nuclear factor (erythroid-derived 2)-like 2 (Nrf2), and its key anti-inflammatory downstream target genes, including those encoding heme oxygenase-1 (HO-1), and possibly TAM (Tyro3, Axl, and Mertk) receptors involved in phagocytosis via C-X3-C motif chemokine receptor 1 (CX3CR1)-dependent and CX3CR1-independent mechanisms. This leads to shift toward more proinflammatory microglial phenotype mirrored in increased expression of proinflammatory cytokines/chemokines (e.g., IL-1β, IL-23, IL-6, CCL2), followed by diminished expression of anti-inflammatory microglial markers (e.g., CD163, IL-10), and consequently, increased infiltration of spinal cord with Th cells, their reactivation/proliferation and differentiation toward pathogenic Th17 cells. (dLN, draining lymph node) NA/A acting through β-adrenoceptor enhance antigen-carrying antigen presenting cell (APC)

(Continued)

FIGURE 1 | migration to dLN, whereas impair their synthesis of Th17 polarizing cytokines (IL-1β, IL-23), and CD4+ cell expression of RORγt and their proliferation. On the other hand, α_1-adrenoceptor–dependent stimulation leads to APC activation/maturation and augmented Th17-polarizing cytokine expression, followed by decrease in Foxp3+ Th cell (Treg) number and expression of Foxp3 and TGF-β leading to increased proliferation of Th cells and their IL-17/GM-CSF synthesis. Proinflammatory NA effects in myeloid cells, including microglia and macrophages (MØ) and peripheral APCs, may be self-amplified through a NA-α_1-adrenoceptor loop.

in vivo and *in vitro* could be reconciled by data indicating that the number of autoantigen-carrying APCs in dLNs critically determines the magnitude of the primary (auto)reactive CD4+ T-cell response and clinical outcome of autoimmune responses (136, 137).

Until recently, role of α-adrenoceptor in EAE was exclusively related to the effector phase of the disease (103, 115, 138). Our recent study showed the expression of α_1-adrenoceptor on Tregs (but not on effector CD4+ T-cells) and APCs from dLNs of DA rats in the inductive phase of EAE (59). More important, it showed that prazosin suppressed proliferation of neuroantigen-stimulated CD4+ T-cells in dLN cell cultures, by increasing the frequency of Tregs and their Foxp3 and TGF-β expression, and decreasing co-stimulatory molecule expression on APCs (59). Moreover, prazosin also decreased IL-1β and IL-23 production in EAE rat dLN cell cultures, and consequently the generation of Th17 cells, including the most pathogenic GM-CSF–producing ones (59).

Putative Research Directions

To fulfill composite picture of sympathoadrenal system modulation of EAE/MS development, several issues need to be resolved. In light of findings suggesting that sympathoneural changes in inflammatory autoimmune diseases may be organ-specific (31), it should be answered if sympathoadrenal influence on (auto)immune response in dLNs changes with progression of EAE, and at which time-point this change occurs, as well as to elucidate adrenoceptor types involved in immunoregulation. Furthermore, as human studies directly linking stress and (auto)immune response are lacking, owing to practical and ethical concerns (139), EAE models, despite limitations (5), should be considered for investigating role of stress in triggering MS, and particularly pharmacological treatments affecting catecholamine action trough distinct types of adrenoceptors. Considering that individual's elevated noradrenergic tone (e.g., due to genetics) may favor MS onset (140), such investigation should encompass animals of different genetic makeup.

CONCLUSIONS

Collectively, available data suggest that alterations in sympathoadrenal system activity due to premorbid/disease-induced stress and disease-associated sympathoneural damage contribute to EAE and possibly MS onset and development (affecting distinct types of immune cells, and particularly

important microglia, as depicted in **Figure 1**), respectively. However, further research to elucidate noradrenaline/adrenaline immunomodulatory action in the target organ and lymphoid organs/blood, in distinct phases of EAE (and in distinct EAE models) and MS alike, is necessary to envisage significance of alterations in sympathoadrenal immunomodulatory action for susceptibility to/progression of EAE/MS, and consequently consider possibilities to manipulate catecholamine action to prevent/mitigate them. To emphasize significance of this research it should be pointed that adrenergic drugs are safe and cost-effective.

AUTHOR CONTRIBUTIONS

GL and IPi wrote the manuscript. All authors participated in data collection and interpretation, critically revised the manuscript, and approved the final version for submission.

FUNDING

This study was supported by the Ministry of Education, Science and Technological Development of the Republic of Serbia (Grant No. 175050).

REFERENCES

1. Filippi M, Bar-Or A, Piehl F, Preziosa P, Solari A, Vukusic S et al. Multiple sclerosis. *Nat Rev Dis Primers*. (2018) 4:43. doi: 10.1038/s41572-018-0041-4
2. Al-Badri G, Castorina A. Insights into the role of neuroinflammation in the pathogenesis of multiple sclerosis. *J Funct Morphol Kinesiol*. (2018) 3:13. doi: 10.3390/jfmk3010013
3. *Atlas of MS 2013: Mapping Multiple Sclerosis Around the World*. London: Multiple Sclerosis International Federation (2013). Available online at: https://www.msif.org/about-us/who-we-are-and-what-we-do/advocacy/atlas/ (accessed September 6, 2019).
4. Constantinescu CS, Farooqi N, O'Brien K, Gran B. Experimental autoimmune encephalomyelitis (EAE) as a model for multiple sclerosis (MS). *Br J Pharmacol*. (2011) 164:1079–106. doi: 10.1111/j.1476-5381.2011.01302.x
5. Lassmann H, Bradl M. Multiple sclerosis: experimental models and reality. *Acta Neuropathol*. (2017) 133:223–44. doi: 10.1007/s00401-016-1631-4
6. Kurschus FC. T cell mediated pathogenesis in EAE: Molecular mechanisms. *Biomed J*. (2015) 38:183–93. doi: 10.4103/2319-4170.155590
7. Kara EE, McKenzie DR, Bastow CR, Gregor CE, Fenix KA, Ogunniyi AD, et al. CCR2 defines *in vivo* development and homing of IL-23-driven GM-CSF-producing Th17 cells. *Nat Commun*. (2015) 6:8644. doi: 10.1038/ncomms9644
8. Koutrolos M, Berer K, Kawakami N, Wekerle H, Krishnamoorthy G. Treg cells mediate recovery from EAE by controlling effector T cell proliferation and motility in the CNS. *Acta Neuropathol Commun*. (2014) 2:163. doi: 10.1186/s40478-014-0163-1
9. Thompson KK, Tsirka SE. The diverse roles of microglia in the neurodegenerative aspects of central nervous system (CNS) autoimmunity. *Int J Mol Sci*. (2017) 18:504. doi: 10.3390/ijms18030504
10. Briones-Buixassa L, Milà R, M Aragonès J, Bufill E, Olaya B, Arrufat FX. Stress and multiple sclerosis: a systematic review considering potential moderating and mediating factors and methods of assessing stress. *Health Psychol Open*. (2015) 2:2055102915612271. doi: 10.1177/2055102915612271
11. Stojanović L, Marisavljević D. Stress as a trigger of autoimmune disease. *Autoimmun Rev*. (2008) 7:209–13. doi: 10.1016/j.autrev.2007.11.007
12. Shepshelovich D, Shoenfeld Y. Prediction and prevention of autoimmune diseases: additional aspects of the mosaic of autoimmunity. *Lupus*. (2006) 15:183–90. doi: 10.1191/0961203306lu2274rr
13. O'Donovan A, Cohen BE, Seal KH, Bertenthal D, Margaretten M, Nishimi K, et al. Elevated risk for autoimmune disorders in iraq and afghanistan veterans with posttraumatic stress disorder. *Biol Psychiatry*. (2015) 77:365–74. doi: 10.1016/j.biopsych.2014.06.015
14. Carletto S, Borghi M, Scavelli F, Francone D, Perucchini ML, Cavallo M, et al. Prevalence of posttraumatic stress disorder in patients with multiple sclerosis. *J Nerv Ment Dis*. (2018) 206:149–51. doi: 10.1097/NMD.0000000000000780
15. Mohr DC, Hart SL, Julian L, Cox D, Pelletier D. Association between stressful life events and exacerbation in multiple sclerosis: a meta-analysis. *BMJ*. (2004) 328:731. doi: 10.1136/bmj.38041.724421.55
16. Gold SM, Mohr DC, Huitinga I, Flachenecker P, Sternberg EM, Heesen C. The role of stress-response systems for the pathogenesis and progression of MS. *Trends Immunol*. (2005) 26:644–52. doi: 10.1016/j.it.2005.09.010
17. Heesen C, Gold SM, Huitinga I, Reul JM. Stress and hypothalamic-pituitary-adrenal axis function in experimental autoimmune encephalomyelitis and multiple sclerosis - a review. *Psychoneuroendocrinology*. (2007) 32:604–18. doi: 10.1016/j.psyneuen.2007.05.002
18. Elenkov IJ, Wilder RL, Chrousos GP, Vizi ES. The sympathetic nerve–an integrative interface between two supersystems: the brain and the immune system. *Pharmacol Rev*. (2000) 52:595–638.
19. Haensch CA, Jörg J. Autonomic dysfunction in multiple sclerosis. *J Neurol*. (2006) 253:I3–9. doi: 10.1007/s00415-006-1102-2
20. Racosta JM, Kremenchutzky M. The role of autonomic dysregulation from pathophysiology to therapeutics of multiple sclerosis: a putative novel treatment target? *J Neurol Neurophysiol*. (2014) 5:212. doi: 10.4172/2155-9562.1000212
21. Pintér A, Cseh D, Sárközi A, Illigens BM, Siepmann T. Autonomic dysregulation in multiple sclerosis. *Int J Mol Sci*. (2015) 16:16920–52. doi: 10.3390/ijms160816920
22. Chelmicka Schorr E, Arnason BG. Nervous system-immune system interactions and their role in multiple sclerosis. *Ann Neurol*. (1994) 36(Suppl):S29–32. doi: 10.1002/ana.410360710
23. Flachenecker P, Reiners K, Krauser M, Wolf A, Toyka KV. Autonomic dysfunction in multiple sclerosis is related to disease activity and progression of disability. *Mult Scler*. (2001) 7:327–34. doi: 10.1177/135245850100700509
24. Merkelbach S, Haensch CA, Hemmer B, Koehler J, König NH, Ziemssen T. Multiple sclerosis and the autonomic nervous system. *J Neurol*. (2006) 253(Suppl 1):I21–5. doi: 10.1007/s00415-006-1105-z
25. Padro CJ, Sanders VM. Neuroendocrine regulation of inflammation. *Semin Immunol*. (2014) 26:357–68. doi: 10.1016/j.smim.2014.01.003
26. Samuels ER, Szabadi E. Functional neuroanatomy of the noradrenergic locus coeruleus: its roles in the regulation of arousal and autonomic function part I: principles of functional organisation. *Curr Neuropharmacol*. (2008) 6:235–53. doi: 10.2174/157015908785777229
27. Benarroch EE. The locus ceruleus norepinephrine system: functional organization and potential clinical significance. *Neurology*. (2009) 73:1699–704. doi: 10.1212/WNL.0b013e3181c2937c
28. O'Donnell J, Zeppenfeld D, McConnell E, Pena S, Nedergaard M. Norepinephrine: a neuromodulator that boosts the function of multiple cell types to optimize CNS performance. *Neurochem Res*. (2012) 37:2496–512. doi: 10.1007/s11064-012-0818-x
29. Deckx N, Lee WP, Berneman ZN, Cools N. Neuroendocrine immunoregulation in multiple sclerosis. *Clin Dev Immunol*. (2013) 2013:705232. doi: 10.1155/2013/705232
30. Miyake S. Mind over cytokines: crosstalk and regulation between the neuroendocrine and immune systems. *Clin Exp Neuroimmunol*. (2012) 3:1–15. doi: 10.1111/j.1759-1961.2011.00023.x
31. Bellinger DL, Lorton D. Sympathetic nerve hyperactivity in the spleen: causal for nonpathogenic-driven chronic immune-mediated inflammatory diseases (IMIDs)? *Int J Mol Sci*. (2018) 19:1188. doi: 10.3390/ijms19041188
32. Godinho-Silva C, Cardoso F, Veiga-Fernandes H. Neuro-immune cell units: a new paradigm in physiology. *Annu Rev Immunol*. (2019) 37:19–46. doi: 10.1146/annurev-immunol-042718-041812

33. Dantzer R. Neuroimmune interactions: from the brain to the immune system and vice versa. *Physiol Rev*. (2018) 98:477–504. doi: 10.1152/physrev.00039.2016
34. ThyagaRajan S, Priyanka HP. Bidirectional communication between the neuroendocrine system and the immune system: relevance to health and diseases. *Ann Neurosci*. (2012) 19:40–6. doi: 10.5214/ans.0972.7531.180410
35. Kaplin A, Bartner S. Reciprocal communication between the nervous and immune systems: crosstalk, back-talk and motivational speeches. *Int Rev Psychiatry*. (2005) 17:439–41. doi: 10.1080/02646830500381419
36. Besedovsky HO, del Rey A. Immune-neuro-endocrine interactions: facts and hypotheses. *Endocr Rev*. (1996) 17:64–102. doi: 10.1210/edrv-17-1-64
37. Racosta JM, Kimpinski K. Autonomic dysfunction, immune regulation, and multiple sclerosis. *Clin Auton Res*. (2016) 26:23–31. doi: 10.1007/s10286-015-0325-7
38. Jiang JL, Qiu YH, Peng YP, Wang JJ. Immunoregulatory role of endogenous catecholamines synthesized by immune cells. *Sheng Li Xue Bao*. (2006) 58:309–17.
39. Qiu YH, Peng YP, Jiang JM, Wang JJ. Expression of tyrosine hydroxylase in lymphocytes and effect of endogenous catecholamines on lymphocyte function. *Neuroimmunomodulation*. (2004) 11:75–83. doi: 10.1159/000075316
40. Kvetnansky R, Sabban EL, Palkovits M. Catecholaminergic systems in stress: structural and molecular genetic approaches. *Physiol Rev*. (2009) 89:535–606. doi: 10.1152/physrev.00042.2006
41. Flierl MA, Rittirsch D, Nadeau BA, Sarma JV, Day DE, Lentsch AB, et al. Upregulation of phagocyte-derived catecholamines augments the acute inflammatory response. *PLoS ONE*. (2009) 4:e4414. doi: 10.1371/journal.pone.0004414
42. Capellino S, Weber K, Gelder M, Härle P, Straub RH. First appearance and location of catecholaminergic cells during experimental arthritis and elimination by chemical sympathectomy. *Arthritis Rheum*. (2012) 64:1110–8. doi: 10.1002/art.33431
43. Vujnović I, Pilipović I, Jasnić N, Petrović R, Blagojević V, Arsenović-Ranin N, et al. Noradrenaline through β-adrenoceptor contributes to sexual dimorphism in primary CD4+ T-cell response in DA rat EAE model? *Cell Immunol*. (2019) 336:48–57. doi: 10.1016/j.cellimm.2018.12.009
44. Staedtke V, Bai RY, Kim K, Darvas M, Davila ML, Riggins GJ, et al. Disruption of a self-amplifying catecholamine loop reduces cytokine release syndrome. *Nature*. (2018) 564:273–7. doi: 10.1038/s41586-018-0774-y
45. Pilipović I, Stojić-Vukanić Z, Prijić I, Jasnić N, Leposavić G. Propranolol diminished severity of rat EAE by enhancing immunoregulatory/protective properties of spinal cord microglia. *Neurobiol Dis*. (2020) 134:104665. doi: 10.1016/j.nbd.2019.104665
46. Tanaka KF, Kashima H, Suzuki H, Ono K, Sawada M. Existence of functional beta1- and beta2-adrenergic receptors on microglia. *J Neurosci Res*. (2002) 70:232–7. doi: 10.1002/jnr.10399
47. Mori K, Ozaki E, Zhang B, Yang L, Yokoyama A, Takeda I, et al. Effects of norepinephrine on rat cultured microglial cells that express alpha1, alpha2, beta1 and beta2 adrenergic receptors. *Neuropharmacology*. (2002) 43:1026–34. doi: 10.1016/s0028-3908(02)00211-3
48. Maestroni GJ, Mazzola P. Langerhans cells beta 2-adrenoceptors: role in migration, cytokine production, Th priming and contact hypersensitivity. *J Neuroimmunol*. (2003) 144:91–9. doi: 10.1016/j.jneuroim.2003.08.039
49. Dimitrijević M, Pilipović I, Stanojević S, Mitić K, Radojević K, Pesić V, et al. Chronic propranolol treatment affects expression of adrenoceptors on peritoneal macrophages and their ability to produce hydrogen peroxide and nitric oxide. *J Neuroimmunol*. (2009) 211:56–65. doi: 10.1016/j.jneuroim.2009.03.014
50. Ramer-Quinn DS, Swanson MA, Lee WT, Sanders VM. Cytokine production by naive and primary effector CD4+ T cells exposed to norepinephrine. *Brain Behav Immun*. (2000) 14:239–55. doi: 10.1006/brbi.2000.0603
51. Loza MJ, Foster S, Peters SP, Penn RB. Beta-agonists modulate T-cell functions via direct actions on type 1 and type 2 cells. *Blood*. (2006) 107:2052–60. doi: 10.1182/blood-2005-08-3265
52. Guereschi MG, Araujo LP, Maricato JT, Takenaka MC, Nascimento VM, Vivanco BC, et al. Beta2-adrenergic receptor signaling in CD4+ Foxp3+ regulatory T cells enhances their suppressive function in a PKA-dependent manner. *Eur J Immunol*. (2013) 43:1001–12. doi: 10.1002/eji.201243005
53. Carvajal Gonczi CM, Tabatabaei Shafiei M, East A, Martire E, Maurice-Ventouris MHI, Darlington PJ. Reciprocal modulation of helper Th1 and Th17 cells by the β2-adrenergic receptor agonist drug terbutaline. *FEBS J*. (2017) 284:3018–28. doi: 10.1111/febs.14166
54. Liu Y, Rui XX, Shi H, Qiu YH, Peng YP. Norepinephrine inhibits Th17 cells via β2-adrenergic receptor (β2-AR) signaling in a mouse model of rheumatoid arthritis. *Med Sci Monit*. (2018) 24:1196–204. doi: 10.12659/msm.906184
55. Maestroni GJ. Dendritic cell migration controlled by alpha 1b-adrenergic receptors. *J Immunol*. (2000) 165:6743–7. doi: 10.4049/jimmunol.165.12.6743
56. Yanagawa Y, Matsumoto M, Togashi H. Enhanced dendritic cell antigen uptake via alpha2 adrenoceptor-mediated PI3K activation following brief exposure to noradrenaline. *J Immunol*. (2010) 185:5762–8. doi: 10.4049/jimmunol.1001899
57. Jetschmann JU, Benschop RJ, Jacobs R, Kemper A, Oberbeck R, Schmidt RE, et al. Expression and *in-vivo* modulation of alpha- and beta-adrenoceptors on human natural killer (CD16+) cells. *J Neuroimmunol*. (1997) 74:159–64. doi: 10.1016/S0165-5728(96)00221-4
58. Slota C, Shi A, Chen G, Bevans M, Weng NP. Norepinephrine preferentially modulates memory CD8 T cell function inducing inflammatory cytokine production and reducing proliferation in response to activation. *Brain Behav Immun*. (2015) 46:168–79. doi: 10.1016/j.bbi.2015.01.015
59. Pilipović I, Vujnović I, Stojić-Vukanić Z, Petrović R, Kosec D, Nacka-Aleksić M, et al. Noradrenaline modulates CD4+ T cell priming in rat experimental autoimmune encephalomyelitis: a role for the α1-adrenoceptor. *Immunol Res*. (2019) 67:223–40. doi: 10.1007/s12026-019-09082-y
60. Grisanti LA, Perez DM, Porter JE. Modulation of immune cell function by α(1)-adrenergic receptor activation. *Curr Top Membr*. (2011) 67:113–38. doi: 10.1016/B978-0-12-384921-2.00006-9
61. Torres MB, Vega VL, Bedri M, Saad D, Trentzsch H, Reeves RH, et al. IL-10 plasma levels are elevated after LPS injection in splenectomized A/J mice. *J Surg Res*. (2005) 129:101–6. doi: 10.1016/j.jss.2005.06.008
62. Flierl MA, Rittirsch D, Huber-Lang M, Sarma JV, Ward PA. Catecholamines-crafty weapons in the inflammatory arsenal of immune/inflammatory cells or opening pandora's box? *Mol Med*. (2008) 14:195–204. doi: 10.2119/2007-00105.Flierl
63. Grisanti LA, Evanson J, Marchus E, Jorissen H, Woster AP, DeKrey W, et al. Pro-inflammatory responses in human monocytes are β1-adrenergic receptor subtype dependent. *Mol Immunol*. (2010) 47:1244–54. doi: 10.1016/j.molimm.2009.12.013
64. Hu XX, Goldmuntz EA, Brosnan CF. The effect of norepinephrine on endotoxin-mediated macrophage activation. *J Neuroimmunol*. (1991) 31:35–42. doi: 10.1016/0165-5728(91)90084-k
65. van der Poll T. Effects of catecholamines on the inflammatory response. *Sepsis*. (2001) 4:159–67. doi: 10.1023/a:1011463006351
66. Hanke ML, Powell ND, Stiner LM, Bailey MT, Sheridan JF. Beta adrenergic blockade decreases the immunomodulatory effects of social disruption stress. *Brain Behav Immun*. (2012) 26:1150–9. doi: 10.1016/j.bbi.2012.07.011
67. Heijnen CJ, Rouppe van der Voort C, Wulffraat N, van der Net J, Kuis W, Kavelaars A. Functional alpha 1-adrenergic receptors on leukocytes of patients with polyarticular juvenile rheumatoid arthritis. *J Neuroimmunol*. (1996) 71:223–6. doi: 10.1016/s0165-5728(96)00125-7
68. Szelenyi I. Animal models of bronchial asthma. *Inflamm Res*. (2000) 49:639–54. doi: 10.1007/s000110050642
69. Sanders VM. The beta2-adrenergic receptor on T and B lymphocytes: do we understand it yet? *Brain Behav Immun*. (2012) 26:195–200. doi: 10.1016/j.bbi.2011.08.001
70. Wohleb ES, Hanke ML, Corona AW, Powell ND, Stiner LM, Bailey MT, et al. β-adrenergic receptor antagonism prevents anxiety-like behavior and microglial reactivity induced by repeated social defeat. *J Neurosci*. (2011) 31:6277–88. doi: 10.1523/JNEUROSCI.0450-11.2011
71. Takenaka MC, Araujo LP, Maricato JT, Nascimento VM, Guereschi MG, Rezende RM, et al. Norepinephrine controls effector T cell differentiation through β2-adrenergic receptor-mediated inhibition of NF-κB and AP-1 in dendritic cells. *J Immunol*. (2016) 196:637–44. doi: 10.4049/jimmunol.1501206

72. Polak PE, Kalinin S, Feinstein DL. Locus coeruleus damage and noradrenaline reductions in multiple sclerosis and experimental autoimmune encephalomyelitis. *Brain*. (2011) 134:665–77. doi: 10.1093/brain/awq362
73. Davidson D, Pullar IA, Mawdsley C, Kinloch N, Yates CM. Monoamine metabolites in cerebrospinal fluid in multiple sclerosis. *J Neurol Neurosurg Psychiatry*. (1977) 40:741–5. doi: 10.1136/jnnp.40.8.741
74. Markianos M, Koutsis G, Evangelopoulos ME, Mandellos D, Karahalios G, Sfagos C. Relationship of CSF neurotransmitter metabolite levels to disease severity and disability in multiple sclerosis. *J Neurochem*. (2009) 108:158–64. doi: 10.1111/j.1471-4159.2008.05750.x
75. Dunn AJ. Effects of cytokines and infections on brain neurochemistry. *Clin Neurosci Res*. (2006) 6:52–68. doi: 10.1016/j.cnr.2006.04.002
76. Berne-Fromell K, Fromell H, Lundkvist S, Lundkvist P. Is multiple sclerosis the equivalent of Parkinson's disease for noradrenaline? *Med Hypotheses*. (1987) 23:409–15. doi: 10.1016/0306-9877(87)90062-4
77. Pacheco R, Contreras F, Zouali M. The dopaminergic system in autoimmune diseases. *Front Immunol*. (2014) 5:117. doi: 10.3389/fimmu.2014.00117
78. Loder C, Allawi J, Horrobin DF. Treatment of multiple sclerosis with lofepramine, L-phenylalanine and vitamin B(12): mechanism of action and clinical importance: roles of the locus coeruleus and central noradrenergic systems. *Med Hypotheses*. (2002) 59:594–602. doi: 10.1016/s0306-9877(02)00261-x
79. Wade DT, Young CA, Chaudhuri KR, Davidson DLW. A randomised placebo controlled exploratory study of vitamin B-12, lofepramine, and L-phenylalanine (the "Cari Loder regime") in the treatment of multiple sclerosis. *J Neurol Neurosurg Psychiatry*. (2002) 73:246–9. doi: 10.1136/jnnp.73.3.246
80. Axelrod S, Bielory L. Beta2-agonists and paresthesias in multiple sclerosis. *Ann Allergy Asthma Immunol*. (2007) 98:100. doi: 10.1016/S1081-1206(10)60871-X
81. Makhlouf K, Weiner HL, Khoury SJ. Potential of beta2-adrenoceptor agonists as add-on therapy for multiple sclerosis: focus on salbutamol (albuterol). *CNS Drugs*. (2002) 16:1–8. doi: 10.2165/00023210-200216010-00001
82. Khoury SJ, Healy BC, Kivisäkk P, Viglietta V, Egorova S, Guttmann CR, et al. A randomized controlled double-masked trial of albuterol add-on therapy in patients with multiple sclerosis. *Arch Neurol*. (2010) 67:1055–61. doi: 10.1001/archneurol.2010.222
83. Zimmer P, Bloch W, Schenk A, Oberste M, Riedel S, Kool J, et al. High-intensity interval exercise improves cognitive performance and reduces matrix metalloproteinases-2 serum levels in persons with multiple sclerosis: a randomized controlled trial. *Mult Scler*. (2018) 24:1635–44. doi: 10.1177/1352458517728342
84. Sandroff BM, Johnson CL, Motl RW. Exercise training effects on memory and hippocampal viscoelasticity in multiple sclerosis: a novel application of magnetic resonance elastography. *Neuroradiology*. (2017) 59:61–7. doi: 10.1007/s00234-016-1767-x
85. Feys P, Moumdjian L, Van Halewyck F, Wens I, Eijnde BO, Van Wijmeersch B, et al. Effects of an individual 12-week community-located "start-to-run" program on physical capacity, walking, fatigue, cognitive function, brain volumes, and structures in persons with multiple sclerosis. *Mult Scler*. (2019) 25:92–103. doi: 10.1177/1352458517740211
86. Gilbertson RM, Klatt MD. Mindfulness in motion for people with multiple sclerosis: a feasibility study. *Int J MS Care*. (2017) 19:225–31. doi: 10.7224/1537-2073.2015-095
87. Willekens B, Perrotta G, Cras P, Cools N. Into the moment: does mindfulness affect biological pathways in multiple sclerosis? *Front Behav Neurosci*. (2018) 12:103. doi: 10.3389/fnbeh.2018.00103
88. Pagnini F, Cavalera C, Rovaris M, Mendozzi L, Molinari E, Phillips D et al. Longitudinal associations between mindfulness and well-being in people with multiple sclerosis. *Int J Clin Health Psychol*. (2019) 19:22–30. doi: 10.1016/j.ijchp.2018.11.003
89. Thakur P, Mohammad A, Rastogi YR, Saini RV, Saini AK. Yoga as an intervention to manage multiple sclerosis symptoms. *J Ayurveda Integr Med*. (2019). doi: 10.1016/j.jaim.2019.04.005. [Epub ahead of print].
90. Tsai CP, Lin FC, Lee CT. Beta2-adrenergic agonist use and the risk of multiple sclerosis: a total population-based case-control study. *Mult Scler*. (2014) 20:1593–601. doi: 10.1177/1352458514528758
91. Khoruzhaia TA, Saakov BA. Change in monoamine content and monoamine oxidase activity in brain structures during experimental allergic encephalomyelitis. *Biull Eksp Biol Med*. (1975) 79:80–2.
92. White SR, Bhatnagar RK, Bardo MT. Norepinephrine depletion in the spinal cord gray matter of rats with experimental allergic encephalomyelitis. *J Neurochem*. (1983) 40:1771–3. doi: 10.1111/j.1471-4159.1983.tb08156.x
93. Krenger W, Honegger CG, Feurer C, Cammisuli S. Changes of neurotransmitter systems in chronic relapsing experimental allergic encephalomyelitis in rat brain and spinal cord. *J Neurochem*. (1986) 47:1247–54. doi: 10.1111/j.1471-4159.1986.tb00747.x
94. Krenger W, Kabiersch A, Honegger CG. Monoamines and related substances in brainstem and spinal cord of Lewis rats during the attack and recovery of experimental autoimmune encephalomyelitis. *Brain Res*. (1989) 491:374–8. doi: 10.1016/0006-8993(89)90074-7
95. Musgrave T, Tenorio G, Rauw G, Baker GB, Kerr BJ. Tissue concentration changes of amino acids and biogenic amines in the central nervous system of mice with experimental autoimmune encephalomyelitis (EAE). *Neurochem Int*. (2011) 59:28–38. doi: 10.1016/j.neuint.2011.03.020
96. Jovanova-Nesic K, Nikolic V, Jankovic BD. Locus ceruleus and immunity. II. Suppression of experimental allergic encephalomyelitis and hypersensitivity skin reactions in rats with lesioned locus ceruleus. *Int J Neurosci*. (1993) 68:289–94. doi: 10.3109/00207459308994284
97. Karpus WJ, Konkol RJ, Killen JA. Central catecholamine neurotoxin administration. 1. Immunological changes associated with the suppression of experimental autoimmune encephalomyelitis. *J Neuroimmunol*. (1988) 18:61–73. doi: 10.1016/0165-5728(88)90135-X
98. Konkol RJ, Wesselmann U, Karpus WJ, Leo GL, Killen JA, Roerig DL. Suppression of clinical weakness in experimental autoimmune encephalomyelitis associated with weight changes, and post-decapitation convulsions after intracisternal-ventricular administration of 6-hydroxydopamine. *J Neuroimmunol*. (1990) 26:25–34. doi: 10.1016/0165-5728(90)90116-5
99. Simonini MV, Polak PE, Sharp A, McGuire S, Galea E, Feinstein DL. Increasing CNS noradrenaline reduces EAE severity. *J Neuroimmune Pharmacol*. (2010) 5:252–9. doi: 10.1007/s11481-009-9182-2
100. Ross SB, Stenfors C. DSP4, a selective neurotoxin for the locus coeruleus noradrenergic system. A review of its mode of action. *Neurotox Res*. (2015) 27:15–30. doi: 10.1007/s12640-014-9482-z
101. Chelmicka-Schorr E, Kwasniewski MN, Thomas BE, Arnason BGW. The β-adrenergic agonist isoproterenol suppresses experimental allergic encephalomyelitis in Lewis rats. *J Neuroimmunol*. (1989) 25:203–7. doi: 10.1016/0165-5728(89)90138-0
102. Dimitrijević M, Rauski A, Radojević K, Kosec D, Stanojević S, Pilipović I, et al. Beta-adrenoceptor blockade ameliorates the clinical course of experimental allergic encephalomyelitis and diminishes its aggravation in adrenalectomized rats. *Eur J Pharmacol*. (2007) 577:170–82. doi: 10.1016/j.ejphar.2007.08.021
103. Brosnan CF, Goldmuntz EA, Cammer W, Factor SM, Bloom BR, Norton WT. Prazosin, an alpha 1-adrenergic receptor antagonist, suppresses experimental autoimmune encephalomyelitis in the Lewis rat. *Proc Natl Acad Sci USA*. (1985) 82:5915–9. doi: 10.1073/pnas.82.17.5915
104. Neil-Dwyer G, Bartlett J, McAinsh J, Cruickshank JM. Beta-adrenoceptor blockers and the blood-brain barrier. *Br J Clin Pharmacol*. (1981) 11:549–53. doi: 10.1111/j.1365-2125.1981.tb01169.x
105. Lastres-Becker I, Innamorato NG, Jaworski T, Rábano A, Kügler S, Van Leuven F, et al. Fractalkine activates NRF2/NFE2L2 and heme oxygenase 1 to restrain tauopathy-induced microgliosis. *Brain*. (2014) 137:78–91. doi: 10.1093/brain/awt323
106. Lee H, Choi YK. Regenerative effects of heme oxygenase metabolites on neuroinflammatory diseases. *Int J Mol Sci*. (2019) 20:78. doi: 10.3390/ijms20010078
107. Castro-Sánchez S, García-Yagüe ÁJ, Kügler S, Lastres-Becker I. CX3CR1-deficient microglia shows impaired signalling of the transcription factor NRF2: implications in tauopathies. *Redox Biol*. (2019) 22:101118. doi: 10.1016/j.redox.2019.101118

108. Dinkova-Kostova AT, Kostov RV, Kazantsev AG. The role of Nrf2 signaling in counteracting neurodegenerative diseases. *FEBS J*. (2018) 285:3576–90. doi: 10.1111/febs.14379
109. Cuadrado A, Martin-Moldes Z, Ye J, Lastres-Becker I. Transcription factors NRF2 and NF-kappaB are coordinated effectors of the Rho family, GTP-binding protein RAC1 during inflammation. *J Biol Chem*. (2014) 289:15244–58. doi: 10.1074/jbc.M113.540633
110. Hinojosa AE, Garcia-Bueno B, Leza JC, Madrigal JL. CCL2/MCP-1 modulation of microglial activation and proliferation. *J Neuroinflammation*. (2011) 8:77. doi: 10.1186/1742-2094-8-77
111. Ji R, Meng L, Li Q, Lu Q. TAM receptor deficiency affects adult hippocampal neurogenesis. *Metab Brain Dis*. (2015) 30:633–44. doi: 10.1007/s11011-014-9636-y
112. Rothlin CV, Lemke G. TAM receptor signaling and autoimmune disease. *Curr Opin Immunol*. (2010) 22:740–6. doi: 10.1016/j.coi.2010.10.001
113. Zhang Z, Zhang ZY, Wu Y, Schluesener HJ. Lesional accumulation of CD163+ macrophages/microglia in rat traumatic brain injury. *Brain Res*. (2012) 1461:102–10. doi: 10.1016/j.brainres.2012.04.038
114. Ahn M, Yang W, Kim H, Jin JK, Moon C, Shin T. Immunohistochemical study of arginase-1 in the spinal cords of Lewis rats with experimental autoimmune encephalomyelitis. *Brain Res*. (2012) 1453:77–86. doi: 10.1016/j.brainres.2012.03.023
115. Brosnan CF, Sacks HJ, Goldschmidt RC, Goldmuntz EA, Norton WT. Prazosin treatment during the effector stage of disease suppresses experimental autoimmune encephalomyelitis in the Lewis rat. *J Immunol*. (1986) 137:3451–6.
116. White SR, Black PC, Samathanam GK, Paros KC. Prazosin suppresses development of axonal damage in rats inoculated for experimental allergic encephalomyelitis. *J Neuroimmunol*. (1992) 39:211–8. doi: 10.1016/0165-5728(92)90255-J
117. Karaszewski JW, Reder AT, Anlar B, Arnason GW. Increased high affinity beta-adrenergic receptor densities and cyclic AMP responses of CD8 cells in multiple sclerosis. *J Neuroimmunol*. (1993) 43:1–7. doi: 10.1016/0165-5728(93)90068-A
118. Mel'nikov MV, Belousova OO, Zhetishev RR, Pashchenkov MV, Boiko AN. Effects of catecholamines on Th17 cells in multiple sclerosis. *Neurosci Behav Phys*. (2018) 48:342–5. doi: 10.1007/s11055-018-0568-6
119. Rajda C, Bencsik K, Vécsei LL, Bergquist J. Catecholamine levels in peripheral blood lymphocytes from multiple sclerosis patients. *J Neuroimmunol*. (2002) 124:93–100. doi: 10.1016/S0165-5728(02)00002-4
120. Cosentino M, Zaffaroni M, Marino F, Bombelli R, Ferrari M, Rasini E, et al. Catecholamine production and tyrosine hydroxylase expression in peripheral blood mononuclear cells from multiple sclerosis patients: effect of cell stimulation and possible relevance for activation-induced apoptosis. *J Neuroimmunol*. (2002) 133:233–40. doi: 10.1016/S0165-5728(02)00372-7
121. Arnason BG, Brown M, Maselli R, Karaszewski J, Reder A. Blood lymphocyte beta-adrenergic receptors in multiple sclerosis. *Ann N Y Acad Sci*. (1988) 540:585–8. doi: 10.1111/j.1749-6632.1988.tb27181.x
122. Karaszewski JW, Reder AT, Maselli R, Brown M, Arnason BG. Sympathetic skin responses are decreased and lymphocyte beta-adrenergic receptors are increased in progressive multiple sclerosis. *Ann Neurol*. (1990) 27:366–72. doi: 10.1002/ana.410270404
123. Zoukos Y, Leonard JP, Thomaides T, Thompson AJ, Cuzner ML. beta-Adrenergic receptor density and function of peripheral blood mononuclear cells are increased in multiple sclerosis: a regulatory role for cortisol and interleukin-1. *Ann Neurol*. (1992) 31:657–62. doi: 10.1002/ana.410310614
124. Zoukos Y, Thomaides TN, Kidd D, Cuzner ML, Thompson A. Expression of beta2 adrenoreceptors on peripheral blood mononuclear cells in patients with primary and secondary progressive multiple sclerosis: a longitudinal six month study. *J Neurol Neurosurg Psychiatry*. (2003) 74:197–202. doi: 10.1136/jnnp.74.2.197
125. Zoukos Y, Kidd D, Woodroofe MN, Kendall BE, Thompson AJ, Cuzner ML. Increased expression of high affinity IL-2 receptors and beta-adrenoceptors on peripheral blood mononuclear cells is associated with clinical and MRI activity in multiple sclerosis. *Brain*. (1994) 117:307–15. doi: 10.1093/brain/117.2.307
126. Mackenzie FJ, Leonard JP, Cuzner ML. Changes in lymphocyte beta-adrenergic receptor density and noradrenaline content of the spleen are early indicators of immune reactivity in acute experimental allergic encephalomyelitis in the Lewis rat. *J Neuroimmunol*. (1989) 23:93–100. doi: 10.1016/0165-5728(89)90027-1
127. Huang HW, Fang XX, Wang XQ, Peng YP, Qiu YH. Regulation of differentiation and function of helper T cells by lymphocyte-derived catecholamines via α1-and β2-adrenoceptors. *Neuroimmunomodulation*. (2015) 22:138–51. doi: 10.1159/000360579
128. Huang HW, Zuo C, Chen X, Peng YP, Qiu YH. Effect of tyrosine hydroxylase overexpression in lymphocytes on the differentiation and function of T helper cells. *Int J Mol Med*. (2016) 38:635–42. doi: 10.3892/ijmm.2016.2639
129. Chelmicka-Schorr E, Checinski M, Arnason BG. Chemical sympathectomy augments the severity of experimental allergic encephalomyelitis. *J Neuroimmunol*. (1988) 17:347–50. doi: 10.1016/0165-5728(88)90125-7
130. Chelmicka-Schorr E, Kwasniewski MN, Wollmann RL. Sympathectomy augments adoptively transferred experimental allergic encephalomyelitis. *J Neuroimmunol*. (1992) 37:99–103. doi: 10.1016/0165-5728(92)90160-M
131. Konkol RJ, Bendeich EG, Breese GR. A biochemical and morphological study of the altered growth pattern of central catecholamine neurons following 6-hydroxydopamine. *Brain Res*. (1978) 140:125–35. doi: 10.1016/0006-8993(78)90242-1
132. Pilipović I, Vujnović I, Petrović R, Stojić-Vukanić Z, Leposavić G. Propranolol impairs primary immune responses in rat experimental autoimmune encephalomyelitis. *Neuroimmunomodulation*. (2019) 27:1–10. doi: 10.1159/000500094
133. Copik AJ, Baldys A, Nguyen K, Sahdeo S, Ho H, Kosaka A, et al. Isoproterenol acts as a biased agonist of the alpha-1a-adrenoceptor that selectively activates the MAPK/ERK pathway. *PLoS ONE*. (2015) 10:e0115701. doi: 10.1371/journal.pone.0115701
134. Hein L, Altman JD, Kobilka BK. Two functionally distinct alpha2-adrenergic receptors regulate sympathetic neurotransmission. *Nature*. (1999) 402:181–4. doi: 10.1038/46040
135. Araujo LP, Maricato JT, Guereschi MG, Takenaka MC, Nascimento VM, de Melo FM, et al. The sympathetic nervous system mitigates CNS autoimmunity via β2-adrenergic receptor signaling in immune cells. *Cell Rep*. (2019) 28:3120–30.e5. doi: 10.1016/j.celrep.2019.08.042
136. Allenspach EJ, Lemos MP, Porrett PM, Turka LA, Laufer TM. Migratory and lymphoid-resident dendritic cells cooperate to efficiently prime naive CD4 T cells. *Immunity*. (2008) 29:795–806. doi: 10.1016/j.immuni.2008.08.013
137. Ludewig B, Junt T, Hengartner H, Zinkernagel RM. Dendritic cells in autoimmune diseases. *Curr Opin Immunol*. (2001) 13:657–62. doi: 10.1016/S0952-7915(01)00275-8
138. Haerter K, Vroon A, Kavelaars A, Heijnen CJ, Limmroth V, Espinosa E, et al. *In vitro* adrenergic modulation of cellular immune functions in experimental autoimmune encephalomyelitis. *J Neuroimmunol*. (2004) 146:126–32. doi: 10.1016/j.jneuroim.2003.10.051
139. Padgett DA, Glaser R. How stress influences the immune response. *Trends Immunol*. (2003) 24:444–8. doi: 10.1016/S1471-4906(03)00173-X
140. Fitzgerald PJ. Noradrenaline transmission reducing drugs may protect against a broad range of diseases. *Auton Autacoid Pharmacol*. (2015) 34:15–26. doi: 10.1111/aap.12019

Conflict of Interest: The authors declare that the research was conducted in the absence of any commercial or financial relationships that could be construed as a potential conflict of interest.

The reviewer DM declared a shared affiliation, with no collaboration, with the authors ZS-V and GL to the handling editor at the time of the review.

frontiers in Endocrinology

CASE REPORT
published: 21 January 2020
doi: 10.3389/fendo.2019.00936

Adrenocorticotropic Hormone-Producing Paraganglioma With Low Plasma ACTH Level: A Case Report and Review of the Literature

Siyue Liu, Zhelong Liu, Fuqiong Chen, Weijie Xu and Gang Yuan**

Department of Endocrinology, Tongji Hospital, Huazhong University of Science and Technology, Wuhan, China

Ectopic adrenocorticotropic hormone (ACTH) syndrome caused by paraganglioma is extremely rare. It usually accompanied by high or normal plasma ACTH level. Here we described a male who presented with ectopic ACTH-producing paraganglioma and a low plasma ACTH level. Immunohistochemistry and immunofluorescence confirmed ACTH production in focal paraganglioma cells. This unusual case expanded the spectrum of ACTH-dependent Cushing's syndrome and revealed a potential mechanism of this unique clinical phenotype. Besides, the literature concerning ACTH-producing paraganglioma is reviewed.

Keywords: Cushing's syndrome, paraganglioma, adrenocorticotropic hormone, ectopic ACTH syndrome, immunohistochemistry, immunofluorescence

OPEN ACCESS

Edited by:
Vinicius Frias Carvalho, Oswaldo Cruz Foundation (Fiocruz), Brazil

Reviewed by:
Victor Alejandro Castillo, University of Buenos Aires, Argentina
Muhammad Yazid Jalaludin, University of Malaya, Malaysia

****Correspondence:***
Weijie Xu
xwj.07@163.com
Gang Yuan
yuangang88@hotmail.com

Specialty section:
This article was submitted to Neuroendocrine Science, a section of the journal Frontiers in Endocrinology

Received: *25 October 2019*
Accepted: *24 December 2019*
Published: *21 January 2020*

Citation:
Liu S, Liu Z, Chen F, Xu W and Yuan G (2020) Adrenocorticotropic Hormone-Producing Paraganglioma With Low Plasma ACTH Level: A Case Report and Review of the Literature. Front. Endocrinol. 10:936. doi: 10.3389/fendo.2019.00936

BACKGROUND

Cushing's syndrome (CS) is a rare disorder with an incidence of five per million. CS is fatal unless appropriate treatment is provided; therefore, the early and correct diagnosis has important implications for patients (1). Most cases (about 80%) are caused by hypersecretion of adrenocorticotropic hormone (ACTH), 70% of which are primary pituitary diseases. Ten percent of CS cases are caused by ectopic ACTH production. The etiology of the remaining 20% of CS patients is not related to ACTH, but adrenal in origin (adrenal adenoma, cancer, or bilateral hyperplasia) (2). Paraganglioma and pheochromocytoma belong to a tumor of the paraganglion system; the former arises from the extra-adrenal regions and the latter from the adrenal medulla (3). Ectopic ACTH syndrome caused by paraganglioma is extremely rare. It usually accompanied by high or normal plasma ACTH level. Here we present an ectopic ACTH-dependent CS, caused by a paraganglioma. This is the first report of ectopic ACTH-producing paraganglioma with a low plasma ACTH level. This unusual case expanded the spectrum of ACTH-dependent CS and revealed a potential mechanism of this unique clinical phenotype. Besides, we review the literature concerning ACTH-producing paraganglioma.

CASE PRESENTATION

A 55-year-old man presented with a 2-month history of severe hypertension (220/160 mmHg). Blood pressure was maintained at 150/100 mmHg with benzenesulfonate levamlodipine 5 mg treatment. There was no apparent headache, palpitation, and hyperhidrosis.

He also suffered from persistent distended upper abdominal pain and fatigue for 2 weeks. There was no family history of Cushing's syndrome or pheochromocytoma. Physical examination revealed a blood pressure of 148/102 mmHg, a heart rate of 98 beats/min. He showed no cushingoid features such as hyperpigmentation, muscle weakness of the limbs, moon face, or buffalo hump. Laboratory examination showed the presence of slight hypokalemia (**Table 1**). The serum level of cortisol was elevated, yet the ACTH level was decreased (**Table 2**). There was no suppression after 2-day 2-mg dexamethasone administration (**Table 2**). There was no elevation of renin, aldosterone, urinary metanephrine, and normetanephrine levels (**Table 2**). Subsequent analysis of 24-h urinary metanephrine, normetanephrine, catecholamines, and vanillylmandelic acid, as well as of blood catecholamines, showed no elevated levels. B-scan ultrasonography, computed tomography (CT) scan, and enhanced scans presented a large mass in Morison's pouch, measuring 17*12*12 cm, possibly derived from the right adrenal gland (**Figure 1**). The images showed no evidence of left adrenal hypertrophy, respectively. According to these findings, our clinical diagnosis was Cushing's syndrome with a retroperitoneal mass. Alpha-blocker and calcium channel blocker were added, and he underwent an exploratory laparotomy, retroperitoneal tumor resection, and right adrenalectomy. His right adrenal gland is compressed and atrophic, carrying no tumor cells, and no hyperplasia was evident. The resected tumor was diagnosed as the ACTH-secreting paraganglioma in the pathological examination. Histological features were typical of paraganglioma, including chief cells arranged in nests, alveolar-like, and stereo-like structures and surrounded by sustentacular cells partly or entirely (a Zellballen pattern). Immunohistochemical analysis revealed scattered and focally positive for synaptophysin in tumor cells and S-100 positivity for sustentacular cells, which are characteristics of paraganglioma. Additional immunohistochemistry and double immunofluorescence technology revealed positive immunostaining for ACTH, and also for synaptophysin, proving that ACTH secretion indeed was derived from paraganglioma cells. Furthermore, immunofluorescence histochemical double staining was positive for both Melan-A and synaptophysin in focal tumor cells, indicating that these ACTH-secreting tumor cells might secrete cortisol as well (**Figure 1**). All of these findings confirmed the diagnosis of ACTH-secreting paraganglioma and Cushing's syndrome. After surgery, his hypertension and the symptoms of abdominal pain and fatigue improved, and the hydrocortisone supplementation slowly tapered. At the last follow-up 1.5 years later, his blood pressure and heart rate became normal (128/80 mmHg and 78 bpm); his plasma ACTH level increased, and the cortisol level dropped to the normal range. Hypokalemia was improved (**Table 2**).

TABLE 1 | Baseline laboratory values of the patient.

Parameter	On admission	Postoperative	Reference range
WBC	10.1	8.3	5.2–11.4 $10^3/\mu L$
Hg	14	14	12–16 g/dL
Plt	246	284	130–400 $10^3/\mu L$
Neutrophil	7.57	5.84	1.9–8 $10^3/\mu L$
Eosinophil	0.1	0.0	0-0.8 $10^3/\mu L$
Lymphocyte	2.5	2.4	0.9–5.2 $10^3/\mu L$
Glucose	85	78	70–100 mg/dL
Na^+	140.6	142.8	136–145 mmol/L
K^+	3.4	4.7	3.5–5.1 mmol/L

WBC, white blood cell; Hg, hemoglobin; Plt, platelet; Na^+, sodium; K^+, potassium.

TABLE 2 | Hormone profiles and dexamethasone suppression test.

Parameter	On admission	Postoperative	Reference range
ACTH	1.0	76.3	7.2–63.3 pg/mL
Cortisol	18.60	10.90	6.02–18.4 μg/dL
Aldosterone	27.1	30.2	0–353.0 pg/mL
Plasma renin activity	13	14	4.4–46.1 μIU/mL
Urinary metanephrine	145.28	150.82	38–266 μg/24 h
Urinary normetanephrine	116.54	114.86	27–561 μg/24 h
Plasma metanephrine	<0.07	<0.07	≤0.21 nmol/L
Plasma normetanephrine	<0.06	<0.06	≤0.59 nmol/L
Urinary epinephrine	1.1	2.5	0–14 μg/24 h
Urinary norepinephrine	38.5	27.9	1–100 μg/24 h
Urinary dopamine	167.83	108.57	18–504 μg/24 h
Urinary vanillylmandelic acid	16.8	21.4	0–41.28 μmol//24 h
Urinary homovanillis acid	15.14	8.66	0–41.86 μmol//24 h
TSH	0.919	ND	0.27–4.2 μIU/mL
fT3	2.11	ND	2.0–4.4 pg/mL
fT4	11.56	ND	9.32–17.09 ng/L
Dexamethasone suppression test before surgical operation			
Dexamethasone	Basal	2 mg	
Cortisol (μg/dL)	18.5	19.10	

ACTH, adrenocorticotropin; TSH, thyroid stimulating hormone; fT3, free triiodothyronine; fT4, free thyroxine; ND, no data.

DISCUSSION

This case represents a very rare cause of ectopic CS caused by an ACTH-producing paraganglioma and illustrates the diagnostic challenges of ACTH-dependent CS. This is the first report of ectopic ACTH-producing paraganglioma with a low plasma ACTH level. It demonstrates that the relative contributions of clinical, biochemical, and radiological clues in establishing the correct underlying cause of CS may differ considerably between Cushing's disease and Cushing's syndrome due to ectopic ACTH production.

In about 90% of cases, tumors arising from chromaffin cells are located in the adrenal medulla and are commonly termed pheochromocytomas, whereas, in 10% of cases, tumors are extra-adrenal and are termed paragangliomas (3). Hormonal and immunobiological studies suggested that our patient suffered from functional paragangliomas with ACTH producing. Only 15 cases of ectopic ACTH caused by paraganglioma were reported (**Table 3**) (4–18). The tumors were located in mediastinum in 4 cases, paranasal sinuses in 5 cases and retroperitoneal in 3

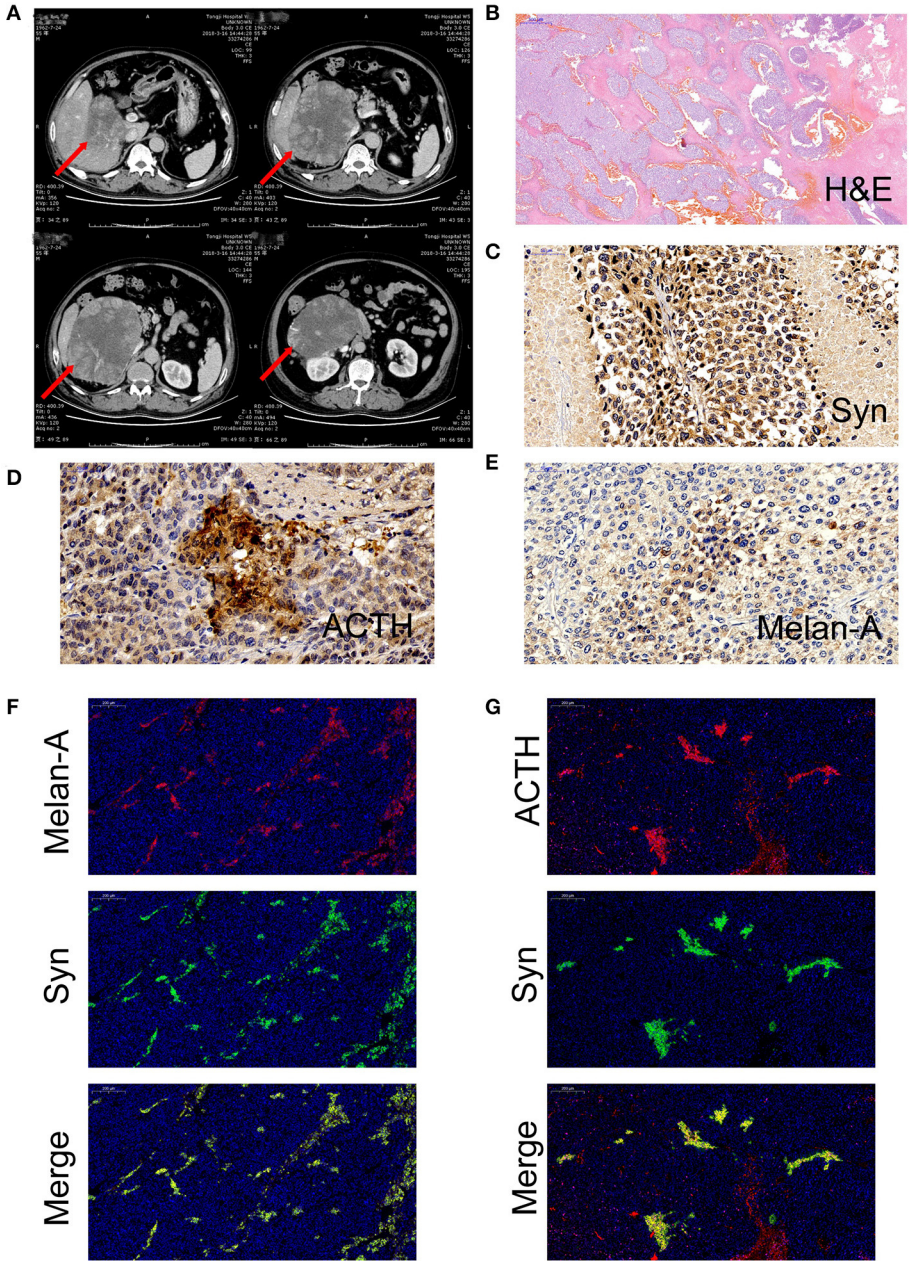

FIGURE 1 | (A) Computed tomography of a large mass in Morison's pouch, measuring 17*12*12 cm (red arrow). **(B)** Hematoxylin and eosin (H&E) stain of paraffin embedded tumor tissue. **(C)** Immunohistochemistry with antibodies specific for synaptophysin (Syn) (Abcam, #ab32127, Cambridge, UK). **(D)** Immunohistochemistry with antibodies specific for adrenocorticotropic hormone (ACTH) (Abcam, #ab74976, Cambridge, UK). **(E)** Immunohistochemistry with antibodies specific for Melan-A (Abcam, #ab210546, Cambridge, UK). **(F)** Double immunofluorescence staining for synaptophysin (green) and Melan-A (red). **(G)** Double immunofluorescence staining for synaptophysin (green) and ACTH (red).

cases. Two cases were malignant. The ages of all the patients ranged from 12–70 years old; 11 of them were female. There were 14 cases of hypertension and 12 cases of hyperglycemia. Hypokalemia occurred in 9 cases. Consistent with previous studies, only three patients experienced excessive catecholamine excretion. Although paraganglioma originated from chromaffin cells, only about 16.9% of the patients showed an increase in catecholamine, which may be due to the fact that the tumor body of paraganglioma is usually large, and catecholamine may breakdown within the tumor body and fail to be released into the blood. It may also be that some paragangliomas do not produce catecholamine at all. On the other hand, about 95% of paraganglioma patients with catecholamine hypersecretion presented with hypertension, while only 33.5% of paraganglioma patients without elevated catecholamine had hypertension (19). For ACTH producing paraganglioma patients, although only

TABLE 3 | Clinical characteristics of patients with ACTH-producing paraganglioma published in the literature.

Authors	Age/gender	AM Cortisol (μg/dl)	ACTH (pg/ml)	Hypertension	Hyperglycemia	Hypokalemia	Catecholamine excess	Location	Clinical outcome
Apple et al. (4)	50/F	52	167	+	+	ND	ND	Right nasal sinuses	Recovery
Kitahara et al. (5)	12/F	107.1	13.6	+	+	–	+	Lung;	Died; malignant paraganglioma
Park et al. (6)	51/F	59	278	+	+	+	–	Anterior mediastinum	Died of mediastinitis
Lieberum et al. (7)	64/M	High, ND	95.6	+	+	+	–	Paranasal sinus	Recovery
Dahir et al. (8)	39/F	30.6	73.0	+	ND	ND	–	Mediastinum	Recovery
Otsuka et al. (9)	55/F	76.5	318.4	+	+	+	+	Retroperitoneum	Recovery
Willenberg et al. (10)	61/F	176.0	1078	+	+	+	+	Retroperitoneum	Died of pulmonary bleeding 6 months after operation
Palau et al. (11)	55/M	High, ND	High, ND	ND	ND	ND	ND	Mediastinum	Recovery
Fohr et al. (12)	23/M	38	287	+	+	ND	ND	Anterior mediastinum	Recovery
Thomas et al. (13)	70/F	74.4	273.0	+	+	+	–	Left paranasal sinus	Recovery
Serra et al. (14)	68/F	98.7	317.0	+	+	+	ND	Right nasal sinuses	Recovery
Chen et al. (15)	53/F	89.6	432.4	+	+	+	–	Retroperitoneum	Recovery
Kumar et al. (16)	46/F	94.6	312.0	+	+	ND	ND	Right nasal sinuses	Recovery
Tufal et al. (17)	40/F	61.1	679	+	+	+	–	Left kidney	Recovery
Li et al. (18)	39/M	37.68	151.50	+	ND	+	–	Thymus	Recovery
Present case	55/M	18.60	1.0	+	–	+	–	Retroperitoneum	Recovery

All are paraganglioma proved by immunohistochemistry. ACTH, adrenocorticotropin; F, female; M, male; ND, not documented.

3 of 15 patients showed catecholamine hypersecretion, 14 patients had hypertension, indicating that the hypertension that occurred in these patients could be derived from Cushing's syndrome.

In general, most patients with ACTH-secreting paraganglioma presented with significantly elevated plasma ACTH levels. In the literature, only one of 15 cases presented with normal plasma ACTH level and small (pg) amounts of ACTH in tumor extract. Interestingly, the plasma ACTH level was suppressed in our patient. Louiset et al. described a complex paracrine regulation of cortisol secretion resulting from the unexpected expression of ACTH in clusters of steroidogenic cells in bilateral macronodular adrenal hyperplasia tissues. Cortisol secretion by the adrenals in patients with macronodular hyperplasia and Cushing's syndrome appears to be regulated by corticotropin, which is produced by a subpopulation of steroidogenic cells in the hyperplastic adrenals (20). Similarly, in our case, ACTH was immunohistochemically detectable in focal tumor cells, as well as Melan-A and synaptophysin. Synaptophysin, an integral membrane protein of small synaptic vesicles in the brain and endocrine cells, is abundant in neuroendocrine cells and tumor tissues with neuroendocrine function. Synaptophysin is mainly expressed in adrenal medulla, pheochromocytoma, and paraganglioma (21, 22). On the other hand, Melan-A is present in the cytoplasm of epithelial cells and steroid hormone-secreting cells. It is often expressed in melanoma and adrenal cortex (23, 24). In conclusion, these results indicate that the paraganglioma in our case indeed produced ACTH and cortisol. The mildly elevated concentrations of plasma cortisol suggest that the tumor cells produced cortisol and secreted it. As for ACTH, biochemistry failed to demonstrate its excess in the blood. These results may suggest that the tumor cells produced a small amount of ACTH, which stimulates the synthesis of cortisol by cortisol-producing cells in the tumor through an autocrine or paracrine pattern. Excessive cortisol would then inhibit the secretion of ACTH in the pituitary as a negative feedback, accounting for the suppressed plasma level of ACTH. After surgery, the patient's plasma ACTH level increased and the cortisol level dropped to the normal range, confirming the above speculation. This is the first and unique report of ectopic ACTH-producing paraganglioma with a low plasma ACTH level.

The hypersecretion of cortisol may result in hyperglycemia and suppression of the immune system. Thus, before tumor resection, patients are commonly susceptible to infections. In the literature, seven out of 15 patients presented with infections, and one patient died of mediastinitis and pneumonia. In our case, the patient had pneumonia, and his pneumonia did not improve until the paraganglioma was resected.

We did not perform a high dose dexamethasone suppression test to distinguish orthotopic and ectopic ACTH secretion, given its relatively low diagnostic value in this diagnostic setting (the retroperitoneal tumor must be treated regardless of test results) and its risk of hypertensive crisis (25).

CS can also manifest as metabolic syndromes, such as hypertension, hyperglycemia, and hypokalemia. It is challenging to detect the ACTH source in CS. In such settings, biochemical and imaging assessments can prove useful. In the present case,

we were confronted by an extremely rare ACTH-producing retroperitoneal paraganglioma with a low plasma ACTH level. Cortisol secretion by the paraganglioma in the patient with CS appears to be regulated by ACTH, which is produced by these steroidogenic tumor cells in the paraganglioma. Surgical resection is the preferred and definitive treatment. This unusual case expanded the spectrum of ACTH-dependent CS and revealed a potential mechanism of this unique clinical phenotype.

DATA AVAILABILITY STATEMENT

All datasets generated for this study are included in the article.

ETHICS STATEMENT

The studies involving human participants were reviewed and approved by Ethics Committee, Tongji Hospital of Tongji Medical College, Huazhong University of Science and Technology. The patients/participants provided their written informed consent to participate in this study. Written informed consent was obtained from the individual(s) for the publication of any potentially identifiable images or data included in this article.

AUTHOR CONTRIBUTIONS

GY and WX conceived and designed the study. SL and ZL performed the experiments and wrote the paper. FC and GY reviewed and edited the manuscript. All authors read and approved the manuscript.

FUNDING

This work was supported by the National Natural Science Foundation of China (81770817).

REFERENCES

1. Plotz CM, Knowlton AI, Ragan C. The natural history of Cushing's syndrome. *Am Med J*. (1952) 13:597–614. doi: 10.1016/0002-9343(52)90027-2
2. Newell-Price J, Bertagna X, Grossman AB, Nieman LK. Cushing's syndrome. *Lancet*. (2006) 367:1605–17. doi: 10.1016/S0140-6736(06)68699-6
3. Neumann H, Young WJ, Eng C. Pheochromocytoma and Paraganglioma. *N Engl J Med*. (2019) 381:552–65. doi: 10.1056/NEJMra1806651
4. Apple D, Kreines K. Cushing's syndrome due to ectopic ACTH production by a nasal paraganglioma. *Am J Med Sci*. (1982) 283:32–5. doi: 10.1097/00000441-198201000-00005
5. Kitahara M, Mori T, Seki H, Washizawa K, Amano Y, Nakahata T, et al. Malignant paraganglioma presenting as Cushing syndrome with virilism in childhood. Production of cortisol, androgens, and adrenocorticotrophic hormone by the tumor. *Cancer Soc*. (1993) 72:3340–5.
6. Park HK, Park CM, Ko KH, Rim MS, Kim YI, Hwang JH, et al. A case of Cushing's syndrome in ACTH-secreting mediastinal paraganglioma. *Korean J Intern Med*. (2000) 15:142–6. doi: 10.3904/kjim.2000.15.2.142
7. Lieberum B, Jaspers C, Munzenmaier R. [ACTH-producing paraganglioma of the paranasal sinuses]. *HNO*. (2003) 51:328–31. doi: 10.1007/s00106-002-0695-8
8. Dahir KM, Gonzalez A, Revelo MP, Ahmed SR, Roberts JR, Blevins LJ. Ectopic adrenocorticotropic hormone hypersecretion due to a primary pulmonary paraganglioma. *Endocr Pract*. (2004) 10:424–8. doi: 10.4158/EP.10.5.424
9. Otsuka F, Miyoshi T, Murakami K, Inagaki K, Takeda M, Ujike K, et al. An extra-adrenal abdominal pheochromocytoma causing ectopic ACTH syndrome. *Am Hypertens J*. (2005) 18:1364–8. doi: 10.1016/j.amjhyper.2005.01.019
10. Willenberg HS, Feldkamp J, Lehmann R, Schott M, Goretzki PE, Scherbaum WA. A case of catecholamine and glucocorticoid excess syndrome due to a corticotropin-secreting paraganglioma. *Ann N Y Acad Sci*. (2006) 1073:52–8. doi: 10.1196/annals.1353.006
11. Palau MA, Merino MJ, Quezado M. Corticotropin-producing pulmonary gangliocytic paraganglioma associated with Cushing's syndrome. *Hum Pathol*. (2006) 37:623–6. doi: 10.1016/j.humpath.2005.12.006
12. Flohr F, Geddert H. Images in clinical medicine. Ectopic Cushing's syndrome. *N Engl J Med*. (2011) 365:e46. doi: 10.1056/NEJMicm1010540
13. Thomas T, Zender S, Terkamp C, Jaeckel E, Manns MP. Hypercortisolaemia due to ectopic adrenocorticotropic hormone secretion by a nasal paraganglioma: a case report and review of the literature. *BMC Res Notes*. (2013) 6:331. doi: 10.1186/1756-0500-6-331
14. Serra F, Duarte S, Abreu S, Marques C, Cassis J, Saraiva M. Cushing's syndrome due to ectopic ACTH production by a nasal paraganglioma. *Endocrinol Diabetes Metab Case Rep*. (2013) 2013:130038. doi: 10.1530/EDM-13-0038
15. Chen F, Wang X, Wang Y, Meng H, Hou X, Zhu Y, et al. Ectopic Cushing's syndrome due to retroperitoneal ACTH-producing paragangliomas. *Can Urol Assoc J*. (2016) 10:E320–3. doi: 10.5489/cuaj.3153
16. Venkitaraman B, Karunanithi S, Kumar A, Bal C, Ammini AC, Kumar R. ^{68}Ga-DOTATOC PET-CT in the localization of source of ectopic ACTH in patients with ectopic ACTH-dependent Cushing's syndrome. *Clin Imaging*. (2014) 38:208–11. doi: 10.1016/j.clinimag.2013.10.007
17. Tutal E, Yilmazer D, Demirci T, Cakir E, Gultekin SS, Celep B, et al. A rare case of ectopic ACTH syndrome originating from malignant renal paraganglioma. *Arch Endocrinol Metab*. (2017) 61:291–5. doi: 10.1590/2359-3997000000240
18. Li ZH, Wang Y, Li DB. A case of cushing syndrome in ACTH-secreting thymic paraganglioma. *J Thorac Oncol*. (2019) 14:e79–81. doi: 10.1016/j.jtho.2018.12.009
19. Erickson D, Kudva YC, Ebersold MJ, Thompson GB, Grant CS, van Heerden JA, et al. Benign paragangliomas: clinical presentation and treatment outcomes in 236 patients. *J Clin Endocrinol Metab*. (2001) 86:5210–6. doi: 10.1210/jcem.86.11.8034
20. Louiset E, Duparc C, Young J, Renouf S, Tetsi NM, Boutelet I, et al. Intraadrenal corticotropin in bilateral macronodular adrenal hyperplasia. *N Engl J Med*. (2013) 369:2115–25. doi: 10.1056/NEJMoa1215245
21. Saeger W, Fassnacht M, Chita R, Prager G, Nies C, Lorenz K, et al. High diagnostic accuracy of adrenal core biopsy: results of the German and Austrian adrenal network multicenter trial in 220 consecutive patients. *Hum Pathol*. (2003) 34:180–6. doi: 10.1053/hupa.2003.24
22. Isidori AM, Kaltsas GA, Pozza C, Frajese V, Newell-Price J, Reznek RH, et al. The ectopic adrenocorticotropin syndrome: clinical features, diagnosis, management, and long-term follow-up. *J Clin Endocrinol Metab*. (2006) 91:371–7. doi: 10.1210/jc.2005-1542
23. Busam KJ, Iversen K, Coplan KA, Old LJ, Stockert E, Chen YT, et al. Immunoreactivity for A103, an antibody to melan-A (Mart-1), in

adrenocortical and other steroid tumors. *Am J Surg Pathol.* (1998) 22:57–63. doi: 10.1097/00000478-199801000-00007

24. Miller AD, Masek-Hammerman K, Dalecki K, Mansfield KG, Westmoreland SV. Histologic and immunohistochemical characterization of pheochromocytoma in 6 cotton-top tamarins (*Saguinus oedipus*). *Vet Pathol.* (2009) 46:1221–9. doi: 10.1354/vp.09-VP-0022-M-FL
25. Aron DC, Raff H, Findling JW. Effectiveness versus efficacy: the limited value in clinical practice of high dose dexamethasone suppression testing in the differential diagnosis of adrenocorticotropin-dependent Cushing's syndrome. *J Clin Endocrinol Metab*. (1997) 82:1780–5. doi: 10.1210/jc.82.6.1780

Conflict of Interest: The authors declare that the research was conducted in the absence of any commercial or financial relationships that could be construed as a potential conflict of interest.

frontiers in Endocrinology

ORIGINAL RESEARCH
published: 22 January 2020
doi: 10.3389/fendo.2019.00944

Transcriptional Analysis of Sepsis-Induced Activation and Damage of the Adrenal Endothelial Microvascular Cells

*Lan-Sun Chen[1,2], Sumeet P. Singh[3], Gregor Müller[2], Stefan R. Bornstein[2] and Waldemar Kanczkowski[2]**

[1] Institute of Medical Microbiology and Hygiene, Technische Universität Dresden, Dresden, Germany, [2] Department of Internal Medicine III, University Hospital Carl Gustav Carus at the Technische Universität Dresden, Dresden, Germany, [3] IRIBHM ULB, Brussels, Belgium

OPEN ACCESS

Edited by:
Ana Rosa Pérez,
National Council for Scientific and Technical Research (CONICET), Argentina

Reviewed by:
Silvina Raquel Villar,
CONICET Instituto de Inmunología Clínica y Experimental de Rosario (IDICER), Argentina
M. Victoria Delpino,
CONICET Institute of Immunology, Genetics and Metabolism (INIGEM), Argentina

***Correspondence:**
Waldemar Kanczkowski
waldemar.kanczkowski@uniklinikum-dresden.de

Specialty section:
This article was submitted to Cellular Endocrinology, a section of the journal Frontiers in Endocrinology

Received: 19 October 2019
Accepted: 31 December 2019
Published: 22 January 2020

Citation:
Chen L-S, Singh SP, Müller G, Bornstein SR and Kanczkowski W (2020) Transcriptional Analysis of Sepsis-Induced Activation and Damage of the Adrenal Endothelial Microvascular Cells. Front. Endocrinol. 10:944. doi: 10.3389/fendo.2019.00944

Bacterial sepsis is a serious threat to the body homeostasis and is often associated with high mortality in non-coronary intensive stations. In order to survive sepsis, rapid activation of the hypothalamus-pituitary-adrenal gland axis and sympathomedullary system is necessary. In many patients with sepsis, the function of those two arms of the stress system is dysregulated with underlying mechanisms remaining unknown. In our previous experimental studies, we have demonstrated that LPS-induced systemic inflammation and CLP-induced peritonitis can result in adrenal gland damage. Histological and transcriptomic analysis revealed a potential involvement of the adrenal microvascular endothelium in this process. However, our knowledge about the function of adrenal microvascular cells during sepsis is scarce. In the present study, we have characterized transcriptomic alterations in isolated mouse adrenal microvascular endothelial cells induced by systemic administration of bacterial LPS. Our results revealed that LPS induced a distinct transcriptomic profile in the adrenal microvascular cells, including multiple genes regulating inflammation, activation of the coagulation cascade and vascular permeability. Activation of those genes may be potentially involved in the damage to the microvascular endothelium and altogether contribute to the sepsis-mediated adrenal dysregulation.

Keywords: the HPA axis, RNAseq, adrenal dysfunction, microvascular endothelial cells, sepsis

INTRODUCTION

Sepsis and septic shock are major causes of death in non-coronary intensive care stations worldwide. Despite decades of intensive basic and clinical research, currently, no specific therapeutic interventions are available and the treatment of patients with sepsis is mostly focused on support of their organ function (1). Sepsis is characterized by progressive dysfunction of multiple organs as a result of the improper host response to systemic microbial infection (2). The mechanisms involved in the latter process are complex, multifactorial, and mostly unexplored (3).

It is generally accepted that prompt activation of the hypothalamic-pituitary-adrenal (HPA) axis and the sympathomedullary system (SAS), known collectively as the stress system, is crucial in surviving sepsis (4). Many patients with a prolonged stay at the intensive care stations develop

adrenal gland dysfunction, which results from an early inhibition of pituitary ACTH secretion due to dysfunctional glucocorticoid hormone metabolism and prolonged activation of the immune-adrenal crosstalk (5, 6). The latter factors may increase the risk of sepsis-related death among those patients (7, 8). However, the diagnosis of the adrenal gland insufficiency and identification of patients that may benefit from glucocorticoid therapy remain as enigmatic as sepsis syndrome itself (9).

In the last years, our group has been investigating potential mechanisms involved in the sepsis mediated adrenal gland dysregulation (4). We have demonstrated that during both LPS- and cecal-ligation and puncture (CLP)-induced sepsis, adrenal gland damage occurs, including a rapid increase in intraadrenal inflammation, enhanced cell death of adrenal cells and occurrence of hemorrhages (10, 11). In our latest study, we have characterized the adrenal gland transcriptome changes induced by LPS using the RNA sequencing technique. Results of that investigation demonstrated that LPS induced a strong inflammation in the adrenal gland along with hypoxia and the coagulation pathway, which suggests the potential involvement of the adrenal microvasculature (12).

In non-stressed conditions, tissue microvascular endothelial cells are involved in the maintenance of tissue homeostasis. In particular, these cells provide an essential barrier between circulation and parenchymal cells, control vascular tone, the coagulation properties of blood, and regulate leukocyte recruitment (13). However, during sepsis, this homeostatic function of the endothelial cells is often dysfunctional (14). In those conditions, elevated plasma and local concentration of proinflammatory cytokines activate endothelial cells, resulting in an increased expression of P- and E-selectins, chemokines, and adhesion molecules e.g., ICAM-1 or VCAM-1 by these cells. As a result, increased infiltration of immune cells triggers inflammation in affected organs (15). Moreover, during activation, endothelial cells enter often a procoagulant phase, which is associated with increased expression of tissue factor and plasminogen activator inhibitor-1 (PAI-1) and decrease in anticoagulants level, including activated protein C or thrombomodulin. This situation together with increased permeability of vasculature and disruption in endothelial barrier integrity often predisposes to hemorrhages (16).

Although vascular damage is undisputedly involved in the sepsis-induced dysfunction of many organs, scarce information is available regarding the adrenal gland vascular endothelial cells (17, 18). Therefore, the main purpose of this study was to study the potential characteristics of microvascular damage by performing a next-generation sequencing analysis of transcriptome changes in adrenal microvascular endothelial cells isolated from mice with LPS-induced systemic inflammation.

Our results, clearly demonstrate that the adrenal microvascular endothelial cells may actively contribute to sepsis-induced adrenal dysfunction. In particular, we have found that sepsis promotes the expression of several genes involved in vascular cell inflammation, leakage, and coagulation, which may ultimately contribute to adrenal gland hemorrhages, and hypoxia.

MATERIALS AND METHODS

Animals

C57BL/6JRj male mice were purchased from the Javier Labs (France). Mice were divided into two groups. A systemic inflammatory response syndrome (SIRS) group ($n = 11$) and a control group ($n = 11$). Both groups were injected intraperitoneally at the age of 10 weeks, either with 1 mg/kg body weight of bacterial LPS (serotype 0111: B4; Invivogen; France) in the SIRS group or with 0.9% NaCl (physiological saline)—in the control group. Three hours after LPS injection mice were killed and adrenals were excised for further analysis. The experiment was approved by the German ethical committee of the Landesdirection Dresden.

Isolation of Mouse Adrenal Gland Endothelial Cells

For isolation of endothelial cells, adrenal glands were digested using a solution containing collagenase I and bovine serum albumin (both at 1.6 mg/ml concentration, Sigma-Aldrich, Germany) dissolved in the phosphate-buffered saline (PBS). Digestion was performed for a total of 30 min at 37°C in a thermomixer with shaking. After digestion, cells were dissociated using a 1 ml tuberculin syringe and 20 Gauge needle (Braun, Germany) and by subsequent passing through 100 μm-pore size strainers. Resulting cell suspensions were centrifuged at 2,900 RPM for 8 min at 4°C, pelleted, and washed in a FACS buffer (PBS solution containing 5% of fetal calf serum). Afterward, cells were incubated for 60 min at 8°C with a mixture of conjugated antibodies in the FACS buffer: including rat against mouse CD45-PE antibody (immune cells), rat against mouse CD31-PE/CY7 antibody (endothelial cells) and rat against mouse Ter119-APC (erythrocytes) antibody. All those monoclonal antibodies were purchased from BD Bioscience (BD Biosciences, USA). Dead cells were excluded using Hoechst 33258 (Invitrogen, Thermo Fisher Scientific). Populations of single, alive, CD31 positive endothelial cells were subsequently isolated by BD FACSAria III sorter (BD Biosciences). From each adrenal gland, 30.000 endothelial cells were sorted out and used for further analysis.

RNA Isolation and Quantitative PCR Analysis

RNA isolation was performed using the RNeasy Plus Micro Kit (Qiagen, Germany), according to a manufacturing protocol. High quality and integrity of RNA samples ($n = 3$ per group) used for the RNA-Sequencing experiment were additionally verified by a Bioanalyzer 2100 (Agilent, USA). Samples used for PCR validation ($n = 5$ per group), were reverse-transcribed using the iScript cDNA Synthesis Assay (Bio-Rad, Germany) in a final volume of 20 ml according to manufacture protocol. Real-time PCR, which was performed using SsoFast Eva Green Supermix (BioRad) and previously reported gene-specific primers (12) in a CFX96 Real-Time PCR detection system (BioRad). Gene expression was calculated based on the ΔΔCt method upon normalization with 18S rRNA gene (19).

Libraries Preparation for RNA Sequencing and Extraction of Data

RNA sequencing was performed by the Deep Sequencing Facility Group (BIOTEC, Center of Regenerative Therapies Dresden, Germany). The procedure of data extraction and analysis has been described in detail in our previous study (12). Briefly, fastq formatted raw reads were trimmed using a "trim-galore" package with default settings for adapter sequences removal (12). Trimmed data were further mapped to the mouse genome GRCm38 by using HISAT2 (20) with default parameters. Htseq-count (21) was used to assign reads to exons thus eventually getting counts per gene. Quality control, normalization, and scaling of the raw read counts were performed by EdgeR (22) package as a part of an integrated Differential Expression and Pathway analysis (iDEP.90) web-based tool for analyzing RNA-seq data (23). Differentially expressed genes were identified using the following criteria: minimum 50 counts per million (CPM) in at least three libraries, an adjusted p-value (padj) < 0.05 and minimal fold change > 2. Unsupervised analysis of the 100 most variable genes between treatments was performed using a cluster analysis based on Euclidean distance as a part of the iDEP.90 software.

Gene Ontology Analysis

A number of top 500 upregulated (UP) and top 500 downregulated (DOWN) genes were submitted to the DAVID software (version 6.7, https://david-d.ncifcrf.gov) for analysis of gene ontology and functional mapping (24). An EASE cut off score of p-value < 0.05 was chosen for gene enrichment in annotation terms (25). P-values from enriched pathways or GO terms were transformed into—log 10 and visualized by pyramid slot transformations.

Gene Set Enrichment Analysis (GSEA)

All significantly changed genes were subjected to GSEA software v4.0.1 from the Broad Institute (http://www.gsea-msigdb.org/gsea/index.jsp) (26) for pathway enrichment and functional annotation analysis. GSEA was performed with a default setting, and annotated Hallmarks gene sets collection v7.0, from Molecular Signatures Database (MSigDB, http://software.broadinstitute.org/gsea/msigdb/index.jsp), was used as an enrichment database. Gene sets with nominal p-value < 0.05 and FDR q-value < 0.25 were considered as enriched and were further investigated.

Immunofluorescent Staining

Adrenal glands were cleaned from surrounding fat and fixed in a 4% paraformaldehyde solution for 1 h. After washing, adrenals were incubated in increasing concentrations (5–30%) of sucrose solution, embedded in Tissue-Tek® O.C.T.™ Compound (Sakura, Japan) and kept at −80°C. For immunofluorescent staining, 6 μm-thick tissue slices were incubated for 1 h in a blocking solution (composed of 0.3% Triton 100 and 5% normal goat serum in PBS) and then incubated overnight at +8°C in a buffer containing antigen-specific primary antibodies (composed of 0.3% Triton 100 and 5% BSA in PBS). The following antibodies were used: polyclonal rabbit antibody anti-mouse thrombomodulin (Thbd, 1:800, ab130152, Abcam), monoclonal rat anti-mouse CD31 antibody (1:100, ab7388, Abcam), monoclonal rat anti-mouse CD34 antibody conjugated with 488 dye (1:50, 11-0341-82, eBioscience) and monoclonal rabbit anti-mouse VCAM-1 antibody (1:200, clone EPR5047, ab134047, Abcam, USA). Primary antibodies were then detected by secondary antibodies conjugated to either Cy3 or 488 fluorescent dyes (VCAM-1, CD31, Thmd1) and counterstained with a nuclear dye (DAPI, 1:10000). Isotype controls were used as controls for CD146 and CD34 antibodies. Pictures were acquired with a × 10 objective using the Axio Imager 2 light microscope (Carl Zeiss, Jena, Germany).

Protein Extraction and Western Blot

For protein isolation, adrenal glands were briefly sonicated in a 1x lysis buffer containing a proteinase/phosphatase inhibitor cocktail (both buffers were from Cell Signaling Technology, USA). Twenty micrograms of proteins were separated on 8% polyacrylamide gel and subsequently blotted onto polyvinylidene fluoride (PVDF) membrane. Membranes were then incubated for 120 min in a blocking solution composed of non-fat milk (5%) dissolved in TBS-T (tris buffered saline buffer containing Tween®20 detergent). For the VCAM-1 and GAPDH detection following antibodies were used rabbit monoclonal anti-mouse VCAM-1 antibody (1:1000, clone EPR5047, ab134047, Abcam), a monoclonal rabbit anti-mouse GAPDH (1:1000; clone 14C10, #2118, Cell Signaling Technology), and goat anti-rabbit HRP conjugated secondary antibodies (1:6000, CST). The expression of VCAM-1 protein was analyzed based on densitometry in ImageJ software (http://rsb.info.nih.gov/ij/index.html).

Protein Cytokine Array

Six adrenals from each experimental group were isolated and immediately homogenized in 500 μl PBS containing protease inhibitor cocktail (P8340, Sigma-Aldrich, Merck). After homogenization, Triton X-100 was supplemented to a total concentration of 1%, and samples were frozen at −80°C. After thawing on ice and centrifuging at 13,000 rpm for 5 min supernatants were collected. Protein concentration was determined and 300 μg of each lysate was applied to the Proteome Profiler Mouse Cytokine Array Kit, Panel A (R&D Systems, catalog ARY006). The chemiluminescence reaction was measured with Syngene G: BOX XT4: Chemiluminescence and Fluorescence Imaging System (Integrated Scientific Solutions, Inc. USA). Densitometry quantitation was performed using FIJI/ImageJ software (NIH, USA).

RESULTS

Identification of the Adrenal Gland Microvascular Endothelial Cells

In order to study transcriptional changes of the adrenal vascular cells, we had to first identify an efficient method that can

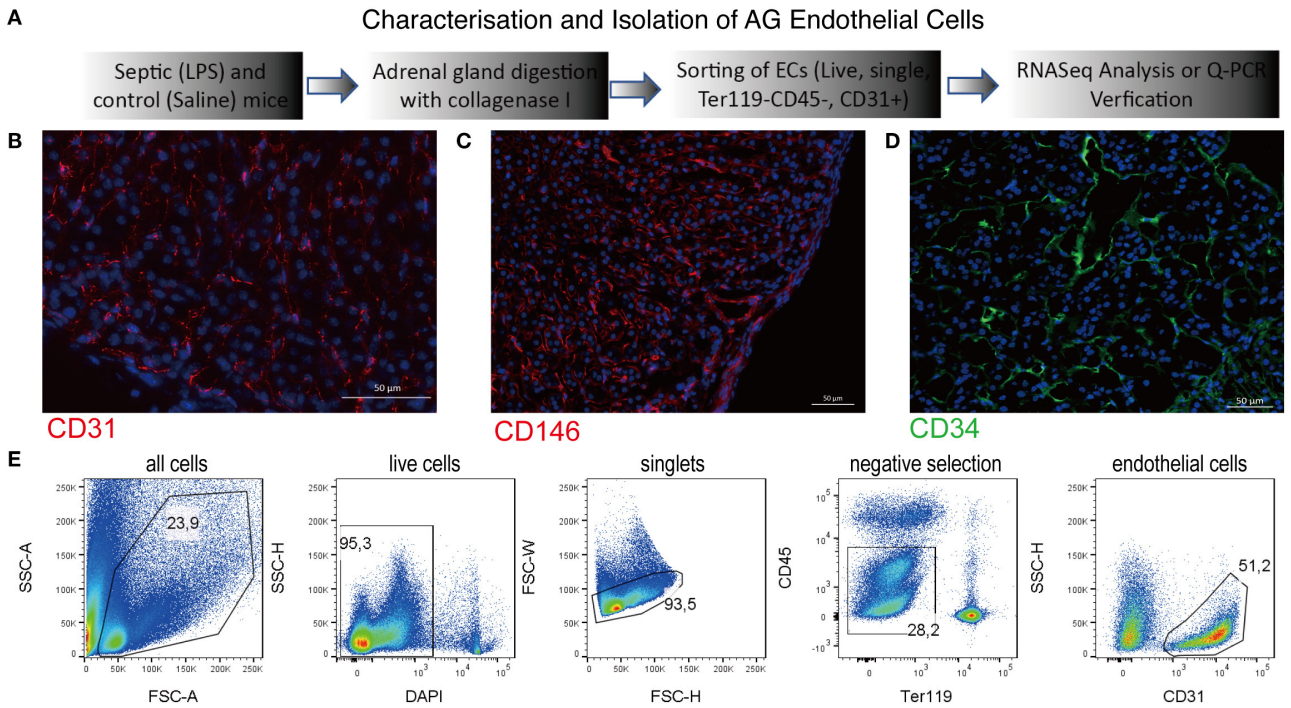

FIGURE 1 | Characterization of the adrenal gland microvascular endothelial cells. Schematic representation of the procedures used to isolate and to characterize the adrenal microvascular endothelial cells **(A)**. Fluorescent staining of the mouse adrenal gland sections for endothelial-specific markers such as CD31 (PECAM) **(B)**, CD146 (MCAM) **(C)**, and CD34 **(D)**. CD31 and CD146 were visualized using secondary antibodies coupled to Cy3 dye (red color), and CD34 was visualized using secondary antibodies coupled to 488 dye (green color). Representation of the multiparametric FACS sorting technique used to isolate adrenal microvascular endothelial cells **(E)**. The gating strategy was based on negative selection. Only alive, single cells that were CD45 negative (devoid of immune cells) and Ter119 negative (devoid of erythrocytes) but CD31 positive (endothelial cells) were sorted.

provide us an exact and high number of alive, single endothelial cells that can be subsequently used for high-quality RNA isolation. Since techniques based on antibody-coated magnetic beads often provide mixed populations of endothelial cells containing also parenchymal and perivascular cells (27), we have decided to use multiparametric flow cytometry sorting. In a search of a specific and stably expressed cell membrane marker, we have performed a series of immunofluorescent staining in adrenal gland tissue sections and a FACS validation of primary cells. We have verified a specific expression of the following endothelial markers in mouse adrenal glands: a cluster of differentiation (CD) member 31, known also as platelet endothelial cell adhesion molecule (PECAM) (**Figure 1B**), melanoma cell adhesion molecule (MCAM; CD146) (**Figure 1C**) and CD34 (**Figure 1D**). Afterwards, we have tested the expression of those markers by FACS in adrenal cells from control and SIRS groups. Based on this analysis, we have chosen the CD31 marker for isolation of endothelial cells from the adrenal gland due to its high and stabile expression among control and SIRS groups. Therefore, in our further studies, we will refer to adrenal microvascular endothelial cells as primary cells expressing CD31, which are negative for pan immune cell marker, CD45, and are devoid of erythrocytes (Ter119-negative; **Figure 1E**).

Bioinformatics Analysis of the Adrenal Microvascular Endothelial Cell Transcriptome During LPS-Induced Systemic Inflammation

Transcriptomic changes triggered by sepsis in the adrenal microvascular cells were evaluated by RNA sequencing using endothelial cells of mice that were injected either with physiological saline (control group) or bacterial LPS (SIRS group) for 3 h according to schema presented in **Figure 1A**. Principal component analysis (PCA) of our RNAseq results demonstrated a high separation of transcriptome patterns between both analyzed groups (PC1, 82 % of variance) and a very low variance among the biological replicates within each group (PC2, 4%), which suggest a clear separation of both analyzed experimental groups (**Figure 2A**).

We have next compared 11,137 differentially expressed genes identified from both groups with the DESeq2 package based on the following threshold—false detection rate (FDR < 0.01) and p-value < 0.05. As depicted in **Figure 2C** in the form of a volcano plot, systemic administration of LPS resulted in significant downregulation of 1,993 and upregulation of 2,494 genes in adrenal vascular cells. We have next performed unsupervised hierarchical clustering of the top 100 highest

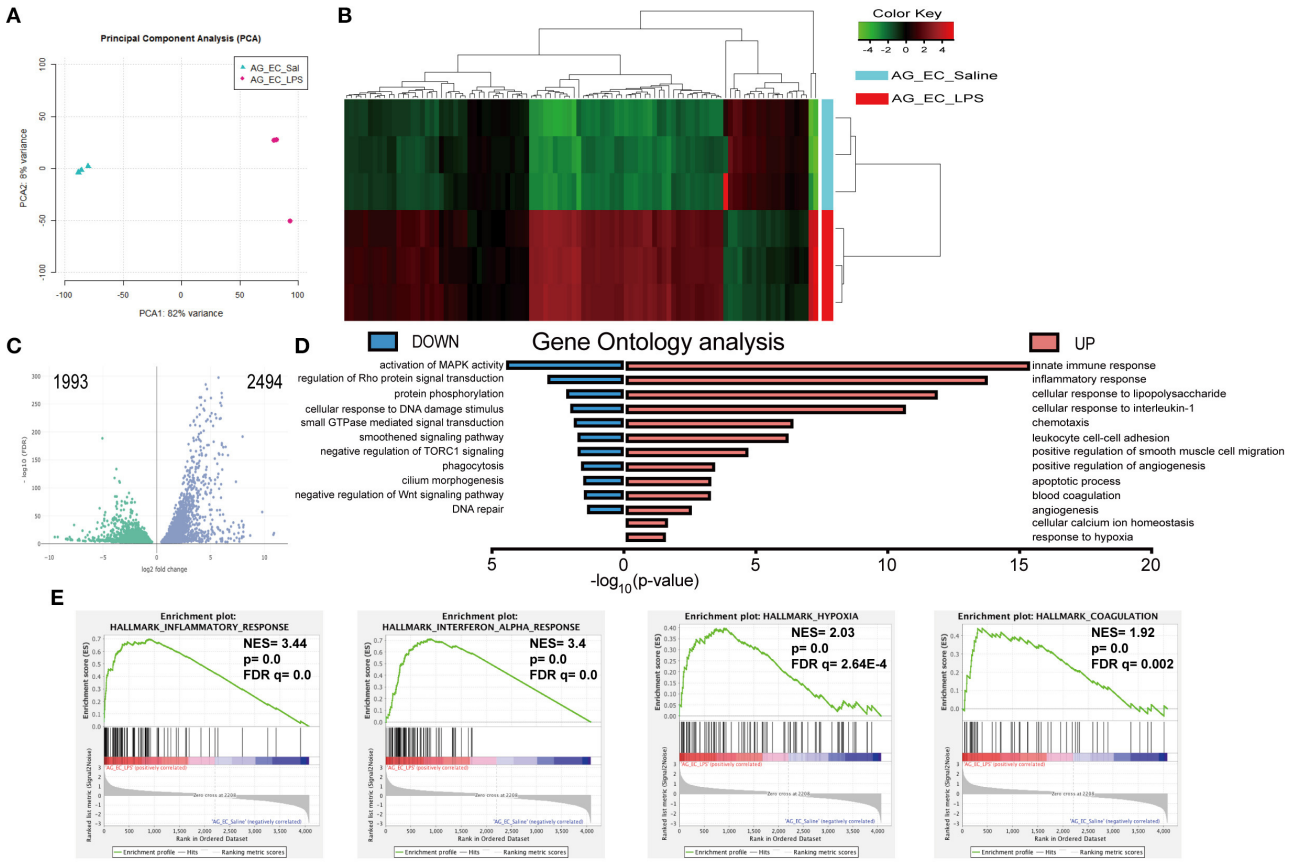

FIGURE 2 | Bioinformatics analysis of the transcriptomes of the adrenal microvascular endothelial cells isolated from saline- and LPS-treated mice. Logarithm transformed counts from RNA-Seq dataset of adrenal microvascular endothelial cells isolated from saline- and LPS-treated adrenal glands were computed for sample correlation or variance by PCA analysis. Percentages in the PCA analysis axis indicated the proportional variance explained by each PC. LPS samples were labeled in red and Saline samples were labeled in blue that represented as condition located in the upper left part of the plot **(A)**. Unsupervised hierarchical clustering of the most 100 up- and down-regulated genes were computed by Euclidean distance clustering and expression heatmap with normalized raw z-scores. The labeling of Condition and DE were adapted as previous panels. **(B)** A volcano plot was depicted with –log10(FDR) against log2FoldChange of all 4487 significantly altered genes that were detected from the RNA-Seq dataset. Differential expression (DE) of genes was colored with green and blue, regarding 1,993 down-regulated and 2,494 up-regulated genes, respectively. Significance of differential gene expression was determined with adjusted *p*-value (p adj.) < 0.05 and counts > 50 **(C)**. Pyramid plot with bidirectional –log10 (*p*-value) demonstrated the involved gene ontology (GO) terms and pathways from submitted UP- or DOWN-regulated gene lists. The EASE score of *p*-value < 0.05 was set by DAVID software. Identical color code was used for showing UP and DOWN groups. $N = 3$ for each condition **(D)**. Representative 4 significantly enriched gene sets from GSEA analysis of 4,487 significantly changed genes in the RNA-Seq dataset. Enrichment plots comparing LPS toward Saline were depicted with the following sets of genes: **(A)** Hallmark Inflammatory response. **(B)** Hallmark Interferon-alpha response, Hallmark Hypoxia and Hallmark Coagulation **(E)**. Comparison of samples, NES, nominal *p*-value, and FDR q-value were determined by the GSEA software and were indicated within each enrichment plot.

up- and down-regulated genes and found that LPS induced a profound and clear differential gene expression patterns in the adrenal endothelial cells with a tight clustering between both experimental groups (**Figure 2B**). Further analysis of the 100 upregulated genes demonstrated a high enrichment of genes involved in the regulation of inflammation (**Table 1**). In particular, LPS induced multiple chemokines such as members of the C-X-C motif ligand (Cxcl) family (Cxcl10, and Cxcl11), members of chemokine family characterized by (C-C motif) ligand including Ccl2, Ccl5, or Ccl7, and colony-stimulating factor 3 (G-CSF) and 2 (GM-CSF). Other top induced genes by LPS were those involved in increased leukocyte recruitment including P- and E-selectins and Vascular cell adhesion protein 1) and in inflammation such as IL-6, cyclooxygenase 2 (Ptgs2), sphingosine kinase 1 (Sphk1), and procoagulant gene encoding for plasminogen activator inhibitor type 1, member 1 (Serpine 1). In addition, endotoxemia resulted in the upregulation of multiple interferon-inducible genes such as an interferon-induced protein with tetratricopeptide Repeats (Ifit1-3), MX Dynamin Like GTPase 1 (Mx1) and Interferon regulatory element 5 (Irf5). Besides initiation of inflammatory genes endothelial cells initiate an anti-inflammatory program represented by Acod1 (Aconitate decarboxylase 1) gene, which is a negative regulator of TLR-signaling (28).

Among the most downregulated genes were those regulating protein phosphorylation, as well as genes involved in the development and vascular endothelial growth factor receptor (VEGFR) signaling, such as Sonic hedgehog (Shh) and Protein

TABLE 1 | Representative top 100 up- and downregulated genes from RNA-Seq analysis (related to **Figure 2**).

	Gene ID	log_2FC
UP-REGULATED		
Chemokines	Csf3	10.89
	Ccl2	9.57
	Cxcl10	8.06
	Cxcl11	7.96
	Ccl11	7.67
	Csf2	7.41
	Ccl7	7.35
	Ccl5	7.18
Leukocyte adhesion	Selp	8.67
	Sele	6.13
	Vcam-1	6.40
	Icosl	5.8
Angiopoiesis	Pdgf	5.84
	Angpt2	5.72
Inflammation	IL6	9.79
	Sphk1	7.59
	IL27	7.18
	Ptgs2	7.1
	IL1rn	6.37
	Acod1	6.56
	Serpin1	6.44
	CD274	5.85
	Saa3	5.71
INF-induced genes	Mx1	8.06
	Ifit2	6.11
	Ifit3	5.99
	Ifit1	5.85
	Irf5	5.78
DOWN-REGULATED		
Wnt & VEGFR signaling	Ptk7	−8
Apoptosis &Autophagy	Dapk2	−4.96
Development	Shh	−5.93
Cell junctions	Rapsn	−8.44
	Dsc2	−6.1
	Zc4gz	−5.42
	Kcnb1	−4.63
	Pcdh12	−4.21

tyrosine kinase 7 (Ptk7), respectively (**Table 1**). The other downregulated genes found were those involved in apoptosis and autophagy including Death associated protein kinase 2 (Dapk2) and genes controlling cell junctions such as Receptor associated protein of the synapse (Rapsn) or Desmocollin 2 (Dsc2).

Functional analysis based on gene ontology identified the innate immunity, inflammation, cellular responses to cytokines and regulation of infiltration, as the most upregulated pathways induced by LPS in the microvascular adrenal endothelial cells (**Figure 2D**). Other highly enriched pathways were angiogenesis, apoptosis, hypoxia, and blood coagulation processes (**Table S1**). Subsequently, LPS suppressed genes regulating protein phosphorylation, activation of MAPK- and Rho-mediated signal transduction, smoothened signaling, cilium morphogenesis and DNA repair (**Figure 2D** and **Table S2**).

Finally, we have analyzed the potential contribution and interconnection of all significantly altered genes by a gene set enrichment analysis (GSEA) method. Based on the following criteria (nominal p-value $< 5\%$ and the false detection rate, FDR below 25%), we have found 22 gene sets that were positively enriched and none from 13 gene sets initially found to be downregulated by LPS. Four of the most induced gene sets by the LPS treatment are presented in **Figure 2E**. Those were gene sets involved in the inflammatory response (normalized enrichment score, NES $= 3.44$, p-value $= 0.0$ and FDR $q = 0.0$), response to interferon-alpha (NES $= 3.4$, $p = 0.0$ and FDR $q = 0.0$), the hypoxia (NES $= 2.03$, p-value $= 0.0$ and FDR $q = 2.64$ E-4) and coagulation pathway (NES $= 1.92$, p-value $= 0.0$ and FDR $q = 0.002$).

Verification of RNA Sequencing Results

In order to validate our RNA sequencing data, we have sorted the adrenal microvascular endothelial cells from mice that received either saline or LPS (5 mice per group) and verified the expression of some genes representing each identified pathway by real-time PCR (**Figure 3**).

We have first evaluated the expression of endothelial-specific genes that were previously reported to be regulated either positively or negatively by LPS action. In particular, we could confirm LPS-reduced mRNA expression of the Tek gene (encoding for an Ang receptor, Tie2), Edil3 gene (the EGF like repeats and discoidin domains 3, Del-1) and Thmd1 gene encoding for thrombomodulin. At the same time endotoxin highly upregulated Anxa 1 gene encoding for annexin A1 (**Figure 3A**). After reconfirming the identity of our sorted cells, we have analyzed the mRNA expression of genes identified by our gene ontology and the GSEA analysis. As presented in **Figure 3B**, we have found that LPS strongly induced expression of genes involved in the inflammatory response hallmark, such as toll-like receptor 4 (Tlr4), P- and E-selectins, Vcam-1 and an intracellular adhesion molecule−1 (Icam-1), chemokines (Ccl2, Cxcl2) and gens involved in prostaglandin synthesis e.g., cyclooxygenase 2 (Cox2, Ptgs2). Additionally, we have also validated the upregulation of genes encoding for hypoxia-inducible factor 1 alpha (Hif-1α), a gene representing the hypoxia hallmark, and the Serpine1 gene encoding for plasminogen activator inhibitor type 1, member 1 (PAI-1), which protein is known to inhibit fibrinolysis and therefore promote tissue coagulation.

In addition, to mRNA analysis, we have also studied the effect of LPS on the protein level using immunofluorescence, western blot and dot blot techniques in the whole adrenal gland. We have first looked at VCAM-1 expression in adrenal gland tissue after LPS administration because of its inducible character. As presented in **Figure 3D**, a strong induction of this adhesion molecule could be observed in the adrenal vascular cells after LPS administration (**Figure 3C**). Furthermore, we have additionally quantified (**Figure 3D**) this VCAM-1 induction by densitometrical analysis of western blot (**Figure 3E**). We have also studied the expression of thrombomodulin protein in

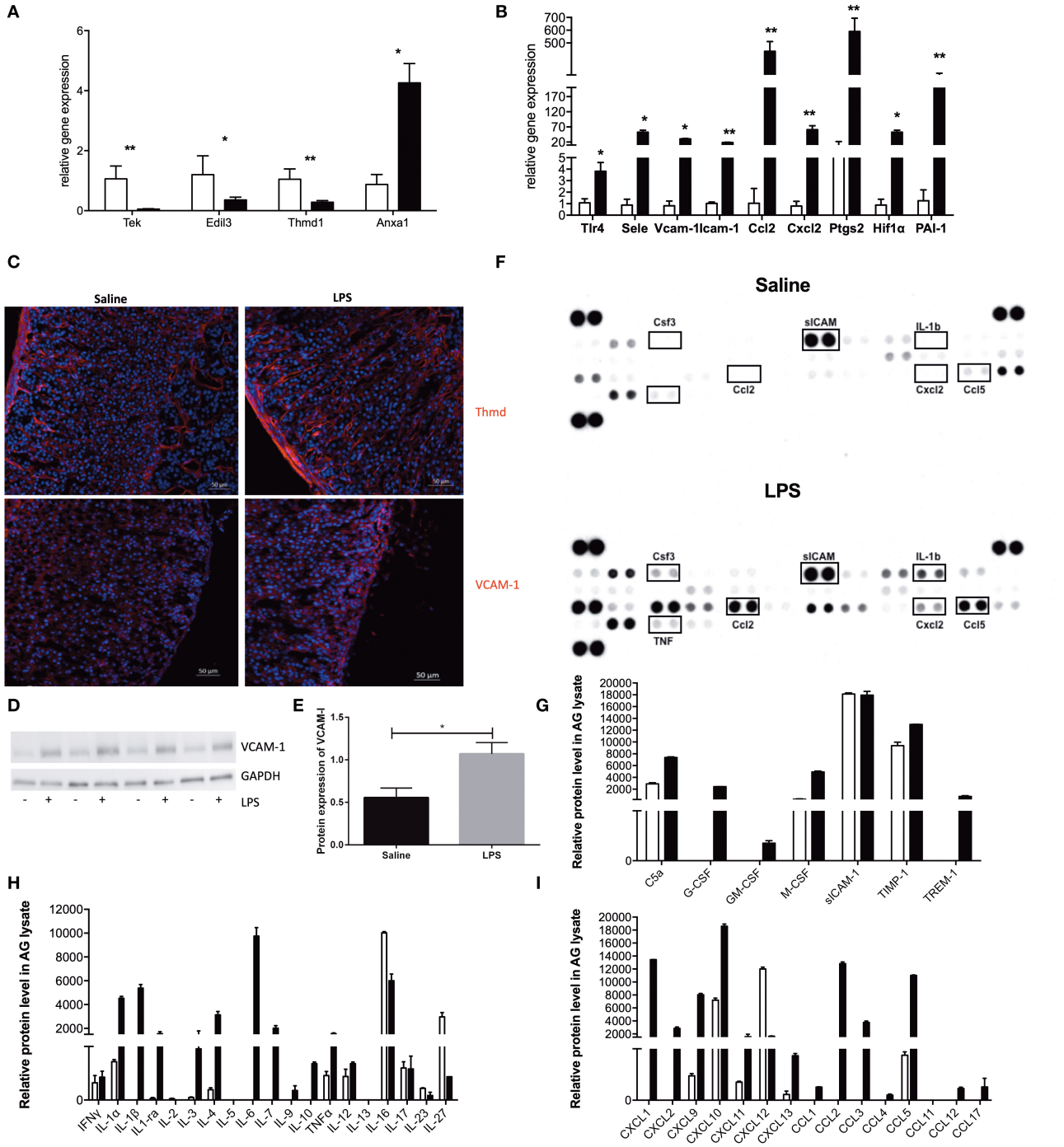

FIGURE 3 | mRNA and protein verification of RNA sequencing analysis. Real-time PCR (qPCR) verification of expression of endothelial-specific genes **(A)** and expression of some of the top 100 most altered genes **(B)** with specific primers. Relative gene expression was determined by the $\Delta\Delta$Ct method with normalization of 18S ribosomal RNA. Saline-treated samples were depicted with open bars, and LPS-treated samples were depicted with black filled bars. $N = 5$ and statistics were calculated with the two-tailed non-parametric Mann-Whitney test. Values are mean with SEM. $^{*}p < 0.05$, $^{**}p < 0.01$. Images of fluorescent staining of thrombomodulin (Thmd) and Vascular adhesion molecule 1 (VCAM-1) **(C)** in adrenal tissue sections of mouse adrenal gland isolated from either Saline or LPS treated mice. Thmd and VCAM-1 were visualized using secondary antibodies coupled to Cy3 dye (red color). Western blot evaluation of VCAM-1 expression in adrenal glands isolated from mice treated either with Saline or LPS ($N = 4$) **(D)**. Graphic representation of the VCAM-1 and GAPDH protein expression quantified in ImageJ Software based on the densitometric evaluation of protein bands **(E)**. Results and evaluation of dot-blot based protein array **(F)** of different inflammatory-related molecules **(G)**, cytokines **(H)** and chemokines **(I)**. Saline-treated samples were depicted with open bars, and LPS-treated samples were depicted with gray filled bars. For each experimental group, two adrenals from three different animals ($N = 6$) were pooled and results are presented as double replicate.

adrenal tissue expression after LPS stimulation. On contrary to VCAM-1 however, LPS injection has not changed Thmd protein expression (**Figure 3C**). This result could imply that 3 h are too early to investigate a change in thrombomodulin protein levels, and later time points should be investigated.

As a part of the adrenal microenvironment, adrenal microvascular endothelial cells are in constant contact with intraadrenal produced pro-inflammatory mediators especially during systemic inflammation initiated by LPS. In addition, based on the above-presented transcriptome analysis, the adrenal endothelial cells may not just be a passive target of those inflammatory mediators, but also a substantial contributor to their production. Our analysis presented in **Figure 3F** revealed that during LPS-induced systemic inflammation, a significant induction of pro-inflammatory (IL-1α, IL-1β, TNF-α, IL-3, or IL-6) and anti-inflammatory (IL-4, IL-10, IL-1ra) cytokines were found. Whereas, the expression of others is either unchanged (IFN-γ, IL-17) or not detected at all (IL-5 and IL-13) **Figure 3H**. Among multiple chemokines detected the expression of CXCL1, CXCL2, CXCL9, CXCL10, CXCL12, CXCL13, CCL2, CCL3, CCL5 proteins were found to be strongly upregulated by LPS. This result corresponds to the induction of Cxcl2, Ccl2 verified by the Q-PCR or other chemokines, which expression was shown to be highly induced in adrenal microvascular endothelial cells by LPS according to our RNA-sequencing analysis (such as Cxcl10, Cxcl11, or Ccl5) presented in **Figure 3I**. Moreover, we have also observed a strong induction of G-CSF (CSF3) protein (**Figure 3G**), which was the highest upregulated gene found by RNA sequencing (**Table 1**). The latter observation is also in accordance with the literature, reporting that the microvascular endothelial cells are the main source of this chemokine.

DISCUSSION

It is generally accepted that endothelial cell dysfunction occurs progressively during sepsis and contributes to the pathophysiological function of many organs (14, 15). More importantly, a positive correlation between endothelial dysfunction and increased mortality rate of patients with sepsis was reported (29). Less is known, however, whether a similar situation occurs also in the adrenal glands.

In the present study, we aimed to investigate LPS-induced damage of the mouse adrenal microvascular cells *in vivo* using next-generation sequencing and protein analysis. To this end, we analyzed the transcriptomic changes in the endothelial microvascular cells isolated from mice 3 h after systemic administration of bacterial LPS. We have chosen LPS-model of systemic inflammation because of various reasons. In particular, LPS was shown to mimic an initial fulminant stage of Gram-negative sepsis induced by meningococcal infection in humans (30). Furthermore, it has the ability to induce a robust transcriptomic response in multiple organs in a highly reproducible manner. Finally, LPS-induced changes in the adrenal gland transcriptome were also previously verified by us in a more clinically relevant model of sepsis—a cecal-ligation and puncture (CLP)-induced peritonitis (12). We have chosen a 3 h time point for analysis because of the transient nature of an *in vivo* action of LPS, especially regarding the transcriptomic response.

Our results from RNA sequencing supported by bioinformatics analysis demonstrated that LPS induced multiple genes and enriched gene sets that are involved in the control of the innate immunity and tissue inflammation. Those include pathogen recognition receptors, cytokines, chemokines, immune cell modulators, and adhesion molecules.

We have found an increased expression of some key pattern recognition receptors, including Tlr2, Tlr3, and Tlr4 along with nuclear oligomerization domain member 2 (Nod2) in the adrenal microvascular endothelial cells. Expression of those receptors sensitizes endothelial cells to the action of several Gram-negative (Tlr4) and positive (Tlr2) bacteria along with several viral infections (Tlr3). The expression of the LPS receptor (Tlr4) was additionally verified by real-time PCR in a separate group of mice. This result is also in accordance with available literature demonstrating the expression of several TLRs in microvascular endothelial cells (31).

In our previous studies, we have shown that activation of TLR4 triggers the expression of multiple cytokines and chemokines in the adrenal gland on the mRNA (12) and protein levels (32). Furthermore, we have found that inactivation of immune but not adrenocortical TLR-signaling could partially decrease this effect (32). Based on this observation, we have postulated that other cells of the adrenal microenvironment, potentially the endothelial cells, may be involved (4). In order to validate this hypothesis, in the present study we have compared the LPS induced cytokines in the adrenal gland with those found only in the adrenal endothelial cells. We have found that systemic administration of LPS increased expression of TNF-α, IFN-α, IFN-γ, IL-12, IL-1α, IL-1β, IL-7, IL-11, IL15, and IL-33 cytokines in the adrenal glands, whereas, at the same time upregulation of only IL-6, IL-27, and IL-15 cytokines was found in endothelial cells. This result suggests that adrenal endothelial cells may contribute to the local inflammation by upregulating IL-6. Limited information is available regarding the transcriptomic analysis of the other microvascular cells during sepsis. However, the existing *in vitro* experiments support our observation, showing that LPS induces mostly IL-6, diverse chemokines and growth factors from cultured endothelial cells (31, 33).

Although endothelial cells might not be substantially the main source of the cytokines during the sepsis, more importantly, those cells are the main target of pro-inflammatory mediators. Indeed, vascular cells are known to express receptors for various pro-inflammatory mediators that are being released into the circulation during sepsis, such as cytokines, chemokines, growth factors, reactive oxygen species (3). Therefore, we have next studied the pro-inflammatory milieu induced by LPS at a 3 h time point in the adrenal gland using a multi cytokine protein array. This assay confirmed a strong induction of IL-6, but also TNF-α, IFN-γ, IL-13, IL-7, and IL-1α or IL-1β cytokines in the adrenal gland lysates.

All those cytokines were shown to contribute to sepsis-mediated activation of the endothelium leading to its increased permeability, altered vascular tone, promotion of a procoagulant state and leukocyte adhesion (13). In order to study whether adrenal microvascular cells are also activated

during endotoxemia, we have compared the expression of diverse chemokines and adhesion molecules between the adrenal gland (12) and isolated endothelial cells. The results of this comparison suggest that the adrenal endothelium may be the main contributor of Csf3, Ccl2, Csf2, and Ccl5, whereas the expression of Cxcl11, Ccl4, or Cxcl5 chemokine can originate also from other cells of the adrenal microenvironment. In addition, the results of our protein array analysis confirmed that indeed the adrenal microvascular endothelial cells contribute substantially to the secretion of CSF (G-CSF), CCL2 and CCL5 chemokines. This observation is in accordance with recent studies using an endothelial cell-specific inactivation of TLR4 signaling. In those mice, a significant decrease in infection-induced plasma CSF3 levels and related lack of emergency granulopoiesis from the bone marrow was observed (34). Furthermore, a significant reduction of LPS-induced expression of adhesion molecules, leukocyte infiltration, and vascular permeability was observed (35). The latter observation was additionally supported in a TNF-induced endothelial damage model, in which inactivation of endothelial TLR signaling decreased plasma CCL5, IL-6, and iNOS levels (36). These observations collectively suggest that LPS activates adrenal endothelium, and promotes expression and secretion of several chemokines (CCL2, CCL5, and CSF3) and adhesion molecules from those cells.

Besides attracting leukocytes, the locally expressed chemokines are also involved in the activation of those immune cells on the endothelium surface (37). Infiltration of immune cells into organs requires multiple steps, including selecting-mediated rolling, chemokine-induced activation, adhesion molecule-mediated firm adhesion, and transmigration through endothelium govern by junctional adhesion molecules and CD31 (37). In the absence of pathogens, the surface of the endothelial cells is rather antiadhesive. Particularly, in the adrenal gland, this process is governed by the secretion of Del-1 protein, which is an antagonist of leukocyte adhesion by preventing the ICAM-1-LFA1 interaction (38). Our study revealed that LPS rapidly induces expression of genes encoding for the P- and E-selectins as well as ICAM-1 and VCAM-1 adhesion molecules. We have verified those changes by real-time PCR and in the case of VCAM-1 also on the protein level in the adrenal gland. Together with decreased expression of Tek and Edil3 genes, which suggest increased vascular permeabilization, increased expression of adhesion molecules may promote the infiltration of immune cells into the adrenal gland. Indeed, in our previous studies, we demonstrated that intraperitoneal injection of LPS to mice results in a rapid infiltration of immune cells into the adrenal gland and that Del-1 deficiency aggravated this process (18). Leading to enhanced apoptosis of adrenal cells, and reduced corticosterone production (18).

An increasing number of studies demonstrate the sepsis-mediated increase in vascular leakiness and their persistent pro-coagulative phenotype, which leads to a progressive hypooxygenation of the affected tissues and can contribute to multi-organ failure (14). In particular, in a study utilizing the cecal ligation and puncture (CLP) model of experimental sepsis, temporary inhibition of the blood flow was demonstrated in skeletal muscle, which led to an improper oxygen distribution and local hypoxia (39). Whether hypoxia can also contribute to the adrenal gland dysfunction is unknown. In our study, we have observed a strong upregulation of hypoxia-inducible factor 1-alpha (Hif-1α), angiopoietin-like 1 (Angptl1) and glycolysis hexokinase 1 and 2 (HK1, 2) in microvascular endothelial cells, which are major hypoxia-related genes. Out of those, we have additionally verified the upregulation of Hif-1α by real-time PCR. On contrary to the results from a transcriptomic analysis of an intact adrenal gland (12), we have not observed any differences in the expression of von Hippel-Lindau tumor suppressor (Vhl) gene in the isolated adrenal endothelial cells. The potential reason of this observation may relate rather to the pro-inflammatory effect of the HIF-1α stabilization and activation induced by LPS and not hypoxia itself. Although activation of HIF-1α was also reported under normoxic conditions preceding the hypoxic conditions (40).

A hallmark of sepsis-induced vascular dysfunction is an increased permeability (13). The endothelial leakage can be initiated either by a loss of protective glycocalyx layer (41), or disturbance in Angiopoietin2 (Angpt2)-Tie2 interaction. In our study, we have investigated the second mechanism. In particular, we have found that LPS injection upregulates the Angpt2 gene in adrenal microvascular cells. This may analogously to the other organs, lead to the increased occupation of Tie2 receptors (42) and increased VEGF-mediated vascular permeability (43). At the same time, LPS-reduced expression of Tek gene, thereby additionally contributing to the Tie2-Anpt2 dysbalance. The loss of this critical tyrosine kinase receptor expressed by endothelial cells was reported recently in diverse critical illnesses including human sepsis, as was correlated with endothelial dysfunction (44).

A well-established hallmark of sepsis is dysregulation of a balance between coagulation and fibrinolysis, which process may lead to disseminated intravascular coagulation (DIC), and subsequently to multiple organ failure. The adrenal gland is an extremely vascularized organ that receives a 10-times higher amount of blood supply in regards to its weight (45, 46), which sensitizes it to hemorrhages. In fact, singular or bilateral adrenal bleedings are being regularly reported, especially after trauma or in patients with meningococcal sepsis (47, 48).

In the present study, systemic inflammation was associated with a strong upregulation of the tissue factor gene, which is one of the main inducers of coagulation (16). Furthermore, we have also observed a strong upregulation of PAI-I (encoded by the Serpin1 gene), which inhibits plasminogen formation and fibrinolysis. Those observations particularly in a view of decreased thrombomodulin gene (thbd1) expression and reported fibrin deposition (49), suggest that LPS increases potentially also the risk of adrenal vascular coagulation. However, a longer time point should be considered when analyzing the adrenal coagulation, as 3 h were not sufficient to alter the protein expression of this important cofactor of protein C activation in the adrenal tissue.

In order to counterbalance the mostly pro-inflammatory effect of LPS on the adrenal microvascular cells, several protective and inflammation resolving factors are subsequently upregulated. Those include first of all IL-4,

and IL-10 cytokines, as well as genes encoding for cis-aconitate decarboxylase (Acod1), annexin 1 (Anxa1) and sphingosine kinase 1 (Sphk1). Upregulation of the Acod1 was reported to antagonize Toll-like receptors (TLRs)-mediated inflammatory innate response (28), whereas induction of annexin 1 was found to mediate the anti-inflammatory action of glucocorticoids (50). Furthermore, as a part of the homeostatic action, adrenal endothelial cells highly upregulated sphingosine kinase 1 (Sphk1) that phosphorylates sphingosine to sphingosine-1-phosphate (S1P), which factors are known to stabilize the endothelial barriers (51). Whether endothelial dysfunction leads to adrenal gland dysfunction, will depend on the delicate balance between pro and anti-inflammatory pathways.

Altogether, this is the first study presenting the LPS-induced global changes in the transcriptome by the adrenal microvascular cells. The results of RNA sequencing and subsequent bioinformatics analysis and protein verification revealed that adrenal vascular endothelial cells are not only involved in the maintenance of the adrenal gland microenvironment but are also active players in pathogen-induced adrenal pathophysiology. Moreover, our results suggest that the damage to the microvascular cells may be an important step preceding the adrenal gland dysfunction, however additional experiments that are ongoing are needed to verify this statement.

DATA AVAILABILITY STATEMENT

Sequencing data are available at the Gene Expression Omnibus database (http://www.ncbi.nlm.nih.gov/geo/) under the following corresponding GSE accession number: GSE139134. Statistical analysis of relative gene expression results and densitometry data were conducted using a non-parametric Mann-Whitney U test in GraphPad Prism Version 6 software (GraphPad Software Inc., USA).

ETHICS STATEMENT

The animal study was reviewed and approved by LANDESDIREKTION SACHSEN.

AUTHOR CONTRIBUTIONS

L-SC, WK, and SS conducted research. L-SC, WK, SS, and GM analyzed data. WK, L-SC, and SB wrote the manuscript.

FUNDING

This study has been funded by the Deutsche Forschungsgemeinschaft (DFG, German Research Foundation) Project A01: 314061271-TRR 205 (to WK and SB).

ACKNOWLEDGMENTS

We are thankful to Andreas Dahl from the Deep Sequencing Group in BIOTEC/Center for Regenerative Therapies Dresden for performing the RNA Sequencing and to Uta Lehnert and Maria Schuster for experiments involving Real-time PCR and immunofluorescent staining.

SUPPLEMENTARY MATERIAL

The Supplementary Material for this article can be found online at: https://www.frontiersin.org/articles/10.3389/fendo.2019.00944/full#Supplementary-Material

REFERENCES

1. Gaieski DF, Edwards JM, Kallan MJ, Carr BG. Benchmarking the incidence and mortality of severe sepsis in the United States. *Crit Care Med*. (2013) 41:1167–74. doi: 10.1097/CCM.0b013e31827c09f8
2. Singer M, Deutschman CS, Seymour CW, Shankar-Hari M, Annane D, Bauer M, et al. The third international consensus definitions for sepsis and septic shock (sepsis-3). *JAMA*. (2016) 315:801–10. doi: 10.1001/jama.2016.0287
3. Van der Poll T, van de Veerdonk FL, Scicluna BP, Netea MG. The immunopathology of sepsis and potential therapeutic targets. *Nat Rev Immunol*. (2017) 17:407–20. doi: 10.1038/nri.2017.36
4. Kanczkowski W, Sue M, Zacharowski K, Reincke M, Bornstein SR. The role of adrenal gland microenvironment in the HPA axis function and dysfunction during sepsis. *Mol Cell Endocrinol*. (2015) 408:241–8. doi: 10.1016/j.mce.2014.12.019
5. Boonen E, Vervenne H, Meersseman P, Andrew R, Mortier L, Declercq PE, et al. Reduced cortisol metabolism during critical illness. *N Engl JMed*. (2013) 368:1477–88. doi: 10.1056/NEJMoa1214969
6. Bornstein SR, Ziegler CG, Krug AW, Kanczkowski W, Rettori V, McCann SM, et al. The role of toll-like receptors in the immune-adrenal crosstalk. *Ann NY Acad Sci*. (2006) 1088:307–18. doi: 10.1196/annals.1366.027
7. Boonen E, Langouche L, Janssens T, Meersseman P, Vervenne H, De SE, et al. Impact of duration of critical illness on the adrenal glands of human intensive care patients. *J Clin Endocrinol Metab*. (2014) 99:4214–22. doi: 10.1210/jc.2014-2429
8. Bornstein SR. Predisposing factors for adrenal insufficiency. *N Engl J Med*. (2009) 360:2328–39. doi: 10.1056/NEJMra0804635
9. Boonen E, Bornstein SR, Van den Berghe G. New insights into the controversy of adrenal function during critical illness. *Lancet Diabet Endocrinol*. (2015) 3:805–15. doi: 10.1016/S2213-8587(15)00224-7
10. Kanczkowski W, Zacharowski K, Wirth MP, Ehrhart-Bornstein M, Bornstein SR. Differential expression and action of Toll-like receptors in human adrenocortical cells. *Mol Cell Endocrinol*. (2009) 300:57–65. doi: 10.1016/j.mce.2008.10.028
11. Jennewein C, Tran N, Kanczkowski W, Heerdegen L, Kantharajah A, Drose S, et al. Mortality of septic mice strongly correlates with adrenal gland inflammation. *Crit Care Med*. (2016) 44:e190–9. doi: 10.1097/CCM.0000000000001373
12. Chen LS, Singh SP, Schuster M, Grinenko T, Bornstein SR, Kanczkowski W. RNA-seq analysis of LPS-induced transcriptional changes and its possible implications for the adrenal gland dysregulation during sepsis. *J Steroid Biochem Mol Biol*. (2019) 191:105360. doi: 10.1016/j.jsbmb.2019.04.009
13. Shapiro NI, Schuetz P, Yano K, Sorasaki M, Parikh SM, Jones AE, et al. The association of endothelial cell signaling, severity ofillness, and organ dysfunction in sepsis. *Crit Care*. (2010) 14:R182. doi: 10.1186/cc9290
14. Ince C, Mayeux PR, Nguyen T, Gomez H, Kellum JA, Ospina-Tascon GA, et al. The endothelium in sepsis. *Shock*. (2016) 45:259–70. doi: 10.1097/SHK.0000000000000473
15. Aird WC. The role of the endothelium in severe sepsis and multiple organ dysfunction syndrome. *Blood*. (2003) 101:3765–77. doi: 10.1182/blood-2002-06-1887

16. Iba T, Levi M, Levy JH. Sepsis-induced coagulopathy and disseminated intravascular coagulation. *Semin Thromb Hemost.* (2019). doi: 10.1055/s-0039-1694995. [Epub ahead of print].
17. Chavakis T, Kanczkowski W, Willenberg HS, Bornstein SR. Endothelial dysfunction: a critical determinant in inflammation-associated adrenal insufficiency? *Eur J Clin Invest*. (2011) 41:917–9. doi: 10.1111/j.1365-2362.2011.02477.x
18. Kanczkowski W, Chatzigeorgiou A, Grossklaus S, Sprott D, Bornstein SR, Chavakis T. Role of the endothelial-derived endogenous anti-inflammatory factor del-1 in inflammation-mediated adrenal gland dysfunction. *Endocrinology*. (2013) 154:1181–9. doi: 10.1210/en.2012-1617
19. Livak KJ, Schmittgen TD. Analysis of relative gene expression data using real-time quantitative PCR and the 2(-Delta Delta C(T)) method. *Methods*. (2001) 25:402–8. doi: 10.1006/meth.2001.1262
20. Kim D, Langmead B, Salzberg SL. HISAT: a fast spliced aligner with low memory requirements. *Nat Methods*. (2015) 12:357–60. doi: 10.1038/nmeth.3317
21. Anders S, Pyl PT, Huber W. HTSeq–a Python framework to work with high-throughput sequencing data. *Bioinformatics*. (2015) 31:166–9. doi: 10.1093/bioinformatics/btu638
22. Robinson MD, McCarthy DJ, Smyth GK. edgeR: a bioconductor package for differential expression analysis of digital gene expression data. *Bioinformatics*. (2010) 26:139–40. doi: 10.1093/bioinformatics/btp616
23. Ge SX, Son EW, Yao R. iDEP: an integrated web application for differential expression and pathway analysis of RNA-Seq data. *BMC Bioinformatics*. (2018) 19:534. doi: 10.1186/s12859-018-2486-6
24. Huang dW, Sherman BT, Lempicki RA. Systematic and integrative analysis of large gene lists using DAVID bioinformatics resources. *Nat Protoc*. (2009) 4:44–57. doi: 10.1038/nprot.2008.211
25. Kanehisa M, Sato Y, Kawashima M, Furumichi M, Tanabe M. KEGG as a reference resource for gene and protein annotation. *Nucleic Acids Res*. (2016) 44:D457–62. doi: 10.1093/nar/gkv1070
26. Subramanian A, Tamayo P, Mootha VK, Mukherjee S, Ebert BL, Gillette MA, et al. Gene set enrichment analysis: a knowledge-based approach for interpreting genome-wide expression profiles. *Proc Natl Acad Sci USA*. (2005) 102:15545–50. doi: 10.1073/pnas.0506580102
27. Nolan DJ, Ginsberg M, Israely E, Palikuqi B, Poulos MG, James D, et al. Molecular signatures of tissue-specific microvascular endothelial cell heterogeneity in organ maintenance and regeneration. *Dev Cell*. (2013) 26:204–19. doi: 10.1016/j.devcel.2013.06.017
28. Michelucci A, Cordes T, Ghelfi J, Pailot A, Reiling N, Goldmann O, et al. Immune-responsive gene 1 protein links metabolism to immunity by catalyzing itaconic acid production. *Proc Natl Acad Sci USA*. (2013) 110:7820–5. doi: 10.1073/pnas.1218599110
29. McGarrity S, Anuforo Ó, Halldórsson H, Bergmann A, Halldórsson S, Palsson S, et al. Metabolic systems analysis of LPS inducedendothelial dysfunction applied to sepsis patient stratification. *Sci Rep*. (2018) 8:6811. doi: 10.1038/s41598-018-25015-5
30. Kamisoglu K, Haimovich B, Calvano SE, Coyle SM, Corbett SA, Langley RJ, et al. Human metabolic response to systemic inflammation: assessment of the concordance between experimental endotoxemia and clinical cases of sepsis/SIRS. *Crit Care*. (2015) 19:71. doi: 10.1186/s13054-015-0783-2
31. Khakpour S, Wilhelmsen K, Hellman J. Vascular endothelial cell toll-like receptor pathways in sepsis. *Innate Immun*. (2015) 21:827–46. doi: 10.1177/1753425915606525
32. Kanczkowski W, Alexaki VI, Tran N, Grossklaus S, Zacharowski K, Martinez A, et al. Hypothalamo-pituitary and immune-dependent adrenal regulation during systemic inflammation. *Proc Natl Acad Sci USA*. (2013) 110:14801–6. doi: 10.1073/pnas.1313945110
33. Zeuke S, Ulmer AJ, Kusumoto S, Katus HA, Heine H. TLR4-mediated inflammatory activation of human coronary artery endothelial cells by LPS. *Cardiovasc Res*. (2002) 56:126–34. doi: 10.1016/S0008-6363(02)00512-6
34. Boettcher S, Gerosa RC, Radpour R, Bauer J, Ampenberger F, Heikenwalder M, et al. Endothelial cells translate pathogen signals into G-CSF-driven emergency granulopoiesis. *Blood*. (2014) 124:1393–403. doi: 10.1182/blood-2014-04-570762
35. Ye X, Ding J, Zhou X, Chen G, Liu SF. Divergent roles of endothelial NF-kappaBin multiple organ injury and bacterial clearance in mouse models of sepsis. *J Exp Med*. (2008) 205:1303–15. doi: 10.1084/jem.20071393
36. Zhou Z, Gengaro P, Wang W, Wang XQ, Li C, Faubel S, et al. Role of NF-kappaB and PI 3-kinase/Akt in TNF-alpha-induced cytotoxicity in microvascular endothelial cells. *Am J Physiol Renal Physiol*. (2008) 295:F932–41. doi: 10.1152/ajprenal.00066.2008
37. Mitroulis I, Alexaki VI, Kourtzelis I, Ziogas A, Hajishengallis G, Chavakis T. Leukocyte integrins: role in leukocyte recruitment and as therapeutic targets in inflammatory disease. *Pharmacol Ther*. (2015) 147:123–35. doi: 10.1016/j.pharmthera.2014.11.008
38. Choi EY, Chavakis E, Czabanka MA, Langer HF, Fraemohs L, Economopoulou M, et al. Del-1, an endogenous leukocyte-endothelial adhesion inhibitor, limits inflammatory cell recruitment. *Science*. (2008) 322:1101–4. doi: 10.1126/science.1165218
39. Ellis CG, Bateman RM, Sharpe MD, Sibbald WJ, Gill R. Effect of a maldistribution of microvascular blood flow on capillary O(2) extraction in sepsis. *Am J Physiol Heart Circ Physiol*. (2002) 282:H156–64. doi: 10.1152/ajpheart.2002.282.1.H156
40. Jantsch J, Wiese M, Schödel J, Castiglione K, Gläsner J, Kolbe S. Toll-like receptor activation and hypoxia use distinct signaling pathways tostabilize hypoxia-inducible factor 1α (HIF1A) and result in differentialHIF1A-dependent gene expression. *J Leukoc Biol*. (2011) 90:551–62. doi: 10.1189/jlb.1210683
41. Iba T, Levy JH. Derangement of the endothelial glycocalyx in sepsis. *J Thromb Haemost*. (2019) 17:283–94. doi: 10.1111/jth.14371
42. Drost CC, Rovas A, Kusche-Vihrog K, Van SP, Kim H, Hoang VC, et al. Tie2 activation promotes protection and reconstitution of the endothelial glycocalyx in human sepsis. *Thromb Haemost*. (2019) 119:1827–38. doi: 10.1055/s-0039-1695768
43. Ziegler T, Horstkotte J, Schwab C, Pfetsch V, Weinmann K, Dietzel S, et al. Angiopoietin 2 mediates microvascular and hemodynamic alterations in sepsis. *J Clin Invest*. (2013) 123:3436–45. doi: 10.1172/JCI66549
44. Thamm K, Schrimpf C, Retzlaff J, Idowu TO, van Meurs M, Zijlstra JG. Molecular regulation of acute Tie2 suppression in sepsis. *Crit Care Med*. (2018) 46:e928–36. doi: 10.1097/CCM.0000000000003269
45. Breslow MJ. Regulation of adrenal medullary and cortical blood flow. *Am J Physiol*. (1992) 262:H1317–30. doi: 10.1152/ajpheart.1992.262.5.H1317
46. Sapirstein LA, Goldman H. Adrenal blood flow in the albino rat. *Am J Physiol*. (1959) 196:159–62. doi: 10.1152/ajplegacy.1958.196.1.159
47. Alves Pereira FD, Hickson ML, Wilson PAJ. Case 268: bilateral adrenal haemorrhage in the context of sepsis. *Radiology*. (2019) 292:503–6. doi: 10.1148/radiol.2019170489
48. Adem PV, Montgomery CP, Husain AN, Koogler TK, Arangelovich V, Humilier M, et al. Staphylococcus aureus sepsis and the Waterhouse-Friderichsen syndrome in children. *N Engl J Med*. (2005) 353:1245–51. doi: 10.1056/NEJMoa044194
49. Yamamoto K, Loskutoff DJ. Fibrin deposition in tissues from endotoxin-treated mice correlates with decreases in the expression of urokinase-type but not tissue-type plasminogen activator. *J Clin Invest*. (1996) 97:2440–51. doi: 10.1172/JCI118691
50. Sawmynaden P, Perretti M. Glucocorticoid upregulation of the annexin-A1 receptor in leukocytes. *Biochem Biophys Res Commun*. (2006) 349:1351–5. doi: 10.1016/j.bbrc.2006.08.179
51. Dennhardt S, Finke KR, Huwiler A, Coldewey SM. Sphingosine-1-phosphate promotes barrier-stabilizing effects in human microvascular endothelial cells via AMPK-dependent mechanisms. *Biochim Biophys Acta Mol Basis Dis*. (2019) 1865:774–81. doi: 10.1016/j.bbadis.2018.12.022

Conflict of Interest: The authors declare that the research was conducted in the absence of any commercial or financial relationships that could be construed as a potential conflict of interest.

frontiers in Endocrinology

REVIEW
published: 31 January 2020
doi: 10.3389/fendo.2020.00025

The Role of Short-Chain Fatty Acids From Gut Microbiota in Gut-Brain Communication

Ygor Parladore Silva[1], *Andressa Bernardi*[2] *and Rudimar Luiz Frozza*[1]*

[1] Laboratory on Thymus Research, Oswaldo Cruz Institute, Oswaldo Cruz Foundation, Rio de Janeiro, Brazil, [2] Laboratory of Inflammation, Oswaldo Cruz Institute, Oswaldo Cruz Foundation, Rio de Janeiro, Brazil

A substantial body of evidence supports that the gut microbiota plays a pivotal role in the regulation of metabolic, endocrine and immune functions. In recent years, there has been growing recognition of the involvement of the gut microbiota in the modulation of multiple neurochemical pathways through the highly interconnected gut-brain axis. Although amazing scientific breakthroughs over the last few years have expanded our knowledge on the communication between microbes and their hosts, the underpinnings of microbiota-gut-brain crosstalk remain to be determined. Short-chain fatty acids (SCFAs), the main metabolites produced in the colon by bacterial fermentation of dietary fibers and resistant starch, are speculated to play a key role in neuro-immunoendocrine regulation. However, the underlying mechanisms through which SCFAs might influence brain physiology and behavior have not been fully elucidated. In this review, we outline the current knowledge about the involvement of SCFAs in microbiota-gut-brain interactions. We also highlight how the development of future treatments for central nervous system (CNS) disorders can take advantage of the intimate and mutual interactions of the gut microbiota with the brain by exploring the role of SCFAs in the regulation of neuro-immunoendocrine function.

Keywords: central nervous system, neuroinflammation, gut-brain axis, gut microbiota, short-chain fatty acids

OPEN ACCESS

Edited by:
Ana Rosa Pérez,
National Council for Scientific and Technical Research (CONICET), Argentina

Reviewed by:
Claude Knauf,
Institut National de la Santé et de la Recherche Médicale (INSERM), France
Douglas Morrison,
University of Glasgow, United Kingdom
Norbert Sprenger,
Nestle Institute of Health Sciences (NIHS), Switzerland

***Correspondence:**
Rudimar Luiz Frozza
rudimar.frozza@ioc.fiocruz.br

Specialty section:
This article was submitted to Neuroendocrine Science, a section of the journal Frontiers in Endocrinology

Received: *31 October 2019*
Accepted: *14 January 2020*
Published: *31 January 2020*

Citation:
Silva YP, Bernardi A and Frozza RL (2020) The Role of Short-Chain Fatty Acids From Gut Microbiota in Gut-Brain Communication. Front. Endocrinol. 11:25. doi: 10.3389/fendo.2020.00025

INTRODUCTION

The human body is inhabited by a wide variety of commensal microorganisms collectively called the microbiota. This host microbiota colonizes the skin and several mucosal cavities (nasal, oral, pulmonary, and vaginal); however, it is in the gastrointestinal (GI) tract that these organisms reach extraordinary densities since trillions of bacteria, fungi, and viruses coexist in symbiosis with the host for potential mutual benefit (1–3). Despite its significant influence on the state of human health and the development or progression of diseases, it is only in the last 20 years that our gut microbiota has become the focus of intense studies. Therefore, its pivotal roles in protecting against pathogens, regulating metabolic, endocrine, and immune functions and in influencing drug metabolism and absorption have started to be elucidated (4, 5). Further, it was recently unveiled that the influence of the microbiota is not restricted to the GI tract; it plays a major role in the bidirectional communication between the GI tract and the central nervous system (CNS). The growing body of evidence indicating that the gut microbiota exerts a profound influence on key brain processes has led to the development of the microbiota-gut-brain axis concept, which has attracted the interest of researchers worldwide (6–11).

Although the precise mechanisms involved in the crosstalk between the gut microbiota and brain remain to be fully determined, there are a number of potential pathways through which the gut microbiota can influence brain function (9). Microorganisms can influence CNS processes bidirectionally via the vagus nerve (12) and through modulation of the immune system (6), the hypothalamic-pituitary-adrenal (HPA) axis (13, 14), and tryptophan metabolism (15), along with their ability to synthetize a number of neurotransmitters (16–18) and produce metabolites, such as short-chain fatty acids (SCFAs), that possess neuroactive properties (17, 19–21).

The SCFAs acetate, propionate, and butyrate are the main metabolites produced in the colon by bacterial fermentation of dietary fibers and resistant starch (22). In addition to the long-known role of the colon in energy supply and trophic factors (22), as well as the regulation of T regulatory (Treg) cell colonies (23, 24), growing evidence supports the idea that SCFAs also exert crucial physiological effects on several organs, including the brain (17, 20, 21). This hypothesis is supported by studies in animals and humans showing that gut microbiota dysbiosis has been implicated in behavioral and neurologic pathologies, such as depression, Alzheimer's (AD) and Parkinson's (PD) diseases and autism spectrum disorder (ASD) (9, 21, 25–27). Furthermore, microbiota manipulation and SCFA administration have been proposed as treatment targets for such diseases (28).

In this review, we outline the current knowledge about the involvement of acetate, propionate, and butyrate in microbiota-gut-brain interactions. We also highlight how the development of future treatments for CNS disorders can take advantage of the intimate and mutual interactions of the gut microbiota with the brain by exploring the role of SCFAs in the regulation of neuro-immunoendocrine function.

THE MICROBIOTA-GUT-BRAIN AXIS

The modulation of gut physiology by the CNS and its effects on gut function such as motility, secretion, blood flow, nociception, and immune function during neurological stressors are well-documented (17, 29, 30). Further, brain to gut signaling can directly affect the microbiota, either via immune system or gut functions such as motility, release of neurotransmitters and intestinal immune tone (12, 17, 21, 31). Comparatively, gut to CNS signaling has been studied for a short period, and the mechanisms underlying this crosstalk are starting to be understood (13, 32). It is noteworthy that several brain disorders have been linked to imbalances in the microbial composition of the gut (17, 19, 29, 33–37); however, whether these alterations in the microbiota are induced by brain signaling or whether brain dysfunction is driven by changes in the gut microbiota remains to be fully determined.

Although a more compelling causal relationship between altered gut microbial composition and brain dysfunction is still needed, it has been shown that disruption in the neuronal and microbial organization in prenatal and postnatal periods of mammalian development may lead to the onset of neurodevelopmental and other brain disorders later in life (9, 38–40). In a similar way, growing evidence has shown that alterations in maternal microbiome during pregnancy, such as use of antibiotics or probiotics (41, 42), variations in diet (43), immune activation (44, 45), and exposure to stress (46) can modulate the microbiome, neurodevelopment, and behavior of offspring in both rodents and humans (9, 29). Furthermore, delivery mode (47) and early-life occurrences such as feeding changes, infection, and antibiotics treatment (48, 49) have a huge effect on the gut microbiota composition with a long-term impact on brain and behavior (9, 29).

Under physiological conditions, activation of immune cells and production of cytokines can have a minor impact in the CNS. However, chronic systemic inflammation, mostly in the form of infections, has long been associated with behavioral alterations and cognitive dysfunction (50, 51). It is now widely known that peripheral insults that cause a systemic inflammatory response might affect ongoing inflammation in the CNS mainly by microglial activation, production of inflammatory molecules, as well as recruitment of peripheral immune cells into the brain, thus shaping a cerebral inflammatory milieu that may seriously affect neuronal function (50, 52, 53). Noteworthy, during gut pathologies with increased permeability of the intestinal barrier, the translocation of bacterial products can increase the production of cytokines and impact the blood-brain barrier (BBB), leading to more intense harmful effects (37). Further, it has already been shown that several bacterial strains can modify levels of neurotransmitter precursors in the gut lumen and even independently synthesize (or modulate the synthesis of) a number of neurotransmitters, including γ-aminobutyric acid (GABA), serotonin (5-HT), dopamine (DA), and noradrenaline (NA) (16–18). These neurotransmitters can potentially influence microglial activation and several cerebral functions (54). Additionally, the sympathetic branch of the autonomic nervous system is also involved in intestinal homeostasis and immune regulation (30). Conversely, the gut microbiota can interact with the CNS via gut modulation or directly via metabolites and endotoxin translocation from the lumen to the circulation (9, 17, 21). Possible signal transducers involved in the communication of the microbiota with the CNS include enterochromaffin cells, which can bind several microbial products and secrete serotonin into the lamina propria, increasing colonic and blood concentrations of 5-HT (55, 56). Gut-brain communication can also be achieved through vagus nerve signaling (57). Changes in enteric neuron activity perceived

Abbreviations: Aβ, amyloid-β peptide; AD, Alzheimer's disease; ASD, autism spectrum disorder; αSyn, α-synuclein; BBB, blood-brain barrier; BDNF, brain-derived neurotrophic factor; BHB, β-hydroxybutyrate; CNS, central nervous system; DA, dopamine; EAE, experimental autoimmune encephalopathy; FFAR, free fatty acid receptor; FMT, fecal microbiota transplantation; GABA, γ-aminobutyric acid; GDNF, glial cell line-derived neurotrophic factor; GF, germ free; GH, growth hormone; GI, gastrointestinal (tract); GLP-1, glucagon-like peptide 1; GOS, galacto-oligosaccharides; GPCR, G protein-coupled receptors; HCAR2, hydrocarboxylic acid receptor; HDACs, histone deacetylases; HDACi, HDAC inhibitor; HPA, hypothalamus-pituitary-adrenal; LPS, lipopolysaccharide; MCT, H^+-coupled monocarboxylate transporter; MS, multiple sclerosis; NA, noradrenaline; NGF, nerve growth factor; PD, Parkinson's disease; PKCδ, protein kinase Cδ; PYY, peptide YY; 5-HT, serotonin; SCFAs, short-chain fatty acids; SMCTs, sodium-coupled monocarboxylate transporters; SPF, specific pathogen-free; Tregs, T-regulatory lymphocytes.

by the vagus nerve are essential for mediating satiety, stress, and mood (12, 58, 59). Given the close physical proximity, gut bacteria can interact with and activate the vagus nerve, thereby exerting effects upstream to the CNS. This notion is in full accordance with early studies showing that oral inoculation with pathogens or probiotics induces activation of the vagal sensory neurons that innervate the GI affecting the regulation of CNS functions, and this effect is absent in vagotomized mice (32, 58, 60). However, whether the vagus nerve is activated by physical interaction with bacteria or through soluble microbial components remain to be determined.

Finally, bacterial metabolic byproducts including SCFAs are often considered key candidate mediators of gut-brain communication, and altered SCFA production has been demonstrated in a variety of neuropathologies (19, 21, 33–35).

METABOLISM AND PERIPHERAL EFFECTS OF SCFAS

SCFAs are small organic monocarboxylic acids with a chain length of up to six carbons atoms and are the main products of the anaerobic fermentation of indigestible polysaccharides such as dietary fiber and resistant starch produced by the microbiota in the large intestine (61, 62). Comprised mostly of acetate (C2), propionate (C3), and butyrate (C4) (63, 64) in an approximate molar rate of 60:20:20, respectively (65), approximately 500–600 mmol of SCFAs are produced in the gut per day depending on the fiber content in the diet, microbiota composition, and gut transit time (66, 67). Although anaerobic fermentation of fibers is the largest source of SCFAs, acetate, propionate, and butyrate can also be produced from amino acid metabolism (68). However, less than 1% of the large intestine microbiota uses these metabolic pathways to produce SCFAs (69, 70). Protein fermentation usually takes place in the distal large intestine where carbohydrates are already depleted and also leads to the production of potentially toxic metabolites, such as ammonia, phenols, and sulfides, as well as unique branched-chain fatty acids (BCFA) (69, 71). Further, acetate produced from acetyl-CoA derived from glycolysis can also be transformed into butyrate by the enzyme butyryl-CoA:acetyl-CoA transferase (72, 73), and bovine milk fats also provide a source of butyrate (74).

Following their production, SCFAs are absorbed by colonocytes, mainly via H^+-dependent or sodium-dependent monocarboxylate transporters (MCTs and SMCTs, respectively) (75). MCTs show different subtypes and expression patterns in different tissues. SCFAs that are not metabolized in the colonocytes are transported into the portal circulation and are used as an energy substrate for hepatocytes (76), except for acetate that is not oxidized in the liver (76). Therefore, only a minor fraction of colon-derived acetate, propionate, and butyrate reaches the systemic circulation and other tissues (65). In this context, it is important to note that most of the recent works regarding microbial-derived SCFA, mainly in human studies, use fecal concentrations as a proxy of the production in the colon (17, 19, 29, 33–37). Although it represents a valid approach, there are many potential sources of bias, such as intestinal transit and permeability, metabolite transportation, and sample handling (77). Thus, these drawbacks must be taken into account when concluding the effects of administered SCFAs, given that some experiments might be conducted under non-physiological conditions.

SCFAs improve the gut health through a number of local effects, ranging from maintenance of intestinal barrier integrity, mucus production, and protection against inflammation to reduction of the risk of colorectal cancer (78–81). Although a thorough comprehension of signaling triggered by SCFAs is still lacking, it is already known that SCFAs bind to G protein-coupled receptors (GPCRs). The best-studied SCFA receptors are GPR43 and GPR41, later renamed free fatty acid receptor (FFAR2) and FFAR3, as well as GPR109a/HCAR2 (hydrocarboxylic acid receptor) and GPR164, which are expressed in a vast array of cells, from the gastrointestinal mucosa to the immune and nervous systems (82, 83). The effects of activation of these receptors differ greatly depending on the cell on which they are expressed. For instance, binding of SCFAs to their receptors on enteroendocrine cells results in stimulated secretion of glucagon-like peptide 1 (GLP-1) and peptide YY (PYY) (84), while signaling in β-pancreatic cells leads to increased insulin secretion (85).

Another mechanism by which SCFAs regulate systemic functions is through the inhibition of histone deacetylase (HDAC) activity, thus promoting the acetylation of lysine residues present in nucleosomal histones throughout various cell populations (20). This intracellular signaling mechanism has been found in both the gut and associated immune tissue (86), as well as in the peripheral nervous system and CNS (20).

Although only a minor fraction of colon-derived SCFAs reaches the systemic circulation and other tissues, their effects on different organ and systems have recently been widely outlined. One of the best-documented effects of SCFAs is on the immune system since butyrate is capable of inducing Treg differentiation and controlling inflammation (17, 23, 24, 87). Although fine-tuning of the gut immune response to the microbiota is still a matter of debate, microbiota metabolites are capable of alleviating or worsening gut conditions such as inflammatory bowel disease (88). Effects on brown adipose tissue activation (89), regulation of liver mitochondrial function (90), whole-body energy homeostasis (91), and control of appetite (89) and sleep (10) have been attributed to all SCFAs. Further, the influence of the microbiota and the effects of SCFAs on the CNS have been a matter of intense debate in the last few years.

SCFAS AND THE BRAIN

In addition to exerting local effects in the colon and in the peripheral tissues, SCFAs are speculated to play a pivotal role in microbiota-gut-brain crosstalk (**Figure 1**). The abundant expression of MCTs in endothelial cells (75, 92) might facilitate crossing of the BBB by SCFAs since brain uptake of SCFAs has previously been demonstrated in rats following injection of ^{14}C-SCFAs into the carotid artery (93). Although studies on physiological concentrations of SCFAs in the brain are scarce, all three metabolites are detectable in the human cerebrospinal fluid (CSF), typically in the range of 0–171 μM for acetate,

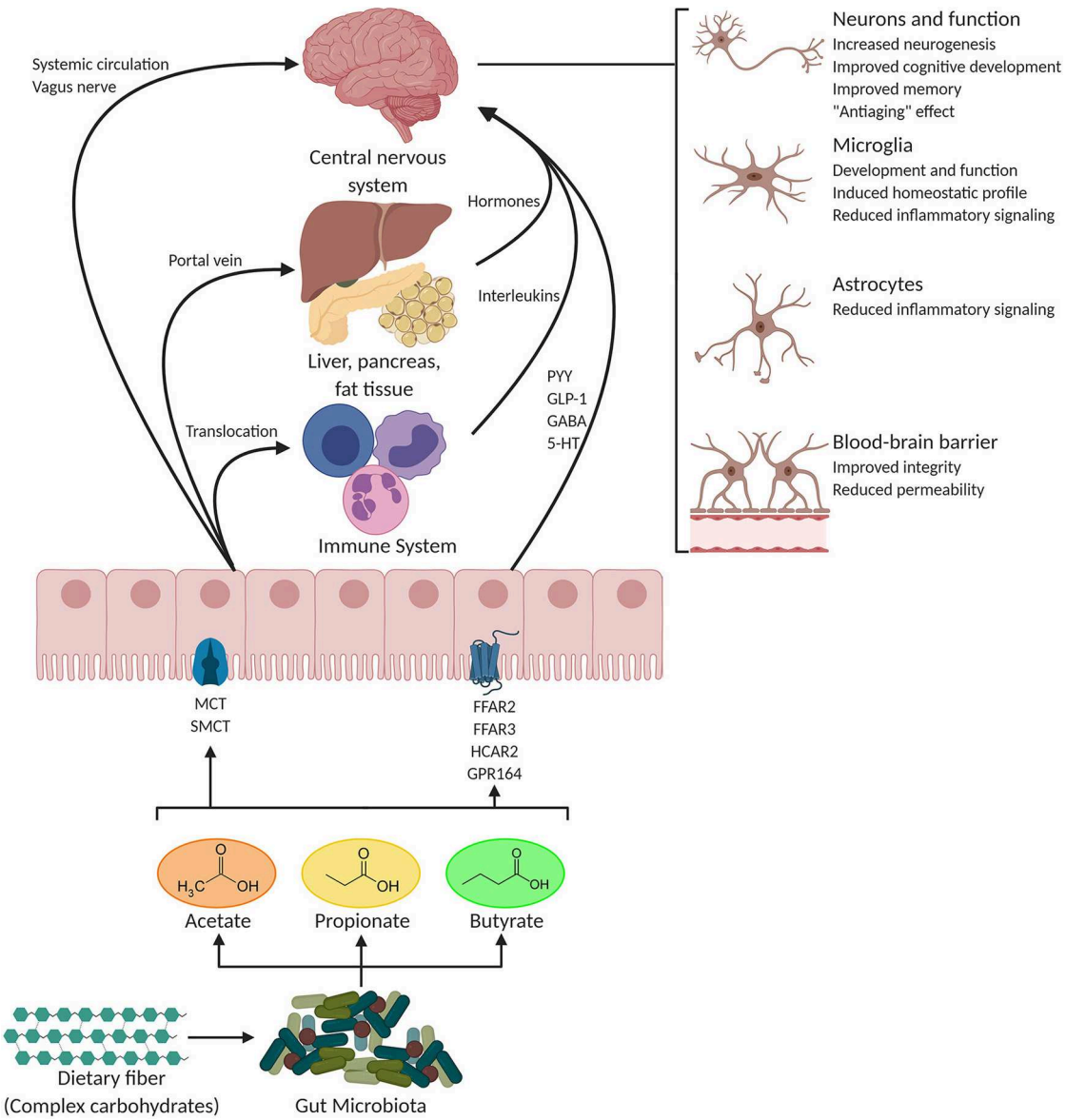

FIGURE 1 | Potential pathways through which SCFAs influence gut-brain communication. Short-chain fatty acids (SCFAs) are the main metabolites produced by the microbiota in the large intestine through the anaerobic fermentation of indigestible polysaccharides such as dietary fiber and resistant starch. SCFAs might influence gut-brain communication and brain function directly or indirectly. Following their production, SCFAs are absorbed by colonocytes, mainly via H^+-dependent monocarboxylate transporters (MCTs) or sodium-dependent monocarboxylate transporters (SMCTs). Through binding to G protein-coupled receptors (GPCRs) such as free fatty acid receptor 2 and 3 (FFAR2 and FFAR3), as well as GPR109a/HCAR2 (hydrocarboxylic acid receptor) and GPR164 or by inhibiting histone deacetylases, SCFAs influence intestinal mucosal immunity, and barrier integrity and function. SCFA interaction with their receptors on enteroendocrine cells promotes indirect signaling to the brain via the systemic circulation or vagal pathways by inducing the secretion of gut hormones such as glucagon-like peptide 1 (GLP1) and peptide YY (PYY), as well as γ-aminobutyric acid (GABA), and serotonin (5-HT). Colon-derived SCFAs reaches the systemic circulation and other tissues, leading to brown adipose tissue activation, regulation of liver mitochondrial function, increased insulin secretion by β-pancreatic cells, and whole-body energy homeostasis. Peripherally, SCFAs influence systemic inflammation mainly by inducing T regulatory cells (Treg) differentiation and by regulating the secretion of interleukins. SCFAs can cross the blood-brain barrier (BBB) via monocarboxylate transporters located on endothelial cells and influence BBB integrity by upregulating the expression of tight junction proteins. Finally, in the central nervous system (CNS) SCFAs also influence neuroinflammation by affecting glial cell morphology and function as well as by modulating the levels of neurotrophic factors, increasing neurogenesis, contributing to the biosynthesis of serotonin, and improving neuronal homeostasis and function. Together, the interaction of SCFAs with these gut-brain pathways can directly or indirectly affect emotion, cognition, and pathophysiology of brain disorders. Figure of this review was created with BioRender (https://biorender.com/).

0–6 μM for propionate, and 0–2.8 μM for butyrate (94). An average concentration of 17.0 pmol/mg of tissue for butyrate and 18.8 pmol/mg of tissue for propionate in the human brain was reported (95). Furthermore, the levels of butyrate in the brain of mice supplemented with live *Clostridium butyricum* reached a range from 0.4 to 0.7 μmol/g, which was about

an order of magnitude higher than concentrations reported in peripheral blood (96, 97). In addition to crossing BBB, SCFAs seem to play an important role in maintaining its integrity, which is tightly associated with controlled passage of molecules and nutrients from the circulation to the brain, playing a central role in brain development and the preservation of CNS homeostasis. Supporting the notion that SCFAs regulate the BBB function, germ-free (GF) mice show reduced expression of tight junction proteins such as claudin and occludin, leading to increased permeability of the BBB from intrauterine life to adulthood (98). Furthermore, recolonization of these adult mice with a complex microbiota or monocolonization with SCFA-producing bacterial strains recovers the integrity of the BBB (98). Similarly, treatment of an *in vitro* model of cerebrovascular endothelial cells with propionate attenuates the permeabilizing effects of exposure to lipopolysaccharide (LPS) (99).

Accumulating evidence suggests that SCFAs that cross into the CNS have neuroactive properties. Although the precise mechanisms involved in the action of SCFAs on the CNS remain largely unknown, a multitude of animal studies have shown that they exert widespread influence on key neurological and behavioral processes and may be involved in critical phases of neurodevelopmental and neurodegenerative disorders (17, 21, 29, 36, 100).

SCFAs and Microglia

The development of the nervous system is marked by the sculpting of the neuronal networks shaping the functional neural circuitry that is critical for normal cognitive, emotional, and social domains. In this context, glial cells, especially microglial cells, have been increasingly recognized to play a critical role in the elimination of excess or unnecessary synaptic connections, which is necessary for the maturation and refinement of circuits and connections in the nervous system (101, 102). Therefore, control of innate immune function in the CNS is critical for brain development, and the gut microbiota seems to play a pivotal role in the development and functionality of the immune system in the CNS. The results reported by Erny and collaborators shed light on how the microbiota might influence microglial maturation and function (6). While microglia from specific pathogen-free (SPF) mice shows normal maturation and function, non-colonized young GF mice exhibit stunted microglia under homeostatic conditions. It is noteworthy that the oral application of a mixture of the three major SCFAs acetate, propionate, and butyrate was sufficient to drive maturation of microglia in GF mice (6). Although the mechanisms involved in the control of maturation and function of microglia by SCFAs remain to be determined, the activation of FFAR2 could be conceivable since FFAR2-deficient mice displayed microglia reminiscent of those found in GF mice (103).

Neuroinflammation is also an important process shaping brain function. Similar to observations in GF mice, perturbations of the gut microbiota by antibiotics systemically produce altered immune responses in experimental models, notably toward a pro-inflammatory profile (6). This is also true in the CNS, which becomes more prone to extreme inflammatory responses when the microbiota is depleted by antibiotics early in life (104). It was shown that antibiotic-induced perturbations in gut microbial diversity influence neuroinflammation with altered microglial morphology (105–107). On the other hand, several studies have reported that sodium butyrate is capable of decreasing microglial activation and pro-inflammatory cytokines secretion (108–110). Also, butyrate treatment *in vitro* and *in vivo* induces morphological and functional changes in the microglia toward a homeostatic profile and inhibits LPS-induced pro-inflammatory modifications (109) and depression-like behavior (110). Likewise, acetate treatment of microglia primary culture has been shown to reduce inflammatory signaling through reduced IL-1β, IL-6, and TNF-α expression and p38 MAPK, JNK, and NF-κB phosphorylation (111). Similarly, acetate was also able to modulate inflammatory cytokines and signaling pathways in astrocyte primary culture (112). Although the precise signaling involved in the effects of SCFAs on microglia remain unveiled, inhibition of HDACs, which results in epigenetically regulated gene expression, has been considered the main effector mechanism triggered by SCFAs (113). In this way, histone acetylation seems to modulate glial cells in an anti-inflammatory and neuroprotective manner. Therefore, taking into account the role of microglia in shaping neuronal networks and the influence of the microbiota on this process, SCFAs might provide new methods to modulate the brain immunity disruption underlying neurodevelopmental and neurodegenerative disorders.

SCFAs and Neurons

Apart from providing the cells with energy and affecting microglia maturation, these microbial metabolites also seem to influence neuronal function. It was described that SCFAs may modulate the levels of neurotransmitters and neurotrophic factors. Acetate has previously been shown to alter the levels of the neurotransmitters glutamate, glutamine and GABA in the hypothalamus and increase anorexigenic neuropeptide expression (114). Propionate and butyrate exert an influence on the intracellular potassium level, which implies the involvement of SCFAs in the operation of cell signaling systems (115). In particular, these SCFAs regulate the expression levels of tryptophan 5-hydroxylase 1, the enzyme involved in synthesis of serotonin, and tyrosine hydroxylase, which is involved in a rate-limiting step in the biosynthesis of dopamine, noradrenaline and adrenaline; therefore, producing an effect on brain neurochemistry (21, 55, 56, 116, 117). Antibiotic depletion of the microbiota also results in hippocampal neurogenesis and memory impairments, which can be partially recovered by the reconstitution of specific SPF microbiota and completely recovered by probiotic treatment or exercise (118). This cognitive deficit might be associated with changes in the expression of cognition-relevant signaling molecules such as brain-derived neurotrophic factor (BDNF), N-methyl-D-aspartate receptor subunit 2B, serotonin transporter and neuropeptide Y system (119).

Neurotrophic factors, such as nerve growth factor (NGF), glial cell line-derived neurotrophic factor (GDNF), and BDNF that regulate the growth, survival and differentiation of neurons and synapses in the CNS also play important parts in learning

and memory and in a range of brain disorders have been also shown to be modulated by SCFAs (120–123). BDNF expression, neurogenesis, and neural proliferation in rodents (124–126), as well as facilitation of long-term memory consolidation, were stimulated by sodium butyrate (127). Further, physiological levels of all three SCFAs were shown to increase the growth rate of human neural progenitor cells and induce more cells to undergo mitosis (128), affording some hints of how SCFAs could regulate early neural system development. Further, SCFAs show effects on several neural functions, such as enhancing sleep (10), suppressing the activity of orexigenic neurons that express neuropeptide Y in the hypothalamus (89), and modulating the signaling triggered by the ghrelin receptor (129), contributing to circadian rhythm and appetite control. The seeking for mechanism involved in the modulation of neuronal function by SCFAs has unveiled that some of these effects are likely mediated by the activation of GPR41/GPR43 receptors. Other SCFA effects, especially of propionate and butyrate, are mediated through their HDAC inhibitory activity (108, 116).

Because of the similarity of SCFAs with the ketone bodies aceto-acetate and β-hydroxybutyrate (BHB), studies have been conducted to elucidate their role during fasting. Accordingly, fasting has been shown to sharply influence the gene regulation and protein expression of several MCTs, which alters the uptake of SCFAs in the gut and their transport to the brain (130). The regulation of the transporter is likely related to the direction of energy supplies to tissues during fasting. Moreover, Miletta and colleagues found that butyrate enhances growth hormone (GH) secretion in pituitary cells via GPR41/43 activation and intracellular accumulation of Ca^{2+} (131). This leads to the hypothesis that butyrate acts as a secondary mediator of metabolic adaptations of GH during fasting, which mainly include increased lipolysis and protein retention.

In summary, SCFAs might directly influence the brain by reinforcing BBB integrity, modulating neurotransmission, influencing levels of neurotrophic factors and promoting memory consolidation. However, further studies are needed to understand the precise mechanisms involved in these neuroactive effects.

SCFAS AND BRAIN DISORDERS

The synthesis of new proteins is necessary for long-term changes in synaptic plasticity and learning (132–134). In this context, learning and long-term memory formation are improved by enhanced histone acetylation (135), which could be improved by HDAC inhibitors (HDACi). Given the HDAC inhibition property of SCFAs, several animal studies have focused mainly on the use of butyrate to elevate histone acetylation in the brain during a critical phase of memory formation. These studies have reported an enhancement of long-term potentiation (LTP) and contextual fear memory induced by HDAC inhibition (124, 127, 136, 137), pointing out enteric SCFAs as a promising learning and memory modulators. Therefore, the discovery that the microbiota can influence brain physiology has led to a plethora of experiments involving neurological disorders. The central hypothesis is supported by experimental and clinical evidence that the microbiota is altered in such diseases, which aggravates the condition, and/or its modulation might prevent or improve the development and progression of CNS pathologies (17, 19, 29, 33–37). Interestingly, several studies have found that the gut microbiome composition and, consequently, metabolome are altered in many brain disorders (138–142). Despite the knowledge that microbiota-gut-brain communication can theoretically occur through multiple systems (including the autonomic nervous system, enteric nervous system, neuroendocrine system, and immune system), increased evidence supports a potential key role of SCFAs in gut-brain axis signaling, and alterations in this signaling might underpin CNS disturbances ranging from neurodevelopmental disorders to neurodegenerative diseases.

SCFAs and Autism Spectrum Disorder

Characterized by behavioral symptoms including communication deficits, repetitive behaviors, and sensitivity to environmental changes, ASD comprises an array of neurodevelopmental disorders (143). Imbalances in the microbial composition of the gut are present in ASD. Support for this notion originates from animal studies and clinical evidence. However, the role of SCFAs in ASD is still controversial. Recently, Sharon and collaborators showed that microbiota transplantation from human ASD donors into mice could transfer ASD-relevant behavioral deficits (27). Although Sharon and coworkers did not evaluate the alteration in SCFAs, children with ASD have been previously reported to have both lower (144) and higher (33) fecal SCFA levels than controls. Interestingly, Wang and coworkers found similar proportions of specific SCFA and protein fermentation metabolites when comparing children with ASD with controls, even though the groups were controlled for gastrointestinal abnormalities, macronutrients intake and usage of probiotics, prebiotics, and antibiotics (33). However, neither of the previous studies performed a comprehensive evaluation of microbiota ecology.

In line with these findings, the microbiota has been suggested to affect the occurrence and severity of the disease through an increase in propionate-producing bacteria and a decrease in butyrate-producing bacteria (145, 146). The study conducted by Finegold and coworkers also found several pathobionts increased in the stool of ASD affected children such as *Proteobacteria* and hydrogen sulfide producing *Desulfovibrio*, raising a question for the causality of microbial metabolites unbalance (145, 146). Further, propionate-induced autism has become a validated animal model to study the disease. Administering high amounts of propionate through subcutaneous, intragastric, intraperitoneal, or intracerebroventricular routes to rodents has been suggested to induce high levels of microglia activation, neurotoxic cytokine production, genetic expression alterations, abnormal hippocampal histology, and abnormal neurobehaviors, such as repetitive actions and impaired social interaction (147). On the other hand, butyrate appears to have a beneficial effect on social and repetitive behavior in the BTBR mouse model, a strain-based ASD-like model (148). Epigenetic changes led to enhanced transcription of inhibitory neurotransmitter pathways in the frontal cortex, especially through HDAC inhibition (148). As described above, improvement of BBB impermeability by butyrate may be another mechanism through which butyrate

can revert abnormalities in propionic acid-induced autism-like disorder (143). This evidence points to the importance of balance of a microbiota but also highlights the difficulty in drawing conclusions on the role of SCFAs in ASD and the need for more research in patients with ASD.

SCFAs and Mood Disorders

Despite the complex pathophysiology of mood disorders, several studies have indicated the participation of the gut microbiota in the severity of these diseases. Major depression is one of the most common mood disorders, seriously impairing the quality of life of patients and is one of the leading causes of social disability. Untreated depression is associated with an increased risk of morbidity and mortality, including suicide. Monoamine deficiency (149) and neurogenesis disruption (150) are two predominant theories underpinning depression. Furthermore, it has been shown that inflammation biomarkers are increased among patients with depression, and pro-inflammatory cytokines play an important role in the physiopathology of the disease (150). The importance of the microbiota in depression is supported by findings that the levels of SCFAs are decreased in a naturally occurring non-human primate model of depression (26). In line with these findings, clinical evidence has shown that fecal SCFA concentrations are lower in patients with depression than in controls (35, 151). Moreover, current knowledge shows that butyrate possesses an antidepressant-like effect that reverses behavioral alterations in mouse models, such as low energy (126, 152), anhedonia (153), and cognitive and sociability impairments (154). Therefore, taking into account the anti-inflammatory property of SCFAs, dysbiosis followed by decreased levels of these metabolites could play a role in the inflammation process related to the development of depression.

Studies on chronic psychosocial stress have also shown a possible application for prebiotics (154) and SCFAs (8) in reverting sociability impairment while also reducing stress-induced corticosterone release. Sodium butyrate has been shown to be capable of reversing behavioral hyperactivity (155) and depressive-like and manic-like behaviors in rats (156). There is also evidence for butyrate's antimanic effect on a rat model of bipolar disorder induced by intracerebroventricular administration of ouabain (157). Contrarily, a microbiome study in schizophrenic patients at risk of developing psychosis reported enriched *Clostridiales*, *Prevotella,* and *Lactobacillus ruminis* and predicted increased SCFA production (141). However, the study did not perform direct measurement of the metabolites and further research to confirm whether it is a case of SCFA overproduction or a specific metabolite unbalance is needed.

SCFAs and Alzheimer's Disease

Accumulating evidence has demonstrated that key neuropathological processes underlying AD might also be modulated by SCFAs (25, 34, 158, 159). Characterized by progressive cognitive impairment, AD is the most common form of dementia (160). Given that AD has a complex pathology and that therapies that effectively halt the disease progression are still lacking, recent studies have focused on environmental components and diet-based possible prevention strategies by using transgenic animal models (161, 162). In this context, several studies have established the benefits of a healthy microbiome on slowing AD and the correlation of dysbiosis with disease progression (7, 138, 163). Consistent with this notion, a study by Zhang and coworkers showed that the microbiota composition and diversity were perturbed and the level of SCFAs was reduced in AD mice, predicting alterations in more than 30 metabolic pathways, which may be associated with amyloid deposition and ultrastructural abnormalities in the APP/PS1 mouse model (25).

It is worth noting that SCFAs interfere with protein-protein interactions between amyloid-β peptides (Aβ), thereby disrupting their assembly into neurotoxic oligomers (34), the main toxins responsible for synapse dysfunction and cognitive deficits in AD (164). Given the close relation between gut dysbiosis and brain dysfunction, fecal microbiota transplantation (FMT) has been considered a promising therapeutic approach for the reestablishment of a healthy gut microbial community and has been shown to have beneficial effects on a plethora of diseases, including AD. Supporting this hypothesis, APP/PS1 mice exhibited significantly relieved cognitive deficits, Aβ accumulation, synaptic dysfunction, and neuroinflammation, mainly by the microglia, after FMT from healthy wild-type mice (165). These protective effects may be related to reversal of changes in the gut microbiota and SCFAs.

Oral bacteriotherapy through probiotic administration has become a potential treatment option for neurodegenerative diseases such as AD. Accordingly, the 3xTg mouse model of AD treated with probiotics in the early stage showed a promising reduction of inflammatory cytokines and decreased cognitive decline associated with reduced brain damage and Aβ aggregate accumulation (166). Moreover, other studies have shown beneficial effects of butyrate and probiotic treatment on cognition and memory in a D-galactose model of aging, a condition known to correlate with AD occurrence and progression (137, 167). The model consists of a long term administration of D-galactose, which can readily be metabolized but eventually leads to an overproduction of reactive oxygen species, thus causing genetic and cell damage impairing cognition (137, 168). Finally, through HDAC inhibition, butyrate administration recovered memory function and increased expression of genes implicated in associative learning in the APP/PS1 mouse model of AD (158).

SCFAs and Parkinson's Disease

SCFAs play a controversial role in Parkinson's disease (PD), a synucleinopathy and a multifactorial disorder with strong environmental influence characterized by tremors, muscle rigidity, bradykinesia, and impaired gait (169). Aggregation of the protein α-synuclein (αSyn) is thought to be the main pathogenic event in PD, which primarily affects dopaminergic neurons (169). Most PD patients also present gastrointestinal manifestations due to disturbances of the enteric nervous system. Hence, there has been great interest in the relationship between the gut microbiota and the development of the disease. Accordingly, sequencing of the microbiota of fecal samples from PD patients revealed reduced populations of *Bacteroidetes*

and *Prevotellaceae* in contrast to increased *Enterobacteriaceae* and reduced production of SCFAs when compared to matched controls (139). However, the presence of gut microbes is necessary to elicit pathophysiological alterations in a mouse model of αSyn overexpression, because elimination of the gut microbiota with antibiotics ameliorated the condition (169). In contrast, FMT from PD patient donors worsens disease progression suggesting the presence of specific disease-promoting microbes (169). Accordingly, Li and colleagues confirmed that PD patients suffer alterations in the microbiota that correlate with disease progression, as there is a continuous decrease in fiber-degrading bacterial strains and an increase in pathobionts (170). This conversion probably leads to a decrease in SCFA production and an increase in endotoxin and neurotoxin production (170). Supporting this hypothesis, growing evidence has shown that FMT from healthy donors (171) as well as butyrate administration in animal models of PD improves motor impairment and dopamine deficiency (172–175).

SCFAs and Sclerosis

Multiple sclerosis (MS) is a neurodegenerative T-cell-mediated autoimmune disease of the CNS that mainly affects the myelin sheath around motor neurons. Among its etiological factors, the imbalance between pro and anti-inflammatory cells in the immune system seems to play an important role, which is highly affected by the gut microbiota composition and can be aggravated by dysbiosis (104, 176, 177). Given that SCFAs, mainly butyrate, are capable of inducing Treg polarization, modulation of the gut microbiota toward increased production of these metabolites could be an interesting therapeutic approach to MS. In fact, it is noteworthy that oral administration of SCFAs ameliorated the disease severity of experimental autoimmune encephalomyelitis (EAE), an animal model of MS (87, 178). Specifically, acetate supplementation is able to induce increased acetyl-CoA metabolism, which increases histone acetylation, resulting in preserved spinal cord lipid content and essentially preventing the onset of clinical symptoms of EAE (179). Furthermore, treatment with butyrate suppresses demyelination and enhances remyelination through oligodendrocyte maturation and differentiation (180).

Efforts to modify the course of amyotrophic lateral sclerosis (ALS) a disease that affects motor neurons but also involves a stronger genetic basis that leads to the premature death of those cells, has focused on the gut microbiota composition and its circulating metabolites (181). A comparative study conducted in human patients showed an elevated relative abundance of pathobionts compared to bacterial strains related to beneficial metabolism function (142). Another study found that transgenic ALS model mice had worse disease progression when raised under antibiotic treatment or GF conditions and identified several bacterial strains correlated with ameliorated or aggravated disease progression. A small assessment of the human microbiome/metabolite configuration was also conducted for comparison (181).

SCFAs and Metabolic Disorders

Much speculation currently surrounds the possible involvement of the gut microbiota in metabolic disorders such as type 2 diabetes and obesity. Compelling evidence have shown that the composition of the gut microbiota is altered in animal models of obesity and subjects with prediabetes or type 2 diabetes compared with controls (182–186). Despite differences in the identification of specific microbiome features responsible for these effects, a shift in the microbiome composition away from species able to produce butyrate was one consistent finding in type 2 diabetes subjects (187). Further, epidemiological and experimental studies have demonstrated that increased intake of dietary fiber reduces the risk for developing metabolic diseases (188–190), possibly by changing gut microbiome composition and diversity with increased production of SCFAs (187–189).

Animal studies suggest that SCFAs have an important role in the prevention and treatment of obesity-associated insulin resistance (89, 114, 191, 192). Mechanisms involved in the effects of SCFAs, mainly propionate and butyrate, in the brain responsible for controlling metabolic disorders include the activation of FFAR2 and FFAR3 receptors (91). It was shown that activation of these receptors leads to suppression of the activity of orexigenic neurons that express neuropeptide Y in the hypothalamus (89), and the modulation of the signaling mediate by the ghrelin receptor (129), contributing to circadian rhythm and appetite control. Studies in rodents show that the administration of prebiotics that influences a shift in the gut microbiome toward increased production of butyrate has beneficial effects associated with higher levels of GLP-1 (193–195), as well as hypothalamic expression of pro-opiomelanocortin (196), thereby influencing the hunger-satiety cycle. Although limited, some of these results were confirmed in human *in vivo* studies, as showed that acute rectal infusions of sodium acetate and SCFA mixtures increased circulating concentrations of PYY in individuals who were overweight (197–199).

CONCLUDING REMARKS

The gut microbiota has attracted considerable attention in recent years, putting it in the spotlight of biomedical research. Recent studies have suggested that an intestinal bacteria imbalance plays a role in the development of several disorders. The bidirectional communication that occurs between the microbiota and its mammalian host can be mediated through a variety of mechanisms, and it is clear that the biochemical messengers produced by the microbiota are an important facet of this crosstalk. Convincing evidence exists that SCFAs produced by the intestinal microbiota are involved in gastrointestinal physiology, immune function, host metabolism, and even in development and homeostasis of the CNS.

Although our understanding of microbiota-host interactions has considerably increased over recent years, there is still an unmet requirement for a deeper understanding of the complex microbiota-gut-brain communication. Furthermore, since most studies have been conducted in rodents, one must be cautious when translating the effects of SCFAs on humans. Given that SCFAs can regulate CNS processes through direct and indirect means and ultimately shape behavior and cognitive function, a thorough comprehension of how these

metabolites participate in these complex gut-brain interactions may aid in developing novel therapeutic targets for treating CNS disorders. Further, through their effects on the development and maintenance of healthy brain function, these metabolites hold the potential for use as dietary interventions with a range of psychological functions.

AUTHOR CONTRIBUTIONS

YS, AB, and RF planned, researched, and wrote the manuscript.

FUNDING

Work in the authors' laboratories has been supported by grants from Brazilian National Council for Development of Science and Technology (CNPq/Brazil), State of Rio de Janeiro Foundation for Funding Research (FAPERJ-JCNE-E-26/203.195/2016), Inova Fiocruz Program (Inova Fiocruz/VPPCB), National Institute of Science and Technology on Neuroimmunomodulation (INCT-NIM), and the Mercosur Program for Structural Convergence (FOCEM).

REFERENCES

1. Hooper LV, Littman DR, Macpherson AJ. Interactions between the microbiota and the immune system. *Science.* (2012) 336:1268–73. doi: 10.1126/science.1223490
2. Erny D, Hrabe de Angelis AL, Prinz M. Communicating systems in the body: how microbiota and microglia cooperate. *Immunology.* (2017) 150:7–15. doi: 10.1111/imm.12645
3. Lynch SV, Pedersen O. The human intestinal microbiome in health and disease. *N Engl J Med.* (2016) 375:2369–79. doi: 10.1056/NEJMra1600266
4. Cho I, Blaser MJ. The human microbiome: at the interface of health and disease. *Nat Rev Genet.* (2012) 13:260–70. doi: 10.1038/nrg3182
5. Palm NW, Zoete MR De, Flavell RA, Haven N. Immune-microbiota interactions in health and disease. *Clin Immunol.* (2016) 159:122–7. doi: 10.1016/j.clim.2015.05.014
6. Erny D, De Angelis ALH, Jaitin D, Wieghofer P, Staszewski O, David E, et al. Host microbiota constantly control maturation and function of microglia in the CNS. *Nat Neurosci.* (2015) 18:965–77. doi: 10.1038/nn.4030
7. Cryan JF, Dinan TG. Mind-altering microorganisms: the impact of the gut microbiota on brain and behaviour. *Nat Rev Neurosci.* (2012) 13:701–12. doi: 10.1038/nrn3346
8. van de Wouw M, Boehme M, Lyte JM, Wiley N, Strain C, O'Sullivan O, et al. Short-chain fatty acids: microbial metabolites that alleviate stress-induced brain–gut axis alterations. *J Physiol.* (2018) 596:4923–44. doi: 10.1113/JP276431
9. Borre YE, O'Keeffe GW, Clarke G, Stanton C, Dinan TG, Cryan JF. Microbiota and neurodevelopmental windows: implications for brain disorders. *Trends Mol Med.* (2014) 20:509–18. doi: 10.1016/j.molmed.2014.05.002
10. Szentirmai É, Millican NS, Massie AR, Kapás L. Butyrate, a metabolite of intestinal bacteria, enhances sleep. *Sci Rep.* (2019) 9:7035. doi: 10.1038/s41598-019-43502-1
11. Wang X, Sun G, Feng T, Zhang J, Huang X, Wang T, et al. Sodium oligomannate therapeutically remodels gut microbiota and suppresses gut bacterial amino acids-shaped neuroinflammation to inhibit Alzheimer's disease progression. *Cell Res.* (2019) 29:787–803. doi: 10.1038/s41422-019-0216-x
12. Forsythe P, Bienenstock J, Kunze WA. Vagal pathways for microbiome-brain-gut axis communication. *Adv Exp Med Biol.* (2014) 817:115–33. doi: 10.1007/978-1-4939-0897-4_5
13. Sudo N, Chida Y, Aiba Y, Sonoda J, Oyama N, Yu XN, et al. Postnatal microbial colonization programs the hypothalamic-pituitary-adrenal system for stress response in mice. *J Physiol.* (2004) 558:263–75. doi: 10.1113/jphysiol.2004.063388
14. Mudd AT, Berding K, Wang M, Donovan SM, Dilger RN. Serum cortisol mediates the relationship between fecal Ruminococcus and brain N-acetylaspartate in the young pig. *Gut Microbes.* (2017) 8:589–600. doi: 10.1080/19490976.2017.1353849
15. O'Mahony SM, Clarke G, Borre YE, Dinan TG, Cryan JF. Serotonin, tryptophan metabolism and the brain-gut-microbiome axis. *Behav Brain Res.* (2015) 277:32–48. doi: 10.1016/j.bbr.2014.07.027
16. Sherwin E, Dinan TG, Cryan JF. Recent developments in understanding the role of the gut microbiota in brain health and disease. *Ann NY Acad Sci.* (2018) 1420:5–25. doi: 10.1111/nyas.13416
17. Fung TC, Olson CA, Hsiao EY. Interactions between the microbiota, immune and nervous systems in health and disease. *Nat Neurosci.* (2017) 20:145–55. doi: 10.1038/nn.4476
18. Calvani R, Picca A, Lo Monaco MR, Landi F, Bernabei R, Marzetti E. Of microbes and minds: a narrative review on the second brain aging. *Front Med.* (2018) 5:53. doi: 10.3389/fmed.2018.00053
19. Tan J, McKenzie C, Potamitis M, Thorburn AN, Mackay CR, Macia L. The role of short-chain fatty acids in health and disease. In: *Advances in Immunology.* Alt FW, editor. Cambridge, MA: Academic Press Inc. (2014). p. 91–119.
20. Stilling RM, van de Wouw M, Clarke G, Stanton C, Dinan TG, Cryan JF. The neuropharmacology of butyrate: the bread and butter of the microbiota-gut-brain axis? *Neurochem Int.* (2016) 99:110–32. doi: 10.1016/j.neuint.2016.06.011
21. Dalile B, Van Oudenhove L, Vervliet B, Verbeke K. The role of short-chain fatty acids in microbiota–gut–brain communication. *Nat Rev Gastroenterol Hepatol.* (2019) 16:461–78. doi: 10.1038/s41575-019-0157-3
22. Pascale A, Marchesi N, Marelli C, Coppola A, Luzi L, Govoni S, et al. Microbiota and metabolic diseases. *Endocrine.* (2018) 61:357–71. doi: 10.1007/s12020-018-1605-5
23. Arpaia N, Campbell C, Fan X, Dikiy S, Van Der Veeken J, Deroos P, et al. Metabolites produced by commensal bacteria promote peripheral regulatory T-cell generation. *Nature.* (2013) 504:451–5. doi: 10.1038/nature12726
24. Smith PM, Howitt MR, Panikov N, Michaud M, Gallini CA, Bohlooly-y M, et al. The microbial metabolites, short-chain fatty acids, regulate colonic treg cell homeostasis. *Science.* (2013) 341:569–74. doi: 10.1126/science.1241165
25. Zhang L, Wang Y, Xiayu X, Shi C, Chen W, Song N, et al. Altered gut microbiota in a mouse model of Alzheimer's disease. *J Alzheimer's Dis.* (2017) 60:1241–57. doi: 10.3233/JAD-170020
26. Deng FL, Pan JX, Zheng P, Xia JJ, Yin BM, Liang WW, et al. Metabonomics reveals peripheral and central shortchain fatty acid and amino acid dysfunction in a naturally occurring depressive model of macaques. *Neuropsychiatr Dis Treat.* (2019) 15:1077–88. doi: 10.2147/NDT.S186071
27. Sharon G, Cruz NJ, Kang DW, Gandal MJ, Wang B, Kim YM, et al. Human gut microbiota from autism spectrum disorder promote behavioral symptoms in mice. *Cell.* (2019) 177:1600–18.e17. doi: 10.1016/j.cell.2019.05.004
28. Dinan TG, Cryan JF. Microbes, immunity, and behavior: psychoneuroimmunology meets the microbiome. *Neuropsychopharmacology.* (2017) 42:178–92. doi: 10.1038/npp.2016.103
29. Sharon G, Sampson TR, Geschwind DH, Mazmanian SK. The central nervous system and the gut microbiome. *Cell.* (2016) 167:915–32. doi: 10.1016/j.cell.2016.10.027
30. Kim HL, Chang BJ, Nam SM, Nahm SS, Lee JH. Increased osteopontin expression and mitochondrial swelling in 3-nitropropionic acid-injured rat brains. *Rom J Morphol Embryol.* (2017) 58:1249–56.
31. Andersson U, Tracey KJ. Reflex principles of immunological homeostasis. *Annu Rev Immunol.* (2012) 30:313–35. doi: 10.1146/annurev-immunol-020711-075015

32. Wang X, Wang BR, Zhang XJ, Xu Z, Ding YQ, Ju G. Evidences for vagus nerve in maintenance of immune balance and transmission of immune information from gut to brain in STM-infected rats. *World J Gastroenterol.* (2002) 8:540–5. doi: 10.3748/wjg.v8.i3.540
33. Wang L, Christophersen CT, Sorich MJ, Gerber JP, Angley MT, Conlon MA. Elevated fecal short chain fatty acid and ammonia concentrations in children with autism spectrum disorder. *Dig Dis Sci.* (2012) 57:2096–102. doi: 10.1007/s10620-012-2167-7
34. Ho L, Ono K, Tsuji M, Mazzola P, Singh R, Pasinetti GM. Protective roles of intestinal microbiota derived short chain fatty acids in Alzheimer's disease-type beta-amyloid neuropathological mechanisms. *Expert Rev Neurother.* (2018) 18:83–90. doi: 10.1080/14737175.2018.1400909
35. Skonieczna-zydecka K, Grochans E, Maciejewska D, Szkup M, Schneider-Matyka D, Jurczak A, et al. Faecal short chain fatty acids profile is changed in Polish depressive women. *Nutrients.* (2018) 10:E1939. doi: 10.3390/nu10121939
36. Kelly JR, Minuto C, Cryan JF, Clarke G, Dinan TG. Cross talk: the microbiota and neurodevelopmental disorders. *Front Neurosci.* (2017) 11:490. doi: 10.3389/fnins.2017.00490
37. Dinan TG, Cryan JF. The microbiome-gut-brain axis in health and disease. *Gastroenterol Clin North Am.* (2017) 46:77–89. doi: 10.1016/j.gtc.2016.09.007
38. Ben-Ari Y. Neuropaediatric and neuroarchaeology: understanding development to correct brain disorders. *Acta Paediatr Int J Paediatr.* (2013) 102:331–4. doi: 10.1111/apa.12161
39. Rapoport JL, Giedd JN, Gogtay N. Neurodevelopmental model of schizophrenia: update 2012. *Mol Psychiatry.* (2012) 17:1228–38. doi: 10.1038/mp.2012.23
40. Clarke G, Grenham S, Scully P, Fitzgerald P, Moloney RD, Shanahan F, et al. The microbiome-gut-brain axis during early life regulates the hippocampal serotonergic system in a sex-dependent manner. *Mol Psychiatry.* (2013) 18:666–73. doi: 10.1038/mp.2012.77
41. Russell SL, Gold MJ, Willing BP, Thorson L, McNagny KM, Finlay BB. Perinatal antibiotic treatment affects murine microbiota, immune responses and allergic asthma. *Gut Microbes.* (2013) 4:158–64. doi: 10.4161/gmic.23567
42. Tochitani S, Ikeno T, Ito T, Sakurai A, Yamauchi T, Matsuzaki H. Administration of non-absorbable antibiotics to pregnant mice to perturb the maternal gut microbiota is associated with alterations in offspring behavior. *PLoS ONE.* (2016) 11:e0138293. doi: 10.1371/journal.pone.0138293
43. Buffington SA, Di Prisco GV, Auchtung TA, Ajami NJ, Petrosino JF, Costa-Mattioli M. Microbial reconstitution reverses maternal diet-induced social and synaptic deficits in offspring. *Cell.* (2016) 165:1762–75. doi: 10.1016/j.cell.2016.06.001
44. Foley KA, Ossenkopp K-P, Kavaliers M, MacFabe DF. Pre- and neonatal exposure to lipopolysaccharide or the enteric metabolite, propionic acid, alters development and behavior in adolescent rats in a sexually dimorphic manner. *PLoS ONE.* (2014) 9:e87072. doi: 10.1371/journal.pone.0087072
45. Estes ML, McAllister AK. Maternal immune activation: implications for neuropsychiatric disorders. *Science.* (2016) 353:772–7. doi: 10.1126/science.aag3194
46. Jašarević E, Rodgers AB, Bale TL. A novel role for maternal stress and microbial transmission in early life programming and neurodevelopment. *Neurobiol Stress.* (2015) 1:81–8. doi: 10.1016/j.ynstr.2014.10.005
47. Dominguez-Bello MG, Costello EK, Contreras M, Magris M, Hidalgo G, Fierer N, et al. Delivery mode shapes the acquisition and structure of the initial microbiota across multiple body habitats in newborns. *Proc Natl Acad Sci USA.* (2010) 107:11971–5. doi: 10.1073/pnas.1002601107
48. Bäckhed F, Roswall J, Peng Y, Feng Q, Jia H, Kovatcheva-Datchary P, et al. Dynamics and stabilization of the human gut microbiome during the first year of life. *Cell Host Microbe.* (2015) 17:690–703. doi: 10.1016/j.chom.2015.04.004
49. Koenig JE, Spor A, Scalfone N, Fricker AD, Stombaugh J, Knight R, et al. Succession of microbial consortia in the developing infant gut microbiome. *Proc Natl Acad Sci USA.* (2011) 108:4578–85. doi: 10.1073/pnas.1000081107
50. Perry VH, Newman TA, Cunningham C. The impact of systemic infection on the progression of neurodegenerative disease. *Nat Rev Neurosci.* (2003) 4:103–12. doi: 10.1038/nrn1032
51. Perry VH, Cunningham C, Holmes C. Systemic infections and inflammation affect chronic neurodegeneration. *Nat Rev Immunol.* (2007) 7:161–7. doi: 10.1038/nri2015
52. Amor S, Peferoen LAN, Vogel DYS, Breur M, van der Valk P, Baker D, et al. Inflammation in neurodegenerative diseases - an update. *Immunology.* (2014) 142:151–66. doi: 10.1111/imm.12233
53. Wendeln AC, Degenhardt K, Kaurani L, Gertig M, Ulas T, Jain G, et al. Innate immune memory in the brain shapes neurological disease hallmarks. *Nature.* (2018) 556:332–8. doi: 10.1038/s41586-018-0023-4
54. Abdel-Haq R, Schlachetzki JCM, Glass CK, Mazmanian SK. Microbiome–microglia connections via the gut–brain axis. *J Exp Med.* (2019) 216:41–59. doi: 10.1084/jem.20180794
55. Reigstad CS, Salmonson CE, Rainey JF, Szurszewski JH, Linden DR, Sonnenburg JL, et al. Gut microbes promote colonic serotonin production through an effect of short-chain fatty acids on enterochromaffin cells. *FASEB J.* (2015) 29:1395–403. doi: 10.1096/fj.14-259598
56. Yano JM, Yu K, Donaldson GP, Shastri GG, Ann P, Ma L, et al. Indigenous bacteria from the gut microbiota regulate host serotonin biosynthesis. *Cell.* (2015) 161:264–76. doi: 10.1016/j.cell.2015.02.047
57. Rhee SH, Pothoulakis C, Mayer EA. Principles and clinical implications of the brain-gut-enteric microbiota axis. *Nat Rev Gastroenterol Hepatol.* (2009) 6:306–14. doi: 10.1038/nrgastro.2009.35
58. Goehler LE, Gaykema RPA, Opitz N, Reddaway R, Badr N, Lyte M. Activation in vagal afferents and central autonomic pathways: early responses to intestinal infection with *Campylobacter jejuni*. *Brain Behav Immun.* (2005) 19:334–44. doi: 10.1016/j.bbi.2004.09.002
59. Browning KN, Verheijden S, Boeckxstaens GE. The vagus nerve in appetite regulation, mood, and intestinal inflammation. *Gastroenterology.* (2017) 152:730–44. doi: 10.1053/j.gastro.2016.10.046
60. Bercik P, Park AJ, Sinclair D, Khoshdel A, Lu J, Huang X, et al. The anxiolytic effect of Bifidobacterium longum NCC3001 involves vagal pathways for gut-brain communication. *Neurogastroenterol Motil.* (2011) 23:1132–9. doi: 10.1111/j.1365-2982.2011.01796.x
61. Miller TL, Wolin MJ. Pathways of acetate, propionate, and butyrate formation by the human fecal microbial flora. *Appl Environ Microbiol.* (1996) 62:1589–92. doi: 10.1128/AEM.62.5.1589-1592.1996
62. Louis P, Flint HJ. Diversity, metabolism and microbial ecology of butyrate-producing bacteria from the human large intestine. *FEMS Microbiol Lett.* (2009) 294:1–8. doi: 10.1111/j.1574-6968.2009.01514.x
63. Fernandes J, Su W, Rahat-Rozenbloom S, Wolever TMS, Comelli EM. Adiposity, gut microbiota and faecal short chain fatty acids are linked in adult humans. *Nutr Diabetes.* (2014) 4:e121. doi: 10.1038/nutd.2014.23
64. Luu M, Pautz S, Kohl V, Singh R, Romero R, Lucas S, et al. The short-chain fatty acid pentanoate suppresses autoimmunity by modulating the metabolic-epigenetic crosstalk in lymphocytes. *Nat Commun.* (2019) 10:760. doi: 10.1038/s41467-019-08711-2
65. Cummings JH, Pomare EW, Branch HWJ, Naylor CPE, MacFarlane GT. Short chain fatty acids in human large intestine, portal, hepatic and venous blood. *Gut.* (1987) 28:1221–7. doi: 10.1136/gut.28.10.1221
66. Bergman EN. Energy contributions of volatile fatty acids from the gastrointestinal tract in various species. *Physiol Rev.* (1990) 70:567–90. doi: 10.1152/physrev.1990.70.2.567
67. Macfarlane S, Macfarlane GT. Regulation of short-chain fatty acid production. *Proc Nutr Soc.* (2003) 62:67–72. doi: 10.1079/PNS2002207
68. Louis P, Flint HJ. Formation of propionate and butyrate by the human colonic microbiota. *Environ Microbiol.* (2017) 19:29–41. doi: 10.1111/1462-2920.13589
69. Smith EA, Macfarlane GT. Dissimilatory amino acid metabolism in human colonic bacteria. *Anaerobe.* (1997) 3:327–37. doi: 10.1006/anae.1997.0121
70. Smith E, Macfarlane G. Enumeration of amino acid fermenting bacteria in the human large intestine: effects of pH and starch on peptide metabolism and dissimilation of amino acids. *FEMS Microbiol Ecol.* (1998) 25:355–68. doi: 10.1111/j.1574-6941.1998.tb00487.x
71. Windey K, de Preter V, Verbeke K. Relevance of protein fermentation to gut health. *Mol Nutr Food Res.* (2012) 56:184–96. doi: 10.1002/mnfr.201100542

72. Duncan SH, Barcenilla A, Stewart CS, Pryde SE, Flint HJ. Acetate utilization and butyryl coenzyme A (CoA): Acetate-CoA transferase in butyrate-producing bacteria from the human large intestine. *Appl Environ Microbiol.* (2002) 68:5186–90. doi: 10.1128/AEM.68.10.5186-5190.2002
73. Duncan SH, Holtrop G, Lobley GE, Calder AG, Stewart CS, Flint HJ. Contribution of acetate to butyrate formation by human faecal bacteria. *Br J Nutr.* (2004) 91:915–23. doi: 10.1079/BJN20041150
74. Bugaut M. Occurrence, absorption and metabolism of short chain fatty acids in the digestive tract of mammals. *Comp Biochem Physiol B.* (1987) 86:439–72. doi: 10.1016/0305-0491(87)90433-0
75. Vijay N, Morris ME. Role of monocarboxylate transporters in drug delivery to the brain. *Curr Pharm Des.* (2014) 20:1487–98. doi: 10.2174/13816128113199990462
76. Schönfeld P, Wojtczak L. Short- and medium-chain fatty acids in energy metabolism: the cellular perspective. *J Lipid Res.* (2016) 57:943–54. doi: 10.1194/jlr.R067629
77. Primec M, Mičetić-Turk D, Langerholc T. Analysis of short-chain fatty acids in human feces: a scoping review. *Anal Biochem.* (2017) 526:9–21. doi: 10.1016/j.ab.2017.03.007
78. Lewis K, Lutgendorff F, Phan V, Söderholm JD, Sherman PM, McKay DM. Enhanced translocation of bacteria across metabolically stressed epithelia is reduced by butyrate. *Inflamm Bowel Dis.* (2010) 16:1138–48. doi: 10.1002/ibd.21177
79. Peng L, Li Z-R, Green RS, Holzman IR, Lin J. Butyrate enhances the intestinal barrier by facilitating tight junction assembly via activation of AMP-activated protein kinase in Caco-2 cell monolayers. *J Nutr.* (2009) 139:1619–25. doi: 10.3945/jn.109.104638
80. Gaudier E, Rival M, Buisine M-P, Robineau I, Hoebler C, Hoebler C. Butyrate enemas upregulate muc genes expression but decrease adherent mucus thickness in mice colon. *Physiol Res.* (2009) 58:111–9.
81. O'Keefe SJD. Diet, microorganisms and their metabolites, and colon cancer. *Nat Rev Gastroenterol Hepatol.* (2016) 13:691–706. doi: 10.1038/nrgastro.2016.165
82. Mohajeri MH, Brummer RJM, Rastall RA, Weersma RK, Harmsen HJM, Faas M, et al. The role of the microbiome for human health: from basic science to clinical applications. *Eur J Nutr.* (2018) 57:1–14. doi: 10.1007/s00394-018-1703-4
83. Bolognini D, Tobin AB, Milligan G, Moss CE. The pharmacology and function of receptors for short-chain fatty acids. *Mol Pharmacol.* (2016) 89:388–98. doi: 10.1124/mol.115.102301
84. Cherbut C, Ferrier L, Rozé C, Anini Y, Blottière H, Lecannu G, et al. Short-chain fatty acids modify colonic motility through nerves and polypeptide YY release in the rat. *Am J Physiol.* (1998) 275:G1415–22. doi: 10.1152/ajpgi.1998.275.6.G1415
85. Puddu A, Sanguineti R, Montecucco F, Viviani GL. Evidence for the gut microbiota short-chain fatty acids as key pathophysiological molecules improving diabetes. *Mediators Inflamm.* (2014) 2014:162021. doi: 10.1155/2014/162021
86. Kien CL, Peltier CP, Mandal S, Davie JR, Blauwiekel R. Effects of the *in vivo* supply of butyrate on histone acetylation of cecum in piglets. *J Parenter Enter Nutr.* (2008) 32:51–6. doi: 10.1177/014860710803200151
87. Haghikia A, Jorg S, Duscha A, Berg J, Manzel A, Waschbisch A, et al. Dietary fatty acids directly impact central nervous system autoimmunity via the small intestine. *Immunity.* (2015) 43:817–29. doi: 10.1016/j.immuni.2015.09.007
88. Brown EM, Sadarangani M, Finlay BB. The role of the immune system in governing host-microbe interactions in the intestine. *Nat Immunol.* (2013) 14:660–7. doi: 10.1038/ni.2611
89. Li Z, Yi CX, Katiraei S, Kooijman S, Zhou E, Chung CK, et al. Butyrate reduces appetite and activates brown adipose tissue via the gut-brain neural circuit. *Gut.* (2018) 67:1269–79. doi: 10.1136/gutjnl-2017-314050
90. Mollica MP, Raso GM, Cavaliere G, Trinchese G, De Filippo C, Aceto S, et al. Butyrate regulates liver mitochondrial function, efficiency, and dynamics in insulin-resistant obese mice. *Diabetes.* 66:1405–18. doi: 10.2337/db16-0924
91. De Vadder F, Kovatcheva-Datchary P, Goncalves D, Vinera J, Zitoun C, Duchampt A, et al. Microbiota-generated metabolites promote metabolic benefits via gut-brain neural circuits. *Cell.* (2014) 156:84–96. doi: 10.1016/j.cell.2013.12.016
92. Kekuda R, Manoharan P, Baseler W, Sundaram U. Monocarboxylate 4 mediated butyrate transport in a rat intestinal epithelial cell line. *Dig Dis Sci.* (2013) 58:660–7. doi: 10.1007/s10620-012-2407-x
93. Oldendorf WH. Carrier mediated blood brain barrier transport of short chain monocarboxylic organic acids. *Am J Physiol.* (1973) 224:1450–3. doi: 10.1152/ajplegacy.1973.224.6.1450
94. Human Metabolome Database. Available online at: http://www.hmdb.ca/ (accessed December 27, 2019).
95. Bachmann C, Colombo JP, Berüter J. Short chain fatty acids in plasma and brain: quantitative determination by gas chromatography. *Clin Chim Acta.* (1979) 92:153–9. doi: 10.1016/0009-8981(79)90109-8
96. Liu J, Sun J, Wang F, Yu X, Ling Z, Li H, et al. Neuroprotective effects of *Clostridium butyricum* against vascular dementia in mice via metabolic butyrate. *Biomed Res Int.* (2015) 2015:1–12. doi: 10.1155/2015/412946
97. Sun J, Ling Z, Wang F, Chen W, Li H, Jin J, et al. *Clostridium butyricum* pretreatment attenuates cerebral ischemia/reperfusion injury in mice via anti-oxidation and anti-apoptosis. *Neurosci Lett.* (2016) 613:30–5. doi: 10.1016/j.neulet.2015.12.047
98. Braniste V, Al-Asmakh M, Kowal C, Anuar F, Abbaspour A, Tóth M, et al. The gut microbiota influences blood-brain barrier permeability in mice. *Sci Transl Med.* (2015) 6:263ra158. doi: 10.1126/scitranslmed.3009759
99. Hoyles L, Snelling T, Umlai U-K, Nicholson JK, Carding SR, Glen RC, et al. Microbiome-host systems interactions: protective effects of propionate upon the blood-brain barrier. *Microbiome.* (2018) 6:55. doi: 10.1186/s40168-018-0439-y
100. Dinan TG, Cryan JF. Gut instincts: microbiota as a key regulator of brain development, ageing and neurodegeneration. *J Physiol.* (2017) 595:489–503. doi: 10.1113/JP273106
101. Hong S, Beja-Glasser VF, Nfonoyim BM, Frouin A, Li S, Ramakrishnan S, et al. Complement and microglia mediate early synapse loss in Alzheimer mouse models. *Science.* (2016) 352:712–6. doi: 10.1126/science.aad8373
102. Wilton DK, Dissing-Olesen L, Stevens B. Neuron-glia signaling in synapse elimination. *Annu Rev Neurosci.* (2019) 42:107–27. doi: 10.1146/annurev-neuro-070918-050306
103. Gautier EL, Shay T, Miller J, Greter M, Jakubzick C, Ivanov S, et al. Gene-expression profiles and transcriptional regulatory pathways that underlie the identity and diversity of mouse tissue macrophages. *Nat Immunol.* (2012) 13:1118–28. doi: 10.1038/ni.2419
104. Stanisavljević S, Cepić A, Bojić S, Veljović K, Mihajlović S, Đedović N, et al. Oral neonatal antibiotic treatment perturbs gut microbiota and aggravates central nervous system autoimmunity in Dark Agouti rats. *Sci Rep.* (2019) 9:1–13. doi: 10.1038/s41598-018-37505-7
105. Minter MR, Zhang C, Leone V, Ringus DL, Zhang X, Oyler-Castrillo P, et al. Antibiotic-induced perturbations in gut microbial diversity influences neuro-inflammation and amyloidosis in a murine model of Alzheimer's disease. *Sci Rep.* (2016) 6:30028. doi: 10.1038/srep30028
106. Minter MR, Hinterleitner R, Meisel M, Zhang C, Leone V, Zhang X, et al. Antibiotic-induced perturbations in microbial diversity during post-natal development alters amyloid pathology in an aged APP SWE /PS1 ΔE9 murine model of Alzheimer's disease. *Sci Rep.* (2017) 7:10411. doi: 10.1038/s41598-017-11047-w
107. Jang H-M, Lee H-J, Jang S-E, Han MJ, Kim D-H. Evidence for interplay among antibacterial-induced gut microbiota disturbance, neuro-inflammation, and anxiety in mice. *Mucosal Immunol.* (2018) 11:1386–97. doi: 10.1038/s41385-018-0042-3
108. Patnala R, Arumugam TV, Gupta N, Dheen ST. HDAC inhibitor sodium butyrate-mediated epigenetic regulation enhances neuroprotective function of microglia during ischemic stroke. *Mol Neurobiol.* (2017) 54:6391–411. doi: 10.1007/s12035-016-0149-z
109. Wang P, Zhang Y, Gong Y, Yang R, Chen Z, Hu W, et al. Sodium butyrate triggers a functional elongation of microglial process via Akt-small RhoGTPase activation and HDACs inhibition. *Neurobiol Dis.* (2018) 111:12–25. doi: 10.1016/j.nbd.2017.12.006
110. Yamawaki Y, Yoshioka N, Nozaki K, Ito H, Oda K, Harada K, et al. Sodium butyrate abolishes lipopolysaccharide-induced depression-like behaviors and hippocampal microglial activation in mice. *Brain Res.* (2018) 1680:13–38. doi: 10.1016/j.brainres.2017.12.004

111. Soliman ML, Puig KL, Combs CK, Rosenberger TA. Acetate reduces microglia inflammatory signaling *in vitro*. *J Neurochem.* (2012) 123:555–67. doi: 10.1111/j.1471-4159.2012.07955.x
112. Soliman ML, Combs CK, Rosenberger TA. Modulation of inflammatory cytokines and mitogen-activated protein kinases by acetate in primary astrocytes. *J Neuroimmune Pharmacol.* (2013) 8:287–300. doi: 10.1007/s11481-012-9426-4
113. Reddy DS, Wu X, Golub VM, Dashwood WM, Dashwood RH. Measuring histone deacetylase inhibition in the brain. *Curr Protoc Pharmacol.* (2018) 81:e41. doi: 10.1002/cpph.41
114. Frost G, Sleeth ML, Sahuri-Arisoylu M, Lizarbe B, Cerdan S, Brody L, et al. The short-chain fatty acid acetate reduces appetite via a central homeostatic mechanism. *Nat Commun.* (2014) 5:3611. doi: 10.1038/ncomms4611
115. Oleskin AV, Shenderov BA. Neuromodulatory effects and targets of the SCFAs and gasotransmitters produced by the human symbiotic microbiota. *Microb Ecol Heal Dis.* (2016) 27:30971. doi: 10.3402/mehd.v27.30971
116. Nankova BB, Agarwal R, MacFabe DF, La Gamma EF. Enteric bacterial metabolites propionic and butyric acid modulate gene expression, including CREB-dependent catecholaminergic neurotransmission, in PC12 cells - possible relevance to autism spectrum disorders. *PLoS ONE.* (2014) 9:e103740. doi: 10.1371/journal.pone.0103740
117. Clarke G, Stilling RM, Kennedy PJ, Stanton C, Cryan JF, Dinan TG. Minireview: gut microbiota: the neglected endocrine organ. *Mol Endocrinol.* (2014) 28:1221–38. doi: 10.1210/me.2014-1108
118. Möhle L, Mattei D, Heimesaat MM, Bereswill S, Fischer A, Alutis M, et al. Ly6Chi monocytes provide a link between antibiotic-induced changes in gut microbiota and adult hippocampal neurogenesis. *Cell Rep.* (2016) 15:1945–56. doi: 10.1016/j.celrep.2016.04.074
119. Fröhlich EE, Farzi A, Mayerhofer R, Reichmann F, Jačan A, Wagner B, et al. Cognitive impairment by antibiotic-induced gut dysbiosis: analysis of gut microbiota-brain communication. *Brain Behav Immun.* (2016) 56:140–55. doi: 10.1016/j.bbi.2016.02.020
120. Savignac HM, Corona G, Mills H, Chen L, Spencer JPE, Tzortzis G, et al. Prebiotic feeding elevates central brain derived neurotrophic factor, N-methyl-d-aspartate receptor subunits and d-serine. *Neurochem Int.* (2013) 63:756–64. doi: 10.1016/j.neuint.2013.10.006
121. Varela RB, Valvassori SS, Lopes-Borges J, Mariot E, Dal-Pont GC, Amboni RT, et al. Sodium butyrate and mood stabilizers block ouabain-induced hyperlocomotion and increase BDNF, NGF and GDNF levels in brain of Wistar rats. *J Psychiatr Res.* (2015) 61:114–21. doi: 10.1016/j.jpsychires.2014.11.003
122. Intlekofer KA, Berchtold NC, Malvaez M, Carlos AJ, McQuown SC, Cunningham MJ, et al. Exercise and sodium butyrate transform a subthreshold learning event into long-term memory via a brain-derived neurotrophic factor-dependent mechanism. *Neuropsychopharmacology.* (2013) 38:2027–34. doi: 10.1038/npp.2013.104
123. Barichello T, Generoso JS, Simões LR, Faller CJ, Ceretta RA, Petronilho F, et al. Sodium butyrate prevents memory impairment by re-establishing BDNF and GDNF expression in experimental pneumococcal meningitis. *Mol Neurobiol.* (2015) 52:734–40. doi: 10.1007/s12035-014-8914-3
124. Kim HJ, Leeds P, Chuang DM. The HDAC inhibitor, sodium butyrate, stimulates neurogenesis in the ischemic brain. *J Neurochem.* (2009) 110:1226–40. doi: 10.1111/j.1471-4159.2009.06212.x
125. Yoo DY, Kim W, Nam SM, Kim DW, Chung JY, Choi SY, et al. Synergistic effects of sodium butyrate, a histone deacetylase inhibitor, on increase of neurogenesis induced by pyridoxine and increase of neural proliferation in the mouse dentate gyrus. *Neurochem Res.* (2011) 36:1850–7. doi: 10.1007/s11064-011-0503-5
126. Wei Y Bin, Melas PA, Wegener G, Mathe AA, Lavebratt C. Antidepressant-like effect of sodium butyrate is associated with an increase in tet1 and in 5-hydroxymethylation levels in the BDNF gene. *Int J Neuropsychopharmacol.* (2015) 18:1–10. doi: 10.1093/ijnp/pyu032
127. Levenson JM, O'Riordan KJ, Brown KD, Trinh MA, Molfese DL, Sweatt JD. Regulation of histone acetylation during memory formation in the hippocampus. *J Biol Chem.* (2004) 279:40545–59. doi: 10.1074/jbc.M402229200
128. Yang LL, Millischer V, Rodin S, MacFabe DF, Villaescusa JC, Lavebratt C. Enteric short-chain fatty acids promote proliferation of human neural progenitor cells. *J Neurochem.* (2019) e14928. doi: 10.1111/jnc.14928. [Epub ahead of print].
129. Torres-Fuentes C, Golubeva AV, Zhdanov AV, Wallace S, Arboleya S, Papkovsky DB, et al. Short-chain fatty acids and microbiota metabolites attenuate ghrelin receptor signaling. *FASEB J.* (2019) 33:13546–59. doi: 10.1096/fj.201901433R
130. Schutkowski A, Wege N, Stangl GI, Konig B. Tissue-specific expression of monocarboxylate transporters during fasting in mice. *PLoS ONE.* (2014) 9:e112118. doi: 10.1371/journal.pone.0112118
131. Miletta MC, Petkovic V, Eblé A, Ammann RA, Flück CE, Mullis PE. Butyrate increases intracellular calcium levels and enhances growth hormone release from rat anterior pituitary cells via the G-protein-coupled receptors GPR41 and 43. *PLoS ONE.* (2014) 9:e107388. doi: 10.1371/journal.pone.0107388
132. Dale N, Kandel ER, Schacher S. Serotonin produces long-term changes in the excitability of aplysia sensory neurons in culture that depend on new protein synthesis. *J Neurosci.* (1987) 7:2232–8. doi: 10.1523/JNEUROSCI.07-07-02232.1987
133. Montarolo PG, Goelet P, Castellucci VF, Morgan J, Kandel ER, Schacher S. A critical period for macromolecular synthesis in long-term heterosynaptic facilitation in Aplysia. *Science.* (1986) 234:1249–54. doi: 10.1126/science.3775383
134. Buffington SA, Huang W, Costa-Mattioli M. Translational control in synaptic plasticity and cognitive dysfunction. *Annu Rev Neurosci.* (2014) 37:17–38. doi: 10.1146/annurev-neuro-071013-014100
135. Gräff J, Tsai LH. Histone acetylation: molecular mnemonics on the chromatin. *Nat Rev Neurosci.* (2013) 14:97–111. doi: 10.1038/nrn3427
136. Zhong T, Qing QJ, Yang Y, Zou WY, Ye Z, Yan JQ, et al. Repression of contexual fear memory induced by isoflurane is accompanied by reduction in histone acetylation and rescued by sodium butyrate. *Br J Anaesth.* (2014) 113:634–43. doi: 10.1093/bja/aeu184
137. Garcez ML, de Carvalho CA, Mina F, Bellettini-Santos T, Schiavo GL, da Silva S, et al. Sodium butyrate improves memory and modulates the activity of histone deacetylases in aged rats after the administration of D-galactose. *Exp Gerontol.* (2018) 113:209–17. doi: 10.1016/j.exger.2018.10.005
138. Hill JM, Bhattacharjee S, Pogue AI, Lukiw WJ. The gastrointestinal tract microbiome and potential link to Alzheimer's disease. *Front Neurol.* (2014) 5:43. doi: 10.3389/fneur.2014.00043
139. Unger MM, Spiegel J, Dillmann KU, Grundmann D, Philippeit H, Bürmann J, et al. Short chain fatty acids and gut microbiota differ between patients with Parkinson's disease and age-matched controls. *Park Relat Disord.* (2016) 32:66–72. doi: 10.1016/j.parkreldis.2016.08.019
140. Li H, Sun J, Wang F, Ding G, Chen W, Fang R, et al. Sodium butyrate exerts neuroprotective effects by restoring the blood-brain barrier in traumatic brain injury mice. *Brain Res.* (2016) 1642:70–8. doi: 10.1016/j.brainres.2016.03.031
141. He Y, Kosciolek T, Tang J, Zhou Y, Li Z, Ma X, et al. Gut microbiome and magnetic resonance spectroscopy study of subjects at ultra-high risk for psychosis may support the membrane hypothesis. *Eur Psychiatry.* (2018) 53:37–45. doi: 10.1016/j.eurpsy.2018.05.011
142. Zhai C-D, Zheng J-J, An B-C, Huang H-F, Tan Z-C. Intestinal microbiota composition in patients with amyotrophic lateral sclerosis. *Chin Med J.* (2019) 132:1815–22. doi: 10.1097/CM9.0000000000000351
143. Downs R, Perna J, Vitelli A, Cook D, Dhurjati P. Model-based hypothesis of gut microbe populations and gut/brain barrier permeabilities in the development of regressive autism. *Med Hypotheses.* (2014) 83:649–55. doi: 10.1016/j.mehy.2014.09.005
144. Adams JB, Johansen LJ, Powell LD, Quig D, Rubin RA. Gastrointestinal flora and gastrointestinal status in children with autism - comparisons to typical children and correlation with autism severity. *BMC Gastroenterol.* (2011) 11:22. doi: 10.1186/1471-230X-11-22
145. Finegold SM, Dowd SE, Gontcharova V, Liu C, Henley KE, Wolcott RD, et al. Pyrosequencing study of fecal microflora of autistic and control children. *Anaerobe.* (2010) 16:444–53. doi: 10.1016/j.anaerobe.2010.06.008
146. Finegold SM. Desulfovibrio species are potentially important in regressive autism. *Med Hypotheses.* (2011) 77:270–4. doi: 10.1016/j.mehy.2011.04.032

147. Choi J, Lee S, Won J, Jin Y, Hong Y, Hur T-Y, et al. Pathophysiological and neurobehavioral characteristics of a propionic acid-mediated autism-like rat model. *PLoS ONE.* (2018) 13:e0192925. doi: 10.1371/journal.pone.0192925
148. Kratsman N, Getselter D, Elliott E. Sodium butyrate attenuates social behavior deficits and modifies the transcription of inhibitory/excitatory genes in the frontal cortex of an autism model. *Neuropharmacology.* (2016) 102:136–45. doi: 10.1016/j.neuropharm.2015.11.003
149. Delgado PL. Depression: the case for a monoamine deficiency. *J Clin Psychiatry.* (2000) 61:7–11.
150. Miller AH, Raison CL. The role of inflammation in depression: from evolutionary imperative to modern treatment target. *Nat Rev Immunol.* (2016) 16:22–34. doi: 10.1038/nri.2015.5
151. Szczesniak O, Hestad KA, Hanssen JF, Rudi K. Isovaleric acid in stool correlates with human depression. *Nutr Neurosci.* (2016) 19:279–83. doi: 10.1179/1476830515Y.0000000007
152. Valvassori S, Resende W, Budni J, Dal-Pont G, Bavaresco D, Reus G, et al. Sodium butyrate, a histone deacetylase inhibitor, reverses behavioral and mitochondrial alterations in animal models of depression induced by early- or late-life stress. *Curr Neurovasc Res.* (2015) 12:312–20. doi: 10.2174/1567202612666150728121121
153. Sun J, Wang F, Hong G, Pang M, Xu H, Li H, et al. Antidepressant-like effects of sodium butyrate and its possible mechanisms of action in mice exposed to chronic unpredictable mild stress. *Neurosci Lett.* (2016) 618:159–66. doi: 10.1016/j.neulet.2016.03.003
154. Burokas A, Arboleya S, Moloney RD, Peterson VL, Murphy K, Clarke G, et al. Targeting the microbiota-gut-brain axis: prebiotics have anxiolytic and antidepressant-like effects and reverse the impact of chronic stress in mice. *Biol Psychiatry.* (2017) 82:472–87. doi: 10.1016/j.biopsych.2016.12.031
155. Moretti M, Valvassori SS, Varela RB, Ferreira CL, Rochi N, Benedet J, et al. Behavioral and neurochemical effects of sodium butyrate in an animal model of mania. *Behav Pharmacol.* (2011) 22:766–72. doi: 10.1097/FBP.0b013e32834d0f1b
156. Resende WR, Valvassori SS, Réus GZ, Varela RB, Arent CO, Ribeiro KF, et al. Effects of sodium butyrate in animal models of mania and depression: implications as a new mood stabilizer. *Behav Pharmacol.* (2013) 24:569–79. doi: 10.1097/FBP.0b013e32836546fc
157. Valvassori SS, Dal-Pont GC, Steckert AV, Varela RB, Lopes-Borges J, Mariot E, et al. Sodium butyrate has an antimanic effect and protects the brain against oxidative stress in an animal model of mania induced by ouabain. *Psychiatry Res.* (2016) 235:154–9. doi: 10.1016/j.psychres.2015.11.017
158. Govindarajan N, Agis-Balboa RC, Walter J, Sananbenesi F, Fischer A. Sodium butyrate improves memory function in an alzheimer's disease mouse model when administered at an advanced stage of disease progression. *J Alzheimer's Dis.* (2011) 26:187–97. doi: 10.3233/JAD-2011-110080
159. Walsh ME, Bhattacharya A, Sataranatarajan K, Qaisar R, Sloane L, Rahman MM, et al. The histone deacetylase inhibitor butyrate improves metabolism and reduces muscle atrophy during aging. *Aging Cell.* (2015) 14:957–70. doi: 10.1111/acel.12387
160. Prince M, Comas-Herrera A, Knapp M, Guerchet M, Karagiannidou M. *World Alzheimer Report 2016: Improving Healthcare for People Living With Dementia: Coverage, Quality and Costs Now and in the Future.* (2016). Available online at: https://www.alz.co.uk/research/world-report-2016 (accessed December 28, 2019).
161. Jankowsky JL, Fadale DJ, Anderson J, Xu GM, Gonzales V, Jenkins NA, et al. Mutant presenilins specifically elevate the levels of the 42 residue β-amyloid peptide *in vivo*: evidence for augmentation of a 42-specific γ secretase. *Hum Mol Genet.* (2004) 13:159–70. doi: 10.1093/hmg/ddh019
162. Frozza RL, Lourenco MV, de Felice FG. Challenges for Alzheimer's disease therapy: insights from novel mechanisms beyond memory defects. *Front Neurosci.* (2018) 12:37. doi: 10.3389/fnins.2018.00037
163. Hoffman JD, Yanckello LM, Chlipala G, Hammond TC, McCulloch SD, Parikh I, et al. Dietary inulin alters the gut microbiome, enhances systemic metabolism and reduces neuroinflammation in an APOE4 mouse model. *PLoS ONE.* (2019) 14:e0221828. doi: 10.1371/journal.pone.0221828
164. Ferreira ST, Lourenco MV, Oliveira MM, De Felice FG. Soluble amyloid-β oligomers as synaptotoxins leading to cognitive impairment in Alzheimer's disease. *Front Cell Neurosci.* (2015) 9:191. doi: 10.3389/fncel.2015.00191
165. Sun J, Xu J, Ling Y, Wang F, Gong T, Yang C, et al. Fecal microbiota transplantation alleviated Alzheimer's disease-like pathogenesis in APP/PS1 transgenic mice. *Transl Psychiatry.* (2019) 9:189. doi: 10.1038/s41398-019-0525-3
166. Bonfili L, Cecarini V, Berardi S, Scarpona S, Suchodolski JS, Nasuti C, et al. Microbiota modulation counteracts Alzheimer's disease progression influencing neuronal proteolysis and gut hormones plasma levels. *Sci Rep.* (2017) 7:1–21. doi: 10.1038/s41598-017-02587-2
167. Ho ST, Hsieh YT, Wang SY, Chen MJ. Improving effect of a probiotic mixture on memory and learning abilities in D-galactose–treated aging mice. *J Dairy Sci.* (2019) 102:1901–9. doi: 10.3168/jds.2018-15811
168. Hsieh HM, Wu WM, Hu ML. Genistein attenuates D-galactose-induced oxidative damage through decreased reactive oxygen species and NF-κB binding activity in neuronal PC12 cells. *Life Sci.* (2011) 88:82–8. doi: 10.1016/j.lfs.2010.10.021
169. Sampson TR, Debelius JW, Thron T, Janssen S, Shastri GG, Ilhan ZE, et al. Gut microbiota regulate motor deficits and neuroinflammation in a model of Parkinson's disease. *Cell.* (2016) 167:1469–80.e12. doi: 10.1016/j.cell.2016.11.018
170. Li W, Wu X, Hu X, Wang T, Liang S, Duan Y, et al. Structural changes of gut microbiota in Parkinson's disease and its correlation with clinical features. *Sci China Life Sci.* (2017) 60:1223–33. doi: 10.1007/s11427-016-9001-4
171. Sun MF, Zhu YL, Zhou ZL, Jia XB, Da Xu Y, Yang Q, et al. Neuroprotective effects of fecal microbiota transplantation on MPTP-induced Parkinson's disease mice: gut microbiota, glial reaction and TLR4/TNF-α signaling pathway. *Brain Behav Immun.* (2018) 70:48–60. doi: 10.1016/j.bbi.2018.02.005
172. Liu J, Wang F, Liu S, Du J, Hu X, Xiong J, et al. Sodium butyrate exerts protective effect against Parkinson's disease in mice via stimulation of glucagon like peptide-1. *J Neurol Sci.* (2017) 381:176–81. doi: 10.1016/j.jns.2017.08.3235
173. Paiva I, Pinho R, Pavlou MA, Hennion M, Wales P, Schütz AL, et al. Sodium butyrate rescues dopaminergic cells from alpha-synuclein-induced transcriptional deregulation and DNA damage. *Hum Mol Genet.* (2017) 26:2231–46. doi: 10.1093/hmg/ddx114
174. St. Laurent R, O'Brien LM, Ahmad ST. Sodium butyrate improves locomotor impairment and early mortality in a rotenone-induced Drosophila model of Parkinson's disease. *Neuroscience.* (2013) 246:382–90. doi: 10.1016/j.neuroscience.2013.04.037
175. Sharma S, Taliyan R, Singh S. Beneficial effects of sodium butyrate in 6-OHDA induced neurotoxicity and behavioral abnormalities: modulation of histone deacetylase activity. *Behav Brain Res.* (2015) 291:306–14. doi: 10.1016/j.bbr.2015.05.052
176. Jangi S, Gandhi R, Cox LM, Li N, Von Glehn F, Yan R, et al. Alterations of the human gut microbiome in multiple sclerosis. *Nat Commun.* (2016) 7:12015. doi: 10.1038/ncomms12015
177. Chen J, Chia N, Kalari KR, Yao JZ, Novotna M, Soldan MMP, et al. Multiple sclerosis patients have a distinct gut microbiota compared to healthy controls. *Sci Rep.* (2016) 6:28484. doi: 10.1038/srep28484
178. Mizuno M, Noto D, Kaga N, Chiba A, Miyake S. The dual role of short fatty acid chains in the pathogenesis of autoimmune disease models. *PLoS ONE.* (2017) 12:e0173032. doi: 10.1371/journal.pone.0173032
179. Chevalier AC, Rosenberger TA. Increasing acetyl-CoA metabolism attenuates injury and alters spinal cord lipid content in mice subjected to experimental autoimmune encephalomyelitis. *J Neurochem.* (2017) 141:721–37. doi: 10.1111/jnc.14032
180. Chen T, Noto D, Hoshino Y, Mizuno M, Miyake S. Butyrate suppresses demyelination and enhances remyelination. *J Neuroinflammation.* (2019) 16:165. doi: 10.1186/s12974-019-1552-y
181. Blacher E, Bashiardes S, Shapiro H, Rothschild D, Mor U, Dori-Bachash M, et al. Potential roles of gut microbiome and metabolites in modulating ALS in mice. *Nature.* (2019) 572:474–80. doi: 10.1038/s41586-019-1443-5
182. Turnbaugh PJ, Hamady M, Yatsunenko T, Cantarel BL, Duncan A, Ley RE, et al. A core gut microbiome in obese and lean twins. *Nature.* (2009) 457:480–4. doi: 10.1038/nature07540
183. Larsen N, Vogensen FK, van den Berg FWJ, Nielsen DS, Andreasen AS, Pedersen BK, et al. Gut microbiota in human adults with type

2 diabetes differs from non-diabetic adults. *PLoS ONE.* (2010) 5:e9085. doi: 10.1371/journal.pone.0009085
184. Karlsson FH, Tremaroli V, Nookaew I, Bergström G, Behre CJ, Fagerberg B, et al. Gut metagenome in European women with normal, impaired and diabetic glucose control. *Nature.* (2013) 498:99–103. doi: 10.1038/nature12198
185. Kootte RS, Levin E, Salojärvi J, Smits LP, Hartstra AV, Udayappan SD, et al. Improvement of insulin sensitivity after lean donor feces in metabolic syndrome is driven by baseline intestinal microbiota composition. *Cell Metab.* (2017) 26:611–9.e6. doi: 10.1016/j.cmet.2017.09.008
186. Zhang X, Shen D, Fang Z, Jie Z, Qiu X, Zhang C, et al. Human gut microbiota changes reveal the progression of glucose intolerance. *PLoS ONE.* (2013) 8:e71108. doi: 10.1371/journal.pone.0071108
187. Sanna S, van Zuydam NR, Mahajan A, Kurilshikov A, Vich Vila A, Võsa U, et al. Causal relationships among the gut microbiome, short-chain fatty acids and metabolic diseases. *Nat Genet.* (2019) 51:600–5. doi: 10.1038/s41588-019-0350-x
188. Kaczmarczyk MM, Miller MJ, Freund GG. The health benefits of dietary fiber: beyond the usual suspects of type 2 diabetes mellitus, cardiovascular disease and colon cancer. *Metabolism.* (2012) 61:1058–66. doi: 10.1016/j.metabol.2012.01.017
189. Keenan MJ, Zhou J, Hegsted M, Pelkman C, Durham HA, Coulon DB, et al. Role of resistant starch in improving gut health, adiposity, and insulin resistance. *Adv Nutr.* (2015) 6:198–205. doi: 10.3945/an.114.007419
190. Edwards CA, Xie C, Garcia AL. Dietary fibre and health in children and adolescents. *Proc Nutr Soc.* 74:292–302. doi: 10.1017/S0029665115002335
191. Den Besten G, Bleeker A, Gerding A, Van Eunen K, Havinga R, Van Dijk TH, et al. Short-chain fatty acids protect against high-fat diet-induced obesity via a pparg-dependent switch from lipogenesis to fat oxidation. *Diabetes.* (2015) 64:2398–408. doi: 10.2337/db14-1213
192. Lu Y, Fan C, Li P, Lu Y, Chang X, Qi K. Short chain fatty acids prevent high-fat-diet-induced obesity in mice by regulating g protein-coupled receptors and gut microbiota. *Sci Rep.* (2016) 6:37589. doi: 10.1038/srep37589
193. Tolhurst G, Heffron H, Lam YS, Parker HE, Habib AM, Diakogiannaki E, et al. Short-chain fatty acids stimulate glucagon-like peptide-1 secretion via the G-protein-coupled receptor FFAR2. *Diabetes.* (2012) 61:364–71. doi: 10.2337/db11-1019
194. Yadav H, Lee JH, Lloyd J, Walter P, Rane SG. Beneficial metabolic effects of a probiotic via butyrate-induced GLP-1 hormone secretion. *J Biol Chem.* (2013) 288:25088–97. doi: 10.1074/jbc.M113.452516
195. Barrea L, Muscogiuri G, Annunziata G, Laudisio D, Pugliese G, Salzano C, et al. From gut microbiota dysfunction to obesity: could short-chain fatty acids stop this dangerous course? *Hormones.* (2019) 18:245–50. doi: 10.1007/s42000-019-00100-0
196. Ahmadi S, Nagpal R, Wang S, Gagliano J, Kitzman DW, Soleimanian-Zad S, et al. Prebiotics from acorn and sago prevent high-fat-diet-induced insulin resistance via microbiome–gut–brain axis modulation. *J Nutr Biochem.* (2019) 67:1–13. doi: 10.1016/j.jnutbio.2019.01.011
197. van der Beek CM, Canfora EE, Lenaerts K, Troost FJ, Damink SWMO, Holst JJ, et al. Distal, not proximal, colonic acetate infusions promote fat oxidation and improve metabolic markers in overweight/obese men. *Clin Sci.* (2016) 130:2073–82. doi: 10.1042/CS20160263
198. Freeland KR, Wolever TMS. Acute effects of intravenous and rectal acetate on glucagon-like peptide-1, peptide YY, ghrelin, adiponectin and tumour necrosis factor-α. *Br J Nutr.* (2010) 103:460–6. doi: 10.1017/S0007114509991863
199. Canfora EE, Van Der Beek CM, Jocken JWE, Goossens GH, Holst JJ, Olde Damink SWM, et al. Colonic infusions of short-chain fatty acid mixtures promote energy metabolism in overweight/obese men: a randomized crossover trial. *Sci Rep.* (2017) 7:2360. doi: 10.1038/s41598-017-02546-x

Conflict of Interest: The authors declare that the research was conducted in the absence of any commercial or financial relationships that could be construed as a potential conflict of interest.

frontiers in Endocrinology

ORIGINAL RESEARCH
published: 31 January 2020
doi: 10.3389/fendo.2019.00943

Exposure to the UV Filter Octyl Methoxy Cinnamate in the Postnatal Period Induces Thyroid Dysregulation and Perturbs the Immune System of Mice

*Fausto Klabund Ferraris[1†], Esdras Barbosa Garcia[1†], Amanda da Silva Chaves[1], Thais Morais de Brito[1], Laís Higino Doro[1], Naína Monsores Félix da Silva[1], Amanda Soares Alves[1], Tatiana Almeida Pádua[2], Maria das Graças M. O. Henriques[2], Tiago Savignon Cardoso Machado[3] and Fabio Coelho Amendoeira[1]**

[1] Laboratory of Pharmacology, Department of Pharmacology and Toxicology, National Institute of Health Quality Control (INCQS)—Oswaldo Cruz Foundation (FIOCRUZ), Rio de Janeiro, Brazil, [2] Laboratory of Applied Pharmacology, Institute of Drug Technology (Far-Manguinhos)—Oswaldo Cruz Foundation (FIOCRUZ), Rio de Janeiro, Brazil, [3] Laboratory of Professional Education in Laboratory Techniques in Health, Polytechnic School of Health Joaquim Venâncio—Oswaldo Cruz Foundation (FIOCRUZ), Rio de Janeiro, Brazil

Evidence demonstrates the bidirectional communication and regulation between the neuroendocrine and immune systems. Thyroid hormones play key roles in nervous system development and can exert influence on various immune cells contributing to pathophysiological conditions. Octyl methoxycinnamate (OMC) is one of the most commonly used UV filters, and *in vitro* and *in vivo* studies have found thyroid disrupting effects. The present study assessed whether OMC administration in mice dams during the lactational period can cause thyroid disruption and generate immunologic alterations in the offspring. Indirect exposure to the OMC (1,000 mg/kg) in the lactational period affected neurodevelopment parameters, such as delayed eye-opening and weight gain in mice of both sexes, and these alterations are corroborated by the decrease in the T4 levels present in the pups' blood. No significant changes were observed in the thymus of these pups, but the number of lymphocytes increased in the spleen of the animals exposed to OMC, similar to the animals treated with propyl-thiouracil (PTU), a well-known thyroid disruptor. OMC modulated the percentage of leukocyte populations in peripheral blood, and the number of circulating polymorphonuclear cells increased two-fold. *In vitro*, OMC exhibited an inhibitory effect on splenocyte proliferation and IL-2 production induced by anti-CD3 antibody; however, this effect was reversed with the addition of T4 in the cell culture. In summary, the results of the present study demonstrate the influence of OMC on thyroid dysregulation and its impact on the modulation of the immune system in mice pups.

Keywords: sunscreen, UV filter, thyroid disruptor, hypothyroidism, octyl methoxycinnamate, OMC, immune system

OPEN ACCESS

Edited by:
Ana Rosa Pérez, National Council for Scientific and Technical Research (CONICET), Argentina

Reviewed by:
Ivan Pilipovic, Institute of Virology, Vaccines and Sera "Torlak", Serbia
Egberto Gaspar Moura, Rio de Janeiro State University, Brazil

****Correspondence:***
Fabio Coelho Amendoeira
fabio.amendoeira@incqs.fiocruz.br

[†]These authors have contributed equally to this work

Specialty section:
This article was submitted to Neuroendocrine Science, a section of the journal Frontiers in Endocrinology

Received: *11 September 2019*
Accepted: *31 December 2019*
Published: *31 January 2020*

Citation:
Ferraris FK, Garcia EB, Chaves AdS, Brito TMd, Doro LH, Félix da Silva NM, Alves AS, Pádua TA, Henriques MdGMO, Cardoso Machado TS and Amendoeira FC (2020) Exposure to the UV Filter Octyl Methoxy Cinnamate in the Postnatal Period Induces Thyroid Dysregulation and Perturbs the Immune System of Mice. Front. Endocrinol. 10:943. doi: 10.3389/fendo.2019.00943

INTRODUCTION

The octyl methoxycinnamate (OMC), also known as octinoxate, is probably the organic ultraviolet (UV) filter used most by the cosmetic industry. UV filters, such as OMC, can be bioaccumulated in organisms due to their high lipophilicity and poor degradability (1–5); therefore, they have become contaminants of emerging concern (5). Studies have previously reported that OMC can penetrate through the epidermis and the dermis, spread through the systemic circulation and can have a systemic action on the body, due to its relatively low molecular weight, and lipophilic character (6). Consequently, OMC has been detected in human bodily fluids such as urine and blood after topical application (7). OMC was reported to induce acute toxicities, and a large number of studies, both *in vivo* and *in vitro*, found multiple endocrine disrupting effects in the estrogen receptor (ER), androgen receptor (AR), progesterone receptor (PR), and hypothalamus-pituitary-thyroid (HPT) axis (8–10).

Several UV filters have already been cataloged and reported as a HPT function deregulators, especially when exposed to during the early stages of development (11). These actions can directly affect the gland and/or the corresponding regulatory centers, such as the hypothalamus and the pituitary, affecting the levels of thyrotropin releasing hormone (TRH) and/or thyroid-stimulating hormone (TSH), which are directly related to the synthesis of thyroid hormones. Most studies have focused on the estrogenic and anti-androgenic effects of OMC in wild and lab animals (12–14); however only a few studies focused on the influence of OMC upon the HPT function (15–17).

Several studies have demonstrated the importance of thyroid hormones in ontogenesis, acting on embryonic and fetal tissues, via active transport of maternal thyroid hormone across the placenta to ensure normal development, until the fetal thyroid gland reaches maturity (18). Thyroid hormones are an important coordinators of embryonic and early postnatal development, conducing the metabolism, thermogenesis, the stimulation of growth and the development of various tissues; thus, abnormalities of thyroid hormone levels in infancy and childhood may result in dysfunctional effects in adults. Alterations of the thyroid function can also affect the immune system. Most studies assessing the interrelationship between thyroid and immune system are based on pathophysiological models where the immune system is already altered, such as autoimmune thyroid diseases (e.g., hyperthyroidism—Grave's Disease and hypothyroidism—Hashimoto's thyroiditis) (19). Different studies have generally shown that hyperthyroidism increases the immune response, antibody production, cell proliferation and migration, reactive oxygen species production, and downmodulation of proinflammatory markers (20–22). On the other hand, cases of hypothyroidism produce antagonistic effects on parameters of the immune function; such as decreased immune response, lower antibody production, and perturbed migratory and proliferative capacity of immune cells (23, 24).

The sensitivity of immune system to thyroid disruptor compounds is poorly explored in the neonatal period, added to the fact that the effects of chemicals may be different when administered to adults and neonates; therefore, the present study assessed whether OMC administration in mice dams during the lactational period can cause thyroid disruption and generate immunologic alterations in the offspring.

MATERIALS AND METHODS

Materials

Phosphate buffered saline (PBS), ethylenedyaminetetracetic sodium salt (EDTA), HEPES, bovine serum albumin (BSA), RPMI 1640 and Hank's balanced salt solution (HBSS) were purchased from Sigma-Aldrich (St. Louis, MO, USA). The 6-propyl-2-thiouracil (PTU) and 2-ethylhexyl-4-methoxycinnamate (Octyl Methoxycinnamate—OMC) were purchased from Sigma-Aldrich (St. Louis, MO, USA). IgG anti-murine CD3 (clone 145-2C11), APC-conjugated hamster IgG anti-murine CD3, PE-conjugated hamster IgG anti-murine CD8, and FITC-conjugated rat IgG anti-murine CD4 were all obtained from EXBIO Praha (Vestec, Czech Republic). Fetal bovine serum was obtained from Hyclone (Logan, UT, USA). Carboxyfluorescein diacetate-succinimidyl ester (CFSE) was obtained from Invitrogen (Carlsbad, CA, USA). Cell Proliferation Kit I (MTT) was purchased from Sigma-Aldrich (St. Louis, MO, USA). Thyroxine (T4) AccuBind® kit was purchased from Monobind Inc. (Lake Forest, CA, USA).

Mouse Line and Animal Care

The Swiss Webster mice used in this study were provided by the Oswaldo Cruz Foundation breeding unit (Rio de Janeiro, Brazil). The animals were kept under standard laboratory conditions, with free access to food and fresh water in a room with the temperature ranging from 22 to 24°C and a 12 h light/dark cycle. The animals were housed at the INCQS experimental animal facility unit until use. After a 3-days cohabitation period, females were removed from the male's cage, and housed individually. Starting on gestational day 15, the cages were daily checked for deliveries. On post-natal day (PN) 1, pups were sexed and allocated into experimental groups. Twenty-four hours after birth pups were divided into two groups (i.e., 4 males and 4 females). Pups were kept with theirs respective mothers inside individual standard plastic cages with stainless steel coverlids and pinewood shavings as bedding. All experimental procedures were performed according to The Committee on Ethical Use of Laboratory Animals of the Fundação Oswaldo Cruz (FIOCRUZ, Brazil; license LW-30/14).

Post-natal Development, Weight Gain, and Weaning

To evaluate the subacute toxicity of the OMC during the lactation period and to define the dose to be used in subsequent trials, lactating female mice were exposed to different doses of OMC (250, 500, or 1,000 mg/Kg/day), PTU—a known thyrotoxic compound (4 mg/Kg/day) or corn oil (vehicle) by gavage for 22 days (9). One day after birth, the offspring was randomized again into three experimental groups designating one couple/group. The lactating female mice received OMC, PTU or corn oil (vehicle) during the lactational period (PN1 to PN22) daily at 10 a.m. by gavage. To investigate the influence of OMC on their

development, pups were observed from PN1 to PN16 to evaluate developmental parameters such as the eruption of the incisors, hair growth and opening of eyes (exact day). On PN23 the Swiss Webster pups, as well as lactating female mice, were euthanized and organs such as thymus and spleen were carefully collected, weighed and processed for cell count and flow cytometry analysis. The peripheral blood from these animals was also collected for leukocyte count and hormone dosage.

Measurement of Total T4 Hormone Serum Levels

Total T4 was determined in mouse serum by enzyme immunosorbent assay (EIA) Thyroxine (T4) AccuBind® kit following the instructions of the manufacturer (Monobind Inc., Lake Forest, CA, USA). Absorbance was read at 450 nm using a Spectramax M5 microplate reader (Molecular Devices, Sunnyvale, CA, USA).

Cell Counts

Total cell counts from the thymus, spleen and peripheral blood were conducted using a Neubauer chamber, under an optical microscope, after dilution in Turk fluid (2% acetic acid). The thymus and spleen cell counts are reported as the number of cells per gram of tissue. The peripheral blood counts are expressed as cells per milliliter.

MTT-Based Proliferation Assay

The splenocyte proliferation was measured by the Cell Proliferation Kit I (MTT) of Sigma-Aldrich (St. Louis, MO, USA) according to the manufacturer's protocol. Splenocytes, recovered from 3 week old male Swiss mice, were treated for 1 h with different concentrations of OMC (1–200 μg/mL) or vehicle; and subsequently cultured in the anti-CD3 mAb-coated wells at a concentration of 10^5 cells/well in RPMI 1640 medium supplemented with 10% FBS (at 5% CO_2 and 37°C). After 72 h, the cells were incubated with the MTT solution for another 4 h. The water insoluble formazan dye was solubilized before the measurement of absorbance using a Spectramax M5 multiwell spectrophotometer (Molecular Devices, Sunnyvale, CA, USA). The absorbance was read at 550 nm (25).

CFSE-Based Proliferation Assay

Splenocytes, recovered from 3 week old male Swiss mice, were labeled with the cell proliferation dye carboxyfluorescein diacetate succinimidyl ester (CFSE) kit (Invitrogen, Carlsbad, CA, USA) according to the manufacturer's protocol and stimulated for 72 h with anti-CD3 antibody after treatment for 1 h with OMC, T4 (10^{-5} M), OMC plus T4, or vehicle. Proliferation was assessed by the percentage of CFSE+ high cells (0 h) compared to CFSE+ low cells (72 h) as analyzed by CyFlow Space flow cytometer (Partec GmbH—a Sysmex Company, Münster, Germany) (26).

Enzyme-Linked Immunosorbent Assay (ELISA)

The concentrations of IL-2 in the supernatants from the proliferation assay were evaluated by sandwich ELISA using matched antibody pairs (Quantikine, R&D Systems, Minneapolis, MN, USA) according to the manufacturer's instructions. The results are expressed as nanograms per milliliter (ng/mL) (26).

Statistical Analysis

All data distributions were used to check normality by Kolmogorov-Smirnov test. In this case, a value of $p > 0.1$ suggests normal distribution. For the data with normal distribution, mean and standard error of the mean (SEM) were calculated. The treatment groups were compared by Student's *t*-test for independent samples. For the evaluation of weight gain, we used ANOVAr (ANOVA repeated measure), with sex and group like between-subject factors. For data with free distribution, proper statistical analyses were performed for each type of data. The variables: ear detachment, hair growth, eruption of the incisors, and opening of eyes were analyzed by Chi-Square test. For all tests, a value of $p < 0.05$ was considered as statistically significant. The statistical analyses were created using Graph Pad Prism Program 3 version 2.01 and SPSS Program version 15.0 for Windows.

RESULTS

Lactating pups fed by females exposed to 1,000 mg/Kg/day of OMC showed a significant reduction in weight gain and a delay in eye opening compared to the vehicle group (**Figures 1A,B** and **Table 1**). These data were in agreement with results obtained by our group in rats (unpublished data), where the direct exposition to OMC interfered in diverse developmental parameters in pups, wich were linked to a decrease of thyroid activity. To test whether the observed alterations in the offspring could have any correlation with thyroid disruption, the plasma T4 levels of pups and dams were evaluated.

The results showed that dams from PTU (4 mg/Kg/day) and OMC (1,000 mg/Kg/day) groups as well as pups from both groups (PTU and OMC) have significantly decreased total T4 levels when measured on PN23 (**Figures 1C,D**). The reduction of T4 levels in the offspring was similar in the PTU and OMC group (**Figure 1C**).

No alteration was found in the thymus for relative weight (data not shown), the relative number of thymocytes, as well as changes in thymocyte subpopulations—double-negative (DN), double-positive (DP), CD4+ cells, and CD8+ cells (**Figures 2A,B**). On the other hand, the relative spleen weight (data not shown) and the relative number of splenocytes of the OMC and PTU groups significantly increased (**Figure 2C**). When we analyzed the numbers of B and T lymphocytes in pups' spleen, only the group exposed to PTU presented a significantly increased number of B lymphocytes (**Figure 2D**); however, both OMC and PTU pups presented an increased, but not statistically significant, number of T lymphocytes compared to the control group (**Figure 2E**). Hematological examination showed an increased level of total leukocytes counts in the PTU group, with no alteration in the OMC group compared to control (**Figure 2F**). The number of mononuclear cells in the PTU group increased by 1.37-fold, but no difference was

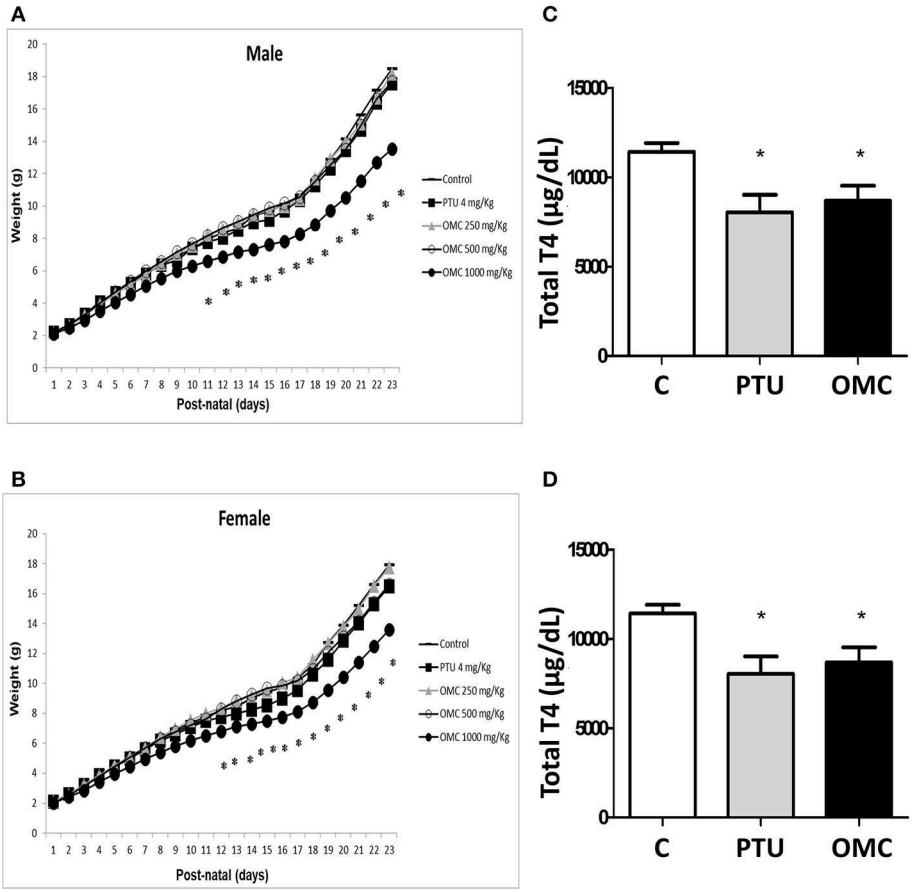

FIGURE 1 | Weight gain and measurement of total T4 hormone in animals exposed to PTU or OMC. Weight gain of **(A)** male and **(B)** female pups following exposure of lactating female mice to different concentrations of OMC. **(C)** Total T4 hormone serum levels in pups and **(D)** lactating female mice on PN23. **(A)** ($N = 17$); **(B)** ($N = 17$); **(C)** ($N = 13$); **(D)** ($N = 13$); *Significant difference between exposed groups and Control ($p < 0.05$). Error bars correspond to ± SEM.

TABLE 1 | Parameters of development of pups exposed to PTU or OMC in postnatal period.

Parameters		**Ear**		**Hair**		**Tooth**		**Eyes**	
		Detachment		**Growth**		**Eruption**		**Open**	
GROUP		**Before**	**After**	**Before**	**After**	**Before**	**After**	**Before**	**After**
		PN4	**PN4**	**PN5**	**PN5**	**PN10**	**PN10**	**PN14**	**PN14**
Control	Count	2	30	0	31	6	22	7	10
	% within GROUP	6.2	93.8	0	100	21.4	78.6	41.2	58.8
PTU 4 mg	Count	0	24	0	24	8	12	5	6
	% within GROUP	0	100	0	100	40	60	45.5	54.5
OMC 250 mg	Count	0	21	0	21	9	10	7	8
	% within GROUP	0	100	0	100	47.4	52.6	46.7	53.3
OMC 500 mg	Count	6	16	0	22	1	21	10	8
	% within GROUP	27.3	72.7	0	100	4.5	95.5	55.6	44.4
OMC 1.000 mg	Count	8	21	7	22	6	23	7	21*
	% within GROUP	27.6	72.4	24.1	75.9	20.7	79.3	25	75*

Postnatal day of ear detachment, hair growth, tooth eruption, and eyes open over 16 days of PTU or OMC administration for pups from both genders. Control: Corn oil (vehicle); Data are displayed as counting and percentage of counting. Animals were observed from PN1 to PN16 (N = 17). The differences were significant at $p < 0.05$ (*).

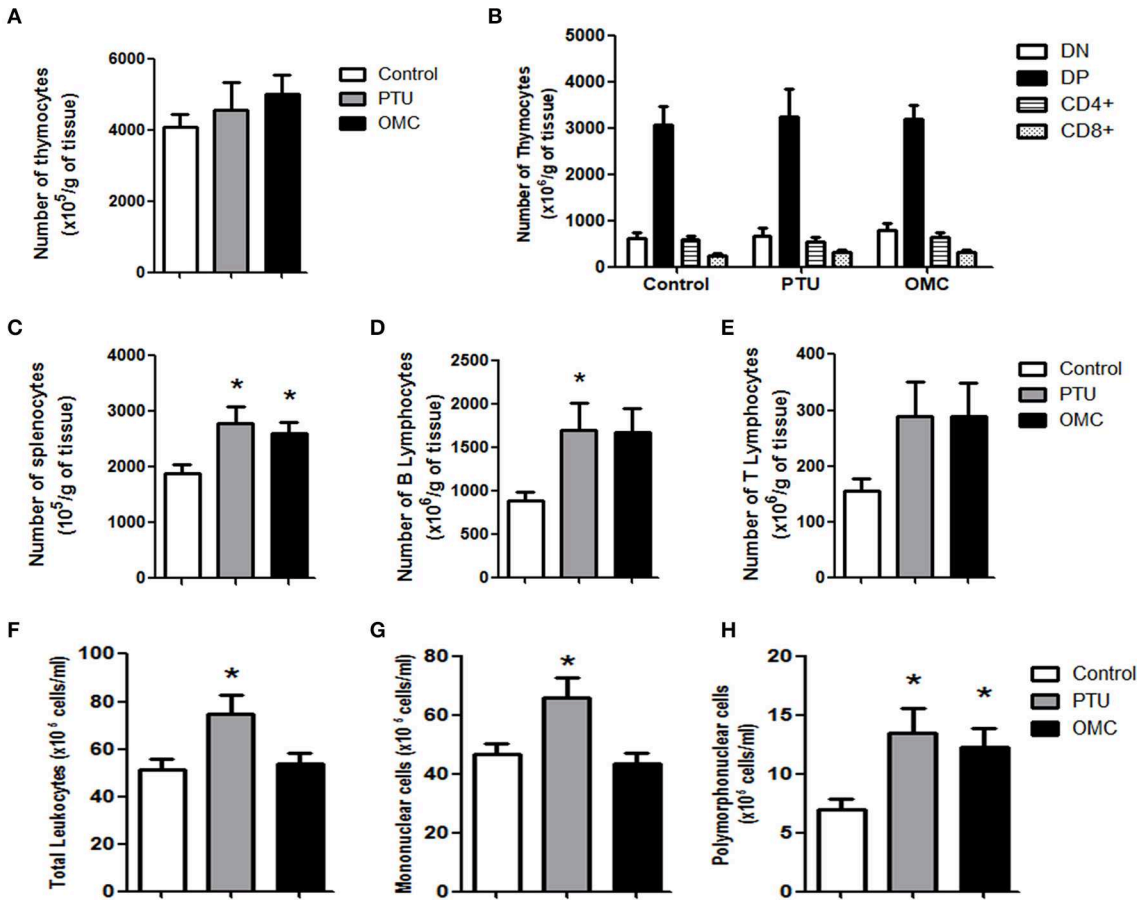

FIGURE 2 | Analysis of thymus, spleen and peripheral blood of animals exposed to PTU or OMC. **(A)** The number of total thymocytes and **(B)** flow cytometry analysis of subpopulations from pups on PN23 exposed to PTU or OMC 1,000 mg/kg. **(C)** The number of total splenocytes, **(D)** B lymphocytes, and **(E)** T lymphocytes from the spleen of pups on PN23 exposed to PTU or OMC 1,000 mg/kg. *Significant difference between exposed groups and Control ($p < 0.05$). **(F)** Total leukocytes and subpopulation counts of **(G)** mononuclear cells and **(H)** polymorphonuclear cells of pups on PN23 exposed to PTU or OMC 1,000 mg/kg. (A) ($N = 26$); **(B)** ($N = 25$); **(C)** ($N = 25$); **(D)** ($N = 7$); **(E)** ($N = 7$); **(F)** ($N = 26$); **(G)** ($N = 25$); **(H)** ($N = 25$); *Significant difference between exposed groups and Control ($p < 0.05$). Error bars correspond to ± SEM.

observed between the OMC and control group (**Figure 2G**). Furthermore, a significant increase occurred in the number of polymorphonuclear (PMN) cells in the groups exposed to PTU (1.86-fold increase) and OMC (1.81-fold increase) over the control group (**Figure 2H**).

Since thyroid hormones may have a direct action on T lymphocytes (27) and considering the ability of the OMC to molecularly modulate the thyroid hormone receptor, we evaluated the *in vitro* effect of OMC on splenocyte activation and proliferation. As observed in **Figure 3A**, OMC, in concentrations ranging from 10 to 200 μg/mL, inhibited anti-CD3 induced splenocyte proliferation. To investigate whether T4 addition could block the inhibitory OMC-induced effect, splenocytes were incubated with a medium containing OMC plus T4 and then stimulated to proliferate. The incubation of splenocytes with OMC impaired cell proliferative response induced by anti-CD3 stimulation within 72 h; however, when T4 was added, the proliferative capacity of the cells increased (**Figure 3B**). Since interleukin (IL)-2 is a critical T-cell growth factor, we evaluated the presence of this cytokine in the supernatant from the splenocytes of the proliferation assay. The treatment of cells with OMC reduced IL-2 production and this effect was reversed when T4 was added (**Figure 3C**), which is in accordance with the cell proliferation data (**Figure 3B**). Our results indicate that the addition of T4 was able to reverse the inhibitory effect caused by the OMC.

DISCUSSION

Our results provide new information on the influence of the OMC on hypothyroxinemia generation and its implications on the immune system in rodents after the lactation phase.

For thyroid hormone support during lactation, the important role of breastfeeding for the passage of T4 through milk is already known (28). The levels of T4 secretion are found to be higher in lactating rats than after weaning (29). Lactating mice pups whose mothers received dietary thyroxine supplementation had higher serum T4 levels than those without this diet, and

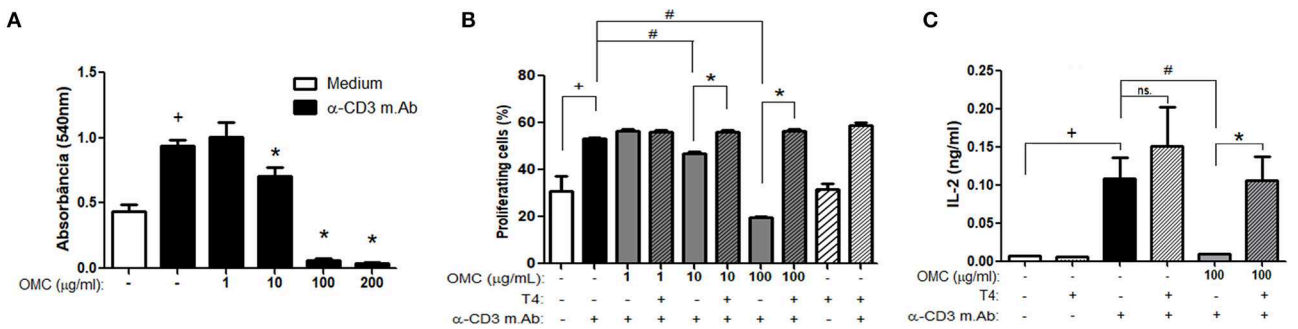

FIGURE 3 | Effect of OMC on splenocyte proliferation. **(A)** Effect of different concentrations of OMC on splenocyte proliferation after anti-CD3 stimulation for 72 h. $^{+}$Significant difference between anti-CD3 stimulated group and non-stimulated ($p < 0.05$). *Significant difference between OMC treated group and anti-CD3 stimulated non-treated group ($p < 0.05$). **(B)** Effect of OMC treatment and T4 supplementation on splenocyte proliferation after anti-CD3 stimulation for 72 h. $^{+}$Significant difference between anti-CD3 stimulated group and non-stimulated ($p < 0.05$). $^{\#}$Significant difference between OMC treated group and anti-CD3 stimulated non-treated group ($p < 0.05$). *Significant difference between OMC treated group and OMC treated and T4 supplemented group ($p < 0.05$). Error bars correspond to ±SEM. **(C)** Effect of OMC treatment and T4 supplementation on IL-2 production after anti-CD3 stimulation for 72 h. $^{+}$Significant difference between anti-CD3 stimulated group and non-stimulated ($p < 0.05$); $^{\#}$Significant difference between OMC treated group and anti-CD3 stimulated non-treated group ($p < 0.05$); *Significant difference between OMC treated group and OMC treated and T4 supplemented group ($p < 0.05$); ns, not significant. Error bars correspond to ±SEM.

this supplementation was responsible for restoring the brain myelination process of the litter (30). Just as thyroid hormones can pass through milk, some authors have also found the presence of the UV filter OMC in breast milk (31, 32), and this has raised concern given its ability to modulate hormones. The data presented here corroborate the findings of several authors in wich OMC led to a hypothyroxinemia condition (15, 17, 32, 33). In our study, the lactating females treated with the OMC had lower T4 levels, which could transfer less T4 to their pups. However, since OMC is an inhibitor of thyroid function in the mother, it could act with the same mechanisms in the pups. The amount of T4 transferred through the milk might not be sufficient to influence T4 serum levels in the pups. It was not possible to determine whether the reduction in puppies T4 levels was due to the lower T4 intake from the mothers, or a direct effect of OMC being passed through the milk and affecting the pups' thyroid or both in a synergistic effect. In any case, the deregulation of thyroid hormones in offspring led to developmental changes similar to those observed by other authors, such as lower body weight gain in animals (9, 34). Moreover, our data indicates that OMC induced an increase in eye-opening time and was similar to results from our group using an experimental rat model (unpublished data). This developmental change in eye-opening time correlates with the formation of the central nervous system. On the other hand, even with a reduction in T4 levels, animals exposed to PTU did not have significant changes in the evaluated developmental parameters. However, even without noticeable developmental changes due to the generated hypothyroxinemia, the PTU group presented other changes that were similar to the animals exposed to the OMC, such as alterations in splenocyte counts and in subpopulations of circulating leukocytes. Another factor that may have to do with the lack of clear signs of developmental change in PTU-treated animals may be the dose used in our study. Mallela et al. (35) administrated different doses of PTU (10–100 mg/kg/day) in pregnant rats and mice. Individual fetuses did not have gross malformations from PTU treatment. Fetuses from rats presented body weights lower in the 100 mg/kg PTU treated group compared to the control group, and weights with lower PTU doses were not significantly different than the control group. In mice, PTU had no adverse effects, such as on placental weight, litter size, resorption rates, or body weights of fetuses after maternal treatment. In addition, histopathological evaluations of mice fetuses did not reveal any significant abnormalities with PTU treatment. In this sense, the lower PTU dose that we used (4 mg/kg/day) was able to induce hypothyroxinemia and correlate with the developmental findings of the study in mice by Mallela et al. (35).

Several neurodevelopmental phenomena are influenced by thyroid hormones, such as axonal and dendritic growth, migration, synaptogenesis, neural survival, oligodendrocyte proliferation and myelinization, as well as synaptic efficacy (36). Several studies have observed that hypothyroidism induced by PTU could significantly compromise rodents in memory and learning tests (37–39); moreover, changes in motor skills and learning related to the effect of the OMC have been described by Axelstad et al. (9).

Experimental and clinical evidence suggests the bidirectional interactions between the neuroendocrine system and the thymus, especially the thymus hormone activity appears to be strongly modulated by thyroid hormone signals (40, 41). Hyperthyroidism increases numbers of thymocytes, leading to thymic hyperplasia in humans, and mice exogenously injected with triiodothyronine have an increase in thymocyte proliferation and volume of the thymus (42, 43). In our study, no changes were found in total numbers of thymocytes or subpopulations of DP, DN, CD4+ and CD8+ T cells. The differences found in our results from other data in the literature could be associated with two factors, indirect exposure to endocrine disruptors through mothers and the fact that animals are in the neonatal phase. The neonatal period can generate different response pattern from those observed in adult mice. The pups from the group exposed to the OMC presented a

higher number of splenocytes in contrast to unaltered number of circulating mononuclear cells in peripheral blood. The increase in splenocyte number also seems to occur with the PTU group, although this group exhibited a considerable leukocyte increase in all cell populations in the peripheral blood. Both cases of hypothyroxinemia generated by OMC or PTU did not present a reduction in leukocytes compared to the control group. Some studies found that rats and chickens with induced hypothyroidism exhibit a reduction in the number of peripheral blood lymphocytes and low responsiveness to mitogenic stimuli (44, 45). The main difference from these studies to ours is that they were performed in adult animals, and our model evaluated the neonatal period, which can lead to a difference in sensitivity and in some generated effects.

In clinical cases of hypothyroidism, PMNs have low migratory capacity when compared to healthy individuals (46); however, individuals with hyperthyroidism present PMN migratory activity similar to normal (47). A curious result was the increased number of circulating PMN cells in both PTU and OMC groups. The increased number of PMNs in the PTU group seems to be associated with a generalized increase in total leukocytes. On the other hand, the OMC group presented higher numbers of circulating PMN, with an imbalance between mononuclear and PMN cells compared to control animals. This increase in the number of circulating PMNs may be due to the accumulation of mononuclear cells in the lymphoid organs (as observed in the spleen) or a compensatory mechanism of the innate immune system to the detriment of a possible low functional activity of lymphocytes affected by low levels of T4 and/or a toxic effect of the OMC.

Some authors have already pointed to a positive correlation between hypothyroxinemia and a decrease in humoral and cell-mediated immune responses (45, 48). Our results indicate that the OMC has a direct dose-dependent blocking effect on the proliferative capacity of T lymphocytes. Curiously, T4 treatment was able to reverse the blocking effect of OMC on lymphocyte proliferation *in vitro*, suggesting that the OMC somewhat perturbs the ability of T lymphocyte activation and proliferation directly rather than by indirect mechanism via interactions between the endocrine and immune systems. Lymphocytes express thyroid receptors, produce TSH, and have enzymes for converting T4 to triiodothyronine (49–52), moreover, studies have shown that thyroid hormones modulate in an autocrine/paracrine mechanism the expression of soluble interleukin-2 receptor (sIL-2R), a marker of T lymphocyte activation (53, 54). Corroborating these data, Klecha et al. demonstrated after antigen challenge that IL-2 and interferon (IFN)-γ release increased in lymphocytes from hyperthyroid mice, while decreasing in cells from hypothyroid animals compared to control (24). We showed that diminished IL-2 production was closely related to inhibited proliferation in OMC-treated splenocytes, and the addition of T4 was able to rescue the cells from an anergic state, allowing IL-2 synthesis and proliferation. The addition of T4 alone without anti-CD3 stimulation failed to induce IL-2 synthesis and cell proliferation. Similar results were observed by Barreiro Arcos et al. (27), where thyroid hormones did not induce cell proliferation in resting T lymphocytes, but promotes cell proliferation in mitogen-stimulated T lymphocytes in a dose-dependent manner.

Surprisingly, our data show that T4 did not alter the proliferation of splenocytes stimulated with anti-CD3 antibody, unlike findings that demonstrated that T4 stimulates mitogen/antigen-induced proliferation of murine T cells (27, 55). We observed a subtle and non-significant increase in the anti-CD3 plus T4 stimulated group compared to the anti-CD3 group (58.9 + 1.8 vs. 53.1 + 1.1%), similarly, IL-2 production data correlate with these findings. The difference among our results and the findings of other groups may be linked to the proliferative stimuli used as well as the mouse strain/cell origin adopted in the studies. Both Barreiro Arcos and Varedi (27, 55) used the BALB/c inbreed strain, while we used the Swiss webster outbreed strain. This difference may imply the proliferative response pattern of the cells analyzed. Another difference was the proliferative stimulus used by us, the anti-CD3 monoclonal antibody, in contrast to the use of Concanavalin A (ConA) (27) and inactivated vírus HSV-1 (55). Anti-CD3 is specific for T lymphocyte stimulation, whereas ConA stimulates indistinctly different kinds of cells, besides, ConA and anti-CD3 have been shown to require activated differential pathways for calcium influx (56). Interestingly, Varedi et al. (55) demonstrated that the presence of T4 was ineffective to significant increase the antigen-induced proliferation of the cells from hyperthyroid animals. Also, the effect on the response to the ConA stimulus was similar to the inactivated vírus HSV-1 (55). Our results showed that the *in vitro* presence of T4 potentiated small increase in cell proliferation and IL-2 production, a similar effect was observed on splenocytes from hyperthyroid mice (55), however, in both cases, the potentiation was not significant.

Many of the immunologic effects of hypothyroidism can be reversed by administering thyroid hormones (40, 57). Data reported by other investigators demonstrated that *in vitro* T4 treatment or alterations in the normal state of the thyroid gland impacted the proliferative and cytokines production of lymphocytes (22, 25–27). Treatment of murine lymphocytes *in vitro* with T4 has been shown to increase the proliferative response to mitogens (27, 55). Klecha et al. (24) achieved similar results by reversing the inhibitory effect of PTU on lymphocyte proliferation following triiodothyronine treatment; nevertheless, the question remains whether the effects generated by the OMC *in vivo* can be reversed by treatment with thyroid hormones. At the same time, some contradictory results demonstrate that the thyroid hormones can have a negative influence on the immune response. Rats with induced hyperthyroidism presented a decrease in the peripheral blood helper/suppressor T cell ratio, while in thyroidectomized rats, this ratio increased, suggesting that thyroid hormones suppress the immune system and that thyroid hormone deficiency is associated with an increase of T lymphocyte activation (48).

In summary, this paper studied the effects of OMC using the non-autoimmune hypothyroidism model to better understand of the role of the thyroid on immune system homeostasis. Our results indicate that the OMC can act directly on lymphocyte

functions; however, T4 supplementation could revive these functions. Our future research will functionally assess the *in vitro* and *in vivo* status of these different cell populations in the immune system in animals exposed to the OMC. The effects of OMC on innate and acquired immunity must be better understood.

DATA AVAILABILITY STATEMENT

All datasets generated for this study are included in the article/supplementary material.

ETHICS STATEMENT

The experimental protocols were in accordance with the Guide for the Care and Use of Animals by the Oswaldo Cruz Foundation prepared by the Comitê de Ética no Uso de Animais (CEUA).

AUTHOR CONTRIBUTIONS

EG, FF, and FA conceived and designed the experiments. FF and FA wrote the paper. TP and MH performed the new experiments required by the referee. All authors performed the experiments and analyzed the data.

FUNDING

This study was financed in part by the Coordenação de Aperfeiçoamento de pessoal de Nível Superior–Brasil (CAPES)-Finance Code 001. We thank the Program PrInt Fiocruz-CAPES for financial support.

REFERENCES

1. Jiménez MM, Pelletier J, Bobin MF, Martini MC. Influence of encapsulation on the *in vitro* percutaneous absorption of octyl methoxycinnamate. *Int J Pharm*. (2004) 272:45–55. doi: 10.1016/j.ijpharm.2003.11.029
2. Puglia C, Damiani E, Offerta A, Rizza L, Tirendi GG, Tarico MS, et al. Evaluation of nanostructured lipid carriers (NLC) and nanoemulsions as carriers for UV-filters: characterization, *in vitro* penetration and photostability studies. *Eur J Pharm Sci.* (2014) 51:211–7. doi: 10.1016/j.ejps.2013.09.023
3. Freitas JV, Peporine Lopes N, Rigo Gaspar L. Photostability evaluation of five UV-filters, trans-resveratrol and beta-carotene in sunscreens. *Eur J Pharm Sci.* (2015) 78:79–89. doi: 10.1016/j.ejps.2015.07.004
4. Gago-Ferrero P, Díaz-Cruz MS, Barceló D. UV filters bioaccumulation in fish from Iberian river basins. *Sci Total Environ.* (2015) 15:518–9:518–25. doi: 10.1016/j.scitotenv.2015.03.026
5. Prado AH, Borges MC, Eloy JO, Peccinini RG, Chorilli M. An ultra-high performance liquid chromatography method to determine the skin penetration of an octyl methoxycinnamate-loaded liquid crystalline system. *Pharmazie.* (2017) 72:563–7. doi: 10.1691/ph.2017.7037
6. Gilbert E, Pirot F, Bertholle V, Roussel L, Falson F, Padois K. Commonly used UV filter toxicity on biologicalfunctions: review of last decade studies. *Int J Cosmet Sci.* (2013) 35:208–19. doi: 10.1111/ics.12030
7. Janjua NR, Kongshoj B, Andersson AM, Wulf HC. Sunscreens in human plasma and urine after repeated whole-body topical application. *J Eur Acad Dermatol Venereol.* (2008) 22:456–61. doi: 10.1111/j.1468-3083.2007.02492.x
8. Schreurs RHMM, Sonneveld E, Jansen JHJ, Seinen W, Burg BVD. Interaction of polycyclic musks and UV Filters with the estrogen receptor (ER), androgen receptor (AR), and progesterone receptor (PR) in reporter gene bioassays. *Toxicol Sci*. (2004) 83:264–72. doi: 10.1093/toxsci/kfi035
9. Axelstad M, Boberg J, Hougaard KS, Christiansen S, Jacobsen PR, Mandrup KR, et al. Effects of pre- and postnatal exposure to the UV-filter octyl methoxycinnamate (OMC) on the reproductive, auditory and neurological development of rat offspring. *Toxicol Appl Pharmacol.* (2011) 250:278–90. doi: 10.1016/j.taap.2010.10.031
10. Jiménez-Díaz I, Molina-Molina JM, Zafra-Gómez A, Ballesteros O, Navalón A, Real M, et al. Simultaneous determination of the UV-filters benzyl salicylate, phenyl salicylate, octyl salicylate, homosalate, 3-(4-methylbenzylidene) camphor and 3-benzylidene camphor in human placental tissue by LC–MS/MS. Assessment of their *in vitro* endocrine activity. *J Chromatogr B.* (2013) 936:80–7. doi: 10.1016/j.jchromb.2013.08.006
11. Krause M, Klit A, Blomberg Jensen M, Søeborg T, Frederiksen H, Schlumpf M, et al. Sunscreens: are they beneficial for health? An overview of endocrine disrupting properties of UV-filters. *Int J Androl.* (2012) 35:424–36. doi: 10.1111/j.1365-2605.2012.01280.x
12. Gelbke HP, Kayser M, Poole A. OECD test strategies and methods for endocrine disruptors. *Toxicology*. (2004) 205:17–25. doi: 10.1016/j.tox.2004.06.034
13. Safe S. Endocrine disruptors and human health: is there a problem. *Toxicology*. (2004) 205:3–10. doi: 10.1016/j.tox.2004.06.032
14. Owens W, Zeiger E, Walker M, Ashby J, Onyon L, Gray LE Jr. The OECD program to validate the rat Hershberger bioassay to screen compounds for *in vivo* androgen and antiandrogen responses. Phase 1: use of a potent agonist and a potent antagonist to test the standardized protocol. *Environ Health Perspect*. (2006) 114:1259–65. doi: 10.1289/ehp.8751
15. Schmutzler C, Hamann I, Hofmann PJ, Kovacs G, Stemmler L, Mentrup B, et al. Endocrine active compounds affect thyrotropin and thyroid hormone levels in serum as well as endpoints of thyroid hormone action in liver, heart and kidney. *Toxicology.* (2004) 205:95–102. doi: 10.1016/j.tox.2004.06.041
16. Hamann I, Hofmann P, Schmutzler C, Mentrup B, Huhne K, Jarry H, et al. 4MBC and OMC, components of UV-sunscreens, exert organ specific alterations on type I 51-Deiodinase activity and expression in female rats. *Exp Clin Endocrinol Diabetes.* (2005) 2005:113–38. doi: 10.1055/s-2005-862997
17. Klammer H, Schlecht C, Wuttke W, Schmutzler C, Gotthardt I, Kohrle J, et al. Effects of a 5-day treatment with the UV-filter octyl-methoxycinnamate (OMC) on the function of the hypothalamo-pituitary–thyroid function in rats. *Toxicology*. (2007) 238:192–9. doi: 10.1016/j.tox.2007.06.088
18. Obregon MJ, Calvo RM, Escobar Del Rey F, Morreale de Escobar G. Ontogenesis of thyroid function and interactions with maternal function. *Endocr Dev*. (2007) 10:86–98. doi: 10.1159/000106821
19. Li Q, Wang B, Mu K, Zhang JA. The pathogenesis of thyroid autoimmune diseases: New T lymphocytes - Cytokines circuits beyond the Th1-Th2 paradigm. *J Cell Physiol*. (2019) 234:2204–16. doi: 10.1002/jcp.27180
20. Ladenson PW. Problems in the management of hypothyroidism. In: Braverman LE, editor. *Diseases of the Thyroid*. Totawa: Humana Press (2003). p. 161–76.
21. Klecha AJ, Barreiro Arcos ML, Frick L, Genaro AN, Cremaschi G. Immunoendocrineinteractions in autoimmune thyroid diseases. *Neuroimmunomodulation*. (2008) 15:68–75. doi: 10.1159/000135626
22. De Vito P, Incerpi S, Pedersen JZ, Luly P, Davis FB, Davis PJ. Thyroid hormones asmodulators of immune activities at the cellular level. *Thyroid.* (2011) 21:879–90. doi: 10.1089/thy.2010.0429
23. Klecha AJ, Genaro AM, Lysionek AE, Caro RA, Coluccia AG, Cremaschi GA. Experimental evidence pointing to the bidirectional interaction between theimmune system and the thyroid axis. *Int J Immunopharmacol.* (2000) 22:491–500. doi: 10.1016/S0192-0561(00)00012-6
24. Klecha AJ, Genaro AM, Gorelik G, Barreiro Arcos ML, Silberman DM, SchumanM, et al. Integrative study of hypothalamus–pituitary–thyroid-immune system interaction: thyroid hormone-mediatedmodulation of

lymphocyte activity through the protein kinase C signaling pathway. *J Endocrinol.* (2006) 189:45–55. doi: 10.1677/joe.1.06137
25. Nikbakht M, Pakbin B, Nikbakht Brujeni G. Evaluation of a new lymphocyte proliferation assay based on cyclic voltammetry; an alternative method. *Sci Rep.* (2019) 9:4503. doi: 10.1038/s41598-019-41171-8
26. Ferraris FK, Rodrigues R, da Silva VP, Figueiredo R, Penido C, Henriques Md. Modulation of T lymphocyte and eosinophil functions *in vitro* by natural tetranortriterpenoids isolated from Carapa guianensis Aublet. *Int Immunopharmacol.* (2011) 11:1–11. doi: 10.1016/j.intimp.2010.09.010
27. Barreiro Arcos ML, Gorelik G, Klecha A, Genaro AM, Cremaschi GA. Thyroid hormones increase inducible nitric oxide synthase gene expression downstream from PKC-zeta in murine tumor T lymphocytes. *Am J Physiol Cell Physiol.* (2006) 291:C327–36. doi: 10.1152/ajpcell.00316.2005
28. Van Wassenaer AG, Stulp MR, Valianpour F, Tamminga P, Stalpers CR, De Randamie JSE, et al. The quantity of thyroid hormone in human milk is too low to influence plasma thyroid hormone levels in the very preterm infant. *Clin Endocrinol.* (2002) 56:621–7. doi: 10.1046/j.1365-2265.2002.01526.x
29. Hapon MB, Simoncini M, Via G, Jahn GA. Effect of hypothyroidism on hormone profiles in virgin, pregnant and lactating rats, and on lactation. *Reproduction.* (2003) 126:371–82. doi: 10.1530/rep.0.1260371
30. Noguchi T, Sugisaki T, Satoh I, Kudo M. Partial restoration of cerebral myelination of the congenitally hypothyroid mouse by parenteral or breast milk administration of thyroxine. *J Neurochem.* (1985) 45:1419–26. doi: 10.1111/j.1471-4159.1985.tb07208.x
31. Janjua NR, Mogensen B, Andersson AM, Petersen JH, Henriksen M, Skakkebaek NE, et al. Systemic absorption of the sunscreens benzophenone-3, octyl-methoxycinnamate, and 3-(4-methyl-benzylidene) camphor after whole-body topical application and reproductive hormone levels in humans. *J Invest Dermatol.* (2004) 123:57–61. doi: 10.1111/j.0022-202X.2004.22725.x
32. Schlumpf M, Durrer S, Faass O, Ehnes C, Fuetsch M, Gaille C, et al. Developmental toxicity of UV filters and environmental exposure: a review. *Int J Androl.* (2008) 31:144–51. doi: 10.1111/j.1365-2605.2007.00856.x
33. Schlumpf M, Kypke K, Wittassek M, Angerer J, Mascher H, Mascher D, et al. Exposure patterns of UV filters, fragrances, parabens, phthalates, organochlor pesticides, PBDEs, and PCBs in human milk: correlation of UV filters with use of cosmetics. *Chemosphere.* (2010) 81:1171–83. doi: 10.1016/j.chemosphere.2010.09.079
34. Schneider S, Deckardt K, Hellwig J, Kuttler K, Mellert W, Schulte S, et al. Octyl methoxycinnamate: two generation reproduction toxicity in Wistar rats by dietary administration. *Food Chem Toxicol.* (2005) 43:1083–92. doi: 10.1016/j.fct.2005.02.013
35. Mallela MK, Strobl M, Poulsen RR, Wendler CC, Booth CJ, Rivkees SA. Evaluation of developmental toxicity of propylthiouracil and methimazole. *Birth Defects Res B Dev Reprod Toxicol.* (2014) 101:300–7. doi: 10.1002/bdrb.21113
36. Anderson GW, Schoonover CM, Jones SA. Control of thyroid hormone action in the developing rat brain. *Thyroid.* (2003) 13:1039–56. doi: 10.1089/105072503770867219
37. Akaike M, Kato N, Ohno H, Kobayashi T. Hyperactivity and spatial maze learning impairment of adult rats with temporary neonatal hypothyroidism. *Neurotoxicol. Teratol.* (1991) 13:317–22. doi: 10.1016/0892-0362(91)90077-A
38. Noda S, Muroi T, Takakura S, Sakamoto S, Takatsuki M, Yamasaki K, et al. Preliminary evaluation of an *in utero*-lactation assay using 6-n-propyl-2-thiouracil. *Arch Toxicol.* (2005) 79:414–21. doi: 10.1007/s00204-004-0641-5
39. Axelstad M, Hansen PR, Boberg J, Bonnichsen M, Nellemann C, Lund SP, et al. Developmental neurotoxicity of propylthiouracil (PTU) in rats: relationship between transient hypothyroxinemia during development and long-lasting behavioural and functional changes. *Toxicol Appl Pharmacol.* (2008) 232:1–13. doi: 10.1016/j.taap.2008.05.020
40. Fabris N, Mocchegiani E, Mariotti S, Pacini F, Pinchera A. Thyroid function modulates thymic endocrine activity. *J Clin Endocrinol Metab.* (1986) 62:474–8. doi: 10.1210/jcem-62-3-474
41. Dardenne M, Savino W, Bach JF. Modulation of thymic endocrine function by thyroid and steroid hormones. *Int J Neurosci.* (1988) 39:325–34. doi: 10.3109/00207458808985719
42. Villa-Verde DM, de Mello-Coelho V, Farias-de-Oliveira DA, Dardenne M, Savino W. Pleiotropic influence of triiodothyronine on thymus physiology. *Endocrinology.* (1993) 133:867–75. doi: 10.1210/endo.133.2.8344222
43. Chen YK, Yeh CL, Chen YL, Wang SC, Cheng RH, Kao PF. The frequency and spectrum of thymus 2-[fluorine-18] fluoro-2-deoxy-D-glucose uptake patterns in hyperthyroidism patients. *Acad Radiol.* (2011) 18:1292–7. doi: 10.1016/j.acra.2011.05.011
44. Yam D, Heller D, Snapir N. The effect of the thyroidal state on the immunological state of the chicken. *Dev Comp Immunol.* (1981) 5:483–90. doi: 10.1016/S0145-305X(81)80060-2
45. Chatterjee S, Chandel AS. Immunomodulatory role of thyroid hormones: *in vivo* effect of thyroid hormones on the blastogenic response of lymphoid tissues. *Acta Endocrinol.* (1983) 103:95–100. doi: 10.1530/acta.0.1030095
46. Hrycek A. Functional characterization of peripheral blood neutrophils in patients with primary hypothyroidism. *Folia Biol.* (1993) 39:304–10.
47. Wolach B, Lebanon B, Jedeikin A, Shapiro MS, Shenkman L. Neutrophil chemotaxis, random migration, and adherence in patients with hyperthyroidism. *Acta Endocrinol.* (1989) 121:817–20. doi: 10.1530/acta.0.1210817
48. Ohashi H, Itoh M. Effects of thyroid hormones on the lymphocyte phenotypes in rats: changes in lymphocyte subsets related to thyroid function. *Endocr Regul.* (1994) 28:117–23.
49. Smekers L, Golstein J, Vanhaelst L. Measurement of thyroxine conversion to triiodothyronine using human lymphocytes. A useful laboratory technique. *J Endocrinol Invest.* (1983) 6:113–7. doi: 10.1007/BF03350582
50. Smith EM, Phan M, Kruger TE, Coppenhaver DH, Blalock JE. Human lymphocyte production of immunoreactive thyrotropin. *Proc Natl Acad Sci USA.* (1983) 80:6010–3. doi: 10.1073/pnas.80.19.6010
51. Csaba G, Kovacs P, Pállinger E. Effect of inhibition of triiodothyronine (T3) production by thiamazole on the T3 and serotonin content of immune cells. *Life Sci.* (2005) 76:2043–52. doi: 10.1016/j.lfs.2004.07.031
52. Csaba G. The immuno-endocrine system: hormones, receptors and endocrine function of immune cells. The packed-transport theory. *Adv Neuroimmune Biol.* (2011) 1:71–85. doi: 10.3233/NIB-2011-007
53. Mariotti S, Caturegli P, Barbesino G, Marinò M, Del Prete GF, Chiovato L, et al. Thyroid function and thyroid autoimmunity independently modulate serum concentration of soluble interleukin 2 (IL-2) receptor (sIL-2R) in thyroid diseases. *Clin Endocrinol.* (1992) 37:415–22. doi: 10.1111/j.1365-2265.1992.tb02352.x
54. Koukkou E, Panayiotidis P, Thalassinos N. Serum soluble interleukin-2 receptors as an index of the biological activity of thyroid hormones in hyperthyroidism. *J Endocrinol Invest.* (1995) 18:253–7. doi: 10.1007/BF03347809
55. Varedi M, Shiri H, Moattari A, Omrani GH, Amirghofran Z. Hyperthyroid state or *in vitro* thyroxine treatment modulates TH1/TH2 responses during exposure to HSV-1 antigens. *J Immunotoxicol.* (2014) 11:160–5. doi: 10.3109/1547691X.2013.816983
56. Pang B, Shin DH, Park KS, Huh YJ, Woo J, Zhang YH, et al. Differential pathways for calcium influx activated by concanavalin A and CD3 stimulation in Jurkat T cells. *Pflugers Arch.* (2012) 463:309–18. doi: 10.1007/s00424-011-1039-x
57. Mocchegiani E, Imberti R, Testasecca D, Zandri M, Santarelli L, Fabris N. Thyroid and thymic endocrine function and survival in severely traumatized patients with or without head injury. *Intensive Care Med.* (1995) 21:334–41. doi: 10.1007/BF01705412

Conflict of Interest: The authors declare that the research was conducted in the absence of any commercial or financial relationships that could be construed as a potential conflict of interest.

frontiers in Endocrinology

ORIGINAL RESEARCH
published: 12 March 2020
doi: 10.3389/fendo.2020.00124

Behavioral Abnormalities in Knockout and Humanized Tau Mice

Rafaella Araujo Gonçalves[1,2], *Nadeeja Wijesekara*[2], *Paul E. Fraser*[2,3]* and *Fernanda G. De Felice*[1,4,5]*

[1] Centre for Neuroscience Studies, Queen's University, Kingston, ON, Canada, [2] Tanz Centre for Research in Neurodegenerative Diseases, University of Toronto, Toronto, ON, Canada, [3] Department of Medical Biophysics, University of Toronto, Toronto, ON, Canada, [4] Department of Psychiatry, Queen's University, Kingston, ON, Canada, [5] Institute of Medical Biochemistry Leopoldo de Meis, Federal University of Rio de Janeiro, Rio de Janeiro, Brazil

Microtubule-associated protein tau assists in stabilizing microtubules and has been particularly implicated in Alzheimer's disease (AD). Given the importance of tau to AD pathogenesis and therapies, it is important to understand non-classic physiological functions for this protein inside and outside the central nervous system (CNS). Our group has previously shown that tau ablation triggers glucose intolerance and pancreatic dysfunction in mice, suggesting that tau plays a role in peripheral metabolic regulation. Little is known about the role of tau in anxiety. Moreover, inconsistent results have been generated regarding the effects of tau deletion in memory. Here, we characterize systemic insulin resistance, anxiety-related behavior and memory in 15 to 20 weeks old Wild-Type (WT), Tau knockout (TauKO) and a distinct hTau mouse model consisting of tau knockout expressing the longest isoform (2N4R) of a non-mutant WT human Tau protein under the prion promoter (hTau). Our findings demonstrate that tau deletion leads to anxiety-related behavior, impaired contextual and cued fear memory. The presence of a human Tau transgene did not ameliorate the phenotypes observed in animals lacking the mouse tau protein and it elicited impairments in learning, memory, and peripheral insulin sensitivity. Our results suggest that tau protein plays a role in memory and anxiety-related behavior. Our findings also indicate that previously unrecognized functions for tau protein may be a complicating factor in using animal models on the TauKO background. Understanding the link between tau pathophysiology and cognitive and metabolic alterations is of great importance to establish the complete contribution of tau protein to AD pathogenesis.

Keywords: Alzheimer's disease, MAPT, Tau protein, insulin, anxiety, metabolism, memory

OPEN ACCESS

Edited by:
Clarissa M. Maya-Monteiro, Oswaldo Cruz Foundation (Fiocruz), Brazil

Reviewed by:
Xavier Xifró, University of Girona, Spain
Sakina Mhaouty-Kodja, Centre National de la Recherche Scientifique (CNRS), France

***Correspondence:**
Paul E. Fraser
paul.fraser@utoronto.ca
Fernanda G. De Felice
felice@bioqmed.ufrj.br

Specialty section:
This article was submitted to Neuroendocrine Science, a section of the journal Frontiers in Endocrinology

Received: *01 October 2019*
Accepted: *24 February 2020*
Published: *12 March 2020*

Citation:
Gonçalves RA, Wijesekara N, Fraser PE and De Felice FG (2020) Behavioral Abnormalities in Knockout and Humanized Tau Mice. Front. Endocrinol. 11:124. doi: 10.3389/fendo.2020.00124

INTRODUCTION

Tau is a microtubule-associated protein abundant in the Central Nervous System (CNS) with its most well-characterized biological function being microtubules polymerization (1, 2). Hyperphosphorylated tau is the main component of Neurofibrillary tangles (NFT) in Alzheimer's Disease (AD) brains (3). In AD, the six Braak stages of the pathology are based on the sequential appearance of NFT in the brain in a hierarchical pattern that correlates with disease severity (4, 5). Tau pathology in the form of NFT correlates with memory loss in normal aging and mild cognitive impairment (MCI) (6, 7). Soluble tau oligomer species isolated from AD patient brains have been implicated in memory impairment, synaptic dysfunction and disease propagation (8–10).

A predominant hypothesis in the AD field is that tau hyperphosphorylation, oligomerization, misfolding, and aggregation into tangles impair synaptic plasticity and contribute to neurodegeneration. These events are probably a result of combined tau gain of toxic function and loss of key physiological function (11, 12). Elucidating unrecognized physiological functions for tau protein is important to better understand the role of this protein in diseases.

The neuropathological spectrum of AD is complex and neuropsychiatric symptoms, particularly depression-related and anxiety, are both reported in patients and considered predictors of disease progression (13–15). Similarly, metabolic alterations are a risk factor and a feature of the AD pathogenesis (16–19). Our group and others have shown that tau ablation triggers glucose intolerance, brain insulin resistance and pancreatic dysfunction in mice, suggesting a physiological role for tau protein in metabolic regulation (20, 21). The effects of tau ablation in mood-related behavior remains to be better elucidated and thus far, inconsistent results have been generated (22–29). Here, we complement our previous metabolic findings on TauKO mouse by investigating the impact of tau loss of function on systemic insulin sensitivity, anxiety-related behavior and memory. We investigate tau gain of toxic function by analyzing the same parameters in a murine Tau knockout mouse expressing the longest isoform of a non-mutant wild type human Tau protein under the prion promoter (hTau).

Our findings show that in the absence of tau, mice develop anxiety-related behavior and memory impairment. Moreover, the insertion of a wild type human tau transgene in TauKO triggered systemic insulin resistance, aggravated memory impairment and did not rescue anxiety phenotype. Notably, hTau present AD-relevant phosphorylation of tau protein and tau oligomers in the neocortex, hippocampus and hypothalamus, when compared to wild type (WT) and TauKO animals.

METHODS

Animal Care

All experiments were approved by the Animal Care Committee at the University of Toronto. TauKO (B6.129X1-Mapttm1Hnd/J) were purchased from Jackson Labs and have been previously described (30). Mice expressing the longest isoform of the microtubule-associated protein tau (MAPT) gene (2N4R) under the control of cos-tet prion promoter were developed using the same technology as previous described (31). Human Tau expressing mice were crossed with TauKO resulting in hTau/TauKO animals on the C57BL/6 background. C57BL/6 mice are referred to as WT and hTau/TauKO as hTau. TauKO and hTau animals were littermates. Male mice were 15 weeks old at the beginning of the experiments. Euthanasia and tissue collection were performed when animals completed 20 weeks of age.

Abbreviations: AD, Alzheimer's disease; BDNF, Brain-derived neurotrophic factor; CNS, Central nervous system; ELISA, Enzyme-linked immunosorbent assay; EZM, Elevated zero maze; FC, Fear Conditioning test; FST, Forced swim test; ITT, Insulin Tolerance Test; LepR, Leptin receptor; LTD, Long-term depression; LTP, Long-term potentiation; MAPT, Microtubule-associated protein tau; MCI, Mild cognitive impairment; NFT, Neurofibrillary tangles; NOR, Novel Object Recognition test; OF, Open Field; TauKO, Tau knockout; TH, Tyrosine hydroxylase; TST, Tail suspension test; WT, Wild type.

Behavioral Analysis

To evaluate anxiety-like behavior and memory, WT, TauKO, and hTau mice were tested for the Open field, Elevated zero maze, Forced swim, Tail suspension, Fear conditioning, Novel object recognition, and Barnes maze behavior tests. Animals were habituated to the testing room at least 1 h prior to testing. The experimenter was blinded to the genotype of the animals for all behavioral studies. All tests were performed between 9:00 and 16:00 in the lights-on cycle. Behavioral effects for each test were observed in at least two independent experiments.

Open Field Test

Open field experiments were carried out in an open field arena measuring 0.3 (w) × 0.3 (d) × 0.45 (h) m and divided into nine squares equal in size as previously described (32, 33). During behavioral sessions, each animal was placed at the center of the open field apparatus in which they were allowed to freely explore the empty arena for a 5-min-long session. The time spent exploring the center vs. the periphery of the arena was recorded by a video camera. Total distance traveled and average speed were evaluated to verify possible effects on locomotor exploratory activities.

Elevated Zero Maze

The elevated zero maze apparatus consists of an annular platform divided into four equal quadrants: Two opposite enclosed and two opposite opened, as previously described (34). In this study, we used a 50 cm in diameter platform elevated 50 cm above the floor. As previously described (35), during behavioral sessions, each animal was placed on one open arm, facing one of the closed arms of the maze, and was then allowed to freely explore the arena for 5 min. The time spent exploring the closed vs. open arms of the apparatus was recorded by a trained researcher blinded to the genotypes.

Forced Swim Test

As previously described (36, 37), one day before the test day, each animal was placed in a 2 L Pyrex glass beaker containing 1,6 L of water at 24 ± 1°C and allowed to freely swim for 15 min. After the 15 min period, the animals were returned to their home cages. On the test day, each mouse was placed individually in a 2 L Pyrex glass beaker containing 1,6 L of water at 24 ± 1°C, for 6 min. A trained researcher blinded to the genotypes recorded immobility time using a stopwatch. The last 4 min of immobility time are plotted in the result graphs. The water was changed between each animal's session.

Tail Suspension Test

As previously described (38, 39), each animal was suspended from a tape on the tail for 6 min and the immobility time was recorded by a trained researcher blinded to the genotypes.

Fear Conditioning

As previously described (40), mice were trained and tested in chambers on three consecutive days in the cued and contextual

fear conditioning paradigm. On Day 1, mice were placed into Context A for a total of 180 s. A tone started at the 60th second and lasted for 90 seconds. A 2 s 0.6 mA foot shock was delivered at 88 and 148th s. On Day 2, mice were placed into Context A and were allowed to explore for 300 s without the tone. Freezing was defined as the absence of movement except that which is required for respiration. On Day 3, mice were placed into Context B and were allowed to explore for 300 s. The tone started at the 120th s and lasted for 180 s. Fear memory for the context (contextual memory) or the tone (cued memory) was obtained by calculating the percentage of freezing on day 2 or 3, respectively. Freezing behavior was recorded by measuring beam breaks in 1 s intervals and analyzed using Freeze Monitor (San Diego Instruments). In our analysis, we set a threshold of two beam breaks to be considered as movement.

Novel Object Recognition Test

As previously described (41, 42), object recognition experiments were carried out in an open field arena measuring 0.3 (w) × 0.3 (d) × 0.45 (h) m^3. Test objects were made of plastic and had different shapes, colors, sizes and textures. During behavioral sessions, objects were fixed with tape to the floor so that the animals could not move it. None of the objects used in our experiments evoked innate preference. Before training, each animal was submitted to a 5-min-long habituation session, in which they were allowed to freely explore the empty arena. Training consisted of a 5-min-long session during which animals were placed at the center of the arena in the presence of two objects. The time spent exploring each object was recorded by a trained researcher. Sniffing and touching the object were considered as exploratory behavior. The arena and objects were cleaned thoroughly between trials with 50% alcohol (vol/vol) to ensure minimal olfactory cues. One hour after training, animals were reinserted into the arena for the test session, when one of the two objects used in the training session was replaced by a new one. The time exploring familiar and novel objects were measured. Results were expressed as percentage of time exploring each object during the training or test sessions.

Barnes Maze

As previously described (43), the Barnes Maze paradigm consists of an elevated and circular platform with 18 equally spaced holes. Under one of the holes, named 'target', a small dark recessed chamber was positioned which the animals could access to escape from the platform. Bright light was used as the aversive stimuli. Visual cues were placed surrounding the maze. Learning, short and long-term memory retention were evaluated. The test consisted of: i. Adaptation period: The animals were placed in the middle of the maze in a cylindrical black chamber for 10 s and then were gently guided to the target hole with the aversive stimuli on. Once the animals reached the target hole, the aversive stimuli were turned off and the animals were kept inside the escape box for 2 min. ii. Spatial acquisition: The animals were placed in the middle of the maze in a cylindrical black chamber for 10 s and then were allowed to freely explore the maze for 3 min with the aversive stimulus on. Primary errors, total errors, primary latency, total latency, were measured by the experimenter. When the animal reached the target hole or when 3 min had elapsed, the mouse was allowed to stay in the target box for 1 min. Animals received 4 trials per day for 4 days, with an inter-trial interval of 15 min. iii. Probe day (short- and long-term memory retention): On day 5 and on day 12, 24 h and 8 days after the last training day, respectively, the probe trials were conducted. The target hole was closed, and the animals were allowed to explore the maze for 90 s. Number of pokes (errors) and latency to reach the virtually target hole, were measured.

Immunoblot Analyses

Mice were euthanatized and the neocortex, hippocampus and hypothalamus were rapidly dissected and frozen in dry ice. For total protein extraction, samples were homogenized in RIPA lysis buffer containing protease and phosphatase inhibitors. Protein concentration was determined using the Pierce BCA Protein Assay Kit. Aliquots containing 20 ug of protein were resolved in 4–20% Mini-PROTEAN TGX Precast Protein Gels (Bio-Rad) and were eletrotransferred to nitrocellulose membranes for 90 min at 100 V. Blots were blocked for 1 h with 10% skim milk in TBS-T at room temperature and were incubated overnight at 4C with primary antibodies diluted in TBS-T. 10 uL of molecular weight markers were run in one lane in every gel (Precision Plus Protein Kaleidoscope, Bio-Rad). The primary antibodies used were the rabbit polyclonal anti-Tau AB0024 (1:100000; DAKO), rabbit polyclonal anti-Tau oligomer T22 (1:100000; Millipore), rabbit polyclonal anti-TauSer199Ser202 (1:1000; ThermoFisher) and mouse monoclonal anti-beta Actin (1:10000; Abcam). After incubation with primary antibodies, membranes were incubated with horseradish peroxidase-conjugated secondary antibody (anti-mouse or anti-rabbit; 1:5000) diluted in TBS-T at room temperature for 2 h. Chemiluminescence was detected using ECL substrate (Amersham) for 5 min and imaged using Azure Biosystems.

Insulin and Leptin Enzyme-Linked Immunosorbent Assay (ELISA)

After 4 h fast, blood was collected in EDTA-coated microvettes (Sarstedt) from tail vein and plasma was isolated. Insulin levels from brain lysates (neocortex, hippocampus, and hypothalamus) and plasma were measured using ultrasensitive insulin ELISA (ALPCO Diagnostics). Leptin levels were measured using a Mouse Leptin ELISA Kit (Crystal Chem).

Insulin Tolerance Test

Following 4 h fast, insulin (1 IU/kg body weight) was injected intraperitoneally and plasma glucose was measured at 0, 15, 30, and 60 from tail vein blood using a glucometer.

Statistical Analysis

Values are expressed as means +/− SEM. Significance was determined using Student's *t*-test or one-way ANOVA followed by Holm-Sidak *post-hoc* test. All analyses were performed with GraphPad Prism6® (GraphPad Software).

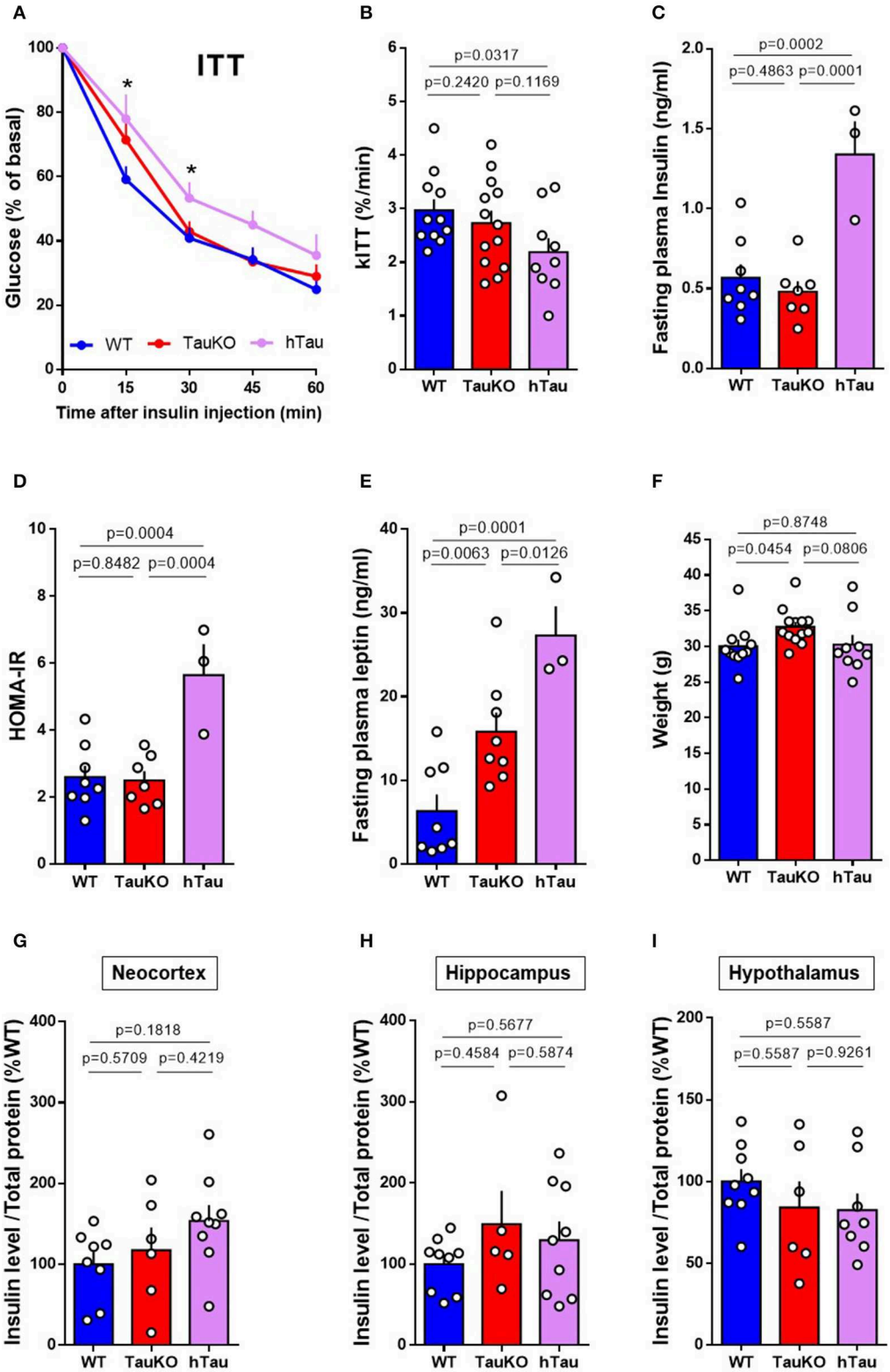

FIGURE 1 | Peripheral insulin sensitivity and brain insulin levels of TauKO and hTau mice. **(A)** Insulin Tolerance Test (ITT) with 20 weeks old WT, TauKO, or hTau mice. After 4 h fasting, mice received 1U/kg of intraperitoneal insulin and blood glucose levels were measured at the designated time points from tail vein blood ($n = 11$ WT; 13 TauKO; 9 hTau). **(B)** Bar graphs representing the kinetic constants for glucose disappearance (Kitt) calculated from the time course plot ($n = 11$ WT; 13 TauKO; 9 hTau). **(C)** Plasma insulin levels after fasting measured by ELISA ($n = 8$ WT; 7 TauKO; 3 hTau). **(D)** HOMA-IR calculated from glucose (mMol/L) and insulin (mU/L)

(Continued)

FIGURE 1 | levels, using the formula: HOMA = fasting glucose (mMol/L) x fasting insulin (mU/L)/22.5 ($n = 8$ WT; 7 TauKO; 3 hTau). **(E)** Plasma leptin levels after fasting measured by ELISA ($n = 8$ WT; 7 TauKO; 3 hTau). **(F)** Body weight ($n = 11$ WT; 13 TauKO; 9 hTau). **(G–I)** Levels of insulin in lysates from the neocortex ($n = 8$ WT; 6 TauKO; 9 hTau), hippocampus ($n = 9$ WT; 5 TauKO; 9 hTau), and hypothalamus ($n = 9$ WT; 6 TauKO; 8 hTau), measured by ELISA. Data are representative of two independent experiments. $^*p < 0.5$.

RESULTS

Peripheral Insulin Sensitivity and Brain Insulin Levels of TauKO and hTau Mice

Tau ablation in mice leads to pancreatic beta cell dysfunction and glucose intolerance (20, 21). In agreement with our previous study (21), here we show that Tau deletion does not affect systemic insulin sensitivity in 20 weeks old mice. WT and TauKO did not show differences in the percentage of blood glucose reduction after intraperitoneal injection of insulin during the Insulin Tolerance Test (ITT) (**Figures 1A,B**). Fasting plasma insulin levels (**Figure 1C**) and HOMA-IR index (**Figure 1D**) also did not differ between WT and TauKO mice. Surprisingly, the insertion of a transgene that encodes the longest isoform of human Tau (2N4R) triggered insulin resistance in TauKO animals. hTau mice displayed insulin resistance in the ITT (**Figures 1A,B**), increased fasting plasma insulin levels (**Figure 1C**) and higher HOMA-IR index (**Figure 1D**) when compared to WT and TauKO.

Augmented body weight and hyperleptinemia were previously reported following tau ablation in mice (20, 21). Interestingly, although in our current study the hTau transgene aggravates hyperleptinemia (**Figure 1E**), hTau expression seems to correct the increase in body weight resulted from tau deletion (**Figure 1F**). Therefore, hyperleptinemia in hTau mice might result from other factors than increased fat mass.

Brain insulin has been implicated in the modulation of metabolism and neurobehavior in rodents (44, 45). Moreover, tau ablation promotes insulin resistance in the brain of mice (20). To investigate whether insulin levels were altered in the brains of TauKO and hTau, the levels of insulin in the neocortex (**Figure 1G**), hippocampus (**Figure 1H**) and hypothalamus (**Figure 1I**) were determined by ELISA. However, no statistical differences were observed between the experimental groups.

In summary, our results show that the presence of a hTau transgene impairs peripheral insulin sensitivity and systemic leptin levels at 20 weeks of age, without affecting insulin levels in different brain regions.

Patterns of Anxiety-Related Behaviors in TauKO and hTau Mice

Impaired metabolic regulation is associated with anxiety symptoms (46, 47). Therefore, we investigated anxiety-related behavior in 15–19 weeks old WT and TauKO mice at the open field (OF), elevated zero maze (EZM), forced swim, and tail suspension behavior tests. TauKO spent significantly less time in the open arms of the EZM (**Figure 2A**), and in the central area of the OF apparatus (**Figure 2B**), when compared to WT animals. In addition to that, TauKO moved more in the periphery of the OF arena (**Figure 2C**). The reduced time exploring the center of the OF and open arms of the EZM indicate higher anxiogenic behavior in TauKO when compared to WT mice (33, 35). Tau ablation also affected the locomotor exploratory activity of mice during the OF test indicated by increased total ambulatory distance (**Figure 2D**) and average speed (**Figure 2E**). Unexpectedly, the insertion of a human tau transgene did not correct anxiety-related behaviors of TauKO animals. Similar to TauKO, hTau mice spent less time in the open arms of the EZM and in the center of the OF apparatus (**Figures 2A,B**), exhibited increased peripheral (**Figure 2C**) and total ambulatory distance (**Figure 2D**), and augmented average speed (**Figure 2E**).

The tail suspension (TST) and forced swim (FST) tests are commonly used for the detection of behavior despair in mice and for the screening of antidepressants (48). In this context, increased immobility time indicates depressive-like behavior (36, 39). However, studies have suggested the use of TST and FST for the detection of anxiety-related behavior arguing that reduced immobility time in these tests results from exacerbated escape-directed behavior caused by an anxiogenic phenotype (49). Here, we report reduced immobility time of 15–19 weeks old TauKO and hTau mice in the FST (**Figure 2F**) and TST (**Figure 2G**) when compared to WT animals. We believe that these results do not represent an antidepressant-like response but is instead caused by the anxiogenic effect of knocking out Tau that is not corrected by the addition of the hTau transgene in the hTau mice. In agreement with this idea, linear regression analysis showed a positive correlation between immobility time in the TST and time spent in center of the OF arena (**Figure 2H**). Similar to previous reports (50, 51), we observed an inverse relationship between behavior despair and anxiety-related behavior in our mouse cohort. In summary, our results indicate that whole-body murine tau deletion leads to anxiety-related behavior that is not corrected by the presence of a human tau transgene.

Performance in the Fear Conditioning, Novel Object Recognition and Barnes Maze Behavior Tests

Poor glycemic control is associated with cognitive decline (52, 53). Therefore, to determine the effect of tau deletion on memory, 15–19 weeks old WT and TauKO mice were subjected to the Fear conditioning (FC), Novel object recognition (NOR) and Barnes maze tests.

Fear conditioning was performed to assess hippocampal and amygdala learning and memory. In contextual fear conditioning, TauKO mice displayed reduced freezing behavior when compared to WT animals (**Figure 3A**). In cued fear, when animals were placed in a new context but with the same auditory conditioned stimulus, TauKO showed a more pronounced reduction in freezing than WT animals (**Figure 3B**).

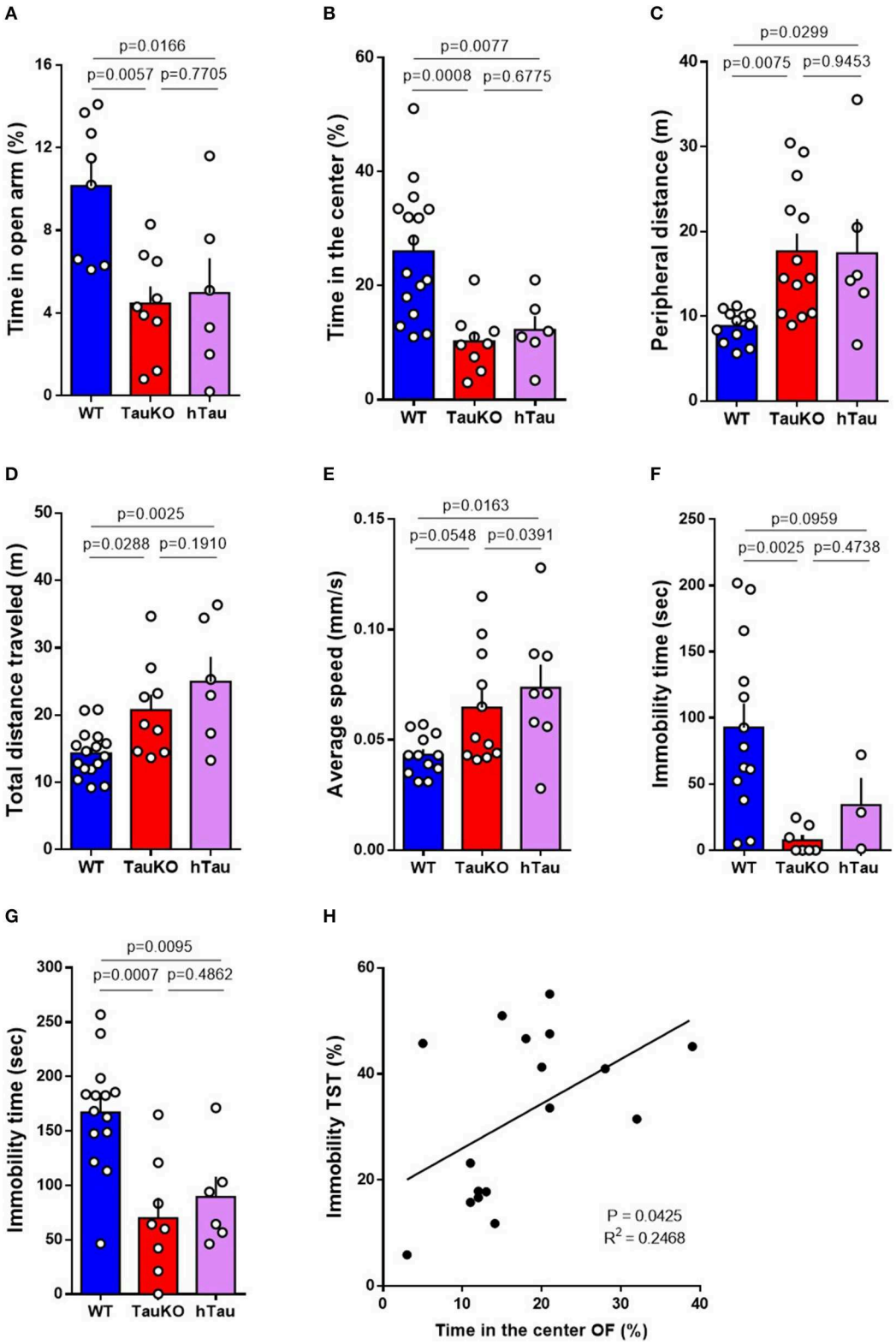

FIGURE 2 | Patterns of anxiety-related behaviors in TauKO and hTau mice. **(A)** Analysis of the time spent in the open arms of the elevated zero maze expressed in percentage of time relative to the 5 min' test length. Test performed with 15–19 weeks old WT, TauKO, and hTau mice (n = 8 WT; 9 TauKO; 6 hTau). **(B–E)** Open field test performed with 15–19 weeks old WT, TauKO, and hTau mice (n = 12–16 WT; 9–13 TauKO; 6–8 hTau). **(B)** Analysis of the time spent in the center of the apparatus expressed in percentage of time relative to the 5 min' test length. **(C)** Analysis of the total distance moved in the periphery of the apparatus. **(D)** Analysis of the total

(Continued)

FIGURE 2 | distance traveled in the whole apparatus. **(E)** Analysis of the average speed during the test. **(F)** Time of immobility during the forced swim test performed with 15–19 weeks old WT, TauKO, and hTau mice ($n = 13$ WT; 7 TauKO; 3 hTau). **(G)** Time of immobility during the tail suspension test performed with 15–19 weeks old WT, TauKO, and hTau mice ($n = 14$ WT; 8 TauKO; 6 hTau). **(H)** Correlation of immobility time during the TST and time spent in the center of the OF for each mouse. Values expressed in percentage of time relative to the total length of the tests. Data are representative of at least two independent experiments.

Similarly, hTau mice had reduced freezing when compared to WT in both tests.

The novel object recognition (NOR) test involves several brain regions of learning and memory. During the acquisition/training phase, WT, TauKO and hTau mice were exposed to two objects for 5 min and no object preference was observed (**Figure S1A**). After 1-h interval, each animal was individually reintroduced to the apparatus and allowed to explore one familiar and one novel object for 5 min. By definition, animals that recognize the familiar object (i.e., normal learning) explore the novel object for a time significantly higher than 50% of the total time. Our results show that while WT and TauKO mice correctly discriminated between familiar and novel object (**Figure 3C**), hTau mice displayed impaired object recognition memory indicated by the lack of preference for the novel object over the familiar one (**Figure 3C**). Total exploration time and time exploring the new object did not exhibit statistically significant differences for the various test groups (**Figures S1B,C**).

Lastly, Barnes maze was performed to assess non-hippocampal contributions to spatial memory. During the acquisition training phase of the test, while WT and TauKO mice displayed similar total latency and errors to enter the target hole during the trials, hTau mice showed impaired learning indicated by increase in total errors and total latency (**Figures 3D,E**). The latency to find the target zone (**Figure 3F**) and the time spent in this area 24 h (**Figure 3G**) after the last training trial, probe day 5, did not differ between the experimental groups. Histograms representing the mean number of nose pokes in each hole of the Barnes Maze during the probe day 5 are depicted (**Figure S2A**) and no statistical difference was detected regarding the % of pokes in the target hole ($p = 0.7537$ between WT and TauKO; $p = 0.6480$ between WT and hTau; $p = 0.7537$ between TauKO and hTau. One-way ANOVA). Similar results were observed when these parameters were analyzed 8 days after the last training trial, probe day 12 (**Figures S2B–D**). Primary errors (**Figure S2E**) and primary latency (**Figure S2F**) were also similar between the experimental groups.

In summary, our results indicate that Tau deletion leads to defective associative fear memory in mice that is not corrected by a hTau transgene. On the other hand, object recognition and spatial memory are not affected by tau ablation and are impaired after the addition of a hTau transgene in the hTau mice.

Phospho-Tau and Tau Oligomers Are Increased in Multiple Brain Regions of hTau Mice

Tau oligomers and pTauSer199Ser202 are detected in *post-mortem* AD brains and are believed to play a role in AD pathophysiology (54, 55). Therefore, to investigate a possible gain of toxic function for tau as an underlying mechanism for the behavioral alterations observed in hTau mice, we investigated the presence of AD-relevant phosphorylation of tau protein and tau oligomers in the neocortex, hippocampus and hypothalamus of hTau mice. Immunoblotting results targeting total tau protein confirmed the absence of tau in the TauKO mice and the presence of tau in the neocortex, hippocampus and hypothalamus of 20 weeks old WT and hTau mice (**Figure 4**). Tau Oligomers (**Figures 4A–C**) and phosphorylated tau at the Serine-202 and Serine-199 residues (**Figures 4D–F**) were detected in the neocortex, hippocampus and hypothalamus of hTau mice by immunoblotting analysis. Intriguingly, while phospho-tau levels were elevated in the neocortex and hippocampus of hTau mice when compared to WT animals, no changes were observed in the hypothalamus. Conversely, tau oligomers were consistently elevated in the different brain regions.

DISCUSSION

The present study provides evidence for a role of tau protein in anxiety and memory. Tau ablation in mice led to anxiety-related behavior and memory impairment. We also showed that the insertion of a human tau transgene in TauKO mice triggered peripheral insulin resistance, aggravated memory impairment and did not ameliorate anxiety phenotype in 15–20 weeks old animals.

Tau protein was first described in 1975 as a factor essential for microtubule assembly and polymerization in the porcine brain (1). In 1986, hyperphosphorylated tau was identified as one the main constituents of neurofibrillary tangles in the AD brain (3). The timeline of the scientific discoveries involving tau led to investigations on the role of this protein in the brain and in diseases. However, tau is expressed in a variety of tissues (56–58) and understanding unknown physiological functions for this protein inside and outside the CNS is key to understand the role of tau in the pathophysiology of diseases. Although tau deletion is not lethal (59), tau knockout mice have been instrumental to the understanding of novel functions for tau protein in physiology and in pathology (60).

Metabolic syndrome and insulin resistance are associated with cognitive dysfunction and AD (53, 61–65). Therefore, because of our previous publication showing impaired glucose-stimulated insulin secretion in TauKO and hTau mice (21), and our recent finding demonstrating insulin resistance in hTau animals, we initially hypothesized that the levels of insulin getting to the brain of these mouse models would be reduced. However, we did not find statistical differences in the levels of insulin in the neocortex, hippocampus and hypothalamus between the experimental groups. Considering the proposed role for tau protein in the regulation of insulin signaling in the hippocampus (20), it is likely that the behavioral alterations of

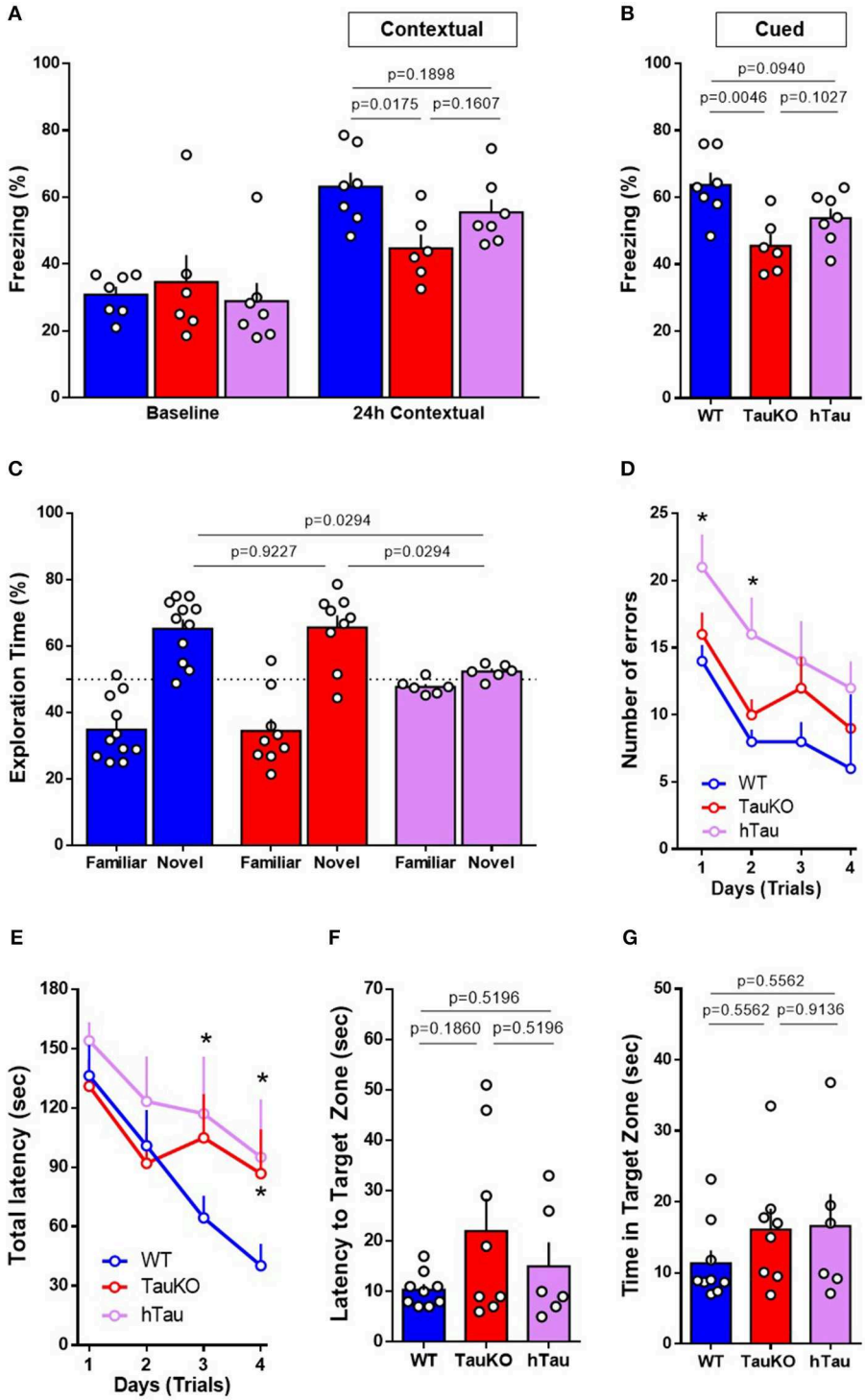

FIGURE 3 | Performance in the Fear Conditioning, Novel Object Recognition and Barnes Maze behavior tests. **(A,B)** Fear conditioning test performed with 15–19 weeks old WT, TauKO, and hTau mice ($n = 7$ WT; 6 TauKO; 7 hTau). Percentage of freezing behavior during the **(A)** contextual and **(B)** cued FC. **(C)** Novel object recognition test performed with 15–19 weeks old WT, TauKO, and hTau mice ($n = 11$ WT; 9 TauKO; 6 hTau). Exploration time of familiar and novel objects during the test phase. Time expressed in percentage. **(D–G)** Barnes maze test performed with 15–19 weeks old WT, TauKO, and hTau mice ($n = 9$ WT; 8 TauKO; 6 hTau). **(D)** Total number of errors and **(E)** Total latency to find the target zone in 4 different trials/day, for 4 days during the acquisition/training phase of the Barnes maze test. **(F)** Latency to find and **(G)** time in the target zone 24 h after the last training trial as a measure of spatial reference memory. Data are representative of at least two independent experiments. $^*p < 0.5$.

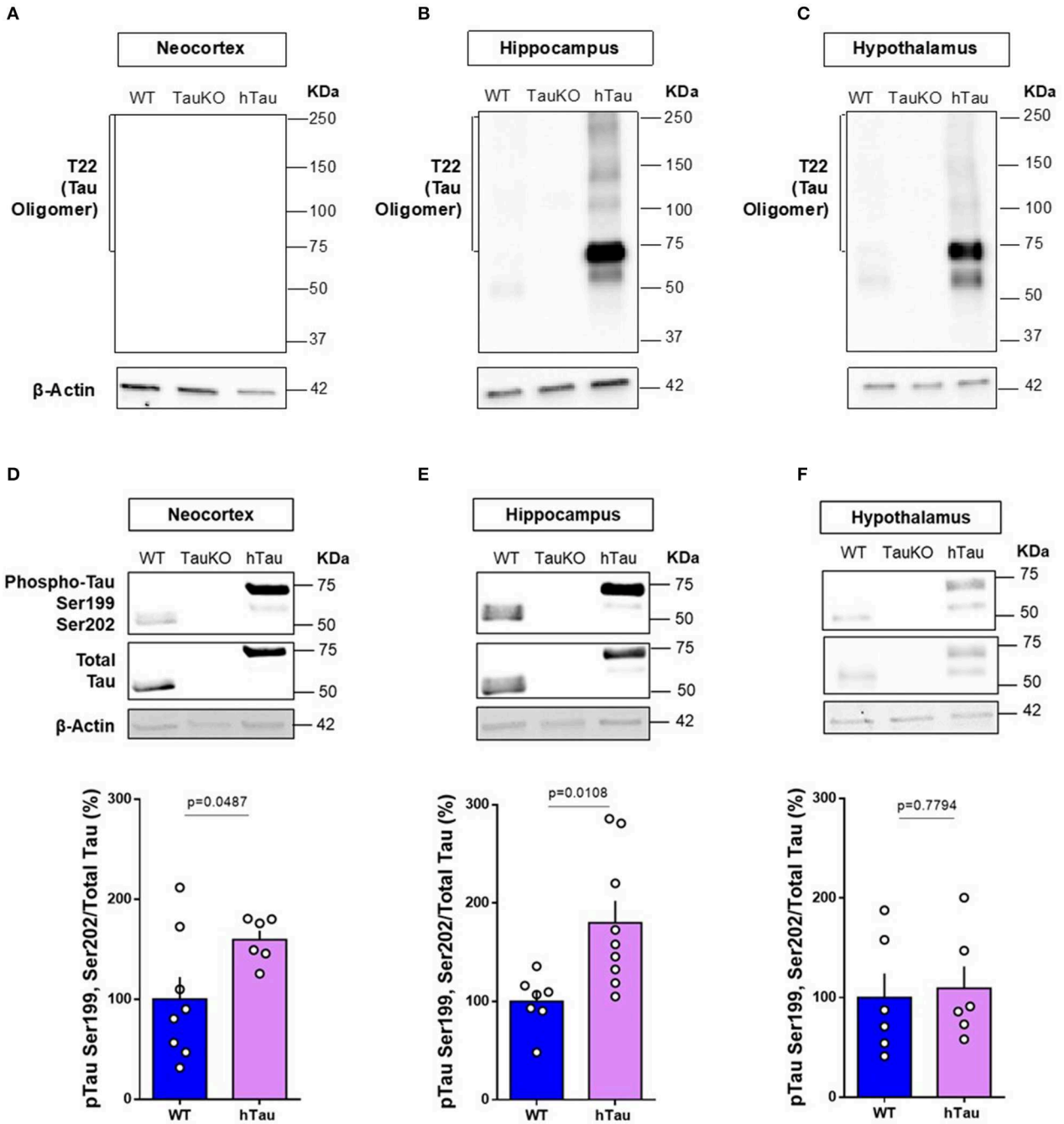

FIGURE 4 | Phospho-tau and tau oligomers are increased in multiple brain regions of hTau mice. Immunoblot analysis of Tau Oligomers in **(A)** cortical, **(B)** hippocampal, and **(C)** hypothalamic lysates from 20 weeks old WT, TauKO, and hTau mice. Immunoblot analysis of pTauSer199Ser202/TotalTau ratio in **(D)** cortical (n = 8 WT; 6 hTau), **(E)** hippocampal (n = 7 WT; 9 hTau) and **(F)** hypothalamic (n = 6 WT; 6 hTau) lysates from 20 weeks old WT, TauKO, and hTau mice.

TauKO and hTau result from impaired insulin signaling instead of reduced hormonal levels in the brain. Further studies aiming to investigate insulin signaling pathway in different brain regions of hTau mice are warranted.

Anxiety is reported in up to 75% of AD patients (66) and it is associated with increased rates of conversion from MCI to AD (14). Here, we show that 15–19 weeks old TauKO and hTau mice displayed anxiety-related behavior in the elevated zero maze, open field, forced swim and tail suspension tests. Hyperactivity was also observed, characterized by increased total ambulatory locomotion and average speed in the OF arena. Interestingly, a positive correlation was found between the time spent in the

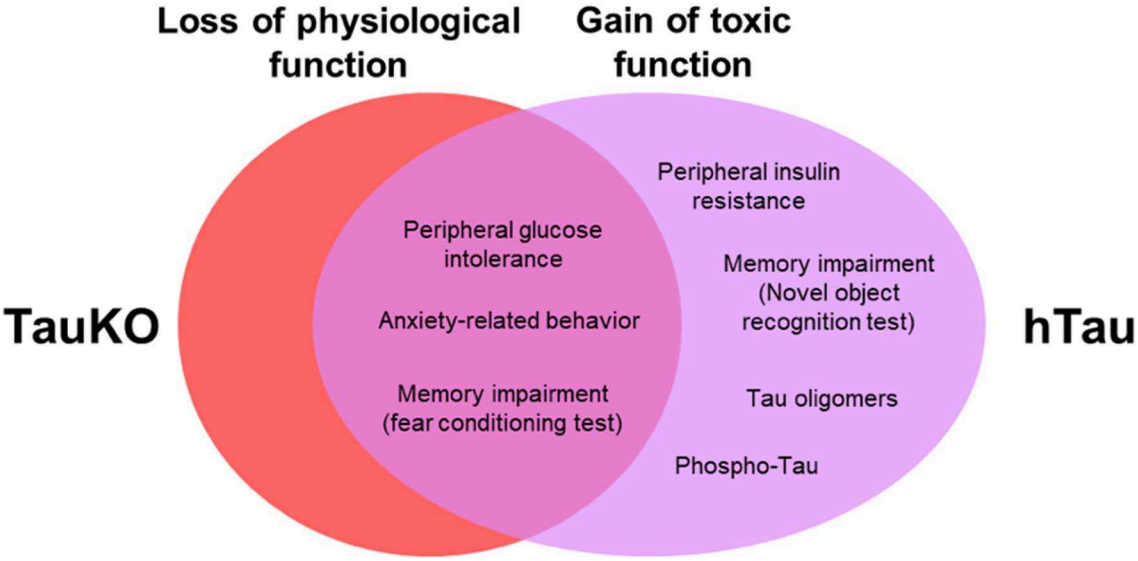

FIGURE 5 | Behavioral and metabolic alterations in TauKO and hTau mice. Here, we hypothesize that tau loss of function in the knockout, and a combined loss and gain of toxic function for tau in the hTau mice, underlie the behavioral and metabolic alterations observed in both mouse models in this study.

center of the OF apparatus and the immobility time during the tail suspension test. As suggested by a recent commentary (49), and in validation of our correlational results, we believe that the reduced immobility in the FST and TST is a measure of anxiety behavior/hyperactivity rather than an antidepressant effect of tau deletion in mice. The mechanisms underlying the increase in anxiety-like behavior following tau ablation in mice are unknown and may involve several mechanisms. Conversely, other studies did not detect an anxiogenic phenotype in 6 or 7-months-old TauKO mice in the zero maze (29) and open field (26) behavior tests. These differences in results might be due to the age, strain and sex of the animals, as well as behavior test protocol used in each study.

Impaired metabolic regulation is associated with anxiety behavior (46, 47). Therefore, it is possible that the severe glucose intolerance in TauKO and hTau mice (21) is involved in the increase of anxiety-related behavior reported in this study. Moreover, leptin is an adipokine-derived hormone upregulation of which triggers anxiolytic phenotype in mice (67) and deficiency results in anxiogenic-like behavior (68, 69). Plasma leptin levels are associated with the emotional state of individuals throughout the day (70) and serum leptin and leptin resistance correlated with anxiety symptoms in patients with type 2 diabetes (T2D) (71). Therefore, the augmented circulating leptin levels reported in TauKO and hTau mice (**Figure 1E**) could be involved in the anxiogenic phenotype observed in these animals, probably as a consequence of leptin resistance following chronic hyperleptinemia.

The dopaminergic system plays an important role in the modulation of anxiety behaviors (72). The enzyme tyrosine hydroxylase (TH) catalyzes the reaction of L-DOPA formation, which precedes its conversion in dopamine. In line with that, although one study reported mild dopaminergic deficits in aged but not in adult TauKO mice (24), other investigators have showed reduced TH-positive nigral neurons and decreased TH expression in the substantia nigra of adult TauKO animals (22, 73). Therefore, it is possible that tau ablation impacts the homeostasis of the dopaminergic system resulting in anxiety-behavior in mice.

Memory loss is a widely known clinical manifestation of AD. However, conflicting results have been generated regarding the impact of tau deletion on memory in mice (22–29). In this study, we investigated memory integrity using three distinct behavior tests. Fifteen to nineteen weeks old TauKO mice showed impaired associative learning in the fear conditioning (FC) paradigm and no alterations in object recognition or spatial and learning memory in the novel object recognition (NOR) and Barnes maze, respectively. Impaired performance in the FC test is associated with defective hippocampal and amygdala function (74, 75), while memory defects in the NOR task are sensitive to cortical injuries (76). Therefore, our results suggest that tau ablation in mice differently impacts memory-related brain regions.

Tau protein plays a role in the regulation of synaptic function (11). Accordingly, a role for tau in synaptic plasticity has been suggested by reports showing deficits in hippocampal long-term potentiation (LTP) and/or long-term depression (LTD) (26, 29, 77), as well as reduced hippocampal brain-derived neurotrophic factor (BDNF) levels following tau deletion or knockdown in mice (22, 78). Therefore, impairments in synaptic plasticity might be involved in the behavioral alterations reported in TauKO and hTau, in this study.

Tau is an intrinsically unfolded and soluble protein that undergoes a number of post-translational modifications that affect its structure and therefore its function inside the cells. Among these modifications, hyperphosphorylation has been

implicated in the pathogenesis of AD due to its capability of affecting tau self-assembly, aggregation and its accumulation into Neurofibrillary tangles (NFT) (3). The phosphorylation of tau at Ser199/Ser202 is particularly increased in human AD brains (54) and tau oligomers were isolated from the brains of patients (8, 55). The cerebral accumulation of soluble small oligomeric tau species correlates with neuronal loss, synaptic dysfunction and behavior alterations associated with AD (9, 10). Therefore, in addition to the physiological function of tau in synaptic activity, pathological tau can induce synaptic damage in AD.

In conjunction with the behavioral changes, elevated tau oligomers were observed in cognitive-related (neocortex and hippocampus) and metabolic-related (hypothalamus) brain regions of hTau mice. Increased tau phosphorylation at Serine-199 and Serine-202 residues were also detected in the neocortex and hippocampus of these animals. Therefore, toxic gain of tau function in hTau mice might be elicited by the phosphorylated and oligomeric tau species detected in these animals. In terms of loss of function, because tau isoforms differ between humans and rodents (79), human tau might not compensate for the absence of endogenous murine tau in the humanized mice. Therefore, an imbalance in the tau isoforms expressed in different brain and peripheral tissues of hTau mice might explain the lack of compensation of this model.

Collectively, our results from TauKO mice suggest a physiological role for tau in anxiety-related behavior and memory. Results from hTau mice demonstrate that the presence of a non-mutant WT human tau triggers insulin resistance, elicit impairments in spatial learning and object recognition memory, and does not restore anxiety, memory and metabolic alterations in mice lacking endogenous murine tau (**Figure 5**). Our findings also suggest that previously unrecognized functions for tau protein is a potentially complicating factor in using animal models on the TauKO background. Understanding the link between tau pathophysiology, and cognitive and metabolic alterations is of great importance to establishing the complete contribution of tau protein to AD pathogenesis.

DATA AVAILABILITY STATEMENT

The datasets generated for this study are available on request to the corresponding author.

ETHICS STATEMENT

The animal study was reviewed and approved by the Local Animal Care Committee (LACC) at the University of Toronto. Animal Use Protocol number 5832.

AUTHOR CONTRIBUTIONS

RG designed the experiments, acquired, analyzed, and interpreted the data, and drafted the manuscript. NW contributed to the acquisition and interpretation of data. FD and PF provided substantial contributions to the conception of the study, experimental design, and data interpretation. All authors revised and approved the final version of the manuscript.

FUNDING

Work from PF laboratory was supported by grants from Canadian Institutes of Health Research (CIHR) (MOP-115056) and the Alzheimer Society of Ontario. Work from FD laboratory was supported by grants from Alzheimer's Society Canada and the Weston Brain Institute, National Institute for Translational Neuroscience (INNT/Brazil) (465346/2014-6), and the Brazilian funding agencies Conselho Nacional de Desenvolvimento Científico e Tecnológico (CNPq) (473324/2013-0) and Fundação de Amparo à Pesquisa do Estado do Rio de Janeiro (FAPERJ) (202.944/2015). NW was supported by a postdoctoral fellowship from Diabetes Canada.

SUPPLEMENTARY MATERIAL

The Supplementary Material for this article can be found online at: https://www.frontiersin.org/articles/10.3389/fendo.2020.00124/full#supplementary-material

REFERENCES

1. Weingarten MD, Lockwood AH, Hwo SY, Kirschner MW. A protein factor essential for microtubule assembly. *Proc Natl Acad Sci USA*. (1975) 72:1858–62. doi: 10.1073/pnas.72.5.1858
2. Cleveland DW, Hwo SY, Kirschner MW. Purification of tau, a microtubule-associated protein that induces assembly of microtubules from purified tubulin. *J Mol Biol*. (1977) 116:207–25. doi: 10.1016/0022-2836(77)90213-3
3. Grundke-Iqbal I, Iqbal K, Quinlan M, Tung YC, Zaidi M, Wisniewski HM. Microtubule-associated protein tau. A component of Alzheimer paired helical filaments. *J Biol Chem*. (1986) 261:6084–9.
4. Braak H, Braak E. Neuropathological stageing of Alzheimer-related changes. *Acta Neuropathol*. (1991) 82:239–59. doi: 10.1007/BF00308809
5. Braak H, Alafuzoff I, Arzberger T, Kretzschmar H, Del Tredici K. Staging of Alzheimer disease-associated neurofibrillary pathology using paraffin sections and immunocytochemistry. *Acta Neuropathol*. (2006) 112:389–404. doi: 10.1007/s00401-006-0127-z
6. Arriagada PV, Marzloff K, Hyman BT. Distribution of Alzheimer-type pathologic changes in non-demented elderly individuals matches the pattern in Alzheimer's disease. *Neurology*. (1992) 42:1681–8. doi: 10.1212/WNL.42.9.1681
7. Guillozet AL, Weintraub S, Mash DC, Mesulam MM. Neurofibrillary tangles, amyloid, and memory in aging and mild cognitive impairment. *Arch Neurol*. (2003) 60:729–36. doi: 10.1001/archneur.60.5.729
8. Maeda S, Sahara N, Saito Y, Murayama S, Ikai A, Takashima A. Increased levels of granular tau oligomers: an early sign of brain aging and Alzheimer's disease. *Neurosci Res*. (2006) 54:197–201. doi: 10.1016/j.neures.2005.11.009
9. Lasagna-Reeves CA, Castillo-Carranza DL, Sengupta U, Clos AL, Jackson GR, Kayed R. Tau oligomers impair memory and induce synaptic and mitochondrial dysfunction in wild-type mice. *Mol Neurodegener*. (2011) 6:39. doi: 10.1186/1750-1326-6-39
10. Castillo-Carranza DL, Gerson JE, Sengupta U, Guerrero-Muñoz MJ, Lasagna-Reeves CA, Kayed R. Specific targeting of tau oligomers in Htau mice prevents cognitive impairment and tau toxicity following injection with brain-derived tau oligomeric seeds. *J Alzheimers Dis*. (2014) 40(Suppl.1):S97–111. doi: 10.3233/JAD-132477

11. Pooler AM, Noble W, Hanger DP. A role for tau at the synapse in Alzheimer's disease pathogenesis. *Neuropharmacology*. (2014) 76:1–8. doi: 10.1016/j.neuropharm.2013.09.018
12. Congdon EE, Sigurdsson EM. Tau-targeting therapies for Alzheimer disease. *Nat Rev Neurol*. (2018) 14:399–415. doi: 10.1038/s41582-018-0013-z
13. Donovan NJ, Locascio JJ, Marshall GA, Gatchel J, Hanseeuw BJ, Rentz DM, et al. Longitudinal association of amyloid beta and anxious-depressive symptoms in cognitively normal older adults. *Am J Psychiatry*. (2018) 175:530–7. doi: 10.1176/appi.ajp.2017.17040442
14. Mah L, Binns MA, Steffens DC, Alzheimer's Disease Neuroimaging Initiative. Anxiety symptoms in amnestic mild cognitive impairment are associated with medial temporal atrophy and predict conversion to Alzheimer disease. *Am J Geriatr Psychiatry*. (2015) 23:466–76. doi: 10.1016/j.jagp.2014.10.005
15. Geda YE, Roberts RO, Mielke MM, Knopman D, Christianson TJ, Pankratz VS, et al. Baseline neuropsychiatric symptoms and the risk of incident mild cognitive impairment: a population-based study. *Am J Psychiatry*. (2014) 171:572–81. doi: 10.1176/appi.ajp.2014.13060821
16. Janson J, Laedtke T, Parisi JE, O'Brien P, Petersen R, Butler PC. Increased risk of type 2 diabetes in Alzheimer disease. *Diabetes*. (2004) 53:474–81. doi: 10.2337/diabetes.53.2.474
17. Turner R, Craft S, Aisen P. Individuals with Alzheimer's disease exhibit a high prevalence of undiagnosed impaired glucose tolerance and type 2 diabetes mellitus. *Alzheimer's Dementia*. (2013) 9:P284–5. doi: 10.1016/j.jalz.2013.05.573
18. Ott A, Stolk RP, van Harskamp F, Pols HA, Hofman A, Breteler MM. Diabetes mellitus and the risk of dementia: the Rotterdam study. *Neurology*. (1999) 53:1937–42. doi: 10.1212/WNL.53.9.1937
19. Wijesekara N, Gonçalves RA, De Felice FG, Fraser P. Impaired peripheral glucose homeostasis and Alzheimer's disease. *Neuropharmacology*. (2017) 136:172–81. doi: 10.1016/j.neuropharm.2017.11.027
20. Marciniak E, Leboucher A, Caron E, Ahmed T, Tailleux A, Dumont J, et al. Tau deletion promotes brain insulin resistance. *J Exp Med*. (2017) 214:2257–69. doi: 10.1084/jem.20161731
21. Wijesekara N, Gonçalves RA, Ahrens R, De Felice FG, Fraser PE. Tau ablation in mice leads to pancreatic β cell dysfunction and glucose intolerance. *FASEB J*. (2018) 32:3166–73. doi: 10.1096/fj.201701352
22. Lei P, Ayton S, Finkelstein DI, Spoerri L, Ciccotosto G, Wright DK, et al. Tau deficiency induces parkinsonism with dementia by impairing APP-mediated iron export. *Nat Med*. (2012) 18:291–5. doi: 10.1038/nm.2613
23. Lei P, Ayton S, Moon S, Zhang Q, Volitakis I, Finkelstein D, et al. Motor and cognitive deficits in aged tau knockout mice in two background strains. *Mol Neurodegener*. (2014) 9:29. doi: 10.1186/1750-1326-9-29
24. Morris M, Hamto P, Adame A, Devidze N, Masliah E, Mucke L. Age-appropriate cognition and subtle dopamine-independent motor deficits in aged tau knockout mice. *Neurobiol Aging*. (2013) 34:1523–9. doi: 10.1016/j.neurobiolaging.2012.12.003
25. Ikegami S, Harada A, Hirokawa N. Muscle weakness, hyperactivity, and impairment in fear conditioning in tau-deficient mice. *Neurosci Lett*. (2000) 279:129–32. doi: 10.1016/S0304-3940(99)00964-7
26. Ahmed TA, Van der Jeugd, Blum D, Galas MC, D'Hooge R, Buee L, et al. Cognition and hippocampal synaptic plasticity in mice with a homozygous tau deletion. *Neurobiol Aging*. (2014) 35:2474–8. doi: 10.1016/j.neurobiolaging.2014.05.005
27. Dawson HN, Cantillana V, Jansen M, Wang H, Vitek MP, Wilcock DM, et al. Loss of tau elicits axonal degeneration in a mouse model of Alzheimer's disease. *Neuroscience*. (2010) 169:516–31. doi: 10.1016/j.neuroscience.2010.04.037
28. Tan DCS, Yao S, Ittner A, Bertz J, Ke YD, Ittner LM, et al. Generation of a New Tau Knockout (tauΔex1) line using CRISPR/Cas9 genome editing in mice. *J Alzheimers Dis*. (2018) 62:571–8. doi: 10.3233/JAD-171058
29. Biundo F, Del Prete D, Zhang H, Arancio O, D'Adamio L. A role for tau in learning, memory and synaptic plasticity. *Sci Rep*. (2018) 8:3184. doi: 10.1038/s41598-018-21596-3
30. Dawson HN, Ferreira A, Eyster MV, Ghoshal N, Binder L, Vitek MP. Inhibition of neuronal maturation in primary hippocampal neurons from tau deficient mice. *J Cell Sci*. (2001) 114:1179–87.
31. Murakami T, Paitel E, Kawarabayashi T, Ikeda M, Chishti MA, Janus C, et al. Cortical neuronal and glial pathology in TgTauP301L transgenic mice: neuronal degeneration, memory disturbance, and phenotypic variation. *Am J Pathol*. (2006) 169:1365–1375. doi: 10.2353/ajpath.2006.051250
32. Fortuna JTS, Gralle M, Beckman D, Neves FS, Diniz L, Frost PS, et al. Brain infusion of α-synuclein oligomers induces motor and non-motor Parkinson's disease-like symptoms in mice. *Behav Brain Res*. (2017) 333:150–60. doi: 10.1016/j.bbr.2017.06.047
33. Prut L, Belzung C. The open field as a paradigm to measure the effects of drugs on anxiety-like behaviors: a review. *Eur J Pharmacol*. (2003) 463:3–33. doi: 10.1016/S0014-2999(03)01272-X
34. Shepherd JK, Grewal SS, Fletcher A, Bill DJ, Dourish CT. Behavioural and pharmacological characterisation of the elevated "zero-maze" as an animal model of anxiety. *Psychopharmacology*. (1994) 116:56–64. doi: 10.1007/BF02244871
35. Biallosterski BT, Prickaerts J, Rahnama'I MS, de Wachter S, van Koeveringe GA, Meriaux C. Changes in voiding behavior in a mouse model of Alzheimer's disease. *Front Aging Neurosci*. (2015) 7:160. doi: 10.3389/fnagi.2015.00160
36. Porsolt RD, Anton G, Blavet N, Jalfre M. Behavioural despair in rats: a new model sensitive to antidepressant treatments. *Eur J Pharmacol*. (1978) 47:379–91. doi: 10.1016/0014-2999(78)90118-8
37. Ledo JH, Azevedo EP, Beckman D, Ribeiro FC, Santos LE, Razolli DS, et al. Cross talk between brain innate immunity and serotonin signaling underlies depressive-like behavior induced by Alzheimer's amyloid-beta oligomers in mice. *J Neurosci*. (2016) 36:12106–16. doi: 10.1523/JNEUROSCI.1269-16.2016
38. Ledo JH, Azevedo EP, Clarke JR, Ribeiro F, Figueiredo CP, Foguel D, et al. Amyloid-β oligomers link depressive-like behavior and cognitive deficits in mice. *Mol Psychiatry*. (2013) 18:1053–54. doi: 10.1038/mp.2012.168
39. Can A, Dao DT, Terrillion CE, Piantadosi S, Bhat S, Gould TD. The tail suspension test. (2012) *J Vis Exp*. 59:e3769. doi: 10.3791/3769
40. Durk MR, Han K, Chow EC, Ahrens R, Henderson J, Fraser PE, et al. 1α,25-Dihydroxyvitamin D3 reduces cerebral amyloid-β accumulation and improves cognition in mouse models of Alzheimer's disease. *J Neurosci*. (2014) 34:7091–101. doi: 10.1523/JNEUROSCI.2711-13.2014
41. Figueiredo CP, Clarke JR, Ledo JH, Ribeiro F, Costa CV, Melo HM, et al. Memantine rescues transient cognitive impairment caused by high-molecular-weight aβ oligomers but not the persistent impairment induced by low-molecular-weight oligomers. *J Neurosci*. (2013) 33:9626–34. doi: 10.1523/JNEUROSCI.0482-13.2013
42. Lourenco MV, Clarke JR, Frozza RL, Bomfim T, Forny-Germano L, Batista AF, et al. TNF-α mediates PKR-dependent memory impairment and brain IRS-1 inhibition induced by Alzheimer's β-amyloid oligomers in mice and monkeys. *Cell Metab*. (2013) 18:831–43. doi: 10.1016/j.cmet.2013.11.002
43. Sunyer B, Patil S, Höger H, Lubec G. Barnes maze, a useful task to assess spatial reference memory in the mice. *Protocol Exchange*. (2007). doi: 10.1038/nprot.2007.390
44. Soto M, Cai W, Konishi M, Kahn CR. Insulin signaling in the hippocampus and amygdala regulates metabolism and neurobehavior. *Proc Natl Acad Sci USA*. (2019) 116:6379–84. doi: 10.1073/pnas.1817391116
45. Kleinridders A, Cai W, Cappellucci L, Ghazarian A, Collins WR, Vienberg SG, et al. Insulin resistance in brain alters dopamine turnover and causes behavioral disorders. *Proc Natl Acad Sci USA*. (2015) 112:3463–8. doi: 10.1073/pnas.1500877112
46. Kahl KG, Schweiger U, Correll C, Müller C, Busch ML, Bauer M, et al. Depression, anxiety disorders, and metabolic syndrome in a population at risk for type 2 diabetes mellitus. *Brain Behav*. (2015) 5:e00306. doi: 10.1002/brb3.306
47. Rebolledo-Solleiro D, Roldán-Roldán G, Díaz D, Velasco M, Larqué C, Rico-Rosillo G, et al. Increased anxiety-like behavior is associated with the metabolic syndrome in non-stressed rats. *PLoS ONE*. (2017) 12:e0176554. doi: 10.1371/journal.pone.0176554
48. Poleszak E, Szopa A, Bogatko K, Wyska E, Wośko S, Swiader K, et al. Antidepressant-like activity of typical antidepressant drugs in the forced swim test and tail suspension test in mice is augmented by DMPX, an Adenosine A. *Neurotox Res*. (2019) 35:344–52. doi: 10.1007/s12640-018-9959-2
49. Anyan J, Amir S. Too depressed to swim or too afraid to stop? A reinterpretation of the forced swim test as a measure of anxiety-like behavior. *Neuropsychopharmacology*. (2018) 43:931–3. doi: 10.1038/npp.2017.260
50. Estanislau C, Ramos AC, Ferraresi PD, Costa N, de Carvalho HM, Batistela S. Individual differences in the elevated plus-maze and the forced

swim test. *Behav Processes*. (2011) 86:46–51. doi: 10.1016/j.beproc.2010.08.008
51. Nishimura H, Ida Y, Tsuda A, Tanaka M. Opposite effects of diazepam and beta-CCE on immobility and straw-climbing behavior of rats in a modified forced-swim test. *Pharmacol Biochem Behav*. (1989) 33:227–31. doi: 10.1016/0091-3057(89)90454-1
52. Yaffe K. Metabolic syndrome and cognitive disorders: is the sum greater than its parts? *Alzheimer Dis Assoc Disord*. (2007) 21:167–71. doi: 10.1097/WAD.0b013e318065bfd6
53. Yaffe K, Falvey C, Hamilton N, Schwartz AV, Simonsick E, Satterfield S, et al. Diabetes, glucose control, and 9-year cognitive decline among older adults without dementia. *Arch Neurol*. (2012) 69:1170–5. doi: 10.1001/archneurol.2012.1117
54. Ikura Y, Kudo T, Tanaka T, Tanii H, Grundke-Iqbal I, Iqbal K, et al. Levels of tau phosphorylation at different sites in Alzheimer disease brain. *Neuroreport*. (1998) 9:2375–9. doi: 10.1097/00001756-199807130-00041
55. Lasagna-Reeves CA, Castillo-Carranza DL, Sengupta U, Sarmiento J, Troncoso J, Jackson GR, et al. Identification of oligomers at early stages of tau aggregation in Alzheimer's disease. *FASEB J*. (2012) 26:1946–59. doi: 10.1096/fj.11-199851
56. Gu Y, Oyama F, Ihara Y. Tau is widely expressed in rat tissues. *J Neurochem*. (1996) 67:1235–44. doi: 10.1046/j.1471-4159.1996.67031235.x
57. Kenner L, El-Shabrawi Y, Hutter H, Forstner M, Zatloukal K, Hoefler G, et al. Expression of three- and four-repeat tau isoforms in mouse liver. *Hepatology*. (1994) 20:1086–9. doi: 10.1002/hep.1840200442
58. Dugger BN, Whiteside CM, Maarouf CL, Walker D, Beach TG, Sue LI, et al. The presence of select tau species in human peripheral tissues and their relation to Alzheimer's disease. *J Alzheimers Dis*. (2016) 54:1249. doi: 10.3233/JAD-169007
59. Harada A, Oguchi K, Okabe S, Kuno J, Terada S, Ohshima T, et al. Altered microtubule organization in small-calibre axons of mice lacking tau protein. *Nature*. (1994) 369:488–91. doi: 10.1038/369488a0
60. Ke YD, Suchowerska AK, van der Hoven J, De Silva DM, Wu CW, van Eersel J, et al. Lessons from tau-deficient mice. *Int J Alzheimers Dis*. (2012) 2012:873270. doi: 10.1155/2012/873270
61. Benedict C, Brooks SJ, Kullberg J, Burgos J, Kempton M, Nordenskjöld R, et al. Impaired insulin sensitivity as indexed by the HOMA score is associated with deficits in verbal fluency and temporal lobe gray matter volume in the elderly. *Diabetes Care*. (2012) 35:488–94. doi: 10.2337/dc11-2075
62. Ekblad LL, Rinne JO, Puukka P, Laine H, Ahtiluoto S, Sulkava R, et al. Insulin resistance predicts cognitive decline: an 11-year follow-up of a nationally representative adult population sample. *Diabetes Care*. (2017) 40:751–8. doi: 10.2337/dc16-2001
63. Luchsinger JA, Tang MX, Shea S, Mayeux R. Hyperinsulinemia and risk of Alzheimer disease. *Neurology*. (2004) 63:1187–92. doi: 10.1212/01.WNL.0000140292.04932.87
64. Neergaard JS, Dragsbæk K, Christiansen C, Nielsen HB, Brix S, Karsdal MA, et al. Metabolic syndrome, insulin resistance, and cognitive dysfunction: does your metabolic profile affect your brain? *Diabetes*. (2017) 66:1957–63. doi: 10.2337/db16-1444
65. Xu WL, von Strauss E, Qiu CX, Winblad B, Fratiglioni L. Uncontrolled diabetes increases the risk of Alzheimer's disease: a population-based cohort study. *Diabetologia*. (2009) 52:1031–9. doi: 10.1007/s00125-009-1323-x
66. Teri L, Ferretti LE, Gibbons LE, Logsdon R, McCurry SM, Kukull WA, et al. Anxiety of Alzheimer's disease: prevalence, and comorbidity. *J Gerontol A Biol Sci Med Sci*. (1999) 54:M348–52. doi: 10.1093/gerona/54.7.M348
67. Liu J, Garza JC, Bronner J, Kim CS, Zhang W, Lu X-Y. Acute administration of leptin produces anxiolytic-like effects: a comparison with fluoxetine. *Psychopharmacology*. (2010) 207:535–45. doi: 10.1007/s00213-009-1684-3
68. Asakawa A, Inui A, Inui T, Katsuura G, Fujino MA, Kasuga M. Leptin treatment ameliorates anxiety in ob/ob obese mice. *J Diabetes Complications*. (2003) 17:105–7. doi: 10.1016/S1056-8727(02)00185-X
69. Finger BC, Dinan TG, Cryan JF. Leptin-deficient mice retain normal appetitive spatial learning yet exhibit marked increases in anxiety-related behaviours. *Psychopharmacology*. (2010) 210:559–68. doi: 10.1007/s00213-010-1858-z
70. Licinio J, Negrao AB, Wong ML. Plasma leptin concentrations are highly correlated to emotional states throughout the day. *Transl Psychiatry*. (2014) 4:e475. doi: 10.1038/tp.2014.115
71. Cernea S, Both E, Hutanu A, Sular FL, Roiban A, Correlations of serum leptin and leptin resistance with depression and anxiety in patients with type 2 diabetes. *Psychiatry Clin Neurosci*. (2019) 73:745–53. doi: 10.1111/pcn.12922
72. Zarrindast MR, Khakpai F. The modulatory role of dopamine in anxiety-like behavior. *Arch Iran Med*. (2015) 18:591–603.
73. Ma QL, Zuo X, Yang F, Ubeda OJ, Gant D, Alaverdyan M, et al. Loss of MAP function leads to hippocampal synapse loss and deficits in the Morris Water Maze with aging. *J Neurosci*. (2014) 34:7124–36. doi: 10.1523/JNEUROSCI.3439-13.2014
74. Marschner A, Kalisch R, Vervliet B, Vansteenwegen D, Büchel C. Dissociable roles for the hippocampus and the amygdala in human cued versus context fear conditioning. *J Neurosci*. (2008) 28:9030–6. doi: 10.1523/JNEUROSCI.1651-08.2008
75. Phillips RG, LeDoux JE. Differential contribution of amygdala and hippocampus to cued and contextual fear conditioning. *Behav Neurosci*. (1992) 106:274–85. doi: 10.1037/0735-7044.106.2.274
76. Barker GR, Bird F, Alexander V, Warburton EC. Recognition memory for objects, place, and temporal order: a disconnection analysis of the role of the medial prefrontal cortex and perirhinal cortex. *J Neurosci*. (2007) 27:2948–57. doi: 10.1523/JNEUROSCI.5289-06.2007
77. Kimura T, Whitcomb DJ, Jo J, Regan P, Piers T, Heo S, et al. Microtubule-associated protein tau is essential for long-term depression in the hippocampus. *Philos Trans R Soc Lond B Biol Sci*. (2014) 369:20130144. doi: 10.1098/rstb.2013.0144
78. Velazquez R, Ferreira E, Tran A, Turner EC, Belfiore R, Branca C, et al. Acute tau knockdown in the hippocampus of adult mice causes learning and memory deficits. *Aging Cell*. (2018) 17:e12775. doi: 10.1111/acel.12775
79. Hernández F, Cuadros R, Ollá I, García C, Ferrer I, Perry G, et al. Differences in structure and function between human and murine tau. *Biochim Biophys Acta Mol Basis Dis*. (2019) 1865:2024–30. doi: 10.1016/j.bbadis.2018.08.010

Conflict of Interest: The authors declare that the research was conducted in the absence of any commercial or financial relationships that could be construed as a potential conflict of interest.

frontiers in Endocrinology

ORIGINAL RESEARCH
published: 20 March 2020
doi: 10.3389/fendo.2020.00126

Evidence for a More Disrupted Immune-Endocrine Relation and Cortisol Immunologic Influences in the Context of Tuberculosis and Type 2 Diabetes Comorbidity

*Rocío D. V. Fernández[1,2], Ariana Díaz[1,2], Bettina Bongiovanni[1], Georgina Gallucci[1], Diego Bértola[2,3], Walter Gardeñez[4], Susana Lioi[5], Yésica Bertolin[6], Romina Galliano[6], María L. Bay[1,2], Oscar Bottasso[1,2] and Luciano D'Attilio[1,2]**

[1] Instituto de Inmunología Clínica y Experimental de Rosario CONICET-UNR, Rosario, Argentina, [2] Facultad de Ciencias Médicas, UNR, Rosario, Argentina, [3] Hospital Provincial del Centenario, Rosario, Argentina, [4] Servicio de Neumonología, Hospital Provincial del Centenario, Rosario, Argentina, [5] Laboratorio Central, Hospital Provincial del Centenario, Rosario, Argentina, [6] Servicio de Medicina Transfusional, Hospital Provincial del Centenario, Rosario, Argentina

OPEN ACCESS

Edited by:
Clarissa M. Maya-Monteiro, Oswaldo Cruz Foundation (Fiocruz), Brazil

Reviewed by:
Terry D. Hinds Jr, University of Toledo, United States
Nils Lambrecht, VA Long Beach Healthcare System, United States

***Correspondence:**
Luciano D'Attilio
dattilio@idicer-conicet.gob.ar

Specialty section:
This article was submitted to Neuroendocrine Science, a section of the journal Frontiers in Endocrinology

Received: 30 November 2019
Accepted: 25 February 2020
Published: 20 March 2020

Citation:
Fernández RDV, Díaz A, Bongiovanni B, Gallucci G, Bértola D, Gardeñez W, Lioi S, Bertolin Y, Galliano R, Bay ML, Bottasso O and D'Attilio L (2020) Evidence for a More Disrupted Immune-Endocrine Relation and Cortisol Immunologic Influences in the Context of Tuberculosis and Type 2 Diabetes Comorbidity. Front. Endocrinol. 11:126. doi: 10.3389/fendo.2020.00126

Pulmonary tuberculosis (PTB), caused by *Mycobacterium tuberculosis* (*Mtb*), is a major health problem worldwide, further aggravated by the convergence of type 2 diabetes mellitus (DM) which constitutes an important risk factor for TB development. The worse scenario of patients with PTB and DM may be partly related to a more unbalanced defensive response. As such, newly diagnosed PTB patients with DM (TB+DM, $n = 11$) or not (TB, $n = 21$), as well as DM ($n = 18$) patients and pair matched controls (Co, $n = 22$), were investigated for the circulating immuno-endocrine-metabolic profile (ELISA), along with studies in peripheral blood mononuclear cells (PBMC) analyzing transcript expression (RT-qPCR) of mediators involved in glucocorticoid functionality. Given the hyperglycemic/hypercortisolemic scenario of TB+DM patients, PBMC were also exposed to stress-related cortisol concentrations (0.1 and 1 μM) and supraphysiologic glucose doses (10, 20, and 40 mM) and assessed for the specific response against *Mtb* stimulation (lymphoproliferation, -thymidine incorporation-, and cytokine production -bead-cytometry). All TB patients displayed increased plasma amounts of cortisol, growth hormone -hGH-, and proinflammatory mediators. In turn, TB+DM showed even higher levels of interferon gamma -IFN-γ- and hGH (vs. TB), or IL-6, C reactive protein, cortisol and hGH (vs. DM). Both DM groups had equally augmented values of IL-10. All TB patients showed decreased dehydroepiandrosterone- sulfate concentrations, even more in TB+DM cases. Leptin was also decreased in both TB cases, particularly in the TB group, revealing a lower body mass index, as well. Unlike PBMC from TB cases showing a decreased relationship between the glucocorticoids receptor (GR) isoforms (GRα/GRβ; functional isoform/negative isoform), cells from TB+DM patients had no changes in this regard, along with an increased expression of 11-beta hydroxysteroid dehydrogenase type-1, the enzyme facilitating intracellular cortisone to cortisol conversion. TB+DM patients also showed an increased *Mtb* antigen-driven lymphoproliferation. Compared to TB, DM and HCo counterparts, PBMC from TB+DM patients had a biased Th1

response to *Mtb* stimulation (increased IL-2 and IFN-γ production), even when exposed to inhibitory cortisol doses. TB+DM patients show a more unbalanced immuno-endocrine relationship, respect the non-diabetic counterparts, with a relative deficiency of cortisol immunomodulatory influences, despite their more favorable microenvironment for cortisol-mediated immune effects.

Keywords: pulmonary tuberculosis, diabetes mellitus type 2, immune-endocrine alterations, cortisol, glucose

INTRODUCTION

Pulmonary tuberculosis (PTB) is a major health problem around the world and the leading cause of death due to a pathogen, *Mycobacterium tuberculosis* (*Mtb*). In 2017, WHO reported 10 million new PTB cases, 15% of them attributed to the TB-type 2 diabetes mellitus (TB-DM) comorbidity (1). Tuberculosis clinical manifestations result from a complex interaction between its etiologic agent, and the defensive reactions developed to control infection, but its proper basis is not fully understood (2). Endocrine disturbances are likely to contribute to disease pathology, since DM increases more than three times the possibility of developing active PTB, which otherwise develop in 5–10% of *Mtb*-infected individuals. In addition to this increased risk, PTB patients with concomitant diabetes are at higher rates of treatment failure and death (3–6). Within this setting, we have recently demonstrated that patients with TB+DM showed a more pronounced adverse immune-endocrine profile than those with PTB alone (TB group) (7), for instance higher circulating amounts of cortisol.

Besides its metabolic functions, cortisol acts as an extrinsic regulator of the immune response (IR) inhibiting, at supraphysiologic concentrations, the proinflammatory response as well as the specific cellular IR against *Mtb* (8). Glucocorticoids (GC) are known to reduce the production of various cytokines such as tumor necrosis factor alpha (TNF-α), interleukins, as well as inflammatory enzymes, e.g., cyclooxygenase 2 and inducible nitric oxide synthase (9). Most immunological effects of GC are mediated by GRα isoform, whereas GRβ lacks the ability to bind GC and seems to function as an inhibitor of GRα-mediated transcriptional activation through the formation of GRα/GRβ heterodimers (10). It follows that this ratio may be related with GC functionality.

While increased susceptibility to PTB in DM patients may be linked to alterations on macrophage and lymphocyte functions (11, 12), partly related to a higher cortisol production, other factors like hyperglycemia and insulin resistance are also likely to account for such detrimental influence (3). Several studies indicate that diabetes and hyperglycemia coexist with impaired innate immune responses like phagocytosis, cytokine secretion and macrophage activation (13–17). Nevertheless, in a more recent *in vitro* study, Lachmandas et al. provided evidence that hyperglycemia failed to affect the functional capacity of macrophages against *Mtb* while being able to increase cytokine production upon mycobacterial and LPS stimulation (18).

Given this background, in the present study we sought to analyze various systemic mediators involved in the immuno-endocrine-metabolic interrelation: IFN-γ, IL-6, IL-10, IL-4, IL-1β, cortisol, dehydroepiandrosterone-sulfate (DHEA-S), prolactin, growth hormone (hGH), adiponectin, and leptin. In addition, we also quantified the expression levels of transcripts, related to the GC activity (α and β isoforms of the GC receptor -GR-), and the 11 beta hydroxysteroid dehydrogenase type 1 (11βHSD1) and type 2 (11βHSD2) enzymes. Experiments were also carried out to analyze whether high doses of cortisol (mirroring a stressful situation) along with physiological and supraphysiological glucose concentrations, or not, modified the *Mtb*-induced response of peripheral blood mononuclear cells (PBMC) from patients with TB+DM when compared to the ones yielded by TB cases, patients with DM and sex and age matched controls (Co). Assessments included lymphoproliferation studies and production of pro and anti-inflammatory cytokines as well as the Th1/Th2/Th17 profiles.

MATERIALS AND METHODS

Sample Population

Patients (14 females and 18 males) with no HIV co-infection and newly diagnosed PTB were included. Diagnosis was based on clinical and radiological examinations together with the identification of *Mtb* bacilli in sputum. Eleven of these patients were diagnosed as also having DM (TB+DM) and 21 with only PTB (TB). For DM diagnosis, the criteria of the American Diabetes Association of 2009 were considered. Those were hyperglycemia (based on two fasting glucose levels >125 mg/dL or a random glucose level equal to or higher than 200 mg/dL) evaluated on EDTA-anticoagulated blood specimens.

The control groups were composed of 22 pair matched Co and 18 individuals with DM, sharing the same socioeconomic conditions of TB patients, unexposed to TB patients, with no clinical or radiological evidence of PTB. Patients and Co had no other respiratory disease, nor immune-compromising diseases.

The control group (Co) was composed of 22 individuals. Another group of 18 patients with DM was also included for comparison purposes. All of them were sex- and age-matched and shared the same socioeconomic conditions of TB patients, in addition to being unexposed to TB patients, with no clinical or radiological evidence of PTB. All volunteers had no other respiratory disease, nor immune-compromising diseases.

Participants were sampled by applying a consecutive non-probabilistic approach. As such, the Co group had a median BMI which fell within the range of overweight, as defined by WHO.

Blood samples were obtained on study admission, in the case of TB patients immediately before the initiation of anti-tuberculosis treatment. Samples were collected at 8 a.m. to avoid differences due to circadian variations. Exclusion criteria included disease states affecting the adrenal glands or the Hypothalamus—Pituitary- Adrenal (HPA) axis, corticosteroid treatment, pregnancy, and age below 18 years. The body mass index (BMI) was also calculated (weight/square of height). The Bioethical Committee of the School of Medical Sciences, National University of Rosario, approved the protocol. All participants gave their consent to participate in the study.

PBMC Isolation and Lymphoproliferation

Plasma and PBMC were obtained from fresh EDTA-treated blood. Samples were centrifuged at 2000 rpm during 30 min and plasma was collected and stored at −20°C. The buffy coat was separated and diluted 1:1 in RPMI 1640 (PAA Laboratories GmbH, Austria), containing standard concentrations of L-glutamine, penicillin, and streptomycin (culture medium, CM). The cell suspension was layered over a Ficoll-Paque Plus gradient (density 1.077, Amersham Biosciences, NJ, USA), and centrifuged at 400 g for 30 min at room temperature (19–22°C). PBMC recovered from the interface were washed three times with CM and resuspended in CM containing 10% heat-inactivated pooled normal AB human sera (PAA Laboratories GmbH, Germany). Cells were cultured in quadruplicate in flat-bottomed microtiter plates (2×10^5 cells/well in 200 µl) with or without addition of γ-irradiated H37Rv *M. tuberculosis* strain (*Mtbi*; 8 µg/ml, Colorado University, USA). Concanavalin A (ConA; 2.5 µg/ml, Sigma-Aldrich) was used as a proliferation positive control. PBMC cultures were incubated for 5 days at 37°C, in a 5%, CO_2 humidified atmosphere and pulsed with ^{3}H-thymidine for 18 h before cell harvesting. The average counts per minute (cpm) of stimulated and non-stimulated cultures were calculated.

Quantification of Cytokines and Hormones in Plasma

Plasma levels of cytokines: IFN-γ (BD Pharmingen, detection limit-DL: 4.7 pg/ml), IL-10 (BD Pharmingen, DL:3.9 pg/ml), IL-6 (DRG Diagnostics, DL: 2 pg/ml), IL-4 (BD Pharmingen, DL: 7.8 pg/ml), IL-1β (BD Pharmingen, DL: 3.9 pg/ml), and hormones like Cortisol (DRG Diagnostics, DL: 2.5 ng/ml), DHEA-S (DRG Diagnostics, DL: 0.108 ng/ml), prolactin (DRG Diagnostics, DL: 0.35 ng/ml), hGH (DRG Diagnostics, DL: 0.17µIU/ml), adiponectin (Invitrogen, DL: 100 pg/ml), and leptin (Invitrogen, DL: 3.5 pg/ml) were assessed by commercial enzyme immune analysis according to the manufacturer instructions. C reactive protein (CRP) levels were measured by high-sensitivity Turbitest (Wiener Lab, DL: 2.5 mg/l). All samples were processed individually and assayed in duplicate.

Studies on the *In vitro* Effects of Cortisol and Glucose

PBMC were cultured as above described (section PBMC Isolation and Lymphoproliferation) with the addition of various concentrations of cortisol (0.1 µM y 1 µM) (19) and/or D-Glucose (Glc; physiological dose−5 mM- and supraphysiological doses−10, 20, 40 mM- Sigma Aldrich) and further stimulated with *Mtbi*, or not. PBMC were seeded in 96-well flat-bottomed microtiter plates for the lymphoproliferation assay as previously described (section PBMC Isolation and Lymphoproliferation). The same protocol was performed in 24-well flat-bottomed microtiter plates (1×10^6 cells/well). Supernatants were obtained, fractionated and preserved at −20°C until the assessment of different cytokine patterns by means of the Cytometric Bead Array Kit (LTCD4+ cells, CBA).

RNA Isolation, cDNA Synthesis and qPCR

Total RNA was isolated from PBMC using TRIreagent (Genbiotech). RNA pellets were dissolved in Diethyl pyrocarbonate (DEPC) sterile water and stored at −80°C. RNA quantity and integrity was assessed as reported earlier (20). cDNA was synthesized from 2 µg of total RNA by extension of oligodT primers with M-MuLV reverse transcriptase (Thermo) in a final volume of 40 µl DEPC sterile water. cDNA was stored at −80°C until use. qPCR was performed with the StepOnePlus (96-well) Real-Time PCR Systems (Applied Biosystems) using 3 µl of cDNA dilution, 0.4 µM of each primer and 3 µl of 5x HOT FIREPol® EvaGreen qPCR Mix Plus (ROX) (Solis BioDyne), final volume of 15 µl. Thermal cycling conditions were as follows: 10 min at 95°C followed by 45 PCR cycles of denaturing at 95°C for 20 s, 30 s for annealing at 60°C and 30 s for elongation at 72°C. Fluorescence readings were performed during 10 s at 80°C before each elongation step. To normalize the expression of every gene, the transcript of peptidylprolyl isomerase A was used as an endogenous control on each mononuclear cell sample (21). Serially diluted cDNA samples synthesized from Jurkat and NCI-H295R cell line expressing GRα, GRβ and 11βHSD1 and 11βHSD2 mRNA, respectively (22, 23), were used as relative external standards curve in each run, to make "The Relative Standard Curve Method" for the relative quantification of gene expression, as performed formerly (20). Similarity and homogeneity of PCR products from samples were confirmed by automated melting curve analysis (StepOne Software, Applied Biosystems), revealing melting temperature values of the PCR products. Primers were designed as described by D'Attilio et al. (24), **Table 1**. Data were expressed as fold change of the relative expression levels of the gene of interest (GOI) normalized by the relative expression levels of PPIA.

Cytometric Bead Array

Cytokine quantification was done using the Human Th1/Th2/Th17 CBA kit (BD Biosciences) which allowed the simultaneous detection of IL-2, IL-4, IL-6, IL-10, TNF-α, IFN-γ, and IL-17A (DL: 2.6; 4.9; 2.4; 4.5; 3.8; 3.7 and 18.9 pg/ml, respectively). CBA analysis was performed according to the manufacturer's instructions. Cytokine supernatant levels were calculated using BD CBA software (version 4.0, BD Biosciences).

Statistical Analysis

Comparisons between groups were made by non-parametric methods: Kruskall–Wallis followed by *post-hoc* comparisons when applicable. Qualitative variables were compared by the

chi square test. Related samples were analyzed by means of Wilcoxon and Friedman tests. Associations between variables were analyzed using the Spearman correlation test. A value of $p < 0.05$ was considered as statistically significant.

RESULTS

General Features of Study Groups

Table 2 shows the general characteristics from the different study groups and diabetes-related biochemical findings. A lower percentage of BCG vaccination was seen in the DM and TB+DM groups with respect to Co, with the TB+DM group showing the lowest percentage of a BCG scar. The TB group showed a significant decrease in the BMI if compared to Co and TB+DM. Patients with DM showed the highest BMI, but their values did not differ from the ones recorded in Co counterparts. Mainly because, by chance, 23% of Co volunteers presented a BMI within the normal weight range, whereas 55% and a 22% of them had values that fell in the overweight and obesity categories, respectively. Regarding diabetes-related biochemical findings (**Table 2**), DM and TB+DM groups had elevated blood glucose levels (much higher in the latter group). The percentage of glycosylated hemoglobin (HbA1c) was higher in both groups of DM patients more pronounced in those with the TB+DM comorbidity. Basal insulinemia was found increased only in the TB+DM group, statistically different from the remaining groups. When calculating the HOMA index (≥3.2 compatible with insulin resistance), 67% of DM patients and 73% of TB+DM fell in this category. It is worth reminding that most DM were under treatment with metformin and fenofibrate. In addition, the erythrocyte sedimentation rate (ESR) was increased in both groups of patients with TB in relation to their respective controls, while the DM group differed from the Co-individuals (**Table 2**).

TABLE 1 | Sequence of qPCR primers.

Transcript	Forward Primer	Reverse Primer	Size
CycA ***PPIA* GeneID:**5478	*CycA-F* 5′-gca tac ggg tcc tgg catc ttg-3′	*CycA-R* 5′-tgc cat cca acc act cag tct tg-3′	101pb
GRα ***NR3C1,* GeneID:**2908 **Transcript variant 1**	*GR-F* 5′gaa gga aac tcc agc cag aac-3′	*GRα-R* 5′-gat gat ttc agc taa catc tcg-3′	159bp
GRβ ***NR3C1,* GeneID:**2908 **Transcript variant 6**	*GR-F* 5′-gaa gga aac tcc agc cag aac-3′	*GRβ –R* 5′-tga gcg cca aga ttg ttg g-3′	144 bp
11βHSD1 ***HSD11B 1*, GeneID:**3290	*11βHSD1 F* 5′- atg ata ttc acc atg tgc gca–3′	*11βHSD1 R* *5′- ata ggc agc aac cat tgg ata ag-3′*	158pb
11βHSD2 ***HSD11B 2*, GeneID:**3291	*11βHSD2 F* *5′-tcg cgc ggt gct cat cac-3′*	*11βHSD2 R* 5′- gta cgc agc tcg atg gca cc-3′	132pb

PPIA, peptidylprolyl isomerase A; NR3C1, nuclear receptor subfamily 3 group C member 1; GR, glucocorticoids receptors; HSD11B1, hydroxysteroid 11-beta dehydrogenase 1; HSD11B2, hydroxysteroid 11-beta dehydrogenase 2.

Plasma Quantification of Immunologic Mediators and Hormones

Plasma Levels of Pro and Anti-inflammatory Cytokines, Adiponectin, Leptin, Prolactin and hGH

Both groups of TB patients showed elevated values of IL-6, CRP, and IFN-γ (**Figures 1A–C**), with TB+DM patients showing even higher amounts of IFN-γ if compared to TB counterparts. Patients with DM also displayed increased CRP levels. As regards IL-10, this cytokine was increased in both groups of DM patients (**Figure 1D**), as well as in the group of TB patients with severe

TABLE 2 | Main features of subjects participating in the study.

Parameters	Co ($n = 22$)	DM ($n = 18$)	TB ($n = 21$)	TB+DM ($n = 11$)	Overall *p*-value
Age (years)	45 (35–62)	54 (51–61)	41 (34–59)	50 (41–62)	n.s.
Sex (F/M)	9/13	10/8	8/13	6/5	n.s.
BCG (%)	95.4	78.9	76.2	45.5$^{*\#\&}$	0.001
BMI (kg/m^2)	27.0 (25.9–29.6)	28.0 (25.1–31.5)	20.9 (19.4–23.9)*	26.9 (23.4–31.9)$^{\&}$	<0.0001
Glycemia (mg/dl) [r.v: 70–100]	89.5 (84.3–106)	111* (94.5–129)	87.0 (81.0–104)	213$^{*,\#,\&}$ (161–285)	<0.0001
$HbA1_C$ (%) [r.v: 4.8-6]	5.5 (5.0–5.8)	7.5* (6.0–10)	5.8 (5.4–6.3)	9.7$^{*,\&}$ (7.0–11)	<0.0001
Insulin (μIU/ml) [r.v: 2.6-25]	6.7 (5.4–9.8)	7.4 (5.7–13)	7.0 (3.9–8.6)	14$^{*,\&}$ (6.4–29)	0.0003
$HOMA_{IR}$ [r.v: ≤3.2]	1.43 (1.08–2.12)	3.22* (1.32–4.45)	1.51 (0.832–2.20)	6.51$^{*,\#,\&}$ (2.31–15.8)	0.0003
ESR (mm/1° hs) [r.v: 1-15]	5.0 (2.3–9.3)	10.0* (7.8–20.5)	57.5* (34.5–89.5)	60.0$^{*,\#}$ (36.0–92.0)	<0.0001

*Co, controls; DM, patients with type 2 diabetes mellitus; TB, patients with pulmonary tuberculosis; TB+DM, patients with pulmonary tuberculosis and type 2 diabetes mellitus; n.s., not significant; F, female; M, male; BCG, Bacillus Calmette-Guerin vaccination; BMI, body mass index. rv, reference values; $HOMA_{IR}$ index, [insulin (μIU/ml)*glycemia (mmol/L)]/22.5; ESR, Erythrocyte Sedimentation Rate. Results are shown as median (25-75 percentiles). *different from HCo, $p < 0.05$; $^{\#}$different from DM, $p < 0.05$; $^{\&}$different from TB, $p < 0.05$.*

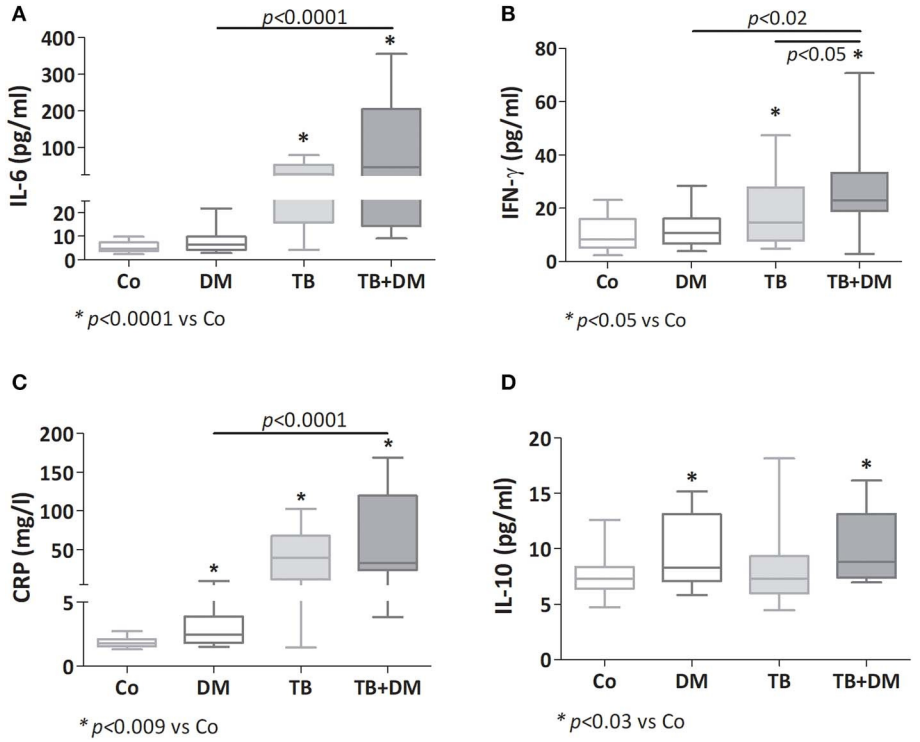

FIGURE 1 | Plasma levels of IL-6 **(A)**, IFN-γ **(B)**, C reactive protein (CRP; **C**) and IL-10 **(D)** in controls (Co), patients with type 2 diabetes (DM), with pulmonary tuberculosis (TB) or with TB and DM (TB-DM). Box plots show median values, 25–75 percentiles from data in each group with maximum and minimum values.

disease (data not shown). Assays for IL-4 and IL-1β yielded values below the detection limits.

While adiponectin and prolactin concentrations showed no differences among study groups (**Figures 2A,C**, respectively), leptin levels appeared decreased in both TB patient groups, much lower in those without DM (**Figure 2B**). hGH levels were increased in both TB groups particularly in TB+DM cases (**Figure 2D**).

An additional analysis by sex revealed that decreased levels of leptin prevailed between both groups of men with TB even more in those cases without DM. Regarding hGH, men with TB+DM were the ones showing significantly increased amounts of this hormone (data not shown).

Plasma Levels of Cortisol, DHEA and DHEA-S

As reported earlier, patients with TB had a higher cortisol concentration ($^*p < 0.04$ vs. Co, **Figure 3A**), as did patients with TB+DM ($p < 0.04$ vs. Co and $p < 0.02$ vs. DM). Plasma concentrations of DHEA were significantly lower in TB group compared to Co, but not in patients with TB+DM, who even showed values higher than TB cases (**Figure 3B**). However, DHEA-S levels were diminished in both groups of TB patients, particularly the TB+DM ones, as well as DM cases (**Figure 3C**). When analyzing the Cort/DHEA ratio (**Figure 3D**), this was significantly increased in the three groups of patients compared with those from Co, a bit less pronounced in the TB+DM group. The same was true when comparing the Cort/DHEA-S ratio (**Figure 3E**), with TB+DM differing in turn from DM.

Relative Levels of mRNAs Expression for GRα, GRβ and the Enzymes 11βHSD1 and 11βHSD2 in PBMC From the Study Groups

As depicted in **Figures 4A,B** there were no significant differences in transcript expression levels for GRα and GRβ, although the GRα/GRβ ratio was found to be diminished in patients with TB when compared with Co (**Figure 4C**). Regarding the 11βHSD1 mRNA, its levels were increased in both groups of patients with DM, respect to those of Co, as well as TB+DM patients if compared to TB (**Figure 4D**). In general terms the 11βHSD2 enzyme was not expressed, or at very low levels, even with optimized reaction conditions (24).

Lymphoproliferation Studies

The effects of different Glc doses on the proliferative capacity of PBMC against *Mtbi* are shown in **Figure 6**. Regardless of the Glc dose, the blastogenic response of cells, expressed as Stimulation Index (SI), from each study group showed a similar pattern (**Figure 5**). For instance, the SI of the TB group was lower than that from Co, and negatively correlated with IL-10 levels ($r = -0.54$, $p < 0.03$), while both groups of DM patients showed the highest responses, in the case of TB+DM statistically significant from TB and Co groups. In essence, increasing Glc concentrations did not modify the *Mtbi*-driven blastogenesis in the four study groups (**Figure 5**). Data from studies by adding cortisol in presence of different Glc concentrations are summarized in **Figure 6**. The higher dose of

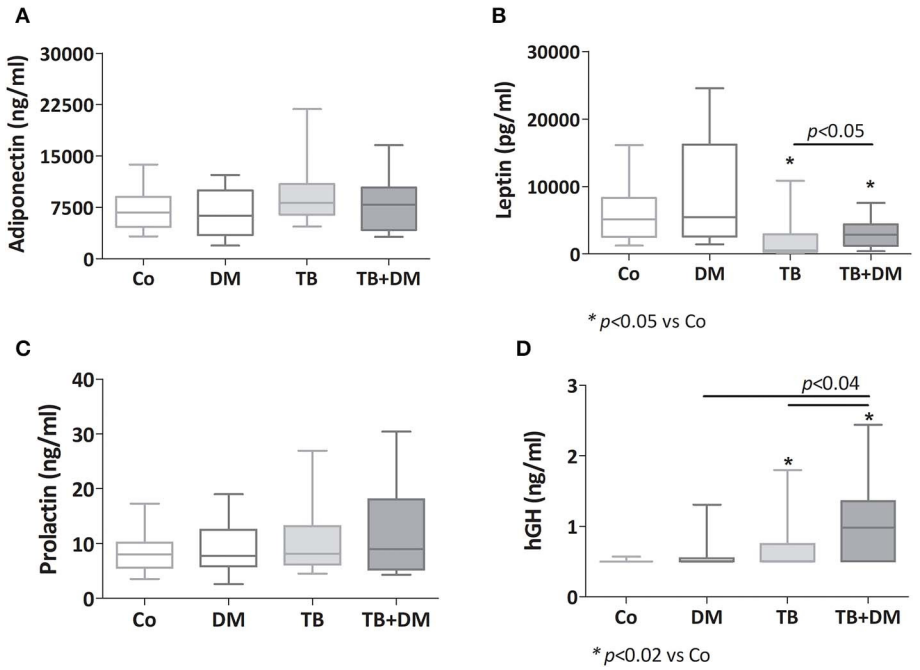

FIGURE 2 | Plasma levels of adiponectin **(A)**, leptin **(B)**, prolactin **(C)** and human growth hormone (hGH, **D**) in controls (Co), patients with type 2 diabetes (DM), with pulmonary tuberculosis (TB) or with TB and DM (TB-DM). Box plots show median values, 25–75 percentiles from data in each group with maximum and minimum values.

cortisol (1 μM) decreased proliferation regardless of the study group or Glc concentration, being significantly lower than the results obtained when using a lower cortisol dose (0.1 μM; **Figures 6A–D**). Between group differences in the blastogenic response continued to show the pattern described in **Figure 6**, regardless of the Glc or cortisol doses (**Figures 6A–D**). Notably, hyperglycemia did not modify the inhibitory cortisol effect (**Figures 7A,B**).

Quantification of Mediators in Culture Supernatants of PBMC

According to the study purposes, 24 h culture supernatants from PBMC subjected to the above described treatments (Materials and Methods section Studies on the *In vitro* Effects of Cortisol and Glucose), were assessed for the levels of proinflammatory (TNF-α, IL-1β, IL-6), and anti-inflammatory (IL-10) cytokines as well as the ones representing the Th1 (IL-2, IFN-γ), Th2 (IL-4) and Th17 (IL-17A) profiles. According to data from the lymphoproliferation studies, we decided to quantify cytokines in six parallel cultures undergoing one of the following stimulation procedures: Glc 5 mM, Glc 20 Mm, Glc 5 mM+ *Mtbi*, Glc 20 Mm+ *Mtbi*, Glc 5 mM + Cortisol 1 μM + *Mtbi*, Glc 20 mM + Cortisol 1 μM + *Mtbi.* All *Mtbi*-stimulated cultures contained increased levels of TNF-α, IL-1β, IL-2, IFN-γ, and IL-10 which remained unmodified by Glc treatment even at the 20 μM dose, except for IL-1β production from PBMC of Co (**Table 3**). IL-6 levels were largely increased before stimulation, beyond the upper detection limits of the Kit, whereas IL-4 and IL-17A remained undetectable.

When comparing cytokine production, cultured PBMC of patients with TB+DM had the highest levels of IL-2 (**Figure 8**) and IFN-γ (**Figure 9**), in the case of IL-2 statistically different from the remaining groups (**Figures 8A,B**). Levels of TNF-α, IL-1β, and IL-10, in stimulated cultures were similar for all study groups (data not shown). Cortisol treatment decreased the production of all above described cytokines, regardless of subject groups or Glc doses (**Figures 8**, **9**). As regards to IL-2 (**Figures 8A,B**), although their levels dropped, they remained significantly elevated in the TB+DM group respect to the remaining groups. The same was true when analyzing IFN-γ concentrations, although differences were only significant in relation to Co and DM (**Figures 9A,B**).

DISCUSSION

TB-DM comorbidity became more relevant in recent decades due to the diabetic population marked increase; particularly in low and middle-income countries, where PTB is prevalent. Both pathologies present, by themselves, alterations in the bidirectional communication between the immune and neuroendocrine systems, with an important impact on the metabolic component (25–27).

Our work evidenced that both groups of PTB patients presented an important inflammatory response, reflected in high systemic levels of IL-6, CRP, and IFN-γ. Several reports

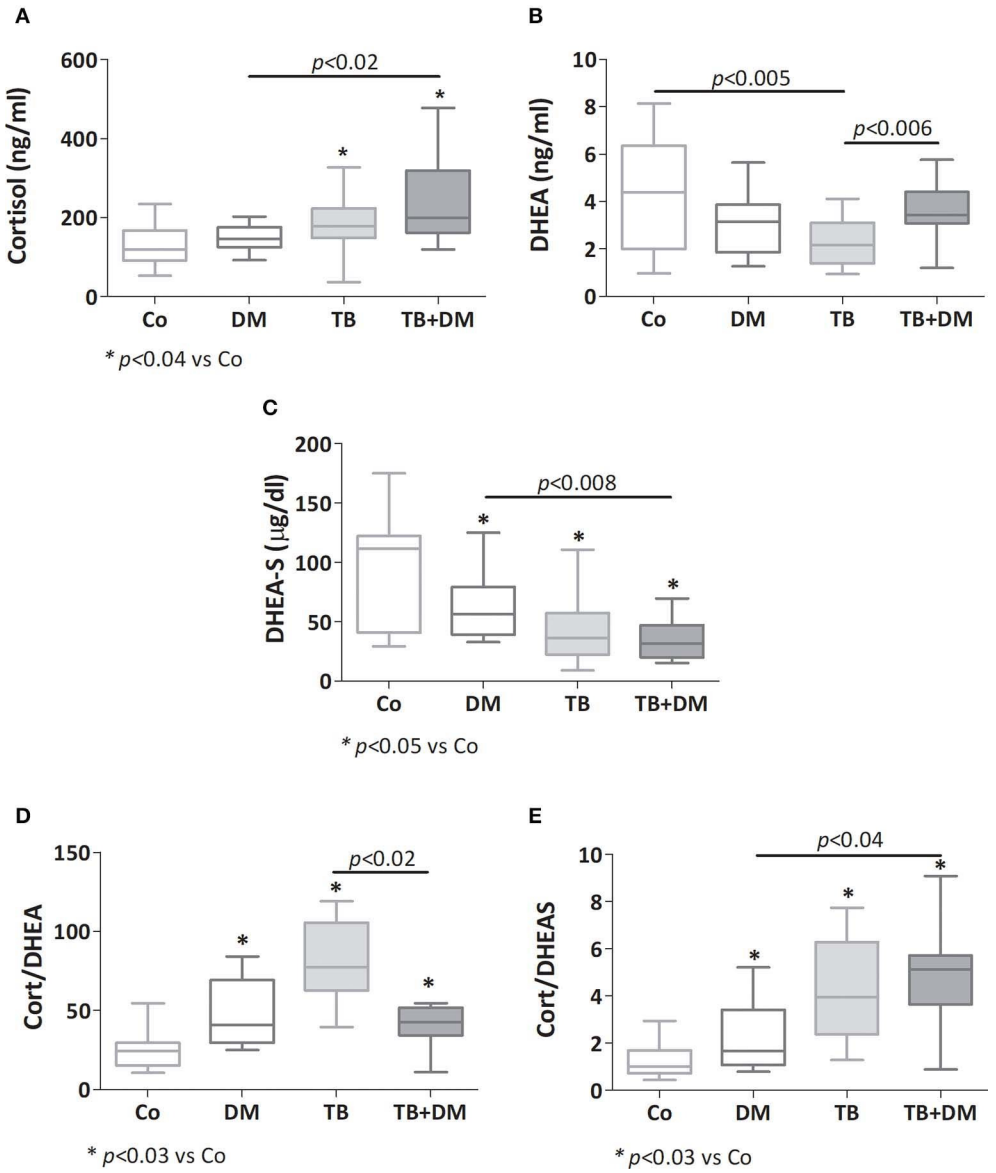

FIGURE 3 | Plasma levels of cortisol **(A)**, dehydroepiandrosterone (DHEA, **B**), dehydroepiandrosterone-sulfate (DHEA-S, **C**), cortisol/DHEA ratio **(D)** and cortisol/DHEA-S ratio **(E)** in controls (Co), patients with type 2 diabetes (DM), with pulmonary tuberculosis (TB) or with TB and DM (TB-DM). Box plots show median values, 25–75 percentiles from data in each group with maximum and minimum values.

indicate a greater increase of proinflammatory mediators in PTB patients suffering DM compared to non-diabetic patients (28, 29). This may reinforced by the increased presence of hGH in plasma from TB+DM cases, considering that this hormone exerts a contributory role for the development of the IR and the accompanying inflammation (30, 31).

As in previous studies (32–34), patients with only TB showed decreased blastogenesis, which in turn correlated negatively with IL-10 levels, a cytokine of recognized inhibitory effect on lymphoproliferation (35). Such decreased specific proliferation may be partly attributed to a recruitment of cells committed toward the site of the lesion (19). This mechanism seems to be altered in diabetic patients with active PTB (27, 36) and could to account for the increased *Mtb*-driven mitogenesis of PBMC.

The systemic increase of IL-10 from TB+DM patients, also reported by Kumar and collaborators (37), may be mirroring a regulatory mechanism of IR, given its well-known anti-inflammatory and anti-proliferative effects (35, 38). At the same time, IL-10 seems to be detrimental in mouse and human TB, as it favors mycobacterial survival in macrophages by inhibiting phagosome maturation, reducing NO production (39) and in turn blocking IFN-γ (40, 41) signaling. Some studies suggest that IL-10 would be a marker of disease progression (42–46). In our cases, analysis according

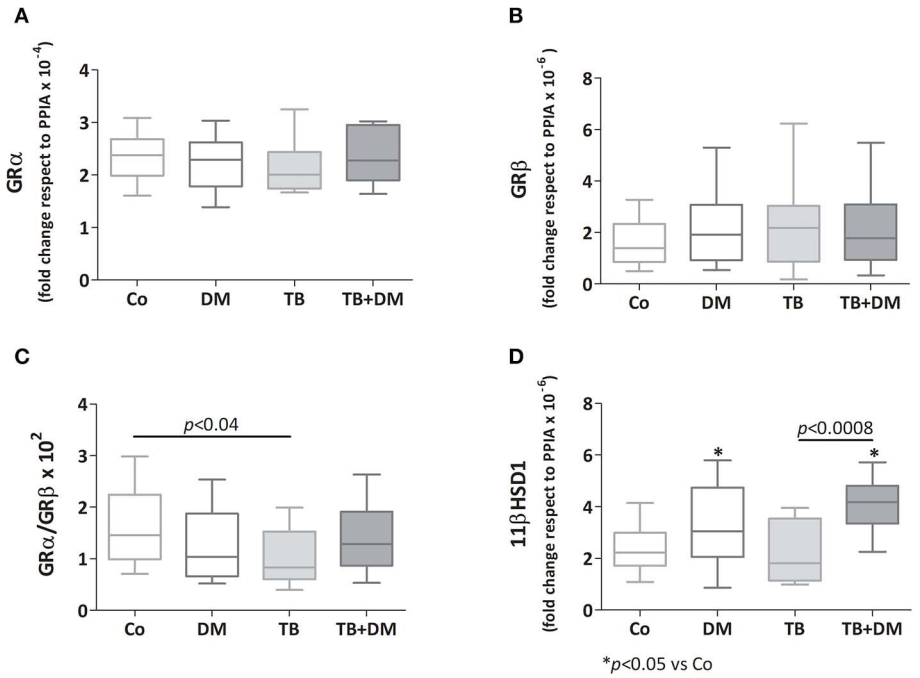

FIGURE 4 | Relative expression of mRNA glucocorticoids receptor (GR) isoforms α (GR α, **A**) and β (GRβ, **B**), 11βHSD1 enzyme **(D)**, and the GRα/GRβ ratio **(C)** in peripheral blood mononuclear cells (PBMC) from controls (Co), patients with type 2 diabetes (DM), with pulmonary tuberculosis (TB) or with TB and DM (TB-DM). Data are expressed as fold change respect to PPIA. Box plots show median values, 25–75 percentiles from data in each group with maximum and minimum values.

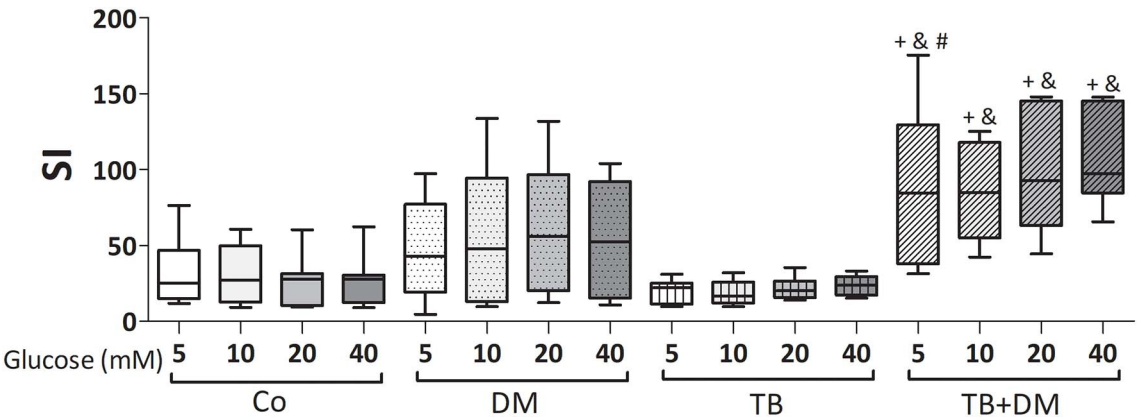

FIGURE 5 | Effects of supraphysiological glucose doses on *Mtbi*-induced proliferation of peripheral blood mononuclear cells (PBMC) from controls (Co), patients with type 2 diabetes (DM), with pulmonary tuberculosis (TB) or with TB and DM (TB-DM). *Mtbi*: γ-irradiated H37Rv *M. tuberculosis* strain. Results are shown as Stimulation index (SI: average of counts per minute -cpm- in *Mtbi* stimulated cultures/average of cpm in unstimulated cultures). Box plots show median values, 25–75 percentiles from data in each group with maximum and minimum values. $^{+}$different from HCo, $p < 0.02$; $^{\&}$different from TB, $p < 0.003$; $^{\#}$different from DM, $p < 0.05$; in each case when comparing with the same glucose dose.

to disease severity showed a significant increase of IL-10 in TB+DM patients with progressive pulmonary involvement (data not shown).

Notably, IL-10 levels were also augmented in DM patients who also displayed increased amounts of CRP together with a high ESR resembling some sort of pro- and anti-inflammatory influences.

As seen in former studies (33, 34, 47, 48), the unbalanced relationship between steroid hormones recorded in TB patients, increased and decreased levels of cortisol and DHEA-DHEA-S, respectively, was also found in TB+DM patients. This may be explained by assuming that the adrenal gland is trying to preserve cortisol production at the expense of DHEA synthesis, to counteract the inflammatory response accompanying active

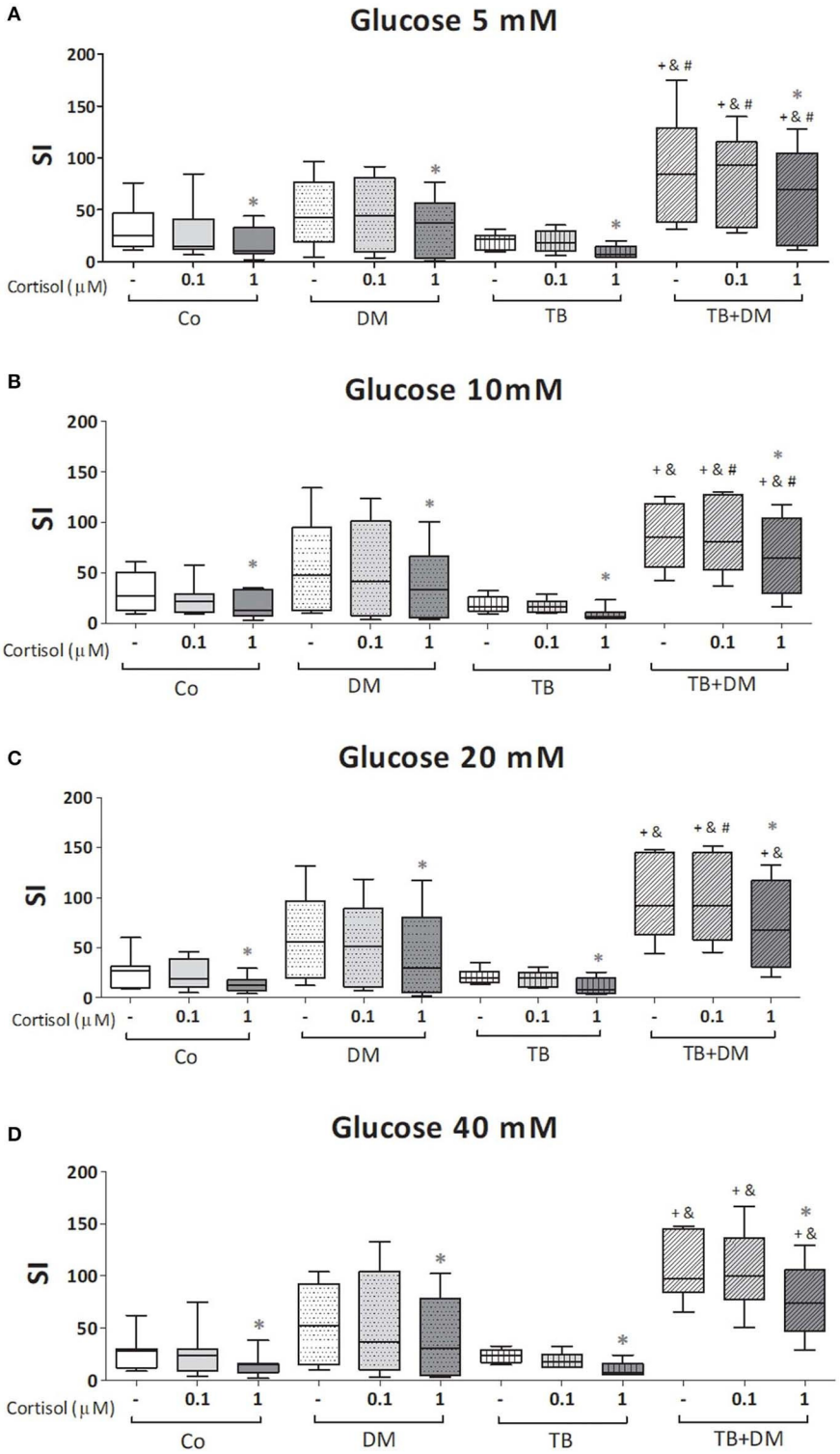

FIGURE 6 | Effects of glucose doses (5 mM, **A**; 10 mM, **B**; 20 mM, **C**; 40 mM, **D**) on cortisol-induced inhibition of *Mtbi*-blastogenesis by peripheral blood mononuclear cells (PBMC) from controls (Co), patients with type 2 diabetes (DM), with pulmonary tuberculosis (TB) or with TB and DM (TB-DM). *Mtbi*: γ-irradiated H37Rv *M. tuberculosis* strain. Results are shown as Stimulation index (SI: average of counts per minute -cpm- in *Mtbi* stimulated cultures/average of cpm in unstimulated cultures). Box plots show median values, 25–75 percentiles from data in each group with maximum and minimum values. $^{+}$different from Co, $p < 0.04$; $^{\&}$different from TB, $p < 0.02$; $^{\#}$different from DM, in each case when comparing the same treatment between groups, $p < 0.05$; *different from cultures without cortisol and from those treated with 0.1 uM cortisol within the same group, $p < 0.05$.

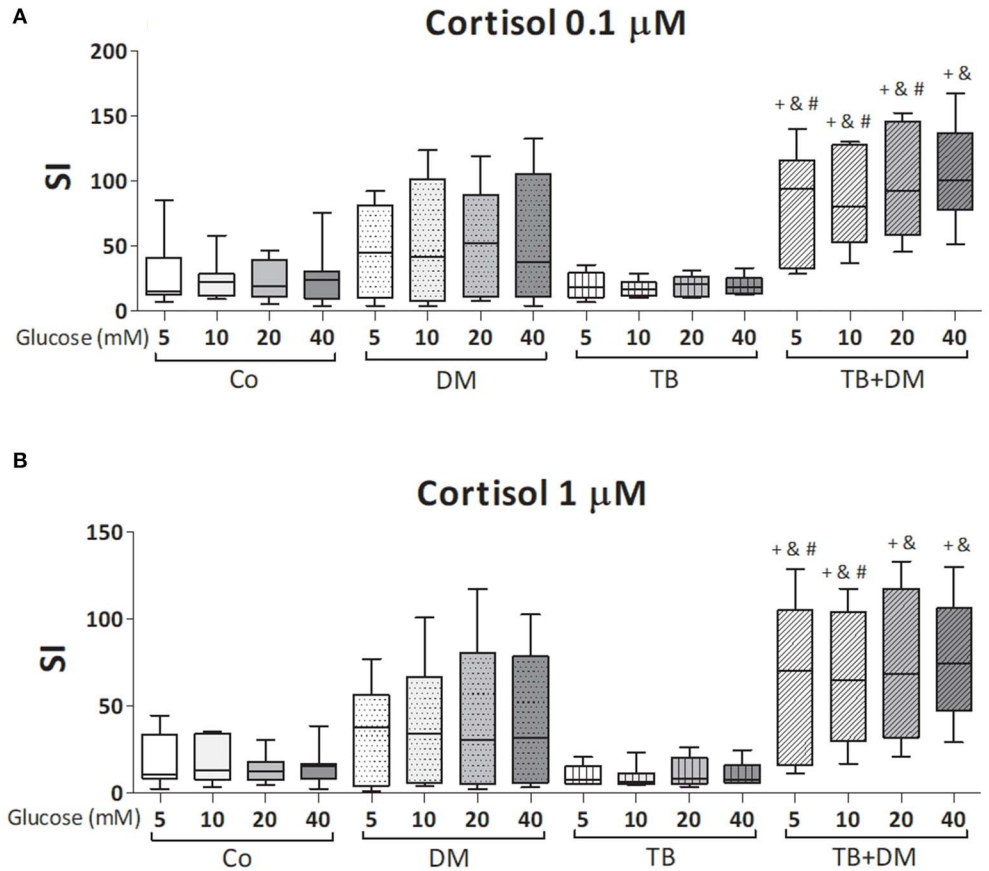

FIGURE 7 | Effects of glucose doses on *Mtbi*-blastogenesis of peripheral blood mononuclear cells (PBMC) from in controls (Co), patients with type 2 diabetes (DM), with pulmonary tuberculosis (TB) or with TB and DM (TB-DM) treated with cortisol 0.1 μM **(A)** or 1 μM **(B)**. *Mtbi*: γ-irradiated H37Rv *M. tuberculosis* strain. Results are shown as Stimulation index (SI: average of counts per minute -cpm- in *Mtbi* stimulated cultures/average of cpm in unstimulated cultures). Box plots show median values, 25–75 percentiles from data in each group with maximum and minimum values. $^{+}$different from Co, $p < 0.04$; $^{\&}$different from TB, $p < 0.02$; $^{\#}$different from DM, $p < 0.05$; in each case when comparing with the same glucose dose.

disease. Decreased levels of DHEA and DHEA-S, may be detrimental in TB, since they preferentially favor the Th1 profile of the IR in addition to exerting anti-inflammatory activities (49–52). DHEA-S is not bioactive; but constitutes the natural reservoir of DHEA being therefore a stable marker of its availability.

As regards GR isoforms, while high GC-responsiveness would typically reduce GRα increasing GRβ and therefore dampening GC effects, this was not so evident in TB, probably because of its chronic nature and several endocrine alterations. The reduced GRα/GRβ ratio seen in TB patients is compatible with a certain degree of resistance to GC endogenous function. In a recent study, Martins et al. reported that GRβ expression levels were dramatically increased in PBMC of patients with the metabolic syndrome compared to lean controls (53). Our present lack of GRβ transcript alterations in control subjects may be explained by considering that their BMI situated below the ones displayed by the group of dysmetabolic Brazilian patients. Mouse studies revealed that GRβ causes higher glucose levels along with and increased immune-inflammatory response (54), but in our hands GRβ expression was not associated to any particular change in the profile of metabolic or immune-endocrine mediators. Despite TB+DM cases showed no differences in the GRα/GRβ ratio, transcriptional levels of 11βHSD1, which favors the availability of cortisol at the cellular level, were clearly elevated in both groups of DM patients. The fact that TB+DM patients presented high levels of plasma cortisol, along with 11βHSD1 transcripts and IFN-γ values points out to some degree of HPA axis dysfunction and/or GC resistance in them (55, 56).

The lower BMI from TB patients is in line with our former demonstrations in this regard, in which we also documented a negative association between BMI and IL-6 levels, probably reflecting the high-energy demand required to support the chronic inflammatory response (48, 57). In the case of TB+DM patients they exhibit a negative association between cortisol levels and BMI (data not shown). With regard to TB+DM patients, 60% of them fell within the overweight category in line with some evidence indicating an association between overweight and obesity with an increased risk for DM and pre-DM development (58–60). While 77% of individuals from the Co group had a high BMI, our findings are in line with a report from WHO

TABLE 3 | Effect of glucose doses on cytokine production by Mtbi-stimulated peripheral mononuclear cells from the different study groups.

***Mtbi* stimulus**	**Co (*n* = 7)**		***p***	**DM (*n* = 9)**		***p***	**TB (*n* = 7)**		***p***	**TB+DM (*n* = 6)**		***p***
	Glc 5 mM	**Glc 20mM**		**Glc 5mM**	**Glc 20mM**		**Glc 5mM**	**Glc 20mM**		**Glc 5mM**	**Glc 20mM**	
TNF-α (pg/ml)	900 (537–1,032)	840 (524–1,239)	n.s.	565 (278–1,729)	876 (35–1,394)	n.s.	1,121 (602–3,298)	1,195 (619–3,086)	n.s.	830 (344–2,904)	1,167 (462–2,877)	n.s.
IL-1β (pg/ml)	4,053 (3,610–5,066)	4,526 (4,153–5,232)	0.03	5,181 (4,516–5,706)	5,286 (4,841–5,857)	n.s.	4,221 (3,776–5,400)	4,746 (4,479–5,579)	n.s.	4,099 (3,706–5,498)	4,302 (3,625–4,754)	n.s.
IL-2 (pg/ml)	17.8 (12.6–29.2)	18.3 (11.2–24.5)	n.s.	10.9 (7.52–32.6)	12,3 (5.99–26.9)	n.s.	16.4 (8.01–38.7)	15.3 (8.13–37.4)	n.s.	91.8 (40.4–323)	85.5 (40.9–254)	n.s.
IFN-γ (pg/ml)	8.72 (6.98–30.6)	9.42 (6.94–34.4)	n.s.	16,0 (3.70–37.4)	11,1 (3,42–48,0)	n.s.	21,5 (12,4–37.4)	22,9 (13.8–43.4)	n.s.	94,2 (21.2–654)	106 (22.5–634)	n.s.
IL-10 (pg/ml)	160 (125–285)	154 (121–253)	n.s.	195 (176–255)	198 (184–243)	n.s.	375 (63.3–490)	380 (66.0–468)	n.s.	208 (50.0–241)	192 (115–262)	n.s.

Co, controls; DM, patients with type 2 diabetes mellitus; TB, patients with pulmonary tuberculosis; TB+DM, patients with pulmonary tuberculosis and type 2 diabetes mellitus; Glc, glucose; n.s., not significant. Results are shown as median (25–75 percentiles).

(GLOBAL STATUS REPORT on non-communicable diseases 2014), referring to an increase in BMI in most developing countries between the 2010–2014 period, in our country from 27.2 to 27.8 (61).

Present results in TB patients are consistent with our earlier studies (48), revealing an orexigenic pattern characterized by low and high levels of leptin and adiponectin, respectively. This not being the case of TB+DM patients in whom leptin levels appeared diminished to a lesser extent, with no changes in adiponectin concentrations. Reduced levels of leptin in both groups of patients with TB may be partly due to the high systemic amounts of proinflammatory mediators, known to suppress leptin synthesis (62, 63). The different pattern seen in TB+DM patients may have to do with their preserved or even increased BMI, implying a greater adiposity. Likewise, leptin has been reported as facilitating the cellular response, particularly that of the Th1 profile (64). Adiponectin was found reduced in dysregulated diabetic patients, compared to slim controls (65), but in our study we found differences in this regard. Between study differences may be explained by considering that most DM patients were being treated for their diabetes, and their BMI was comparable to the one recorded in Co group.

The inflammatory component observed in DM and TB+DM patients is likely to account for their insulin resistance, mainly in the former group (66–68). Decreased amounts of both androgens (DHEA and DHEA-S) may be also implied in insulin resistance, since they favor body weight (69, 70) and adipose tissue reduction (71) while stimulating Glc uptake (70, 72).

Moving to the immune-metabolic communication, innate and adaptive immune cells must respond rapidly in the presence of noxious stimuli, for which they must drastically alter their metabolism to achieve a high rate of cell division, as well as the synthesis and secretion of various molecules necessary for the development of a protective IR. While leukocytes use several types of energy sources (fatty acids, cholesterol, vitamins, trace elements, amino acids, monosaccharides), Glc and glutamine emerge as the main metabolic substrates, representing 70% of energy sources (73).

Studies assessing the immune status of DM patients against several microbial antigens showed a dysfunctionality of innate and adaptive cells, particularly in cases with chronic hyperglycemia (high HbA1c levels) (14, 74). Such alterations appeared to reverse under a proper glycemic control (14, 75–77), although transient and chronic hyperglycemia induce epigenetic modifications, known under the term "metabolic memory" likely to influence substantially immunocompetent cell activity (78, 79).

In the present study, *Mtbi*-stimulated PBMCs from TB+DM patients showed the highest mitogenic response together with an abundant production of IL-2 and IFN-γ. Present results are in line with the study by Restrepo et al. showing a predominant Th1 profile upon PPD stimulation of PBMC from patients with this comorbidity (28). Kumar et al. reported the presence of a Th1/Th17 profile when studying cells from TB+DM cases (80), while Stalenhoef et al. found no differences in IFN-γ production levels when comparing TB patients with or without DM (81).

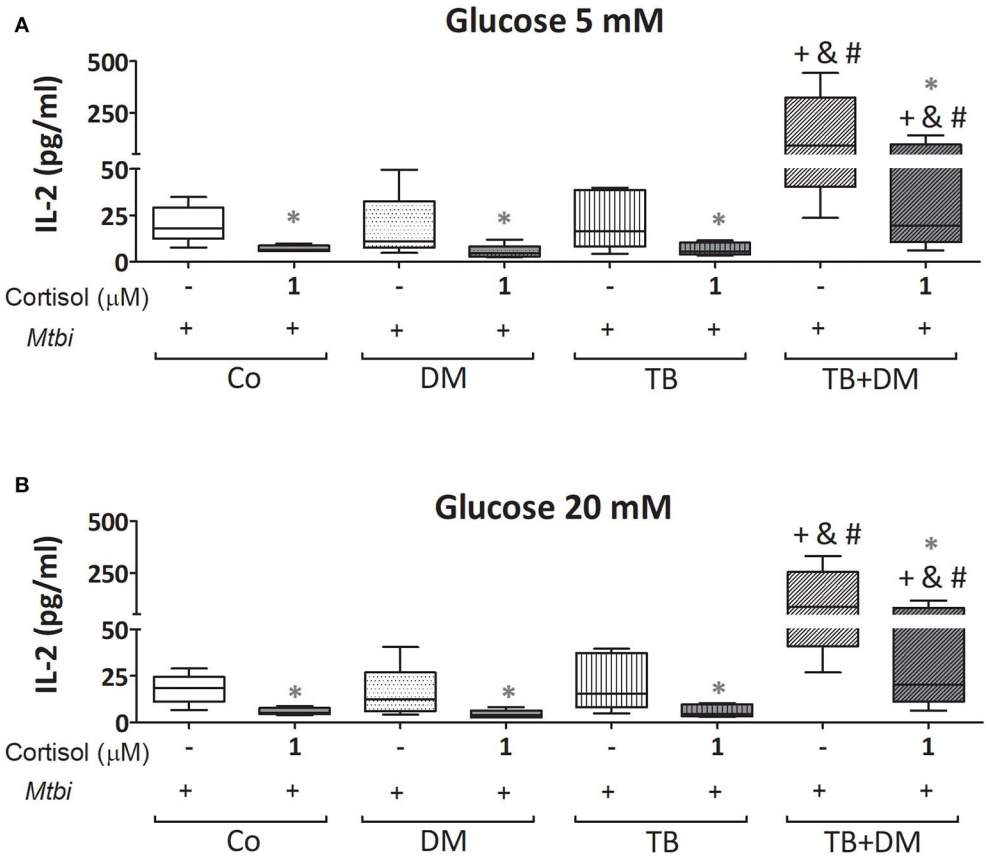

FIGURE 8 | IL-2 production by cultures of peripheral blood mononuclear cells (PBMC) from in controls (Co), patients with type 2 diabetes (DM), with pulmonary tuberculosis (TB) or with TB and DM (TB-DM), stimulated with *Mtbi* and treated with glucose 5 mM **(A)** and 20 mM **(B)** with or without cortisol (1 μM). *Mtbi*: γ-irradiated H37Rv *M. tuberculosis* strain. Box plots show median values, 25–75 percentiles from data in each group with maximum and minimum values. $^{+}$different from Co, $p < 0.03$; $^{\&}$different from TB, $p < 0.04$; $^{\#}$different from DM, $p < 0.04$; in each case when performing between-group comparisons for the same treatment; *different from cultures without cortisol within the same group. $p < 0.03$.

Such dissimilarities may be due to ethnical differences, control status of DM and experimental conditions, among others.

In line with the well-known immunostimulant effects of IL-2 (82), in our case IL-2 levels were positively associated with *Mtb*-driven proliferation in DM and Co individuals, as well as with IFN-γ in all study groups. The increased *in vitro* synthesis of IFN-γ by stimulated PBMC from TB+DM patients was paralleled by augmented amounts of this cytokine in circulation. While being critical for mycobacterial elimination (83, 84), IFN-γ also exerts proinflammatory effects likely to mediate tissue damage when improperly regulated. As such, and over-expansion of cells with a Th1 profile may constitute a double-edged sword in the context of TB+DM.

Hyperglycemia can lead to an inflammatory state through several pathways (85–87) with advanced glycation end products playing a substantial role is this regard. These products, which are abundant in uncontrolled diabetic patients, promote inflammation not only by activating NF-kB (88) but also by working in combination with other inflammatory mediators like the high mobility group box 1 protein to aggravate the inflammatory process (89, 90). Consequently, DM individuals with uncontrolled hyperglycemia are likely to show a greater inflammatory and lymphoproliferative response upon exposure to an infectious agent, increasing tissue damage as well. In our hands, both groups of DM patients had the greatest SI, statistically significant in TB+DM, who in turn showed an increased IL-2 and IFN-γ production.

In vitro studies have shown an increased release of inflammatory cytokines by PBMC from healthy individuals when exposed to supraphysiological doses of Glc (91, 92). Lachmandas et al. observed that PBMC from healthy people produced higher levels of TNF-α, IL-1β, and IL-6 before stimulation in a hyperglycemic microenvironment, without changes in the levels of IFN-γ, IL-17A, and IL-22, suggesting that Glc would have a greater effect on monocytes than in lymphocytes (18, 83, 84).

In our case, specific stimulation under a hyperglycemic scenario led to an increased IL-1β production only in Co cells, with the specific lymphoproliferation and production of other mediators being unmodified no matter the study groups. Differences in technical approaches, i.e., stimulation procedures

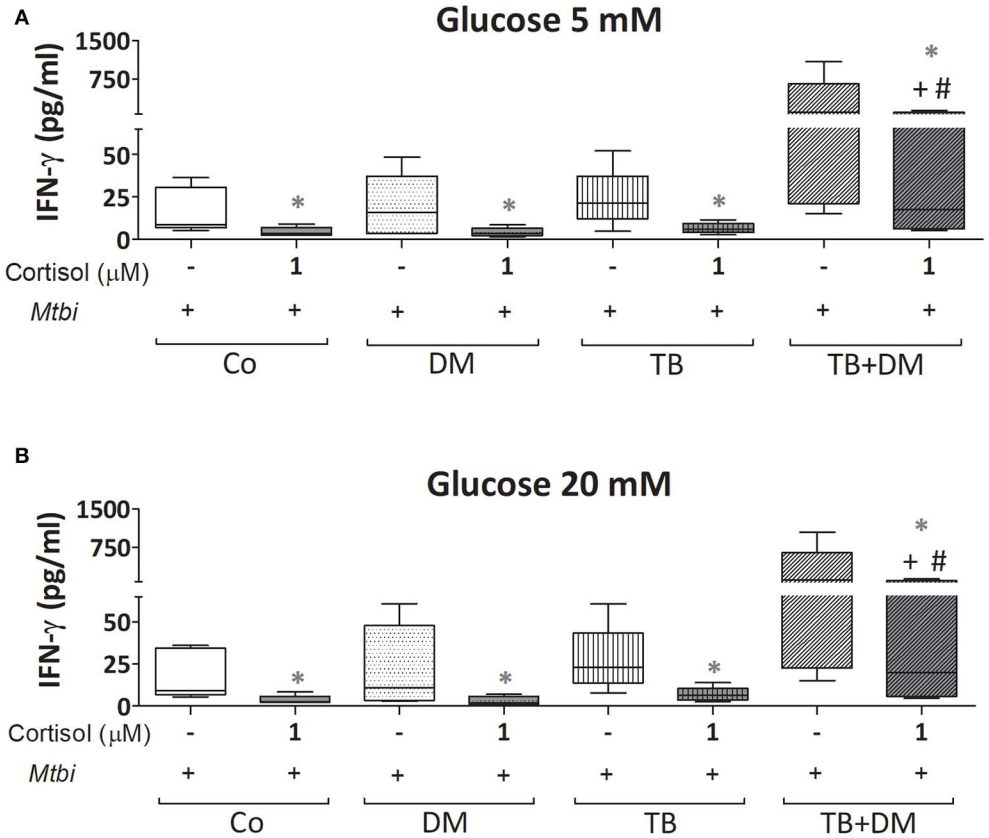

FIGURE 9 | IFN-γ production by cultures of peripheral blood mononuclear cells (PBMC) from controls (Co), patients with type 2 diabetes (DM), with pulmonary tuberculosis (TB) or with TB and DM (TB-DM), stimulated with *Mtbi* and treated with glucose 5 mM **(A)** and 20 mM **(B)** with or without cortisol (1 μM). *Mtbi*: γ-irradiated H37Rv *M. tuberculosis* strain. Box plots show median values, 25–75 percentiles from data in each group with maximum and minimum values. $^{+}$different from Co, $p < 0.04$; $^{\#}$different from DM, $p < 0.05$; in each case when performing between-group comparisons for the same treatment; *different from cultures without cortisol within the same group $p < 0.03$.

and time point evaluations, may account for inconsistencies between present studies and former reports.

Our former demonstration that cortisol treatment, at doses resembling an acute stress situation, inhibited the specific proliferative response and synthesis of IFN-γ by PBMC of TB patients and Co (19) along with the increased systemic levels of cortisol of TB+DM patients, prompted us to analyze cortisol effects in them. As seen in TB patients, high cortisol doses inhibited proliferative capacity and production of TNF-α, IL-1β, IL-2, IFN-γ, and IL-10, in TB+DM and DM patients as well as Co. Although TB+DM continued to show a remarkable response despite this steroid treatment. Cortisol inhibitory effects on pro-inflammatory cytokine production are achieved by several transcriptional repression mechanisms (93–97), with some inconsistencies as to its role in the production of anti-inflammatory mediators in light of evidence reporting a stimulating or inhibitory influences on IL-10 *in vitro* synthesis (98–102). Whether the present diminished IL-10 production is to some extent related to the decreased TNF-α and IFN-γ synthesis, which by themselves may promote IL-10 production (103), remains to be established.

Although the effects of Glc and cortisol on IR have been extensively analyzed, their combined effect on PBMC had not been studied so far. As shown, high Glc doses did not modify the cortisol-induced inhibition on mitogenesis, nor cytokine production from different study groups.

The bulk of presented results points out that the deregulated immune-endocrine-metabolic status from DM patients becomes more pronounced in those with the TB comorbidity. This is supported not only by the further increased systemic proinflammatory response of TB+DM patients but also for the demonstration that PBMC are more likely to develop an exacerbated response against *Mtb*, reflected in a more pronounced Th1 profile. A better control of the diabetic status will promote a more favorable course of TB in the context of TB+DM comorbidity.

DATA AVAILABILITY STATEMENT

All datasets generated for this study are included in the article/supplementary material.

ETHICS STATEMENT

The studies involving human participants were reviewed and approved by The Bioethical Committee of the School of Medical Sciences, National University of Rosario. The patients/participants provided their written informed consent to participate in this study.

AUTHOR CONTRIBUTIONS

RF, AD, BB, GG, and LD'A designed and carried out experimental procedures. DB, WG, SL, YB, and RG selected voluntaries and performed blood samples extraction. RF, LD'A, MB, and OB performed data analysis and wrote the paper.

FUNDING

This work was supported by grants from the Foundation for Scientific and Technological Research–FONCyT– (PICT 2012-1523, PICT 2016-0279), the Ministry of Science, Technology and Productive Innovation of Santa Fe Province, Rosario, Argentina (IO-2017-00142) and the Foundation for Medical Sciences of Rosario, Argentina. Grant for accredited projects of the National University of Roario (1MED485).

ACKNOWLEDGMENTS

The authors thank Wiener Labs, Rosario, for providing a CRP Turbitest High-Sensitivity kit and the Federada Foundation, Rosario, Argentina.

REFERENCES

1. Global Tuberculosis Report (2018). Geneva: World Health Organization. Licence: CC BY-NC-SA 3.0 IGO. Available online at: https://apps.who.int/medicinedocs/documents/s23553en/s23553en.pdf (accessed March 9, 2020).
2. Ernst JD. The immunological life cycle of tuberculosis. *Nat Rev Immunol*. (2012) 12:581–91. doi: 10.1038/nri3259
3. Dooley KE, Chaisson RE. Tuberculosis and diabetes mellitus: convergence of two epidemics. *Lancet Infect Dis*. (2009) 9:737–46. doi: 10.1016/S1473-3099(09)70282-8
4. Stevenson CR, Forouhi NG, Roglic G, Williams BG, Lauer JA, Dye C, et al. Diabetes and tuberculosis: the impact of the diabetes epidemic on tuberculosis incidence. *BMC Public Health*. (2007) 7:234. doi: 10.1186/1471-2458-7-234
5. Jeon CY, Murray MB. Diabetes mellitus increases the risk of active tuberculosis: a systematic review of 13 observational studies. *PLoS Med*. (2008) 5:1091–101. doi: 10.1371/journal.pmed.0050152
6. Lonnroth K, Roglic G, Harries AD. Improving tuberculosis prevention and care through addressing the global diabetes epidemic: from evidence to policy and practice. *Lancet Diabetes Endocrinol*. (2014) 2:730–9. doi: 10.1016/S2213-8587(14)70109-3
7. Fernández R, Díaz A, D'Attilio L, Bongiovanni B, Santucci N, Bertola D, et al. An adverse immune-endocrine profile in patients with tuberculosis and type 2 diabetes. *Tuberculosis (Edinb)*. (2016) 101:95–101. doi: 10.1016/j.tube.2016.09.001
8. Bottasso O, Bay ML, Besedovsky H, Del Rey A. The immuno-endocrine component in the pathogenesis of tuberculosis. *Scand J Immunol*. (2007) 66:166–75. doi: 10.1111/j.1365-3083.2007.01962.x
9. Barnes PJ. Glucocorticosteroids: current and future directions. *Br J Pharmacol*. (2011) 163:29–43. doi: 10.1111/j.1476-5381.2010.01199.x
10. Cain DW, Cidlowski JA. Immune regulation by glucocorticoids. *Nat Rev Immunol*. (2017) 17:233–47. doi: 10.1038/nri.2017.1
11. Martinez N, Kornfeld H. Diabetes and immunity to tuberculosis. *Eur J Immunol*. (2014) 44:617–26. doi: 10.1002/eji.201344301
12. Restrepo BI, Schlesinger LS. Host-pathogen interactions in tuberculosis patients with type 2 diabetes mellitus. *Tuberculosis (Edinb)*. (2013) 93 (Suppl. 0):S10–4. doi: 10.1016/S1472-9792(13)70004-0
13. Gomez DI, Twahirwa M, Schlesinger LS, Restrepo BI. Reduced association of mycobacteria with monocytes from diabetes patients with poor glucose control. *Tuberculosis (Edinb)*. (2013) 93:192–7. doi: 10.1016/j.tube.2012.10.003
14. Lecube A, Pachón G, Petriz J, Hernández C, Simó R. Phagocytic activity is impaired in type 2 diabetes mellitus and increases after metabolic improvement. *PLoS ONE*. (2011) 6:e23366. doi: 10.1371/journal.pone.0023366
15. Sun C, Sun L, Ma H, Peng J, Zhen Y, Duan K, et al. The phenotype and functional alterations of macrophages in mice with hyperglycemia for long term. *J Cell Physiol*. (2012) 227:1670–9. doi: 10.1002/jcp.22891
16. Liu HF, Zhang HJ, Hu QX, Liu XY, Wang ZQ, Fan JY, et al. Altered polarization, morphology, and impaired innate immunity germane to resident peritoneal macrophages in mice with long-term type 2 diabetes. *J Biomed Biotechnol*. (2012) 2012:867023. doi: 10.1155/2012/867023
17. Devaraj S, Venugopal SK, Singh U, Jialal I. Hyperglycemia induces monocytic release of interleukin-6 via induction of protein kinase C-α and -β. *Diabetes*. (2005) 54:85–91. doi: 10.2337/diabetes.54.1.85
18. Lachmandas E, Vrieling F, Wilson LG, Joosten SA, Netea MG, Ottenhoff TH, et al. The effect of hyperglycaemia on *in vitro* cytokine production and macrophage infection with *Mycobacterium tuberculosis*. *PLoS ONE*. (2015) 10:e0117941. doi: 10.1371/journal.pone.0117941
19. Mahuad C, Bay ML, Farroni M, Bozza V, Del Rey A, Besedovsky H, et al. Cortisol and dehydroepiandrosterone affect the response of peripheral blood mononuclear cells to mycobacterial antigens during tuberculosis. *Scand J Immunol*. (2004) 60:639–46. doi: 10.1111/j.0300-9475.2004.01514.x
20. D'Attilio L, Trini E, Bongiovanni B, Dídoli G, Gardeñez W, Nannini LJ, et al. mRNA expression of alpha and beta isoforms of glucocorticoid receptor in peripheral blood mononuclear cells of patients with tuberculosis and its relation with components of the immunoendocrine response. *Brain Behav Immun*. (2011) 25:461–7. doi: 10.1016/j.bbi.2010.11.006
21. He J-Q, Sandford AJ, Wang I-M, Stepaniants S, Knight DA, Kicic A, et al. Selection of housekeeping genes for real-time PCR in atopic human bronchial epithelial cells. *Eur Respir J*. (2008) 32:755–62. doi: 10.1183/09031936.00129107
22. Mazzocchi G, Rossi GP, Neri G, Malendowicz LK, Albertin G. 11β-Hydroxysteroid dehydrogenase expression and activity in the human adrenal cortex. *FASEB J*. (1988) 12:1533–9. doi: 10.1096/fasebj.12.14.1533
23. Orii F, Ashida T, Nomura M, Maemoto A, Fujiki T, Ayabe T, et al. Quantitative analysis for human glucocorticoid receptor alpha/beta mRNA in IBD. *Biochem Biophys Res Commun*. (2002) 296:1286–94. doi: 10.1016/S0006-291X(02)02030-2
24. D'Attilio L, Díaz A, Santucci N, Bongiovanni B, Gardeñez W, Marchesini M, et al. Levels of inflammatory cytokines, adrenal steroids, and mRNA for GRα, GRβ and 11βHSD1 in TB pleurisy. *Tuberculosis (Edinb)*. (2013) 93:635–41. doi: 10.1016/j.tube.2013.07.008
25. Hackett RA, Steptoe A. Type 2 diabetes mellitus and psychological stress — a modifiable risk factor. *Nat Rev Endocrinol*. (2017) 13:547–560. doi: 10.1038/nrendo.2017.64
26. Bottasso O, Bay ML, Besedovsky H, del Rey A. The immune-endocrine-metabolic unit during human tuberculosis. *Curr Immunol Rev*. (2010) 6:314–22. doi: 10.2174/1573395511006040314
27. Vallerskog T, Martens GW, Kornfeld H. Diabetic mice display a delayed adaptive immune response to *Mycobacterium tuberculosis*. *J Immunol*. (2010) 184:6275–82. doi: 10.4049/jimmunol.1000304
28. Restrepo BI, Fisher-hoch SP, Pino P, Salinas A, Mohammad H, Mora F, et al. Tuberculosis in poorly controlled Type 2 diabetes: altered cytokine expression in peripheral white blood cells. *Clin Infect Dis*. (2008) 47:634–41. doi: 10.1086/590565

29. Kumar NP, Banurekha VV, Nair D, Sridhar R, Kornfeld H, Nutman TB, et al. Coincident pre-diabetes is associated with dysregulated cytokine responses in pulmonary tuberculosis. *PLoS ONE*. (2014) 9:e112108. doi: 10.1371/journal.pone.0112108
30. Besedovsky H, Del Rey A. Immune-neuro-endocrine interactions: facts and hypotheses. *Endocr Rev*. (1996) 17:64–102. doi: 10.1210/edrv-17-1-64
31. Saito H, Inoue T, Fukatsu K, Ming-Tsan L, Inaba T, Fukushima R, et al. Growth hormone and the immune response to bacterial infection. *Horm Res*. (1996) 45:50–4. doi: 10.1159/000184759
32. Leung CC, Lam TH, Chan WM, Yew WW, Ho KS, Leung GM, et al. Original contribution diabetic control and risk of tuberculosis: a cohort study. *Am J Epidemiol*. (2008) 167:1486–94. doi: 10.1093/aje/kwn075
33. Díaz A, Bongiovanni B, D'Attilio L, Santucci N, Dídoli G, Fernández RdV, et al. The clinical recovery of tuberculosis patients undergoing specific treatment is associated with changes in the immune and neuroendocrine responses. *Pathog Dis*. (2017) 75:ftx087. doi: 10.1093/femspd/ftx087
34. Bongiovanni B, Díaz A, D'Attilio L, Santucci N, Dídoli G, Lioi S, et al. Changes in the immune and endocrine responses of patients with pulmonary tuberculosis undergoing specific treatment. *Ann N Y Acad Sci*. (2012) 1262:10–5. doi: 10.1111/j.1749-6632.2012.06643.x
35. Del Prete G, de Carli M, Almerigogna F, Giudizi MG, Biagiotti R, Romagnani S. Human IL-10 is produced by both type 1 helper (Th1) and type 2 helper (Th2) T cell clones and inhibits their antigen-specific proliferation and cytokine production. *J Immunol*. (1993) 150:353–60.
36. Stew SS, Martinez PJ, Schlesinger LS, Restrepo BI. Differential expression of monocyte surface markers among TB patients with diabetes co-morbidity. *Tuberculosis (Edingb)*. (2013) 93:S78–82. doi: 10.1016/S1472-9792(13)70015-5
37. Pavan Kumar N, Sridhar R, Banurekha VV, Jawahar MS, Fay MP, Nutman TB, et al. Type 2 diabetes mellitus coincident with pulmonary tuberculosis is associated with heightened systemic Type 1, Type 17, and other proinflammatory cytokines. *Ann Am Thorac Soc*. (2013) 10:441–9. doi: 10.1513/AnnalsATS.201305-112OC
38. Sabat R, Grütz G, Warszawska K, Kirsch S, Witte E, Wolk K GJ. Biology of interleukin-10. *Cytokine Growth Factor Rev*. (2010) 21:331–44. doi: 10.1016/j.cytogfr.2010.09.002
39. Schreiber T, Ehlers S, Heitmann L, Rausch A, Mages J, Murray PJ, et al. Autocrine IL-10 induces hallmarks of alternative activation in macrophages and suppresses anti-tuberculosis effector mechanisms without compromising T cell immunity. *J Immunol*. (2009) 183:1301–12. doi: 10.4049/jimmunol.0803567
40. de Paus RA, van Wengen A, Schmidt I, Visser M, Verdegaal EME, van Dissel JT, et al. Inhibition of the type I immune responses of human monocytes by IFN-α and IFN-β. *Cytokine*. (2013) 61:645–55. doi: 10.1016/j.cyto.2012.12.005
41. Dallagi A, Girouard J, Hamelin-Morrissette J, Dadzie R, Laurent L, Vaillancourt C, et al. The activating effect of IFN-γ on monocytes/macrophages is regulated by the LIF–trophoblast–IL-10 axis via Stat1 inhibition and Stat3 activation. *Cell Mol Immunol*. (2015) 12:326–41. doi: 10.1038/cmi.2014.50
42. Olobo JO, Geletu M, Demissie A, Eguale T, Hiwot K, Aderaye G, et al. Circulating TNF-alpha, TGF-beta, and IL-10 in tuberculosis patients and healthy contacts. *Scand J Immunol*. (2001) 53:85–91. doi: 10.1046/j.1365-3083.2001.00844.x
43. Jamil B, Shahid F, Hasan Z, Nasir N, Razzaki T, Dawood G, et al. Interferonγ/IL10 ratio defines the disease severity in pulmonary and extra pulmonary tuberculosis. *Tuberculosis (Edingb)*. (2007) 87:279–87. doi: 10.1016/j.tube.2007.03.004
44. Barnes PF, Lu S, Abrams JS, Wang E, Yamamura M MR. Cytokine production at the site of disease in human tuberculosis. *Infect Immun*. (1993) 61:3482–9. doi: 10.1128/IAI.61.8.3482-3489.1993
45. Awomoyi AA, Marchant A, Howson JMM, McAdam KPWJ, Blackwell JM, Newport MJ. Interleukin-10, polymorphism in SLC11A1 (formerly NRAMP1), and susceptibility to tuberculosis. *J Infect Dis*. (2002) 186:1808–14. doi: 10.1086/345920
46. Abdalla AE, Lambert N, Duan X, Xie J. Interleukin-10 family and tuberculosis: an old story renewed. *Int J Biol Sci*. (2016) 12:710–7. doi: 10.7150/ijbs.13881
47. Del Rey A, Mahuad CV, Bozza VV, Bogue C, Farroni MA, Bay ML, et al. Endocrine and cytokine responses in humans with pulmonary tuberculosis. *Brain Behav Immun*. (2007) 21:171–9. doi: 10.1016/j.bbi.2006.06.005
48. Santucci N, D'Attilio L, Kovalevski L, Bozza V, Besedovsky H, del Rey A, et al. A multifaceted analysis of immune-endocrine-metabolic alterations in patients with pulmonary tuberculosis. *PLoS ONE*. (2011) 6:e26363. doi: 10.1371/journal.pone.0026363
49. Suzuki T, Suzuki N, Daynes RA, Engleman EG. Dehydroepiandrosterone enhances IL2 production and cytotoxic effector function of human T cells. *Clin Immunol Immunopathol*. (1991) 61:202–11. doi: 10.1016/S0090-1229(05)80024-8
50. Kipper-Galperin M, Galilly R, Danenberg HD, Brenner T. Dehydroepiandrosterone selectively inhibits production of tumor necrosis factor α and Interlukin-6 in astrocytes. *Int J Dev Neurosci*. (1999) 17:765–75. doi: 10.1016/S0736-5748(99)00067-2
51. Hazeldine J, Arlt W, Lord JM. Dehydroepiandrosterone as a regulator of immune cell function. *J Steroid Biochem Mol Biol*. (2010) 120:127–36. doi: 10.1016/j.jsbmb.2009.12.016
52. Svec F, Porter JR. The actions of exogenous dehydroepiandrosterone in experimental animals and humans. *Proc Soc Exp Biol Med*. (1998) 218:174–91. doi: 10.3181/00379727-218-44285
53. Martins CS, Elias D, Colli LM, Couri CE, Souza MCLA, Moreira AC, et al. HPA axis dysregulation, NR3C1 polymorphisms and glucocorticoid receptor isoforms imbalance in metabolic syndrome. *Diabetes Metab Res Rev*. (2017) 33:e2842. doi: 10.1002/dmrr.2842
54. Marino JS, Stechschulte LA, Stec DE, Nestor-Kalinoski A, Coleman S HTJ. Glucocorticoid receptor β induces hepatic steatosis by augmenting inflammation and inhibition of the Peroxisome Proliferator-Activated Receptor (PPAR) α. *J Biol Chem*. (2016) 291:25776–88. doi: 10.1074/jbc.M116.752311
55. Bottasso O, Bay ML, Besedovsky H, del Rey A. Adverse neuro-immune-endocrine interactions in patients with active tuberculosis. *Mol Cell Neurosci*. (2013) 53:77–85. doi: 10.1016/j.mcn.2012.11.002
56. Straub RH, Besedovsky HO. Integrated evolutionary, immunological, and neuroendocrine framework for the pathogenesis of chronic disabling inflammatory diseases. *FASEB J*. (2003) 17:2176–83. doi: 10.1096/fj.03-0433hyp
57. Mahuad C, Bozza V, Pezzotto SM, Bay ML, Besedovsky H, Del Rey A, et al. Impaired immune responses in tuberculosis patients are related to weight loss that coexists with an immunoendocrine imbalance. *Neuroimmunomodulation*. (2007) 14:193–9. doi: 10.1159/000110646
58. Leung CC, Lam TH, Chan WM, Yew WW, Ho KS, Leung G, et al. Lower risk of tuberculosis in obesity. *Arch Intern Med*. (2007) 167:1297. doi: 10.1001/archinte.167.12.1297
59. Kim SJ, Ye S, Han YJ, Ha E, Chun EM. The association of body mass index with incidence of tuberculosis in Korea. *Eur Respir J*. (2017) 50(Suppl. 61):PA2715.
60. Hanrahan CF, Golub JE, Mohapi L, Tshabangu N, Modisenyane T, Chaisson RE, et al. Body mass index and risk of tuberculosis and death. *AIDS*. (2010) 24:1501–8. doi: 10.1097/QAD.0b013e32833a2a4a
61. World Health Organization. *Global Status Report on Noncommunicable Diseases* (2014). Available online at: https://www.who.int/nmh/publications/ncd-status-report-2014/en/
62. Popa C, Netea MG, Radstake DS, van Riel PL, Barrera P, van JWM, et al. Markers of inflammation are negatively correlated with serum leptin in rheumatoid arthritis. *Ann Rheum Dis*. (2005) 64:1195–8. doi: 10.1136/ard.2004.032243
63. Thaler JP, Choi SJ, Schwartz MW, Wisse BE. Hypothalamic inflammation and energy homeostasis: Resolving the paradox. *Front Neuroendocrinol*. (2010) 31:79–84. doi: 10.1016/j.yfrne.2009.10.002
64. Martín-Romero C, Santos-Alvarez J, Goberna R, Sánchez-Margalet V. Human leptin enhances activation and proliferation of human circulating T Lymphocytes. *Cell Immunol*. (2000) 199:15–24. doi: 10.1006/cimm.1999.1594
65. Liu C, Feng X, Li Q, Wang Y, Li Q, Hua M. Adiponectin, TNF-α and inflammatory cytokines and risk of type 2 diabetes: a systematic review and meta-analysis. *Cytokine*. (2016) 86:100–9. doi: 10.1016/j.cyto.2016.06.028
66. Pradhan AD, Manson JE, Rifai N, Buring JE, Ridker PM. C-reactive protein, interleukin 6, and risk of developing type 2 diabetes mellitus. *JAMA*. (2001) 286:327–34. doi: 10.1001/jama.286.3.327

67. Duncan BB, Schmidt MI, Pankow JS, Ballantyne CM, Couper D, Vigo A, et al. Low-grade systemic inflammation and the development of type 2 diabetes: the atherosclerosis risk in communities study. *Diabetes*. (2003) 52:1799–805. doi: 10.2337/diabetes.52.7.1799
68. Spranger J, Kroke A, Mo M, Hoffmann K, Bergmann MM. Inflammatory cytokines and the risk to develop Type 2 diabetes results of the prospective population-based european prospective investigation into cancer and nutrition (EPIC)-potsdam study. *Diabetes*. (2003) 52:812–7. doi: 10.2337/diabetes.52.3.812
69. Gómez-Santos C, Hernández-Morante JJ, Tébar FJ, Granero E, Garaulet M. Differential effect of oral dehydroepiandrosterone-sulphate on metabolic syndrome features in pre- and postmenopausal obese women. *Clin Endocrinol (Oxf)*. (2012) 77:548–54. doi: 10.1111/j.1365-2265.2011.04306.x
70. Villareal DT, Holloszy JO. Effect of DHEA on abdominal fat and insulin action in elderly women and men. *JAMA*. (2004) 292:2243. doi: 10.1001/jama.292.18.2243
71. Hernández-Morante JJ, Pérez-de-Heredia F, Luján JA, Zamora S, Garaulet M. Role of DHEA-S on body fat distribution: gender- and depot-specific stimulation of adipose tissue lipolysis. *Steroids*. (2008) 73:209–15. doi: 10.1016/j.steroids.2007.10.005
72. Casson P, Hornsby P, Buster J. Adrenal androgens, insulin resistance, and cardiovascular disease. *Semin Reprod Med*. (1996) 14:29–34. doi: 10.1055/s-2007-1016306
73. Wolowczuk I, Verwaerde C, Viltart O, Delanoye A, Delacre M, Pot B, et al. Feeding our immune system: impact on metabolism. *Clin Dev Immunol*. (2008) 2008:639803. doi: 10.1155/2008/639803
74. Foss-Freitas MC, Foss NT, Donadi EA, Foss MC. Effect of metabolic control on interferon-gamma and interleukin-10 production by peripheral blood mononuclear cells from type 1 and type 2 diabetic patients. *Brazilian J Med Biol Res*. (2007) 40:671–7. doi: 10.1590/S0100-879X2007000500010
75. Bagdade JD, Nielson KL, Bulger RJ. Reversible abnormalities in phagocytic function in poorly controlled diabetic patients. *Am J Med Sci*. (1972) 263:451–6. doi: 10.1097/00000441-197206000-00005
76. Bagdade JD, Stewart M, Walters E. Impaired granulocyte adherence. A reversible defect in host defense in patients with poorly controlled diabetes. *Diabetes*. (1978) 27:677–81. doi: 10.2337/diabetes.27.6.677
77. MacRury SM, Gemmell CG, Paterson KR, MacCuish AC. Changes in phagocytic function with glycaemic control in diabetic patients. *J Clin Pathol*. (1989) 42:1143–7. doi: 10.1136/jcp.42.11.1143
78. Berezin A. Metabolic memory phenomenon in diabetes mellitus: achieving and perspectives. *Diabetes Metab Syndr Clin Res Rev*. (2016) 10:S176–83. doi: 10.1016/j.dsx.2016.03.016
79. Bianchi C, Miccoli R, Del Prato S. Hyperglycemia and vascular metabolic memory: truth or fiction? *Curr Diab Rep*. (2013) 13:403–10. doi: 10.1007/s11892-013-0371-2
80. Kumar NP, Sridhar R, Banurekha VV, Jawahar MS, Nutman TB, Babu S. Expansion of pathogen-specific T-helper 1 and T-helper 17 cells in pulmonary tuberculosis with coincident type 2 diabetes mellitus. *J Infect Dis*. (2013) 208:739–48. doi: 10.1093/infdis/jit241
81. Stalenhoef JE, Alisjahbana B, Nelwan EJ, Ven-Jongekrijg J, Ottenhoff THM, Meer JWM, et al. The role of interferon-gamma in the increased tuberculosis risk in type 2 diabetes mellitus. *Eur J Clin Microbiol Infect Dis*. (2008) 27:97–103. doi: 10.1007/s10096-007-0395-0
82. Kelso A, MacDonald HR, Smith KA, Cerottini JC, Brunner KT. Interleukin 2 enhancement of lymphokine secretion by T lymphocytes: analysis of established clones and primary limiting dilution microcultures. *J Immunol*. (1984) 132:2932–8.
83. Scriba TJ, Coussens AK, Fletcher HA. Human immunology of tuberculosis. *Microbiol Spectr*. (2016) 4:1–23. doi: 10.1128/microbiolspec.TBTB2-0016-2016
84. Flynn JL, Chan J, Triebold KJ, Dalton DK, Stewart TA, Bloom BR. An essential role for interferon gamma in resistance to *Mycobacterium tuberculosis* infection. *J Exp Med*. (1993) 178:2249–54. doi: 10.1084/jem.178.6.2249
85. Ahmed M, de Winther MPJ, van den Bossche J. Epigenetic mechanisms of macrophage activation in type 2 diabetes. *Immunobiology*. (2017) 222:937–43. doi: 10.1016/j.imbio.2016.08.011
86. Chang S-C, Yang W-CV. Hyperglycemia, tumorigenesis, and chronic inflammation. *Crit Rev Oncol Hematol*. (2016) 108:146–53. doi: 10.1016/j.critrevonc.2016.11.003
87. Ramasamy R, Yan SF, Schmidt AM. Receptor for AGE (RAGE): signaling mechanisms in the pathogenesis of diabetes and its complications. *Ann N Y Acad Sci*. (2011) 1243:88–102. doi: 10.1111/j.1749-6632.2011.06320.x
88. Guglielmotto M, Aragno M, Tamagno E, Vercellinatto I, Visentin S, Medana C, et al. AGEs/RAGE complex upregulates BACE1 via NF-κB pathway activation. *Neurobiol Aging*. (2012) 33:196.e13–27. doi: 10.1016/j.neurobiolaging.2010.05.026
89. Ingels C, Derese I, Wouters PJ, Van den Berghe G, Vanhorebeek I. Soluble RAGE and the RAGE Ligands HMGB1 and S100A12 in critical illness. *Shock*. (2015) 43:109–16. doi: 10.1097/SHK.0000000000000278
90. Nogueira-Machado JA, Volpe CM de O, Veloso CA, Chaves MM. HMGB1, TLR and RAGE: a functional tripod that leads to diabetic inflammation. *Expert Opin Ther Targets*. (2011) 15:1023–35. doi: 10.1517/14728222.2011.575360
91. Morohoshi M, Fujisawa K, Uchimura I, Numano F. Glucose-dependent interleukin 6 and tumor necrosis factor production by human peripheral blood monocytes vitro. *Diabetes*. (1996) 45:954–9. doi: 10.2337/diabetes.45.7.954
92. Hu R, Xia C-Q, Butfiloski E, Clare-Salzler M. Effect of high glucose on cytokine production by human peripheral blood immune cells and type I interferon signaling in monocytes: implications for the role of hyperglycemia in the diabetes inflammatory process and host defense against infection. *Clin Immunol*. (2018) 195:139–48. doi: 10.1016/j.clim.2018.06.003
93. Brattsand R, Linden M. Cytokine modulation by glucocorticoids: mechanisms and actions in cellular studies. *Aliment Pharmacol Ther*. (1996) 10(Suppl. 2):81–90–2. doi: 10.1046/j.1365-2036.1996.22164025.x
94. He Y, Luo Y, Lao X, Tan L, Sun E. Cytokine signatures of human whole blood for monitoring immunosuppression. *Cent Eur J Immunol*. (2014) 39:271–8. doi: 10.5114/ceji.2014.45936
95. Liu Z, Yuan X, Luo Y, He Y, Jiang Y, Chen ZK, et al. Evaluating the effects of immunosuppressants on human immunity using cytokine profiles of whole blood. *Cytokine*. (2009) 45:141–7. doi: 10.1016/j.cyto.2008.12.003
96. Devin LH, Remick DG. Delayed addition of glucocorticoids selectively suppresses cytokine production in stimulated human whole blood. *Clin Vaccine Immunol*. (2010) 17:979–85. doi: 10.1128/CVI.00404-09
97. Rhen T, Cidlowski JA. Antiinflammatory action of glucocorticoids — new mechanisms for old drugs. *N Engl J Med*. (2005) 353:1711–23. doi: 10.1056/NEJMra050541
98. Mozo L, Suárez A, Gutiérrez C. Glucocorticoids up-regulate constitutive interleukin-10 production by human monocytes. *Clin Exp allergy*. (2004) 34:406–12. doi: 10.1111/j.1365-2222.2004.01824.x
99. Olnes MJ, Kotliarov Y, Biancotto A, Cheung F, Chen J, Shi R, et al. Effects of systemically administered hydrocortisone on the human immunome. *Sci Rep*. (2016) 6:23002. doi: 10.1038/srep25215
100. Kunicka JE, Talle MA, Denhardt GH, Brown M, Prince LA, Goldstein G. Immunosuppression by glucocorticoids: inhibition of production of multiple lymphokines by *in vivo* administration of dexamethasone. *Cell Immunol*. (1993) 149:39–49. doi: 10.1006/cimm.1993.1134
101. Fushimi T, Okayama H, Seki T, Shimura S, Shirato K. Dexamethasone suppressed gene expression and production of lnterleukin-10 by human peripheral blood mononuclear cells and monocytes. *Int Arch Allergy Immunol*. (1997) 112:13–8. doi: 10.1159/000237425
102. Borish L, Aarons A, Rumbyrt J, Cvietusa P, Negri J, Wenzel S. Interleukin-10 regulation in normal subjects and patients with asthma. *J Allergy Clin Immunol*. (1996) 97:1288–96. doi: 10.1016/S0091-6749(96)70197-5
103. Saraiva M, O'Garra A. The regulation of IL-10 production by immune cells. *Nat Rev Immunol*. (2010) 10:170–81. doi: 10.1038/nri2711

Conflict of Interest: The authors declare that the research was conducted in the absence of any commercial or financial relationships that could be construed as a potential conflict of interest.

frontiers in Neuroscience

CASE REPORT
published: 15 April 2020
doi: 10.3389/fnins.2020.00331

Hashimoto's Encephalopathy Mimicking Viral Encephalitis: A Case Report

*Miaomiao Yu, Yu Yang, Xianyi Ma, Yinyin Xie, Ningning Sun and Hongmei Meng**

Department of Neurology and Neuroscience Center, The First Hospital of Jilin University, Changchun, China

Hashimoto's encephalopathy (HE) is a rare neuropsychiatric syndrome characterized by elevated levels of anti-thyroid antibodies. Diverse manifestations make timely diagnosis of HE difficult. Herein, we report a case of HE, in which the clinical symptoms and laboratory test results mimicked viral encephalitis. A 59-year-old male patient, who presented with a fever, headache, slow and unclear speech, sentence confusion, elevated levels of anti-thyroid antibodies in the serum, an increased white blood cell count, and positivity for anti-thyroid antibodies in the CSF, was finally diagnosed with HE and responded well to a small dose of methylprednisolone. This report helps bring the attention of clinicians to the fact that HE should be considered when cases of unexplained encephalopathy are encountered.

Keywords: Hashimoto's encephalopathy, viral encephalitis, differential diagnosis, anti-thyroid antibodies, therapy

OPEN ACCESS

Edited by:
Ana Rosa Pérez, National Scientific and Technical Research Council (CONICET), Argentina

Reviewed by:
Kumaran Deiva, Hôpitaux Universitaires Paris-Sud (APHP), France
Tadanori Hamano, University of Fukui, Japan

***Correspondence:**
Hongmei Meng
hongmeiyp@126.com

Specialty section:
This article was submitted to Neuroendocrine Science, a section of the journal Frontiers in Neuroscience

Received: *21 October 2019*
Accepted: *20 March 2020*
Published: *15 April 2020*

Citation:
Yu M, Yang Y, Ma X, Xie Y, Sun N and Meng H (2020) Hashimoto's Encephalopathy Mimicking Viral Encephalitis: A Case Report. Front. Neurosci. 14:331. doi: 10.3389/fnins.2020.00331

BACKGROUND

Hashimoto's encephalopathy (HE) is a rare neuropsychiatric syndrome associated with thyroid antibodies and was first reported by Brain in 1996 (Brain et al., 1966). HE presents with a broad range of clinical symptoms, including neurological manifestations such as stroke-like episodes, seizures, confusion, myoclonus, ataxia, tremors, and dementia, as well as psychiatric manifestations, including acute psychosis, depressive disorders, personality changes, hallucinations, and schizophrenia (Kirshner, 2014; Menon et al., 2017). In this case report, we describe a patient with HE whose clinical symptoms and laboratory test results mimicked viral encephalitis.

CASE REPORT

A 59-year-old man who presented with fever, headache, and awkward speech which specifically manifested as slow and unclear speech, was admitted to the hospital. He denied recent infections such as flu or gastroenteritis, travel, and other possible reasons, which could be responsible for the fever, which peaked at 39.5°C. Previous medical history revealed gout for 20 years, but no drugs were prescribed. His neurological examination and cranial computed tomography (CT) and magnetic resonance imaging (MRI) (**Figure 1**) scans were normal. EEG results showed minor irregularities in waves (5–20 μv 14–20 Hz β) emitted from the bilateral hemispheres. Blood routine, C-reactive protein, serum vitamin B12, and folic acid, as well as other autoimmunity makers containing

antinuclear antibody (ANA), anti-neutrophil cytoplasmic antibodies (ANCA), and rheumatoid factors were all unremarkable. The cerebrospinal fluid (CSF) showed an increased white blood cell (WBC) count (104×10^6/L, reference range 0–8 × 10^6/L) and elevated protein levels (1.68 g/L, reference range 0.15–0.45 g/L). Culture, smear, and bacterial, fungal, viral, and tubercle bacillus antibodies in the serum and CSF were negative. He was diagnosed with viral encephalitis and treated with antiviral agents. His symptoms eased within a week and he was discharged from the hospital. Five months later, he was referred to our hospital again due to a fever of 38.5°C and occasional sentence confusion. Another lumbar puncture was performed; the CSF had a WBC count of 39 × 10^6/L and the protein content was 1.32 g/L. The cranial MRI and laboratory test findings were almost normal except for decreased thyroid function and increased anti-thyroid autoantibody (ATA) levels in the serum and CSF. The initial findings were as follows: in the serum, the thyroid stimulating hormone (TSH) concentration was 43.39 uIU/ml (reference range (RR): 0.27–4.2 uIU/ml), free triiodothyronine (FT3) concentration was 2.89 pmol/ml (RR: 3.1–6.8 pmol/ml), free thyroxine (FT4) concentration was 7.18 pmol/ml (RR: 12.0–22.0 pmol/ml), total triiodothyronine (TT3) concentration was 1.17 pmol/ml (RR: 1.3–3.1 pmol/ml), and total thyroxine (TT4) concentration was 44.26 pmol/ml (RR: 66–181 pmol/ml); the titer of anti-thyroglobulin autoantibodies (TgAb) was 1274 IU/ml (RR: < 115 IU/ml) and the titer of anti-thyroperoxidase autoantibodies (TPOAb) was 600 IU/ml (RR: < 35 IU/ml). In the CSF, ATA was positive (TPOAb 17.06 IU/ml, TgAb 16.02 IU/ml). Ultrasound imaging indicated diffuse lesions of the thyroid. Antibody analysis of anti-NMDAR, AMPA1, AMPA2, LGI1, CASPR2, GABA, GAD, anti-Hu, Yo, Ri, MAI, MA2, CV2, Amphiphysin, SOX-1, Tr, Zic4, and GAD65, were all negative in both the serum and CSF. The patient was ultimately diagnosed with HE, Hashimoto's Thyroiditis, and hypothyroidism and prescribed methylprednisolone and Euthyrox. Methylprednisolone was started at a dose of 80 mg/day for 1 week and reduced to 40 mg/day in the 2 week; subsequently, oral prednisolone was prescribed, which was weaned at a rate of 5 mg per week, that is oral prednisolone was used for a total of 8 weeks. His symptoms were relieved in 3 days. The patient remained healthy during a follow up period of 1 year.

DISCUSSION

The estimated prevalence rate of HE is 2.1 in 100,000 and the sex ratio (female to male) is 4:1 (Ferracci et al., 2004). The course of HE may be progressive, relapsing-remitting, or even self-limiting. In the present case, the patient appeared to have a relapsing-remitting course.

Combined with the patient's symptoms, normal MRI results, high titers of ATA in the serum and ATA positivity of the CSF, the patient was finally diagnosed with HE after excluding other potential causes including stroke, tumor, central nervous system infection, autoimmune encephalitis, and paraneoplastic syndrome.

Overall, the pathophysiology of HE is still inconclusive. On the basis of the neuropathological findings, an autoimmune vasculitis mechanism has been proposed. In a previous study, brain biopsies revealed that lymphocytic infiltration around the venules and arterioles may be involved (Duffey et al., 2003). Another possible mechanism involved is that ATAs attack antigens that are shared by the thyroid and the brain, and for this reason high titers of ATAs including TPOAb, TgAb, and anti-TSH receptor (TSH-R) antibodies in the serum, and sometimes in CSF, are considered hallmark features of HE (Yoneda, 2018). Similarly, high titers of ATA and CSF-ATA were found in our case. In a previous study, plasma exchange therapy resulted in a profound improvement of the patients' symptoms (Tran et al., 2018). Together, these findings suggest that ATA plays an important role in HE. However, elevated ATA levels in the serum are also found within the general population and are especially common in elderly individuals. Further, the extent of ATA elevation is not related to the severity of HE. Although the patients' serum ATA levels still remained high after methylprednisolone therapy, his symptoms were resolved (titer of anti-thyroglobulin autoantibodies (TgAb): 041 IU/ml, RR: < 115 IU/ml; titer of anti-thyroperoxidase autoantibodies (TPOA): 600 IU/ml, RR: <35 IU/ml). Our results confirm that there is no relationship between the extent of ATA elevation and the severity of HE.

Although the correlation between ATA and HE is still unclear (Kirshner, 2014), diagnostic criteria for HE were proposed by a team of experts in Lancet Neurology in 2016. The criteria are as follows: (1) encephalopathy with seizures, myoclonus, hallucinations, or stroke-like episodes; (2) subclinical or mild

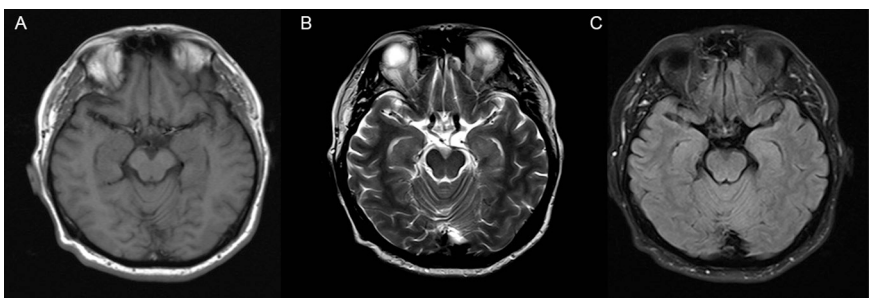

FIGURE 1 | MRI imaging of brain. There are no abnormal findings in the brain MRI imaging of the patient. **(A)** T1-weighted image; **(B)** T2-weighted image; **(C)** FLAIR image.

overt thyroid disease (usually hypothyroidism); (3) normal findings or non-specific abnormalities shown by brain MRI; (4) presence of thyroid antibodies in the serum (thyroid peroxidase, thyroglobulin); (5) absence of well-characterized neuronal antibodies in the serum and CSF; and (6) reasonable exclusion of alternative causes. HE can be diagnosed if a patient meets all the criteria (Graus et al., 2016). Our patient met all the above criteria, and he could therefore be diagnosed with HE. Most patients with HE respond well to steroids; however, when patients are steroid-resistant, other immunosuppression therapies including plasma exchange, IVIg, methotrexate, and mycophenolate have been shown to be effective. High doses of methylprednisolone (500–1000 mg) are most frequently used. Because the patient showed mild symptoms and refusal the use of high dose of methylprednisolone, we prescribed a low dose of methylprednisolone. Our patient underwent steroid therapy and has since remained healthy. The patient did not receive any other immunotherapy treatments during follow-up. In a retrospective observational study performed by Mamoudjy et al. (2013) the research results indicated that some HE patients underwent a relapse, even a third attack, which had a shorter interval time (mean 18 days) compared with that of the second attack (mean 213 days). Patients with relapses needed methylprednisolone or immunosuppressive therapy again (Mamoudjy et al., 2013). Our patient suffered one relapse about 150 days after the first attack and steroid therapy was effective. Sequelae, such as headache, memory disorders and so on, was also frequent (Mamoudjy et al., 2013), however, our patient did not have any sequelae left luckily.

Hashimoto's encephalopathy is difficult to diagnose accurately, because of its association with a broad range of clinical symptoms, as well its non-specific neuroimaging and electroencephalogram presentation. A previous article reported a case of HE that was initially misdiagnosed as viral encephalitis (He et al., 2013), in which the patient presented with progressively impaired cognitive function and uncontrolled seizures without fever. In our case, the increased WBC count and CSF protein combined with a fever and headache lead us to diagnose it as viral encephalitis. Fever has been described in several patients with HE with and without thyroid disorders (Huang et al., 2011; Lu et al., 2015). Although the reason for fever in HE is unclear, Lu et al. (2015) suggested it may be a direct result of inflammation combined with the autoimmune vasculitis.

Hashimoto's encephalopathy can manifest in many different ways, including stroke-like episodes, seizures, confusion, myoclonus, acute psychosis, depressive disorders, and hallucinations, causing HE to be confused with other diseases. Uwatoko et al. (2018) reported a case of a patient who presented with parkinsonism and a tumor-like lesion revealed by brain MRI. After biopsy, it was found that the lesion was not a tumor, and HE was finally confirmed (Uwatoko et al., 2018). Patients with HE can also present with unusual symptoms such as pseudobulbar palsy, sensorimotor polyneuropathy, catatonic symptoms, vertigo, muscle weakness, chorea, opsoclonus, and a trigeminal neuralgia type headache, among others (Beckmann et al., 2011; Salazar et al., 2012; Sharan et al., 2015; Ueno et al., 2016; Karthik et al., 2017; Emeksiz et al., 2018; Oz Tuncer et al., 2018). Rapidly progressive dementia, as a common manifestation of HE, makes it necessary to distinguish HE from other diseases caused by vascular, infectious, toxic-metabolic, and autoimmune factors, metastasis/neoplasia, iatrogenic/inborn errors of metabolism, neurodegenerative diseases, and systemic diseases/seizures (Paterson et al., 2012).

CONCLUSION

In conclusion, the diagnosis of HE is rather complex but valuable because of its dramatic response to immunosuppressive therapy. When clinicians are faced with unexplained encephalitis, thyroid function and ATA levels should be considered as conventional tests. HE can be excluded as a diagnosis for patients with normal serum levels of ATA. For patients with increased levels of ATA, HE should be considered after ruling out other possible diseases.

DATA AVAILABILITY STATEMENT

The datasets generated for this study are available on request to the corresponding author.

ETHICS STATEMENT

The studies involving human participants were reviewed and approved by the Ethics Committee of The First Hospital of Jilin University, China. The patients/participants provided their written informed consent to participate in this study. Written informed consent was obtained from the individual(s) for the publication of any potentially identifiable images or data included in this article.

AUTHOR CONTRIBUTIONS

HM contributed to the conception and design of the manuscript. MY wrote the first draft of the manuscript. YY, XM, YX, and NS wrote sections of the manuscript. All authors contributed to manuscript revision, read, and approved the submitted version.

FUNDING

This work was supported by National Key R&D Program of China (No. 2017YFC0110304).

REFERENCES

Beckmann, Y. Y., Top, D., and Yigit, T. (2011). Unusual presentations of Hashimoto's encephalopathy: trigeminal neuralgiaform headache, skew deviation, hypomania. *Endocrine* 40, 495–496. doi: 10.1007/s12020-011-9506-x

Brain, L., Jellinek, E. H., and Ball, K. (1966). Hashimoto's disease and encephalopathy. *Lancet* 2, 512–514.

Duffey, P., Yee, S., Reid, I. N., and Bridges, L. R. (2003). Hashimoto's encephalopathy: postmortem findings after fatal status epilepticus. *Neurology* 61, 1124–1126.

Emeksiz, S., Kutlu, N. O., Alacakir, N., and Caksen, H. (2018). A case of steroid-resistance Hashimoto's encephalopathy presenting with sensorimotor polyneuropathy. *Turk. J. Pediatr.* 60, 310–314. doi: 10.24953/turkjped.2018.03.012

Ferracci, F., Bertiato, G., and Moretto, G. (2004). Hashimoto's encephalopathy: epidemiologic data and pathogenetic considerations. *J. Neurol. Sci.* 217, 165–168.

Graus, F., Titulaer, M. J., Balu, R., Benseler, S., Bien, C. G., Cellucci, T., et al. (2016). A clinical approach to diagnosis of autoimmune encephalitis. *Lancet Neurol.* 15, 391–404.

He, L., Li, M., Long, X. H., Li, X. P., and Peng, Y. (2013). A case of Hashimoto's encephalopathy misdiagnosed as viral encephalitis. *Am. J. Case Rep.* 14, 366–369.

Huang, W., Xia, C., and Chatham, M. (2011). Infectious disease or Hashimoto's encephalopathy flares: a case report. *Seizure* 20, 717–719. doi: 10.1016/j.seizure.2011.04.011

Karthik, M. S., Nandhini, K., Subashini, V., and Balakrishnan, R. (2017). Hashimoto's Encephalopathy Presenting with Unusual Behavioural Disturbances in an Adolescent Girl. *Case Rep. Med.* 2017, 3494310. doi: 10.1155/2017/3494310

Kirshner, H. S. (2014). Hashimoto's encephalopathy: a brief review. *Curr. Neurol. Neurosci. Rep.* 14:476.

Lu, T., Zhou, Z., Wu, A., Qin, B., and Lu, Z. (2015). Febrile Hashimoto's encephalopathy associated with Hashitoxicosis. *Acta Neurol. Belg.* 115, 811–813.

Mamoudjy, N., Korff, C., Maurey, H., Blanchard, G., Steshenko, D., Loiseau-Corvez, M. N., et al. (2013). Hashimoto's encephalopathy: identification and long-term outcome in children. *Eur. J. Paediatr. Neurol.* 17, 280–287. doi: 10.1016/j.ejpn.2012.11.003

Menon, V., Subramanian, K., and Thamizh, J. S. (2017). Psychiatric presentations heralding Hashimoto's encephalopathy: a systematic review and analysis of cases reported in literature. *J. Neurosci. Rural. Pract.* 8, 261–267. doi: 10.4103/jnrp.jnrp_440_16

Oz Tuncer, G., Teber, S., Kutluk, M. G., Albayrak, P., and Deda, G. (2018). Hashimoto's encephalopathy presenting as pseudobulbar palsy. *Childs Nerv. Syst.* 34, 1251–1254. doi: 10.1007/s00381-018-3720-2

Paterson, R. W., Takada, L. T., and Geschwind, M. D. (2012). Diagnosis and treatment of rapidly progressive dementias. *Neurol Clin. Pract.* 2, 187–200.

Salazar, R., Mehta, C., Zaher, N., and Miller, D. (2012). Opsoclonus as a manifestation of Hashimoto's encephalopathy. *J. Clin. Neurosci.* 19, 1465–1466. doi: 10.1016/j.jocn.2012.02.012

Sharan, A., Sengupta, S., Mukhopadhyay, S., and Ghosh, B. (2015). Hashimoto's Encephalopathy Presenting with Chorea. *J. Assoc. Physicians India* 63, 83–84.

Tran, M. H., Mkhikian, H., Sy, M., Perez-Alvarez, I., and Demetriou, M. (2018). Long-term plasma exchange as maintenance therapy for cerebellar-type Hashimoto's encephalopathy, a case report. *Transfus. Apher. Sci.* 57, 418–420. doi: 10.1016/j.transci.2018.05.027

Ueno, H., Nishizato, C., Shimazu, T., Watanabe, H., Mizukami, T., Kosuge, H., et al. (2016). Hashimoto's encephalopathy presenting with vertigo and muscle weakness in a male pediatric patient. *No Hattatsu* 48, 45–47.

Uwatoko, H., Yabe, I., Sato, S., Abe, M., Shirai, S., Takahashi, I., et al. (2018). Hashimoto's encephalopathy mimicking a brain tumor and its pathological findings: a case report. *J. Neurol. Sci.* 394, 141–143. doi: 10.1016/j.jns.2018.09.008

Yoneda, M. (2018). Hashimoto's Encephalopathy and Autoantibodies. *Brain Nerve* 70, 305–314. doi: 10.11477/mf.1416201004

Conflict of Interest: The authors declare that the research was conducted in the absence of any commercial or financial relationships that could be construed as a potential conflict of interest.

frontiers in Endocrinology

REVIEW
published: 21 April 2020
doi: 10.3389/fendo.2020.00195

OPEN ACCESS

Edited by:
Ana Rosa Pérez, National Council for Scientific and Technical Research (CONICET), Argentina

Reviewed by:
Antonio Torsello, University of Milano-Bicocca, Italy
Takefumi Suzuki, University of Yamanashi, Japan

***Correspondence:**
Lenin Pavón
lkuriaki@imp.edu.mx

†ORCID:
Samantha Alvarez-Herrera
orcid.org/0000-0001-9747-885X
Raúl Escamilla
orcid.org/0000-0002-6772-9731
Oscar Medina-Contreras
orcid.org/0000-0002-4432-7780
Ricardo Saracco
orcid.org/0000-0002-0004-1318
Yvonne Flores
orcid.org/0000-0002-4508-8734
Gabriela Hurtado-Alvarado
orcid.org/0000-0002-6137-663X
José Luis Maldonado-García
orcid.org/0000-0003-2694-1290
Gilberto Pérez-Sánchez
orcid.org/0000-0003-3878-0631
Enrique Becerril-Villanueva
orcid.org/0000-0001-7210-9775
Lenin Pavón
orcid.org/0000-0002-6067-6868

‡*These authors have contributed equally to this work*

Specialty section:
This article was submitted to Neuroendocrine Science, a section of the journal Frontiers in Endocrinology

Received: *14 October 2019*
Accepted: *18 March 2020*
Published: *21 April 2020*

Citation:
Alvarez-Herrera S, Escamilla R, Medina-Contreras O, Saracco R, Flores Y, Hurtado-Alvarado G, Maldonado-García JL, Becerril-Villanueva E, Pérez-Sánchez G and Pavón L (2020) Immunoendocrine Peripheral Effects Induced by Atypical Antipsychotics. Front. Endocrinol. 11:195. doi: 10.3389/fendo.2020.00195

Immunoendocrine Peripheral Effects Induced by Atypical Antipsychotics

Samantha Alvarez-Herrera[1†‡], Raúl Escamilla[2†‡], Oscar Medina-Contreras[3†], Ricardo Saracco[2†], Yvonne Flores[2†], Gabriela Hurtado-Alvarado[4†], José Luis Maldonado-García[1†], Enrique Becerril-Villanueva[1†], Gilberto Pérez-Sánchez[1†] and Lenin Pavón[1†]*

[1] *Laboratorio de Psicoinmunología, Dirección de Investigaciones en Neurociencias del Instituto Nacional de Psiquiatría Ramón de la Fuente Muñiz, Ciudad de México, Mexico,* [2] *Clínica de Esquizofrenia, Instituto Nacional de Psiquiatría Ramón de la Fuente Muñiz, Ciudad de México, Mexico,* [3] *Laboratorio de Investigación en Inmunología y Proteómica, Hospital Infantil de México Federico Gómez, Ciudad de México, Mexico,* [4] *Area of Neurosciences, Department of Biology of Reproduction, CBS, Universidad Autonoma Metropolitana-Iztapalapa, Mexico City, Mexico*

Atypical antipsychotics (AAP) or second-generation antipsychotics are the clinical option for schizophrenia treatment during acute psychoses, but they are also indicated for maintenance during lifetime, even though they are being used for other psychiatric conditions in clinical practice such as affective disorders and autism spectrum disorder, among others. These drugs are differentiated from typical antipsychotics based on their clinical profile and are a better choice because they cause fewer side effects regarding extrapyramidal symptoms (EPS). Even though they provide clear therapeutic benefits, AAP induce peripheral effects that trigger phenotypic, functional, and systemic changes outside the Central Nervous System (CNS). Metabolic disease is frequently associated with AAP and significantly impacts the patient's quality of life. However, other peripheral changes of clinical relevance are present during AAP treatment, such as alterations in the immune and endocrine systems as well as the intestinal microbiome. These less studied alterations also have a significant impact in the patient's health status. This manuscript aims to revise the peripheral immunological, endocrine, and intestinal microbiome changes induced by AAP consumption recommended in the clinical guidelines for schizophrenia and other psychiatric disorders.

Keywords: atypical antipsychotics (AAP), peripheral effects, inflammatory response, endocrine response, microbiome

INTRODUCTION

Antipsychotics have been widely used in clinical psychiatry and neuroscience research for over 68 years since chlorpromazine demonstrated sedative effects in psychotic patients (1). Antipsychotics drugs are classified as typical or atypical according to the clinical effects that they cause (2). Atypical (AAP) or second-generation antipsychotics (SGA) are effective against positive and negative symptoms and improve some domains of cognition of schizophrenia. AAP are the first clinical option to treat various psychiatric conditions because they produce significantly fewer EPS and pose a lower risk of pseudo-parkinsonism and catalepsy in comparison to typical antipsychotics (3, 4).

Even though AAP were initially prescribed for psychotic disorders like schizophrenia, the Food and Drug Administration (FDA) has approved the use of these drugs for the treatment of other psychiatric conditions, including bipolar disorder, major depressive disorder with psychotic features, acute agitation, Tourette syndrome, borderline personality disorder,

dementia, and substance-induced psychotic disorder (5) as well as diagnosed psychiatric conditions in children (6).

The pharmacological and adverse effects related to AAP consumption are due to the affinity of these drugs to a broad range of neurotransmitter receptors located in the CNS, peripheral organs, tissues, and cells. Each AAP has its own unique affinity pattern that generates psychiatric and peripheral effects acting at dopamine (DA) D1, D2, D3, D4, adrenergic α-1 and α-2, serotoninergic 5-HT_{2A} and 5-HT_{2C}, histaminergic, and muscarinic receptors (7). Despite their enormous efficacy on psychiatric symptoms and their low rate of EPS, AAP are not without adverse side effects. It is well-known that AAP produce peripheral effects related with metabolic alterations (8) like weight gain, type 2 diabetes, dyslipidemia, and subsequent cardiovascular complications (9, 10).

However, AAP consumption induces other peripheral changes that are clinically relevant but commonly dismissed, such as alterations in the immune and endocrine function as well as the intestinal microbiome. These sets of changes play a significant role in triggering inflammatory and metabolic chronic changes that affect the adequate recovery of patients and their quality of life.

A wide variety of hormones show alterations in their circulatory levels in human and animal models during AAP consumption. Among the affected hormones are those related to glucose metabolism, orexigenic and anorexigenic molecules, and hormones secreted by the hypothalamus or pituitary (11–14).

In patients and experimental models, AAP consumption modifies leukocyte phenotype, and cell count. The evidence demonstrates that macrophages (MQs), dendritic cells (DCs), T and B lymphocytes, neutrophils, and other leukocytes modify their function as well as cytokine production and release, apoptosis, phagocytosis, and Th1-Th2 differentiation (15–17). Additionally, other reports show AAP can change the peripheral levels of pro-inflammatory, anti-inflammatory, and growth factors molecules like C-reactive protein (CRP), interleukin (IL)-1β, IL-6, IL-12, IL-10, tumor necrosis factor (TNF)-α, interferon (IFN)-γ, and other molecules, affecting the systemic condition of the organism (18, 19).

Changes in hormonal and inflammatory levels in patients that consume AAP impact intestinal microbiota. It is important to note that the growing evidence suggests the intestinal microbiome could be involved in the treatment response. Moreover, gut microorganisms might be necessary to the occurrence of adverse effects such as weight gain (20).

In this review, we summarize the clinical and experimental studies that demonstrated the immunological, endocrine, and intestinal microbiome changes induced by the consumption of each AAP approved by the FDA for the treatment of schizophrenia and other psychiatric disorders.

Why Is It Important to Make Evident the Neuroendocrine Effects Induced by AAP Consumption?

Antipsychotic therapy prevails as a standard and fundamental component for major psychiatric disorders like acute episode of psychoses and the maintenance phase of schizophrenia and schizoaffective disorders (21). These drugs do not act exclusively on the CNS, and the more evident problem related with AAP treatment is the higher risk of developing hyperphagia, hyperglycemia, dyslipidemia, weight gain, diabetes mellitus, and insulin resistance (22), which further develops metabolic and cardiac complications with subsequent reduction in life expectancy, poor patient compliance, and sudden death (4).

Daily clinical practice not only identifies metabolic problems but also three clinically relevant issues that are the result of the chronic consumption of AAP by patients (23), often disregarded by healthcare professionals. The first are the endocrine and immune effects that AAP cause in patients and that will be listed in subsequent sections. The second is that the effects of the cotreatment with AAP and psychiatric medication, despite being more common than which is acknowledged (approximately 66% of psychiatrists use AAPs in combination), (24). The most common causes of co-treatment are: Patients seemed resistant to treatment instead of a monotherapy assay with clozapine or had been diagnosed with two or more psychiatric diagnoses, the clinician overlapped one antipsychotic while another was titrated (switching medication because of lack of response or better security profile), and finally, an effective dose of an AP was not achieved because of intolerance or side effects. Finally, the third issue is the joint effect of AAP consumption together with other drugs as benzodiazepines (adjunctive therapy for acute agitation, comorbid anxiety, or distress), antidepressants (as the adjunctive therapy in schizophrenia for persistent negative symptoms, comorbid major depressive disorder, and suicide risk) (25), APs also are used as adjunctive therapy for treatment-resistant major depressive disorder and major depressive disorder with psychotic features, and mood stabilizers as adjunctive therapy in bipolar disorder, schizoaffective disorder, and ultra-resistant schizophrenia (26).

This evidences the wide therapeutic use of AAP, which have become first-choice drugs to treat schizophrenia and other psychoses due to the lower risk of developing EPS. However, these drugs are highly promiscuous in their interaction with several neurotransmitter receptors as 5-HT and D, expressed in different peripheral cell types, such as leukocytes and gland cells (27–30), which constitutively express these receptors AAP can bind to.

To understand the diversity of effects these drugs systemically induce, we must consider that AAP do not behave equivalently, as shown in **Figure 1**. They are structurally heterogeneous, and the therapeutic effects, albeit generally equivalent, have particularities firstly explained by their heterogeneous physicochemical interactions with several receptors (see **Table 1**). The interactions between these drugs and their receptor firstly induces the conformational changes within the receptor structure that result in the activation of the associated heterotrimeric G protein (GPCR) and its consequent activation (53).

In addition, over the past decade new mechanisms associated with GPCR function have been discovered, such as the ability of β-arrestins to act as multifunctional proteins and activate multiple mediators like ERK, proto-oncogene tyrosine-protein kinase SRC, nuclear factor-κB, and phosphoinositide 3-kinase

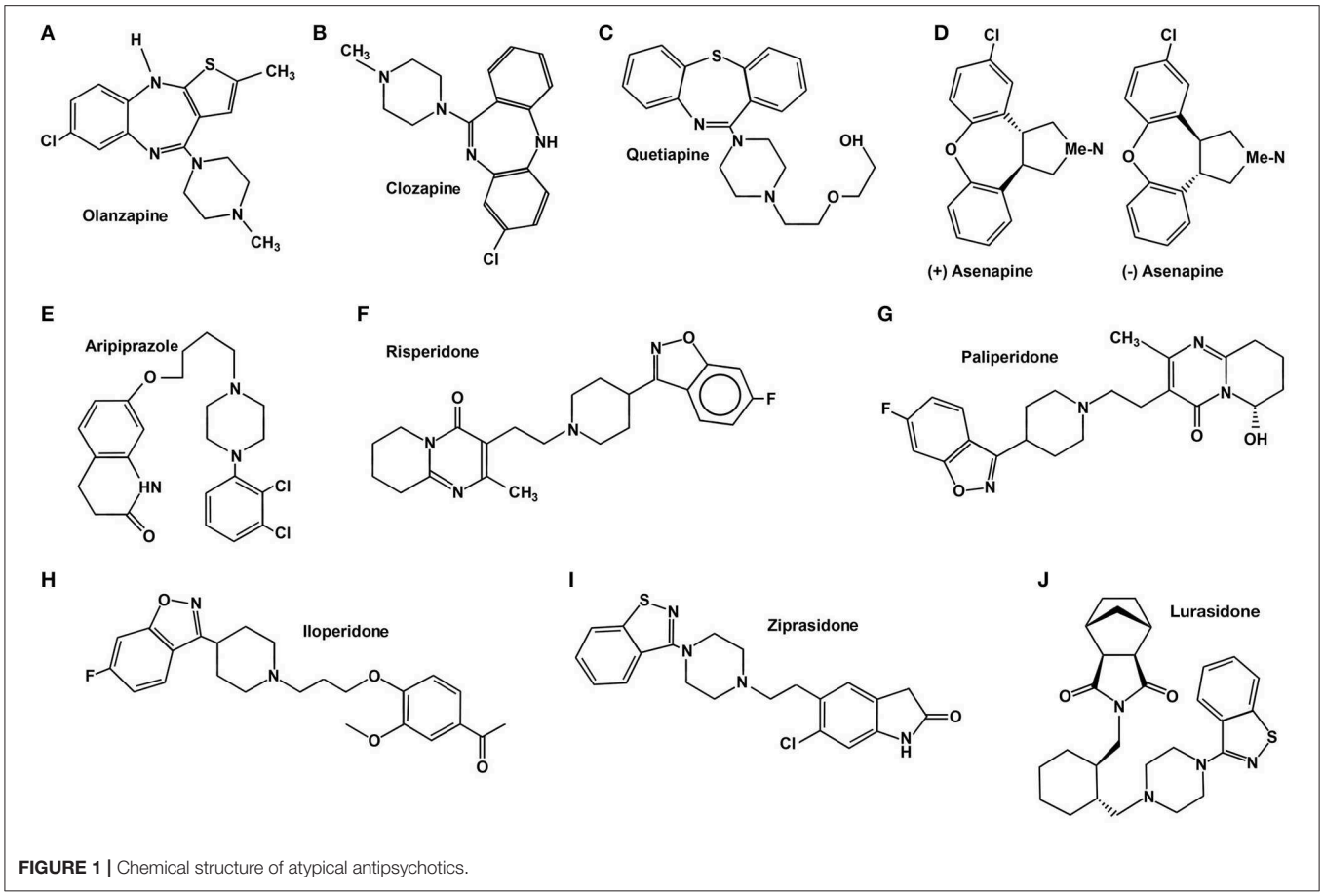

FIGURE 1 | Chemical structure of atypical antipsychotics.

(54). The capacity of a ligand to preferentially activate either G protein-dependent signaling or G protein-independent signaling is called "biased agonism" or "functional selectivity." This innovative new concept reflects the heterogeneity and complexity of the different receptor conformation states it can be transitioning when specifically interacting with stimulants (55). In addition, recent data have demonstrated how receptor functional selectivity is a dynamic and adaptable process, which can also be modified by physiopathological conditions (56).

In addition, it must be considered that, in cases such as cotreatment, the combined effect of two or more AAP or polypharmacy can induce a phenomenon called Convergence of signaling pathways occurring in cells. It can change the overall outcome of signals initiated with different relative strengths of signal, while initial events at the cell membrane may also pose differential consequences for the whole cell (57). These phenomena are reflected in the fluctuations of soluble mediators such as cytokines and hormones in AAP consumers.

Immunoendocrine Peripheral Effects Induced by AAP

In this section we will exhibit the specific immunoendocrine peripheral effects of the 10 most prescribed APs drugs approved by the FDA: olanzapine, clozapine, quetiapine, asenapine, aripiprazole, risperidone, paliperidone, iloperidone, ziprasidone, and lurasidone.

CLOZAPINE

Clozapine was the first AAP developed in 1958 and it was approved by the FDA in 1989 after 31 years of investigations and clinical trials for treatment-resistant schizophrenia (58). Currently, it is considered to be one of the most effective antipsychotics for the treatment of schizophrenia, psychosis, and depression. Nevertheless, it is not the first-line drug of choice due to its range of adverse effects, making compliance an issue for many patients (59).

Clozapine is often discontinued (18) since it has some other potentially dangerous and life-threatening side effects, such as myocarditis, seizures, agranulocytosis, or granulocytopenia, and gastrointestinal hypomotility. It is a 5-HT_{2A} and D4 receptor antagonist. It also shows affinity to D1, D2, D3, D5, α-adrenergic, histaminergic H1, and cholinergic receptors (37) (see **Table 1**). This fact hinders the understanding of its molecular mechanisms of action and the identification of drug response predictors (60). In addition, this drug is an antagonist of other receptors, such as H1, 5-HT_{2C}, and M3, leading to weight gain and metabolic side effects (61) that include both glycemic dysregulation and insulin resistance (62) (see **Table 1**).

TABLE 1 | Characteristics of APPs interaction with different neurotransmitter receptors.

	M1	1/2	D1	1/2	D2	1/2	D3	1/2	D4	1/2	$5HT_{1A}$	1/2	$5HT_{2A}$	1/2	$5HT_{2C}$	1/2	$5HT_6$	1/2	$5HT_7$	1/2	α 1A	1/2	α2A	1/2	H1	1/2	References
Olanzapine	73.0	1	11.0	2	14.4	2	43.0	2	50.0	2	3442.0	1	4.0	2	11.00	2	5.00	2	nd	-	19.0	2	nd	-	7.0	2	(31–36)
Clozapine	6.1	2	266.2	1	157.0	1	269.0	1	26.3	1	123.7	2	5.3	1	9.44	1	13.4	1	17.9	1	1.6	1	37.0	2	1.1	1	(36, 37)
Quetiapine	858.0	1	712.0	1	245.0	1	483.0	1	1202.0	1	432.0	2	101.0	1	2502.0	1	1865.0	1	307.0	1	22.0	1	3630.0	1	11.0	1	(36, 38)
Asenapine	-	-	1.4	1	1.3	1	0.4	1	1.1	1	2.5	1	0.1	1	0.03	1	1.10	1	1.4	1	1.2	1	1.2	1	1.0	1	(39)
Aripiprazole	6780.0	nd	265.0	nd	66.0	2	0.8	2	44.0	2	5.5	2	8.7	1	22.00	2	214.0	1	9.6	1	26.0	1	74.0	1	30.0	nd	(40–42)
Risperidone	>10,000	-	580.0	1	3.2	1	18.0	1	22.0	1	282.0	1	0.5	2	19.00	2	4118.0	1	3.5	1	8.0	1	9.5	1	34.0	2	(36, 43)
Paliperidone	>10,000	-	554.0	1	2.8	1	7.5	1	38.0	1	1030.0	1	0.8	2	19.00	2	3425.0	1	3.8	1	11.0	1	111.0	1	34.0	2	(44, 45)
Iloperidone	nd	-	216.0	2	7.1	2	7.1	2	25.0	2	168.0	1	5.6	2	14.00	2	43.0	2	22.0	2	>10000	2	162.0	2	437.0	2	(46–51)
Ziprasidone	300.0	nd	130.0	nd	4.8	1	7.2	1	105.0	1	76.0	2	1.4	1	13.00	2	76.0	1	9.3	1	18.0	1	160.0	1	130.0	1	(52)
Lurasidone	>1,000	nd	262.0	nd	1.6	1	15.7	1	30.0	nd	6.7	2	2.0	1	415.00	nd	-	-	0.5	1	48.0	nd	10.8	nd	>1000	nd	(32)

The binding affinity (Ki) are expressed in nM by each AAPs and receptor when the information was available. 1 = antagonist; 2 = agonist; nd = non determined.

Clozapine may have several interactions with other drugs as it is metabolized by the hepatic cytochrome P450 (CYP) system. Clozapine is transformed into norclozapine by CYP3A4 and 1A2 and clozapine N-oxide by CYP3A4. Nevertheless, CYP2C19 is also significant at clozapine therapeutic concentration (24%) while the influence of CYP2C9 (12%) and 2D6 (6%) is more modest. Then, blood-level monitoring of clozapine may be needed when inhibitors (such as antifungals, oral contraceptives, fluvoxamine, ciprofloxacin, caffeine, and disulfiram) or inducers (such as rifampicin, omeprazole, phenytoin, phenobarbital, and tobacco smoke) of CYP1A2 and both inhibitors (such as cimetidine, erythromycin, and clarithromycin) and inducers (as carbamazepine and rifampicin) of CYP13A4 are used. It is important to note that tobacco smoking may affect clozapine metabolism through CYP1A2 induction (59).

Endocrine alterations induced in animal models by clozapine administration have been observed at doses of 1–10 mg/kg (63), 7.5 mg/kg (64), 10 mg/kg (65), and 2–20 mg/kg (66). Additionally, clozapine significantly increased leptin levels (67) due to its affinity to M3 receptors, which have been linked to decreased insulin released by β-cells (63, 68), regulated glucose homeostasis, and body weight (69, 70). Indeed, studies have shown that only olanzapine and clozapine have a substantial affinity to M3 receptors. In this sense, the overall increase in leptin levels and its association with BMI suggest that leptin acts as a negative feedback signal in the event of fat increase (63).

A potential metabolic impairment by clozapine via the hypothalamic insulin signaling pathway has been reported *in vitro*. Using mHypoE-46 and rHypoE-19 neuron cell lines, clozapine impaired insulin-induced phosphorylation of AKT (63). Although clozapine is known to inhibit 5-HT_{2A}R signaling through G protein-dependent mechanisms, it differs from classic GPCR antagonists in that it also induces 5-HT_{2A}R internalization and activates AKT signaling through a 5-HT_{2A}R-mediated event (71). An animal model, where this drug (2.5, 5, 10 mg/kg) was applied intravenously to Wistar rats, showed an acute increase in corticosterone and glucagon levels, which explains the establishment of hyperglycemia (72).

The vasoactive intestinal peptide (VIP) of parasympathetic origin may contribute to clozapine (muscarinic M1-receptor)-induced sialorrhea, an adverse effect created by its synergistic interaction with the antipsychotic in some patients with schizophrenia (73). Therapeutic doses of clozapine may induce reproductive dysfunction through mechanisms involving ovarian mitochondrial dysfunction and oxidative stress (74), an effect explained by the impairment of the mitochondrial respiratory chain. This phenomenon is supported by a study with thirty adult female albino rats that received clozapine (20 mg/kg/day) for 28 days. It was observed that reduced complex I activity (25%) resulted in a 35% decrease in ATP and mitochondrial respiration, thus severely impairing energy production and leading to apoptosis (75).

Resistin is a biomarker of systemic inflammation and likely plays a role as a marker of cardiovascular comorbidity. A study showed that Clozapine (40 μM) inhibited resistin mRNA expression in mouse brown adipocytes (76). However, in 121 schizophrenia patients treated with clozapine (403 mg/day),

high serum levels of resistin were associated with smokers in comparison with non-smokers (77).

The interaction between clozapine and its pharmacological target in leukocytes induced inflammatory alterations in cell lines, primary cultures, animal models, and humans. The principal immune alteration associated with clozapine is agranulocytosis (neutrophils < 500 cells/mm^3), the most severe form of leukopenia affecting approximately 3.9% of users, and others as neutropenia (neutrophil count <1,500 cells/mm^3) (78). The risk of neutropenia/agranulocytosis is 0.38% approximately with monitoring and 2.5% without it (79). This was mainly observed in female patients and was directly associated with the time of clozapine use (37, 80). Clozapine by itself was not directly toxic to neutrophils or their progenitors at therapeutic concentrations (79). However, the bioactivation/oxidation of clozapine in neutrophils produced reactive and unstable clozapine metabolites, which induced toxic oxidative stress, leading to neutrophil apoptosis. Metabolites may be cytotoxic to bone marrow stroma, potentially leading to accelerated neutrophil or myelocyte precursor apoptosis (81, 82). An associated genetic susceptibility was detected in 31 patients who developed clozapine-induced agranulocytosis and 38 patients who developed neutropenia in a group of 310 clozapine users. The most significant association was found with mutation NQO2 G1541A, making it one of the candidate markers for the prediction of these adverse effects (83).

The current pharmacovigilance processes, carried out worldwide, have allowed for the identification of three uncommon cases of clozapine-induced drug reaction with eosinophilia and systemic symptoms (84). These three reported cases took place in adults older than 57 years, all of them consuming different drugs previously. Two patients were diagnosed with acute exacerbation of a chronic paranoid schizophrenia and the third presented schizoaffective disorder. In the three cases, 15–22 days into the treatment (200–400 mg/day), the blood levels of clozapine were within the toxic range, while eosinophilia, leukocytosis, and liver abnormalities were detected along with a significant increase in CRP without infection (85, 86).

The phenomenon observed in these patients was secondary to the inflammatory process leading to an increase in circulatory levels of clozapine. It is known that cytokines can inhibit the metabolism of clozapine through cytochrome 4501A2 inhibition (87).

Clozapine is also associated with changes in lymphocyte phenotype and differentiation as well as changes in cytokine secretion. Some evidence showed that clozapine primarily inhibited the expression of 5-$HT_{2A/2C}$ on the membrane of primary T cell cultures and Jurkat and CEM cell lines (29, 72). Additionally, it is known that clozapine *in vitro* (1.5–7.5 μg/mL) inhibits Th1 differentiation by preventing the expression of transcription factor T-bet but not that of STAT-4 in T cells; clozapine also inhibited Th1 differentiation by blocking the AKT activation pathway (88). Moreover, clozapine (20 μM) promoted the *in vitro* differentiation of Treg cells and the expression of Foxp3 in splenocytes and lymph node cells from C57BL6/J mice in a model of experimental autoimmune encephalomyelitis (EAE) (15).

Regarding the effects of clozapine in MQs it has been described that clozapine increased IL-10 production and decreased IL-12 secretion in MQs after 5 days of incubation and when it is stimulated with lipopolysaccharide (LPS) for 24 h (89). Similarly, clozapine (10–100 μM) reduced nitric oxide (NO) and IL-12p40 production by LPS-stimulated bone marrow-derived macrophages (BMDM) from female C57BL/6 mice (90).

In studies carried out in animal models, similar effects to those described above in cell cultures have been observed in MQs. In a perinatal phencyclidine rat model, the administration of clozapine increased IL-6 and TNF-α with sex-specific changes (91), which can fit in the theory of "cytokine signature" observed in blood leukocytes from healthy volunteers incubated with clozapine (1 μM) (92). It has also been reported that, in Wistar rats, clozapine (45 mg/kg/day) induced myocarditis related with lymphocytic infiltrates, which induced the release of reactive oxygen species (ROS), cytokines, and TNF-α (93). Additionally, a perinatal model of 90 day-old Wistar rats prenatally treated with LPS reported that daily clozapine (10 mg/kg) significantly reduced IL-1β, TNF-α, and IL-2 levels (60, 94).

Finally, consideration should be given to the changes in the profile of circulating cytokines induced by clozapine consumption. For instance, nine patients with diagnosed schizophrenia or schizoaffective disorder, who were treated with clozapine 100–400 mg/day, showed increased risk of developing fever after the first intake, and IL-6 might play a specific role in the interaction effect between treatment duration and fever development (94, 95). Clozapine has also been shown to increase soluble IL-2 receptor (sIL-2R) and IL-6 levels (96, 97). Similarly, the adipokine resistin was associated with several acute and chronic inflammatory states and promoted the expression of TNF-α and IL-6 by human mononuclear cells (97) (see **Table 2**).

RISPERIDONE

Risperidone was the second AAP approved by the FDA and is among the most prescribed worldwide (98). Its use was authorized for the treatment of schizophrenia in 1993; it was approved to treat acute manic or mixed episodes of bipolar I disorder as monotherapy or adjunctive drug in 2003 and autism-related irritability in 2006 (99). There are also many varied non-FDA approved uses for risperidone, such as Tourette syndrome (100), major depressive disorder (MDD) (101), anorexia nervosa (102), dementia (103), borderline personality disorder (104), Parkinson's disease psychosis (105), posttraumatic stress disorder (106), and some other psychiatric conditions (107). This drug has liver metabolism; it mainly undergoes 9-hydroxylation that produces active 9-hydroxy-risperidone (OH-RIS) metabolite by CYP2D6 and CYP3A4 to a lesser extent (107). The available formulations of risperidone in the market are oral solution formulation, oral disintegrating tablets, and long-acting injectable (LAI) formulation (108).

TABLE 2 | Immunoendocrine peripheral effects induced by atypical antipsychotics.

AAPs	Diseases	Endocrine effects	Immune effects
Olanzapine	• Schizophrenia • Bipolar disorder (mixed or manic episodes)	• Lower concentrations of BNDF • Insulin-resistance • Increase in serum prolactin (only female in short term treatment) • Decrease in serum prolactin (long term treatment) • Hyperinsulinemia • Diabetic ketoacidosis • Increase in leptin • Decrease in ghrelin • Increase in postprandial ghrelin (rats) • Decrease in cortisol	• Increased levels of IL-1, IL-6, and TNF-α (mice) • Eosinophilia • Hypersensitivity syndrome • Leukopenia • Decrease in IL-6 and TNF-α production (THP-1 cells)
Clozapine	• Treatment-resistant schizophrenia • Psychosis • Depression	• Glycemic deregulation • Insulin resistance • Increase in leptin levels • Increased cholesterol concentration • Sialorrhea (secondary to VIP interaction with muscarinic receptor) • Ovarian mitochondrial dysfunction	• Increased levels of IL-10, IL-6, and TNF-α • Decreased levels of IL-12 • Reduction in NO levels • Decreased expression of 5-$HT_{2A/2C}$ in T lymphocytes • Inhibits Th1 differentiation
Quetiapine	• Schizophrenia • Bipolar disorders • Depression • Bipolar depression • Anxiety • Delirium • Obsessive compulsive disorder	• Low incidence of hyperprolactinemia • Insulin resistance • Low levels of insulin • Hyperglycemia • High levels of glucagon • High levels of growth hormone • Low levels of T4 and free T4 • High levels of TSH • Low levels of cortisol	• Neutropenia • Leukopenia • Agranulocytosis, • Thrombocytopenia • *In vitro*: low levels of IL-2 • *In vitro*: high levels of TNF-α and IL-17 • *In vitro*: high levels of IL-4 and IL-10 • *In vitro*: low levels of IFN-γ • High plasma levels of BDNF
Asenapine	• Schizophrenia • Bipolar disorders • Bipolar disorder in children and adolescents	• Hyperinsulinemia • Variation in glucagon release • Hypoprolactinemia	• No available data
Aripiprazole	• Bipolar disorder (manic and mixed episodes) • Schizophrenia • Irritability associated ASD • Tourette syndrome • Adjunctive treatment for MDD	• Increased DNA methylation of GLUT1 • Increased fatty acid synthesis and hypertriglyceridemia • Decreased levels hyperprolactinemia	• Decreased levels of TNF-α, IL-8, IL-21, IL-13, IL-17, CXCL1, CXCL10, CCL4, IFN-γ, IL-1-β, IL-6, IL-12, IL-23, and IL-4. • Reduction of levels of PGE2, COX2, and NO. • Increase Glutathione peroxidase (GSH-Px) and Superoxide Dismutase (SOD)
Risperidone	• Schizophrenia • Schizoaffective disorder • Schizophrenia in pediatric population s (13-17 years) • Bipolar mania in pediatric population (10-17 years) • Autism-related irritability (>5 years)	• Hyperprolactinemia (human and pigtail macaques). • Decrease in testosterone levels in women and estradiol levels in both genders. • Increase in leptin and insulin levels. • Increase in TSH levels. • Decrease in adiponectin levels. • Increase in insulin levels in FVB/N line (mice). • Decrease in α-MSH, AgRP, and CART (rats). • Increase in glucagon, leptin, and ghrelin levels (rats). • Ovarian mitochondrial dysfunction (rats).	• Leukopenia • Neutropenia • Lymphopenia • Thrombocytopenia • Fever • Development of acute eosinophilic pneumonia • Elevated BDNF levels only in relapsing males • Increase in IL–6, TNF-α, and CRP levels (rats) • Decreased IL-1β, IL-6, IL-8, MIP-1β, fraktaline, TNF-α, IL-7, IL-13 IL-17a, IL-23, IL-21, IL-4, IL-10, eotaxin, and MCP-1 levels. • Increase in IL-10, IL-RA, and TNF-α levels. • Increase in Igγ chain levels. • Decrease in titers of platelet-associated antibodies titers. • Reduced platelet aggregation. • Reduction in IFN-γ production and Th1 differentiation by PBMCs.

(Continued)

TABLE 2 | Continued

AAPs	Diseases	Endocrine effects	Immune effects
			• Reduction in IFN-γ production by CD4 T cells. • Increased IL-10, IL-6, IL-8, and TNF-α production by MDDCs. • Decreased IP-10 and IL-12 production by MDDCs with neutrophil death and decreased IFN-γ secretion by T cells • Inhibition of adhesion, phagocytosis, and ROS in U-937 cells • Decrease in IL-6 and IL-8 and increase IL-10 production by macrophages. • Decreased Th17 cell count. • Induction of NF-κB target genes in adipocytes. • Increased TLR2 expression in T cells. • Decreased TLR4 expression in monocytes. • Up-regulation of genes in blood cells: cytokine receptors, PRRs, molecules involved in apoptosis, *BDKRB1*, *IGF1R*, and *CR1*. • Increased of VCAM, ICAM, E-selectin, MCP-1, and TNF-α levels in aortic tissue (rats) • Decreased IL-17, IL-2, and IL-4 secretion in acute EAE; increase splenocytes Tregs, $CD4^+$ T cells and IFN-γ levels in chronic EAE (mice) • Decrease IL-12 and increase IL-10 production; reduction of IFN-γ, IL-17, and increase IL-10 production by T cells (mice). • Increased NO levels and apoptosis; decreased Bcl/BAX, IL-10 production and increase IL-1, IL-6, TNF-α and IFN-γ in RAW 264.7 line (mice).
Paliperidone	• Schizophrenia • Schizoaffective disorder • Schizophrenia in pediatric population (12-17 years)	• Hyperprolactinemia • Elevated insulin levels.	• Leukopenia • Neutropenia • Lymphopenia • Agranulocytosis • Increase in BDNF levels • Enrichment of NF-κB pathways • Decrease in cell survival (U-937 cell line)
Iloperidone (see **Supplementary Material** section)	• Acute phase of schizophrenia in adults • Stabilization phase of schizophrenia	• Hypoprolactinemia • Hyperprolactinemia with galactorrhea	• No available data
Ziprasidone	• Schizophrenia • Bipolar disorders	• Hyperprolactinemia with galactorrhea • Hypocortisolemia	• Agranulocytosis • Low levels of IL-10 • It induced allergic responses: high levels of IgG and complement proteins C3 and C4 • *In vitro*: high levels of NO and ROS • *In vitro*: high levels of IL-1, IL-6, TNF-α, and IFN-γ
Lurasidone (see **Supplementary Material** section)	• Schizophrenia • Depression associated with bipolar disorder	• Decrease in levels triglyceride levels • Increase in HDL cholesterol	• Decrease in C-reactive protein (CRP) • Leukopenia • Thrombocytopenia

The presumed action mechanism of risperidone is associated with the combination of 5-HT_{2A} agonist and D2 antagonist effects with a strong binding affinity for the first one (see **Table 1**) (109). This drug is also active as an antagonist for other receptors with a lower affinity, such as dopamine D3 and D4, serotonin 5-HT_6, 5-HT_7, and α-1 and α-2 adrenergic. Risperidone acts as agonist on 5-HT_{2C} serotoninergic receptors and H1 histaminergic receptors (43).

Risperidone consumption has demonstrated to generate hormone alterations in human and animal models. Reports on this AP refer to hormones related with glucose metabolism, adipokines, appetite, and those linked to the adrenal, and gonadal axes, among others. One of the main effects associated with risperidone consumption is elevated PRL levels in patients (110), having a significant incidence of HPRL compared with other APs (111–113). In human and adult studies, the drug caused significant PRL elevation after 44 days of treatment (1–6 mg/day) in 27 of 37 schizophrenic patients, while in a 1 year follow-up (1–6 mg/day) 6 out of 20 patients reported HPRL with decreased PRL, without reaching baseline levels (114). These results were similar to those obtained by Perez-Islas et al., whose report showed that 90% of the men and 87% of the women in the study had PRL levels above the reference range 3 months into the treatment (unspecified dose). These levels were still elevated in 70% of the subjects at 1 year of follow-up with a tendency to decrease (115).

During an acute follow-up (4 weeks), the patients with an increase of more than 20% in PRL levels had a better chance of responding to risperidone (116). However, the chronic consumption gave more information on PRL concentration and its effects; the reports proved that risperidone is associated with chronic HPRL (117). Female patients presented a significant incidence of HPRL as compared with their male counterparts (118). Elevated PRL by risperidone consumption could be associated to higher concentrations of osteocalcin in both genders (119), breast symptoms, discomfort, menstrual changes, and erectile dysfunction (120). In fact, patients who consumed risperidone and showed menstrual disorders had a significant increase in serum PRL levels, showing a correlation between the incidence of elevated PRL and menstrual disorders (121). Other organic and rare alterations, in adult and/or children patients, as granulomatous mastitis (122), amenorrhea (123), galactorrhea (124), acute pancreatitis (125), and pituitary adenoma (126) have also been associated with risperidone consumption.

The reports on PRL levels in children and adolescent patients have shown that these populations present elevated HPRL, which has been reported in 44.9% of autism spectrum disorder (ASD) patients as unrelated to the duration of risperidone treatment (0.25–5 mg/kg, 1.03–158.03 months) (127). Still, there is evidence exposing the possible relation between plasma metabolite levels of risperidone and elevated PRL concentrations (128). Patients from the same population presented an increase in serum PRL during 3 months of follow-up (0.5–4 mg/day); gender, pubertal status, risperidone dosage, psychiatry diagnosis, and personal/family history of autoimmune diseases also affected PRL elevation during treatment (129). Similarly, a meta-analysis reported that pediatric patients treated with risperidone (4–6 mg/day) were found to experience the most significant increase in PRL, followed by patients treated with 1–3 mg/day of risperidone compared with other APs at a different dose (130). In fact, the occurrence of HPRL in this population has been associated to the presence of the C allele of the rs6318 single nucleotide polymorphism (SNP) of the *HTR2C* gene (0.25–6 mg/day, 0.1–143 months) (131). In addition, HPRL during treatment with risperidone/paliperidone in schizophrenic patients showed an association with rs40184 and rs3863145 variants in *SLC6A3* gene of blood leukocyte DNA (132). All the studies that showed elevated PRL levels in the pediatric population are in accordance with a meta-analysis that presented a relation between risperidone treatment and high PRL (130). The possible mechanism by which risperidone causes HPRL is associated with the transcriptional upregulation of neuropeptide Y (NPY) secreted by the arcuate hypothalamic nucleus due to the high affinity of risperidone to 5-HT_{2A} receptors. NPY inhibits tyrosine hydroxylase expression in the paraventricular nucleus and thus reduces DA synthesis, which in turn would diminish the inhibition of PRL expression induced by DA. The reduction in DA would cause the overexpression of PRL in the pituitary and ultimately induce HPRL (133).

Studies have shown that, in addition to PRL increase, other hormone profiles such as estradiol, testosterone, leptin, adiponectin, and insulin could be altered during risperidone treatment. The acute consumption of this drug (2–4 mg/Kg) decreased testosterone and estradiol levels in female patients after a 6-week treatment (134), and the same decrease in estradiol levels was reported in male patients with schizophrenia during 1 year of treatment (2–6 mg/day) (135), although other studies showed that risperidone consumption did not alter the testosterone or estradiol levels in male or female patients (136, 137). Although the mechanism is not clear, risperidone could affect estradiol and testosterone levels by a direct effect on the hypothalamic-hypophysis-gonadal axis, decreasing hormone production (135).

The concentration of leptin has also been proven to increase by 60% in psychotic patients after 4 weeks of risperidone consumption (4–8 mg/day) (138). Other studies showed that the leptin levels of schizophrenic patients with risperidone consumption were higher than those of healthy controls (139, 140). Similarly, there was an increase in leptin among ASD patients during at least 12 months of treatment (0.25–1 mg/day) (141). In treatment-naïve children and adolescents, leptin increased after 3 and 6 months of treatment (unspecified dose) when compared with baseline (142). However, a 5-month treatment (6.1 $\pm$ 1.8 mg/day) yielded no changes in leptin concentrations when compared with baseline (143); this data is supported by a meta-analysis that found no significant changes in leptin after risperidone treatment (63). The serum leptin elevation is attributed to weight gain rather than the direct effect of risperidone on leptin metabolism. This hormone is secreted by adipocytes and it is proportional to the mass of stored fat, so the elevation in blood of patients with antipsychotic-induced weight gain could be the result of the increased weight itself (144).

Adiponectin is a molecule with conflicting results on the effect of risperidone consumption. Schizophrenia patients treated with risperidone (unspecified dose, 50.1 $\pm$ 82.4 months) reduced plasma levels of adiponectin when compared with healthy subjects (145), and medication-free children showed a decrease in adiponectin levels after 16 weeks of treatment (3–91 months) (146). However, these data do not match with the results of two meta-analysis that reported no association between risperidone treatment and low adiponectin (147, 148).

According with most reports, risperidone consumption increases insulin levels in blood. The treatment with LAI-risperidone (38 $\pm$ 2 mg/15 days) for 18 $\pm$ 1.6 months showed

higher insulin concentrations in patients compared with the control group (140). Children studies show that the treatment for at least 12 months (0.25–1 mg/day) increased insulin levels in ASD patients (141). Similar results were obtained in medication-free children (3–91 months) after 16 weeks of treatment (146).

The changes in hormone levels related with risperidone treatment are also evident in animal models. In a pigtail macaque model, PRL was higher at low (0.025 mg/Kg) and high doses (0.05 mg/Kg) of risperidone during 4-month consumption, with a gradual decline until reaching placebo levels in the post-drug phase (149). In an animal model, male Wistar rats showed reduced α-MSH, agouti-related protein (AgRP), and cocaine- and amphetamine-regulated transcript (CART) concentrations and increased leptin levels vs. the vehicle group after 4 weeks of treatment (2 mg/kg/day) (150). In addition, female Sprague-Dawley rats with depot risperidone exhibited higher glucagon levels (20 mg/day), while daily risperidone (40 mg) increased leptin and ghrelin levels at 4 and 6 weeks (151). In rat ovarian theca cells, risperidone inhibited mitochondrial bioenergetics and steroidogenesis by reducing ATP content (0.1–100 μM, 24 h) and the production of progesterone and androstenedione (1–37 μM, 24 h) (151). Finally, mouse models have reported plasma insulin increased over 8-fold in FVB/N mice 3 h after consumption of risperidone (152).

The adverse effects, involving immune alterations, caused by risperidone have been widely studied. In the immune system, this drug alters leukocyte numbers and levels of humoral inflammatory molecules, and it directly effects the phenotype and function of leukocytes (16, 153, 154).

Risperidone does not require regular clinical monitoring of white blood cell (WBC) count; however, anecdotal evidence has shown that it could modify and reduce the leukocyte count. Different risperidone doses (2–4 mg/day) and the combined treatment of risperidone/paliperidone (2 mg/day/100 mg) caused leukopenia with neutropenia (155) or lymphopenia (153, 156–158) as well as fever (159). Other leukocyte alterations have been described. A case report showed the development of thrombocytopenia in a male paranoid schizophrenia patient with risperidone treatment (4 mg/day) (160). Risperidone has demonstrated the association between its consumption (3 mg/day) and the development of acute eosinophilic pneumonia (AEP) in a male patient under a 6-month treatment (161). All count alterations and developed diseases improved after discontinuing the drug. Nevertheless, there are reported cases of neutropenia induced by risperidone but the incidence rate of cytopenia alterations seems to be very low (162).

The reports that analyze the effect of risperidone consumption on soluble molecules with immune function are very diverse. Even though CRP levels did not show changes in schizophrenic patients during risperidone treatment vs. healthy volunteers (163), there is evidence showing the relationship between elevated CRP and the effects on risperidone metabolism. A case report demonstrated that two females who had consumed risperidone during acute inflammation indicated by elevated CRP exhibited an increase in dose-related serum concentrations of risperidone up to the therapeutic concentration (164, 165). Furthermore, high CRP vs. common CRP values increased risperidone and OH-RIS serum levels by 58.4 and 20%, respectively, in patients with risperidone consumption (166). Contrastingly, other reports showed no correlation between CRP levels and affected risperidone levels in serum concentration (95).

The studies of changes in BDNF levels during treatment are controversial; only relapse schizophrenic males patients showed elevated BDNF after 4 weeks of risperidone consumption (3–6 mg/day), a result that suggests gender should be considered when choosing the pharmacological treatment (167–169). However, other studies reported no alteration whatsoever after risperidone consumption (170, 171).

Cytokines, chemokines, and immunoglobulins (Ig) are inflammatory molecules that have been measured during risperidone treatment and results show changes in blood levels in some of them. In an animal model, risperidone decreased and normalized the plasma levels of IL-6 and TNF-α in n-3 fatty-acid deficient rats when compared with elevated levels of n-3 fatty-acid adequate rats after 40 days of treatment (3 mg/kg/day) (172).

In patients with schizophrenia, the measurement of these molecules in blood has proven the immunomodulatory effect of risperidone at different times of consumption. A 3-month treatment with risperidone (1–6 mg/day) showed significant decreases in serum levels of IL-8, macrophage inflammatory protein (MIP)-1β, fractalkine, TNF-α, IL-7, IL 13, IL-17a, IL-23, and IL-21 (173). The same effect in TNF-α was observed at 40 days of treatment (unspecified doses) with increased IL-10 serum levels in patients with risperidone or clozapine consumption (174). Elevated levels of Interleukin-1 receptor antagonist (IL-1RA) and IL-10 have also been reported after 6 weeks of treatment (unspecified doses) (175) as well as significant decreases in IL-6, IL-10, TNF-α, and IL-4 after 10 weeks of risperidone consumption (4 ± 1.8 mg/day) (176). During 6 months of risperidone treatment (2–6 mg/day), TNF-α levels increased compared with baseline while IL-1β and IL-6 decreased at 1 month and then gradually increased at the end of the follow-up (154). In ASD patients, eotaxin and monocyte chemoattractant protein-1 (MCP-1) levels significantly decreased after 8 weeks of treatment (0.5–1.5 mg/day) (177). Regarding Igs, a report showed that a 4-week treatment with risperidone increased Igγ (IgG) chain levels significantly when compared with baseline (178). Another report showed that from 17 schizophrenic children with high blood titers of platelet-associated antibodies (PAA) only two became PAA-negative following 3 years of treatment. Most of the reports above show evidence that risperidone could reduce the production of the pro-inflammatory molecules caused by psychiatric conditions and support an anti-inflammatory response.

When talking about phenotype and function alterations in immune cells, it seems that risperidone causes significant changes such as a shift in cytokine secretion, cell differentiation, adhesion and phagocytic functions, receptor expression on leukocytes, and gene expression. Firstly, this drug reduces ATP-induced platelet aggregation when platelet-rich plasma of healthy donors is incubated *in vitro* with risperidone (65 ng/mL) for 30 min (179). An *in vitro* assay showed that activated peripheral blood mononuclear cell (PBMC) from healthy adults

incubated with risperidone (10^{-7} M, 3–5 days) reduced IFN-γ production and inhibited AKT phosphorylation and T-bet expression, causing reduced Th1 differentiation. During chronic treatment (10^{-7} M, 28 days), risperidone reduced IFN-γ released by $CD4^+$ T cell subpopulation (180). Similarly, this drug affected cytokine and chemokine production of activated mature monocyte-derived dendritic cells (DCs) of healthy adults, increasing IL-10, IL-6, IL-8, and TNF-α levels and decreasing interferon γ-inducible protein−10 (IP-10) and IL-12 levels (10^{-7}-10^{-5} M, 3 days). These changes in mature DCs produced a reduction in IFN-γ secretion by activated T cells, causing Th1 suppression and leading to neutrophil death (15, 17).

The increase in IL-10 levels and/or the decrease in IFN-γ production by activated PBMC with risperidone treatment were reproducible in other reports (16). Risperidone also inhibited the adhesion, phagocytosis, and ROS production by activated U937 cells (10^{-5}-10^{-4} M), decreased IL-6, IL-8, and IL-12, and increased IL-10 production in healthy, stimulated human MQs *in vitro* (10^{-6}-10^{-5} M). This effect could support the inhibition of Th1 differentiation (181, 182), although some evidence proposes that this drug suppresses inflammatory (M1 MQs, Th1 lymphocytes) and anti-inflammatory (Th2 lymphocytes, Treg) responses (90).

In the blood of schizophrenic patients, the treatment with risperidone (2–6 mg/day) for 4 weeks showed a decrease in the number of Th17 cells (183). *In vitro*, differentiated human adipocytes incubated with risperidone (100 ng/ml, 11 days) induced transcription factor NF-κB target genes of IL-1β and IL-8 molecules (184). In schizophrenic patients, risperidone (8 weeks, 2–6 mg/day) modifies the expression of toll-like receptors (TLR), while monocytes $CD14^+$, $CD3^+CD4^+Foxp3^+$ T, and $CD3^+CD4^+CD25^+$ T cells increased TLR2 expression, and $CD14^+$ monocytes decreased TLR4 expression (185). Effects on gene expression have been reported; in blood cells of first-episode psychosis patients, risperidone (unspecified doses, 20 days) was associated to the up-regulation of 11 immune system genes, including cytokines and cytokine receptors (*SPP1, IL1R1, IL1R2*), pattern recognition molecules *(TLR1, TLR2, TLR6*, dectin-1/*CLEC7a*), molecules involved in apoptosis (FAS), and *BDKRB1, IGF1R*, and *CR1* (186).

In animal models, a 3-week treatment with risperidone (1.25 mg/Kg/day) in diabetic Wistar rats showed that this drug altered the vascular function by the significant up-regulation of vascular cell adhesion molecule-1 (VCAM-1), intercellular adhesion molecule-1 (ICAM-1), E-selectin, and MCP-1 and TNF-α in aortic tissue homogenate (187). In an experimental autoimmune encephalitis (EAE) model with C57BL/6 mice, risperidone (3 mg/kg/day) reduced the severity of the disease in a dose-dependent manner and down-regulated IL-17a, IL-2, and IL-4 secretion by splenocytes at peak disease (day 15). During chronic EAE phase, risperidone significantly increased the number of splenocytes, Tregs, and $CD4^+$ T cells and increased IFN-γ levels, showing that T cells responded differently to risperidone during the acute and chronic phases of EAE. In addition, activated BMDM of treated mice decreased IL-12 levels but increased IL-10 concentration. These cells modified T cell activation reducing IFN-γ and IL-17 production and enhancing IL-10 levels (188). In RAW 264.7, a macrophage mice line, risperidone activated these cells (20–40 μM for 24, 48, and 72 h) and increased nitric oxide (NO) levels (30–40 μM) as well as apoptosis events by modulating levels of caspases 8 and 3 (20–40 μM at 72 h). The drug also reduced Bcl-2/BAX gene expression ratio (24 h) and, contrary to the above data, increased IL-1, IL-6, TNF-α, and IFN-γ and decreased IL-10 production in a dose-dependent manner. Results of the RAW 264.7 line could show that the continued activation of MQs likely contributes to the development of endocrine disturbances caused by risperidone (91) (see **Table 2**).

OLANZAPINE

Olanzapine (2-methyl-4-(4-methyl-1-piperazinyl)-10H-thieno[2,3-b][1,5]benzodiazepine) belongs to the thienobenzodiazepine class and is structurally similar to clozapine (see **Figure 1**) (189). It was authorized for the treatment of schizophrenia in 1996 and bipolar I acute manic or mixed episodes in 2000 (43, 109, 190). There are also many varied non-FDA-approved uses for quetiapine, such as dementia-related behavioral problems, bipolar depression, psychotic depression, SSRI-resistant major depression, personality disorders, post-traumatic stress disorder, and Tourette syndrome in children and adolescents (191). Olanzapine is metabolized in the liver by direct glucuronidation and cytochrome P450 (CYP) oxidation and generates two metabolites, 10-N-glucuronide and 4'-N-desmethylolanzapine, which lack pharmacological activity (192).

The therapeutic effect of this drug is associated to the antagonism of D2, D3, $5HT_{2a}$, and $5\text{-}HT_{2c}$ receptors, although it exhibits an antagonist effect on other receptors such as $5\text{-}HT_{1C}$, $5\text{-}HT_6$, $5\text{-}HT_7$, α-1A, α-2A, H1, M1, M3, and $5\text{-}HT_{1A}$ (see **Table 1**) (31–35).

This drug has been associated with the decrease in cell counts. There are few reports that evidence leukopenia is induced by olanzapine consumption (2.5–10 mg/day) during the first 35 days of treatment (193, 194). This phenomenon is associated with the covalent bonding between neutrophils and a reactive nitrenium ion, the oxidized form of olanzapine. It has been proposed that this reactive metabolite is responsible for the effect in neutrophils (195). Other studies have reported that this drug is associated with a decrease in eosinophils. Three reported cases showed that males with schizophrenia developed eosinophilia during olanzapine treatment (10–20 mg); in all cases, the problem was solved suspending the medication (193, 194, 196). This drug also modifies receptor expression; according to a report, 30 first-episode psychotic patients treated with olanzapine (15–25 mg/day) for 30 days showed a decrease in D1, D2, $5\text{-}HT_{2A}$, and transforming growth factor (TGF)-β mRNA expression in PBMC as well as an increase in IL-6, IL-1β, and TGF-β blood levels (197).

The increase in PRL caused by the consumption of most of the AAPs is also observed in the consumption of olanzapine. However, the evidence of this effect is contradictory since there

is also proof of the decrease during the consumption of this drug. It has been reported that according to the period of consumption, the effects on PRL blood levels change (111, 198, 199): The consumption during short periods (<2 weeks) or the intake of a single dose does not alter PRL levels (111, 200).

There are two case reports of women aged 29 and 49 years with bipolar affective disorder and delusional disorder who exhibited HPRL associated with olanzapine consumption during 24 weeks (5–20 mg/day) (201). Most reports evidence the increase of this hormone: A study with 72 patients (33 women and 39 men) who were administered olanzapine (10–20 mg/day) for 3 weeks or more showed an increase in PRL levels only in female patients (202). Similar effects were detected in 49 schizophrenia patients (24 women and 25 men) treated with 15–30 mg/day of olanzapine for 4 weeks (203) and those patients (27) with chronic consumption (10–15 mg/day, 8 years) (204). In fact, a study with healthy volunteers showed that participants with no psychopathology who received one dose of olanzapine (10 mg) exhibited an increase in PRL levels (58). On the other hand, other studies showed the decrease of PRL after olanzapine consumption. In a study with 22 participants, PRL levels were reduced only in women with schizophrenia or schizoaffective disorder at 6 and 12 months of treatment (5–20 mg/day), while levels in men showed no difference (198). The decrease in PRL levels was also reported in 37 first-episode psychosis patients who consumed olanzapine (unspecified dose) for 1 year (115). The PRL elevation is associated with the interaction between olanzapine and D2 receptors on lactotroph cells. This phenomenon hampers the interaction between DA and its receptor, so DA cannot inhibit PRL production. The alterations depend on gender, genetic predisposition, dose, and time of consumption (115, 190, 201, 205).

Interestingly, the chronic administration of olanzapine is associated with the development of hyperinsulinemia and insulin resistance; the decrease in insulin sensitivity was reported in 29 healthy individuals after 10 days of olanzapine treatment (10 mg/day) (206). The increase in fasting insulin was reported in 25 schizophrenic patients with olanzapine consumption (5–20 mg/day) for 13 weeks (207). It has been postulated that alterations in insulin synthesis may be due to the stimulation of M3 receptors in β-pancreatic cells (70, 208).

It has also been described that olanzapine is associated with an increase in leptin blood levels (63), although there is little evidence that shows no changes in leptin blood levels during treatment. The increase in this hormone was shown in 18 schizophrenic male patients after 9 months of olanzapine consumption (5–20 mg/day) (209). Another study reported that 23 schizophrenic patients showed the same effect after 8 weeks of olanzapine treatment, and the increase in leptin concentration was correlated with elevated IL-1 receptor antagonist (IL-1ra) serum levels (210). In fact, the report of Tsuneyama and cols. described that the increase in leptin levels was observed only in schizophrenic female participants treated with olanzapine for 1 year (12 male and 19 female) (211). However, 12 schizophrenic patients exhibited no changes in appetite or leptin concentrations after a 5-month treatment (mean: 25 mg/day) (143). Although the mechanism by which this drug affects leptin secretion is unclear, the effect could be secondary to the interaction between the drug and H1 receptors on the hypothalamus and nucleus accumbens. Additionally, the genetic predisposition is crucial for the development of alterations associated with leptin function (212).

The data of reports on the olanzapine effect in ghrelin levels exhibit contradictions in the conclusions; some studies in schizophrenic patients show that this drug reduces ghrelin concentration after a 6-week treatment (213) and chronic consumption (8.3 ± 7.5 years, 10–20 mg/day) (214). In contrast, no changes in ghrelin levels or appetite were shown in 13 patients with schizophrenia treated with olanzapine for 5 months (143). However, an animal model with Wistar rats showed that the acute consumption of this drug (1 mg/kg) increased the concentration of postprandial ghrelin compared to controls (215). The mechanism of ghrelin alterations is not clear but these changes are associated with leptin resistance. It has been proposed that olanzapine exhibits a direct effect on hypothalamic neurocircuits that regulate ghrelin synthesis, causing an altered leptin/ghrelin ratio (212). There is only one report that measured cortisol levels during olanzapine treatment: Hahn and cols. reported that healthy individuals who received a single dose of olanzapine (10 mg) exhibited a decrease in cortisol serum levels compared with baseline (58).

Other immune alterations associated with olanzapine consumption are the modulation of cytokine secretion and production, depending on the consumption time of the drug (216). There are *in vitro* studies in PBMC of healthy individuals and THP-1 line (10^{-4} M for 72 h) that demonstrate a reduction in mRNA expression of IL-1β, IL-6, IL-10, and TNF-α, IL-6, TNF-α, and IL-10. Similarly, stimulation in THP-1 cells resulted in a significant decrease in the expression and secretion of IL-1β and TNF-α (217). Other studies in schizophrenic patients with prolonged consumption reported changes in cytokine levels. After a 24-month olanzapine treatment (unspecified dose), 95 schizophrenic patients with metabolic syndrome showed lower concentrations of BDNF ($P < 0.012$) and higher values of TNF-α as compared to 121 patients only diagnosed with schizophrenia (218). Also, out of 28 patients with chronic olanzapine consumption (unspecified dose) 14 were insulin-resistant and had a higher concentration of TNF-α, IL-6, IL-1β, and IL-8 with a positive correlation between these values and insulin resistance (210). Similarly, female Sprague-Dawley rats and female BALB/c mice, after 8 weeks of treatment (10 mg/kg/day), exhibited a significant increase in TNF-α, IL-6, IL-1β, and IL-8 levels, in addition to insulin resistance (219). Some evidence suggests that the effect of olanzapine under cytokine secretion is gender-dependent; female Sprague-Dawley rats given olanzapine (low dose 2 mg/day; high dose 4 mg/day) for 3 weeks showed increased IL-8 levels, while males showed TNF-α concentration during low dose consumption, proving a gender-dependent difference. Also, compared with those of the control group, IL-6 levels were reduced in males after both doses of olanzapine while IL-1β concentration was reduced in females after a low dose (208).

Olanzapine can also modulate TLR expression in leukocytes. A study that evaluated 24 schizophrenic patients after 8

weeks of treatment (10–25 mg/day) exhibited that this drug increased TLR2 expression and decreased TLR4 and TLR5 in $CD14^+$ monocytes. Treg and Tact cells reduced TLR2 and increased TLR5 expression (186). In 23 patients diagnosed with schizophrenia and treated with olanzapine for 8 weeks, IL-1RA was overexpressed, which correlated with the increase in leptin (210) (see **Table 2**).

QUETIAPINE

Quetiapine is an AAP derived from benzothiazepine (220) (see **Figure 1**) and used for the treatment of psychotic symptoms in a wide range of disorders. Its use was authorized for the treatment of schizophrenia in 1997; it was authorized to treat unipolar and bipolar disorders in 2003 and bipolar depression in 2006. There are also many varied non-FDA-approved uses for quetiapine, such as anxiety, delirium, obsessive compulsive disorder, and the combined treatment of major depressive disorder (MDD) with antidepressants (221). Quetiapine metabolism, which comprises several steps as sulfoxidation, *N*- and *O*- dealkylation, and 7-hydroxilation by the CYP3A of the cytochrome P-450 system, produces *N*-desalkylquetiapine (norquetiapine), an active metabolite of quetiapine (222). Quetiapine is considered a multifunctional drug since it acts on three systems: dopaminergic, serotonergic, and noradrenergic (223). It shows high affinity for serotonin (5-HT) and DA type-2 receptors, slightly higher for the serotonergic than the dopaminergic. Contrastingly, lower affinity has been reported for type-1 receptors of both systems: D1 and 5-HT_{1A}. Moreover, it is known that quetiapine also has affinity for histaminergic (H_1) and adrenergic systems (α-$_1$ and α-$_2$) (see **Table 1**) (38).

It is well-known that most SGAs produce HPRL; however, quetiapine is considered among the safest medications due to its lower incidence of HPRL. Such properties have been associated to its lower affinity to Sackett et al. (149) and fast dissociation rate from DA receptors (224). In schizophrenia patients with sexual dysfunction, the treatment usually begins with PRL-sparing antipsychotics, switching to quetiapine in a second phase (225). In fact, quetiapine has been reported to revert HPRL in 175 patients with schizophrenia after a 2-week treatment (300–700 mg/day) (226).

On the other hand, several studies have shown the adverse endocrine effects produced by the administration of APs. In patients (12) with schizophrenia, quetiapine consumption induced significant insulin resistance. Nine months after administration, it led to a reduction in insulin sensitivity, as a result of a deficient secretion of insulin by the β-pancreatic cells (227). After a 10-month treatment with quetiapine, 16 youths (9–18 years) showed decreased levels of insulin associated with an impairment in β-pancreatic cell function (228). In mice, quetiapine administration (10 mg/kg) induced an increase in plasma levels of glucose but not in insulin, suggesting an insulin-blocker role of quetiapine in the insulin-secretory compensation mechanism (152), a finding supported by *in vitro* studies (229). McNamara et al., demonstrated that stearoyl-CoA desaturase-1 (scd-1), an enzyme involved in triglyceride biosynthesis and whose up-regulation showed a positive correlation with quetiapine consumption, could be involved in both sensitivity and insulin resistance (230). Moreover, the higher activity of scd-1 has been suggested as a risk factor for diabetes in humans (231), which reinforces the link between scd-1 and the adverse effects of quetiapine consumption. On the other hand, studies in rats have suggested that quetiapine-induced hyperglycemia was produced by increased levels of glucagon and suppressed glucagon-like peptide-1 (GLP-1) more than insulin resistance (66). Disturbances in glucagon and GLP-1 caused serious alterations in glucose metabolism because of stimulated hepatic glucose production (232).

In healthy volunteers aged 18–21 years, a dose of 150 mg/day of quetiapine was tested and the results showed an increase in PRL and growth hormone (GH) after 60 and 210 min of administration, respectively; in contrast, cortisol showed a decrease at 240 min and no changes were observed in ACTH (233). The alterations observed in GH levels by quetiapine consumption might be attributed to the high affinity and antagonism between the drug and H1 receptors. It should be noted that PRL in healthy volunteers showed a different behavior than that observed in patients, but, importantly, the sampling time used in healthy volunteers was very short. However, data in healthy volunteers are controversial, since other reports have shown no effects on PRL, but on ACTH due to the consumption of quetiapine in short sampling periods (234). Disturbances in ACTH and cortisol could be due to alterations in functioning of hypothalamus-pituitary-adrenal (HPA) axis in psychiatric patients, but the exact mechanism remains unclear. Moreover, quetiapine has revealed affectations in the levels of thyroxine (T4) and thyroid-stimulating hormone (TSH) (cases reports) with doses of 300–350 mg/day which induced a decrease in T4 and free T4, whereas TSH was increased (235).

Although the precise mechanism by which quetiapine induces adverse endocrine effects is not fully clear yet, some studies have focused their efforts on shedding light on this issue; nevertheless, more works are required to clarify this point.

Quetiapine consumption also affects the immune system. In patients with schizophrenia, quetiapine (600–1,200 mg/day, case reports) is associated with neutropenia, leukopenia (236–239), agranulocytosis, and thrombocytopenia (240). The mechanism by which quetiapine causes these adverse effects is still unclear, but some authors have proposed that this drug acts directly as a cytotoxic agent on immune cells, thus producing cell death; additionally, some products of quetiapine oxidation could induce apoptosis by oxidative stress (241). Other authors have suggested a bone marrow depression by quetiapine consumption, which could be produced by an inhibitory effect on leukopoiesis. It has even been proposed that quetiapine may act as a hapten, inducing antibody formation, complement activation, and cell death (237).

Studies *in vitro* have demonstrated the capability of quetiapine to alter the levels of some cytokines (242). Himmerich et al. demonstrated that this drug reduced IL-2 levels in whole blood cells, whereas it increased the levels of TNF-α and IL-17 (243). In PBMC cultures (LPS-stimulated) from patients with schizophrenia, quetiapine raised the levels of anti-inflammatory cytokines (IL-4 and IL-10) and lowered the pro-inflammatory ones (IFN-γ) (181). The anti-inflammatory properties of quetiapine may be explained by its capacity to suppress the NF-κB pathway activation. Quetiapine not only inhibited the

expression NF-κB but also reverted its translocation from the cytosol to the nucleus, thus affecting its activation as well. These properties could explain quetiapine effects on cytokine expression (244) and have led experts to consider it a therapeutic alternative in some neuroinflammatory diseases.

Neurotrophins (NTs) are a group of neural growth factors that regulate survival, maintenance, cell differentiation, and synaptic plasticity in the CNS. But, their activity is not limited to the CNS: Cells of the immune system also express both NTs and their receptors (245), which in turn strongly contributes to the connection between neuronal dysregulation and inflammation (246). BDNF has been considered a potential biomarker of psychiatric disorders (247, 248). In patients with first episode psychosis, serum BDNF levels were increased after a 12-week treatment with quetiapine (200 or 400 mg/day). This rise in BDNF showed a positive correlation with the clinical improvement of patients, suggesting an indirect neurotrophic role of quetiapine through BDNF (249) (see **Table 2**).

ZIPRASIDONE

Ziprasidone is a psychotropic agent commonly used in the treatment of schizophrenia (250) and bipolar disorder (251, 252) since its approval by the FDA in 2001. It is a benzisothiazolyl-3-yl-piperazine-type AAP (see **Figure 1**) with potent pharmacological antagonism to 5-HT_{2A} and D2 receptors. However, it also acts on H1, M1, α1 and α2 receptors with less affinity (253, 254). The high affinity of ziprasidone to 5-HT_{2A} as compared to D2 is an important characteristic of this drug. However, the pharmacological antagonism of ziprasidone toward D2 makes a lot of sense considering its antipsychotic effects, whereas the role of 5-HT_{2A} receptors is still unclear (see **Table 1**). Still, it has been proposed that the antagonism against 5-HT_{2A} stimulates the activity of DA in mesocortical pathways (52). Ziprasidone is metabolized almost fully, excreting only 5 % of the original drug intact. Aldehyde oxidase and cytochrome CYPA34 are the two main pathways by which ziprasidone is metabolized (255).

Ziprasidone slightly disturbs PRL levels and causes low extrapyramidal effects (256). There is a case study that reported elevated PRL levels after 9 days of ziprasidone administration (80 mg/day) (257, 258). Moreover, other studies have shown that ziprasidone suppresses the activity of the HPA-axis ($n = 11$, healthy volunteers; 40 mg/day), reducing the levels of nocturnal cortisol excretion, likely due to its antagonism toward H1 and α1 adrenergic receptors (259). Studies on the adverse effects produced by ziprasidone are scarce and more research is needed.

On the other hand, the immune alterations caused by ziprasidone consumption are few. There is no sufficient evidence supporting ziprasidone causes neutropenia, but there is a case report of agranulocytosis (120 mg/day); however, this effect was attributed to a combined activity of ziprasidone and mirtazapine (260). *In vitro* studies have shown that ziprasidone and its metabolites have cytotoxic, cytostatic, and genotoxic effects on peripheral blood lymphocyte cultures, causing a reduction in mitotic, proliferation, and nuclear division indexes (261).

In RAW macrophage cell line cultures, ziprasidone can induce inflammatory response. RAW cells exposed to ziprasidone (75 ng/L) showed increased levels of NO and ROS; moreover, they showed significantly higher levels of IL-1, IL-6, TNF-α, and IFN-γ but reduced levels of IL-10 (262). Several case reports have shown that ziprasidone induced allergic responses, such as Kounis syndrome (20 mg; IM) (263), pedal edema (80 mg/day) (264), urticaria, and angioedema (120 mg/day) (265). Little is known about the adverse effects of ziprasidone, but some studies have demonstrated minor effects in the endocrine system. On the other hand, special attention should be paid to the allergic response observed after ziprasidone administration, which can be explained by the high levels of IgE and the complement proteins C3 and C4 observed in patients (264). However, it is still unclear how ziprasidone induces this response (see **Table 2**).

ARIPIPRAZOLE

Aripiprazole acts as a stabilizer of the dopamine-serotonin system. Its use was authorized for the treatment of schizophrenia in 2002 (266); in 2006 it was approved to treat bipolar disorder (mania or mixed episodes) (267), and major depressive disorder (as adjunctive drug) (268). In 2009 it was finally approved for the treatment of autism-related irritability (269). There are also non-FDA-approved uses for this drug such as Tourette syndrome and substance abuse disorders (270–273). Aripiprazole is metabolized in the liver by cytochrome P450, CYP2D6, and CYP3A4 by dehydrogenation, hydroxylation, and N-dealkylation. Its active metabolite, dehydro-aripiprazole, represents around 40% of the parent drug levels in plasma (274, 275). Despite the use of SGAs, this drug has several advantages for the treatment of multiple mood disorders, even if its consumption affects patients' metabolism (276–278).

Aripiprazole is a quinolinone derivate (see **Figure 1**); its pharmacological activity is based on its activity as a partial agonist of D2 and 5-HT_{1A} receptors and as an antagonist of 5HT_{2A}. Furthermore, aripiprazole exhibits a moderate affinity to α1 adrenergic and histaminergic H1 receptors. When compared to other typical and atypical APs, aripiprazole has a higher affinity to both states of D2 receptors (see **Table 1**) (40–42).

There are few reports of hormonal alterations caused by the consumption of aripiprazole, possibly because this drug develops fewer hormonal effects than other AAPs. There are multicentric studies that evaluate the tolerability, efficacy, and safety of aripiprazole in schizophrenia and other mood disorders for up to 52 weeks of treatment (15 mg/day) (279–282). The administration of aripiprazole (15 mg/day) is recommended for the control of HPRL associated to chronic consumption of other AAPs such as risperidone, amisulpride, olanzapine (270, 275, 283), and benzamide, and it helps to maintain improvement in the positive and negative symptoms of patients (134, 284, 285). In fact, aripiprazole is prescribed as a substitute for treatments with AAPs when the patients show no signs of clinical response or when they exhibit severe symptoms of sexual dysfunction associated with HPRL (134, 282, 286, 287). Although there are few cases of patients with an increase in PRL during treatment (288–290), aripiprazole is considered a safe drug.

There is minimal evidence on its metabolic activity, yet aripiprazole is known to play a partially protective role (291–295). Concerning research of aripiprazole-induced effects in

animal models (Wistar rats) and cell lines (rHypoE-19), beneficial changes over metabolic parameters such as risk dyslipidemia and body weight have been found (72, 296).

Regarding the immune effects caused by aripiprazole consumption, there is evidence that shows this drug produces significant changes, such as cell count and changes in cytokine secretion, response to ROS, and gene expression. Although reports on the adverse effects of aripiprazole are scant compared to other AAPs, there is minimal evidence of its effect on the decrease in white blood cell count (297). A 10-year old with attention deficit hyperactivity disorder (ADHD) treated with aripiprazole (5 mg/day) showed a lower absolute neutrophil count (ANC). Additionally, a 50-year old Caucasian woman with schizophrenia developed neutropenia after aripiprazole consumption (15 mg/day) for 5 days (298), and a 21-year old Asian man with a conduct disorder showed a drop in WBC and neutropenia during aripiprazole treatment (297, 298). In all cases, the discontinuation of aripiprazole resulted in the normalization of WBC count and ANC, suggesting that the long-term bone marrow suppression by this drug plays a role in repeated antipsychotic consumption.

Some studies have shown that this drug affect cytokines secretion toward an anti-inflammatory profile: A meta-analysis involving 505 patients treated with aripiprazole showed a relationship between cytokine levels (TNF-α and IFN-γ) and their possible role as state and trait markers (86, 299). Another report described that aripiprazole consumption (5–30 mg/day, 3 months) reduced TNF-α, IL-8, IL-21, IL-13, IL-17, and fractalkine (CXCL1) levels in 31 first-episode psychotic patients; the effect in these molecules exhibited a positive correlation with clinical improvement (174). Another study also demonstrated a decrease in IL−1β, IL-6, TNF-α, IL-12, IL-23, IL-4, and IFN-γ under aripiprazole treatment with a dose from 10 mg/day (week 1) to a maximum of 30 mg/day (weeks 2, 3, and 4) (300).

In vitro studies confirm those data, since PBMC from healthy subjects and THP-1 cells incubated with aripiprazole (10–5 μM) exhibited a decrease in the expression of pro-inflammatory cytokines IL-1β, IL-6, and TNF-α and reduced the levels of IL-2, IL-9, IP-10 (CXCL10), and MIP-1β (CCL4) in the supernatant (217). The anti-inflammatory effect shown by this drug could be associated to the decrease in gene expression of cyclooxygenase (COX)-2 and inducible nitric oxide synthase (iNOS), causing lower levels of NO, prostaglandin 2 (PGE 2), and TNF-α (301). Furthermore, It is known that RAW264.7 cells treated with aripiprazole (20 μM) inhibited the interaction of the second messengers TAK1, MKK4, and MKK7 on AP-1, and, and Syk, which play a key role in the NF-κB signaling pathway (301). Aripiprazole also acts as an antioxidant improving the response to ROS. Studies in murine (2 mg/kg) and *in vitro* (5 μM) models showed that this drug increased the activity of glutathione peroxidase (GSH-Px) and superoxide dismutase (SOD) enzymes, promoting a decrease in the concentration of NO in supernatants and TNF-α, IL-1α, IL-2, and IL-10 in mice serum levels. This antioxidant activity is related to the input of intracellular [Ca^{2+}], which allows for ROS regulation and the decrease in inflammation cytokines (302, 303).

Some evidence suggests that this drug also modifies the gene expression of relevant genes; an *in vitro* study using primary human adipose-derived stem cells (ADSCs) demonstrated that aripiprazole (100 ng/mL) increased the expression of key genes involved in cell cycle (*ANAPC2, CD14*), apoptosis (*BCL2)*, nuclear and transporter receptors (*PPARα, PPARγ, ABCA1, LEPR, INSR*), transcript factors (*CEBPA, SREBF1*, *NF-KB1*), signal transduction (*IRS1, SIRT1*), adipogenic markers, lipid metabolism, adipokines (*ADFP, FABPN, LPL, ACSL1, ADIPOQ, LEP*) and cytokines and chemokines (TNF-α, IL-1β, IL-8, MCP-1). These results support the role of AAPs in the recruitment of MQs to adipose tissue by increasing MCP-1 and the risk of metabolic syndrome associated with drug treatment (185). However, this drug showed no significant immunotoxic effects in ICR mice and C6 glioma and RAW264.7 cells (50 mg/kg) when no alterations in organs or cell lines were found (304).

In summary, there is little evidence on the hormonal and immune effects of aripiprazole, as well as its partially protective role (291–295). These effects allow aripiprazole to suitably treat schizophrenia and bipolar disorder (304) (see **Table 2**).

PALIPERIDONE

Paliperidone, or 9-hydroxy-risperidone (see **Figure 1**), is the most significant active metabolite of risperidone. The FDA approved this drug for the treatment of schizophrenia in 2006 (305). Paliperidone is a monotherapy drug for short-term and maintenance treatment of schizophrenia as well as monotherapy or adjunct drug for the short-term treatment of schizoaffective disorder (306–308). It has also been used in the treatment of bipolar disorder (309), borderline personality disorder (310), Huntington's disease (311), ASD, and ADHD (312); however, it has not been approved to treat any of these last clinical conditions. Paliperidone is a racemic mixture of (+)-paliperidone and (−)-paliperidone enantiomers that undergo minimal hepatic metabolism (44). The available pharmaceutical formulations of this drug are oral immediate-release formulation, oral extended-release (ER) formulation, and intramuscular depot formulation (305).

The therapeutic activity of paliperidone is comparable with that of risperidone itself; its action mechanism is unknown, but it likely acts through a combination of 5-HT_{2A} agonism and D2 receptor antagonism (see **Table 1**) (44). This drug is also active as an antagonist for other receptors such as D3, D4 dopaminergic receptors, 5-HT_{1A}, 5-HT_{1B}, and 5-HT_{1D} serotoninergic receptors, and α-1 and α-2 adrenergic receptors, although it also acts as agonist to 5-HT_{2C} and 5- H1 histaminergic receptors (45).

The immunoendocrine alterations cited in this section are related to paliperidone; effects on 9-hydroxy-risperidone by risperidone consumption and its subsequent metabolism are not mentioned. The most representative endocrine alteration reported after paliperidone consumption is the increase in PRL or HPRL (207, 308, 313, 314). This alteration can produce prolactin-related adverse effects (PRL-RAEs) or be asymptomatic (315).

HPRL induced by risperidone/paliperidone treatment in schizophrenic patients was presented in association with rs40184 and rs3863145 variants in the *SLC6A3* gene of blood leukocyte DNA (132). According to several reports, paliperidone produced high HPRL incidence when compared vs. other SGAs in adults (dosage 7.03 ± 3.63 mg/day) (111) and pediatric patients (130). Paliperidone consumption showed an association between PRL, sex, and age (113, 130), although Druyts and cols. reported no differences between females and males (314). This drug increased PRL levels, yet some reports have shown that the switch from risperidone or paliperidone ER to paliperidone palmitate treatment (PP, an intramuscular depot formulation) reduced PRL concentration (316, 317) as well as sexual dysfunction (316), a common PRL-RAE. Similarly, patients with sexual dysfunction presented higher PRL as compared with no sexual dysfunction patients (318). Adolescent patients with PRL-RAE showed higher PRL levels when compared against patients without PRL-RAE (1.5–12 mg/day) (319). According to the literature above, different formulations of paliperidone could cause this alteration in pediatric and adult patients. The precise mechanism by which paliperidone increases PRL levels is unclear; however, it corresponds to D2 receptor blockade (320).

There are a few reports that show changes in other hormonal profiles in patients during paliperidone consumption. Although other AAPs mentioned in this review induce dysregulation in glucose metabolism, paliperidone does not modify serum levels of insulin. The acute and chronic treatment with paliperidone did not alter serum insulin levels and β-cell function with the homeostatic model assessment (HOMA-B) (207, 313, 321). However, a case report showed increased insulin secretion, causing hypoglycemia in a schizophrenic female patient (322).

The reports on immune alterations induced by paliperidone consumption are a few yet diverse. Several cases of schizophrenic patients showed that paliperidone treatment decreased leukocyte counts. Monotherapy with paliperidone produced leukopenia and neutropenia (323); still, the combined use of paliperidone depot/risperidone (100–2 mg/day) resulted in leukopenia and lymphopenia but risperidone alone did not (159). Agranulocytosis was reported in a patient when switching from risperidone to paliperidone treatment (6 mg/day) (324). The treatment with paliperidone ER/valproic acid (12–1,000 mg/day) caused leukopenia and neutropenia in a patient with schizoaffective disorder (325). In all cases, the cytopenic alterations were normalized after discontinuing the consumption of paliperidone. Some proposed mechanisms of AP-induced blood dyscrasia, such as paliperidone, include direct bone marrow suppression, antibody formation against hematologic precursors, and peripheral WBC destruction (326).

Paliperidone increases BDNF concentration during acute treatment. The serum levels of BDNF in first-episode schizophrenia patients increased after a 12-week paliperidone treatment negatively correlated with a reduction rate of the positive and negative symptoms scale (PANSS) score (unspecified dose) (327). However, the paliperidone ER treatment during 8 weeks did not increase BDNF serum concentration (unspecified dose) (328).

In blood, peripheral cells of patients with EPS (acute dystonia and drug-induced parkinsonism) showed a constructed network enriched in different biological processes related to pathways of NF-κB, an important transcription factor for immune response, (12.85 ± 2.85 mg/day) (329) in patients with paliperidone or risperidone treatment. *In vitro*, U-937 human cell line decreased cell survival with 25 and 50 μM/mL of paliperidone (330) (see **Table 2**).

ASENAPINE

The FDA approved asenapine for the treatment of schizophrenia (331) and bipolar disorders (332) in 2019. This drug is a new AAP with unique features that was introduced in Japan in 2016, and it is the only AP used sublingually; its chemical structure of (±)-Asenapine can be described as a tetracyclic framework wherein N-methylpyrrolidine ring fuses at third and fourth positions with chlorophenyl phenyl ether in a trans geometry (333) (see **Figure 1**). This drug is metabolized rapidly in a process mediated by glucuronidation and demethylation pathways that induce two non-active metabolites, asenapine N-glucuronide and asenapine N-desmethyl carbamoyl glucuronide (334). Asenapine has subnanomolar and nanomolar affinities for diverse and numerous subtypes of aminergic G protein coupled receptors (GPCRs) associated to 5-HT, norepinephrine (NE), DA, and histamine (H) (335, 336). Still, the antagonist activity at 5-HT_{1A}, 5-HT_{1B}, 5-HT_{2A}, 5-HT_{2C}, 5-HT_{5A}, 5-HT_6, and 5-HT_7 may contribute to the antimanic and antidepressant effects of asenapine (see **Table 1**) (39).

Endocrine deleterious side effects induced by asenapine consumption were reported in PRL and insulin blood levels. Asenapine displays more potent antagonist activity toward 5-HT_{2A} receptor than D2 receptor (337, 338), that is why it has a low propensity to cause PRL elevation (331, 339, 340); Therefore, this drug is one of the AP treatments of choice for breast cancer patients (341). Nevertheless, research groups reported that 2.3% of patients with bipolar disorder who received asenapine monotherapy had PRL levels ≥ 4 times the upper limit of the normal range, compared with those who received a placebo (332, 342), In contrast, 9% of patients with schizophrenia who received asenapine (5 and 10 mg twice daily) had PRL levels over 2-fold the upper limit of the normal range compared with those who received a placebo (343).

Insulin altered levels are associated with glucose metabolism disturbances and the evidence shows that asenapine modifies the blood levels of these hormones. In 302 patients (aged 10–17 years) with bipolar I disorder in manic or mixed episodes who were treated with asenapine (2, 5, or 10 mg twice, daily) for 3 weeks, the mean change from baseline in fasting insulin was significant when compared to controls. In all cases, the patients treated with asenapine increased their body weight (344). Contrastingly, no changes in insulin resistance were detected in adult female Sprague Dawley rats treated with asenapine (0.01, 0.05, 0.1, 0.5, 1.0 mg/kg) (67).

As described above, asenapine can interact with 5-HT, NE, DA, and H receptors expressed in leukocytes (28, 29, 345,

346). Then, the administration or consumption of this drug could induce changes in the inflammatory response in patients, although the evidence of this effect is very scarce. There is only one report of a case of pityriasis rosea secondary to asenapine consumption. A biopsy of the lesions evidenced superficial and deep perivascular and interstitial dermatitis with eosinophils and dermal perivascular lymphocytic infiltrate, as well as minimal parakeratosis and spongiosis (347). Although there was no molecular explanation of this phenomenon, we may speculate that this patient had an alteration in neurotransmitter receptors (density or functional alteration) expressed by leukocytes, becoming more susceptible to this aberrant inflammatory response secondary to asenapine consumption (see **Table 2**).

MICROBIOTA

Little is known about the effects of AAPs on the microbiota; however, a small body of evidence suggests they cause severe adverse effects. Olanzapine and risperidone induced an increase in Firmicutes and a decrease in *Bacteroidetes*, as well as metabolic alterations as a result of a shift toward a potentially obesogenic bacterial profile associated with short-chain fatty acids and inflammation in adults (348), children (349, 350), and rodents (351). These changes were also gender-dependent (349, 352, 353), with females showing a higher pro-inflammatory cytokine (IL-8 and IL-1β) response in circulation and macrophage infiltration; still, microbiota dysbiosis was equally present in males and females.

AAPs have a potent antibiotic effect, inducing a profound dysbiosis in the gut microbiota, either chronically or after short-term administration (205). Antibiotic co-administration resulted in further changes in microbiota composition. Interestingly, these antibiotic-dependent changes in microbiota diversity reduced the side effects, including macrophage infiltration. Furthermore, experiments in germ-free mice showed no alteration in their metabolic profile (352–355), indicating a clear role of the microbiota in the metabolic dysfunction associated with AAPs (352). Finally, fecal transplants from risperidone-treated mice induced excess weight gain in control mice (354). These alterations have been associated to a decrease in *Bifidobacterium*, *Escherichia coli*, and *Lactobacillus* and an increase in *Clostridium coccoides* (353).

Risperidone *in vitro* altered the colon microbiota just 24 h after administration, inducing specific metabolites (350). Probiotic treatment has shown a protective effect, restoring the *Bacteroidetes:Firmicutes* ratio, without reducing the AAPs effect (356).

EPILOG

The bidirectional communication between the SNC with other peripheral systems occurs by the release of soluble molecules that interact with their receptors. Any cell in the organism that bears a functional receptor for a molecule will respond when they interact. The complex structure that confers pharmacological non-specificity to AAPs allows for the interaction with the receptors they have an affinity for, not only in the CNS but also in all body cells. This result leads to the therapeutic effect of AAPs in various psychiatric conditions and their possible ability to modify the endocrine and immune systems as well as the gut microbiota. The therapeutic effect of AAPs is exhibited by the antagonism in CNS receptors that are involved in the pathophysiology of the disease. In schizophrenia, for example, the positive and negative symptoms decrease due to the AAP-receptor interaction in the mesocortical and mesolimbic pathways, although HPRL is caused by the antagonism of receptors in the tuberoinfundibular pathway. In addition, the antagonism of neurotransmitter receptors on leukocytes and glandular cells have immune and endocrine effects. The effect of each AAP is unique and depends on specificity and affinity characteristics.

AAPs are drugs prescribed for various psychiatric conditions due to their high efficiency and low rate of extrapyramidal effects. However, these drugs have systemic effects that are not only metabolic but also related to changes in endocrine and immune responses. Having greater knowledge of these immune, endocrine, and microbiota effects, allows clinicians to have a broader point of view and more significant criteria to prescribe these drugs to patients, considering that the adverse effects can modify the systemic response and generate undesirable effects, with a direct impact on the patients' quality of life. It is necessary to start a new generation of drugs that support the resolution of psychiatric symptoms with higher specificity to prevent acute adverse effects and the patients' systemic deterioration by chronic consumption.

AUTHOR CONTRIBUTIONS

SA-H, RE, and LP: conceptualization. All authors: writing-original draft preparation and writing-review and editing. LP: supervision.

FUNDING

The study was supported by Instituto Nacional de Psiquiatría Ramón de la Fuente Muñiz Projects SC-15-24-14; NC150048SECITI; SECITI 0048/2014; NC16044.0; NC092318.0 and FOSISS: SALUD-2017-1-289800. SA-H is a doctoral student from Programa de Doctorado en Ciencias Biomédicas, Universidad Nacional Autónoma de México (UNAM) and she was supported by CONACYT-fellowship number 594780.

ACKNOWLEDGMENTS

We acknowledge and appreciate the support of Raul Cardoso and José L. Calderon, from the Department of Biomedical Illustration of INPRFM. Thanks to León Luka for breaking paradigms and taking us beyond our limits.

SUPPLEMENTARY MATERIAL

The Supplementary Material for this article can be found online at: https://www.frontiersin.org/articles/10.3389/fendo.2020.00195/full#supplementary-material

REFERENCES

1. Cunningham Owens D, Johnstone EC. The development of antipsychotic drugs. *Brain Neurosci Adv.* (2018) 2:2398212818817498. doi: 10.1177/2398212818817498
2. Meltzer HY. Update on typical and atypical antipsychotic drugs. *Annu Rev Med.* (2013) 64:393–406. doi: 10.1146/annurev-med-050911-161504
3. Zhang J-P, Gallego JA, Robinson DG, Malhotra AK, Kane JM, Correll CU. Efficacy and safety of individual second-generation vs. first-generation antipsychotics in first-episode psychosis: a systematic review and meta-analysis. *Int J Neuropsychopharmacol.* (2013) 16:1205–18. doi: 10.1017/S1461145712001277
4. Singh R, Bansal Y, Medhi B, Kuhad A. Antipsychotics-induced metabolic alterations: recounting the mechanistic insights, therapeutic targets and pharmacological alternatives. *Eur J Pharmacol.* (2019) 844:231–40. doi: 10.1016/j.ejphar.2018.12.003
5. Chokhawala K, Stevens L. *Antipsychotic Medications*. Treasure Island, FL: StatPearls Publishing (2019).
6. Lee ES, Vidal C, Findling RL. A focused review on the treatment of pediatric patients with atypical antipsychotics. *J Child Adolesc Psychopharmacol.* (2018) 28:582–605. doi: 10.1089/cap.2018.0037
7. Xu H, Zhuang X. Atypical antipsychotics-induced metabolic syndrome and nonalcoholic fatty liver disease: a critical review. *Neuropsychiatr Dis Treat.* (2019) 15:2087–99. doi: 10.2147/NDT.S208061
8. Murray R, Correll CU, Reynolds GP, Taylor D. Atypical antipsychotics: recent research findings and applications to clinical practice: proceedings of a symposium presented at the 29th Annual European college of neuropsychopharmacology congress, 19 September 2016, Vienna, Austria. *Ther Adv Psychopharmacol.* (2017) 7:1–14. doi: 10.1177/2045125317693200
9. Wei Xin Chong J, Hsien-Jie Tan E, Chong CE, Ng Y, Wijesinghe R. Atypical antipsychotics: a review on the prevalence, monitoring, and management of their metabolic and cardiovascular side effects. *Ment Heal Clin.* (2016) 6:178–84. doi: 10.9740/mhc.2016.07.178
10. De Hert M, Detraux J, van Winkel R, Yu W, Correll CU. Metabolic and cardiovascular adverse effects associated with antipsychotic drugs. *Nat Rev Endocrinol.* (2012) 8:114–26. doi: 10.1038/nrendo.2011.156
11. Kowalchuk C, Castellani LN, Chintoh A, Remington G, Giacca A, Hahn MK. Antipsychotics and glucose metabolism: how brain and body collide. *Am J Physiol Metab.* (2019) 316:E1–15. doi: 10.1152/ajpendo.00164.2018
12. Guest PC. Insulin resistance in schizophrenia. *Adv Exp Med Biol.* (2019) 1134:1–16. doi: 10.1007/978-3-030-12668-1_1
13. Misiak B, Bartoli F, Stramecki F, Samochowiec J, Lis Michałand Kasznia J, Jarosz K, et al. Appetite regulating hormones in first-episode psychosis: a systematic review and meta-analysis. *Neurosci Biobehav Rev.* (2019) 102:362–70. doi: 10.1016/J.NEUBIOREV.2019.05.018
14. Karanikas E, Ntouros E, Oikonomou D, Floros G, Griveas I, Garyfallos G. Evidence for hypothalamus-pituitary-adrenal axis and immune alterations at prodrome of psychosis in males. *Psychiatry Investig.* (2017) 14:703–7. doi: 10.4306/pi.2017.14.5.703
15. Chen ML, Tsai TC, Lin YY, Tsai YM, Wang LK, Lee MC, Tsai FM. Antipsychotic drugs suppress the AKT/NF-κB pathway and regulate the differentiation of T-cell subsets. *Immunol Lett.* (2011) 140:81–91. doi: 10.1016/j.imlet.2011.06.011
16. Chen ML, Tsai TC, Wang LK, Lin YY, Tsai YM, Lee MC, et al. Risperidone modulates the cytokine and chemokine release of dendritic cells and induces TNF-α-directed cell apoptosis in neutrophils. *Int Immunopharmacol.* (2012) 12:197–204. doi: 10.1016/j.intimp.2011.11.011
17. Chen ML, Tsai TC, Wang LK, Lin YY, Tsai YM, Lee MC, et al. Clozapine inhibits Th1 cell differentiation and causes the suppression of IFN-γ production in peripheral blood mononuclear cells. *Immunopharmacol Immunotoxicol.* (2012) 34:686–94. doi: 10.3109/08923973.2011.651535
18. Petrikis P, Voulgari PV, Tzallas AT, Boumba VA, Archimandriti DT, Zambetas D, et al. Changes in the cytokine profile in first-episode, drug-naïve patients with psychosis after short-term antipsychotic treatment. *Psychiatry Res.* (2017) 256:378–83. doi: 10.1016/J.PSYCHRES.2017.07.002
19. Capuzzi E, Bartoli F, Crocamo C, Clerici M, Carrà G. Acute variations of cytokine levels after antipsychotic treatment in drug-naïve subjects with a first-episode psychosis: a meta-analysis. *Neurosci Biobehav Rev.* (2017) 77:122–8. doi: 10.1016/j.neubiorev.2017.03.003
20. Cussotto S, Clarke G, Dinan TG, Cryan JF. Psychotropics and the microbiome: a chamber of secrets. *Psychopharmacology.* (2019) 236:1411–32. doi: 10.1007/s00213-019-5185-8
21. Jeon S, Kim Y-K. Unresolved issues for utilization of atypical antipsychotics in schizophrenia: antipsychotic polypharmacy and metabolic syndrome. *Int J Mol Sci.* (2017) 18:2174. doi: 10.3390/ijms18102174
22. Reynolds GP, Kirk SL. Metabolic side effects of antipsychotic drug treatment – pharmacological mechanisms. *Pharmacol Ther.* (2010) 125:169–79. doi: 10.1016/j.pharmthera.2009.10.010
23. Correll CU, Rummel-Kluge C, Corves C, Kane JM, Leucht S. Antipsychotic combinations vs monotherapy in schizophrenia: a meta-analysis of randomized controlled trials. *Schizophr Bull.* (2009) 35:443–57. doi: 10.1093/schbul/sbn018
24. Fleischhacker WW, Uchida H. Critical review of antipsychotic polypharmacy in the treatment of schizophrenia. *Int J Neuropsychopharmacol.* (2014) 17:1083–93. doi: 10.1017/S1461145712000399
25. Liu Y, Zhou X, Qin B, Del Giovane C, Zhang Y, Xie P. Efficacy, quality of life, and acceptability outcomes of atypical antipsychotic augmentation treatment for treatment-resistant depression: protocol for a systematic review and network meta-analysis. *Syst Rev.* (2014) 3:133. doi: 10.1186/2046-4053-3-133
26. Baandrup L. Polypharmacy in schizophrenia. *Basic Clin Pharmacol Toxicol.* (2020) 126:183–92. doi: 10.1111/bcpt.13384
27. Kapur S, Zipursky RB, Remington G. Clinical and theoretical implications of 5-HT2 and D2 receptor occupancy of clozapine, risperidone, and olanzapine in schizophrenia. *Am J Psychiatry.* (1999) 156:286–93. doi: 10.1176/ajp.156.2.286
28. Arreola R, Alvarez-Herrera S, Pérez-Sánchez G, Becerril-Villanueva E, Cruz-Fuentes C, Flores-Gutierrez EO, et al. Immunomodulatory effects mediated by dopamine. *J Immunol Res.* (2016) 2016:3160486. doi: 10.1155/2016/3160486
29. Arreola R, Becerril-Villanueva E, Cruz-Fuentes C, Velasco-Velázquez MA, Garcés-Alvarez ME, Hurtado-Alvarado G, et al. Immunomodulatory effects mediated by serotonin. *J Immunol Res.* (2015) 2015:354957. doi: 10.1155/2015/354957
30. Zhang Y, Zheng R, Meng X, Wang L, Liu L, Gao Y. Pancreatic endocrine effects of dopamine receptors in human islet cells. *Pancreas.* (2015) 44:925–9. doi: 10.1097/MPA.0000000000000357
31. Chue P, Chue J. A review of olanzapine pamoate. *Expert Opin Pharmacother.* (2012) 13:1661–70. doi: 10.1517/14656566.2012.686169
32. Ishibashi T, Horisawa T, Tokuda K, Ishiyama T, Ogasa M, Tagashira R, et al. Pharmacological profile of lurasidone, a novel antipsychotic agent with potent 5-hydroxytryptamine 7 (5-HT 7) and 5-HT 1A receptor activity. *J Pharmacol Exp Ther.* (2010) 334:171–81. doi: 10.1124/jpet.110.167346
33. Zajdel P, Kos T, Marciniec K, Satała G, Canale V, Kaminski K, et al. Novel multi-target azinesulfonamides of cyclic amine derivatives as potential antipsychotics with pro-social and pro-cognitive effects. *Eur J Med Chem.* (2018) 145:790–804. doi: 10.1016/J.EJMECH.2018.01.002
34. Fernández J, Alonso JM, Andrés JI, Cid JM, Díaz A, Iturrino L, et al. Discovery of new tetracyclic tetrahydrofuran derivatives as potential broad-spectrum psychotropic agents. *J Med Chem.* (2005) 48:1709–12. doi: 10.1021/jm049632c
35. Ablordeppey SY, Altundas R, Bricker B, Zhu XY, Suresh Kumar EVK, Jackson T, et al. Identification of a butyrophenone analog as a potential atypical antipsychotic agent: 4-[4-(4-Chlorophenyl)-1,4-diazepan-1-yl]-1-(4-fluorophenyl)butan-1-one. *Bioorg Med Chem.* (2008) 16:7291–301. doi: 10.1016/j.bmc.2008.06.030
36. Cutler AJ, Kalali AH, Mattingly GW, Kunovac J, Meng X. Long-term safety and tolerability of iloperidone: results from a 25-week, open-label extension trial. *CNS Spectr.* (2013) 18:43–54. doi: 10.1017/S1092852912000764
37. Munshi T, Mazhar M, Hassan T. Clozapine reinitiation following a "red result" secondary to chemotherapy. *Neuropsychiatr Dis Treat.* (2013) 9:1267–71. doi: 10.2147/NDT.S49028
38. Keating GM, Robinson DM. Quetiapine: a review of its use in the treatment of bipolar depression. *Drugs.* (2007) 67:1077–95. doi: 10.2165/00003495-200767070-00008

39. Reynolds GP. Receptor mechanisms of antipsychotic drug action in bipolar disorder – focus on asenapine. *Ther Adv Psychopharmacol.* (2011) 1:197–204. doi: 10.1177/2045125311430112
40. Keck PE, McElroy SL. Aripiprazole: a partial dopamine D2 receptor agonist antipsychotic. *Expert Opin Investig Drugs.* (2003) 12:655–62. doi: 10.1517/eoid.12.4.655.23750
41. Burris KD, Molski TF, Xu C, Ryan E, Tottori K, Kikuchi T, et al. Aripiprazole, a novel antipsychotic, is a high-affinity partial agonist at human dopamine D2 receptors. *J Pharmacol Exp Ther.* (2002) 302:381–9. doi: 10.1124/jpet.102.033175
42. Goodnick PJ, Jerry JM. Aripiprazole: profile on efficacy and safety. *Expert Opin Pharmacother.* (2002) 3:1773–1781. doi: 10.1517/14656566.3.12.1773
43. Mauri MC, Paletta S, Maffini M, Colasanti A, Dragogna F, Di Pace C, et al. Clinical pharmacology of atypical antipsychotics: an update. *EXCLI J.* (2014) 13:1163–91.
44. Chue P, Chue J. A review of paliperidone palmitate. *Expert Rev Neurother.* (2012) 12:1383–97. doi: 10.1586/ern.12.137
45. Wang SM, Han C, Lee SJ, Patkar AA, Pae CU, Fleischhacker WW. Paliperidone: a review of clinical trial data and clinical implications. *Clin Drug Investig.* (2012) 32:497–512. doi: 10.2165/11634440
46. Kalkman HO, Subramanian N, Hoyer D. Extended radioligand binding profile of iloperidone: a broad spectrum dopamine/serotonin/norepinephrine receptor antagonist for the management of psychotic disorders. *Neuropsychopharmacology.* (2001) 25:904–14. doi: 10.1016/S0893-133X(01)00285-8
47. Kalkman HO, Feuerbach D, Lötscher E, Schoeffter P. Functional characterization of the novel antipsychotic iloperidone at human D2, D3, α2C, 5-HT6, and 5-HT1A receptors. *Life Sci.* (2003) 73:1151–59. doi: 10.1016/S0024-3205(03)00419-3
48. Richelson E, Souder T. Binding of antipsychotic drugs to human brain receptors focus on newer generation compounds. *Life Sci.* (2000) 68:29–39. doi: 10.1016/s0024-3205(00)00911-5
49. Roth BL, Lopez E, Patel S, Kroeze WK. The multiplicity of serotonin receptors: uselessly diverse molecules or an embarrassment of riches? *Neuroscientist.* (2000) 6:252–62. doi: 10.1177/107385840000600408
50. Kongsamut S, Roehr JE, Cai J, Hartman HB, Weissensee P, Kerman LL, et al. Iloperidone binding to human and rat dopamine and 5-HT receptors. *Eur J Pharmacol.* (1996) 317:417–23. doi: 10.1016/S0014-2999(96)00840-0
51. Caccia S, Pasina L, Nobili A. New atypical antipsychotics for schizophrenia: iloperidone. *Drug Des Devel Ther.* (2010) 4:33–48. doi: 10.2147/dddt.s6443
52. Conley RR, Kelly DL. Current status of antipsychotic treatment. *Curr Drug Targets CNS Neurol Disord.* (2002) 1:123–8. doi: 10.2174/1568007024606221
53. Aringhieri S, Carli M, Kolachalam S, Verdesca V, Cini E, Rossi M, et al. Molecular targets of atypical antipsychotics: from mechanism of action to clinical differences. *Pharmacol Ther.* (2018) 192:20–41. doi: 10.1016/j.pharmthera.2018.06.012
54. Rajagopal S, Rajagopal K, Lefkowitz RJ. Teaching old receptors new tricks: biasing seven-transmembrane receptors. *Nat Rev Drug Discov.* (2010) 9:373–86. doi: 10.1038/nrd3024
55. Kenakin T. New concepts in pharmacological efficacy at 7TM receptors: IUPHAR review 2. *Br J Pharmacol.* (2013) 168:554–75. doi: 10.1111/j.1476-5381.2012.02223.x
56. Kaya AI, Onaran HO, Özcan G, Ambrosio C, Costa T, Balli S, et al. Cell contact-dependent functional selectivity of β2-adrenergic receptor ligands in stimulating cAMP accumulation and extracellular signal-regulated kinase phosphorylation. *J Biol Chem.* (2012) 287:6362–74. doi: 10.1074/jbc.M111.301820
57. Kenakin T. Signaling bias in drug discovery. *Expert Opin Drug Discov.* (2017) 12:321–33. doi: 10.1080/17460441.2017.1297417
58. Hahn MK, Wolever TMS, Arenovich T, Teo C, Giacca A, Powell V, et al. Acute effects of single-dose olanzapine on metabolic, endocrine, and inflammatory markers in healthy controls. *J Clin Psychopharmacol.* (2013) 33:740–46. doi: 10.1097/JCP.0b013e31829e8333
59. De Berardis D, Rapini G, Olivieri L, Di Nicola D, Tomasetti C, Valchera A, et al. Safety of antipsychotics for the treatment of schizophrenia: a focus on the adverse effects of clozapine. *Ther Adv drug Saf.* (2018) 9:237–56. doi: 10.1177/2042098618756261
60. Nikolić-Kokić A, Tatalović N, Nestorov J, Mijović M, Mijusković A, Miler M, et al. Clozapine, ziprasidone, and sertindole-induced morphological changes in the rat heart and their relationship to antioxidant enzymes function. *J Toxicol Environ Health A.* (2018) 81:844–53. doi: 10.1080/15287394.2018.1495587
61. Yuen JWY, Wu C, Wang CK, Kim DD, Procyshyn RM, Honer WG, et al. A comparison of the effects of clozapine and its metabolite norclozapine on metabolic dysregulation in rodent models. *Neuropharmacology.* (2019) 23:107717. doi: 10.1016/j.neuropharm.2019.107717
62. Nakazawa T, Kikuchi M, Ishikawa M, Yamamori H, Nagayasu K, Matsumoto T, et al. Differential gene expression profiles in neurons generated from lymphoblastoid B-cell line-derived iPS cells from monozygotic twin cases with treatment-resistant schizophrenia and discordant responses to clozapine. *Schizophr Res.* (2017) 181:75–82. doi: 10.1016/j.schres.2016.10.012
63. Potvin S, Zhornitsky S, Stip E. Antipsychotic-induced changes in blood levels of leptin in schizophrenia: a meta-analysis. *Can J Psychiatry.* (2015) 60:S26–34. Available at: http://www.ncbi.nlm.nih.gov/pubmed/25886677
64. Houseknecht KL, Robertson AS, Zavadoski W, Gibbs EM, Johnson DE, Rollema H. Acute effects of atypical antipsychotics on whole-body insulin resistance in rats: implications for adverse metabolic effects. *Neuropsychopharmacology.* (2007) 32:289–97. doi: 10.1038/sj.npp.1301209
65. Tulipano G, Rizzetti C, Bianchi I, Fanzani A, Spano P, Cocchi D. Clozapine-induced alteration of glucose homeostasis in the rat: the contribution of hypothalamic-pituitary-adrenal axis activation. *Neuroendocrinology.* (2007) 85:61–70. doi: 10.1159/000100981
66. Smith GC, Vickers MH, Cognard E, Shepherd PR. Clozapine and quetiapine acutely reduce glucagon-like peptide-1 production and increase glucagon release in obese rats: implications for glucose metabolism and food choice behaviour. *Schizophr Res.* (2009) 115:30–40. doi: 10.1016/j.schres.2009.07.011
67. Boyda HN, Procyshyn RM, Pang CCY, Hawkes E, Wong D, Jin CH, et al. Metabolic side-effects of the novel second-generation antipsychotic drugs asenapine and iloperidone: a comparison with olanzapine. *PLoS ONE.* (2013) 8:e53459. doi: 10.1371/journal.pone.0053459
68. Tschoner A, Engl J, Rettenbacher M, Edlinger M, Kaser S, Tatarczyk T, et al. Effects of six second generation antipsychotics on body weight and metabolism - risk assessment and results from a prospective study. *Pharmacopsychiatry.* (2009) 42:29–34. doi: 10.1055/s-0028-1100425
69. Bymaster FP, Felder CC, Tzavara E, Nomikos GG, Calligaro DO, Mckinzie DL. Muscarinic mechanisms of antipsychotic atypicality. *Prog Neuropsychopharmacol Biol Psychiatry.* (2003) 27:1125–43. doi: 10.1016/j.pnpbp.2003.09.008
70. Weston-Green K, Huang X-F, Deng C. Second generation antipsychotic-induced type 2 diabetes: a role for the muscarinic M3 receptor. *CNS Drugs.* (2013) 27:1069–80. doi: 10.1007/s40263-013-0115-5
71. Schmid CL, Streicher JM, Meltzer HY, Bohn LM. Clozapine acts as an agonist at serotonin 2A receptors to counter MK-801-induced behaviors through a βarrestin2-independent activation of Akt. *Neuropsychopharmacology.* (2014) 39:1902–13. doi: 10.1038/npp.2014.38
72. Kowalchuk C, Kanagasundaram P, Belsham DD, Hahn MK. Antipsychotics differentially regulate insulin, energy sensing, and inflammation pathways in hypothalamic rat neurons. *Psychoneuroendocrinology.* (2019) 104:42–8. doi: 10.1016/j.psyneuen.2019.01.029
73. Heppner KM, Perez-Tilve D. GLP-1 based therapeutics: simultaneously combating T2DM and obesity. *Front Neurosci.* (2015) 9:92. doi: 10.3389/fnins.2015.00092
74. Ekström J, Godoy T, Loy F, Riva A. Parasympathetic vasoactive intestinal peptide (VIP): a likely contributor to clozapine-induced sialorrhoea. *Oral Dis.* (2014) 20:90–6. doi: 10.1111/odi.12139
75. Khalaf HA, Elmorsy E, Mahmoud E-HM, Aggour AM, Amer SA. The role of oxidative stress in ovarian toxicity induced by haloperidol and clozapine-a histological and biochemical study in albino rats. *Cell Tissue Res.* (2019) 378:371–83. doi: 10.1007/s00441-019-03067-x
76. Margulska A, Kozłowska E, Wysokinski A. Effect of clozapine dose and concentration on fasting concentration of appetite regulating peptides. *Psychiatry Res.* (2018) 260:473–7. doi: 10.1016/j.psychres.2017.12.018

77. Oh J-E, Cho YM, Kwak S-N, Kim J-H, Lee KW, Jung H, et al. Inhibition of mouse brown adipocyte differentiation by second-generation antipsychotics. *Exp Mol Med.* (2012) 44:545–53. doi: 10.3858/emm.2012.44.9.062
78. Basta-Kaim A, Szcz?eny E, Leśkiewicz M, Głombik K, Slusarczyk J, Budziszewska B, et al. Maternal immune activation leads to age-related behavioral and immunological changes in male rat offspring - The effect of antipsychotic drugs. *Pharmacol Rep.* (2012) 64:1400–10. doi: 10.1016/S1734-1140(12)70937-4
79. Tunsirimas N, Pariwatcharakul P, Choovanichvong S, Ratta-apha W. Clozapine-induced agranulocytosis and leukopenia: incidence, associated factors, and rate of hematologic adverse-effects monitoring in psychiatric out-patient services in Thailand. *Asian J Psychiatr.* (2019) 41:13–6. doi: 10.1016/j.ajp.2019.03.002
80. Capllonch A, de Pablo S, de la Torre A, Morales I. Increase in white cell and neutrophil counts during the first eighteen weeks of treatment with clozapine in patients admitted to a long-term psychiatric care inpatient unit. *Rev Psiquiatr Salud Ment.* (2018) 11:94–100. doi: 10.1016/j.rpsm.2016.03.005
81. Pessina A, Turlizzi E, Bonomi A, Guizzardi F, Cavicchini L, Croera C, et al. *In vitro* toxicity of clozapine, olanzapine, and quetiapine on granulocyte-macrophage progenitors (GM-CFU). *Pharmacopsychiatry.* (2006) 39:20–2. doi: 10.1055/s-2006-931475
82. Goto A, Yoshimi A, Nagai T, Ukigai M, Mouri A, Ozaki N, et al. Human neutrophils show decreased survival upon long-term exposure to clozapine. *Hum Psychopharmacol.* (2017) 32:1–5. doi: 10.1002/hup.2629
83. Gardiner E, Carroll A, Tooney PA, Cairns MJ. Antipsychotic drug-associated gene-miRNA interaction in T-lymphocytes. *Int J Neuropsychopharmacol.* (2014) 17:929–43. doi: 10.1017/S1461145713001752
84. Van Der Weide K, Loovers H, Pondman K, Bogers J, Van Der Straaten T, Langemeijer E, et al. Genetic risk factors for clozapine-induced neutropenia and agranulocytosis in a Dutch psychiatric population. *Pharmacogenomics J.* (2017) 17:471–8. doi: 10.1038/tpj.2016.32
85. Petrikis P, Voulgari PV, Tzallas AT, Boumba VA, Archimandriti DT, Zambetas D, et al. Changes in the cytokine profile in first-episode, drug-naïve patients with psychosis after short-term antipsychotic treatment. *Psychiatry Res.* (2017) 256:378–83. doi: 10.1016/j.psychres.2017.07.002
86. Capuzzi E, Bartoli F, Crocamo C, Clerici M, Carrà G. Acute variations of cytokine levels after antipsychotic treatment in drug-naïve subjects with a first-episode psychosis: a meta-analysis. *Neurosci Biobehav Rev.* (2017) 77:122–8. doi: 10.1016/J.NEUBIOREV.2017.03.003
87. Sanader B, Grohmann R, Grötsch P, Schumann T, Toto S, Fernando P, et al. Clozapine-induced DRESS syndrome: a case series from the AMSP multicenter drug safety surveillance project. *Pharmacopsychiatry.* (2019) 52:156–9. doi: 10.1055/a-0586-8983
88. Yin J, Albert RH, Tretiakova AP, Jameson BA. 5-HT1B receptors play a prominent role in the proliferation of T-lymphocytes. *J Neuroimmunol.* (2006) 181:68–81. doi: 10.1016/j.jneuroim.2006.08.004
89. Zareie P, Connor B, La Flamme AC. Amelioration of experimental autoimmune encephalomyelitis by clozapine is not associated with defective CD4 T cell responses. *J Neuroinflammation.* (2017) 14:1–10. doi: 10.1186/s12974-017-0842-5
90. Chen ML, Wu S, Tsai TC, Wang LK, Tsai FM. Regulation of macrophage immune responses by antipsychotic drugs. *Immunopharmacol Immunotoxicol.* (2013) 35:573–80. doi: 10.3109/08923973.2013.828744
91. O'Sullivan D, Green L, Stone S, Zareie P, Kharkrang M, Fong D, et al. Treatment with the antipsychotic agent, risperidone, reduces disease severity in experimental autoimmune encephalomyelitis. *PLoS ONE.* (2014) 9: e104430. doi: 10.1371/journal.pone.0104430
92. Nikolić T, Petronijević M, Sopta J, Velimirović M, Stojković T, Jevtić DoŽudić G, et al. Haloperidol affects bones while clozapine alters metabolic parameters - sex specific effects in rats perinatally treated with phencyclidine. *BMC Pharmacol Toxicol.* (2017) 18:65. doi: 10.1186/s40360-017-0171-4
93. Szuster-Ciesielska A, Słotwinska M, Stachura A, Marmurowska-Michałowska H, Kandefer-Szerszen M. Neuroleptics modulate cytokine and reactive oxygen species production in blood leukocytes of healthy volunteers. *Arch Immunol Ther Exp.* (2004) 52:59–67.
94. Haack MJ, Bak MLFJ, Beurskens R, Maes M, Stolk LML, Delespaul PAEG. Toxic rise of clozapine plasma concentrations in relation to inflammation. *Eur Neuropsychopharmacol.* (2003) 13:381–5. doi: 10.1016/S0924-977X(03)00042-7
95. Hefner G, Shams MEE, Unterecker S, Falter T, Hiemke C. Inflammation and psychotropic drugs: the relationship between C-reactive protein and antipsychotic drug levels. *Psychopharmacology.* (2016) 233:1695–705. doi: 10.1007/s00213-015-3976-0
96. Hung YP, Wang CSM, Yen CN, Chang HC, Chen PS, Lee IH, et al. Role of cytokine changes in clozapine-induced fever: a cohort prospective study. *Psychiatry Clin Neurosci.* (2017) 71:395–402. doi: 10.1111/pcn.12508
97. Miller BJ, Buckley P, Seabolt W, Mellor A, Kirkpatrick B. Meta-analysis of cytokine alterations in schizophrenia: clinical status and antipsychotic effects. *Biol Psychiatry.* (2011) 70:663–71. doi: 10.1016/j.biopsych.2011.04.013
98. Ayano G. Second generation antipsychotics: pharmacodynamics, therapeutic effects indications and associated metabolic side effects: review of articles. *J Schizophr Res.* (2016) 3:1027.
99. Chopko TC, Lindsley CW. Classics in chemical neuroscience: risperidone. *ACS Chem Neurosci.* (2018) 9:1520–9. doi: 10.1021/acschemneuro.8b00159
100. Roth J. The colorful spectrum of tourette syndrome and its medical, surgical and behavioral therapies. *Park Relat Disord.* (2018) 46:S75–9. doi: 10.1016/j.parkreldis.2017.08.004
101. Spielmans GI, Berman MI, Linardatos E, Rosenlicht NZ, Perry A, Tsai AC. Adjunctive atypical antipsychotic treatment for major depressive disorder: a meta-analysis of depression, quality of life, and safety outcomes. *PLoS Med.* (2013) 10:e1001403. doi: 10.1371/journal.pmed.1001403
102. Couturier J, Isserlin L, Spettigue W, Norris M. Psychotropic medication for children and adolescents with eating disorders. *Child Adolesc Psychiatr Clin N Am.* (2019) 28:583–92. doi: 10.1016/j.chc.2019.05.005
103. Kassm SA, Naja W, Hoertel N, Limosin F. Prise en charge pharmacologique des idées délirantes associées à un syndrome démentiel. *Gériatrie Psychol Neuropsychiatr du Vieil.* (2019) 17:317–26. doi: 10.1684/PNV.2019.0813
104. Belli H, Ural C, Akbudak M. Borderline personality disorder: bipolarity, mood stabilizers and atypical antipsychotics in treatment. *J Clin Med Res.* (2012) 4:301–8. doi: 10.4021/jocmr1042w
105. Yuan M, Sperry L, Malhado-Chang N, Duffy A, Wheelock V, Farias S, et al. Atypical antipsychotic therapy in Parkinson's disease psychosis: a retrospective study. *Brain Behav.* (2017) 7:1–6. doi: 10.1002/brb3.639
106. Courtois C, Sonis J, Brown L, Seattle W, Cook J, Fairbank J, et al. Summary of the clinical practice guideline for the treatment of posttraumatic stress disorder (PTSD) in adults. *Am Psychol.* (2019) 74:596–607. doi: 10.1037/amp0000473
107. McNeil SE, Cogburn M. *Risperidone*. Treasure Island, FL: StatPearls Publishing (2019).
108. Madaan V, Bestha DP, Kolli V, Jauhari S, Burket RC. Clinical utility of the risperidone formulations in the management of schizophrenia. *Neuropsychiatr Dis Treat.* (2011) 7:611–20. doi: 10.2147/NDT.S14385
109. Kusumi I, Boku S, Takahashi Y. Psychopharmacology of atypical antipsychotic drugs: from the receptor binding profile to neuroprotection and neurogenesis. *Psychiatry Clin Neurosci.* (2015) 69:243–58. doi: 10.1111/pcn.12242
110. Grahovac T, RuŽić K, Medved P, Pavešić-Radonja A, Dadić-Hero E. Hyperprolactinaemia - a risperidone side-effect. *Psychiatr Danub.* (2010) 22:120–22.
111. Park YM, Lee SH, Lee BH, Lee KY, Lee KS, Kang SG, et al. Prolactin and macroprolactin levels in psychiatric patients receiving atypical antipsychotics: a preliminary study. *Psychiatry Res.* (2016) 239:184–9. doi: 10.1016/j.psychres.2016.03.015
112. Lally J, Ajnakina O, Stubbs B, Williams HR, Colizzi M, Carra E, et al. Hyperprolactinaemia in first episode psychosis - A longitudinal assessment. *Schizophr Res.* (2017) 189:117–25. doi: 10.1016/j.schres.2017.07.037
113. Bonete Llácer JM, Martínez Hortelano A, Richart Albelda B. Hyperprolactinemia in psychotic patients treated in monotherapy with long-acting injectable antipsychotics. *Int J Psychiatry Clin Pract.* (2019) 23:189–93. doi: 10.1080/13651501.2019.1576905
114. Cešková E, Prikryl R, Kašpárek T, Ondrušová M. Prolactin levels in risperidone treatment of first-episode schizophrenia. *Int J Psychiatry Clin Pract.* (2004) 8:31–6. doi: 10.1080/1365150031004786

115. Pérez-Iglesias R, Mata I, Martínez-García O, Garcia-Unzueta MT, Amado JA, Valdizán EM, et al. Long-term effect of haloperidol, olanzapine, and risperidone on plasma prolactin levels in patients with first-episode psychosis. *J Clin Psychopharmacol.* (2012) 32:804–8. doi: 10.1097/JCP.0b013e318272688b
116. Charan A, Shewade DG, Rajkumar RP, Chandrasekaran A. Relation between serum prolactin levels and antipsychotic response to risperidone in patients with schizophrenia. *Psychiatry Res.* (2016) 240:209–13. doi: 10.1016/j.psychres.2016.04.001
117. Liu J, Sun J, Shen X, Guo W, Zhi S, Song G, et al. Randomized controlled trial comparing changes in serum prolactin and weight among female patients with first-episode schizophrenia over 12 months of treatment with risperidone or quetiapine. *Shanghai Arch Psychiatry.* (2014) 26:88–94. doi: 10.3969/j.issn.1002-0829.2014.02
118. Suzuki Y, Fukui N, Watanabe J, Ono S, Sugai T, Tsuneyama N, et al. Gender differences in the relationship between the risperidone metabolism and the plasma prolactin levels in psychiatric patients. *Prog Neuro-Psychopharmacol Biol Psychiatry.* (2010) 34:1266–8. doi: 10.1016/j.pnpbp.2010.07.003
119. Kinon BJ, Liu-Seifert H, Stauffer VL, Jacob J. Bone loss associated with hyperprolactinemia in patients with schizophrenia: are there gender differences? *Clin Schizophr Relat Psychoses.* (2013) 7:115–23. doi: 10.3371/CSRP.KISE.020113
120. An F-R, Yang R, Wang Z-M, Ungvari GS, Ng CH, Chiu HFK, et al. Hyperprolactinemia, prolactin-related side effects and quality of life in Chinese psychiatric patients. *Compr Psychiatry.* (2016) 71:71–6. doi: 10.1016/j.comppsych.2016.08.009
121. Takechi K, Yoshioka Y, Kawazoe H, Tanaka M, Takatori S, Kobayashi M, et al. Psychiatric patients with antipsychotic drug-induced hyperprolactinemia and menstruation disorders. *Biol Pharm Bull.* (2017) 40:1775–8. doi: 10.1248/bpb.b17-00053
122. Holla SN, Vittalrao AMB, Kamath A, Kamalkishore MK, Ommurugan B. Risperidone induced granulomatous mastitis secondary to hyperprolactinemia in a non-pregnant woman-a rare case report in a bipolar disorder. *J Clin Diagnostic Res.* (2017) 11:FD01–3. doi: 10.7860/JCDR/2017/20733.9278
123. Shagufta S, Farooq F, Khan AM, Dar K, Mohit A. Risperidone-induced amenorrhea in floridly psychotic female. *Cureus.* (2017) 9:e1683. doi: 10.7759/cureus.1683
124. Sakaguchi S, Aizawa K. Galactorrhea induced by risperidone. *Intern Med.* (2020) 58:3609–10. doi: 10.2169/internalmedicine.3224-19
125. Kawabe K, Ueno SI. A case of acute pancreatitis associated with risperidone treatment. *Clin Psychopharmacol Neurosci.* (2014) 12:67–8. doi: 10.9758/cpn.2014.12.1.67
126. Rad F, Buica AM, Anghel GC, Stancu M, Dobrescu I. Hormonal imbalance and pituitary adenoma during antipsychotic treatment in an adolescent with bipolar affective disorder. *Riv Psichiatr.* (2019) 54:37–9. doi: 10.1708/3104.30939
127. Hongkaew Y, Ngamsamut N, Puangpetch A, Vanwong N, Srisawasdi P, Chamnanphon M, et al. Hyperprolactinemia in thai children and adolescents with autism spectrum disorder treated with risperidone. *Neuropsychiatr Dis Treat.* (2015) 11:191–6. doi: 10.2147/NDT.S76276
128. Roke Y, Buitelaar JK, Boot AM, Tenback D, Van Harten PN. Risk of hyperprolactinemia and sexual side effects in males 10-20 years old diagnosed with autism spectrum disorders or disruptive behavior disorder and treated with risperidone. *J Child Adolesc Psychopharmacol.* (2012) 22:432–9. doi: 10.1089/cap.2011.0109
129. Margari L, Matera E, Petruzzelli MG, Simone M, Lamanna AL, Pastore A, et al. Prolactin variations during risperidone therapy in a sample of drug-naive children and adolescents. *Int Clin Psychopharmacol.* (2015) 30:103–8. doi: 10.1097/YIC.0000000000000063
130. Balijepalli C, Druyts E, Zoratti MJ, Wu P, Kanji S, Rabheru K, et al. Change in prolactin levels in pediatric patients given antipsychotics for schizophrenia and schizophrenia spectrum disorders: a network meta-analysis. *Schizophr Res Treat.* (2018) 2018:543034. doi: 10.1155/2018/1543034
131. Dos Santos Júnior A, Henriques TB, De Mello MP, Neto APF, Paes LA, Torre OH Della, et al. Hyperprolactinemia in children and adolescents with use of risperidone: clinical and molecular genetics aspects. *J Child Adolesc Psychopharmacol.* (2015) 25:738–48. doi: 10.1089/cap.2015.0094
132. Osmanova DZ, Freidin MB, Fedorenko OY, Pozhidaev IV, Boiko AS, Vyalova NM, et al. A pharmacogenetic study of patients with schizophrenia from West Siberia gets insight into dopaminergic mechanisms of antipsychotic-induced hyperprolactinemia. *BMC Med Genet.* (2019) 20(Suppl. 1):47. doi: 10.1186/s12881-019-0773-3
133. Sun WW, Li LY, Huang XF, Shi YC, Yang HQ, Song ZY, et al. The central mechanism of risperidone-induced hyperprolactinemia. *Prog Neuro-Psychopharmacology Biol Psychiatry.* (2017) 76:134–9. doi: 10.1016/j.pnpbp.2017.03.009
134. Jiang XJ, Wu FX, Zhang JP, Shi L, Hu JQ, Zhu HZ, et al. Effects of risperidone and aripiprazole on serum levels of prolactin, testosterone and estradiol in female patients with schizophrenia. *Drug Res.* (2018) 68:410–14. doi: 10.1055/s-0044-102093
135. Piriu G, Torac E, Gaman LE, Iosif L, Tivig IC, Delia C, et al. Clozapine and risperidone influence on cortisol and estradiol levels in male patients with schizophrenia. *J Med Life.* (2015) 8:548–51.
136. Konarzewska B, Galinska-Skok B, Waszkiewicz N, Łazarczyk-Kirejczyk J, Małus A, Simonienko K, et al. Association between serum testosterone levels, body mass index (BMI) and insulin in male patients with schizophrenia treated with atypical antipsychotics - Olanzapine or risperidone. *Neuroendocrinol Lett.* (2014) 35:50–7.
137. Bishop JR, Rubin LH, Reilly JL, Pavuluri MN, Sweeney JA. Risperidone-associated prolactin elevation and markers of bone turnover during acute treatment. *Ther Adv Psychopharmacol.* (2012) 2:95–102. doi: 10.1177/2045125312442080
138. Yanik T, Kursungoz C, Sutcigil L, Ak M. Weight Gain in risperidone therapy: investigation of peripheral hypothalamic neurohormone levels in psychotic patients. *J Clin Psychopharmacol.* (2013) 33:608–13. doi: 10.1097/JCP.0b013e318297980e
139. Tsai MC, Chang CM, Liu CY, Chang PY, Huang TL. Association of serum levels of leptin, ghrelin, and adiponectin in schizophrenic patients and healthy controls. *Int J Psychiatry Clin Pract.* (2011) 15:106–11. doi: 10.3109/13651501.2010.550400
140. Doknic M, Maric NP, Britvic D, Pekic S, Damjanovic A, Miljic D, et al. Bone remodeling, bone mass and weight gain in patients with stabilized schizophrenia in real-life conditions treated with long-acting injectable risperidone. *Neuroendocrinology.* (2011) 94:246–54. doi: 10.1159/000329391
141. Srisawasdi P, Vanwong N, Hongkaew Y, Puangpetch A, Vanavanan S, Intachak B, et al. Impact of risperidone on leptin and insulin in children and adolescents with autistic spectrum disorders. *Clin Biochem.* (2017) 50:678–85. doi: 10.1016/j.clinbiochem.2017.02.003
142. Baeza I, Vigo L, de la Serna E, Calvo-Escalona R, Merchán-Naranjo J, Rodríguez-Latorre P, et al. The effects of antipsychotics on weight gain, weight-related hormones and homocysteine in children and adolescents: a 1-year follow-up study. *Eur Child Adolesc Psychiatry.* (2017) 26:35–46. doi: 10.1007/s00787-016-0866-x
143. Smith RC, Rachakonda S, Dwivedi S, Davis JM. Olanzapine and risperidone effects on appetite and ghrelin in chronic schizophrenic patients. *Psychiatry Res.* (2012) 199:159–63. doi: 10.1016/J.PSYCHRES.2012.03.011
144. Endomba FT, Tankeu AT, Nkeck JR, Tochie JN. Leptin and psychiatric illnesses: does leptin play a role in antipsychotic-induced weight gain? *Lipids Health Dis.* (2020) 19:22. doi: 10.1186/s12944-020-01203-z
145. Sugai T, Suzuki Y, Fukui N, Ono S, Watanabe J, Tsuneyama N, et al. Dysregulation of adipocytokines related to second-generation antipsychotics in normal fasting glucose patients with schizophrenia. *J Clin Psychopharmacol.* (2012) 32:390–93. doi: 10.1097/JCP.0b013e3182524393
146. Scahill L, Jeon S, Boorin SJ, McDougle CJ, Aman MG, Dziura J, et al. Weight gain and metabolic consequences of risperidone in young children with autism spectrum disorder. *J Am Acad Child Adolesc Psychiatry.* (2016) 55:415–23. doi: 10.1016/j.jaac.2016.02.016
147. Bartoli F, Lax A, Crocamo C, Clerici M, Carrà G. Plasma adiponectin levels in schizophrenia and role of second-generation antipsychotics: a meta-analysis. *Psychoneuroendocrinology.* (2015) 56:179–89. doi: 10.1016/j.psyneuen.2015.03.012
148. Bartoli F, Crocamo C, Clerici M, Carrà G. Second-generation antipsychotics and adiponectin levels in schizophrenia: a comparative

meta-analysis. *Eur Neuropsychopharmacol.* (2015) 25:1767–74. doi: 10.1016/j.euroneuro.2015.06.011
149. Sackett G, Unis A, Crouthamel B. Some effects of risperidone and quetiapine on growth parameters and hormone levels in young pigtail macaques. *J Child Adolesc Psychopharmacol.* (2010) 20:489–93. doi: 10.1089/cap.2010.0018
150. Kursungoz C, Ak M, Yanik T. Effects of risperidone treatment on the expression of hypothalamic neuropeptide in appetite regulation in Wistar rats. *Brain Res.* (2015) 1596:146–55. doi: 10.1016/j.brainres.2014.10.070
151. Horska K, Ruda-Kucerova J, Karpisek M, Suchy P, Opatrilova R, Kotolova H. Depot risperidone-induced adverse metabolic alterations in female rats. *J Psychopharmacol.* (2017) 31:487–99. doi: 10.1177/0269881117691466
152. Savoy YE, Ashton MA, Miller MW, Nedza FM, Spracklin DK, Hawthorn MH, et al. Differential effects of various typical and atypical antipsychotics on plasma glucose and insulin levels in the mouse: evidence for the involvement of sympathetic regulation. *Schizophr Bull.* (2010) 36:410–8. doi: 10.1093/schbul/sbn104
153. Manfredi G, Solfanelli A, Dimitri G, Cuomo I, Sani G, Kotzalidis GD, et al. Risperidone-induced leukopenia: a case report and brief review of literature. *Gen Hosp Psychiatry.* (2013) 35:102.e3–102.e6. doi: 10.1016/j.genhosppsych.2012.03.009
154. Noto C, Ota VK, Gouvea ES, Rizzo LB, Spindola LMN, Honda PHS, et al. Effects of risperidone on cytokine profile in drug-naïve first-episode psychosis. *Int J Neuropsychopharmacol.* (2014) 18:1–8. doi: 10.1093/ijnp/pyu042
155. Elmorsy E, Al-Ghafari A, Aggour AM, Mosad SM, Khan R, Amer S. Effect of antipsychotics on mitochondrial bioenergetics of rat ovarian theca cells. *Toxicol Lett.* (2017) 272:94–100. doi: 10.1016/j.toxlet.2017.03.018
156. Tseng CC. Neutropenia during risperidone treatment. *J Neuropsychiatry Clin Neurosci.* (2011) 23:E19. doi: 10.1176/jnp.23.4.jnpe19
157. Morrison M, Schultz A, Sanchez DL, Catalano MC, Catalano G. Leukopenia associated with risperidone treatment. *Curr Drug Saf.* (2017) 12:126–30. doi: 10.2174/1574886312666170531072837
158. Sy-Cherng Woon L, Tee CK, Gan LLY, Deang KT, Chan LF. Olanzapine-induced and risperidone-induced leukopenia: a case of synergistic adverse reaction? *J Psychiatr Pract.* (2018) 24:121–4. doi: 10.1097/PRA.0000000000000292
159. Raj V, Druitt T, Purushothaman S, Dunsdon J. Risperidone/paliperidone induced neutropenia and lymphopenia. *Aust N Z J Psychiatry.* (2013) 47:291–2. doi: 10.1177/0004867412460594
160. Kailasam VK, Chima V, Nnamdi U, Sharma K, Shah K. Risperidone-induced reversible neutropenia. *Neuropsychiatr Dis Treat.* (2017) 13:1975–77. doi: 10.2147/NDT.S141472
161. Bhattacharjee D, Yerrapragada D, Chogtu B, Thomson SR. Risperidone induced isolated thrombocytopenia: a rare adverse event. *Psychopharmacol Bull.* (2018) 48:47–9.
162. Rizos E, Tsigkaropoulou E, Lambrou P, Kanakaki M, Chaniotou A, Alevyzakis E, et al. Risperidone-induced acute eosinophilic pneumonia. *In Vivo.* (2013) 27:651–4.
163. Rettenbacher MA, Hofer A, Kemmler G, Fleischhacker WW. Neutropenia induced by second generation antipsychotics: a prospective investigation. *Pharmacopsychiatry.* (2010) 43:41–4. doi: 10.1055/s-0030-1249071
164. Diaz FJ, Pérez-Iglesias R, Mata I, Martínez-Garcia O, Vázquez-Barquero JL, de Leon J, et al. Possible effects of some antipsychotic drugs on C-reactive protein in a drug-naïve psychotic sample. *Schizophr Res.* (2010) 121:207–12. doi: 10.1016/j.schres.2010.06.002
165. Lin CC, Chang CM, Liu CY, Huang TL. Increased high-sensitivity C-reactive protein levels in Taiwanese schizophrenic patients. *Asia-Pacific Psychiatry.* (2013) 5:E58–63. doi: 10.1111/appy.12078
166. Hefner G, Falter T, Bruns K, Hiemke C. Elevated risperidone serum concentrations during acute inflammation, two cases. *Int J Psychiatry Med.* (2015) 50:335–44. doi: 10.1177/0091217415610313
167. Ajami A, Hosseini SH, Taghipour M, Khalilian A. Changes in serum levels of brain derived neurotrophic factor and nerve growth factor-beta in schizophrenic patients before and after treatment. *Scand J Immunol.* (2014) 80:36–42. doi: 10.1111/sji.12158
168. Kudlek Mikulic S, Mihaljevic-Peles A, Sagud M, Bajs Janovic M, Ganoci L, Grubisin J, et al. Brain-derived neurotrophic factor serum and plasma levels in the treatment of acute schizophrenia with olanzapine or risperidone: 6-week prospective study. *Nord J Psychiatry.* (2017) 71:513–20. doi: 10.1080/08039488.2017.1340518
169. Yoshimura R, Ueda N, Hori H, Ikenouchi-Sugita A, Umene-Nakano W, Nakamura J. Different patterns of longitudinal changes in plasma levels of catecholamine metabolites and brain-derived neurotrophic factor after administration of atypical antipsychotics in first episode untreated schizophrenic patients. *World J Biol Psychiatry.* (2010) 11:256–61. doi: 10.3109/15622970802309617
170. Scherf-Clavel M, Weidner A, Deckert J, Menke A, Unterecker S. Pathological concentration of c-reactive protein is correlated to increased concentrations of quetiapine, but not of risperidone, olanzapine and aripiprazole in a naturalistic setting. *Pharmacopsychiatry.* (2019) 53:30–5. doi: 10.1055/a-0869-8053
171. Rizos EN, Papadopoulou A, Laskos E, Michalopoulou PG, Kastania A, Vasilopoulos D, et al. Reduced serum BDNF levels in patients with chronic schizophrenic disorder in relapse, who were treated with typical or atypical antipsychotics. *World J Biol Psychiatry.* (2010) 11:251–5. doi: 10.3109/15622970802182733
172. Bosshart H. Supra-therapeutic plasma concentrations of haloperidol induce moderate inhibition of lipopolysaccharide-induced interleukin-8 release in human monocytes. *Ann Transl Med.* (2016) 4:396. doi: 10.21037/atm.2016.10.56
173. McNamara RK, Jandacek R, Rider T, Tso P. Chronic risperidone normalizes elevated pro-inflammatory cytokine and C-reactive protein production in omega-3 fatty acid deficient rats. *Eur J Pharmacol.* (2011) 652:152–6. doi: 10.1016/j.ejphar.2010.11.010
174. Juncal-Ruiz M, Riesco-Dávila L, Ortiz-García de la Foz V, Martínez-Garcia O, Ramírez-Bonilla M, Ocejo-Viñals JG, et al. Comparison of the anti-inflammatory effect of aripiprazole and risperidone in 75 drug-naïve first episode psychosis individuals: a 3 months randomized study. *Schizophr Res.* (2018) 202:226–33. doi: 10.1016/j.schres.2018.06.039
175. Ajami A, Abedian F, Hamzeh Hosseini S, Akbarian E, Alizadeh-Navaei R, Taghipour M. Serum TNF-α, IL-10 and IL-2 in schizophrenic patients before and after treatment with risperidone and clozapine. *Iran J Immunol.* (2014) 11:200–09.
176. De Witte L, Tomasik J, Schwarz E, Guest PC, Rahmoune H, Kahn RS, et al. Cytokine alterations in first-episode schizophrenia patients before and after antipsychotic treatment. *Schizophr Res.* (2014) 154:23–9. doi: 10.1016/j.schres.2014.02.005
177. Lo LH, Shiea J, Huang TL. Rapid detection of alteration of serum IgG in patients with schizophrenia after risperidone treatment by matrix-assisted laser desorption ionization/time-of-flight mass spectrometry. *Rapid Commun Mass Spectrom.* (2016) 30:2645–9. doi: 10.1002/rcm.7753
178. Song X, Fan X, Li X, Zhang W, Gao J, Zhao J, et al. Changes in pro-inflammatory cytokines and body weight during 6-month risperidone treatment in drug naïve, first-episode schizophrenia. *Psychopharmacology.* (2014) 231:319–25. doi: 10.1007/s00213-013-3382-4
179. Choi JE, Widjaja F, Careaga M, Bent S, Ashwood P, Hendren RL. Change in plasma cytokine levels during risperidone treatment in children with autism. *J Child Adolesc Psychopharmacol.* (2014) 24:586–9. doi: 10.1089/cap.2013.0108
180. Chen ML, Wu S, Tsai TC, Wang LK, Tsai FM. Regulation of neutrophil phagocytosis of *Escherichia coli* by antipsychotic drugs. *Int Immunopharmacol.* (2014) 23:550–7. doi: 10.1016/j.intimp.2014.09.030
181. Al-Amin MM, Uddin MMN, Reza HM. Effects of antipsychotics on the inflammatory response system of patients with schizophrenia in peripheral blood mononuclear cell cultures. *Clin Psychopharmacol Neurosci.* (2013) 11:144–51. doi: 10.9758/cpn.2013.11.3.144
182. Krause D, Weidinger E, Dippel C, Riedel M, Schwarz MJ, Müller N, et al. Impact of different antipsychotics on cytokines and tryptophan metabolites in stimulated cultures from patients with schizophrenia. *Psychiatr Danub.* (2013) 25:389–97.
183. Noto MN, Maes M, Nunes SOV, Ota VK, Rossaneis AC, Verri WA, et al. Activation of the immune-inflammatory response system and the compensatory immune-regulatory system in antipsychotic naive first episode psychosis. *Eur Neuropsychopharmacol.* (2019) 29:416–31. doi: 10.1016/j.euroneuro.2018.12.008

184. Ding M, Song X, Zhao J, Gao J, Li X, Yang G, et al. Activation of Th17 cells in drug naïve, first episode schizophrenia. *Prog Neuro-Psychopharmacology Biol Psychiatry*. (2014) 51:78–82. doi: 10.1016/j.pnpbp.2014.01.001
185. Sárvári AK, Veréb Z, Uray IP, Fésüs L, Balajthy Z. Atypical antipsychotics induce both proinflammatory and adipogenic gene expression in human adipocytes *in vitro*. *Biochem Biophys Res Commun.* (2014) 450:1383–9. doi: 10.1016/j.bbrc.2014.07.005
186. Kéri S, Szabó C, Kelemen O. Antipsychotics influence Toll-like receptor (TLR) expression and its relationship with cognitive functions in schizophrenia. *Brain Behav Immun.* (2017) 62:256–64. doi: 10.1016/j.bbi.2016.12.011
187. Mantere O, Trontti K, García-González J, Balcells I, Saarnio S, Mäntylä T, et al. Immunomodulatory effects of antipsychotic treatment on gene expression in first-episode psychosis. *J Psychiatr Res.* (2019) 109:18–26. doi: 10.1016/j.jpsychires.2018.11.008
188. Aboul-Fotouh S, Elgayar N. Atypical antipsychotics such as risperidone, but not paliperidone, worsen vascular endothelial function via upregulation of adhesion molecules VCAM-1, ICAM-1, and E-selectin in diabetic rats. *Can J Physiol Pharmacol.* (2013) 91:1119–26. doi: 10.1139/cjpp-2013-0185
189. Da Cruz Jung IE, Machado AK, Da Cruz IBM, Barbisan F, Azzolin VF, Duarte T, et al. Haloperidol and risperidone at high concentrations activate an *in vitro* inflammatory response of RAW 264.7 macrophage cells by induction of apoptosis and modification of cytokine levels. *Psychopharmacology.* (2016) 233:1715–23. doi: 10.1007/s00213-015-4079-7
190. Bymaster FP, Calligaro DO, Falcone JF, Marsh RD, Moore NA, Tye NC, et al. Radioreceptor binding profile of the atypical antipsychotic olanzapine. *Neuropsychopharmacology.* (1996) 14:87–96. doi: 10.1016/0893-133X(94)00129-N
191. Eisenberg Center at Oregon Health & Science University EC at OH& S. *Off -Label Use of Atypical Antipsychotic Drugs: A Summary for Clinicians and Policymakers*. Agency for Healthcare Research and Quality (US) (2007). Available online at: http://www.ncbi.nlm.nih.gov/pubmed/21938813 (accessed February 20, 2020)
192. Thomas K, Saadabadi A. *Olanzapine.* (2019). Available at: https://www.ncbi.nlm.nih.gov/books/NBK532903/ (accessed February 24, 2020)
193. Evison M, Holme J, Alaloul M, Doran H, Bishop P, Booton R, et al. Olanzapine-induced eosinophilic pleuritis. *Respir Med Case Rep.* (2015) 14:24–6. doi: 10.1016/J.RMCR.2014.11.007
194. Huang J, Yu Y, Lin W, Zhang D, Deng Z, Ding Q. Olanzapine-induced peripheral eosinophilia and eosinophilic pleural effusion: a case report. *Medicine.* (2018) 97:e9996. doi: 10.1097/MD.0000000000009996
195. Ng W, Kennar R, Uetrecht J. Effect of clozapine and olanzapine on neutrophil kinetics: implications for drug-induced agranulocytosis. *Chem Res Toxicol.* (2014) 27:1104–08. doi: 10.1021/tx500183x
196. Raz A, Bergman R, Eilam O, Yungerman T, Hayek T. A case report of olanzapine-induced hypersensitivity syndrome. *Am J Med Sci.* (2001) 321:156–8. doi: 10.1097/00000441-200102000-00008
197. Thomas K, Saadabadi A. *Olanzapine*. Treasure Island, FL: StatPearls Publishing (2019).
198. Matei VP, Purnichi T, Mihailescu A, Grigoras R. Prolactin level in patients with first episode schizophrenia treated for one year with atypical antipsychotics. *Acta Endocrinol.* (2018) 14:483–90. doi: 10.4183/aeb.2018.483
199. Kishimoto T, Hagi K, Nitta M, Kane JM, Correll CU. Long-term effectiveness of oral second-generation antipsychotics in patients with schizophrenia and related disorders: a systematic review and meta-analysis of direct head-to-head comparisons. *World Psychiatry.* (2019) 18:208–24. doi: 10.1002/wps.20632
200. Yasui-Furukori N, Furukori H, Sugawara N, Tsuchimine S, Fujii A, Inoue Y, et al. Prolactin fluctuation over the course of a day during treatments with three atypical antipsychotics in schizophrenic patients. *Hum Psychopharmacol Clin Exp.* (2010) 25:236–42. doi: 10.1002/hup.1110
201. Barata PC, Santos MJ, Melo JC, Maia T. Olanzapine-induced hyperprolactinemia: two case reports. *Front Pharmacol.* (2019) 10:846. doi: 10.3389/fphar.2019.00846
202. Suzuki Y, Sugai T, Fukui N, Watanabe J, Ono S, Tsuneyama N, et al. Differences in plasma prolactin levels in patients with schizophrenia treated on monotherapy with five second-generation antipsychotics. *Schizophr Res.* (2013) 145:116–9. doi: 10.1016/J.SCHRES.2012.12.027
203. Wu XL, Wang JH, Hu SH, Tao J. Serum prolactin levels and the acute-phase efficacy in drug-naïve schizophrenia treated with ziprasidone and olanzapine (translated version). *East Asian Arch Psychiatry.* (2012) 22:7–11.
204. Feng S, Melkersson K. Metabolic parameters and long-term antipsychotic treatment: a comparison between patients treated with clozapine or olanzapine. *Neuro Endocrinol Lett.* (2012) 33:493–8.
205. Davey KJ, O'Mahony SM, Schellekens H, O'Sullivan O, Bienenstock J, Cotter PD, et al. Gender-dependent consequences of chronic olanzapine in the rat: effects on body weight, inflammatory, metabolic and microbiota parameters. *Psychopharmacology.* (2012) 221:155–69. doi: 10.1007/s00213-011-2555-2
206. Sacher J, Mossaheb N, Spindelegger C, Klein N, Geiss-Granadia T, Sauermann R, et al. Effects of olanzapine and ziprasidone on glucose tolerance in healthy volunteers. *Neuropsychopharmacology.* (2008) 33:1633–41. doi: 10.1038/sj.npp.1301541
207. Huang M, Yu L, Pan F, Lu S, Hu S, Hu J, et al. A randomized, 13-week study assessing the efficacy and metabolic effects of paliperidone palmitate injection and olanzapine in first-episode schizophrenia patients. *Prog Neuro-Psychopharmacology Biol Psychiatry.* (2018) 81:122–30. doi: 10.1016/j.pnpbp.2017.10.021
208. Li H, Peng S, Li S, Liu S, Lv Y, Yang N, et al. Chronic olanzapine administration causes metabolic syndrome through inflammatory cytokines in rodent models of insulin resistance. *Sci Rep.* (2019) 9:1582. doi: 10.1038/s41598-018-36930-y
209. Raposo NRB, Ferreira AS, Gattaz WF. Body mass index increase, serum leptin, adiponectin, neuropeptide y and lipid levels during treatment with olanzapine and haloperidol. *Pharmacopsychiatry.* (2011) 44:169–72. doi: 10.1055/s-0031-1280793
210. Lin Y, Peng Y, He S, Xu J, Shi Y, Su Y, et al. Serum IL-1ra, a novel biomarker predicting olanzapine-induced hypercholesterolemia and hyperleptinemia in schizophrenia. *Prog Neuro-Psychopharmacology Biol Psychiatry.* (2018) 84:71–8. doi: 10.1016/J.PNPBP.2018.01.020
211. Tsuneyama N, Suzuki Y, Sawamura K, Sugai T, Fukui N, Watanabe J, et al. Effect of serum leptin on weight gain induced by olanzapine in female patients with schizophrenia. *PLoS ONE.* (2016) 11:e0149518. doi: 10.1371/journal.pone.0149518
212. Panariello F, Polsinelli G, Borlido C, Monda M, De Luca V. The role of leptin in antipsychotic-induced weight gain: genetic and non-genetic factors. *J Obes.* (2012) 2012:572848. doi: 10.1155/2012/572848
213. Basoglu C, Oner O, Ates AM, Algul A, Semiz UB, Ebrinc S, et al. Association between symptom improvement and change of body mass index, lipid profile, and leptin, ghrelin, and cholecystokinin levels during 6-week olanzapine treatment in patients with first-episode psychosis. *J Clin Psychopharmacol.* (2010) 30:636–8. doi: 10.1097/JCP.0b013e3181f0580e
214. Chen VC-H, Wang T-N, Lu M-L, Chou J-Y, Ju P-C, Wu J-Y, et al. Weight gain and ghrelin level after olanzapine monotherapy. *Prog Neuro-Psychopharmacology Biol Psychiatry.* (2011) 35:632–5. doi: 10.1016/j.pnpbp.2011.01.010
215. Goetz RL, Miller BJ. Meta-analysis of ghrelin alterations in schizophrenia: effects of olanzapine. *Schizophr Res.* (2019) 206:21–6. doi: 10.1016/J.SCHRES.2018.11.036
216. Zabotina T, Nasyrova RF, Sosin DN, Sosina, Ershov, Grunina N, Krupitsky. The effect of antipsychotic drug on monoamine receptors in peripheral blood mononuclear cells: Affinity linked mechanism. *Biomeditsinskaya Khimiya.* (2018) 64:201–07. doi: 10.18097/PBMC20186402201
217. Stapel B, Sieve I, Falk CS, Bleich S, Hilfiker-Kleiner D, Kahl KG. Second generation atypical antipsychotics olanzapine and aripiprazole reduce expression and secretion of inflammatory cytokines in human immune cells. *J Psychiatr Res.* (2018) 105:95–102. doi: 10.1016/j.jpsychires.2018.08.017
218. Zhang C, Fang X, Yao P, Mao Y, Cai J, Zhang Y, et al. Metabolic adverse effects of olanzapine on cognitive dysfunction: a possible relationship between BDNF and TNF-alpha. *Psychoneuroendocrinology.* (2017) 81:138–43. doi: 10.1016/J.PSYNEUEN.2017.04.014
219. Hatziagelaki E, Tsiavou A, Gerasimou C, Vavougios G, Spathis A, Laskos E, et al. Effects of olanzapine on cytokine profile and brain-derived neurotrophic factor in drug-naive subjects with first-episode psychosis. *Exp Ther Med.* (2019) 17:3071–6. doi: 10.3892/etm.2019.7285

220. DeVane CL, Nemeroff CB. Clinical pharmacokinetics of quetiapine. *Clin Pharmacokinet.* (2001) 40:509–22. doi: 10.2165/00003088-200140070-00003
221. Riedel M, Müller N, Strassnig M, Spellmann I, Severus E, Möller H-J. Quetiapine in the treatment of schizophrenia and related disorders. *Neuropsychiatr Dis Treat.* (2007) 3:219–35. doi: 10.2147/nedt.2007.3.2.219
222. Kim D-W, Weon K-Y, Hong E-P, Chung EK, Lee K-T. Comparative physicochemical and pharmacokinetic properties of quetiapine and its active metabolite norquetiapine. *Chem Pharm Bull.* (2016) 64:1546–54. doi: 10.1248/cpb.c16-00223
223. López-Muñoz F, Álamo C. Active metabolites as antidepressant drugs: the role of norquetiapine in the mechanism of action of quetiapine in the treatment of mood disorders. *Front Psychiatry.* (2013) 4:102. doi: 10.3389/fpsyt.2013.00102
224. Carboni L, Negri M, Michielin F, Bertani S, Fratte SD, Oliosi B, et al. Slow dissociation of partial agonists from the D_2 receptor is linked to reduced prolactin release. *Int J Neuropsychopharmacol.* (2012) 15:645–56. doi: 10.1017/S1461145711000824
225. Nunes LVA, Moreira HC, Razzouk D, Nunes SOV, Mari JDJ. Strategies for the treatment of antipsychotic-induced sexual dysfunction and/or hyperprolactinemia among patients of the schizophrenia spectrum: a review. *J Sex Marital Ther.* (2012) 38:281–301. doi: 10.1080/0092623X.2011.606883
226. Bushe C, Sniadecki J, Bradley AJ, Poole Hoffmann V. Comparison of metabolic and prolactin variables from a six-month randomised trial of olanzapine and quetiapine in schizophrenia. *J Psychopharmacol.* (2010) 24:1001–9. doi: 10.1177/0269881108101783
227. Oriot P, Feys J-L, Mertens de Wilmars S, Misson A, Ayache L, Fagnart O, et al. Insulin sensitivity, adjusted beta-cell function and adiponectinaemia among lean drug-naive schizophrenic patients treated with atypical antipsychotic drugs: a nine-month prospective study. *Diabetes Metab.* (2008) 34:490–6. doi: 10.1016/j.diabet.2008.03.003
228. Ngai YF, Sabatini P, Nguyen D, Davidson J, Chanoine J-P, Devlin AM, et al. Quetiapine treatment in youth is associated with decreased insulin secretion. *J Clin Psychopharmacol.* (2014) 34:359–64. doi: 10.1097/JCP.0000000000000118
229. Melkersson K, Jansson E. The atypical antipsychotics quetiapine, risperidone and ziprasidone do not increase insulin release *in vitro*. *Neuro Endocrinol Lett.* (2005) 26:205–8.
230. McNamara RK, Jandacek R, Rider T, Tso P, Cole-Strauss A, Lipton JW. Atypical antipsychotic medications increase postprandial triglyceride and glucose levels in male rats: relationship with stearoyl-CoA desaturase activity. *Schizophr Res.* (2011) 129:66–73. doi: 10.1016/j.schres.2011.03.016
231. Ran H, Zhu Y, Deng R, Zhang Q, Liu X, Feng M, et al. Stearoyl-CoA desaturase-1 promotes colorectal cancer metastasis in response to glucose by suppressing PTEN. *J Exp Clin Cancer Res.* (2018) 37:54. doi: 10.1186/s13046-018-0711-9
232. Smith GC, Chaussade C, Vickers M, Jensen J, Shepherd PR. Atypical antipsychotic drugs induce derangements in glucose homeostasis by acutely increasing glucagon secretion and hepatic glucose output in the rat. *Diabetologia.* (2008) 51:2309–17. doi: 10.1007/s00125-008-1152-3
233. De Borja Gonçalves Guerra A, Castel S, Benedito-Silva AA, Calil HM. Neuroendocrine effects of quetiapine in healthy volunteers. *Int J Neuropsychopharmacol.* (2005) 8:49–57. doi: 10.1017/S1461145704004705
234. Cohrs S, Röher C, Jordan W, Meier A, Huether G, Wuttke W, et al. The atypical antipsychotics olanzapine and quetiapine, but not haloperidol, reduce ACTH and cortisol secretion in healthy subjects. *Psychopharmacology.* (2006) 185:11–8. doi: 10.1007/s00213-005-0279-x
235. Kontaxakis VP, Karaiskos D, Havaki-Kontaxaki BJ, Ferentinos P, Papadimitriou GN. Can quetiapine-induced hypothyroidism be reversible without quetiapine discontinuation? *Clin Neuropharmacol.* (2009) 32:295–6. doi: 10.1097/WNF.0b013e3181a8cbcc
236. Crépeau-Gendron G, L'Heureux S. Quetiapine XR-induced neutropenia: is a clozapine trial still possible for treatment-resistant schizophrenia? A case report. *Early Interv Psychiatry.* (2015) 9:151–5. doi: 10.1111/eip.12134
237. Croarkin P, Rayner T. Acute neutropenia in a patient treated with quetiapine. *Psychosomatics.* (2001) 42:368. doi: 10.1176/appi.psy.42.4.368
238. Cowan C, Oakley C. Leukopenia and neutropenia induced by quetiapine. *Prog Neuropsychopharmacol Biol Psychiatry.* (2007) 31:292–4. doi: 10.1016/j.pnpbp.2006.07.003
239. Almaghrebi AH. Safety of a clozapine trial following quetiapine-induced leukopenia: a case report. *Curr Drug Saf.* (2019) 14:80–3. doi: 10.2174/1574886313666180807094654
240. Shankar BR. Quetiapine-induced leucopenia and thrombocytopenia. *Psychosomatics.* (2007) 48:530–31. doi: 10.1176/appi.psy.48.6.530
241. Arslan FC, Aykut DS, Ince C, Tiryaki A. Klinik Psikofarmakoloji Bülteni-bulletin of clinical psychopharmacology neutropenia and thrombocytopenia induced by quetiapine monotherapy: a case report and review of literature. *Bull Clin Psychopharmacol.* (2016) 26:319–23. doi: 10.5455/bcp.20151219072235
242. Tourjman V, Kouassi É, Koué M-È, Rocchetti M, Fortin-Fournier S, Fusar-Poli P, et al. Antipsychotics' effects on blood levels of cytokines in schizophrenia: a meta-analysis. *Schizophr Res.* (2013) 151:43–7. doi: 10.1016/j.schres.2013.10.011
243. Himmerich H, Schönherr J, Fulda S, Sheldrick AJ, Bauer K, Sack U. Impact of antipsychotics on cytokine production in-vitro. *J Psychiatr Res.* (2011) 45:1358–65. doi: 10.1016/j.jpsychires.2011.04.009
244. Zhu S, Shi R, Li V, Wang J, Zhang R, Tempier A, et al. Quetiapine attenuates glial activation and proinflammatory cytokines in APP/PS1 transgenic mice via inhibition of nuclear factor-κB pathway. *Int J Neuropsychopharmacol.* (2014) 18:pyu022. doi: 10.1093/ijnp/pyu022
245. Hillis J, O'Dwyer M, Gorman AM. Neurotrophins and B-cell malignancies. *Cell Mol Life Sci.* (2016) 73:41–56. doi: 10.1007/s00018-015-2046-4
246. Manti S, Brown P, Perez MK, Piedimonte G. The role of neurotrophins in inflammation and allergy. In: G. Litwack editor. *Vitamins and Hormones*. Cambridge MA: Elsevier. p. 313–41. doi: 10.1016/bs.vh.2016.10.010
247. Polyakova M, Stuke K, Schuemberg K, Mueller K, Schoenknecht P, Schroeter ML. BDNF as a biomarker for successful treatment of mood disorders: a systematic & quantitative meta-analysis. *J Affect Disord.* (2015) 174:432–40. doi: 10.1016/j.jad.2014.11.044
248. Fernandes BS, Gama CS, Maria Ceresér K, Yatham LN, Fries GR, Colpo G, et al. Brain-derived neurotrophic factor as a state-marker of mood episodes in bipolar disorders: a systematic review and meta-regression analysis. *J Psychiatr Res.* (2011) 45:995–1004. doi: 10.1016/j.jpsychires.2011.03.002
249. Murphy BP, Pang TY, Hannan AJ, Proffitt T-M, McConchie M, Kerr M, et al. Vascular endothelial growth factor and brain-derived neurotrophic factor in quetiapine treated first-episode psychosis. *Schizophr Res Treat.* (2014) 2014:1–10. doi: 10.1155/2014/719395
250. Kul D, Gumustas M, Uslu B, Ozkan SA. Electroanalytical characteristics of antipsychotic drug ziprasidone and its determination in pharmaceuticals and serum samples on solid electrodes. *Talanta.* (2010) 82:286–95. doi: 10.1016/j.talanta.2010.04.036
251. Gitlin M, Frye MA. Maintenance therapies in bipolar disorders. *Bipolar Disord.* (2012) 14(Suppl. 2):51–65. doi: 10.1111/j.1399-5618.2012.00992.x
252. Sacchetti E, Galluzzo A, Valsecchi P. Oral ziprasidone in the treatment of patients with bipolar disorders: a critical review. *Expert Rev Clin Pharmacol.* (2011) 4:163–79. doi: 10.1586/ecp.10.139
253. Warrington L, Lombardo I, Loebel A, Ice K. Ziprasidone for the treatment of acute manic or mixed episodes associated with bipolar disorder. *CNS Drugs.* (2007) 21:835–49. doi: 10.2165/00023210-200721100-00004
254. Schmidt AW, Lebel LA, Howard HR, Zorn SH. Ziprasidone: a novel antipsychotic agent with a unique human receptor binding profile. *Eur J Pharmacol.* (2001) 425:197–201. doi: 10.1016/s0014-2999(01)01188-8
255. Beedham C, Miceli JJ, Obach RS. Ziprasidone metabolism, aldehyde oxidase, and clinical implications. *J Clin Psychopharmacol.* (2003) 23:229–32. doi: 10.1097/01.jcp.0000084028.22282.f2
256. Ben Amor L. Antipsychotics in pediatric and adolescent patients: a review of comparative safety data. *J Affect Disord.* (2012) 138:S22–30. doi: 10.1016/j.jad.2012.02.030
257. Raza S, Haq F. Ziprasidone-induced galactorrhea in an adolescent female: a case report. *Prim Care Companion J Clin Psychiatry.* (2010) 12:PCC.09l00855. doi: 10.4088/PCC.09l00855gry
258. Kopecek M, Bares M, Mohr P. Ziprasidone-induced galactorrhea: a case report. *Neuro Endocrinol Lett.* (2005) 26:69–70. doi: 10.4088/PCC.09l00855gry
259. Meier A, Neumann AC, Jordan W, Huether G, Rodenbeck A, Rüther E, et al. Ziprasidone decreases cortisol excretion in healthy subjects.

Br J Clin Pharmacol. (2005) 60:330–6. doi: 10.1111/j.1365-2125.2005.02431.x

260. Montgomery J. Ziprasidone-related agranulocytosis following olanzapine-induced neutropenia. *Gen Hosp Psychiatry.* (2006) 28:83–5. doi: 10.1016/j.genhosppsych.2005.08.005
261. Kefelioglu H, Atli Sekeroglu Z, Coşguner G, Kontaş Yedier S, Sekeroglu V. Ziprasidone induces cytotoxicity and genotoxicity in human peripheral lymphocytes. *Drug Chem Toxicol.* (2017) 40:425–31. doi: 10.1080/01480545.2016.1252920
262. Duarte T, Barbisan F, do Prado-Lima PAS, Azzolin VF, da Cruz Jung IE, Duarte MMMF, et al. Ziprasidone, a second-generation antipsychotic drug, triggers a macrophage inflammatory response *in vitro*. *Cytokine.* (2018) 106:101–7. doi: 10.1016/j.cyto.2017.10.017
263. Hamera L, Khishfe BF. Kounis syndrome and ziprasidone. *Am J Emerg Med.* (2017) 35:493–4. doi: 10.1016/j.ajem.2016.11.061
264. Ku HL, Su TP, Chou YH. Ziprasidone-associated pedal edema in the treatment of schizophrenia. *Prog Neuro-Psychopharmacology Biol Psychiatry.* (2006) 30:963–4. doi: 10.1016/j.pnpbp.2006.01.020
265. Akkaya C, Sarandol A, Aydogan K, Kirli S. Urticaria and angio-oedema due to ziprasidone. *J Psychopharmacol.* (2007) 21:550–2. doi: 10.1177/0269881106075273
266. Swainston Harrison T, Perry CM. Aripiprazole. *Drugs.* (2004) 64:1715–36. doi: 10.2165/00003495-200464150-00010
267. Li DJ, Tseng PT, Stubbs B, Chu CS, Chang HY, Vieta E, et al. Efficacy, safety and tolerability of aripiprazole in bipolar disorder: an updated systematic review and meta-analysis of randomized controlled trials. *Prog Neuro-Psychopharmacology Biol Psychiatry.* (2017) 79:289–301. doi: 10.1016/j.pnpbp.2017.06.023
268. Jing Y, Guo Z, Kalsekar I, Forbes RA, Hebden T, Thase ME. Dosing patterns of aripiprazole and quetiapine for adjunctive treatment of major depressive disorder (2006–2010). *Int Clin Psychopharmacol.* (2013) 28:87–90. doi: 10.1097/YIC.0b013e32835ce232
269. Blankenship K, Erickson CA, Stigler KA, Posey DJ, McDougle CJ. Aripiprazole for irritability associated with autistic disorder in children and adolescents aged 6–17 years. *Ped Health.* (2010) 4:375–81. doi: 10.2217/phe.10.45
270. Stip E, Tourjman V. Aripiprazole in schizophrenia and schizoaffective disorder: a review. *Clin Ther.* (2010) 32(Suppl. 1):S3–20. doi: 10.1016/j.clinthera.2010.01.021
271. Hirsch LE, Pringsheim T. Aripiprazole for autism spectrum disorders (ASD). *Cochrane Database Syst Rev.* (2016) 26:CD009043. doi: 10.1002/14651858.CD009043.pub3
272. Brunetti M, Di Tizio L, Dezi S, Pozzi G, Grandinetti P, Martinotti G. Aripiprazole, alcohol and substance abuse: a review. *Eur Rev Med Pharmacol Sci.* (2012) 16:1346–54.
273. Marcus RN, McQuade RD, Carson WH, Hennicken D, Fava M, Simon JS, et al. The efficacy and safety of aripiprazole as adjunctive therapy in major depressive disorder: a second multicenter, randomized, double-blind, placebo-controlled study. *J Clin Psychopharmacol.* (2008) 28:156–65. doi: 10.1097/JCP.0b013e31816774f9
274. McGavin JK, Goa KL. Aripiprazole. *CNS Drugs.* (2002) 16:779–86. doi: 10.2165/00023210-200216110-00008
275. Belmonte C, Ochoa D, Román M, Saiz-Rodríguez M, Wojnicz A, Gómez-Sánchez CI, et al. Influence of CYP2D6, CYP3A4, CYP3A5 and ABCB1 Polymorphisms on pharmacokinetics and safety of aripiprazole in healthy volunteers. *Basic Clin Pharmacol Toxicol.* (2018) 122:596–605. doi: 10.1111/bcpt.12960
276. Perez Rodriguez A, Tajima-Pozo K, Lewczuk A, Montañes-Rada F. Atypical antipsychotics and metabolic syndrome. *Cardiovasc Endocrinol.* (2015) 17:460–6. doi: 10.1097/XCE.0000000000000063
277. Pramyothin P, Khaodhiar L. Metabolic syndrome with the atypical antipsychotics. *Curr Opin Endocrinol Diabetes Obes.* (2010) 17:460–6. doi: 10.1097/MED.0b013e32833de61c
278. Newcomer JW. Second-generation (atypical) antipsychotics and metabolic effects: a comprehensive literature review. *CNS Drugs.* (2005) 19(Suppl 1):1–93. doi: 10.2165/00023210-200519010-00001
279. Keck PE, Marcus R, Tourkodimitris S, Ali M, Liebeskind A, Saha A, et al. A placebo-controlled, double-blind study of the efficacy and safety of aripiprazole in patients with acute bipolar mania. *Am J Psychiatry.* (2003) 160:1651–8. doi: 10.1176/appi.ajp.160.9.1651
280. Casey DE, Carson WH, Saha AR, Liebeskind A, Ali MW, Jody D, et al. Aripiprazole Study Group. Switching patients to aripiprazole from other antipsychotic agents: a multicenter randomized study. *Psychopharmacology.* (2003) 166:391–9. doi: 10.1007/s00213-002-1344-3
281. Kane JM, Meltzer HY, Carson WH, McQuade RD, Marcus RN, Sanchez R. Aripiprazole for treatment-resistant schizophrenia: results of a multicenter, randomized, double-blind, comparison study versus perphenazine. *J Clin Psychiatry.* (2007) 68:213–23. doi: 10.4088/JCP.v68n0206
282. Fleischhacker WW, Baker RA, Eramo A, Sanchez R, Tsai LF, Peters-Strickland T, et al. Effects of aripiprazole once-monthly on domains of personal and social performance: results from 2 multicenter, randomized, double-blind studies. *Schizophr Res.* (2014) 59:415–20. doi: 10.1016/j.schres.2014.09.019
283. Zhao J, Song X, Ai X, Gu X, Huang G, Li X, et al. Adjunctive aripiprazole treatment for risperidone-induced hyperprolactinemia: an 8-week randomized, open-label, comparative clinical trial. *PLoS ONE.* (2015) 10:e0139717. doi: 10.1371/journal.pone.0139717
284. Chen CK, Huang YS, Ree SC, Hsiao CC. Differential add-on effects of aripiprazole in resolving hyperprolactinemia induced by risperidone in comparison to benzamide antipsychotics. *Prog Neuro-Psychopharmacology Biol Psychiatry.* (2010) 134:1495–9. doi: 10.1016/j.pnpbp.2010.08.012
285. Kelly DL, Powell MM, Wehring HJ, Sayer MA, Kearns AM, Hackman AL, et al. Adjunct aripiprazole reduces prolactin and prolactin-related adverse effects in premenopausal women with psychosis: results from the DAAMSEL clinical trial. *J Clin Psychopharmacol.* (2018) 38:317–26. doi: 10.1097/JCP.0000000000000898
286. Berardis D, Fornaro M, Serroni N, Marini S, Piersanti M, Cavuto M, et al. Treatment of antipsychotic-induced hyperprolactinemia: an update on the role of the dopaminergic receptors D2 partial agonist aripiprazole. *Recent Pat Endocr Metab Immune Drug Discov.* (2014) 8:30–7. doi: 10.2174/1872214807666131229125700
287. Fujioi J, Iwamoto K, Banno M, Kikuchi T, Aleksic B, Ozaki N. Effect of adjunctive aripiprazole on sexual dysfunction in schizophrenia: a preliminary open-label study. *Pharmacopsychiatry.* (2017) 50:74–8. doi: 10.1055/s-0042-116323
288. Joseph SP. Aripiprazole-induced hyperprolactinemia in a young female with delusional disorder. *Indian J Psychol Med.* (2016) 38:260–2. doi: 10.4103/0253-7176.183082
289. Saraf G, Behere RV, Venkatasubramanian G, Rao NP, Varambally S, Gangadhar BN. Hyperprolactinemia with aripiprazole: understanding the paradox. *Am J Ther.* (2014) 21:e80–1. doi: 10.1097/MJT.0b013e3182456de7
290. Luo T, sheng Liu Q, jian Yang Y, Wei B. Aripiprazole for the treatment of duloxetine-induced hyperprolactinemia: a case report. *J Affect Disord.* (2019) 250:330–2. doi: 10.1016/j.jad.2019.03.006
291. Stroup TS, McEvoy JP, Ring KD, Hamer RH, LaVange LM, Swartz MS, et al. A randomized trial examining the effectiveness of switching from olanzapine, quetiapine, or risperidone to aripiprazole to reduce metabolic risk: comparison of antipsychotics for metabolic problems (CAMP). *Am J Psychiatry.* (2011) 168:947–56. doi: 10.1176/appi.ajp.2011.10111609
292. Stroup TS, Byerly MJ, Nasrallah HA, Ray N, Khan AY, Lamberti JS, et al. Effects of switching from olanzapine, quetiapine, and risperidone to aripiprazole on 10-year coronary heart disease risk and metabolic syndrome status: results from a randomized controlled trial. *Schizophr Res.* (2013) 146:190–5. doi: 10.1016/j.schres.2013.01.013
293. Bak M, Fransen A, Janssen J, Van Os J, Drukker M. Almost all antipsychotics result in weight gain: a meta-analysis. *PLoS ONE.* (2014) 9:e94112. doi: 10.1371/journal.pone.0094112
294. Parabiaghi A, Tettamanti M, D'Avanzo B, Barbato A, GiSAS study group. Metabolic syndrome and drug discontinuation in schizophrenia: a randomized trial comparing aripiprazole olanzapine and haloperidol. *Acta Psychiatr Scand.* (2016) 133:63–75. doi: 10.1111/acps.12468
295. Kasteng F, Eriksson J, Sennfält K, Lindgren P. Metabolic effects and cost-effectiveness of aripiprazole versus olanzapine in schizophrenia and bipolar disorder. *Acta Psychiatr Scand.* (2011) 124:214–25. doi: 10.1111/j.1600-0447.2011.01716.x

296. Horska K, Ruda-Kucerova J, Drazanova E, Karpisek M, Demlova R, Kasparek T, et al. Aripiprazole-induced adverse metabolic alterations in polyI: C neurodevelopmental model of schizophrenia in rats. *Neuropharmacology.* (2017) 123:148–58. doi: 10.1016/j.neuropharm.2017.06.003
297. Felin T, Naveed S, Chaudhary AM. Aripiprazole-induced neutropenia: case report and literature review. *J Psychosoc Nurs Ment Health Serv.* (2018) 56:21–4. doi: 10.3928/02793695-20180419-02
298. Lim MH, Park J-I, Park TW. A case with neutropenia related with the use of various atypical antipsychotics. *Psychiatry Investig.* (2013) 10:428. doi: 10.4306/pi.2013.10.4.428
299. Upthegrove R, Manzanares-Teson N, Barnes NM. Cytokine function in medication-naive first episode psychosis: a systematic review and meta-analysis. *Schizophr Res.* (2014) 155:101–8. doi: 10.1016/j.schres.2014.03.005
300. Sobis J, Rykaczewska-Czerwinska M, wietochowska E, Gorczyca P. Therapeutic effect of aripiprazole in chronic schizophrenia is accompanied by anti-inflammatory activity. *Pharmacol Rep.* (2015) 67:353–9. doi: 10.1016/j.pharep.2014.09.007
301. Yoo S, Kim MY, Cho JY. Syk and Src-targeted anti-inflammatory activity of aripiprazole, an atypical antipsychotic. *Biochem Pharmacol.* (2018) 148:1–12. doi: 10.1016/j.bcp.2017.12.006
302. Kato T, Mizoguchi Y, Monji A, Horikawa H, Suzuki SO, Seki Y, et al. Inhibitory effects of aripiprazole on interferon-γ-induced microglial activation via intracellular Ca^{2+} regulation *in vitro*. *J Neurochem.* (2008) 106:815–25. doi: 10.1111/j.1471-4159.2008.05435.x
303. Zargar S, Al-Majed ARA, Wani TA. Potentiating and synergistic effect of grapefruit juice on the antioxidant and anti-inflammatory activity of aripiprazole against hydrogen peroxide induced oxidative stress in mice. *BMC Complement Altern Med.* (2018) 18:106. doi: 10.1186/s12906-018-2169-x
304. Baek KS, Ahn S, Lee J, Kim JH, Kim HG, Kim E, et al. Immunotoxicological effects of a ripiprazole: *in vivo* and *in vitro* studies. *Korean J Physiol Pharmacol.* (2015) 19:365–72. doi: 10.4196/kjpp.2015.19.4.365
305. Citrome L. Paliperidone: Quo vadis? *Int J Clin Pract.* (2007) 61:653–62. doi: 10.1111/j.1742-1241.2007.01321.x
306. Greenberg WM, Citrome L. Paliperidone palmitate for schizoaffective disorder: a review of the clinical evidence. *Neurol Ther.* (2015) 4:81–91. doi: 10.1007/s40120-015-0030-4
307. INVEGA SUSTENNA ® *Paliperidone Palmitate Product Information*. Available online at: https://www.janssen.com/australia/sites/www_janssen_com_australia/files/prod_files/live/invega_sustenna_pi.pdf (accessed October 2, 2019)
308. Nussbaum AM, Stroup TS. Paliperidone for treatment of schizophrenia. *Schizophr Bull.* (2008) 34:419–22. doi: 10.1093/schbul/sbn015
309. Marino J, English C, Caballero J, Harrington C. The role of paliperidone extended release for the treatment of bipolar disorder. *Neuropsychiatr Dis Treat.* (2012) 2012:181–9. doi: 10.2147/NDT.S20675
310. Palomares N, Montes A, Díaz-Marsá M, Carrasco JL. Effectiveness of long-acting paliperidone palmitate in borderline personality disorder. *Int Clin Psychopharmacol.* (2015) 30:338–41. doi: 10.1097/YIC.0000000000000095
311. van Oosterom N, Theodoros T. Paliperidone long-acting injections in huntington's disease for motor and behavioural disturbances. *Clin Drug Investig.* (2019) 39:407–10. doi: 10.1007/s40261-019-00759-8
312. Naguy A, Adel T, Almazeedi I. Paliperidone use in child psychiatry: evidence or diffidence? *Pharmacology.* (2019) 104:67–70. doi: 10.1159/000500629
313. Hu S, Yao M, Peterson BS, Xu D, Hu J, Tang J, et al. A randomized, 12-week study of the effects of extended-release paliperidone (paliperidone ER) and olanzapine on metabolic profile, weight, insulin resistance, and β-cell function in schizophrenic patients. *Psychopharmacology.* (2013) 230:3–13. doi: 10.1007/s00213-013-3073-1
314. Druyts E, Zoratti MJ, Toor K, Wu P, Kanji S, Rabheru K, et al. Prolactin-related adverse events and change in prolactin levels in pediatric patients given antipsychotics for schizophrenia and schizophrenia spectrum disorders: a systematic review. *BMC Pediatr.* (2016) 16:1–14. doi: 10.1186/s12887-016-0710-y
315. Skopek M, Manoj P. Hyperprolactinaemia during treatment with paliperidone. *Australas Psychiatry.* (2010) 18:261–3. doi: 10.3109/10398561003686763
316. Montalvo I, Ortega L, López X, Solé M, Monseny R, Franch J, et al. Changes in prolactin levels and sexual function in young psychotic patients after switching from long-acting injectable risperidone to paliperidone palmitate. *Int Clin Psychopharmacol.* (2013) 28:46–9. doi: 10.1097/YIC.0b013e32835ba832
317. Nakamura M, Nagamine T, Sato G, Besho K. Prolactin levels after switching to paliperidone palmitate in patients with schizophrenia. *Innov Clin Neurosci.* (2016) 13:28–30.
318. Potkin SG, Loze JY, Forray C, Baker RA, Sapin C, Peters-Strickland T, et al. Reduced sexual dysfunction with aripiprazole once-monthly versus paliperidone palmitate: results from QUALIFY. *Int Clin Psychopharmacol.* (2017) 32:147–54. doi: 10.1097/YIC.0000000000000168
319. Gopal S, Lane R, Nuamah I, Copenhaver M, Singh J, Hough D, et al. Evaluation of potentially prolactin-related adverse events and sexual maturation in adolescents with schizophrenia treated with paliperidone extended-release (ER) for 2 years: a post hoc analysis of an open-label multicenter study. *CNS Drugs.* (2017) 31:797–808. doi: 10.1007/s40263-017-0437-9
320. Ngamsamut N, Hongkaew Y, Vanwong N, Srisawasdi P, Puangpetch A, Chamkrachangpada B, et al. 9-Hydroxyrisperidone-induced hyperprolactinaemia in thai children and adolescents with autism spectrum disorder. *Basic Clin Pharmacol Toxicol.* (2016) 119:267–72. doi: 10.1111/bcpt.12570
321. Sliwa JK, Fu DJ, Bossie CA, Turkoz I, Alphs L. Body mass index and metabolic parameters in patients with schizophrenia during long-term treatment with paliperidone palmitate. *BMC Psychiatry.* (2014) 2014:1–11. doi: 10.1186/1471-244X-14-52
322. Omi T, Riku K, Fukumoto M, Kanai K, Omura Y, Takada H, et al. Paliperidone induced hypoglycemia by increasing insulin secretion. *Case Rep Psychiatry.* (2016) 2016:1–3. doi: 10.1155/2016/1805414
323. Kim JN, Lee BC, Choi IG, Jon DI, Jung MH. Paliperidone-induced leukopenia and neutropenia: a case report. *Prog Neuro-Psychopharmacology Biol Psychiatry.* (2011) 35:284–5. doi: 10.1016/j.pnpbp.2010.09.018
324. Wakuda T, Suzuki A, Hasegawa M, Ichikawa D, Yamasue H. Acute agranulocytosis when switching from risperidone to paliperidone. *Aust N Z J Psychiatry.* (2019) 53:586–7. doi: 10.1177/0004867418821441
325. Matsuura H, Kimoto S, Harada I, Naemura S, Yamamuro K, Kishimoto T. Lithium carbonate as a treatment for paliperidone extended-release-induced leukopenia and neutropenia in a patient with schizoaffective disorder; a case report. *BMC Psychiatry.* (2016) 16:1–3. doi: 10.1186/s12888-016-0874-x
326. Flanagan RJ, Dunk L. Haematological toxicity of drugs used in psychiatry. *Hum Psychopharmacol.* (2008) 23(Suppl 1):27–41. doi: 10.1002/hup.917
327. Wu RQ, Lin CG, Zhang W, Lin XD, Chen XS, Chen C, et al. Effects of risperidone and paliperidone on brain-derived neurotrophic factor and N400 in first-episode schizophrenia. *Chin Med J.* (2018) 131:2297–301. doi: 10.4103/0366-6999.241802
328. Chung YC, Cui Y, Sumiyoshi T, Kim MG, Lee KH. Associations of fatty acids with cognition, psychopathology, and brain-derived neurotrophic factor levels in patients with first-episode schizophrenia and related disorders treated with paliperidone extended release. *J Psychopharmacol.* (2017) 31:1556–63. doi: 10.1177/0269881117731169
329. Mas S, Gassó P, Parellada E, Bernardo M, Lafuente A. Network analysis of gene expression in peripheral blood identifies mTOR and NF-κB pathways involved in antipsychotic-induced extrapyramidal symptoms. *Pharmacogenomics J.* (2015) 15:452–60. doi: 10.1038/tpj.2014.84
330. Schmidt AJ, Krieg JC, Clement HW, Hemmeter UM, Schulz E, Vedder H, et al. Effects of quetiapine, risperidone, 9-hydroxyrisperidone and ziprasidone on the survival of human neuronal and immune cells *in vitro*. *J Psychopharmacol.* (2010) 24:349–54. doi: 10.1177/0269881108096506
331. Leucht S, Cipriani A, Spineli L, Mavridis D, Örey D, Richter F, et al. Comparative efficacy and tolerability of 15 antipsychotic drugs in schizophrenia: a multiple-treatments meta-analysis. *Lancet.* (2013) 382:951–62. doi: 10.1016/S0140-6736(13)60733-3
332. Vieta E, Montes JM. A review of asenapine in the treatment of bipolar disorder. *Clin Drug Investig.* (2018) 38:87–99. doi: 10.1007/s40261-017-0592-2
333. Anugu RR, Mainkar PS, Sridhar B, Chandrasekhar S. The Ireland-claisen rearrangement strategy towards the synthesis of the schizophrenia drug,

(+)-asenapine. *Org Biomol Chem.* (2016) 14:1332–7. doi: 10.1039/c5ob02047f
334. van de Wetering-Krebbers SFM, Jacobs PL, Kemperman GJ, Spaans E, Peeters PAM, Delbressine LPC, et al. Metabolism and excretion of asenapine in healthy male subjects. *Drug Metab Dispos.* (2011) 39:580–90. doi: 10.1124/dmd.110.036715
335. Hounsou C, Baehr C, Gasparik V, Alili D, Belhocine A, Rodriguez T, et al. From the promiscuous asenapine to potent fluorescent ligands acting at a series of aminergic G-protein-coupled receptors. *J Med Chem.* (2018) 61:174–88. doi: 10.1021/acs.jmedchem.7b01220
336. Delcourte S, Abrial E, Etiévant A, Rovera R, Arnt J, Didriksen M, et al. Asenapine modulates mood-related behaviors and 5-HT1A/7 receptors-mediated neurotransmission. *CNS Neurosci Ther.* (2017) 23:518–25. doi: 10.1111/cns.12698
337. Meltzer HY, Massey BW. The role of serotonin receptors in the action of atypical antipsychotic drugs. *Curr Opin Pharmacol.* (2011) 11:59–67. doi: 10.1016/j.coph.2011.02.007
338. Bobo WV. Asenapine, iloperidone and lurasidone: critical appraisal of the most recently approved pharmacotherapies for schizophrenia in adults. *Expert Rev Clin Pharmacol.* (2013) 6:61–91. doi: 10.1586/ecp.12.70
339. Samalin L, Charpeaud T, Llorca PM. Asenapine in bipolar I disorder: evidence and place in patient management. *Ther Adv Chronic Dis.* (2013) 4:5–14. doi: 10.1177/2040622312468933
340. Peuskens J, Pani L, Detraux J, De Hert M. The effects of novel and newly approved antipsychotics on serum prolactin levels: a comprehensive review. *CNS Drugs.* (2014) 28:421–53. doi: 10.1007/s40263-014-0157-3
341. Rahman T, Clevenger CV, Kaklamani V, Lauriello J, Campbell A, Malwitz K, et al. Antipsychotic treatment in breast cancer patients. *Am J Psychiatry.* (2014) 171:616–21. doi: 10.1176/appi.ajp.2013.13050650
342. Citrome L. Asenapine review, part II: clinical efficacy, safety and tolerability. *Expert Opin Drug Saf.* (2014) 13:803–30. doi: 10.1517/14740338.2014.908183
343. Citrome L. Role of sublingual asenapine in treatment of schizophrenia. *Neuropsychiatr Dis Treat.* (2011) 7:325–39. doi: 10.2147/NDT.S16077
344. Findling RL, Landbloom RL, Szegedi A, Koppenhaver J, Braat S, Zhu Q, et al. Asenapine for the acute treatment of pediatric manic or mixed episode of bipolar i disorder. *J Am Acad Child Adolesc Psychiatry.* (2015) 54:1032–41. doi: 10.1016/j.jaac.2015.09.007
345. Mommert S, Ratz L, Stark H, Gutzmer R, Werfel T. The histamine H4 receptor modulates the differentiation process of human monocyte-derived M1 macrophages and the release of CCL4/MIP-1β from fully differentiated M1 macrophages. *Inflamm Res.* (2018) 67:503–13. doi: 10.1007/s00011-018-1140-0
346. Anstead MI, Hunt TA, Carlson SL, Burki NK. Variability of peripheral blood lymphocyte beta-2-adrenergic receptor density in humans. *Am J Respir Crit Care Med.* (1998) 157:990–2. doi: 10.1164/ajrccm.157.3.9704071
347. Makdisi J, Amin B, Friedman A. Pityriasis rosea-like drug reaction to asenapine. *J Drugs Dermatol.* (2013) 12:1050–51.
348. Klemettilä JP, Kampman O, Seppälä N, Viikki M, Hämäläinen M, Moilanen E, et al. Resistin as an inflammatorymarker in patients with schizophrenia treated with clozapine. *Nord J Psychiatry.* (2017) 71:89–95. doi: 10.1080/08039488.2016.1230649
349. Skonieczna-Zydecka K, Łoniewski I, Misera A, Stachowska E, Maciejewska D, Marlicz W, et al. Second-generation antipsychotics and metabolism alterations: a systematic review of the role of the gut microbiome. *Psychopharmacology.* (2019) 236:1491–512. doi: 10.1007/s00213-018-5102-6
350. Kao AC-C, Spitzer S, Anthony DC, Lennox B, Burnet PWJ. Prebiotic attenuation of olanzapine-induced weight gain in rats: analysis of central and peripheral biomarkers and gut microbiota. *Transl Psychiatry.* (2018) 8:66. doi: 10.1038/s41398-018-0116-8
351. Yuan X, Zhang P, Wang Y, Liu Y, Li X, Kumar BU, et al. Changes in metabolism and microbiota after 24-week risperidone treatment in drug naïve, normal weight patients with first episode schizophrenia. *Schizophr Res.* (2018) 201:299–306. doi: 10.1016/j.schres.2018.05.017
352. Bahra SM, Weidemann BJ, Castro AN, Walsh JW, deLeon O, Burnett CML, et al. Risperidone-induced weight gain is mediated through shifts in the gut microbiome and suppression of energy expenditure. *EBioMedicine.* (2015) 2:1725–34. doi: 10.1016/j.ebiom.2015.10.018
353. Bahr SM, Tyler BC, Wooldridge N, Butcher BD, Burns TL, Teesch LM, et al. Use of the second-generation antipsychotic, risperidone, and secondary weight gain are associated with an altered gut microbiota in children. *Transl Psychiatry.* (2015) 5:e652. doi: 10.1038/tp.2015.135
354. Davey KJ, Cotter PD, O'Sullivan O, Crispie F, Dinan TG, Cryan JF, et al. Antipsychotics and the gut microbiome: olanzapine-induced metabolic dysfunction is attenuated by antibiotic administration in the rat. *Transl Psychiatry.* (2013) 3:e309. doi: 10.1038/tp.2013.83
355. Cussotto S, Strain CR, Fouhy F, Strain RG, Peterson VL, Clarke G, et al. Differential effects of psychotropic drugs on microbiome composition and gastrointestinal function. *Psychopharmacology.* (2019) 236:1671–85. doi: 10.1007/s00213-018-5006-5
356. van de Steeg E, Schuren FHJ, Obach RS, van Woudenbergh C, Walker GS, et al. An ex vivo fermentation screening platform to study drug metabolism by human gut microbiota. *Drug Metab Dispos.* (2018) 46:1596–607. doi: 10.1124/dmd.118.081026

Conflict of Interest: The authors declare that the research was conducted in the absence of any commercial or financial relationships that could be construed as a potential conflict of interest.

frontiers in Endocrinology

ORIGINAL RESEARCH
published: 17 June 2020
doi: 10.3389/fendo.2020.00388

Intranasal Flunisolide Suppresses Pathological Alterations Caused by Silica Particles in the Lungs of Mice

Tatiana Paula Teixeira Ferreira[1†], *Januário Gomes Mourão e Lima*[1†], *Francisco Alves Farias-Filho*[1], *Yago Amigo Pinho Jannini de Sá*[1], *Ana Carolina Santos de Arantes*[1], *Fernanda Verdini Guimarães*[1], *Vinicius de Frias Carvalho*[1], *Cory Hogaboam*[2], *John Wallace*[3], *Marco Aurélio Martins*[1] and *Patrícia Machado Rodrigues e Silva*[1*]

[1] Laboratory of Inflammation, Oswaldo Cruz Institute, Oswaldo Cruz Foundation, Rio de Janeiro, Brazil, [2] Department of Medicine, Cedars-Sinai Medical Center, Women's Guild Lung Institute, Los Angeles, CA, United States, [3] Departments of Physiology and Pharmacology, and Medicine, Cumming School of Medicine, University of Calgary, Calgary, AB, Canada

OPEN ACCESS

Edited by:
Rachida Guennoun,
Institut National de la Santé et de la Recherche Médicale (INSERM), France

Reviewed by:
Nils Lambrecht,
VA Long Beach Healthcare System, United States
Ben Nephew,
Worcester Polytechnic Institute, United States

***Correspondence:**
Patrícia Machado Rodrigues e Silva
patsilva1910@gmail.com

[†]These authors have contributed equally to this work

Specialty section:
This article was submitted to Neuroendocrine Science, a section of the journal Frontiers in Endocrinology

Received: 03 December 2019
Accepted: 15 May 2020
Published: 17 June 2020

Citation:
Ferreira TPT, Lima JGM, Farias-Filho FA, Jannini de Sá YAP, de Arantes ACS, Guimarães FV, Carvalho VF, Hogaboam C, Wallace J, Martins MA and Silva PMR (2020) Intranasal Flunisolide Suppresses Pathological Alterations Caused by Silica Particles in the Lungs of Mice. Front. Endocrinol. 11:388. doi: 10.3389/fendo.2020.00388

Silicosis is an occupational disease triggered by the inhalation of fine particles of crystalline silica and characterized by inflammation and scarring in the form of nodular lesions in the lungs. In spite of the therapeutic arsenal currently available, there is no specific treatment for the disease. Flunisolide is a potent corticosteroid shown to be effective for controlling chronic lung inflammatory diseases. In this study, the effect of flunisolide on silica-induced lung pathological changes in mice was investigated. Swiss-Webster mice were injected intranasally with silica particles and further treated with flunisolide from day 21 to 27 post-silica challenge. Lung function was assessed by whole body invasive plethysmography. Granuloma formation was evaluated morphometrically, collagen deposition by Picrus sirius staining and quantitated by Sircol. Chemokines and cytokines were evaluated using enzyme-linked immunosorbent assay. The sensitivity of lung fibroblasts was also examined in *in vitro* assays. Silica challenge led to increased leukocyte numbers (mononuclear cells and neutrophils) as well as production of the chemokine KC/CXCL-1 and the cytokines TNF-α and TGF-β in the bronchoalveolar lavage. These alterations paralleled to progressive granuloma formation, collagen deposition and impairment of lung function. Therapeutic administration of intranasal flunisolide inhibited granuloma and fibrotic responses, noted 28 days after silica challenge. The upregulation of MIP-1α/CCL-3 and MIP-2/CXCL-2 and the cytokines TNF-α and TGF-β, as well as deposition of collagen and airway hyper-reactivity to methacholine were shown to be clearly sensitive to flunisolide, as compared to silica-challenge untreated mice. Additionally, flunisolide effectively suppressed the responses of proliferation and MCP-1/CCL-2 production from IL-13 stimulated lung fibroblasts from silica- or saline-challenged mice. In conclusion, we report that intranasal treatment with the corticosteroid flunisolide showed protective properties on pathological features triggered by silica particles in mice, suggesting that the compound may constitute a promising strategy for the treatment of silicosis.

Keywords: lung, fibrosis, silica particles, therapy, flunisolide

INTRODUCTION

Silicosis is a work-related and occupational disease caused by long-term exposure to inhaled dust containing crystalline silica particles which can progress to severe lung inflammation and fibrosis (1). There are three forms of silicosis (acute, accelerated, and chronic) dependent on the amount and time of silica particle exposure (2), which can be complicated by increased risk of infections (3) and/or chronic obstructive pulmonary disease (4). It became a greater public health problem worldwide after the Industrial Revolution, which increased dust levels and the number of workers exposed around the world (5). Among activities with elevated risk are those involving sandblasting, brickworks, civil construction, mining and many others (6).

Silicosis persists mainly in developing countries due to a lack of application of protective measures against environmental dust (5). Existing evidence shows that about 6 million workers are exposed to silica in Brazil, 11.5 million in India and 23 million are at risk of getting the disease in China, and more than 24 thousand deaths are reported annually (6–8). The incidence of silicosis is also on the rise in workers of the stonecutting industry in Australia (9) and sandblast fashion denim in Turkey (10). Since no effective treatment exists for silicosis currently, new therapies are badly needed in this field (1).

It is noteworthy that daily oral prednisolone therapy suppressed alveolitis in some patients with chronic silicosis, improving lung function and gas exchange, under conditions where responders and non-responders did not differ with regard to simple or complicated silicosis (11). However, systemic use of corticosteroids is often associated with significant adverse effects such as pituitary-adrenal suppression, cataract formation, hypertension and osteoporosis, among others (12). Flunisolide is a well-known intranasal corticosteroid molecule reported to be effective in inhibiting adverse remodeling in the peripheral airways of mild and moderate asthmatic patients by reducing expression the α-SMA (13). It also inhibited idiopathic pulmonary hemosiderosis, a rare disease characterized by bleeding into the pulmonary alveoli and progressive lung fibrosis (14).

Thus, considering the lack of an appropriate therapy for silicotic patients, in the present study we evaluated the effectiveness of intranasal administration of flunisolide on the chronic pulmonary inflammation caused by instillation of silica particles into mice.

Abbreviations: AHR, airway hyper-reactivity; α-SMA, α-smooth muscle actin; BAL, bronchoalveolar lavage; NF-κB, nuclear factor-κB; AP-1, activator protein-1; MCP-1, monocyte chemoatractive protein-1; MIP-1α, monocyte inducible protein-1 alpha; MIP-2, monocyte inducible protein-2; TNF-α, tumor necrosis factor-alpha; TGF-β, tumor growth factor-beta; F4/80, also known EGF-like module-containing mucin-like hormone receptor-like 1 (EMR1); HRP, horseradish peroxidase; Tris-HCl, tris (hydroxymethyl) aminomethane hydrochloride; DMEM, Dulbecco's Modified Eagle Medium; IL-13, interleukin-13; IL-13PE, Interleukin-13 conjugated to mutated *Pseudomonas aeruginosa* exotoxin.

MATERIALS AND METHODS

Animals

Male Swiss Webster mice (18–20 g) were obtained from the Oswaldo Cruz Foundation (Rio de Janeiro, Brazil) breeding unit and kept in the care facility of Oswaldo Cruz Institute. Animals were kept in ventilated cages (in groups of five) at 22–25°C and relative humidity (40–70%), on a 12 h light/dark cycle with food and water *ad libitum*. All the animal experiments were conducted in accordance with the guidelines of the Committee on Use of Laboratory Animals of the Oswaldo Cruz Foundation (license LW057/14).

Silicosis Induction and Treatment

Animals were anesthetized with isofluorane (5%) (Cristália, São Paulo) and then instilled, intranasally, with crystalline silica (10 mg/50 μL/mouse) (particle size 0.5–10 μm; Sigma Chemical Co, St. Louis, MO) diluted in sterile 0.9% NaCl (15). Sham-challenged mice were instilled with similar volume of 0.9% NaCl. Analyses were performed at 7, 14, and 28 days post-silica challenge. Flunisolide (0.3–10 μg/mouse) was dissolved in 0.9% NaCl and intranasally administered, daily, from days 21–27 and analyses were performed on day 28 (**Figure 1**). Silica-challenged mice received the same volume (20 μL) of the treatment vehicle.

Bronchoalveolar Lavage (BAL)

Animals were killed with sodium pentobarbital (500 mg/kg, i.p.), and the bronchoalveolar lavage (BAL) was performed as previously described (16). Total leukocytes were counted in a Neubauer chamber and differential cell counts performed in cytospin preparations stained with May-Grunwald-Giemsa dye. Analyses were made under light microscopy (BX50, Olympus).

Lung Histology

After bronchoalveolar lavage and lung perfusion, the left lung was removed and fixed in Milloning buffer solution (pH 7.4) with 4% paraformaldehyde, and sections of 4 μm were stained with hematoxylin & eosin (H&E) or Picrus sirius. Lung morphometric analysis was performed by an integrating eyepiece with a coherent system consisting of a grid with 100 points and 50 lines (known length) (17) coupled to a light microscope (Olympus BX50), connected to a video camera (Optronics Engineering, DEI-750). The camera output was processed and examined by

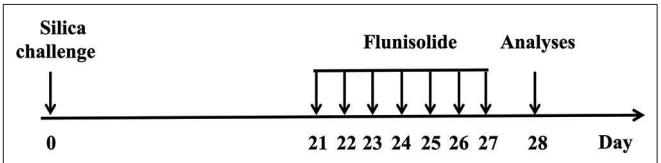

FIGURE 1 | Schematic study protocol for induction of silicosis and treatment in mice. Silica particles (10 mg/mice) were instilled intranasally, and animals were treated with intranasal flunisolide (0.3–10 μg/mouse) once a day from days 21 to 27 post-silica challenge. The analyses were performed on day 28.

image analyzer software Image-Pro Plus Version 4. Silica crystals were quantitatively analyzed, in 15 independent fields, with a light microscope (Olympus BX50) equipped with polarizing attachment for detecting birefringent particles and Image-Pro Plus Version 4. The results were expressed as number of pixels per μm^2 of tissue. To avoid experimental bias, the slides were evaluated in blind fashion.

Immunohistochemistry

Left lung tissue samples were evaluated for immunohistochemical localization of F4/80 and α-SMA (α-smooth muscle actin). The antibodies were obtained from the following sources: anti-mouse F4/80 (MCA497G) from AbD Serotec (Kidlington, UK) and anti-α-SMA (A2547) from Sigma-Aldrich (St. Louis, USA). Secondary antibodies conjugated with horseradish peroxidase (HRP) were all obtained from R&D Systems (Minneapolis, USA). To determine the specificity of staining, no primary antibody was used followed by incubation of section with secondary antibodies and detection reagents (18).

Quantification of Lung Collagen

Right lung was homogenized in Tris-HCl 0.05M, NaCl 1M containing protease inhibitor cocktail (Hoffmann-La Roche Ltd, Switzerland) (pH = 7.4). Total soluble collagen was extracted overnight at 4°C and quantification performed using the Sircol™ kit (Biocolor Ltd, Newton Abbey, UK). Results were expressed as mg of collagen per right lung.

ELISA Analysis

The concentration of murine KC/CXCL-1, MIP-2/CXCL-2, MIP-1α/CCL-3, MCP-1/CCL-2, TNF-α and TGF-β, was measured in the supernatant of BAL and/or in homogenates from right lung samples by means of ELISA as previously described (15). For lung tissue, samples were homogenized in PBS containing 0.05% Triton X-100 and protease inhibitor cocktail (Hoffmann-La Roche, Basel, Switzerland). Reagents from commercial DuoSet kits (R&D Systems, Minneapolis, MN, USA) were used in accordance with the instructions of the manufacturer.

Invasive Assessment of Respiratory Mechanics

Mice were anesthetized with nembutal (60 mg/kg) and the neuromuscular activity was blocked with bromide pancuronium (1 mg/kg). Tracheostomized animals were mechanically ventilated and the lung function assessed. Airway resistance ($cmH_2O.s/mL$) and lung elastance (mL/cmH_2O) were assessed using a FinePointe R/C Buxco Platform (DSI™, Minneapolis) (15). Animals were allowed to stabilize for 5 min and increasing concentrations of methacholine (3–81 mg/mL) were aerosolized for 5 min each. Baseline pulmonary parameters were assessed with aerosolized PBS.

Lung Fibroblast Isolation and Activation

The whole lung was removed from mice, 7 d after silica-challenge, perfused under aseptic conditions and gently dispersed on steel mesh followed by enzymatic digestion with collagenase 1A (1 mg/mL in 10 mL) (Sigma-Aldrich) for 1 h at 37 C. Lung fibroblasts from saline-challenged mice were used as control group. Dispersed cells were submitted to a continuous Percoll gradient (GE Healthcare) to eliminate silica particles and then placed in DMEM medium plus 10% of FBS, 1% penicillin-streptomycin at 37 C, and 5% CO2. Cells were stimulated with rmIL-13 (40 ng/mL), for 24 h. After centrifugation, 0.25×10^6 cells were added to 6-well plates, incubated with flunisolide (0.1–100 μM) at 37°C and a 5% CO_2, for 24 h. Proliferation was assessed via [^{3}H] thymidine incorporation (0.5 mCi/well). In another set of experiments, after centrifugation, the supernatant was recovered and quantified for chemokine MCP-1/CCL2 by ELISA.

Statistical Analysis

Results were expressed as mean ± standard error of mean (SEM) and statistical analysis was done with one-way ANOVA followed by the multiple comparison test of Newman-Keuls-Student. Values of $p < 0.05$ were considered statistically significant for both tests.

RESULTS

Time Course of the Airways Inflammation Caused by Exposure to Silica in Mice

Intranasal instillation of crystaline silica particle suspension in mice resulted in an increased number of leukocytes in the bronchoalveolar space at days 7, 14, and 28 post-challenge as compared to sham-challenged mice (**Figure 2A**). Although the maximal response was at day 7 post-silica, the absolute number of leukocytes remained significantly increased over the saline-challenged mice at days 14 and 28 (**Figure 2A**). Standard staining of cytospin preparations revealed a predominant mononuclear cell infiltration into the airways after silica challenge (**Figure 2B**), while a slight but significant elevation in polymorphonuclear neutrophil counts was noted from 7 to 28 days (**Figure 2C**). The profile of chemokines and cytokines was also investigated. As shown in **Figure 2D**, KC/CXCL-1 levels in the BAL effluent appeared significantly increased at all timepoints analyzed, in a clear association with the polymorphonuclear neutrophl influx (**Figure 2C**). In contrast, levels of the cytokines TNF-α and TGF-β appeared elevated at later timepoints, day 14 and 28 concerning the former (**Figure 2E**) and only at day 28 (**Figure 2F**) concerning the latter.

Time Course of Lung Pathological Changes Caused by Exposure to Silica in Mice

In order to evaluate the impact of silica particle instillation in the lungs, tissue sections were examined under light microscopy. Specimens obtained from sham-challenged mice at days 7, 14, and 28, stained with either H&E (**Figures 3A,E,I**, respectively) or Picrus sirius (**Figures 3C,G,K**, respectively), showed no pathological changes as expected. In contrast, H&E-staining revealed a clear thickening of alveolar walls as well as progressive increase in areas of parenchyma occupied by granuloma in silica-challenged mice at day 7 (**Figure 3B**), day 14 (**Figure 3F**) and

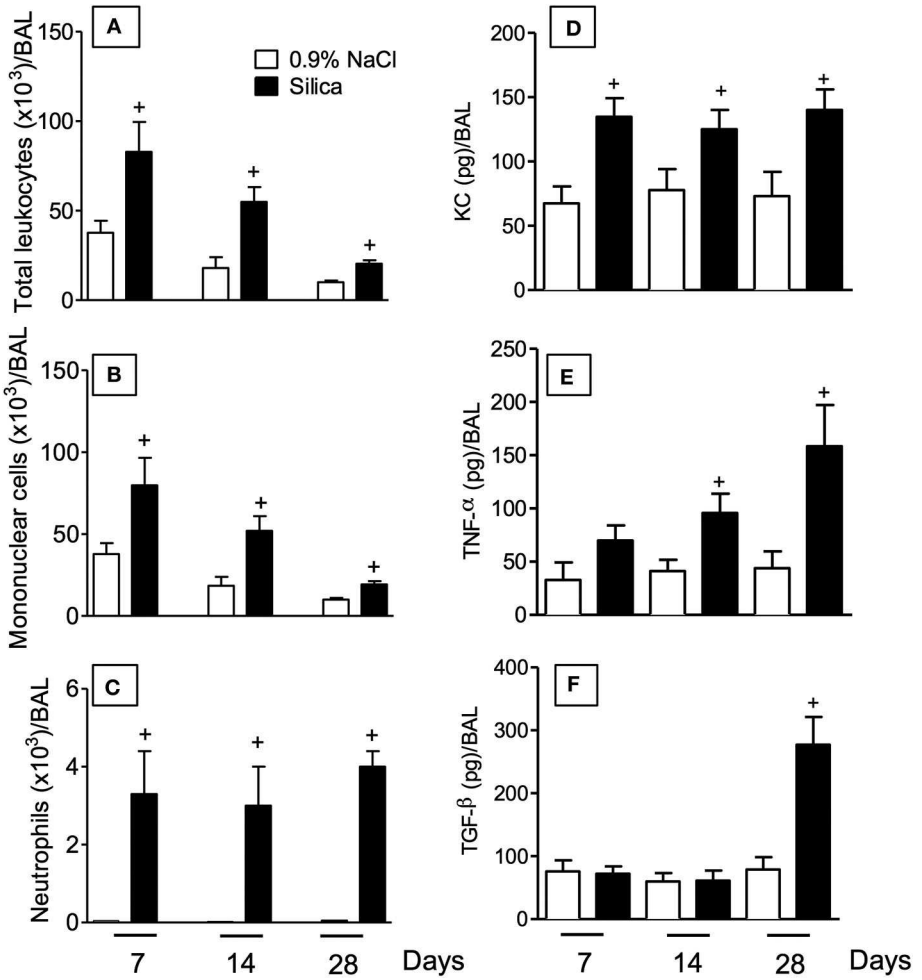

FIGURE 2 | Inflammatory changes in BAL effluent following silica particle instillation. BAL effluent samples were obtained from sham-challenged mice (open column) or silica-challenged mice (closed column) for quantification of total leukocytes **(A)**, mononuclear cells **(B)**, neutrophils **(C)**, KC/CXCL1 **(D)**, TNF-α **(E)**, and TGF-β **(F)** on days 7, 14, and 28. Values represent mean ± SEM from 5 animals per group. Statistical analysis was done with one-way ANOVA followed by Newman-Keuls-Student test. $^{+}P < 0.05$ as compared to saline-challenged animals.

day 28 (**Figure 3J**) post-challenge. Quantitative morphometric analyses confirmed the time-dependent formation of granulomas in the lungs of silica-challenged mice (**Figure 3M**). In parallel, Picrus sirius staining of lung sections from silicotic mice revealed a time-dependent increase in the amount of collagen deposition in the parenchyma at day 7 (**Figure 3D**), day 14 (**Figure 3H**), and day 28 (**Figure 3L**). These histological findings close-correlated with the levels of total collagen content in the lungs, quantified by the Sircol assay (**Figure 3N**). Silica challenge did not cause death of animals during the course of the experiments.

Treatment With Flunisolide Inhibits Lung Inflammation, Fibrosis, and Airway Hyper-Reactivity in Silicotic Mice

Interventional local treatment with flunisolide (10 μg/mouse), given daily from day 21 to 27, via nasal instillation, reduced both granulomatous response (**Figure 4C**) and collagen deposition (**Figure 4F**) caused by silica particles as compared to untreated silicotic mice, concerning granuloma formation (**Figure 4B**) and collagen deposition (**Figure 4E**), respectively. Flunisolide treatment reduced, but did not abolish, these changes as can be attested by the comparison with lung sections from negative controls (**Figures 4A,D**). Quantitative values are shown in **Figures 4G,H** for granulomatous and fibrotic response, respectively. There was no effect on silica-induced granulomatous and fibrotic response when flunisolide was given at the doses of 0.3 or 1 μg/mouse.

We then examined the effect of flunisolide (0.3, 1 and 10 μg/mouse) on pro-inflammatory and pro-fibrotic mediators generated in the lung tissue of silicotic mice. **Figure 4** shows that silica particle exposure upregulated the levels of MIP-1α/CCL-3 (**Figure 5A**) and MIP-2/CXCL-2 (**Figure 5B**), TNF-α (**Figure 5C**), and TGF-β (**Figure 5D**), all of which being partially inhibited by flunisolide (10 μg/mouse). As shown in this figure,

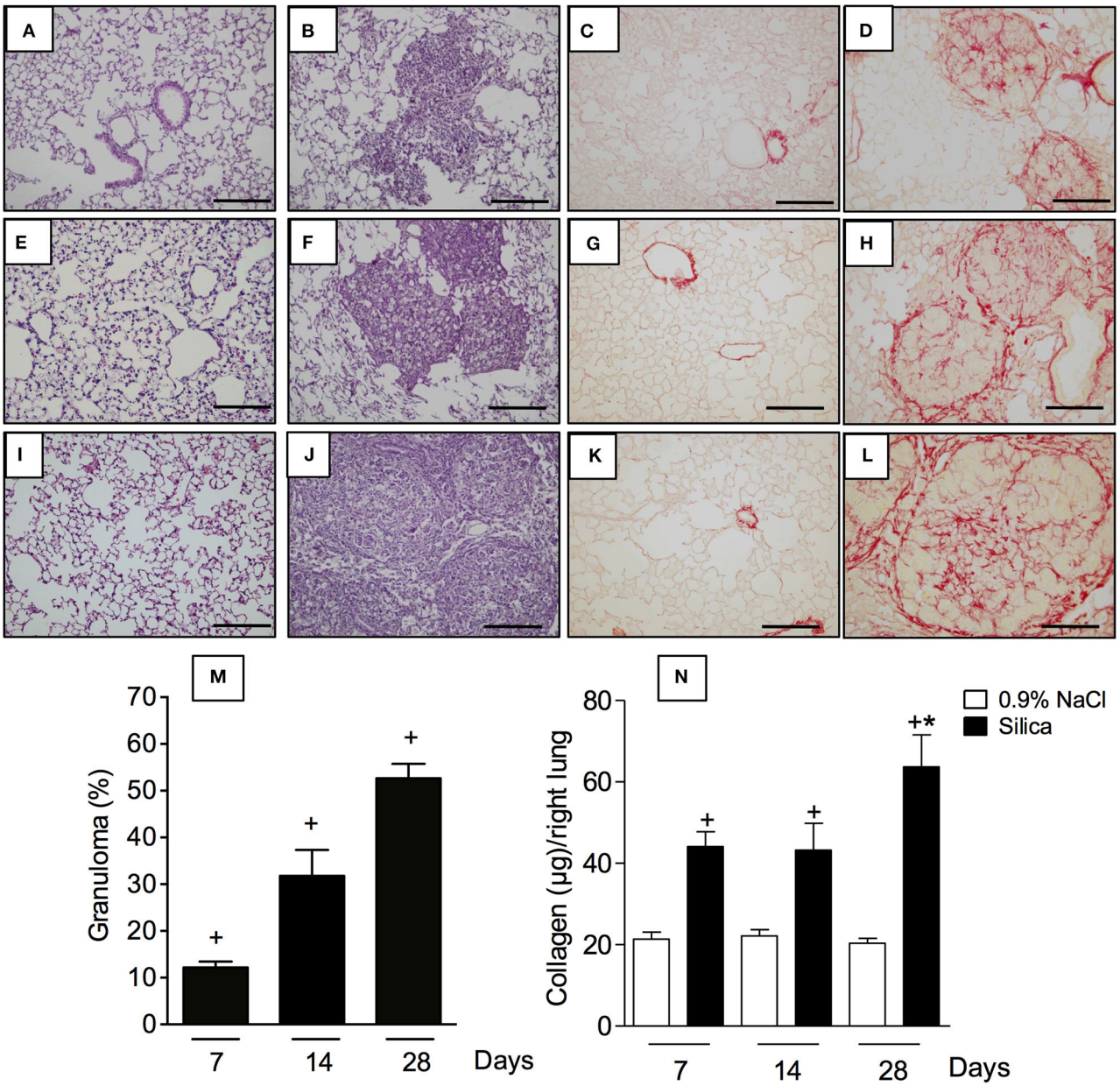

FIGURE 3 | Pathological changes caused by silica particle instillation. Lung sections were obtained from sham-challenged mice **(A,E,I/C,G,K)** or silica-challenged mice **(B,F,J/D,H,L)** (**H,E**/Picrus Sirius staining) on days 7, 14, and 28, respectively. Quantitative evaluation of area occupied by granuloma and lung collagen content are seen in **(M)** and **(N)**, respectively. Scale bar = 200 µm. Values represent mean ± SEM from 5 animals per group. Statistical analysis was done with one-way ANOVA followed by Newman-Keuls-Student test. $^{+}P < 0.05$ as compared to saline-challenged animals. $^{*}P < 0.05$ as compared to silica-challenged animals.

doses as low as 0.3 µg/mouse and 1 µg/mouse inhibited MIP-1α/CCL-3 and MIP-2/CXCL-2, respectively, but did not affect the cytokines.

We then employed invasive barometric plethysmography to assess whether flunisolide could repair the lung function disorder caused by silica particle exposure. As shown in **Figure 6**, silicotic mice reacted with exacerbation of the increase in airway resistance (**Figure 6A**) and lung elastance (**Figure 6B**) caused by aerosolized methacholine. Intranasal flunisolide, administered daily from days 21 to 27, significantly inhibited silica-induced airway hyper-reactivity concerning both airway resistance (**Figure 6A**) and lung elastance (**Figure 6B**).

Treatment With Flunisolide Improves Clearance of Silica Particles From the Lungs

Residual silica particles present inside the lungs trigger and perpetuate inflammation and development of fibrosis. By means of polarized light, crystalline silica particles can be visualized

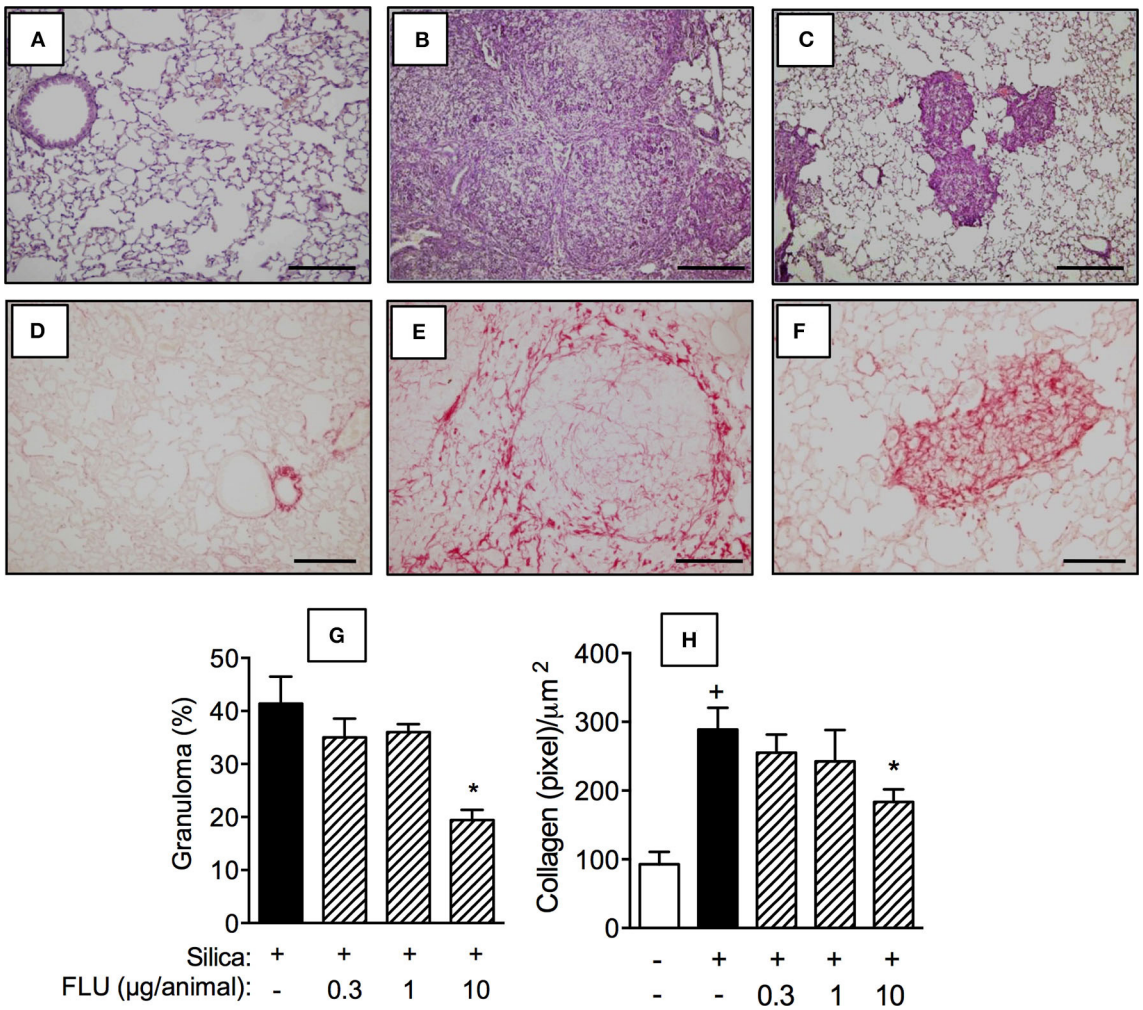

FIGURE 4 | Effect of flunisolide on granulomatous and fibrotic response caused by silica particle instillation. Lung sections were obtained from sham-challenged mice (negative control) **(A/D)**, silica-challenged mice treated with vehicle (positive control) **(B/E)** and silica-challenged mice treated with flunisolide (10 μg/mouse, intranasal, daily from days 21–27) **(C/F)** (**H,E**/Picrus sirius staining) on day 28. Quantitative evaluation of the area occupied by granuloma and lung collagen content from silicotic mice treated or not with flunisolide are seen in **(G)** and **(H)**, respectively. Scale bar = 200 μm. Values represent mean ± SEM from 6 animals per group. Statistical analysis was done with one-way ANOVA followed by Newman-Keuls-Student test. $^{+}P < 0.05$ as compared to saline-challenged animals. $^{*}P < 0.05$ as compared to silica-challenged animals.

based on their property to exhibit birefringence (19). By means of polarized microscopy, we detected the presence of small bright crystals in the lungs of silica-challenged mice (**Figure 7A**), and that treatment with flunisolide (10 μg/animal) reduced the number of these particles (**Figure 7B**). Quantitative data are shown in **Figure 7C**.

Treatment With Flunisolide Inhibits Silica-Induced Macrophage and Myofibroblast Accumulation in the Lung Tissue

In comparison to sham-challenged mice (**Figures 8A,E**), the silicotic ones presented increased lung tissue levels of macrophages (**Figure 8B**) and myofibroblasts (**Figure 8F**), as revealed by F4/80 and α-SMA immunelabelling, respectively. Flunisolide (10 μg/mouse) given daily from day 21 to 27 reduced the number of F4/80 (**Figure 8C**) and α-SMA positive cells (**Figure 8G**). Quantitative data for F4/80 and α-SMA positive cells are shown in **Figures 8D,H**, respectively.

Treatment With Flunisolide Inhibited Lung Fibroblast Activation *in vitro*

Finally, we examined the capacity of flunisolide to directly modulate the IL-13-induced activation of fibroblasts *in vitro*. Cells were recovered from the lungs of saline- and silica-challenged mice, and proliferative (**Figure 9A**) and secretory (**Figure 9B**) activities were evaluated. Incubation of normal fibroblasts with the pro-fibrotic cytokine IL-13 (40 ng/mL) triggered proliferation and MCP-1/CCL2 production

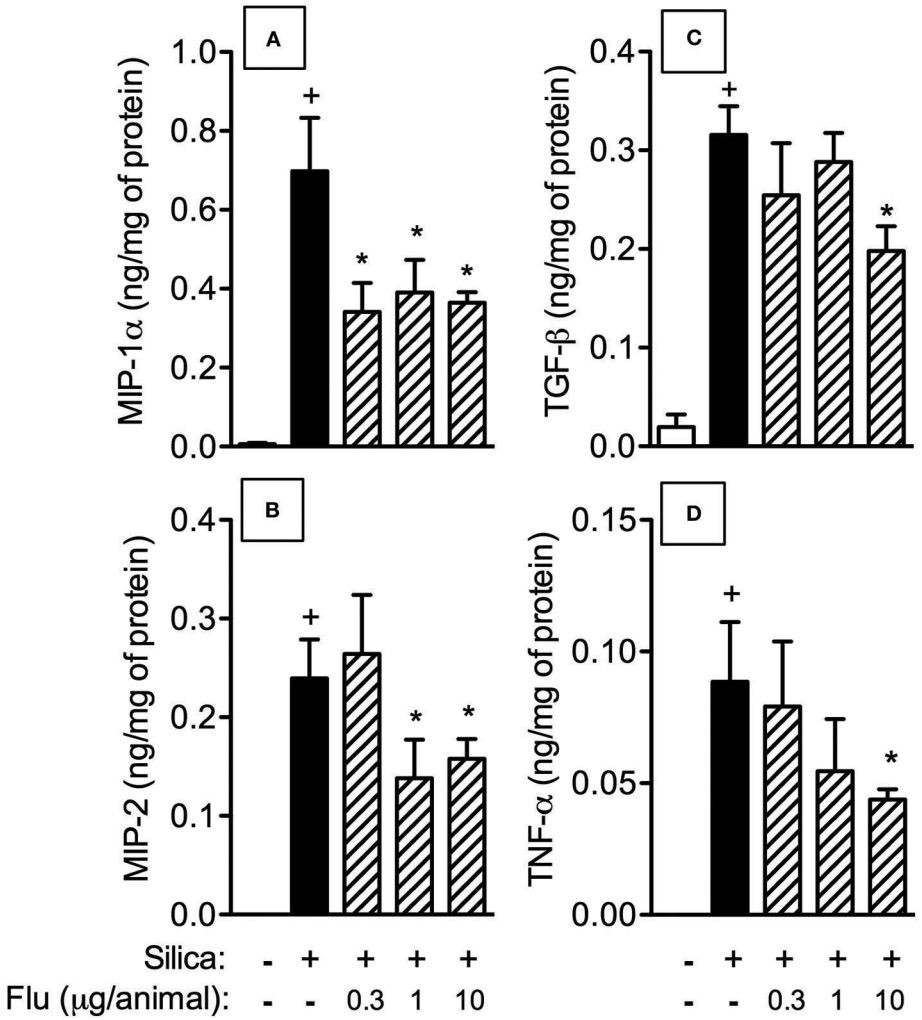

FIGURE 5 | Effect of flunisolide on generation of inflammatory mediators caused by silica particle instillation. Chemokines MIP-1α/CCL3 **(A)**, MIP-2/CXCL2 **(B)** and cytokines TGF-β **(C)** and TNF-α **(D)** were measured in the lung tissue obtained from sham-challenged mice (negative control), silica-challenged mice treated with vehicle (positive control) and silica-challenged mice treated with flunisolide (0.3–10 μg/mouse, intranasal, daily from days 21–27) on day 28. Values represent mean ± SEM from 6 animals per group. Statistical analysis was done with one-way ANOVA followed by Newman-Keuls-Student test. $^{+}P < 0.05$ as compared to saline-challenged animals. $^{*}P < 0.05$ as compared to silica-challenged animals.

(**Figures 9A,B**, respectively). Interestingly, silicotic fibroblasts showed increased baseline levels of MCP-1/CCL-2 production as compared to those from normal controls (**Figure 9B**). Stimulation with IL-13 increased proliferation and MCP-1/CCL-2 production in silicotic fibroblasts at higher levels when compared to control fibroblasts, suggesting a primed phenotype. Fibroblasts from saline- and silica-challenged mice showed IL-13-induced proliferation and MCP-1/CCL-2 production, responses significantly reduced following incubation with flunisolide (0.1 to 10 μM) (**Figure 9**).

DISCUSSION

The current study addressed the effect of therapeutic treatment with flunisolide on silica-induced pulmonary inflammation and fibrogenesis in mice. The nasal instillation of crystalline silica promoted a pulmonary fibro-granulomatous response, starting as lung inflammatory process and evolving to form granuloma rich in collagen fibers. Flunisolide inhibited granuloma formation and collagen deposition induced by silica in the mouse lungs. This effect appeared related to the decrease in the content of F4/80 and α-SMA positive cells in the lungs, which paralleled with reduction of pro-inflammatory and pro-fibrotic cytokines and chemokines. Flunisolide also suppressed IL-13-induced proliferation and MCP-1/CCL-2 release from lung myofibroblasts recovered from saline- and silica-challenged mice. These findings indicate that flunisolide seems to be an encouraging therapeutic strategy to be used in the case of silicosis.

Our current understanding of the precise mechanistic connection between inflammation and fibrogenesis is limited, in

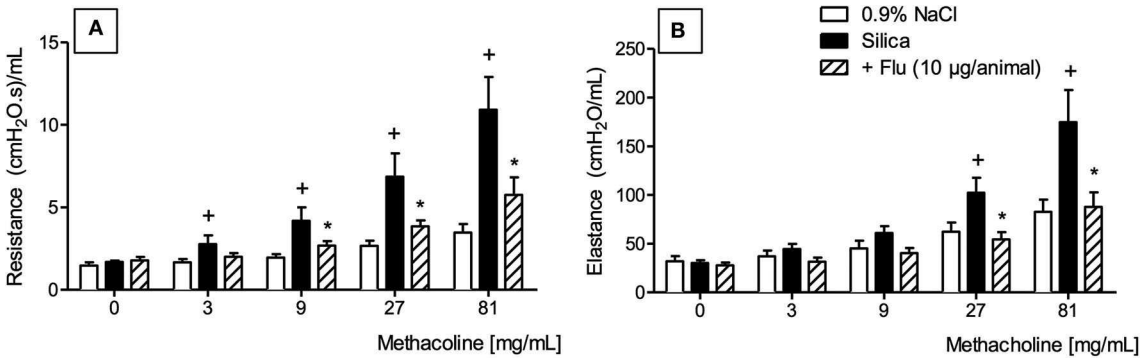

FIGURE 6 | Effect of flunisolide on airway hyper-reactivity caused by silica particle instillation. Airway resistance **(A)** and pulmonary elastance **(B)** were evaluated in the presence of increasing concentrations of methacholine (3–81 mg/mL) in sham-challenged mice (negative control), silica-challenged mice treated with vehicle (positive control) and silica-challenged mice treated with flunisolide (10 μg/mouse, intranasal, daily from days 21–27) on day 28. Values represent mean ± SEM from 6 animals per group. Statistical analysis was done with one-way ANOVA followed by Newman-Keuls-Student test. $^{+}P < 0.05$ as compared to saline-challenged animals. $^{*}P < 0.05$ as compared to silica-challenged animals.

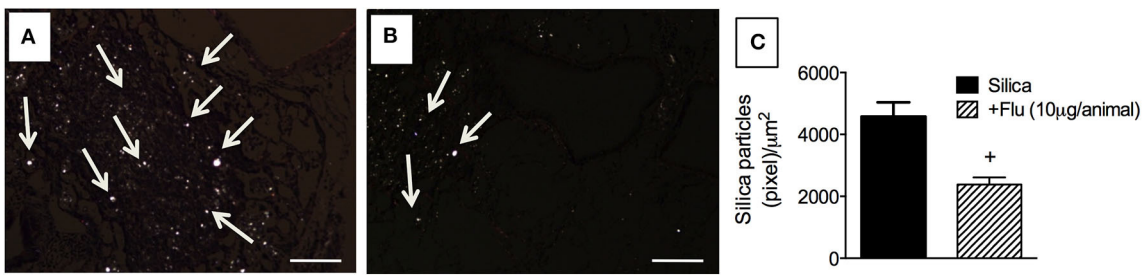

FIGURE 7 | Effect of flunisolide on the presence of crystalline silica particles in the lungs. Tissue sections were obtained from silica-challenged mice treated with vehicle (positive control) **(A)** and silica-challenged mice treated with flunisolide (10 μg/mouse, intranasal, daily from days 21–27) **(B)**. Quantitative evaluation of silica particles is seen in **(C)** (Picrus sirius staining/polarized microscopy). Arrows indicate silica particles. Scale bar = 200 μm. Values represent mean ± SEM from 6 animals per group. Statistical analysis was done with one-way ANOVA followed by Newman-Keuls-Student test. $^{+}P < 0.05$ as compared to saline-challenged animals.

spite of intensive research in the field (20). Existing evidence strongly suggests that in the lung, as well as in many other tissues, fibrosis is underlined by a complex multistep inflammatory response driven by a network of cytokines/chemokines, growth factors and signaling processes, often associated with leucocyte infiltration and fibroblast activation (20, 21). In the murine model of silicosis used in this study, Swiss Webster was the mouse strain of choice as this is not an inbred mouse strain, thereby modeling the outbred human condition associated with clinical silicosis as previously reported (15, 22–24). The kinetics of leukocyte infiltration in BAL fluid revealed that there was a marked increase in the number of total leukocytes at 7 days, which reduced progressively with time. A similar profile was noted in the case of mononuclear cells, while neutrophil numbers remained elevated for at least 28 days after nasal instillation of silica into mice. The latter paralleled with the increased levels of KC/CXCL-1 detected in the BAL of silica challenged-mice. Tissue analyses showed that there was a marked inflammatory cell infiltration at day 7, peribronchiolar granuloma formation at day 14, followed by an extensive tissue fibrosis 28 days post-silica challenge. In parallel, a marked increase in the levels of fibrogenic cytokines namely TGF-β and TNF-α was detected in both BAL and lung tissue. These responses directly correlated with alteration of lung function as attested by the state of airway hyper-reactivity to the spasmogenic methacholine.

Despite the sustained incidence of silicosis, little has been achieved concerning treatment development. Studies aiming to identify an effective therapy for silicosis are occurring, though management of silicosis still consists of supportive therapy including the use of bronchodilators and cough medication, as well as oxygen therapy (25–27). We demonstrated, herein, the efficacy of the therapeutic administration of flunisolide in reversing granuloma formation and collagen deposition triggered by silica particles. Our results are in line with those which showed glucocorticoids inhibiting remodeling and fibrosis in experimental models of lung allergic inflammation (13) and carbon tetrachloride-stimulated spleen in mice (28). Our findings are also supported by earlier clinical studies showing acute and chronic silicosis somehow responding to glucocorticoid therapy (11, 29, 30). Glucocorticoids are known for their ability to down-regulate inflammatory signaling, a response attributed to repression of the transcription of target pro-inflammatory genes

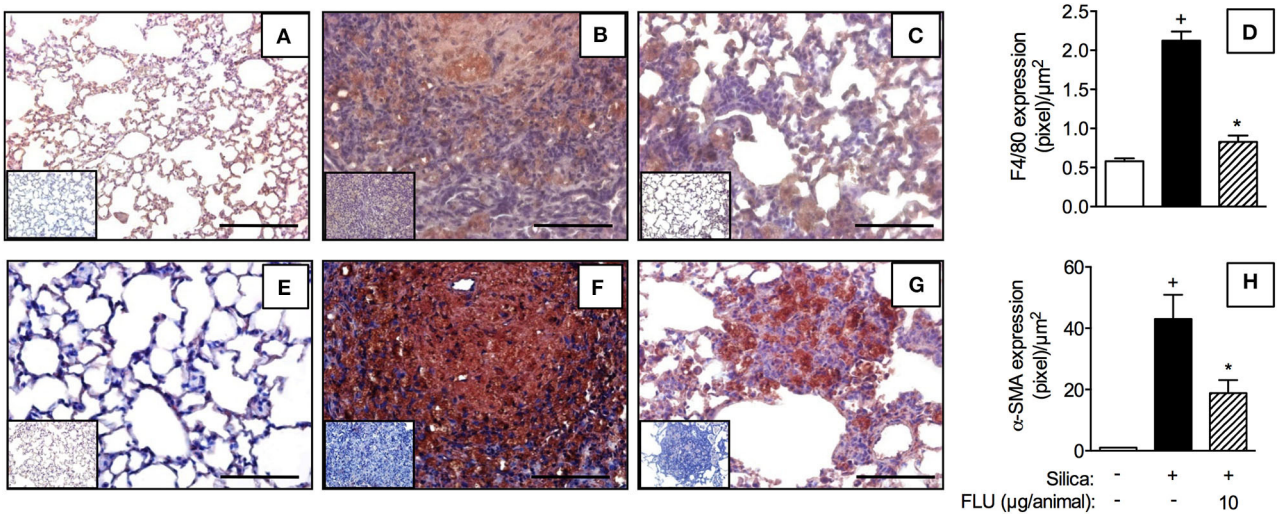

FIGURE 8 | Effect of flunisolide on accumulation of macrophages and myofibroblasts caused by silica particle instillation. Lung sections were obtained from sham-challenged mice (negative control) **(A,E)**, silica-challenged mice treated with vehicle (positive control) **(B,F)** and silica-challenged mice treated with flunisolide (10 μg/mouse, intranasal, daily from days 21–27) **(C,G)** (F4/80 and α-SMA imunohistochemical labeling) on day 28. Measurements of pixels per micrometer square for F4/80 and α-SMA positive cells are shown in **(D)** and **(H)**, respectively. IHC negative control (inset) consisted in the absence of primary antibody. Scale bar = 200 μm. Values represent mean ± SEM from 6 animals per group. Statistical analysis was done with one-way ANOVA followed by Newman-Keuls-Student test. $^{+}P < 0.05$ as compared to saline-challenged animals. $^{*}P < 0.05$ as compared to silica-challenged animals.

through inhibition of nuclear factor-κB (NF-κB) and activator protein-1 (AP-1) activation (31). Consistently, treatment with flunisolide effectively inhibited cytokine generation as well as labeling of α-SMA-positive fibroblasts into granulomatous areas in lungs of silicotic mice, phenomena that can be correlated to the reduction of pro-fibrotic cytokine generation as TGF-β and TNF-α.

A lot of attention has been directed toward myofibroblasts as central cells in the development of lung fibrosis based on their capacity to generate extracellular matrix components (32), thus being considered important targets for antifibrotic drugs. We also assessed the direct effect of flunisolide on lung fibroblasts recovered from normal or silica-challenged mice in the presence and absence of IL-13. Interestingly, the basal levels of MCP-1/CCL-2 generated in the case of fibroblasts from silica-stimulated mice were significantly higher when compared to normal mice, suggesting a change in the cell phenotype. MCP-1/CCL-2 is a chemokine known to up-regulate collagen gene expression (33), being implicated in lung fibrosis. We detected increased levels of MCP-/CCL-2 in the lungs of silicotic mice already on day 7 post-challenge (24), suggesting that the chemokine might be implicated in the lung fibrotic response to silica crystals. It was reported that fibroblasts are key cells involved not only in physiological but also several pathological processes (34) including fibrosis, when they can be activated and change their phenotype, particularly after being in contact with pro-fibrotic cytokines including TGF-β (35) and IL13 (34). We found that flunisolide inhibited fibroblast proliferation as well as MCP-1/CCL-2 production *in vitro*, from both normal and silica-challenged mice. These data can help to explain the reduction of the granulomatous response and labeling of α-SMA-positive fibroblasts noted in the flunisolide-treated silicotic mice.

Macrophages also play an important role in regulating the fibrotic process, based on their phagocytic activity (36, 37). Inhalation of crystalline silica is a persistent process that reflects multiple ingestion and re-ingestion cycles of particles by macrophages, causing activation and release of various pro-inflammatory and pro-fibrotic factors, resulting in sustained inflammation and ultimately fibrosis (38). We found that treatment with flunisolide reduced the number of F4/80 positive cells and levels of lung cytokines (TNF-α and TGF-β) and chemokines (MIP-1α/CCL-3 and MIP-2/CXCL-2), suggesting that mediators released by macrophages were inhibited by flunisolide. Down-regulation of macrophage functionality can be associated with the effect of glucocorticoids on the cytoskeleton, leading to reduction of cell adherence and/or migration to the inflammatory site (39–43) or even induction of apoptosis (44–46), thus contributing to the inhibition of fibrosis by flunisolide. Alternatively, macrophages that have taken up silica particles could be carried off the lungs by the lymphatics (15). Although silicosis is primarily a lung-associated disease, it also affects draining intrathoracic lymph nodes (47). In parallel to typical silicotic alterations in the lungs, changes in the mediastinal lymph nodes were already described including fibrosis and the presence of silica particles. Our group reported that amelioration, by the immunotoxin IL-13PE, of the granulomatous fibrosis in silica-challenged mice, was clearly associated with the reduction in the amount of free silica particles present in the lung parenchyma (15). In the current study, treatment with flunisolide showed a marked tendency for reduction in the amount of silica particles in the lungs. Moreover, the reversal of lung granulomatous fibrosis

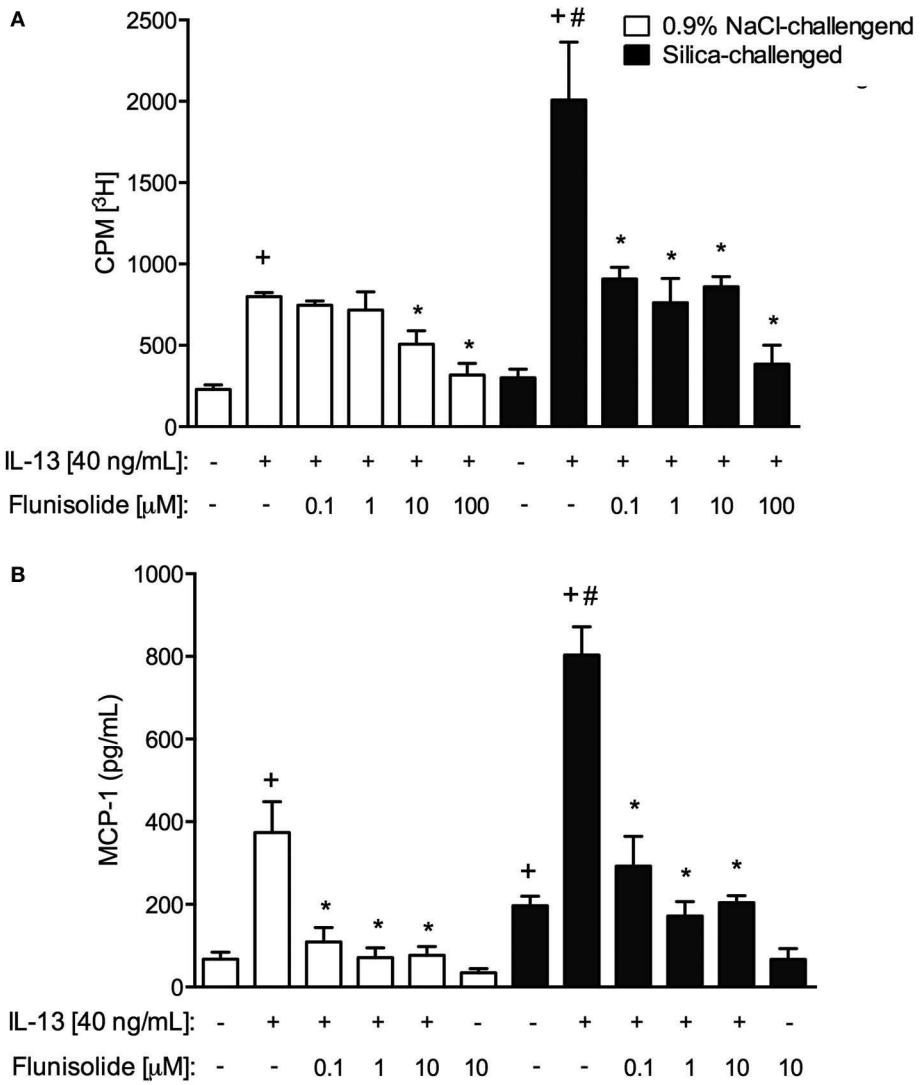

FIGURE 9 | Proliferation **(A)** and chemokine MCP-1 production **(B)** in cultured lung fibroblasts recovered from normal (white columns) and silica-challenged mice (black columns). Cells were exposed with flunisolide (Flu) (0.1–100 μM), 1 h before stimulation with IL-13 (40 ng/mL), and the analysis was performed 24 h later. Values represent mean ± SEM of quadruplicates from 3 independent experiments. Statistical analysis was done with one-way ANOVA followed by Newman-Keuls-Student test. $^{+}P < 0.05$ compared to respective medium-stimulated group; $^{\#}P < 0.05$ compared to IL-13-challenged normal group; $^{*}P < 0.05$ compared to respective IL-13-challenged group.

caused by flunisolide could lead to an enlargement of alveolar spaces, supporting the idea that the treatment might be acting in favor of the exhalation of free silica particles through the airways.

Finally, previous reports stated that patients with silicosis exhibit a respiratory deficit and airway hyper-reactivity (48), and in more severe cases increased airways resistance and residual volume were reported (6, 49, 50). By means of whole-body invasive plethysmography, it became evident that flunisolide decreased silica-induced state of airway hyper-reactivity, as attested by the reduction in lung resistance and elastance following methacholine aerosolization. It is noteworthy that TNF-α is implicated in airway hyper-reactivity (51), adding support to the interpretation that the suppressive effect of flunisolide on airway hyper-reactivity and other pathological features of silicosis is at least in part accounted for by a decrease in the generation of cytokines.

Since silicosis is a chronic inflammatory disfunction, this study had its inherent limitations in being based in a short-term murine model of the disease, imposed in some extent by ethical restrictions concerning the use of laboratory animals. In addition, although the findings from this study pointed out the positive influence of the flunisolide interventional treatment, the lack of data on the persistence of the protective effects on time-points later than 28 days post-challenge is also a limitation.

Overall, our findings show that therapeutic treatment with the intranasal glucocorticoid flunisolide improved granulomatous

inflammation and fibrosis, leading to restoration of lung function in silica-challenged mice. They also indicate that local flunisolide seems to constitute a promising therapeutic alternative for treatment of lung fibrotic diseases such as silicosis.

DATA AVAILABILITY STATEMENT

All datasets generated for this study are included in the article/supplementary material.

ETHICS STATEMENT

The animal study was reviewed and approved by Committee on Use of Laboratory Animals of the Oswaldo Cruz Foundation (license LW057/14).

AUTHOR CONTRIBUTIONS

TF, JL, AA, FF-F, FG, and YJ: data acquisition, analysis and interpretation of data for the work, provided illustration. VC: drafting of the work. JW and CH: revising it critically for important intellectual content. MM: substantial contributions to design of the work, revising it critically for important intellectual content, financing. PS: design of the work, supervision and final approval, financing, agreement to be accountable for all aspects of the work in ensuring that questions related to the accuracy or integrity of any part of the work are appropriately investigated and resolved. All authors contributed to the article and approved the submitted version.

FUNDING

This study was supported by grants from PRINT/FIOCRUZ/CAPES, Conselho Nacional de Desenvolvimento Científico e Tecnológico (CNPq) (304080/2013-6), INCT/INOFAR (465249/2014-0), Fundação Carlos Chagas de Amparo à Pesquisa do Estado do Rio de Janeiro (FAPERJ) (E-26.211.783/2015; E26/202.884/2018) and Fundação Oswaldo Cruz (INOVA/FIO 18-2-75).

ACKNOWLEDGMENTS

The authors thank Magda Fráguas Serra, Thiago José Figueira Ramos, Camila Dantas da Silva and Rodrigo Bandeira de Azevedo for technical assistance.

REFERENCES

1. Sato T, Shimosato T, Klinman DM. Silicosis and lung cancer: current perspectives. *Lung Cancer*. (2018) 9:91–101. doi: 10.2147/LCTT.S156376
2. Wagner GR. Asbestosis and silicosis. *Lancet*. (1997) 349:1311–5. doi: 10.1016/S0140-6736(96)07336-9
3. Rees D, Murray J. Silica, Silicosis and Tuberculosis. *Int. J. Tuberc. Lung Dis.* (2007) 11:474–84.
4. Morgan WK. Industrial bronchitis. *Br J Ind Med*. (1978) 35:285–91. doi: 10.1136/oem.35.4.285
5. Ghio AJ. Pneumoconiosis in the Twenty-First Century. In: Huang YT, Ghio AJ, Maier LA, editors. *A Clinical Guide to Occupational and Environmental Lung Diseases.* New York, NY; Heidelberg; Dordrecht; London: Humana Press, Springer (2012). p. 171–87.
6. Leung CC, YuI T, Chen W. Silicosis. *Lancet*. (2012) 379:2008–18. doi: 10.1016/S0140-6736(12)60235-9
7. Terra Filho M, Santos Ude P, Silicosis. *J. Bras. Pneumol.* (2006) 32(Suppl. 2):S41–7. doi: 10.1590/S1806-37132006000800008
8. Jindal SK. Silicosis in India: past and present. *Curr Opin Pulm Med*. (2013) 19:163–8. doi: 10.1097/MCP.0b013e32835bb19e
9. Kirby T, Australia reports on audit of silicosis for stonecutters. *Lancet*. (2019) 393:861. doi: 10.1016/S0140-6736(19)30478-7
10. Akgun M. Denim production and silicosis. *Curr Opin Pulm Med.*(2016) 22:165–9. doi: 10.1097/MCP.0000000000000249
11. Sharma SK, Pande JN, Verma K.Effect of prednisolone treatment in chronic silicosis. *Am Rev Respir Dis*. (1991) 143:814–21. doi: 10.1164/ajrccm/143.4_Pt_1.814
12. BarnesPJ. Glucocorticosteroids. *Handb Exp Pharmacol.* (2017) 237:93–115. doi: 10.1007/164_2016_62
13. Bergeron C, Hauber HP, Gotfried M, Newman K, Dhanda R, Servi RJ, et al. Evidence of remodeling in peripheral airways of patients with mild to moderate asthma: effect of hydrofluoroalkane-flunisolide. *J Allergy Clin Immunol*. (2005) 116:983–9. doi: 10.1016/j.jaci.2005.07.029
14. Tutor JD, Eid NS, Treatment of idiopathic pulmonary hemosiderosis with inhaled flunisolide. *South Med J*. (1995) 88:984–6. doi: 10.1097/00007611-199509000-00021
15. Ferreira TP, de Arantes AC, do Nascimento CV, Olsen PC, Trentin PG, Rocco PR, et al. IL-13 immunotox in accelerates resolution oflung pathological changes triggered by silica particles in mice. *Immunol J*. (2013) 191:5220–9. doi: 10.4049/jimmunol.1203551
16. Serra MF, Cotias AC, Pao CRR, Daleprane JB, Jurgilas PB, Couto GC, et al. Repeated allergen exposure in A/J mice causes steroid-insensitive asthma via a defect in glucocorticoid receptor bioavailability. *Immunol J*. (2018) 201:851–60. doi: 10.4049/jimmunol.1700933
17. Gundersen HJ, Bendtsen TF, Korbo L, Marcussen N, Moller A, Nielsen K, et al. Some new, simple and efficient stereological methods and their use in pathological research and diagnosis. *APMIS*. (1988) 96:379–94. doi: 10.1111/j.1699-0463.1988.tb05320.x
18. de Carvalho VF, de Barreto EO, Farias-Filho FA, Gomes LH, de Mendonca LL, Cordeiro RS, et al. Reduced expression ofIL-3 mediates intestinal mast cell depletion in diabetic rats: role of insulin and glucocorticoid hormones. *Int J Exp Pathol*. (2009) 90:148–55. doi: 10.1111/j.1365-2613.2008.00620.x
19. Wolman M, Kasten FH. Polarized light microscopy in the study of the molecular structure of collagen and reticulin. *Histochemistry*. (1986) 85:41–9. doi: 10.1007/BF00508652
20. Lee SB, Kalluri R. Mechanistic connection between inflammation and fibrosis. *Kidney Int.* (2010) 78:S22–6. doi: 10.1038/ki.2010.418
21. White ES, Mantovani AR. Inflammation, wound repair, and fibrosis: reassessing the spectrum of tissue injury and resolution. *Pathol J*. (2013) 229:141–4. doi: 10.1002/path.4126
22. Carvalho VF, Ferreira TPT, de Arantes ACS, Noel F, Tesch R, Sant'Anna CMR, et al. LASSBio-897 Reduces Lung Injury Induced by Silica Particles in Mice: Potential Interaction with the A2A Receptor. *Front. Pharmacol*. (2017) 8:778. doi: 10.3389/fphar.2017.00778
23. Ferreira TPT, Mariano LL, Bortolini RG, Arantes ACS, Fernandes A, Berni M, et al. Potential of PE Gylated toll-like receptor 7 ligands for controlling inflammation and functional changes in mouse models of asthma and silicosis. *Front. Immunol.* (2016) 7:95. doi: 10.3389/fimmu.2016.00095
24. Trentin PG, Ferreira TP, Arantes AC, Ciambarella BT, Cordeiro RS, Flower RJ, et al. Annexin A1 mimetic peptide controls the inflammatory and fibrotic effects of silica particles in mice. *Br J Pharmacol*. (2015) 172:3058–71. doi: 10.1111/bph.13109

25. Hoshi S, Tamai Y, Tamura A, Ishida H, Yoshida N, Ogawa C, et al. Silico-asbestosis that responded to steroid therapy. *Intern Med*. (2006) 45:917–21. doi: 10.2169/internalmedicine.45.1656
26. Barnes H, Goh NSL, Leong TL, Hoy R. Silica-associated lung disease: an old-world exposure in modern industries. *Respirology*. (2019) 24:1165–75. doi: 10.1111/resp.13695
27. Tani K, Bando M. Clinical course of silicotic patients receiving home oxygen therapy. *Nihon Kyobu Shikkan Gakkai Zasshi*. (1993) 31:341–5.
28. Kim KH, Lee JM, Zhou Y, Harpavat S, Moore DD. Glucocorticoids have opposing effects on liver fibrosis in hepatic stellate and immune cells. *Mol Endocrinol*. (2016) 30:905–16. doi: 10.1210/me.2016-1029
29. Goodman GB, Kaplan PD, StachuraI, Castranova V, Pailes WH, Lapp NL, Acute silicosis responding to corticosteroid therapy. *Chest*. (1992) 101:366–70. doi: 10.1378/chest.101.2.366
30. Bando T, Fujimura M, Shinagawa S, Mizuhashi K, Noda Y, Ohta G, et al. Effect of beclomethasone dipropionate inhalation on eosinophilic bronchitis in patients with silicosis. *Arzneimittelforschung*. (1997) 47:1370–4.
31. Sudlow AW, Carey F, Forder R, Rothwell NJ. The role of lipocortin-1 in dexamethasone-induced suppression ofPGE2 andTNF alpha release from human peripheral blood mononuclear cells. *Br J Pharmacol*. (1996) 117:1449–56. doi: 10.1111/j.1476-5381.1996.tb15305.x
32. Kendall RT, Feghali-Bostwick CA. Fibroblasts in fibrosis: novel roles and mediators. *Front Pharmacol*. (2014) 5:123. doi: 10.3389/fphar.2014.00123
33. Galindo M, Santiago B, Rivero M, Rullas J, Alcami J, Pablos JL. Chemokine expression by systemic sclerosis fibroblasts: abnormal regulation of monocyte chemoattractant protein 1 expression. *Arthritis Rheum*. (2001) 44:1382–6. doi: 10.1002/1529-0131(200106)44:6<1382::AID-ART231>3.0.CO;2-T
34. Tomasek JJ, Gabbiani G, Hinz B, Chaponnier C, Brown RA. Myofibroblasts and mechano-regulation of connective tissue remodelling. *Nat Rev Mol Cell Biol*. (2002) 3:349–63. doi: 10.1038/nrm809
35. Rockey DC, Bell PD, Hill JA. Fibrosis—A common pathway to organ injury and failure. *N Engl J Med*. (2015) 373:96. doi: 10.1056/NEJMc1504848
36. Wynn TA, Vannella KM. Macrophages in tissue repair, regeneration, and fibrosis. *Immunity*. (2016) 44:450–62. doi: 10.1016/j.immuni.2016.02.015
37. Smigiel KS, Parks WC. Macrophages, Wound Healing, and Fibrosis: recentInsights. *Curr Rheumatol Rep*. (2018) 20:17. doi: 10.1007/s11926-018-0725-5
38. Gilberti RM, Joshi GN, *Knecht* DA.The phagocytosis of crystalline silica particles by macrophages. *Am J Respir Cell Mol Biol*. (2008) 39:619–27. doi: 10.1165/rcmb.2008-0046OC
39. Ehrchen J, Steinmuller L, Barczyk K, Tenbrock K, Nacken W, Eisenacher M, et al. Glucocorticoids induce differentiation of a specifically activated, anti-inflammatory subtype of human monocytes. *Blood*. (2007) 109:1265–74. doi: 10.1182/blood-2006-02-001115
40. Abraham SM, Lawrence T, Kleiman A, Warden P, Medghalchi M, Tuckermann J, et al. Antiinflammatory effects of dexamethasone are partly dependent on induction of dual specificity phosphatase 1. *J Exp Med*. (2006) 203:1883–9. doi: 10.1084/jem.20060336
41. Giles KM, Ross K, Rossi AG, Hotchin NA, Haslett C. DransfieldI, Glucocorticoid augmentation of macrophage capacity for phagocytosis of apoptotic cells is associated with reduced p130Cas expression, loss of paxillin/pyk2 phosphorylation, and high levels of active Rac. *J Immunol*. (2001) 167:976–86. doi: 10.4049/jimmunol.167.2.976
42. Yamada K, Naito M, Hayashi T, Asai K, Yoshimine N, Iguchi A, Effects of dexamethasone on migration of human monocytes in response to oxidized beta-very low density lipoprotein. *Artery*. (1993) 20:253–67.
43. Getting SJ, Flower RJ, Perretti M. Inhibition of neutrophil and monocyte recruitment by endogenous and exogenous lipocortin 1. *Br J Pharmacol*. (1997) 120:1075–82. doi: 10.1038/sj.bjp.0701029
44. Schmidt M, Pauels HG, Lugering N, Lugering A, Domschke W, Kucharzik T. Glucocorticoids induce apoptosis in human monocytes: potential role of IL-1 beta. *J Immunol*. (1999) 163:3484–90.
45. Schmidt M, Lugering N, Lugering A, Pauels HG, Schulze-Osthoff K, Domschke W, et al. Role of theCD95/CD95 ligand system in glucocorticoid-induced monocyte apoptosis. *J Immunol*. (2001) 166:1344–51. doi: 10.4049/jimmunol.166.2.1344
46. Zeng S, Qiao H, Lv XW, Fan D, Liu T, Xie D, High-dose dexamethasone induced LPS-stimulated rat alveolar macrophages apoptosis. *Drug Des Devel Ther*. (2017) 11:3097–104. doi: 10.2147/DDDT.S147014
47. Cox-Ganser JM, Burchfiel CM, Fekedulegn D, Andrew ME, Ducatman BS. Silicosis in lymph nodes: the canary in the miner*? J Occup Environ Med*. (2009) 51:164–9. doi: 10.1097/JOM.0b013e31818f6a0f
48. Tripathi M, Pandey M. Heterogeneity in ventilation during positive end-expiratory pressure. *Crit Care*. (2010) 14:436. doi: 10.1186/cc9212
49. de Mesquita Junior JA, Lopes AJ, JansenJ M, de Melo PL. Using the forced oscillation technique to evaluate respiratory resistance in individuals with silicosis. *J Bras Pneumol*. (2006) 32:213–20. doi: 10.1590/S1806-37132006000300007
50. Sa PM, Lopes AJ, Jansen JM, Melo PL. Oscillation mechanics of the respiratory system in never-smoking patients with silicosis: pathophysiological study and evaluation of diagnostic accuracy. *Clinics*. (2013) 68:644–51. doi: 10.6061/clinics/2013(05)11
51. Tripathi SS, Mishra V, Shukla M, Verma M, Chaudhury BP, Kumar P, et al. IL-6 receptor-mediated lung Th2 cytokine networking in silica-induced pulmonary fibrosis. *Arch Toxicol*. (2010) 84:947–55. doi: 10.1007/s00204-010-0559-z

Conflict of Interest: The authors declare that the research was conducted in the absence of any commercial or financial relationships that could be construed as a potential conflict of interest.

frontiers in Endocrinology

ORIGINAL RESEARCH
published: 18 September 2020
doi: 10.3389/fendo.2020.585923

Brucella abortus Infection Modulates 3T3-L1 Adipocyte Inflammatory Response and Inhibits Adipogenesis

Ayelén Ivana Pesce Viglietti[1], *Guillermo Hernán Giambartolomei*[1], *Jorge Quarleri*[2*†] *and María Victoria Delpino*[1*†]

[1] *Instituto de Inmunología, Genética y Metabolismo (INIGEM), Facultad de Farmacia y Bioquímica, Universidad de Buenos Aires (UBA), Consejo Nacional de Investigaciones Científicas y Técnicas (CONICET), Buenos Aires, Argentina,* [2] *Instituto de Investigaciones Biomédicas en Retrovirus y Sida (INBIRS), Facultad de Medicina, Universidad de Buenos Aires (UBA), Consejo Nacional de Investigaciones Científicas y Técnicas (CONICET), Buenos Aires, Argentina*

Brucellosis is a prevalent global zoonotic infection but has far more impact in developing countries. The adipocytes are the most abundant cell type of adipose tissue and their secreted factors play an important role in several aspects of the innate and adaptive immune response. Here, we demonstrated the ability of *Brucella abortus* to infect and replicate in both adipocytes and its precursor cells (pre-adipocytes) derived from 3T3-L1 cell line. Additionally, infection of pre-adipocytes also inhibited adipogenesis in a mechanism independent of bacterial viability and dependent on lipidated outer membrane protein (L-Omp19). *B. abortus* infection was able to modulate the secretion of IL-6 and the matrix metalloproteases (MMPs) -2 and-9 in pre-adipocytes and adipocytes, and also modulated de transcription of adiponectin, leptin, and resistin in differentiated adipocytes. *B. abortus*-infected macrophages also modulate adipocyte differentiation involving a TNF-α dependent mechanism, thus suggesting a plausible interplay between *B. abortus*, adipocytes, and macrophages. In conclusion, *B. abortus* is able to alter adipogenesis process in adipocytes and its precursors directly after their infection, or merely their exposure to the *B. abortus* lipoproteins, and indirectly through soluble factors released by *B. abortus*-infected macrophages.

Keywords: Brucella, TNF-α, adipogenesis, macrophage, inflammation

OPEN ACCESS

Edited by:
Vinicius Frias Carvalho, Oswaldo Cruz Foundation (Fiocruz), Brazil

Reviewed by:
Rubén Cereijo, University of Barcelona, Spain
Tobias Fromme, Technical University of Munich, Germany
P Trayhurn, University of Liverpool, United Kingdom

****Correspondence:***
María Victoria Delpino
mdelpino@ffyb.uba.ar
Jorge Quarleri
quarleri@fmed.uba.ar

†ORCID:
María Victoria Delpino
orcid.org/0000-0003-2077-8509
Jorge Quarleri
orcid.org/0000-0001-5110-8773

Specialty section:
This article was submitted to Cellular Endocrinology, a section of the journal Frontiers in Endocrinology

Received: *22 July 2020*
Accepted: *08 September 2020*
Published: *18 September 2020*

Citation:
Pesce Viglietti AI, Giambartolomei GH, Quarleri J and Delpino MV (2020) Brucella abortus Infection Modulates 3T3-L1 Adipocyte Inflammatory Response and Inhibits Adipogenesis. Front. Endocrinol. 11:585923. doi: 10.3389/fendo.2020.585923

INTRODUCTION

Brucellosis is a prevalent global zoonotic infection but has far more impact in developing countries (1). Clinical manifestations of brucellosis are frequently associated with inflammatory responses in the organs affected (2). Adipose tissue represents one of the largest organs and constitutes up to 25% of the mass of the body in normal weight individuals (3). It is distributed throughout the body and is made up of different cell types that are involved in storing energy, regulating metabolism in addition to fulfilling neuroendocrine and immunological functions (3). Adipocytes secrete a multiplicy of adipokines, including adiponectin, leptin, and various cytokines such as IL-1β and IL-6. The resident immune cells—which include lymphocytes and macrophages—also secrete multiple inflammatory mediators, again including classical cytokines and chemokines (4, 5).

Adipocytes are the most abundant cell type of adipose tissue and their secreted factors play an important role in several aspects of the innate and adaptive immune response among other functions (6). Therefore, these cells could participate in the modulation of the immune response during *Brucella* infection. On the other hand, adipocytes are specialized for fat storage regulating the balance of energy and homeostasis (7). The pathogens could take advantage of this characteristic, turning adipose tissue into a survival niche. In fact, *Mycobacterium tuberculosis*, *Trypanosoma cruzi*, influenza virus A, *Chlamydia pneumoniae*, HIV -among other pathogens- are housed in adipose tissue (8–11). The cell and tissue in which *Brucella* persists during chronic infection remain largely unknown. Most studies describe the location of the bacteria based on the site of isolation or the histopathology of the disease, but the place where the bacterium resides has not been elucidated (12, 13).

Adipocytes differentiate from mesenchymal stem cells. During the differentiation process, the transcriptional factor CCAAT/enhancer-binding protein (C/EBP)β is transiently induced leading to activation of two master adipogenic transcription factors, peroxisome proliferator-activated receptor (PPAR)γ, and C/EBPα. These mediators stimulate each other to activate the transcription of genes implicated in lipid metabolism (14). Adipocyte differentiation is regulated by hormones, cytokines, growth factors, and also by matrix metalloproteinase (MMPs) (15, 16). A recent study performed in canine fetuses and neonates naturally infected with *B. canis* revealed its intracellular localization in adipocytes. *B. canis* was localized near to the lipid droplet and in the same place of the endoplasmic reticulum. The adipocytes from neonates and fetuses are immature and present features of pre-adipocytes. During their differentiation process, the pre-adipocytes express unfolded proteins as occurs during the intracellular replication of *Brucella* spp. (17, 18). This finding suggests that pre-adipocytes could be a replicative niche for *Brucella* spp. during the differentiation process. In the present study, we investigate whether *B. abortus* can infect and survive in differentiated adipocyte and its precursors, as well as the incumbency on both adipogenesis and immune response modulation, on the inflammatory response during brucellosis.

MATERIALS AND METHODS

Bacterial Culture

Brucella abortus S2308, DsRed-expressing *B. abortus* 2308 (provided by Diego Comerci, UNSAM University, Argentina), were grown for 18 h in 10 ml tryptic soy agar supplemented with yeast extract (Merck) with constant agitation (150 rpm) at 37°C. Bacteria were collected and inoculums prepared as previously described (19). To obtain heat-killed *B. abortus* (HKBA), bacteria were washed with sterile physiological solution and heat-killed at 70°C for 20 min. Absence of bacterial viability was verified by the lack of its *in vitro* growth on trypticase soy agar (TSA). Live *B. abortus* manipulations were performed in biosafety level 3 facilities.

Cell Culture

3T3-L1 fibroblasts were obtained from the American Type Culture Collection (ATCC, Manassas, VA) and were culture in DMEM (Gibco) containing 10% of heat-inactivated fetal bovine serum (FBS) (Gibco), 2 mM of L-glutamine (Gibco), 1 mM of sodium pyruvate (Gibco), and penicillin-streptomycin. The murine macrophage cell line J774 was grown in DMEM with 10% FBS and supplemented as previously described.

Adipocyte Differentiation

3T3-L1 cells were seeded at 5 x 10^4 cells/well in 24-well plates and allowed to reach confluence. After 2 days (day 0), the medium was changed to differentiation medium (DMEM, 0.5 mM 3-isobutyl-1-methylxanthine (IBMX), 1 μM dexamethasone (DM), and 1 μg/ml human insulin), all from SIGMA. At day 2, the medium was replaced by a maintenance medium (10% FBS and 1 μg/ml insulin). Full differentiation was reached at day 10–15.

Adipocyte differentiation was evaluated by oil red O staining (Sigma). Cultures in 24-well plates were fixed for 1 h with 10% formalin and then washed with 60% isopropanol, stained for 30 min by complete immersion in a working solution of 6% oil red O, and wash repeatedly with water. Ten microscopic fields per well in three wells per condition were quantified for each experiment. The percentage of adipocytes was calculated for the nontreated/noninfected controls.

Cellular Infection

3T3-L1 preadipocytes and adipocytes were separately seeded in two different densities: 2x10^4 cells per well in 24 well plate, and 1x10^5 cell per well in 6 well plate. Besides, J774.A1 macrophages were seeded at a density of 3x10^5 cells per well in 24 well plates. These three cell types were infected with *B. abortus* S2308 or DsRed-expressing *B. abortus* S2308 at different multiplicities of infection (MOI) 100 to 1,000 or at MOI 100 for J774.A1 cell line. After the bacterial suspension was dispensed, the plates were centrifuged for 10 min at 2,000 rpm and then incubated for 2 h at 37°C under a 5% CO2 atmosphere. Cells were extensively washed with DMEM to remove extracellular bacteria and incubated in medium supplemented with 100 μg/ml gentamicin and 50 μg/ml streptomycin to kill extracellular bacteria. Adipocytes and preadipocytes were harvested at different times to determine cytokine production, MMP secretion, lipid droplets staining and adiponectin, leptin, PPAR-γ, C/EBP-α, C/EBP-β gene transcription. Supernatants from J774.A1 macrophages were harvested at 24 h post-infection and sterilized by filtration through a 0.22 nitrocellulose filter. To evaluate the intracellular replication of *B. abortus*, the infected cells were washed and lysed at different time post-infection with 0.2% (vol/vol) of triton X-100. The number of viable intracellular bacteria was determined by the count of CFU/ml from serial dilutions to the tenth in TSA plates.

Brucella-Derived Lipoproteins and LPS

B. abortus L-Omp19 and U-Omp19 were obtained as previously described (20). Both recombinant proteins contained 0.25 endotoxin U/μg protein, as assessed by Limulus amoebocyte lysates (Associates of Cape Cod, East Falmouth, MA, USA). Protein concentration was determined by the BCA method (Pierce, Rockford, IL, USA). Ignacio Moriyon from the University of Navarra, Pamplona, Spain kindly provided *B. abortus* S2308 LPS and *E. coli* O111K58H2 LPS. Pam_3Cys was acquired from Boehringer Mannheim (Indianapolis, IN, USA).

Confocal Microscopy

3T3-L1 differentiated cells seeded onto glass coverslips were infected with DsRed expressing-*B. abortus* S2308 at MOI 100 as was previously described. At different time points, cells were fixed with paraformaldehyde, permeabilized with 0.3% Triton X-100, and then lipid droplets were stained with 1 μg/ml of Bodipy 493/503 (Invitrogen), and nucleus were stained with TO-PRO®-3 (Invitrogen). The coverslips were mounted in PBS-glycerin (9:1 vol/vol) and analyzed in a FV-1000 confocal microscope with an oil-immersion Plan Apochromatic 60X NA1.42 objective (Olympus). Ten microscopic fields per well in 3 wells per condition were quantified for each experiment. The percentage of adipocytes was calculated to the noninfected controls. To determine *B. abortus* replication we visualized DsRed-expressing *B. abortus* positive areas by confocal microscopy and quantified using Image J software (National Institutes of Health).

The amount and individual diameter size of the lipid droplets in the image were measured using Image J software and data were loaded into GraphPad Prism 5.0 (GraphPad Software, La Jolla, CA, USA) and evaluated for average lipid droplet size and size-frequency distribution for individual adipocytes. The adipocytes containing lipid droplets with a mean diameter >1 μM were classified as cells with big lipid droplets size.

Measurement of Cytokine Concentrations

Secretion of IL-1β, IL-6, and TNF-α were quantified by ELISA in culture supernatants following the manufacturer's instructions (BD Pharmingen, San Diego, CA).

No cross-reactivity with other mouse cytokines was identified. For IL1β ELISA were tested IL-1β IL-2, IL-3, IL-4, IL-5, IL-6, IL-7, IL-9, IL-10, IL-12 (p70), IL-15, IFN-γ, MCP-1, TCA3, and TNF-α; for IL-6 ELISA were tested IL-1β, IL-2, IL-3, IL-4, IL-5, IL-7, IL-9, IL-10, IL-12 (p70), IL-15, IFN-γ, GM-CSF, MCP-1, TCA3, and TNF-α; for IL1 β ELISA were tested IL-2, IL-3, IL-4, IL-5, IL-6, IL-7, IL-9, IL-10, IL-12 (p70), IL-15, IFN-γ, MCP-1, TCA3, and TNF-α. Sensitivity for IL-1 β, IL-6, and TNF-α the limit of detection is 15.6 pg/ml.

Zymography

Gelatinase activity was assayed by the method of Hibbs et al. with modifications, as described (21, 22). Briefly, a total of 20 μl of cell culture supernatants from infected cells or untreated controls were mixed with 5 μl of 5X loading buffer [0.25 M Tris (pH 6.8), 50% glycerol, 5% SDS, and bromophenol blue crystals] and loaded onto 10% SDS-PAGE gels containing 1 mg/ml gelatin (Sigma-Aldrich, Buenos Aires, Argentina). Following electrophoresis, gels were washed with a solution containing 50 mM Tris-HCl (pH 7.5) and 2.5% Triton X-100 (buffer A) for 30 min and with buffer A added with 5 mM CaCl2 and 1 μM ZnCl2 for 30 min and were later incubated with buffer A with additional 10 mM CaCl2 and 200 mM NaCl for 48 h at 37°C. Gelatin activity was visualized by the staining of the gels with 0.5% Coomassie blue. Unstained bands indicated the presence of gelatinase activity.

Gelatinase Activity Under Native Conditions

Gelatinase activity in unprocessed culture supernatants (native conditions) was measured by using a gelatinase/collagenase fluorometric assay kit (EnzChek; Invitrogen, Carlsbad, CA) according to the manufacturer's instructions. The EnzChek kit contains DQ gelatin, a fluorescein-conjugated gelatin so heavily labeled with fluorescein that fluorescence is quenched. When this substrate is digested by gelatinases or collagenases it yields highly fluorescent peptides, and fluorescence increase is proportional to proteolytic activity. Collagenase purified from *Clostridium histolyticum* provided in the assay kit serves as a control enzyme. Plates were read in a fluorescence plate reader (Victor3; Perkin-Elmer, Waltham, MA).

mRNA Extraction and Quantitative Real-Time PCR

Total RNA was extracted from cells using the kit Quick-RNA MiniPrep Kit (Zymo Research) according to the manufacturer's instructions. cDNA was synthesized from 1 μg total RNA with the enzyme reverse transcriptase Improm-II (Promega). Real-time PCR was done with a SYBR green as a DNA binding fluorescent dye using a StepOne Real-Time PCR System (Applied Biosystems). The pairs of primers used were the following: adiponectin sense:5′-GACGACACCAAAAGGGCTCA-3′, antisense: 5′-GAGTGCC ATCTCTGCCATCA-3′, leptin sense: 5′-TCCCTGCCTCAGAC CAGTG-3′, antisense: 5′-TAGAGTGAGGCTTCCAGGACG-3′, PPAR-γ sense: 5′-CTGATGGCATTGTGAGACAT-3′, antisense: 5′-ATGTCTCACAATGCCATCAG-3′, C/EBP-α sense: 5′-TGT GCGAGCACGAGACGTC-3′, antisense: 5′-AACTCGTCGT TGAAGGCGG-3′, C/EBP-β sense: 5′-GCTGAGCGACG AGTACAAGA-3′, antisense: 5′-CAGCTCCAGCACCTTGTG-3′, β-actin sense: 5′-AACAGTCCGCCTAGAAGCAC-3′, antisense: 5′-CGTTGACATCCGTAAAGACC-3′.

The amplification cycle for adiponectin, leptin, PPAR-γ, C/EBP-α, and C/EBP-β was the following 10 min 95 °C, 40 cycles for 15 s at 95°C, 60°C for 30 s, and 72°C for 60 s. All primer sets yielded a single product of the correct size. The fold change (relative expression) in gene expression was calculated using the relative quantitation method ($2^{-\Delta\Delta Ct}$). Relative expression levels were normalized against β-actin. Intra experiment CT values differences between samples were less than 0.5.

Statistical Analysis

Each experiment was performed at least three times with different culture preparations. Data were represented as mean ± SD measured in triplicate from at least three individual experiments. Statistical analysis was performed with one-way ANOVA. Multiple comparisons between all pairs of groups were made with Tukey's posttest, and those against two groups were made with Student's *t* test, Mann-Whitney test. To determine normality, the Shapiro-Wilk normality test was used. Graphical and statistical analyses were performed with GraphPad Prism 5.0 software. $P<0.05$ was the minimum level for accepting a statistically significant difference between groups.

RESULTS

B. abortus Infects and Replicates in Both Pre-Adipocytes and Adipocytes, and Inhibits Adipogenesis

There are no former reports about the interaction between *B. abortus* and adipogenic cells. Thus, we first determined the differential capacity of *B. abortus* to infect pre-adipocytes and adipocytes. As shown in **Figures 1A**. *B. abortus* was internalized by both, pre-adipocytes and adipocytes *in vitro*. However, the multiplication efficiency was dissimilar between them. In pre-adipocytes the number of intracellular bacteria was increased by more than one log at 24 h post-infection and continued growing thereafter. By contrast, adipocytes were less permissive for *B. abortus* growth, and the number of bacteria in adipocytes was significantly lower than that observed for pre-adipocytes ($p < 0.01$). The number of intracellular bacteria in adipocytes increased by one log at 48 h post-infection and then decline.

At seven days of adipogenic differentiation, the culture is heterogeneous with cells that present small and big lipid droplets (more than 1 μm in diameter). At this time, cells were infected with DsRed-expressing *B. abortus* and lipid droplets were stained with Bodipy 493/503, and cells were evaluated at different times post-infection. Our results indicate that *B. abortus* invades adipocytes in a manner that was independent of the lipid droplets size (**Figures 1B–D**). However, *B. abortus* preferentially replicates in adipocytes with small lipid droplets (**Figure 1E**).

To assess whether the infection affects adipocyte differentiation, pre-adipocytes were infected with *B. abortus* at MOI 100 and 1,000, in the presence of differentiation medium for 2 days, and then incubated with maintenance medium. *E. coli* LPS was used as a control. At 15 days post-infection cells were fixed. The presence of differentiated adipocytes was revealed by lipid droplets staining with Bodipy 493/503 and Oil Red O (**Figures 1F–I**). *B. abortus* infection inhibited adipocyte differentiation as was revealed by a reduction of lipid droplets formation.

Given the ability of *B. abortus* infection to inhibit adipocyte differentiation, subsequent experiments were carried out to determine whether such infection could also modulate the transcription of the essential pro-adipogenic factors C/EBP-α, C/EBP-β, and PPAR-γ (14). For this purpose, pre-adipocytes were infected, incubated with a differentiation/maintenance medium, and mRNA levels of mentioned pro-adipogenic factors were measured at 15 days. *B. abortus* infection promoted a decrease in the transcription of C/EBP-α and PPAR-γ genes despite an increase in the transcription of C/EBP-β gen (**Figures 1J–L**). Altogether, these results indicate that *B. abortus* replicates preferentially in pre-adipocytes slowing down their normal adipogenesis.

B. abortus Infection Modulates Proinflammatory Cytokines and Adipokines Secretion in Pre-Adipocytes and Adipocytes

The adipose tissue physiology is committed to the expression of cytokines and adipokines. They not only control fat metabolism but also immune homeostasis (6). Infection with *B. abortus* at MOI 100 and 1,000 induced IL-6 (**Figures 2A, B**) but not IL-1β nor TNF-α (not shown) secretion by both pre-adipocytes and adipocytes. In adipocytes, the mRNA transcription level of leptin remained unaltered after the *B. abortus* infection, but the levels of mRNA of adiponectin and resistin are significantly ($p < 0.01$) inhibited respect to uninfected control cells (**Figures 2C–E**). This is in concordance with the inhibitory effect of *B. abortus* infection on adipogenesis, since transcription of adipokine genes are controlled by the transcription factor PPAR-γ (23). These results indicate that *B. abortus* infection modulates the expression of cytokines and adipokines in pre-adipocytes and adipocytes.

B. abortus Infection Induces MMPs Secretion in Pre-Adipocytes but Was Unable to Modulate MMPs in Adipocytes

Cytokines and adipokines have been shown to stimulate MMPs secretion from different cell types (24–30). Additionally, pre-adipocytes and adipocytes can produce MMP-2 and MMP-9 (15). To analyze whether *B. abortus* is capable of modulating their MMP-2 and MMP-9 activity, separated pre-adipocyte and adipocyte cells were infected with *B. abortus* at MOI 100 and 1,000, and after 24 h MMPs activity was evaluated, in culture supernatants, by gelatin zymography. Supernatants, from *B. abortus*-infected pre-adipocyte displayed a significant increase in MMP-2 and MMP-9 gelatinase activity than that of uninfected cells (**Figures 3A–C**). By contrast, in adipocytes, no further increase of the MMP-2 and MMP-9 activity was detected for any MOI of infection (**Figures 3D–F**). The activity of MMPs *in vivo* is counterbalanced by the tissue inhibitor's action including TIMPs (31). Therefore, the net gelatinase or collagenase activity in a complex sample, such as culture supernatants, depends on the balance between MMP and TIMP activities. This net activity is not revealed by zymography, since MMP-TIMP complexes may dissociate during gel electrophoresis. To assess whether the environment surrounding *Brucella*-infected pre-adipocytes and adipocytes has an increased net gelatinase activity, culture supernatants from these cells were incubated with a non-fluorescent gelatin-fluorescein conjugate, and the fluorescence unmasked as a consequence of gelatin degradation was measured in a fluorometer. Our results indicated that enzymatic activity is increased significantly in *B. abortus*-infected supernatants from pre-adipocytes supernatants but it remained unaltered in supernatants from *B. abortus*-infected adipocytes (**Figures 3G, H**). Therefore, *B. abortus* infection increases the MMP-2 and MMP-9 activity in pre-adipocytes, but no in adipocytes.

B. abortus Lipoproteins Inhibit Adipocyte Differentiation

Previously, we have reported that *Brucella* lipoproteins are crucial for many responses induced by *B. abortus* infection (19–21, 32–36). Additionally, adipogenesis inhibition may be a process involving TLR-ligand interactions (37, 38). At first, we evaluated whether viable *B. abortus* was necessary to inhibit

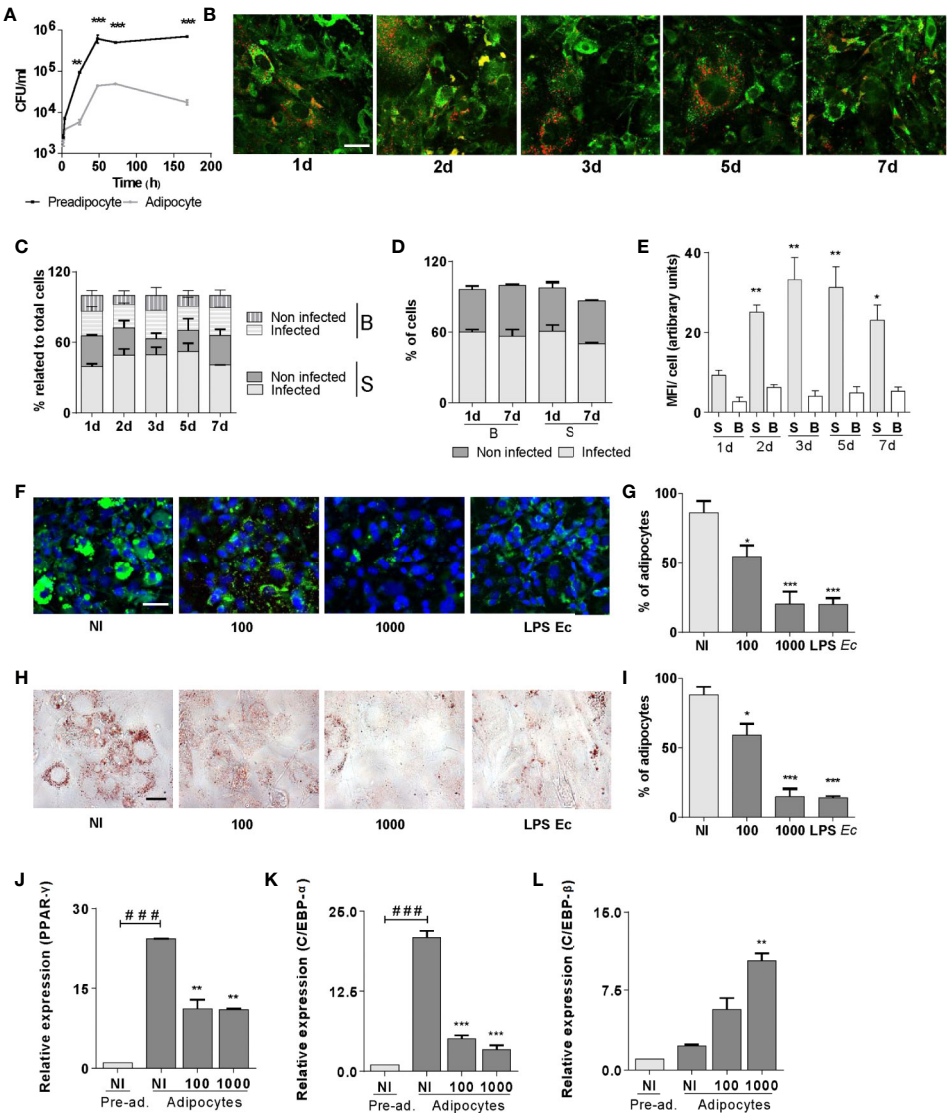

FIGURE 1 | *B. abortus* replicates in pre-adipocytes and adipocytes and inhibits adipogenesis. Infection with *B. abortus* was performed at a multiplicity of infection (MOI)= 100, and CFU was determined at different times of infection in pre-adipocytes and adipocytes. **(A)**. Intracellular DsRed-expressing *B. abortus* in adipocytes assessed by confocal microscopy, lipid droplets were stained with Bodipy 493/503 **(B)**. Quantification of the experiment performed in B **(C–E)**. Percentage of infected and non-infected adipocytes with small (S) and big **(B)** lipids droplets respect to total cells at each time **(C)**. Percentage of infected and non-infected cells at 1 and 7 d post infection present in adipocytes with S or B droplets cells respect to total S o B cells at each time. Quantification of bacterial replication is measured as means of fluorescence intensity (MFI) **(E)**. Effect of *B. abortus* infection at MOI 100 and 1,000 on adipocyte differentiation determined by lipid droplets staining with Bodipy 493/503 **(F)**, quantified by cell counts **(G)** and Oil Red O staining **(H)**, quantified by cell counts **(I)**. Effect of *B. abortus* infection on PPAR-γ **(J)**, C/EBP-α **(K)**, and C/EBP-β **(L)** transcription determined by RT-qPCR in adipocytes after 24 h post-infection. LPS from *E. coli* (LPS *Ec*) was used as a positive control. Scale bar: 30 µm. Data are given as the mean ± SD measured in triplicate from at least three individual experiments. Ten microscopic fields per condition were quantified for each experiment. Data shown are from a representative experiment of three performed. *P < 0.05; **P < 0.01; ***P < 0.001vs non infected cells (NI). ###P< 0.001 vs non infected pre-adipocytes (NI/Pre-ad.).

adipocyte differentiation. Oil red staining of adipocytes differentiated in the presence of HKBA revealed a markedly reduced adipocyte differentiation compared with the unstimulated cells. We further assessed the *B. abortus* LPS or its lipoproteins involvement on adipocyte differentiation inhibition. To this end, pre-adipocytes were differentiated in the presence of *B. abortus* LPS, or *B. abortus* lipidated outer membrane protein 19 (L-Omp19), used as a model of *Brucella* lipoprotein, and compared against unlipidated (U)-Omp19 (20). LPS from *E. coli* and $Pamp_3Cys$ were used as positive controls. As shown in **Figure 4**, L-Omp19, but not *B. abortus* LPS, mimicked the inhibition of lipid droplets accumulation induced by *B. abortus* infection. Nonetheless, the U-Omp19 was not capable to inhibit lipid droplets accumulation (**Figure 4**). Together these

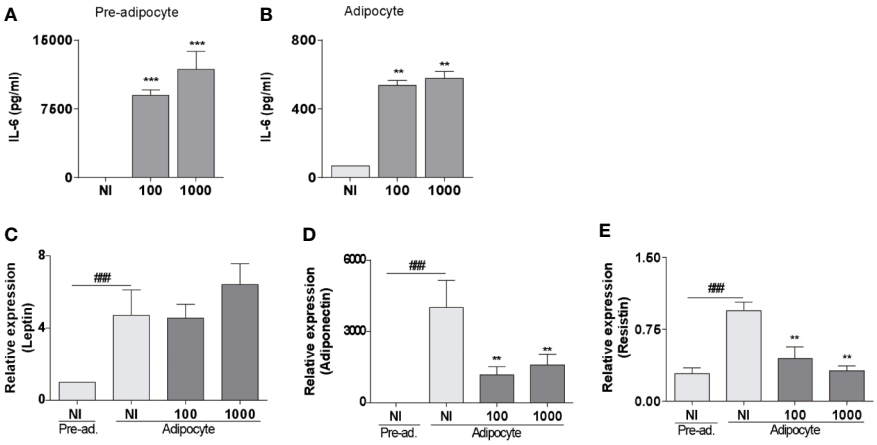

FIGURE 2 | *B. abortus* infection modulates proinflammatory cytokines and adipokines secretion in pre-adipocytes and adipocytes. ELISA determination of IL-6 in pre-adipocytes **(A)** and adipocytes **(B)** measured in culture supernatants at 24 h post-infection. Determination of leptin **(C)**, adiponectin **(D)**, and resistin **(E)** by RT-qPCR in *B. abortus* -infected adipocyte cells at MOI 100 and 1,000 at 24 h post-infection. Data are given as the mean ± SD measured in triplicate from five individual experiments. Data shown are from a representative experiment of five performed **P < 0.01; ***P < 0.001vs non infected cells (NI). ###P< 0.001 vs non infected pre-adipocytes (NI/Pre-ad.)

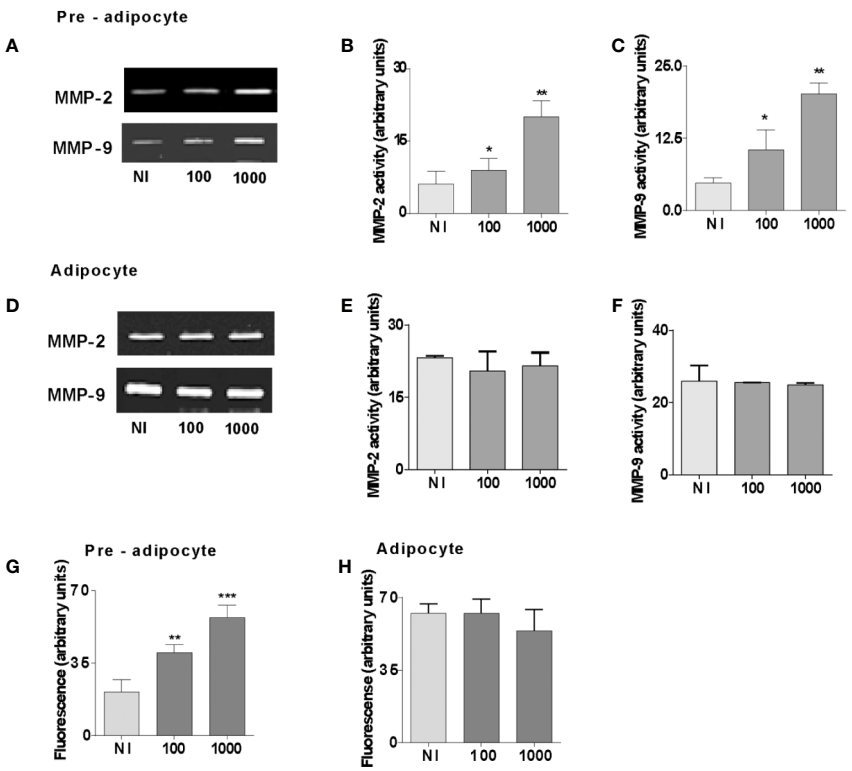

FIGURE 3 | *B. abortus* infection induces MMPs secretion in pre-adipocytes but was unable to modulate MMPs in adipocytes. MMP-2 and MMP-9 activity were measured by gelatin zymography in culture supernatants from *B. abortus*-infected preadipocytes **(A)** and adipocytes **(D)** at 24 h post-infection. **(B, C, E**, and **F)**. Densitometric analysis of results from three independent experiments performed in A and D. For MMP activities, the culture supernatants from B. abortus infected preadipocytes **(G)** and adipocytes **(H)** with a fluorescein-conjugated gelatin substrate that produces highly fluorescent peptides when gelatin is digested. Data are expressed in fluorescence units informed by the fluorometer. Data are given as the mean ± SD measured in triplicate from four individual experiments. Data shown are from a representative experiment of five performed *P < 0.05; **P < 0.01; ***P < 0.001 vs non infected cells (NI).

results indicate that the lipoproteins (L-Omp19) from *B. abortus* but not its LPS participates in the inhibition of adipogenesis among infected pre-adipocytes.

B. abortus-Infected Macrophages Modulate Adipocyte Differentiation

Macrophages constitute the main host cell for *B. abortus* replication (39). We hypothesized that *B. abortus*-infected macrophages release soluble mediators that may affect adipocyte differentiation. For this goal, the adipocyte differentiation process was studied in the presence of conditioned media from *B. abortus*-infected macrophages, or uninfected macrophages as control. As shown in **Figure 5**, the adipocyte differentiation was significantly reduced by conditioned media from *B. abortus*-infected macrophages but it was not modified by conditioned media from uninfected macrophages (**Figure 5**).

To determine whether conditioned media from *B. abortus*-infected macrophages affects at early and/or late stage of the adipocyte differentiation process, we added the conditioned media from *B. abortus*-infected macrophages during the incubation with adipocyte differentiation medium or, during the cultivation with maintenance medium. As a control, conditioned media from uninfected macrophages was included. The adipocyte differentiation was inhibited when conditioned media from *B. abortus*-infected macrophages was added during the culture of cells with adipocyte differentiation media indicating that suppresses the pre-adipocyte differentiation at an early stage while the addition of conditioned medium during the cultivation with maintenance medium did not affect adipocyte differentiation (**Figure 6**). Together, these results indicate that soluble factors released from *B. abortus*- infected macrophages inhibit adipogenesis at an early state.

B. abortus-Infected Macrophages Inhibit Adipocyte Differentiation *via* a Mechanism Dependent on TNF-α

TNF-α is a proinflammatory cytokine able to downregulate the adipocyte differentiation (40). Previously, we have reported that *B. abortus*-infected macrophages secrete TNF-α (21, 32). To test whether TNF-α released from *B. abortus*-infected macrophages inhibits adipogenesis, we performed experiments with culture supernatants preincubated with a TNF-α neutralizing antibodies. As shown in **Figure 7**, the inhibitory effect of *B. abortus*-infected macrophages on adipocyte differentiation was inhibited by the treatment with TNF-α neutralizing antibody. Also, the isotype control does not affect. Thus, we concluded that TNF-α plays a key role in the inhibition of adipogenesis induced by macrophages-infected with *B. abortus*.

DISCUSSION

The role of adipose tissue in the pathogenesis of infectious diseases has increased attention in recent years (41–45). Adipose tissue constitutes a nutritionally rich organ for the survival of pathogens such as *Mycobacterium tuberculosis*, *Trypanosoma cruzi*, HIV, among others (9, 46, 47). Cell types composing adipose tissue include, fibroblasts, smooth muscle, endothelial, and immune cells. In the setting of infectious or non-infectious diseases like diabetes or obesity, adipose-resident immune cells are derived to a proinflammatory phenotype due to a proinflammatory microenvironment. However, adipocytes are the most abundant cell type (48).

Cell types composing adipose tissue include, fibroblasts, smooth muscle, endothelial and immune cells. In the setting of

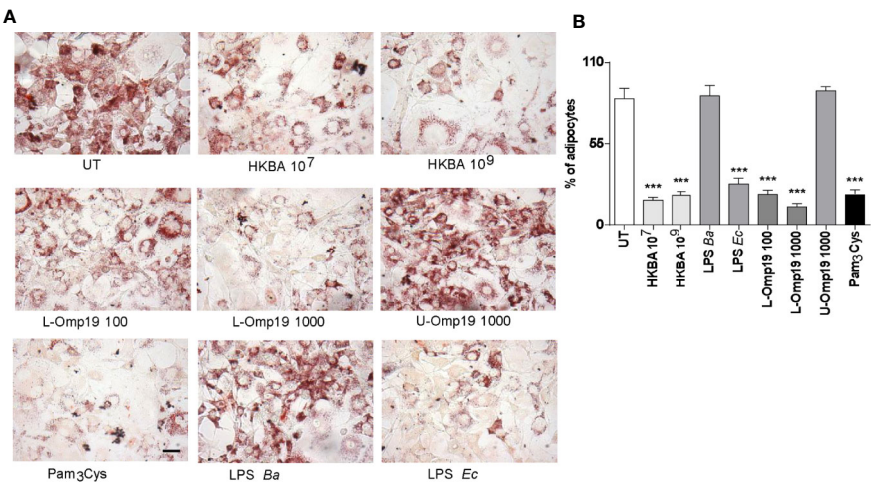

FIGURE 4 | *B. abortus* lipoproteins inhibits adipocyte differentiation. Pre-adipocytes were differentiated in the presence of HKBA (1x106 and 1x109 bacteria/ml) and *E. coli* LPS (LPS *Ec*) (10 ng/ml), *B. abortus* LPS (LPS *Ba*) (1,000 ng/ml), L-Omp19 (10, 100, or 1,000 ng/ml), U-Omp19 (1,000 ng/ml), or Pam3Cys (50 ng/ml) or untreated (UT). The presence of adipocytes was revealed by staining of lipid droplets with Oil Red O **(A)**. Quantification of Oil Red O was determined by cell counts **(B)**. Ten microscopic fields per well in three wells per condition were quantified for each experiment. The percentage of adipocytes was calculated to the untreated cells (UT). Scale bar: 30 μm. Data are given as the mean ± SD measured in triplicate from five individual experiments. Data shown are from a representative experiment of five performed ***P < 0.001 vs untreated cells (UT).

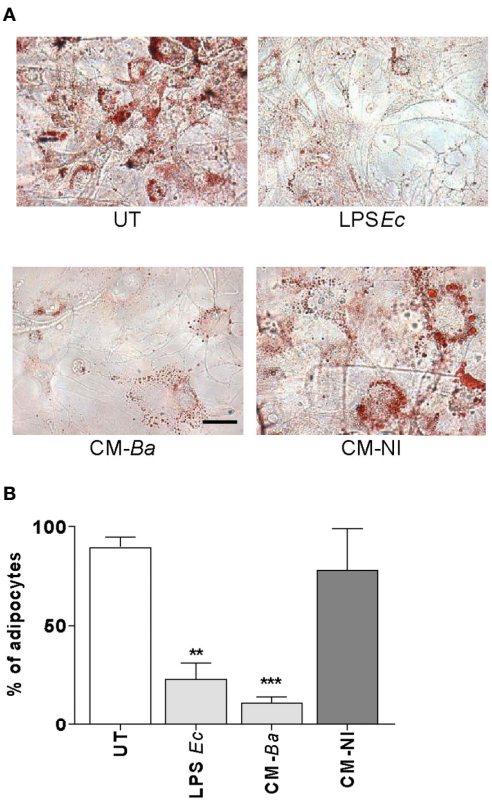

FIGURE 5 | *B. abortus*-infected macrophages modulate adipocyte differentiation. Pre-adipocytes were differentiated in the presence of culture supernatants from *B. abortus* infected macrophages at MOI 100 (CM-Ba) or culture supernatants from non-infected macrophages as control (CM-NI). The presence of adipocytes was revealed by staining of lipid droplets with Oil Red O **(A)**. Quantification of Oil Red O was determined by cell counts **(B)**. LPS from *E. coli* (LPS *Ec*) was used as a positive control. Ten microscopic fields per well in three wells per condition were quantified for each experiment. The percentage of adipocytes was calculated with respect to untreated cells (UT). Scale bar: 30 µm. Data are given as the mean ± SD measured in triplicate from five individual experiments. Data shown are from a representative experiment of five performed. **P < 0.01; ***P < 0.001 vs untreated cells (UT).

infectious or non-infectious diseases like diabetes or obesity, adipose-resident immune cells are derived to a proinflammatory phenotype due to a proinflammatory microenvironment.

In brucellosis, the tissue and cell type in which the bacteria persist during chronic infection remains unknown. Previous findings have reported the capacity of *B. abortus* for intracellular replication in several cell types (17, 21, 49). In particular, the *Brucella* capability to localize intracellularly in adipocytes and its precursors was recently revealed for *B. canis* (13, 17). Here, we show that *B. abortus* infects and replicates in both adipocyte and even with higher efficiency, in pre-adipocyte.

An impairment in adipogenesis process may involve an adipokine misbalance induced by *B. abortus* infection. Adiponectin and resistin have been associated with adipogenesis (50, 51). Leptin acts largely on the hypothalamus, informing the nutritional status of the adipocytes and controlling adipokines and the endocrine role of adipose tissues and food intake, thus regulating energy balance (23).

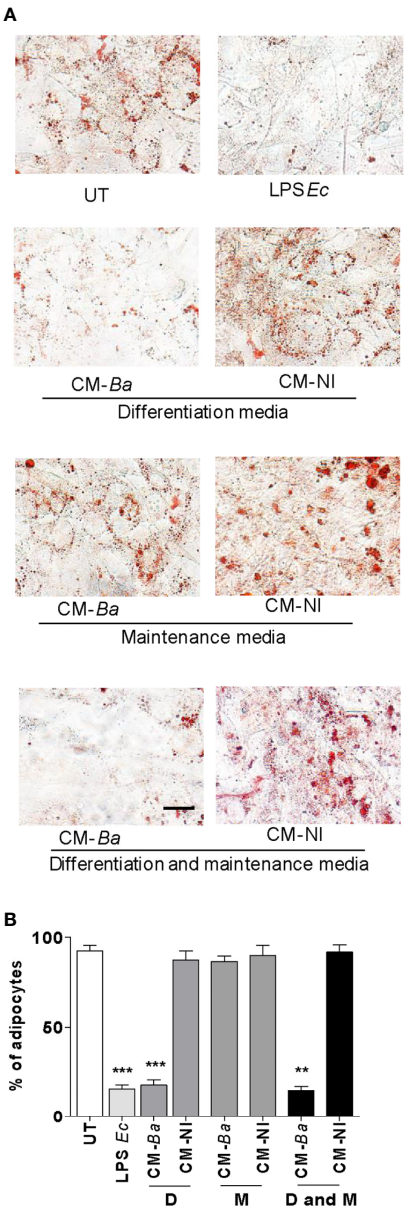

FIGURE 6 | *B. abortus*-infected macrophages modulate early adipocyte differentiation. Pre-adipocytes were differentiated in the presence of culture supernatants from *B. abortus*—infected macrophages at MOI 100 (CM-Ba) or culture supernatants from non-infected macrophages as control (CM-NI). Supernatants were added during the early differentiation process (differentiation media, D), later differentiation process (maintenance media, M) or during all differentiation process (differentiation and maintenance media, D and M). The presence of adipocytes was revealed by staining of lipid droplets with Oil Red O **(A)**. Quantification of Oil Red O was determined by cell counts **(B)**. LPS from *E. coli* (LPS *Ec*) was used as a positive control. Ten microscopic fields per well in three wells per condition were quantified for each experiment. The percentage of adipocytes was calculated to the untreated cells (UT). Scale bar: 30 µm. Data are given as the mean ± SD from three individual experiments. **P < 0.01; ***P < 0.001 vs untreated cells (UT).

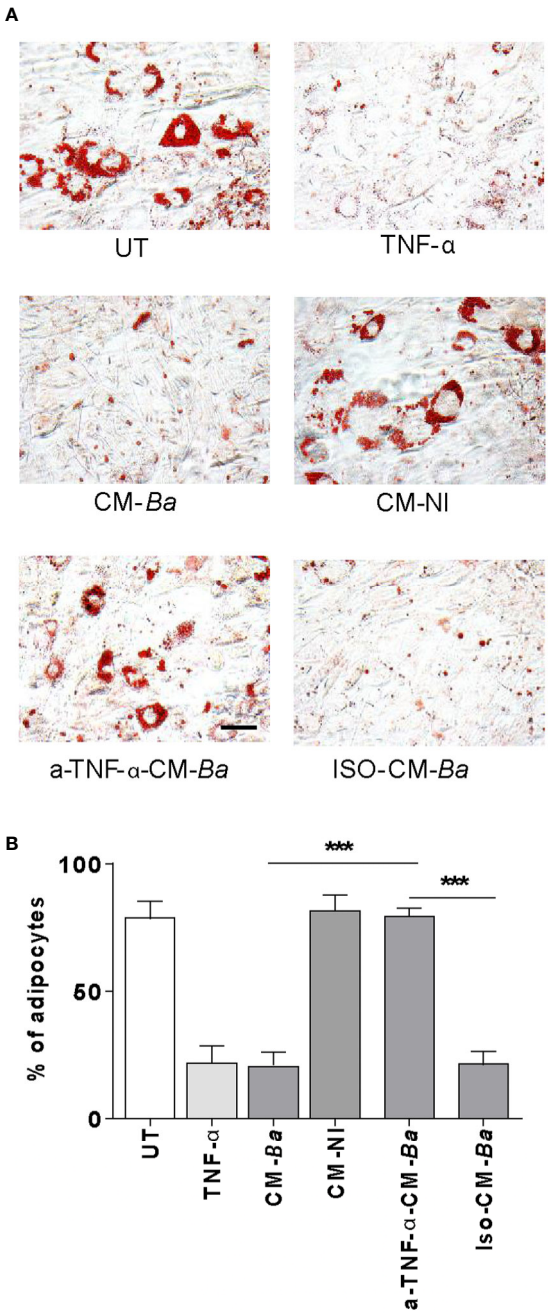

FIGURE 7 | *B. abortus*-infected macrophages inhibit adipocyte differentiation *via* a mechanism dependent on TNF-α. Pre-adipocytes were differentiated in the presence of culture supernatants from *B. abortus*-infected macrophages at MOI 100 (CM-Ba) or culture supernatants from non-infected macrophages as control (CM-NI). Supernatants were incubated with an anti-TNF-α neutralizing antibody (a-TNF-α-CM-Ba) or isotype control (ISO-CM-Ba). TNF-α (1 ng/ml) was used as a positive control. The presence of adipocytes was revealed by staining of lipid droplets with Oil Red O **(A)**. Quantification of Oil Red O was determined by cell counts **(B)**. Ten microscopic fields per well in three wells per condition were quantified for each experiment. The percentage of adipocytes was calculated to the untreated cells (UT). Scale bar: 30 μm. Data are given as the mean ± SD from three individual experiments. ***P < 0.001.

Additionally, leptin could significantly reduce lipid accumulation during the adipocyte differentiation process, indicating an inhibitory effect on adipogenesis. The loss of expression of adipokines and the acquisition of an inflammatory phenotype may also involve the secretion of IL-1β, TNF-α, and IL-6 (52). Here, we have demonstrated an increased secretion of adipokines such as IL-6, but not IL-1β and TNF-α, among infected pre-adipocytes and adipocytes after *B. abortus* infection, being higher among the former. Likewise, pre-adipocytes depict a higher number of intracellular bacteria than adipocyte cells. Considering that IL-6 could be able to inhibit the anti-inflammatory adipokines adiponectin and resistin in an autocrine and paracrine manner (53), we have measured their transcriptional level after *B. abortus* infection. For both, the mRNA level appeared significantly diminished after infection. However, although IL-6 also induces leptin production (54, 55), leptin levels were not significantly altered after infection with *Brucella abortus*. Several transcription regulators, such as PPAR-γ, C/EBP-α, and C/EBP-β are well-known to mediate adipogenesis. The main role of PPAR-γ in adipogenesis during infection has been revealed using *in vivo* models of infectious diseases (41, 44). Moreover, the expression level of the critical adipogenic transcription factor PPAR-γ was downregulated after *B. abortus* infection, thus affecting its role in the maintenance of mature adipocyte phenotype (56, 57). C/EBPα is expressed in the late phase of adipocyte differentiation. In contrast, C/EBPβ is expressed very early during adipogenesis and is also required to sustain the expression of PPAR-γ and C/EBPα. After the treatment of preadipocytes with inducers of differentiation, a rapid and transient increase in transcription and expression of C/EBPβ occurs and then decrees during the differentiation process (14). As we expected, *B. abortus* infection also inhibited C/EBPα transcription (58). On the contrary, *B. abortus* infection increases the transcription of C/EBPβ. These contradictory results could be explained, at least in part, by the fact that the transcriptional activity of C/EBPβ is regulated by several posttranscriptional modifications (59), including acetylation (60, 61), phosphorylation, and polyubiquitination (62). Additionally, it could be also speculated that overexpression of C/EBPβ may be a compensatory mechanism in response to C/EBPα reduction as was described for brown adipocyte differentiation (63). Further studies are needed to define the mechanism involved during *B. abortus* infection and the significance of this regulation.

We have observed that *B. abortus* infection of pre-adipocytes may also alter the extracellular matrix by inducing MMP-2 and MMP-9 secretion. Despite this, finding appears to be opposed to previous studies that reported that these MMPs are involved in extracellular matrix remodeling during adipocyte differentiation (15, 64, 65), two plausible explanations should be considered. First, it is known that other MMPs such as MMP-3 could have the opposite effects and down modulate the adipogenic differentiation (66, 67). Second, the MMPs action is controlled by regulators such as tissue inhibitor of metalloproteinases (TIMPs) as well as members of protease family of ADAMs (68). *In vivo*, TIMPs counterbalanced the activity of MMPs, and these complexes are dissociated during gelating zymography procedure. However, in general, in inflammatory conditions, TIMPs do not increase in the

same degree as MMPs do, thus increasing the MMP/TIMP ratio (4, 69). Accordingly, supernatants from *B. abortus*-infected pre-adipocytes produced gelatin cleavage when evaluated under native conditions in the fluid phase, with MMP-TIMP complex are not dissociated as occurs during gel electrophoresis. This indicates that other mechanisms are involved during adipogenesis inhibition by *B. abortus* infection.

Adipogenesis inhibition may be a process involving TLR-ligand interactions (37, 38). Here, we have demonstrated that *B. abortus*-mediated inhibition of the adipocyte differentiation was independent of the bacterial viability, thus insinuating a potential role elicited by a structural bacterial component. As in our previous studies, the bacteria lipoprotein L-Omp19 plays again a critical role in this sense but not the LPS (20). Such lipid moiety but not its non-lipidated counterpart U-Omp19, was able to mimic adipogenesis inhibition induced by *B. abortus* infection. The effect was elicited by the lipid moiety, which is likely shared by all bacterial lipoproteins. The genome of *B. abortus* codifies no less than 80 putative lipoproteins (70). This indicates that lipoproteins present in *Brucella* could be sufficient to modulate adipocyte physiology.

In adipose tissue, immune cells including macrophages and T cells are the main responsible for inflammatory cytokine production (71, 72). In particular, macrophages participate in adipose tissue dysfunction and reduced adipogenesis (73, 74). *Brucella* infection is accompanied by the infiltration of inflammatory cells, and the macrophages represent the main replication niche for these bacteria (75). Even though the role of macrophage polarization in the pathogenesis of *Brucella* species is poorly described until now (76, 77). Here, we have demonstrated that proinflammatory cytokines -such as TNF-α- secreted by macrophages in response to *B. abortus* infection exert an inhibitory effect on adipogenic differentiation (52). However, we cannot rule out that other cytokines are also present in the conditioned media and contribute to these observations.

Overall, these results suggest a possible scenario in which *B. abortus* infection *via* its lipoproteins modulates adipogenesis process and soluble mediators secreted by *B. abortus*—infected macrophages may contribute to this phenomenon, as a mechanism in which TNF-α is involved.

In conclusion, our results suggest that adipogenesis process could be altered directly after exposure—even without effective multiplication—of the adipocytes and their precursors to *Brucella*, or their lipoproteins. Furthermore, this same process could be indirectly altered, thanks to soluble mediators such as TNF-α released by macrophages infected by the same bacteria.

These early studies using murine cell lines provide clues regarding potential mechanisms involved during the interaction of *B. abortus* with adipocytes. Further studies using primary human adipocytes, human adipose tissue explants, and the *in vivo* murine model will be needed to confirm whether the responses described here have a role in the chronic inflammation and chronicity of the infection.

DATA AVAILABILITY STATEMENT

The raw data supporting the conclusions of this article will be made available by the authors, without undue reservation.

AUTHOR CONTRIBUTIONS

AP performed the experiments. All authors analyzed the data. MD and JQ wrote the article. MD and JQ designed the experiments, revised the article, and obtained research funding. GG performed a critical read of the manuscript. All authors contributed to the article and approved the submitted version.

FUNDING

This work was supported by grants from Agencia Nacional of Promoción Científica y Tecnológica (ANPCYT, Argentina), PICT 2014-1111, PICT 2015-0316, PICT 2017-2859 to MD and PICT-2015-1921 to JQ. Funding agencies had no role in study design, data collection and analysis, decision to publish, or preparation of the manuscript.

ACKNOWLEDGMENTS

We thank Horacio Salomón and the staff of the Instituto de Investigaciones Biomédicas en Retrovirus y Sida (INBIRS), for their assistance with biosafety level 3 laboratory uses.

REFERENCES

1. Franc, KA, Krecek, RC, Hasler, BN, and Arenas-Gamboa, AM. Brucellosis remains a neglected disease in the developing world: a call for interdisciplinary action. *BMC Public Health* (2018) 18(1):125. doi: 10.1186/s12889-017-5016-y
2. Pappas, G, Akritidis, N, Bosilkovski, M, and Tsianos, E. Brucellosis. *N Engl J Med* (2005) 352(22):2325–36. doi: 10.1056/NEJMra050570
3. Wu, BN, and O'Sullivan, AJ. Sex differences in energy metabolism need to be considered with lifestyle modifications in humans. *J Nutr Metab* (2011) 2011:391809. doi: 10.1155/2011/391809
4. Kershaw, EE, and Flier, JS. Adipose tissue as an endocrine organ. *J Clin Endocrinol Metab* (2004) 89(6):2548–56. doi: 10.1210/jc.2004-0395
5. Ouchi, N, Parker, JL, Lugus, JJ, and Walsh, K. Adipokines in inflammation and metabolic disease. *Nat Rev Immunol* (2011) 11(2):85–97. doi: 10.1038/nri2921
6. Ferrante, AW, Jr. The immune cells in adipose tissue. *Diabetes Obes Metab* (2013) 15 (Suppl 3):34–8. doi: 10.1111/dom.12154
7. Birsoy, K, Festuccia, WT, and Laplante, M. A comparative perspective on lipid storage in animals. *J Cell Sci* (2013) 126(Pt 7):1541–52. doi: 10.1242/jcs.104992
8. Bouwman, JJ, Visseren, FL, Bouter, KP, and Diepersloot, RJ. Infection-induced inflammatory response of adipocytes in vitro. *Int J Obes (Lond)* (2008) 32(6):892–901. doi: 10.1038/ijo.2008.36
9. Damouche, A, Lazure, T, Avettand-Fenoel, V, Huot, N, Dejucq-Rainsford, N, Satie, AP, et al. Adipose Tissue Is a Neglected Viral Reservoir and an Inflammatory Site during Chronic HIV and SIV Infection. *PLoS Pathog* (2015) 11(9):e1005153. doi: 10.1371/journal.ppat.1005153

10. Maurin, T, Saillan-Barreau, C, Cousin, B, Casteilla, L, Doglio, A, and Penicaud, L. Tumor necrosis factor-alpha stimulates HIV-1 production in primary culture of human adipocytes. *Exp Cell Res* (2005) 304(2):544–51. doi: 10.1016/j.yexcr.2004.12.003
11. Kim, JS, Ryu, MJ, Byun, EH, Kim, WS, Whang, J, Min, KN, et al. Differential immune response of adipocytes to virulent and attenuated Mycobacterium tuberculosis. *Microbes Infect* (2011) 13(14-15):1242–51. doi: 10.1016/j.micinf.2011.07.002
12. Poester, FP, Samartino, LE, and Santos, RL. Pathogenesis and pathobiology of brucellosis in livestock. *Rev Sci Tech* (2013) 32(1):105–15. doi: 10.20506/rst.32.1.2193
13. de Souza, TD, de Carvalho, TF, Mol, J, Lopes, JVM, Silva, MF, da Paixao, TA, et al. Tissue distribution and cell tropism of Brucella canis in naturally infected canine foetuses and neonates. *Sci Rep* (2018) 8(1):7203. doi: 10.1038/s41598-018-25651-x
14. Darlington, GJ, Ross, SE, and MacDougald, OA. The role of C/EBP genes in adipocyte differentiation. *J Biol Chem* (1998) 273(46):30057–60. doi: 10.1074/jbc.273.46.30057
15. Bouloumie, A, Sengenes, C, Portolan, G, Galitzky, J, and Lafontan, M. Adipocyte produces matrix metalloproteinases 2 and 9: involvement in adipose differentiation. *Diabetes* (2001) 50(9):2080–6. doi: 10.2337/diabetes.50.9.2080
16. Kuri-Harcuch, W, Velez-delValle, C, Vazquez-Sandoval, A, Hernandez-Mosqueira, C, and Fernandez-Sanchez, V. A cellular perspective of adipogenesis transcriptional regulation. *J Cell Physiol* (2019) 234(2):1111–29. doi: 10.1002/jcp.27060
17. Smith, JA, Khan, M, Magnani, DD, Harms, JS, Durward, M, Radhakrishnan, GK, et al. Brucella induces an unfolded protein response via TcpB that supports intracellular replication in macrophages. *PLoS Pathog* (2013) 9(12):e1003785. doi: 10.1371/journal.ppat.1003785
18. Sha, H, He, Y, Chen, H, Wang, C, Zenno, A, Shi, H, et al. The IRE1alpha-XBP1 pathway of the unfolded protein response is required for adipogenesis. *Cell Metab* (2009) 9(6):556–64. doi: 10.1016/j.cmet.2009.04.009
19. Scian, R, Barrionuevo, P, Fossati, CA, Giambartolomei, GH, and Delpino, MV. Brucella abortus invasion of osteoblasts inhibits bone formation. *Infect Immun* (2012) 80(7):2333–45. doi: 10.1128/IAI.00208-12
20. Giambartolomei, GH, Zwerdling, A, Cassataro, J, Bruno, L, Fossati, CA, and Philipp, MT. Lipoproteins, not lipopolysaccharide, are the key mediators of the proinflammatory response elicited by heat-killed Brucella abortus. *J Immunol* (2004) 173(7):4635–42. doi: 10.4049/jimmunol.173.7.4635
21. Scian, R, Barrionuevo, P, Giambartolomei, GH, Fossati, CA, Baldi, PC, and Delpino, MV. Granulocyte-macrophage colony-stimulating factor- and tumor necrosis factor alpha-mediated matrix metalloproteinase production by human osteoblasts and monocytes after infection with Brucella abortus. *Infect Immun* (2011) 79(1):192–202. doi: 10.1128/IAI.00934-10
22. Hibbs, MS, Hasty, KA, Seyer, JM, Kang, AH, and Mainardi, CL. Biochemical and immunological characterization of the secreted forms of human neutrophil gelatinase. *J Biol Chem* (1985) 260(4):2493–500.
23. Giralt, M, Cereijo, R, and Villarroya, F. Adipokines and the Endocrine Role of Adipose Tissues. *Handb Exp Pharmacol* (2016) 233:265–82. doi: 10.1007/164_2015_6
24. Schram, K, and Sweeney, G. Implications of myocardial matrix remodeling by adipokines in obesity-related heart failure. *Trends Cardiovasc Med* (2008) 18(6):199–205. doi: 10.1016/j.tcm.2008.10.001
25. Park, HY, Kwon, HM, Lim, HJ, Hong, BK, Lee, JY, Park, BE, et al. Potential role of leptin in angiogenesis: leptin induces endothelial cell proliferation and expression of matrix metalloproteinases in vivo and in vitro. *Exp Mol Med* (2001) 33(2):95–102. doi: 10.1038/emm.2001.17
26. Moon, HS, Lee, HG, Seo, JH, Chung, CS, Guo, DD, Kim, TG, et al. Leptin-induced matrix metalloproteinase-2 secretion is suppressed by trans-10,cis-12 conjugated linoleic acid. *Biochem Biophys Res Commun* (2007) 356(4):955–60. doi: 10.1016/j.bbrc.2007.03.068
27. Oku, T, Shimada, K, Kenmotsu, H, Ando, Y, Kurisaka, C, Sano, R, et al. Stimulation of Peritoneal Mesothelial Cells to Secrete Matrix Metalloproteinase-9 (MMP-9) by TNF-alpha: A Role in the Invasion of Gastric Carcinoma Cells. *Int J Mol Sci* (2018) 19(12):1–14. doi: 10.3390/ijms19123961
28. Harris, JE, Fernandez-Vilaseca, M, Elkington, PT, Horncastle, DE, Graeber, MB, and Friedland, JS. IFNgamma synergizes with IL-1beta to up-regulate MMP-9 secretion in a cellular model of central nervous system tuberculosis. *FASEB J* (2007) 21(2):356–65. doi: 10.1096/fj.06-6925com
29. Kohno, Y, Tanimoto, A, Cirathaworn, C, Shimajiri, S, Tawara, A, and Sasaguri, Y. GM-CSF activates RhoA, integrin and MMP expression in human monocytic cells. *Pathol Int* (2004) 54(9):693–702. doi: 10.1111/j.1440-1827.2004.01682.x
30. Krubasik, D, Eisenach, PA, Kunz-Schughart, LA, Murphy, G, and English, WR. Granulocyte-macrophage colony stimulating factor induces endothelial capillary formation through induction of membrane-type 1 matrix metalloproteinase expression in vitro. *Int J Cancer* (2008) 122(6):1261–72. doi: 10.1002/ijc.23234
31. Brinckerhoff, CE, and Matrisian, LM. Matrix metalloproteinases: a tail of a frog that became a prince. *Nat Rev Mol Cell Biol* (2002) 3(3):207–14. doi: 10.1038/nrm763
32. Delpino, MV, Barrionuevo, P, Macedo, GC, Oliveira, SC, Genaro, SD, Scian, R, et al. Macrophage-elicited osteoclastogenesis in response to Brucella abortus infection requires TLR2/MyD88-dependent TNF-alpha production. *J Leukoc Biol* (2012) 91(2):285–98. doi: 10.1189/jlb.04111185
33. Garcia Samartino, C, Delpino, MV, Pott Godoy, C, Di Genaro, MS, Pasquevich, KA, Zwerdling, A, et al. Brucella abortus induces the secretion of proinflammatory mediators from glial cells leading to astrocyte apoptosis. *Am J Pathol* (2010) 176(3):1323–38. doi: 10.2353/ajpath.2010.090503
34. Scian, R, Barrionuevo, P, Giambartolomei, GH, De Simone, EA, Vanzulli, SI, Fossati, CA, et al. Potential role of fibroblast-like synoviocytes in joint damage induced by Brucella abortus infection through production and induction of matrix metalloproteinases. *Infect Immun* (2011) 79(9):3619–32. doi: 10.1128/IAI.05408-11
35. Zwerdling, A, Delpino, MV, Barrionuevo, P, Cassataro, J, Pasquevich, KA, Garcia Samartino, C, et al. Brucella lipoproteins mimic dendritic cell maturation induced by Brucella abortus. *Microbes Infect* (2008) 10(12-13):1346–54. doi: 10.1016/j.micinf.2008.07.035
36. Zwerdling, A, Delpino, MV, Pasquevich, KA, Barrionuevo, P, Cassataro, J, Garcia Samartino, C, et al. Brucella abortus activates human neutrophils. *Microbes Infect* (2009) 11(6-7):689–97. doi: 10.1016/j.micinf.2009.04.010
37. Aamir, K, Khan, HU, Sethi, G, Hossain, MA, and Arya, A. Wnt signaling mediates TLR pathway and promote unrestrained adipogenesis and metaflammation: Therapeutic targets for obesity and type 2 diabetes. *Pharmacol Res* (2020) 152:104602. doi: 10.1016/j.phrs.2019.104602
38. Ajuwon, KM, Banz, W, and Winters, TA. Stimulation with Peptidoglycan induces interleukin 6 and TLR2 expression and a concomitant downregulation of expression of adiponectin receptors 1 and 2 in 3T3-L1 adipocytes. *J Inflamm (Lond)* (2009) 6:8. doi: 10.1186/1476-9255-6-8
39. Baldwin, CL, and Winter, AJ. Macrophages and Brucella. *Immunol Ser* (1994) 60:363–80.
40. Cawthorn, WP, Heyd, F, Hegyi, K, and Sethi, JK. Tumour necrosis factor-alpha inhibits adipogenesis via a beta-catenin/TCF4(TCF7L2)-dependent pathway. *Cell Death Differ* (2007) 14(7):1361–73. doi: 10.1038/sj.cdd.4402127
41. Ayyappan, JP, Ganapathi, U, Lizardo, K, Vinnard, C, Subbian, S, Perlin, DS, et al. Adipose Tissue Regulates Pulmonary Pathology during TB Infection. *mBio* (2019) 10(2):1–16. doi: 10.1128/mBio.02771-18
42. Nagajyothi, JF, and Weiss, LM. Advances in understanding the role of adipose tissue and mitochondrial oxidative stress in Trypanosoma cruzi infection. *F1000Res* (2019) 8:1–7. doi: 10.12688/f1000research.19190.1
43. Lizardo, K, Ayyappan, JP, Cui, MH, Balasubramanya, R, Jelicks, LA, and Nagajyothi, JF. High fat diet aggravates cardiomyopathy in murine chronic Chagas disease. *Microbes Infect* (2019) 21(1):63–71. doi: 10.1016/j.micinf.2018.07.001
44. Gonzalez, FB, Villar, SR, Toneatto, J, Pacini, MF, Marquez, J, D'Attilio, L, et al. Immune response triggered by Trypanosoma cruzi infection strikes adipose tissue homeostasis altering lipid storage, enzyme profile and adipokine expression. *Med Microbiol Immunol* (2019) 208(5):651–66. doi: 10.1007/s00430-018-0572-z
45. Wanjalla, CN, McDonnell, WJ, and Koethe, JR. Adipose Tissue T Cells in HIV/SIV Infection. *Front Immunol* (2018) 9:2730. doi: 10.3389/fimmu.2018.02730
46. Neyrolles, O, Hernandez-Pando, R, Pietri-Rouxel, F, Fornes, P, Tailleux, L, Barrios Payan, JA, et al. Is adipose tissue a place for Mycobacterium

tuberculosis persistence? *PLoS One* (2006) 1:e43. doi: 10.1371/journal.pone.0000043
47. Combs, TP, Nagajyothi, Mukherjee, S, de Almeida, CJ, Jelicks, LA, Schubert, W, et al. The adipocyte as an important target cell for Trypanosoma cruzi infection. *J Biol Chem* (2005) 280(25):24085–94. doi: 10.1074/jbc.M412802200
48. Esteve Rafols, M. Adipose tissue: cell heterogeneity and functional diversity. *Endocrinol Nutr* (2014) 61(2):100–12. doi: 10.1016/j.endonu.2013.03.011
49. Arriola Benitez, PC, Scian, R, Comerci, DJ, Serantes, DR, Vanzulli, S, Fossati, CA, et al. Brucella abortus induces collagen deposition and MMP-9 down-modulation in hepatic stellate cells via TGF-beta1 production. *Am J Pathol* (2013) 183(6):1918–27. doi: 10.1016/j.ajpath.2013.08.006
50. Ikeda, Y, Tsuchiya, H, Hama, S, Kajimoto, K, and Kogure, K. Resistin affects lipid metabolism during adipocyte maturation of 3T3-L1 cells. *FEBS J* (2013) 280(22):5884–95. doi: 10.1111/febs.12514
51. Fu, Y, Luo, N, Klein, RL, and Garvey, WT. Adiponectin promotes adipocyte differentiation, insulin sensitivity, and lipid accumulation. *J Lipid Res* (2005) 46(7):1369–79. doi: 10.1194/jlr.M400373-JLR200
52. Jiang, N, Li, Y, Shu, T, and Wang, J. Cytokines and inflammation in adipogenesis: an updated review. *Front Med* (2019) 13(3):314–29. doi: 10.1007/s11684-018-0625-0
53. Fasshauer, M, Kralisch, S, Klier, M, Lossner, U, Bluher, M, Klein, J, et al. Adiponectin gene expression and secretion is inhibited by interleukin-6 in 3T3-L1 adipocytes. *Biochem Biophys Res Commun* (2003) 301(4):1045–50. doi: 10.1016/s0006-291x(03)00090-1
54. Wueest, S, and Konrad, D. The role of adipocyte-specific IL-6-type cytokine signaling in FFA and leptin release. *Adipocyte* (2018) 7(3):226–8. doi: 10.1080/21623945.2018.1493901
55. Trujillo, ME, Sullivan, S, Harten, I, Schneider, SH, Greenberg, AS, and Fried, SK. Interleukin-6 regulates human adipose tissue lipid metabolism and leptin production in vitro. *J Clin Endocrinol Metab* (2004) 89(11):5577–82. doi: 10.1210/jc.2004-0603
56. Nielsen, R, Pedersen, TA, Hagenbeek, D, Moulos, P, Siersbaek, R, Megens, E, et al. Genome-wide profiling of PPARgamma:RXR and RNA polymerase II occupancy reveals temporal activation of distinct metabolic pathways and changes in RXR dimer composition during adipogenesis. *Genes Dev* (2008) 22(21):2953–67. doi: 10.1101/gad.501108
57. Lefterova, MI, Zhang, Y, Steger, DJ, Schupp, M, Schug, J, Cristancho, A, et al. PPARgamma and C/EBP factors orchestrate adipocyte biology via adjacent binding on a genome-wide scale. *Genes Dev* (2008) 22(21):2941–52. doi: 10.1101/gad.1709008
58. Lechner, S, Mitterberger, MC, Mattesich, M, and Zwerschke, W. Role of C/EBPbeta-LAP and C/EBPbeta-LIP in early adipogenic differentiation of human white adipose-derived progenitors and at later stages in immature adipocytes. *Differentiation* (2013) 85(1-2):20–31. doi: 10.1016/j.diff.2012.11.001
59. Nerlov, C. C/EBPs: recipients of extracellular signals through proteome modulation. *Curr Opin Cell Biol* (2008) 20(2):180–5. doi: 10.1016/j.ceb.2008.02.002
60. Cesena, TI, Cardinaux, JR, Kwok, R, and Schwartz, J. CCAAT/enhancer-binding protein (C/EBP) beta is acetylated at multiple lysines: acetylation of C/EBPbeta at lysine 39 modulates its ability to activate transcription. *J Biol Chem* (2007) 282(2):956–67. doi: 10.1074/jbc.M511451200
61. Wiper-Bergeron, N, Salem, HA, Tomlinson, JJ, Wu, D, and Hache, RJ. Glucocorticoid-stimulated preadipocyte differentiation is mediated through acetylation of C/EBPbeta by GCN5. *Proc Natl Acad Sci U S A* (2007) 104(8):2703–8. doi: 10.1073/pnas.0607378104
62. Hattori, T, Ohoka, N, Inoue, Y, Hayashi, H, and Onozaki, K. C/EBP family transcription factors are degraded by the proteasome but stabilized by forming dimer. *Oncogene* (2003) 22(9):1273–80. doi: 10.1038/sj.onc.1206204
63. Linhart, HG, Ishimura-Oka, K, DeMayo, F, Kibe, T, Repka, D, Poindexter, B, et al. C/EBPalpha is required for differentiation of white, but not brown, adipose tissue. *Proc Natl Acad Sci U S A* (2001) 98(22):12532–7. doi: 10.1073/pnas.211416898
64. Chavey, C, Mari, B, Monthouel, MN, Bonnafous, S, Anglard, P, Van Obberghen, E, et al. Matrix metalloproteinases are differentially expressed in adipose tissue during obesity and modulate adipocyte differentiation. *J Biol Chem* (2003) 278(14):11888–96. doi: 10.1074/jbc.M209196200
65. Lilla, J, Stickens, D, and Werb, Z. Metalloproteases and adipogenesis: a weighty subject. *Am J Pathol* (2002) 160(5):1551–4. doi: 10.1016/S0002-9440(10)61100-5
66. Woessner, JFJr. MMPs and TIMPs. An historical perspective. *Methods Mol Biol* (2001) 151:1–23. doi: 10.1385/MB:22:1:033
67. Alexander, CM, Selvarajan, S, Mudgett, J, and Werb, Z. Stromelysin-1 regulates adipogenesis during mammary gland involution. *J Cell Biol* (2001) 152(4):693–703. doi: 10.1083/jcb.152.4.693
68. Brew, K, and Nagase, H. The tissue inhibitors of metalloproteinases (TIMPs): an ancient family with structural and functional diversity. *Biochim Biophys Acta* (2010) 1803(1):55–71. doi: 10.1016/j.bbamcr.2010.01.003
69. Malemud, CJ, Islam, N, and Haqqi, TM. Pathophysiological mechanisms in osteoarthritis lead to novel therapeutic strategies. *Cells Tissues Organs* (2003) 174(1-2):34–48. doi: 10.1159/000070573
70. Chain, PS, Comerci, DJ, Tolmasky, ME, Larimer, FW, Malfatti, SA, Vergez, LM, et al. Whole-genome analyses of speciation events in pathogenic Brucellae. *Infect Immun* (2005) 73(12):8353–61. doi: 10.1128/IAI.73.12.8353-8361.2005
71. Weisberg, SP, McCann, D, Desai, M, Rosenbaum, M, Leibel, RL, and Ferrante, AWJr. Obesity is associated with macrophage accumulation in adipose tissue. *J Clin Invest* (2003) 112(12):1796–808. doi: 10.1172/JCI19246
72. Wu, H, Ghosh, S, Perrard, XD, Feng, L, Garcia, GE, Perrard, JL, et al. T-cell accumulation and regulated on activation, normal T cell expressed and secreted upregulation in adipose tissue in obesity. *Circulation* (2007) 115(8):1029–38. doi: 10.1161/CIRCULATIONAHA.106.638379
73. Constant, VA, Gagnon, A, Landry, A, and Sorisky, A. Macrophage-conditioned medium inhibits the differentiation of 3T3-L1 and human abdominal preadipocytes. *Diabetologia* (2006) 49(6):1402–11. doi: 10.1007/s00125-006-0253-0
74. Lacasa, D, Taleb, S, Keophiphath, M, Miranville, A, and Clement, K. Macrophage-secreted factors impair human adipogenesis: involvement of proinflammatory state in preadipocytes. *Endocrinology* (2007) 148(2):868–77. doi: 10.1210/en.2006-0687
75. Atluri, VL, Xavier, MN, de Jong, MF, den Hartigh, AB, and Tsolis, RM. Interactions of the human pathogenic Brucella species with their hosts. *Annu Rev Microbiol* (2011) 65:523–41. doi: 10.1146/annurev-micro-090110-102905
76. Wang, Y, Li, Y, Li, H, Song, H, Zhai, N, Lou, L, et al. Brucella Dysregulates Monocytes and Inhibits Macrophage Polarization through LC3-Dependent Autophagy. *Front Immunol* (2017) 8:691. doi: 10.3389/fimmu.2017.00691
77. Thiriot, JD, Martinez-Martinez, YB, Endsley, JJ, and Torres, AG. Hacking the host: exploitation of macrophage polarization by intracellular bacterial pathogens. *Pathog Dis* (2020) 78(1):1–14. doi: 10.1093/femspd/ftaa009

Conflict of Interest: The authors declare that the research was conducted in the absence of any commercial or financial relationships that could be construed as a potential conflict of interest.

frontiers in Endocrinology

ORIGINAL RESEARCH
published: 29 September 2020
doi: 10.3389/fendo.2020.572113

Leptin Elicits *In Vivo* Eosinophil Migration and Activation: Key Role of Mast Cell-Derived PGD_2

Natália R. T. Amorim[1], Glaucia Souza-Almeida[2,3], Tatiana Luna-Gomes[1,4], Patricia T. Bozza[2], Claudio Canetti[1], Bruno L. Diaz[1], Clarissa M. Maya-Monteiro[2†] and Christianne Bandeira-Melo[1*†]*

[1] Laboratório de Inflamação, Instituto de Biofísica Carlos Chagas Filho, Universidade Federal do Rio de Janeiro, Rio de Janeiro, Brazil, [2] Laboratório de Imunofarmacologia, Instituto Oswaldo Cruz - IOC, FIOCRUZ, Rio de Janeiro, Brazil, [3] Laboratório de Imunoinflamação, Instituto de Biologia, Universidade de Campinas, Campinas, Brazil, [4] Departamento de Ciências da Natureza, Instituto de Aplicação Fernando Rodrigues da Silveira, Universidade do Estado do Rio de Janeiro, Rio de Janeiro, Brazil

OPEN ACCESS

Edited by:
Jae B. Kim,
Seoul National University, South Korea

Reviewed by:
Akos Heinemann,
Medical University of Graz, Austria
Jong Bae Seo,
Mokpo National University, South Korea
Jiyoung Park,
Ulsan National Institute of Science and Technology, South Korea

***Correspondence:**
Christianne Bandeira-Melo
cbmelo@biof.ufrj.br
Clarissa M. Maya-Monteiro
clarissa@ioc.fiocruz.br

†These authors have contributed equally to this work and share senior authorship

Specialty section:
This article was submitted to Cellular Endocrinology, a section of the journal Frontiers in Endocrinology

Received: 12 June 2020
Accepted: 09 September 2020
Published: 29 September 2020

Citation:
Amorim NRT, Souza-Almeida G, Luna-Gomes T, Bozza PT, Canetti C, Diaz BL, Maya-Monteiro CM and Bandeira-Melo C (2020) Leptin Elicits In Vivo Eosinophil Migration and Activation: Key Role of Mast Cell-Derived PGD_2. Front. Endocrinol. 11:572113. doi: 10.3389/fendo.2020.572113

Eosinophils are key regulators of adipose tissue homeostasis, thus characterization of adipose tissue-related molecular factors capable of regulating eosinophil activity is of great interest. Leptin is known to directly activate eosinophils *in vitro*, but leptin ability of inducing *in vivo* eosinophilic inflammatory response remains elusive. Here, we show that leptin elicits eosinophil influx as well as its activation, characterized by increased lipid body biogenesis and LTC_4 synthesis. Such leptin-triggered eosinophilic inflammatory response was shown to be dependent on activation of the mTOR signaling pathway, since it was (i) inhibited by rapamycin pre-treatment and (ii) reduced in PI3K-deficient mice. Local infiltration of activated eosinophils within leptin-driven inflammatory site was preceded by increased levels of classical mast cell-derived molecules, including TNFα, CCL5 (RANTES), and PGD_2. Thus, mice were pre-treated with a mast cell degranulating agent compound 48/80 which was capable to impair leptin-induced PGD_2 release, as well as eosinophil recruitment and activation. In agreement with an indirect mast cell-driven phenomenon, eosinophil accumulation induced by leptin was abolished in TNFR-1 deficient and also in HQL-79–pretreated mice, but not in mice pretreated with neutralizing antibodies against CCL5, indicating that both typical mast cell-driven signals TNFα and PGD_2, but not CCL5, contribute to leptin-induced eosinophil influx. Distinctly, leptin-induced eosinophil lipid body (lipid droplet) assembly and LTC_4 synthesis appears to depend on both PGD_2 and CCL5, since both HQL-79 and anti-CCL5 treatments were able to inhibit these eosinophil activation markers. Altogether, our data show that leptin triggers eosinophilic inflammation *in vivo via* an indirect mechanism dependent on activation of resident mast cell secretory activity and mediation by TNFα, CCL5, and specially PGD_2.

Keywords: eosinophils, mast cells, lipid droplets, leptin, prostaglandin D2, leukotriene C4, RANTES, TNF-alpha

INTRODUCTION

Eosinophils are recognized as classical effectors of Type 2 immune responses; and yet, eosinophil anti-helminthic and allergy-related deleterious roles are continually reexamined, with frequent descriptions of novel eosinophil-driven molecular mechanisms emerging all the time (1). Moreover, recent groundbreaking studies had further widened the understanding of eosinophil functions from disease-related pro-inflammatory to homeostatic immunomodulatory roles (2, 3). Eosinophils are now acknowledged as key regulators of adipose tissue homeostasis, with roles in control of thermogenic energy expenditure and resident macrophages modulation (4, 5). Therefore, characterization of adipose tissue-related molecular factors capable of regulating eosinophil activity is of particular interest.

Leptin is a pleiotropic adipose tissue-derived cytokine with significant immuno-neuro-endocrine roles (6). Leptin is considered a key factor to integrate adipose tissue with the systemic metabolism (7). Also, many studies have demonstrated important roles of leptin within the adaptative and innate immune systems regulation, inflammation and response to infection (8–12). Our hypothesis is that leptin is a key physiological stimulus that modulates adipose eosinophils, since (i) significant leptin levels are present in either lean or obese adipose tissue; (ii) adipose eosinophils are continuously exposed to adipocyte-derived leptin; (iii) the full length leptin receptor is present on eosinophil surface (13); and (iv) leptin is known to activate human and mouse eosinophils *in vitro*. Indeed, stimulation of eosinophils with leptin directly elicits a variety of activities, including: survival, chemokinesis (14, 15), secretion of cytokines (14), lipid body biogenesis, as well as synthesis of lipid mediators as prostaglandins (PGs) and leukotrienes (16). Straightforward research aiming to characterize the direct impact of *in situ* leptin on triggering eosinophil recruitment and activation are still missing, despite the fact that some reports indicate that leptin may regulate eosinophils in low-*versus* high-fat diets mouse models of obesity (17, 18).

Numerous studies on the cellular mechanisms governing allergy-driven inflammatory diseases have established mast cells as canonical orchestrators of eosinophilic inflammation (19, 20). Ubiquitously distributed in tissues and preferentially localized in close proximity to vascular vessels, mast cells are strategically localized and ready to coordinate eosinophil recruitment and activation under specific stimulation. Among mast cell repertoire of molecules responsible for eliciting both eosinophil migration to sites of allergic reaction and *in situ* activation of infiltrating eosinophils, important examples are the cytokines IL-5 and eotaxin (19, 20), as well as *de novo* synthesized lipid mediators notably PGD_2 (21). Furthermore, mast cells do express bioactive leptin receptors (22), whose stimulation is able to trigger activation of mast cells secretory activities (23). More importantly, mast cells are able to intermediate leptin effects in even non-conventional mast cell-regulated physiological conditions, like for instance leptin-induced altered sympathetic activity (24), diarrhea-predominant irritable bowel syndrome (25) or coronary atherosclerosis (26). Therefore, it seems reasonable to hypothesize that activation of leptin receptor in mast cells would be capable to elicit one of the utmost archetypal functions of mast cells—the induction of eosinophilic reactions.

Our study aims to investigate the ability of leptin to trigger *in vivo* eosinophilic inflammation, characterized by cell migration and cellular activation. Without any disregard to potential direct impacts of exogenous leptin on eosinophils *in vivo*—as well-established by a series of *in vitro* studies, including one of ours (16)—here, efforts were focused on characterizing indirect mast cell-driven effects of leptin on triggering eosinophilic response *in vivo*. We further defined the roles of mast cell-derived molecules on leptin-elicited eosinophil response, identifying PGD_2 as a key mediator.

MATERIAL AND METHODS

Animals

We used male mice of different strains: C57BL/6, BALB/cBALB/c tumor necrosis factor receptor 1-deficient ($TNFR1^{-/-}$; C57BL/6 background), and PI3Kγ-deficient ($PI3K\gamma^{-/-}$; C57BL/6 background) mice and respective wild types (WTs), obtained as previously described (27). Mice were from either the CCS/UFRJ or FIOCRUZ breeding centers, raised and maintained under the same housing conditions. All animal care and experimental protocols were conducted following the guidelines of the Brazilian Council for Care and Use of Experimentation Animals (CONCEA). The Animal Use Welfare Committees of both Federal University of Rio de Janeiro (CEUA-CCS/UFRJ license number 090/18) and Oswaldo Cruz Institute (CEUA-IOC license number L-011/2015) approved all protocols used in this study.

Mouse Models of Leptin-Induced Eosinophilic Inflammation

Two distinct approaches of leptin *in vivo* stimulation to trigger eosinophil inflammatory response were performed: (i) intraperitoneal (i.p.) administration of murine leptin (0.5, 1, or 2 mg/kg; Peprotech) or its vehicle (sterile LPS-free saline) in naive mice of C57BL/6 background (as indicated) (8); or (ii) intrapleural (i.pl.) injection of leptin (0.5, 1, or 2 mg/kg) or its vehicle (sterile LPS-free saline) in naïve or in previously sensitized BALB/cBALB/c mice (as indicated). As previously described (28), mice were sensitized with a subcutaneous (s.c.) injection (0.2 ml) of ovalbumin (OVA; 50 μg; Sigma-Aldrich) and $Al(OH)_3$ (5 mg) in 0.9% NaCl solution (sterile saline) at days 1 and 7. Animals were euthanized 6 or 24 h after leptin administration. Peritoneal and pleural cavities were rinsed with 3 and 0.5 ml of HBSS (Hank's balanced salted solution), respectively. Total leukocyte count was performed in Neubauer chambers and differential eosinophil count in May-Grunwald-Giemsa stained cytospin slides in a blinded fashion.

Treatments to study the involvement of mTOR pathway in leptin-elicited eosinophil influx, C57BL/6 mice received three i.p. injections of rapamycin (12.5 μg/kg; Sigma-Aldrich), 12 h and 15 min before, and 12 h after leptin or saline challenge (8), followed by the peritoneal lavage at 24 h after challenge. For

determination of CCL5 and PGD_2 potential role in leptin-induced eosinophilic inflammation, sensitized BALB/cBALB/c mice were treated, respectively, either by means of i.pl. injection of neutralizing antibody anti-CCL5 (10 μg/cavity; Peprotech) or i.p. injection of selective inhibitor of PGD synthase HQL-79 (1 mg/kg; Cayman Chemicals), both 1 h before leptin injection. To investigate the participation of resident mast cells on leptin-induced eosinophilic reaction, sensitized BALB/cBALB/c mice were treated by means of local (i.pl.) injection of mast cell degranulating agent compound 48/80 (12 μg/cavity; Sigma-Aldrich) 72 h before leptin i.pl. administration (29). The efficacy of a selective impact on resident mast cell population was ascertained by absence of toluidine blue-stained cells in pleural lavage with no changes in other pleural cell populations.

Production and Stimulation of Bone Marrow-Derived Mast Cells (BMMC)

With slight modifications, mast cells were differentiated *in vitro* from mouse bone marrow cells as previously described (30). Briefly, femurs and tibiae bone marrow of BALB/cBALB/c mice were rinsed with RPMI 1640, and cells were then cultured at 10^3 cells/ml in medium containing IL-3 (2 ng/ml; Peprotech), 20% FBS (VitroCell), 100 IU/ml penicillin, and 10 μg/ml streptomycin (cell medium was replaced on days 7, 14, 21, and 28). After 4 weeks, more than 99% of the cells in the culture were mast cells with characteristic metachromatic granules as assessed by toluidine blue staining. Cell viability was always >95% as determined by Trypan blue exclusion.

To study mast cell activation, bone marrow-differentiated mast cells (3×10^6 cells/ml) in HBSS were pre-treated or not with HQL-79 (10 μM) for 30 min and then incubated with murine leptin (50 nM; Peprotech) for 1 h at 37°C. Cells were then pelleted at 200 × *g*, and supernatants were stored at −80°C for further measurements. It is noteworthy to mention that classical mast cell stimuli, including IgE receptor crosslinking or SCF, typically evoke at least 100× larger responses than leptin effect, reaching levels of ng of PGD_2 or $LTC_4/10^6$ BMMC within 1 h of *in vitro* stimulation.

Measurements of Mediators Release

The lipid mediators PGD_2 and cysteinyl LTs (cysLTs; as a surrogate marker of LTC_4 synthesis) found either in cell-free pleural fluids or mast cell supernatants were detected by commercial EIA kits, according to the manufacturer´s instructions (Cayman Chemicals). The levels of TNFα and CCL5 found in cell-free peritoneal lavages or pleural fluids were quantified by Duo Set ELISA kits, according to manufacturer's protocol (R&D Systems). For determination of secretory granule exocytosis, release of β-hexosaminidase was measured in the supernatant and lysed cell pellets, as described (31, 32).

Lipid Body Staining and Enumeration

For lipid body counting, cells in cytospin slides were fixed in 3.7% formaldehyde and stained with 1.5% OsO_4 in 0.1 M cacodylate buffer, as previously described (16). Fifty consecutively eosinophils/slide were evaluated in a blinded fashion by more than one observer by bright field microscopy.

Statistical Analysis

Results are expressed as the mean ± SEM. *In vivo* data were analyzed by one-way ANOVA followed by Student-Newman-Keuls test. *In vitro* results regarding leptin-stimulated mast cells were analyzed by paired *t*-test. Differences were considered to be significant when $p < 0.05$.

RESULTS

Leptin Elicits Both Eosinophil Migration and Activation *In Vivo*

Eosinophils express leptin receptors, whose direct activation *in vitro* induces mobility, rapid assembly of cytoplasmic lipid bodies (also known as lipid droplets) as well as eicosanoid synthesis (16). Firstly, we aimed to establish whether leptin is capable to trigger an eosinophilic inflammatory response *in vivo*, comprising both cell recruitment and activation. As shown in **Figures 1**, **2**, leptin was able to elicit eosinophil migration into its site of administration. In naïve C57BL/6 mice leptin triggered peritoneal eosinophil accumulation within 24 h in a dose-dependent manner (**Figure 1B**); but not in a selective fashion, since neutrophils also accumulate in response to leptin administration (8). Such effect is dependent on the PI3K/mTOR activation, known to be downstream the leptin receptor signaling. As shown in **Figures 1C, D**, respectively, either pharmacological treatment with rapamycin or the use of $PI3K\gamma^{-/-}$ mice impaired leptin-induced eosinophil recruitment. Of note, $PI3K\gamma^{-/-}$ mice show no defects on bone marrow production or blood availability of eosinophils (33).

Although significant and reproducible, the discreet phenomenon achieved by leptin in naïve C57BL/6 mice demanded experimental adjustments to allow mechanistic studies. Aiming at a more prominent reaction which would enable characterization of cellular and molecular mechanisms involved in leptin-induced eosinophil inflammation *in vivo*, we evaluated the profile of leptin administration in BALB/cBALB/c mice (**Figure 2A**)—a mouse strain known to be more predisposed to mount eosinophil-enriched inflammatory responses (34, 35). Nevertheless, in naïve BALB/cBALB/c mice just a small eosinophilia of about 2×10^5 eosinophils per cavity (similar magnitude observed in naïve C57BL/6 mice) was observed at sites of leptin administration (0.5, 1, or 2 mg/kg; i.pl.) within 24 h (**Figure 2C**). Also, leptin-triggered pleural eosinophil population from naïve BALB/c mice did not display signs of cellular activation; neither lipid body biogenesis nor LTC_4 synthesis (**Figure 2C**). In order to favor a robust eosinophil influx in conjunction with cellular activation of infiltrating eosinophils, we moved to a strategy previously described for other eosinophilic stimuli using a protocol of pre-sensitization of BALB/c mice (**Figure 2B**) (28). As shown in **Figure 2D**, the leptin injection (1mg/kg; i.pl.) into previously sensitized BALB/c mice induced: (i) a modest but significant eosinophil accumulation as soon as 6 h after leptin stimulation; (ii) a major pleural eosinophilia within 24 h, that reached a magnitude about 6 times higher than that triggered by leptin in naïve BALB/c mice; (iii) a selective pleural eosinophilic phenomenon, since no pleural neutrophilia or increased numbers of mononuclear cells were found in parallel to 6 and 24 h eosinophil

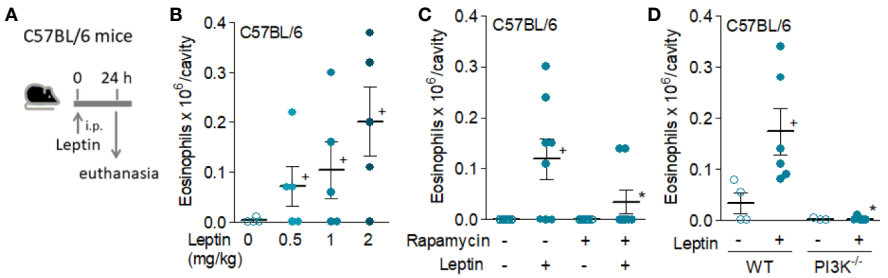

FIGURE 1 | *Leptin induces in vivo eosinophil migration in naive C57/BL6 mice by a mechanism involving activation of mTOR and PI3K.* Panel **(A)** shows a brief schematic representation of the peritonitis model induced by i.p. injection of leptin in C57BL/6 mice employed in this study [data shown in **(B–D)**]. Leptin was injected into peritoneal cavities of naïve C57BL/6 mice. Peritoneal cells were collected and stained by May–Grünwald–Giemsa for eosinophil recruitment analysis within 24 h of leptin stimulation. In **(B)**, different concentrations of leptin (0.5, 1, and 2 mg/kg) were used. In **(C)**, pre-treatment with rapamycin (12.5 μg/kg per injection) 12 h before, 15 min before, and 12 h after leptin injection (1 mg/kg) was performed. In **(D)**, naïve wild type or PI3K deficient C57BL/6mice received i.p. injection of leptin (1 mg/kg) and peritoneal fluids were collected within 24 h of stimulation. There are no significant differences between the number of peritoneal eosinophils recovered from the control groups of wild type and PI3Kγ–/– C57BL/6 mice. Values are expressed as the mean ± SEM (experiments were repeated at least once). $^{+}p < 0.05$ compared to control group.$^{*}p < 0.05$ compared to leptin-stimulated group.

influx (**Supplementary Figure S1**); (iv) a parallel drop in circulatory eosinophil numbers noted 24 h after leptin stimulation that was not accompanied by alterations in bone marrow eosinophil population (**Supplementary Figure S2**), indicating that pleural eosinophils were mobilized from the blood pool; and more remarkable, (v) clear activation of pleural infiltrating eosinophils.

By employing an *in vitro* functional approach, we demonstrated that the sensitization of BALB/c mice does not modulate eosinophil chemotactic response, since the magnitude of eotaxin-, PGD_2-, or leptin-induced *in vitro* chemotaxis of eosinophils recovered from naïve *versus* sensitized animals were not significantly different (**Supplementary Figure S3**). While this finding does not explain why sensitization is required to leptin-driven robust eosinophilic response in BALB/c mice (**Figure 2**), it indicates that the difference may lay, for instance, on *in situ* changes on resident cell populations, like the small pleural mast cell hyperplasia raised by sensitization (described below). In addition, systemic increases in eosinophil population availability could also contribute to it, since in sensitized BALB/c mice both bone marrow and circulating eosinophil populations appear to be slightly (although not statistically significantly) increased in comparison to basal numbers found in naive BALB/c mice (**Supplementary Figure S2**).

Exclusively detected in sensitized BALB/c mice, the *in vivo* eosinophil activation elicited by leptin was characterized by increased biogenesis of cytoplasmic lipid bodies within infiltrating eosinophils and enhanced synthesis of LTC_4 in 24 h (**Figure 2D**). Of note, although LTC_4 levels were found elevated within 24 h in parallel to the intense eosinophilic reaction triggered by leptin stimulation, no production was found within 6 h— when leptin-elicited pleural eosinophilia was still negligible and the few infiltrating eosinophils showed no sign of cellular activation displaying basal intracellular numbers of lipid bodies (**Figure 2C**). On the other hand, by analyzing other soluble mediators potentially produced within 6 h and therefore prior to the establishment of leptin-induced eosinophilic inflammation at 24 h, we detected increased amounts of PGD_2 in pleural lavage fluids of sensitized BALB/c mice (**Figure 3**). Leptin-induced pleural PGD_2 levels remained elevated until 24 h after leptin stimulation in sensitized, but not in naïve BALB/c mice (**Figure 3**), another difference that may represent one of the main mechanisms responsible for the robust eosinophilic response displayed by sensitized in contrast to naïve BALB/c mice.

Sensitized BALB/c mice, besides PGD_2, also displayed augmented amounts of the chemokine CCL-5 in pleural lavage fluids as early as 6 h after *in vivo* stimulation with leptin (from 14.7 ± 4.9 to 42.3 ± 5.4 pg/ml in control and leptin-stimulated sensitized BALB/c mice, respectively; mean ± SEM of five animals per group; + $p < 0.05$ compared to control group). Even in peritoneal fluids of the naïve C57BL/6 mice, leptin increased CCL5 levels (from 8.3 ± 0.1 to 15.5 ± 2.6 pg/ml in control and leptin-stimulated C57BL/6 mice; respectively; mean ± SEM of at least five animals per group; + $p < 0.05$ compared to control group) and TNFα (8) preceding the minor eosinophilia triggered by leptin in these animals. Taken together, these data suggest that in order to induce eosinophil influx, leptin may first activate one or more resident cell types.

Mast cells emerge as the most plausible cellular candidate to be the target of direct activation by injected leptin, inasmuch as (i) mast cells are prominent resident cells in both peritoneal and pleural cavities; (ii) the number of resident mast cells augments marginally, but significantly, in pleural spaces of sensitized BALB/c mice—0.3 ± 0.06 *versus* 0.1 ± 0.05 × 10^6 mast cells/cavity in sensitized *versus* naïve BALB/c mice, respectively (mean ± SEM of five animals; $p < 0.05$ compared to naïve animals); (iii) mast cells are well-established regulators of eosinophil migration in a variety of inflammatory conditions (20); (iv) mast cells are known to express leptin receptors (5, 22); (v) TNFα is known to be stored as a preformed cytokine within mast cell granules and therefore are ready for rapid secretion by degranulation (36); and more important and specific (vi) mast cells are acknowledged as the main cellular source of PGD_2 which is one of the strongest eosinophil chemotactic mediator identified yet (21), also capable

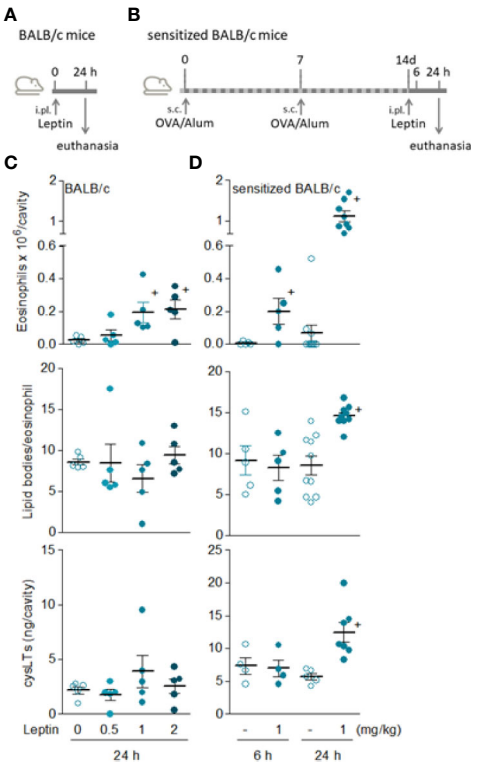

FIGURE 2 | *Leptin induces both in vivo eosinophil migration and activation in sensitized BALB/c mice.* **(A, B)** show, respectively, brief schematic representations of pleurisy models induced by i.pl. injection of leptin in naïve [data shown in **(C)**] and sensitized [data shown in **(D)**] BALB/c mice employed in this study. In **(C)**, naïve BALB/c mice received i.pl. injection with different concentrations of leptin (0.5, 1 and 2 mg/kg) and pleural fluids were collected within 24 h. In **(D)**, sensitized BALB/c mice received i.pl. injection of leptin (1 mg/kg) and pleural fluids were collected within 6 or 24 h, as indicated. Analyses include pleural eosinophil counts evaluated in cells stained by May-Grünwald-Giemsa (upper panels), numbers of cytoplasmic lipid bodies counted within osmium-stained pleural eosinophils (middle panels) and cysLTs levels found in cell-free pleural fluids measured by specific EIA kit (bottom panels). Values are expressed as the mean ± SEM (experiments were repeated at least once). $^{+}p < 0.05$ compared to control group.

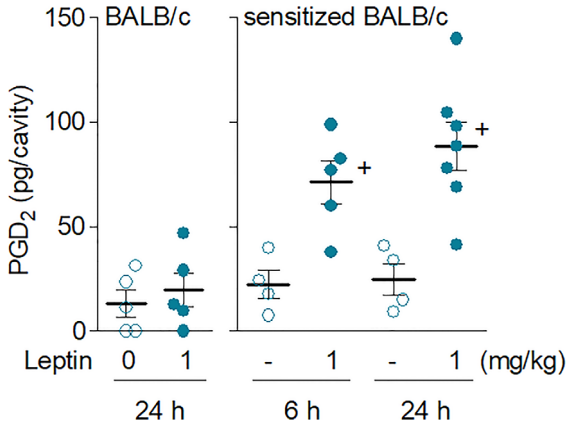

FIGURE 3 | *Leptin administration in vivo elicits rapid secretion of PGD_2 in sensitized BALB/c mice.* Leptin (1 mg/kg; i.pl.) was injected in naïve (left panel) or sensitized BALB/c mice (right panel). PGD_2 levels found 6 or 24 h (as indicated) after leptin stimulation in pleural fluids were evaluated as described in Methods. Values are expressed as the mean ± SEM. $^{+}p < 0.05$ compared to control group.

to trigger eosinophil activation characterized by lipid body biogenesis and LTC_4 synthesis (16).

It is worth mentioning that pleural macrophages were our first candidates, rather than pleural mast cells, as the orchestrators of leptin-driven eosinophilic response in sensitized BALB/c mice. However, we focused our studies on resident mast cell population, first because no change on numbers of pleural mononuclear cells was found in leptin-stimulated sensitized BALB/c mice (**Supplementary Figure S1**). More important and exactly alike i.pl. administration of PGD_2 in sensitized BALB/c mice (28), i.pl. administration of leptin failed to induce lipid body formation within pleural mononuclear cells (data not shown)—a feature consistent with lack of local macrophage activation and enhanced eicosanoid generation. Of note, leptin is known to trigger activation of C57BL/6 peritoneal macrophages, characterized by induced *in vivo* assembly of new highly functional lipid bodies (9). Further studies would be important to evaluate possible interactions between mast cells and macrophages in the C57BL/6 peritoneal cavity.

Altogether, these data consolidates pleurisy in sensitized BALB/c mice as a better suited experimental model to further mast cell/eosinophil studies under leptin stimulation *in vivo*.

Leptin-Induced Eosinophil Influx and Activation Are Dependent on Resident Mast Cells and PGD_2 Synthesis

In order to study the involvement of resident mast cells on leptin-induced eosinophil migration, we assessed the effect of experimental strategies that selectively interfered with *in vivo* mast cell activity as well as reduced synthesis of the distinctive eosinophilotactic mast cell-derived mediator PGD_2. The mast cell degranulating agent compound 48/80 did inhibit leptin-induced eosinophil influx and activation detected 24 h after stimulation of sensitized BALB/c mice (**Figure 4A**), since pleural eosinophil numbers and lipid body content within infiltrating eosinophils were reduced. Of key interest and supporting the role of mast cells-derived PGD_2 on leptin-induced eosinophilic response, compound 48/80 treatment also reduced leptin-induced PGD_2 amounts detected within pleural spaces of sensitized BALB/c mice (**Figure 4A**). The role of mast cells as the direct cellular target of leptin stimulation *in vivo* was reinforced by the observation of leptin being also capable to trigger both *in vitro* degranulation, measured by release of granule protein marker β-hexosaminidase enzyme from BMMC (**Figure 4C**), as well as discreet but significant and reproducible *in vitro* PGD_2 and LTC_4 synthesis (**Figure 4B**). As also shown in **Figure 4B**, pretreatment with HQL-79, a selective inhibitor of PGD synthase, impaired the acute (detected within 1 h) leptin-induced PGD_2 synthesizing activity within BMMC, without affecting LTC_4. Moreover and as previously demonstrated for eosinophils (16), leptin-stimulated BMMC pre-treated with the PI3K inhibitor

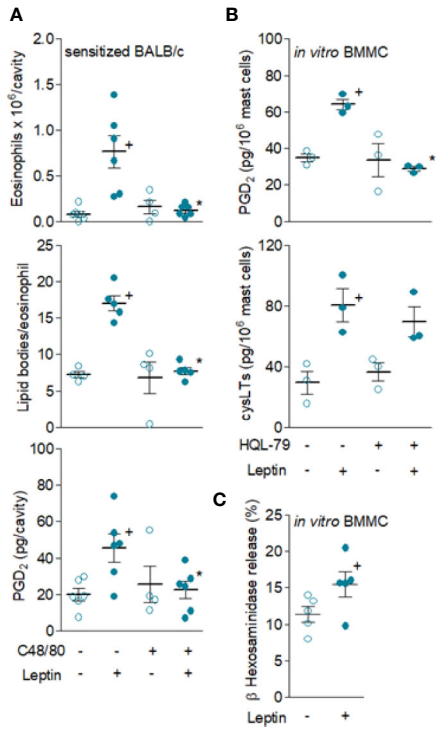

FIGURE 4 | *Resident mast cells are leptin targets and are responsible for in vivo leptin-induced eosinophil migration and activation.* In **(A)**, sensitized BALB/c mice were pre-treated with degranulating mast cell agent compound 48/80 and stimulated with leptin (1 mg/kg; i.pl.). Pleural fluids were collected after 24 h of leptin stimulation. Analyses include pleural eosinophil counts evaluated in cells stained by May-Grünwald-Giemsa (upper panels), PGD_2 levels found in cell-free pleural fluids measured by specific EIA kit (middle panels) and numbers of cytoplasmic lipid bodies counted within osmium-stained pleural eosinophils (bottom panels). Values are expressed as the mean ± SEM (experiments were repeated at least once). $^{+}p < 0.05$ compared to control group and $^{*}p < 0.05$ compared to leptin-stimulated group. In **(B, C)**, mouse *in vitro* differentiated bone marrow-derived mast cells (BMMC) were pre-treated or not (as indicated) with HQL-79 for 30 min and then stimulated with 50 nM of leptin for 1 h. **(B)** shows PGD_2 and cysLTs levels found in BMMC supernatants quantified by specific EIA kits. **(C)** shows BMMC degranulation by means of detection of extracellular activity of the intragranular enzyme β-hexosaminidase. Values are expressed as the mean ± SEM of different *in vitro* differentiation mast cells cultures (as indicated). $^{+}p < 0.05$ compared to control cells.

LY294002 (10 μM) exhibited decreased LTC_4 synthesis (supernatant levels of cysLTs dropped from 80.4 ± 10.8 to 39.3 ± 12.0 pg/ml in non-treated and LY294002-treated leptin-stimulated BMMC, respectively; mean ± SEM of three *in vitro* differentiated mast cell cultures; + $p < 0.05$ compared to non-treated group). This data indicates that leptin is able to activate cannonical signaling pathways in mast cells that culminate in the generation of relevant inflammatory mediators.

PGD_2 is a major mast cell product that appears to be critical for the pathogenesis of a variety of eosinophilic disorders (37, 38), mostly because it is a potent chemoattractant for eosinophils both *in vitro* (39, 40) and *in vivo* (28, 41, 42). Of note, and precisely as observed here for leptin, PGD_2's ability to induce local eosinophilia in BALB/c mice also depends on specific experimental strategies to create a proper PGD_2-sensitive environment (34, 43, 44), such as the sensitization of BALB/c mice protocol employed elsewhere (45) and here. Therefore, to investigate the role of PGD_2 in eosinophil influx triggered by leptin administration, sensitized BALB/c mice were pretreated with HQL-79. As expected, concurrent to inhibition of leptin-induced PGD_2 synthesis *in vivo*, HQL-79 also inhibited leptin-induced eosinophil influx detected 24 h after i.pl. injection in sensitized BALB/c mice (**Figure 5A**), showing that endogenous PGD_2 produced during leptin-elicited reaction has an important role in the *in vivo* eosinophil migration. Interestingly, HQL-79 pretreatment also reduced the leptin-induced CCL-5 found within 24 h in sensitized BALB/c mice (**Figure 5A**). This indicates that PGD_2 may be a central molecule also capable of controlling the secretion of additional mediators from leptin-elicited eosinophilic responses *in vivo*. In line with such autocrine/paracrine activity of PGD_2 shown here for *in vivo* leptin-stimulated mast cells, we have previously observed some PGD_2/CCL-5 loop for *in vitro* leptin-stimulated eosinophils (16).

Likewise PGD_2, it is well established that CCR3 activation by some CC chemokines, including CCL5, promotes potent eosinophil chemoattraction and mast cells have been reported to produce and release CCL5 (46). As shown in **Figure 5B**, the pre-treatment with a neutralizing antibody against mouse CCL5 failed to interfere with eosinophil accumulation triggered by leptin administration in sensitized BALB/c mice, therefore indicating that those earlier elevated levels of CCL5 found in leptin-elicited inflammatory sites do not participate in eosinophil migration. Differently, leptin-driven enhanced TNFα levels—which precede eosinophil influx—appear to contribute to it, as evidenced by the lack of eosinophil migration in TNFR1 deficient mice (C57BL/6 background) after leptin injection (**Figure 5C**). This result indicates that activation of TNFα receptor TNFR1 by endogenous TNFα may contribute to leptin-induced eosinophil migration *in vivo*.

PGD_2 and CCL5 Mediate *In Situ* Eosinophil Activation Triggered by Leptin *In Vivo*

Recently, we have identified leptin as a novel mediator capable of activating the biogenesis of lipid bodies and enhanced LTC_4 production within eosinophils (16), suggesting that part of the *in vivo* mechanisms of leptin-induced lipid body-driven LTC_4 production would be due to a direct stimulatory effect of leptin on recruited eosinophils. However, as virtually no resident eosinophils are present in the pleural or peritoneal cavities neither in naïve nor sensitized mice (not shown), the leptin-induced cellular activation of infiltrating eosinophils seem to be an indirect phenomenon. Therefore, the initial response to leptin *in vivo* may depend on direct activation of resident cells and triggered by mediators produced upon exogenous leptin stimulation.

Among very few other specific stimuli (21), PGD_2 and CCL5 are known to directly promote activation of *de novo* formation of lipid bodies and LTC_4 synthesis by eosinophils both *in vitro* and

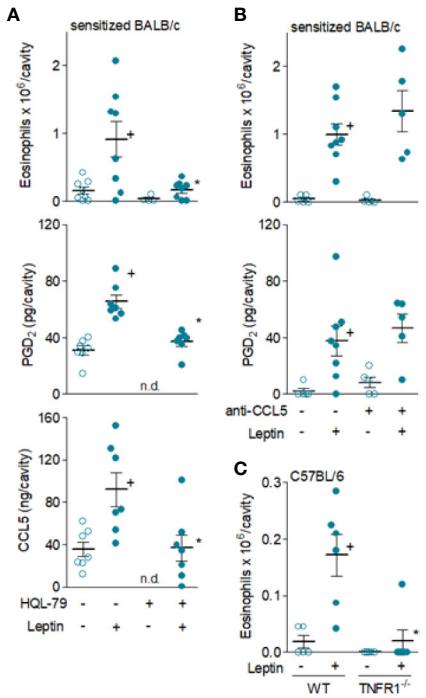

FIGURE 5 | *Leptin-induced in vivo eosinophil migration is mediated by PGD_2 and TNFα, but not by CCL5.* In **(A, B)**, sensitized BALB/c mice received i.pl. injection of leptin (1 mg/kg) and pleural fluids were collected within 24 h. While in **(A)**, animals were pre-treated with HQL-79 (1 mg/kg, i.p.), in **(B)** mice were pre-treated with a neutralizing anti-CCL5 antibody (10 µg/cavity, i.pl.). In **(C)**, naïve wild type or TNFR1 deficient C57BL/6 mice received i.p. injection of leptin (1 mg/kg) and peritoneal fluids were collected within 24 h of stimulation. As indicated, analyses include pleural eosinophil counts evaluated in cells stained by May-Grünwald-Giemsa as well as PGD_2 and CCL-5 levels found in cell-free pleural fluids measured by specific EIA and ELISA kits (middle panels). Values are expressed as the mean ± SEM (experiments were repeated at least once). $^{+}p < 0.05$ compared to control group and $^{*}p < 0.05$ compared to leptin-stimulated group. n.d.; not determined.

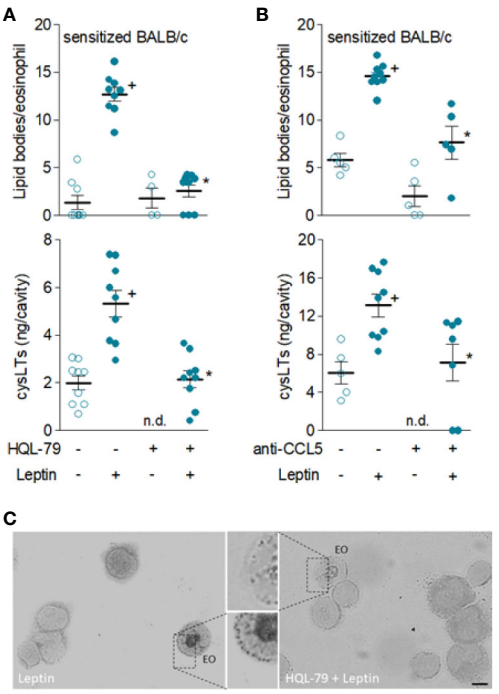

FIGURE 6 | *Leptin-induced in vivo eosinophil activation in sensitized BALB/c mice is mediated by PGD_2 and CCL5.* Sensitized BALB/c mice received i.pl. injection of leptin (1 mg/kg) and pleural fluids were collected within 24 h of stimulation. While in **(A)**, animals were pre-treated with HQL-79 (1 mg/kg, i.p.), in **(B)** mice were pre-treated with a neutralizing anti-CCL5 antibody (10 µg/cavity, i.pl.). Analyses include numbers of cytoplasmic lipid bodies counted within osmium-stained pleural eosinophils (upper panels) and cysLTs levels found in cell-free pleural fluids measured by specific EIA kit (bottom panels). **(C)** shows representative images of osmium-stained pleural cells recovered from leptin-stimulated sensitized BALB/c mice which were pre-treated or not (as indicated) with HQL-79. Values are expressed as the mean ± SEM (experiments were repeated at least once). $^{+}p < 0.05$ compared to control group and $^{*}p < 0.05$ compared to leptin-stimulated group. n.d.; not determined. EO; eosinophil. Scale bar = 5 µm.

in vivo (28, 47). Here, several of our findings confirm that leptin-induced eosinophil activation *in vivo* appears to be dependent on mast cell-derived PGD_2-driven paracrine activity in sensitized BALB/c mice, since (i) increased PGD_2 levels detected as early as 6 h (**Figure 3B**) of leptin administration are kept elevated for at least 24 h in eosinophilic inflammatory site of leptin-challenged sensitized BALB/c; (ii) pretreatment with compound 48/80 reduced *in vivo* leptin-induced production of PGD_2 (**Figure 4A**) in sensitized BALB/c mice; (iii) mast cell degranulating agent compound 48/80 blocked leptin-induced assembly of new cytoplasmic lipid bodies within recruited eosinophils as detected 24 h after leptin stimulation of sensitized BALB/c mice (**Figure 4A**); and, more significantly, (iv) specific inhibition of PGD_2 synthesis by HQL-79 disrupted both biogenesis of cytoplasmic lipid bodies and LTC_4 synthesis within recruited eosinophils in leptin-stimulated sensitized BALB/c mice (**Figures 6A, C**).

Remarkably, even though CCL5 did not appear to participate on the induction of leptin-elicited eosinophil migration *in vivo*, it does mediate leptin-induced *in vivo* eosinophil activation, inasmuch as the pre-treatment with the neutralizing antibody to CCL5 did inhibit leptin-driven assembly of new lipid bodies within recruited eosinophils and LTC_4 synthesis (**Figure 6B**).

DISCUSSION

It is now broadly accepted that eosinophils are fundamental keepers of adipose tissue homeostasis, capable of thwarting obesity-related metabolic syndrome (18, 48). As adipose sentinel cells which express leptin receptors, eosinophils may be under constant leptin stimulation. *In vitro* studies unveiled leptin as a wide-ranging stimulus for eosinophils, eliciting eosinophil kinesis, cytokine secretion, lipid body biogenesis, and the highly regulated events of eicosanoid synthesis (13–16). However, in contrast to the well documented leptin-induced

in vitro eosinophil activation, studies addressing whether leptin affects eosinophil population *in vivo* are scarse.

Here, we demonstrated the capability of leptin in triggering eosinophilic inflammation *in vivo* in naïve C57BL/6 or BALB/c mice. Interestingly, the leptin induced eosinophil migration was more prominent in sensitized BALB/c mice. In addition, leptin was successful in triggering activation of the infiltrating eosinophils only in pre-sensitized BALB/c mice. Evaluation of these two mouse backgrounds are currently of key relevance; inasmuch as recent reports employing BALB/c mice have defied the paradigm derived from C57BL/6 studies that eosinophils are absent from obese adipose tissue, while revealed even far-reaching protective functions of adipose tissue eosinophils (18, 48).

It has been shown that, no matter the metabolic state displayed by the adipose micro-environment, both the homeostatic functions of eosinophils and the general mechanisms regulating eosinophil presence within adipose tissue are alike; including the mediation by a common tripod of type 2 innate lymphoid cells (ILC2s), IL-5, and eotaxin (4, 5). However, the multiplicity of adipose micro-environmental factors potentially capable of establishing adipose eosinophilia and/or properly activate eosinophil functions is far more abundant and obviously not restricted to these three key players, and as shown here, may involve leptin as an additional molecular modulator.

It seems definitive that eosinophilia is a hallmark of lean adipose niches and that eosinophils counteract the obesity related chronic inflammation (18, 48). This knowledge is derived from a large body of data using C57BL/6 mouse experimental models of obesity which established the reduction of homeostatic eosinophils in adipose tissue undergoing metabolic syndrome (4, 5). Nevertheless, Lee et al. found contrasting results in adipose tissue eosinophils of BALB/c mice under high-fat diet (18). The adipose tissue eosinophils appear to increase in numbers, rather than vanish. Such difference in eosinophil dynamics has been immediately attributed to the well-established feature of preferential responsive shifts toward Type 1 *versus* Type 2 immune profiles by C57BL/6 *versus* BALB/c mice, respectively (49). Consistent with this proposition, we have shown here a more robust leptin-stimulated eosinophilic response seen in BALB/c mice which were submitted to previous sensitization—an experimental procedure known to promptly evoke intense Type 2 response characterized by eosinophilic outcomes. While we did not focus on characterizing the mechanisms explaining why sensitization of BALB/c mice promotes the establishment of a more intense, selective and whole (migration *plus* activation) leptin-driven eosinophilic response, we have identified at least three factors that in association may contribute to the overall more robust pleural eosinophilic reaction. These factors are: (i) an increased number of mast cells residing in pleural cavities; (ii) an increased availability of bone marrow and blood eosinophils; and (iii) the local production of PGD_2. Of note, recent clinical results showed similar results to BALB/c mice with increased adipose eosinophilia in a group of obese patients (50); therefore indicating that BALB/c models may reproduce better adipose tissue-related human eosinophilic events.

According to the study by Lee and coworkers (18), rather than the size of eosinophil population within adipose niche, the profile of eosinophil activation emerges as the central element of tissue function. Overall, these authors reported that, even though eosinophils accumulate in adipose tissue of obese BALB/c mice, they display homeostatic functions as proposed for the lean adipose tissue (18). Therefore, evaluating *in vivo* eosinophil activation, instead of the exclusive assessment of their migration pattern, was germane here. So far, the acknowledged mechanism of eosinophil homeostatic roles lays essentially on activation of eosinophil secretory activity of immune-modulator proteins, mostly cytokines like IL-4 and IL-13 (48, 51, 52). However, eosinophils have a much diverse secretory capability, which is not limited to cytokine secretion, but eosinophils are remarkable sources of multifunctional lipid mediators. Within physiologically stimulated eosinophils, bioactive lipids from arachidonic acid metabolism are synthesized primarily in cytoplasmic lipid bodies (53, 54). Of note, cytoplasmic lipid body numbers are characteristically increased within eosinophils following *in vitro* stimulation, as well as in *in vivo* inflammatory disorders, and are used as a marker of eosinophil activation (55). Besides the previously reported direct activation of lipid body biogenesis *in vitro* within eosinophils by leptin (16), we demonstrated that leptin administration in sensitized BALB/c mice promotes formation of new lipid bodies within the eosinophils recruited to the leptin ability to evoke eosinophil activation *in vivo*.

The assembly of these highly active organelles within eosinophils is often linked to intense synthesis of eicosanoids, notably LTC_4, which was produced upon *in vivo* stimulation with leptin. LTC_4 may drive adipose homeostasis since it (i) potentiates IL-5 release from ILC2s (56) and (ii) elicits IL-4 secretion from eosinophils (57). Noteworthy, we have recently demonstrated that leptin prompts LTC_4 synthesis within the newly formed cytoplasmic lipid bodies in human and mouse eosinophils *in vitro* (16). Besides LTC_4, increased leptin levels triggered by adipose tissue dysfunction, may also unbalance eosinophil lipid body-compartmentalized synthesis of other eicosanoids known to interfere with adipogenesis and inflammation (58, 59), such as the prostanoids PGE_2 and PGD_2 (16). Eosinophil lipid bodies are highly active intracellular sites of eicosanoid synthesis (54, 55) and may have important roles, not only in the adipose tissue physiology, but also in metabolic disease states, therefore indicating that further studies on the potential impacts of activation of eosinophilic lipid bodies on adipose tissue are germane.

Considering both leptin receptor expression by eosinophils (13) and *in vitro* leptin capability to activate eosinophils (14), one could assume that *in vivo* leptin-induced eosinophil activation described here is a consequence of direct stimulation of leptin receptors on eosinophil surface. Without precluding a partial direct effect of leptin onto eosinophils in the overall leptin-driven eosinophilic response *in vivo* described here, as eosinophils are not resident cells within the pleural cavity and, therefore, absent at the moment of leptin administration; leptin ability to induce *in vivo* eosinophil activation may mostly depend on indirect components. Among the various resident cellular targets for leptin stimulation *in vivo*, we identified mast cells as a key cell population. Importantly, our results identify mast cells as modulators of leptin-driven eosinophilic reaction are in line with recent postulations that

adipose tissue resident mast cells or the obesity-related increased mast cell population are modulators of adipose tissue homeostasis and inflammation (60, 61).

Several pieces of evidence indicate that mast cells secretory activity is involved in leptin-elicited eosinophil influx and lipid body-driven LTC_4 synthesis *in vivo*, since: (i) the understanding that mast cells express active leptin receptors (22, 62); (ii) the ability of leptin to directly arouse mast cell secretory activities, as showed here and by others (63); (iii) the leptin-elicited increased local levels of classical mast cell-derived eosinophil-relevant stimuli which precede eosinophil arrival but may remain elevated during installed eosinophilia; (iv) the *in vivo* inhibitory effect achieved by selectively targeting mast cells with the compound 48/80; and (v) the paracrine role of classical mast cell-derived molecules in the leptin-driven induction of eosinophil recruitment and activation. Among mast cells-derived molecules, PGD_2 may represent one of the most classical and unambiguous products (37). Here, PGD_2 synthesis in mast cells was promoted by leptin both *in vitro* and *in vivo*. Moreover, increased local levels of mast cell-derived PGD_2 were crucial for both influx and activation of eosinophils induced by leptin. Besides a potent eosinophilotactic factor, this prostanoid is undeniably also a known eosinophil activator (64). In an analogous manner to leptin, PGD_2 is able to trigger lipid body biogenesis and compartmentalized LTC_4 synthesis both *in vitro* within human and mice eosinophils, as well as *in vivo* only in sensitized BALB/c mice.

In addition to PGD_2, the mechanisms involved in leptin-induced lipid body-driven LTC_4 synthesis also include CCL5 as another mediator of the *in vivo* phenomenom in sensitized BALB/c mice. Strikingly, even though CCL5 is a chemokine capable of promoting both eosinophilotaxis and LTC_4 synthesis within newly formed lipid bodies (47), it did not participate in eosinophil migration while mediated *in vivo* eosinophil activation triggered by leptin. Therefore, we concluded that although both eosinophilic events depend on paracrine activities mediated by mast cell-derived PGD_2, eosinophil migration and activation triggered by leptin *in vivo* seem to be independent phenomena mediated by different sets of locally produced factors. Additional chemotactic mediators may synergize with PGD_2 to promote leptin-induced eosinophil. Of note, another classical mast cell-derived molecule addressed here—the pro-inflammatory cytokine TNFα—appears to also contribute to eosinophil accumulation in response to leptin stimulation, even though it is not recognized as a direct eosinophil chemotactic molecule.

We have previously shown that leptin is capable of eliciting pro-adipogenic and pro-inflammatory signaling in adipocytes, as well as eicosanoid production in macrophages, neutrophils, eosinophils (8, 16, 65). Here, by further evidencing the capacity of leptin to modulate the interplay between eosinophils and mast cells, we suggest leptin as a key factor of the inflammation-modulated homeostasis in the adipose tissue.

By extrapolating the findings presented here to adipose tissue, one can speculate that leptin continuously produced by mature adipocytes may elicit local synthesis of bioactive PGD_2 by PGDS-expressing resident cells, such as mast cells and eosinophils. Functioning in a paracrine fashion within adipose tissue, locally produced PGD_2 may trigger a variety of adipose housekeeping mechanisms with potential impact on metabolic syndrome

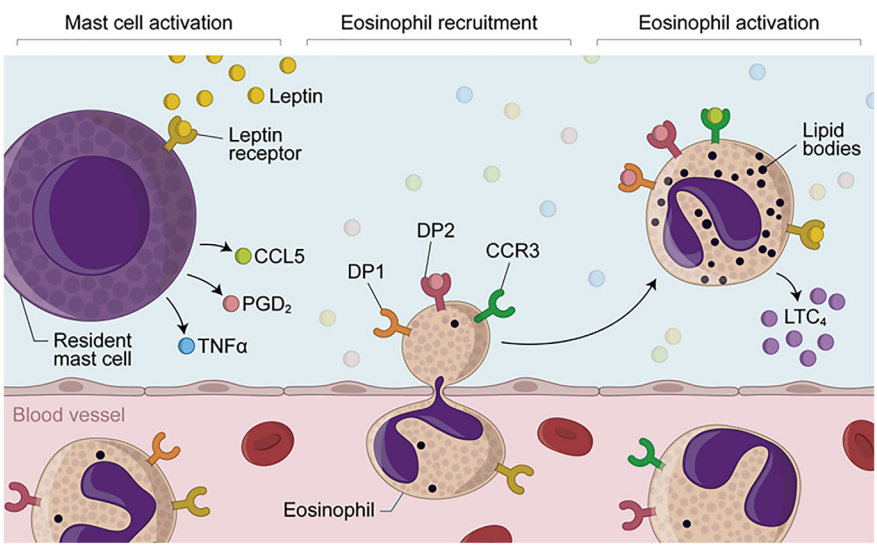

FIGURE 7 | *Proposed mechanisms of leptin-induced in vivo eosinophilic inflammation mediated by mast cell-derived PGD_2.* Eosinophilic inflammation triggered by *in vivo* stimulation with leptin depends on sequential events, including (i) initial activation of resident mast cell secretory activity; (ii) increased local levels of TNFα, CCL5 and PGD_2; (iii) induction of eosinophil migration by TNFα and PGD_2 and then; (iv) cellular activation of recruited eosinophils, characterized by lipid body biogenesis and LTC_4 synthesis. While mast cell-derived PGD_2 may induce eosinophil influx *via* activation of its chemotactic DP2 receptor which is highly expressed on eosinophils, leptin-driven *in situ* eosinophil activation is mediated by both CCL5 and PGD_2 throughout simultaneous activation of CCR3 and PGD_2 receptors DP1 and DP2— whose downstream signaling are known to culminate with *in vitro* lipid body-compartmentalized synthesis of LTC_4 within leptin-stimulated eosinophils.

evasion, including (i) down-regulation of leptin production (66), secretion of Type 2 cytokines IL-5 as well as IL-4 by ILC2s (67, 68), activation of adipose eosinophils (16) and/or polarization of macrophages toward a M2 anti-inflammatory state (69).

Collectively, our data unveiled a scenario where leptin interacts with resident mast cells, which in turn govern eosinophil numbers as well as set up a proper *in situ* eosinophil activation (for proposed mechanisms see **Figure 7**). Moreover, PGD_2 emerges as an important player of leptin-mediated cell crosstalk between mast cells and eosinophils, which culminates with LTC_4 production. Therefore, it seems clear that further investigations addressing eosinophil-driven homeostatic roles in adipose tissue must include studies on the role of leptin-driven immune-modulatory lipid mediators in addition to the well-established role of eosinophil-derived cytokines.

DATA AVAILABILITY STATEMENT

The raw data supporting the conclusions of this article will be made available by the authors, without undue reservation.

ETHICS STATEMENT

The animal study was reviewed and approved by both Animal Use Welfare Committees of Federal University of Rio de Janeiro (CEUA-CCS/UFRJ license number 090/18) and Oswaldo Cruz Institute (CEUA-IOC license number L-011/2015).

AUTHOR CONTRIBUTIONS

CM-M and CB-M conceived and designed the study. NA, GS-A, and TL-G designed and performed the experiments, analyzed, and interpreted data. NA, GS-A, TL-G, PB, CC, and BD participated in the data acquisition, analysis, and interpretation. PB, CC, BD, CM-M and CB-M wrote and revised the manuscript. All authors contributed to the article and approved the submitted version.

FUNDING

This work was supported by the Fundação de Amparo à Pesquisa do Estado do Rio de Janeiro_Faperj (grants E-26/202.926/2015 to CB-M and E-26/110.374/2014 to CM-M); the Conselho Nacional de Desenvolvimento Científico e Tecnológico (CNPq; grants 453826/2014-8 to CB-M and 306290/2014-6 to CM-M); and Coordenação de Aperfeiçoamento de Pessoal de Nível Superior_CAPES (fellowship to GS-A); PAPES/FIOCRUZ (grant 407442/2012-0 to CM-M), and aboratory financial support from Oswaldo Cruz Institute (IOC/FIOCRUZ) (to CM-M and PB). Disclaimer: The funders had no role in study design, data collection/analysis, decision to publish, or preparation of the manuscript.

SUPPLEMENTARY MATERIAL

The Supplementary Material for this article can be found online at: https://www.frontiersin.org/articles/10.3389/fendo.2020.572113/full#supplementary-material

REFERENCES

1. Klion AD, Rothenberg ME. Advances in eosinophilic diseases in 2018. *J Allergy Clin Immunol* (2019) 144:1490–4. doi: 10.1016/j.jaci.2019.10.010
2. Weller PF, Spencer LA. Functions of tissue-resident eosinophils. *Nat Rev Immunol* (2017) 17:746–60. doi: 10.1038/nri.2017.95
3. Shah K, Ignacio A, McCoy KD, Harris NL. The emerging roles of eosinophils in mucosal homeostasis. *Mucosal Immunol* (2020) 13(4):574–83. doi: 10.1038/s41385-020-0281-y
4. Calco GN, Fryer AD, Nie Z. Unraveling the connection between eosinophils and obesity. *J Leukoc Biol* (2020) 108(1):123–8. doi: 10.1002/JLB.5MR0120-377R
5. Vohralik EJ, Psaila AM, Knights AJ, Quinlan KGR. EoTHINophils: Eosinophils as key players in adipose tissue homeostasis. *Clin Exp Pharmacol Physiol* (2020) 47(8):1495–505. doi: 10.1111/1440-1681.13304
6. Larabee CM, Neely OC, Domingos AI. Obesity: a neuroimmunometabolic perspective. *Nat Rev Endocrinol* (2020) 16:30–43. doi: 10.1038/s41574-019-0283-6
7. Francisco V, Pino J, Campos-Cabaleiro V, Ruiz-Fernández C, Mera A, Gonzalez-Gay MA, et al. Obesity, Fat Mass and Immune System: Role for Leptin. *Front Physiol* (2018) 9:640. doi: 10.3389/fphys.2018.00640
8. Souza-Almeida G, D'Avila H, Almeida PE, Luna-Gomes T, Liechocki S, Walzog B, et al. Leptin Mediates In Vivo Neutrophil Migration: Involvement of Tumor Necrosis Factor-Alpha and CXCL1. *Front Immunol* (2018) 9:111. doi: 10.3389/fimmu.2018.00111
9. Maya-Monteiro CM, Almeida PE, D'Avila H, Martins AS, Rezende AP, Castro-Faria-Neto H, et al. Leptin induces macrophage lipid body formation by a phosphatidylinositol 3-kinase- and mammalian target of rapamycin-dependent mechanism. *J Biol Chem* (2008) 283:2203–10. doi: 10.1074/jbc.M706706200
10. Procaccini C, Pucino V, De Rosa V, Marone G, Matarese G. Neuro-endocrine networks controlling immune system in health and disease. *Front Immunol* (2014) 5:143. doi: 10.3389/fimmu.2014.00143
11. Mancuso P, Curtis JL, Freeman CM, Peters-Golden M, Weinberg JB, Myers MG. Ablation of the leptin receptor in myeloid cells impairs pulmonary clearance of Streptococcus pneumoniae and alveolar macrophage bactericidal function. *Am J Physiol-Lung Cell Mol Physiol* (2018) 315:L78–86. doi: 10.1152/ajplung.00447.2017
12. Mancuso P. Obesity and respiratory infections: does excess adiposity weigh down host defense? *Pulm Pharmacol Ther* (2013) 26:412–9. doi: 10.1016/j.pupt.2012.04.006
13. Conus S, Bruno A, Simon H-U. Leptin is an eosinophil survival factor. *J Allergy Clin Immunol* (2005) 116:1228–34. doi: 10.1016/j.jaci.2005.09.003
14. Wong CK, Cheung PF-Y, Lam CWK. Leptin-mediated cytokine release and migration of eosinophils: implications for immunopathophysiology of allergic inflammation. *Eur J Immunol* (2007) 37:2337–48. doi: 10.1002/eji.200636866
15. Kato H, Ueki S, Kamada R, Kihara J, Yamauchi Y, Suzuki T, et al. Leptin has a priming effect on eotaxin-induced human eosinophil chemotaxis. *Int Arch Allergy Immunol* (2011) 155:335–44. doi: 10.1159/000321195
16. Amorim NRT, Luna-Gomes T, Gama-Almeida M, Souza-Almeida G, Canetti C, Diaz BL, et al. Leptin Elicits LTC4 Synthesis by Eosinophils Mediated by Sequential Two-Step Autocrine Activation of CCR3 and PGD2 Receptors. *Front Immunol* (2018) 9:2139. doi: 10.3389/fimmu.2018.02139
17. Calixto MC, Lintomen L, Schenka A, Saad MJ, Zanesco A, Antunes E. Obesity enhances eosinophilic inflammation in a murine model of allergic asthma. *Br J Pharmacol* (2010) 159:617–25. doi: 10.1111/j.1476-5381.2009.00560.x
18. Lee E-H, Itan M, Jang J, Gu H-J, Rozenberg P, Mingler MK, et al. Eosinophils support adipocyte maturation and promote glucose tolerance in obesity. *Sci Rep* (2018) 8:9894. doi: 10.1038/s41598-018-28371-4
19. Stone KD, Prussin C, Metcalfe DD. IgE, mast cells, basophils, and eosinophils. *J Allergy Clin Immunol* (2010) 125:S73–80. doi: 10.1016/j.jaci.2009.11.017

20. Robida PA, Puzzovio PG, Pahima H, Levi-Schaffer F, Bochner BS. Human eosinophils and mast cells: Birds of a feather flock together. *Immunol Rev* (2018) 282:151–67. doi: 10.1111/imr.12638
21. Luna-Gomes T, Bozza PT, Bandeira-Melo C. Eosinophil recruitment and activation: the role of lipid mediators. *Front Pharmacol* (2013) 4:27. doi: 10.3389/fphar.2013.00027
22. Taildeman J, Pérez-Novo CA, Rottiers I, Ferdinande L, Waeytens A, De Colvenaer V, et al. Human mast cells express leptin and leptin receptors. *Histochem Cell Biol* (2009) 131:703–11. doi: 10.1007/s00418-009-0575-3
23. Żelechowska P, Brzezińska-Błaszczyk E, Wiktorska M, Różalska S, Wawrocki S, Kozłowska E, et al. Adipocytokines leptin and adiponectin function as mast cell activity modulators. *Immunology* (2019) 158:3–18. doi: 10.1111/imm.13090
24. Wang Y, Yu L, Meng G, Wang Z, Zhou Z, Zhang Y, et al. Mast cells modulate the pathogenesis of leptin-induced left stellate ganglion activation in canines. *Int J Cardiol* (2018) 269:259–64. doi: 10.1016/j.ijcard.2018.07.126
25. Liu D-R, Xu X-J, Yao S-K. Increased intestinal mucosal leptin levels in patients with diarrhea-predominant irritable bowel syndrome. *World J Gastroenterol* (2018) 24:46–57. doi: 10.3748/wjg.v24.i1.46
26. Chaldakov GN, Fiore M, Stankulov IS, Hristova M, Antonelli A, Manni L, et al. BDNF, leptin, and mast cells in human coronary atherosclerosis and metabolic syndrome. *Arch Physiol Biochem* (2001) 109:357–60. doi: 10.1076/apab.109.4.357.4249
27. Zheng L, Fisher G, Miller RE, Peschon J, Lynch DH, Lenardo MJ. Induction of apoptosis in mature T cells by tumour necrosis factor. *Nature* (1995) 377:348–51. doi: 10.1038/377348a0
28. Mesquita-Santos FP, Vieira-de-Abreu A, Calheiros AS, Figueiredo IH, Castro-Faria-Neto HC, Weller PF, et al. Cutting edge: prostaglandin D2 enhances leukotriene C4 synthesis by eosinophils during allergic inflammation: synergistic in vivo role of endogenous eotaxin. *J Immunol Baltim Md 1950* (2006) 176:1326–30. doi: 10.4049/jimmunol.176.3.1326
29. Diaz BL, Serra MF, Alves AC, Pires AL, Corrêa FM, Cordeiro RS, et al. e Silva PM. Alloxan diabetes reduces pleural mast cell numbers and the subsequent eosinophil influx induced by allergen in sensitized rats. *Int Arch Allergy Immunol* (1996) 111:36–43. doi: 10.1159/000237343
30. Diaz BL, Fujishima H, Kanaoka Y, Urade Y, Arm JP. Regulation of prostaglandin endoperoxide synthase-2 and IL-6 expression in mouse bone marrow-derived mast cells by exogenous but not endogenous prostanoids. *J Immunol Baltim Md 1950* (2002) 168:1397–404. doi: 10.4049/jimmunol.168.3.1397
31. Murakami M, Austen KF, Arm JP. The immediate phase of c-kit ligand stimulation of mouse bone marrow-derived mast cells elicits rapid leukotriene C4 generation through posttranslational activation of cytosolic phospholipase A2 and 5-lipoxygenase. *J Exp Med* (1995) 182:197–206. doi: 10.1084/jem.182.1.197
32. Diaz BL, Satake Y, Kikawada E, Balestrieri B, Arm JP. Group V secretory phospholipase A2 amplifies the induction of cyclooxygenase 2 and delayed prostaglandin D2 generation in mouse bone marrow culture-derived mast cells in a strain-dependent manner. *Biochim Biophys Acta* (2006) 1761:1489–97. doi: 10.1016/j.bbalip.2006.09.009
33. Pinho V, Souza DG, Barsante MM, Hamer FP, De Freitas MS, Rossi AG, et al. Phosphoinositide-3 kinases critically regulate the recruitment and survival of eosinophils in vivo: importance for the resolution of allergic inflammation. *J Leukoc Biol* (2005) 77:800–10. doi: 10.1189/jlb.0704386
34. Hsieh CS, Macatonia SE, O'Garra A, Murphy KM. T cell genetic background determines default T helper phenotype development in vitro. *J Exp Med* (1995) 181:713–21. doi: 10.1084/jem.181.2.713
35. Jovicic N, Jeftic I, Jovanovic I, Radosavljevic G, Arsenijevic N, Lukic ML, et al. Differential Immunometabolic Phenotype in Th1 and Th2 Dominant Mouse Strains in Response to High-Fat Feeding. *PloS One* (2015) 10:e0134089. doi: 10.1371/journal.pone.0134089
36. Gordon JR, Galli SJ. Release of both preformed and newly synthesized tumor necrosis factor alpha (TNF-alpha)/cachectin by mouse mast cells stimulated via the Fc epsilon RI. A mechanism for the sustained action of mast cell-derived TNF-alpha during IgE-dependent biological responses. *J Exp Med* (1991) 174:103–7. doi: 10.1084/jem.174.1.103
37. Raible DG, Schulman ES, DiMuzio J, Cardillo R, Post TJ. Mast cell mediators prostaglandin-D2 and histamine activate human eosinophils. *J Immunol Baltim Md 1950* (1992) 148:3536–42.
38. Matsuoka T, Hirata M, Tanaka H, Takahashi Y, Murata T, Kabashima K, et al. Prostaglandin D2 as a mediator of allergic asthma. *Science* (2000) 287:2013–7. doi: 10.1126/science.287.5460.2013
39. Hirai H, Tanaka K, Yoshie O, Ogawa K, Kenmotsu K, Takamori Y, et al. Prostaglandin D2 selectively induces chemotaxis in T helper type 2 cells, eosinophils, and basophils via seven-transmembrane receptor CRTH2. *J Exp Med* (2001) 193:255–61. doi: 10.1084/jem.193.2.255
40. Monneret G, Gravel S, Diamond M, Rokach J, Powell WS. Prostaglandin D2 is a potent chemoattractant for human eosinophils that acts via a novel DP receptor. *Blood* (2001) 98:1942–8. doi: 10.1182/blood.v98.6.1942
41. Spik I, Brénuchon C, Angéli V, Staumont D, Fleury S, Capron M, et al. Activation of the prostaglandin D2 receptor DP2/CRTH2 increases allergic inflammation in mouse. *J Immunol Baltim Md 1950* (2005) 174:3703–8. doi: 10.4049/jimmunol.174.6.3703
42. Kagawa S, Fukunaga K, Oguma T, Suzuki Y, Shiomi T, Sayama K, et al. Role of prostaglandin D2 receptor CRTH2 in sustained eosinophil accumulation in the airways of mice with chronic asthma. *Int Arch Allergy Immunol* (2011) 155 Suppl 1:6–11. doi: 10.1159/000327257
43. Almishri W, Cossette C, Rokach J, Martin JG, Hamid Q, Powell WS. Effects of prostaglandin D2, 15-deoxy-Delta12,14-prostaglandin J2, and selective DP1 and DP2 receptor agonists on pulmonary infiltration of eosinophils in Brown Norway rats. *J Pharmacol Exp Ther* (2005) 313:64–9. doi: 10.1124/jpet.104.079079
44. Honda K, Arima M, Cheng G, Taki S, Hirata H, Eda F, et al. Prostaglandin D2 reinforces Th2 type inflammatory responses of airways to low-dose antigen through bronchial expression of macrophage-derived chemokine. *J Exp Med* (2003) 198:533–43. doi: 10.1084/jem.20022218
45. Mesquita-Santos FP, Bakker-Abreu I, Luna-Gomes T, Bozza PT, Diaz BL, Bandeira-Melo C. Co-operative signalling through DP(1) and DP(2) prostanoid receptors is required to enhance leukotriene C(4) synthesis induced by prostaglandin D(2) in eosinophils. *Br J Pharmacol* (2011) 162:1674–85. doi: 10.1111/j.1476-5381.2010.01086.x
46. Mukai K, Tsai M, Saito H, Galli SJ. Mast cells as sources of cytokines, chemokines, and growth factors. *Immunol Rev* (2018) 282:121–50. doi: 10.1111/imr.12634
47. Bandeira-Melo C, Phoofolo M, Weller PF. Extranuclear lipid bodies, elicited by CCR3-mediated signaling pathways, are the sites of chemokine-enhanced leukotriene C4 production in eosinophils and basophils. *J Biol Chem* (2001) 276:22779–87. doi: 10.1074/jbc.M101436200
48. Wu D, Molofsky AB, Liang H-E, Ricardo-Gonzalez RR, Jouihan HA, Bando JK, et al. Eosinophils sustain adipose alternatively activated macrophages associated with glucose homeostasis. *Science* (2011) 332:243–7. doi: 10.1126/science.1201475
49. Watanabe H, Numata K, Ito T, Takagi K, Matsukawa A. Innate immune response in Th1- and Th2-dominant mouse strains. *Shock Augusta Ga* (2004) 22:460–6. doi: 10.1097/01.shk.0000142249.08135.e9
50. Moussa K, Gurung P, Adams-Huet B, Devaraj S, Jialal I. Increased eosinophils in adipose tissue of metabolic syndrome. *J Diabetes Complications* (2019) 33:535–8. doi: 10.1016/j.jdiacomp.2019.05.010
51. Goh YPS, Henderson NC, Heredia JE, Red Eagle A, Odegaard JI, Lehwald N, et al. Eosinophils secrete IL-4 to facilitate liver regeneration. *Proc Natl Acad Sci U S A* (2013) 110:9914–9. doi: 10.1073/pnas.1304046110
52. Heredia JE, Mukundan L, Chen FM, Mueller AA, Deo RC, Locksley RM, et al. Type 2 innate signals stimulate fibro/adipogenic progenitors to facilitate muscle regeneration. *Cell* (2013) 153:376–88. doi: 10.1016/j.cell.2013.02.053
53. Pereira-Dutra FS, Teixeira L, de Souza Costa MF, Bozza PT. Fat, fight, and beyond: The multiple roles of lipid droplets in infections and inflammation. *J Leukoc Biol* (2019) 106:563–80. doi: 10.1002/JLB.4MR0119-035R
54. Bozza PT, Bakker-Abreu I, Navarro-Xavier RA, Bandeira-Melo C. Lipid body function in eicosanoid synthesis: an update. *Prostagland Leukot Essent Fatty Acids* (2011) 85:205–13. doi: 10.1016/j.plefa.2011.04.020
55. Melo RCN, Weller PF. Lipid droplets in leukocytes: Organelles linked to inflammatory responses. *Exp Cell Res* (2016) 340:193–7. doi: 10.1016/j.yexcr.2015.10.028
56. Lund SJ, Portillo A, Cavagnero K, Baum RE, Naji LH, Badrani JH, et al. Leukotriene C4 Potentiates IL-33-Induced Group 2 Innate Lymphoid Cell Activation and Lung Inflammation. *J Immunol Baltim Md 1950* (2017) 199:1096–104. doi: 10.4049/jimmunol.1601569

57. Bandeira-Melo C, Hall JC, Penrose JF, Weller PF. Cysteinyl leukotrienes induce IL-4 release from cord blood-derived human eosinophils. *J Allergy Clin Immunol* (2002) 109:975–9. doi: 10.1067/mai.2002.124269
58. Reginato MJ, Krakow SL, Bailey ST, Lazar MA. Prostaglandins promote and block adipogenesis through opposing effects on peroxisome proliferator-activated receptor gamma. *J Biol Chem* (1998) 273:1855–8. doi: 10.1074/jbc.273.4.1855
59. Rahman MS. Prostacyclin: A major prostaglandin in the regulation of adipose tissue development. *J Cell Physiol* (2019) 234:3254–62. doi: 10.1002/jcp.26932
60. Elieh Ali Komi D, Shafaghat F, Christian M. Crosstalk Between Mast Cells and Adipocytes in Physiologic and Pathologic Conditions. *Clin Rev Allergy Immunol* (2020) 58:388–400. doi: 10.1007/s12016-020-08785-7
61. Milling S. Adipokines and the control of mast cell functions: from obesity to inflammation? *Immunology* (2019) 158:1–2. doi: 10.1111/imm.13104
62. Żelechowska P, Wiktorska M, Różalska S, Stasikowska-Kanicka O, Wągrowska-Danilewicz M, Agier J, et al. Leptin receptor is expressed by tissue mast cells. *Immunol Res* (2018) 66:557–66. doi: 10.1007/s12026-018-9029-0
63. Żelechowska P, Agier J, Różalska S, Wiktorska M, Brzezińska-Błaszczyk E. Leptin stimulates tissue rat mast cell pro-inflammatory activity and migratory response. *Inflammation Res Off J Eur Histamine Res Soc Al* (2018) 67:789–99. doi: 10.1007/s00011-018-1171-6
64. Xue L, Gyles SL, Wettey FR, Gazi L, Townsend E, Hunter MG, et al. Prostaglandin D2 causes preferential induction of proinflammatory Th2 cytokine production through an action on chemoattractant receptor-like molecule expressed on Th2 cells. *J Immunol Baltim Md 1950* (2005) 175:6531–6. doi: 10.4049/jimmunol.175.10.6531
65. Palhinha L, Liechocki S, Hottz ED, Pereira JA da S, de Almeida CJ, Moraes-Vieira PMM, et al. Leptin Induces Proadipogenic and Proinflammatory Signaling in Adipocytes. *Front Endocrinol* (2019) 10:841. doi: 10.3389/fendo.2019.00841
66. Peeraully MR, Sievert H, Bulló M, Wang B, Trayhurn P. Prostaglandin D2 and J2-series (PGJ2, Delta12-PGJ2) prostaglandins stimulate IL-6 and MCP-1, but inhibit leptin, expression and secretion by 3T3-L1 adipocytes. *Pflugers Arch* (2006) 453:177–87. doi: 10.1007/s00424-006-0118-x
67. Xue L, Salimi M, Panse I, Mjösberg JM, McKenzie ANJ, Spits H, et al. Prostaglandin D2 activates group 2 innate lymphoid cells through chemoattractant receptor-homologous molecule expressed on TH2 cells. *J Allergy Clin Immunol* (2014) 133:1184–94. doi: 10.1016/j.jaci.2013.10.056
68. Mjösberg JM, Trifari S, Crellin NK, Peters CP, van Drunen CM, Piet B, et al. Human IL-25- and IL-33-responsive type 2 innate lymphoid cells are defined by expression of CRTH2 and CD161. *Nat Immunol* (2011) 12:1055–62. doi: 10.1038/ni.2104
69. Virtue S, Masoodi M, de Weijer B a. M, van Eijk M, Mok CYL, Eiden M, et al. Prostaglandin profiling reveals a role for haematopoietic prostaglandin D synthase in adipose tissue macrophage polarisation in mice and humans. *Int J Obes 2005* (2015) 39:1151–60. doi: 10.1038/ijo.2015.34

Conflict of Interest: The authors declare that the research was conducted in the absence of any commercial or financial relationships that could be construed as a potential conflict of interest.

frontiers in Neuroscience

ORIGINAL RESEARCH
published: 19 November 2020
doi: 10.3389/fnins.2020.585604

Intracerebroventricular Administration of Interferon-Alpha Induced Depressive-Like Behaviors and Neurotransmitter Changes in Rhesus Monkeys

Zhifei Li[1], Zhaoxia Li[1], Xiaoman Lv[2], Zhaofu Li[2], Lei Xiong[2], Xintian Hu[1,3,4,5]* and Dongdong Qin[1,2]**

[1] Key Laboratory of Animal Models and Human Disease Mechanisms of the Chinese Academy of Sciences and Yunnan Province, Kunming Institute of Zoology, Chinese Academy of Sciences, Kunming, China, [2] Yunnan University of Chinese Medicine, Kunming, China, [3] National Resource Center for Non-Human Primates, Kunming Primate Research Center, National Research Facility for Phenotypic & Genetic Analysis of Model Animals (Primate Facility), Kunming Institute of Zoology, Chinese Academy of Sciences, Kunming, China, [4] Kunming Primate Research Center, Kunming Institute of Zoology, Chinese Academy of Sciences, Kunming, China, [5] Center for Excellence in Brain Science and Intelligence Technology, Chinese Academy of Sciences, Shanghai, China

OPEN ACCESS

Edited by:
Clarissa M. Maya-Monteiro, Oswaldo Cruz Foundation (Fiocruz), Brazil

Reviewed by:
Sarah Haas Lockie, Monash University, Australia
Richard G. Hunter, University of Massachusetts Boston, United States

***Correspondence:**
Lei Xiong
xlluck@sina.com
Xintian Hu
xthu@mail.kiz.ac.cn
Dongdong Qin
qindong108@163.com

Specialty section:
This article was submitted to Neuroendocrine Science, a section of the journal Frontiers in Neuroscience

Received: *21 July 2020*
Accepted: *19 October 2020*
Published: *19 November 2020*

Citation:
Li Z, Li Z, Lv X, Li Z, Xiong L, Hu X and Qin D (2020) Intracerebroventricular Administration of Interferon-Alpha Induced Depressive-Like Behaviors and Neurotransmitter Changes in Rhesus Monkeys. Front. Neurosci. 14:585604. doi: 10.3389/fnins.2020.585604

Interferon-alpha (IFN-α) is a cytokine widely used in the treatment of brain cancers and virus infections with side effects including causing depression. Monoamine neurotransmitter systems have been found playing important roles in peripheral IFN-α-induced depression, but how peripheral IFN-α accesses the central nervous system and contributes to the development of depression is poorly known. This study aimed to develop a non-human primate model using long-term intracerebroventricular (i.c.v.) administration of IFN-α (5 days/week for 6 weeks), to observe the induced depressive-like behaviors and to explore the contributions of monoamine neurotransmitter systems in the development of depression. In monkeys receiving i.c.v. IFN-α administration, anhedonia was observed as decreases of sucrose consumption, along with depressive-like symptoms including increased huddling behavior, decreases of spontaneous and reactive locomotion in home cage, as well as reduced exploration and increased motionless in the open field. Chronic central IFN-α infusion significantly increased the cerebrospinal fluid (CSF) concentrations of noradrenaline (NA), and 3,4-dihydroxyphenylacetic acid (DOPAC), but not 5-hydroxyindoleacetic acid (5-HIAA) and homovanillic acid (HVA). These CSF monoamine metabolites showed associations with some specific depression-related behaviors. In conclusion, central IFN-α administration induced anhedonia and depression-related behaviors comparable to the results with peripheral administration, and the development of depression was associated with the dysfunction of monoamine neurotransmitters.

Keywords: interferon-alpha, intracerebroventricular administration, rhesus monkeys, depressive-like behaviors, neurotransmitters

INTRODUCTION

Interferon-alpha (IFN-α) is a pleiotropic cytokine released in response to viral infection, which enhances the cellular immune response. IFN-α is usually used to treat certain cancers and infectious diseases because of its antiproliferative and antiviral effects. For example, intraventricular administration of IFN-α was used to treat central nervous system (CNS) diseases induced by viral infection such as subacute sclerosing panencephalitis (SSPE) (Yalaz et al., 1992; Kwak et al., 2019). However, 30–50% of the patients receiving IFN-α treatment suffer from major depressive disorder (MDD) (Hepgul et al., 2018; Su et al., 2019). Recruitment of cytokines including the IFN-α during CNS inflammation also contributes to the development of depression (Bodnar et al., 2018; Su et al., 2019).

How peripherally administrated IFN-α (e.g., intravenous and intramuscular injection) induces depression has been well studied in animal models including rodents (Hoyo-Becerra et al., 2015) and non-human primates (Felger et al., 2007). Rhesus monkeys receiving chronic (4 weeks) subcutaneous IFN-α administration showed increased anxiety-like and depression-like behaviors as well as diminished environmental exploration, accompanied by increased levels of plasma adrenocorticotropic hormone (ACTH) and cortisol, which tended to improve after the administration terminated. Monkeys that showed IFN-α-induced huddling behavior had lower cerebrospinal fluid (CSF) concentrations of homovanillic acid (HVA), a dopamine metabolite (Felger et al., 2007).

The study of mechanisms underlying IFN-α-induced depression has been largely focused on the monoamine neurotransmitter systems (Lotrich et al., 2009; Felger and Miller, 2012; Ping et al., 2012; Felger et al., 2013b). Monoamine neurotransmitters in the brain, especially serotonin (5-HT), play critical roles in the development of depression. Most antidepressants target at the functioning of 5-HT, such as selective serotonin reuptake inhibitors (SSRIs). Studies in both humans and laboratory animals have found that IFN-α administration can disrupt the functions of monoamine neurotransmitters by decreasing their synthesis and release (Anderson et al., 2013; Felger and Lotrich, 2013; Felger et al., 2013a), inhibiting their binding to the receptors (Ping et al., 2012; Felger et al., 2013b) and/or upregulating the reuptake from synapses (Tsao et al., 2008; Capuron et al., 2012).

It should be noted that IFN-α was peripherally administrated in most studies, and they are relatively large molecules (∼15–25 kD) that do not freely pass through the blood–brain barrier (BBB) (Collins et al., 1985; Smith et al., 1985), while some studies have reported that IFNs can enter the CNS from the periphery but with regional differences, and the spinal cord had greater permeability to IFNs than did the brain (Pan et al., 1997). Therefore, much attention should be paid to the pathways by which peripheral IFN-α signals reach the brain. Laboratory studies have shown that cytokines administered peripherally can access the brain through several routes including (1) passage through leaky regions in the BBB, (2) active transport via saturable transport molecules, (3) activation of endothelial cells (as well as other cells lining the cerebral vasculature), which then release inflammatory mediators within the brain parenchyma, and (4) binding to cytokine receptors associated with peripheral afferent nerve fibers (e.g., the vagus nerve) which in turn relay signals to relevant brain nuclei (Goehler et al., 2000; Quan and Banks, 2007; Dantzer et al., 2008). Nevertheless, it remains to be established whether peripheral IFN-α can access the brain and affect the brain functioning. Moreover, it has yet to be determined whether IFN-α-induced changes in behavior in humans are related to effects of central cytokines on the metabolism of behaviorally relevant neurotransmitter systems. Thus, it will be interesting to know: (1) whether direct administration of IFN-α into the brain can cause similar depression-like behaviors in rhesus monkeys as observed with peripheral administration; and (2) whether IFN-α can induce changes in monoamine neurotransmitters and contribute to the development of depression. In this study, IFN-α was directly delivered into the CNS via intracerebroventricular (i.c.v) administration. We analyzed the effects of central IFN-α on anhedonia, depression-related behaviors in both home cage and the open field, as well as the CSF concentrations of monoamine neurotransmitters and their metabolites.

MATERIALS AND METHODS

Animals

All animal care and experimental protocols were approved by the National Animal Research Authority (China) and the Institutional Animal Care and Use Committee (IACUC) of Kunming Institute of Zoology, Chinese Academy of Sciences. Eight male rhesus monkeys (*Macaca mulatta*) ranging from 7 to 10 years old (8.00 ± 1.20, mean ± SD) were purchased from Kunming Primate Research Center of the Chinese Academy of Sciences. All monkeys were individually housed in a stainless-steel cage (80 × 80 × 80 cm) on the same side of the housing room with relatively constant temperature of 21 ± 2°C. Artificial illumination (800 lx) was provided from 07:00 to 19:00. Monkeys were supplied with commercial monkey biscuits and fruits, as well as *ad libitum* access to tap water, except for the days of sucrose preference test. Routine veterinary care was provided throughout the experiment by professional keepers and veterinarians. All possible efforts were made to minimize the suffering of animals.

Surgical Procedures

After 1 week of habituation to the housing environment, all animals received the surgery of intraventricular intubation. The surgical procedures have been described in previous studies (Li et al., 2015; Zhai et al., 2018). Animals were anesthetized with intramuscular injections of atropine (20 mg/kg), ketamine (10 mg/kg), and sodium pentobarbital (20 mg/kg). Anesthesia was confirmed by pinching toes of the monkey, before fixing its head on a stereotaxic instrument (Model 1504 Heavy-Duty Research Stereotaxic for Monkeys, KOPF, United States). The skull over the parietal lobe was exposed by a longitudinal incision of the scalp, and tissues on the skull were removed. A small hole (about 2 mm in diameter) in the skull was

drilled (anterioposterior: + 17 mm; mediolateral: −2 mm, with reference to the midpoint of the interaural line). A stainless-steel cannula (21 gauge, 40 mm, New England Small Tube Corporation, United States) was vertically inserted through the hole into the right lateral ventricle with depths ranging from 18 to 22 mm beneath the surface of the skull. Outflow or pulsation of the CSF at the orifice indicated that the cannula had reached the lateral ventricle. The cannula was then blocked with a removable stainless-steel plug, and protected with a truncated plastic centrifuge tube (15 ml) with the cap. Three titanium alloy screws were fixed on the skull surface to anchor the dental cement to the skull. Postoperative care was conducted by a veterinarian with daily observation and intramuscular injections of Penicillin (1,600 K Unit, Harbin Pharmaceutical Group Sixth Pharm Factory, Harbin, China) for 7 days, before any behavioral observation and i.c.v. administration.

Intraventricular Administration of IFN-α

Postoperative monkeys were trained to sit in a customized monkey chair until they were habituated to the manipulations of intraventricular injection without anesthesia and experience of stress. All monkeys were then randomly separated into two administration groups with four animals in each group. Recombinant human IFN-α (1.4×10^5 IU/kg bodyweight) or saline in equivalent volume was injected into the lateral ventricle gradually over a period of 15 min between 9:30 and 12:00 for 6 weeks (5 days/week). On the first and second administration day, the injected doses were, respectively, 1/4 and 1/2 of the normal dose in order to adapt monkeys to the drugs. A stainless-steel needle (42 mm) connected to a syringe with silicone capillary tube was inserted into the cannula for the injection. The injection was conducted with a microinjection pump (Smith WZ-50C6, Zhejiang Smith Medical Instrument Co Ltd, Hangzhou, China) when the animal was sitting awake in the monkey chair. The injection needle was retained in place for 5 min after the completion of injection.

Sucrose Preference Tests

Sucrose preference tests were conducted in three 3-week phases, with 14 tests in each phase, namely, preadministration (Pre), the first half (Adm1) and second half (Adm2) of the administration period. Each phase lasted for 3 weeks, and the sucrose preference test was measured in a water-deprived state to maximize the motivation of monkeys. Briefly, a 1.5% sucrose solution and tap water was available in two adjacent bottles fixed to every home-cage from 8:30 to 9:30 every day, with no extra water available during the days of sucrose preference tests. Positions of these two liquids were switched every day to avoid the potential effects of position preference (Paul et al., 2000; Qin et al., 2015a). The consumed volume of each liquid was quantified and recorded. The sucrose preference was calculated as a percentage of consumed sucrose solution of the total amount of water drunk. Sucrose water and tap water intake were, respectively, calculated as ml consumed per kg body weight.

Behaviors in Home Cage

Each monkey was videotaped for 30 min a day. Before the administration, the video recording lasted for 14 days. After completion of the injection, each monkey was again videotaped for another 14 days (30 min per day). The video recordings were evenly distributed in the light phase, with 3.5 h in the morning (8:00–8:30 a.m., 8:30–9:00 a.m., 9:00–9:30 a.m., 9:30–10:00 a.m., 10:00–10:30 a.m., 10:30–11:00 a.m., and 11:00–11:30 a.m.), and 3.5 h in the afternoon (14:00–14:30 p.m., 14:30–15:00 p.m., 15:00–15:30 p.m., 15:30–16:00 p.m., 16:00–16:30 p.m., 16:30–17:00 p.m., and 17:00–17:30 p.m.). The recordings were analyzed by three trained raters blinded to the experiment design, with an inter-rater correlation coefficient of >0.90 after a period of training. The ethogram in the home cage included huddling, exploration, spontaneous locomotion, reactive locomotion, anxiety-like behaviors, stereotyped behaviors, self-grooming, and masturbating.

Huddling, measured as a depression-like behavior in monkeys, was defined as a fetal-like and self-enclosed posture with the head at or below the shoulders during the waking state (Harlow and Suomi, 1971; Shively et al., 2005; Qin et al., 2015a,b, 2019, 2016). Exploration consisted of oral or tactile manipulation of surroundings and body parts except self-grooming and masturbating (Felger et al., 2007; Davenport et al., 2008). Spontaneous locomotion included walking, running, and jumping other than stereotyped behaviors. Reactive locomotion was locomotor activities inspired by environmental stimuli. All behaviors were quantified as frequency and duration per 30-min, and the data were presented as an average of 14 days.

Open-Field Test

The floor (2.06 × 1.80 m) of the open-field test room (2.20-m high) was equally divided into 5 × 5 rectangles with red-painted lines. The monkeys were individually transported into the test room with a transport cage. Each monkey was tested for 7 days, respectively, before and after the administration without stimulus from the experimenters (15 min/day). The test for each monkey was performed at the same time of the day to minimize the effects of time. The animals were leashed with a flexible rope to help in retreating them from the test room. The rope was long enough to reach every position in the room. Videotaped behaviors of all tests were scored by raters blinded to the treatment condition. Behaviors related to anxiety and depression were analyzed, namely, urination, defecation, spontaneous locomotion, grids crossed, exploration, motionless, stereotypical behaviors, huddling, masturbating, self-grooming, attacking, and vocalization. All behaviors were presented as the mean of seven open-field tests.

Sampling and Measurement of Cerebrospinal Fluid Neurochemicals

The CSF samples was obtained the day before the first and the day after the last administration under ketamine (10 mg/kg) anesthesia within 10–20 min of the initial experimenter contact. Lumbar CSF was collected passively into chilled polypropylene tubes via a spinal needle inserted into the dorsolumbar vertebrae. The collected samples were immediately frozen in liquid nitrogen and stored at −80°C until assayed. The CSF samples were centrifuged at 8,000 × g for 10 min at 4°C. Concentrations of noradrenaline (NA) and its metabolite HVA,

5-hydroxyindole acetic acid (5-HIAA, the metabolite of 5-HT), as well as 3,4-dihydroxyphenylacetic acid (DOPAC, the metabolite of DA), were assessed using high-performance liquid chromatography (HPLC) (Yu et al., 2003). Samples from a given animal obtained before and after administration were paired and run in a single assay. Details about the HPLC system and procedures have been described previously (Qin et al., 2019). Data of each sample represent the average of at least two assessments.

Statistical Analysis

All statistics and plotting were performed with GraphPad (GraphPad Prism 7.04), except that the extraction of principal components from log-transformed CSF concentrations of monoamine metabolites was conducted with SPSS (IBM SPSS Statistics 19). Two-way ANOVA with repeated measures were used to analyze the differences between the Ctrl and IFN group in sucrose preference, sucrose intake, relative sucrose intake (normalized to sucrose intake before the administration), and all measured behaviors in the home cage and the open field, with Bonferroni multiple comparisons. Pearson linear correlation was used to assess the associations among the CSF concentrations of monoamine metabolites, sucrose intake, and behaviors in the home cage and the open field. All data were presented as mean ± SD (standard deviation), and all p-values in the results were two tailed with an α level of $p < 0.050$.

RESULTS

Anhedonia Induced by Long-Term Interferon-Alpha Intracerebroventricular Administration

The bodyweight of IFN and Ctrl groups was comparable before and after the administration of IFN-α or saline (**Figure 1A**). The bodyweights of all animals were slightly increased after the administration, and the changes were significant in the Ctrl group (**Figure 1A**, $^{\$}p = 0.016$).

Long-term i.c.v. IFN-α administration tended to decrease the sucrose preference (IFN group: Pre, 84.78%; Adm2, 68.34%), but the changes were not significant (**Figure 1B**, all $p > 0.050$). Thereafter, we compared the volume of sucrose intake, which was significantly decreased in Adm2 compared with the Pre phase in the IFN group (**Figure 1C**, $^{*}p = 0.049$). In order to diminish the effect of individual difference, the sucrose intake in Adm2 was normalized to Pre for each individual animal. The sucrose intake of IFN group was reduced into 65.65 and 60.28%, respectively, in Adm1 and Adm2, and the difference between IFN group and the Ctrl group in Adm2 was significant (**Figure 1D**, $^{\#}p = 0.036$), with a significant effect of time revealed by two-way ANOVA ($p = 0.037$). Finally, no significant change was observed in the consumption of tap water.

Depression-Related Behaviors Induced by Long-Term Interferon-Alpha Intracerebroventricular Administration

The IFN group showed increased post-Adm huddling frequency (**Figure 2A**, $^{*}p = 0.019$) and duration (**Figure 2B**, $^{*}p = 0.037$) compared with pre-Adm. The IFN group exhibited higher frequency of huddling behavior than the Ctrl group (**Figure 2A**, $^{\#}p = 0.021$) after the IFN-α i.c.v. administration. Two-way ANOVA revealed significant effect of interaction between time and treatment on both frequency ($p = 0.022$) and duration ($p = 0.047$) of huddling behavior. Consistently, inhibited duration of spontaneous locomotion (**Figure 2C**, $^{*}p = 0.016$) as well as reduced frequency (**Figure 2D**, $^{*}p = 0.044$) and duration (**Figure 2E**, $^{*}p = 0.020$) of reactive locomotion was observed in the IFN group after IFN-α i.c.v. administration. Finally, no significant change in exploration, anxiety-like behaviors, self-grooming, masturbating, and stereotyped behaviors was observed in either group after the i.c.v. administration of IFN-α or saline.

One monkey in the IFN group was excluded when the behaviors were analyzed in the open field because it barely moved in the test room both before and after the IFN-α administration. Different from the behaviors in home cage, no huddling behavior was observed in the open field. Long-term

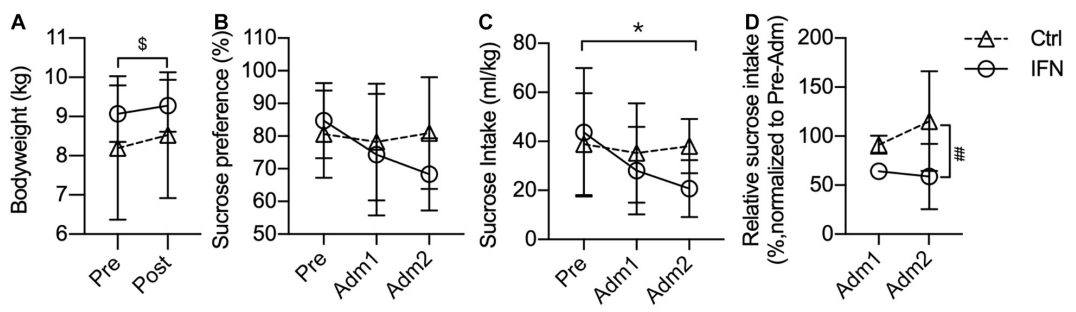

FIGURE 1 | Long-term IFN-α i.c.v. administration significantly reduced the sucrose intake. The bodyweight of the Ctrl and IFN groups was comparable before and after the administration period **(A)**. Long-term IFN-α i.c.v. administration tended to decrease the sucrose preference **(B)**, and significantly reduced the sucrose intake of monkeys in the IFN group compared with the Pre phase **(C)**, as well as with the Ctrl group **(C)**. The sucrose intake was normalized to Pre for each individual animal, and they were reduced in the IFN group **(D)**. Adm1, the first 3-week of administration. Adm2, the second 3-week of administration. Ctrl, control group ($n = 4$). IFN, IFN-α administration group ($n = 4$). NS, not significant. Pre, pre-administration. Ctrl-Pre vs Ctrl-Post: $^{\$}p < 0.050$. IFN-Pre vs IFN-Adm2: $^{*}p < 0.050$. Ctrl-Adm2 vs IFN-Adm2: $^{\#\#}p < 0.010$. Error bar: mean ± S D.

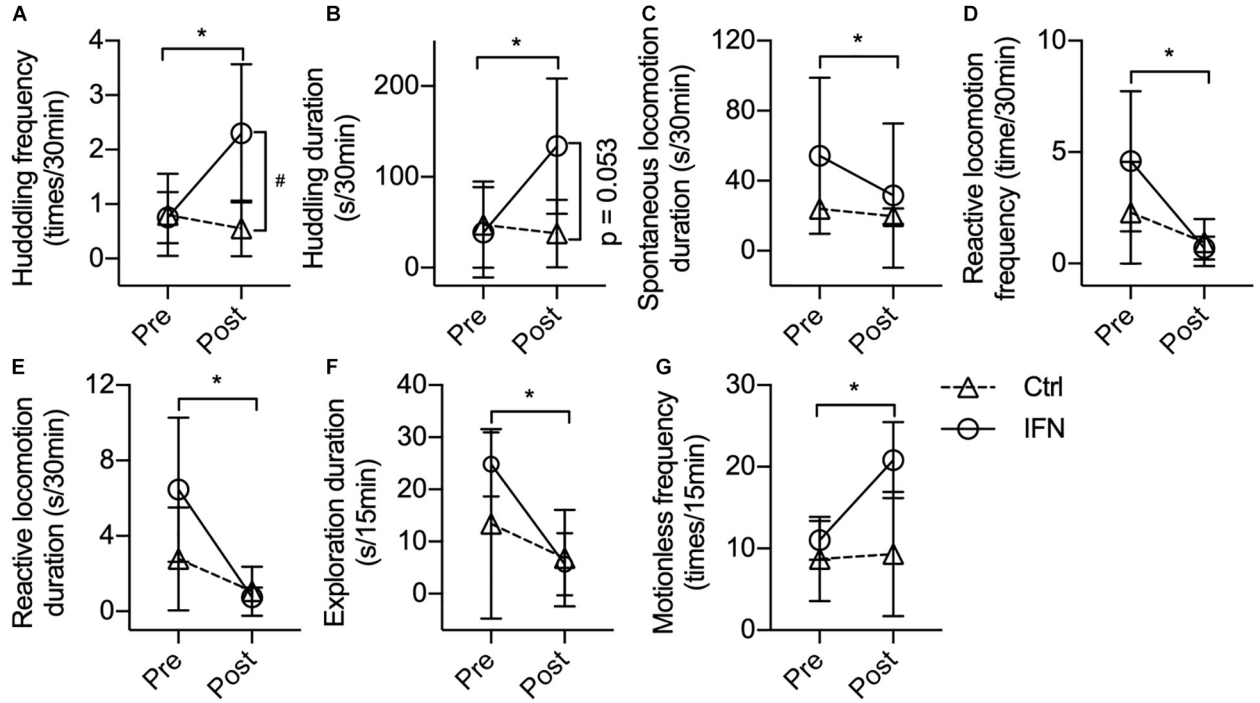

FIGURE 2 | Long-term IFN-α i.c.v. administration induced depressive-like behavioral changes in rhesus monkeys in the home cage and open-field test. Six weeks of IFN-α i.c.v. administration enhanced huddling behavior. **(A,B)** while inhibiting spontaneous locomotion **(C)** and reactive locomotion **(D,E)** in the home cage. In the open-field test, IFN-α reduced the exploration duration **(F)** and increased motionless frequency **(G)** of the IFN group. Behaviors with a time scale of 30 and 15 min were observed in the home cage **(A–E)** and in the open-field **(F,G)** tests, respectively. Ctrl, control group ($n = 4$). IFN, IFN-α administration group [$n = 4$ for **(A–E)**; $n = 3$ for **(F,G)]**. Post, post-administration; Pre, pre-administration. IFN-Pre vs. IFN-Post: $^{*}p < 0.050$. Ctrl-Post vs. IFN-Post: $^{\#}p < 0.050$. Error bar: mean ± SD.

IFN-α i.c.v. administration significantly reduced the duration of environmental exploration of the IFN group (**Figure 2F**, $p = 0.012$), with a significant effect of time ($p = 0.006$) revealed by two-way ANOVA. The IFN group showed significantly higher post-Adm motionless frequency than the Ctrl group (**Figure 2G**, $^{*}p = 0.044$) in the open field after 6 weeks of IFN-α administration. No significant change was observed in the frequency and duration of locomotion and grids crossed during locomotion. Finally, some behaviors including urinating, defecating, self-grooming, masturbating, attacking, or vocalization were too scarce in the open field to do a statistical analysis.

Interferon-Alpha Intracerebroventricular Administration Increased Cerebrospinal Fluid Concentrations of Noradrenaline and 3,4-Dihydroxyphenylacetic Acid

The IFN group had increased the CSF concentrations of NA (**Figure 3A**, $^{*}p = 0.007$) and DOPAC (**Figure 3B**, $^{*}p = 0.023$) after IFN-α administration. Further way-way ANOVA revealed a significant effect of time ($p = 0.006$) and interaction between time and group ($p = 0.044$) on the CSF NA, as well as a significant effect of group ($p = 0.022$) on the DOPAC. However, the CSF concentrations of 5-HIAA (**Figure 3C**, $p > 0.050$) and HVA (**Figure 3D**, $p > 0.050$) were not significantly changed by i.c.v. administration of saline or IFN-α. In order to assess the integrated functions of monoamines on the behaviors, two principal components were derived from the log-transformed CSF concentrations of all four monoamine metabolites as log(NT)s-PC1 and log(NT)s-PC2 with principal component analysis (PCA). After long-term IFN-α i.c.v. administration, the IFN group had increased log(NT)s-PC1 compared with pre-Adm (**Figure 3E**, $^{\#}p = 0.031$), as well as higher log(NT)s-PC2 compared with the Ctrl group (**Figure 3F**, $^{**}p = 0.007$). Two-way ANOVA revealed significant effect of group on log(NT)s-PC1 ($p = 0.011$) and effect of time on log(NT)s-PC2 ($p = 0.006$). The CSF concentrations of 5-HIAA showed positive correlations with those of DOPAC and HVA (**Figures 3G,H**).

Correlations Between the Cerebrospinal Fluid Concentrations of Monoamine Metabolites and Depression-Related Behaviors

Sucrose preference could be predicted by the CSF concentrations of NA and log(NT)s-PC1 with negative correlations (**Figures 4A,B**). Similarly, sucrose intake showed negative correlations with the CSF concentrations of 5-HIAA and log(NT)s-PC1 (**Figures 4C,D**, respectively). In the home cage, the CSF levels of both NA and DOPAC were strong predictors of huddling frequency (**Figures 4E,F**, respectively), and the duration of huddling behavior could also be predicted by the CSF NA levels (**Figure 4G**). Both the frequency and

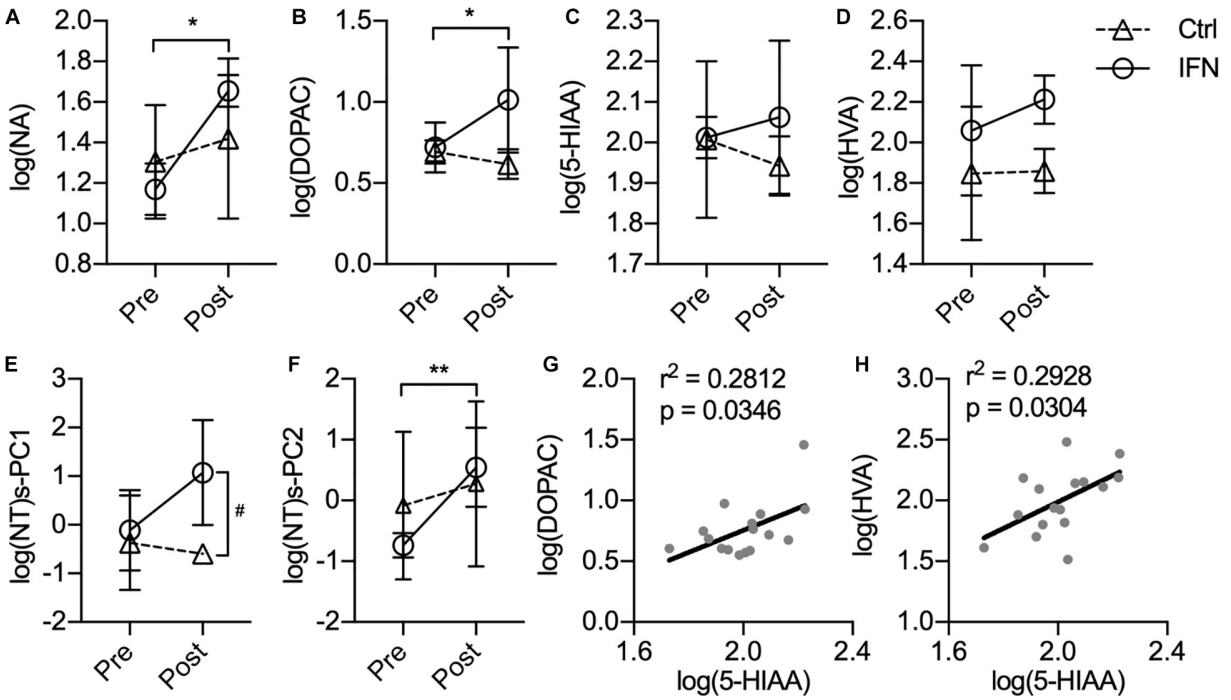

FIGURE 3 | Long-term IFN-α i.c.v. administration increased the cerebrospinal fluid (CSF) concentrations of monoamine metabolites. The CSF concentrations of NA **(A)** and DOPAC **(B)** were significantly increased after IFN-α i.c.v. administration, but not 5-hydroxyindole acetic acid (5-HIAA) **(C)** and homovanillic acid (HVA) **(D)**. The principal components extracted from the log-transformed CSF concentrations of these four monoamine metabolites were also augmented by IFN-α administration **(E,F)**. The CSF concentrations of 5-HIAA showed positive correlation with those of DOPAC **(G)** and HVA **(H)**. Ctrl, control group ($n = 4$). IFN, IFN-α administration group ($n = 4$). log(NT)s-PC1 and log(NT)s-PC2, principal components derived from the log-transformed CSF concentrations of four measured monoamine metabolites. NT, neurotransmitter. Post, post-administration. Pre, pre-administration. IFN-Pre vs. IFN-Post: $^{*}p < 0.050$. Ctrl-Post vs. IFN-Post: $^{\#}p < 0.050$. Error bar: mean ± SD. IFN-Pre vs. IFN-Post: $^{**}p < 0.010$.

duration of reactive locomotion in the home cage showed a negative correlation with log(NT)s-PC2 (**Figures 4H,I**). In the open field, a negative correlation was found between the duration of exploration and the CSF 5-HIAA concentrations (**Figure 4J**). Motionless frequency in the open field was positively correlated with the CSF HVA levels (**Figure 4K**). Finally, the CSF concentrations of NA showed positive correlations with the locomotion duration, number of crossed grids, and speed of locomotion in the open field (**Figures 4L–N**).

Correlations Between Behaviors in Different Tests

Until now, depression-like behavioral changes induced by long-term i.c.v. administration of IFN-α have been observed in sucrose preference test, in home cage, and in the open-field test. Monkeys in the IFN group displayed different aspects of depression-related behaviors. It would be interesting to know whether behaviors displayed in different tests had some innate relation with each other. In **Figure 4**, we can see that some neurotransmitters showed correlations with behaviors in different tests, indicating that behaviors in different tests could be modulated by the same changes in neurotransmitters. Thus, the correlations between behaviors in different tests were analyzed. Sucrose preference was positively correlated with both frequency and duration of masturbating behavior in home cage (**Figures 5A,B**). Sucrose intake was positively correlated with both frequency and duration of the exploration behaviors in the open field (**Figures 5C,D**). The frequency of locomotion in the open field showed strong positive correlations with the frequency and duration of locomotion (**Figures 5E,F**) and exploration (**Figures 5G,H**), as well as the masturbating frequency in the home cage (**Figure 5I**). Finally, the frequency and duration of the self-grooming behavior in the home cage were negatively correlated with the frequency of motionless in the open field (**Figures 5J,K**).

DISCUSSION

In humans, peripheral IFN-α-induced depression is more associated with somatic symptoms and less associated with symptoms of mood and negative cognition, compared with patients with major depressive disorder (Capuron et al., 2009; Su et al., 2019). Consistently, the anxiety-like behaviors and stereotypical behaviors were not changed by IFN-α administration in this study. The increased huddling and motionless frequency, as well as decreased spontaneous locomotion and reactive locomotion were more likely to be a manifestation of depressed mood or loss of interest and motivation, rather than physical retardation (e.g., fatigue) because the mobility was not reduced in the open field. In support of this possibility, the locomotor behaviors in both home cage

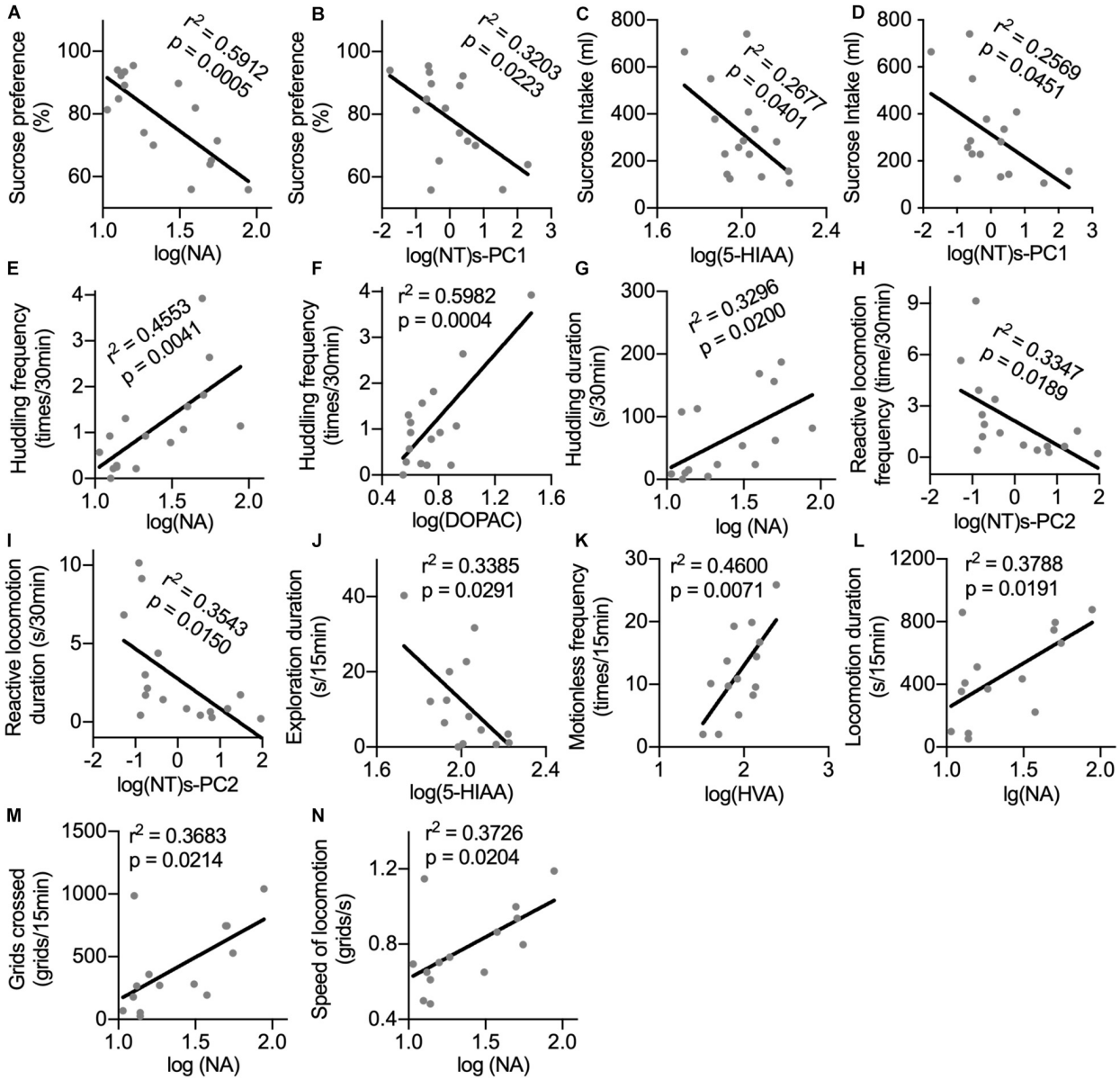

FIGURE 4 | Correlations between the CSF concentrations of monoamine metabolites with anhedonia and depression-related behaviors. For the correlation analysis of the CSF monoamine metabolites with sucrose consumption **(A–D)** and behaviors in home cage **(E–I)**, the sample size was $n = 16$. For the correlation analysis between the CSF monoamine metabolites and behaviors in the open field test **(J–N)**, the sample size was $n = 14$ because one monkey was excluded from the IFN group. Behaviors with time scale of 30 and 15 min were observed in the home cage and in the open-field test, respectively. NT, neurotransmitter. log(NT)s-PC1 and log(NT)s-PC2, principal components derived from the log-transformed CSF concentrations of four measured monoamine metabolites.

and the open field were positively associated with intrinsically motivated behaviors including masturbating, self-grooming, and exploratory behaviors. We also found correlations between behaviors in different tests. For example, monkeys, which showed lower sucrose preference, tended to show lower masturbating behavior in the home cage, and monkeys which showed lower sucrose intake also tended to have less exploratory behavior in the open-field test. Moreover, both sucrose intake and exploratory behavior were positively correlated with the CSF concentrations of 5-HIAA, indicating that these behaviors in the different tests could be influenced by the same changes in neurotransmitters.

Huddling behavior was observed in monkeys even before saline/IFN-α administration in this study. It was different from Felger's study (Felger et al., 2007), possibly because of the small and isolated housing environment (Suomi and Harlow, 1972). Thus, IFN-α induced depressive-like behaviors in monkeys, but the development and expression of the depressive symptoms was also environment dependent. In support of this hypothesis, huddling behavior was only observed in the home cage, and IFN-α administration only inhibited exploration in the open field. Another interesting finding was that the association between CSF monoamine metabolites and specific behaviors only existed in

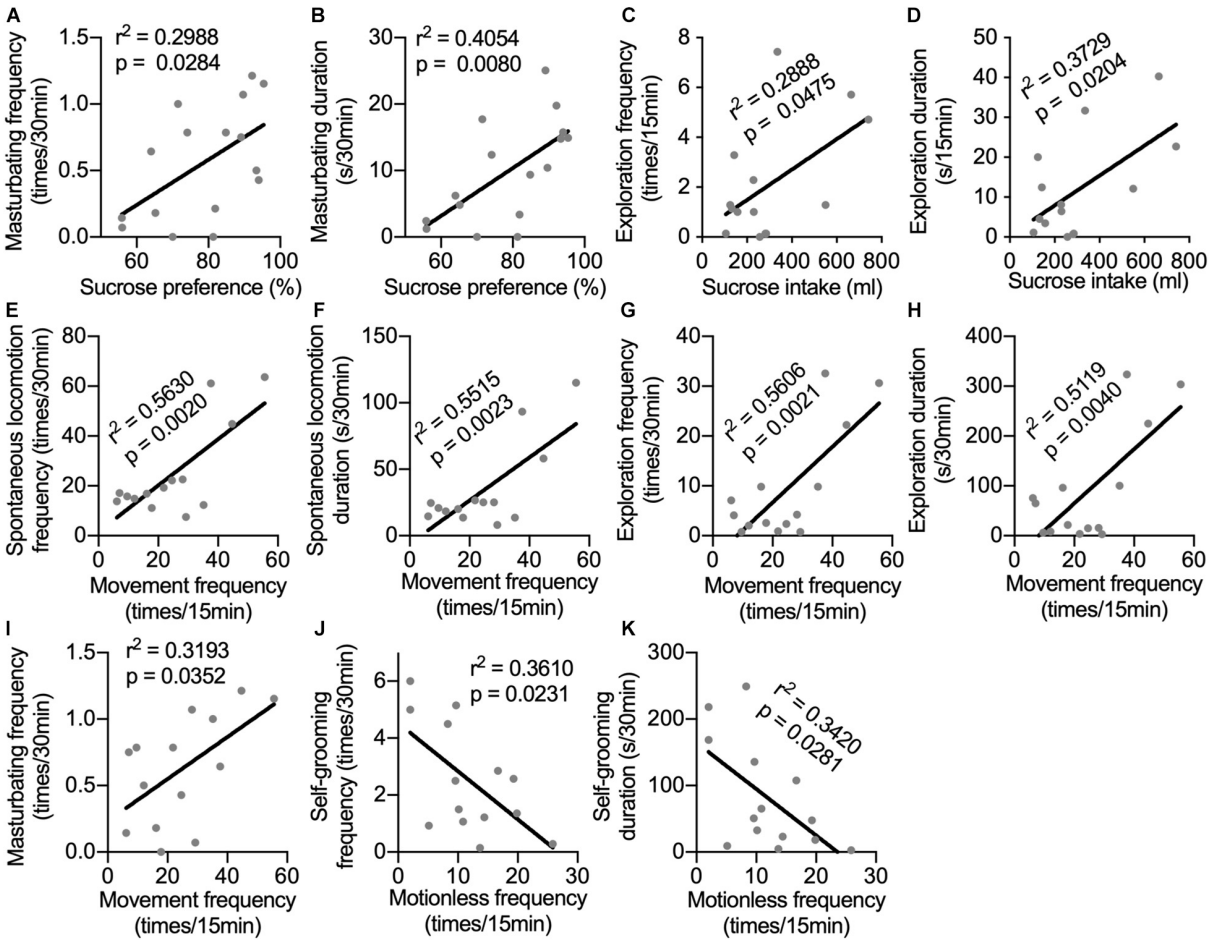

FIGURE 5 | Correlations between behaviors in different tests. The correlations were analyzed between sucrose preference and frequency **(A)** and duration of masturbating behavior in home cage **(B)**; between sucrose intake and frequency **(C)** and duration of the exploration behaviors in the open field **(D)**; between movement frequency in the open field and the frequency **(E)** and duration of spontaneous locomotion **(F)**, as well as the frequency **(G)**, duration of exploration **(H)** and the masturbating frequency **(I)** in the home cage; between the frequency **(J)** and duration of the self-grooming behavior in the home cage **(K)** and the frequency of motionless in the open field. Behaviors in different tests showed significant correlations indicating that they were possibly influenced by the same mental status. Behaviors with time scale of 30-min and 15-min were observed in home cage and in the open-field test respectively.

one environment, in either home cage or the open field. For example, CSF concentrations of 5-HIAA was associated with the exploration duration in the open field, but not in the home cage. Then, whether and to what extent the social isolation housing environment might potentiate the development and expression of IFN-α-induced depression are interesting questions and worth further investigation. Thus, attention should be payed to the housing and evaluating/testing environment when developing non-human primate animal models of mental disorders.

In patients subcutaneously treated with IFN-α for 4–6 weeks, fMRI revealed significantly reduced bilateral activation of the ventral striatum during a reward-related task, and this change was correlated with anhedonia and depressive symptoms (Capuron et al., 2012). Anhedonia-like behavior was also observed in rhesus monkeys accompanied by decreased dopamine release and dopamine 2 receptor (D2R) binding in the striatum after 4 weeks of subcutaneous administration of IFN-α (Felger et al., 2013b). Consistently, 6 weeks of IFN-α i.c.v. administration significantly reduced the sucrose consumption, accompanied by significant change in DA metabolite DOPAC in the CSF. Besides, the change in sucrose consumption might be directly explained by the IFN-α-induced increase in CSF concentrations of 5-HIAA and NA, together with their negative correlation with sucrose consumption and sucrose preference.

Although IFN-α i.c.v. administration only significantly changed the CSF concentrations of NA and DOPAC, the correlations between all measured monoamine metabolites and depression-related behaviors indicated their involvement in regulating these behaviors. Moreover, the correlations of the principal components derived from the CSF concentrations of these monoamine metabolites with depression-related behaviors suggested that some behaviors could possibly be mediated by multiple neurotransmitters.

The concentrations of neurotransmitters and their metabolites in the CSF were dependent on the balance between synthesis and metabolism. Although the 5-HIAA concentrations in the CFS

was not significantly changed by IFN-α i.c.v. administration in this study, a change in functional 5-HT levels in the brain was still possible. IFN-α induces depression by activating IL-6 (Schaefer et al., 2003), which disrupts the function of tetrahydrobiopterin (BH4) in the synthesis of 5-HT (Felger and Lotrich, 2013). IL-6 can also inhibit the 5-HT synthesis via induction of indoleamine-2,3-dioxygenase (IDO) enzyme, which facilitates the metabolism of tryptophan into kynurenine (KYN) (Anderson et al., 2013). For example, a single i.c.v. IFN-α injection in rats significantly reduced the 5-HT levels in the frontal cortex, midbrain, and stratum of rats in a dose-dependent manner (Kamata et al., 2000).

It was found in mice that repeated peripheral administration of IFN-α induced depressive-like behaviors via downregulating the serotoninergic receptor 5-HT1A and promoting apoptosis in the hippocampus (Ping et al., 2012). Increase in IFN-α and serotonin transporter (SERT) expression happen together in central inflammation (Katafuchi et al., 2005), and IFN-α administration itself has been found to stimulate SERT expression (Schaefer et al., 2003). In both situations, the 5-HT uptake from the synapses is enhanced (Tsao et al., 2008). However, with upregulated 5-HT reuptake, the CSF concentrations of 5-HIAA should be decreased instead of unchanged as observed in the current study. A more plausible possibility was that IFN-α increased the metabolism of 5-HT into 5-HIAA (Schaefer et al., 2003), leading to an increased 5-HIAA/5-HT ratio (De La GarzaII, and Asnis, 2003) via inhibiting SERT function (Foley et al., 2007) and increasing platelet monoamine oxidase-B (MAO) activities (Bannink et al., 2005). The result will induce reduced recycling of 5-HT, even less material for 5-HT synthesis, and finally a deficiency of functional 5-HT in the synapses. In support of this possibility, decreased sucrose preference and exploratory behaviors, as well as increased immobility in forced swim test was observed in SERT knock-out mice and rats (Olivier et al., 2008; Popa et al., 2008). Patients with long-form of the SERT gene (L_A/L_A genotype) are more resistant to IFN-α-induced depression (Lotrich et al., 2009).

Similarly, peripheral IFN-α has been found to decrease the DA functions in the brain by inhibiting the conversion of the phenylalanine (Phen) to Tyr, the primary amino acid precursor of DA (Felger and Miller, 2012; Felger et al., 2013a). Moreover, rhesus monkeys receiving 4 weeks of IFN-α subcutaneous injections exhibited decreased striatal DA release and DA binding to receptors D2R, without change in the DA transporter (Felger et al., 2013b). However, significantly increased DA uptake and decreased DA turnover in caudate, putamen, and ventral striatum was observed in human patients receiving IFN-α for 4–6 weeks (Capuron et al., 2012). These changes in DA functions were similar to the 5-HT changes in peripheral IFN-α administration and might contribute to the IFN-α-induced anhedonia and depression. Nevertheless, the CSF concentrations of DOPAC were upregulated by i.c.v. IFN-α administration in this study, possibly because of increased metabolism of DA.

In conclusion, we hypothesize that i.c.v. IFN-α administration reduced the synthesis and increased the metabolism of 5-HT and DA, leading to a deficiency in functional 5-HT and DA in the brain (Kamata et al., 2000). It can explain the positive correlations of CSF concentrations of 5-HIAA and DOPAC with the severity of depression in rhesus monkeys in this study. The correlations of the CSF concentrations of 5-HIAA with DOPAC and HVA was probably a result of dose-dependent activation of monoamine metabolism by IFN-α. Nevertheless, the functioning and metabolism of NA is relatively special and more complicated among these monoamines because NA can be taken up by the DAT of dopaminergic neurons (Haenisch and Bönisch, 2011). It means that the depletion of noradrenaline transporters (NATs) can be partially compensated by other monoamine transporters, retaining the proportion between NA in the CSF and functional NA in the brain. The recruitment of DATs by NA further decreased the recycling/turnover of DA, making NA positively correlated with the severity of depressive symptoms including anhedonia and huddling behavior. Another possibility was that NA directly promoted depressive symptoms. In genetically modified mice, increased NA levels in the brain was accompanied with decreased sucrose preference and intake (Aizawa et al., 2016).

The mechanisms about how peripheral IFN-α regulates the metabolism and functioning of monoamines are relatively well studied (Felger and Miller, 2012). However, the behavioral and physical effects of both long-term and acute IFN-α i.c.v. administration have been scarcely studied. Little is known about how IFN-α in the CNS changes the process of monoamine synthesis, packaging, release, reuptake and metabolism, let alone how these changes contribute to the development of IFN-induced depression.

Accumulating studies have found that some possible mechanisms were involved in the development of IFN-α-induced depression, including dysregulation of monoaminergic and glutamatergic neurotransmitter systems (Capuron et al., 2003; Haroon et al., 2014), alterations of activities of the HPA axis (Felger et al., 2016), and impairment of neuronal survival and plasticity (Hoyo-Becerra et al., 2014; Zheng et al., 2015). However, most of these observations was obtained from patients with preexisting health problems or laboratory animals receiving IFN-α treatment through peripheral administration. However, the central nervous system is separated from the circulating blood by the blood–brain barrier. In rhesus monkeys, peripherally administrated IFN-α can hardly be detected in the CSF; on the other hand, the IFN-α in plasma is not detectable following an i.c.v. administration (Collins et al., 1985). Specifically, the initial CSF concentrations of IFN-α exceeded 100,000 U/ml with a dose of 120,000 U/kg i.c.v. administration and remained at levels above 100 U/ml for 2 days. Central administration of IFN-α provided a total exposure (area under the concentrations vs. time curve) for the CSF 3,000-fold greater than peripheral administration with a 20-fold larger dose (Collins et al., 1985). Thus, studies with central IFN-α administration are urgently necessary to answer these pivotal questions.

This animal model is the first non-human primate model of depression induced by central administration of IFN-α, which is necessary to explore the mechanisms of depression induced by i.c.v. IFN-α treatment and the CNS inflammation. Rhesus monkeys showed considerable depressive-like symptoms accompanied with changes in the CSF concentrations of monoamine metabolites after 6 weeks of i.c.v. IFN-α administration. Anhedonia was observed as significantly reduced

sucrose intake during the IFN-α administration. Monkeys receiving i.c.v. IFN-α infusion spent more time huddling in a corner of their home cages and showed less interests in their physical and living environment even when they were stimulated. Bodyweights of both Ctrl and IFN groups were increased, suggesting that the i.c.v. administration of IFN-α or saline with the dose in this study did not cause health problem to these monkeys. In other words, the behavioral changes in the IFN group was not a result of IFN-α-induced sickness. This study also found that increased metabolism of monoamines in the brain might play an important role in central IFN-α-induced depression. Thus, even though both peripheral and central administration of IFN-α can induce depressive symptoms in humans and animal models, the underlying mechanisms and involved pathways are likely to be different. Restoration of normal monoamine metabolisms in the brain is a potential therapeutic strategy to prevent and cure depression induced by central IFN-α and CNS inflammation.

DATA AVAILABILITY STATEMENT

All datasets generated for this study are included in the article/supplementary material, further inquiries can be directed to the corresponding authors.

ETHICS STATEMENT

The animal study was reviewed and approved by the National Animal Research Authority (China) and the Institutional Animal Care and Use Committee (IACUC) of Kunming Institute of Zoology, Chinese Academy of Sciences.

AUTHOR CONTRIBUTIONS

All authors listed have made a substantial, direct and intellectual contribution to the work, and approved it for publication.

FUNDING

This work was supported by the Key Realm R&D Program of Guangdong Province (2019B030335001), the National Natural Science Foundation of China (31700897, 31960178, and 82074421), the Applied Basic Research Programs of Science and Technology Commission Foundation of Yunnan Province (2018FB053 and 2019FA007), the China Postdoctoral Science Foundation (2018M631105), and the Yunnan Provincial Academician and Expert Workstation (202005AF150017 and 2019IC051).

REFERENCES

Aizawa, F., Nishinaka, T., Yamashita, T., Nakamoto, K., Kurihara, T., Hirasawa, A., et al. (2016). GPR40/FFAR1 deficient mice increase noradrenaline levels in the brain and exhibit abnormal behavior. *J. Pharmacol. Sci.* 132, 249–254. doi: 10.1016/j.jphs.2016.09.007

Anderson, G., Kubera, M., Duda, W., Lasoń, W., Berk, M., and Maes, M. (2013). Increased IL-6 trans-signaling in depression: focus on the tryptophan catabolite pathway, melatonin and neuroprogression. *Pharmacol. Rep.* 65, 1647–1654. doi: 10.1016/s1734-1140(13)71526-3

Bannink, M., Kruit, W. H. J., Van Gool, A. R., Mulder, P. G. H., Sleijfer, S., Eggermont, A. M. M., et al. (2005). Platelet MAO activity during treatment with pegylated interferon-alfa in melanoma patients. *Prog. Neuro Psychopharmacol. Biol. Psychiatr.* 29, 109–114. doi: 10.1016/j.pnpbp.2004.10.012

Bodnar, C. N., Morganti, J. M., and Bachstetter, A. D. (2018). Depression following a traumatic brain injury: uncovering cytokine dysregulation as a pathogenic mechanism. *Neural Regen. Res.* 13:1693. doi: 10.4103/1673-5374.238604

Capuron, L., Fornwalt, F. B., Knight, B. T., Harvey, P. D., Ninan, P. T., and Miller, A. H. (2009). Does cytokine-induced depression differ from idiopathic major depression in medically healthy individuals?. *J. Affect. Disord.* 119, 181–185. doi: 10.1016/j.jad.2009.02.017

Capuron, L., Neurauter, G., Musselman, D. L., Lawson, D. H., Nemeroff, C. B., Fuchs, D., et al. (2003). Interferon-alpha-induced changes in tryptophan metabolism: relationship to depression and paroxetine treatment. *Biol. Psychiatr.* 54, 906–914. doi: 10.1016/s0006-3223(03)00173-2

Capuron, L., Pagnoni, G., Drake, D. F., Woolwine, B. J., Spivey, J. R., Crowe, R. J., et al. (2012). Dopaminergic mechanisms of reduced basal ganglia responses to hedonic reward during interferon alfa administration. *Archiv. Gen. Psychiatr.* 69, 1044–1053. doi: 10.1001/archgenpsychiatry.2011.2094

Collins, J. M., Riccardi, R., Trown, P., O'Neill, D., and Poplack, D. G. (1985). Plasma and cerebrospinal fluid pharmacokinetics of recombinant interferon alpha A in monkeys: comparison of intravenous, intramuscular, and intraventricular delivery. *Cancer Drug Deliv.* 2, 247–253. doi: 10.1089/cdd.1985.2.247

Dantzer, R., O'Connor, J. C., Freund, G. G., Johnson, R. W., and Kelley, K. W. (2008). From inflammation to sickness and depression: when the immune system subjugates the brain. *Nat. Rev. Neurosci.* 9, 46–56. doi: 10.1038/nrn2297

Davenport, M. D., Lutz, C. K., Tiefenbacher, S., Novak, M. A., and Meyer, J. S. (2008). A rhesus monkey model of self-injury: effects of relocation stress on behavior and neuroendocrine function. *Biol. Psychiatry* 63, 990–996. doi: 10.1016/j.biopsych.2007.10.025

De La Garza, R. II, and Asnis, G. M. (2003). The non-steroidal anti-inflammatory drug diclofenac sodium attenuates IFN-α induced alterations to monoamine turnover in prefrontal cortex and hippocampus. *Brain Res.* 977, 70–79. doi: 10.1016/s0006-8993(03)02757-4

Felger, J. C., Alagbe, O., Hu, F., Mook, D., Freeman, A. A., Sanchez, M. M., et al. (2007). Effects of interferon-alpha on rhesus monkeys: a nonhuman primate model of cytokine-induced depression. *Biol. Psychiatry* 62, 1324–1333. doi: 10.1016/j.biopsych.2007.05.026

Felger, J. C., Haroon, E., Woolwine, B. J., Raison, C. L., and Miller, A. H. (2016). Interferon-alpha-induced inflammation is associated with reduced glucocorticoid negative feedback sensitivity and depression in patients with hepatitis C virus. *Physiol. Behav.* 166, 14–21. doi: 10.1016/j.physbeh.2015.12.013

Felger, J. C., Li, L., Marvar, P. J., Woolwine, B. J., Harrison, D. G., Raison, C. L., et al. (2013a). Tyrosine metabolism during interferon-alpha administration: association with fatigue and CSF dopamine concentrations. *Brain Behav. Immun.* 31, 153–160. doi: 10.1016/j.bbi.2012.10.010

Felger, J. C., Mun, J., Kimmel, H. L., Nye, J. A., Drake, D. F., Hernandez, C. R., et al. (2013b). Chronic interferon-α decreases dopamine 2 receptor binding and striatal dopamine release in association with anhedonia-like behavior in nonhuman primates. *Neuropsychopharmacology* 38, 2179–2187. doi: 10.1038/npp.2013.115

Felger, J. C., and Lotrich, F. E. (2013). Inflammatory cytokines in depression: neurobiological mechanisms and therapeutic implications. *Neuroscience* 246, 199–229. doi: 10.1016/j.neuroscience.2013.04.060

Felger, J. C., and Miller, A. H. (2012). Cytokine effects on the basal ganglia and dopamine function: the subcortical source of inflammatory malaise. *Front. Neuroendocrinol.* 33, 315–327. doi: 10.1016/j.yfrne.2012.09.003

Foley, K. F., Pantano, C., Ciolino, A., and Mawe, G. M. (2007). IFN-γ and TNF-α decrease serotonin transporter function and expression in Caco2 cells. *Am. J. Physiol. Gastrointest. Liver Physiol.* 292, G779–G784.

Goehler, L. E., Gaykema, R. P. A., Hansen, M. K., Anderson, K., and Watkins, L. R. (2000). Vagal immune-to-brain communication: a visceral chemosensory pathway. *Auton. Neurosci. Basic Clin.* 85, 49–59. doi: 10.1016/s1566-0702(00)00219-8

Haenisch, B., and Bönisch, H. (2011). Depression and antidepressants: insights from knockout of dopamine, serotonin or noradrenaline re-uptake transporters. *Pharmacol. Therap.* 129, 352–368. doi: 10.1016/j.pharmthera.2010.12.002

Harlow, H. F., and Suomi, S. J. (1971). Production of depressive behaviors in young monkeys. *J. Autism Dev. Disord.* 1, 246–255. doi: 10.1007/bf01557346

Haroon, E., Woolwine, B. J., Chen, X., Pace, T. W., Parekh, S., Spivey, J. R., et al. (2014). IFN-alpha-induced cortical and subcortical glutamate changes assessed by magnetic resonance spectroscopy. *Neuropsychopharmacology* 39, 1777–1785. doi: 10.1038/npp.2014.25

Hepgul, N., Pariante, C. M., Baraldi, S., Borsini, A., Bufalino, C., Russell, A., et al. (2018). Depression and anxiety in patients receiving interferon-alpha: the role of illness perceptions. *J. Health Psychol.* 23, 1405–1414. doi: 10.1177/1359105316658967

Hoyo-Becerra, C., Liu, Z., Yao, J., Kaltwasser, B., Gerken, G., Hermann, D. M., et al. (2015). Rapid regulation of depression-associated genes in a new mouse model mimicking interferon-α-related depression in hepatitis C virus infection. *Mol. Neurobiol.* 52, 318–329. doi: 10.1007/s12035-014-8861-z

Hoyo-Becerra, C., Schlaak, J. F., and Hermann, D. M. (2014). Insights from interferon-α-related depression for the pathogenesis of depression associated with inflammation. *Brain Behav. Immun.* 42, 222–231. doi: 10.1016/j.bbi.2014.06.200

Kamata, M., Higuchi, H., Yoshimoto, M., Yoshida, K., and Shimizu, T. (2000). Effect of single intracerebroventricular injection of α-interferon on monoamine concentrations in the rat brain. *Eur. Neuropsychopharmacol.* 10, 129–132. doi: 10.1016/s0924-977x(99)00067-x

Katafuchi, T., Kondo, T., Take, S., and Yoshimura, M. (2005). Enhanced expression of brain interferon-α and serotonin transporter in immunologically induced fatigue in rats. *Eur. J. Neurosci.* 22, 2817–2826. doi: 10.1111/j.1460-9568.2005.04478.x

Kwak, M., Yeh, H.-R., Yum, M.-S., Kim, H.-J., You, S. J., and Ko, T.-S. (2019). A long-term subacute sclerosing panencephalitis survivor treated with intraventricular interferon-alpha for 13 years. *Korea. J. Pediatr.* 62, 108–112. doi: 10.3345/kjp.2018.06730

Li, H., Lei, X., Huang, B., Rizak, J. D., Yang, L., Yang, S., et al. (2015). A quantitative approach to developing Parkinsonian monkeys (*Macaca fascicularis*) with intracerebroventricular 1-methyl-4-phenylpyridinium injections. *J. Neurosci. Methods* 251, 99–107. doi: 10.1016/j.jneumeth.2015.05.008

Lotrich, F. E., Ferrell, R. E., Rabinovitz, M., and Pollock, B. G. (2009). Risk for depression during interferon-alpha treatment is affected by the serotonin transporter polymorphism. *Biol. Psychiatr.* 65, 344–348. doi: 10.1016/j.biopsych.2008.08.009

Olivier, J., Van Der Hart, M., Van Swelm, R., Dederen, P., Homberg, J., Cremers, T., et al. (2008). A study in male and female 5-HT transporter knockout rats: an animal model for anxiety and depression disorders. *Neuroscience* 152, 573–584. doi: 10.1016/j.neuroscience.2007.12.032

Pan, W., Banks, W. A., and Kastin, A. J. (1997). Permeability of the blood-brain and blood-spinal cord barriers to interferons. *J. Neuroimmunol.* 76, 105–111. doi: 10.1016/s0165-5728(97)00034-9

Paul, I. A., English, J. A., and Halaris, A. (2000). Sucrose and quinine intake by maternally-deprived and control rhesus monkeys. *Behav. Brain Res.* 112, 127–134. doi: 10.1016/s0166-4328(00)00173-x

Ping, F., Shang, J., Zhou, J., Zhang, H., and Zhang, L. (2012). 5-HT1A receptor and apoptosis contribute to interferon-α-induced "depressive-like" behavior in mice. *Neurosci. Lett.* 514, 173–178. doi: 10.1016/j.neulet.2012.02.087

Popa, D., Léna, C., Alexandre, C., and Adrien, J. (2008). Lasting syndrome of depression produced by reduction in serotonin uptake during postnatal development: evidence from sleep, stress, and behavior. *J. Neurosci.* 28, 3546–3554. doi: 10.1523/jneurosci.4006-07.2008

Qin, D., Chu, X., Feng, X., Li, Z., Yang, S., Lü, L., et al. (2015a). The first observation of seasonal affective disorder symptoms in Rhesus macaque. *Behav. Brain Res.* 292, 463–469. doi: 10.1016/j.bbr.2015.07.005

Qin, D., Rizak, J., Chu, X., Li, Z., Yang, S., Lu, L., et al. (2015b). A spontaneous depressive pattern in adult female rhesus macaques. *Sci. Rep.* 5:11267.

Qin, D., Li, Z., Li, Z., Wang, L., Hu, Z., Lu, L., et al. (2019). Chronic glucocorticoid exposure induces depression-like phenotype in rhesus Macaque (*Macaca Mulatta*). *Front. Neurosci.* 13:188. doi: 10.3389/fnins.2019.00188

Qin, D. D., Rizak, J., Feng, X. L., Yang, S. C., Lü, L. B., Pan, L., et al. (2016). Prolonged secretion of cortisol as a possible mechanism underlying stress and depressive behaviour. *Sci. Rep.* 6:30187.

Quan, N., and Banks, W. A. (2007). Brain-immune communication pathways. *Brain Behav. Immun.* 21, 727–735. doi: 10.1016/j.bbi.2007.05.005

Schaefer, M., Schwaiger, M., Pich, M., Lieb, K., and Heinz, A. (2003). Neurotransmitter changes by interferon-alpha and therapeutic implications. *Pharmacopsychiatry* 36, 203–206. doi: 10.1055/s-2003-45131

Shively, C. A., Register, T. C., Friedman, D. P., Morgan, T. M., Thompson, J., and Lanier, T. (2005). Social stress-associated depression in adult female cynomolgus monkeys (*Macaca fascicularis*). *Biol. Psychol.* 69, 67–84. doi: 10.1016/j.biopsycho.2004.11.006

Smith, R. A., Norris, F., Palmer, D., Bernhardt, L., and Wills, R. J. (1985). Distribution of alpha interferon in serum and cerebrospinal fluid after systemic administration. *Clin. Pharmacol. Therap.* 37, 85–88. doi: 10.1038/clpt.1985.16

Su, K.-P., Lai, H.-C., Peng, C.-Y., Su, W.-P., Chang, J. P.-C., and Pariante, C. M. (2019). Interferon-alpha-induced depression: comparisons between early- and late-onset subgroups and with patients with major depressive disorder. *Brain Behav. Immun.* 80, 512–518. doi: 10.1016/j.bbi.2019.04.032

Suomi, S. J., and Harlow, H. F. (1972). Depressive behavior in young monkeys subjected to vertical chamber confinement. *J. Comparat. Physiol. Psychol.* 80:11. doi: 10.1037/h0032843

Tsao, C., Lin, Y.-S., Cheng, J., Lin, C.-F., Wu, H., Wu, S., et al. (2008). Interferon-α-induced serotonin uptake in Jurkat T cells via mitogen-activated protein kinase and transcriptional regulation of the serotonin transporter. *J. Psychopharmacol.* 22, 753–760. doi: 10.1177/0269881107082951

Yalaz, K., Anlar, B., Oktem, F., Aysun, S., Ustacelebi, S., Gurcay, O., et al. (1992). Intraventricular interferon and oral inosiplex in the treatment of subacute *Sclerosing panencephalitis*. *Neurology* 42, 488–488. doi: 10.1212/wnl.42.3.488

Yu, P. H., Cauglin, C., Wempe, K. L., and Gubisne-Haberle, D. (2003). A novel sensitive high-performance liquid chromatography/electrochemical procedure for measuring formaldehyde produced from oxidative deamination of methylamine and in biological samples. *Analyt. Biochem.* 318, 285–290. doi: 10.1016/s0003-2697(03)00211-2

Zhai, R., Rizak, J., Zheng, N., He, X., Li, Z., Yin, Y., et al. (2018). Alzheimer's disease-like pathologies and cognitive impairments induced by formaldehyde in non-human primates. *Curr. Alzheimer Res.* 15, 1304–1321. doi: 10.2174/1567205015666180904150118

Zheng, L.-S., Kaneko, N., and Sawamoto, K. (2015). Minocycline treatment ameliorates interferon-alpha-induced neurogenic defects and depression-like behaviors in mice. *Front. Cell. Neurosci.* 9:5. doi: 10.3389/fncel.2015.00005

Conflict of Interest: The authors declare that the research was conducted in the absence of any commercial or financial relationships that could be construed as a potential conflict of interest.

frontiers in Endocrinology

REVIEW
published: 19 April 2021
doi: 10.3389/fendo.2021.613983

Current Aspects of the Role of Autoantibodies Directed Against Appetite-Regulating Hormones and the Gut Microbiome in Eating Disorders

Kvido Smitka[1,2]*, *Petra Prochazkova*[3], *Radka Roubalova*[3], *Jiri Dvorak*[3], *Hana Papezova*[4], *Martin Hill*[5], *Jaroslav Pokorny*[1], *Otomar Kittnar*[1], *Martin Bilej*[3] *and Helena Tlaskalova-Hogenova*[3]

[1] First Faculty of Medicine, Institute of Physiology, Charles University, Prague, Czechia, [2] First Faculty of Medicine, Institute of Pathological Physiology, Charles University, Prague, Czechia, [3] Laboratory of Cellular and Molecular Immunology, Institute of Microbiology of the Czech Academy of Sciences, Prague, Czechia, [4] Psychiatric Clinic, Eating Disorder Center, First Faculty of Medicine, Charles University and General University Hospital in Prague, Prague, Czechia, [5] Steroid Hormone and Proteofactors Department, Institute of Endocrinology, Prague, Czechia

OPEN ACCESS

Edited by:
Ana Rosa Pérez, Consejo Nacional de Investigaciones Científicas y Técnicas (CONICET), Argentina

Reviewed by:
Sergueï O. Fetissov, Université de Rouen, France
Ludmila Prokesova, Charles University, Czechia

***Correspondence:**
Kvido Smitka
kvido.smitka@f1.cuni.cz

Specialty section:
This article was submitted to Neuroendocrine Science, a section of the journal Frontiers in Endocrinology

Received: *04 October 2020*
Accepted: *09 March 2021*
Published: *19 April 2021*

Citation:
Smitka K, Prochazkova P, Roubalova R, Dvorak J, Papezova H, Hill M, Pokorny J, Kittnar O, Bilej M and Tlaskalova-Hogenova H (2021) Current Aspects of the Role of Autoantibodies Directed Against Appetite-Regulating Hormones and the Gut Microbiome in Eating Disorders. Front. Endocrinol. 12:613983. doi: 10.3389/fendo.2021.613983

The equilibrium and reciprocal actions among appetite-stimulating (orexigenic) and appetite-suppressing (anorexigenic) signals synthesized in the gut, brain, microbiome and adipose tissue (AT), seems to play a pivotal role in the regulation of food intake and feeding behavior, anxiety, and depression. A dysregulation of mechanisms controlling the energy balance may result in eating disorders such as anorexia nervosa (AN) and bulimia nervosa (BN). AN is a psychiatric disease defined by chronic self-induced extreme dietary restriction leading to an extremely low body weight and adiposity. BN is defined as out-of-control binge eating, which is compensated by self-induced vomiting, fasting, or excessive exercise. Certain gut microbiota-related compounds, like bacterial chaperone protein *Escherichia coli* caseinolytic protease B (ClpB) and food-derived antigens were recently described to trigger the production of autoantibodies cross-reacting with appetite-regulating hormones and neurotransmitters. Gut microbiome may be a potential manipulator for AT and energy homeostasis. Thus, the regulation of appetite, emotion, mood, and nutritional status is also under the control of neuroimmunoendocrine mechanisms by secretion of autoantibodies directed against neuropeptides, neuroactive metabolites, and peptides. In AN and BN, altered cholinergic, dopaminergic, adrenergic, and serotonergic relays may lead to abnormal AT, gut, and brain hormone secretion. The present review summarizes updated knowledge regarding the gut dysbiosis, gut-barrier permeability, short-chain fatty acids (SCFA), fecal microbial transplantation (FMT), blood-brain barrier permeability, and autoantibodies within the ghrelin and melanocortin systems in eating disorders. We expect that the new knowledge may be used for the development of a novel preventive and therapeutic approach for treatment of AN and BN.

Keywords: anorexia nervosa and bulimia, ghrelin, alpha-MSH, caseinolytic peptidase B, gut and blood-brain barrier permeability, fecal microbial transplantation, microbiome, autoantibody

INTRODUCTION

Anorexia nervosa (AN) and bulimia nervosa (BN) are serious eating disorders with a substantial impact on the long-term quality of life and broad psychological, social and economic implications. These psychiatric disorders affect as many as 2-3% of young women and adolescents (1) and exhibit substantial mortality (with a mortality rate of 5-10% after 10 years) (2). Both AN and BN are disorders with severe disturbances in eating behavior. While AN is characterized by self-induced starvation, amenorrhea, severe weight loss due to reduction of both fat mass and fat free mass mainly at the expense of adipose tissue (AT), refusal to gain and maintain a minimal normal body weight (weight criterion for the diagnosis is under 85% of normal body weight), manifestations of BN include recurrent episodes of binge eating followed by inappropriate compensatory behavior such as self-induced vomiting, laxative and diuretics misuse (3).

Despite extensive research efforts worldwide, the etiopathogenesis of AN and BN has not been elucidated to date. Fetissov et al. hypothesized that AN is an autoimmune disease caused by delayed exposure to microorganisms (such as *Group A β-hemolytic Streptococcus*, *Escherichia coli*, and *Helicobacter pylori*) in which autoantibodies against appetite-regulating neuropeptides, neurotransmitters, peptide hormones, and hypothalamic neurons disturb appetite and mood and lead to decreased intake of food (4). A higher prevalence of autoimmune diseases such as type 1 diabetes and Crohn's disease was observed among patients with eating disorders (5). In this vein, the development of type 1 diabetes in adolescence seems to be a risk factor for the subsequent development of AN and BN (6). Further, patients with AN are suggested to be susceptible to autoimmune diseases and thus, a bi-directional relationship between eating disorders and autoimmunity was considered (7–9).

Recently, Watson et al. (10) identified multiple genetic loci for AN and reconceptualized AN as a metabo-psychiatric disorder. Negative genetic correlations were documented between anorexic patients and metabolic traits such as type 2 diabetes, insulin resistance, blood plasma insulin, leptin, and a significant positive genetic correlation was found with high-density lipoprotein (HDL) cholesterol. Disordered niacin metabolism leading to niacin deficiency was shown to provoke schizophrenia-like symptoms in neuropsychiatric diseases such as pellagra (11), which was seen as a secondary complication associated with a tryptophan-deficient diet in AN and BN (12, 13).

The gut, enteric nervous system, central nervous system, gut microbiome, and adipose tissue (AT) newly introduced as the AT-microbiome-gut-brain axis produce a variety of neuroactive factors with orexigenic and anorexigenic effects which are important in the regulation of food intake and body weight control (14–16) (**Figure 1**). The differential release of these compounds may act to initiate, maintain, or exacerbate cycles of food restriction or binge-purge behavior observed in AN and BN (17). In particular, translocation of intestinal bacterial antigens including enterobacterial caseinolytic protease B (ClpB) and food-derived antigens across the intestinal wall can trigger the production of autoantibodies cross-reacting with appetite-regulating hormones (18). This cross-reactivity is a phenomenon affecting the AT-microbiome-gut-brain axis.

In the present review we show that the regulation of appetite, emotion, nutritional status, and adiposity is also under the control by secretion of autoantibodies directed against neuropeptides, neurotransmitters, and neuromodulators. This may lead to the onset, development, and perpetuation of severe food restriction or binge-eating behavior and psychopathological traits in eating disorders. Better understanding of the AT-microbiome-gut-brain axis in eating disorders and elucidation of its interactions with adipocyte lipolysis and adipogenesis may provide a novel therapeutic approach for treatment of anorexia and bulimia nervosa.

The goals of the present review were to: (i) describe the role of autoantibodies cross-reacting with appetite-regulating hormones and the gut microbiome in etiopathogenesis of AN and BN, and to (ii) discuss bi-directional communication along the AT-microbiome-gut-brain axis in eating disorders.

Abbreviations: ACTH, adrenocorticotropin; AGRP, agouti-related protein; α-MSH, alpha-melanocyte-stimulating hormone; AN, anorexia nervosa; anti-ClpB Ig, enterobacterial caseinolytic protease B immunoglobulin; ARC, arcuate nucleus; AT, adipose tissue; autoAbs, autoantibodies; BCFA, branched-chain fatty acids; BMI, body mass index; BN, bulimia nervosa; CART, cocaine- and amphetamine-regulated transcript; CIPO, chronic intestinal pseudo-obstruction syndrome; ClpB, enterobacterial caseinolytic protease B; CNS, central nervous system; EC, enterochromaffin serotonin cells; FFA, free fatty acids; FFAR, free fatty acid receptor; FMT, fecal microbiota transplantation; GABA, gamma-aminobutyric acid; GH, growth hormone; GHS-R1a, growth hormone secretagogue receptor type 1a; GLP-1, glucagon-like peptide-1; GLP-2, glucagon-like peptide-2; GOAT, ghrelin O-acyltransferase; HCA, hydroxy-carboxylic acid; HDL, high-density lipoprotein; HOMA-IR, homeostasis model assessment of insulin resistance; HPA, hypothalamic-pituitary-adrenal axis; 5-HT, 5-hydroxytryptamine; HW, healthy women; I-FABP, intestinal fatty acid binding protein; Ig, immunoglobulin; Ig, immunoglobulin (IgA, IgG, and IgM classes); IL-1β, interleukin-1 beta; IL-6, interleukin-6; MC4R, melanocortin 4 receptor; NE, norepinephrine; NPY, neuropeptide tyrosine; PANDAS, Pediatric Autoimmune Neuropsychiatric Disorders Associated with Streptococcal infection; POMC, pro-opiomelanocortin; PP, pancreatic polypeptide; PYY, peptide tyrosine tyrosine; SCFA, short-chain fatty acids; SIBO, small intestinal bacterial overgrowth syndrome; SNS, sympathetic nervous system; TNF-α, tumor necrosis factor-alpha.

INVOLVEMENT OF AUTOIMMUNITY IN AN AND BN PATHOGENESIS

Various microorganisms have been shown to exhibit protein sequence homologies with some autoantigens including appetite-regulating peptides, which can lead to the production of autoantibodies (autoAbs) cross-reacting with these peptides and to the changed appetite regulation. Molecular mimicry concept was proposed to explain autoantibodies formation directed against microbial antigens and cross-reacting with host proteins, which can explain some microorganism-triggered autoimmune diseases (19, 20).

Such homology was reported for anorexigenic/anxiogenic peptide α-melanocyte-stimulating hormone (α-MSH) and bacterial protein *Escherichia coli* caseinolytic protease B (ClpB) (21). ClpB, α-MSH conformational mimetic produced by the bacterial *Enterobacteriaceae* family induces the production of antibodies cross-reacting with human α-MSH. In patients with

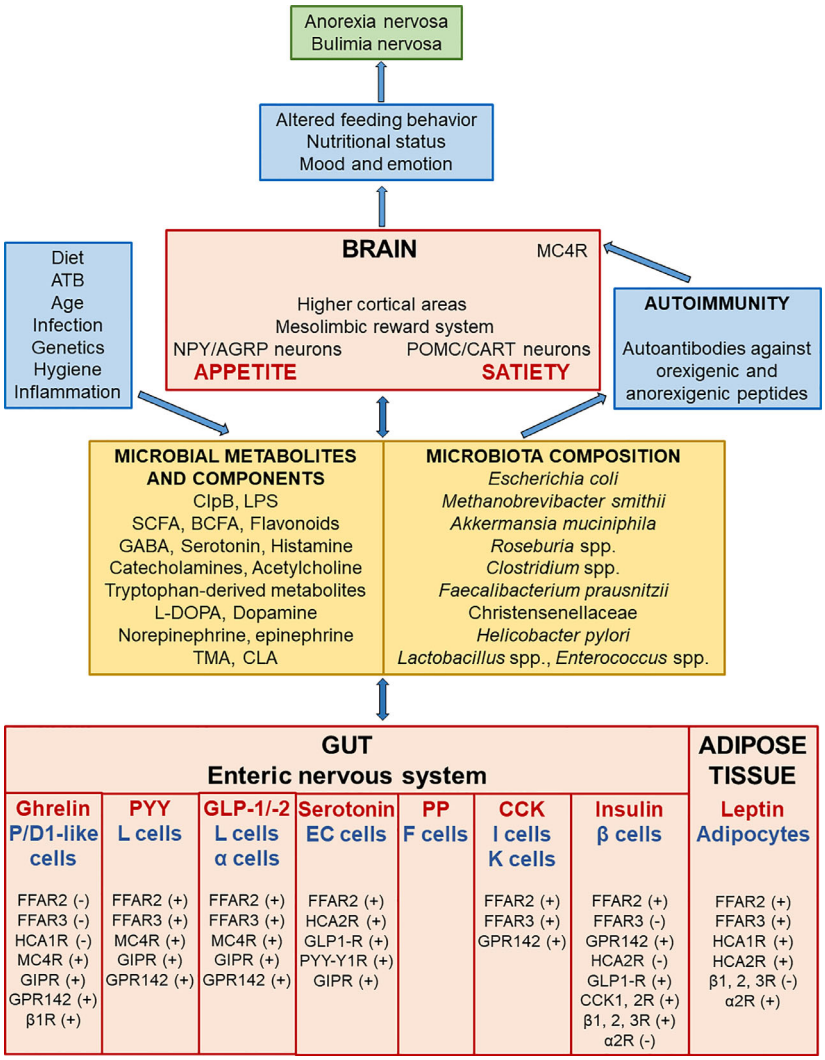

FIGURE 1 | Scheme demonstrating the bi-directional interactions along the adipose tissue, microbiome, gut and brain leading to the development of eating disorders. Microbial composition and consequently the amount of microbial metabolites and components are affected by various factors like diet, antibiotics, infection and so on. Gut microbial metabolites and components act as signals to influence enteric nervous system and adipose tissue responses through various receptors. P/D1 like ghrelin cells in humans (or termed X/A like ghrelin cells in rodents) are localized in the oxyntic mucosa of the gastric fundus and duodenum. Enteroendocrine L cells secrete PYY and GLP-1/-2 (and/or co-release GLP-1/-2 together with PYY) in the mucosa of the distal ileum and colon. F (or PP) cells, which secrete pancreatic polypeptide (PP) under cholinergic control, are localized in the periphery of pancreatic islets of Langerhans, and also expressed in the distal gut. Enteroendocrine I and K cells, which secrete CCK and glucose-dependent insulinotropic peptide (GIP), are located in the mucosa of the upper small intestine. Short-chain fatty (FFA2-3) and hydroxy-carboxylic (HCA1-2) acid receptors are expressed on gastric P/D1 like ghrelin cells, ileal L cells, pancreatic α cells, enterochromaffin (EC) serotonin cells, duodeno-jejuno-ileal I and K cells, pancreatic β cells, and adipocytes. The signalization leads to ghrelin secretion inhibition or produce PYY, GLP-1/-2, serotonin, CCK, insulin, and leptin production. Leptin, an adipocyte-secreted hormone, is an indicator of energy stores and acts to reduce food intake and increase energy expenditure. These appetite-regulating hormones signal to NPY/AGRP and POMC/CART neurons, the mesolimbic reward system, and higher cortical areas, which all play a pivotal role in the regulation of metabolism. GABA has an inhibitory input from NPY/AGRP neurons to POMC/CART neurons in the hypothalamic arcuate nucleus. Activation of hypothalamic NPY/AGRP neurons stimulates hunger and inhibits energy expenditure and lipolysis in AT; however, stimulation of hypothalamic POMC/CART neurons together with MC4R leads to inhibition of food intake and enhancing of energy expenditure and lipolysis in AT. IgG immune complexes with orexigenic and anorexigenic peptides chronically activate MC4R leading to increased satiety in both AN and BN. Dysregulation of appetite-regulating circuits may affect altered feeding behavior leading to the onset, development, and maintenance of AN and BN. α2R, alpha-2 adrenoceptors; AGRP, agouti-related protein; AT, adipose tissue; β 1, 2, 3R, beta-1, 2, 3 adrenoceptors; BCFA, branched-chain fatty acids (isobutyrate, 2-methyl-butyrate, and isovalerate); ATB, antibiotics; CART, cocaine- and amphetamine-regulated transcript; CCK, cholecystokinin, CCK1, 2 R; cholecystokinin 1, 2 receptors; CLA, conjugated linoleic acid; ClpB, enterobacterial caseinolytic protease B; EC, enterochromaffin serotonin cells; FFAR, free fatty acid receptor; GABA, gamma-aminobutyric acid; GIP, glucose-dependent insulinotropic peptide; GIPR, glucose-dependent insulinotropic peptide receptor; GLP-1/-2, glucagon-like peptide-1 and 2; GLP1-R, glucagon-like peptide-1 receptor; GPR142, G protein receptor 142 for tryptophan, HCAR, hydroxy-carboxylic acid receptor; L-DOPA, L-3,4-dihydroxyphenylalanine; LPS, lipopolysaccharide; MC4R, melanocortin 4 receptor; NPY, neuropeptide tyrosine; POMC, pro-opiomelanocortin; PP, pancreatic polypeptide; PYY, peptide tyrosine tyrosine; PYY-Y1R, peptide tyrosine tyrosine-1 receptor, SCFA, short-chain fatty acids (butyrate, acetate, and propionate); TMA, trimethylamine; (+) = the stimulatory effect of ligands on hormone or serotonin secretion; (-) = the inhibitory effect of ligands on hormone secretion.

AN, increased levels of IgM autoantibodies against α-MSH were detected (22). Another study showed lower levels of IgG autoantibodies against α-MSH in obese patients, but increased levels in anorectic and bulimic patients (23). Furthermore, IgG from patients with AN can form immunocomplexes with α-MSH, which chronically activate the melanocortin (MC) system involved in the feeding behavior regulation (24, 25). α-MSH signals *via* the MC type 4 receptor (MC4R), a key molecular pathway regulating appetite (23). This interaction may thus represent a pathophysiological trigger of both AN and BN (21).

α-MSH–reactive autoAbs as well as autoAbs directed against other appetite-regulating peptides are present also in the plasma of healthy people. Fetissov et al. (25) screened the plasma of healthy women for the presence of autoantibodies directed against 14 key appetite-regulating neuropeptides or peptide hormones including α-MSH, ACTH, NPY, ghrelin, leptin, insulin, or PYY suggesting a link between IgG and IgA classes of such autoantibodies and antigenic stimulation by gut microbiota in healthy subjects (25) (**Table 1**). High affinity autoantibodies are responsible for the neutralization of neuropeptides preventing them from immune complexes formation, while low affinity autoantibodies do not exhibit blocking properties and can bind neuropeptides reversibly and thus play a role in peptide transport or protection from degradation by peptidases (33, 34).

Except higher levels of α-MSH (IgM class), higher levels of ACTH (IgG class) autoantibodies were also found in the plasma of patients with AN (22, 35). On the contrary, lower levels of acylated ghrelin (IgM class) autoantibodies (26) and lower levels of NPY (IgG class) autoantibodies in depressive disorder, a common comorbidity of eating disorders, were found (28). This is in contrast to increased levels of plasma NPY in BN and AN patients, which can act as a protective mechanism that prevents the exhaustion of energy reserves (36). Garcia et al. supported NPY protective role in depression by detection of decreased plasma levels of NPY IgG autoantibodies in patients with depression while their increased affinities were associated with lower body mass index (BMI) and reduced appetite (28).

IgG leptin-neutralizing autoantibodies were found in healthy subjects with a lower BMI; however, a decreased affinity of these antibodies was found in obese patients, which might be relevant to leptin resistance in obesity (30) (**Table 1**). Fetissov et al. reported that levels and affinities of autoantibodies against orexigenic and anorexigenic neuropeptides correlated with psychopathological traits in patients with eating disorders and these neutralizing autoantibodies were suggested as important attributors to mechanisms controlling motivation in AN and BN (22).

Moreover, immunoglobulin class switching of autoantibodies reacting with appetite-regulating hormones could be responsible for the differences in pathological manifestations of AN and BN.

In AN, the dysregulated immune profile includes an over-expression of anorexigenic and pro-inflammatory cytokines such as tumor necrosis factor-alpha (TNF-α), interleukin-6 (IL-6), and interleukin-1β (IL-1β). IL-1β and TNF-α influence the expression of certain crucial neuropeptides, which are known

TABLE 1 | Summary of changes in autoantibodies against appetite-regulating hormones, the ClpB-mimetic protein, and neurotransmitters in AN, BN, depression, in healthy subjects, in obesity, and diabetes.

Antigen	Healthy subjects / disease	Ig class	Changes	Reference
Ghrelin	Healthy women	IgG, IgA	present	(25)
Acylated ghrelin	AN	IgG, IgA, IgM	IgG ↓, IgA ↓, IgM ↓ before renourishment (associated with ghrelin resistance), IgM ↑ after renourishment	(26)
Ghrelin	Obese humans	IgG	IgG affinity ↑	(27)
NPY	Healthy women	IgG, IgA	present	(25)
NPY	Depressive disorder	IgG	IgG ↓	(28)
α-MSH	AN, BN	IgG	IgG ↑	(23)
α-MSH	AN	IgM	IgM ↑	(22)
α-MSH	Obese female patients	IgG	IgG ↓	(23)
ClpB	AN, BN	IgG, IgM	ClpB correlated positively with anti-ClpB IgM in BN anti-ClpB IgG, IgM present in AN	Breton et al. (2016) in the (29)
ClpB	Healthy women	IgG	ClpB correlated positively with anti-ClpB IgG in HW	Breton et al. (2016) in the (29)
Leptin	Healthy women	IgG, IgA	present	(25)
Leptin	Healthy subjects with lower BMI	IgG	IgG affinity ↑	(30)
Leptin	Obesity and type 2 DM	IgG	IgG affinity ↓ (associated with leptin resistance)	(30)
Insulin	Type 1 DM	IgG, IgM	IgG, IgM affinity ↑ and/or ↓	(31)
Insulin	Type 2 DM	IgG, IgM	IgG, IgM affinity ↑ (associated with insulin resistance)	(31)
PYY	Healthy women	IgG, IgA	present	(25)
Dopamine, dopamine-beta-hydroxylase and serotonin	BN	IgG, IgM	IgG, IgM ↓ in BN	(32)

α-MSH, alpha-melanocyte-stimulating hormone; anti-ClpB Ig, enterobacterial caseinolytic protease B immunoglobulin; AN, anorexia nervosa; BMI, body mass index, BN, bulimia nervosa; ClpB, enterobacterial caseinolytic protease B; DM, diabetes mellitus; Ig, immunoglobulin (IgA, IgG, and IgM classes); NPY, neuropeptide tyrosine; PYY, peptide tyrosine tyrosine. ↑ = higher than healthy controls, ↓ = lower than healthy controls.

to be associated with anxiety states and AN. Importantly, it has been surmised that AN may result from an inability to produce neutralizing antibodies to TNF-α and/or IL-1β (37). Direct TNF-α, IL-1β, and IL-6 down-regulating monoclonal antibodies such as infliximab, adalimumab, etanercept, and tocilizumab as well as monoclonal antibodies against appetite-regulating hormones have not been evaluated as a treatment of AN and BN so far, although there is a strong theoretical rationale that could justify such a study (38, 39). Beneficial effects of anti-TNF-α therapy and an improvement in psychopathological traits in a case of AN with comorbid Crohn's disease and with juvenile idiopathic arthritis were reported (40, 41).

In our previous studies, we observed *in vivo* increased sympathetic nervous system (SNS) activity, especially elevated norepinephrine (NE) concentrations in subcutaneous abdominal adipose tissue (AT) in AN and BN patients (36, 42, 43). NPY is synthesized in AT and co-localized with NE in perivascular sympathetic nerve fibers of the AT. NPY is also co-localized with NE and gamma-aminobutyric acid (GABA) in the brain. NPY amplifies growth hormone (GH) release, and stimulates appetite and lipogenesis (36, 44). Corcos et al. hypothesized that dopamine, dopamine-β-hydroxylase, and serotonin could be the antigenic cerebral targets reacting with "anti-brain" antibodies in BN (32). The role of up- or down-regulated neutralizing autoantibodies (IgM, IgG, and IgA classes), and changes of their affinity directed against appetite-regulating neuropeptides and neurotransmitters (dopamine, dopamine-beta-hydroxylase, and serotonin) in neuropeptidergic transmission was documented in the pathogenesis of eating disorders (26, 32) (**Table 1**). Moreover, a link between CNS neuroinflammation, autoimmunity, and neuropsychiatric disorders was reported (45–47).

"LEAKY GUT" AND THE BLOOD-BRAIN BARRIER PERMEABILITY IN AN AND BN

The gut microbiota transform dietary components, including macro- and micronutrients, fibers, and polyphenols, into a range of metabolites, including amino acid derivatives, vitamins, short-chain fatty acids (SCFA), and trimethylamines. These microbial-derived metabolites and dietary components can modulate host homeostasis, including gut and blood-brain barrier integrity (48–50).

SCFA (in particular butyrate, acetate, propionate), and other microbial metabolites can act on the intestinal epithelial barrier, the blood-brain barrier, and directly on brain neurons; they can regulate the endocrine and immune system to protect against the pathological inflammation (49). SCFA-producing gut microbiota was shown to up-regulate the expression of blood-brain barrier tight junction proteins occludin, claudin-5, and zonulin, and to reduce the permeability of the blood-brain barrier (51).

SCFA can mediate appetite reduction *via* increased POMC/CART neurotransmission of glutamatergic neurons and *via* decreased NPY/AGRP neurotransmission of GABAergic neurons in the hypothalamic arcuate nucleus (52, 53). Starvation and weight loss of AN patients may decrease the gut-barrier permeability (54) and increase the permeability of the blood-brain barrier through increased plasma free fatty acids levels and increased ketone bodies production (55, 56). Disruption of blood-brain barrier integrity in parallel with decreased expression of tight junction proteins occludin and claudin-5 have been also related to stress, post-streptococcal autoimmune disorders (*PANDAS*), and increased pro-inflammatory anorexigenic cytokines including TNF-α, IL-6, and IL-1β (37, 57–59). Autoantibodies against appetite-regulating peptides, and neurotransmitters can also disrupt the blood-brain barrier permeability and the gut-barrier permeability referred to as "leaky gut" underlying low-grade inflammation in AN and BN patients (18, 24). Indeed, penetration of circulating neuropeptides to the brain may be assisted by neuropeptide autoantibodies (60).

It is believed that the access of high-affinity autoantibodies against appetite-regulating neuropeptides and peptides to the brain centers, otherwise protected by the blood-brain barrier, can trigger the development of AN and BN. The increased affinity of plasmatic IgG for acyl-ghrelin in obesity was associated with increased ghrelin function, while increased plasma IgG/α-MSH affinity in obesity was shown to decrease activation of MC4R (23, 61). Monteleone et al. reported a decrease of intestinal permeability in the small intestine by measuring lactulose/mannitol absorption in AN patients (54). Jésus et al. observed increased colonic permeability with decreased expression of the tight junction protein claudin-1 in an activity-based anorexia model in mice (62). Methotrexate-induced intestinal inflammation was shown to acutely disrupt the gut-barrier permeability and induce anorexia in rats (63). Coquerel et al. linked intestinal inflammation to the production of autoantibodies against neuropeptides and showed that changes in anti-α-MSH autoAb plasma levels may participate in the body weight control relevant to the pathophysiology of AN (64).

Intestinal fatty acid binding protein (I-FABP) was proposed as a biomarker for small intestinal epithelial damage and subsequently for potentially altered gut permeability in Crohn's and celiac diseases (65, 66). It is a small (14-15 kD) protein, which constitutes up to 2% of the cytoplasmic protein content of mature enterocytes (67). Upon death of the enterocyte, its cytoplasmic content is liberated into the circulation. I-FABP is present in very small amounts in the plasma of healthy individuals, probably representing the normal turnover of enterocytes, but its levels rise rapidly after episodes of acute intestinal ischemia and inflammation.

We determined a significantly increased I-FABP level in patient with severe and enduring AN suffering from the small intestinal bacterial overgrowth syndrome. Patient treatment with fecal microbiota transplantation (FMT) led to an improvement of the gut barrier function reflected by a decrease in I-FABP levels within 6 months post-FMT with non-detectable values 1 year post-FMT (68).

THE GHRELIN, LEPTIN, AND MELANOCORTIN SYSTEM IN AN AND BN

Ghrelin is a 28-amino-acid peptide produced mainly by the neuroendocrine cells named P/D1 in humans in the oxyntic

mucosa of the gastric fundus, and to a far lesser extent in the duodenum, and also in the *epsilon* pancreatic islet cells (69, 70). Ghrelin is cleaved from the 117-amino-acid preproghrelin protein encoded by the human ghrelin gene on chromosome 3p25-26. Two major molecular forms of ghrelin were found in the stomach and plasma, *i.e.* acyl ghrelin with n-octanoylated serine in position 3 attached by the GOAT (Ghrelin O-Acetyltransferase), and des-acyl ghrelin. Acyl ghrelin is involved in the regulation of growth hormone (GH) secretion, energy homeostasis, gastric emptying, cardiac performance, cardiac output and contractility, antidepressant-like and anxiolytic responses (71–73). It was reported that in contrast to acyl ghrelin, des-acyl ghrelin induces a negative energy balance by decreasing food intake and delaying gastric emptying (71, 74). The physiological role of ghrelin in food intake regulation is reflected by an increase in its plasma level before eating and its decrease after the meal (75).

Thus, des-acyl ghrelin does not bind to growth hormone secretagogue receptor type 1a (GHS-R1a). Moreover, it has anti-ghrelin effects including the loss of ghrelin's appetite-stimulating effect *via* increasing expression of melanocortin 4 receptor (MC4R) in the hypothalamic arcuate nucleus (76). It was found that des-acyl ghrelin level was higher in symptomatic AN patients than in healthy controls, which may elucidate why AN patients report being less hungry compared to healthy women. On the other hand, the des-acyl ghrelin level was lower in AN patients after renourishment than in heathy women (71, 77).

Acyl ghrelin binds to GHS-R1a and its plasma levels have been documented to be decreased in AN when compared to age-matched and weight-healthy women (71, 78, 79). Therefore, treatment with acyl ghrelin and/or Relamorelin, a pentapeptide ghrelin receptor agonist, may be useful for stimulating appetite, gastric emptying, and weight regain in AN patients (80).

Plasma total ghrelin levels are increased in patients with AN; however, anorexic patients report less hunger when compared to healthy women. This discordance may be explained on the basis of ghrelin resistance in anorectic women (71, 78) or a changed acyl/des-acyl ghrelin ratio and/or ghrelin reactive autoantibodies (77, 81). Patients with AN display lower levels of autoantibodies (IgG) against acyl-ghrelin and higher levels of autoantibodies against des-acyl ghrelin present in immune complexes compared to healthy controls. Moreover, negative correlations between plasma ghrelin autoantibodies (IgG) and ghrelin peptides were found. The observed decrease in the levels of bioavailable ghrelin autoantibodies (IgG) was suggested to lead to increased ghrelin levels and ghrelin resistance in patients with AN (26) (**Table 1**). Moreover, a decrease in IgM and IgA classes of acyl ghrelin autoantibodies in AN was also detected (26). Subsequently, the refeeding of AN patients led to an increase in IgM acyl ghrelin autoantibodies levels, which may indicate new antigenic stimulation resulting from realimentation-induced changes in the gut-barrier permeability. Furthermore, high affinity anti-ghrelin IgG autoantibodies were proposed to enhance ghrelin's orexigenic effect, which may contribute to increased appetite and overeating and may enhance the bioactivity of endogenous or exogenous ghrelin in obese patients (27, 61) (**Table 1**). In addition, this shows that ghrelin degradation is inhibited by these autoantibodies, *i.e.* by forming ghrelin-IgG immune complexes in obese patients (27).

The presence of immune complexes prevents des-acyl ghrelin from occurring with a decrease of the free fraction of autoantibodies binding ghrelins resulting in elevated levels of free acylated ghrelin in AN patients, and eventually in ghrelin resistance in AN (26). High-affinity insulin autoantibodies have been proposed to be involved in a mechanism underlying severe insulin resistance after insulin administration (31) and have also been also studied as a marker of type 1 diabetes (**Table 1**). Low-affinity autoantibodies against insulin may influence the levels of bioavailable insulin with potential effects on hypoglycemia (31). Using a homeostasis model assessment of insulin resistance (HOMA-IR), significantly lower values of HOMA-IR in malnourished and underweight patients with AN were found when compared to healthy controls (82). However, refeeding led to the onset of insulin resistance in patients with AN (83). Indeed, the onset of type 1 diabetes in adolescence seems to place female patients at risk for the subsequent development of AN and BN (5, 6, 78, 84). Importantly, a decrease in leptin-reacting immunoglobulin affinity kinetics may also be related to hyperinsulinemia, insulin resistance, and leptin resistance in patients with type 2 diabetes (30). Intravenous injection of leptin-neutralizing antibodies was reported to induce hyperinsulinemia in mice (85). Conversely, an increase in IgG affinity kinetics for leptin was found in healthy controls with lower BMI suggesting an enhancing role of IgG in leptin transduction with anorexigenic and antidiabetic properties (30) (**Table 1**).

Obestatin, a 23-amino-acid peptide cleaved of the pro-hormone preproghrelin, appears to function as a part of the anorexigenic gut-brain axis that decreases food intake and reduces body weight in rats (86). Obestatin has been postulated to antagonize ghrelin action on energy balance and gastrointestinal function. However, controversies exist as regards its specific effects on food intake in animals and humans (71, 87). Patients with AN displayed increased circulating levels of both obestatin and ghrelin and an increased ghrelin/obestatin ratio, whereas patients with BN did not (88).

Gastric ghrelin stimulates appetite, while gut hormones pancreatic polypeptide (PP) and peptide tyrosine tyrosine (PYY) have the opposite effect on the hypothalamic level. PP and PYY, 36 amino acid peptides, are secreted from pancreatic F cells and enteroendocrine L-cells following meals, respectively (89, 90). Importantly, G protein receptor 142 for tryptophan (GPR142) is expressed on gastro-enteroendocrine and pancreatic islet cells to stimulate ghrelin, PYY, glucagon-like peptide-1 (GLP-1), cholecystokinin (CCK), and insulin secretagogue activities, respectively (91, 92) (**Figure 1**). It was shown that SCFA including butyrate and lactate are ligands of FFA2, FFA3, and HCA1 receptors which are expressed on gastric ghrelin cells and ileal L cells. Their activation reduces ghrelin secretion and increases PYY secretion, respectively (69, 73, 93). Furthermore,

PYY and GLP-1 stimulate serotonin (5-hydroxytryptamine, 5-HT) secretion from small intestinal and colonic enterochromaffin (EC) cells (94) (**Figure 1**). The SCFA receptors FFA2, FFA3, and HCA1 were found in AT where they increase the secretion of the anorexigenic hormone leptin (95, 96), and the blood-brain barrier is endowed with FFA3 (97). Interestingly, an endogenous ligand for HCA2 and FFA2 receptor is 3-hydroxy-butyrate. Thus, FFA2 and HCA2 receptors are activated by the endogenous ligand 3-hydroxy-butyrate as well as the exogenous ligand anti-dyslipidemic drug niacin having protective effects of the prebiotic fiber-derived butyrate in the gut-barrier permeability (42, 98, 99). We documented reduced ghrelin levels and increased PP, PYY, and leptin levels after administration of the niacin-like anti-dyslipidemic drug Olbetam in bulimic patients when compared to healthy-weight Czech women (42).

The subpeptide PYY_{3-36} is the major form of PYY in the circulation. This peptide reduces food intake in humans. In AN, unlike ghrelin, plasma levels of anorexigenic PYY are paradoxically increased (100). Elevated levels of PYY might contribute to decreased food intake and disordered eating psychopathology in AN. PYY levels remain elevated despite renourishment and weight regain (101, 102). Healthy humans showed a negative correlation between ghrelin plasma concentrations and BMI (103) and a negative correlation of PYY and body weight (104). However, two independent research groups documented that BN patients, despite of higher BMI, had increased plasma ghrelin levels before food ingestion with a decreased response of ghrelin after food ingestion (105, 106). In those patients with BN, the increase of plasma PYY levels after food ingestion was also blunted. Depressed and blunted PYY levels may result from reduced and impaired CCK secretion in BN. The anorexigenic hormone CCK is a stimulant of PYY secretion (107). PYY_{3-36} is known as meal terminator opposed to ghrelin considered as meal initiator in the feeding behavior. The suppression of plasma ghrelin and the increase of plasma PYY_{3-36} after food ingestion may indicate compensatory activation of peripheral signals promoting termination of food ingestion in healthy humans. Thus, the altered CCK, PYY, and ghrelin response to food intake may play a role in the perpetuating post-binge eating behavior in bulimic patients (108).

Ghrelin has an important role in regulation of energy homeostasis and appetite by acting centrally through GHS-R1a or *via* vagal afferents. Furthermore, ghrelin can activate hypothalamic GABAergic arcuate neurons that secrete the orexigenic peptides NPY and the agouti-related peptide (AGRP). It can inhibit anorexigenic neurons secreting α-MSH resulting in higher energy intake to be induced by increased GABA-mediated inhibitory inputs from NPY/AGRP neurons to hypothalamic glutamatergic arcuate neurons, which express anorexigenic pro-opiomelanocortin (a precursor of α-MSH), and cocaine- and amphetamine-regulated transcript (POMC/CART) (42, 89). Anorexigenic/anxiogenic α-MSH is a 13-amino-acid-long neuropeptide derived from POMC. Activation of POMC neurons leads to stimulation of the melanocortin satiety pathway. Cone has demonstrated that the central melanocortin system operating through α-MSH on MC4R provides the final common pathway signaling satiety (109). High plasma levels and changes of affinity kinetics of autoantibodies reacting with α-MSH and ACTH seem to be caused by the exposure to stress as a result of concomitant hypothalamic-pituitary-adrenal (HPA) axis activation (110, 111). These results support the hypothesis that changes in affinity of autoantibodies reacting with α-MSH and ACTH are involved in the pathogenesis of AN and BN and that increased levels of high-affinity anti-α-MSH or anti-ClpB (α-MSH conformational mimetic produced by *Enterobacteriaceae)* autoantibodies can induce bulimia, while increased levels of low-affinity anti-α-MSH autoantibodies can induce anorexia (24, 110, 112) (**Table 1**).

α-MSH and ClpB may exert a dual effect on the anorexigenic/orexigenic pathway. A key role in appetite regulation is played by the melanocortin 4 receptor (MC4R), which is activated by its main ligand α-MSH in both peripheral and central sites. In this vein, α-MSH and ClpB can induce the activation of MC4R expressed on intestinal enteroendocrine L cells which regulate the release of satiating hormones PYY or GLP-1/-2 leading to activation of the POMC neurons releasing α-MSH *via* the vagal and endocrine pathways (29, 113, 114) (**Figure 1**). Surprisingly, α–MSH can also induce activation of MC4R expressed on gastric ghrelin cells which stimulate orexigenic hormone ghrelin secretion (73, 92, 93) (**Figure 1**). In AN patients, plasma α-MSH were significantly lower all over the day. Thus, lower circadian α-MSH levels integrate the adaptive profile of appetite regulation in AN (115).

As mentioned above, the gut microbiota serving as a direct source of antigens was shown to produce molecules that share similar sequence and conformational homologies with some neuroactive peptides (25). Healthy humans display IgG and IgA autoantibodies directed against appetite-regulating hormones and neuropeptides, such as leptin, ghrelin, PYY, neuropeptide Y and others. These neuropeptides share sequence homology with various peptides produced by some commensal and pathogenic microorganisms including *Lactobacilli*, *Bacteroides*, *Helicobacter pylori*, *Escherichia coli*, and *Candida* species. The autoAbs may thus affect hunger and satiety pathways (25). The presence of *H. pylori* was also associated with decreased adiposity, high levels of stomach leptin, and insulin resistance. On the other hand, decreased ghrelin and increased obestatin were found after *H. pylori* eradication (116, 117). Psychological stress was shown to alter the gut microbiome, *e.g.* to decrease *Bacteroides* and to increase *Clostridium* abundance (118). Certain bacterial proteins of *Clostridium perfringens* and *Enterococcus faecalis* were shown to have sequence homology with orexigenic ghrelin (24, 25).

Appetite-stimulating hormone ghrelin (increased in AN) was associated with greater levels of *Bacteroides* and *Prevotella* and reduced levels of *Bifidobacterium* and *Lactobacillus*. Simultaneously, appetite-suppressing hormone leptin (decreased in AN) showed an inverse association with reduced levels of *Bacteroides* and *Prevotella* and higher levels of *Bifidobacterium* and *Lactobacillus* in rats (119). In another

study incorporating an activity-based anorexia mouse model mimicking the core features of AN, bacterial taxa that correlate positively or negatively with body weight, food intake, and fat mass as well as with hypothalamic mRNA levels of orexigenic NPY and satiety inducer POMC, were identified (120).

Recently, Schalla & Stengel (121) discussed the link between ghrelin and gut microbiota. They surmised that positive effectors such as exercise, prebiotics, probiotics, and food supplements are efficient to increase *Blautia cocoides*, *Bacteroidetes/Firmicutes* ratio, *Faecalibacterium*, *Prevotellaceae*, *Streptococcus*, *Escherichia coli*, *Shigella*, and SCFA leading to a suppression of plasma acylated ghrelin and a decrease of GHS-R1a-induced food intake and weight regain. Conversely, negative effectors including the gut dysbiosis, food restriction, fasting, antibiotics, and pesticides are able to stimulate *Coriobacteriaceae*, *Veillonellaceae*, *Clostridium sensu stricto 1*, *Ruminococcus*, *Prevotella*, and *Coprococcus*, which may result in an increased plasma acylated ghrelin and its orexigenic and the obesogenic side effects (121).

THE GUT MICROBIOME IN AN AND BN

It is now generally accepted that the immune and nervous systems maintain a state of systemic homeostasis by continuous communication. The gut microbial content plays an important role in this communication. Disruption of the pathways connecting gut and brain can lead to various psychopathologies (122, 123). In our studies we described the role of gut microbiota and the gut-barrier permeability in the pathogenesis of inflammatory, autoimmune diseases, including neurological, and psychiatric diseases (19, 124–126). Kleiman et al. showed that the intestinal microbiota plays a role in key features of AN, including weight regulation, energy metabolism, anxiety, and depression as well as a role in the development, maintenance, and recovery from BN (127).

Microbial diversity seems to be essential for health and disease prevention (14, 15). The predominant bacterial phyla in the human gut microbiome are obligate anaerobes *Bacteroidetes* (e.g. genera *Bacteroides* and *Prevotella*) and *Firmicutes* (e.g. genera *Lactobacillus*, *Clostridium*, *Enterococcus*, and *Streptococcus*), and facultative anaerobes present in lesser abundance such as *Actinobacteria* (e.g. *Bifidobacteria*), *Proteobacteria* (e.g. *Escherichia coli*), *Verrucomicrobia* (e.g. *Akkermansia muciniphila*), and *Archaea* (e.g. *Methanobrevibacter smithii*) (128). Microbiome dysbiosis is characterized by either expansion of pathobionts, loss of commensals, loss of microbial diversity, or their combinations (129). There are conflicting results regarding specific changes in microbiome composition in patients with AN (**Table 2**). Current research and microbiota signature associated with acute ill AN patients show a relative depletion of *Firmicutes* (*e.g. Roseburia*, *Clostridium, Anaerostipes*, and *Faecalibacterium prausnitzii*) for the benefit of *Bacteroidetes* (133, 134, 136–138) together with increased abundance in the archeon *Methanobrevibacter smithii* (130, 131, 134, 136), the mucin-degrader *Akkermansia muciniphila* (134, 139) and *Proteobacteria* (*Escherichia coli*) (131, 136) (**Table 2**).

Simultaneously, inconsistent results were reported on bacterial alpha and beta diversity in AN. The gut microbiome exerted lower alpha microbial diversity (describes intra-sample variance) in five studies in underweight AN patients (133, 135, 137, 138, 140); in three additional studies, no difference in alpha diversity was found (126, 134, 136). A significant increase in alpha microbial diversity after weight rehabilitation of patients with AN was shown in two studies (133, 134). Recently, we measured parameters of microbial alpha diversity and detected only an increased Chao 1 index in patients with AN before their renourishment considering their interindividual variation. In this study, weight gain in patients with AN led to a modification of the Chao 1 index which reached healthy control values (126).

Furthermore, differences in beta microbial diversity (describes inter-sample variation) were found in three studies showing higher heterogeneity in AN patients (126, 133, 134). This beta microbial diversity was modified during weight regain in AN patients (126, 133). Bacterial composition of the control and of patients with AN was similar in two studies (136, 138).

Various studies of the gut microbiota in patients with AN revealed an increase in *Methanogens (e.g. Methanobrevibacter smithii)*, while *Lactobacillus* species were linked to obese patients (130, 131). *M. smithii* is known to recycle and convert hydrogen and carbon dioxide to methane, increase the transformation of nutrients to calories by free hydrogen reduction in the colon, increase the fermentation of prebiotic fiber and resistant starch generating SCFA (butyrate, acetate, and propionate), thus increasing energy harvest. *Methanogens* in AN may be thus associated with an adaptive response to very low caloric diet (130) (**Table 2**). However, *M. smithii* may contribute to delay gastric emptying and constipation in AN (78). Archaeal family *Methanobacteriaceae* co-occur with the bacterial family *Christensenellaceae* and are more abundant in lean individuals with lower BMI (141). *Christensenella* spp. can efficiently support the metabolism of *M. smithii* by H_2 production (142).

FMT of *Christensenella minuta* to microbiome-lacking mice, *i.e.* germ-free mice, led to weight gain and adiposity reduction suggesting a role of the gut microbiome in the altered metabolism of AN (141). Furthermore, FMT from lean donors increased insulin sensitivity in patients with the metabolic syndrome and obesity-associated insulin resistance (143). Conversely, FMT from obese mice to germ-free mice led to greater adiposity and increased weight gain indicating that manipulation of gut microbiome might be a possible approach in the treatment of obesity (144, 145).

Lactobacillus intake may be associated with weight gain, anxiolytic or antidepressant effects and may reduce intestinal permeability. In a recent study, *Lactobacillus rhamnosus* decreased anxiety and depression and reduced stress-induced ACTH and corticosterone levels in mice. This study demonstrated that these effects are dependent on the vagus nerve and that parasympathetic innervation is necessary for *Lactobacillus rhamnosus* participation in the gut microbiota-brain interaction (146). Consumption of *Bifidobacterium* species by rats was found to change serotonin metabolism in the brain (147).

TABLE 2 | Gut microbial studies in patients with AN.

Year of publication	Author, reference	Population	Bacterial differences
2009	Armougom et al. (130)	AN=9 C=20	↑ *M. smithii* ↔ *Bacteroidetes* ↔ *Firmicutes* ↔ *Lactobacillus*
2013	Million et al. (131)	AN=15 C=76	↑ *M. smithii* ↑ *E. coli* ↓ *L. reuteri*
2013	Pfleiderer et al.	AN=1	Composition of gut microbiota
2014	Gouba et al.	AN=1	Composition and diversity of gut microbiota
2015	Morita et al. (132)	AN=25 C=21	↓ *Streptococcus* ↓ *Cl. coccoides* ↓ *Cl. leptum* ↓ *L. plantarum* ↓ *B. fragilis*
2015	Kleiman et al. (133)	AN=15 C=12	↑ *Bacilli* ↓ *Clostridium spp.* ↓ *Anaerostipes spp.* ↓ *Faecalibacterium spp.*
2016	Mack et al. (134)	AN=55 C=55	↑ mucin-degraders (*Verrucomicrobia, Bifidobacteria, Anaerotruncus*) ↑ *Clostridium clusters I, XI and XVIII* ↓ *Roseburia spp.* ↓ *Gemminger spp.*
2017	Mörkl et al. (135)	AN=18 C=26	↑ *Coriobacteriaceae*
2017	Borgo et al. (136)	AN=15 C=15	↑ *Enterobacteriaceae* ↑ *Proteobacteria* ↑ *M. smithii* ↓ *Firmicutes* ↓ *Ruminococcaceae* ↓ *Roseburia spp.* ↓ *Ruminococcus spp.* ↓ *Clostridium spp.*
2017	Kleiman et al.	AN=3	Composition and diversity changes over time
2019	Hanashi et al. (137)	AN=33 C=22	↑ *Turicibacter spp.* ↑ *Anaerotruncus spp.* ↑ *Salmonella spp.* ↑ *Klebsiella spp.* ↓ *Eubacterium spp.* ↓ *Roseburia spp.* ↓ *Anaerostipes spp.* ↓ *Peptostreptococcaceae*
2019	Prochazkova et al. (68)	AN=1	Composition and diversity changes over time after the FMT
2021	Prochazkova et al. (126)	AN=59 C=67	↑ *Alistipes spp.* ↑ *Clostridiales* ↑ *Christensenellaceae* ↑ *Ruminococcaceae* ↓ *Faecalibactrium spp.* ↓ *Agathobacter spp.* ↓ *Bacteroides spp.* ↓ *Blautia spp.* ↓ *Lachnospira*

AN, anorexia nervosa; C, healthy persons.

↑ = higher than healthy persons, ↓ = lower than healthy persons, ↔ = not different from healthy persons.

Bacterial species produce a number of neuroactive compounds including serotonin (*Bacillus* spp., *Lactobacillus plantarum*, *Clostridium ramosum*, and *Escherichia coli*), dopamine, the major disruptor of the mesolimbic-neocortical reward circuit in the brain (*Lactobacillus plantarum, Clostridium* spp., *Escherichia coli*, *Bacillus* spp., *Serratia* spp.), norepinephrine (*Clostridium* spp., *Escherichia coli*, and *Bacillus* spp.), and acetylcholine (*Lactobacillus plantarum*), and they synthesize the inhibitory neurotransmitter GABA from glutamate, reducing anxiety and stress (*Bacteroides*, *Escherichia coli*, *Lactobacillus reuteri, Bifidobacterium, Lactobacillus rhamnosus, Lactobacillus brevis*, and *Lactobacillus plantarum*) (146, 148–158). These microbially-derived neurotransmitters may induce intestine epithelial cells to release molecules that in turn modulate neural signaling within the enteric nervous system and consequently signal brain function and host behavior. Mood and depressive-like behavior regulators include serotonin which is an important neurotransmitter implicated in psychiatric

disorders including AN and BN. Hata et al. observed significantly lower brainstem serotonin levels in anorectic mice, which may be associated with reduced tryptophan intake resulting from restricted food intake (159). Recently, Prochazkova et al. (126) detected lower levels of serotonin, dopamine and GABA in fecal samples of patients with AN when compared with healthy women.

The central nervous system (CNS) modulation by microbiota occurs primarily through neuroimmune and neuroendocrine mechanisms. Except neurotransmitters and hormones, this communication is mediated by gut microbial metabolites, including SCFA, bile acids, and tryptophan metabolites. SCFA are generated by microbial fermentation of non-digestible colon polysaccharides.

Overall, there are inconsistent results for fecal concentrations of SCFA and branched-chain fatty acids (BCFA; isobutyrate, 2-methyl-butyrate, and isovalerate) in AN patients (132, 134, 136, 160). In our study, we detected reduced butyrate and acetate in AN, which were not changed after weight recovery (126). Reduced levels of acetate and propionate were found in another study (132), while Borgo et al. found decreased butyrate and propionate concentrations in patients with AN (136).

FMT is a therapeutic procedure to modify the recipient's gut microbiota. FMT is commonly used for the treatment of recurrent pseudomembranous colitis caused by toxin-producing *Clostridium difficile* (161). Moreover, FMT was also used to alleviate chronic intestinal pseudo-obstructive syndrome (CIPO) mimicking mechanical intestinal obstruction (162, 163) or the small intestinal bacterial overgrowth syndrome (SIBO). SIBO is a gastrointestinal disorder diagnosed as an excessive and/or abnormal bacterial colonization in the small intestine (more than 10^5 colony-forming units of bacteria per mL of jejunal aspirate) associated with various metabolic disorders and serious malnutrition found also in patients with AN (68, 163) who suffer from delayed gastric emptying and constipation (164, 165).

CONCLUSIONS

Various stressors, especially infectious, but also components of diet, mental stress, and others can modify the gut and the blood-brain barrier function leading to the production of antibodies directed against microbial compounds and cross-reacting with human neuropeptides and neurotransmitters. The interplay between the gut microbiome, immune, hormonal, behavioral, and emotional regulation provides a complex mechanism underlying AN pathophysiology as well as other neuropsychiatric diseases. Immunization against ClpB could be validated as a potential preventive and therapeutic option for AN and BN. The current long-term pharmacological therapy of AN and BN patients is rather inefficient, is associated with adverse side effects, and given that these disorders tend to relapse. New approaches to prevention and therapy could be suggested. The gut microbiota modulation realized by lifestyle changes and by application of prebiotics, probiotics (psychobiotics), FMT could represent an useful tool for prevention and treatment of eating and other neuropsychiatric disorders.

AUTHOR CONTRIBUTIONS

KS, PP, RR, JD, HP, OK, MB, and HT-H: conceptualization. All authors: writing-original draft preparation, editing, and revising. HT-H: supervision. All authors contributed to the article and approved the submitted version.

FUNDING

This study was supported by the grant No. 17-28905A provided by the AZV Grant Agency of the Ministry of Health, Czech Republic.

REFERENCES

1. Hsu LK. Epidemiology of the eating disorders. *Psychiatr Clin North Am* (1996) 19:681–700c. doi: 10.1016/S0193-953X(05)70375-0
2. Arcelus J, Mitchell AJ, Wales J, Nielsen S. Mortality rates in patients with anorexia nervosa and other eating disorders. A meta-analysis of 36 studies. *Arch Gen Psychiatry* (2011) 68:724–31. doi: 10.1001/archgenpsychiatry.2011.74
3. American Psychiatric Association. *Diagnostic and Statistical Manual of Mental Disorders, 5th ed. (DSM-5R). 5th ed.* Washington, DC: American Psychiatric Association Publishing (2013). doi: 10.1176/appi.books.9780890425596
4. Fetissov SO, Hallman J, Oreland L, Af Klinteberg B, Grenbäck E, Hulting AL, et al. Autoantibodies against alpha -MSH, ACTH, and LHRH in anorexia and bulimia nervosa patients. *Proc Natl Acad Sci U S A* (2002) 99(26):17155–60. doi: 10.1073/pnas.222658699
5. Raevuori A, Haukka J, Vaarala O, Suvisaari JM, Gissler M, Grainger M, et al. The increased risk for autoimmune diseases in patients with eating disorders. *PloS One* (2014) 9(8):e104845. doi: 10.1371/journal.pone.0104845
6. Takii M, Uchigata Y, Kishimoto J, Morita C, Hata T, Nozaki T, et al. The relationship between the age of onset of type 1 diabetes and the subsequent development of a severe eating disorder by female patients. *Pediatr Diabetes* (2011) 12:396–401. doi: 10.1111/j.1399-5448.2010.00708.x
7. Hedman A, Breithaupt L, Hübel C, Thornton LM, Tillander A, Norring C, et al. Bidirectional relationship between eating disorders and autoimmune diseases. *J Child Psychol Psychiatry* (2019) 60:803–12. doi: 10.1111/jcpp.12958
8. Zerwas S, Larsen JT, Petersen L, Thornton LM, Quaranta M, Koch SV, et al. Eating Disorders, Autoimmune, and Autoinflammatory Disease. *Pediatrics* (2017) 140:e20162089. doi: 10.1542/peds.2016-2089
9. Hommer RE, Swedo SE. Anorexia and Autoimmunity: Challenging the Etiologic Constructs of Disordered Eating. *Pediatrics* (2017) 140:e20173060. doi: 10.1542/peds.2017-3060
10. Watson HJ, Yilmaz Z, Thornton LM, Hübel C, Coleman JRI, Gaspar HA, et al. Genome-wide association study identifies eight risk loci and implicates metabo-psychiatric origins for anorexia nervosa. *Nat Genet* (2019) 51:1207–14. doi: 10.1038/s41588-019-0439-2
11. Periyasamy S, John S, Padmavati R, Rajendren P, Thirunavukkarasu P, Gratten J, et al. Association of Schizophrenia Risk With Disordered Niacin Metabolism in an Indian Genome-wide Association Study. *JAMA Psychiatry* (2019) 76:1026–36. doi: 10.1001/jamapsychiatry.2019.1335

12. Portale S, Sculati M, Sanford FC, Cena H. Pellagra and anorexia nervosa: a case report. *Eat Weight Disord* (2020) 25:1493–96. doi: 10.1007/s40519-019-00781-x
13. Haleem DJ. Improving therapeutics in anorexia nervosa with tryptophan. *Life Sci* (2017) 178:87–93. doi: 10.1016/j.lfs.2017.04.015
14. Roubalová R, Procházková P, Papežová H, Smitka K, Bilej M, Tlaskalová-Hogenová H. Anorexia nervosa: Gut microbiota-immune-brain interactions. *Clin Nutr* (2020) 39:676–84. doi: 10.1016/j.clnu.2019.03.023
15. Cryan JF, O'Riordan KJ, Cowan CSM, Sandhu KV, Bastiaanssen TFS, Boehme M, et al. The Microbiota-Gut-Brain Axis. *Physiol Rev* (2019) 99:1877–2013. doi: 10.1152/physrev.00018.2018
16. Lundgren P, Thaiss CA. The microbiome-adipose tissue axis in systemic metabolism. *Am J Physiol Gastrointest Liver Physiol* (2020) 318(4):G717–24. doi: 10.1152/ajpgi.00304.2019
17. Prince AC, Brooks SJ, Stahl D, Treasure J. Systematic review and meta-analysis of the baseline concentrations and physiologic responses of gut hormones to food in eating disorders. *Am J Clin Nutr* (2009) 89:755–65. doi: 10.3945/ajcn.2008.27056
18. Fetissov SO. Role of the gut microbiota in host appetite control: bacterial growth to animal feeding behaviour. *Nat Rev Endocrinol* (2017) 13(1):11–25. doi: 10.1038/nrendo.2016.150
19. Tlaskalová-Hogenová H, Stepánková R, Hudcovic T, Tucková L, Cukrowska B, Lodinová-Zádníková R, et al. Commensal bacteria (normal microflora), mucosal immunity and chronic inflammatory and autoimmune diseases. *Immunol Lett* (2004) 93(2-3):97–108. doi: 10.1016/j.imlet.2004.02.005
20. Oldstone MB. Molecular mimicry, microbial infection, and autoimmune disease: evolution of the concept. *Curr Top Microbiol Immunol* (2005) 296:1–17. doi: 10.1007/3-540-30791-5_1
21. Fetissov SO, Hökfelt T. On the origin of eating disorders: altered signaling between gut microbiota, adaptive immunity and the brain melanocortin system regulating feeding behavior. *Curr Opin Pharmacol* (2019) 48:82–91. doi: 10.1016/j.coph.2019.07.004
22. Fetissov SO, Harro J, Jaanisk M, Järv A, Podar I, Allik J, et al. Autoantibodies against neuropeptides are associated with psychological traits in eating disorders. *Proc Natl Acad Sci U S A* (2005) 102:14865–70. doi: 10.1073/pnas.0507204102
23. Lucas N, Legrand R, Bôle-Feysot C, Breton J, Coëffier M, Akkermann K, et al. Immunoglobulin G modulation of the melanocortin 4 receptor signaling in obesity and eating disorders. *Transl Psychiatry* (2019) 9(1):87. doi: 10.1038/s41398-019-0422-9
24. Fetissov SO, Déchelotte P. The new link between gut-brain axis and neuropsychiatric disorders. *Curr Opin Clin Nutr Metab Care* (2011) 14:477–82. doi: 10.1097/MCO.0b013e32834936e7
25. Fetissov SO, Sinno MH, Coëffier M, Bole-Feysot C, Ducrotte P, Hökfelt T, et al. Autoantibodies against appetite-regulating peptide hormones and neuropeptides: Putative modulation by gut microflora. *Nutrition* (2008) 24:348–59. doi: 10.1016/j.nut.2007.12.006
26. Terashi M, Asakawa A, Harada T, Ushikai M, Coquerel Q, Sinno MH, et al. Ghrelin reactive autoantibodies in restrictive anorexia nervosa. *Nutrition* (2011) 27:407–13. doi: 10.1016/j.nut.2011.01.002
27. Takagi K, Legrand R, Asakawa A, Amitani H, François M, Tennoune N, et al. Anti-ghrelin immunoglobulins modulate ghrelin stability and its orexigenic effect in obese mice and humans. *Nat Commun* (2013) 4:2685. doi: 10.1038/ncomms3685
28. Garcia FD, Coquerel Q, do Rego JC, Cravezic A, Bole-Feysot C, Kiive E, et al. Anti-neuropeptide Y plasma immunoglobulins in relation to mood and appetite in depressive disorder. *Psychoneuroendocrinology* (2012) 37 (9):1457–67. doi: 10.1016/j.psyneuen.2012.01.015
29. Breton J, Jacquemot J, Yaker L, Leclerc C, Connil N, Feuilloley M, et al. Host Starvation and Female Sex Influence Enterobacterial ClpB Production: A Possible Link to the Etiology of Eating Disorders. *Microorganisms* (2020) 8 (4):530. doi: 10.3390/microorganisms8040530
30. Bouhajja H, Bougacha-Elleuch N, Lucas N, Legrand R, Marrakchi R, Kaveri SV, et al. Affinity kinetics of leptin-reactive immunoglobulins are associated with plasma leptin and markers of obesity and diabetes. *Nutr Diabetes* (2018) 8(1):32. doi: 10.1038/s41387-018-0044-y
31. Hu X, Chen F. Exogenous insulin antibody syndrome (EIAS): a clinical syndrome associated with insulin antibodies induced by exogenous insulin in diabetic patients. *Endocr Connect* (2018) 7(1): R47–R55. doi: 10.1530/EC-17-0309
32. Corcos M, Atger F, Lévy-Soussan P, Avrameas S, Guilbert B, Cayol V, et al. Bulimia nervosa and autoimmunity. *Psychiatry Res* (1999) 87:77–82. doi: 10.1016/S0165-1781(99)00048-7
33. Fetissov SO. Neuropeptide autoantibodies assay. *Methods Mol Biol* (2011) 789:295–302. doi: 10.1007/978-1-61779-310-3_19
34. François M, Takagi K, Legrand R, Lucas N, Beutheu S, Bôle-Feysot C, et al. Increased Ghrelin but Low Ghrelin-Reactive Immunoglobulins in a Rat Model of Methotrexate Chemotherapy-Induced Anorexia. *Front Nutr* (2016) 3:23. doi: 10.3389/fnut.2016.00023
35. Wheatland R. Chronic ACTH autoantibodies are a significant pathological factor in the disruption of the hypothalamic-pituitary-adrenal axis in chronic fatigue syndrome, anorexia nervosa and major depression. *Med Hypotheses* (2005) 65(2):287–95. doi: 10.1016/j.mehy.2005.02.031
36. Smitka K, Papezova H, Vondra K, Hill M, Hainer V, Nedvidkova J. A higher response of plasma neuropeptide Y, growth hormone, leptin levels and extracellular glycerol levels in subcutaneous abdominal adipose tissue to Acipimox during exercise in patients with bulimia nervosa: single-blind, randomized, microdialysis study. *Nutr Metab* (2011) 8:81. doi: 10.1186/1743-7075-8-81
37. Holden RJ, Pakula IS. Tumor necrosis factor-alpha: is there a continuum of liability between stress, anxiety states and anorexia nervosa? *Med Hypotheses* (1999) 52(2):155–62. doi: 10.1054/mehy.1997.0641
38. Patsalos O, Dalton B, Leppanen J, Ibrahim MAA, Himmerich H. Impact of TNF-α Inhibitors on Body Weight and BMI: A Systematic Review and Meta-Analysis. *Front Pharmacol* (2020) 11:481. doi: 10.3389/fphar.2020.00481
39. Patsalos O, Dalton B, Himmerich H. Effects of IL-6 Signaling Pathway Inhibition on Weight and BMI: A Systematic Review and Meta-Analysis. *Int J Mol Sci* (2020) 21(17):6290. doi: 10.3390/ijms21176290
40. Solmi M, Santonastaso P, Caccaro R, Favaro A. A case of anorexia nervosa with comorbid Crohn's disease: beneficial effects of anti-TNF-α therapy? *Int J Eat Disord* (2013) 46(6):639–41. doi: 10.1002/eat.22153
41. Barber J, Sheeran T, Mulherin D. Anti-tumour necrosis factor treatment in a patient with anorexia nervosa and juvenile idiopathic arthritis. *Ann Rheum Dis* (2003) 62(5):490–1. doi: 10.1136/ard.62.5.490
42. Smitka K, Nedvidkova J, Vondra K, Hill M, Papezova H, Hainer V. Acipimox Administration With Exercise Induces a Co-feedback Action of the GH, PP, and PYY on Ghrelin Associated With a Reduction of Peripheral Lipolysis in Bulimic and Healthy-Weight Czech Women: A Randomized Study. *Front Endocrinol (Lausanne)* (2019) 10:108. doi: 10.3389/fendo.2019.00108
43. Nedvidkova J, Dostalova I, Bartak V, Papezova H, Pacak K. Increased subcutaneous abdominal tissue norepinephrine levels in patients with anorexia nervosa: an in vivo microdialysis study. *Physiol Res* (2004) 53:409–13.
44. Bi S, Kim YJ, Zheng F. Dorsomedial hypothalamic NPY and energy balance control. *Neuropeptides* (2012) 46(6):309–14. doi: 10.1016/j.npep.2012.09.002
45. Lancaster E, Dalmau J. Neuronal autoantigens–pathogenesis, associated disorders and antibody testing. *Nat Rev Neurol* (2012) 8(7):380–90. doi: 10.1038/nrneurol.2012.99
46. Najjar S, Pearlman DM, Alper K, Najjar A, Devinsky O. Neuroinflammation and psychiatric illness. *J Neuroinflamm* (2013) 10:43. doi: 10.1186/1742-2094-10-43
47. Margutti P, Delunardo F, Ortona E. Autoantibodies associated with psychiatric disorders. *Curr Neurovasc Res* (2006) 2:149–57. doi: 10.2174/156720206776875894
48. Caspani G, Swann J. Small talk: microbial metabolites involved in the signaling from microbiota to brain. *Curr Opin Pharmacol* (2019) 48:99–106. doi: 10.1016/j.coph.2019.08.001
49. Parker A, Fonseca S, Carding SR. Gut microbes and metabolites as modulators of blood-brain barrier integrity and brain health. *Gut Microbes* (2020) 11(2):135–57. doi: 10.1080/19490976.2019.1638722
50. Fasano A. All disease begins in the (leaky) gut: role of zonulin-mediated gut permeability in the pathogenesis of some chronic inflammatory diseases. *F1000Res* (2020) 9:F1000 Faculty Rev–69. doi: 10.12688/f1000research.20510.1

51. Braniste V, Al-Asmakh M, Kowal C, Anuar F, Abbaspour A, Tóth M, et al. The gut microbiota influences blood-brain barrier permeability in mice. *Sci Transl Med* (2014) 6(263):263ra158. doi: 10.1126/scitranslmed.3009759
52. Frost G, Sleeth ML, Sahuri-Arisoylu M, Lizarbe B, Cerdan S, Brody L, et al. The short-chain fatty acid acetate reduces appetite via a central homeostatic mechanism. *Nat Commun* (2014) 5:3611. doi: 10.1038/ncomms4611
53. Chambers ES, Morrison DJ, Frost G. Control of appetite and energy intake by SCFA: what are the potential underlying mechanisms? *Proc Nutr Soc* (2015) 74(3):328–36. doi: 10.1017/S0029665114001657
54. Monteleone P, Carratu R, Carteni M, Generoso M, Lamberti M, De Magistris L, et al. Intestinal permeability is decreased in anorexia nervosa. *Mol Psychiatry* (2004) 9:76–80. doi: 10.1038/sj.mp.4001374
55. Naisberg Y, Modai I, Weizman A. Metabolic bioenergy homeostatic disruption: a cause of anorexia nervosa. *Med Hypotheses* (2001) 56:454–61. doi: 10.1054/mehy.2000.1199
56. Morris AA. Cerebral ketone body metabolism. *J Inherit Metab Dis* (2005) 28 (2):109–21. doi: 10.1007/s10545-005-5518-0
57. Puxley F, Midtsund M, Iosif A, Lask B. PANDAS anorexia nervosa–endangered, extinct or nonexistent? *Int J Eat Disord* (2008) 41:15–21. doi: 10.1002/eat.20462
58. Vincenzi B, O'Toole J, Lask B. PANDAS and anorexia nervosa–a spotters' guide: suggestions for medical assessment. *Eur Eat Disord Rev* (2010) 8 (2):116–23. doi: 10.1002/erv.977
59. Kılıç F, Işık Ü, Demirdaş A, Doğuç DK, Bozkurt M. Serum zonulin and claudin-5 levels in patients with bipolar disorder. *J Affect Disord* (2020) 266:37–42. doi: 10.1016/j.jad.2020.01.117
60. Fu A, Hui EK, Lu JZ, Boado RJ, Pardridge WM. Neuroprotection in stroke in the mouse with intravenous erythropoietin-Trojan horse fusion protein. *Brain Res* (2011) 1369:203–7. doi: 10.1016/j.brainres.2010.10.097
61. Fetissov SO, Lucas N, Legrand R. Ghrelin-Reactive Immunoglobulins in Conditions of Altered Appetite and Energy Balance. *Front Endocrinol (Lausanne)* (2017) 8:10. doi: 10.3389/fendo.2017.00010
62. Jésus P, Ouelaa W, François M, Riachy L, Guérin C, Aziz M, et al. Alteration of intestinal barrier function during activity-based anorexia in mice. *Clin Nutr* (2014) 33(6):1046–53. doi: 10.1016/j.clnu.2013.11.006
63. Sinno MH, Coquerel Q, Boukhettala N, Coëffier M, Gallas S, Terashi M, et al. Chemotherapy-induced anorexia is accompanied by activation of brain pathways signaling dehydration. *Physiol Behav* (2010) 101(5):639–48. doi: 10.1016/j.physbeh.2010.09.016
64. Coquerel Q, Sinno MH, Boukhettala N, Coëffier M, Terashi M, Bole-Feysot C, et al. Intestinal inflammation influences α-MSH reactive autoantibodies: relevance to food intake and body weight. *Psychoneuroendocrinology* (2012) 37(1):94–106. doi: 10.1016/j.psyneuen.2011.05.008
65. Wiercinska-Drapalo A, Jaroszewicz J, Siwak E, Pogorzelska J, Prokopowicz D. Intestinal fatty acid binding protein (I-FABP) as a possible biomarker of ileitis in patients with ulcerative colitis. *Regul Pept* (2008) 147(1-3):25–8. doi: 10.1016/j.regpep.2007.12.002
66. Henderson AL, Brand MW, Darling RJ, Maas KJ, Detzel CJ, Hostetter J, et al. Attenuation of Colitis by Serum-Derived Bovine Immunoglobulin/Protein Isolate in a Defined Microbiota Mouse Model. *Dig Dis Sci* (2015) 60 (11):3293–303. doi: 10.1007/s10620-015-3726-5
67. Bass N. The cellular fatty acid binding proteins: aspects of structure, regulation, and function. *Int Rev Cytol* (1988) 111:143–84. doi: 10.1016/S0074-7696(08)61733-7
68. Prochazkova P, Roubalova R, Dvorak J, Tlaskalova-Hogenova H, Cermakova M, Tomasova P, et al. Microbiota, Microbial Metabolites, and Barrier Function in A Patient with Anorexia Nervosa after Fecal Microbiota Transplantation. *Microorganisms* (2019) 7(9):338. doi: 10.3390/microorganisms7090338
69. Monteiro MP, Batterham RL. The Importance of the Gastrointestinal Tract in Controlling Food Intake and Regulating Energy Balance. *Gastroenterology* (2017) 152:1707–17.e2. doi: 10.1053/j.gastro.2017.01.053
70. Sakata N, Yoshimatsu G, Kodama S. Development and Characteristics of Pancreatic Epsilon Cells. *Int J Mol Sci* (2019) 20(8):1867. doi: 10.3390/ijms20081867
71. Smitka K, Papezova H, Vondra K, Hill M, Hainer V, Nedvidkova J. The role of "mixed" orexigenic and anorexigenic signals and autoantibodies reacting with appetite-regulating neuropeptides and peptides of the adipose tissue-gut-brain axis: relevance to food intake and nutritional status in patients with anorexia nervosa and bulimia nervosa. *Int J Endocrinol* (2013) 2013:483145. doi: 10.1155/2013/483145
72. Mani BK, Zigman JM. Ghrelin as a Survival Hormone. *Trends Endocrinol Metab* (2017) 8(12):843–54. doi: 10.1016/j.tem.2017.10.001
73. Müller TD, Nogueiras R, Andermann ML, Andrews ZB, Anker SD, Argente J, et al. Ghrelin. *Mol Metab* (2015) 4:437–60. doi: 10.1016/j.molmet.2015.03.005
74. Asakawa A, Inui A, Fujimiya M, Sakamaki R, Shinfuku N, Ueta Y, et al. Stomach regulates energy balance via acylated ghrelin and desacyl ghrelin. *Gut* (2005) 54(1):18–24. doi: 10.1136/gut.2004.038737
75. Cummings DE, Purnell JQ, Frayo RS, Schmidova K, Wisse BE, Weigle DS. A preprandial rise in plasma ghrelin levels suggests a role in meal initiation in humans. *Diabetes* (2001) 50(8):1714–9. doi: 10.2337/diabetes.50.8.1714
76. Hassouna R, Labarthe A, Tolle V. Hypothalamic regulation of body growth and appetite by ghrelin-derived peptides during balanced nutrition or undernutrition. *Mol Cell Endocrinol* (2016) 438:42–51. doi: 10.1016/j.mce.2016.09.027
77. Koyama KI, Yasuhara D, Nakahara T, Harada T, Uehara M, Ushikai M, et al. Changes in acyl ghrelin, des-acyl ghrelin, and ratio of acyl ghrelin to total ghrelin with short-term refeeding in female inpatients with restricting-type anorexia nervosa. *Horm Metab Res* (2010) 42(8):595–8. doi: 10.1055/s-0030-1252017
78. Igudesman D, Sweeney M, Carroll IM, Mayer-Davis EJ, Bulik CM. Gut-Brain Interactions: Implications for a Role of the Gut Microbiota in the Treatment and Prognosis of Anorexia Nervosa and Comparison to Type I Diabetes. *Gastroenterol Clin North Am* (2019) 48:343–56. doi: 10.1016/j.gtc.2019.04.003
79. Hotta M, Ohwada R, Katakami H, Shibasaki T, Hizuka N, Takano K. Plasma levels of intact and degraded ghrelin and their responses to glucose infusion in anorexia nervosa. *J Clin Endocrinol Metab* (2004) 89(11):5707–12. doi: 10.1210/jc.2004-0353
80. Fazeli PK, Lawson EA, Faje AT, Eddy KT, Lee H, Fiedorek FT, et al. Treatment With a Ghrelin Agonist in Outpatient Women With Anorexia Nervosa: A Randomized Clinical Trial. *J Clin Psychiatry* (2018) 79 (1):17m11585. doi: 10.4088/JCP.17m11585
81. Gorwood P, Blanchet-Collet C, Chartrel N, Duclos J, Dechelotte P, Hanachi M, et al. New Insights in Anorexia Nervosa. *Front Neurosci* (2016) 10:256. doi: 10.3389/fnins.2016.00256
82. Dostalova I, Smitka K, Papezova H, Kvasnickova H, Nedvidkova J. Increased insulin sensitivity in patients with anorexia nervosa: the role of adipocytokines. *Physiol Res* (2007) 56:587–94.
83. Prioletta A, Muscogiuri G, Sorice GP, Lassandro AP, Mezza T, Policola C, et al. In anorexia nervosa, even a small increase in abdominal fat is responsible for the appearance of insulin resistance. *Clin Endocrinol* (2011) 75:202–6. doi: 10.1111/j.1365-2265.2011.04046.x
84. Yahya AS, Khawaja S, Chukwuma J, Chukwuma C. Early Diagnosis and Management of Bulimia Nervosa in Type 1 Diabetes. *Prim Care Companion CNS Disord* (2020) 22(6):20nr02707. doi: 10.4088/PCC.20nr02707
85. Martínez-Ansó E, Pérez M, Martínez JA. Induction of hypothermia, hypoglycemia and hyperinsulinemia after acute leptin immunoneutralization in overnight fasted mice. *Int J Mol Med* (1998) 2 (6):681–3. doi: 10.3892/ijmm.2.6.681
86. Zhang JV, Ren PG, Avsian-Kretchmer O, Luo CW, Rauch R, Klein C, et al. Obestatin, a peptide encoded by the ghrelin gene, opposes ghrelin's effects on food intake. *Science* (2005) 310(5750):996–9. doi: 10.1126/science.1117255
87. Garg A. The ongoing saga of obestatin: is it a hormone? *J Clin Endocrinol Metab* (2007) 92(9):3396–8. doi: 10.1210/jc.2007-0999
88. Monteleone P, Serritella C, Martiadis V, Scognamiglio P, Maj M. Plasma obestatin, ghrelin, and ghrelin/obestatin ratio are increased in underweight patients with anorexia nervosa but not in symptomatic patients with bulimia nervosa. *J Clin Endocrinol Metab* (2008) 93(11):4418–21. doi: 10.1210/jc.2008-1138
89. Matafome P, Eickhoff H, Letra L, Seiça R. Neuroendocrinology of Adipose Tissue and Gut-Brain Axis. *Adv Neurobiol* (2017) 19:49–70. doi: 10.1007/978-3-319-63260-5_3
90. Manning S, Batterham RL. The role of gut hormone peptide YY in energy and glucose homeostasis: twelve years on. *Annu Rev Physiol* (2014) 76:585–608. doi: 10.1146/annurev-physiol-021113-170404

91. Rudenko O, Shang J, Munk A, Ekberg JP, Petersen N, Engelstoft MS, et al. The aromatic amino acid sensor GPR142 controls metabolism through balanced regulation of pancreatic and gut hormones. *Mol Metab* (2019) 19:49–64. doi: 10.1016/j.molmet.2018.10.012
92. Engelstoft MS, Schwartz TW. Opposite Regulation of Ghrelin and Glucagon-like Peptide-1 by Metabolite G-Protein-Coupled Receptors. *Trends Endocrinol Metab* (2016) 27(9):665–75. doi: 10.1016/j.tem.2016.07.001
93. Engelstoft MS, Park WM, Sakata I, Kristensen LV, Husted AS, Osborne-Lawrence S, et al. Seven transmembrane G protein coupled receptor repertoire of gastric ghrelin cells. *Mol Metab* (2013) 2:376–92. doi: 10.1016/j.molmet.2013.08.006
94. Lund ML, Egerod KL, Engelstoft MS, Dmytriyeva O, Theodorsson E, Patel BA, et al. Enterochromaffin 5-HT cells - A major target for GLP-1 and gut microbial metabolites. *Mol Metab* (2018) 11:70–83. doi: 10.1016/j.molmet.2018.03.004
95. Zaibi MS, Stocker CJ, O'Dowd J, Davies A, Bellahcene M, Cawthorne MA, et al. Roles of GPR41 and GPR43 in leptin secretory responses of murine adipocytes to short chain fatty acids. *FEBS Lett* (2010) 584(11):2381–6. doi: 10.1016/j.febslet.2010.04.027
96. Al-Lahham SH, Roelofsen H, Priebe M, Weening D, Dijkstra M, Hoek A, et al. Regulation of adipokine production in human adipose tissue by propionic acid. *Eur J Clin Invest* (2010) 40(5):401–7. doi: 10.1111/j.1365-2362.2010.02278.x
97. Hoyles L, Snelling T, Umlai UK, Nicholson JK, Carding SR, Glen RC, et al. Microbiome-host systems interactions: protective effects of propionate upon the blood-brain barrier. *Microbiome* (2018) 6(1):55. doi: 10.1186/s40168-018-0439-y
98. Friedrichs P, Saremi B, Winand S, Rehage J, Dänicke S, Sauerwein H, et al. Energy and metabolic sensing G protein-coupled receptors during lactation-induced changes in energy balance. *Domest Anim Endocrinol* (2014) 48:33–41. doi: 10.1016/j.domaniend.2014.01.005
99. Macia L, Tan J, Vieira AT, Leach K, Stanley D, Luong S, et al. Metabolite-sensing receptors GPR43 and GPR109A facilitate dietary fibre-induced gut homeostasis through regulation of the inflammasome. *Nat Commun* (2015) 6:6734. doi: 10.1038/ncomms7734
100. Schorr M, Miller KK. The endocrine manifestations of anorexia nervosa: mechanisms and management. *Nat Rev Endocrinol* (2017) 13(3):174–86. doi: 10.1038/nrendo.2016.175
101. Lawson EA, Eddy KT, Donoho D, Misra M, Miller KK, Meenaghan E, et al. Appetite-regulating hormones cortisol and peptide YY are associated with disordered eating psychopathology, independent of body mass index. *Eur J Endocrinol* (2011) 164(2):253–61. doi: 10.1530/EJE-10-0523
102. Nakahara T, Kojima S, Tanaka M, Yasuhara D, Harada T, Sagiyama K, et al. Incomplete restoration of the secretion of ghrelin and PYY compared to insulin after food ingestion following weight gain in anorexia nervosa. *J Psychiatr Res* (2007) 41(10):814–20. doi: 10.1016/j.jpsychires.2006.07.021
103. Otto B, Cuntz U, Fruehauf E, Wawarta R, Folwaczny C, Riepl RL, et al. Weight gain decreases elevated plasma ghrelin concentrations of patients with anorexia nervosa. *Eur J Endocrinol* (2001) 145(5):669–73. doi: 10.1530/EJE-1450669
104. Tong J, D'Alessio D. Eating disorders and gastrointestinal peptides. *Curr Opin Endocrinol Diabetes Obes* (2011) 18(1):42–9. doi: 10.1097/MED.0b013e328341e12b
105. Kojima S, Nakahara T, Nagai N, Muranaga T, Tanaka M, Yasuhara D, et al. Altered ghrelin and peptide YY responses to meals in bulimia nervosa. *Clin Endocrinol (Oxf)* (2005) 62(1):74–8. doi: 10.1111/j.1365-2265.2004.02176.x
106. Monteleone P, Martiadis V, Rigamonti AE, Fabrazzo M, Giordani C, Muller EE, et al. Investigation of peptide YY and ghrelin responses to a test meal in bulimia nervosa. *Biol Psychiatry* (2005) 57(8):926–31. doi: 10.1016/j.biopsych.2005.01.004
107. Feltrin KL, Little TJ, Meyer JH, Horowitz M, Rades T, Wishart J, et al. Comparative effects of intraduodenal infusions of lauric and oleic acids on antropyloroduodenal motility, plasma cholecystokinin and peptide YY, appetite, and energy intake in healthy men. *Am J Clin Nutr* (2008) 87(5):1181–7. doi: 10.1093/ajcn/87.5.1181
108. Hannon-Engel SL, Filin EE, Wolfe BE. CCK response in bulimia nervosa and following remission. *Physiol Behav* (2013) 122:56–61. doi: 10.1016/j.physbeh.2013.08.014
109. Cone RD. Anatomy and regulation of the central melanocortin system. *Nat Neurosci* (2005) 8:571–8. doi: 10.1038/nn1455
110. Sinno MH, Do Rego JC, Coëffier M, Bole-Feysot C, Ducrotté P, Gilbert D, et al. Regulation of feeding and anxiety by alpha-MSH reactive autoantibodies. *Psychoneuroendocrinology* (2009) 34(1):140–9. doi: 10.1016/j.psyneuen.2008.08.021
111. Schaefer JM, Fetissov SO, Legrand R, Claeyssens S, Hoekstra PJ, Verhulst FC, et al. Corticotropin (ACTH)-reactive immunoglobulins in adolescents in relation to antisocial behavior and stress-induced cortisol response. The TRAILS study. *Psychoneuroendocrinology* (2013) 38(12):3039–47. doi: 10.1016/j.psyneuen.2013.08.015
112. Galmiche M, Lucas N, Déchelotte P, Deroissart C, Solliec ML, Rondeaux J, et al. Plasma Peptide Concentrations and Peptide-Reactive Immunoglobulins in Patients with Eating Disorders at Inclusion in the French EDILS Cohort (Eating Disorders Inventory and Longitudinal Survey). *Nutrients* (2020) 12(2):522. doi: 10.3390/nu12020522
113. Dominique M, Legrand R, Galmiche M, Azhar S, Deroissart C, Guérin C, et al. Changes in Microbiota and Bacterial Protein Caseinolytic Peptidase B During Food Restriction in Mice: Relevance for the Onset and Perpetuation of Anorexia Nervosa. *Nutrients* (2019) 11(10):2514. doi: 10.3390/nu11102514
114. Panaro BL, Tough IR, Engelstoft MS, Matthews RT, Digby GJ, Møller CL, et al. The melanocortin-4 receptor is expressed in enteroendocrine L cells and regulates the release of peptide YY and glucagon-like peptide 1in vivo. *Cell Metab* (2014) 20(6):1018–29. doi: 10.1016/j.cmet.2014.10.004
115. Galusca B, Prévost G, Germain N, Dubuc I, Ling Y, Anouar Y, et al. Neuropeptide Y and α-MSH circadian levels in two populations with low body weight: anorexia nervosa and constitutional thinness. *PloS One* (2015) 10(3):e0122040. doi: 10.1371/journal.pone.0122040
116. Budzyński J, Kłopocka M. Brain-gut axis in the pathogenesis of Helicobacter pylori infection. *World J Gastroenterol* (2014) 20:5212–25. doi: 10.3748/wjg.v20.i18.5212
117. Yanagi H, Tsuda A, Matsushima M, Takahashi S, Ozawa G, Koga Y, et al. Changes in the gut microbiota composition and the plasma ghrelin level in patients with *Helicobacter pylori*-infected patients with eradication therapy. *BMJ Open Gastroenterol* (2017) 4(1):e000182. doi: 10.1136/bmjgast-2017-000182
118. Bailey MT, Dowd SE, Galley JD, Hufnagle AR, Allen RG, Lyte M. Exposure to a social stressor alters the structure of the intestinal microbiota: implications for stressor-induced immunomodulation. *Brain Behav Immun* (2011) 25(3):397–407. doi: 10.1016/j.bbi.2010.10.023
119. Queipo-Ortuño MI, Seoane LM, Murri M, Pardo M, Gomez-Zumaquero JM, Cardona F, et al. Gut microbiota composition in male rat models under different nutritional status and physical activity and its association with serum leptin and ghrelin levels. *PloS One* (2013) 8(5):e65465. doi: 10.1371/journal.pone.0065465
120. Breton J, Tirelle P, Hasanat S, Pernot A, L'Huillier C, do Rego JC, et al. Gut microbiota alteration in a mouse model of Anorexia Nervosa. *Clin Nutr* (2021) 40(1):181–9. doi: 10.1016/j.clnu.2020.05.002
121. Schalla MA, Stengel A. Effects of microbiome changes on endocrine ghrelin signaling - A systematic review. *Peptides* (2020) 133:170388. doi: 10.1016/j.peptides.2020.170388
122. Dinan TG, Cryan JF. Microbes, Immunity and Behaviour: Psychoneuroimmunology Meets the Microbiome. *Neuropsychopharmacology* (2016) 42(1):178–92. doi: 10.1038/npp.2016.103
123. Collins SM, Surette M, Bercik P. The interplay between the intestinal microbiota and the brain. *Nat Rev Microbiol* (2012) 10(11):735–42. doi: 10.1038/nrmicro2876
124. Tlaskalová-Hogenová H, Stěpánková R, Kozáková H, Hudcovic T, Vannucci L, Tučková L, et al. The role of gut microbiota (commensal bacteria) and the mucosal barrier in the pathogenesis of inflammatory and autoimmune diseases and cancer: contribution of germ-free and gnotobiotic animal models of human diseases. *Cell Mol Immunol* (2011) 8(2):110–20. doi: 10.1038/cmi.2010.67

125. Kostovcikova K, Coufal S, Galanova N, Fajstova A, Hudcovic T, Kostovcik M, et al. Diet Rich in Animal Protein Promotes Pro-inflammatory Macrophage Response and Exacerbates Colitis in Mice. *Front Immunol* (2019) 10:919. doi: 10.3389/fimmu.2019.00919
126. Prochazkova P, Roubalova R, Dvorak J, Kreisinger J, Hill M, Tlaskalova-Hogenova H, et al. The intestinal microbiota and metabolites in patients with anorexia nervosa. *Gut Microbes* (2021) 13(1):1–25. doi: 10.1080/19490976.2021.1902771
127. Kleiman SC, Carroll IM, Tarantino LM, Bulik CM. Gut feelings: A role for the intestinal microbiota in anorexia nervosa? *Int J Eat Disord* (2015) 48 (5):449–51. doi: 10.1002/eat.22394
128. Breton J, Dechelotte P, Ribet D. Intestinal microbiota and anorexia nervosa. *Clin Nutr Exp* (2019) 28:11–21. doi: 10.1016/j.yclnex.2019.05.001
129. Levy M, Kolodziejczyk AA, Thaiss CA, Elinav E. Dysbiosis and the immune system. *Nat Rev Immunol* (2017) 17(4):219–32. doi: 10.1038/nri.2017.7
130. Armougom F, Henry M, Vialettes B, Raccah D, Raoult D. Monitoring bacterial community of human gut microbiota reveals an increase in *Lactobacillus* in obese patients and Methanogens in anorexic patients. *PloS One* (2009) 4(9):e7125. doi: 10.1371/journal.pone.0007125
131. Million M, Angelakis E, Maraninchi M, Henry M, Giorgi R, Valero R, et al. Correlation between body mass index and gut concentrations of *Lactobacillus reuteri*, *Bifidobacterium animalis*, *Methanobrevibacter smithii* and *Escherichia coli*. *Int J Obes (Lond)* (2013) 37(11):1460–6. doi: 10.1038/ijo.2013.20
132. Morita C, Tsuji H, Hata T, Gondo M, Takakura S, Kawai K, et al. Gut Dysbiosis in Patients with Anorexia Nervosa. *PloS One* (2015) 10(12): e0145274. doi: 10.1371/journal.pone.0145274
133. Kleiman SC, Watson HJ, Bulik-Sullivan EC, Huh EY, Tarantino LM, Bulik CM, et al. The Intestinal Microbiota in Acute Anorexia Nervosa and During Renourishment: Relationship to Depression, Anxiety, and Eating Disorder Psychopathology. *Psychosom Med* (2015) 77(9):969–81. doi: 10.1097/PSY.0000000000000247
134. Mack I, Cuntz U, Gramer C, Niedermaier S, Pohl C, Schwiertz A, et al. Weight gain in anorexia nervosa does not ameliorate the faecal microbiota, branched chain fatty acid profiles, and gastrointestinal complaints. *Sci Rep* (2016) 6:1–16. doi: 10.1038/srep26752
135. Mörkl S, Lackner S, Müller W, Gorkiewicz G, Kashofer K, Oberascher A, et al. Gut microbiota and body composition in anorexia nervosa inpatients in comparison to athletes, overweight, obese, and normal weight controls. *Int J Eat Disord* (2017) 50(12):1421–31. doi: 10.1002/eat.22801
136. Borgo F, Riva A, Benetti A, Casiraghi MC, Bertelli S, Garbossa S, et al. Microbiota in anorexia nervosa: The triangle between bacterial species, metabolites and psychological tests. *PloS One* (2017) 12(6):e0179739. doi: 10.1371/journal.pone.0179739
137. Hanachi M, Manichanh C, Schoenenberger A, Pascal V, Levenez F, Cournède N, et al. Altered host-gut microbes symbiosis in severely malnourished anorexia nervosa (AN) patients undergoing enteral nutrition: An explicative factor of functional intestinal disorders? *Clin Nutr* (2019) 38(5):2304–10. doi: 10.1016/j.clnu.2018.10.004
138. Monteleone AM, Troisi J, Fasano A, Dalle Grave R, Marciello F, Serena G, et al. Multi-omics data integration in anorexia nervosa patients before and after weight regain: A microbiome-metabolomics investigation. *Clin Nutr* (2021) 40(3):1137–46. doi: 10.1016/j.clnu.2020.07.021
139. Di Lodovico L, Mondot S, Doré J, Mack I, Hanachi M, Gorwood P. Anorexia nervosa and gut microbiota: A systematic review and quantitative synthesis of pooled microbiological data. *Prog Neuropsychopharmacol Biol Psychiatry* (2021) 22:110114. doi: 10.1016/j.pnpbp.2020.110114
140. Mörkl S, Lackner S, Meinitzer A, Gorkiewicz G, Kashofer K, Painold A, et al. [Pilot study: Gut microbiome and intestinal barrier in anorexia nervosa]. *Fortschr Neurol Psychiatr* (2019) 87:39–45. doi: 10.1055/s-0043-123826
141. Goodrich JK, Waters JL, Poole AC, Sutter JL, Koren O, Blekhman R, et al. Human genetics shape the gut microbiome. *Cell* (2014) 159(4):789–99. doi: 10.1016/j.cell.2014.09.053
142. Ruaud A, Esquivel-Elizondo S, de la Cuesta-Zuluaga J, Waters JL, Angenent LT, Youngblut ND, et al. Syntrophy via Interspecies H_2 Transfer between *Christensenella* and *Methanobrevibacter* Underlies Their Global Cooccurrence in the Human Gut. *mBio* (2020) 11(1):e03235–19. doi: 10.1128/mBio.03235-19
143. Vrieze A, Van Nood E, Holleman F, Salojärvi J, Kootte RS, Bartelsman JF, et al. Transfer of intestinal microbiota from lean donors increases insulin sensitivity in individuals with metabolic syndrome. *Gastroenterology* (2012) 143(4):913–6.e7. doi: 10.1053/j.gastro.2012.06.031
144. Ley RE, Turnbaugh PJ, Klein S, Gordon JI. Microbial ecology: human gut microbes associated with obesity. *Nature* (2006) 444(7122):1022–3. doi: 10.1038/4441022a
145. Turnbaugh PJ, Ley RE, Mahowald MA, Magrini V, Mardis ER, Gordon JI. An obesity-associated gut microbiome with increased capacity for energy harvest. *Nature* (2006) 444(7122):1027–31. doi: 10.1038/nature05414
146. Bravo JA, Forsythe P, Chew MV, Escaravage E, Savignac HM, Dinan TG, et al. Ingestion of *Lactobacillus* strain regulates emotional behaviour and central GABA receptor expression in a mouse via the vagus nerve. *Proc Natl Acad Sci USA* (2011) 108:16050–55. doi: 10.1073/pnas.1102999108
147. Desbonnet L, Garrett L, Clarke G, Bienenstock J, Dinan TG. The probiotic *Bifidobacteria infantis*: An assessment of potential antidepressant properties in the rat. *J Psychiatr Res* (2008) 43:164. doi: 10.1016/j.jpsychires.2008.03.009
148. Valles-Colomer M, Falony G, Darzi Y, Tigchelaar EF, Wang J, Tito RY, et al. The neuroactive potential of the human gut microbiota in quality of life and depression. *Nat Microbiol* (2019) 4):623–32. doi: 10.1038/s41564-018-0337-x
149. Liu WH, Chuang HL, Huang YT, Wu CC, Chou GT, Wang S, et al. Alteration of behavior and monoamine levels attributable to Lactobacillus plantarum PS128 in germ-free mice. *Behav Brain Res* (2016) 298(Pt B):202–9. doi: 10.1016/j.bbr.2015.10.046
150. Shishov VA, Kirovskaia TA, Kudrin VS, Oleskin AV. Amine neuromediators, their precursors, and oxidation products in the culture of Escherichia coli K-12. *Appl Biochem Mikrobiol* (2009) 45:494–7. doi: 10.1134/S0003683809050068
151. Asano Y, Hiramoto T, Nishino R, Aiba Y, Kimura T, Yoshihara K, et al. Critical role of gut microbiota in the production of biologically active, free catecholamines in the gut lumen of mice. *Am J Physiol Gastrointest Liver Physiol* (2012) 303(11):G1288–95. doi: 10.1152/ajpgi.00341.2012
152. Tsavkelova EA, Botvinko IV, Kudrin VS, Oleskin AV. Detection of neurotransmitter amines in microorganisms with the use of high-performance liquid chromatography. *Dokl Biochem* (2000) 372(1-6):115–7.
153. Stanaszek PM, Snell JF, O'Neill JJ. Isolation, extraction, and measurement of acetylcholine from Lactobacillus plantarum. *Appl Environ Microbiol* (1977) 34(2):237–9. doi: 10.1128/AEM.34.2.237-239.1977
154. Strandwitz P, Kim KH, Terekhova D, Liu JK, Sharma A, Levering J, et al. GABA-modulating bacteria of the human gut microbiota. *Nat Microbiol* (2019) 4(3):396–403. doi: 10.1038/s41564-018-0307-3
155. Kunze WA, Mao YK, Wang B, Huizinga JD, Ma X, Forsythe P, et al. Lactobacillus reuteri enhances excitability of colonic AH neurons by inhibiting calcium-dependent potassium channel opening. *J Cell Mol Med* (2009) 13(8B):2261–70. doi: 10.1111/j.1582-4934.2009.00686.x
156. De Vadder F, Grasset E, Mannerås Holm L, Karsenty G, Macpherson AJ, Olofsson LE, et al. Gut microbiota regulates maturation of the adult enteric nervous system via enteric serotonin networks. *Proc Natl Acad Sci U S A* (2018) 115(25):6458–63. doi: 10.1073/pnas.1720017115
157. Barrett E, Ross RP, O'Toole PW, Fitzgerald GF, Stanton C. gamma-Aminobutyric acid production by culturable bacteria from the human intestine. *Appl Microbiol* (2012) 113(2):411–7. doi: 10.1111/j.1365-2672.2012.05344.x
158. Siragusa S, De Angelis M, Di Cagno R, Rizzello CG, Coda R, Gobbetti M. Synthesis of gamma-aminobutyric acid by lactic acid bacteria isolated from a variety of Italian cheeses. *Appl Environ Microbiol* (2007) 73(22):7283–90. doi: 10.1128/AEM.01064-07
159. Hata T, Miyata N, Takakura S, Yoshihara K, Asano Y, Kimura-Todani T, et al. The Gut Microbiome Derived From Anorexia Nervosa Patients Impairs Weight Gain and Behavioral Performance in Female Mice. *Endocrinology* (2019) 160(10):2441–52. doi: 10.1210/en.2019-00408
160. Monteleone P, Monteleone AM, Troisi J, Dalle Grave R, Corrivetti G, Calugi S, et al. Metabolomics signatures of acutely ill and short-term weight recovered women with anorexia nervosa. *Mol Psychiatry* (2019). doi: 10.1038/s41380-019-0573-3
161. Cammarota G, Masucci L, Ianiro G, Bibbò S, Dinoi G, Costamagna G, et al. Randomised clinical trial: faecal microbiota transplantation by colonoscopy

vs. vancomycin for the treatment of recurrent Clostridium difficile infection. *Aliment Pharmacol Ther* (2015) 41(9):835–43. doi: 10.1111/apt.13144
162. Zenzeri L, Tambucci R, Quitadamo P, Giorgio V, De Giorgio R, Di Nardo G. Update on chronic intestinal pseudo-obstruction. *Curr Opin Gastroenterol* (2020) 36(3):230–7. doi: 10.1097/MOG.0000000000000630
163. Quigley EMM. The Spectrum of Small Intestinal Bacterial Overgrowth (SIBO). *Curr Gastroenterol Rep* (2019) 21(1):3. doi: 10.1007/s11894-019-0671-z
164. Santonicola A, Gagliardi M, Guarino MPL, Siniscalchi M, Ciacci C, Iovino P. Eating Disorders and Gastrointestinal Diseases. *Nutrients* (2019) 11 (12):3038. doi: 10.3390/nu11123038
165. Vendrik KEW, Ooijevaar RE, de Jong PRC, Laman JD, van Oosten BW, van Hilten JJ, et al. Fecal Microbiota Transplantation in Neurological Disorders. *Front Cell Infect Microbiol* (2020) 10:98. doi: 10.3389/fcimb.2020.00098

Conflict of Interest: The authors declare that the research was conducted in the absence of any commercial or financial relationships that could be construed as a potential conflict of interest.

The reviewer LP declared a shared affiliation with several of the authors to the handling editor at time of review.

Advantages of publishing in Frontiers

OPEN ACCESS
Articles are free to read for greatest visibility and readership

FAST PUBLICATION
Around 90 days from submission to decision

HIGH QUALITY PEER-REVIEW
Rigorous, collaborative, and constructive peer-review

TRANSPARENT PEER-REVIEW
Editors and reviewers acknowledged by name on published articles

Frontiers
Avenue du Tribunal-Fédéral 34
1005 Lausanne | Switzerland

Visit us: www.frontiersin.org
Contact us: frontiersin.org/about/contact

REPRODUCIBILITY OF RESEARCH
Support open data and methods to enhance research reproducibility

DIGITAL PUBLISHING
Articles designed for optimal readership across devices

FOLLOW US
@frontiersin

IMPACT METRICS
Advanced article metrics track visibility across digital media

EXTENSIVE PROMOTION
Marketing and promotion of impactful research

LOOP RESEARCH NETWORK
Our network increases your article's readership